A. TREMBLAY · L. VARFALVY
C. ROEHM · M. GARNEAU
Editors

Greenhouse Gas Emissions – Fluxes and Processes

Hydroelectric Reservoirs and Natural Environments

Springer

Environmental Science

Series Editors: R Allan • U. Förstner • W. Salomons

Alain Tremblay, Louis Varfalvy,
Charlotte Roehm and Michelle Garneau
(Eds.)

Greenhouse Gas Emissions - Fluxes and Processes

Hydroelectric Reservoirs and Natural Environments

With 200 Figures

Springer

Dr. ALain Tremblay
Hydro-Québec Production
Direction Barrages et
Environnement
10nd floor
75 Boul. René-Lévasque
Montréal, Québec H2Z 1A4
Canada

Dr. Louis Varfalvy
Hydro-Québec
Direction Environnement
2nd floor
75 Boul. René-Lévasque
Montréal, Québec H2Z 1A4
Canada

Dr. Charlotte Roehm
Université du Québec à
Montréal
Département des sciences
biologiques
Case Postal 8888, Succursale
Centre-ville
Montréal, Québec H3C 3P8
Canada

Dr. Michelle Garneau
Université du Québec à
Montréal
Centre de Modélisation
Régionale du Climat-Ouranos
Département de Géographie
Case Postal 8888, Succursale
Centre-ville
Montréal, Québec H3C 3P8
Canada

Library of Congress Control Number: 2004114231

ISBN 3-540-23455-1 **Springer Berlin Heidelberg New York**

Springer is a part of Springer Science+Business Media
springeronline.com

Printed in Germany

Cover design: E. Kirchner, Heidelberg
Production: A. Oelschläger
Typesetting: Camera-ready by the Editors
Printing: Mercedes-Druck, Berlin
Binding: Stein + Lehmann, Berlin

Printed on acid-free paper 30/2132/AO 5 4 3 2 1 0

Foreword

In a time when an unquestionable link between anthropogenic emissions of greenhouse gases and climatic changes has finally been acknowledged and widely documented through IPCC* reports, the need for precise estimates of greenhouse gas (GHG) production rates and emissions from natural as well as managed ecosystems has risen to a critical level. Future agreements between nations concerning the reduction of their GHG emissions will depend upon precise estimates of the present level of these emissions in both natural and managed terrestrial and aquatic environments.

From this viewpoint, the present volume should prove to a benchmark contribution because it provides very carefully assessed values for GHG emissions or exchanges between critical climatic zones in aquatic environments and the atmosphere. It also provides unique information on the biases of different measurement methods that may account for some of the contradictory results that have been published recently in the literature on this subject. Not only has a large array of current measurement methods been tested concurrently here, but a few new approaches have also been developed, notably laser measurements of atmospheric CO_2 concentration gradients. Another highly useful feature of this book is the addition of monitoring and process studies as well as modeling.

Indeed, the prospect of mitigation measures and of better management practices of aquatic environments requires an in-depth knowledge of processes governing GHG production and an exhaustive knowledge of those involved in the global carbon cycle. Here again, the present volume provides new information and highly original research projects on the carbon fate in aquatic systems. Most compartments of the carbon cycle in such systems have been investigated using state-of-the-art methodologies. The roles of primary production and of the bacterial and photochemical degradation of organic matter are carefully addressed as well as the fate of soil-derived dissolved organic carbon (DOC) in the aquatic environments. The degradation site and rates of DOC seem to be key elements in this respect.

---

* International Panel on Climate Change (see http:// www.ipcc.ch)

As illustrated in the volume, the present state of knowledge does not permit the unequivocal conversion of "gross GHG emissions" of impounded basins into "net GHG emissions," mainly due to uncertainties concerning the fate of terrestrially derived DOC and of soil-atmosphere budgets. In other words, GHG emissions resulting strictly from the impoundment of terrestrial and aquatic ecosystems, particularly in high latitude environments, are certainly lower than the measured emissions, but are still difficult to assess.

As a matter of fact, the focus on the boreal forest and equatorial systems described here is interesting in the way that it provides information on the two end-members of large aquatic bodies with respect to their GHG emissions into the atmosphere, from primarily CO_2-emitters in the Boreal domain to primarily CH_4-emitters in the equatorial forest domain. More concern, indeed, arises from the role of the latter in the capture of atmospheric CO_2 through primary production and its replacement by the much longer residence time of CH_4.

Nevertheless, despite the contributions of nearly 60 co-authors, this volume has well-balanced content and a coherent view of GHG production and emissions in terrestrial water bodies. The efforts of the editorial committee have been instrumental in this respect. However, one specific advantage of the involvement of such a large group of scientists in such a hotly debated topic cannot be ignored: a consensus among so many specialists is likely to provide ground for policy decisions.

It is very much to the credit of Hydro-Québec and its partners that supported most of the studies illustrated in the present volume that they have devoted so much time and effort to studying GHG emissions from hydroelectric reservoirs. Indeed, from the strict viewpoint of Hydro-Québec, this problem is relatively less serious than for many other energy producers, since hydropower from boreal forest reservoirs remains one of the most cost-effective processes with respect to GHG emissions.

Claude Hillaire-Marcel, D. ès Sci,, F.R.S.C.
UNESCO Chair for Global Change Study
Université du Québec à Montréal

Contents

Gross Emissions

Processes Leading to GHG Production

Modelling

Editorial Committee

External Reviewers

The editorial committee would like to thank the external reviewers for their highly relevant comments and useful suggestions to improve the monograph.

Eric Duchemin, Ph.D.
DREX Environnement
2669 Knox
Montréal, Québec, H3K 1R3
Canada

George W. Kling, Ph.D.
Department of Ecology
and Evolutionary Biology
University of Michigan
Ann Arbor, Michigan, 48109-1048
USA

Peter Kuhry, Ph.D.
Department of Physical Geography
and Quaternary Geology
Stockholm University,
SE-106 91 Stockholm,
Sweden

List of contributors

Gwenaël Abril, Ph.D.
Université Bordeaux 1
Département de Géologie et Océanographie
CNRS-UMR EPOC 5805
Avenue des Facultés, F 33405 Talence
France

Donald Adams, Ph.D.
Center for Earth and Environmental Science
State University of New York
Plattsburgh, New York 12901
U.S.A.

Nathalie Barrette, Ph.D.
Université Laval
Département de Géographie
Sainte-Foy, Québec, G1K 7P4
Canada

Julie Bastien, M.Sc.
Institut national de la recherche scientifique
Centre Eau, Terre et Environnement
2800, rue Einstein
C.P. 7500
Ste-Foy, Québec, G1V 4C7
Canada

Kenneth G. Beaty
Fisheries and Oceans Canada,
Freshwater Institute,
501 University Crescent,
Winnipeg, MB R3T 2N6
Canada

Anne-Marie Blais, M.Sc.
Environnement Illimité inc.
1453 Saint-Timothée
Montréal, Québec, H2L 3N7
Canada

Philippe Chrétien, B.Sc.
Université Laval
Département de physique
Laboratoire de Physique Atomique et Moléculaire
Cité universitaire, Québec, G1K 7P4
Canada

François Courchesne, Ph.D.
Département de Géographie,
Université de Montréal,
C.P. 6128, Succursale Centre-Ville,
Montréal, Québec, H3C 3J7
Canada

Claire Delon, Ph.D.
Laboratoire d'Aérologie,
UMR CNRS 5560, OMP,
14 Avenue E. Belin 31 400,
Toulouse, France

Robert Delmas, Ph.D.
Laboratoire d'Aérologie,
UMR CNRS 5560, OMP,
14 Avenue E. Belin 31 400,
Toulouse, France

Claude Demers, M.Sc.
Hydro-Québec
Direction Environnement
2nd floor
75 Boul. René-Lévesque
Montréal, Québec, H2Z 1A4
Canada

Ednaldo Oliveira dos Santos, M.Sc.
IVIG/COPPE/UFRJ - Centro de Tecnologia,
Bloco I, Sala 129, Cidade Universitária
Zip Code: 21945-970
Rio de Janeiro , Brazil

Jean-Louis Fréchette
Groupe Conseil Génivar
5355 Boul. des Gradins
Québec, Québec, G2J 1C8
Canada

Philippe Gosse, Senior Eng.
EDF-R&D,
6 Quai Watier,
78 401 Chatou Cedex,
France

Alain Grégoire, Ph.D.
EDF-CIH,
Savoie Technolac,
73 373 le Bourget du Lac Cedex,
France

Bill Hamlin, P. Eng.
Resource Planning & Market Analysis Department
Manitoba Hydro
820 Taylor Avenue
P.O. Box 815
Winnipeg, Manitoba, R3C 2P4
Canada

Marco Aurelio dos Santos, D.Sc.
IVIG/COPPE/UFRJ - Centro de Tecnologia,
Bloco I, Sala 129, Cidade Universitária
Zip Code: 21945-970
Rio de Janeiro, Brazil

Rachel A. Dwilow, B.Sc.
Fisheries and Oceans Canada,
Freshwater Institute,
501 University Crescent,
Winnipeg, MB R3T 2N6
Canada

Corinne Galy-Lacaux, Ph.D.
Laboratoire d'Aérologie,
UMR CNRS 5560, OMP,
14 Avenue E. Belin 31 400,
Toulouse, France

Charles W. Greer, Ph.D.
Biotechnology Research Institute,
National Research Council Canada,
6100 Royalmount Ave.,
Montreal Quebec, H4P 2R2
Canada

Frédéric Guérin
(Ph.D. Student)
Laboratoire d'Aérologie,
UMR CNRS 5560, OMP,
14 Avenue E. Belin 31 400,
Toulouse, France

Jean-François Hélie, Ph.D.
Université du Québec à Montréal
GEOTOP
C.P. 8888, Succursale Centre-ville
Montréal, Québec, H3C 3P8
Canada

Claude Hillaire-Marcel, Ph.D.
Université du Québec à Montréal
GEOTOP
C.P. 8888, Succursale Centre-ville
Montréal, Québec, H3C 3P8
Canada

Raymond H. Hesslein, Ph.D.
Fisheries and Oceans Canada,
Freshwater Institute,
501 University Crescent,
Winnipeg, MB R3T 2N6
Canada

Robert B. Jacques, M.Sc., P. Eng.
E Cubed Inc.
2603 Toulouse Drive
Austin, Texas, 78748-6015
USA

Louis B. Jugnia, Ph.D.
Université du Québec à Montréal
Biotechnology Research Institute
GEOTOP
C.P. 8888, Succursale Centre-ville
Montréal, Québec, H3C 3P8
Canada

Maryse Lambert, M.Sc.
Hydro-Québec
Direction Environnement
2nd floor
75 Boul. René-Lévesque
Montréal, Québec,H2Z 1A4
Canada

René Laprise, Ph.D.
Université du Québec à Montréal
Centre de Modélisation Régionale du Climat - Ouranos
Département des sciences de la Terre et de l'Atmosphère
C.P. 8888, Succursale Centre-ville
Montréal, Québec, H3C 3P8
Canada

Michel Larzillière Ph.D.
Université Laval
Département de physique
Laboratoire de Physique Atomique et Moléculaire
Cité universitaire, Québec, G1K 7P4
Canada

Lawrence J. LeDrew, M.Sc.
Newfoundland and Labrador Hydro
P.O. Box 12,400
500 Columbus Drive
St.John's, NewFoundland, A1B 4K7
Canada

Mark E. Lyng
Fisheries and Oceans Canada,
Freshwater Institute,
501 University Crescent,
Winnipeg, MB R3T 2N6
Canada

Stéphane Lorrain, M.Sc.
Environnement Illimité inc.
1453 Saint-Timothée
Montréal, Québec, H2L 3N7
Canada

Jérôme Marty, M.Sc.
(Ph.D. Student)
Université du Québec à Montréal
GEOTOP
C.P. 8888, Succursale Centre-ville
Montréal, Québec, H3C 3P8
Canada

Bohdan Matvienko, D.Sc.
Hydraulics Department,
University of São Paulo – São Carlos
SP 13560-970, Brazil

Cory Matthews, M.Sc.
Department of Biological Sciences,
University of Alberta,
Edmonton, Alberta, T6H 4R3
Canada

Ginette Méthot, M.Sc.
Département des sciences biologiques
Faculté des arts et des sciences
Université de Montréal
90 rue Vincent d'Indy
C.P. 6128, Succursale Centre-ville
Montréal Québec, H3C 3J7
Canada

Carlos B. Miguez, Ph.D.
Biotechnology Research Institute,
National Research Council Canada,
6100 Royalmount Ave.,
Montreal Quebec, H4P 2R2
Canada

Ken Morrison, Ph.D.
Faculté de génie
Université de Sherbrooke
2500 Boul de l'Université
Sherbrooke, Québec, J1K 2R1
Canada

Maria C. Pacheco-Oliver, B.Sc.
Biotechnology Research Institute,
National Research Council Canada,
6100 Royalmount Ave.,
Montreal Quebec, H4P 2R2
Canada

Serge Paquet, M.Sc.
Université du Québec à Montréal
GEOTOP
C.P. 8888, Succursale Centre-ville
Montréal, Québec, H3C 3P8
Canada

Bernadette Pinel-Alloul, Ph.D.
Département des sciences biologiques
Faculté des arts et des sciences
Université de Montréal
90 rue Vincent d'Indy
C.P. 6128, Succursale Centre-ville
Montréal Québec, H3C 3J7
Canada

Dolors Planas, Ph.D.
Université du Québec à Montréal
GEOTOP
C.P. 8888, Succursale Centre-ville
Montréal, Québec, H3C 3P8
Canada

Yanick Plourde, M.Sc.
Groupe Conseil Génivar
5355 Boul. des Gradins
Québec, Québec, G2J 1C8
Canada

Sandrine Richard, Ph.D.
Laboratoire Environnement,
Hydreco,
BP 823, 97 388 Kourou Cedex,
France

Tommy Ringuette, M.Sc.
Université Laval
Département de physique
Laboratoire de Physique Atomique et Moléculaire
Cité universitaire, Québec, G1K 7P4
Canada

Luiz Pinguelli Rosa, D.Sc.
IVIG/COPPE/UFRJ - Centro de Tecnologia,
Bloco I, Sala 129, Cidade Universitária
Zip Code: 21945-970
Rio de Janeiro, Brazil

Réal Roy, Ph.D.
University of Victoria
Department of Biology
P.O. Box 3020 Stn CSC
Victoria, British Columbia, V8W 3N5
Canada

Denis Roy, Ph.D.
Université Laval
Département de physique
Laboratoire de Physique Atomique et Moléculaire
Cité universitaire, Québec, G1K 7P4
Canada

Sherry Schiff, Ph.D.:
Department of Earth Sciences
University of Waterloo
200 University Ave W
Waterloo, Omtario, N2L 3G1
Canada

Elizabeth Sikar, B.Sc.
Construmaq
C.P. 717 – São Carlos
SP – 13560-970, Brazil

Vincent St. Louis, Ph.D.
Department of Biological Sciences,
University of Alberta,
Edmonton, Alberta, T6H 4R3
Canada

Annick St-Pierre, B.Sc.
(M.Sc. Student)
Université du Québec à Montréal
GEOTOP
C.P. 8888, Succursale Centre-ville
Montréal, Québec, H3C 3P8
Canada

Rémy D. Tadonléké, Ph.D.
Université du Québec à Montréal
GEOTOP
C.P. 8888, Succursale Centre-ville
Montréal, Québec, H3C 3P8
Canada

Normand Thérien, Ph.D.
Département de génie chimique
Faculté de génie
Université de Sherbrooke
2500 Boul de l'Université
Sherbrooke, Québec, J1K 2R1
Canada

Jean Therrien, B.Sc.
Groupe Conseil Génivar
5355 Boul. des Gradins
Québec, Québec, G2J 1C8
Canada

Marie-Claude Turmel, M.Sc.
Département de Géographie,
Université de Montréal,
C.P. 6128, Succursale Centre-Ville,
Montréal, Québec, H3C 3J7
Canada

Jason Venkiteswaran, M.Sc.
Department of Earth Sciences
University of Waterloo
200 University Ave W
Waterloo, Ontario, N2L 3G1
Canada

Alberto Vieira Borges" Ph.D.
Université de Liège
Unité d'Océanographie Chimique,
MARE, Institut de Physique (B5),
B 4000, Liège, Belgium.

Eva Wichmann, BSc., R.P.Bio
BC Hydro
Generation Sustainability
6911 Southpoint Drive, E 16
Burnaby, British Columbia, V3N 4X8
Canada

The editorial committee would like to thank the following contributors for their help in editing this monograph.

Lise Blais
En Toutes Lettres
1453, Saint-Timothée
Montréal, Québec, H2L 3N7
Canada

Daniel Cloutier
Carto-Média
1453, Saint-Timothée
Montréal, Québec, H2L 3N7
Canada

Nicole Paré
Hydro-Québec
Centre de documentation
2nd floor
75 Boul. René-Lévesque
Montréal, Québec, H2Z 1A4
Canada

Glossary

nm:	nanometer
UV:	Ultra-violet light
DOM:	Dissolved organic matter
DOC:	Dissolved organic carbon
DIC:	Dissolved inorganic carbon
Gross emission:	The gross emissions are those measured at the water-air interface or soil-air interface or soil-water interface.
Net emission:	The net reservoir emissions are gross emissions minus pre-impoundment natural emission (both terrestrial and aquatic ecosystems) at the whole watershed level, including downstream and estuary.
NDIR:	None-dispersive Infrared
FTIR:	Fourier Transform Infrared
CO_2:	Carbon dioxide (44 g per mole, 1 mmole of CO_2 = 44 mg of CO_2)
CH_4:	Methane (16 g per mole, 1 mmole of CH_4 = 16 mg of CH_4)
N_2O:	Nitrous oxide
$mg \cdot m^{-2} \cdot d^{-1}$:	milligram per square meter per day ($mg/m^2/d$)

Résumé-Synthèse

Alain Tremblay, Louis Varfalvy, Charlotte Roehm et Michelle Garneau

Ce chapitre a pour but de faire le point sur l'état des connaissances et d'identifier les lacunes relatives à la problématique de l'émission de gaz à effet de serre (GES) par les réservoirs hydroélectriques et les écosystèmes naturels. Il est devenu essentiel d'intégrer nos connaissances du cycle du carbone à des échelles temporelles et spatiales plus vastes de façon à mieux définir l'ampleur des flux de GES associés aux réservoirs[1] et aux écosystèmes naturels. Les données disponibles proviennent d'études à petite échelle et de courte durée (1 à 10 ans), effectuées surtout en région boréale, mais aussi en régions semi-aride et tropicale. La variabilité naturelle des flux de GES due à des variations climatiques régionales et leurs impacts sur la production biologique globale est plus importante que celle des méthodes de mesures. Il faut donc garder à l'esprit que les incertitudes concernant les flux de GES sont avant tout le résultat de variations spatiales et temporelles naturelles des flux, et non pas des techniques de mesure disponibles. La présente synthèse se base sur les résultats de plus de dix ans de suivis obtenus par différentes équipes de recherche de plusieurs universités, institutions gouvernementales et compagnies d'électricité.

[1] Pour évaluer l'ampleur des flux de GES, nous avons calculé les émissions brutes et les émissions nettes. Les émissions brutes sont celles mesurées à l'interface eau-air. Les émissions nettes des réservoirs correspondent à la différence entre les émissions brutes et les émissions naturelles des écosystèmes terrestres et aquatiques avant la mise en eau, pour l'ensemble du bassin versant, incluant la portion avale et l'estuaire. Ces définitions sont celles de WCD (2000).

Les gaz à effet de serre dans les milieux naturels

Écosystèmes terrestres

Les forêts et les milieux humides constituent des écosystèmes dynamiques notamment par leur contribution au cycle global du carbone. La teneur en carbone des forêts des différentes régions climatiques est similaire ; toutefois, la répartition du carbone entre les sols et la végétation varie selon la latitude. Les plus hautes latitudes sont caractérisées par des taux de décomposition plus lents et des saisons de croissance plus courtes (chapitre 6, Malhi et al. 1999). Les sols typiques des forêts boréales ont une teneur plus élevée en carbone organique (24 ± 94 %) que les sols des forêts tempérées (10 ± 77 %) ou tropicales (11 ± 63 %). Cependant, les estimés de carbone organique retenu dans la végétation de la forêt tropicale sont de deux à cinq fois plus élevés (15-23 kg C m^{-2}) que ceux des forêts boréale et tempérée (4-6 kg C m^{-2}) (chapitre 6, Goodale et al. 2002, FAO 2001, Malhi and Grace 2000).

Les estimations courantes des bilans de GES des forêts indiquent que ces écosystèmes sont des puits de carbone, peu importe la région climatique du globe. La rétention de GES par les forêts est le résultat de la différence entre une absorption substantielle de dioxide de carbone (CO_2) par la biomasse et le dégagement de CO_2 par la respiration du sol, l'oxydation du méthane (CH_4) par des bactéries méthanotrophiques, et une émission plus ou moins importante de d'oxyde nitreux (N_2O) par le sol, un sous-produit des réactions de nitrification et de dénitrification. Selon les bilans estimés de GES, le puits de carbone de la forêt boréale (-873 mg CO_2-éq. m^{-2} j^{-1}) est plus faible que celui de la forêt tempérée et et de la forêt tropicale (-1 288 et -1 673 mg CO_2-éq m^{-2} j^{-1}, respectivement). Durant les années particulièrement chaudes et sèches, les forêts boréales peuvent devenir des sources nettes de CO_2 (chapitre 4, Goulden et al. 1998 ; Lindroth et al. 1998 ; Carrara et al. 2003). La durée de la saison de croissance, qui augmente des hautes vers les basses latitudes, contribue à ce patron général. Au contraire des forêts boréale et tempérée, la forêt tropicale a un flux de N_2O qui semble jouer un rôle important dans le bilan de GES, représentant une perte moyenne de 30 % (en CO_2-éq.) de l'échange net de l'écosysteme (ENE, Net Ecosystem Exchange). Ceci est dû à un taux relativement élevé d'émission de N_2O par les sols de la forêt tropicale, ainsi qu'au potentiel de réchauffement global de N_2O, lequel est environ 300 fois plus élevé que celui du CO_2 (IPCC 2001, Livingston et al. 1988, Clein et al. 2002). De plus, comme le suggère la plage estimée des flux de GES pour la forêt tropicale, la production de GES sous forme de N_2O pourrait dépasser, à cer-

tains sites, l'absorption de CO_2, transformant ces sites en sources de GES (2 758 mg CO_2-éq. m^{-2} j^{-1}) (chapitre 4).

Il est probable que les conditions climatiques changeantes augmentent la fréquence et l'étendue des perturbations naturelles (feu, défoliation par les insectes, zone de chablis) (IPCC 2001). Cependant, les bilans actuels de GES des forêts ne tiennent pas compte de l'influence de ces perturbations naturelles sur la dynamique à grande échelle du carbone des forêts boréales. Sur de grandes étendues, ces perturbations naturelles (surtout les feux de forêt) peuvent provoquer, à court et à long terme, des émissions significatives ; elles devraient être prises en considération pour une évaluation plus précise de la rétention de carbone ou de la production nette de biomes d'un écosystème (Amiro et al. 2001 ; Kasischke and Bruhwiler 2002, chapitres 4 et 6).

Les milieux humides couvrent 3 % de la surface de la Terre, mais ils représentent approximativement 30 % du puits de carbone du sol terrestre Les tourbières représentent environ 30 % du paysage circumboréal (Gorham 1991, McLaughlin 2004). Elles ont une forte tendance à émettre du CH_4 à cause de leurs sols saturés d'eau qui favorisent la décomposition anaérobique de la matière organique. Les milieux humides tropicaux, caractérisés par les marais et marécages, émettent de plus grandes quantités de CH_4 dans l'atmosphère (71 mg CH_4 m^{-2} j^{-1}), par comparaison avec les émissions des tourbières boréales (34 mg CH_4 m^{-2} j^{-1}), résultant en un bilan global de GES d'environ 11 000 mg CO_2-éq. m^{-2} j^{-1} et 1400 mg CO_2-éq. m^{-2} j^{-1} pour les milieux humides tropicaux et boréaux, respectivement. Cependant, le nombre de données disponibles étant limité, ces bilans ne donnent qu'un ordre de grandeur des flux de GES. Tout comme pour les forêts, les flux de GES des milieux humides varient en fonction de paramètres environnementaux et climatiques (chapitre 6, McLaughlin 2004). De plus, les bilans de GES estimés pour les milieux humides ne tiennent généralement pas compte des étangs ou mares qui ponctuent ces écosystèmes et qui sont aussi une source potentielle de GES (Kling et al. 1991, Roulet et al. 1994 ; Waddington and Roulet 2000) et d'exportation de carbone organique dissous (COD, Carroll and Crill 1997 ; Alm et al. 1999b ; Waddington and Roulet 2000). La prise en compte de ces exportations pourrait modifier significativement les bilans de GES des milieux humides.

La majorité de l'information disponible dans la documentation scientifique couvre une saison de croissance partielle ou complète sur quelques années seulement (chapitre 4). Peu importe le type d'écosystème, il existe très peu d'études qui prennent en considération le cycle annuel complet dans l'évaluation des bilans de carbone. Puisque les flux de GES varient de façon saisonnière et annuelle selon les conditions climatiques, il est impor-

tant de tenir compte des échelles temporelle et spatiale utilisées pour estimer les bilans nets de GES pour les écosystèmes terrestres. Par exemple, il est généralement admis qu'après une période de croissance de 30 à 50 ans (puits de carbone), les écosystèmes naturels forêts atteignent un stade de maturité qui dure quelques années, pendant lequel ils ne sont ni un puits, ni une source de carbone. Il s'ensuit par après une période de lente décomposition où ces écosystèmes se transforment en une source de carbone (Grace et al. 1995, International Science Conference, 2000). Étant donné la forte variabilité observée dans les flux de GES sur de petites échelles, une période temporelle de 100 ans et une couverture spatiale à l'échelle du bassin versant seraient plus adéquates pour évaluer le bilan massique de GES dans les écosystèmes terrestres. Cette approche minimiserait la variation saisonnière ou locale induite par la variabilité climatique et biologique naturelle et donnerait des estimés plus réalistes des flux nets de GES.

Écosystèmes aquatiques

Bien que les eaux intérieures constituent moins de 2 % de la surface de la terre, elles peuvent contribuer de façon importante au cycle global du carbone puisqu'une portion significative du carbone organique terrestre transite par les rivières et les lacs avant d'atteindre les estuaires et les océans. Des études récentes ont démontré que jusqu'à 15 % de la production annuelle de carbone des forêts est exportée via le système de drainage et que le flux de CO_2 des habitats limnétiques vers l'atmosphère peut représenter jusqu'à 50 % des pertes continentales de carbone organique vers les océans (Cole et al. 1994, Dillon and Molot 1997). Ceci est particulièrement vrai dans l'hémisphère nord où se trouve la majorité des lacs d'eau douce de la planète. Le transfert de carbone des écosystèmes terrestres vers les écosystèmes aquatiques, sous forme de COD et CID, peut contribuer à augmenter les bilans de carbone (Richey et al. 2002, chapitre 6).

Approximativement 90 % du carbone organique dans les lacs et les rivières se retrouve en phase dissoute (COD) et 10 % sous forme particulaire (COP) (Naiman 1982 ; Hope et al. 1994 ; Pourriot and Meybeck 1995). Les teneurs en COD et COP sont supérieures à la quantité de carbone organique présente sous forme de matériel vivant tel que les bactéries, le plancton, la flore et la faune (Wetzel 2001). La source première de matériel et d'énergie dans la plupart des écosystèmes aquatiques provient des apports allochtones de la matière organique terrestre. La quantité de matière organique qui entre dans un lac et la composition chimique de ces composés organiques varient de façon saisonnière en fonction du taux d'écoulement dans le cours d'eau, et du cycle de croissance et de décom-

position de la végétation terrestre et de la végétation des milieux humides (chapitres 6, 8 et 9). En comparaison du ruissellement, l'apport de la nappe phréatique ne contribue qu'à de petites quantités de COD (environ 5 %) dans les écosystèmes aquatiques (Devol et al. 1987 ; Cole et al. 1989 ; Prairie et al. 2002, Schiff et al. 2001).

Une grande partie du COD est constituée de composés réfractaires complexes et résistants à la dégradation microbienne (Lindell et al. 1995 ; Moran et al. 2000). Les composés organiques dissous labiles sont recyclés rapidement, même à de faibles concentrations, et représentent les voies principales de transformation énergétique du carbone. Les composés organiques labiles sont utilisés soit par les bactéries ou le phytoplancton. Ils sont transformés à l'intérieur de ces organismes vivants et sont transférés vers le haut de la chaîne alimentaire. Bien que les composés réfractaires complexes peuvent être scindés en fractions plus petites par les rayons ultraviolets (chapitre 21), puis assimilés et utilisés par les bactéries (Gennings et al. 2001), la plupart d'entre eux se déposent au niveau des sédiments lacustres.

Les lacs et les rivières agissent comme des zones de transition pour le carbone entre les écosystèmes terrestres et les estuaires, et sont généralement une source de gaz vers l'atmosphère. Il semble y avoir une relation positive entre la quantité de carbone entrant dans le lac, calculée comme étant le rapport entre la surface du bassin versant et la surface du lac, et l'ampleur des émissions à l'interface eau-air (Engstrom 1987 ; Sobek et al. 2003, Chapter 8). Puisque les apports allochtones terrestres à un lac sont généralement déterminés par les caractéristiques de son bassin versant et qu'ils sont relativement constants dans le temps, l'émission de CO_2 vers l'atmosphère ou son transfert vers l'aval devrait aussi être relativement constant à long terme (Wetzel 2001). Dans les lacs profonds, la contribution en carbone organique provenant des sédiments est très faible en comparaison à l'apport terrestre du bassin versant. Cependant, dans les lacs peu profonds, l'ampleur des flux de carbone provenant des sédiments peut être significative, puisque la température de l'eau est généralement plus élevée favorisant la décomposition de la matière organique (chapitres 5, 11, 22).

Dans les écosystèmes aquatiques, le carbone est transformé par les producteurs primaires (bactéries, phytoplancton) et/ou par les consommateurs secondaires (zooplancton, benthos, poisson), et à mesure qu'il se déplace vers le haut de la chaîne alimentaire, il est respiré ou consommé à des taux différents selon la productivité du système. En plus de la physicochimie de l'eau, ces taux de respiration vont influencer la quantité de CO_2 dissous dans l'eau ainsi que et les flux de CO_2 à l'interface eau-air. Approximativement 90 % des lacs boréaux naturels sont sursaturés en CO_2 et émettent entre 50 et 10 000 mg CO_2 m^{-2} j^{-1} vers l'atmosphère (ex. : Cole et al. 1994,

Prairie et al. 2002, Therrien 2003). Les rivières des zones boréale et tempérée ont des flux plus élevés ou du même ordre de grandeur que les lacs (Hinton et al., 1998, Hope et al., 1997, Cole and Caraco 2001, Sobek et al. 2003). Par contre, les lacs ayant un pH supérieur à 8, soit à cause d'une production primaire élevée ou soit encore par l'effet tampon des sols alcalins du bassin versant, ont tendance à être non-saturés en CO_2. Ces systèmes ont des taux d'émission plus faibles, ou encore ils agissent comme des puits de CO_2 (chapitres 8, 9).

La plupart des lacs, des rivières et des *varzéas* des régions tropicales ont des émissions de CO_2 généralement plus élevées que dans les milieux similaires en région boréale (Richey et al. 2002, Chapter 22). Bien que les flux de CH_4 à l'interface eau-air soient faibles et que les flux de N_2O soient négligeables (Therrien, chapitres 8, 9) autant dans les régions tropicales que boréales, les émissions de CH_4 peuvent être significatives dans des milieux peu profonds comme les barrages de castor, les rizières et les *varzéas* (chapitres 4, 6, 22).

Les sédiments de subsurface présentent souvent des conditions anoxiques qui favorisent la production de CH_4 et en augmentent les concentrations. La production et la diffusion de CH_4 à l'interface sédiment-eau augmentent toutes deux en fonction de la productivité globale du lac, des lacs oligotrophes aux lacs eutrophes (chapitre 5). Cependant, plus de 95 % de la production sédimentaire de CH_4 dans les sédiments est oxydée dans la colonne d'eau et/ou à l'interface sédiment-eau contribuant très peu, de façon directe, aux émissions de GES du lac (Lidstrom and Somers 1984, Frenzel et al. 1990, King 1990, King and Blackburn 1996). La production de CH_4 dans les sédiments augmente normalement en fonction de la profondeur du lac à cause des conditions anoxiques qui y sont plus fréquentes. Toutefois, dans les eaux chaudes peu profondes des régions tropicales, avec des sédiments riches en matière organique, par exemple dans les varzéas, ou dans les lacs très eutrophes des régions tempérées, le CH_4 peut former des bulles qui ne seront pas oxydées et qui pourraient contribuer significativement aux émissions de GES (chapitres 5, 11, Keller and Stallard 1994 , Huttunen et al. 1999) (figure 26.1). Dans les zones peu profondes (< 1 m), le CH_4 émis à l'interface eau-air représente jusqu'à 45 % de la production de CH_4 à l'interface sédiment-eau (Scranton et al. 1993, Duchemin et al. 1995, Duchemin et al. 2000, Huttunen et al. 2002) et jusqu'à 10 % de la production de CH_4 dans les zones plus profondes (>3 m) (Rudd et Taylor, 1980). Dans certains milieux, la production de GES par les sédiments peut donc représenter une proportion significative des gaz émis à l'interface eau-air du lac (chapitre 5).

Estuaires

Les estuaires représentent des lieux où les processus de sédimentation sont intenses Cette sédimentation est soit formée de matériel provenant du ruissellement de surface, soit de matériel terrestre érodé et transporté par les rivières. En plus des apports de matériel inerte, il s'y produit aussi une respiration bactérienne hétérotrophe où la majorité des bactéries sont attachées aux particules et au plancton.

À long terme, les marais salés sont généralement un puits net de CO_2 atmosphérique entraînant une accumulation nette de matière organique dans les sédiments (Smith and Hollibaugh 1993 ; Gattuso et al. 1998). Cependant, à cause d'un recyclage intensif de matière organique avec le jeu des marées, les estrans et les marais intertidaux émettent aussi de grandes quantities de CO_2 directement dans l'atmosphère. Le transport latéral de CO_2 à partir de ces 2 zones peut aussi contribuer significativement au pCO_2 élevé mesuré dans les eaux estuariennes adjacentes. Les estuaires sont des écosystèmes hétérotrophes très dynamiques dont les émissions de CO_2 vers l'atmosphère varient de 44 à 44 000 $mg \cdot m^{-2} \cdot j^{-1}$ (chapitre 7). Les panaches estuariens sont des sites de production primaire intense et ils sont sujets à des variations saisonnières importantes de sorte qu'à n'importe quel moment, certains panaches se comportent comme des puits nets de CO_2 alors que d'autres en sont une source nette de CO_2. La teneur élevée en matière organique dans les sédiments et la faible concentration en oxygène dans les marais intertidaux se traduisent par des émissions faibles de CH_4 vers l'atmosphère, variant de 0,32-8 $mg \cdot m^{-2} \cdot j^{-1}$.

Malgré qu'environ 60 % de l'apport d'eau douce et de carbone organique aux océans surviennent aux latitudes tropicales, la plupart des flux de CO_2 mesurés dans les estuaires le sont aux latitudes tempérées (Ludwig et al. 1996). Globalement, la source de CO_2 des estuaires intérieurs et les sources ou les puits des panaches de rivières pourraient représenter des composantes significatives des cycles régionaux et peut-être du cycle complet du carbone. Cependant, les émissions de CH_4 des estuaires semblent contribuer très peu aux émissions globales de méthane (chapitre 7, Bange et al. 1994).

La problématique des gaz à effet de serre dans les réservoirs hydroélectriques

Selon différents auteurs (IAEA 1996, tableau 26.1), l'hydroélectricité est une des formes de production d'énergie les plus propres en terme

d'émission de gaz à effet de serre. Cette tendance a été confirmée par la plupart des études conduites dans les réservoirs boréaux au cours de la dernière décennie, où les émissions brutes moyennes de GES sont de un ou deux ordres de grandeur plus basses que les émissions produites par les centrales thermiques. Cependant en région tropicale, les émissions par les réservoirs pourraient dépasser, sous certaines conditions, les émissions des sources thermiques (ex. le réservoir Petit Saut en Guyane Française et certains réservoirs au Brésil). Un débat à l'échelle mondiale est présentement cours sur la contribution des réservoirs d'eau douce à l'augmentation des GES dans l'atmosphère. Un débat parallèlle est aussi en cours sur la comparaison entre les différentes méthodes de production d'énergie (Rosa and Scheaffer 1994, 1995, Fearnside 1996, Gagnon and van de Vate 1997, St. Louis et al. 2000, Tremblay et al. 2003). Il en résulte que de nombreuses études ont été menées au cours des dix dernières années pour tenter de cerner les processus qui causent des émissions de GES dans les réservoirs et pour en déterminer la durée.

Les processus chimiques, géomorphologiques et biologiques qui influencent le sort du carbone dans les réservoirs sont similaires à ceux se produisant dans les écosystèmes aquatiques naturels. Cependant, certains de ces processus peuvent être temporairement modifiés à cause de l'inondation d'écosystèmes terrestres suite à la mise en eau des réservoirs (Chartrand et al. 1994, Schetagne 1994, Deslandes et al. 1995). Dans les réservoirs boréaux, des programmes de suivi environnemental ont clairement démontré que ces changements durent généralement moins de dix ans. Par contre, dans les réservoirs tropicaux, ces changements peuvent s'étendre sur une période plus longue, dépendamment des conditions de mise en eau.

Les conclusions tirées dans cette section sont fondées sur les résultats obtenus dans le contexte des plus grands programmes de suivis environnementaux au monde. Il faut garder à l'esprit que la plupart des données proviennent de recherche et de mesures prises en région boréale (surtout au Canada) et, dans une moindre mesure, d'un programme de suivi environnemental au réservoir tropical Petit Saut en Guyane Française. D'autres résultats proviennent de mesures de terrain entreprises dans les régions tropicales du Panama et du Brésil, dans la région semi-aride du sud-ouest des États-Unis, ainsi que de d'autres secteurs de la région boréale (figure 26.2 à 26.5, tableau 26.2).

Sols inondés et sédiments

Des expériences *in vitro* ont été menées en inondant différents types de sol et en reproduisant différentes conditions environnementales rencontrées lors de la mise en eau d'écosystèmes terrestres boréaux (chapitre 13). Ces expériences ont révélé des émissions significatives de CO_2 et de CH_4 des sols ennoyés vers la colonne d'eau des incubateurs. Peu importe les conditions environnementales appliquées sur une durée de 340 jours, la quantité totale de carbone cumulatif variait entre 200 et 450 mg $CO_2.g^{-1}$ et se chiffrait à environ 1,7 mg $CH_4.g^{-1}$ pour la végétation inondée. Pour les sols inondés, les quantités cumulatives moyennes produites durant la même période variaient entre 72 et 140 g CO_2 m^{-2} et entre 0,2 et 0,6 g CH_4 m^{-2} (chapitre 13). Pour la partie vivante de la végétation, une proportion significative de la teneur initiale en carbone a été émise vers la phase aqueuse au cours des six premiers mois, les plus grandes quantités provenant des mousses vertes. Pour les sols inondés, lesquels supportent une masse de matière organique beaucoup plus grande, seule une petite fraction de la teneur initiale en carbone a été relâchée dans la colonne d'eau au cours de l'expérience. Étant donné la grande variabilité de la charge en carbone dans les échantillons de sol, le pourcentage de la teneur initiale en carbone qui est relâché est donc difficile à estimer avec précision.

Dans les réservoirs boréaux, des mesures *in situ* des sols inondés confirment que seulement une petite fraction du carbone disponible est relâchée dans la colonne d'eau (Houel 2002). Après dix ans, la plupart des sols inondés, à l'exception de ceux érodés dans la zone de marnage à la périphérie des réservoirs, ne montrent aucune perte significative de la teneur en carbone (Houel 2003). Ces résultats sont liés à de petits changements physiques structuraux et à une dégradation partielle de la matière organique après l'inondation. Bien que l'activité bactérienne soit suffisamment intense pour provoquer une forte demande en oxygène dans les sols inondés et dans les eaux profondes pendant quelques années après la mise en eau (Schetagne 1994), les pertes de carbone dans ces sols inondés sont plus petites que la variabilité inhérente de la teneur en carbone des sols avoisinants. La matière organique dans les sols podzoliques semble plus sensible à la dégradation après la mise en eau que la matière organique des tourbières déjà saturées en eau avant la mise en eau. Les composantes ligneuses de la végétation inondée sont demeurées virtuellement inchangées après plusieurs décennies et dans le réservoir Gouin, les troncs des épinettes ont perdu moins de 1 % de leur biomasse après 55 ans d'inondation (Québec boréal, Van Coillie et al. 1983). De plus, des résultats provenant de réservoirs artificiels (ELARP and FLUDEX, chapitre 15) ayant des émissions similaires de GES ont démontré que la composition de la matière organi-

que était plus importante que sa quantité. Les réservoirs expérimentaux permettent une meilleure compréhension des mécanismes liés aux flux de GES. Cependant, à cause de leur faible profondeur et de leur petite superficie, les résultats ne peuvent pas être extrapolés facilement à de plus grands réservoirs.

En Guyane Française, région tropicale, les résultats au réservoir Petit Saut ont révélé une augmentation rapide des émissions de GES suite à la mise en eau (chapitres 12, 22, Galy-Lacaux et al. 1997, 1999). La grande quantité de végétation inondée associée à une température moyenne élevée de l'eau (> 25°C) favorise la décomposition de la matière organique et la consommation d'oxygène dissous dans la colonne d'eau, créant des conditions anoxiques qui augmentent la production de CH_4 à l'interface sol-eau. Sept ans après la mise en eau, la production de CH_4 dans les sédiments avait diminué de 30 % (chapitres 12, 22). Cependant, l'apport de carbone provenant du bassin versant pourrait maintenir les conditions anoxiques favorables à la production de CH_4, ce qui pourrait allonger la période de production de CH_4 dans certains réservoirs tropicaux (chapitres 12, 22, figure 26.4 et 26.5).

Il y a une convergence dans les résultats illustrant, dans les réservoirs boréaux autant que dans les réservoirs tropicaux, que la contribution en carbone des sols inondés est importante durant les premières années suivant la mise en eau des réservoirs (chapitres 9, 11, 12). Après cette période, l'apport terrestre allochtone de COD peut excéder de plusieurs fois la quantité de carbone organique particulaire (COP) et de COD produite dans le réservoir par la lixivation des sols ou par la production primaire (Wetzel 2001). Ce phénomène est particulièrement important dans les réservoirs car le temps de séjour de l'eau est généralement court, de quelques semaines à quelques mois, alors que dans les lacs il varie de plusieurs années à plusieurs décennies (chapitre 8). Le modèle des émissions de GES qui prédit qu'après 5 à 8 ans, la contribution en carbone provenant des sols inondés est très petite et que la source majeure de carbone est la matière terrestre allochtone confirme ces résultats. De plus, dans les réservoirs expérimentaux peu profonds FLUDEX et ELARP, où les apports terrestres allochtones sont très petits, une diminution de la production globale de CID et de CO_2 a suivi la production maximale. Il est toutefois difficile de déterminer si ces émissions sont liées à la perte de carbone par les sols inondés ou à la décomposition de la biomasse d'algues produite dans les réservoirs (chapitre 15).

Colonne d'eau

L'hypolimnion (couche inférieure de la colonne d'eau) et l'épilimnion (couche supérieure de la colonne d'eau) sont affectés différemment par les paramètres extérieurs. L'hypolimnion est peu affecté par des processus externes et est généralement caractérisé par la diffusion moléculaire des gaz de l'interface sol-eau à quelques mètres au-dessus du fond (chapitres 5, 22, Duchemin 2000). L'épilimnion est généralement une couche plus épaisse, allant de 1 ou 2 mètres à 35-50 mètres. La dynamique de cette couche est généralemet influencée par des paramètres extérieurs comme le vent, les vagues, les radiations UV, et les échanges gazeux avec l'atmosphère (chapitres 10, 12,13, 14, 20, 22).

Dans le Québec boréal, les résultats obtenus au Complexe La Grande montrent que la décomposition intensive de la matière organique immergée est de courte durée et la fraction facilement décomposable s'épuise rapidement (chapitre 1 et Schetagne 1994). Les modifications de la qualité de l'eau résultant de cette décomposition, telle que la déplétion de l'oxygène dissous, la production accrue de CO_2 et le largage d'éléments nutritifs, durent de 8 à 14 ans après la mise en eau. La durée dépend des caractéristiques hydrauliques et morphologiques du réservoir (Schetagne 1994, Chartrand et al. 1994). Les expériences d'inondation *in vitro* ont confirmé qu'à la température de l'eau du Complexe La Grande (environ 10-20^{o}C), virtuellement tout le carbone labile était décomposé en quelques années, et surtout au cours des premiers mois (chapitre 13). De plus, un modèle expérimental prédisant la qualité de l'eau a démontré une tendance similaire ; après moins de dix ans, la qualité de l'eau dans les réservoirs boréaux était comparable à celle des lacs naturels (chapitre 25). Dans le réservoir tropical de Petit Saut, il y a eu une décomposition très intense de la matière organique inondée, résultant en une consommation rapide de presque tout l'oxygène dissous dans la colonne d'eau. Les modifications de la qualité de l'eau induites par la décomposition ont été plus grandes que dans les réservoirs boréaux. Il s'est produitune stratification presque permanente où la couche supérieure oxygénée s'est épaissie, passant de moins de 1 mètre lors de la mise en eau à près de 7 mètres, 5 ans après la mise en eau. Bien qu'il y ait une nette amélioration de la qualité de l'eau après 5 ans, les modifications pourraient durer plus de 10 ans, contrairement aux réservoirs boréaux (chapitres 12, 22).

Le rapport entre la production primaire brute et la respiration planctonique, qui réflète le métabolisme de la communauté, varie de façon saisonnière à l'intérieur d'un plan d'eau, mais il est similaire dans les lacs et les réservoirs âgés de plus de 7 ans (chapitre 20). Ce rapport indique aussi que la contribution la plus faible de carbone autochtone à la respiration sur-

vient dans les réservoirs les plus jeunes et dans les zones peu profondes où les sols larguent de la matière organique. Ceci est aussi mis en évidence par une activité bactérienne similaire dans les lacs et les réservoirs de plus de 7 ans, quoiqu'il n'y ait pas de preuve évidente que l'âge du réservoir ait un effet important sur l'activité bactérienne mesurée (chapitres 18, 19). Toutefois, l'âge du réservoir a un effet sur la disponibilité du COD et des éléments nutritifs, qui influencent positivement l'activité bactérienne (figures 26.2 à 26.5).

La communauté zooplanctonique a aussi été affectée par la production primaire plus élevée dans les années suivant la mise en eau, la biomasse de la communauté ayant augmenté. Cependant, le zooplancton a été plus affecté par le temps de séjour de l'eau et la température de l'eau que par la disponibilité de nourriture. Dans les réservoirs boréaux, ces conditions ont favorisé la croissance des communautés de cladocères et de rotifères et ont influencé la dynamique des échanges de carbone avec l'atmosphère. Par exemple, la respiration totale de la communauté planctonique dans les réservoirs et dans les lacs représentait plus de 90 % des flux de CO_2 mesurés à l'interface eau-air (chapitre 20).

Échange à l'interface eau-air

Les apports terrestres allochtones de carbone, la physicochimie de l'eau, la dynamique sédimentaire et la production biologique dans un système déterminent la concentration de CO_2 et de CH_4 dissous dans l'eau, et affectent les flux de GES à l'interface eau-air. Cependant, les mécanismes qui prennent place à cet interface sont plutôt complexes et rendent difficile l'estimation des coefficients d'échange (ex. : k_{600}) requis pour calculer les flux de GES par des méthodes indirectes (couche limite, gradients de concentration, etc.) (chapitres 2, 3, 14 ; Guérin et al. 2003, Duchemin et al. 1995). Ainsi, les mesures directes des flux à l'interface eau-air doivent intégrer tous les processus et indiquer la direction réelle des flux, hors du système (source de GES) ou vers le système (puits de GES). Avec moins de 20 % de variation entre les techniques, les méthodes directes et indirectes sont comparables (Lannemezan 2004). Les erreurs associées aux techniques de mesure des flux de GES sont plus faibles que les variations naturelles GES. Il est donc très important de connaître le plus précisement possible les variations spatiales et temporelles des flux de GES.

Lorsqu'ils atteignent leur maximum 3 à 5 ans après la mise en eau, les flux dans les réservoirs réservoirs sont généralement 3 à 6 fois plus élevés que dans les lacs naturels. Dans les réservoirs boréaux de plus de 10 ans, les flux varient entre -1 800 et 11 200 mg $CO_2 \cdot m^{-2} \cdot jour^{-1}$ et sont similaires à

ceux des systèmes naturels dont les valeurs varient entre -460 et 10800 mg $CO_2 \cdot m^{-2} \cdot jour^{-1}$. De façon générale, les émissions provenant du dégazage en aval des barrages et les émissions sous forme de bulles (ébullition) sont très peu rapportées dans les régions boréales où les émissions diffuses sont considérées comme la voie principale d'émission des GES. Les émissions de méthane sont généralement très faibles dans les régions boréales ; cependant, elles peuvent être substantielles dans certaines zones tropicales où l'ébullition est une voie importante d'émission (chapitres 11, 12, 22).

Au Québec, où la plus importante série de données est disponible (10 ans de mesures systématiques), le suivi de l'évolution temporelle des émissions de CO_2 et de CH_4 a été réalisé sur plusieurs réservoirs d'âges différents (de 2 à 90 ans). Les résultats indiquent une augmentation rapide des émissions de GES peu après la mise en eau, suivie d'un retour aux valeurs mesurées dans des lacs naturels ou des rivières (après 10 ans pour le CO_2 et 4 ans pour le CH_4). Les valeurs moyennes de CO_2 varient entre – 3 400 et 16 700 mg $CO_2 \cdot m^{-2} \cdot jour^{-1}$ pour les réservoirs et entre –5 700 et 10 900 mg $CO_2 \cdot m^{-2} \cdot jour^{-1}$ pour les lacs naturels. Bien qu'il y ait moins de données disponibles, des tendances similaires ont été observés dans la plupart des réservoirs étudiés dans d'autres régions boréales (Finlande, Colombie-Britannique, Manitoba, Terre-Neuve-Labrador), semi-arides (Arizona, Nouveau-Mexique, Utah) et tropicales (Panama, Brésil, Guyane Française, chapitres 8, 9, 11, 12). Dans les régions tropicales, le temps requis pour un retour à des valeurs naturelles est parfois plus long, dépendamment des conditions de qualité de l'eau. Par exemple, lorsque des conditions anoxiques prévalent, la production de CH_4 diminue lentement et peut être maintenue pour de plus longues périodes par un apport de carbone provenant du bassin versant. Cependant, de telles situations sont rares dans la plupart des réservoirs étudiés (chapitres 11, 12).

Alors que les mesures directes révèlent l'ampleur des flux de GES, ces flux ne sont pas nécessairement reliés à l'effet réservoir, mais peuvent être parfois reliés à d'autres paramètres comme les apports provenant du bassin versant et des échanges atmosphériques. Tel que mentionné précédemment, il est difficile de séparer la contribution individuelle de chaque paramètre au cycle du carbone. Cependant, l'emploi d'isotopes stables comme traceurs (^{13}C, ^{15}N, ^{18}O) a permis de distinguer entre le CO_2 d'origine terrestre de celui d'origine atmosphérique (chapitre 15). Cette technique permet de distinguer la contribution de la décomposition de la matière organique dans les sols inondés de la matière organique autochtone produite par la production primaire (chapitre 15). Les émissions de surface obtenues par des mesures directes sont habituellement surévaluées par rapport à celles résultant de processus propres aux réservoirs. Par exemple, les flux moyens de diffusion de CO_2 estimés sur le réservoir Robert-Bourassa

(Complexe La Grande) par la technique des isotopes stables étaient 2 à 3 fois plus faibles que ceux obtenus par des mesures directes. À cet égard, des modèles développés pour mesurer les échanges gazeux eau-air peuvent aider à déterminer la contribution des mécanismes principaux responsables des émissions de GES. Les résultats fournis par un tel modèle calibré sur deux réservoirs boréaux (nord du Québec) ont révélé que le vent et la température de l'eau exercent une influence sur les flux de GES (chapitre 21).

Caractéristiques des réservoirs

L'action mécanique du vent, des vagues et de la glace, et les caractéristiques biophysiques du réservoir ont un effet sur le cycle du carbone et peuvent affecter significativement les émissions de GES par les plans d'eau. La proportion de la superficie totale de terre inondée dans la zone de marnage est un bon indicateur de l'ampleur et de la durée de l'action active des vagues sur le transfert du carbone des sols inondés à la colonne d'eau. Cette érosion de matériel organique augmente la disponibilité du carbone (dissous ou particulaire) et des éléments nutritifs pour la production primaire. Dans les zones peu profondes normalement protégées de l'action des vagues, ce processus actif joue un rôle durant des périodes prolongées, où la matière organique n'a pas été érodée. Par exemple, dans les réservoirs du Complexe La Grande, les sols inondés sont généralement minces, érodés rapidement et déposés subséquemment dans des zones profondes plus froides, ce qui devient peu propice à la décomposition bactérienne (Chartrand et al. 1994, tableau 26.2, figures 26.2 et 26.3). Dans les eaux peu profondes où les taux de dilution de l'eau sont réduits, les flux de CO_2 et de CH_4 sont 2 ou 3 fois plus élevés que dans des lacs naturels. Ce phénomène confirme que certaines quantités de carbone et d'éléments nutritifs provenant des sols inondés sont recyclées et maintenues dans la colonne d'eau pour des périodes excédant 10 ans.

Les sols organiques (tourbes) qui sont inondés périodiquement ou en permanence contribuent plus activement à la production de méthane que les sols émergés (chapitre 18). Les taux d'oxydation du méthane sont donc plus élevés dans les tourbières exondés que dans les sols forestiers inondés ou dans les sédiments lacustres. Les taux les plus faibles d'oxydation du méthane se rencontrent dans le sol forestier, composé de sols typiques non perturbés, où les taux de production de CH_4 sont près des valeurs les plus faibles des réservoirs. La plupart du CH_4 produit dans les zones peu profondes des réservoirs peut être oxydé dans la colonne d'eau. Dans les secteurs peu profonds de la zone de marnage, les émissions de GES à partir de substrats inondés ne sont probablement pas importantes à long terme, car

la majorité des sols dans ces zones sont erodés rapidement (figures 26.3). Les résultats obtenus dans les réservoirs du Complexe La Grande, ont révélé que l'érosion de la matière organique dans la zone de marnage était à son maximum durant les premières années et qu'elle diminue rapidement après 5 à 10 ans (Chartrand et al. 1994, chapitre 8). Des résultats similaires ont été obtenus dans le réservoir Petit Saut (Lannemezan, 2004, figures 26.4 et 26.5).

Le rapport entre la surface inondée et le volume annuel d'eau s'écoulant dans le réservoir est un autre indicateur de l'ampleur de l'augmentation en carbone labile et en éléments nutritifs après la mise en eau. Le volume annuel d'eau s'écoulant dans un réservoir est considéré comme un facteur de premier plan parce que : (1) il est un indicateur de la capacité de dilution des éléments nutritifs et du carbone largués dans la colonne d'eau, (2) il joue un rôle dans l'étendue de l'épuisement de l'oxygène et de la production de méthane, et (3) il contribue à l'exportation d'éléments nutritifs et de carbone hors du réservoir, réduisant la production autochtone.

Les réservoirs construits dans les vallées escarpées des montagnes sont généralement profonds, couvrent une petite superficie, ont des couts temps de séjour de l'eau et possèdent d'importants volumes d'eau pour la production d'énergie. Ces réservoirs en montagne sont donc les plus performants en terme d'émissions de GES par unité d'énergie produite. D'un autre côté, les réservoirs construits sur des plateaux sont les moins performants en terme d'émissions de GES par unité d'énergie produite. Ce sont généralement des réservoirs peu profonds, avec de très grandes superficies inondées où les temps de séjour de l'eau sont plus longs (chapitres 8, 9, 11 12).

Évaluation des émissions nettes de GES par les réservoirs

Les émissions plus élevées de GES par les réservoirs durant les premières années suivant la mise en eau sont la conséquence directe de l'immersion des forêts, de leurs sols et des sédiments de tourbière. Ces émissions proviennet du largage de carbone labile et d'éléments nutritifs disponibles pour les organismes de production lors de la mise en eau. Cependant, après une période d'environ 10 ans, tous les paramètres biologiques, de qualité de l'eau et les flux de GES, montrent que les réservoirs se comportent comme des lacs naturels (chapitres 8, 17 18, Schetagne 1994, Chartrand et al. 1994, Therrien 2003). Devant ces résultats, les réservoirs devraient docn être considérés comme des lacs naturels lors de l'évaluation des émissions nettes de GES à long terme .

Pour les lacs naturels, les apports terrestres allochtones sont généralement déterminés par les caractéristiques biophysiques du bassin versant

qui varient relativement peu dans le temps ; ainsi, les émissions de CO_2 vers l'atmosphère devraient aussi être relativement constantes. Ceci est probablement encore plus important pour les réservoirs puisque les temps de séjour de l'eau y sont beaucoup plus courts que dans les lacs.

Les résultants présentés dans cette monographie et plusieurs autres études suggèrent que les lacs naturels et les rivières sont des émetteurs substantiels de CO_2 et de CH_4 alors que les estuaires et les écosystèmes terrestres peuvent être soit des sources ou des puits de GES selon les stades de successions biologiques (chapitres 4, 6). De plus, cette monographie démontrent que la création de réservoirs a un impact direct sur la production accrue de GES durant les premières années suivant la mise en eau. Afin d'évaluer adéquatement les émissions nettes de GES des réservoirs, il est devenu essentiel dans le cadre des projets futurs de déterminer les émissions des différents écosystèmes du bassin versant avant et après la création du réservoir. Cependant, le processus d'évaluation quantitative des changements induits dans les émissions de GES par l'inondation demeure très complexe, long et coûteux, car il requiert une compréhension du cycle du carbone à l'échelle du bassin versant incluant le segment aval de la rivière entre le barrage et l'estuaire. À cause de leur complexité, de telles évaluations quantitatives sont rarement entreprises. Quoiqu'il en soit, il importe dès maintenant d'élaborer une méthodologie pour déterminer les émissions nettes induites par les réservoirs (World Commision of Dams, 2000). Une approche mise de l'avant par le WCD propose de considérer les émissions de GES comme des émissions nettes pour (1) évaluer les sites futurs de réservoirs spécifiques, tel que les barrages hydroélectriques, et (2) pour estimer l'ensemble des changements anthropiques affectant les sources et les puits de CO_2 et de CH_4. Le WCD (2000) estime aussi que plusieurs paramètres biochimiques majeurs qui influencent les émissions de GES des régions tropicale et boréale (tel que la teneur initiale en carbone, l'hydrodynamique, le temps de séjour, les apports et les sorties de COD et de COP, etc.) devraient faire l'objet de recherches plus intenses. De plus, puisqu'il existe d'importantes variations temporelles et spatiales dans les flux de GES provenant autant des écosystèmes aquatiques que terrestres, nous suggérons d'utiliser une échelle temporelle de 100 ans qui intégrerait la plupart des variations naturelles au niveau du bassin versant, tel que proposé par le WCD (2000).

Selon cette approche globale, les émissions nettes des réservoirs devraient être inférieures à celles mesurées directement à l'interface eau-air comme celles présentées dans cette monographie ou dans d'autres publications scientifiques. Une première estimation effectuée au réservoir Petit Saut a démontré que les émissions nettes sont environ 30 % inférieures à celles mesurées directement sur le réservoir (chapitre 12). Une étude utili-

sant les isotopes stables conduite sur le réservoir Robert-Bourassa suggère une tendance similaire (chapitres 8, 14, Therrien 2003).

Comparaison des émissions de GES des différentes sources d'énergie

La planification énergétique dans un contexte de développement durable requiert une comparaison des avantages et des inconvénients des différentes sources d'énergie, sur la base d'un cycle de vie des installations, pour l'estimation des facteurs d'émission des polluants les plus nocifs (SO_x, NO_x, PM, etc.) et des principaux gaz à effet de serre (CO_2, CH_4, N_2O, etc.) inclus dans le Protocole de Kyoto (US DOE 1998, Spath et al. 1999, Sones et al. 1999, Spath and Mann 2000, US EPA 2000, Hydro-Québec 2000, IAEA 2001).

Sur la base des facteurs d'émission de GES identifiés pour les réservoirs hydroélectriques par l'IAEA (1996) et par différentes études effectuées au cours de la dernière décennie sur une variété et un grand nombre de réservoirs (tableau 26.1), on peut conclure à la grande performance de l'hydroélectricité, les facteurs d'émission étant d'un ou deux ordres de grandeur inférieurs aux facteurs d'émission des centrales thermiques. Toutefois dans le cas de certains réservoirs tropicaux, tel que le réservoir Petit Saut en Guyane Française ou certains réservoirs au Brésil, les émissions de GES pourraient, durant une certaine période, excéder significativement les émissions produites par les centrales thermiques. Des valeurs similaires ont été obtenues par différentes études (ex. : Rosa and Scheaffer 1994, 1995, Fearnside 1996, Gagnon and van de Vate 1997). L'utilisation de technologies plus efficaces, telles que les centrales à gaz à cycle combiné, réduirait les émissions de GES reliées aux centrales thermiques. Ces centrales ont les facteurs d'émission parmi les plus faibles (400 – 500 g CO_2 équiv./ $kWh(e)\cdot h^{-1}$, tableau 26.1). Comme les coûts associés à la réduction des émissions de GES par cette technologie sont raisonnables (Spath 2000, US EPA 2000), cette dernière est déjà utilisée à travers le monde. La réduction des émissions de GES des centrales au charbon est également possible (US.DOE, 1998), quoique les coûts sont beaucoup plus élevés.

Dans le contexte de ce volume, seuls les facteurs d'émission des GES ont été pris en considération ; cependant, les comparaisons environnementales globales entre les différentes options énergétiques devraient aussi inclure d'autres polluants (SO_x, NO_x, PM, etc.). En ce qui concerne les émissions de GES, les observations générales découlant des résultats présentés dans cette monographie et des données apparaissant dans le tableau 26.1 :

- les facteurs d'émission de GES par l'hydroélectricité produite dans les régions boréales sont significativement inférieurs aux facteurs d'émission correspondants aux centrales thermiques (de < 2 % à 8 % de n'importe quelle type de production thermique conventionelle) ;
- les facteurs d'émission de GES par l'hydroélectricité produite dans les régions tropicales couvrent une plage beaucoup plus vaste de valeurs (par exemple, une plage de plus de deux ordres de grandeur pour les 9 réservoirs brésiliens). Pour un cycle de vie de 100 ans, ces facteurs d'émission pourraient atteindre des valeurs très faibles ou très élevées, variant de moins de 1 % à plus de 200 % des facteurs d'émission obtenus pour les centrales thermiques ;
- les facteurs d'émission nette de GES pour l'hydroélectricité devraient être, à première vue, de 30 % à 50 % moins élevés que les valeurs couramment rapportées.

Conclusions et recherches futures

Avec cette synthèse, nous avons fait progresser d'un pas notre compréhension de la dynamique des GES dans les réservoirs. Les processus responsables de l'émission de GES dans les réservoirs boréaux, semi-arides et tropicaux sont similaires (tableaux 26.2, figures 26.1 à 26.5). Les différences majeures sont reliées à la présence plus fréquente de conditions anoxiques dans les réservoirs tropicaux, lesquelles favorisent et maintiennent la méthanogénèse sur de plus longues périodes (>10 ans). De plus, dans les réservoirs boréaux et semi-arides, les émissions de GES entre les lacs naturels et les réservoirs âgés de plus de 10 ans d'un même bassin versant sont similaires.

Cette monographie a traité de plusieurs enjeux et problèmes soulevés lors de la réunion de l'atelier d'experts de la World Commission on Dams tenue à Montréal en 2000. Bien que plusieurs études menées sur différents réservoirs boréaux et tropicaux aient porté sur les processus responsables des émissions de GES et que des tentatives aient été faites pour évaluer les émissions nettes de GES pour de grands bassins versants et sur une échelle temporelle de 100 ans, plusieurs questions doivent encore être abordées.

Puisque les estimés d'émission de GES devraient être établis pour des échelles temporelles > 100 ans, il est crucial de développer des outils (ex. : le modèle du chapitre 12) pour prédire les émissions de GES pour les projets de réservoirs futurs, incluant les impacts des changements climatiques à long terme sur ces milieux (www.cics.uvic.ca/scenarios). L'emploi de

modèles prédictifs sera très important pour la diminution du coût des projets et la réduction de leurs impacts.

Pour utiliser adéquatement de tels modèles, l'information suivante doit être obtenue :

- inter calibration des techniques d'échantillonnage et de mesures des GES et optimisation des stratégies d'échantillonnage pour accroître la couverture spatiale et temporelle ;
- mesure des GES sur une plus grande diversité de réservoirs pour déterminer l'hétérogénéité temporelle et spatiale des émissions par ébullition et par diffusion ;
- mesure des GES à des sites de référence, tels que des rivières, des lacs, des forêts et des milieux humides pour en déterminer l'hétérogénéité temporelle et spatiale ;
- détermination de la proportion de GES émis en relation avec les apports de carbone provenant des sols ou des sédiments inondés dans un bassin versant ;
- détermination de la durée de séjour du carbone dans les réservoirs, les lacs naturels et les segments avals des réservoirs jusqu'aux estuaires.

L'intégration des flux au niveau du bassin versant avant et après la mise en eau des réservoirs en tenant compte des types de milieux mis en eau est essentielle avant de pouvoir tirer des conclusions majeures. La simple comparaison des flux par unité de surface entre les réservoirs et les lacs n'est pas suffisante. Les données générées par des études intégrées permettront une évaluation plus adéquate des émissions de GES par les réservoirs et les milieux naturels.

1 Introduction

Alain Tremblay, Maryse Lambert and Claude Demers

1.1 Greenhouse Gases and Reservoirs

The major greenhouse gases (GHGs) are carbon dioxide (CO_2), methane (CH_4) and nitrous oxide (N_2O) (IPCC 2001). These gases are emitted from both natural aquatic (lakes, rivers, estuaries, wetlands) and terrestrial ecosystems (forest, soils) as well as from anthropogenic sources (e.g. Cole et al. 1994; Hope et al. 1994; Borges and Frankignoulle 2002; Rosa et al. 2002; Therrien 2003; Tremblay et al. 2003; Blais et al. 2003).

Retention of heat by these gases, through absorption of the infrared light reflected or produced by the Earth, is called the "greenhouse effect". This is a natural phenomenon that keeps worldwide average temperatures around $18^{O}C$, which would otherwise be close to $-15^{O}C$. This mechanism allows for life on Earth. In recent times, GHG concentrations in the atmosphere have increased significantly due to anthropogenic emissions from fossil fuel burning, deforestation, the creation of artificial wetlands, cattle, etc. It is clear that only part of this excess GHGs has been taken up by natural sinks, resulting in increased concentrations and, likely, and enhanced greenhouse effect.

According to both the European Environment Agency and the United States Environmental Protection Agency, CO_2 emissions account for the largest share of GHGs equivalent of 80–85% of the emissions. Fossil fuel combustion for transportation and electricity generation are the main sources of CO_2 contributing to more than 50% of the emissions (Fig. 1.1). Generation of electricity with thermal power plants represents 66% of the world's electric generation capacity (Fig. 1.2, EIA). Hydroelectricity and nuclear power represent respectively only 22% and 11.5% of the world electric generation capacity. Although hydropower represents about 22% of the world generation capacity, it represents a much smaller fraction of the GHG emissions worldwide, since it emits 35 to 70 times less GHG per TWh than thermal power plants (IAEA 1996). Nevertheless, for the last few years GHG emissions from freshwater reservoirs and their contribu-

tion to the increase of GHG in the atmosphere are actually at the heart of a worldwide debate concerning methods of energy generation (Rosa and Scheaffer 1994, 1995; Fearnside 1996; Gagnon and van de Vate 1997; St. Louis et al. 2000; Duchemin et al. 2002; Tremblay et al. 2003).

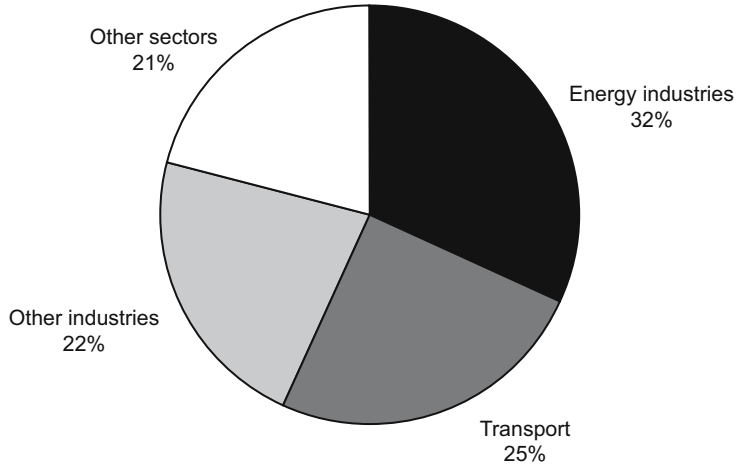

Fig. 1.1. Carbon dioxide emissions per sector of European Union-15, 1999 (Modified from: European Environment Agency, Annual European Community Greenhouse Gas Inventory 1990-1999. Technical Report No. 60, 11 April 2001)

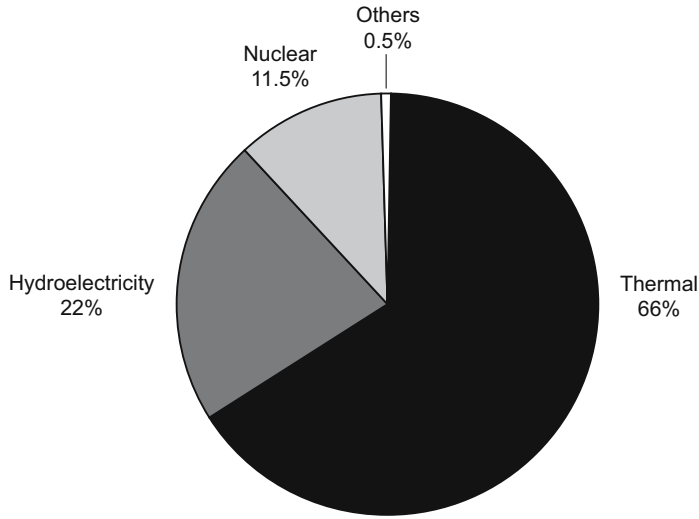

Fig. 1.2. Technology used to generate electricity in the world (modified from EIA, site www.eia.doe.gov)

It must be pointed out, however, that 71% of the worldwide single-use dams are used for irrigation or water related purposes and only 20% of the reported dams are built to generate electricity (Fig. 1.3, ICOLD 1998). Moreover, multi-purpose dams account for nearly 30% of the total number of large dams reported. Worldwide, most of the single-purpose dams (approx. 48%) are for irrigation and therefore contribute greatly to food production. Multi-purpose dams are increasingly important for regional economic development. Irrigation is the first use of multi-purpose dams followed by flood control, hydropower, domestic and industrial water supply, recreation, fish farming and navigation.

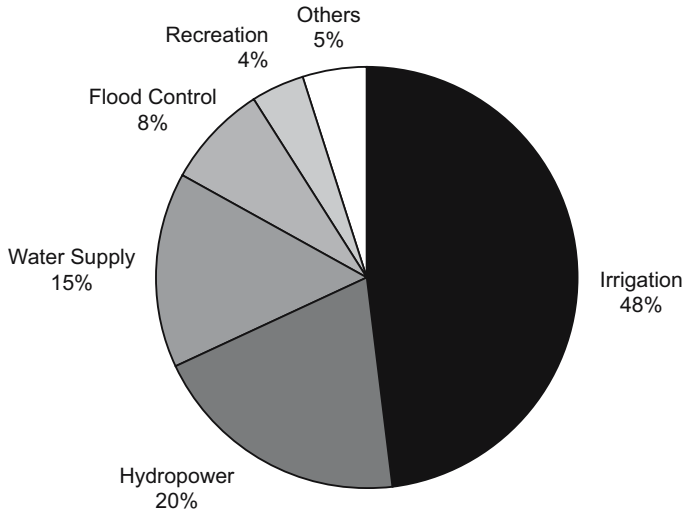

Fig. 1.3. Distribution of single uses of reservoirs in the world (taken from: ICOLD's World register 1998)

This monograph represents the first comprehensive synthesis on GHG fluxes from natural and modified aquatic ecosystems. Other issues related to multiple use of land, biophysical characterization, social and climatic charge impacts of reservoirs are beyond the scope of this monograph. This monograph regroups research results from many countries around the world, representing years of collaboration and activities between research institutes, universities and power facilities. This monograph covers the processes of GHG production as well as carbon dynamics in aquatic and terrestrial ecosystems. It must be pointed out, however, that the information from both terrestrial or aquatic ecosystems comes from three major regions of the world: Europe, Canada-USA and Brazil (Fig. 1.4 and 1.5).

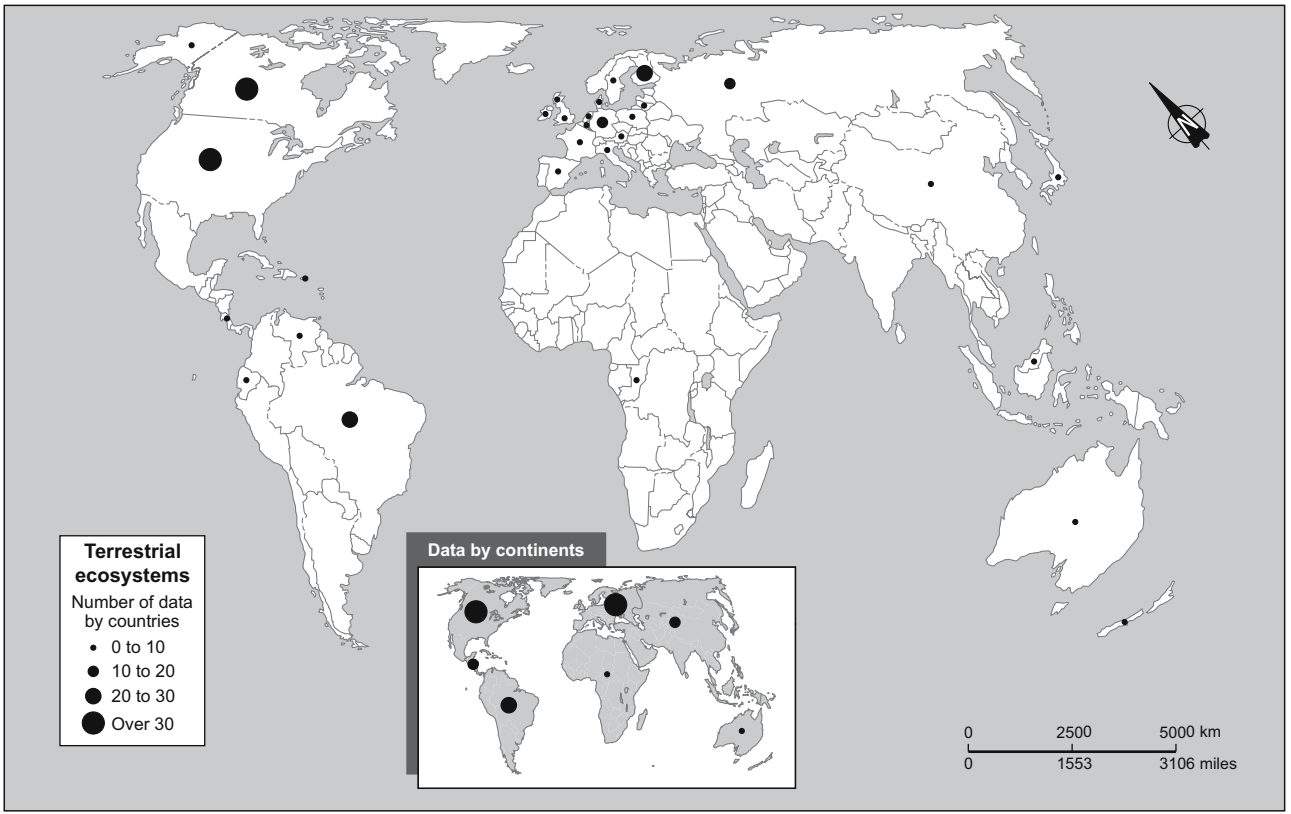

Fig. 1.4. Qualitative world distribution of studies data on greenhouse gas flux or carbon mass balances and processes in terrestrial environments

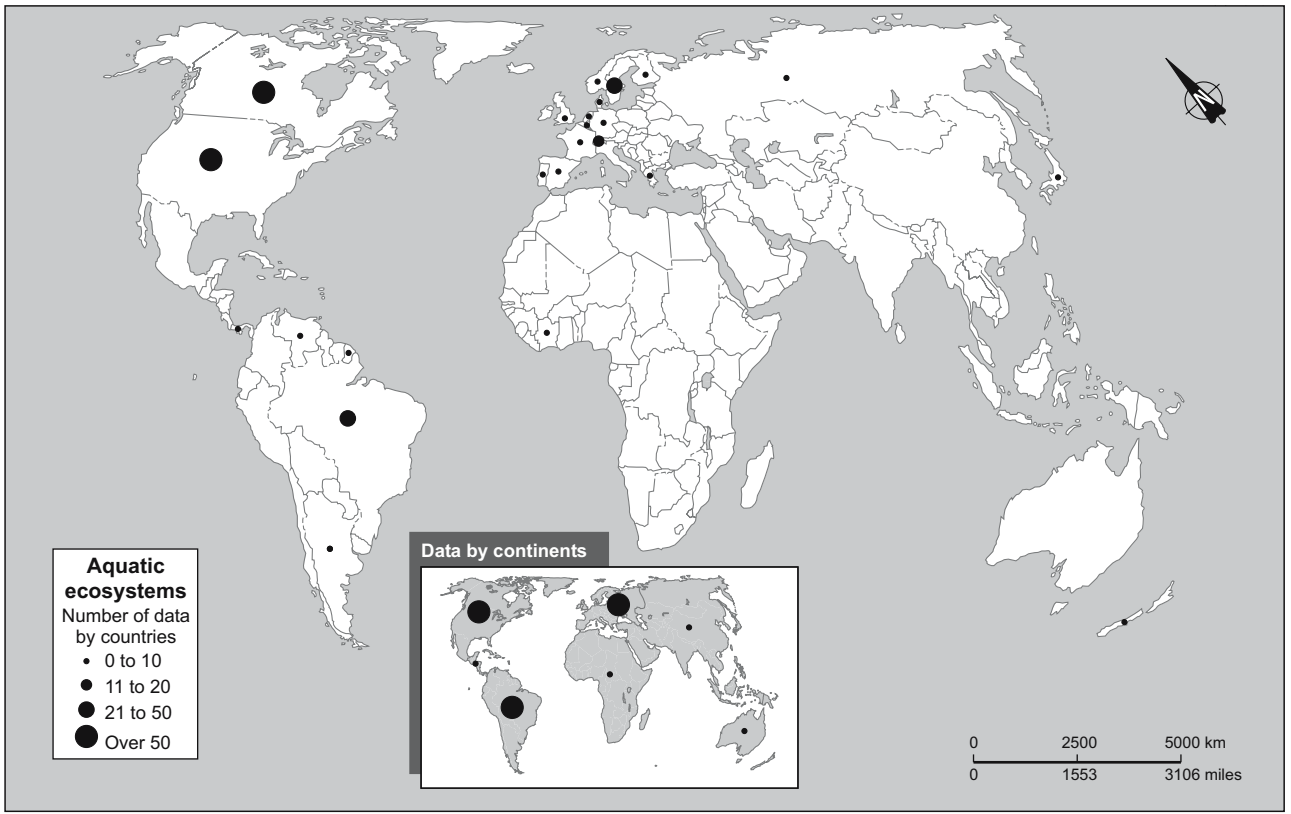

Fig. 1.5. Qualitative world distribution of studies data on greenhouse gas flux measurements and processes in aquatic environments

These regions contain only 28% of the world reported dams (Table 1.1). There is very little information, however, from Asia, which contains 68% of the reported dams.

Table 1.1. Top 20 countries by number of large dams (modified from WCD 2000)

Country	ICOLD, World register of dams 1998	Other sources	Percentage of total
Asia			
China	1855	22000	
India	4011	4291	
Japan	1077	2675	
South Korea	765	765	
Australia	486	486	
Total Asia	8194	30217	63
Europe			
Spain	1187	1196	
Turkey	625	625	
France	569	569	
Italy	524	524	
United Kingdom	517	517	
Norway	335	335	
Germany	311	311	
Albania	306	306	
Romania	246	246	
Total Europe	4620	4629	10
America			
United States	6375	6375	
Canada	793	793	
Brazil	594	594	
Mexico	537	537	
Total America	8299	8299	18
Africa and others			
South Africa	539	539	
Zimbabwe	213	213	
Others	3 558	3558	
Total Africa and others	4310	4310	9
Total	25423	47655	100

1.2 Reservoir Dynamics

The flooding of forest, soils, rivers and lakes generated by the creation of reservoir modifies, for a period of time the biochemical parameters, which influence the GHG dynamics of that new environment. The ecology of reservoirs has been relatively well documented in the literature. However, most studies have focused on short-time scale observation getting a snapshot of reservoir mechanisms. To better understand GHG dynamics in reservoirs, it is better to use a long term approach, since these environments are dynamic in terms of the carbon cycle mostly in the first few years after impoundment. For this purpose, we will use data generated by the La Grande hydroelectric complex follow-up environment program, the world's largest and longest environmental follow up program to our knowledge.

The biophysical characteristics of La Grande hydroelectric complex (Fig. 1.6) have been studied for more than 20 years, as part of Hydro-Québec's environmental follow-up program. This follow-up program tracked changes occurring in water quality, plankton, benthos and fish in different modified environments of the La Grande hydroelectric complex. As demonstrated in the monograph, these long term follow-up studies have been extremely useful for developing our understanding of the carbon dynamics in boreal reservoirs.

1.2.1 Water Quality

The evolution of major water quality parameters measured in the photic zone of three reservoirs of the La Grande complex, during the ice-free period, is shown in Fig. 1.7. The changes observed in this zone were generally limited and remained within the range of values favourable to strong biological productivity. The slight variations observed from one reservoir to another may be explained by their specific characteristics: flooded land area, density and type of flooded vegetation, length of filling period, configuration, average depth and water residence time. Changes in water quality are explained mainly by the following three phenomena:

- Submersion of vegetation and forest soils, which causes mineral salts and soil nutrients to dissolve in water—a process that is accelerated by wave action on forest soils. This phenomenon, which occurs at the start of impoundment, partly explains the rapid increase in total phosphorus concentration and decrease in pH.

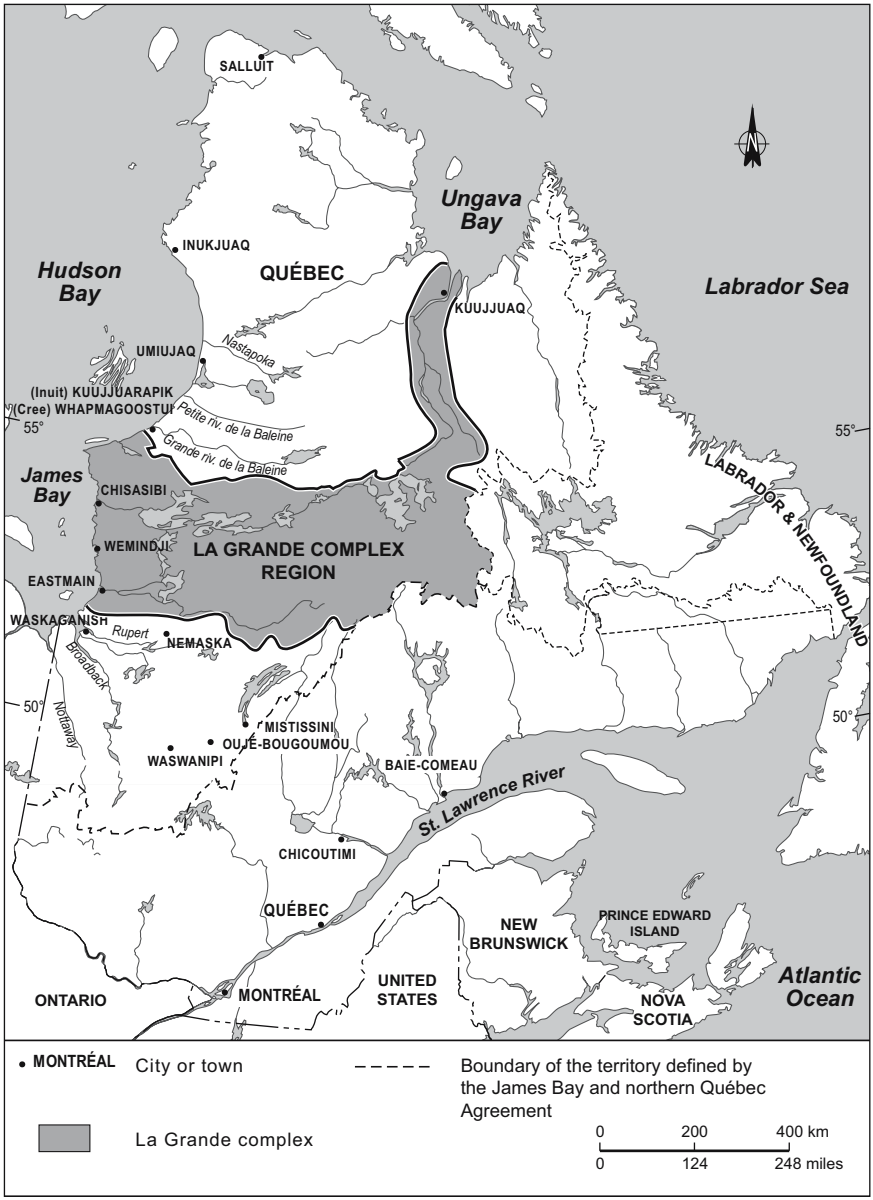

Fig. 1.6. Location of La Grande River hydroelectric complex

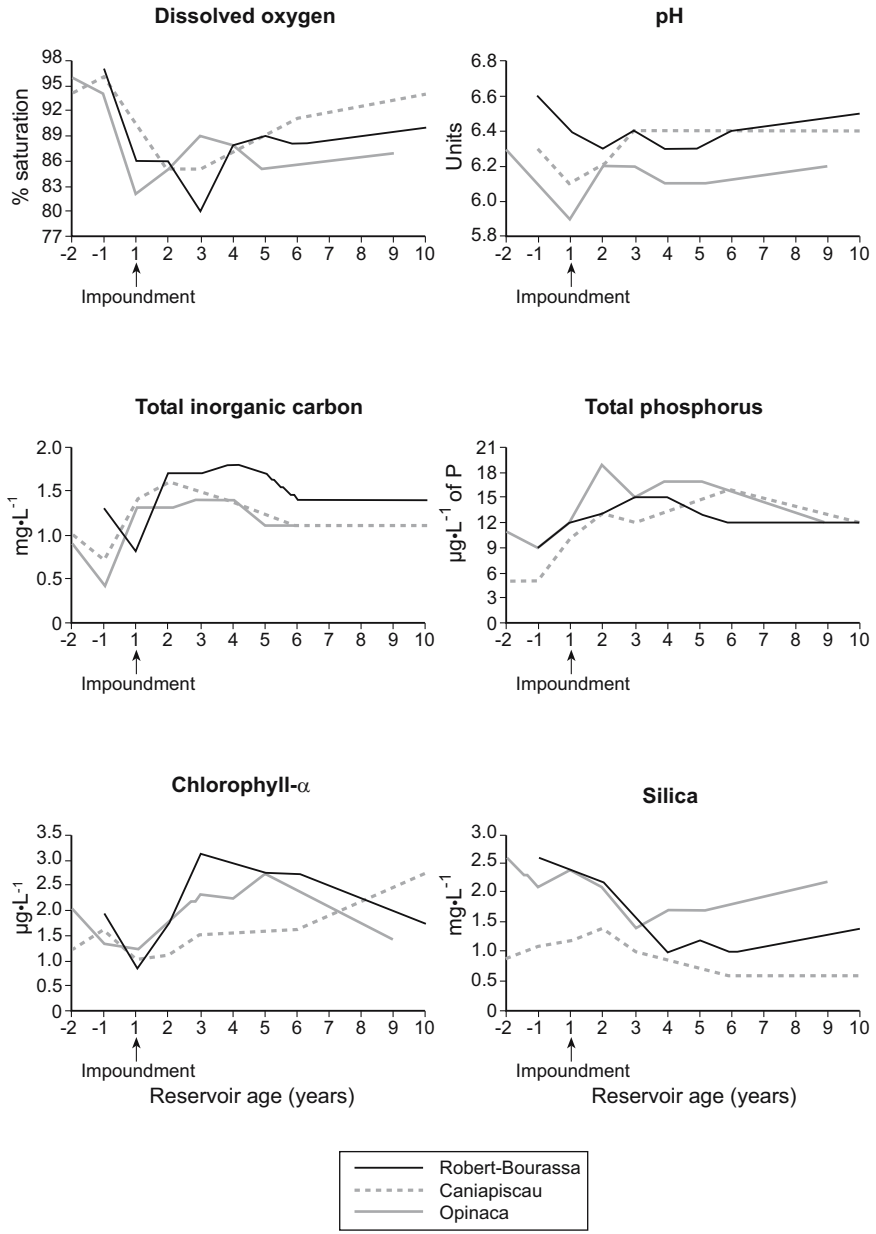

Fig. 1.7. Changes in main parameters linked with decomposition of submerged organic matter in the photic zone (ice-free period, La Grande Complex reservoirs)

- Mixing of waters of various qualities coming from rivers and lakes in the flooded zone.
- Decomposition of vegetation and humus in flooded soils by a series of micro-organisms, such as bacteria. In decomposing this organic matter, the micro-organisms consume dissolved oxygen and release CO_2, resulting in a decrease in pH. This phenomenon is accompanied by a release of minerals and nutrients such as phosphorus.

Greater variations in oxygen, major ions and nutrients were measured in bottom layers of the reservoirs where drops in redox potential permitted better exchanges between flooded substrates and overlying waters. However, these restricted areas had very little effect on the overall water quality of these large and deep reservoirs. Follow-up of reservoirs in the La Grande hydroelectric complex clearly indicates that maximum water quality changes are reached within 2 or 3 years after impoundment and reservoirs regain physical and chemical characteristics similar to those found in natural waters within 10 to 15 years (Schetagne 1994).

The short duration of changes is largely due to the fact that only a small portion of flooded organic matter (forest soils, tree branches, trunks and vegetation) is readily and rapidly decomposable in the cold water of boreal reservoirs. Trees branches, trunks and roots, as well as the underlying soil humus, have been found still intact in 60-year-old reservoirs (Van Coillie et al. 1983).

The duration of water quality parameter changes could be longer in some tropical reservoirs. This is likely due to warmer water temperatures that favour the decomposition of flooded organic matter or fresh material coming from run-off under anoxic conditions. These conditions favour methane production. However, one must keep in mind that not all tropical reservoirs have anoxic conditions and therefore, are emitting methane (Tremblay and Lambert 2003). There are very few data from tropical regions (e.g. Galy-Lacaux 1996) and to our knowledge only Petit Saut reservoir in tropical French Guiana (flooded in early 1994) has a follow-up program (Galy-Lacaux et al. 1997; Gosse et al. 1998; Galy-Lacaux et al. 1999).

1.2.2 Plankton

Phytoplankton biomass (through measure of chlorophyll-*a*) monitored in La Grande Complex increased for a number of years after impoundment inducing a depletion of silica as diatoms which are an important phytoplankton group in this region (Fig. 1.7 and 1.8). Increased water residence

time and nutrient enrichment contributed to temporary increases in zooplankton and benthos biomass in most of the modified bodies of water. Both phytoplankton and zooplankton reached a maximum biomass within 3 to 5 years after impoundment, then declined and stabilized after about 10 to 15 years to levels comparable to natural values (Schetagne 1994; Chartrand et al. 1994).

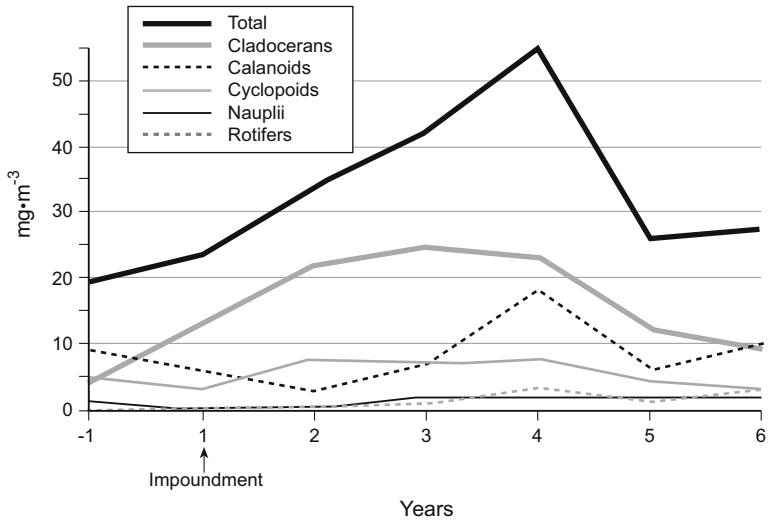

Fig. 1.8. Changes in zooplanktonic biomass: Robert-Bourassa reservoir (in La Grande complex)

1.2.3 Benthos

Benthic organisms of La Grande Complex had to adapt to the major physical transformations related to reservoir creation. After a slight decline in their biodiversity due to the increased scarcity of less mobile species and of species better adapted to fast-running water, the new aquatic environments were rapidly occupied by lake dwelling species. The presence of extensive substrate, supplied by submerged plants, considerably increased the surface available for species in search of food.

In addition, examinations of fish stomach contents and monitoring of fish populations revealed that the diversity and quantity of benthic organisms were sufficient to bring about substantial increases in growth rates and condition factors (plumpness index) of fish species that feed on the benthos, such as lake whitefish, and their predators, such as pike.

1.2.4 Fish

Following the first year after impoundment, we saw a decrease in fish yields due to the dispersal of populations in a larger volume of water. This decline was quickly followed, in subsequent years, by an increase in yields resulting from overall water enrichment and fish growth. After 15 years or so, yields returned to levels comparable to those observed in undisturbed natural environments surrounding La Grande Complex (Fig. 1.9).

Northern pike and lake whitefish are the species that benefited the most from the creation of large reservoirs. Reproduction rates for these species suggest that much of their increase in yield was attributable to better recruitement, associated with a better survival rate in the first years after impoundment (Deslandes et al. 1995). The growth rate of the principal species in Robert-Bourassa reservoir increased markedly after impoundment. Like growth, the condition factor of almost all the species increased after impoundment. After several years, the fish's condition factor gradually returns to those of natural systems.

The data provided by the environmental follow-up program of the La Grande hydroelectric complex have demonstrated that all the parameters measured (water quality, plankton, benthos, fish, etc.) in boreal reservoirs return to values similar to those found in natural lakes within 10 to 20 years depending on the parameter measured. Therefore, after biological upsurge following impoundment, all the parameters measured indicate that a reservoir behaves like a lake. Since greenhouse gas production in aquatic ecosystems is related to whole biological productivity and water quality, fluxes of GHG from boreal reservoirs should follow the same patterns as these over time. This might not be the case in tropical regions due to the possible presence of anoxic zones.

1.3 Contents and Rationales

In order to fulfill the objectives of determining sources and processes of carbon leading to greenhouse gases emissions from both natural and modified aquatic ecosystems, methodological improvements were required, especially for the determination of spatial variability of fluxes from large water bodies. Large water bodies are quite often remote from laboratory facilities, hence real time *in situ* techniques had to be developed to reduce costs and facilitate logistics. These developments, as well as other methodological aspects, are presented in Chap. 2 and 3.

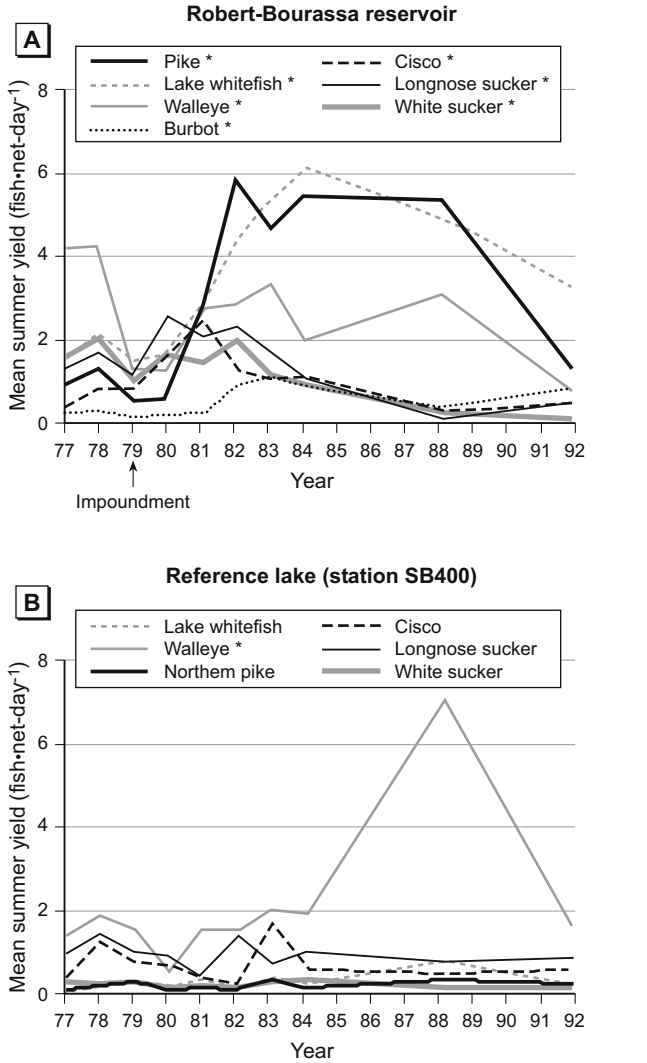

Evolution of species composition of catches, overall yield (all species combined) and mean annual yields of the main fish species in the Robert-Bourassa reservoir and its reference lake (lac Detcheverry; station SB400).

* Significant variations over time detected using single-classification ANOVA (reference) or repeated-measures ANOVA (reservoir)

Figure 1.9

Fig. 1.9. Evolution of fish biomass and captures per unit of effort in Robert-Bourassa reservoir (in La Grande Complex) and a natural lake

To compare reservoirs with other methods of energy generation (based on a life cycle approach), it became important to consider different natural reference ecosystems to reveal the amplitude of GHG fluxes from these environments. A priority was given to document natural ecosystems in terms of GHG or carbon fluxes from terrestrial sources (Chap. 4 and 6), from drainage basins (Chap. 16), from lake sediments (Chap. 5), from lake surfaces (Chap. 8 and 9) and from estuaries (Chap. 7).

In reservoirs, emphasis was put on processes related to the role of freshly flooded soils which favour GHG emissions in young reservoirs (< 10 years). Using reservoirs of different ages, we documented the approximate duration of modified fluxes in reservoirs (Chap. 8, 9, 10, 11 and 12). The role of primary producers and food web structure (Chap. 17), planktonic CO_2 respiration/consumption ratios (Chap. 20), and bacterial activity (Chap. 18 and 19) in GHG fluxes from water bodies were investigated. The origin of carbon related to GHG emissions was also investigated using stable isotope tracers (Chap. 14 and 15) as well as its transformation in the water column (Chap. 21 and 22).

Since the potential for hydroelectric development is very important, particularly in Asia and South America, and the cost of impact assessment are increasing over time, there was a need to develop models to predict CO_2 and CH_4 fluxes in reservoirs (Chap. 12 and 25), and to simulate different situations and identify missing information (Chap. 23 and 24). The development of these models is based mainly on data collected in La Grande Complex (boreal ecosystem, 25 years of data) and Petit Saut (tropical ecosystem, 7 years of data) follow-up programs as well as from ELARP-FLUDEX experimental reservoirs and from in vitro experiments (Chap. 8, 10, 12, 15, 22, 24, 25).

Findings of all these studies are presented in 24 separate articles, each forming a distinct chapter. In addition, a final chapter presents a general synthesis and future prospects for research for GHG emissions from reservoirs.

Gross Emissions

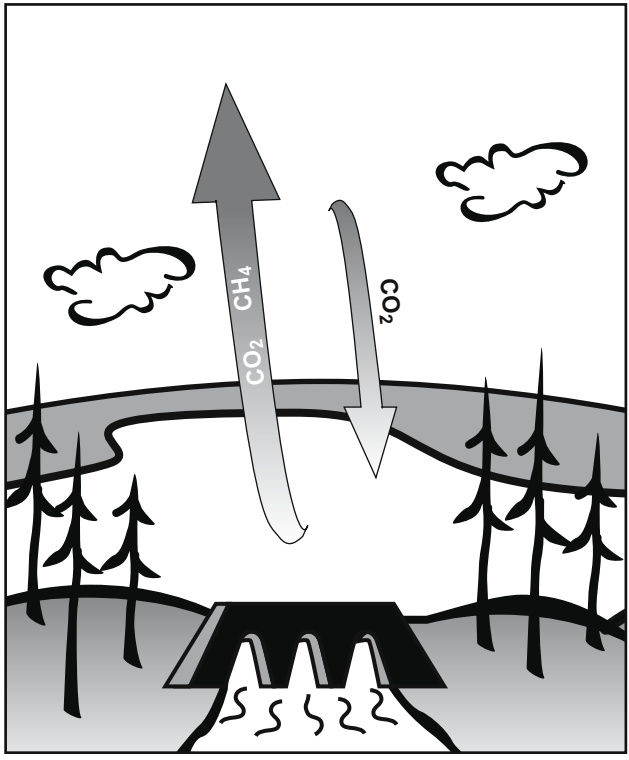

2 Analytical Techniques for Measuring Fluxes of CO_2 and CH_4 from Hydroelectric Reservoirs and Natural Water Bodies

Maryse Lambert and Jean-Louis Fréchette

Abstract

Hydro-Québec and its partners have been measuring greenhouse gases (GHG) gross fluxes from hydroelectric reservoirs and natural water bodies since 1993. Over the years the methods have changed with a constant aim for improvement. The methods used are: the thin boundary layer, the use of floating chambers with *in situ* or *ex situ* laboratory analysis and the use of floating chambers coupled to an automated instrument (NDIR or FTIR). All these methods have their pros and their cons. Over the years many tests were done to compare the methods.

There is no significant difference in the results obtained with the *in situ* or *ex situ* laboratory analysis. For CO_2 fluxes, the number of results rejected is similar for the NDIR and the laboratory analysis methods. For CH_4 fluxes, the number of results rejected is three times lower with the floating chamber with *in situ* laboratory analysis than with the other methods. The precision for duplicate measurements of fluxes is similar for all methods with floating chambers. In general, the thin boundary layer method tends to measure lower fluxes than the floating chamber method with laboratory analysis and there is no good correlation between the two methods. Fluxes measured with automated instruments (specially for fluxes > 5000 $mg \bullet m^{-2} \bullet d^{-1}$) tend to be higher compared with the laboratory analysis method but the correlation between the two methods is very good ($R^2 = 0.92$ for CO_2). The method with the less logistical constraints is the floating chamber coupled to an automated instrument. This method enables the sampling of about 5 times more sites in the same amount of time as the method with laboratory analysis. The floating chamber coupled to an automated instrument has therefore been retained as the method of choice by Hydro-Québec for GHG gross flux measurements over water bodies.

2.1 Introduction

Hydroelectric reservoirs have been suspected to emit GHG for quite some time (Rudd et al. 1993; Rosa et al. 1994; Duchemin et al. 1995). Many elements need to be considered before we can quantify a net flux from reservoir or natural water bodies.

However, to be able to determine net emissions, we need to adequately address the gross emissions from the air-water interface. Different methods are used in the field to measure gross GHG fluxes between the water and the atmosphere (Canuel et al. 1997; Raymond et al. 1997; Carignan 1998; Duchemin et al. 1999; Rosa et al. 2002). The methods can be split in three major types:

1. Fluxes calculated by measuring the dissolved gas concentrations in the water;
2. Fluxes calculated by measuring an integrated concentration of the GHG above the water surface;
3. Fluxes calculated by measuring the GHG across the air-water interface.

Type 1 methods include for example thin boundary layer (TBL) and carbon isotope analysis. Type 2 methods include for example infrared laser and eddy correlation (Grelle et al. 1996). Type 3 methods include different floating chambers methods. Laser and isotopes methods are described in detail in Chap. 4 and 12 respectively. In this chapter, we will describe and compare only the methods that were used by Hydro-Québec and its partners to measure gross GHG fluxes from hydroelectric reservoirs and natural water bodies. The methods compared in this chapter measure diffusive emission only. For boreal water bodies, diffusive emissions are the major form of emission. The contribution of ebullitive emission is very small but is more important in tropical water bodies (Canuel et al. 1997; Therrien 2003).

2.2 History of the Methods Used by Hydro-Québec

Hydro-Québec, in collaboration with University of Québec at Montréal (UQAM) and Groupe Conseil Génivar, have been doing GHG measurements over hydroelectric reservoirs and natural water bodies since 1993. Over the years the methods have changed with a continuous aim to improve the technique. All the methods used are described in the following section.

Between 1993 and 1999, the measurements were done by UQAM personnel using a floating chamber with *in situ* laboratory analysis of the air samples. Most of this sampling was done with other types of measurements in order to determine the mechanisms of production of GHG. Only a few sampling campaigns were done exclusively to obtain representative data from specific reservoirs. In 2000, Hydro-Québec decided to begin representative measurements from specific reservoirs. In 2000 and 2001, the measurements were done by Hydro-Québec and Groupe Conseil Génivar personnel with a floating chamber with *ex situ* laboratory analysis of the air samples. The goal was to try to determine a representative average of the gross flux over a water body (lake or reservoir). Since 2002, the measurements are conducted by Groupe Conseil Génivar personnel with a floating chamber and an NDIR or FTIR instrument. Before 1999, travel from site to site was done by boat. This enabled us to measure sites located mostly near the shores or near boat ramps. Since 1999, hydroplanes were also used for travel between sites. This enabled us to sample sites in remote areas that were impossible to reach by boat.

2.3 Description of the Methods

2.3.1 Floating Chambers with *in situ* Laboratory Analysis

Field Sampling

The method is described in detail in Canuel et al. 1997. The floating chambers are rectangular boxes made of acrylic. The box is 30 cm wide and long and 50 cm high over water. The outside surface of the chamber is covered with Mylar paper to prevent overheating inside the chamber. About 10 cm of the chamber is under water and the level is kept in position by Styrofoam collars (Fig. 2.1A). The intake of the air sample is located on the top center of the chamber. It is connected to Tygon tubing of 4 m long with an internal diameter of 3.2 mm.

At each site, two to four floating chambers are placed at a distance of about 2 m from the boat. The floating chambers are placed upside down for a few minutes to allow equilibration with local air. The chambers are then placed on the water. A 60 mL polypropylene syringe is then connected under water to the tubing of the floating chamber and is pumped several times. This changes the air in the tube and homogenizes the air in the chamber. A first sample is then collected, which is entitled t_0. Four other samples are taken at 15 minutes intervals for a total of one hour (15,

30, 45 and 60 minutes). The five concentrations enabled us to calculate a flux by linear regression (Fig. 2.2 and Eq. 2.1). Only sites with a correlation coefficient higher than 0.85 for CO_2 and 0.9 for CH_4 are kept.

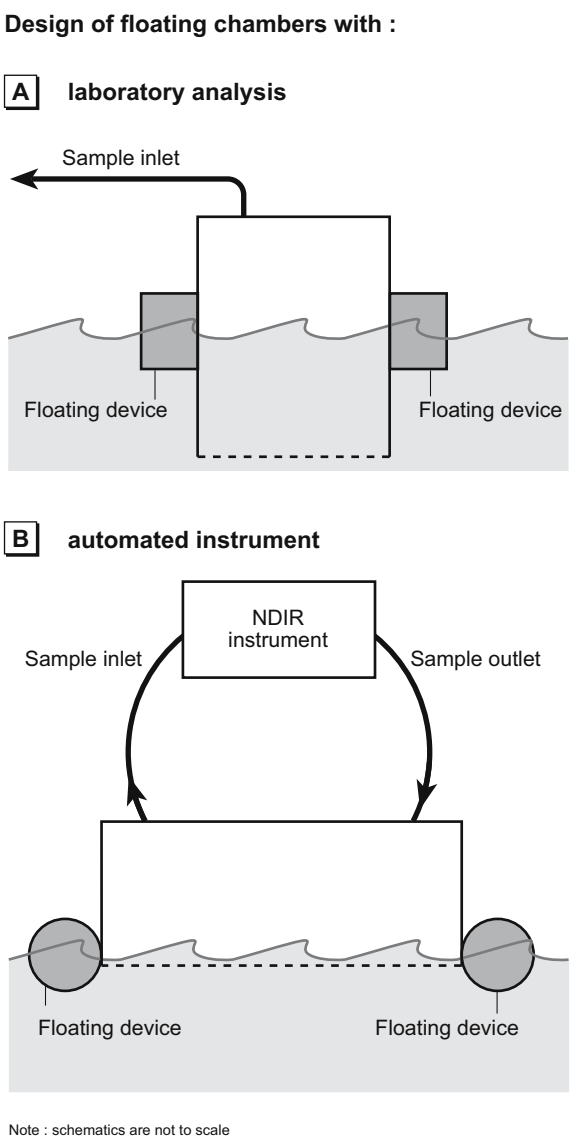

Fig. 2.1. Design of floating chambers with: A) laboratory analysis; B) automated instrument. Schematics are not to scale

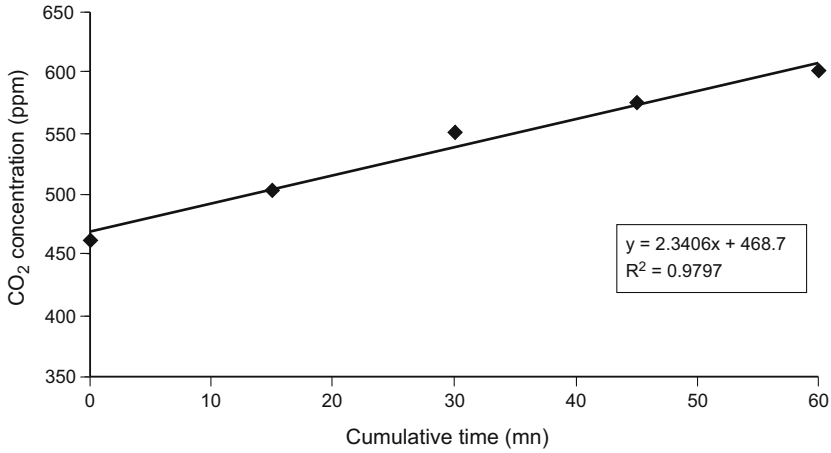

Fig. 2.2. Typical graph of results with laboratory analysis

Calculation of the flux with laboratory analysis

$$\text{Flux} = \frac{\text{slope} \times \text{F1} \times \text{F2} \times \text{volume}}{\text{surface} \times \text{F3}} \tag{2.1}$$

with slope = slope from graph of concentration versus time in ppm/mn
F1 = conversion factor from ppm to $\mu g \cdot m^{-3}$ (1798.45 for CO_2 and 655.47 for CH_4)
F2 = conversion factor from minutes to day (1440)
volume = volume of air trapped in the chamber (m^3)
surface = surface of the floating chamber over the water (m^2)
F3 = conversion factor from µg to mg (1000)
flux = $mg \bullet m^{-2} \bullet d^{-1}$

Laboratory Analysis

At the beginning of each sampling campaign, the laboratory is setup on site and the instruments tested prior to analysis. Air samples are injected into a sample loop in a gas chromatograph (GC). A thermal conductivity detector (TCD) is used for CO_2 and a flame ionization detector (FID) is used for CH_4. Standards of 10000 ppm of CO_2 are used to verify the calibration of the instrument. Standards are injected at the beginning and the end of each set of analysis and at the end of every 10 samples. The detection limit for CO_2 is estimated at 25 ppm and for CH_4 at 0.375 ppm. The

reproducibility of the laboratory analysis in less than 5%. (Canuel et al. 1997).

2.3.2 Floating Chambers with *ex situ* Laboratory Analysis

Field Sampling

The field sampling is very similar to the one described in Sect. 2.3.1. The design of the floating chambers is based on Canuel et al. 1997.

A Tygon tube of 2.5 m is used for the air sampling. It has a 3.2 mm internal diameter and thick walls to prevent breaking. The sampling end of the tube is connected to a two-way valve. The air volume of the tube is 30 mL. A Styrofoam float is made to ensure the flotation of the chamber. Plastic markers are fixed to the side of the chambers to ensure that the floats are always placed at the same height.

At each site, two floating chambers are installed on each side of the hydroplane or boat. The floating chambers are placed upside down for approximately 5 minutes to allow equilibration with local air. The chambers are then placed on the water, with the valve open, with a little push on the top to initiate equilibrium. The chambers are left in place for one or two minutes to allow a complete equilibrium. Then a 60 mL syringe equipped with a valve is fixed to the valve of the floating chamber and is pumped six times. This changes the air in the tube and homogenizes the air in the chamber. As for the method with *in situ* laboratory analysis, five air samples are taken. The same equation and correlation coefficients are used (Fig. 2.2 and Eq. 2.1).

Laboratory Analysis

The method is described in detail in Dumas 2002. Air samples are analysed with a gas chromatograph (GC) equipped with a mass spectrometer detector (MS). The detector is in selective ion mode. The detection and quantification limits are 0.2 and 0.6 ppm respectively for CO_2 and 0.1 and 0.3 ppm for CH_4. The laboratory analysis have an accuracy of 5% for CO_2 and 4% for CH_4. The repeatability is 4% for CO_2 and 3% for CH_4. Standards of 100 and 1000 ppm are used for CO_2 and a standard of 100 ppm is used for CH_4. All standards are injected after 10 samples, the 100 ppm CO_2 standard is also injected after 5 samples and one out of ten samples is analysed in duplicate.

2.3.3 Floating Chambers Coupled to an NDIR or FTIR Instrument

The floating chambers coupled to an automated instrument technique was used for a trial period in 2001 and since 2002 has replaced the floating chambers used with syringes. The design is based on work done by Dr. Richard Carignan of Université de Montréal. The design of the floating chamber is slightly different to the one used with laboratory analysis. It is a one piece Rubbermaid dish (polyethylene container) with a surface area of 0.2 m^2 and a height of 15 cm of which 1 or 2 cm are below the surface of the water. The volume of air trapped over the water is about 20 L. A floating chamber with no sides going underwater seems to create more disturbance to the air-water interface than a chamber with sides going 2 cm underwater.

The air is sampled from the top of the floating chamber and returned at the opposite end of the chamber (Fig. 2.1B). The air coming from the chamber is passed through a desiccant (magnesium perchlorate) to prevent condensation of water in the tubing. Another column of desiccant is placed just before the input to the instrument.

Air is analyzed with an automated instrument, a NDIR (Non-Dispersive Infrared) instrument or FTIR (Fourier Transform Infrared). In 2001, the equipment used was a NDIR LI-COR model LI-6251. Since 2002, we used instruments from LI-COR (NDIR, model LI-7000), PP-Systems (NDIR, model CIRAS-2SC) and Temet Instruments (FTIR, Gasmet model DX-4010). Table 2.1 compares some characteristics of those instruments.

Table 2.1. Characteristics of the NDIR and FTIR instruments

Parameter	LI-6251	LI-7000	CIRAS-2SC	Gasmet DX-4010
Manufacturer	LI-COR	LI-COR	PP Systems	Temet Instruments
Analyzer type	NDIR	NDIR	NDIR	FTIR
Range (ppm)				
CO_2	0-3000	0-3000	0-2000	0-2000
CH_4	—	—	—	0-100
N_2O	—	—	—	0-100
Accuracy (ppm)				
CO_2	1-3 (at 350 ppm) 2-6 (at 1000 ppm)	< 1% range	0.2 (at 300 ppm) 0.5 (at 1750 ppm)	< 1% range
CH_4	—	—	—	< 1% range
N_2O	—	—	—	< 1% range

The data from the LI-COR and PP Systems instruments are collected either on a data logger (Campbell Scientific, model CR10X) or on a portable computer. All sampling equipment are installed in a rigid box (type Pelican) to prevent breakings during transportation from site to site.

Air is circulated through a closed loop in the floating chamber and the instrument takes readings at 20 seconds intervals. The chamber is deployed over the water for about 5 to 10 minutes. All readings are plotted on a graph and the slope is calculated in ppm/s (Fig. 2.3). The flux is calculated with Eq. 2.2 or 2.3. Only samples with a correlation coefficient higher than those specified on Table 2.2 are kept. The coefficient of correlation accepted is different according to the flux measured. As the flux measured approaches zero the difference between consecutive readings is close to the precision of the instrument, resulting in more fluctuation in the concentrations and a lower coefficient.

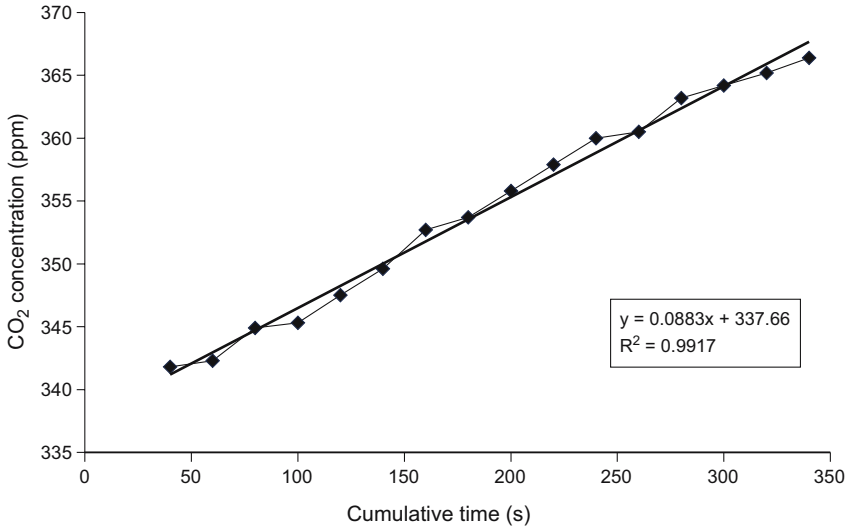

Fig. 2.3. Typical graph of results with NDIR instrument

Calculation of the flux with NDIR instrument for 2001 (with correction for temperature and pressure)

$$\text{Flux} = \frac{\text{slope} \times \text{pressure} \times \text{F1} \times \text{F2} \times \text{volume}}{\text{SP} \times \text{R} \times (273.15 + \text{T}) \times \text{surface}} \tag{2.2}$$

with slope = slope from graph of concentration versus time in µatm/s or ppm/s

pressure = ambient pressure measured in kPa

F1 = molecular weight (44 for CO_2)
F2 = conversion factor from seconds to day (86400)
volume = volume of air trapped in the chamber (m^3)
SP = standard pressure (101.33 kPa)
R = constant (0.08207 L-atm/mole/K)
273.15 = conversion from °C to K
T = ambient temperature (°C)
surface = surface of the floating chamber over the water (m^2)
flux = $mg \cdot m^{-2} \cdot d^{-1}$

Global conversion of µatm to atm, L to m^3 and g to mg is equal to 1.

Calculation of the flux with NDIR and FTIR instrument for 2002 and 2003

$$\text{Flux} = \frac{\text{slope} \times \text{F1} \times \text{F2} \times \text{volume}}{\text{surface} \times \text{F3}} \tag{2.3}$$

with slope = slope from graph of concentration versus time in $ppm \cdot s^{-1}$
F1 = conversion factor from ppm to $\mu g \cdot m^{-3}$ (1798.45 for CO_2, 655.47 for CH_4 and 1798.56 for N_2O)
F2 = conversion factor from seconds to day (86400)
volume = volume of air trapped in the chamber (m^3)
surface = surface of the floating chamber over the water (m^2)
F3 = conversion factor from µg to mg (1000)
flux = $mg \cdot m^{-2} \cdot d^{-1}$

The correction for temperature and ambient pressure is done automatically by the instruments.

The coefficients of correlation are different for the NDIR and FTIR instrument (see Table 2.2). For a maximum stability, the FTIR instrument needs a continuous purge of zero gas (nitrogen). As it is not always possible to do this in the field, there is more fluctuation in the measurements which results in a lower coefficient of correlation. To obtain a better precision, the PP Systems instrument does an automatic zero measurement. To do this ambient air is passed through two absorber columns filled with soda lime and Drierite to remove CO_2 and moisture.

2.3.4 Thin Boundary Layer

Field Sampling

This method is very different from the previous ones. It does not involve a floating chamber and does not directly measure the flux over water. The

Table 2.2. Coefficient of correlation for accepting fluxes

Instrument	Gas	Flux	R^2
NDIR	CO_2	≥ 200	≥ 0.85
		≥ 100 to < 200	≥ 0.75
		> 100 (including all negatives)	≥ 0.50
		- 50 to 50	all
FTIR	CO_2	≥ 200	≥ 0.80
		≥ 100 to < 200	≥ 0.70
		> 100 (including all negatives)	≥ 0.45
		- 50 to 50	all
	CH_4	≥ 2.0	≥ 0.70
		≥ 1.0 to < 2.0	≥ 0.60
		> 1.0 (including all negatives)	≥ 0.35
		- 0.5 to 0.5	all

These criterion are determined considering the number of data collected and the precision of the instrument.

thin boundary layer method calculates a flux using semi-empirical equations (Liss and Slater, 1974; Canuel et al. 1997; Duchemin et al. 1999). The local parameters necessary for the calculation are the concentration of the dissolved gas in the water, the wind speed and the temperature of the water. The wind speed is a major factor affecting the flux. The equations used for the calculations are not validated at low and high wind speeds (< 5 m/s and > 10 m/s, Duchemin et al. 1999).

At each site a sample of water is taken at a depth of about 15 to 30 cm. The bottle is sealed underwater to avoid the presence of air bubbles in the sample. For years 1993 to 1999, the samples were analysed at the *in situ* laboratory. Some samples taken in 1999 and all samples taken in 2000 and 2001 were analyzed by the *ex situ* laboratory.

Laboratory Analysis

After extraction from the water, the gases are analysed by the same method used for the floating chamber with *in situ* or *ex situ* laboratory analysis. Between 1993 and 2000, all water samples were extracted in the laboratory. The sample is shaken to allow an equilibration with an equal volume of inert gas. Nitrogen and argon are used as inert gases for *in situ* and *ex situ* laboratory analysis respectively. For CO_2, tests demonstrated that there is no difference between extraction with nitrogen or argon. For CH_4, argon is a better choice since the tailing of the nitrogen peak in the GC-MS analysis could interfere (Dumas 2002).

2.4 Comparison of the Different Methods

It was important to verify the impact of the change in methods used over the years on the results. Different tests were therefore designed to compare the methods and verify if the results are comparable to one another.

2.4.1 Stability of Air and Water Samples in Syringes and Bottles

For the *in situ* laboratory method, the stability of the air samples in the syringes was tested with a CO_2 standard of 10000 ppm. Samples are stable for at least 48 hours, with losses of < 5%. No stability test was done at concentrations near those measured.

For the *ex situ* laboratory method, the stability of the air samples was tested at ten concentrations ranging from zero to 1200 ppm CO_2 (Dumas 2002). Samples near the ambient air concentration (350-530 ppm) are stable for 21 days. For other concentrations there seems to be some diffusion of CO_2 from or into the syringe with time. An equation was defined to correct the concentration of the sample according to the delay between sampling and analysis for samples with a concentration higher than 530 ppm. In 2000 and 2001, respectively 7% and 32% of the samples had a concentration higher than 530 ppm. The stability was also tested for the CH_4 in the air around 4 and 8000 ppm (Dumas 2002). Samples are stable for about 7 days, after that there is a slight loss in concentration. On average, samples were analyzed within 12 days of sampling in 2000 and 8 days in 2001 (Lambert 2002).

For the *in situ* laboratory method, no stability tests of the water samples were made. For the *ex situ* laboratory method, several stability tests were made. Contrary to air samples, no standard was available to confirm the real concentration measured. For CO_2, the results were inconclusive as the results varied for different types of water. For CH_4, samples with a dissolved CH_4 concentration lower than 10 ppm are stable for about 4 days (Dumas 2001).

2.4.2 Effect on the Mode of Transportation of the Samples

Usually, samples can be shipped to the *ex situ* laboratory by overland or aerial transportation. Depending on the location of the sampling site, one of the modes of transportation may not be available. It is important to verify the impact of the mode of transportation on the integrity of the sample. Since gas samples can be sent by plane, we must check the impact of

changes in air pressure resulting from aerial transportation. A study done in 2000 showed no significant difference between samples transported by air or land (Lambert et al. 2001).

2.4.3 Effect of the Mode of Transportation Between Sites

Before 1999, transportation to each site was done by boat. For this reason, sites far away from roads and boat ramps could not be sampled. In 1999, we began to move from site to site using an hydroplane for more remote areas. Since then, the sites are accessed either by boat or by hydroplane.

It is not possible to directly compare access by boat or by plane at the same site. We therefore compared the two approaches indirectly. We compared the average flux values obtained for a specific reservoir that was sampled both by plane and by boat in different years. The sites are not the same for each year. While similar average CO_2 fluxes were obtained from the sites sampled with both modes of transport, differences were observed in average CH_4 fluxes. This difference may be explained by the fact that most sites sampled by boat between 1993 and 1997 were located near the shores or in small bays. Usually these sites have a higher CH_4 flux than sites located in the middle of the reservoir (Lambert et al. 2001).

During transportation between sites, all the equipment is stored in the boat or in the hydroplane. It is possible that gases may accumulate in both the chambers and the tubing during transportation. This is why it is important to aerate the chambers before sampling. But with both methods of laboratory analysis (*in situ* or *ex situ*), it is impossible to verify whether the chamber and the tubing are ventilated well enough prior to sampling. With the automated instruments, the problem does not occur since we can verify the concentration in real time. The sampling does not begin until the concentration in the chamber and tubing has stabilized at ambient air level, usually between 370 and 400 ppm of CO_2.

2.4.4 Quality Control for all Methods

Precision – Analysis of Duplicate

Precision is obtained by comparing two results of the same sample, usually duplicates. As such, there can be different types of duplicates. In the case of this study, the following types of duplicates were done:

- Duplicate analysis in the laboratory of the same air or water sample
- Duplicate sampling of an air or water sample

- Duplicate flux (method with laboratory analysis)
  - if all air sample were taken in duplicate
  - if two or more chambers were installed side by side
- Duplicate flux (method with automated instrument)
  - if flux is measured by two different instruments simultaneously with one or two chambers
  - if two fluxes are measured one immediately after the other

The precision is calculated with Eq. 2.4. A lower percentage means a better precision. For example, two identical results would have a precision of 0% because there is no difference between the results. The precision is different for each method and varies from year to year (Table 2.3). For the method with laboratory analysis *in situ*, no recorded information to ascertain the precision was obtained.

Calculation of the precision for duplicates

$$\text{Precision coefficient} = \sqrt{\frac{\sum_{i}^{n} (d_i)^2}{2\,n}} \tag{2.4}$$

with d_i = difference between two duplicates
n = number of pair of duplicates

The precision is then converted in percentage with the following equation:

$$\text{Precision (\%)} = \frac{\text{precision coefficient}}{\text{mean of the duplicates}} \times 100\%$$

As seen in Table 2.3, the precision of the *ex situ* laboratory analysis is fairly good, lower than 7%. The precision of analysis of field duplicate samples is lower than for laboratory duplicate samples, between 8 to 26% for air samples and between 7 to 35% for water samples. One of the possible causes of this lower precision is the lack of real mixing of the air in the chamber and therefore consecutive samples taken may have some difference in concentration. For water samples, sometimes the duplicates have been taken at the beginning and the end of a flux measurement and one hour may have occurred between the sampling of each duplicate.

The precision for the fluxes measured with the *in situ* laboratory method is lower than that measured with the *ex situ* laboratory method. This is

Table 2.3. Precision for different methods and type of duplicate

Method	Year	Type of duplicate	CO_2		CH_4	
			n	%	n	%
Laboratory in situ	1993 to 1999	Flux from different chambers	414	52	430	62
Laboratory ex situ	2000 and 2001		77	31	39	30
NDIR	2001 to 2003		1025	34	—	—
FTIR	2002 and 2003		228	24	131	52
Laboratory ex situ	2000 and 2001	Flux from duplicate samples of the same chamber	13	36	3	15
	1999 to 2001	Laboratory analysis of the same water sample	32	5.9	31	6.2
	2000 to 2002	Laboratory analysis of the same air sample	142	3.1	142	6.7
	1999 to 2001	Laboratory analysis of duplicate water samples taken at the same time	20	6.6	20	35
	2000 and 2001	Laboratory analysis of duplicate air samples taken at the same time	133	7.7	133	26

n represents the number of pairs of duplicates not the number of sites sampled.

likely due to the method still being in the process of development during the first couple of years of measurements. For the last three years, the precision for the two methods was similar, around 30% for CO_2. For the automated method, the duplicates used for the calculation of the precision are not real duplicates. They are fluxes measured one after the other, usually in a short period of time (often less than 15 minutes and no more than one hour). Globally, the precision of the automated instruments (24 to 34%) is the same as the laboratory analysis for CO_2 fluxes.

The precision of the CH_4 fluxes measured with laboratory analysis methods is also better for the last three years (around 30%). The precision of the measurements obtained with the FTIR is lower (52%) due to the greater ability to measure very low fluxes with this instrument. There is more variation for duplicates of those fluxes than for higher fluxes. This situation leads to lower precision for NDIR and FTIR in some sampling campaigns (with very low fluxes) which affects the overall precision of the method.

The precision is not the same for each instrument used (Table 2.4). The LI-COR instruments obtained the lowest precision. These instruments are

also the least user friendly in the field. That's why most of the measurements were made with the PP Systems and the Gasmet instruments.

Table 2.4. Precision for each NDIR instrument used for CO_2 measurement

Company	Instrument	Year	N	Precision (%)
LI-COR	206	2002	8	27
	208	2002	50	45
	209	2002	5	64
	All LI-COR	2002	63	43
PP Systems	528	2002	193	32
	528	2003	116	40
	527	2003	235	28
	577	2003	275	25
	578	2003	74	31
	All PP Systems	2002 and 2003	893	31

n represents the number of pairs of duplicates not the number of sites sampled.

Completeness – Percentage of Rejected Fluxes

As specified in Sect. 2.3, each flux is accepted or rejected according to the coefficient of correlation. Also if some problem occurred during sampling, the flux can be rejected. The number of samples accepted or rejected is different for each method. Table 2.5 lists the number and percentage of rejected fluxes for all methods (Bourassa 2001; Lambert 2001; Lambert 2002). The percentage of fluxes rejected is variable for each method but is also variable for each year of sampling.

For CO_2 fluxes, the percentage of rejected fluxes is slightly better for NDIR (20%) compared to the laboratory methods (24 to 26%). The percentage of rejected fluxes is highest for the FTIR.

For CH_4 fluxes, the method with less rejection of fluxes is with laboratory analysis *in situ*. The other two methods (laboratory analysis *ex situ* and FTIR) have a similar percentage of rejected fluxes, between 51 and 58% on average.

For the NDIR and FTIR, the number of rejected fluxes is very different for each campaign. In some cases, there are no rejected fluxes. The percentage of rejected fluxes is very high in those sampling campaigns where most of the fluxes were very low or negative. For these fluxes, there is a lot of variation between samples and as a consequence the coefficient of correlation is lower and the number of fluxes rejected is higher. Without these campaigns, the number of rejected fluxes would overall be lower for the automated instrument.

Table 2.5. Number and percentage of CO_2 and CH_4 fluxes rejected for each method

Method	Year	Number of fluxes		% of fluxes
		Measured	Rejected	Rejected
CO_2				
Floating chamber with analysis *in situ*	1993 to 1999	833	201	24
Floating chamber with analysis *ex situ*	2000 and 2001	243	64	26
Floating chamber with NDIR	2001 to 2003	2702	547	20
Floating chamber with FTIR	2002 and 2003	916	399	44
CH_4				
Floating chamber with analysis *in situ*	1993 to 1999	833	127	15
Floating chamber with analysis *ex situ*	2000 and 2001	243	123	51
Floating chamber with FTIR	2002 and 2003	902	527	58

2.4.5 Comparison of the two Methods with Syringe

Due to logistical constraints, we were not able to do a direct comparison of the two different methods in the field. Instead we did an indirect comparison of the two methods, as for the mode of transportation. We used the average flux measured in the same area at the same period of the year (Lambert et al. 2001).

For CO_2, the average flux is similar for both methods except for the year 1994. For that year, there are some sites with very high fluxes that result in a higher average and standard deviation. For CH_4, the fluxes measured in 2000 and 2001 with the *ex situ* laboratory are lower than those measured with the *in situ* laboratory between 1993 and 1997. This difference may be explained by the fact that most sites sampled between 1993 and 1997 were located near the shores or in small bays. Usually these sites have a higher flux of CH_4 than sites located in the middle of the reservoir.

2.4.6 Comparison of Syringe and Thin Boundary Layer Methods

Duchemin et al. 1999 did a comparison of the two methods with 1994 data. For the sites studied, it was shown that the thin boundary layer method obtains lower fluxes compared to the floating chamber method with *in situ* analysis. The same observation was made in 1999 (with *in situ* laboratory analysis) and in 2001 (with *ex situ* laboratory analysis) (Lambert 2001; Lambert 2002). Also, the correlation between the two methods is very low for 1999 and 2001 data (R^2 of 0.09 for CO_2 and 0.54 for CH_4, see Fig. 2.4 and 2.5). Matthews et al. 2003 also observed that in calm conditions the fluxes obtained with the floating chambers are higher than those obtained with the TBL method. The design of the floating chamber may affect the fluxes measured.

Because of the logistical constraints related to the analysis of the water samples and the fact that the TBL method gives lower fluxes compared to the floating chamber method, the use of this method was not retained.

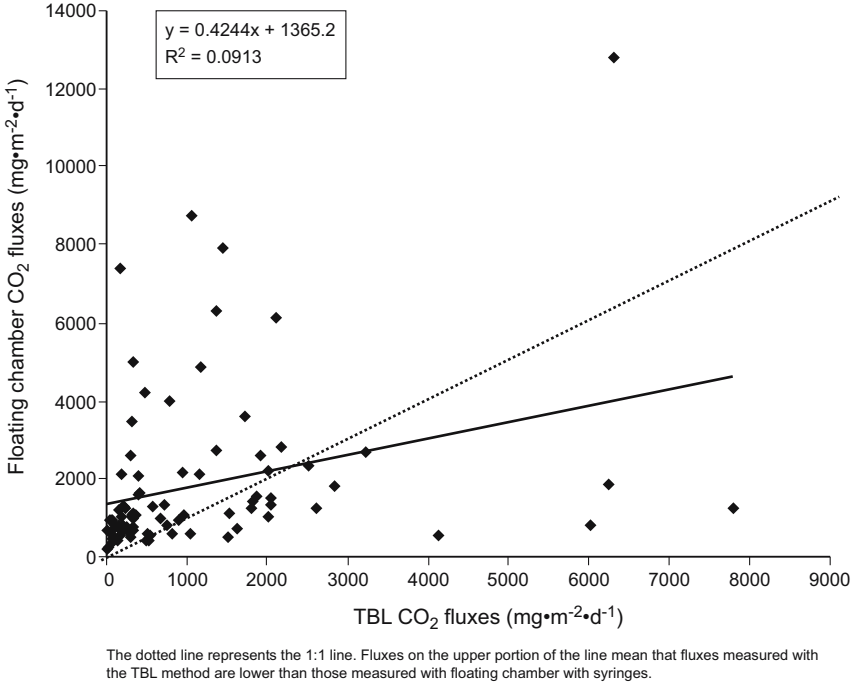

Fig. 2.4. Comparison of CO_2 fluxes ($mg \cdot m^{-2} \cdot d^{-1}$) measured with TBL and with floating chambers with syringes

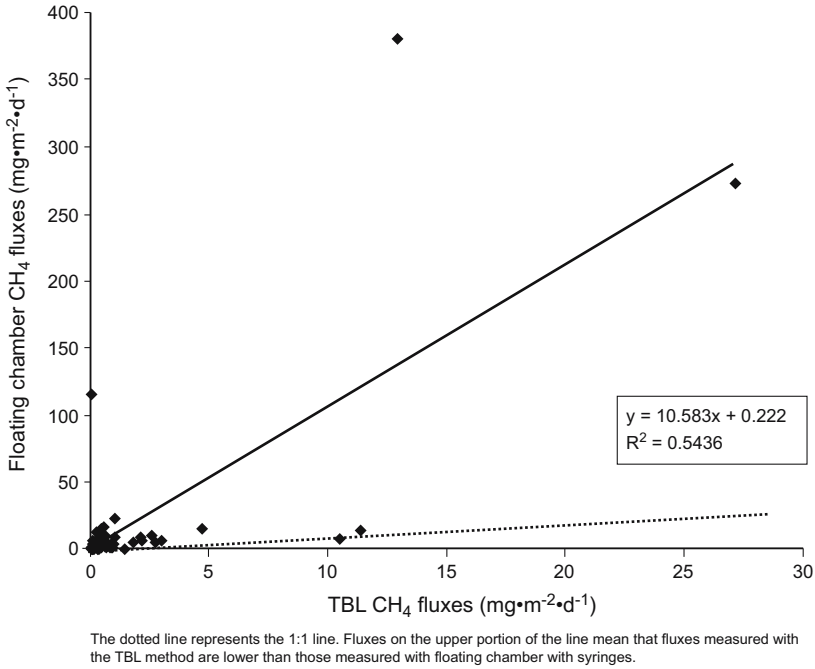

Fig. 2.5. Comparison of CH_4 fluxes ($mg \cdot m^{-2} \cdot d^{-1}$) measured with TBL and with floating chambers with syringes

2.4.7 Comparison of Syringe and Automated Instrument Methods

To be able to compare the results obtained with the method using syringes to those obtained with the method using automated instruments, we must first compare the fluxes measured by both methods at the same site. This was done at 24 sites in 2001 and 2002 (Lambert 2001; Lambert 2002).

The two chambers are installed at the same site. During the sampling of the chamber with syringes, one or more fluxes are measured with the automated instrument. There is a good correlation between the two series (R^2 of 0.92 for CO_2 and 0.84 for CH_4, see Fig. 2.6 and 2.7).

For CH_4, the fluxes measured with the syringes are usually slightly higher than those measured with the FTIR instrument. On average, the fluxes are 19% higher if we consider all sites. If we exclude the site SM294 (lowest flux measured, highest difference between methods), the average difference is then of 0.8%.

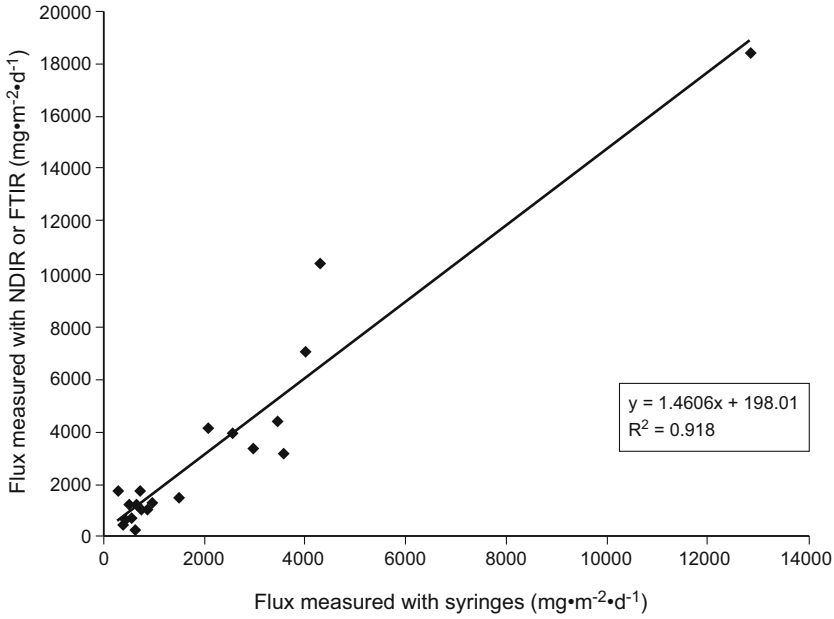

Fig. 2.6. Comparison of CO_2 fluxes ($mg \cdot m^{-2} \cdot d^{-1}$) measured with syringes and with NDIR/FTIR instrument

We noted that the CO_2 fluxes measured with the automated instrument are usually higher than those measured with the syringes. The difference is more important for fluxes bigger than 1000 $mg \cdot m^{-2} \cdot d^{-1}$ (96% difference in average) than for smaller fluxes (19% difference in average). The differences between the two methods are mostly caused by the different design of the floating chambers.

2.4.8 Comparison of NDIR and FTIR Instruments

When we receive a new piece of equipment, prior to the field, we compare the readings to a certified gas cylinder of CO_2 (concentration in the range of 400-450 ppm). There is always a slight difference between the instrument and the gas cylinder, usually around 10 ppm and less than 30 ppm. This does not significantly affect the results since we use the increase of concentration in ppm/s and not the absolute concentration to calculate the flux.

In 2002 and 2003, we used instruments of three different models (LI-COR, PP Systems and Gasmet). It was necessary to compare the

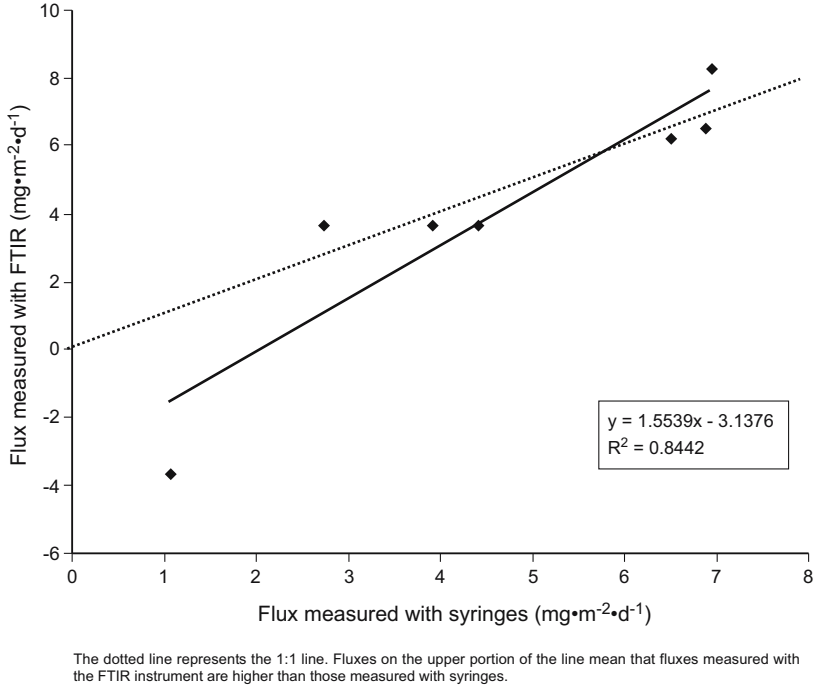

The dotted line represents the 1:1 line. Fluxes on the upper portion of the line mean that fluxes measured with the FTIR instrument are higher than those measured with syringes.

Fig. 2.7. Comparison of CH_4 fluxes ($mg \cdot m^{-2} \cdot d^{-1}$) measured with syringes and with FTIR instrument

instruments to ensure that the results are similar. We measured fluxes in the field at the same time with two or more instruments. The comparison can be done in three different ways:

- instruments connected to the same chamber in a closed loop;
- instruments connected to different chambers at the same time;
- flux measured by different instrument one after the other with the same chamber.

We did this in 2002 and 2003 with a total of 312 measurements. As the fluxes measured by different instruments at the same site and at the same time can be considered as duplicates, we calculated the precision with the equations used in Sect. 2.4.4. We can see in Table 2.6 that the instruments with the more comparable results are the Gasmet and the PP Systems (#528) with a precision of 14%. The PP Systems are comparable between themselves with a precision around 10%. The LI-COR have lower precision when compared with the Gasmet and the PP Systems (precision rang-

ing from 23 to 74%). As we saw in Sect. 2.4.4, those are also the instruments with the lowest precision for duplicates from the same instrument.

Table 2.6. Comparison of fluxes measured with different NDIR/FTIR instruments at the same site, at the same time

Instruments compared	Number of duplicates	Precision (%)
2002		
Gasmet – PP Systems 528	76	14
Gasmet – LI-COR 206	17	27
Gasmet – LI-COR 208	23	74
Gasmet – LI-COR 209	7	68
PP Systems 528 – LI-COR 206	15	23
PP Systems 528 – LI-COR 208	30	45
PP Systems 528 – LI-COR 209	8	61
2003		
PP Systems 527 – 528	44	10
PP Systems 577 – 528	46	9
PP Systems 577 – 528	46	10

In general, the Gasmet has fluxes slightly lower than those of the PP Systems and the LI-COR have fluxes higher than those obtained with both the Gasmet and the PP Systems. Since the LI-COR is less user friendly in the field and has the lowest precision, these instruments were used only in the first month of field measurements in 2002. For all other field measurements, only the Gasmet and the PP Systems were used.

2.4.9 Advantages and Disadvantages for Each Method

There is no perfect method for measuring GHG diffusive fluxes from water bodies. The advantages and disadvantages for all methods used by Hydro-Québec are listed in the following tables. Nevertheless, the method that is most reliable and most flexible in terms of logistics is the floating chamber coupled to an automated instrument.

Floating chambers coupled to an NDIR or FTIR instrument	
Advantages	Disadvantages
• It is possible to see in real time the concentration measured and the rise of the concentration under the chamber. Problems with the measurement can be detected rapidly. Contamination of the chamber or the tubing can be easily detected. • The results are known rapidly and it is possible to return the next day to the site if needed to measure again the flux. • The FTIR enables us to measure simultaneously fluxes of CO_2, CH_4 and N_2O. • There is mixing of the air trapped under the chamber during sampling. • Measurement of a flux is fairly quick, about 10 to 15 minutes for one measurement. Ten to twenty sites can be sampled each day.	• The instruments are costly initially but the investment is made profitable in a year with the avoided laboratory analysis costs. • We need to have a backup instrument in case of breakdown since it may take a couple of weeks to send an instrument to the manufacturer for repairs. • The NDIR enables us to measure only fluxes of CO_2. • The absorber columns of the PP Systems for zero air must be changed regularly. • Without use of continuous nitrogen, the FTIR is less stable. At the beginning of each day the zero of the FTIR must be done with nitrogen zero gas. If we run out of gas we can use ambient air passed through solid absorbents to make zero air. This results in less precision. • This method results in fluxes that are generally higher than those measured with floating chambers with laboratory analysis.
Thin boundary layer	
Advantages	Disadvantages
• This method is very quick, one site can be sampled in less than five minutes. Twenty to forty sites can be easily sampled each day.	• The water samples need to be analyzed rapidly because in some cases samples are not very stable. • In some remote areas, it is very hard to send the samples to the laboratory by plane or by bus. • Compared to theoretical concentrations of dissolved CO_2, the concentration measured by the laboratory are low. • The fluxes obtained by this method are based on theoretical equations that are not validated at low and high wind speeds.

Thin boundary layer (cont.)	
Advantages	Disadvantages
	• On a day with calm winds, the resulting fluxes are automatically zero. Also some times the wind speed is very low and cannot be measured precisely with some anemometers. The error on the wind speed measurement induces a major error on the flux. • This method results in fluxes that are usually lower than those measured with floating chambers with laboratory analysis.
Floating chambers with *in situ* laboratory analysis	
Advantages	Disadvantages
• The air samples are generally analyzed in less than 24 hours after sampling. There is no loss of stability of the samples. • The results are known rapidly and it is possible if needed to return to the site to measure the flux again a couple of days after sampling.	• We need to install a laboratory on site which may be impossible in remote areas or when we stay only a couple of days in the same region. If the instrument breaks there is no backup and it may take some time to repair. • The instrument is calibrated with standards of 10000 ppm which does not correspond to the range of actual measurements (usually less than 1000 ppm). • We need to have an extra technician on site to make the laboratory analysis which increase the logistical costs. • It is impossible to know if the aeration of the chamber and the tubing between sites is sufficient. • There is no real mixing of the air trapped under the chamber during sampling. • This method is long to sample on site, it takes about one and a half to two hours to measure a flux. With this method it is possible to sample only two to four sites per day.
Floating chambers with *ex situ* laboratory analysis	
Advantages	Disadvantages
• The analysis with a GC-MS is more precise than with other detectors. The standards used are closer to the range of actual measurements. • These is no need to install a laboratory on site. It is useful for remote sites where it is impossible to install a laboratory on site or when we stay only a couple of days in the same region.	• When the delay between the sampling and the analysis is too long, there is a loss of stability of the sample mostly for CO_2. • In some remote areas, it is very hard to send the samples to the laboratory by plane or by bus. • There is no real mixing of the air trapped under the chamber during sampling. • It is impossible to know if the aeration of the chamber and the tubing between sites is sufficient. • The results are not known rapidly, most of the time a week or more after sampling. It is not possible to return on site if needed to measure again the flux. • This method is long to sample on site, it takes about one and a half to two hours to measure a flux. With this method it is possible to sample only two to four sites per day.

2.5 Conclusion

It is almost impossible to find a perfect method to accurately measure GHG diffusive fluxes over bodies of water. As such, when gross emission of GHG are measured with floating chambers, the air-water interface is disturbed, which affects the flux measured. Only methods that measure an integrated concentration of GHG over water (for example laser, eddy correlation) do not affect the air-water interface. But these methods require logistics that limit the type of site that can be sampled. It is not possible with the latter to obtain data from a variety of different areas of a water body especially in remote areas.

As we have seen in this chapter each method that was used by Hydro-Québec has its pros and cons. To obtain an adequate representation of the mean flux for a reservoir or a natural water body, it is important to have a large number of results from all the different areas present in the water body. The method that enables us to sample at a great number of sites in a relatively short time with a fairly good precision is the floating chamber with an automated instrument (NDIR or FTIR). This method however tends to measure higher fluxes compared to the laboratory analysis and the thin boundary layer methods which enables us to obtain more conservative data. That's the reasons why Hydro-Québec uses this method since 2002 to measure gross fluxes of GHG from reservoirs and natural water bodies.

3 Development and Use of an Experimental near Infrared Open Path Diode Laser Prototype for Continuous Measurement of CO_2 and CH_4 Fluxes from Boreal Hydro Reservoirs and Lakes

Michel Larzillière, Denis Roy, Philippe Chrétien, Tommy Ringuette and Louis Varfalvy

Abstract

Diode laser second derivate modulation spectroscopy combined with an open atmospheric path is a well suited technique for trace gas monitoring above wide areas. This paper presents the development of a portable long optical path near infrared spectrometer based on telecommunication laser diodes in order to provide a powerful tool for real time simultaneous measurements of greenhouse gas (GHG) concentrations above lakes and hydro reservoirs. CO_2 and CH_4 are respectively monitored at 1572 and 1653 nm along optical paths of several hundreds of meters above the area of interest. Simultaneous measurements of the target gases at two different heights above the water surface allows to detect concentration gradients on a continuous basis. A simplified turbulent diffusion model involving both the measured concentration gradients and local wind data has been used to estimate average GHG fluxes emitted by lakes and hydro reservoirs in different regions. Recent optimizations of the developed prototype allow quick on site set-up and operation of the laser device, even in remote areas without local facilities, as well as the continuous measurement of low GHG concentration gradients during long time periods with a minimum of local surveillance. Further improvements of this laser system would allow simultaneous detection of other trace gases such as N_2O emitted by agricultural soils and other gases present in various environments.

3.1 Introduction

Carbon dioxide (CO_2) is known as the major greenhouse gas and its mixing ratio is increasing in the global troposphere at a rate of 0.7% per year (IPCC 2001), corresponding to an increase in concentration of about 2.5 ppmv per year. Both anthropogenic and biogenic sources contribute to this effect. During the last decades, it has been demonstrated that peatlands, wetlands, forested soils, and various type of surface waters may play an important role in the carbon cycle by releasing greenhouse gases such as CO_2, CH_4 and N_2O in response to the degradation of organic matter (Duchemin et al. 1995; IPCC 1995; IGBP 1996; Kelly et al. 1997; Galy-Lacaux et al.1999; WCD 2000; IPCC 2001).

Reliable quantification of GHG fluxes originating from aquatic sources such as natural lakes and man made reservoirs is required to evaluate the net contributions of these elements to overall GHG emissions. Use of conventional techniques for flux measurements or estimates, such as various types of floating or submerged chambers (Duchemin et al. 1999; Kelly et al. 1997; Lambert 2001; Matthews et al. 2003) or the TBL (thin boundary layer) approach (Broeker and Peng 1974; Duchemin et al. 1999) based on empirical relationships between dissolved GHG concentrations, temperature and wind speed, have serious technical limitations, especially in order to integrate spatial and temporal variations of GHG fluxes over large water bodies (WCD 2000; Tremblay 2002). On the other hand, the use of spectroscopic methods, such as the "eddy correlation" or the "relaxed eddy accumulation" (REA) techniques (Desjardins et al. 1992; Bowling et al. 1998) are complex to operate in remote areas and they are quite expensive. These techniques also have logistical and space coverage limitations. The ultimate goal of this project was to provide a powerful tool for real time simultaneous assessment of CO_2 and CH_4 fluxes above a wide area of various environments, especially natural lakes and hydroelectric reservoirs.

Optical sensors have the advantages of high sensitivity, reliability, high-speed operation and absorption path length up to several hundred meters can be achieved (Ku et al. 1975; Schiff et al. 1994). Tunable Diode Laser Absorption Spectroscopy (TDLAS) combined with Wavelength Modulation and second harmonic detection (WM(2f)) (Silver 1992) are ideal candidates for trace gases detection in the atmosphere. The necessity to carry the apparatus prevents the use of cooling diode systems. Furthermore, near IR diode lasers have been proved to be a viable alternative to the mid IR diodes lasers (Féher and Martin 1995). They have the advantage of single mode output of milliwatts and near room temperature operation in addition to the availability of inexpensive auxiliary equipment, such as low noise current drivers, thermoelectric cooler, detectors and optical components.

The portable solid state near IR laser developed, according to specific needs of Hydro-Quebec for GHG flux estimates in hydro reservoirs and natural lakes, should have low power requirements and be easy to operate in various natural and remote environments.

This chapter succinctly describes the concentrations gradient approach used for GHG flux estimates, the experimental set-up used for the measurements, as well as the major results of the field measurements made respectively on a small experimental reservoir in the Experimental Lakes Area (ELA) of Ontario (FWI 2002), a large boreal hydroelectric reservoir (Robert-Bourassa) located in James Bay area in northern Quebec, and a small shallow lake (Lake Piché), containing high levels of organic matter, located in the experimental forest area (Montmorency Forest in "Réserve faunique des Laurentides") of Laval University. The major advantages of this technique and its potential use for monitoring other trace gases are highlighted by comparison with conventional flux measurement techniques.

3.2 Methodology

3.2.1 Choice of the Gradient Technique for Flux Estimates

Evaluating average fluxes of GHG over wide areas is a difficult task taking into account the different types of environments involved, spatial and temporal variations of the local emissions and/or absorptions, as well as physical, chemical and climatic factors of the area under investigation. For practical reasons, most of the time, flux measurements involved different types of soils (Wienhold et al 1994; IGBP 1996), rather than different types of surface waters (rivers, lakes, reservoirs, estuaries). As mentioned earlier, different conventional techniques could be used for flux measurements of short duration and at small scales, such as various chamber techniques or the use of empirical relationships involving air-water exchange mechanisms, such as the TBL technique. For estimating average fluxes for wider areas, concentration gradient techniques could be used, as described in several recent studies (Baldocchi et al. 1988; Desjardins et al. 1992; Schiff et al. 1994; Smith et al. 1994; Bowling et al. 1998). Indeed, when wind blows over a surface with a given roughness, trace gases released at the surface level are taken up by the small scale atmospheric eddies. Trace gas concentrations in upward eddies are most of the time a little bit higher than trace gas concentrations in downward eddies. This phenomenon is attributed to the natural dispersion mechanism in the atmosphere as air parcels

are carried away from the emitting surface. A very fast measurement technique should be used simultaneously at two different heights, with recording speeds of 0.1 Hz or better, as allowed by TDLAS, in order to determine concentration gradients with accuracy. This gradient technique is based on the hypothesis that the transfer of a given trace gas emitted by a uniform surface, from one point to another in the atmosphere nearby the source, could be correctly represented by simple diffusion processes (Baldocchi et al. 1998).

Our approach for estimating average GHG fluxes emitted by water surfaces is based essentially on this technique, combined with the use of a unique solid state near IR diode laser developed for this study. As it will be shown in the next sections, the use of this technique, along with optical path of several hundreds of meters, allows the more accurate estimation of representative average CO_2 and CH_4 fluxes originating from natural lakes and hydroelectric reservoirs.

3.2.2 Assessing Average CO_2 and CH_4 Concentration Gradients

Technical details of the external cavity diode laser device developed during this project are described elsewhere (Larzillière 1997-2002). This device is operating according to the same principles as the ones used by commercial infrared spectrometers, where the relative absorption of the luminous power is a function of the wavelength according to the Beer-Lambert law.

$$\frac{P(L)}{P(0)} = \exp(-kNL) \tag{3.1}$$

Where:
P(L) = transmitted power (W)
P(0) = power at the beginning of the absorption path (W)
k = cross section of absorption (m^2.molecule^{-1})
N = voluminal concentration of the absorbing molecules (molecule.m^{-3})
L = optical path length (m)

This law could be also expressed as follows:

$$\frac{P(L)}{P(0)} = \exp(-\alpha(\nu)L) \tag{3.2}$$

Where $\alpha(\nu)$ is the frequency (ν) dependent absorption coefficient

The magnitude of the signal measured by the spectrometer is proportional to the relative absorption of the laser beam. To determine the concentration of the trace gas, it is necessary to carry out a calibration of the laser device in the range of the measured values. Two absorption spectra are thus recorded: one in a reference cell containing a known pressure of the absorbing gas and the other in the atmosphere. Absorption being relatively weak ($\alpha(\nu)$ L « 1), there is a ratio of proportionality between the magnitudes measured on the two spectra. Let us call R the value of this ratio which is determined with a linear regression by a software. Using Eq. 3.2, the partial pressure of the absorbing molecule along the path of the beam is thus written in the following form:

$$P_{atm} = \frac{RP_{cell}L_{cell}}{L_{atm}} \tag{3.3}$$

and its relative concentration is given by:

$$C_{atm} = \frac{P_{atm}}{P_{ATM}} x10^{-6} \tag{3.4}$$

Where:

C_{atm} = concentration of the absorbing molecule in the atmosphere (ppm)
P_{cell} = partial pressure of CO_2 or CH_4 in the cell (Torr)
P_{atm} = partial pressure of CO_2 or CH_4 in the atmosphere (Torr)
P_{ATM} = total atmospheric pressure (Torr)
L_{cell} = optical path length of the cell (m)
L_{atm} = optical path length in the atmosphere (m)
R = ratio of the magnitudes on the two spectra (determined by a linear regression)

3.2.3 Assessing Average GHG fluxes

The gradient technique, as mentioned earlier, uses measured concentration gradients to estimate the corresponding fluxes according to a simple diffusion process (using the similarity principle) in the atmosphere near the trace gas emitting source (Baldocchi et al. 1988). The following equations (Zannetti 1990) represent this approach:

$$F = K\frac{\Delta C}{\Delta Z} \tag{3.6}$$

$$K = \frac{0{,}4U^{*}Z}{(1+5\frac{Z}{L})} \qquad \text{(Neutral, stable)} \tag{3.7}$$

$$K = (0{,}4 \times U^{*} \times Z) \times (1-16\frac{Z}{L})^{\frac{1}{2}} \qquad \text{(Unstable)} \tag{3.8}$$

$$U^{*} = 0{,}4U\left(\ln\left(\frac{Z}{Z_0}\right) - \Psi_m\left(\frac{Z}{L}\right)\right)^{-1} \tag{3.9}$$

$$\Psi_m = -5\frac{Z}{L} \tag{3.10}$$

Where:
F = flux ($mg \cdot m^{-2} \cdot d^{-1}$)
K = turbulent diffusion coefficient ($m^2 \cdot s^{-1}$)
U = wind speed ($m \cdot s^{-1}$)
U* = Roughness speed ($m \cdot s^{-1}$)
ψ_m = the universal function in the diabatic surface layer wind profile (in neutral conditions $\psi_m = 0$)
Roughness length (m): Z_0 (10^{-4} for H_2O)
Roughness speed (m/s): U* = 2.0; 0.2; 0.1 (unstable, neutral, stable)
Obukov length (1/m): 1/L = -0.2; 0.0; +0.2 (unstable, neutral, stable)
Superior measure of Concentration: H1 (m)
Inferior measure of Concentration: H2 (m)
Distance between 2 paths (m): ΔZ
Geometric average (m): $Z = \sqrt{H1 \times H2}$

Stability Class (1/L)

A: Very unstable	-0.2	D: Neutral	0
B: Unstable	-0.187	E: Stable slightly	0.134
C: Slightly unstable	-0.134	F: Stable	0.2

3.3 Experimental Set-Up and Technique

3.3.1 Description of the Optical Paths

The optical set-up designed and used during various field campaigns is shown in Fig. 3.1. Concentration gradients of the greenhouse gas of

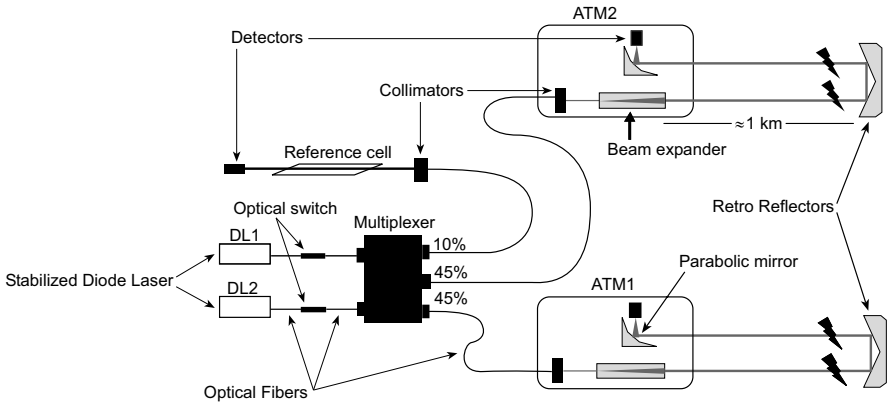

Fig. 3.1. Optical set-up of the solid state near infrared laser prototype

interest are measured simultaneously at two different heights (0.5 and 1.5 m) above the water surface for a given time period (usually several days) by using two laser diodes, DL1 at 1572 nm for CO_2 and DL2 at 1653 nm for CH_4. Only one laser diode is operated at once. The laser beam is split in to three parts by a multiplexer. A fraction (~ 10%) of the laser beam goes through the reference cell and the remaining two fractions (~ 45% each) go through the atmosphere simultaneously at the two different heights chosen for the experimental design. The atmospheric laser beams are shaped by a telescope, sent to the retro-reflector tower, located at a distance from several hundreds of meters to about 1 km from the portable laser device, and reflected back toward a parabolic mirror which one focalizes the received light on the photodiode detectors in order to evaluate accurately the remaining intensity of the reflected laser beams. The maximum optical path length obtained by this set-up design was about 2 km, using a retro-reflector located to a distance of about 1 km from the laser device. It is technically possible to use longer optical paths lengths. This would however require the use of more powerful distance meters.

To assure a good stability of the laser beams in the atmosphere during the measurements, two metallic towers (made of aluminum columns) are strongly fixed to the ground. These towers are equipped with platforms to support, at one end, the telescopes and the detection system (a parabolic mirror, detector and pre-amplifier), and, at the other end, the retro-reflectors. The laser beams coming from the multiplexer are directed through optical fibers to the platform. Figure 3.2 shows the typical laser tower set-up used for the concentration gradient technique over water surfaces. A second tower, equipped with two retro-reflectors at the same

height, is located far away at a given remote distance. For both towers, a solid concrete base was used in order to assure the required focus and stability of the optical signals.

Fig. 3.2. Experimental set-up of the laser tower for dual beam measurements

3.3.2 Spectral Resolution of the Laser Device

The presence of water vapour in the atmosphere is a major problem when using absorption spectroscopy in trace gas analysis, taking into account its strong absorption bands in the infrared region. To overcome this problem, laser diodes with very good spectral resolution of 20 MHz were chosen for this project (30000 MHz is corresponding to one wave number), a width smaller than the Doppler line width of the rotational absorption lines. Only weak absorption lines of water are present in the tuning range chosen for CO_2 monitoring, as it can be seen in Fig. 3.3, illustrating partly the rotational structure of the 301-000 CO_2 vibration band. For example, R(38) and R(16) absorption bands of CO_2 are completely free of water interference and can be used for efficient trace gas monitoring. The R(16) rotational line was chosen for measuring CO_2 concentration gradients by our portable laser device. On the other hand, the spectral region (vicinity of 1572 nm) of the laser diode commercially available for CH_4 monitoring is

completely free of water vapour interference, allowing convenient trace gas analysis of this compound, even above large water bodies.

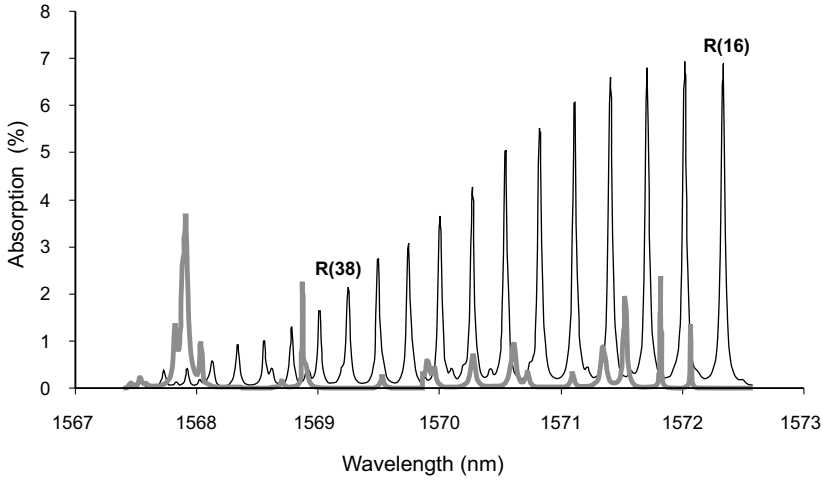

Fig. 3.3. Rotational structure of the 301-100 CO_2 vibration band overlapped by water vapour rotational lines (absorption lines R38 and R16 are free from interference)

3.3.3 Description of the Signal Detection

Only weak absorption lines, in the order of 10^{-3} units, are available in the spectral regions for interference free trace gas monitoring of CO_2 and CH_4. Consequently, the noise control in these spectral regions becomes a major problem. This noise has several origins, such as the laser power itself, the atmospheric turbulence, the optical elements transporting the laser beams (patterns of interference), and the detectors. In order to decrease, to an acceptable level, the noise effects on the monitoring results, the laser light should be modulated either in terms of frequency and intensity. On one hand, frequency modulation reduces the noise due to atmospheric turbulence, and, on the other hand, modulation of the laser power allows the reduction of the noise originating from the laser itself.

In order to compare efficiently absorption intensities of the laser light for the two optical paths, located at two different heights, the so called ratio method should be used. According to this approach, the signal coming from the detector is sent to a lock-in amplifier equipped with two entries, allowing the detection at two different frequencies. The first entry detects the absorption and the laser intensity, while the second entry allows the de-

tection of the laser power only. The ratio of these two signals produces a new signal depending only on the absorption parameter. This technique allows an efficient comparison of the laser light absorptions occurring simultaneously in the laser beam at the two different heights, as shown on Fig. 3.4. This figure contains three signals: the first one, the smallest, is coming from the reference cell, and the two others, strongly overlapped, are coming from the atmosphere. These signals are corresponding to the absorption width of the R(16) rotational line for CO_2 according to the Wavelength Modulation and second harmonic detection (WM(2f)) technique, mentioned previously (Silver 1992, p 372). According to the two strongly overlapped atmospheric signals, the difference of the laser light absorption at the two different heights is very weak in this example. In order to get a better resolution of the absorption difference between the two laser beams, we decided to stabilize the laser diode at the wavelength corresponding to the maximum of absorption and to monitor the absorption gradients at this position continuously (several hours) during the data acquisition periods. Figure 3.5 illustrates a typical example of this approach. It shows the temporal variations of CH_4 concentration gradients, observed at Lake Piché during a period of about 6 hours, computed from the simultaneous measurement of this gas at 0.5 and 1.5 m above the water surface, using a total optical path of 390 m. It should be noted that each point on this graphic represents the average absorption difference between the two laser beams according to 2500 individual records.

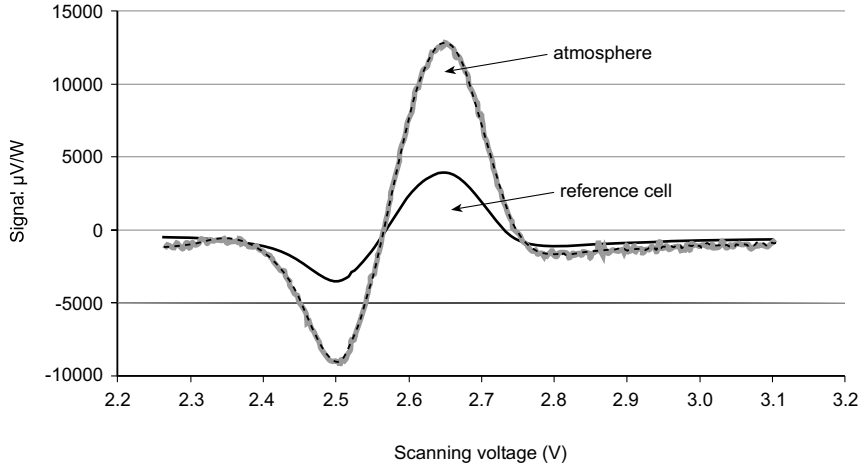

Fig. 3.4. Typical absorption signals of the CO_2 reference cell and atmospheric CO_2 monitored at two different heights (0.5 and 1.5 m above water surface)

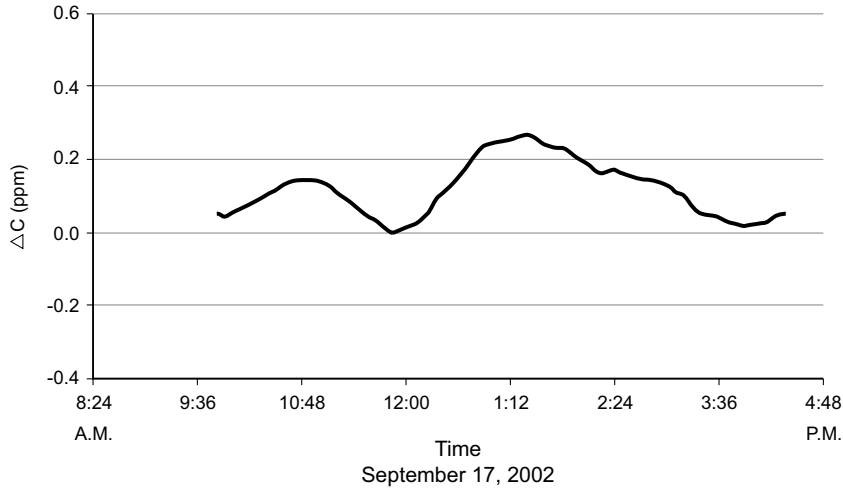

Fig. 3.5. Temporal variations of positive CH_4 concentration gradients recorded at Lake Piché, Montmorency Forest experimental site, September 17, 2002

3.4 Major Results and Discussion

3.4.1 Technical Developments and Optimizations

The technical development of the portable and versatile long optical path length solid state near IR laser device required by the specific needs of Hydro-Quebec was initiated at the LPAM laboratory of Laval University in 1995, after a previous feasibility study. The ultimate goal of the project was to develop a laser device for continuous and simultaneous measurement of CO_2 and CH_4 fluxes above wide water bodies in remote environments. Besides portability, versatility, and durability, the expected optical path length of the laser device was fixed at about 1 km in order to allow detection and precise quantification of low concentration gradients of CO_2 and CH_4, from which the average fluxes could be computed knowing the micrometeorology of the area under investigation. Several major development steps were performed during a five years R&D program, financed by Hydro-Quebec and NSERC, including the choice and experimentation of appropriate laser diodes, optimal treatment of the laser signals, exploratory laboratory and field measurements of CO_2 and CH_4 concentrations using single and dual beams laser prototypes, further optimisations of the laser beam splitting system, as well as the thermal stabilisation of the whole system in various environmental conditions, etc.

Among the major difficulties encountered during the development stage of this project, it is useful to mention here the difficulty to focalize efficiently the invisible laser beams during the field campaigns. The only way to overcome this difficulty was the in situ use of specific photo-detectors, sensitive to the near IR in order to visualize the laser beams. However, because the weakness of the laser signal, overnight work was required in order to accomplish this activity. A remote lake site (Lake Piché), located in the experimental forest of Laval University (Forêt Montmorency), at about 70 km north from Quebec City, far from city and traffic light sources, was chosen for experimental field measurements and investigations in order to optimize the laser system under development. Figure 3.6 shows a view of this site, seen from the retro-laser towers. Figures 3.7 to 3.8 show an example of CO_2 and CH_4 temporal variations recorded over Lake Piché surface water, in order to illustrate situations with either positive and negative concentration gradients occurring during the same day, as well as to illustrate the stability of the laser signals following final optimizations of the whole system. It should be also noted that the present laser prototype no longer uses the previously mentioned photo-detector approach for the laser beam alignment purpose, which approach was difficult and time consuming. The optimized laser prototype is now using a specific He/Ne laser beam which one is oriented parallel to the IR laser beams in order to allow a fast and appropriate alignment of the laser beams and an optimal signal reception from the retro-reflectors. Finally, Fig. 3.9 shows the simultaneous recording of CO_2 and CH_4, using the concentration gradient technique, following several additional technical improvements of the experimental laser device during 2002. This example clearly illustrates the present potential of the open path near IR laser device developed by Laval University for GHG flux assessments over wide water surfaces, as well as over or other type of surfaces (ex.: forested areas, grasslands, wetlands, bogs, etc.).Further details can be found in several reports describing above mentioned technical developments and optimizations (Larzillière 1997-2002).

3.4.2 CO_2 and CH_4 Fluxes at FLUDEX - ELA Experimental Reservoir

The FLooded Uplands Dynamics EXperiment (FLUDEX) reservoirs, located in the Experimental Lakes Area (ELA) are three small and shallow experimental reservoirs in northwestern Ontario, about 50 km east-southeast of Kenora, created in spring 1999 for a joint study purpose, involving Freshwater Institute of Canada, Manitoba Hydro and Hydro-Quebec. These reservoirs were dedicated for detailed mechanistic studies,

Fig. 3.6. General view of Lake Piché dual-beam infrared laser monitoring site (Montmorency experimental forest site of Laval University)

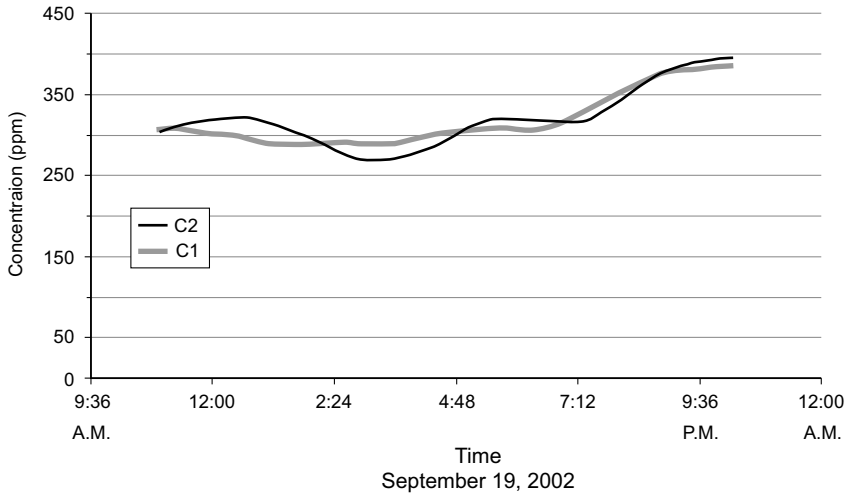

Fig. 3.7. Temporal variations of CO_2 concentrations recorded at Lake Piché, Montmorency Forest experimental site, by the dual-beam infrared laser technique at 0.5 and 1.5 m (C1 and C2) above water surface, September 19, 2002

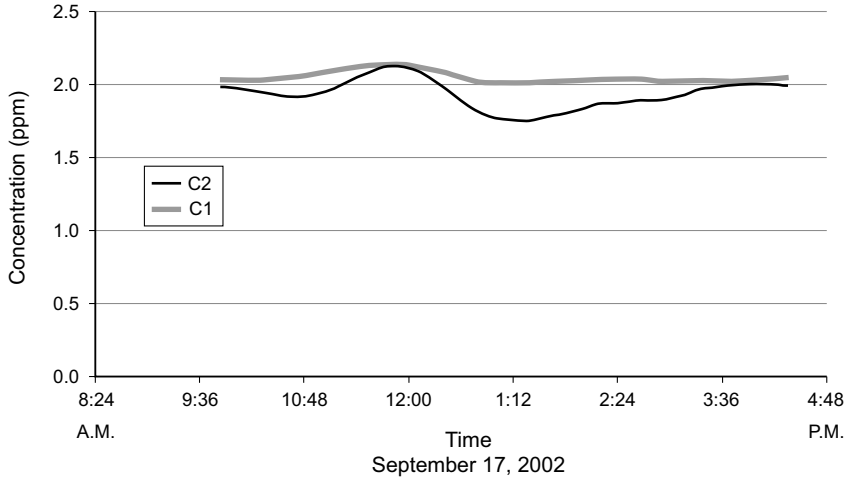

Fig. 3.8. Temporal variations of CH_4 concentrations recorded at Lake Piché, Montmorency Forest experimental site, by the dual-beam infrared laser technique at 0.5 and 1.5 m (C1 and C2) above water surface, September 17, 2002

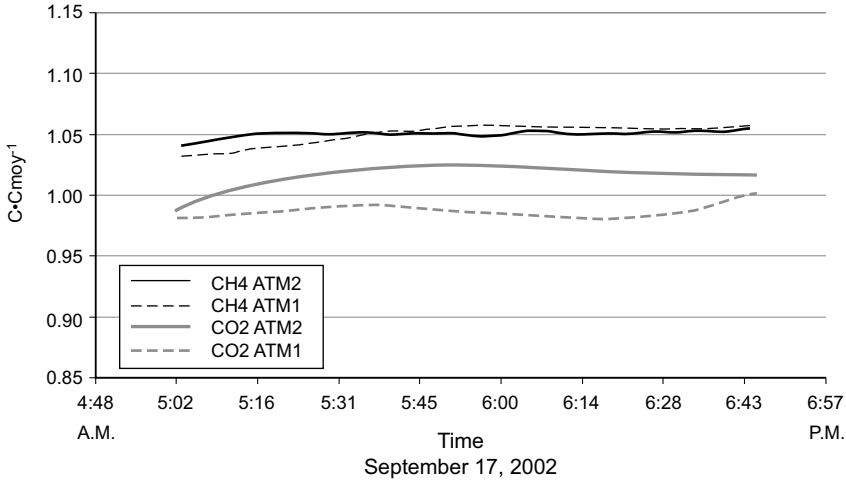

Fig. 3.9. Temporal variations of $C0_2$ and CH_4 concentration gradients recorded simultaneously at Lake Piché, Montmorency Forest experimental site, using the double beam infrared laser technique at 0.5 and 1.5 m above water surface, September 19, 2002

in a totally controlled environment, for assessing, among other goals, the impact of reservoir creation on carbon and nitrogen cycling in boreal forests, in order to evaluate the net effect of reservoir creation on greenhouse gas emissions (CO_2, CH_4 and N_2O). Details can be found in recent FLUDEX reports and publications (FWI 2001; FWI 2002; Matthews et al. 2003; Matthews et al. 2003b; Venkiteshvaran et al. 2003). Several approaches were used at FLUDEX reservoirs, especially during summers 2000 and 2001, to quantify diffusive gas exchanges at the sediment-water and water-air interfaces, such as the use of the thin boundary layer (TBL) empirical relationship, use of SF_6 tracer in order to quantify gas transfer velocities, and the use of benthic and static floating chambers to define individual fluxes during several time periods (Matthews et al. 2003).

The use of the second generation of portable near IR laser prototype, described previously, during summer 2001 was decided early that year, in order to facilitate the interpretation and analysis of the estimated CO_2 and CH_4 fluxes by the laser technique, based on the gradient approach, at least for one of the well characterized FLUDEX experimental reservoirs. This approach gave us the opportunity to experiment the laser device after several technical improvements and optimizations, described previously, in order to evaluate the precision of the measurements, as well as the detailed technical performance of the apparatus. Reservoir No. 1 was chosen for the field programs of CO_2 and CH_4 fluxes, from 23 to 28 August and from 28 to 31 August 2001 respectively.

Figure 3.10 shows the optical path of 340 m (forward and backward) chosen for the measurement at the FUDEX reservoir. Figures 3.11 and 3.12 illustrate examples of concentrations gradients observed at this site, respectively for CH_4 and CO_2, corresponding to the difference between the laser signals measured simultaneously at 0.5 and 1.5 m above the surface water. The average CH_4 flux estimated for this reservoir, from August 28 to August 31, 2001 was about 11 $mg{\cdot}m^{-2}{\cdot}d^{-1}$, with daily values varying from 7.0 to 14.7 $mg{\cdot}m^{-2}{\cdot}d^{-1}$ (cf. Table 3.1). This value is in the same order of magnitude as the average values of CH_4 fluxes (about 15 $mg{\cdot}m^{-2}{\cdot}d^{-1}$) reported for this reservoir for the same time period by other independent flux estimate techniques (SF_6 injection, TBL approach and use of static floating chambers), as mentioned earlier in this section (FWI 2001; FWI 2002; Matthews et al. 2003).

The average flux estimated for CO_2, between August 23 and August 28, 2001, for the same reservoir is about 530 $mg{\cdot}m^{-2}{\cdot}d^{-1}$, with daily values ranging from -580 to 1331 $mg{\cdot}m^{-2}{\cdot}d^{-1}$ as shown in Table 3.2. Negative fluxes were observed at several occasions during nighttime for CO_2. At first sight this phenomenon could be attributed to a lack of representative

Fig. 3.10. FLUDEX-ELA experimental reservoir No 1, dual-beam infrared laser monitoring site of CO_2 and CH_4, optical path of 340 m (forward and backward), August 2001

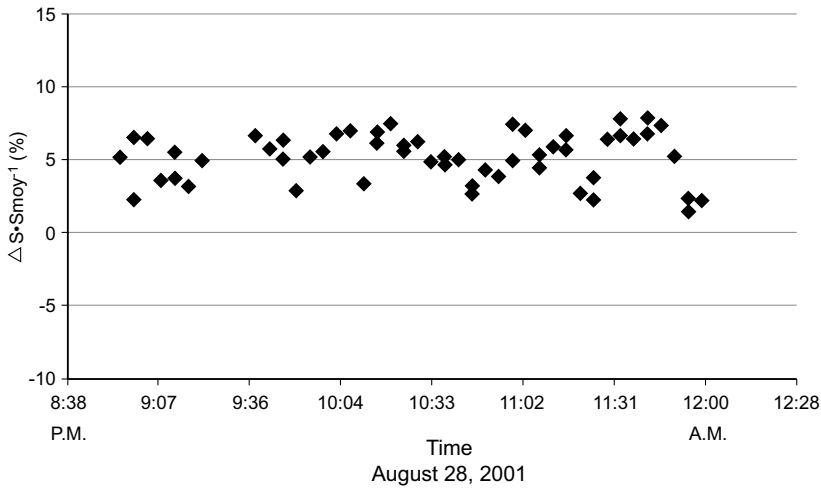

Fig. 3.11. CH_4 concentration gradients measured at FLUDEX-ELA experimental reservoir No.1 by the dual-beam laser technique at 0.5 and 1.5 m above the water surface, August 28, 2001

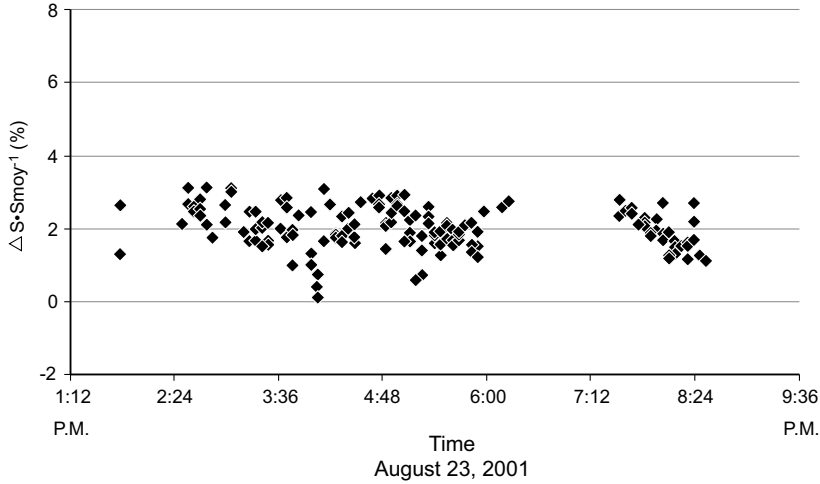

Fig. 3.12. CO_2 concentration gradients measured at FLUDEX-ELA experimental reservoir No.1 by the dual-beam laser technique at 0.5 and 1.5 m above the water surface, August 23, 2001

Table 3.1. Average fluxes of CH_4 estimated for FLUDEX-ELA experimental reservoir No 1 in August 2001 by the laser-gradient technique

Date	Flux [mg·m^{-2}·d^{-1}] Day	n	Flux [mg·m^{-2}·d^{-1}] Night	n	Flux [mg·m^{-2}·d^{-1}] Whole day	n
28-08-01	n.a.	n.a.	9.5	55	9.5	55
29-08-01	20.4	160	9.0	128	14.7	288
30-08-01	19.8	104	8.0	173	13.9	277
31-08-01	10.6	102	3.4	16	7.0	118
Average	16.9	366	7.5	317	11.3	683

local wind speed data. In fact, the wind data used for flux estimates was recorded by a tower located on a small hill a few hundreds of meters from the measurement site. The strong forested coverage of the FLUDEX site provides an efficient shelter against the low wind speeds prevailing during nighttime, as well as during daytime to a lower extent. However, during nighttime with low wind situations, temperature inversions over the shielded water surface could be also favoured. In such situations, artificial negative fluxes could be observed by the gradient technique used here. However, the real occurrence of such situations is still to be demonstrated.

More accurate local wind and temperature measurements should avoid the occurrence of such situations, if any.

Table 3.2. Average fluxes of CO_2 estimated for FLUDEX-ELA experimental reservoir No 1 in August 2001 by the laser-gradient technique

Date	Flux [mg·m^{-2}·d^{-1}] Day	n	Flux [mg·m^{-2}·d^{-1}] Night	n	Flux [mg·m^{-2}·d^{-1}] Whole day	n
23-08-01	2090	127	573	130	1331	257
24-08-01	n.a.	n.a.	-580	254	-580	254
25-08-01	946	146	-178	59	384	205
26-08-01	1116	148	67	101	591	249
27-08-01	598	133	-61	115	268	248
28-08-01	1183	39	n.a.	n.a.	1183	39
Average	1186	593	-36	659	530	1252

Table 3.3 summarizes the average CO_2 and CH_4 fluxes estimated for the FLUDEX-ELA reservoir, during the last week of August 2001, as well as the average daily flux variations observed for these gases during this period. It should be noted here that CO_2 and CH_4 fluxes were not measured at the same time, for technical considerations. Additional improvements of the laser prototype, accomplished during 2002, allow now quasi-simultaneous measurement of both gases at a given site. Finally, Table 3.4 shows the average ambient concentrations of CO_2 and CH_4 estimated during this first field campaign at the FLUDEX experimental site. As expected, average ambient concentrations of CO_2 and CH_4, and their daily variations, are very close to the expected ambient values, taking into account site characteristics (cf. forested areas in boreal regions), according to the ambient values reported for these trace gases by the World Meteorological Organization (WMO 2002).

Table 3.3. Summary of average fluxes and daily variations estimated for CH_4 and CO_2 for the FLUDEX-ELA experimental reservoir No.1 in August 2001 by the laser-gradient technique

Gas	Flux (average) [mg·m^{-2}·d^{-1}]	Daily variation [mg·m^{-2}·d^{-1}]	Number of measurements
CH_4	11	7 to 15	683 (4 days)
CO_2	530	-580 to 1330	1252 (6 days)

Table 3.4. Average ambient CO_2 and CH_4 values measured at the FLUDEX-ELA experimental reservoir No 1 in August 2001 by the open path near IR laser device under development

Gas	C (average) [ppm]	Standard Deviation [ppm]
CH_4	1.731	0.0018
CO_2	351.1	2

3.4.3 CO_2 and CH_4 Fluxes at Robert-Bourassa Hydroelectric Reservoir

Robert-Bourassa reservoir, created in 1979, is one of the largest reservoirs (3100 km^2) of the James Bay La Grande hydroelectric complex located in northern part of Quebec Province. Several sites were investigated by the near IR laser device under development, during various field campaigns performed on this reservoir between 1999 and 2001. Figure 3.13 illustrates one of these sites (cf. optical path no.1) chosen for the field campaign of September 2001, located in a bay, nearby the major dams and the water intakes of the reservoir. This site allowed the use of an optical path length of 870 m (i.e. a total of 1740 m forward and backward). During this field campaign, CH_4 concentration gradients above the water surface, at two heights (0.5 and 1.5 m) were measured during two consecutive days (August 18-19, 2001). CO_2 gradients were measured at this site during a total of 10 days, between September 5 and September 16, 2001. The major results of this campaign are presented here succinctly.

An average flux of about 3.3 $mg{\cdot}m^{-2}{\cdot}d^{-1}$ (cf. Table 3.5) was estimated for CH_4, which is quite close to the average CH_4 fluxes of a few $mg{\cdot}m^{-2}{\cdot}d^{-1}$ reported for this reservoir during the last years by using floating chambers (Duchemin et al. 1999; Duchemin 2000; Lambert 2001; Lambert 2002) However, the average daily values were quite different and varied from 7 to 13 $mg{\cdot}m^{-2}{\cdot}d^{-1}$ between the first and the second day of the field campaign (cf. Table 3.7). Unfortunately, only two days of data are available for CH_4 on this site. A significantly longer measurement period would be required in order to explain such large variations of CH_4 flux variations from one day to another. Figure 3.14 illustrate an example of the CH_4 concentration gradients recorded at this site during September 19, 2001.

During the 10 days of measurement, daily average CO_2 fluxes (Tables 3.6 and 3.7) fluctuated between quite high negative values (down to -6280 $mg{\cdot}m^{-2}{\cdot}d^{-1}$) and positive flux values up to 2130 $mg{\cdot}m^{-2}{\cdot}d^{-1}$, with this latter value being close to the average CO_2 fluxes reported for floating

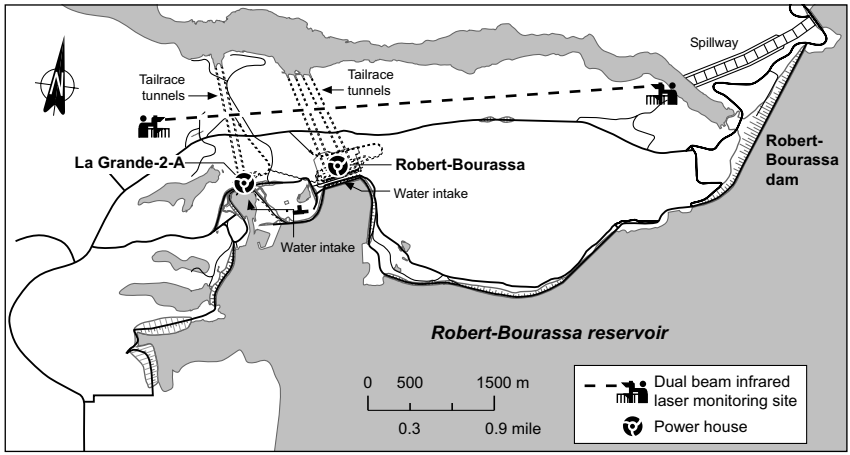

Fig. 3.13. Robert-Bourassa hydroelectric reservoir, dual-beam infrared laser monitoring site (red line) of CO_2 and CH_4 fluxes, optical path of 1940 m (forward and backward), September 2001

Table 3.5. Average fluxes of CH_4 estimated for the Marina monitoring site of Robert-Bourassa hydroelectric reservoir in September 2001 by the laser-gradient technique

Date	Flux [mg·m^{-2}·d^{-1}] Day	n	Flux [mg·m^{-2}·d^{-1}] Night	n	Flux [mg·m^{-2}·d^{-1}] Whole day	n
18-09-01	-1.8	52	-11.9	81	-6.8	133
19-09-01	10.8	90	15.9	138	13.3	228
Average	4.5	142	2.0	219	3.3	361

chamber measurements, during various the field campaigns mentioned earlier (Duchemin et al. 1999; Duchemin 2000; Lambert 2000; Lambert 2001). Figures 3.15 and 3.16 illustrate an example of positive and negative CO_2 concentration gradients recorded at this site, respectively during September 6 and 9, 2001.

The occurrence of negative CO_2 fluxes is not really an uncommon situation for lakes or even hydroelectric reservoirs (BCH 1994; Rosa et al. 2000). They can be explained by various local conditions, such as high photosynthesis periods and/or the prevalence of situations of CO_2 under saturation in the surface water layer. This latter situation could occur, at first, for example during high wind events for long time periods, producing a significant degassing of the dissolved trace gases in the surface water

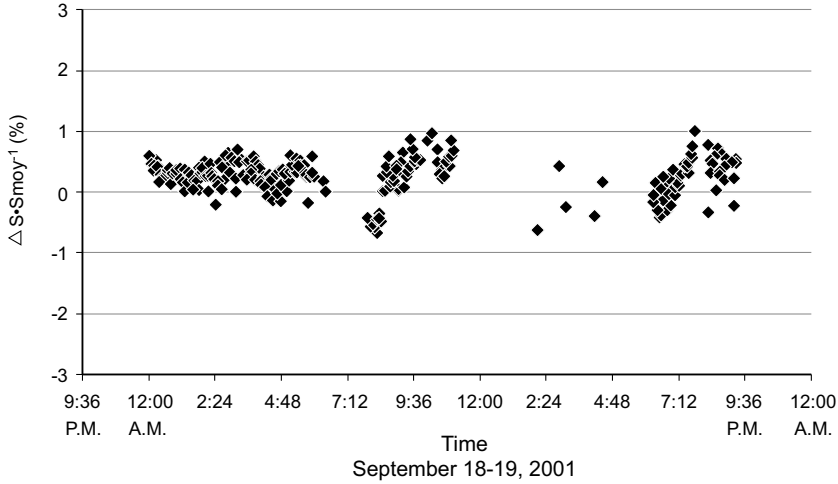

Fig. 3.14. CH_4 concentration gradients measured at Robert-Bourassa hydroelectric reservoir site by the dual-beam infrared laser technique at 0.5 and 1.5 m above the water surface, September 19, 2001

Table 3.6. Average fluxes of CO_2 estimated for Marina site of Robert-Bourassa hydroelectric reservoir in September 2001 by the laser-gradient technique

Date	Flux [mg·m^{-2}·d^{-1}] Day	n	Flux [mg·m^{-2}·d^{-1}] Night	n	Flux [mg·m^{-2}·d^{-1}] Whole day	n
05-09-01			2131	59	2131	59
06-09-01	-2485	152	568	215	-958	367
07-09-01	-414	150	-2983	143	-1699	293
08-09-01	-5194	27	-7365	135	-6280	262
09-09-01	n.a.	n.a.	-2437	109	-2437	109
12-09-01	-1827	37	-6047	10	-3937	47
13-09-01	-509	187	-2056	79	-1283	266
14-09-01	-7310	44	-2592	181	-4951	225
15-09-01	-1254	184	279	173	-488	357
16-09-01	n.a.	n.a.	13	66	13	66
Average	-2713	781	-2049	1170	-1989	2051

layer. In fact, most of the time during the measurement period of CO_2 concentration high wind events prevailed, with winds often over 50 km·h^{-1}, and wind peaks of 90 km·h^{-1}.

Table 3.7. Summary of average fluxes of CH_4 and CO_2 for the Marina site of Robert-Bourassa hydroelectric reservoir in September 2001 by the laser gradient technique

Gas	Flux (average) [mg·m^{-2}·d^{-1}]	Daily Variation [mg·m^{-2}·d^{-1}]	Number of Measurements
CH_4	3	-7 to 13	361 (2 days)
CO_2	-1990	-6280 to 2130	2051 (10 days)

Events also occurred several times during this campaign and the average water level of the reservoir raised very quickly. In fact, during this campaign, we were obliged to change several times the position of the two laser towers because of the rapid water level increase. Accordingly, a significant amount of fresh rain water, originating from a huge water basin, certainly caused significant surface water dilution which could contribute, at first, to events with CO_2 under saturation in the surface water layer of the reservoir under investigation. Available data do not allow to assess, on a scientific basis, this working hypothesis. However, we think that the unusual meteorological conditions could probably explain, at least partly, the unexpected CO_2 results observed for Robert-Bourassa reservoir during this field campaign. Further investigations of this site would be required, in different meteorological conditions, in order to interpret and explain the occurrence of these negative CO_2 flux occurrences.

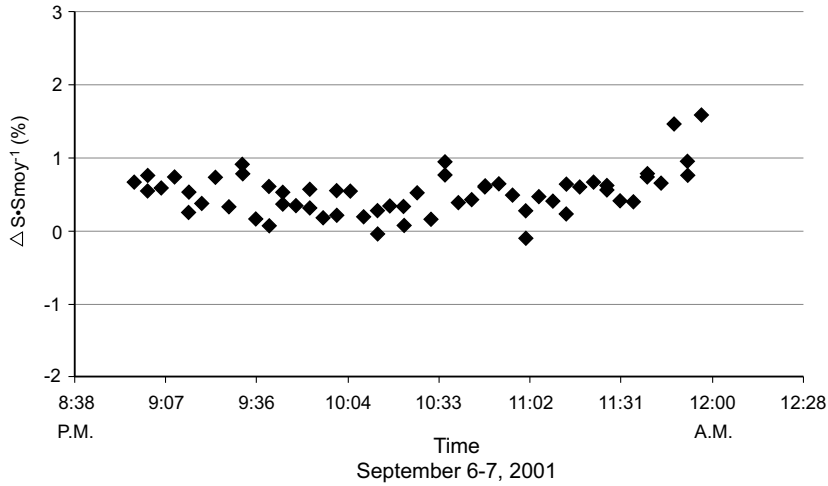

Fig. 3.15. CO_2 concentration gradients measured at Robert-Bourassa hydroelectric reservoir site by the dual-beam infrared laser technique at 0.5 and 1.5 m above the water surface, September 6-7, 2001

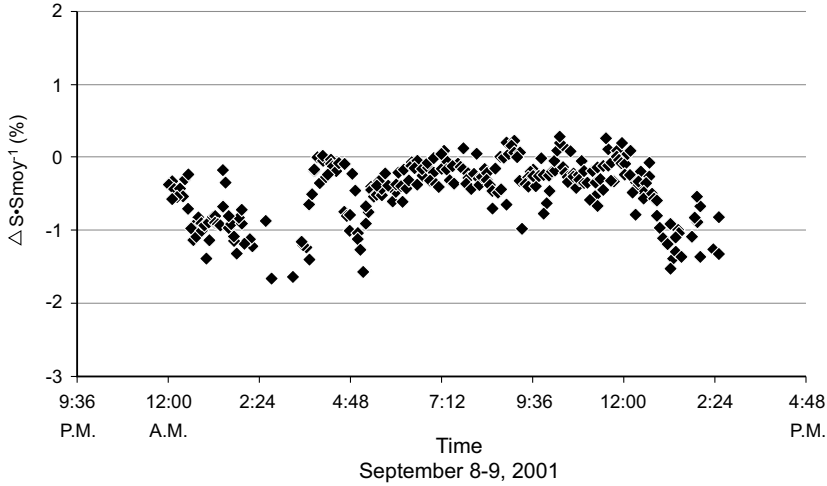

Fig. 3.16. CO_2 concentration gradients (an example of mainly negative values) measured at Robert-Bourassa hydroelectric reservoir. September 9, 2001

Table 3.8. Average ambient CH_4 and CO_2.values measured at the Marina site of Robert-Bourassa reservoir in September 2001 by the open path near IR laser device under development

Gas	C (average) [ppm]	Standard Deviation [ppm]
CH_4	1.737	0.0019
CO_2	350.9	1.8

3.4.4 Major Benefits of Flux Measurements by Tunable Diode Lasers

According to our experience, at the end of these five years of research and development, several major benefits and advantages could be attributed to the use of solid state tunable diode lasers to monitor atmospheric trace gases, among which the major ones could be summarized as follows:

- state of the art solid state tunable diode lasers (TDLs) emit in the near infrared at room temperature, avoiding the necessity of hard logistics for cooling down the laser systems, as well as for stabilizing operating temperatures;

- TDLs can be used for single or multiple gas monitoring by choosing the proper, and unique, absorption line(s) of the given gas(es), virtually without any interference between the concerned gases;
- the open path design of the solid state near IR laser device, developed by the LPAM laboratory of Laval University, in collaboration with Hydro-Quebec, allows presently the convenient and simultaneous monitoring of the major greenhouse gases (CO_2 and CH_4) above wide areas of water surfaces, up to about 2 km of total optical path, without significant interference due to the presence of water vapours or caused by local atmospheric turbulences;
- the high signal to noise ratio achieved by the last portable laser prototype, as well as the very rapid response time of the laser system (< 1 s), combined with the use of long optical paths, allow accurate measurements of trace gases in the sub-ppm, and even in the ppb ranges;
- the versatility of the developed system, also allows the eventual addition of other trace gases, for individual or combined multi-analysis purpose, such as N_2O for example, another greenhouse gas presenting a major interest for present agricultural practices.

3.5 Conclusion and Directions for Future Work

To our knowledge, this is the first study reporting successful CO_2 and CH_4 flux measurements above wide water bodies, such as hydroelectric reservoirs or natural lakes, using a portable solid state, dual beam near IR laser device. One of the greatest advantages of this technique, beyond its capability to assess simultaneously, with high spatial and temporal resolution, both major greenhouse gases (CO_2 and CH_4) concerned by the present global warming issue, is the total absence of water vapor interference along the optical path, allowing for a very high specificity of the laser system at ppb levels. One other unique feature of our present laser prototype concerns its high precision for trace gas measurements in the atmosphere. In fact, with the actual precision of 0.09 ppm for CO_2 concentration gradients and 0.001 ppm for CH_4 gradients, very weak fluxes of greenhouse gases can be measured above wide areas of water surface, or other type of surfaces, such as forested areas, wetlands, bogs, etc.

It should be also mentioned, that the solid state near IR laser technique presented in this chapter could be certainly considered as a very good complementary technique for CO_2 and CH_4 flux measurements, by comparison with the other potential techniques mentioned previously (such as SF_6 injections, TBL approach, or the use of static floating chambers), tak-

ing into account that this technique does not present any interference between the target gas and the measurement system, as is unfortunately the case with other techniques mentioned previously. Several intercomparative studies of different GHG measurement systems are presently going on or planned for the near future (Tremblay 2002; Varfalvy et al. 2002; Matthews et al. 2003; Helie and Marcel 2003), in order to validate the available candidate technique for specific case studies in various field conditions.

The technical results presented here are very promising and reveal a potential interest for future developments, such as, for example, the optimization of the whole electronic system of the laser prototype by replacing the present amplificators and generators by a unique system for the generation and modulation of the laser signals. This would greatly facilitate transportation logistics of the laser system, as well as to reduce the final cost of a commercial prototype. Among other ameliorations of the present system, there are also further possibilities to increase the signal noise ratio, as well as to eliminate of the reference cell (replaced by a system of absolute calibration) using the total laser power for the dual laser beam system.

Several other industrial trace gases of interest could be added easily to the present laser device, such as N_2O, mentioned previously, as well as several other industrial gases of interest (CO, H_2S, NH_3, HX, etc.). Sheltering and powering the actual laser system will greatly facilitate its transportation and use in remote areas. Finally, the use of a state of the art portable micrometeorological system would greatly reduce present uncertainties on local wind speeds, characterizing the site of interest, as well as the uncertainties associated with the atmospheric stability classification by 15 minute time periods, an important input for trace gas flux assessments. These modifications would be a major step and should facilitate further investigations of the various processes involved in greenhouse gas generation and emissions, taking into account, for a given reservoir, the whole carbon cycle at the watershed level.

4 Greenhouse Gas Fluxes (CO_2, CH_4 and N_2O) in Forests and Wetlands of Boreal, Temperate and Tropical Regions

Anne-Marie Blais, Stéphane Lorrain and Alain Tremblay

Abstract

Current estimates of GHG budgets of forests indicate that these ecosystems act, over all, as C sinks, regardless of climatic region. The sequestering of GHGs by forests is the result of the balance between a substantial uptake of CO_2 by vegetation and CO_2 release through soil respiration, a weak consumption of CH_4 by methanotrophic bacteria, and a more or less significant emission of N_2O from soil, a by-product of nitrification and denitrification reactions. According to the estimated GHG budgets, the forest C sink is weaker in the boreal region (mean -236 $mgC \cdot m^{-2} \cdot d^{-1}$) than in the temperate and tropical regions (-398 and -632 $mgC \cdot m^{-2} \cdot d^{-1}$, respectively), in agreement with the NEE (Net Ecosystem Exchange in CO_2) pattern observed with latitude. The increase in solar radiation and growing season length from north to south could be responsible for such a pattern. The C sinks typical of tropical forests can be offset by nearly 30% by N_2O emissions from the soils. In northern forests, some sites have been found to be net sources of CO_2, particularly during warm and dry years.

In wetlands, water-saturated soils are conducive to anaerobic decomposition of organic matter and methane production. CH_4 largely dominates the GHG budget of wetlands. Overall, northern peatlands are sources of GHGs (mostly as CH_4) (173 $gCO_2\text{-eq.} \cdot m^{-2} \cdot yr^{-1}$), while accumulating small quantities of CO_2 as peat (-22 $gC \cdot m^{-2} \cdot yr^{-1}$). Our GHG budgets for peatlands do not generally take into account the high CO_2 and CH_4 emissions from ponds. Tropical wetlands, dominated by marshes and swamps, emit large amounts of CH_4 into the atmosphere (mean 71 $mgCH_4 \cdot m^{-2} \cdot d^{-1}$) compared to northern peatlands (34 $mgCH_4 \cdot m^{-2} \cdot d^{-1}$).

The estimated GHG budget values for forests depends on a) the error in NEE measurements, which dominate the forest GHG budgets and whose

percent correction for calm nights can represent up to 50% of their initial value; b) the small number of published data on NEE for boreal and, especially, tropical forests, for which two out of the three available NEE data sets are contested; and c) the lack of NEE data in certain stands, such as in boreal forests post-fire stands, to which a certain potential for GHG emission is attributed. In wetlands, the popular use of the chamber method for CH_4 flux measurements, along with a sampling period of less than a year, make it difficult to estimate an annual GHG budget that would integrate these systems' considerable spatial and temporal variability. The use of flux towers in forests, and recently in peatlands, allows for estimations of annual CO_2 fluxes (NEE) typical of the local variability of environmental conditions within these systems.

4.1 Introduction

Carbon dioxide (CO_2), methane (CH_4) and nitrous oxide (N_2O) are radiatively active greenhouse gases (GHG) contributing to global warming. Moreover, CH_4 is involved in atmospheric chemical reactions leading to the formation of tropospheric ozone or urban smog (Cicerone and Oremland 1988). Since the industrial revolution, the atmospheric concentrations of CO_2, CH_4 and N_2O have been increasing at mean annual rates over the last two decades of 0.4% for CO_2 and CH_4, and 0.3% for N_2O (IPCC 2001).

Because of the potential effects of increased atmospheric concentrations of CO_2, CH_4, and N_2O on the global energy budget, considerable efforts have been recently made to quantify the strength of terrestrial sources and sinks for these gases. Forests and wetlands are key components of global CO_2, CH_4 and N_2O budgets (Schlesinger 1997). According to recent budgets, close to 20% of the CO_2 found in the atmosphere would transit annually through forests (Schlesinger 1997), and around 2 PgC per year (excluding deforestation) would have been sequestered in the biomass and forest soils in the 1980s (IPCC 2001), reducing the impact of anthropogenic GHG emissions, such as those from fossil-fuel burning. Theoretically, mature forests are in balance with atmospheric CO_2 (Grace et al. 1995), but the higher atmospheric concentration in CO_2 (Keeling et al. 1996; DeLucia et al. 1999; Hamilton et al. 2002) and the increase in atmospheric nitrogen deposition (Nilsson 1995; Mellilo 1996; Clein et al. 2002) could have transformed these systems into carbon sinks, by having stimulated their productivity. The importance of forest soils as methane sinks are significant, with a consumption estimated at around 5% (30 Tg

CH_4/yr) of the CH_4 emitted worlwide (Schlesinger 1997). On the other hand, wetlands are responsible for more than 20% of the CH_4 annually released into the atmosphere (Cao et al. 1998).

It is difficult to accurately assess the net contribution of forests and wetlands to global warming due to the complexity of the processes involved. This evaluation is intimately linked to local environmental conditions and controlled by spatio-temporal factors.

The following chapter gathers the currently available information on CO_2, CH_4 and N_2O gas fluxes from boreal, temperate and tropical forests and wetlands. This overview, based on an extensive review and a critical analysis of literature data, has allowed us to draw up a greenhouse gas (GHG) budget for forests and wetlands and characterize the spatio-temporal variability of gas fluxes within them.

4.2 Net Ecosystem Exchange of CO_2 (NEE) in Forests

Net CO_2 fluxes in forests (or NEE for Net Ecosystem Exchange of CO_2) represent the balance between CO_2 uptake through photosynthesis and CO_2 release through plant respiration and decomposition (Randerson 2002). NEE only approximates net ecosystem production (NEP), since it does not take into account carbon losses other than through local respiration, such as riverine export of dissolved organic carbon (Aitkenhead and McDowell 2000; Richey et al. 2002), volatile organic carbon emissions (Adams et al. 2001; Guenther 2002) and carbon emitted during forest fires or insect outbreaks (Amiro et al. 2001; Kasischke and Bruhwiler, 2003). Continuous NEE measurements with high-time resolution (half-hour) are being made using the eddy covariance method within the FLUXNET network (http://www-eosdis.ornl.gov/FLUXNET/), which includes over 200 sites distributed in all continents, but mainly in North America and Europe.

Northern Forests as Sources or Sinks of Atmospheric CO_2

Annual NEE values compiled in Table 4.1 suggest that northern forests (n = 34) can behave as sinks as well as sources of atmospheric CO_2, with NEE values ranging from -5230 to 271 $mgCO_2 \cdot m^{-2} \cdot d^{-1}$ in boreal stands and from -16605 to 1115 $mgCO_2 \cdot m^{-2} \cdot d^{-1}$ in temperate forests. The majority of stands investigated with flux towers in boreal and temperate forests consume CO_2 over a whole year, meaning that carbon uptake in the biomass and soil exceeds carbon removals through decomposition. CO_2 emissions, rather weak compared to the maximum sink capacity of these forests

Table 4.1. Annual net ecosystem exchange of CO_2 ($mgCO_2 \cdot m^{-2} \cdot d^{-1}$) in forests

Country	Site	Lat.	Long.	Forest type/ Dominant species	Land-use[a]	Age	Year	Mean	Min	Max	Reference(s)
								[$mgCO_2 \cdot m^{-2} \cdot d^{-1}$]			
BOREAL FORESTS (n = 11)											
Canada	Churchill, ON	59°N	94°W	Woodland	N		1997 (G)[b]	-329			Lafleur et al. (1999)
Canada	Schefferville, QC	56°N	67°W	Lichen woodland	N		1994 (G)	-1507			Fan et al. (1995)
Canada	BOREAS NSA[c]	56°N	98°W	Black spruce	N	90	1995-97	271[d]	-101	704	Goulden et al. (1998)
Canada	BOREAS NSA	56°N	98°W	Jack pine	N	~30	1994, 1996 (G)	-2345	-2682	-2008	Joiner et al. (1999)
Canada	BOREAS SSA[c]	54°N	106°W	Black spruce	N	100-150	1995, 2000	-523	-682	-351	Malhi et al. (1999); Griffis et al. (2003)
Canada	BOREAS SSA	54°N	105°W	Jack pine	N	100-150	2000	-784			Griffis et al. (2003)
Canada	BOREAS SSA	54°N	106°W	Aspen	N	~80	1994, 96-2000	-1488	-2912	-803	Black et al. (2000); Griffis et al. (2003)
Russia	Yakutsk	61°N	128°E	Larch	N	~130	1993 (S)[b]	52			Hollinger et al. (1995)
Sweden	Flakaliden	64°N	19°E	Norway spruce	P	37	1997	-5230			Valentini et al. (2000)
Sweden	Norunda	60°N	16°E	Evergreen forest	SG	~80	1995-97	-351	-1910	904	Lindroth et al. (1998)
Finland	Hyytiala	62°N	24°E	Scots pine	P	31	1997-99	-2301	-2633	-1918	Markkanen et al. (2001)
							Average	-863	-2633	904	
TEMPERATE FORESTS (n = 23)											
Canada	Camp Borden	44°N	80°W	Deciduous forest	SG	100	1996-98	-1578	-2411	-603	Barr et al. (2002)
USA	Niwot Ridge	40°N	106°W	Evergreen forest			1999-2000	-693	-803	-584	Monson et al. (2002)
USA	Wind River Crane	46°N	122°W	Douglas fir	N	500	1998	-5323			Paw U et al. (2000)[e]
USA	Howland Forest	45°N	69°W	Mixed forest		90	1996	-2110			Hollinger et al. (1999)
USA	Metolius	44°N	122°W	Ponderosa pine	N	50/250	1996-97	-2964	-3255	-2671	Law et al. (2001)
USA	Harvard Forest	43°N	72°W	Deciduous forest	N	55-75	1991-2000	-2099	-2814	-1205	Goulden et al. (1996); Barford et al. (2001)
USA	Morgan Monroe	39°N	86°W	Deciduous forest	N	60-80	1998-2000	-2562	-2882	-2381	Schmid et al. (2000); Ehman et al. (2002)
USA	Walker Branch	36°N	84°W	Deciduous forest	SG	50-120	1994-99	-5707	-6318	-4720	Wilson and Baldocchi (2000)
Denmark	Soroe	55°N	12°E	Beech	NM	80	1997-99	-1405	-2279	-712	Granier et al. (2002)
Netherlands	Loobos	52°N	6°E	Scots pine	P	80	1997	-2110			Valentini et al. (2000)
Germany	Solling	52°N	10°E	Norway spruce	P	110	1996-97	-4019	-4923	-3115	Valentini et al. (2000)

Table 4.1. (cont.)

Country	Site	Lat.	Long.	Forest type/ Dominant species	Land-use[a]	Age	Year	Mean	Min	Max	Reference(s)
								[$mgCO_2 \cdot m^{-2} \cdot d^{-1}$]			
TEMPERATE FORESTS (n = 23) (cont.)											
Germany	Hainich	51°N	10°E	Beech	N	Mature	2000-01	-4942	-4962	-4923	Knohl et al. (2003)
Germany	Tharandt	51°N	14°E	Norway spruce	NM	105	1996-98	-4520	-5425	-3315	Valentini et al. (2000)
Germany	WeidenBrunnen	50°N	12°E	Norway spruce	NM	45	1997	-773			Valentini et al. (2000)
Belgium	Brasschaat	51°N	4°E	Mixed forest	P	70	1997-2001	1115	-90	2562	Carrara et al. (2003)
Belgium	Vielsalm	50°N	6°E	Mixed forest	P	75	1997	-4320			Valentini et al. (2000)
France	Hesse	49°N	7°E	Beech	NM	30	1996-99	-2120	-2973	-682	Valentini et al. (2000); Granier et al. (2000)
France	Le Bray	45°N	1°E	Maritime pine	P	29	1997	-4320			Valentini et al. (2000)
Italy	Reno/Ritten	47°N	11°E	Norway spruce	NM	80	1998	-4520			Valentini et al. (2000)
Italy	Collelongo	42°N	14°E	Beech	NM	98	1994, 1997	-5677	-6630	-4720	Valentini et al. (2000)
Italy	Castelporziano	42°N	12°E	Oak	N	50	1997	-6630			Valentini et al. (2000)
Japan	Takayama	36°N	137°E	Birch and oak			1994, 1999	-1677	-2151	-1205	Yamomoto et al. (1999); Saigusa (2002)
New Zealand		43°N	173°E	Monterey pine	P	10	1995-97	-16605			Arneth et al. (1998)
							Average	-1455	-2411	2561	
SUBTROPICAL FORESTS											
USA	Gainesville	30°N	82°W	Slash pine	M	24	1996-97	-6781	-7 433	-6 129	Clark et al. (1999)
TROPICAL RAINFORESTS (n = 3)											
Brazil		3°S	50°W	Rainforest	N	Mature	1995-96	-5926			Malhi et al. (1998)
Brazil	Rondonia, Tower A	10°S	62°W	Rainforest	N	Mature	1992, 93	-1025			Grace et al. (1995)
Brazil				Rainforest	N	Mature		~0			Miller et al. (2004)
							Average	-2317			
TROPICAL SAVANA (n = 1)											
Australia	Howard Springs	12°S	131°E	Tropical savanna			1996-98	-1027			Eamus et al. (2001)

[a]: *N*: natural forest; *NM*: naturally-managed forest; *P*: plantation; *SG*: secondary growth.
[b]: NEE estimated over a summer (S) or growing season (G).
[c]: Northern study area (NSA); Southern study area (SSA).
[d]: Unpublished NEE results for 1998 and 1999 indicate that this stand is in equililbrium with atmospheric CO_2 http://www-as.harvard.edu/chemistry/boreas/boreasflux.html.
[e]: Unpublished manuscript cited in Baldocchi et al. (2001).

(-5230 and -16605 $mgCO_2 \cdot m^{-2} \cdot d^{-1}$), were nonetheless measured at a few sites, most of them being located in the boreal region (Canada: 271 $mgCO_2 \cdot m^{-2} \cdot d^{-1}$, Goulden et al. 1998; Europe: 904 $mgCO_2 \cdot m^{-2} \cdot d^{-1}$, Lindroth et al. 1998; Russia: 52 $mgCO_2 \cdot m^{-2} \cdot d^{-1}$ (summer), Hollinger et al. 1995) and only one in the temperate forest (Belgium, 1115 $mgCO_2 \cdot m^{-2} \cdot d^{-1}$, Carrara et al. 2003). To our knowledge, among the preceding studies, only Goulden et al. (1998) cross-validated their eddy correlation results with biometric measurements.

The CO_2 emissions measured in mature stands (Goulden et al. 1998 and Hollinger et al. 1995), which are theoretically in balance with atmospheric CO_2 (Grace et al. 1995), reflect the dynamic equilibrium between NEE and climate. This means that carbon losses at these sites would probably be compensated during years of more favorable weather conditions (Goulden et al. 1998). Besides, unpublished NEE results for the years 1998-99 at the NSA (Northern Study Area) OBS (Old Black Spruce) site indicate a net uptake of CO_2 for both years, which confirms that this site is in near equilibrium with atmospheric CO_2 (http://www-as.harvard.edu/chemistry/boreas/boreasflux. html).

The net efflux of CO_2 at the NSA OBS site, located in the discontinuous permafrost zone of Canada, resulted from a 10-fold increase in soil respiration (measured with soil gas-exchange chambers) upon soil thawing during peak summer temperature in July (Goulden et al. 1998). Higher than normal temperatures and the legacy of past management practices (e.g., intensive thinning and removing of invasive species at the Belgium site, producing dead organic matter for decomposition) may explain the net efflux of CO_2 observed at the mid-succession sites in Sweden and Belgium (Lindroth et al. 1998 and Carrara et al. 2003). A lower photosynthesis in post-fire stands (due to low leaf-area and biomass) or a higher respiration in recently cut stands (fueled with harvest residues) would also result in these stands emitting more CO_2 than they consume (Schulze et al. 2000; Litvak et al. 2003). However, only partial annual NEE measurements are available for early successional stands.

Stronger Sink in Temperate Forests

In spite of the net CO_2 emission at certain sites, the entire boreal forest is thought to be a weak sink of CO_2. Considering our average NEE for the boreal forest (-863 $mgCO_2 \cdot m^{-2} \cdot d^{-1}$, Table 4.1) and a total area of 1343 Mha (Goodale et al. 2002), it is possible to estimate a sink of 1 $PgC \cdot yr^{-1}$ for the 1994-2000 period. However, the results from a few tower fluxes in the boreal region, with an average footprint of 1 km^2 (Baldocchi et al. 2001), are unlikely to be representative of the entire biome, which can be thought of

as a heterogeneous mosaic composed of stands at different successional stages (Larsen 1980). Atmospheric inverse modeling and forest inventories, which incorporate much of the large-scale spatial variability of the boreal forest, estimate for this biome a sink of 0.3 to 0.5 $PgC \cdot yr^{-1}$ (Dixon et al. 1994; Bousquet et al. 2000; Kurz and Apps 1999; Nilsson et al. 2000; Goodale et al. 2002; Gurney et al. 2002). Contrary to the preceding values, our estimate of 1 $PgC \cdot yr^{-1}$ does not consider anything other than respiratory carbon losses.

The boreal forest sink term is concentrated in Eurasia (Goodale et al. 2002; Gurney et al. 2002) and is caused mainly by the replacement of old-growth forests with highly productive young stands (Nilsson et al. 2000). In Canada, forests are either a weak source or sink of carbon. According to Kurz and Apps (1999), Canadian forests became a source of carbon in the 1980s (0.05 $PgC \cdot yr^{-1}$) as a consequence of large-scale disturbances. However, a recent study, with better spatial resolution and incorporating the effect of nitrogen deposition and CO_2 enrichment, suggests that the Canadian forest was a weak sink of carbon during the 80s and 90s (Chen et al. 2003). Tracking down biomass changes with NDVI (normalized difference vegetation index) and remote sensing, Myneni et al. (2001) also found that green biomass was stable between 1995 and 1999 in Canada.

The terrestrial sink of 2 $PgC \cdot yr^{-1}$ (1980-1989) is thought to be concentrated in mid-latitude forests (IPCC 2001; Houghton 2003). The NEE values in Table 4.1 can be extrapolated to estimate the contribution of forests to this sink. In Europe, measurements of NEE at the CARBOEUROFLUX forest sites, which encompass a wide range of European climates and tree species (Valentini et al. 2000), have been combined with climatic maps and NDVI in a neural network to give an aggregated, European-wide forest NEE estimate of -185 $gC \cdot m^{-2} \cdot yr^{-1}$ (Papale and Valentini 2003). Extrapolated to the entire European forest area (149 Mha), a net uptake of 0.3 $PgC \cdot yr^{-1}$ can be estimated. In the USA, flux tower results imply an average net uptake of 300 $gC \cdot m^{-2} \cdot yr^{-1}$ by forest stands for a total of 0.7 $PgC \cdot yr^{-1}$ (246 Mha, Birdsey and Heath 1995). These carbon uptakes, estimated from NEE, are more than twice as high as estimates based on forest inventories (-80 $gC \cdot m^{-2} \cdot yr^{-1}$ for the early 1990s in Europe and -104 $gC \cdot m^{-2} \cdot yr^{-1}$ for the USA, Birdsey and Heath 1995; Nabuurs et al. 1997; UNECE/FAO 2000; Goodale et al. 2002). This would partly reflect the currently biased distribution of flux tower sites towards regrowing forests in the North Hemisphere (IPCC 2001), as well as methodological differences, with forest inventories integrating non-respiratory carbon losses and not directly measuring soil organic carbon sequestration (Janssens et al. 2003).

Combining our estimates for Europe and the USA (and excluding China for which we do not have NEE values) we obtain a total gross sink for temperate forests (n = 23), before perturbations, of 1 $PgC \cdot yr^{-1}$. According to recent estimates combining atmospheric inverse models and forest inventories, the magnitude of the temperate forest sink in Europe and the USA would lie somewhere between 0.4 and 0.8 $PgC \cdot yr^{-1}$ (Pacala et al. 2001; Janssens et al. 2003).

Our estimated total gross sink for temperate forests (1 $PgC \cdot yr^{-1}$) is relatively low compared to the terrestrial sink of 2 $PgC \cdot yr^{-1}$ mentioned previously. This is because, in the USA, about one half of the gross sink is assumed to be located outside the forest sector, resulting from the woody encroachment of grasslands and savannas after large-scale abandonment of agricultural land and cessation of fire suppression practices (Houghton et al. 1999; Pacala et al. 2001). Recent results indicate, however, no carbon gain following woody plant invasion of wet grasslands (Jackson et al. 2002).

Temperate forests take up more C than boreal stands on a per area unit. Average NEE suggest an uptake 1.6 times higher in temperate forests (-1455 mg $CO_2 \cdot m^{-2} \cdot d^{-1}$) compared to boreal ones (-863 mg $CO_2 \cdot m^{-2} \cdot d^{-1}$) (Table 4.1). A higher net uptake of carbon by stands of comparable age in temperate forests, would reflect the predominance of deciduous species with greater productivity, a longer growing season (around 170 days compared to 125) and higher light intensity at southern latitudes, which variables are conducive to plant photosynthesis without directly affecting the organic matter degradation rate. The stronger sink in the temperate forest as a whole (0.4-0.8 $PgC \cdot yr^{-1}$) compared to the boreal forest (0.3-0.5 $PgC \cdot yr^{-1}$) would be due to the comparatively large areas occupied by mid-succession forests (30 to 100 years old) (Birdsey and Heath 1995; Kauppi 1992). Moreover, in western Europe, forests are intensively managed and impacts from natural disturbances, such as fire, are markedly less than in North America and Siberia (Fyles et al. 2002).

Uncertainty Regarding Tropical Forest Sink

The net flux of CO_2 of tropical forests is uncertain (Houghton 2003). Initial NEE values suggested the existence of an important carbon sink in undisturbed tropical forests (Grace et al. 1995; Malhi et al. 1998). Phillips et al. (1998) who estimated, based on long-term plots and biometry, a biomass sink of around 50 $gC \cdot m^{-2} \cdot yr^{-1}$ (1958-1996), supported these results. However, Phillips et al. (1998) were criticized for having included in their data set many plots for which trees had been measured at breast height, where tropical trees typically have buttresses with a greater radial growth

compared to the trunk, or plots located on recent floodplains (Clark 2002). Clark (2002) reanalyzed Phillips et al.'s 1998 data set and, after having excluded the problematic plots, obtained a smaller biomass sink of 13.5 $gC \cdot m^{-2} \cdot yr^{-1}$.

Recent NEE measurements, supported by biometry, suggest, on the contrary, that mature tropical forests are in near equilibrium with atmospheric CO_2 (Miller et al. 2004). Miller et al. (2004) demonstrate that the lateral transfer of CO_2 during calm nights, assumed by Malhi et al. (1998) to be unimportant, is large enough to eliminate the apparent uptake of CO_2 when taken into account. Estimations based on CO_2 concentrations measured from aircraft during the Amazon boundary layer experiment (April-May 1987) indicate that Central and Eastern Amazonia were in balance with CO_2 late in the wet season of 1987 (Chou et al. 2002). Even a small net CO_2 source was measured with a flux tower (Saleska et al. In review), cited in Houghton, 2003) and forest inventory (Rice et al. 2004) in an old-growth forest of the Tapajós National Forest (Brazil). According to Rice et al. (2004), the stand is recovering from a past disturbance, with the decay of dead wood releasing more carbon than the growth of living trees.

Spatial and Temporal Variability of Forest NEE

NEE so far measured in northern forests show spatial variability at their scale of measurement (1 km^2), with values ranging over more than an order of magnitude in both boreal and temperate forests (Table 4.1). In temperate forest, the sites in Table 4.1 differ considerably from one another regarding species composition, stand age (10 to 500 years), mean annual temperature (4.1 to 13.9°C), mean annual precipitation (392 to 2528 cm) and past management. Considering the habitat diversity represented, it is not surprising that measured NEE of temperate forests vary so much.

Moreover, the eddy covariance method, allowing the measurement of net fluxes of CO_2 with high-time resolution (half an hour), has revealed the existence of an important variability of fluxes on a time-scale of days, seasons and from year to year. It was not possible to appreciate short-time variability with biometric methods, which, by following changes in carbon pools, integrate carbon fluxes over several years.

Factors Governing Forest NEE

The response of NEE to seasonal and inter-annual climatic variability was studied by several authors (Goulden et al. 1996, 1998; Lindroth et al. 1998; Chen et al. 1999; Black et al. 2000; Valentini et al. 2000; Barford et al. 2001). They found that NEE was generally sensitive to five climate vari-

ables: 1) the duration of the growing season, determined by air temperature in spring (for leaf expansion) and light in fall (leaf senescence); 2) air temperature in summer; 3) the duration and frequency of drought events; 4) cloud cover; and 5) snow cover thickness during winter (protecting soil from deep freezing). In the Goulden et al. (1996) study, the annual carbon budget has shown to be more sensible to climatic conditions during certain critical periods (e.g., during budding) than to mean annual values of temperature or precipitation.

Generalizing the effects of climatic factors on NEE is quite complex, since different stands respond differently to the same climatic event. This complexity is illustrated by the contrasting impact of a warm spring on annual NEE of stands of differing species composition and climatic regime (Arain et al. 2002; Barr et al. 2002). A warm spring initially enhanced NEE in both an aspen (*Populus tremuloides*) and a black spruce (*Picea mariana*) forests of the BOREAS study sites, but subsequent high mid summer temperatures resulted in reduced annual carbon sequestration at the black spruce stand, due to higher ecosystem respiration, whereas that of the aspen stand increased (Arain et al. 2002). In a temperate deciduous forest, whose age, height and leaf area indices are comparable to the boreal aspen stand, the earlier warm spring also caused early leafout but resulted, unlike the aspen stand, in a reduced annual NEE. The reduced NEE at the temperate deciduous forest was caused by increased soil temperature and drought stress in mid-summer, which promoted ecosystem respiration and reduced photosynthesis (Barr et al. 2002).

Scientists do not agree on the relative importance of the preceding climatic factors on NEE. Valentini et al. (2000), who reported an increase in ecosystem respiration with latitude across European flux tower sites, with no concurrent change in gross ecosystem production, concluded that respiration, and by extension the factors controlling it, was the main determinant of forest carbon balance. Others, supporting Valentini et al., observed that inter-annual changes in temperature and ecosystem respiration exceeded those in photosynthesis, resulting in respiration controlling NEE year to year (Lee et al. 1999; Pilegaard et al. 2001; Arain et al. 2002). However, a reinterpretation of Valentini et al.'s results shows quite the reverse, that is an intimate coupling between ecosystem respiration and production, suggesting that changes in production will likely limit soil respiration (Jarvis et al. 2001; Janssens et al. 2001). Besides, other studies suggest that soil respiration would be stimulated only temporarily by higher temperatures, as it would rapidly become substrate limited (Giardina et Ryan 2000; Jarvis et Linder 2000). Results from Goulden et al. (1996) and Barford et al. (2001) suggest that factors affecting GEP, such as the length of the growing season, are more important in determining annual NEE.

Stand age is critical to understanding the carbon balance of northern forests on a regional basis (Fyles et al. 2002). Some authors have reported a change in NEE with stand age (Arneth et al. 1998; Schulze et al. 2000; Law et al. 2001; Litvak et al. 2003). The pattern observed by these authors is a carbon loss in young stands (NEP > 0), a maximum carbon sequestration rate in mid-age stands (NEP < 0), and a state of equilibrium with atmospheric CO_2 in mature stands (NEP ~ 0). However, Knohl et al. (2003) reported a large C uptake for a mature beech stand in Germany (-4942 $mgCO_2 \cdot m^{-2} \cdot d^{-1}$). Moreover, stand age in Table 4.1 does not seem to correlate with measured NEE as a whole.

Disturbance types (fire, insect defoliation, windthrow, permafrost collapse), frequency and extent have a strong impact on large-scale carbon dynamics of northern forests, through their influence on age-class structure and species composition (Bardford et al. 2001; Fyles et al. 2002). Over wide areas, disturbances (especially fire) can result in large short and long-term emissions (Amiro et al. 2001; Kasischke and Bruhwiler 2003). For example, large-scale increases in fire and insect outbursts since the 1980s in Canada have greatly reduced the carbon uptake by this forest (Kurz and Apps 1999; Chen et al. 2003). Disturbances should be taken into account to really assess the long-term carbon storage of an ecosytem or net biome production (NEP minus disturbance loss) at large scale (Schulze and Heimann 1998). Under conditions of a changing climate predicted by the IPCC (2001), natural disturbances are expected to increase in frequency and extent (Fyles et al. 2002).

4.3 Net Ecosystem Exchange of CO_2 in Wetlands

Data on NEE in wetlands comes mainly from northern peatlands. Peatlands can be distinguished from swamps and marshes by the accumulation of a deep layer (> 30 cm, Gorham 1991) of organic carbon as peat, whose organic carbon content is higher than 40%. Moreover, while swamps are seasonally flooded, most peatlands are permanently wet (Keddy 2000).

In wetlands, the decomposition of organic matter in water-saturated soils follows an anaerobic pathway, which leads to both CH_4 and CO_2 production. Therefore, the net CO_2 flux in wetlands does not represent the balance between gross photosynthesis and ecosystem respiration. For that matter, both CO_2 and CH_4 fluxes must be taken into account when assessing the carbon budget of these systems.

NEE in Peatlands

According to compiled NEE data (Table 4.2), northern peatlands can be either CO_2 sinks (e.g., -350 $mgCO_2 \cdot m^{-2} \cdot d^{-1}$ in Thompson, Manitoba or -2750 $mgCO_2 \cdot m^{-2} \cdot d^{-1}$ in Alberta) or sources (e.g., 491 $mgCO_2 \cdot m^{-2} \cdot d^{-1}$ in Schefferville, Quebec or 2400 $mgCO_2 \cdot m^{-2} \cdot d^{-1}$ in New Hampshire). On average, however, northern peatlands are a net sink for atmospheric CO_2 (-410 $mgCO_2 \cdot m^{-2} \cdot d^{-1}$, n = 13).

Spatial Heterogeneity of NEE in Peatlands

Net CO_2 fluxes can differ largely (direction and magnitude) within a peatland (Bubier et al. 2003), reflecting the spatial heterogeneity of environmental conditions within these systems. This heterogeneity is due notably to the variable microtopography of peatlands, which is characterized by the presence of hummocks, depressions, pools, laggs, strings, ridges and other structuring components (Keddy 2000; Payette and Rochefort 2001). Several authors have measured somewhat different fluxes with changes in microtopography. Hamilton et al. (1994), for example, measured an outgassing of CO_2 in pools along with an uptake of CO_2 by adjacent vegetated areas, with both fluxes being of comparable magnitude but in reverse direction. Waddington and Roulet (2000) also observed that ridges remained dry and were systematically behaving as CO_2 sinks, whereas pools constantly emitted large amounts of CO_2. The net CO_2 efflux measured at a raised open bog in the Hudson Bay Lowlands (216 $mgCO_2 \cdot m^{-2} \cdot d^{-1}$) could be due to the chamber method's inability to integrate the spatial variability of peatlands, because of the chamber's small area (about 1 m^2). In fact, the same site at the same period, but investigated at a larger scale (1 km^2) with a flux tower, was found to be a rather important CO_2 sink (-1700 $mgCO_2 \cdot m^{-2} \cdot d^{-1}$) (Table 4.2).

Temporal Variability of NEE in Peatlands

Peatlands can change from CO_2 source to sink from one year to another, with varying climatic conditions. For example, Shurpali et al. (1995) observed a CO_2 loss (900 $mgCO_2 \cdot m^{-2} \cdot d^{-1}$) in a bog during a year characterized by drought conditions and a CO_2 gain (-400 $mgCO_2 \cdot m^{-2} \cdot d^{-1}$) the following year with wetter conditions. A deeper water table during dry conditions led to increased peat aeration and CO_2 production, whereas moist conditions would have promoted photosynthesis by sphagnum mosses and CO_2 uptake. A correlation between CO_2 fluxes and water level depth has been reported by several authors (Carroll and Crill 1997; Alm et al. 1999a; Lafleur et al. 2001; Bubier et al. 2003), but was not observed experimentally by Updegraff et al. (2001).

Table 4.2. Net ecosystem exchange of CO_2 ($mgCO_2 \cdot m^{-2} \cdot d^{-1}$) in peatlands, marshes and swamps of different climatic regions

Country	Site	Lat.	Long.	Site description	Season[a]	Year	Mean	Min.	Max.	Method[b]	M[c]	J[d]	Reference(s)
							[$mgCO_2 \cdot m^{-2} \cdot d^{-1}$]						
BOREAL REGION (n = 10)													
Sweden	Stor-Amyran	64°N	20°E	Eccentric bog	G	1992-93	-111	-315	92	DC + SC (0.1 h)	50	~8	Waddington and Roulet (2000)
Canada	Churchill, MA	59°N	94°W	Non patterned bog	S	1993-94, 1996-99	-900	-3100	1100	FG		75	Griffis et al. (2000)
Canada	Schefferville, QC	56°N	67°W	Fen	S	1984	491			SC (24 h)	16	5	Moore and Knowles (1987)
Canada	Thompson, MA	56°N	98°W	Fen	G	1994, 1996	-350	-1000	300	EC		124	Lafleur et al. (1997); Joiner et al. (1999)
Canada	Kinosheo Lake, HBL ON	52°N	82°W	Raised open bog	S	1990	-1700			EC		33	Neumann et al. (1994)
Canada	Kinosheo Lake, HBL ON	52°N	82°W	Raised open bog	S	1990	216			SC	6	3	Whiting (1994)
Canada	Hudson Bay Lowlands, ON	52°N	81°W	Interior fen	S	1990	502			SC	4	3	Whiting (1994)
Canada	Hudson Bay Lowlands, ON	51°N	81°W	Coastal fen	S	1990	-143			SC	4	3	Whiting (1994)
Canada	Alberta	54°N	113°W	Carex-dominated fen	G + W	1994-96	-2750	-4200	-1400	DC	6	~13	Whiting and Chanton (2001)
Canada	Prince Albert, SK	53°N	105°W	Patterned fen	G	1994	-2700			EC		136	Suyker et al. (1997)
						Average	-744	-4200	1100				
TEMPERATE REGION (n = 3)													
Canada	Mer bleue, ON	45°N	76°W	Slightly raised bog, fen and wetlands	Y	1998-2001	-540	-693	-100	EC			Lafleur et al. (2003)
USA	Sallie's Fen, NH	43 N	71°W	Poor fen	G + W	1994	2400			DC	9		Carroll and Crill (1997)
USA	Bog Lake Peatland, MN	48°N	93°W	Open bog	G	1991-92	250	-400	900	EC + DC			Shurpali et al. (1995)
						Average	703	-693	900				

Table 4.2. (cont.)

Country	Site	Lat.	Long.	Site description	Season[a]	Year	Mean	Min.	Max.	Method[b]	M[c]	J[d]	Reference(s)
							[$mgCO_2 \cdot m^{-2} \cdot d^{-1}$]						
SUBTROPICAL/TROPICAL REGION (n = 5)													
USA	Virginia	37°N	76°W	Cattail marsh	Y	1992	-9005			DC	4	~10	Whiting and Chanton (2001)
USA	Virginia	37°N	76°W	Arrow arum marsh	Y	1992	-11634			DC	3	~10	Whiting and Chanton (2001)
USA	Florida	30°N	84°W	Cattail marsh	Y	1992-93	-10633	-11500	-9800	DC	2	~24	Whiting and Chanton (2001)
USA	Gainesville, FL	29°N	82°W	Cypress swamp	Y	1996-97	-609	-800	-400	EC			Clark et al. (1999)
Brazil	Amazonia	~3°S		Varzea	Flood	1985	3443			SC (0.3 h)	9		Devol et al. (1988)
						Average	-5688	-11500	-400				

[a]: *G*: growing season; *S*: summer; *W*: winter; *Y*: yearlong.
[b]: *DC*: dynamic chamber method; *EC*: eddy-covariance method; *FG*: flux-gradient method; *SC*: static chamber method (length of measurement); *SGP*: soil-gas profile.
[c]: Number of sites or subsites sampled.
[d]: Number of days studied.

The climatic sensitivity of the processes governing CO_2 fluxes (photosynthesis and respiration) also induces daily (Nykänen et al. 1995) and seasonal (Lafleur et al. 2001) NEE variations. Some studies have considered the daily CO_2 flux variations in their annual NEE estimate (e.g., Waddington and Roulet 2000), but Griffis et al. (2000) and Lafleur et al. (2001) are the only ones who, to our knowledge, conducted NEE measurements in peatlands over a whole year. Half the data in Table 4.2 was obtained over a complete or partial growing season, although CO_2 fluxes in winter can contribute up to 30% of the annual NEE (Alm et al. 1999a; Roehm and Roulet 2003; Lafleur et al. 2003).

Factors Governing NEE in Wetlands

As in forests, climatic conditions govern NEE in wetlands. Those controlling water level depths, such as air temperature and precipitation, are especially important. The length of the growing season (Griffis et al. 2000), cloud cover (Lafleur et al. 2001), peat temperature (Silvola et al. 1996; Updegraff et al. 2001) and species composition (differing between fens and bogs) (Bubier et al. 2003) also influence NEE.

NEE in Marsh and Swamp

The only two NEE estimates for tropical swamps show completely different behaviors (Table 4.2). On one hand, the cypress swamp in Florida is, on an annual basis, an important CO_2 sink (-609 $mgCO_2 \cdot m^{-2} \cdot d^{-1}$), whereas, on the other hand, the seasonally flooded forest of the Amazon Basin (or *varzéas*), emits large amounts of CO_2 (3443 $mgCO_2 \cdot m^{-2} \cdot d^{-1}$). The Amazon River, which is already oversaturated with CO_2 (Richey et al. 2002), flows through the *varzéas*, itself contributing CO_2 through the oxidation of the methane it produces.

Marshes differ clearly from peatlands with their high CO_2 uptake, ranging between -11633 and -9005 $mgCO_2 \cdot m^{-2} \cdot d^{-1}$, which reflect their relatively high productivity (Bradbury and Grace 1983).

4.4 CH_4 Fluxes in Wetlands

The emission or uptake of methane by a natural system depends on the balance between CH_4 production and oxidation, and the transport mode of CH_4 from the deep anoxic layer to the atmosphere (Fiedler and Sommer 2000). In the absence of oxygen, methanogenic bacteria produce CH_4 by acetate fermentation or CO_2 reduction (Schlesinger 1997). Part of the CH_4

produced in the anoxic zone can be oxidized by methanotrophic bacteria when it transits upwards through the upper oxygenated layer in contact with the atmosphere. An important quantity of the CH_4 produced in lakes, peatlands and rice fields would be oxidized before even reaching the atmosphere (Happell and Chanton 1993).

The transport mode of CH_4 influences the CH_4 flux as it determines the amount of CH_4 that will be oxidized. The transport of CH_4 through the soil matrix can be made by diffusion, bubbling (Wassmann et al. 1992) or through plant aerenchyma [e.g. *Carex sp.* (Whiting et al. 1991), *Phragmites sp.* (Kim et al. 1998) and black alder (Rusch and Rennenberg 1998)]. The CH_4 emitted by bubbling or transported through plant aerenchyma avoids the oxidative zone, contrary to the CH_4 transported by diffusion, and results in greater CH_4 emission. In wetlands of the Amazon Basin, bubbling can account for up to 80% of the CH_4 emitted, especially in shallow-water areas (Wassmann et al. 1992). Moreover, up to 91% of the CH_4 produced can bypass the oxidative zone in systems where *Carex sp.* are present (Whiting et al. 1991).

Wetlands have a strong propensity to emit CH_4 because of their water-saturated soils. CH_4 fluxes in wetlands are analyzed separately for peatlands, marshes and swamps, which differ in their productivity level and their water-saturation degree, two variables having the potential to influence CH_4 fluxes.

Main Factors Controlling CH_4 Emission in Wetlands

The water-saturation degree has a deep influence on CH_4 fluxes in wetlands. In peatlands, water table depth, which varies from one peatland to another, as well as within the same peatland given changes in microtopography (e.g., between hummocks and depressions), explains a large part of the CH_4 flux variability. Water table level exercises a particularly strong influence on CH_4 fluxes in peatlands by delimiting both the extent of the CH_4 production zone and that of the oxydative layer (Roulet et al. 1992; Fiedler and Sommer 2000). Generally, wetter sites, such as depressions, tend to emit more CH_4 than drier ones, such as hummocks (Dise 1993). Several studies have established a correlation between CH_4 emissions and water table depth in peatlands (Roulet et al. 1992; Roulet et Moore 1995; Bellisario et al. 1999). As well, a reduction in CH_4 emissions in peatlands drained for forestry is often observed (Roulet and Moore 1995; Nykänen et al. 1998; Minkkinen 1999). However, such a relationship can be difficult to establish (e.g., Rask et al. 2002). CH_4 fluxes in swamps are also sensitive to the soil water-saturation level, which can either vary spatially along a slope gradient or temporally based on water table level fluctuations or

hydrological cycles (flooding versus low water periods) (Bartlett et al. 1990; Tathy et al. 1992; Pulliam 1993).

The productivity level, determining the input of organic matter to methanogenic bacteria, directly influences CH_4 production rates. Accordingly, many authors have found a correlation between CH_4 flux and net primary production (Aselmann and Crutzen 1989), net ecosystem production (Whiting and Chanton 1993), net ecosystem CO_2 exchange (Alm et al. 1997; Waddington et al. 1996) and plant biomass (Bellisario et al. 1999). Rask et al. (2002) also reported a positive relationship between CH_4 flux and phosphorus concentration in the interstitial water. Organic matter biodegradability is also important for CH_4 production, and will depend on the vegetation's species composition (Fiedler and Sommer 2000). For example, certain plant species, such as Sphagnum mosses, which dominate in Northern peatlands, produce a carbon particularly resistant to bacterial decomposition, compared to Cyperaceae (e.g. *Carex sp., Eriophorum sp.*) for example.

Methanogenesis, as well as all bacteria-mediated reactions, is controlled by temperature. A relationship between CH_4 flux and temperature in peatlands is generally observed (Moore and Knowles 1987; Roulet et al. 1992; Frolking and Crill 1994; Saarnio et al. 1997; Nykänen et al. 1998; Bellisario et al. 1999; Rask et al. 2002).

CH_4 Fluxes in Peatlands

Vourlitis and Oechel (1997) have already reviewed CH_4 fluxes in northern peatlands and the tundra published before 1995. This section adds more recent data to Vourlitis and Oechel's review, while maintaining their peatland classification system. This classification allows different peatland comparisons based on their productivity level (bog versus fen), their water-saturation degree (forested versus open peatlands) and their climate (boreal, temperate and tropical region). For tropical peatlands, data is fairly scarce due to the lack of studies undertaken in these regions.

Peatlands clearly contribute to CH_4 emission to the atmosphere. Most mean CH_4 flux values in peatlands range between 0 and 100 $mgCH_4 \cdot m^{-2} \cdot d^{-1}$, with some peatlands characterized by very high CH_4 emission (e.g., 153 $mgCH_4 \cdot m^{-2} \cdot d^{-1}$ for a sedge fen in Alberta, 199 $mgCH_4 \cdot m^{-2} \cdot d^{-1}$ for bogs and 349 $mgCH_4 \cdot m^{-2} \cdot d^{-1}$ for fens at the Marcell Experimental Forest in Minnesota, Table 4.3). Two of the CH_4 flux values among the highest (271 and 509 $mgCH_4 \cdot m^{-2} \cdot d^{-1}$) are from Russian bogs (Panikov and Zelenev 1991; Panikov and Dedysh 2000) and seems to be aberrant when compared to the mean CH_4 fluxes of peatlands in the same category (31 $mgCH_4 \cdot m^{-2} \cdot d^{-1}$) (Table 4.3).

Table 4.3a. Methane fluxes ($mgCH_4 \cdot m^{-2} \cdot d^{-1}$) in boreal peatlands

Country	Region	Lat.	Long.	Description	Season[a]	Year	Mean	Min	Max	SD	Method[b]	M[c]	J[d]	Reference(s)
							[$mgCH_4 \cdot m^{-2} \cdot d^{-1}$]							
FORESTED BOG (n = 15)														
Finland	Ilomantsi	63°N	31°E	Pine bog (I6)	Y[e]		15.8							Nykänen et al. (1996)
Finland	Lakkasuo	62°N	24°E	Cottongrass pine bog with hummocks (L8)	Y[e]		19.1							Nykänen et al. (1996)
Canada	HBL, MB	59°N	94°W	Treed bog	G	1990	0.2	-1	6.1	13	SC (0.5 h) + SGP			Roulet et al. (1994)
Russia	Tver, East Siberia			Treed bog (Tver site 8, Komi site 9)	Y	1990	13.9			35	C	2		Panikov and Zelenev (1991)[g]
Canada	Thompson, MB	56°N	98°W	Lowland forests (Spruce 1, 3, 4, Palsa, Aspen 2, Pine 2)	G	1994	-0.6				SC (0.5 h)	6	12	Savage et al. (1997)
Canada	HBL, ON	52°N	81°W	Treed bog	G	1990	1.8	-1.7	65.7	9	SC (0.5 h) + SGP			Roulet et al. (1994)
Canada	HBL, ON	52°N	81°W	Lowland mixed forest	G	1990	3.3	-2.2	49.7	11	SC (1.3 h)	12		Roulet et al. (1994)
Canada	Kinosheo Lake, ON	52°N	81°W	Forested bog	S	1990	14.5			8	EC	1		Edwards et al. (1994)[g]
Canada				Treed bog (sites 9, 14)	G	1991	5.1			2	C	2		Bubier et al. (1993)[g]
Canada				Treed bog (sites K1-K3)	S	1990	4.3			17	C	3		Klinger et al. (1994)[g]
Canada				Treed bog (sites 31, 33, 34)	G	1990	47.3			70	C	3		Moore et al. (1994)[g]
Canada	Cochrane, ON	49°N	81°W	Lowland spruce forest (site 1)	S	1992	-0.02	-0.4	0.3		SC (3 h)	1	>6	Schiller and Hastie (1996)
Canada	Cochrane, ON	49°N	81°W	Forested bog	G	1991	3.8				SC (2 h)	1	~18	Roulet and Moore (1995)
Canada	Cochrane, ON	49°N	81°W	Treed bog	G	1991	0.3				SC (2 h)	1	~18	Roulet and Moore (1995)
Canada	ON	45°N	79°W	Treed bog (B-T)	G	1990	5.8	-0.1	107	17	SC (20 h)	1	~15	Roulet et al. (1992)
					Average		8.9 (-0.6 to 47.3)							
FORESTED FEN (n = 10)														
Finland	Salmisuo	63°N	31°E	Pine fen with sphagnum cover (centre, lagg)	Y[e]		103				SC (1 h)	1		Alm et al. (1999a); Saarnio et al. (1997)
Russia	Tver, East Siberia			Treed fen (Tver sites 6, 7)	Y	1991	0.8			1	C	2		Panikov and Zelenev (1991)[g]
Canada	Schefferville, QC	55°N	67°W	Fen treed lagg (sites T1, T4, T5, T8, T11, T19)	G	1989	28.0				SC (24 h)	6	~9	Moore et al. (1990)
Canada	HBL, Moosonee, ON	52°N	81°W	Shrub-rich fen	G	1990	2.5	-2.4	32.0	5	SC (0.5 h) + SGP			Roulet et al. (1994)
Canada				Treed fen (site 4)	G	1991	21.3			36	C			Bubier et al. (1993)[g]
Canada				Treed fen (sites 6, 16, 10-15)	G	1990	6.3			6	C	7		Moore et al. (1994)[g]
Canada	Cochrane, ON	49°N	81°W	Treed fen	G	1991	6.6				SC (2 h)	1	~18	Roulet and Moore (1995)
Canada	ON	45°N	79°W	Conifer swamp (depression, hummock, lagg, interior)	G	1990	1.9	-0.2	236		SC (20 h)	4	~15	Roulet et al. (1992)
Canada	ON	45°N	79°W	Peaty swamp	G	1990	0.7	-5.8	27.6		SC (20 h)	2	~15	Roulet et al. (1992)

Table 4.3a. (cont.)

Country	Region	Lat.	Long.	Description	Season[a]	Year	Mean	Min	Max	SD	Method[b]	M[c]	J[d]	Reference(s)
							[$mgCH_4 \cdot m^{-2} \cdot d^{-1}$]							
FORESTED FEN (n = 10) (cont.)														
Canada	ON	45°N	79°W	Thicket swamp (depression, hummock)	G	1990	34.9	-0.3	305		SC (20 h)	2	~15	Roulet et al. (1992)
					Average		20.6 (0.7 to 103)							
OPEN BOG (n = 13)														
Finland	Ilomantsi	66°N	31°E	Open bog (Ahvensalo (I1))	Y[e]		13.1							Alm et al. (1999a, 1999b)
Finland							21.9							Nykänen et al. (1998)
Sweden	Umea	64°N	20°E	Eccentric bog (Stor-Amyran)	G	1992-93	28.8				SC (2 h)			Waddington and Roulet (2000)
Russia	Southwest Siberia			Vasyugan bog			29-42				C			Panikov et al. (1995)
Russia	West Siberia	57°N	82°E	Bakchar Bog	W	1995	5			4	SC (1.5 h)	5		Panikov and Dedysh (2000)
Russia	West Siberia	57°N	82°E	Bakchar Bog	S	1993-97	271				SC (1.5 h)	5		Panikov and Dedysh (2000)
Russia	Tver, East Siberia			Open bog (Tver sites 2-5)	Y	1990	509			885	C	4		Panikov and Zelenev (1991)[g]
Canada	HBL, Moosonee, ON	51°N	81°W	Open bog	G	1990	53.5	-1.7	1356	152	SC (0.5 h) + SGP			Roulet et al. (1994)
Canada	HBL, Moosonee, ON	51°N	81°W	Shrub-rich bog	G	1990	47.5	-1.5	1627	154	SC (0.5 h) + SGP			Roulet et al. (1994)
Canada				Sites 1, 7, 15	G	1991	26.1			36	C	3		Bubier et al. (1993)[g]
Canada				C1, C2, K4	S	1990	54.3			86	C	3		Klinger et al. (1994)[g]
Canada				Sites 24, 25, 36-39	G	1990	34.7			40	C	6		Moore et al. (1994)[g]
Canada	ON	45°'N	79°W	Bog (B-O)	G	1990	20.6	-0.1	140.2	28	SC (20 h)	1	~15	Roulet et al. (1992)
					Average		31 (5 to 54.3)[f]							
OPEN FEN (n = 19)														
	Scandinavia							-2	388					Granberg et al. (1997)
Finland							52.1							Nykänen et al. (1998)
Finland	Ilomantsi	63°N	31°E		Y	1991-92	74.5[h]				SC + DC		~16	Nykänen et al. (1995)
Finland	Lakkasuo	62°N	24°E	Tall sedge fen (L19)	Y[e]		118.6							Alm et al. (1999a); Nykänen et al. (1996)
Canada	HBL, MB	59°N	94°W	Open fen	G	1990	78.6	-0.6	1585	243	SC (0.5 h) + SGP			Roulet et al. (1994)
Canada	Schefferville, QC	56°N	67°W	Fen (sites 1-4)	S	1984	30.9	0	112.3	20	SC	4	5	Moore and Knowles (1987)

Table 4.3a. (cont.)

Country	Region	Lat.	Long.	Description	Season[1]	Year	Mean	Min	Max	SD	Method[2]	M[3]	J[4]	Reference(s)
							[$mgCH_4 \cdot m^{-2} \cdot d^{-1}$]							
OPEN FEN (n = 19) (cont.)														
Canada	MA							13	112.3		C			Bellisario et al. (1996)
Canada	Central Alberta				G		24	0	1520		C			Vitt et al. (1990)
Canada	AL	54°N	113°W	Sedge fen	G, W	1994-96	153.4				SC	1	~42	Whiting and Chanton (2001)
Canada	Schefferville, QC	55°N	67°W	Open fen	S	1990	49.4				EC	1		Moore et al. (1994)[g]
Canada	Schefferville, QC	55°N	67°W	Poor nutrient fen (sites T2, 9, 25, C-M, T10, 13, 15, C-C, T3, 7, 12, C-F)	G	1989	59.7				SC	4	~9	Moore et al. (1990)
Canada	Schefferville, QC	55°N	67°W	Patterned fen (Sites T6, 16, PS, T20, PP)	G	1989	34.7				SC	3	~8	Moore et al. (1990)
Canada	SK	54°N	105°W	Ribbed fen (edge, shallow bay, deep bay, string, flark)	G	1994. 95	121.8				SC	1	~33	Rask et al. (2002)
Canada							194.4				EC	1		Suyker et al. (1996)
Canada	HBL, Moosonee, ON	52°N	81°W	Open fen	G	1990	7.9	-1.6	297.5	19	SC (0.5 h) + SGP			Roulet et al. (1994)
Canada				Sites 3, 5, 6, 13	G	1991	27.6			19	C	4		Bubier et al. (1993)[g]
Canada				CF, IF, MF	S	1990	14.8			20	C	3		Klinger et al. (1994)[g]
Canada				Sites 7-9, 17-22, 26-30	G	1990	18.1			15	C	14		Moore et al. (1994)[g]
Canada	ON	45°N	79°W	Fen with shrub and grass cover (F-O)	G	1990	3	-0.2	78.3	12	SC	1	~15	Roulet et al. (1992)
					Average		62 (3 to 194)							

[a]: *G*: growing season; *S*: summer; *Y*: yearlong.
[b]: *DC*: dynamic chamber method; *EC*: eddy-covariance method; *SC*: static chamber method (length of measurement); *SGP*: soil-gas profil.
[c]: Number of sites or subsites sampled.
[d]: Number of days studied.
[e]: Calculated from Alm et al. (1999) data.
[f]: Calculated without the following values: 271 and 509 mg $CH_4 \cdot m^{-2} \cdot d^{-1}$.
[g]: Cited in Vourlitis and Oechel (1997).
[h]: Measured without vegetation and litter.

Table 4.3b. Methane fluxes in peatlands of temperate and tropical regions

Country	Region	Lat.	Long.	Description	Season[a]	Year	Mean	Min	Max	SD	Method[b]	M[c]	J[d]	Reference (s)
							[$mgCH_4 \cdot m^{-2} \cdot d^{-1}$]							
TEMPERATE REGION														
FORESTED BOG (n = 2)														
USA	Marcell Exp. Forest, MN	48°N	98°W	Red Lake forested bogs, S1, S2	S	1986	89	11	694		SC + DC	4	12	Crill et al. (1988)
USA	Marcell Exp. Forest, MN	48°N	98°W	Forested bog (S2, hollow, hummock)	Y	1989	24	2	246		SC (0.3 h)	2	36	Dise (1993)
					Average		57 (24 to 89)							
FORESTED FEN (n = 2)														
USA	Marcell Exp. Forest, MN	48°N	98°W		S	1986	142	68	263	66	SC + DC	1	12	Crill et al. (1988)
Canada	Kejimkujik National Park, NS	44°N	65°W	Poor nutrient fen	G	1996-97	9.6				SC	18		Clair et al. (2002)
					Average		76 (9.6 to 142)							
OPEN BOG (n = 7)														
Germany				Moor				11	155					Pfeiffer (1994), cited in Boeckx and Van Cleemput (1997)
Germany	Allgau, Wangen	48°N	10°E	Peaty depression	Y	1997-1998	21	-5	208		SC (0.5 h)	4	104	Fiedler and Sommer (2000)
USA	Marcell Exp. Forest, MN	48°N	98°W	Red Lake open bogs, S4, Bena bog	S	1986	199	18	866		SC + DC	4	12	Crill et al. (1988)
USA	Marcell Exp. Forest, MN	48°N	98°W	Open bog (S4)	Y	1989	118	0	1056		SC (0.3 h)	2	34	Dise (1993)
USA	Marcell Exp. Forest, MN	48°N	98°W	Open bogs (WS-1, WS-2, WS-4)	S	1983	132	19	468		DC (0.3 h)	3	6	Harriss et al. (1985)
USA	Chippewa National Forest, MN			Bog Lake Peatland	S	1990	177			50	EC			Verma et al. (1992)
USA	Virginia (W.)	39°N		Mountain bog			251			292	SC + DC	14		Crill et al. (1988)
					Average		150 (21 to 251)							

Table 4.3b. (cont.)

Country	Region	Lat.	Long.	Description	Season[a]	Year	Mean	Min	Max	SD	Method[b]	M[c]	J[d]	Reference (s)
							[$mgCH_4 \cdot m^{-2} \cdot d^{-1}$]							
OPEN FEN (n = 6)														
Germany		48°N	11°E	Fen seasonnaly inundated (Murnauer Moos)	S	1996	130	40.8	214		EC		6	Kormann et al. (2001)
USA	Marcell Exp. Forest, MN	48°N	98°W	Red Lake open fens, Junction fen	S	1986	349	152	711		SC + DC	3	12	Crill et al. (1988)
USA	Marcell Exp. Forest, MN	48°N	98°W	Poor nutrient fen (Junction Fen)	Y	1989	180	11	767		SC (0.3 h)	1	37	Dise (1993)
USA	Marcell Exp. Forest, MN	48°N	98°W	Lagg fen of a forested peaty depression (S2)	Y	1989	35	-1	482		SC (0.3 h)	1	27	Dise (1993)
USA	Marcell Exp. Forest et Lake Itasca, MN	48°N	93-95°W	WS-3 and Shoreline Fen of Lake Itasca	S	1983	85	3	171		DC (0.3 h)	2		Harriss et al. (1985)
USA	Durham, NH	43°N	71°W	Poor nutrient fen	Y	1991-92	190				SC (0.3 h)	3	48	Frolking and Crill (1994)
					Average		161 (35 to 349)							
TROPICAL REGION (n = 3)														
USA	Okeefenokee swamp, GA	30°N		Peaty swamp			141			142	SC + DC	12		Crill (1988)
USA	Corkscrew swamp, FL	26°N		Peaty swamp			128			259	SC + DC	11		Crill (1988)
Malaysia		~5°N		Peaty soil			260							Inubushi (1993), cited in Rask et al. (2002)
					Average		176							

[a]: *G*: growing season; *S*: summer; *Y*: yearlong.
[b]: *DC*: dynamic chamber method ; *EC*: eddy-covariance method; *SC*: static chamber method (length of measurement); *SGP*: soil-gas profile.
[c]: Number of sites or subsites sampled.
[d]: Number of days studied.

Table 4.3c. Methane fluxes ($mgCH_4 \cdot m^{-2} \cdot d^{-1}$) in marshes and swamps

Country	Region	Lat.	Long.	Description	Season[a]	Year	Mean	Min	Max	SD	Method[b]	M[c]	J[d]	Reference(s)
							[$mgCH_4 \cdot m^{-2} \cdot d^{-1}$]							
MARSH/WET MEADOW														
BOREAL REGION (n = 1)														
Canada	ON	45°N	79°W	Open peaty marsh (M1, M2)	G	1990	0.9	-0.3	36		SC (20 h)	2	~15	Roulet et al. (1992)
TEMPERATE REGION (n = 6)														
Denmark		~56°N		Freshwater wetland				0.1	6					Prieme (1994), cited in Rask et al. (2002)
Belgium	Bourgoyen-Osssemeersen	51°N	4°E	Wet meadow	G	1994	20	0	102		SC (1 h)			Boeckx and Van Cleemput (1997)
Germany	Allgau, Aichstetten	48°N	10°E	Alluvial plain used for grazing (AE, ME sites)	Y	1997-98	2	-15	262		SC (0.5 h)	10	104	Fiedler and Sommer (2000)
Germany	Allgau, Artisberg	48°N	10°E	Colluvial pond margin (TH, FH sites)	Y	1997-98	127	0	6775		SC (0.5 h)	10	104	Fiedler and Sommer (2000)
USA	Virginia	37°N	76°W	Cattail marsh and arrow arum marsh	Y	1992-93	390				DC	2	35	Whiting et al. (2001)
USA	Newport News Swamp, VA	37°N		Arrow arum marsh and smartweed marsh	Y	1985	119	BDL[e]	469		SC + DC	2	26	Wilson et al. (1989)
					Average		132 (2 to 390)							
SUBTROPICAL REGION (n = 5)														
USA	FL	30°N	84°W	Cattail marsh	Y	1992-93	226				SC	1	48	Whiting and Chanton (2001)
USA	Okefenokee Swamp, GA	31°N		Wet meadow	Y		130	-7.9	1000					K.B. Bartlett et al. (unpubl. data 1989)[g]
USA	Everglades, FL	25°N		Sawgrass	W		69			81				Bartlett et al. (1989)[f]
USA	Everglades, FL	25°N		Wet meadow and sawgrass	W		61	BDL	624	77	DC (0.3 h)	8	15	Harriss et al. (1988)[g]
USA	Everglades, FL	25°N		Sawgrass	Y		107	9	2390			2	30	Burke et al. (1988)[g]
					Average		119 (61 to 226)							
SWAMP														
TEMPERATE REGION (n = 5)														
Austria	Vienna	~48°N		Klausenleopoldsdorf 2	G	1997	0.7			2	SC (4 h)	3	~16	Hahn et al. (2000)
USA	Newport News Swamp, VA	37°N	76°W	Swamp bank (dry site)	Y	1985	117	BDL	475		SC + DC	1		Wilson et al. (1989)
USA	Newport News Swamp, VA	37°N	76°W	Ash stand	Y	1985	152	BDL	1005		SC + DC	1		Wilson et al. (1989)

Table 4.3c. (cont.)

Country	Region	Lat.	Long.	Description	Season[a]	Year	Mean	Min	Max	SD	Method[b]	M[c]	J[d]	Reference(s)
							[$mgCH_4 \cdot m^{-2} \cdot d^{-1}$]							
TEMPERATE REGION (n = 5) (cont.)														
USA	Great Dismal Swamp, VA	~37°N			W		9.2			8				Harris et al. (1982)[f]
USA	Great Dismal Swamp, VA	~37°N			D		-3.0			2				Harris et al. (1982)[f]
					Average		55 (-3 to 152)							
TROPICAL/SUBTROPICAL REGION (n = 21)														
USA	Four Holes Swamp, SC	~33-26°N			W		10.1			7				Harriss and Sebacher (1981)[f]
USA	Ogeechee River, GA	~32°N		Flooded forest	W		13.6							Pulliam (1993)[f]
USA	Ogeechee River, GA	~32°N		Flooded forest	D		-2.2							Pulliam (1993)[f]
USA	Okefenokee Swamp, GA	31°N			W		92			142				Harriss and Sebacher (1981)[f]
USA	Okefenokee Swamp, GA	31°N		Shrubby swamp	Y		149	-7.5	1250					K.B. Bartlett et al. (unpubl. data 1989)[g]
USA	Okefenokee Swamp, GA	31°N		Cypress and gum-tree swamp	Y		55	-10	442					K.B. Bartlett et al. (unpubl. data 1989)[g]
USA	St. Marks National Wildlife Refuge, FL	~27°N		Swamp composed of red maple, black ash, black gum and cypress	W	1989, 90, 91	94.7			98	SC (0.5 h)		20	Happell and Chanton (1993)
USA		~27°N			D	1990	-0.7			0.2	SC (0.5 h)		6	Happell and Chanton (1993)
USA	Everglades, FL	25°N		Swampy forest	W	1980, 84, 85	59	-3	274	80	DC (0.25 h)	4		Harriss et al. (1988)[g]
Brazil	near Calado Lake	3°S	61°W	Varzea	D	1985	192	BDL	1224	256	DC			Bartlett et al. (1988
Congo	Mayombe	~4°S			W		190			163				Delmas et al. (1992)[f]
Congo	Mayombe	~4°S			D		-1.9			1.2				Delmas et al. (1992)[f]
Brazil	Amazonia	~3°S		Varzea	W	1987	126	BDL	840	152	DC			Bartlett et al. (1990)
Brazil	Amazonia	~3°S		Varzea	D	1985	75	0.8	505	135	SC (0.3 h)			Devol et al. (1988)

Table 4.3c. (cont.)

Country	Region	Lat.	Long.	Description	Season[a]	Year	Mean	Min	Max	SD	Method[b]	M[c]	J[d]	Reference(s)
							[$mgCH_4 \cdot m^{-2} \cdot d^{-1}$]							
TROPICAL/SUBTROPICAL REGION (n = 21) (cont.)														
Brazil	Vargem Grande and Obidos	~3°S		Recently wet, but not flooded, forest soil	D	1985	14	-12	145	36	SC (0.3 h)			Devol et al. (1988)
Brazil	Manaus	~3°S		Varzea	W	1988	76				DC			Wassmann et al. (1992)
	Congo River basin	~0°		Permanently inundated forest (inundated soil)			105	10	549		SC (0.3 h)			Tathy et al. (1992)
	Congo River basin	~0°		Permanently inundated forest (wet soil)			4.9	1.1	8		SC (0.3 h)			Tathy et al. (1992)
	Congo River basin	~0°		Permanently inundated forest (dry soil)			-1.9	-4.6	-1		SC (0.3 h)			Tathy et al. (1992)
Ecuador	Campana Cocha	1°S	78°W	Virgin forest on Napo River banks	D	1984	0.6	-0.6	3		SC (0.5 h)			Keller et al. (1986)
Ecuador	Campana Cocha	1°S	78°W	Secondary forest on Napo River banks	D	1984	-0.8	-0.6	8		SC (0.5 h)			Keller et al. (1986)
					Average		60 (-2 to 192)							

[a]: *D*: dry season; *G*: growing season; *W*: wet sites or rainy season; *Y*: yearlong.
[b]: *DC*: dynamic chamber method; *SC*: static chamber method (length of measurement).
[c]: Number of sites or subsites sampled.
[d]: Number of days studied.
[e]: BDL: Below detection level.
[f]: Cited in Bartlett and Harriss (1993).
[g]: Cited in Bartlett et al. (1990).

CH_4 fluxes in peatlands are highly variable. In general, mean fluxes vary along one to two orders of magnitude within each peatland category, with the largest variation range observed in boreal open bogs, even when excluding seemingly aberrant fluxes from Russian bogs (271 and 509 $mgCH_4 \cdot m^{-2} \cdot d^{-1}$) (Table 4.3). Within the same peatland, CH_4 fluxes can easily vary along three orders of magnitude (Mosier 1990). The CH_4 emission rate within a peatland can reach between 107 and 1627 $mgCH_4 \cdot m^{-2} \cdot d^{-1}$ depending on the site. CH_4 uptake can occasionally be measured at some sites within a peatland, generally at elevated ones (e.g., hummocks), but rates are relatively low, varying between -5.8 and -0.1 $mgCH_4 \cdot m^{-2} \cdot d^{-1}$ (Table 4.3). The important variability of CH_4 fluxes measured within and between peatlands reflects the structural heterogeneity of these systems.

Relationship between CH_4 Flux, Peatland Type and Climatic Region

It is possible to indirectly emphasize the effect of productivity level, water table depth and temperature on CH_4 fluxes by means of a multiple regression comparing CH_4 fluxes (log-transformed) by peatland category (bog, -1; fen, +1, forested, -1; open, +1) and climatic region (boreal: 1, temperate: 2; tropical: 3). Such an analysis indicates that CH_4 fluxes are significantly higher in open peatlands, which are generally characterized by a water table close to the surface, compared to fluxes in forested peatlands, which usually have a deeper water table ($p < 0.001$). What's more, CH_4 emissions by unit area increase from north to south ($p < 0.001$), which is most likely related to the increase in temperature. These two variables explain more than half of the total data set variation ($r^2 = 58\%$). The observed differences in CH_4 fluxes with climatic regions remain when excluding data from the tropical region, which, because they are particularly high, could have alone been responsible for the observed relationship. Compared to bogs, fens are known to be more productive and to have higher water tables and pH, all of which promote CH_4 production (Keddy 2000). Although mean CH_4 fluxes seem to be higher in fens, no significant difference in CH_4 fluxes could be detected between these two peatland types.

Temporal Variability of CH_4 Fluxes in Peatlands

Most of the studies compiled in this chapter have evaluated CH_4 fluxes over a growing season or during summer. Very few studies have measured CH_4 over a complete year. Yet, winter has the potential to contribute significantly to the annual CH_4 emission. Winter contribution to the annual CH_4 budget was estimated to be 20% in Finland (Alm et al. 1999), more

than 20% in New Hampshire (Frolking and Crill 1994) and between 8 and 21%, varying along peatland types, in Minnesota (Dise 1993). However, CH_4 emissions in winter represented only 2 to 9% (averages for 1990 to 1995) of the CH_4 annual emission in a low productive fen of the temperate region (Melloh and Crill 1996). Finally, contrary to NEE, there are few long-term studies of CH_4 fluxes in peatlands, that could actually allow to portray the inter-annual variability of CH_4 emissions in these systems.

CH_4 Fluxes in Marshes and Swamps

Peatlands are concentrated in northern latitudes, whereas marshes and swamps dominate in the tropical region. As can be seen in Table 4.3, tropical wetlands, especially seasonally flooded forests of the Amazon Basin (*varzéas*), emit large amounts of CH_4 into the atmosphere compared to northern peatlands (Table 4.3). As in peatlands, CH_4 fluxes in marshes and swamps are very variable, ranging over more than two orders of magnitude (Table 4.3). The great variability of CH_4 fluxes measured in swamps (-3 to 192 $mgCH_4 \cdot m^{-2} \cdot d^{-1}$, Table 4.3) can be partly explained by the importance of bubbling, a CH_4 transport mechanism, which is an unpredictable and irregular processes (Crill 1988). In the Amazon basin, where half of the CH_4 measured in swamps comes from, up to 80% of it can be released through bubbling (Wassmann et al. 1992).

4.5 CH_4 Fluxes in Forests

Forested soils are generally well oxygenated in their deeper parts and consequently offer a favorable medium for atmospheric CH_4 oxidation. Accordingly, most of the sites investigated in boreal, temperate and tropical forests consume CH_4 (Table 4.4). The CH_4 emission reported by certain authors in boreal and tropical forests occurred at sites with poorly drained soils (Keller et al. 1986; Simpson et al. 1997). It should be noted that relatively weak positive CH_4 fluxes have been measured in black spruce stands (Table 4.3), but since these stands accumulate peat (> 30 cm), they were considered along with forested peatlands (Gorham 1991). Contrary to the other biomes, the temperate forest (-1.4 $mgCH_4 \cdot m^{-2} \cdot d^{-1}$), where no CH_4 emission was documented, seems to contribute more to atmospheric CH_4 oxidation than boreal (-0.39 $mgCH_4 \cdot m^{-2} \cdot d^{-1}$) and tropical (-0.30 $mgCH_4 \cdot m^{-2} \cdot d^{-1}$) forests, even though the ranges of CH_4 fluxes in these forests are generally similar from one to another (Table 4.4).

Table 4.4. Methane fluxes ($mgCH_4 \cdot m^{-2} \cdot d^{-1}$) of forest soils

Country	Region	Lat.	Long.	Forest type	Season[a]	Year	Mean [$mgCH_4 \cdot m^{-2} \cdot d^{-1}$]	Method[b]	M[c]	J[d]	Reference(s)
BOREAL FORESTS (n = 6)											
Canada	SK	54°N	106°W	Aspen stand	G	1994	1.36	FG + EC			Simpson et al. (1997)
Canada	MA	56°N	98°W	Deciduous forest	G	1994	-0.85	SC (0.5 h)	12	12	Savage et al. (1997)
Canada	MA	56°N	98°W	Recently burned site	G	1994	-1.80	SC	1	12	Savage et al. (1997)
Canada	MA	56°N	98°W	Black spruce stand	G	1994	-0.40	SC (0.5 h)	6	12	Savage et al. (1997)
Canada	MA	56°N	98°W	Jack pine stand	G	1994	-0.48	SC (0.5 h)	6	~20	Savage et al. (1997)
Canada	ON	49°N	81°W	Mixed upland forest	S	1992	-0.16	SC (3 h)	>6	>6	Schiller and Hastie (1996)
						Average	-0.39				
TEMPERATE FORESTS (n = 14)											
USA		44°N	72°W	Coniferous forest (15 $kgN \cdot ha \cdot yr^{-1}$)	G	1990	-1.31	SC (0.5 h)	18	6	Castro et al. (1993)
USA	ME	44°N	68°W	Coniferous forest (6 $kgN \cdot ha \cdot yr^{-1}$)	G	1990	-0.64	SC (0.5 h)	6	6	Castro et al. (1993)
USA	VT	43°N	72°W	Coniferous forest (0 $kgN \cdot ha \cdot yr^{-1}$)	G	1990	-1.06	SC (0.5 h)	6	6	Castro et al. (1993)
USA	MA	43°N	72°W	Deciduous forest	G	1988	-4.16	SC (0.5 h)	9	~10	Steudler et al. (1989)
USA	MA	43°N	72°W	Red pine plantation	G	1988	-3.52	SC (0.5 h)	9	~10	Steudler et al. (1989)
USA	NH	43°N	72°W	Mixed forest	Y	1989	-1.65	SC (0.3 h)	2	57	Crill (1991)
Austria	Vienna			Beech stand	G	1997	-0.38	SC (4 h)	8	~16	Hahn et al. (2000)
Ireland	Ballyhooly			Coniferous forest (low atm. N-input)	Nov.	1994	-1.34	SC (2 h)	2	2-3	Butterbach-Bahl et al. (1998)
Germany	Munich			Spruce stand (high atm. N-input)	G	93, 94, 95	-0.46	SC	5	1	Butterbach-Bahl et al. (1998)
	Darmstadt	50°N	9°E	Beech and oak forest	Y	1991	-1.75	SC (0.5 h)	1	43	Dong et al. (1998)
Scotland	Peebles			Coniferous plantation	Y	1995	-0.27	SC (1 h)	6	~12	MacDonald et al. (1997)
Spain	Malaga	37°N		Semiurban forest (ficus and eucalyptus)	Y	1992	-0.54	SGP (^{222}Rn)	1	32	Dueñas et al. (1999)
Spain	Malaga	37°N		Semiurban pine forest	Y	1992-93	-0.84	SGP (^{222}Rn)	1	31	Dueñas et al. (1999)

Table 4.4. (cont.)

Country	Region	Lat.	Long.	Forest type	Season[a]	Year	Mean [$mgCH_4 \cdot m^{-2} \cdot d^{-1}$]	Method[b]	M[c]	J[d]	Reference(s)
TEMPERATE FORESTS (n = 14) (cont.)											
Spain	Malaga	37°N		Semiurban bare soil	Y	1991-92	-0.12	SGP (^{222}Rn)	1	31	Dueñas et al. (1999)
						Average	-1.29				
TROPICAL FORESTS (n = 9)											
Puerto Rico		18°N	66°W	Tabonuco forest	D	1984	-0.57	SC (0.5 h)	18	1	Keller et al. (1986)
Puerto Rico		18°N	66°W	Mahogany plantation	D	1984	-0.28	SC (0.5 h)	10	1	Keller et al. (1986)
Puerto Rico		18°N	66°W	Sierra palm forest	D	1984	0.87	SC (0.5 h)	8	1	Keller et al. (1986)
Puerto Rico		18°N	66°W	Elfin cloud forest	D	1984	1.49	SC (0.5 h)	10	1	Keller et al. (1986)
Costa Rica		10°N	84°W	Rainforest	R	92, 93	-1.02	SC (0.5 h)	72	4	Reiners et al. (1986)
Costa Rica		10°N	84°W	Rainforest	Y	1991	-1.26	SC (0.5 h)	24	12	Keller and Reiners (1994)
Costa Rica		10°N	84°W	Secondary forest	Y	1991	-1.20	SC (0.5 h)	24	12	Keller and Reiners (1994)
Brazil	Manaus	~3°S		Terra firme forest	R	1983	0.02	SC (0.5 h)	7	1	Keller et al. (1986)
Brazil	Manaus	~3°S		Terra firme forest	D	1984	-0.71	SC (0.5 h)	9	1	Keller et al. (1986)
						Average	-0.30				
SAVANA (n= 1)											
Africa				Savana			-1.25	SC			Seiler et al. (1984), cited in Whalen et al. (1992)

[a]: *D*: dry season; *G*: growing season; *R*: rainy season; *Y*: yearlong.
[b]: *EC*: eddy-covariance method; *FG*: flux-gradient method; *SC*: static chamber method (length of measurement); *SGP*: soil-gas profile.
[c]: Number of sites or subsites sampled.
[d]: Number of days studied.

Factors Affecting CH_4 Uptake in Forest Soils

Soil texture and water content are two variables affecting CH_4 fluxes in forests by modulating the diffusion of O_2 and CH_4 throughout the soil matrix (Mancinelli 1995). For example, CH_4 fluxes measured in tropical regions during a rainy season tend to be higher than those measured during a dry season (Reiners et al. 1998). Besides, soils receiving high nitrogen input from the atmosphere or through fertilization consume often less CH_4 than undisturbed soils (Steudler et al. 1989; Castro et al. 1993; Butterbachbahl et al. 1998). Finally, some authors noted a relationship between CH_4 consumption rates and soil temperature (Boeckx and Van Cleemput 1997; MacDonald et al. 1997; Savage et al. 1997), whereas others found a rather weak influence (Dunfield et al. 1993; Crill 1991).

4.6 N_2O Fluxes in Forest and Wetland Soils

Nitrous oxide is produced in soils by nitrification and denitrification reactions (Hahn et al. 2000). Nitrification is an aerobic microbial processes that converts ammonium (NH_4^+) to nitrate (NO_3^-) in the presence of oxygen. During denitrification, nitrates are transformed into nitrogen (N_2). Denitrification requires anoxic conditions, but denitrifying bacteria are facultative anaerobes (Schlesinger 1997).

Greater N_2O Fluxes in Tropical Forests

Atmospheric concentrations of N_2O above the Amazon Basin are recognized as being the highest on the planet (Livingston et al. 1988). As a matter of fact, this is one of the reasons tropical rainforests have long been considered as the main natural source of N_2O at the global scale (Reiners et al. 1998). N_2O fluxes shown in Table 4.5 support the existence of higher emissions of N_2O from tropical soils than from northern soils. It is important to note, however, that the three highest flux values (3.2, 5.1 and 9.0 $mgN_2O \bullet m^{-2} \bullet d^{-1}$) were measured using a vented field chamber (Keller and Reiners 1994; Reiners et al. 1998). This method, which involves using a fan inside the chamber to re-create the surrounding wind conditions that were eliminated from the chamber, can induce an over-estimation of fluxes if the fan wind speed is greater than that of the outside surroundings. When excluding these flux values, the mean N_2O flux estimated for tropical forest soils (0.73 $mgN_2O \cdot m^{-2} \cdot d^{-1}$, n = 7) still exceeds that for boreal forest soils (0.05 $mgN_2O \cdot m^{-2} \cdot d^{-1}$, n = 3), but becomes comparable to the mean N_2O flux for temperate ones (0.84 $mgN_2O \cdot m^{-2} \cdot d^{-1}$, n = 16) (Table 4.5).

Table 4.5. Nitrous oxide ($mgN_2O \cdot m^{-2} \cdot d^{-1}$) fluxes of forest soils

Country	Region	Lat.	Long.	Forest type	Season[a]	Year	Mean [$mgN_2O \cdot m^{-2} \cdot d^{-1}$]	Method[b]	M[c]	J[d]	Reference(s)
BOREAL FORESTS (n = 3)											
Canada	SK	54°N	106°W	Aspen stand	G	1994	0.12	FG + EC			Simpson et al. (1997)
Canada	ON	49°N	81°W	Upland mixed forest	S	1992	0.01	SC (3 h)	>6	>6	Schiller and Hastie (1996)
Canada	MA			Upland forests	G	1998	0.01	SC	15	7	Hendzel (2002)
						Average	0.05				
TEMPERATE FORESTS (n = 16)											
USA	MA			Deciduous forest			0.13				Keller et al. (1983)[e]
USA	NY			Deciduous forest			0.39				Duxbury et al. (1982), cited in Keller et al. (1986)
USA	NH	44°N	71°W	Coniferous forest (15 $kgN \cdot ha \cdot yr^{-1}$)	G	1990	-0.02	SC (0.5 h)	6	6	Castro et al. (1993)
USA	NY	44°N	73°W	Coniferous forest (16 $kgN \cdot ha \cdot yr^{-1}$)	G	1990	0.16	SC (0.5 h)	6	6	Castro et al. (1993)
USA	ME	44°N	68°W	Coniferous forest (6 $kgN \cdot ha \cdot yr^{-1}$)	G	1990	0.03	SC (0.5 h)	6	6	Castro et al. (1993)
USA	VT	43°N	72°W	Coniferous forest (10 $kgN \cdot ha \cdot yr^{-1}$)	G	1990	-0.08	SC (0.5 h)	6	6	Castro et al. (1993)
USA	VT	44°N	72°W	Coniferous forest (16 $kgN \cdot ha \cdot yr^{-1}$)	G	1990	0.15	SC (0.5 h)	6	6	Castro et al. (1993)
USA	MA			Pine stand			0.01				Bowden et al. (1990)[e]
USA	WS			Pine stand			2.09				Goodroad et Keeney (1984)[e]
Austria	Vienna			Beech stand	G	1997	3.67	SC (4 h)	8	~16	Hahn et al. (2000)
Denmark				Beech stand			0.69	C			Ambus and Christensen (1995), cited in Simpson et al. (1997)
Germany	Darmstadt	50°N	9°E	Oak and beech forest	Y	1991	0.14	SC (0.5 h)	1	42	Dong et al. (1998)
Germany	Solling			Beech stand			5.28				Brumme and Beese (1992)[e]

Table 4.5. (cont.)

Country	Region	Lat.	Long.	Forest type	Season[a]	Year	Mean [$mgN_2O \cdot m^{-2} \cdot d^{-1}$]	Method[b]	M[c]	J[d]	Reference(s)
TEMPERATE FORESTS (n = 16) (cont.)											
Germany	Höglwald			Spruce stand (high atm. N-input)	G	93, 94, 95	0.65	SC	5		Butterbach-bahl et al. (1998)
Ireland	Ballyhooly			Spruce stand (low atm. N-input)	G	93, 94, 95	0.09	SC (2 h)	2	2-3	Butterbach-bahl et al. (1998)
Scotland	Peebles			Coniferous plantation	Y	1995	0.06	SC (1 h)	6	~12	MacDonald et al. (1997)
						Average	0.84				
TROPICAL FORESTS (n = 10)											
Puerto Rico		18°N	66°W	Tabonuco	D	1984	1.60	SC (0.5 h)	18	1	Keller et al. (1986)
Puerto Rico		18°N	66°W	Sierra palm forest	D	1984	0.11	SC (0.5 h)	10	1	Keller et al. (1986)
Puerto Rico		18°N	66°W	Elfin cloud forest	D	1984	0.41	SC (0.5 h)	10	1	Keller et al. (1986)
Puerto Rico		18°N	66°W	Mahogany plantation	D	1984	0.30	SC (0.5 h)	10	1	Keller et al. (1986)
Costa Rica		10°N	84°W	Old growth forest	Y	1991	5.05	SC (0.5 h)	24	12	Keller and Reiners (1994)
Costa Rica		10°N	84°W	Secondary forest	Y	1991	3.22	SC (0.5 h)	24	12	Keller and Reiners (1994)
Costa Rica		10°N	84°W	Virgin forest (hilltop. slope and swale)	R	92, 93	9.00	SC (0.5 h)	72	4	Reiners et al. (1998)
Brazil	Manaus			Terra firme forest	R	83, 84	0.83	SC (0.5 h)	6		Keller et al. (1986)
Brazil		3°S	60°W	Upland secondary forest	D	1985	0.88	SC (0.3 h)	1	4	Keller et al. (1986)
Brazil		3°S	60°W	Terra firme forest (ridge. slope and bottom)	D	1985	0.98	SC (0.5 h)	48	2	Livingston et al. (1988)
						Average	2.24				

[a]: *D*: dry season; *G*: growing season; *R*: rainy season; *S*: summer; *Y*: yearlong.
[b]: *EC*: eddy-covariance method; *FG*: flux-gradient method; *SC*: static chamber method (length of measurement).
[c]: Number of sites or subsites sampled.
[d]: Number of days studied.
[e]: Cited in Dong et al. (1998).

The higher N_2O emission from tropical forest soils could reflect the influence of temperature on nitrification and denitrification reactions (Sitaula and Bakken 1993; Stange et al. 2000). Nitrogen availability, which is greater in tropical than in boreal and temperate forests (Clein et al. 2002), could also be responsible, along with temperature, for the greater amount of N_2O emitted from tropical forest soils compared to northern ones.

Although temperate forests show, on average, a lower N_2O emission rate than tropical forests, some sites in the temperate region have the potential to emit almost as large amounts of N_2O as the tropical ones. N_2O fluxes in the temperate forests vary from -0.08 to 5.28 $mgN_2O \cdot m^{-2} \cdot d^{-1}$, with a mean flux of 0.84 $mgN_2O \cdot m^{-2} \cdot d^{-1}$ (n = 16, Table 4.5). Some of the large fluxes of N_2O could be explained by a relatively important nitrogen deposition from the atmosphere, which would stimulate nitrification and denitrification rates. Many authors have observed higher N_2O fluxes in temperate forests stands receiving high inputs of nitrogen (Castro et al. 1993; Butterbach-Bahl et al. 1998; Hahn et al. 2000). The N_2O uptake, measured at two sites in the temperate forest (-0.02 and -0.08 $mgN_2O \cdot m^{-2} \cdot d^{-1}$, Table 4.5), could be due to a slow upward diffusion of N_2O in soil anoxic microsites or water-filled pores, leaving more time for the microbial reduction of N_2O to N_2 (Regina et al. 1996).

The only three N_2O flux results available for the boreal forest indicate a relatively low rate of N_2O emission from this type of forest (average of 0.05 $mgN_2O \cdot m^{-2} \cdot d^{-1}$) (Table 4.5). It is important to mention that no data on N_2O fluxes could be found for black spruce, pine and larch stands, which occupy large areas of the boreal biome (FAO, 2001). Cold temperatures and water-saturated soils, frequent in black spruce stands and resulting from precipitations exceeding evapotranspiration (Schiller and Hastie 1996), are not conducive to N_2O production by nitrification.

N_2O production appears to be higher in wet but not completely water-saturated soils, because of lack of oxygen limiting nitrification (Granli and Bockman 1994). Maddock et al. (2001) and Dong et al. (1998) were able to establish a correlation between N_2O fluxes and the degree of soil water-saturation. Likewise, some authors have observed higher fluxes in wetter soils, such as in depressions, rather than on tropical forest slopes or hilltops (Reiners et al. 1998; but see Livingston et al. 1988), or in peaty podzols, as opposed to well-drained brown forest soils in a temperate forest (UK) (Macdonald et al. 1997).

4.7 N_2O in Wetlands

Very few studies have measured N_2O fluxes in wetlands, for the simple reason that the water-saturated and anoxic soils typical of these systems offer particularly unfavorable conditions for N_2O production. The nitrification rate is quite low in these systems because of very low oxygen content, pH and nitrogen availability (Bridgham et al. 2001). As for denitrification, it is often limited by the lack of nitrates, a direct consequence of slow nitrification rates (Regina et al. 1996).

Given the above information, it is not surprising that the N_2O fluxes measured in peatlands are extremely low, varying between 2.3 and 27 $\mu gN_2O \cdot m^{-2} \cdot d^{-1}$ (Table 4.6). Drier sites within peatlands, such as hummocks, would tend to emit more N_2O than wetter sites, such as depressions (Regina et al. 1996). Likewise, peatland drainage is generally followed by an increase in N_2O emission (Nykänen et al. 1995), which can be explained by an improved peat aeration and a stimulation of the activity of nitrifying bacteria and also, indirectly, of denitrifying bacteria (Regina et al. 1996). The N_2O consumption observed in certain peatlands reflects the highly reducing conditions of these systems.

In swamps, N_2O emission rates are similar to those measured in forests, with fluxes varying between 0.3 and 1.1 $mgN_2O \cdot m^{-2} \cdot d^{-1}$ (Table 4.6).

4.8 GHG Budgets in Forests and Wetlands

Using the available data on CO_2, CH_4 and N_2O fluxes, it is possible to estimate a GHG budget for most of the terrestrial systems treated in this chapter, three of which are the main forest biomes and the northern peatlands (Table 4.7). The GHG budgets in Table 4.7 were estimated on the basis of the relative global warming potentials of the aforementioned gases established over a period of 100 years (CO_2, 1; CH_4, 23; N_2O, 296) (IPCC, 2001).

Forest GHG Budget

The GHG budget estimated for forests indicates that these systems are GHG sinks, regardless of climatic region (Table 4.7). The uptake of GHGs by forests is the result of the balance between an important CO_2 sink, a weak CH_4 consumption by soil methanotrophic bacteria and a low N_2O emission. According to the estimated GHG budgets (Table 4.7), the boreal forest sink ($-873\ mgCO_2\text{-eq.} \cdot m^{-2} \cdot d^{-1}$) is weaker than the temperate and

Table 4.6. Nitrous oxide fluxes ($\mu gN_2O \cdot m^{-2} \cdot d^{-1}$) in wetlands

Country	Lat.	Long.	Wetland description	Season[1]	Year	Mean [$\mu gN_2O \cdot m^{-2} \cdot d^{-1}$]	Method[2]	M[3]	J[4]	Reference(s)
BOREAL PEATLANDS (n = 11)										
Canada	49°N	81°W	Lowland spruce forest (flat. hollow and hummock)	S	1992	16	SC (3 h)	>6	>6	Schiller and Hastie (1996)
Finland	62-63°N	24-31°E	Carex-dominated fen	G + W	1991	2.3	SC (0.5 h)	2-3	6-15	Regina et al. (1996)
			Carex-dominated fen with scattered pine	G + W	1991	14	SC (0.5 h)	2-3	6-15	
			Lagg fen	G + W	1991	-26	SC (0.5 h)	2-3	6-15	
			Dwarf-shrub pine bog	G + W	1991	5.6	SC (0.5 h)	2-3	6-15	
			Cottongrass pine bog	G + W	1991	-30	SC (0.5 h)	2-3	6-15	
			Cottongrass pine bog	G + W	1991	-9.6	SC (0.5 h)	2-3	6-15	
			Sphagnum-dominated bog with scattered pine	G + W	1991	-1.2	SC (0.5 h)	2-3	6-15	
			Carex-dominated bog	G + W	1991	-15	SC (0.5 h)	2-3	6-15	
			Ridge-hollow pine bog	G + W	1991	-0.6	SC (0.5 h)	2-3	6-15	
Finland	63°N	31°E	Herb-rich wet flark fen	G	1991	~70	SC (0.5 h)	2	~13	Nykänen et al. (1995)
				Average		2.3				
TEMPERATE SWAMPS (n = 1)										
Austria			Swamp forest	G	1997	1139	SC (4 h)	4	~16	Hahn et al. (2000)
TROPICAL SWAMPS (n = 2)										
Ecuador	1°S	78°W	Virgin forest on Napo river banks	D	1984	284	SC (0.5 h)	9		Keller et al. (1986)
	1°S	78°W	Secondary forest on Napo river banks	D	1984	278	SC (0.5 h)	8		Keller et al. (1986)
				Average		281				

[a]: *D*: dry season; *G*: growing season; *S*: summer; *W*: winter.
[b]: *SC*: static chamber method (length of measurement).
[c]: Number of sites or subsites sampled.
[d]: Number of days studied.

Table 4.7. Estimated greenhouse gases budgets ($mgCO_2 \cdot eq \cdot m^{-2} \cdot d^{-1}$) of forests and wetlands of different climatic region

	Forest					Peatland					Marsh/Swamp				
	CO_2	CH_4	N_2O	GES	C	CO_2	CH_4	N_2O	GES	C	CO_2	CH_4	N_2O	GES	C
	[$mgCO_2 \cdot eq \cdot m^{-2} \cdot d^{-1}$]				[$mgC \cdot m^{-2} \cdot d^{-1}$]	[$mgCO_2 \cdot eq \cdot m^{-2} \cdot d^{-1}$]				[$mgC \cdot m^{-2} \cdot d^{-1}$]	[$mgCO_2 \cdot eq \cdot m^{-2} \cdot d^{-1}$]				[$mgC \cdot m^{-2} \cdot d^{-1}$]
BOREAL REGION (50-55°N – 65-70°N)															
Mean	-863	-25	15	-873	-236	-744	2131	1	1387	-178		57		57	1
Min	-5230	-114	3	-5341	-1427	-2750	-38	-9	-2797	-750					
Max	271	86	36	393	75	502	12270	21	12793	282					
n	11	6	3	20	17	10	57	11	78	67		1		1	1
TEMPERATE REGION (20°N – 50-55°N)															
Mean	-1455	-82	249	-1288	-398	703 (-2953)	8488		9191 (6238)	292 (-705)		5914	337	6251	70
Min	-16605	-263	-24	-16892	-4532	-540	607		67	-140		-190		-190	-2
Max	1115	-8	1563	2 670	304	2400	22074		24474	916		24668		24668	293
n	23	14	16	53	37	3	17		20	20		10	1	11	10
TROPICAL REGION (20°S – 20°N)															
Mean	-2317	-19	663	-1673	-632		11132		11132	132	-5688	4513	83	-1092	-1498
Min	-5926	-80	33	-5973	-1616		8096		8096	96	-11634	-127		-11761	-3713
Max	0	94	2664	2758	1		16445		16445	195	3443	14294		17737	1108
n	3	9	10	22	11		3		3	3	5	26	2	33	31

(In parenthesis): was estimated from a CO_2 :CH_4 molar ratio of 8.0 (see text).

tropical ones (-1288 and -1673 $mgCO_2\text{-}eq.\cdot m^{-2}\cdot d^{-1}$, respectively), thus reproducing the observed pattern from NEE data (Table 4.1). The solar radiation intensity and growing season duration, which increases from north to south, could contribute to such a pattern. It is important to note, however, that the estimated GHG budget for tropical forests are based on two values of NEE out of three (Grace et al. 1995; Malhi et al. 1998), which have been challenged by recent results (Miller et al. 2004; Rice et al. 2004).

Unlike boreal and temperate forests, the N_2O flux seems to play an important role in the GHG budget of the tropical forest, representing on average 30% (in CO_2-eq.) of the NEE of this biome (Table 4.7). This is due to a relatively high N_2O emission rate from tropical forest soils, as well as to the global warming potential of N_2O, which is 296 times higher than that of CO_2 (IPCC 2001). Furthermore, such as the estimated range of GHG fluxes for the tropical forest suggests, GHG production in the form of N_2O could exceed, at some sites, the CO_2 uptake, transforming them into GHG sources (2758 $mgCO_2\text{-}eq.\cdot m^{-2}\cdot d^{-1}$). Unlike N_2O emissions, CH_4 consumption by forested soils seems to be a relatively minor component of the GHG budget of forests in general.

Peatland GHG Budget

The gathered data indicate that boreal peatlands behave on average as GHG sources (mostly as CH_4) (1387 $mgCO_2\text{-}eq.\cdot m^{-2}\cdot d^{-1}$), while, at the same time, sequestering low amounts of carbon as peat (-178 $mgC\cdot m^{-2}\cdot d^{-1}$) (Table 4.7). This result, which, at first glance seems paradoxical, is due to the global warming potential of CH_4 that is 23 times higher than CO_2, combined to the low molar ratio (8.0 CO_2: CH_4) of CO_2 influx (towards the peatland) over CH_4 efflux (towards the atmosphere). This molar ratio of 8.0, as estimated from the compiled data, is similar to the ratio observed by the authors having simultaneously studied both CO_2 and CH_4 fluxes in peatlands (3 to 10, as estimated by Moore and Knowles 1987; 6.3 to 7.7 by Whiting and Chanton 2001). It should be pointed out that the N_2O contribution to the GHG budget of peatlands is negligible, although only a few data on N_2O fluxes are available in these systems.

The gathered data do not allow establishing the temperate peatlands' GHG budget with certainty. As a matter of fact, the mean CO_2 flux estimated for temperate peatlands relies on only three studies, one of which (Shurpali et al. 1995) has been carried out during an abnormally warm and dry year. Such climatic conditions adversely affect photosynthesis by *Sphagnum* mosses, while favoring microbial degradation through increased peat aeration. Applying our molar ratio of 8.0 (CO_2: CH_4) to temperate

peatlands, while knowing that they are likely to have a higher molar ratio than boreal peatlands (Whiting and Chanton 2001), the GHG budget for these systems would be close to 6238 mg CO_2-eq. $\cdot m^{-2} \cdot d^{-1}$ (Table 4.7). This represents a GHG production four times higher than the estimated GHG budget for boreal peatlands.

The GHG budget estimated for peatlands do not generally take into account the high CO_2 and CH_4 emissions from ponds (Chap. 9). Although they occupy small areas, ponds emit large amounts of CO_2 and CH_4 (Roulet et al. 1994; Waddington and Roulet 2000) and adding these emissions to the GHG budget of peatlands should raise the estimated GHG budget for peatlands in general. Furthermore, the carbon budget estimated from CO_2 and CH_4 fluxes neglects to take into account the export of carbon as DOC (Carroll and Crill 1997; Alm et al. 1999b; Waddington and Roulet 2000). Fraser et al. (2001), for example, estimated northern peatlands as exporting 8.3 ± 3.7 $gC \cdot m^{-2} \cdot yr^{-1}$. Nevertheless, the annual peat accumulation rates estimated from the compiled data (21 $gC \cdot m^{-2} \cdot yr^{-1}$ for boreal peatlands and 61 $gC \cdot m^{-2} \cdot yr^{-1}$ for temperate peatlands, with a growing season length of 125 and 170 days, respectively) compare well with Gorham's (1991) (23 $gC \cdot m^{-2} \cdot yr^{-1}$) and Botch et al.'s (1995) (12 to 80 $gC \cdot m^{-2} \cdot yr^{-1}$) estimates.

Peatlands are one of the most important carbon pools on the planet (Gorham 1991). Over centuries, carbon sequestration in these systems has benefited from cold temperatures and water-saturated conditions, which resulted in slow rate of organic matter degradation. Several authors have put forth the hypothesis that global warming will cause a drying of peatlands and an increase aeration of peat benefiting the release of CO_2 (Oechel et al. 1993). However, as a counterpart to this hypothesis, it is thought that global warming will induce the melting of the permafrost and increase the water-saturation of peatlands beneficial to large carbon uptakes (Camill et al. 2001).

Marsh and Swamp GHG Budget

Limited data has been gathered on CO_2 and CH_4 fluxes in marshes and swamps. This data suggests that marshes and swamps of the temperate region are generally GHG sinks (Table 4.7). In the tropical region, the GHG budget of these systems is even more uncertain, since it is based on only two CO_2 flux data for swamps. One of which is from the *varzéas* during flooding, a period during which the *varzéas* is an important source of GHG (Devol et al. 1988). During low water period, the *varzéas* could be an important sink of CO_2, with its productivity stimulated by the newly deposited nutrients from flood waters (Junk 1997).

Comparison of GHG Budgets

The CO_2 sink capacity of peatlands seems to be similar to that of forests within the same climatic region (Table 4.7). However, the predominance of anaerobic decomposition under water-saturated conditions in peatlands, leading to the production of CH_4, makes these systems net sources of GHG. On the opposite, forests with well-aerated soils tend to be GHG sinks (Table 4.7). The boreal forests acting as GHG sinks (11.7 $TgCO_2 \cdot eq \cdot d^{-1}$ for 1343 Mha, Goodale et al. 2002) would largely compensate for peatland GHG emissions (3.5 $TgCO_2 \cdot eq \cdot d^{-1}$ for 250 Mha). These estimates do not consider, however, CO_2 losses by natural disturbances in forests, such as fire and insect defoliation (Amiro et al. 2001).

All the patterns observed in this chapter rely on the comparison of mean fluxes measured per system. However, the ranges of flux data, such as those of NEE in forest or CH_4 fluxes in peatlands, are considerable and more or less overlap each other from one climatic region to another (NEE: -5230 to 271 $mgCO_2 \cdot m^{-2} \cdot d^{-1}$ in boreal forests, -16605 to 1115 $mgCO_2 \cdot m^{-2} \cdot d^{-1}$ in temperate forests and -5926 to 0 $mgCO_2 \cdot m^{-2} \cdot d^{-1}$ in tropical forests, CH_4: -1 to 194 $mgCH_4 \cdot m^{-2} \cdot d^{-1}$ in boreal peatlands, 10 to 349 $mgCH_4 \cdot m^{-2} \cdot d^{-1}$ in temperate peatlands and -2 to 226 $mgCH_4 \cdot m^{-2} \cdot d^{-1}$ in tropical wetlands). Accordingly, the global GHG budget of the different forest biomes, and of wetlands in general, will depend on the relative area of the different forest stands (age, species composition, climatic conditions) or wetland types (open or forested bog and fen), as well as on the number and quality of the gathered data.

4.9 General Evaluation of Gas Flux Data

Some of the estimated budgets from compiled data are more uncertain that others, because of the limited available data on gas fluxes, which play an important role in these budgets. This is the case of the GHG budget for boreal and tropical forests, for which we have relatively little data on NEE. Tropical forests are of particular concern, since two out of three NEE values raise more and more doubt (Houghton 2003). Temperate peatlands and tropical swamps GHG budgets are also arguable, since only one net CO_2 flux data was collected in temperate peatlands and two in tropical swamps.

Another source of concern regarding the estimated GHG budgets in this chapter is the fact that the inherent variability within the studied terrestrial systems is not always considered. Many environmental variables having a strong influence on gas fluxes vary in space (locally and regionally) and in time (on a daily, seasonal and inter-annual basis), such as soil or peat water-saturation level (Roulet et al. 1994; Shurpali et al. 1995; Savage et al.

1997), air temperature (Lindroth et al. 1998; Arain et al. 2002), stand age (Litvak et al. 2003) and solar radiation (Waddington and Roulet 2000). Yet, this variability is not always taken into account in gas flux studies.

In forests, and since recently in peatlands, the use of flux towers combined with the eddy covariance method allows to estimate CO_2 fluxes (NEE) representative of the local variability over an approximate area of 1 km^2 (Baldocchi et al. 2001). However, other variables can affect forest NEE at a regional scale, such as stand age. A NEE estimate typical of the boreal forest at regional or national scales should take into account the relative area occupied by stands of different age-classes. In the boreal forest, such information is just starting to become available (Litvak et al. 2003).

In peatlands, where the chamber techniques are most often used to measure CH_4 fluxes, several studies have made an effort to account for the spatial heterogeneity of these systems by measuring gas fluxes at different sites within them. These sites are characterized by different water table depths (Dise 1993) or different species composition (Bubier et al. 2003). However, it can never be entirely sure that the chosen sites are typical of the average conditions of the investigated systems. Moreover, for a mean gas flux to be representative of a wetland as a whole, it should be weighted by the area occupied by these different sites. This has only been done by a few authors in Canadian boreal peatlands (Roulet et al. 1994; Waddington and Roulet 2000).

The integration of the temporal variability of gas fluxes is also crucial for estimating annually representative GHG budgets. The estimated budgets for peatlands are based on CH_4 and CO_2 flux data generally covering a complete or partial growing season, even though winter has been found to contribute one tenth to one third of their annual gas budgets (Alm et al. 1999a; Roehm and Roulet 2003; Lafleur et al. 2003). This is not the case for forest, for which NEE, which dominate the GHG budgets of these systems, have been measured over one or several years. Consequently, the GHG budgets estimated for peatlands probably underestimate the real annual contribution of these systems to GHG emissions. Moreover, in view of the potentially important inter-annual variability of CO_2 fluxes in peatlands, data collected over more than one year, such as in forests, will be required to gain a better appreciation of the GHG budget value for these systems.

The estimated budgets cannot be more accurate than the methods used to characterize gas fluxes. NEE values for forests should be interpreted keeping the methods' limitations in mind. The NEE correction needed to consider the accumulation of CO_2 under the forest cover during calm nights is the main uncertainty when using micrometeorological methods.

When CO_2 accumulates under the forest cover during calm nights, it is transferred to the atmosphere only during intermittent events before being evacuated rapidly in the morning when turbulent transport restarts (Grace et al. 1995). A fraction of the CO_2 emitted through respiration can escape measurement when transported outside the study zone by lateral wind movements or because of an overflow during CO_2 evacuation in the morning. This "unseen" CO_2 can lead to overestimating the net carbon uptake of forests (Baldocchi et al. 2001). In order to limit the extent of this problem, many studies eliminate data measured below a certain threshold (characterizing the turbulent transport) (e.g., Barr et al. 2002), whereas others directly measure night-time soil and plant respiration with flux gas chambers and link these fluxes to air or soil temperature to extrapolate them to the entire study period (e.g., Goulden et al. 1998; Shurpali et al. 1995). Depending on the threshold used to reject low wind speed data at night, NEE can be reduced by up to half the initial value (Jarvis et al. 1997; Barr et al. 2002). NEE estimates can also vary following the gap-filling strategy used (e.g., linear interpolation or regressions between NEE and environmental variables) to compensate for the loss of data during the frequent system calibration or during unstable climatic conditions, such as thunderstorm (Carrara et al. 2003). Because of these uncertainties, NEE estimates are more often cross-validated with biometric approaches (Bradford et al. 2001; Curtis et al. 2002).

Closed chambers are generally used for measuring soil-atmosphere CH_4 and N_2O fluxes in forests and peatlands. The disadvantage with using gas flux chambers is the small surface area sampled (~1 m^2) that can not take into account the high heterogeneity of natural ecosystems, resulting in gas fluxes affected by high variation coefficients. Moreover, the use of closed chambers can affect measured fluxes by isolating the sampled area from ambient environmental conditions, such as atmospheric pressure and wind speed, thus affecting gas flux magnitudes (Denmead 1991; Nay et al. 1994; Living and Hutchinson 1995). When the flux is directed towards the atmosphere, the increasing concentration of the gas within the chamber and the resulting decrease of the diffusion gradient can eventually result in a lower flux. This is less important in dynamic chambers (equipped with an automated measurement apparatus designed to detect low gas concentrations) than static ones (the gas being sampled with syringes), because of the smaller sampling period (Rochette et al. 1992; Healy et al. 1996).

Finally, the spatial coverage of the flux data gathered both for forests and wetlands is mostly concentrated in North and South America and Western Europe. This data does not allow an appreciation of the behavior of more than half of the boreal biome of Siberian peatlands or of Asian tropical forests for example.

5 Diffuse Flux of Greenhouse Gases – Methane and Carbon Dioxide – at the Sediment-Water Interface of Some Lakes and Reservoirs of the World

Donald D. Adams

Abstract

Sediments were cored from 19 lakes and 4 reservoirs and were analyzed for CO_2 and CH_4. Additionally sediment concentration profiles were measured in 107 cores. Concentrations of methane in the surface (2 $\pm$ 1.7 cm, n=107) sediment porewater in 4 oligotrophic lakes was in the order of 0.04 $\pm$ 0.03 mM (0-0.14, n=25), 0.24 mM in one oligotrophic reservoir to high values of 1.4 $\pm$ 0.96 mM (0-2.8, n=18) in 5 eutrophic-hypereutrophic lakes and 1.4 $\pm$ 1.0 mM (0-3.5, n=24) in 2 eutrophic reservoirs. Concentrations of porewater CO_2 in oligotrophic lakes were ten times higher than methane concentration with values in the order of 0.4 $\pm$ 0.36 mM but slightly lower for the same eutrophic lakes with values around 1.35 $\pm$ 0.9 mM and reservoirs [1.0 $\pm$ 0.8 (0.1-3.2, n=23)]. Surface sediment CH_4 concentrations were low in 3 acidotrophic lakes [0.2 $\pm$ 0.3 (0-1, n=22)] and very high in geothermal lakes [2.4 $\pm$ 0.6 (1.8-3, n=3)]. The CO_2 concentrations in acidotrophic lakes were, however, high [0.9 $\pm$ 0.7 (0.1-2, n=14)]. Diffuse flux of the two greenhouse gases - CH_4 and CO_2 – from the surficial sediments across the sediment-water interface (SWI) were calculated from Fick's first law of diffusion. These resulted in low methane fluxes from oligotrophic systems (lakes and reservoirs) of 0.2-0.4 mM $CH_4 \cdot m^{-2} \cdot d^{-1}$ (3-6 mg $CH_4 \cdot m^{-2} \cdot d^{-1}$) to much higher fluxes from eutrophic systems [3.9 mM $CH_4 \cdot m^{-2} \cdot d^{-1}$ (62 mg $CH_4 \cdot m^{-2} \cdot d^{-1}$) for lakes and 5.2 mM (83 mg) for reservoirs] to very high fluxes at the two geothermal lakes [14 mM $CH_4 \cdot m^{-2} \cdot d^{-1}$ (220 mg $CH_4 \cdot m^{-2} \cdot d^{-1}$)]. Dissolved CO_2 fluxes were double the methane fluxes in oligotrophic lakes, about equal for eu-

trophic lakes [3.8 mM $CO_2 \cdot m^{-2} \cdot d^{-1}$ (167 mg $CO_2 \cdot m^{-2} \cdot d^{-1}$)] and slightly lower than methane fluxes in eutrophic reservoirs [4.3 mM $CO_2 \cdot m^{-2} \cdot d^{-1}$ (190 mg $CO_2 \cdot m^{-2} \cdot d^{-1}$)]. Diffuse fluxes of CO_2 in acidotrophic systems [3.3 mM $CO_2 \cdot m^{-2} \cdot d^{-1}$ (143 mg $CO_2 \cdot m^{-2} \cdot d^{-1}$)] were almost the same as observed in eutrophic lakes. Even though it is unclear why there are such great differences between temperate and tropical ecosystems, CO_2 gas fluxes at the SWI in one tropical reservoir [Lobo Broa at 16 mM $CO_2 \cdot m^{-2} \cdot d^{-1}$ (700 mg $CO_2 \cdot m^{-2} \cdot d^{-1}$)] were much higher than temperate ecosystems while CH_4 diffuse fluxes [9 mM $CH_4 \cdot m^{-2} \cdot d^{-1}$ (140 mg $CH_4 \cdot m^{-2} \cdot d^{-1}$)] are only slightly higher than temperate ones. There are few data to evaluate the importance of sediment diffuse fluxes of these two greenhouse gases as related to aquatic surface emissions. One study in an 11-m deep tropical high elevation reservoir observed that surface losses represented 10% of the sediment diffuse flux of CH_4 (thus, 90% was oxidized at the SWI or in the water column). For CO_2 it is suspected that 20% of the surface emissions come from sediment sources. The sediments represent an important repository of carbon which contributes gases to overlying waters. These fuel the activities of microorganisms and substantially contribute to oxygen depletion in overlying waters as well as contributing to climate change.

5.1 Introduction

Aquatic and terrestrial ecosystems are of great importance in regulating the natural abundance of the atmospheric components of carbon-, nitrogen-, hydrogen- and sulfur-containing gases (Bouwman 1986, Mooney et al. 1987, Seiler and Conrad 1987, Detwiller and Hall 1988, Gammon and Charlson 1993 and Adams 1996). The natural exchange between these ecosystems and the atmosphere is closely related to processes occurring in soils and vegetation (Bouwman 1990), as well as in submerged aquatic environments, including their bottom deposits (Adams 1996). The anaerobic habitat, located in fine-grained sediments of lakes and reservoirs, represents one of the major sites for the production of reduced trace gases (Adams 1999, Abe et al., submitted). The decomposition of organic matter in these submerged ecosystems provides the energy for the growth of microorganisms, either through fermentation or anaerobic respiration. Within these habitats, at or near oxic-anoxic boundaries sometimes occurring in the water column but usually at the sediment-water interface, there is a sequence of oxidation-reduction reactions mediated by microbes which results in the production, consumption and accumulation of a wide spectrum of gases. These can range from fully (CO_2) to partially oxidized (CO, NO,

N_2O, COS, etc.) species as well as completely reduced (H_2, CH_4, H_2S, N_2, NH_3, etc.) gases. Many of these gaseous species are considered intermediate or end products of organic matter decomposition and are involved in a variety of associated redox reactions. Most are infrared absorbers and could be radiatively important trace (RIT) gases if it were not for their low abundance and short residence times in the atmosphere. The major sediment gases observed in these mostly anaerobic sedimentary environments are methane (CH_4), carbon dioxide (CO_2) and dinitrogen (N_2). Two of these gases (CH_4 and CO_2) are important greenhouse gases (GHGs). Other gaseous species (Ar, H_2, CO, N_2O, H_2S, COS, etc.) also occur but are usually in much lower concentrations; therefore, they are difficult to routinely measure. It has been shown that stratified lakes and reservoirs could present favorable environments for the production of the two major carbon GHGs, CO_2 and CH_4, as described in a review of reduced gases and their hydrosphere to atmosphere transport (Adams 1996) and a recent evaluation of Brazilian reservoirs (Rosa et al. 2004). The focus of this chapter will, therefore, be an evaluation of the production, cycling and diffuse flux of CH_4 and CO_2 at the sediment-water interface of temperate reservoirs and lakes of the world. An evaluation of the trophic conditions (from oligotrophic to hypereutrophic) for these aquatic systems will be included in order to determine if any relationships might exist between sediment gas accumulation, diffuse transport at the sediment-water interface and changing conditions in the trophic status of these water bodies.

Greenhouse gases (GHGs) can be produced both in the water column and sediments; this article will focus on bottom deposits, the major source of the two carbon GHGs – CH_4 and CO_2. These gases, produced in the surficial sediments during the degradation of organic material, can be emitted to the atmosphere through three distinct pathways: 1) molecular diffusion from deeper sediments to the sediment-water interface (SWI), coupled with diffusion or advection through the interface to the overlying water column, 2) transport through plant roots (Chanton et al. 1989, Boon and Sorrell 1995, Hamilton et al. 1995, Boon 2000) and 3) bubble ebullition (Sorrel and Boon 1992, Martens et al. 1992, Casper et al. 2000, Liikanen et al. 2003). Advective transport across the SWI could take place during windy conditions, or possibly from overturn of the water column from differential heating or cooling (MacIntyre and Melack 1995, Melack 1996). Water turbulence and mixing from wind and boat/ship propellers could also resuspend surface sediments, releasing trapped gases. In the third pathway, supersaturation of gases in sediment pore water would produce bubbles, composed mainly of CH_4 and N_2. Disturbance of surficial sediments would result in bubble loss, one of the most important pathways for direct transport of CH_4 to the atmosphere. Because of hydrostatic pressure,

bubble formation and transport is likely a major pathway only in the littoral zone of lakes and reservoirs, while diffusion would be the major transport pathway for sediments located in deeper environments. Since CO_2 is a minor component of gas bubbles (Rothfuss and Conrad, 1998, Adams and Naguib 1999), it is expected that ebullition is not a major pathway for this gas. Therefore, production and accumulation of the two carbon gases (CO_2 and CH_4) in surface sediments underlying deep (> 20–30 m) waters, and their diffusion to – and across – the sediment-water interface should be considered important factors in carbon cycling within the profundal zones of lakes and reservoirs.

CO_2 is produced by respiration throughout the water column and is also a product of sediment anaerobic processes. CO_2 is consumed by photosynthesis (and to a lesser extent by chemosynthesis) and, because light is required for uptake, its loss can be highly variable both vertically and temporally. Microbial respiration, also an important factor in carbon flow as CO_2, can at times exceed photosynthesis (del Giorgio et al. 1997). In contrast to methane, CO_2 is highly soluble and therefore high concentrations can accumulate at depth in the water column. Many lakes are oversaturated with CO_2 resulting in its release to the atmosphere, particularly in winter when productivity is low and the water column is isothermal.

Because of methane's current annual tropospheric increase of about one percent (four times faster than that of CO_2), this gas has received a major research emphasis for developing a better understanding concerning its biogeochemical cycling (Adams 1996). As with CO_2, the internal cycling of CH_4 is important to the overall carbon (C) balance of aquatic freshwater ecosystems. Rudd and Hamilton (1978) reported that production of methane (55% of total C) and its subsequent oxidation (36%) represented a large percentage of the total C budget for a eutrophic Canadian shield lake. It is likely that the difference, or 19%, would have been lost to the atmosphere. There are also numerous publications on the importance of CH_4 in the cycling of carbon, where values range from 7% of the sedimented C being decomposed to CH_4 gas (oligotrophic freshwater reservoir in the Netherlands; Adams and van Eck 1988) to as high as 65% for eutrophic Lake Suwa in Japan (Koyama 1990). Because of methane oxidation in the aerobic waters of lakes (Cicerone and Oremland 1988), at the oxic-anoxic chemocline in the water column of eutrophic, stratified lakes (Casper et al. 2000), or at the same boundary near the sediment-water interface (Frenzel et al. 1990, Adams 1992), Hessen and Nygaard (1992) reported that microbial cellular production by methanotrophs can be as important a carbon source to pelagic food webs as microbial secondary production. These organisms represent the "bacterial filter" which lower CH_4 emissions to the troposphere (by 60–90%) from inundated terrestrial surfaces (Galchenko et

al. 1989**).** Therefore, the internal cycling of gases and their production and utilization are important ecosystem processes whereby carbon is returned to the water column of freshwater lakes. Eventual loss to the atmosphere will depend on a variety of pathways involving carbon gas uptake or production within the water column.

As described, a wide spectrum of oxic to anoxic environments is a prerequisite for GHG production: CO_2 is produced in both oxic, low-oxygen and anoxic environments during respiration and organic matter decomposition. However, anoxia is required for CH_4 production through microbial methanogenesis. Conversion of carbon to CH_4 rather than CO_2 is important for climate change considerations since its infrared absorption and warming potential are 21 times greater than that of carbon dioxide (21 CH_4: 1 CO_2 for a 100-year time horizon, IPCC 1995; Environment Canada 1997). So, understanding the processes which control these fluxes as well as the effectiveness of the "bacterial filter", one of the most active microbial sinks whereby methane is lost from the transport pathway to the atmosphere, is important for a better knowledge of climate change.

5.2 Lakes and Reservoirs Sampled in this Study

The lakes and reservoirs sampled during these studies are listed according to their trophic status (Table 5.1) with the exception of 2 systems (Lake Tanganyika in tropical Africa and Lobo Broa Reservoir; the latter, in Brazil, is considered high altitude tropical), most are located in the temperate zone. The two reservoirs of Chile lay in arid to semi-arid zones. All were gravity cored for sediment gases.

The 19 lakes and 4 reservoirs (Table 5.1) evaluated for this chapter were sampled for extended periods of time (1–1.5 years) or sporadically (sometimes only once) during a 20-year period. Since the initial development of the CASS system in 1985 (Adams 1994) at the Max Planck Institute in Plön, Germany, procedures for processing cored sediments remained reasonably consistent over the years. Coring techniques and processing of sediments for their gas content, which were standardized over this period, have undergone recent (2003–04) major modifications, as described below. CO_2 was not always reported because of changes in gas analysis techniques. Modifications were also instituted over the years to improve the accuracy of measuring N_2 and argon in sediment pore water; however, this information will not be included in this chapter. A total of 107 cores were used for the statistics reported in this chapter on methane and carbon dioxide concentrations in sediment pore waters and incorporated into the calculations of diffuse gas flux.

Table 5.1. Characteristics of the 23 lakes and reservoirs sampled in this investigation (average depth)

Region of the world	Reservoir or lake name	Max depth [m] (Average depth)	Additional information	Reference(s)
OLIGOTROPHIC LAKES AND RESERVOIR				
New Zealand	Taupo	163 (98)	North Island TVZ Oligotrophic; largest lake in Australasia; 20 m secchi depth	Timperley 1987; Forsyth and Howard-Williams 1983; Adams 1992
New Zealand	Tikitapu	27.5 (19)	North Island, Taupo Volcanic Zone (TVZ)	Viner 1987; McColl 1977; Adams 1992
NE Germany	Stechlin	69.5 (23.3)	Intensive studies since 1958; glacially formed; groundwater fed	Casper 1985; Koschel and Adams 2003; Casper et al. 2003a
Africa	Tanganyika	1410	Second largest lake in the world, permanently anoxic	Adams and Ochola 2002
The Netherlands	Grote Rug Reservoir	40	Drinking water reservoir, built in 1962	Adams and van Eck 1988
OLIGOTROPHIC TO MESOTROPHIC RESERVOIR				
Brazil	Lobo Broa Reservoir	12 (3)	São Paulo State; 770 m; tropical	Abe et al. submitted
MESOTROPHIC LAKES				
New Zealand	Okareka	33.5 (18.4)	North Island, Taupo Volcanic Zone	Viner 1987; McColl 1977; Adams 1992
Switzerland	Alpnach	34 (21.6)	Prealpine lake near Lucern; sometimes anoxic hypo in fall	Wüest et al. 2000; Müller et al. 2002; Lorke et al. 2003
Japan	Kizaki	29	Dimictic lake	Abe et al. 2000
MESOTROPHIC TO EUTROPHIC LAKES AND RESERVOIRS				
New Zealand	Ngapouri	25 (13.5)	North Island, Taupo Volcanic Zone	Viner 1987; McColl 1977; Adams 1992
NE Germany	Schmaler Luzin	two basins 33 or 34 (18.1 or 13.3)	Remediated by hypoaeration and $Ca(OH)_2$ injection	Dittrich et al. 2000; Casper and Adams, in prep.
NE Germany	Dagow	9 (5)	Tending towards mesotrophic with watershed controls	Casper 1996; Casper and Adams in prep.
EUTROPHIC LAKES AND RESERVOIRS				
New Zealand	Ngahewa	7.5 (4)	North Island, Taupo Volcanic Zone	Forsyth and McColl 1975; Adams 1992
N Germany	Pluβsee	29 (9.4)	Intensive research Max Planck Institute, Plön	Adams and Naguib 1999

Table 5.1. (cont.)

Region of the world	Reservoir or lake name	Max depth [m] Average depth	Additional information	Reference(s)
EUTROPHIC LAKES AND RESERVOIRS (cont.)				
Switzerland	Sempach	87 (46)	Remediated by hypo aeration in winter and oxygen in summer	Gächter and Wehrli 1998; Müller et al. 2003
Chile, semi arid	Rapel Reservoir	90	Hydroelectric, built in 1968	Vila et al. 2000
Chile, arid	La Paloma Reservoir	69.5 (25.6)	Built for irrigation, arid area, 380 km North of Santiago	Adams et al. 2000
HIGHLY EUTROPHIC (HYPEREUTROPHIC) LAKE				
New Zealand	Okaro	18 (7)	High nutrients; watershed runoff from farming	Viner 1987; McColl 1977; Adams 1992;
GEOTHERMAL LAKES				
New Zealand	Rotokawau	(44)	Oligotrophic crater lake	Timperley and Vigor-Brown 1986; Viner 1987; Adams 1992
New Zealand	Rotorua	44.5 (7)	Eutrophic, but cored in geothermal area	White et al. 1978; Adams 1992
ACIDOTROPHIC LAKES				
N Germany	Tonteich	3.2	Clay pit for bricks now used for swimming; pH 3.5	Naguib and Adams 1996
NE Germany	Grosse Fuchskule	5.5 (3.3)	Peat drainage humic acids, partitioned into 4 sections for research	Casper et al. 2003b
Italy	Orta; sixth largest lake by volume in Italy; largest acid lake in the world in 1900s	4 basins (S to N): southern 30 middle 120 northern 140 Omegna 50 (lake outlet basin)	Acidification 1929 from denitrification ammonia discharge from rayon factory; remediated in 1990, 14500 tons lime	Adams and Baudo 2001

5.2.1 Sediment Sampling for Gases

Since 1985 sediments were routinely collected by gravity coring using two systems: a Phleger corer with 4.4-cm o.d. plastic liner and a UWITEC corer with 6-cm o.d. core liner. In both cases the core barrel was not used because of the loose sediment consistency and the need for processing with

the CASS system (Adams 1994). A third technique for sampling sediment gases is an *in situ* sediment equilibration device called a peeper (Hesslein 1976) or memocell (Van Eck and Smits 1986). There are other methods such as microelectrodes which are capable of directly measuring some gases (O_2, H_2, N_2O, H_2S, etc.) and gas diffusion probes (silicon-covered tubing) for collecting pore water gases, with direct coupling to measuring devices (see Rothfuss et al. 1994; Kühl et al. 1998). Methane in anoxic paddy soils was measured by the latter technique (Rothfuss and Conrad 1998). Sampling with the Phleger corer and sediment processing with the CASS system (Adams 1994) was used for years to collect sediments for pore water gases at 1–2 cm depth intervals. Presently, fine structure (mm) measurements of sediment gases at the sediment-water interface are now possible with a modern slicing system developed for 5-mm sediment core sectioning for gases (A-N sediment gas sampler; UWITEC, Mondsee, Austria; www.uwitec.at). This system is robust and has been tested under numerous field conditions. Some problems occur with sampling sediments containing sand or large leaf fragments, which jam the sliding devices; however, the CASS system also suffered these failures. The *in situ* equilibration technique (peeper) is useful for measuring the interface but the equilibrator needs to remain at a given site for at least two weeks. These devices are normally deployed with scuba divers, but other techniques are available for deeper placements with special landers (Müller et al. 2002). The presence of clays also hinders full gas equilibration with peepers (Adams and van Eck 1988). The greatest criticism of the peeper technique is the rapid gas loss during processing (Adams et al., in prep.), which suggests that *in situ* equilibrators should not be used for gases. With the exception of microelectrodes, all of these techniques require special instrumentation to measure gases in the collected sediment pore water sample.

For routine work, bottom sediments were collected with gravity corers. Depending on the weight of the corer, consistency of the bottom deposits, and distance of the "free fall", 50–100 cm penetration was typical (Mudroch and MacKnight 1994). If lowered slowly into the bottom sediments so as not to disturb and disrupt bubbles, methane concentrations in gravity core-collected sediments compared favorably with other sampling techniques, such as coring with the aid of scuba divers (Adams and Baudo 2001) and subsampling of box cores (Adams 1991). As described above, comparisons with in situ equilibrators suggested problems of gas loss during sub-sampling of the equilibration devices after their recovery (Adams et al., in prep.). In the case of gravity coring for sediment gases, the time period between sampling and sediment processing was minimized and the cores were kept cold to inhibit further methanogenesis (Adams 1994). Vibration and agitation of the cores were avoided to lower bubble disruption

and gas loss. Sediment cores were extruded horizontally within a glove bag flushed with helium within a few hours after collection. Horizontal processing avoids gas bubble migration. Atmospheric contamination during processing was minimized by using an inert gas, usually helium (this is only necessary if measurements of N_2 and argon are required). Sediments sampled at 1–2 cm depth intervals were transferred directly into tarred 25-ml Sarstedt (Sarstedt, Numbrecht-Rommelsdorf, Germany) plastic syringes and glass scintillation vials, using a core adapter syringe sampling (CASS) system (Adams 1994). The recently developed A-N sediment gas sampler (UWITEC, Mondsee, Austria) allows for 0.5-cm (5 mm) depth-interval sediment sampling when a gravity corer with a 6-cm diameter core liner is deployed. The internal air of the glove bag should be kept at about 0.2 ppm O_2, or lower, during sediment processing (Fendinger and Adams 1986). In the field, sediment gas syringes were immediately placed in helium-filled, heavy-duty freezer bags and kept on ice. These bags were flushed daily with helium or submerged in cold sediments to avoid oxygen contamination during storage. These techniques for processing cored sediments lowered the possibility of introducing atmospheric contamination so that Ar and N_2 gases were safely measured in sediment pore waters (Fendinger and Adams, 1987, Adams 1994). A simpler method for collecting and measuring sediment methane is described in Casper (1992). If only CH_4 and CO_2 are measured, it is suspected that a glove bag and inert gas are not necessary for sediment processing (Abe et al., submitted).

Techniques for manipulation of sediments to remove gases have changed very little since 1985. Gas analysis has been modified only slightly as new analytical techniques became available. The following description represents the latest methodology for sediment gas analysis, including N_2 and argon gases. Analysis of sediment gases usually took place no later than 1–2 days after coring and immediate sediment processing (Fendinger and Adams 1986). At this time the sediment gas syringes were submerged in a water bath at constant temperature (20^{o}C) and 5.0 ml helium was added to each syringe; manipulations were kept under water to avoid atmospheric contamination. Extraction of sediment gases into the helium headspace was facilitated by vibration for 4–5 minutes (with the sediment syringe kept in a helium-filled bag) followed by removal of most of the headspace (at least 3–4 ml) into a gas-tight syringe. About 1.5–2 ml of headspace was flushed through a sampling valve containing a 1.0-ml loop for direct injection into a gas chromatograph (GC). The following gases were measured: headspace extractable argon (Ar), oxygen (O_2), dinitrogen (N_2), methane (CH_4) and carbon dioxide (CO_2). Only the last two gases are reported here. These gases, especially the last three, represent the major sediment pore water dissolved gases. The GC was equipped with a

flame ionization detector (FID) for measuring carbon gases (with a C-H bond) and an in-line methanizer (operated at 380°C with H_2) to convert CO_2 to CH_4 for measurement with the FID and to remove O_2 for Ar analyses. The methanizer with FID was used for analyzing low levels of CH_4 and CO_2, for example, in the surface sediments of oligotrophic systems and the overlying water. Caution must be employed not to allow O_2 or H_2S to pass through the methanizer because this will deactivate the catalyst. An in-line thermal conductivity detector (TCD), also used with the methanizer, is employed to measure Ar (with or without O_2), N_2, CH_4 and CO_2. Since Ar and O_2 are measured at the same retention time by these GC techniques, the methanizer is switched into the gas flow (to remove O_2 for Ar analysis) or switched out of the gas flow (to assess the presence of O_2 in the injected sample); with two injections 3-4 ml of headspace sample are required for proper flushing of the 1.0-ml gas sampling loop. Measurement of low levels of O_2 in the sample suggests atmospheric contamination; in this case either the gas data are not reported or corrections are made for air contamination to the Ar and N_2 values. Argon is used as an inert tracer for calculating gas-to-Ar ratios to normalize gas data and improve accuracy for: 1) gas extraction temperatures effecting Bunsen coefficients (Weiss 1970, 1974, Wiesenburg and Guinasso 1979), 2) assessing possible air contamination and 3) calculations of potential denitrification (N_2/Ar ratio; Nishio et al. 1981; Fendinger and Adams 1987). Dinitrogen (N_2) values, however, will not be reported here since it is not a greenhouse gas and a further evaluation of the N_2 data is required.

5.2.2 Diffuse Flux Calculations

The diffusive fluxes of pore water gases to the sediment water interface from layers deeper in the sediments and flux across the interface, i.e. out of the sediments, were calculated using Fick's first law of diffusion:

$$J = - \Phi D_S (dc/dz),$$

where J = the diffusive flux,

Φ = porosity at the sediment-water interface,

D_S= sediment diffusion coefficient for each individual gas, and

dc/dz = the concentration change of each gas with depth.

D_S was calculated two ways from the molecular diffusion coefficient in pure water (D_o) for each of the two carbon gases using the empirical formulae:

$$D_S = D_o \Phi^2 \text{ (from Lerman 1979) and}$$
$$D_S = D_o / \Theta^2 \text{ (from Berner 1980)}$$

Gas diffuse flux, J, using D_S from the two different equations, resulted in a 23.9 $\pm$ 10.7 % (range 0.2 to 39%, n = 514) difference between the two flux calculations. An arithmetic average of the two calculations was used for the diffusion values listed in Tables 5.2 and 5.3. Values for D_o at different temperatures were taken from Lerman (1979). *In situ* temperatures, used for assignment of the D_o value, were measured in the water immediately above each core after its collection. Porosity (Φ) at the sediment-water interface was approximated by fitting the interface and two subsequent deeper porosity values to a linear least squares regression and calculating the porosity at z = 0; this was done only for some of the cores. Sediment tortuosity was estimated using the empirical relationship developed by Sweerts et al. (1991) for numerous fresh water environments:

$$\Theta^2 = -0.73\Phi + 2.17$$

where Θ = sediment tortuosity and
Φ = sediment porosity

Changes in pore water gas (CO_2, CH_4) concentrations with depth (dc/dz) were calculated from 0.5 cm above the sediment-water interface (depth z = +0.5) to the first sediment pore water measurement. The concentrations of gases were obviously never measured at z = 0, but sometimes just above the sediment-water interface (SWI). If these values were not available, gas concentrations from the literature or other data (Adams 1992, Adams and Baudo 2001) were assigned to the +0.5 cm depth interval in order to provide a dc/dz calculation. The best estimate for dc/dz would be from actual core overlying water measurements, with collections next to the SWI (for example, with diffusion probes or micromanipulators). In oligotrophic systems CH_4 was usually assigned zero for the +0.5 cm value; this represents complete methane consumption (oxidation) at the sediment-water interface during periods where the overlying water is aerobic. A CO_2 concentration of 0.5 mM was usually assigned to the +0.5 cm depth.

Table 5.2. Calculated theoretical diffusive fluxes of carbon greenhouse gases (GHGs) across the sediment-water interface (mean, standard deviation, min, max, n) of 23 lakes and reservoirs worldwide. Values are given in average ± one std. dev. (range of values, number of observations)

		Calculated diffusion across sediment-water interface (SWI)		Water and gas content in the uppermost surface layer		
		CH_4 [mM•m^{-2}•d^{-1}]	CO_2 [mM•m^{-2}•d^{-1}]	H_2O [%]	CH_4 [mM]	CO_2 [mM]
Acidotrophic lakes (3)		0.67±1.3	3.26±3.07	0.82±0.13	0.17±0.30	0.89±0.67
		(0.02-4.61, 21)	(0.17-8.88, 15)	(0.58-0.99, 22)	(0.00-1.04, 22)	(0.13-2.03, 14)
Oligotrophic Reservoirs		0.39±0.01		0.76±0.03	0.24±0.05	
(2 but only used 1)		(0.38-0.39, 2)		(0.74-0.78, 2)	(0.21-0.28, 2)	
Oligotrophic Lakes (4)		0.19±0.12	0.34±1.67	0.90±0.05	0.04±0.03	0.41±0.36
		(0.02-0.57, 25)	(-2.39-2.46, 6)	(0.82-0.97, 25)	(0.00-0.14, 25)	(0.00-0.94, 8)
Mesotrophic Lakes (5)		2.07±1.53	2.60±1.07	0.84±0.15	0.42±0.34	0.70±0.30
		(0.0-4.39, 11)	(1.47-3.93, 6)	(0.53-0.96, 11)	(0.00-0.98, 11)	(0.39-1.21, 6)
Eutrophic Reservoirs (2)		5.24±5.10	4.26±3.90	0.76±0.11	1.41±1.02	1.00±0.84
		(0.20-19.27, 24)	(-0.06-17.70, 23)	(0.54-1.00, 24)	(0.00-3.52, 24)	(0.11-3.19, 23)
Eutrophic Lakes (5)		3.90±3.14	3.80±2.58	0.94±0.04	1.40±0.96	1.35±0.87
		(0.01-12.00, 19)	(0.74-8.57, 9)	(0.83-0.98, 18)	(0.00-2.82, 18)	(0.12-2.88, 9)
Geothermal Lakes (2)		13.71±6.08		0.79±0.13	2.38±0.58	
		(6.69-17.35, 3)		(0.69-0.94, 3)	(1.80-2.96, 3)	
Lobo Broa Reservoir[1]		8.67±5.49	15.88±9.02	0.93±0.02	0.67±0.33	1.63±0.54
		(5.34-15.00, 3)	(8.80-26.05, 3)	(0.92-0.95, 3)	(0.36-1.01, 3)	(1.03-2.08, 3)
All Lakes and Reservoirs Across SWI Values [2]	Positive	2.89±4.20	4.30±4.46	0.85±0.12	0.73±0.93	0.95±0.75
		(0.00-19.27, 107)	(0.17-26.05, 58)	(0.53-1.00, 107)	(0.00-3.52, 107)	(0.00-3.19, 63)
	Negative		-0.71±1.12			
			(-2.39--0.06, 4)			
All Lakes and Reservoirs to the SWI values	Positive	1.04±1.24	1.69±2.40			
		(0.01-5.92, 74)	(0.01-11.56, 36)			
	Negative	-0.68±1.30	-0.56±0.47			
		(-0.001--4.44, 32)	(-0.01--1.61, 25)			

[1]: In Brazil, unknown classification, but considered as oligo- to mesotrophic, high altitude, tropical reservoir (Abe pers. comm.). It is included in the "All lakes and reservoirs" statistical calculations.
[2]: Positive = upward flux, negative = downwards flux.

Table 5.3. Theoretical diffusive fluxes of methane and carbon dioxide in the sediments of 23 lakes and reservoirs. Diffusion is calculated in the near surface sediments from the area of highest concentrations. Diffuse flux is calculated in both directions: downwards from surface to deeper sediments (negative) and upwards from deeper towards the sediment-water interface (positive). Values are given in average ± one std. dev. (range of values, number of observations)

	CH_4 (millimoles·m^{-2}·d^{-1} diffuse flux rate)		CO_2 (millimoles·m^{-2}·d^{-1} diffuse flux rate)	
	Downwards (-)	Upwards (+)	Downwards (-)	Upwards (+)
Acidotrophic lakes (3)	-0.06±0.08 (0.19--0.01, 5)	0.25±0.24 (0.01-0.76, 17)	-0.01±.0.00 (-0.02--0.02, 2)	0.76±0.90 (0.01-3.15, 13)
Oligotrophic Reservoirs (2 but only 1 used)	-0.02 (1)	0.23 (1)		
Oligotrophic Lakes (4)	-0.03±0.08 (-0.30-0.00, 13)	0.24±0.20 (0.03-0.77, 12)	-0.74±0.33 (-1.06--0.33, 5)	0.84±0.65 (0.36-1.58, 3)
Mesotrophic Lakes (5)	-0.05±0.04 (-0.10--0.02, 3)	1.14±0.42 (0.38-1.54, 7)	-0.78±0.55 (-1.59--0.37, 4)	0.34
Eutrophic Reservoirs (2)	-1.57±1.31 (-3.40--0.31, 4)	1.67±1.37 (0.13-4.66, 21)	-0.31±0.25 (-0.73--0.02, 9)	1.63±1.24 (0.08-5.18, 14)
Eutrophic Lakes (5)	-2.34±1.81 (-4.44--0.06, 4)	1.05±0.65 (0.27-2.08, 12)	-0.88±0.63 (-1.62--0.18, 5)	1.88±2.23 (0.30-3.46, 2)
Geothermal Lakes (2)	-2.80±2.32 (-4.45--1.16, 2)	0.88	-1.87±1.35 (-3.34--0.69, 3)	
Lobo Broa Reservoir[1]		4.49±2.04 (3.04-5.93, 2)		10.29±1.80 (9.01-11.56, 2)
All Lakes and Reservoirs	-0.69±1.31 (-4.45-0.00, 32)	1.05±1.24 (0.01-5.93, 74)	-0.56±0.48 (-1.62--0.01, 25)	1.69±2.40 (0.01-11.56, 36)
Total combined flux calculated by using absolute values		0.94±1.27 (0.00-5.93, 106)		1.23±1.94 (0.01-11.56, 61)

[1]: From Brazil: Unknown classification, supposedly classified as oligo- to mesotrophic, high elevation, tropical.

5.3 Results and Discussion

5.3.1 Sediment Gas Diffuse Flux

Decomposition of recently deposited organic matter results in the accumulation of the two greenhouse gases – methane and carbon dioxide – in surface sediments. The resulting concentration gradient requires that carbon is transported from these zones of high gas concentrations to either overlying waters by diffusion across the sediment-water interface (SWI), or to deeper sediments if concentrations are lower. The concentrations of CH_4 averaged 0.73 $\pm$ 0.93 mM (0–3.5 mM; n = 107) while CO_2 was slightly higher at 0.95 $\pm$ 0.75 mM (0–3.2 mM; n = 63) in the near surface deposits of 23 lakes and reservoirs (Table 5.2). The concentrations of gases are expressed in mmole (mM) per liter of sediment pore water.

The calculated diffuse fluxes of both methane and carbon dioxide are shown in Fig. 5.1 for all of the reservoirs and lakes sampled, with the exception of Lobo Broa Reservoir. Both diffusion and gas concentrations in the uppermost surface sediments are assigned to lakes of different trophic status (Table 5.2). Diffusive fluxes of these same two gases from sites of high gas concentrations in the deeper sediments were either upwards towards the SWI (flux = positive) or downwards towards deeper layers (flux = negative); these are listed in Table 5.3. Because of coring and sediment processing conditions, which sometimes resulted in the loss of the uppermost few mm of sediments when sampling high water content sediments, gas concentrations were not always measured in the surface sediments but at lower depths where the sediments became firmer. For the flux calculations given in Table 5.2 the overlying water depth was fixed at +0.5 cm (the extent of the assumed diffuse boundary layer) while the average depth below the SWI was 2.0 $\pm$ 1.7 cm (range of 0.3 to 9.3 cm, n = 107). In Table 5.3, diffusive flux towards the surface sediments (upwards = positive flux) or towards the deeper sediments (downwards = negative flux) were calculated over the following depth intervals: the lowest depth averaged 5.3 $\pm$ 2.6 cm (range of 0.8 to 13 cm, n = 104) while the surface depth was 1.7 $\pm$ 1.5 cm (range of 0.3 to 9.3, n = 107). The distance between these two depths averaged 3.6 $\pm$ 1.9 cm with a range of 0.5 to 9.5 cm. It is assumed that these would be the best flux estimates because they are calculated between two known concentrations within the sediment profile. In the case of fluxes across the SWI, an arbitrary value was assigned to the +0.5 cm depth above the SWI, so these estimated fluxes carry a larger degree of uncertainty.

Diffusion takes place along a gradient from higher to lower concentrations, therefore, diffusion can take place both upwards (positive, towards

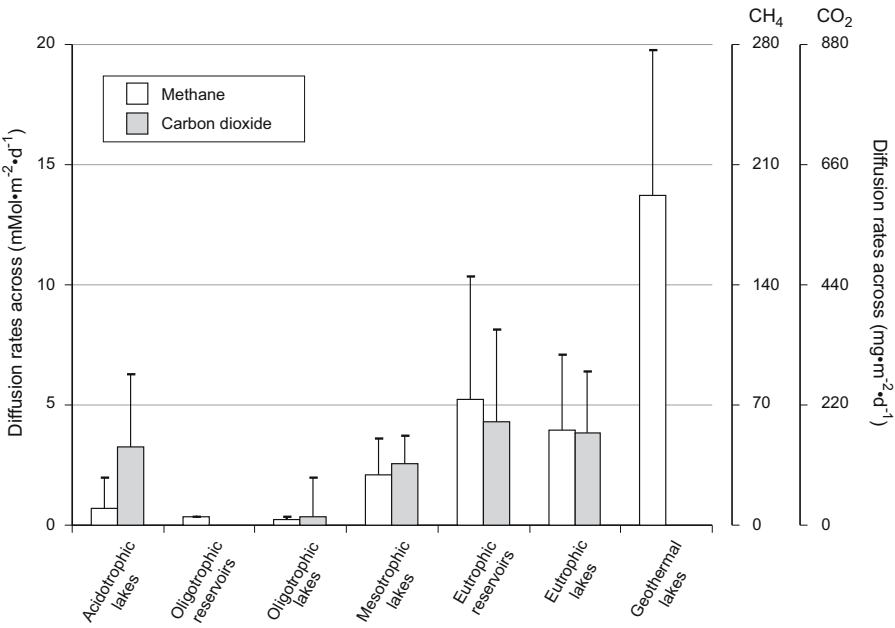

Fig. 5.1. Calculated theoretical diffuse fluxes ($mM \cdot m^{-2} \cdot d^{-1}$) of methane and carbon dioxide across the sediment-water interface (SWI) at 22 reservoirs and lakes (Lobo Broa Reservoir in Brazil is not included because of its high flux values). Averages and one standard deviation are shown for both gases. Carbon dioxide was not measured at the 2 geothermal lakes and the one oligotrophic reservoir used in this data set

the surface and eventually across the SWI) or downwards (negative) into the sediments (Table 5.3). The recently deposited organic material at the SWI represents a rich source of carbon-containing easily decomposable organic substrates, resulting in gaseous products of decomposition. As a result, diffuse flux from the sediments to the overlying water column at the sediment-water interface (SWI) of the 23 lakes and reservoirs (Table 5.2) was:

Methane (CH_4)	2.89 ± 4.20 (0.0 to 19.3, n = 107) $mM \cdot m^{-2} \cdot d^{-1}$ or 46 ± 67 (0.0 to 309, n = 107) mg $CH_4 \cdot m^{-2} \cdot d^{-1}$
Carbon dioxide (CO_2)	4.3 ± 4.5 (0.17 to 26, n = 58) $mM \cdot m^{-2} \cdot d^{-1}$ or 189 ± 196 (7.5 to 1144, n = 58) mg $CH_4 \cdot m^{-2} \cdot d^{-1}$

As described earlier, one major problem in the initial sampling was obtaining sediments close to the SWI with the Phleger gravity corer. The average depth of collection (2 ± 1.7 cm, n = 107) was likely below the zone of maximum decomposition and gas (CH_4 and CO_2) accumulation. For example, Adams et al. (1982) reported a large difference in calculated flux rates at the same site in Lake Erie for CH_4: 0.3 $mM \cdot m^{-2} \cdot day^{1}$ for samples collected by coring (first sediment sampling depth was 2 cm) versus 1.9 $mM \cdot m^{-2} \cdot d^{-1}$ (30 mg $CH_4 \cdot m^{-2} \cdot d^{-1}$) for measurements from peeper-collected samples (where gases were processed from water collected at 0 and -1 cm depths). For surface gas fluxes across the SWI at the 23 lakes and reservoirs there were no negative CH_4 fluxes, while 4 out of 62 CO_2 fluxes were negative (downwards). The downward fluxes took place only in Lake Stechlin, an oligotrophic lake, rich in calcium and carbonate and exhibiting autochothonous calcite precipitation during the summers (Casper et al. 2003a) and for one core which was transported 4 hours in a truck in Chile (where the data are highly suspect). This was not the case for subsurface diffusion calculations, where almost a third of the CH_4 fluxes were downwards (negative) and 66% of the fluxes upwards (positive, Table 5.3). Total gas diffusion from the location of maximum methane concentration in the sediment surface layers would, therefore, be a summation of the absolute values of the upward and downward diffuse fluxes (Fig. 5.2, Table 5.3):

upward fluxes = from deeper sediments towards the SWI = 1.05 $mM \cdot m^{-2} \cdot d^{-1}$, and

downward fluxes = from surface sediments to deeper strata = -0.69 $mM \cdot m^{-2} \cdot d^{-1}$,

resulting in
total fluxes from the zone of CH4 gas production/accumulation = 1.74 $mM \cdot m^{-2} \cdot d^{-1}$.

In the case of CO_2 40% of the fluxes were negative, accounting for 52% of the upwards gas diffusion. From the area of maximum CO_2 gas generation, total diffusion was calculated as (Fig. 5.3, Table 5.3):

upward fluxes (average of all positive fluxes) = 1.69 $mM \cdot m^{-2} \cdot d^{-1}$ and
downward fluxes (average of all negative fluxes) = -0.56 $mM \cdot m^{-2} \cdot d^{-1}$,

resulted in
total diffuse flux of CO_2 in both directions = 2.25 $mM \cdot m^{-2} \cdot d^{-1}$.

These values of total diffuse flux in both directions, 1.74 $mM \cdot m^{-2} \cdot d^{-1}$ CH_4 and 2.25 CO_2, represented only 50–60% of the calculated surface flux

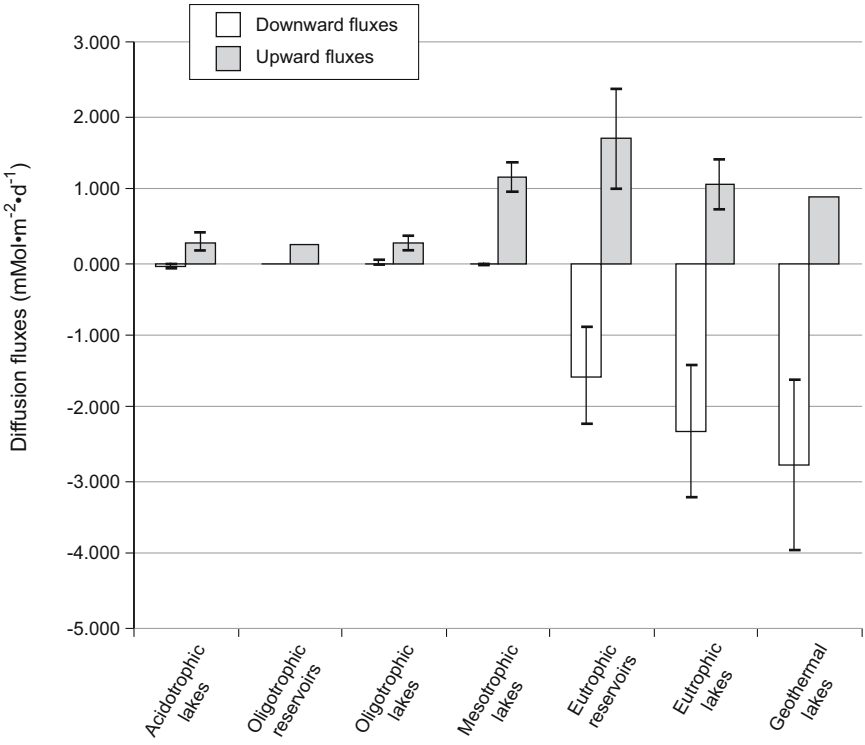

Fig. 5.2. Calculated theoretical diffuse fluxes ($mM \cdot m^{-2} \cdot d^{-1}$) of methane towards the sediment-water interface (upwards flux) and deeper into the sediments (downward flux) from zones of higher concentrations within the sediment profile. Averages and one standard deviation are shown

across the SWI into the overlying water column (2.9 $mM \cdot m^{-2} \cdot d^{-1}$ CH_4 and 4.3 CO_2, Table 5.2), while upwards fluxes were even lower (36–39% for the two gases). This suggested that either: 1) the +0.5 cm assigned gas concentrations were too low, 2) the assigned depth of +0.5 cm (5 mm) above the SWI was too close to the interface, or 3) some other factor. Gächter and Wehrli (1998) stated that the diffuse boundary layer (DBL) is less than 5 mm for Lake Sempach (depth of 87 m) similar to Furrer and Wehrli (1996) calculated a DBL for Lake Alpnach of approximately 2 mm. Other factors could be sediment compression and/or unobserved losses of surface sediments during coring (where concentrations deeper in the sediments were moved upwards), yet visual observations during core retrieval and processing did not substantiate these possibilities. Rothfuss and Conrad (1998) suggested that a transport process other than molecular

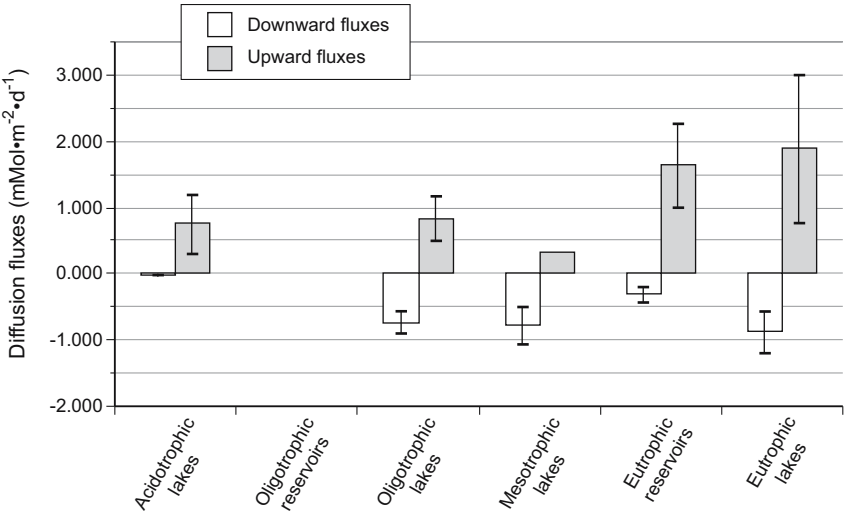

Fig. 5.3. Calculated theoretical diffuse fluxes ($mM \cdot m^{-2} \cdot d^{-1}$) of carbon dioxide gas towards the sediment-water interface (upwards flux) and deeper into the sediments (downward flux) from zones of higher concentrations within the sediment profile. Averages and one standard deviation are shown. There were no data for the one oligotrophic reservoir in the Netherlands

diffusion seemed to be active in the upper soil layers of a flooded paddy soil; this could be bioirrigation, resulting in higher flux. Rapid oxidation of methane at the SWI would also produce a greater dc/dz gradient and higher calculated diffuse flux, but this would likely have little effect on the CO_2 gradient. It is possible that gas diffusion calculations across the SWI were correct and approximately twice the fluxes which occurred within the surficial sediments. This is not unreasonable since the sediments are extremely liquid (high water content) at the SWI and the organic matter arriving at the SWI is readily decomposed resulting in high levels of sediment gases. These processes would result in high diffuse losses to overlying waters from the SWI, which would likely not be observed in deeper sediments containing recalcitrant carbon.

5.3.2 Relationships Between Sediment Gas Fluxes and Lake and Reservoir Trophic Conditions

Diffuse flux data from the 23 lakes and reservoirs have been summarized in Tables 5.2 and 5.3 according to their tropic status. Table 5.2 contains in-

formation about diffuse flux across the SWI while Table 5.3 provides flux data for deeper sediment layers (both upwards diffuse flux towards the SWI and downwards into deeper sediments). For comparison, diffuse fluxes from other aquatic environments are listed in Table 5.4.

For diffusion of gases through the SWI it should be assumed that these gases could be partially consumed at the interfacial zone of high microbial activity. Presently, it is not known how much CO_2 would be produced or consumed at the SWI, but it is suspected that more than 90% of diffusively transported CH_4 would be oxidized to CO_2 and incorporated into the biomass of methanotrophic microorganisms (Frenzel et al. 1990). Therefore, Fickian diffuse flux of methane across the SWI and its incorporation into overlying waters must be viewed with caution because of the microbial processes occurring at the SWI. The diffuse flux of carbon gases to the SWI was calculated from the sediment concentration profile using Fick's first law; this should be a reasonable representation of gas transport. As described above, numerous assumptions were made concerning the flux across the SWI. Regardless, it is obvious that most of the methane transported from the sediments to the water column is consumed at the interface, especially when lakes and reservoirs are oligotrophic. If one compares CH_4 flux for oxic versus anoxic conditions (for water overlying incubated cores in Table 5.4), the greater emissions for cores incubated under anoxic overlying waters (3–145 times higher) illustrate the high methanotroph consumption of methane during oxic conditions at the SWI. Thus, there is a rapid turnover of CH_4-carbon to CO_2 at the sediment-water interface (Adams and Fendinger 1986), or methane is incorporated into microbial biomass (Hessen and Nygaard 1992). For example, the oxidized surface layer of the sediments in Lake Constance accounted for the loss of 93% of the methane produced in deeper strata (Frenzel et al. 1990). Maximum oxidation rates also occurred in the surface 0.5 cm of sediment in Lake Washington (Lidstrom and Somers 1984). Further studies on this lake showed that half of the upward flux of methane, representing 20% of the sedimented organic C, was oxidized in this surface zone; only 2% of the carbon fixed by primary productivity was returned to the hypoliminion as CH_4 (Kuivila et al. 1988). Because of these oxidative losses, diffusive CH_4 flux across the water-atmosphere interfaces of lakes, saltwater marshes and the oceans were considered as minor contributors to global budgets (Schütz and Seiler 1989). In addition, if bottom deposits are located within the photic zone of littoral areas, the increased sediment penetration of O_2 during daytime photosynthesis would likely result in greater methane oxidation and a lower diffuse flux (King 1990, King and Blackburn 1996).

Table 5.4. Diffuse flux (mM m^{-2} day^{-1}) of methane and carbon dioxide across the sediment-water interface as reported for some other lakes and reservoirs and two lakes used in this chapter. To convert diffuse flux from mM m^{-2} day^{-1} to mg (gas) m^{-2} day^{-1} multiply CH_4 by 16 and CO_2 by 44

Methane	Carbon Dioxide	Techniques	Location, name	Reference
0.6			LakeWashington USA mesotrophic	Kuivila et al. 1988
0.4			LakeConstance Switzerland oligotrophic	Frenzel et al. 1990
0.0 – 9.4			Lake Vechten The Netherlands mesotrophic	Sweerts et al. 1991
0.02		flux calculated from profile of CH_4 in water overlying seds	Lake Fryxell, Antarctica, permanent ice	Smith et al. 1993
1.4 littoral 3.1 profundal 1.6 at 87 m		calculated from peeper profiles benthic boxes	Lake Sempach Switzerland eutrophic	Urban et al. 1997
	2.4 littoral HCO_3 2.5 profundal 13.7 at 87 m	HCO_3 fluxes from cores sediment profiles	remediated with hypo O_2 injection in summer and air in winter along with forced circulation	Müller et al. 1998, 2003
	4.5 littoral 22.4 profundal	with minielectrodes		Müller pers. comm.
1.53 from SWI to + 0.2 cm 1.5 from -1.5 cm to SWI	8.1 from SWI to +0.2 cm 2.3 from -1.5 cm to SWI	steady state model of organic matter diagenesis		Furrer and Wehrli 1996
	2.2 littoral 3.09 profundal	calculated from peeper profiles	Lake Baldegg Switzerland	Urban et al. 1997
0.016 max at 23 °C (overlying H_2O) 2.9 (anoxic) 0.02 (oxic) 1.25 2.2		*in situ* benthic chambers microcosms, CH_4 diffusion probes 3–5 mm profile 6–8 mm profile	Tomales Bay estuary, Calif. submerged paddy soil from Italy, air-dried, 25°C for the microcosms	Sansone et al. 1998 Rothfuss and Conrad 1998
before liming 0.13 southern 6.6 central 7.4 northern 4 yrs post liming 2.1 southern	before liming 4 yrs post liming CO_2 flux was not reported	flux calculated from sediment porewater gas profiles, same sites cored 1989 and 1994	Lake Orta, Italy discharge from rayon factory 1929 south basin – NH_4 and Cu 1990 limed	Adams and Baudo 2001
0.08 0.16		during spring circulation during summer stagnation	Lake Stechlin NE Germany oligotrophic	Gonsiorczyk 2002

Table 5.4. (cont.)

Methane	Carbon Dioxide	Techniques	Location, name	Reference
1.9 – 6.0 annual means		Lakes Wittwe Roofen, Peetsch N&S Nehmitz	4 lakes in NE Germany, all mesotrophic	
~ 3 (anoxic) < 1 (oxic)	~ 13 (both anoxic and oxic)	Incubated cores 4 m profundal	Lake Kevätön Finland	Liikanen[1] et al. 2002
6 (anoxic) <1 (oxic)	~ 22 (anoxic) ~ 27 (oxic)	incubated cores, 9 m profundal	hypereutrophic 15°C,	
max ~ 6 (anoxic) max ~ 1.7 (oxic)	max~ 23 (anoxic) max~ 25 (oxic)	incubated cores 1 m littoral cores for 6/98	Lake Kevätön this time listed as eutrophic, cores incubated at 15°C	Liikanen[1] et al. 2003a (flux values taken from
max ~ 3 (anoxic) max ~ 0.4 (oxic)	max ~20 (anoxic) max ~33 (oxic)	incubated cores 4 m profundal cores for 8/98	from 3 sites, collected during 6/98,	Fig. 5.3 so errors are likely
max ~ 8 (anoxic) max ~ 1.7 (oxic)	max ~ 33 (anoxic) max ~ 37 (oxic)	incubated cores 9 m profundal cores 6/ or 8/98	8/98 and 4/99	high)
23[2] (1.5 SE)	404[2] (19 SE) (SE = std error)	incubated cores plant stems cut at 10 cm above sediment, water table at 0 cm	Lake Kevätön hypereutrophic temp variable, 14–18 °C	Liikanen[1] et al. 2003b
1.4 (0.2 SE) max 7.9 (anoxic) 84% less w oxic overlying H_2O[1]		incubated cores changed from 15°C (1 wk) to 23°C for CH_4 stabilization	Lake Kevätön 4 m profundal	Liikanen and Martikainen 2003
0.05 south basin 0.2 central basin	2.3 south basin 35 m 3.4 central basin 68m	flux calculated from sediment porewater gas profile	Lake Stechlin NE Germany oligotrophic	Casper et al. 2003a
~ 3 (at 5°C) to ~ 45 (at 20°C)		regressions for net emission vs. °C in vegetative stands, sand and mud microcosm	Lake Pääjärvi, southern Finland	Kankaala and Berström 2004

1 For the Liikanen publications, collected cores were incubated under different temperature conditions with overlying water being oxic or anoxic. Fluxes were calculated from gas accumulation in the overlying water.
2 Very high gas flux rates likely induced by cutting the plant stems.

Galchenko et al. (1989) predicted that CH_4 emission rates from the water surfaces of aquatic environments for the year 2000 represent about 40% of the global budget of 627 Tg yr^{-1}. Of this amount, freshwater lakes contribute only 1% because of oxidative factors. Depending on the percentage of lake surface area considered productive with respect to methane emissions (Smith and Lewis 1992), the global annual source from aquatic ecosystems was estimated to range from 11 Tg (emission from 10% of lake surface area) to 55 Tg (for 50% of the lake area). These values are higher than the 2 Tg reported by Aselmann and Crutzen (1989) but within the range of 2–70 Tg yr^{-1} provided by Galchenko et al. (1989). Casper et al. (2000), on the other hand, calculated that lakes could provide 72 Tg yr^{-1} of CH_4 (and 156 Tg yr^{-1} of CO_2) to the troposphere. It is obvious that there is a large deficiency in knowledge concerning the sources and sinks of methane, one of the supposedly “best understood” RIT gases. Even though methane emissions are not well correlated with measurements of biological activity, such as biomass or primary production, it is expected that the inherent great variability in the processing of carbon by microorganisms will always result in these large uncertainties. As aptly pointed out by Whitman and Rogers (1991), identifying the sources and sinks for methane and carbon dioxide (and other biogenic traces gases) is analogous in trying to measure gases leaking from pinholes in a large pipe representing the flux of C, N, and S in the geochemical cycle.

This balance between CH_4 production in the deeper subsurface anaerobic zone of aquatic environments and consumption at the anoxic-oxic boundary during upward diffusion has been the subject of numerous investigations (Lidstrom and Somers 1984, Frenzel et al. 1990). Galchenko et al. (1989) called this the "bacterial filter" for retaining methane as C within the aquatic environment; about 60–90% of the newly generated methane in aquatic systems (both fresh and marine waters) is oxidized. Of this percentage, Galchenko et al. (1989) calculated that 50–95% of the emitted CH_4 is oxidized in aerobic waters. Another estimate for anaerobic methane oxidation was 5–20% of the global atmospheric flux, or about 25–94 Tg CH_4 yr^{-1} (Reeburgh and Alperin 1988). Aerobic and anaerobic oxidation thus provide an important mechanism for controlling the flux of RIT gases, such as CH_4, to the troposphere.

In the 23 lakes and reservoirs reviewed in this study the aquatic ecosystems were combined, for statistical averaging, into their assigned trophic status in Tables 5.2 and 5.3. Two “oligotrophic” reservoirs were sampled but diffuse fluxes from Lobo Broa Reservoir in Brazil (Abe et al., submitted) are far above the values observed at oligotrophic sites. Therefore, this reservoir has been placed into its own category (high altitude tropical). Comparisons with the one remaining reservoir, oligotrophic de Grote Rug

in the Netherlands, with four oligotrophic lakes show that CH_4 flux was approximately double (CO_2 was not measured in De Grote Rug) at the reservoir compared to oligotrophic lakes; however, such comparisons are likely not statistically valid because of the poor data set. Comparisons between the two eutrophic reservoirs and the 5 eutrophic lakes suggest that both CH_4 and CO_2 sediment diffuse fluxes might be slightly higher in the reservoirs (Table 5.2). Evaluation of surface sediment gas concentrations, from oligotrophic to mesotrophic to eutrophic (and hypereutropic) aquatic systems, showed that both CH_4 and CO_2 concentrations in surface sediments progressively increased with trophic status. This change in gas concentrations resulted in elevated diffuse fluxes across the SWI, from lower values in oligotrophic lakes and reservoirs to much higher levels in eutrophic lakes (20 times for CH_4 and 11 times higher for CO_2). It is a matter of conjecture how much of these gases, diffusing from the sediments, actually reach the surface of these water bodies. Simultaneous surface water and sediment sampling of the Lobo Broa Reservoir in August 2003 indicated that 80% of the CO_2 lost from surface waters came from sources other than the sediments (Abe et al., submitted), while only 10% of the CH_4 lost from the sediments ($3.4\ mM{\cdot}m^{-2}{\cdot}d^{-1}$) was transported across the water-atmosphere interface ($0.31\ mM{\cdot}m^{-2}{\cdot}d^{-1}$, or $5\ mg\ CH_4{\cdot}m^{-2}{\cdot}d^{-1}$). This suggests that 90% of this gas is oxidized at the sediment-water interface or within the water column, which is in agreement with other authors.

Both methane and carbon dioxide are exported from the sediments. The importance of methanotrophs in remediating the emissions of methane cannot be overemphasized. As lakes become more eutrophic, with nutrient and carbon loadings from surrounding watersheds, generation of these two GHGs from sedimentary sources will become greater. Losses of CH_4 from sediments to overlying waters will result in oxygen depletion and conditions of hypolimnetic anoxia. Along with the formation of anaerobic conditions would be the production of more sediment and water column methane. This situation will likely be exacerbated in tropical lakes and reservoirs because of water column stratification, resulting in permanent anoxic conditions. An emphasis should be placed on controlling external loadings to these water bodies, otherwise the natural biogeochemical carbon cycles will become more influential – resulting in greater problems of anoxia and higher GHG emissions.

5.4 Conclusions

Over a hundred cores from 23 lakes and reservoirs were evaluated for their sediment gases within their surficial deposits. This included 19 lakes and 4 reservoirs of different trophic status. Theoretical diffuse flux was calculated for methane and carbon dioxide within the sediment-water interfacial zone and slightly deeper in the sediments. As lakes and reservoirs become eutrophied, carbon will accumulate in their bottom deposits. This organic material is utilized by a myriad of microbial organisms, resulting in gaseous intermediate and end-products. Two of the decomposition gases, methane and carbon dioxide, are important greenhouse gases, and as such their pathways at the sediment-water interface were examined to evaluate their losses to overlying waters. Their concentrations in the surface sediments indicated accumulation along a gradient of trophic conditions, i.e. the greater the trophic status the higher the sediment carbon gases. This resulted in greater calculated diffusion of gases from the sediments to overlying waters for these two greenhouse gases – oligotrophic<mesotrophic< eutrophic<hypereutrophic. The eutrophic (hypereutrophic) and geothermal lakes had the highest diffuse losses of gases at the sediment-water interface. This was also the case for CO_2 at the sediment-water interface of acid lakes. Methane diffuse flux was minimal for the oligotrophic and acidotrophic lakes, since surface sediment concentrations of CH_4 were also the lowest. It was observed (from this study and literature sources) that methane was consumed during diffuse transport across the SWI (and within the water column). In the case of carbon dioxide, possible changes during diffuse transport at the SWI are relatively unknown since there are many pathways, both in the water column and sediments, which involve its consumption and production. Overall, the sediments represent an important source of these two greenhouse gases to aquatic ecosystems.

Acknowledgements

There were so many individuals that helped in the collecting and processing of sediments, assisting in data interpretation, writing joint publications and providing inspiration that this list would be too lengthy. I am deeply grateful to all of them for their dedicated assistance and cooperation. Many organizations provided financial assistance for the research and lengthy stays in their countries: Germany (Max-Planck Institute, Plön; Max-Planck Fellowship from the Max Planck Society; stipends from the Leibniz-Institut für Gewässerökologie und Binnenfischerei, in particular, the ab-

teilung Limnologie Geschichteter Seen, Stechlin-Neugobsow and a SUNY Presidential Scholarship), New Zealand (DSIR, Dept. Scientific and Industrial Research fellowship; Taupo Research Laboratory and Petroleum Research Fund grant), Chile (International Atomic Energy Commission, Vienna; Comisión Chilena de Energía Nuclear, Dirección General de Aguas, Andes Foundation and Facultad de Ciencias and Ecologicas, Universidad de Chile, Santiago), Tanzania (Fulbright Research Fellowship to Kenya and Tanzania through CIES; START, Washington, DC; Nyanza Project NSF grant), Switzerland (EAWAG's Center for Lake Research, Kastanienbaum), Brazil (a fellowship from FAPESP - Foundation for Support of Research in the State of São Paulo and Institute for International Ecology, São Carlos-SP), Japan (Institute for Hydrospheric Atmospheric Sciences, Nagoya University) and Italy (Istituto Italiano di Idrobiologia, Palanza and a fellowship from CNR - Italian National Research Council). P. Casper is gratefully acknowledged for helping with the figures and editing the first draft and B. Müller is thanked for providing unpublished flux data for Lake Sempach. My wife, Gerlinde Adams, has assisted me throughout with laboratory and field work. Lastly, I would like to thank HydroQuébec for making this publication possible.

6 Organic Carbon Densities of Soils and Vegetation of Tropical, Temperate and Boreal Forests

Anne-Marie Blais, Stéphane Lorrain, Yanick Plourde and Louis Varfalvy

Abstract

Available estimates of the soil organic carbon (SOC) density in northern and tropical forests vary between 8.5 and 13.9 $kgC \cdot m^{-2}$ for the top first meter. Values of SOC for boreal forests are higher when considering the carbon stored as peat and in the forest floor. Overall, current SOC estimates often underestimate the total soil carbon content of boreal and tropical forests, because in many cases sampling is often limited to the soil's first meter.

The estimates of organic carbon sequestered in the vegetation of Amazonian forests (15.2 to 23.3 $kgC \cdot m^{-2}$) are two to five times higher compared to boreal (4.0 to 6.4 $kgC \cdot m^{-2}$) and temperate forests (4.8 to 5.7 $kgC \cdot m^{-2}$). Apart from their greater productivity, the more stable natural conditions prevailing in tropical rainforests have contributed to the accumulation of large amounts of carbon as biomass. On the other hand, the frequent recurrence of forest fires and insect outbursts in northern forests greatly limit carbon storage in the biomass.

The distribution of the total organic carbon stock between soil and vegetation varies with latitude. In northern forests, 72% of the organic carbon is found in the soil, with the remainder (28%) in the plant biomass. In tropical forests, the distribution is reversed, with 38% of the organic carbon stored in the soil and 62% in the vegetation. This difference can be explained by slower decomposition rates and a shorter growing season in relatively cold and humid boreal regions.

The boreal peatland carbon pool (98 to 335 PgC) is comparable to that of the whole boreal forest (180 to 330 PgC), but its surface area is five

times smaller with an organic carbon content two to 10 times greater (39 to 134 $kgC \cdot m^{-2}$).

Export rates of organic carbon from terrestrial to aquatic ecosystems are small compared to their total stock but could be significant in the global forest carbon balance.

6.1 Introduction

Damming for hydroelectric production involves the flooding of vegetation and soils containing significant amounts of organic matter (Poulin-Thériault and Gauthier-Guillemette 1993; Dyck and Shay 1998). This organic matter can decompose more or less rapidly depending on local physico-chemical conditions and can lead to the formation of greenhouse gases that are released at the reservoirs' surface (Kelly et al. 1997; Huttunen et al. 2002; Tremblay et al. 2004).

Carbon accumulates in vegetation as a result of the imbalance between input (i.e., photosynthesis) and loss processes (i.e., respiration, herbivory, natural perturbations such as fire, and harvesting). In soils, the amount of organic matter is regulated mainly by the input of plant residues, either falling at the soil's surface (e.g., leaves and coarse woody debris) or leaching from roots and shoots (e.g., photosynthates), and the rate at which these various compounds decompose (Batjes 1996). Plant residues, which ultimately depend on the type of vegetation and its productivity, are gradually altered through physical and faunal fragmentation, as well as through microbial mineralization (Post et al. 1982; Batjes 1996). The soil organic carbon content is also controlled by the water-mediated movement of carbon within the soil matrix and towards aquatic ecosystems, which is significant and exceeds the riverine export of carbon (Waddington and Roulet 2000; Aitkenhead and McDowell 2000; Richey et al. 2002).

Climatic conditions, such as temperature and precipitation, are thought to have a strong influence on the amount of carbon stored in vegetation and soils, through their influence on plant productivity and organic matter degradation rates (Schlesinger 1997). As such, the carbon densities (carbon mass per unit area) of forest vegetation and soils are expected to differ between climatic regions (e.g., boreal, temperate or tropical ones).

Soil and vegetation carbon densities of forests and peatlands result from historic land-atmosphere gas fluxes, natural and anthropogenic disturbances and the terrestrial-aquatic transfer of carbon since the last glaciation. Understanding how organic carbon is distributed in the terrestrial biosphere is important in view of its role as potential sink for anthropogenic

greenhouse gas emissions (IPCC 2001). Underlying processes for this terrestrial sink, as well as its precise location have, however, still not been clearly established (Houghton 2003).

Measures of vegetation and soil organic carbon densities have been compiled in several studies in order to provide global-scale mean estimates (e.g., Post et al. 1982; Schlesinger 1984; Dixon et al. 1994; Goodale et al. 2002). This chapter reviews available carbon density estimates for soil and vegetation of forests and peatlands of the boreal, temperate and tropical regions. It also stresses upon the high spatial and temporal heterogeneity of soil organic carbon and vegetation biomass.

6.2 Soil Organic Carbon Density

The amount of organic carbon stored in forest mineral soils has been estimated in several studies (Post et al. 1982; Dixon et al. 1994; Batjes 1996; Siltanen et al. 1997, etc.; Table 6.1). When comparing compiled estimates (Table 6.1), the boreal forest soils appear to have a higher soil organic carbon (SOC) content (12.1 to 16.4 $kgC \cdot m^{-2}$, ~1 m) than temperate (8.7 to 13.4 $kgC \cdot m^{-2}$) and tropical (9.8 to 12.7 $kgC \cdot m^{-2}$) forests' soils, where SOC values tend to be similar (Table 6.1). Many authors present results supporting this trend (Post et al. 1982; Schlesinger 1984; Goodale et al. 2002). Batjes (1996) also reports that podzols, typical of boreal forests, have a higher organic carbon content (24.2 ± 94% (CV) $kgC \cdot m^{-2}$) than soils from temperate forests (cambisols: 9.6 ± 77% $kgC \cdot m^{-2}$, phaeozems: 14.6 ± 47% $kgC \cdot m^{-2}$) or tropical ones (ferrasols: 10.7 ± 63% $kgC \cdot m^{-2}$, acrisols: 9.4 ± 82% $kgC \cdot m^{-2}$). Cold temperatures and water-saturated conditions in the boreal region are conducive to organic matter accumulation in soils by limiting microbial decomposition rates (Schlesinger 1997).

However, Jobbágy and Jackson (2000) report a different trend, with tropical soils having a greater amount of organic carbon. Moreover, it appears that some of the available estimates of SOC density (carbon mass per unit area) of boreal forests are overestimated. This would be related to studies based on data from the Oak Ridge National Laboratory (Post et al. 1982; Dixon et al. 1994; Goodale et al. 2002). Data from the ORNL ($n = 177$, data for Canada) was compared to the more complete database ($n = 1462$) from the Canadian Forest Service in a study where both data sets were used to estimate the SOC content of Canadian forests (Siltanen et al. 1997). The results show an overestimation by a factor of two of the SOC density of the Canadian boreal forest when using the smaller ORNL data set (6.8 compared to 14.0 $kgC \cdot m^{-2}$).

Table 6.1. Soil organic carbon densities[a] ($kgC \cdot m^{-2}$) estimated in different biomes [CV%, n]

	Mineral soil							Mineral soil, peat and litter	
	Post et al. (1982)				Jobbágy and Jackson (2000)	Goodale et al. (2002)[b]	Other recent studies [ref. n°] (see Table 6.2)	Schlesinger (1984)[c]	Dixon et al. (1994)[b,d]
	Dry	Moist	Wet	Total					
TUNDRA		10.9 [59%; 12]	25.4 [61%; 36]	21.8[e]	14.2 [99%; 51]			20.4	
BOREAL FOREST		11.6 [71%; 222]	19.3 [50%; 30]	16.4[e]	9.3 [75%; 648]	15.2[e]		20.6 [93%, 13]	34.3 (12.1)[d]
Canada						14.0	6.8 [1][b]		48.4 (14.0)[d]
Alaska						23.1			21.2
Russia						15.3	21.0[CC] to 27.7[W] [2]		28.1 (10.7)[d]
TEMPERATE FOREST	7.9[W] [49%; 94]	6.0[W] [43%; 63] 12.1[C] [68%; 616]	13.9[CC] [63%; 344]	8.7[e]	15.5 [60%; 183]	9.3[e]		13.4	9.6
Australia									8.3
United States						8.7	9.1 [3]		10.8
Europe						6.7	Netherlands: 10.9 [4]		9.0
China						13.4			13.6
TROPICAL FOREST	10.2 [110%; 173]	11.5 [102%; 162]	21.0 [42%; 12]	12.7[e]	18.6[M] [56%, 36] 15.8[MD] [58%, 29]			12.0	12.3
Americas							Brazil: 10.3 [5], 9.8 [6]		12.0
Africa									12.0

Table 6.1. (cont.)

	Mineral soil							Mineral soil, peat and litter	
	Post et al. (1982)				Jobbágy and Jackson (2000)	Goodale et al. (2002)[b]	Other recent studies [ref. n°] (see Table 6.2)	Schlesinger (1984)[c]	Dixon et al. (1994)[b,d]
	Dry	Moist	Wet	Total					
Asia							India: 10.0 [135] [7] 13.9^{M} [65%, 36] 11.2^{MD} [57%, 64] 7.0^{DD} [86%, 35]		13.9
TEMPERATE GRASSLAND	13.3 [71%; 374]			13.3	11.7 [56%; 121]		China: 20.6 [8] Russia: 10.5 [9]	18.9	
SAVANNAS				6.9	13.2 [66%; 35]			5.8	

[a]: Most SOC estimates were calculated for the soil's first meter. However, some authors used a different integration depth. For example, Schlesinger (1984) included in his estimates soil profiles sampled to variable depths (e.g., for the boreal forest, sampling depths vary between 0.3 m to 3.2 m). Siltanen et al. (1997) used a maximum integration depth of 1 m, with soil profiles sampled to depths smaller than 1 m. Genxu et al. (2002) [ref. n°8] used a sampling depth of 0.75 m. The integration depth of the following studies is unknown: Kokorin et al. (1996) [ref. n°2] and Nabuurs and Mohren (1995) [ref. n°4].

[b]: SOC densities estimated by Dixon et al. (1994), Goodale et al. (2002) and Siltanen et al. (1997) for the Canadian and Russian boreal forests include the subarctic region (50°N to 75°N). In other studies, the subarctic region may have been included, but this was not specified.

[c]: Estimates from Schlesinger (1984) include the litter layer and data from forested bogs.

[d]: Estimates from Dixon et al. (1994) include the litter layer and the organic horizon of peatlands. Data in parenthesis excludes peatlands. Peatlands were excluded by considering a peatland carbon pool of 134 PgC for Canada (CCMF, 1997) and 94.3 PgC for Russia (Nilsson et al. 2000) and a forest surface area of 440 Mha and 881 Mha for both countries respectively (Goodale et al. 2002).

[e]: Calculated from the data provided by the authors.

W: Warm region; *CC*: Cold region; *M*: Moist tropical forest, *MD*: Moist deciduous forest, *DD*: Dry deciduous forest

Table 6.2. References cited by authors from Table 6.1

	Dixon et al. (1994)	Goodale et al. (2002)	Other recent studies [ref. n°]
TUNDRA			
BOREAL FOREST			
Canada	Apps and Kurz (1991); Kurz and Apps (1993)	Kurz and Apps (1999)	[1] Siltanen et al. (1997)
United States (Alaska)	Birdsey et al. (1993); Turner et al. (1995)	Birdsey and Heath (1995)	
Russia	Krankina and Dixon (1994); Kolchugina and Vinson (1993)	Nilsson et al. (2000)	[2] Kokorin et al. (1996)
TEMPERATE FOREST			
Australia	Gifford et al. (1992)		
United States	Birdsey et al. (1993); Turner et al. (1995)	Birdsey et Heath (1995)	[3] Turner et al. (1995)
Europe	Kauppi et al. (1992)	Nabuurs et al. (1997)	[4] Nabuurs and Mohren (1995)
China	Deying (1992)	Zhou et al. (2000)	
TROPICAL FOREST			
Americas	Singh (1993)		[5] Moraes et al. (1995) [6] Batjes and Dijkshoorn (1999)
Africa	Singh (1993)		
Asia	Singh (1993); Brown et al. (1993)		[7] Chhabra et al. (2003)
TEMPERATE GRASSLANDS			[8] Genxu et al. (2002) [9] Nilsson et al. (2000)

Using Siltanen et al.'s (1997) estimate for the Canadian boreal forest (6.8 $kgC \cdot m^{-2}$, 404 Mha), and the latest estimates for the Russian taiga (15.3 $kgC \cdot m^{-2}$, 881 Mha) (Nilsson et al. 2000) and the Alaskan forest (23.1 $kgC \cdot m^{-2}$, 52 Mha) (Birdsey and Heath 1995), we estimate approximately 13 $kgC \cdot m^{-2}$ for the mineral soil of the boreal forest as a whole, with values ranging from 8.5 to 13 $kgC \cdot m^{-2}$ (once the estimates from the studies that used ORNL data are adjusted, Blais 2003). This range is now comparable to that of temperate and tropical forests.

Although boreal mineral soils do not appear to store more organic carbon than temperate and tropical soils, large deposits of peat are found in northern regions, with an estimated stock of around 400 PgC (Gorham 1991; Zoltai and Martikainen 1996) compared to 144 PgC for tropical regions (Zoltai and Martikainen 1996) (Table 6.3). Estimates of SOC densities for peatlands vary greatly among studies (39 to 288 $kgC \cdot m^{-2}$) (Table 6.3), partly as a result of the use of different integration depths (from 0.5 to 3.5 m).

Moreover, the amount of carbon stored in the forest floor (including litter, duff, humus, and small woody debris) above the mineral soil can be quite important at northern latitudes under forest cover (Eswaran et al. 1993). According to data in Table 6.4, the litter layer would store between 0.3 to 5.5 $kgC \cdot m^{-2}$ in northern forests but only 0.1 $kgC \cdot m^{-2}$ in tropical ones, as a result of high turnover rates of litter under warm temperatures. Vucetich et al. (2000) found no difference in the litter layer carbon content between latitudes 50°N and 70°N for stands of Scots pine (*Pinus sylvestris*). On the other hand, Simmons et al. (1996, cited in Vucetich et al. 2000) report that mature deciduous forests in north-eastern North America have thicker forest floors and a slower C and N turnover in cool and dry regions (2°C, precipitation ~900 mm) compared to warm and wet ones (6.2°C, precipitation ~1,400 mm). In addition to climate, there seems to be a relationship between the age of the forest and the litter layer thickness (Auclair 1985; Conkling et al. 2002), but it still has not been clearly established (Vucetich et al. 2000; Klopatek 2002). In the boreal region, the litter layer's thickness is also related to the time of the last forest fire (Rapalee et al. 1998).

Most estimates from Table 6.1 neglect the vast amount of carbon stored as peat and in the forest floor. SOC densities estimated by Dixon et al. (1994) for the boreal forest, shown in Table 6.1, are three times higher when peatlands are included compared to mineral soils alone. Likewise, Schlesinger (1984), who not only included the litter and some data from forested peatlands but also data from depths greater than 1 m, estimated a value (20.6 $kgC \cdot m^{-2}$) generally exceeding SOC estimates for the mineral

Table 6.3. Carbon density ($kgC \cdot m^{-2}$) of peatlands of different regions

Location	Study area	Surface area [Mha]	Stock [PgC]	Average [$kgC \cdot m^{-2}$]	Sampling depth [m]	References
GLOBAL/REGIONAL SCALE						
BOREAL REGION						
World	Boreal and subarctic peatlands	335	448	134	2.3	Gorham (1991)
Canada	Canadian peatlands	111	134	121[a]		CCMF (1997)
Russia		139	54	39[a]		Alexeyev and Birdsey (1994)
		139	138	99[a]		Kolchugina et al. (1992)
		139	115	83[a]		Vompersky (1994) Efremova et al. (1997)
	Bog			81	1	Nilsson et al. (2000)
Soviet Union	Wetlands			130 (40-239) 39 to 134	0.5–3.5	Botch et al. (1995)
TEMPERATE AND BOREAL REGIONS						
World	Northern peatlands	302	397	131		Zoltai and Martikainen (1996)
TROPICAL REGION						
World	Tropical peatlands	50	144	288		Zoltai and Martikainen (1996)
SITE-SPECIFIC STUDIES						
Canada (MA)	Palsa, fen and collapse scar bog			59-144		Rapalee et al. (1998)

Table 6.4. Organic carbon density ($kgC \cdot m^{-2}$) of the litter layer of boreal and temperate forests

Countries	Regions	Lat.	Long.	Air Temp. [°C]	Precipitation [$mm \cdot y^{-1}$]	Type of forests	Age [yr]	Average content [$kgC \cdot m^{-2}$]	Reference
BOREAL FOREST									
Canada	Grande-Baleine (QC)	56°N	76°W	-5	685	Spruce-lichen-moss forest		2.2[a]	P-T & G-G (1993)
	Laforge (QC)	54°N	72°W	-5	750	Spruce-lichen-moss forest		2.7[a]	P-T & G-G (1993)
	La Grande (QC)	54°N	76°W	-3.5	680	Spruce-lichen-moss forest		3.2[a]	P-T & G-G (1993)
	Nottaway-Broadback-Rupert (QC)	50°N	76°W	-1.5	710	Coniferous forest		3.4[a]	P-T & G-G (1992)
	Ashuapmushuan (QC)	49°N	73°W	-0.5	950	Coniferous and deciduous forest		3.4[a]	P-T & G-G (1992)
	Haut St-Maurice (QC)	48°N	73°W	1	1000	Coniferous and deciduous forests		3.3[a]	P-T & G-G (1992)
	Schefferville (QC)	56°N	67°W			Spruce-lichen forest	47 to 110	1.8 (47 yr) to 2.5 (110 yr)	Auclair (1985)
	NSA, BOREAS (MA)					Spruce-moss forest and jack pine stands	13->90	0.8 to 4.8	Rapalee et al. (1998)
Alaska						Spruce moss forest		3.8 to 5.5	Van Cleve et al. (1981)
Finland		70°N	27°E	-1	~450	Scots pine forest	66, 98, 178	1.5 (98 yr) to 2.6 (66 yr)	Vucetich et al. (2000)
						Range (min-max)		0.8 to 5.5	

Table 6.4. (cont.)

Countries	Regions	Lat.	Long.	Air Temp. [°C]	Precipitation [mm·y^{-1}]	Type of forests	Age [yr]	Average content [kgC·m^{-2}]	Reference
TEMPERATE FOREST									
Belgium		51°N	4°E	10.1	791	Oak-beech forest	80	3.6	Vande Walle et al. (2001)
Lithuania		55°N	26°E	6	~600	Scots pine forest	116	2.2	Vucetich et al. (2000)
Poland		50°N	23°E	8	~600	Scots pine forest	68	3.9	Vucetich et al. (2000)
USA	Washington					Douglas fir forest	20, 40, mature	1.2 (20 yr) to 1.6 (40 yr)	Klopatek (2002)
	Georgia					Oak-hickory and oak-pine forests	26-37	0.3	Conkling et al. (2002)
	Georgia					Pine forest	14 and 48	0.6 (14 yr) to 1.0 (48 yr)	Conkling et al. (2002)
	Oregon	44°N	122°W	7.5	552	Ponderosa pine forest	15 and 50/250	0.7 (15 yr) to 1.2 (50/250 yr)	Law et al. (2001)
						Range (min-max)		0.3 to 3.9	

[a]: Weighted average for the various stands (willow and alder forest, peatlands, burn, regenerated burn, open spruce- lichen stand, open spruce-moss stand, young spruce stand). Poulin-Thériault (1992) used a maximum sampling depth of 20 cm. Poulin-Thériault (1993) sampled the L, F and H horizons down to 60 cm.

soil. Therefore, including peat and forest floor organic carbon would change the overall picture and result in the boreal biome having the largest SOC density.

SOC densities are more often estimated for the top first meter. However, many soils are thicker than 1 m (Batjes 1996) and large amounts of carbon can be stored at greater depths (Sombroeck et al. 1993; Tarnocai 1994). For example, Amazonian soils can reach 8 m in thickness due to long periods of weathering, with as much as 15.5 $kgC \cdot m^{-2}$ stored between 1 and 8 m (Trumbore et al. 1995). Northern peatland soils (i.e. histosols), which have a high organic carbon content (77.6 $kgC \cdot m^{-2}$: Batjes 1996), are on average 2.3 m deep (Gorham 1991). Adding the second meter's would increase by 180% the carbon density estimated from the first meter (Batjes 1996). In a coniferous forest of Finland, Liski and Westman (1995) report that 18 to 28% of the podzol soil's total carbon stock is stored between 1 m and the water table depth (2.4 to 4.6 m). In Russia, 25% of the carbon would be found between 1 and 2 m, indicating an important flux of dissolved organic carbon typical of boreal humid soils (Nilsson et al. 2000). These results indicate the need to consider the deep layers of soils in order to correctly assess the total amount of carbon stored in them. Therefore, the soil total carbon density is probably underestimated when the first meter of the soil profile is considered, especially for thick soils with high organic carbon content, such as those found under tropical and boreal latitudes.

6.3 Physical and Biological Factors Affecting SOC Density

As indicated by the high coefficients of variation of the estimates from Table 6.1 (CV ranging from 42 to 110%), the distribution of organic carbon in soils is characterized by a high spatial variability (Post et al. 1999). Likewise, the range of values of SOC densities measured at different sites within the boreal, temperate and tropical forests (3 to 20 $kgC \cdot m^{-2}$) is quite large (Table 6.5). Even at a small scale (48 m^2), Liski (1995) obtained a CV of 21% for 126 soil profiles (0.01 m^2) sampled in a Scots pine forest.

This large spatial heterogeneity of SOC implies that many factors control the organic carbon distribution in soils from global to local scales. These factors primarily include climate, soil texture (clay content), topography, vegetation, land-use, parent material and the age of the soil profile (Schimel et al. 1994; Schlesinger 1997).

Climatic conditions (temperature and precipitation) exert a strong influence on the amount of organic carbon stored in soils (Schlesinger 1997).

Table 6.5. Organic carbon density ($kgC \cdot m^{-2}$) of the mineral soil of different sites in the boreal, temperate and tropical forests

Countries	Type of forests	Age	Type of soil	Average content [$kgC \cdot m^{-2}$]	Sampling depth [m]	Reference
BOREAL FOREST						
Canada (SK)	Aspen poplar			3.6		Gower et al. (1997)
Canada (MA)	Spruce forest	13 to > 90	Poor drainage	9.6 to 19.7[a]	0.2 to 5	Rapalee et al. (1998)
Canada (MA)	Cypress pine	30 to > 90	Good drainage	2.8 to 3.1	0.2 to 5	Rapalee et al. (1998)
Finland	Scots pine stands	66, 98, 178	Sandy	2.7 to 4.7	0.25	Vucetich et al. (2000)
		Range (min-max)		2.7 to 19.7		
TEMPERATE FOREST						
Belgium	Oak-beech and ash stands (tree density ~ 375 trees/ha)	80		13.5 to 17.1	1	Vande Walle et al. (2001)
Belgium	Oak-beech and ash stands			10.2 to 12.2	1	Nabuurs and Mohren (1995)
Belgium	Scots pine stands		Sandy	11.5	1	Janssens et al. (1999)
Netherlands	Mixed stands (pine, fir, larch, spruce, oak, beech, etc.)	50–60		6.4 to 20.7		Nabuurs and Mohren (1995)
Lithuania and Poland	Scots pine stands	68, 116	Sandy	5.0	0.25	Vucetich et al. (2000)
USA (WA)	Douglas fir stands	20, 40, 450-550		9.7 (mature) to 15.7–17.5 (young)	0.2	Klopatek (2002)
USA (GA)	Mixed forest (pine, oak-hickory, oak-pine)	25-37		2.8 to 3.1	0.2	Conkling et al. (2002)
USA	Mixed forest (oak-pine, douglas fir-fir, spruce-fir, etc.)			6.5 to 15.1		Turner et al. (1995)

Table 6.5. (cont.)

Countries	Type of forests	Age	Type of soil	Average content [kgC·m^{-2}]	Sampling depth [m]	Reference
USA (GA)	Mixed forest (pine, oak-hickory, oak-pine)			7.7	1	Birdsey (1996)
USA (GA)	Mixed forest (pine, oak-hickory, oak-pine)			4.5 to 7.5	1	STATSGO
USA (OR)	Ponderosa pine stands	15 and 50/250		4.3 (15) to 5.3 (50/250)	1	Law et al. (2001)
		Range (min-max)		2.8 to 20.7		
SUBTROPICAL FOREST						
USA (NC)	Oak, hickory, maple, birch stands	>50		9.5		Mattson and Swank (1989)
USA (FL)	Tropical pine stands	25		10.6		Harding and Jokela (1994)
USA (GA)	Oak, hickory, pine stands	60-80 and mature	Sandy	8.2 to 12.2 (mature)		Huntington (1995)
USA (South-West)	Mixed forest (spruce-fir, maple-beech, etc.) and surrounding peatlands			4.2 to 7.5[b]	1	Heath et al. (2002)
USA	Mixed forest (pine, oak-cypress) and surrounding peatlands			16.6 to 18.2[b]	1	Heath et al. (2002)
		Range (min-max)		4.2 to 18.2		
TROPICAL FOREST						
Venezuela	Semi-deciduous forest			12.2	1	San Jose et al. (1998)

[a]: Includes peatlands.
[b]: Includes litter layer.

Within a given biome, more carbon is usually found in soils where precipitations are highest and temperature coldest, due to slower rates of microbial degradation. For example, Post et al. (1982) report a difference of a factor 2 between SOC densities of moist (11.6 $kgC \cdot m^{-2}$) and wet (19.3 $kgC \cdot m^{-2}$) boreal forests. According to Schimel et al. (1994), SOC density is correlated to mean annual temperature by a negative exponential function. At a regional scale, a decline in SOC density along with a temperature increase and precipitation decrease was observed by Burke et al. (1989) in the Central Grasslands of USA and by Homann et al. (1995) in Western Oregon forests. Kern et al. (1997) also report for the West coast of USA, relationships between SOC density and actual evapotranspiration, mean annual precipitation and available soil holding capacity.

Other factors, not well correlated with climate, affect the SOC content, such as soil texture (clay content). The relationship between SOC density and clay content is possibly one of the best established after those involving climatic factors (Schimel et al. 1994). Several authors have observed a relationship between SOC density and clay content (Burke et al. 1989; Homann et al. 1995; Moraes et al. 1995; Jobbagy and Jackson 2000) or related variables such as soil drainage (Davidson and Lefebvre 1993; Rapalee et al. 1998) and water holding capacity (Kern et al. 1997). Such relationships would reflect the strong interaction between clay minerals and organic carbon to form stable organo-mineral aggregates (Lal and Kimble 2001).

Topography also influences the SOC content and varies, as does clay content, independently of climate. Homann et al. (1995) and Manies et al. (2001) have found a lower SOC content in steeper sites within western Oregon forests and prairies from Iowa.

Vegetation characteristics, such as stand age and specific composition, do not usually show as strong a relationship with SOC density as the previous variables. However, land-use change such as forest conversion to agricultural lands is known to have induced an important decrease (10 to 25%) of the carbon content of soils (Moraes et al. 1995; Trumbore et al. 1995). Moreover, Grigal and Ohmann (1992) have concluded that the SOC content of forests around the Great Lakes varies significantly with forest type, as well as, but to a lesser extent, with stand age, water retention capacity, actual evapotranspiration and clay content. Using the type of vegetation as a fertility indicator, Liski and Westman (1995) have also observed an increase in the SOC content as a function of fertility for 30 sites of mature coniferous forests in Finland. Stand age has been found to have opposite effects on SOC (Law et al. 2001; Klopatek 2002), or no effect at all (Rapalee et al. 1998).

6.4 Uncertainties of SOC Estimates

Estimates of mineral SOC density are quite variable (factor 2 difference) from one study to another for a given biome (Table 6.1). A large part of the uncertainties of currently available estimates arises from a) data processing approaches, which, for example, integrate to different extents the environmental variables controlling SOC distribution when extrapolating site-specific data to a larger scale, or use different integration depths, b) the small number of data relied upon given the high spatial heterogeneity of SOC, c) the biased spatial coverage of pedon data, with some regions being more represented than others, and d) poor reliability of available bulk density and organic carbon content (%) estimates used to calculate SOC density.

The uncertainty related to current estimates of SOC density for forest biomes can be due to authors taking into account none or only a few environmental variables affecting the distribution of SOC when extrapolating site-specific measures to a global scale (biome). For example, some authors simply average site-specific data for a given biome, as if it was a homogeneous category (Schlesinger 1984; Jobbagy and Jackson 2000; Batjes 1996). Others will group carbon data per bioclimatic regions before extrapolating to the biome (Post et al. 1982; Siltanen et al. 1997; Kurz and Apps 1999). Some will add an additional step to the former by grouping data by country, considering possible differences in the SOC densities between regions and countries within a given biome (Dixon et al. 1994; Goodale et al. 2002). Finally, some authors (Batjes and Dijkshoorn 1999) working on Amazonian data have grouped their data following the SOTER (Soils and Terrain) approach, which allows to consider physiographic characteristics (topography, parent material, etc.) before attributing a SOC density value to a given area.

Large differences in SOC density estimates arise when the influence of environmental conditions are not taken into account during extrapolation. For example, Davidson and Lefebvre (1993) have found a 49% difference between estimates obtained from simple averaging of all data and averaging of stratified data according to soil maps. Bhatti et al. (2002) have also found large differences when comparing results for three regions (subarctic, boreal, grassland) in some Canadian provinces (Alberta, Saskatchewan, Manitoba). These differences range from –43% to 16% between estimates based on data from Siltanen et al. (1997) (average by region) and those derived from the Canadian Soil Organic Carbon Database, which takes into account the spatial coverage and SOC content of various soil types within each region.

Current estimates of the amount of carbon stored in forest biomes rely on a relatively small number of soil profiles to represent large areas. The lack of data considerably limits the precision of the estimates, as well as prevents, in many cases, the stratifying of data before extrapolation.

The lack of spatially representative data, with data coming only from certain regions of a biome, is a problem recognized by several authors as greatly limiting the capacity to obtain accurate estimates of SOC at global scales (Eswaran et al. 1993; Batjes 1996). Often, databases do not detail the geographic location of their soil profiles (FAO-UNESCO) or pool together data from studies pursuing different goals (Canadian Forest Service Database). However, there are no statistical methods for correcting potential bias due to soil profiles that have not been sampled randomly. Better estimates could be obtained if sampling was stratified and representative sites were selected (Liski and Westman 1995).

Furthermore, the lack of measured data of organic carbon content (%) and bulk density, especially in peatlands and in the former USSR and Mongolia, is another problem in obtaining reliable estimates of SOC densities (Eswaran et al. 1993). Very often, bulk density must be estimated from imprecise models (Post et al. 1982; Siltanen et al. 1997; Chhabra et al. 2003). In peatlands, measurements of the maximum depth are lacking (Botch et al. 1995).

6.5 Organic Carbon in Vegetation

Tropical forests store larger amounts of carbon into plant biomass than northern forests. Estimates of carbon stored in the vegetation of the Amazonian tropical forest range from 15.2 to 23.3 $kgC \cdot m^{-2}$ (Table 6.6). However, the global biomass of tropical forests would be less, close to 12.1 $kgC \cdot m^{-2}$ (Dixon et al. 1994), when including dry tropical forests, which cover about the same surface area as tropical rainforests but with half the biomass (Schlesinger 1997). Overall, the biomass of tropical rainforests is approximately two to five times greater than that of boreal (4.0 to 6.4 $kgC \cdot m^{-2}$) and temperate forests (4.8 to 5.7 $kgC \cdot m^{-2}$) (Table 6.6).

The greater biomass of the Amazonian tropical forest, compared to that of northern ones, is due to its higher productivity. Plant photosynthetic activity is stimulated by the warmer temperatures and higher humidity and light intensity found at tropical latitudes (Clark 2002). As such, the productivity rate of the Amazonian rainforest, which is close to the maximum potential growth rate of vegetation (1.3 $kgC \cdot m^{-2} \cdot yr^{-1}$), is almost twice the

Table 6.6. Organic carbon biomass (kgC·m^{-2}) in vegetation[a-b] of different biomes

	Dixon et al. (1994) 1987–1990	Goodale et al. (2002) ~1987–1995	Myneni et al. (2001) 1995–1999	Recent regional studies [ref. n°] (see Table 6.7)
BOREAL FOREST	6.4	4.8[f] (3.8)[c]	4.0[f]	
Canada	2.8	4.6 (3.6)[c]	4.4	~1988: (2.3)[h] Botkin and Simpson (1990)
Alaska	3.9	(4.6)[c]	n.a.[g]	
Russia	8.3	4.9 (3.9)[c]	3.8	1993: 6.1[f] (4.0)[c] [1]
TEMPERATE FOREST	5.7	4.8[f] (4.6)[c]	4.8[f]	
Australia	4.5			
United States	6.2	(5.9)[c]	5.8[g]	1989-90: 8,1 (6.3)[c] [2]
Europe[e]	3.2	4.6 (4.1)[c]	5.5	England 1980: ((3.7))[d] [3]; Netherlands, 1984–89: ((5.9))[d] [4]
China	11.4	(3.3)[c]	2.6	
MOIST TROPICAL FOREST	12.1			
Americas	13.0			19,2 [5]; 15.2[h] (13.7)[c] (RADAMBRASIL) [6]; 23.2 (RADAMBRASIL) [7]; 18.3 [8]
Africa	9.9			
Asia	13.2–17.4			India : ((3.2))[d] [9]

[a]: Includes the aboveground and belowground vegetation, the understory (shrubs and herbaceous plants), coarse woody debris (CWD) such as standing dead trees and macroscopic debris (> 2 mm). Goodale et al. (2002) included CWD from forest exploitation in addition to those produced naturally.
[b]: The following studies have included woodlands (eg. from the subartic region) in their estimates: Dixon et al. 1994; Goodale et al. 2002 (except for China); Cannell and Milne (1995); Nabuurs and Mohren (1995). The following studies have excluded woodlands: Houghton (1999); Turner et al. (1995).
[c]: Values in parenthesis exclude coarse woody debris.
[d]: Values in double parenthesis exclude both coarse woody debris and the understory.
[e]: Estimates for Europe include northern countries such as Finland and Sweden.
[f]: Values calculated from data published in the referenced paper.
[g]: Alaska is included in the coterminous USA.
[h]: The original value was multiplied by 1.2 to take into account a root/stem ratio of 0.2 (Houghton et al. 2001) and by 0.5 to convert anhydrous biomass into carbon mass (Schlesinger 1997).

productivity rate of temperate forests (0.8 $kgC \cdot m^{-2} \cdot yr^{-1}$) and close to seven times that of boreal forests (0.2 $kgC \cdot m^{-2} \cdot yr^{-1}$) (Roy et al. 2001).

In addition to its higher productivity, the more stable natural conditions prevailing (i.e., fewer disturbances) in the tropical rainforest have also contributed to its accumulation of a larger amount of carbon as biomass (Turcq et al. 2002). The undisturbed rainforest is typically uneven-aged, which is characteristic of a forest at an advanced stage of succession. The large trees found in this forest, which can be 200 years old (diam. ~80 cm, 1/ha) (Cummings et al. 2002) or even older (500 to 1400 years old, >250 cm diam., Chambers et al. 1998), testify of the stability of environmental conditions over the past centuries (Turcq et al. 2002). On the opposite, the frequent recurrence of forest fires and insect outbursts in northern forests greatly limit carbon storage in the biomass. Large areas of the boreal forest are regularly burned or devastated by insect infestations (CCMF 1997). As a result, the boreal forest is typically composed of a mosaic of even-aged stands, each being at a more or less advanced stage of regeneration. Given a forest fire cycle of 40 to 500 years (Bergeron 1991; Payette 1992), depending on the region, old stands in the boreal region are no more than a hundred years old (on average).

The biomass of the boreal forest has decreased markedly since the beginning of its exploitation. But contrary to the deforestation of tropical forests, the boreal forest is usually replanted to establish new growth for future harvest (Botkin and Simpson 1990). Tropical forests, especially the Brazilian forest, are under intense deforestation and conversion to other land uses (Schroeder and Winjum 1995). Since the beginning of the 20th century, nearly 30% (170 Mha) of the initial surface area of the Amazonian rainforest (540 Mha) has been converted mostly to agriculture and cattle raising and only 20% of the affected area has regenerated as secondary forests. The biomass of the temperate forest has also decreased over the past centuries following colonization (Kauppi 1992). There are practically no remaining original natural stands in temperate forests (Kauppi 1992), which have been replaced by secondary forests or plantations under extensive exploitation or not.

Estimates of boreal and temperate forests biomass of relatively intact and mature stands (9.0 $kgC \cdot m^{-2}$ for the boreal forest and 15.0 $kgC \cdot m^{-2}$ for the temperate forest, Whittaker and Likens 1973; Atjay et al. 1979; Olson et al. 1983, 1985; Houghton 1999) are higher than recent ones based on forest inventories and including the effect of natural and anthropogenic perturbations (4.0 to 6.4 $kgC \cdot m^{-2}$ for the boreal forest and 4.8 to 5.7 $kgC \cdot m^{-2}$ for the temperate forest, Table 6.6). Biomass estimates for the tropical rainforest, which most often represent undisturbed forest, would be reduced slightly if considering the lower biomass of secondary forests

(4.6 kgC·m^{-2}, Olson 1983, 1985), whose areas are relatively small (35 Mha compared to 370 Mha of intact forest, Stone et al. 1994, cited in Schroeder and Winjum 1995). This is because deforested areas, converted to agricultural use, are no longer accounted for in forest statistics, contrary to replanted areas in northern regions. Lal and Singh (2000) included both natural and disturbed forests in their estimate of the Indian forest biomass (3.2 kgC·m^{-2}), which explains why their estimated value is lower than Dixon et al.'s (1994) estimate for Asian forests (13.2 to 17.4 kgC·m^{-2}) based mostly on intact forests.

6.6 High Spatial Heterogeneity of Biomass

The distribution of biomass in forests is characterized by an important spatial heterogeneity. Estimates of biomass vary considerably from site to site within a biome, ranging from 0.8 to 12.3 kgC·m^{-2} in the boreal forest, 2.1 to 17.7 kgC·m^{-2} in the temperate forest and 5.8 to 31.9 kgC·m^{-2} in the tropical rainforest (Table 6.8). As an example, Fearnside et al. (2001) measured a coefficient of variation of 51% within 6 replicates of a plot under study in Manaus, Brazil.

In the boreal forest, this high variability in biomass is related to variations in edaphic conditions, natural disturbances (forest fire and insect defoliation) and cutting in exploited regions (Botkin and Simpson 1990). In tropical rainforests, the biomass varies according to the distribution of large trees, which contribute significantly to the forest's biomass (Cummings et al. 2002). The presence/absence of large trees can be affected by catastrophic climatic events (forest fire or windfall) (Nelson et al. 1994) or soil nutrient availability (Brown and Lugo 1992).

Variations in climate, edaphic factors and disturbances result in species, age, growth rate and density differences between sites, all affecting the carbon storage as biomass. For example, Law et al. (2001) measured a biomass 12 times greater in a mature (50–250 years) pine stand than in a similar stand of 15 years of age. Moreover, subarctic woodlands, which are sparse and unproductive forests, have a biomass two to three times smaller than that of forests located more in the south. The exclusion of subarctic woodlands in Turner et al.'s (1995) estimate for US forests would explain why they obtain higher values compared to other studies which included them (Table 6.6).

Table 6.7. References cited by authors from Table 6.6

	Dixon et al. (1994)	Goodale et al. (2002)	Other recent studies [ref. n°]
BOREAL FOREST			
Canada	Apps and Kurz (1991); Kurz and Apps (1993)	Kurz and Apps (1999)	
Alaska	Birdsey et al. (1993); Turner et al. (1995)	Birdsey and Heath (1995)	
Russia	Krankina and Dixon (1994); Kolchugina and Vinson (1993)	Nilsson et al. (2000); Shvidenko et al. (2000)	[1] Kokorin et al. (1996)
TEMPERATE FOREST			
Australia	Gifford et al. (1992)		
United States	Birdsey et al. (1993); Turner et al. (1995)	Birdsey and Heath (1995)	[2] Turner et al. (1995)
Europe	Kauppi et al. (1992)	UNECE/FAO (2000)	[3] Cannell and Milne (1995) [4] Nabuurs and Mohren (1995)
China	Deying (1992)	Fang et al. (2001)	
TROPICAL FOREST			
Americas	Singh (1993)		[5] Houghton et al. (2001) [6] Brown and Lugo (1992)[a] [7] Fearnside (1997)[b] [8] Brown (unpublished data)[b]
Africa	Singh (1993)		
Asia	Singh (1993); Brown et al. (1993)		[9] Lal and Singh (2000)

[a]: Cited in Schroeder and Winjum (1995)
[b]: Cited in Houghton et al. (2001)

Table 6.8. Organic carbon stored in the vegetation ($kgC \cdot m^{-2}$) (generally including the above- and belowground parts of trees, the understory and coarse woody debris) at different sites in the forested biomes

Country		Type of forest	Age [yr]	Mean (± CV%) [$kgC \cdot m^{-2}$]	Min.	Max.	Measurement methods	Reference(s)
BOREAL FOREST								
Canada	Grande-Baleine (QC)	Sphagnum and lichen spruce forests		1.5[a]			Destructive sampling (understory and dead woody debris) and allometric equations (living trees). A total of 186 plots sampled for the tree stratum.	Poulin-Thériault & Gauthier-Guillemette (1993)
Canada	Laforge (QC)	Sphagnum and lichen spruce forests		1.7[a]				
Canada	La Grande (QC)	Sphagnum and lichen spruce forests		2[a]				
Canada	NBR (QC)	Coniferous forests		2.8[a]				P-T & G-G (1992)
Canada	Schefferville (QC)	Lichen-spruce forests	47 to 110	1.8[a] (47 yr) to 2.3[a] (110 yr)			n.a.	Auclair (1985)
Canada	SSA, BOREAS (SK)	Spruce stand	115	6.7			n.a.	Malhi et al. (1999)
Canada	SSA, BOREAS (SK)	Aspen stand		12.3 (9.9)			n.a.	Gower et al. (1997), Chen et al. (1999)
Finland		Scots pine forest	66	(4.1)			Allometric equations, 3 sample plots (0.04 ha/site), 3 sites	Vucetich et al. (2000)
Finland		Scots pine forest	98	(5.1)				
Finland		Scots pine forest	178	(2.8)				
Russia		Larch forests (North and south forests)	120	(1.8)-(7.7) N (10.1) S			Literature review (60 studies) including 360 sample plots	Usol'tsev and Koltunova (2001)
USA	Alaska	Sphagnum-spruce forests		0.8[a] to 1.2[a]				Van Cleve et al. (1981)
		Range (min-max)		0.8[a] to 12.3				

Table 6.8. (cont.)

Country		Type of forest	Age [yr]	Mean (± CV%) [kgC•m^{-2}]	Min.	Max.	Measurement methods	Reference(s)
TEMPERATE FOREST								
Belgium		Ash stand (403 trees/ha)	80	15.1			Destructive sampling (understory and roots) and allometric equations (trees), 10 plots (0.003 ha) in each stand.	Vande Walle et al. (2001)
Belgium		Oak-beech stand (345 trees/ha)	80	15.7				
Russia		Larch forests (North and south forests)	120	(11.1) N - (17.7) S			Literature review (60 studies) including 360 sample plots	Usol'tsev and Koltunova (2001)
Netherlands		Various stands (alder, pine, … oak)		((3.1))-((12.4))			Forest inventory data (growing stock volumes)	Nabuurs and Mohren (1995)
England		Coniferous and deciduous forests		((2.1)) C - ((5.8)) D			Forest inventory data (growing stock volumes)	Cannell and Milne (1995)
USA	Oak Ridge	Deciduous forest	55	8.5			n.a.	Malhi et al. (1999)
Lithuania		Scots pine forest	116	(11.5)			Allometric equations, 3 sample plots (0.04 ha/site), 3 sites	Vucetich et al. (2000)
Poland		Scots pine forest	68	(10.5)				
Australia		Pine plantation	20	(7.1)			n.a.	Ryan et al. (1996)
New Zealand		Pine plantation	8	(3.8)[a]			Allometric equations, 1 site (0.08 ha)	Arneth et al. (1998)
USA	North Carolina	Pine plantation (1700 trees/ha)	15	(6.1)	(4.9)	(7.0)	Allometric equations	Hamilton et al. (2002)
USA	Oregon	Pine plantation	15	4.9 (1.5)[a]			Allometric equations, 5 plots (0.03 ha)	Law et al. (2001)
USA	Oregon	Pine stand	50/250	14.4[a] (12.7)			Allometric equations, 5 plots (0.03 ha)	Law et al. (2001)
		Range (min-max)		((2.1)) to (17.7)				
DRY TROPICAL FOREST								
Venezuela		Semi-decidous forest		((9.2))			Allometric equations, 1 site	San Jose et al. (1998)

Table 6.8. (cont.)

Country		Type of forest	Age [yr]	Mean (± CV%) [kgC·m^{-2}]	Min.	Max.	Measurement methods	Reference(s)
RAINFOREST[b]								
Brazil	Amazonia	Rainforest	Mature	19.2[a]	5.8	24.7	Literature review. Allometric equations and forest inventory data (growing stock volumes) (11/44 sites), total of 44 sites (0.4 to 415 ha)	Houghton et al. (2001)
Brazil	Rondônia	Rainforest and ecotone (savanna)	Mature	20.1[a] ± 19%	17.3	31.9	Allometric equations. All components measured. 20 sites (0.8 ha)	Cummings et al. (2002)
Brazil	Manaus	Dense moist tropical forest	Mature	22.1[a] ± 51%	16.5	31.2	Destructive sampling. 6 sites (0.006 ha)	Fearnside et al. (2001)
Brazil	Manaus	Rainforest	Mature	21.3[a] ± 13%			Allometric equations, 65 sites (1 ha)	Laurance et al. (1999)
Brazil	Manaus	Rainforest	Mature	28.5			n.a.	Malhi et al. (1999)
Brazil	Pará	Rainforest	Mature	21.3-24.7[a]			Allometric equations, 4 transects (20 ha)	Rice et al. (2004)
Brazil	Amazonia	Rainforest	Mature	21.7[a]	17.6	26.1	6 sites (slashed forests)	Kauffman et al. (1995), Guild et al. (1998)
		Range (min-max)		19.2 to 28.5	5.8	31.9		

( ) or (( )): Values in parenthesis exclude coarse woody debris ( ) and understory (( )).
[a] : Values were multiplied by 1.2 to take into account a root/shoot ratio of 0.2 (Houghton et al., 2001; Hamilton et al., 2002), as well as by 0.5 to convert dry mass values into carbon mass (Schlesinger, 1997).
[b]: Only Kauffman et al. (1995) study is included in Houghton et al. (2001) review. All other studies for the rainforest were published after Houghton et al. (2001) review.

6.7 Uncertainties in Evaluating the Organic Carbon in Vegetation

Carbon density estimates of forest biomass vary considerably from one study to another for the same biome (Table 6.6). Part of the difference between biomass estimates for boreal and temperate forests is due to different sampling period lengths. For example, Goodale et al. (2002) estimated a higher biomass for Alaskan and European forests (4.6 $kgC \cdot m^{-2}$ each) using 5 additional years (1987–1995) of green biomass growth (Fig. 6.1) compared to Dixon et al. (1994) who estimated 3.9 and 3.2 $kgC \cdot m^{-2}$ respectively (1987-1990).

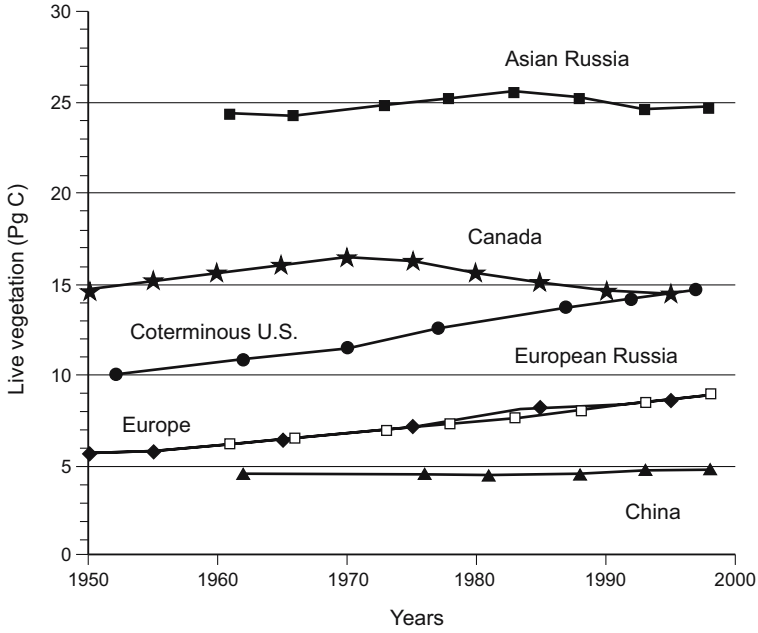

Fig. 6.1. Evolution of the green biomass (PgC) over the past 50 years in countries of the Northern Hemisphere. Source: Goodale et al. (2002)

The large spatial heterogeneity of biomass and difficulties in taking into account this heterogeneity when assessing the carbon stock of an entire forest or biome can also explain why the available estimates of forest biomass are so variable. Few studies, in particular in tropical regions, are based on a sufficient number of data and appropriate methods to integrate the large variability and estimate a carbon stock in vegetation representative of the entire biome.

In many countries of the northern hemisphere (Canada, USA, Europe, Russia and China), forest inventories are statistically devised to estimate growth and wood volumes across large heterogeneous areas. Over the entire northern hemisphere, there are approximately 1 million sample plots (Goodale et al. 2002), which makes it possible to estimate the total wood volume to within 1–5% with a 95% confidence level (Powell et al. 1993; Shvidenko and Nilsson 1997, cited in Goodale et al. 2002). New methods using remote sensing (Mynemi et al. 2001) are powerful tools for containing spatial heterogeneity, but are still uncertain. In Table 6.6, most estimates of forest biomass for northern regions (except Botkin and Simpson 1990) are derived from forest inventory data.

All the uncertainty in using forest inventory data comes from the conversion of wood volumes into carbon stock of an entire forest (Dixon et al. 1994). Wood volumes are calculated from the DBH (diameter at breast height) of trees of merchantable size and essence measured during forest inventories. However, additional steps using allometric equations, conversion factors or models (Kurz and Apps 1999) are required to estimate from wood volumes the biomass of vegetation components which are not directly measured during forest inventories, such as the different parts of trees (branches, roots), the understory, young trees and coarse woody debris (Heath et al. 2002).

Conversion factors can be somewhat complex and more or less consider variables affecting carbon allocation between tree parts (trunk, branches and roots) or vegetation components. Carbon allocation varies from one species to another (Turner et al. 1995), according to site characteristics, with stands growing on poor and dry soils tending to allocate more carbon to roots (Vande Walle et al. 2001), and stand age, with the proportion of woody tissue increasing with age (Vande Walle et al. 2001). In the tropical forest, the understory may represent an important component of the forest biomass (especially in low density forest), and there is no reason not to suspect the same pattern in temperate and boreal forests. Yet, the understory biomass is thought to represent a very small component of an entire forest biomass, and is often assessed as a constant fraction of the total wood volume (Goodale et al. 2002).

The use of species and region-specific conversion factors has led to a decrease of the carbon densities of Russia's and China's forest biomass between earlier studies (Dixon et al. 1994) and more recent ones (Kokorin et al. 1996; Goodale et al. 2002) (Table 6.4). Moreover, revised estimates of stocks of coarse woody debris (CWD) in Canada and Europe are partly responsible for the higher values of forest carbon densities estimated by Goodale et al. (2002) compared to Dixon et al. (1994) for Canada (4.3 vs. 2.8 $kgC \cdot m^{-2}$) and Europe (4.6 vs. 3.2 $kgC \cdot m^{-2}$) (Table 6.6). Such estimates

of CWD would be based on more data and improved methods to quantify the effect of disturbances on CWD production and dead organic matter dynamic (Kurz and Apps 1999; Goodale et al. 2002). The readjustment would have been proportionately more important for Canada, which has seen its green biomass decrease since 1970 because of forest fires and insect outbursts (CCMF 1997).

The uncertainty surrounding biomass estimates appears greater in tropical forests, because of a general lack of detailed national forest inventories. Although some studies used the forest inventory approach, there is no structured network of sampling plots in tropical regions, such as in the northern hemisphere (Clark 2002), but rather regional surveys (Brown and Lugo 1992; Philips et al. 1998). A more direct approach involving the measurement of the biomass of all vegetation components through allometric equations and/or destructive sampling is more often used. The increased effort involved at each site however greatly limits the number of plots sampled and the spatial coverage of such an approach, compared to forest inventories which rely on only a few variables (e.g., DBH of merchantable trees).

The forest inventory approach would tend to produce lower values of biomass in the tropical forest (15.2 $kgC \cdot m^{-2}$; Brown and Lugo 1992) than the more direct approach (around 20 $kgC \cdot m^{-2}$; Houghton et al. 2001; Cummings et al. 2002) based on site-specific measures of biomass and use of vegetation maps for extrapolation. The reasons put forward to explain such differences are that direct methods may be biased with sites being preferably selected from lush areas, whereas forest inventories may underestimate or omit some significant components of the vegetation, such as the understory (trees with a diameter < 10 cm BHP) and CWD, which account for nearly 20% of the aboveground biomass (Cummings et al. 2002). However, these differences may also reflect real differences in biomass since sites used in respective studies are different (Turcq et al. 2002). In India, Dadhwal and Nayak (1993; cited in Chhabra et al. 2003) report a difference by a factor 4 between both methods, which was attributed to the direct method not accounting for the spatial variability of vegetation density.

However, both approaches show deficiencies in the tropics related to an incoherence in the tree diameter measurement method, a lack of specific allometric equations and inadequate sampling plot size.

To date, there is no standard method for measuring trees in tropical regions (Cummings et al. 2002). Trees in the tropical forest will often display buttresses at breast height where trees are measured in northern forests. Diameter measurements should be taken at a height where buttresses of most trees have disappeared, which is often at more than 3 m high, and

allometric equations should be based on such diameter. However, several studies still measure tropical tree diameters at breast height (Philips et al. 1998; Laurance et al. 1999; Cummings et al. 2002; Rice et al. In press).

Moreover, few allometric equations are available for tropical forests and, despite recent studies on the Amazonian tropical forest (Araújo et al. 1999; Nelson et al. 1999, cited in Houghton et al. 2001), these include few large trees which have a marked influence on regression models and errors (Houghton et al. 2001). Equations for estimating belowground biomass are also needed (Houghton et al. 2001).

Finally, the size of sample plots has a potentially important influence over the biomass estimated in tropical forests, by determining whether large trees are represented or not. Large trees are rare, but contribute significantly to the overall biomass of tropical forests (Cummings et al. 2002; Rice et al. 2004). In Cummings et al.'s study (2002), the large tree density was approximately 1/ha, but their average contribution to the biomass of the overstory was 23% (>70 cm BHP) and 13% (>200 cm BHP) for the 20 sites characterized. In Brown and Lugo's (1992) study, large trees accounted for up to 40% of the overstory biomass.

6.8 Total Carbon Densities and Stocks of Forest Biomes

The ranges of average organic carbon densities of the mineral soil, forest floor and vegetation are summarized in Table 6.9 for each of the major biomes. When these different components are pooled together, it appears that the tropical forest contains a higher organic carbon content per square meter (25.3 and 33.4 $kgC \cdot m^{-2}$) than the other two biomes (boreal forest: 13.3 to 24.9 $kgC \cdot m^{-2}$, temperate forest: 14.1 to 23.0 $kgC \cdot m^{-2}$), whose organic carbon density is comparable (Table 6.9).

Differences between the major biomes are not only found in their overall organic carbon content but also in carbon distribution between soil and vegetation. In the tropical forest, approximately 62% (45 to 92%) of the organic carbon is found in vegetation compared to 38% (30 to 55%) in soil, whereas in northern forests, soils store close to 72% (37 to 100%) of the total amount of organic carbon, compared to only 28% (16 to 48%) for vegetation. The higher proportion of carbon stored in soils of northern forests can be explained by lower decomposition rates of organic matter under cold and humid conditions at high latitudes and a shorter growing season (Malhi et al. 1999). On the opposite, warmer temperatures in the tropics favor faster nutrient mineralization and their recycling into vegetation growth.

Table 6.9. Range of average organic carbon density ($kgC \cdot m^{-2}$) of forests (vegetation, mineral soil and litter) and peatlands of the boreal, temperate and tropical regions. Estimates of the corresponding carbon pools are also presented.

	Forests						Peatlands		
	Organic carbon density [$kgC \cdot m^{-2}$]				Surface area[a]	Pool	C density	Surface area[a]	Pool
Region	Vegetation	Soil	Litter[c]	Total	[10^4 km^{-2}]	[PgC]	[$kgC \cdot m^{-2}$]	[10^4 km^2]	[PgC]
Boreal	4.0 to 6.4	8.5 to 13.0	0.8 to 5.5	13.3 to 24.9	1343	180 to 330	39 to 134	250	98 to 335
Temperate	4.8 to 5.7	9.0 to 13.4	0.3 to 3.9	14.1 to 23.0	500	70 to 110	n.a.	n.a.	
Moist tropical	15.2 to 23.3	10.0 to 13.9	0.1	25.3 to 33.4	1510	380 to 560	288	n.a.[b]	

n.a.: Not available.

[a]: Surface area values are taken from Goodale et al. (2002) for the boreal forest, FAO (2001) for the temperate forest and Malhi and Grace (2000) for the tropical forest.

[b]: Peatlands are scarce in sub-tropical and tropical regions. However, some regions accumulate peat when adequate and stable hydrologic conditions are met such as in the Peatswamp forest of Southeast Asia (Borneo, Malaysia, etc.) (Keddy 2000).

[c]: The range is based upon site specific estimates for the litter content whereas ranges for soils, vegetation and peat are based on average estimates for the whole biomes.

Using compiled estimates of organic carbon densities and surface areas from Table 6.9, we estimate for the major biomes a total organic carbon stock of 630 to 1000 PgC, of which 58% is found in the tropical forest, 31% in the boreal forest and only 11% in the temperate forest. The carbon pool estimated for boreal peatlands (98 to 335 PgC) is similar to that of the boreal forest (180 to 330 PgC), despite a surface area five times smaller.

6.9 Export of Organic Carbon to Aquatic Ecosystems

Boreal forest watersheds export high amounts of organic carbon to aquatic ecosystems, with export rates averaging 13.5 $gC \cdot m^{-2} \cdot yr^{-1}$ (range of 1.4 to 51.8 $gC \cdot m^{-2} \cdot yr^{-1}$) for total organic carbon (TOC) (Table 6.10, Hope et al. 1994). Most of the carbon is exported as dissolved organic carbon (DOC: 75 to 90%), and a small portion as particulate organic carbon (POC: 10 to 25%). Export rates vary across a drainage basin, and are inversely related to the stream's order (Naiman 1982).

Many factors control the export of organic carbon from watersheds to aquatic ecosystems. Lakes and rivers located in watersheds dominated by wetlands, especially peatlands, have a high concentration of DOC (Kling et al. 1991; Dillon and Molot 1997; Hope et al. 1994). Eckhardt and Moore (1990) report an intimate relationship between the surface ratio of peatland to watershed and DOC concentration in streams. Moreover, concentration of humic acids (DOC) has been linked to the drainage ratio (the ratio between the drainage area and lake area), with a small ratio implying a greater dilution of carbon inputs into lakes (Engstrom 1987; Sobek et al. 2003). The concentration of DOC is also inversely related to the catchment's slope (D'Arcy and Carignan 1997; Prairie et al. 2002). Periods of intense precipitation saturate the soils' organic layer on gentle slopes, enhancing the formation of DOC which is ultimately exported to lakes.

There is a relationship between precipitation volume and the amount of DOC leached out from soils (McDowell and Likens 1988; Eckhardt and Moore 1990). High precipitation rates favor runoff and leaching of the soil's organic layer, which has a relatively high content in DOC (Mulholland et al. 1990). Hope et al. (1994) have been able to explain 94% of the variability in the amount of DOC exported from 17 drainage basins in England, from precipitation volume and the amount of organic carbon stored in soils. Compared to runoff, groundwater flow contributes small amounts of DOC to aquatic ecosystems (Devol et al. 1987; Cole et al. 1989; Prairie et al. 2002), less than 5% of total DOC inputs according to Schiff et al. (2001).

Table 6.10. Export of carbon from terrestrial to aquatic ecosystems

Biome[a]	DOC[b] [gC·m^{-2}·yr^{-1}]		POC[c] [gC·m^{-2}·yr^{-1}]		TOC[d] [gC·m^{-2}·yr^{-1}]	
	Range	Average (n)	Range	Average	Range	Average
Boreal forest	2.5-48.4	13.8 (6)	0.5-3.4	1.2 (5)	1.4-51.8	13.5 (7)
Temperate forest	0.3-41.7	3.4 (52)	0.1-1.2	0.6 (18)	0.3-8.1	3.1 (17)
Temperate grassland	0.2-0.5	0.3 (3)	0.2-0.6	0.4 (3)	0.4-1.3	0.9 (4)
Wetlands	0.2-14.2	6.6 (5)	0.4-2.0	5.6 (3)	1.9-14.6	6.7 (12)
Total	0.2-48.5	4.7 (67)	0.1-3.4	1.2 (30)	0.3-51.8	5.6 (41)

[a]: Studies done in North America, Russia and New Zealand.
[b]: Dissolved organic carbon.
[c]: Particulate organic carbon.
[d]: TOC (total organic carbon) does not correspond to the sum of DOC and POC because it was measured in different studies.
Adapted from Hope et al. (1994).

Land use changes also affect the transfer of DOC from terrestrial to aquatic ecosystems. Forest clear-cutting in New Zealand and in the Canadian Shield has resulted in an increase in the amount of DOC exported to streams and lakes, in part as a result of the decomposition of cut residues (Moore 1989; Lamontagne et al. 2000).

The above mentioned factors refer mostly to the physical processes affecting the export of DOC from watersheds. According to Aitkenhead and McDowell (2000), the C/N ratio is intimately linked to the biological production and alteration of DOC within soils. These authors obtained a strong direct relationship ($r^2 = 0.99$) between terrestrial DOC inputs and C/N ratios for 164 rivers from all around the world. From their model, they predicted an export rate for boreal forests of 63.4 kgC·ha^{-1}·yr^{-1} (6.34 gC·m^{-2}·yr^{-1}), slightly lower than the average value (13.8 gC·m^{-2}·yr^{-1}, Table 6.10) reported by Hope et al. (1994).

Terrestrial export of carbon to oceans is minimal (Cole and Caraco 2001), represents only 1 to 2% of DOC in oceans (Opsahl and Benner 1997). This suggests that most of the DOC exported from terrestrial ecosystems is trapped or metabolized in aquatic ecosystems. A recent estimate indicates that close to 15% of the annual forest carbon production is exported through the drainage system, of which 5% finds its way back to the atmosphere as CO_2 (Dillon and Molot 1997). The export of carbon, as DOC and CO_2, may contribute to balance the carbon budget of forests (Richey et al. 2002).

6.10 Conclusion

The review of the various studies has emphasized the great variability and uncertainty surrounding the estimates of organic carbon densities in the soil and vegetation of forests. In forest soils, this is due in part to the lack of spatially representative data given the high SOC spatial heterogeneity and the use of extrapolation methods that do not integrate sufficient parameters controlling the distribution of organic carbon in soils (e.g., parent material, climate, clay content). In the vegetation, the uncertainty surrounding the estimates of organic carbon densities is greater for tropical forests where, in most countries, detailed national forest inventories have not been conducted. In northern countries, the conversion of wood volumes estimated from forest inventories into the whole forest carbon content is the main source of uncertainty.

7 Carbon Dioxide and Methane Emissions from Estuaries

Gwenaël Abril and Alberto Vieira Borges

Abstract

Carbon dioxide and methane emissions from estuaries are reviewed in relation with biogeochemical processes and carbon cycling. In estuaries, carbon dioxide and methane emissions show a large spatial and temporal variability, which results from a complex interaction of river carbon inputs, sedimentation and resuspension processes, microbial processes in waters and sediments, tidal exchanges with marshes and flats and gas exchange with the atmosphere. The net mineralization of land- and marsh-derived organic carbon leads to high CO_2 atmospheric emissions (10-1000 mmol·m^{-2}·d^{-1} *i.e.* 44-44 000 mg·m^{-2}·d^{-1}) from inner estuarine waters and tidal flats and marsh sediments. Estuarine plumes at sea are sites of intense primary production and show large seasonal variations of pCO_2 from undersaturation to oversaturation; on an annual basis, some plumes behave as net sinks of atmospheric CO_2 and some others as net sources; CO_2 atmospheric fluxes in plumes are usually one order of magnitude lower than in inner estuaries. Methane emissions to the atmosphere are moderate in estuaries (0.02-0.5 mmol·m^{-2}·d^{-1} *i.e.* 0.32-8 mg·m^{-2}·d^{-1}), except in vegetated tidal flats and marshes, particularly those at freshwater sites, where sediments may be CH_4-saturated. CH_4 emissions from subtidal estuarine waters are the result of lateral inputs from river and marshes followed by physical ventilation, rather than intense in-situ production in the sediments, where oxic and suboxic conditions dominate. Microbial oxidation significantly reduces the CH_4 emissions at low salinity (<10) only.

7.1 Introduction

At the land-ocean interface, estuaries receive large amounts of dissolved and particulate material carried by rivers, including carbon and nutrients. They are highly dynamic systems, characterized by strong physico-chemical gradients, enhanced biological activity (both autotrophic and heterotrophic) and intense sedimentation and resuspension. For twenty years it has been well known that riverine material undergoes profound transformations in estuaries before being transferred to the adjacent coastal zone (Wollast 1983). Although such intense biogeochemical processes in estuaries suggested a potential for high gas emissions, very little was known until recently about estuaries and their atmospheric coupling. Intensive gas emissions studies in estuaries started in the 80s in tidal marshes of the US Eastern coast, then in the 90s in various estuarine channels. Recently, the BIOGEST project (BIOGas transfer in ESTuaries, 1996-1999), supported by the European Union, aimed to describe the distributions, cycling and emissions of several biogenic gases in European tidal estuaries (Frankignoulle and Middelburg 2002). The aim of the present paper is to synthesize the recent advances in our understanding of carbon dioxide and methane emissions from estuarine systems. An effort is made to describe the factors controlling the variability of these emissions and to relate them to the carbon cycling in estuaries.

7.2 Estuaries: Some Useful Definitions for Describing Carbon Cycling and Gas Emissions

The most exhaustive definition of an estuary was first given by Cameron and Pritchard (1963): “a semi-enclosed coastal body of water, which has free connection with the open sea, and within which seawater is measurably diluted with freshwater derived from land drainage”. However, this definition includes many coastal systems with different morphologies. This paper will focus on estuaries classified by Perillo (1995) in two categories: (1) *former fluvial valleys,* which include *coastal plain* estuaries and (2) *river dominated* estuaries. These cases correspond to the majority of large world rivers (Fjords and coastal lagoons will not be considered). Within this definition, the estuary has a channelled or funnelled shape and can be divided in several regions with distinct biogeochemical properties (Fig. 7.1).

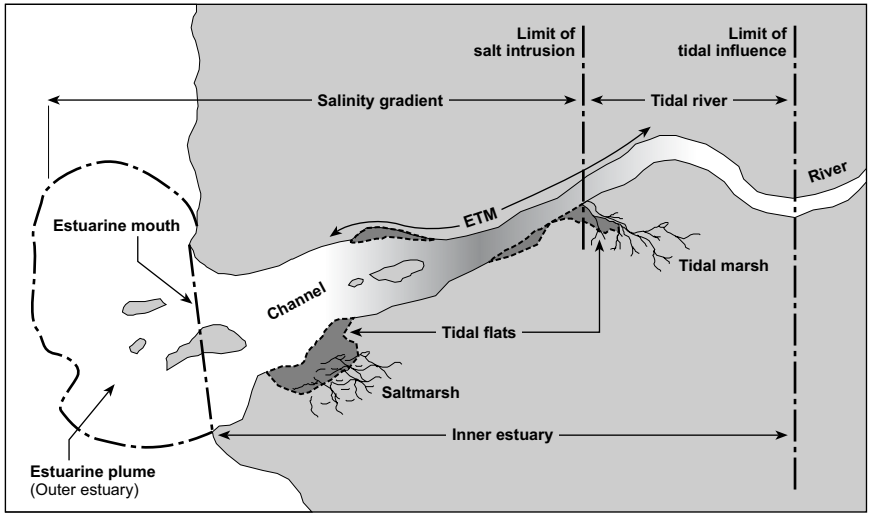

Fig.7.1. Schematic representation of an idealized estuary, with the geographic definitions used in this chapter

Upstream, the inner estuary starts at the limit of the tidal influence, where currents and sedimentary processes become drastically different from those in the river, and stops at the geographic limit of the coast (estuarine or river *mouth*). The surface of the inner estuary divides into the subtidal area that includes the main channels and tidal flats, that are periodically emerged and in direct contact with the atmosphere due to the tide oscillations. The surface of tidal flats varies with tidal amplitude, estuarine morphology and human transformations (*e.g.* damming-up). Tidal marshes are wetlands influenced by the tide oscillations and sometimes occupy an important surface all around the inner estuary, as in the case of the US Eastern coast (Cai et al. 1999). The region of the inner estuary, submitted to the tide but containing only freshwater is generally called the *tidal river*, and may include freshwater tidal flats and marshes. Downstream, the mixing of freshwater with seawater starts inside the geographical limit of the coast, a region that also comprises tidal flats and saltmarshes, and continues at sea, in an area called the *plume* (Ketchum 1983). The surface of this plume is commonly defined on the basis of salinity in surface waters, a value of 1 lower than the adjacent oceanic basin being arbitrary used as the offshore boundary (e.g. Borges and Frankignoulle 2002). Although the surface of the inner estuary is easy to evaluate, the one of the plume is highly variable, both in a given system (seasonal variability) and from one system to another. River-dominated estuaries like the Amazon, (Brazil),

the Mississippi (US) and the Rhine (The Netherlands) have an extended plume, salinity at the mouth being relatively low. By contrast, in coastal plain estuaries with moderate river discharge like the Gironde (France), the Scheldt (Belgium/Netherlands) and the Thames (UK), a large part of the salinity gradient is located within the inner estuary.

The residence time of freshwaters in an estuary may vary from days to months, depending on the river discharge -that lowers it- and the tidal amplitude -that increases it-. Estuaries are sites of intense sedimentation in particular of fine material eroded from land. Due to the asymmetry of the tide, to density gradients and to flocculation processes when freshwater mixes with seawater, an estuarine turbidity maximum (ETM) is commonly found, often most concentrated at low salinities (Allen et al. 1980; Uncles 2002). The high currents (sometimes exceeding 2 $m \cdot s^{-1}$) and their rapid change at the tidal and fortnightly timescales result in intense sedimentation and resuspension cycles in ETMs, where residence time of suspended matter may exceed several years before being definitively sedimented or exported to the adjacent shelf (Allen et al. 1980; Uncles 2002). Tidal flats and marshes exchange sediment, water and porewater with the adjacent subtidal estuary, at the tidal, fortnightly and seasonal times scales.

7.3 Organic Carbon Sources and Mineralization in Estuaries

Both aquatic and terrestrial organic matter are found in estuaries. Rivers carry terrestrial soil particles, humic substances and litters from land, but also freshwater phytoplankton and domestic loads (sewage) (Wollast 1983; Meybeck 1993; Veyssy et al. 1999; Abril et al. 2002). A large part the riverine particulate organic carbon is lost during its transit in estuaries (Ittekkot and Laane 1991; Keil et al. 1996; Abril et al. 2002). Indeed, on an annual basis, total respiration exceeds gross primary production in estuaries that are net heterotrophic ecosystems (Smith and Hollibaugh 1993; Gattuso et al. 1998). Mineralization affects in priority the most labile material (phytoplankton and sewage) but also a significant fraction of terrestrial organic matter (Keil et al. 1997; Veyssy et al. 1999). Estuarine sedimentary environments like ETMs and deltaic muds are characterized by frequent sedimentation/erosion events, which induce redox oscillations and particle mixing and favor particulate organic matter decomposition and recycling (Aller 1998; Abril et al. 1999).

In tidal flats and marshes, like in many wetlands worldwide, primary production by microphytobenthos and periodically submerged plants

(rooted macrophytes) is intense (Nienhuis 1992). It constitutes a major source of organic matter to the flat and marsh sediments (Goni and Thomas 2000; Delaune and Pezeshki 2003), but also to the adjacent estuarine waters and sediments, tidal flushing resulting in an outwelling process of carbon and nutrients (Dame et al. 1986). Consequently, heterotrophic activity in the adjacent estuary is also partly fueled by tidal inputs from flats and marshes. Inversely, intertidal sediments trap estuarine suspended particles, especially when they are colonized by plants (Widdows et al. 2000). This leads to high organic carbon sedimentation rates of a mixture of relatively organic-poor particles from the ETM and highly reactive plant debris (Goni and Thomas 2000). Globally, tidal marshes appear to be slightly autotrophic (Gattuso et al. 1998), meaning that more organic matter is produced by plants than is remineralized in the sediment and exported to adjacent waters. Little is known about the net metabolism of tidal flats, which is probably different from marshes, owing to greater carbon exchanges with the estuarine channel.

In riverine plumes, turbidity is much lower than in inner estuaries. In many sites, like in the Gironde and Loire estuaries in France, depending on river discharge, light starts seasonally to penetrate deeper into the water upstream the estuarine mouth (Fig. 7.1), and the lower part of the inner estuary has similar characteristics as the plume at sea. This availability of light, together with the input of nutrients from the river and the stratification of waters due to vertical salinity gradients, create favorable conditions for phytoplankton blooms (Cloern 1996). In addition, enrichment in nutrients by agricultural practices in watershed has significantly modified the intensity and community structure of these blooms as exemplified by the Mississippi plume (Justic et al. 1995) and the Southern North Sea coast (Reid et al 1990). However, in macrotidal tidal systems and especially those with large ETMs, phytoplankton biomass in estuarine plumes represents a seasonal carbon stock one to two orders of magnitude lower than the terrestrial organic matter in the ETM (Abril et al. 2002).

7.4 Estuarine Specificity for Gas Transfer

The flux of a gas across the air-water interface is governed by the following equation:

$$F = k\alpha\Delta p \tag{7.1}$$

where α is the solubility coefficient of the gas, Δp is the air-water gradient of the gas partial pressure and k is the gas transfer velocity. For sparingly soluble gases such as carbon dioxide and methane, k mainly depends

on turbulence in the liquid phase (Wanninkhof 1992) that is affected by a number of forcings in estuarine environments. As in the ocean and in lakes, wind stress is the main generator of water turbulence. For that reason, a parameterization of k as a function of wind speed is generally used to calculate gas fluxes from Δp in estuaries (Marino and Howard 1993; Raymond and Cole 2001). However, tidal currents may also contribute to water turbulence, especially in inner estuaries with shallow waters and high frictions on the bottom (rugosity). In streams, the generation of turbulence by friction due to flow over the bottom dominates. Therefore, k is parameterized as function of the ratio between water velocity and water depth (O'Connor and Dobbins 1958). In a recent review that compiles measurements in various systems, Raymond and Cole (2001) suggested that k could be significantly higher in estuaries than in open oceanic waters at the same wind speed. Borges et al. (2004a) calculated k from CO_2 flux measurements with a floating chamber in three European estuaries. They found very different relationships between k and wind speed, with significantly higher values in the two macrotidal systems than in the microtidal system (Fig. 7.2). In addition, using low to moderate wind speed data, they calculated a contribution of water current, consistent with the formulation of O'Connor and Dobbins (1958) in streams. In the macrotidal Scheldt estuary, the tidally and yearly integrated contribution of water currents was estimated to account for 24% of the total gas transfer velocity, the remaining part being attributed to wind (Borges et al. 2004b). Zappa et al. (2003) carried out concomitant measurements of k with the gradient flux technique and of water turbulence in the aqueous boundary layer in a macrotidal estuary (Plum Island Sound) over a tidal cycle during a low wind day ($1.9\ m{\cdot}s^{-1}$). They found a large variation of k from 2.2 to $12.0\ cm{\cdot}h^{-1}$ that correlated well with tidal speed and turbulence. The tidal averaged k was 6.2±0.4, that is 1.6 times higher than the one calculated from wind speeds with the Raymond and Cole (2001) relationship. The comparison of all these different k – wind relationships (Fig. 7.2) clearly suggests the occurrence of another controlling factor besides tidal currents, which is site-specific. Fetch (diameter of the inner estuary in the direction of the prevailing wind) is probably a good candidate (Borges et al. 2004a submitted manuscript). A long fetch favors the formation of waves, eventually forming whitecaps and enhances the potential for wind to favor gas transfer. An interesting result was obtained recently by Kauppila et al. (2003), who analysed a database of chemical, meteorological and morphometric parameters from 19 microtidal Finnish estuaries. They concluded that fetch could explain 30% of the variation in oxygen concentrations, being the second variable after a function of mean water depth and the percentage of watershed under agriculture (55%).

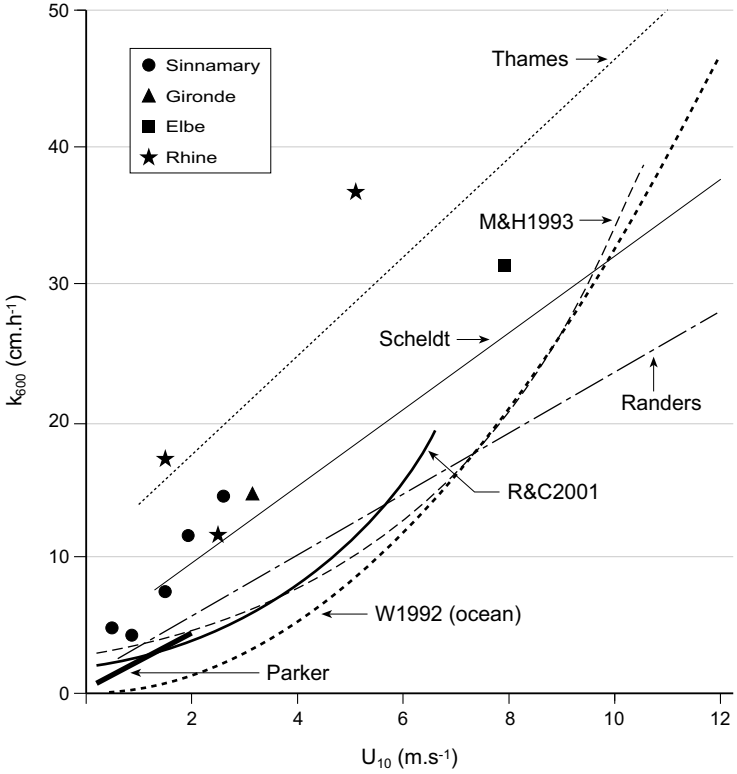

Fig. 7.2. Relationships between the gas transfer velocity k_{600} (normalized to a Schmidt number of 600) and the wind speed at 10 m height obtained in estuaries with different tidal range (TR) and average depth (AD).

The relationships are from the following references: W1992: Wanninkhof (1992) for the ocean; R&C2001: Raymond and Cole (2001) who compiled data in various estuaries with different techniques; M&H1993: Marino and Howard (1993) based on floating chamber oxygen flux measurements in the Hudson estuary (US-New York, TR 1.3 m, AD 15 m) and various rivers; Parker estuary (US-Massachussets, TR 2.9 m, AD 4 m): Carini et al. (1996) based on a SF_6 experiment; Randers Fjord estuary (Denmark, TR 0.2, AD 2 m), Scheldt estuary (Belgium/Netherlands, TR 3.8 m, AD 10 m) and Thames estuary (UK, TR 4.5 m, AD 8 m): Borges et al. (2004a), based on floating chamber CO_2 flux measurements; Gironde (France, TR 4 m, AD 10 m), Elbe (Germany, TR 3 m, AD 9 m) and Rhine (The Netherlands, TR 2.5 m, AD 11 m) are based on floating chamber CO_2 flux measurements (data were averaged over wind speed bins of 1 m·s^{-1}) (Borges et al. unpublished data). Sinnamary estuary (French Guiana, TR 1.8 m, AD 3.5 m) are some preliminary results derived from 5 individual methane flux measurements at low wind speeds (Guérin, Abril et al. unpublished data).

Kremer et al. (2003) and Borges et al. (2004a) concluded that a simple parameterization of k as a function of wind speed is still appropriate for estuaries, but it is site-specific, each relation integrating a combination of current, depth and fetch effects. They added that the floating chamber method, when used cautiously (Lagrangian measurements in a drifting boat and at moderate wind speed) provides a convenient and inexpensive approach for quantifying these cross-system differences. Anyhow, there is an evident need for techniques of gas exchange flux measurements adapted to the physical characteristics of estuaries. Classic natural or released tracer techniques provide gas transfer velocity estimates at time scales (>1 d) that do not allow to adequately describe the short term variability (min to h) of k in these very dynamic environments. Direct techniques as those used by Zappa et al (2004) (gradient flux, dissipation rate and controlled flux) appear promising if they can be adapted to highly dynamic environments with high currents, wind and waves.

Nevertheless, all these recent advances in our understanding of gas exchange processes converge to the idea that gas transfer velocities in estuaries are higher than in lakes and in the ocean at a same wind speed. In addition to temporal variations, k is highly variable spatially. Indeed, tidal currents, depth and wind are geographically highly variable inducing large differences k (Borges et al. 2004b). Dissolved gases can consequently be advected from less dynamic regions (e.g. from tidal marshes) and get further ventilated in more dynamics regions (e.g. the main channel and the plume). This is of major importance when interpreting the spatial distributions of gases in estuarine waters, and when calculating carbon budgets that include input from the river, exchanges with tidal flats and marsch, and outputs to the atmosphere and the ocean.

7.5 Carbon Dioxide Emissions

As heterotrophic ecosystems, estuaries are a source of CO_2 to the atmosphere (Frankignoulle et al. 1996; 1998). Indeed, oxygen deficits and CO_2 supersaturations are common features in estuaries. Examples of classical distribution of pCO_2, oxygen and CO_2 fluxes to the atmosphere are shown in Fig. 7.3. River waters entering estuaries have pCO_2 generally higher than the atmosphere, due to organic carbon mineralization in soils, river waters and sediments (Jones and Mulholland 1998a; Neal et al. 1998; Cole and Caraco 2001; Richey et al. 2002). Nevertheless, pCO_2 further increases in estuaries, especially in the tidal river and at low salinities (Fig. 7.3). This region often corresponds to the location of the ETM where

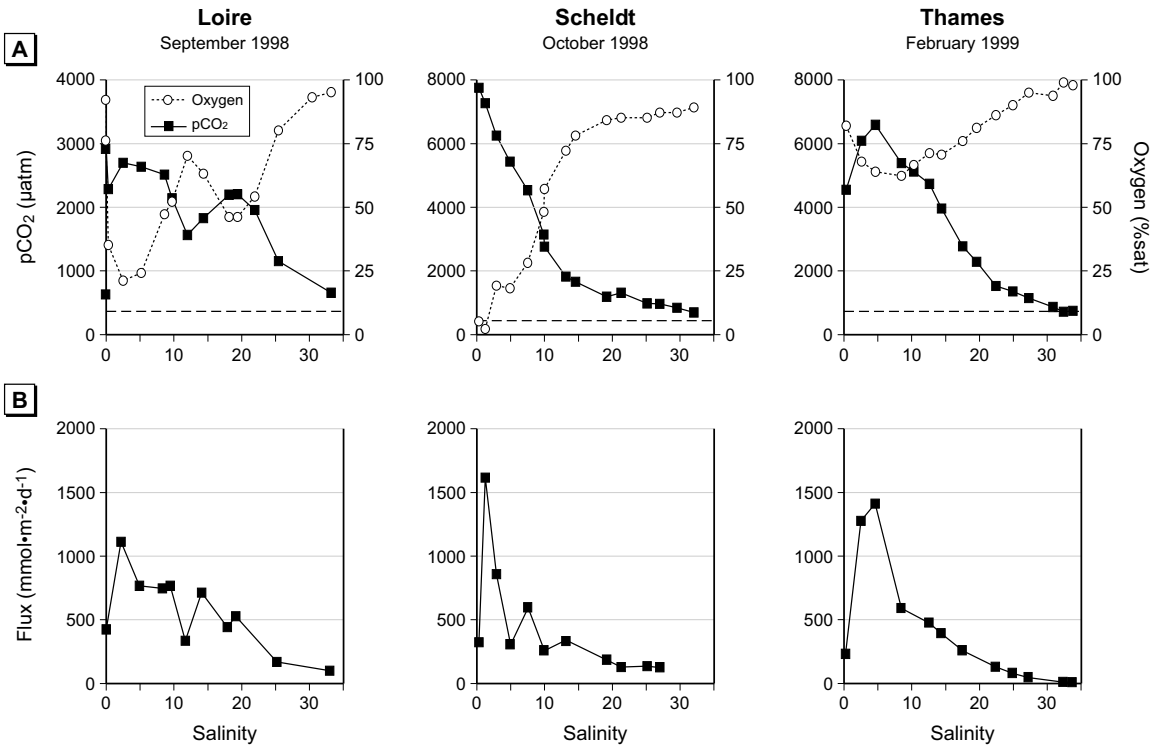

Fig. 7.3. Typical distributions versus salinity of: A. pCO_2 (black squares in µatm) and Oxygen (open squares%Saturation) in surface waters, showing the net anti-parallelism between the two parameters. B. water-air CO_2 fluxes (floating chamber method) measured in three European estuaries studied during the BIOGEST project (Frankignoulle et al. 1998; Abril et al. 2003). Dotted lines are the atmospheric pCO_2 value of 365 µatm. Note the different scale for the Scheldt estuary

heterotrophy is intense as revealed by important oxygen depletions. Indeed, in ETM, steep light extinction inhibits photosynthesis, whereas high suspended matter enhance respiration, heterotrophic bacteria occurring in majority attached to the particles (Crump et al. 1998; Goosen et al. 1999).

Table 7.1 summarizes pCO_2 and CO_2 fluxes measured so far in inner estuaries. Besides some differences from one site to another, it can be seen that a large oversaturation is the general situation and that CO_2 fluxes to the atmosphere can occasionally reach one $mol \cdot m^{-2} \cdot d^{-1}$ (Fig. 7.3). Based on fluxes measured with the floating chamber method in nine European estuaries and during 26 cruises, Frankignoulle et al. (1998) proposed a realistic average CO_2 flux of 170 $mmol \cdot m^{-2} \cdot d^{-1}$ (*i.e.* 7500 $mg \cdot m^{-2} \cdot d^{-1}$) for inner estuaries.

Tidal marshes are generally a net sink of atmospheric CO_2 leading to a net burial of organic matter in the sediment (Gattuso et al. 1998; Delaune and Pezeshki 2003). However, due to an intense recycling of sedimentary organic matter, sediments and soils from tidal flats and marshes emit large amounts of CO_2, directly to the atmosphere at low tide and across a water column of variable height when submerged. It can be seen in Table 7.2 that direct sediment-atmosphere fluxes measured at low tide in flats and marshes fit well within the range of water-atmosphere fluxes measured in subtidal inner estuaries (Table 7.1).

Lateral transport of CO_2 from tidal flats and marshes can also significantly contribute to the high pCO_2 in adjacent estuarine waters. In the freshwater intertidal marshes complex of five rivers in the southeastern U.S., Cai et al. (1999) found that respiratory activity in estuarine waters and sediments was not sufficient to account for the observed oxygen concentrations and pCO_2. In their system, advection of excess CO_2 from marshes with tidal flushing largely contributes to the CO_2 flux in the main channel. This in due to the conjunction of two facts: high respiratory activity in marsh sediments; and lower gas exchange rates in the marsh than in the channel.

Another important process for carbon cycling in inner estuaries is a net production of alkalinity at low to moderate salinities, observed in several systems (Abril et al. 1999; 2003; Cai et al. 2000; Raymond et al. 2000; Bouillon et al. 2003). Production of alkalinity from dissolved CO_2 generated during respiration represents a long term sink for atmospheric CO_2. Basically, there are two potential processes (Stumm and Morgan 1996) that can result in a long term alkalinity production in estuaries: 1) carbonate dissolution, when dissolved CO_2 reacts with calcium carbonate particles to produce two bicarbonate anions and dissolved calcium; this process is responsible for large alkalinity generations in the Loire (Abril et al.

Table 7.1. pCO_2 ranges and fluxes reported in inner estuaries

Estuary	Number of cruises	Average pCO_2 range [µatm]	Average CO_2 flux range [$mmol \cdot m^{-2} \cdot d^{-1}$]	Method used for k §	References
Altamaha (US-Georgia)	1	380–7800			1
Scheldt (Belgium/Netherlands)	10	495–6650	260–660	Floating chamber	2
Sado (Portugal)	1	575–5700	760	Floating chamber	2
Satilla (US-Georgia)	2	420–5475	50	k =12 $cm.h^{-1}$	1
Seine (France)	2	826–5345	–		3
Thames (UK)	1	560–3755	210–290	Floating chamber	2
Gironde (France)	5	500–3535	50–110	Floating chamber	2
Loire (France)	3	770–2780	100–280	Floating chamber	4
Mandovi-Zuavi (India)	2	400–2500	11–67	W92	5
Douro (Portugal)	1	1330–2200	240	Floating chamber	2
York (US-Virginia)	12	350–1895	12–17	C95&C96	6
Tamar (UK)	2	390–1825	90–120	k =8 $cm.h^{-1}$	2
Rhine (Netherlands)	4	570–1870	70–160	Floating chamber	2
Hudson (US-New York)	6	515–1795	16–36	M&H93 & C95	7
Rappanhannock (US-Virginia)	9	474–1613	–		6
James (US-Virginia)	10	284–1361	–		6
Elbe (Germany)	1	580–1100	180	Floating chamber	2
Columbia (Oregon)	1	560–950	–		8
Potomac (Maryland)	12	646–878	–		6

The average pCO_2 range was obtained by averaging the lowest and highest values for each transect and gives information on the spatial variability from the upper part (highest pCO_2) to the estuarine mouth (lowest pCO_2). By contrast, the average CO_2 flux range is composed by the lowest and highest fluxes averaged over the estuarine surface for each cruise and gives information on the temporal variability from one cruise to another.
1 Cai and Wang (1998) and Cai et al. (1999); 2 Frankignoulle et al. (1998) and additional unpublished data from the BIOGEST project; 3 Abril et al., unpublished data; 4 Abril et al. (2003) and unpublished data; 5 Sarma et al. (2001); 6 Raymond et al (2000); 7 Raymond et al. (1997); 8 Park et al. (1969). §Fluxes were either measured directly with a floating chamber or calculated using either a constant piston velocity (value indicated) or using various wind speed relationships: W92 is Wanninkhof (1992); C95&C96 is a combined relationship of Clark et al. (1994) and Carini et al. (1996); M&H93 & C95 is a combined relationship of Marino and Howard (1993) and Clark et al. (1995).

Table 7.2. CO_2 emission from tidal marshes and flats soils and sediments at various salinities

Site	Salinity	CO_2 emission [$mmol \cdot m^{-2} \cdot d^{-1}$]	Reference
Oyster Landing salt marsh (US-South Carolina)	5-7	50-75	1
Dipper Harbour salt marsh (Canada-New Brunswick)	20.6-23.5	40	2
	31-35	60	2
Scheldt estuary, tidal flats (Belgium/the Netherlands)	1	375	3
	25	50	3
Mississipi deltaic coastal marshes (US-Louisiana)	3-5	100-140	4

1 Morris and Whiting (1986); 2 Magenheimer et al. (1996); 3 Middelburg et al. (1996); 4 Delaune and Pezeshki (2003).

2003) and in the Godavari estuary in India (Bouillon et al. 2003). In the Loire ETM, carbonate dissolution is enhanced by the presence of authigenic carbonate carried by the eutrophic river and increases by ~30% the summer alkalinity export to the ocean (Abril et al. 2003); 2) diagenetic processes in anoxic sediments; primary diagenetic reactions (nitrate, manganese, iron or sulfate reductions) consume protons and produce alkalinity, whereas secondary reactions (ammonia, manganese, iron and sulfide oxidations) release protons and decrease the alkalinity. If primary reactions are incompletely compensated by secondary reactions (*e.g.* if iron-sulfides precipitate and get buried), a net release of alkalinity occurs. In addition, anaerobic fermentative processes (*e.g.* decarboxilation) may spontaneously generate alkalinity. For that reason, significant amounts of alkalinity were found to be outwelled from tidal marshes anoxic sediments (Cai et al. 2000; Raymond et al. 2000). There is a need today for a better understanding of the alkalinity generation by these two kinds of processes in estuaries.

The outer estuary has substantial different properties with respect to carbon dioxide, intense phytoplanktonic blooms consuming significant amounts of dissolved CO_2. pCO_2 in estuarine plume depends on its primary production/respiration balance but also on the quantity of excess dissolved CO_2 advected from the inner estuary. Thus, CO_2 atmospheric exchanges in plumes are affected by a large number of parameters, among which, the river discharge, the degree of heterotrophy in the inner estuary, the availability of nutrients and light and the stratification of the water column are the most important. Consequently, pCO_2 is highly variable in

plumes both seasonally in a given system and from one system to another. During 13 cruises in 7 European Atlantic and North Sea estuarine plumes Frankignoulle et al. (1998) observed pCO_2 variations from 240 µatm in the Scheldt plume at salinity 34 in March 1997 to 1330 µatm at the mouth of the Douro (salinity 9) in September 1997. Borges and Frankignoulle (2002) carried out intensive pCO_2 measurements during three years in the Scheldt plume, a highly eutrophic region of the Southern North Sea. They could observe important CO_2 undersaturation (pCO_2 down to 90 µatm) in April and May, associated with a high algal biomass. However, oversaturation (pCO_2 up to 700 µatm) was the general situation the rest of the year, CO_2 advection from the inner Scheldt and mineralization of phytoplanktonic carbon being very important. They concluded that the Scheldt plume behaves as a source of CO_2 with an annually integrated water-air flux of $+4\ mmol \cdot m^{-2} \cdot d^{-1}$. Brasse et al. (2002) carried out similar measurements in the Elbe plume (German Bight, southern North Sea) and found undersaturation (down to 140 µatm) was predominant. However, their dataset was restricted to the spring and summer period, and pCO_2 higher than 500 µatm occurred during their only cruise with high river runoff. Finally, Ternon et al. (2000) showed that the plume of the Amazon, that may extend up to 2000 km northwestward along the coast of Brazil, French Guiana and Surinam, behaves as a large sink of atmospheric CO_2 with pCO_2 values ranging between 200 and 400 µatm. Körtzinger (2003) observed similar pCO_2 values and using sea surface salinity data, calculated an average integrated flux for the Amazon river plume of $-1.4\ mmol \cdot m^{-2} \cdot d^{-1}$. The significance of CO_2 fluxes in estuarine plumes in the overall estuarine system is difficult to apprehend because few studies have investigated both inner and outer estuaries. Borges and Frankignoulle (2002) showed that the CO_2 emission from the Scheldt plume represents 17 to 29% of the estimate for the Scheldt inner estuary. On the other hand, Körtzinger (2003) estimated the sink of CO_2 in the Amazon plume to $0.014\ 10^{15} \cdot g \cdot C \cdot yr^{-1}$ that is more than one order of magnitude smaller than the total CO_2 source of $0.5\ 10^{15} \cdot g \cdot C \cdot yr^{-1}$ from Amazonian rivers and wetlands (Richey et al. 2002). All these studies reveal the variable properties of estuarine plumes with respect to air-sea CO_2 exchange. They also illustrate the high temporal variability in each site and the necessity of sustained investigation in order to adequately quantify the CO_2 exchanges between estuarine plumes and the atmosphere, at the regional and global scale.

7.6 Methane Emissions

Methane emissions from estuarine surfaces vary over a wide range of spatial and temporal scales. The processes of methane production, transport, oxidation and emission are complex and very different in tidal flats and marshes compared to estuarine main channels. However, these processes have been studied in several systems worldwide so it becomes possible nowadays to give a general picture of methane cycling and emissions in estuaries.

Similarly to continental wetlands (Richey et al. 1988), methane emissions from tidal flats and marshes are high (Bartlett et al. 1987; Chanton et al. 1989; Kelley et al. 1995; Middelburg et al. 1996), with annual averages typically in the range of few $mmol \cdot m^{-2} \cdot d^{-1}$ (Table 7.3). Methane production is particularly intense in tidal flats and marshes because of large inputs of organic matter at anoxic depths by plants rooted in the sediments (Kelley et al. 1995; Van der Nat and Middelburg 2000). Methane emissions vary seasonally, closely following the growing, maturing and dying cycle of plants (Bartlett et al. 1987; Kelley et al. 1995). Another crucial parameter is the availability of sulfate that increases with salinity. Sulfate availability allows sulfate-reducing bacteria to outcompete methanogenic bacteria in anoxic sediments (Capone and Kiene 1988). For that reason, methane emissions from estuarine tidal flats (Middelburg et al. 1996) and marshes (Bartlett et al. 1987) decrease by two orders of magnitude from fresh-water sites to saltwater sites (Table 7.3). Methane in tidal flats and marshes is emitted to the atmosphere by diffusion, ebullition (Chanton et al. 1989) and possibly transport through plants (Kelley 1995). In freshwater tidal marshes and flats, ebullition may equal diffusion and the variations in hydrostatic pressure induced by the diurnal tidal cycle control the ebullition rate (Chanton et al. 1989; Kelley et al. 1995; Middelburg et al. 1996). Finally, the tidal flushing of flats and marshes may export laterally large quantities of methane to the adjacent estuarine waters (Bartlett et al. 1985; Kelley et al. 1995).

Methane concentrations in estuarine waters vary over a wide range but are almost always higher than the atmospheric equilibrium (2-3 $nmol \cdot l^{-1}$) and generally show a decrease from fresh to salt waters (De Angelis and Lilley 1987; Scranton and McShane 1991; De Angelis and Scranton 1993; Bange et al. 1998; Sansone et al. 1998 and 1999; Upstill-Goddard et al. 2000; Jayakumar et al. 2001; Middelburg et al. 2002; Abril and Iversen 2002). This general pattern is due to river inputs which are a major contributor to the methane found in estuarine waters. In river main streams,

Table 7.3. Methane fluxes from estuarine regions

Sites	Comments	CH_4 emission [$mmol \cdot m^{-2} \cdot d^{-1}$]	References
Inner estuaries main channel			
Yaquina and Alsea (US-Oregon)	Annual average	0.18	1
Hudson tidal river (US-New-York)	Annual average	0.35	2
Bodden (Germany)	Annual average, spatial range	0.03–0.21	3
Tomales Bay (US-California)	Seasonal range, spatial average	0.007–0.01	4
European tidal estuaries	Median 9 estuaries, 18 cruises	0.13	5
Randers Fjord estuary (Denmark)	Annual average, spatial range	0.07–0.41	6
Estuarine plumes			
Rhine and Scheldt (Southern North Sea)	Spatial range in Marsh 1989	0.006–0.6	7
Amvrakikos bay (Aegean Sea)	Spatial average in July 1993	0.014	8
Danube (North-western Black-Sea)	Spatial range in July 1995	0.26–0.47	9
Tidal flats			
White Oak (US-North Carolina)	Annual average	1.2	10
(Freshwater sites)	Seasonal range	1–45	10
	Tidal variation	2.5–6.3	10
Choptank river estuary	Annual average (salinity 1–10)	2.4	11
Scheldt (Belgium/the Netherlands)	Annual averages		
	Fresh water site	500	12
	Salt water site (salinity 25)	0.1	12
Tidal marshes			
White Oak (US-North Carolina)	Annual averages		
(freshwater marsh)	Total	7.1	13
	Ebullitive	3.5	13
	Diffusive	3.5	13

Table 7.3. (cont.)

Sites	Comments	CH_4 emission [$mmol \cdot m^{-2} \cdot d^{-1}$]	References
Bay Tree Creek Salt Marsh (Virginia)	Annual averages, three sites (salinity 5–23)	2.6–8.1	14
York River (US-Viginia)	Annual averages		
	Salinity 2.6	3.0	15
	Salinity 5.5	3.8	15
	Salinity 8.8	0.9	15
Dipper Harbour	Annual averages		
(Canada-New Brunswick)	Salinity 20.6–23.5	0.13	16
	Salinity 31–35	0.03	16

1 De Angelis and Lilley (1987); 2 De Angelis and Scranton (1993); 3 Bange et al. (1998); 4 Sansone et al. (1998); 5 Middelburg et al. (2002); 6 Abril and Iversen (2002); 7 Scranton and McShane (1991); 8 Bange et al. (1996); 9 Amouroux et al. 2002; 10 Kelley et al. (1995), the seasonal average is from 4 bank stations and the seasonal range is the average of the 4 bank stations in October-March and in August-September; the tidal variation is from a single bank station in August 1991; 11 Lipschultz (1981); 12 Middelburg et al. (1996) (the extremely high value is from an area polluted by sewage loads); 13 Chanton et al (1989); 14 Bartlett et al. (1985); 15 Bartlett et al. (1987); 16 Magenheimer et al. (1996).

the lowest methane concentration reported so far was 5 $nmol \cdot l^{-1}$ (200% saturation relative to the atmosphere) in the McKenzie River (De Angelis and Lilley 1987) and the highest was 2.4 $\mu mol \cdot l^{-1}$ (90 000% saturation) in the Picassic River (Sansone et al. 1999), both systems also showing large temporal variations (for recent compilations of river concentrations refer to Upstill-Goddard et al. 2000 and Middelburg et al. 2002). This supersaturation is mostly due to inputs of methane-rich waters from surrounding anoxic environments rather than important production in the river system itself. In particular, groundwater inputs (Jones and Mulholland 1998b) and transport of river waters over wetlands and floodplains (Richey et al. 1988) are major mechanisms that contribute to the high methane concentrations in rivers.

As discussed previously, due to tidal currents and exposure to wind, gas exchange rates are generally much higher in estuarine main channels and plumes than in rivers and in tidal marshes. This results in a physical ventilation of a large part of the methane carried by rivers or advected from tidal marshes, both in inner estuaries (Upstill-Goddard et al. 2000; Middelburg et al. 2002) and in plumes at sea (Scranton and McShane 1991, Bange et al. 1994). Among the methane distributions observed during the BIOGEST project, the one in the Thames estuary (Fig. 7.4) is typical of a dominant river input followed by an emission (and oxidation, see below) in the upper part of the estuary. By contrast, in the Scheldt and Sado estuaries (Fig. 7.4), the increases in concentrations observed at salinities 20-30 are examples of significant input from tidal flats, highly extended at these salinities in both estuaries (Middelburg et al. 2002).

Methane fluxes in inner estuaries and plumes in Table 7.2 are around 0.2 $mmol \cdot m^{-2} \cdot d^{-1}$. A simple calculation that considers this flux value and a concentration of 200 $nmol \cdot l^{-1}$ in an inner estuary with a 10 m depth, leads to a turnover time of methane in the water column of 10 days, relative to atmospheric emission alone. This is shorter than the residence time of waters in many macrotidal inner estuaries. It means that due to atmospheric emission alone, very little methane from rivers or freshwater marshes reaches the estuarine mouth in long residence time systems like the Hudson (US-New York), Gironde and Loire (France), Scheldt (Belgium/Netherlands), etc. Thus, more methane needs to be produced in the inner estuary in order to export methane to the plume (De Angelis and Scranton 1993; Middelburg et al. 2002). By contrast, in the case of the Rhine (The Netherlands), a river-dominated system with high methane concentrations in freshwater and a short residence time (2-7 days) in the inner estuary, riverine methane can be tracked over long a distance offshore (Scranton and McShane 1991).

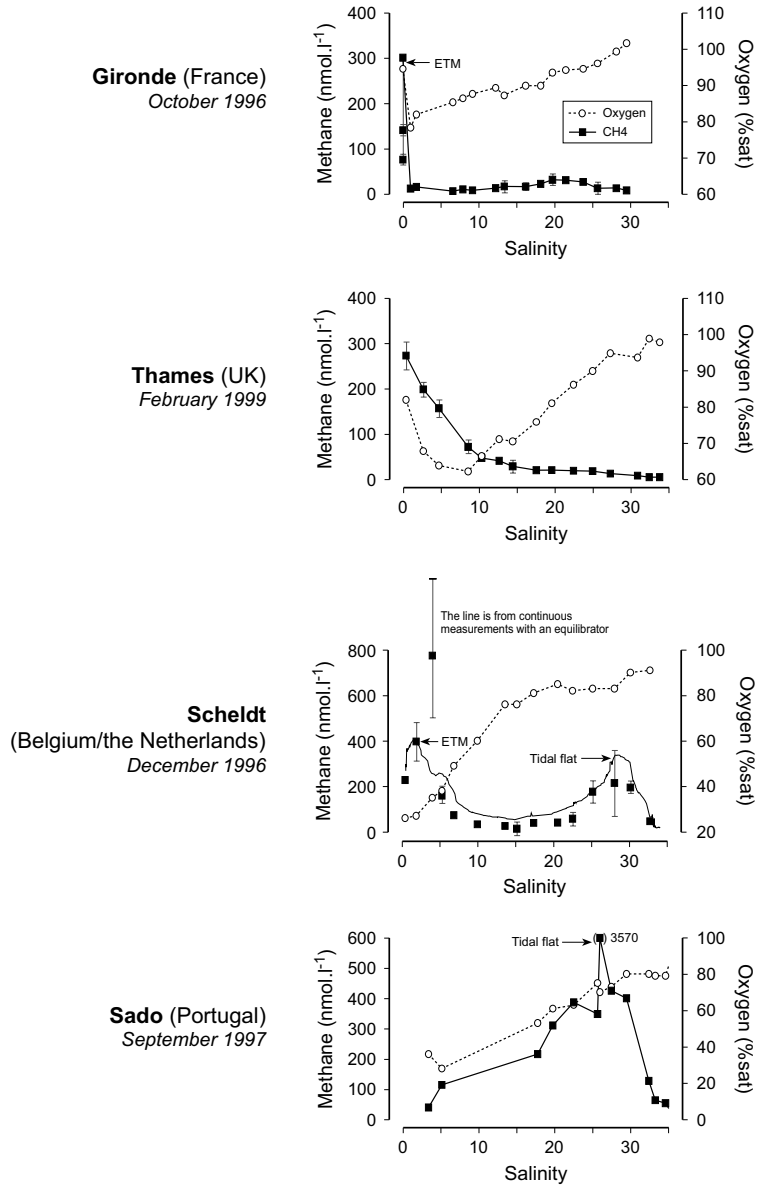

Fig. 7.4. Some examples of non-conservative methane (black squares) and oxygen (open circles) distributions versus salinity measured in European estuaries

Studied during the BIOGEST project (Middelburg et al. 2002). Gironde (France) October 1996; Thames (UK) February 1999; Scheldt (Belgium/the Netherlands) December 1996, the line is from continuous measurements with an equilibrator; Sado (Portugal) September 1997.

Together with gas evasion, aerobic oxidation is also a significant sink for methane in estuarine waters and sediments, particularly at low salinities. In the Hudson estuary, De Angelis and Scanton (1993) found that methane oxidation in waters could turnover the methane pool in 1.4 to 9 days, but only at salinities below 6, oxidation rates at higher salinities being 1-2 orders of magnitude lower. Adding salt and filtered seawater to their freshwater samples resulted in a strong inhibition of methane oxidation. In the Columbia river and estuary, similar oxidation rates were measured by Lilley et al. (1996), consistent with a net shift in $\delta^{13}C\text{-}CH_4$ at low to intermediate salinities (Sansone et al. 1999). In the low salinity (3-7) region of the Randers Fjord, a microtidal and shallow estuary in Denmark, Abril and Iversen (2002) observed intense methane oxidation at the sediment surface, which resulted in a net uptake of riverine methane by the estuarine sediment (downward methane flux through the sediment-water interface). They could not detect any methanotrophic activity at ambient concentrations in sediments at salinities 17-23. The relative contribution of microbial oxidation and atmospheric emission as sinks for dissolved methane was estimated in these three systems. The methane emission/oxidation ratio was on average 4 in the Columbia river and estuary (Lilley et al. 1996), ranged between 0.4 and 23 in the Hudson estuary (De Angelis and Scranton 1993) and between 0.8 and 5.1 in the low salinity regions of the Randers fjord (Abril and Iversen 2002). Ratios lower than one were restricted to summer periods, low salinities and high methane concentrations. Abril and Iversen (2002) discussed that wind speed has a multiplicative effect on this ratio: at low wind, methane builds-up in the water, enhancing microbial oxidation (typically a first order process), whereas at high wind, methane is stripped out the water to the atmosphere, decreasing water concentrations and inhibiting oxidation.

When considering the moderate emissions rates from estuarine channels and plumes in Table 7.2, the large contribution to this flux of methane inputs from rivers, tidal flats and marshes, the modest (though significant) contribution of oxidation, it appears that sub-tidal regions of estuaries are environments where methane production is relatively low. Unlike tidal flats and marshes, submerged estuarine sediments have no rooted macrophytes to inject labile organic matter at depths were methanogenesis occurs. In the freshwater area of the White Oak river estuary, Kelley et al (1995) found lower methane production rates in submerged sediments compared to tidal flat sediments. The organic matter undergoes several phases of degradation in the water column and at the sediment surface and looses most of its labile fraction before being incorporated into the methanogenic active zone of the sediment. In ETMs, periodic resuspensions of surface sediments with tidal currents make oxic and suboxic proc-

esses (nitrate, manganese and iron reductions) dominate the oxidation of organic matter (Abril et al. 1999). In addition, as soon as salinity and sulfate increase, sedimentary carbon remineralization generates in majority dissolved inorganic carbon and little methane (Martens and Goldhaber 1978; Kelley et al. 1990). Nevertheless, biogenic methane production occurs in estuarine channels, as evidenced by the more negative values of $\delta^{13}C\text{-}CH_4$ in the Great Bay estuary (US-New Hampshire) (Sansone et al. 1999). Methane production is also responsible for net methane inputs at very low salinities, observed in macrotidal systems like the Tyne and Humber estuaries (UK) (Upstill-Goddard et al. 2000), and the Gironde and Scheldt estuaries (Fig. 7.4). These regions correspond to the entrance of ETMs, a zone very active for mineralization of riverine organic matter and generally showing the maximum hypoxia.

7.7 Significance at the Global Scale

Owing to this large spatial heterogeneity, estimations of carbon dioxide and methane emissions at the global scale suffer from large uncertainties. In addition, there is also a large uncertainty on the surface of world estuaries. To our best knowledge, the only estimation of world estuarine surface available is the one by Woodwell et al. (1973), i.e. 1400.10^3 km^2. They estimated an inner estuarine surface/coast length ratio in the US which varied between 0.12 km^2·km^{-1} in the North Atlantic coast and 5.97 km^2·km^{-1} in the Gulf of Mexico with an average of 0.78 km^2·km^{-1} for the entire US. Then, Woodwell et al. (1973) extrapolated the latter average value to the entire world coastline but added that: "*It would be surprising if estimates derived in this way were accurate within ±50%*". Nevertheless, almost all gas emission budgets at the global scale were calculated with this estuarine surface. An average CO_2 flux of 100 mmol·m^{-2}·d^{-1} (Table 7.1) integrated over this surface gives a global flux of ~600.10^{12} gC·y^{-1}. This first order estimates is however higher than the total organic carbon transported by world rivers (~400.10^{12} gC·y^{-1} Ludwig et al. 1996). Owing to the fact that only about one half of the particulate organic carbon (representing 170.10^{12} gC·y^{-1}; Ludwig et al. 1996) is generally lost in estuaries (Abril et al. 2002) the overestimation is around a factor 3 to 5. This might be due to an overestimation of the estuarine surface, rather than an overestimation of the flux density from Table 7.1. However, it should also be noted that the estimate of Ludwig et al. (1996) only accounts for fluvial carbon inputs and does not account for lateral inputs (in particular from marshes and flats). No global estimates are at present time available for these, but local studies show they are significant (Cai et al. 1999). Most of the CO_2 fluxes

in estuaries have been reported so far in temperate latitudes, despite the fact that about 60% of the fresh water discharge and organic carbon inputs occurs at tropical latitudes (Ludwig et al. 1996). Anyhow, the carbon dioxide source from inner estuaries and sources or sinks from riverine plumes represent significant components of the global carbon cycle, which need to be further investigated both in terms of magnitude and in terms of processes involved. Methane emissions from estuaries (excluding tidal marshes) have been recently integrated at the global scale by several authors, using the same estuarine surface from Woodwell et al. (1973). Estimates are $0.8\text{-}1.3.10^{12}$ $gCH_4{\cdot}y^{-1}$ (Bange et al. 1994); $0.9\text{-}1.7.10^{12}$ $gCH_4{\cdot}y^{-1}$ (Upstill-Goddard et al. 2000) and $1.8\text{-}3.0.10^{12}$ $gCH_4{\cdot}y^{-1}$ (Middelburg et al. 2002). This is less than 10% of the global oceanic emission, which itself represents only 1-10% of all natural and anthropogenic sources (Bange et al. 1994). Thus, estuaries are a very minor contributor to the global methane emissions.

Acknowledgments

We thank Henri Etcheber (DGO-Bordeaux), Michel Frankignoulle (University de Liège, Belgium), Niels Iversen (Aalborg University), Jack Middelburg (NIOO, the Netherlands) and Roland Wollast (Université Libre de Bruxelles), for their continuous guidance and support during the BIOGEST project. This work benefited from funding by the European Union, through the several doctoral and post-doctoral grants between 1996 and 2001.

8 GHG Emissions from Boreal Reservoirs and Natural Aquatic Ecosystems

Alain Tremblay, Jean Therrien, Bill Hamlin, Eva Wichmann
and Lawrence J. LeDrew

Abstract

Carbon dioxide (CO_2), methane (CH_4) and nitrous oxide (N_2O) gross fluxes were measured at the air-water interface of 205 aquatic ecosystems in the Canadian boreal region from 1993 to 2003. Fluxes were obtained with a floating chamber connected to an automated NDIR or a FTIR instrument. The results show a temporary increase in CO_2 and CH_4 fluxes, followed by a gradual return to values comparable to those observed in natural aquatic ecosystems (lakes, rivers and estuaries). Mean values for CO_2 and CH_4 measured in Québec's reservoirs older than 10 years were 1508±1771 mg $CO_2 \cdot m^{-2} \cdot d^{-1}$ and 8.8±12 mg $CH_4 \cdot m^{-2} \cdot d^{-1}$. Our results showed a strong similarity between lakes, rivers, and old reservoirs across a 5000 km transect from the west coast to the east cost of Canada. These values are comparable to those observed in Finland or in the sub-tropical semi-arid western USA. Although several limnological parameters can influence these fluxes, none showed a statistical relationship. However, levels of CO_2 or CH_4 fluxes are influenced by pH, wind speed, depth at sampling stations and latitude.

8.1 Introduction

Carbon dioxide, CH_4 and N_2O, the global main greenhouse gases (GHGs), are emitted from both natural aquatic ecosystems (lakes, rivers, estuaries, wetlands) and man-made reservoirs (Lemon and Lemon 1981; Richey et al. 1988, 2002; Badr et al. 1991; Franken et al. 1992; Bartlett and Harris 1993; Cole et al. 1994; Hope et al. 1994; Bange et al. 1994, 1996; Bates et

al. 1996; IAEA 1996; Makhov and Bazhin 1999; Riera et al. 1999; Takahashi et al. 1999; Smith et al. 2000; Wickland et al. 2001; Borges and Frankignoulle 2002; Gurney et al. 2002; de Lima et al. 2002; Rosa et al. 2002ab). Greenhouse gas (GHGs) emissions from freshwater reservoirs and their contribution to the increase of GHGs in the atmosphere are actually at the heart of a worldwide debate (Rosa and Scheaffer 1994, 1995; Fearnside 1996; Gagnon and van de Vate 1997; St. Louis et al. 2000; Tremblay et al. In press). However, it must be pointed out that very few studies base their conclusions on direct systematic flux measurements at the water-air interface of reservoirs or natural systems. The uncertainties about the gross flux (measured) as well as the net flux (gross flux minus pre-impoundment natural emissions) are presently at the heart of the debate concerning methods of energy production.

In that perspective, Hydro-Québec and its partners have adapted a technique to measure gross GHG emission at the water-air interface that allows for a high rate of sampling in a short period of time, while increasing the accuracy of the results and decreasing the confidence intervals of the mean flux measured (Lambert and Fréchette, Chap. 2). Large reservoirs in the province of Québec have been sampled for a decade. Since 2002, the sampling has been extended to other provinces, in order to better assess the gross emission of GHGs from aquatic ecosystems in boreal regions, and to adequately estimate the contribution of reservoirs versus natural water bodies in these regions. Ultimately, the results will enable a better comparison of energy production methods.

8.2 Material and Methods

8.2.1 Study Areas

Natural lakes (122), rivers (24), estuaries (4) and man-made reservoirs (55) were sampled in the boreal region of Canada from 1993 to 2003. Sampling was conducted in British-Columbia (July and August 2002), Manitoba (July 2002), Québec (May to October, not systematically, 1993–2003) and Newfoundland (July 2003) (Fig. 8.1). The northern part of these sampling regions is characterized by a moist subarctic climate, while in the southern parts of the provinces of Ontario and Québec the climate is of a moist humid continental type, and the West coast of British-Columbia is under the influence of a maritime West Coast climate (Espenshade and Morrison 1980). Summers are usually warm (10 to 20ºC in July) in the subarctic and marine West Coast regions, and hot (21 to 32ºC) in the others, while the

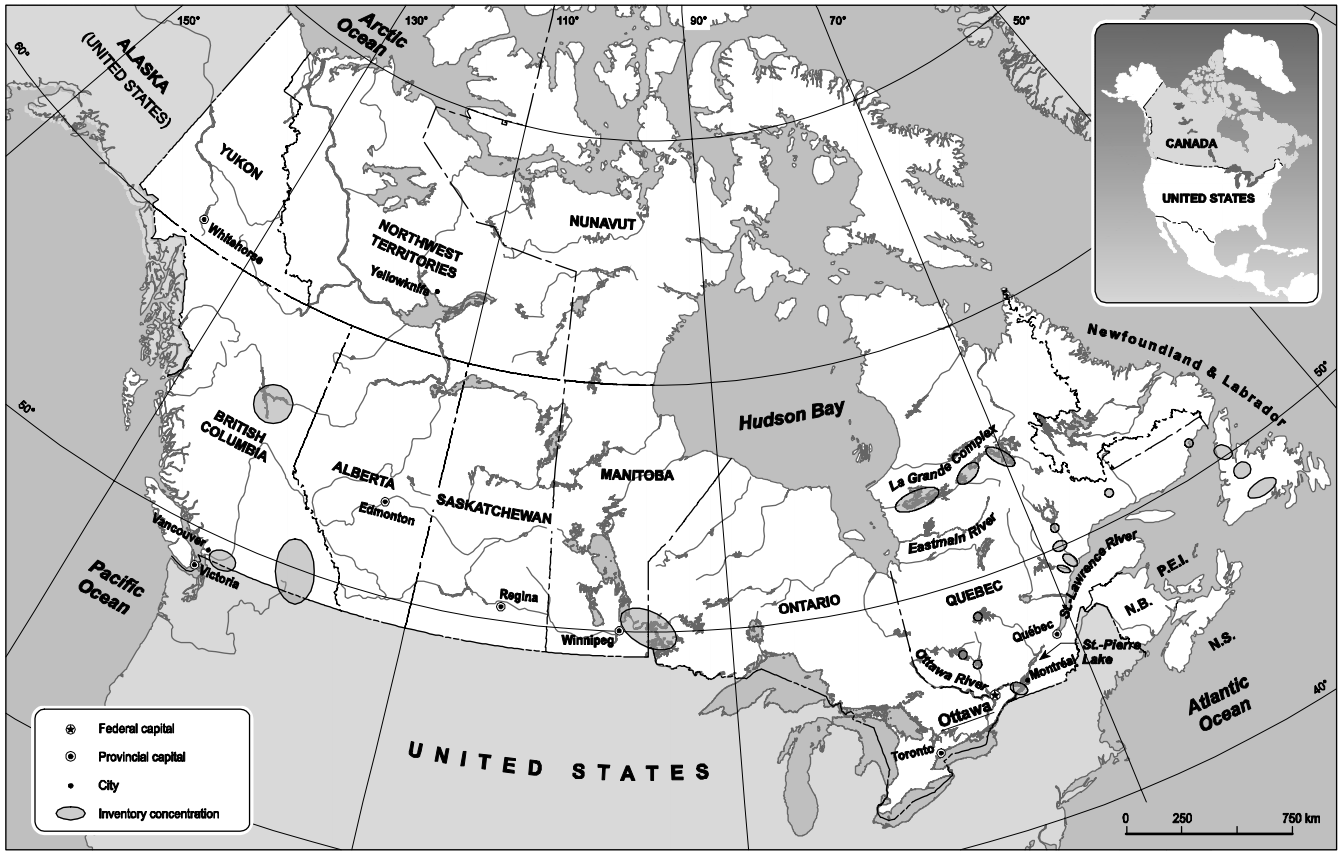

Fig. 8.1. Location of the Canadian regions where gross fluxes of GHG at air-water interface were sampled in 1993-2003

winters are cold (-23 to -12ºC in January) in the subarctic region, cool (-12 to -1ºC) in the humid continental region and mild (-1 to 10ºC) in the marine West Coast region. Mean annual water precipitation is of 750–1250 mm in the eastern provinces, 500–750 mm in the Hudson Bay region, 250–500 mm in the plains (Manitoba and eastern British-Columbia), and 1250–2500 mm on the West Coast. Dominant vegetation is evergreen needleleaf trees, except for the southern parts of Ontario and Québec where deciduous vegetation prevails. Characteristics of the ecosystems sampled are given in Table 8.1.

8.2.2 Measurement of GHG Fluxes and Other Variables

The GHG fluxes were measured with a floating chamber. More details about the different apparatus used and the comparison of the various sampling methods are available in Lambert and Fréchette (Chap. 2). Dimensions of the chamber varied from year to year, the volume of air trapped in the chamber being about 30L from 1993 to 2000, and 20L afterward. From 1993 to 2000, the air was sampled with syringes and analysed afterward in labortory. Since 2001, the chamber is linked to a Non-Dispersive Infrared (NDIR) and Fourier Transform Infrared (FTIR) instruments (Li-Cor, PP-Systems or Gasmet) which takes continuous readings. The first two instruments measure only CO_2 while the Gasmet measures the three GHGs. The NDIR data logger (Campbell Scientific, model CR10X) stores a value every 20 seconds over a sampling period of 5–10 min. Several locations were sampled from each site with a minimum of two fluxes per location. A regression curve is fitted on the results for every flux measured, and its slope determines the average flux (mg $CO_2 \cdot m^{-2} \cdot d^{-1}$) using the following equation:

$$\text{Flux} = \text{slope} \times F1 \times F2 \times \text{volume} \times \text{surface}^{-1} \qquad (8.1)$$

where F1 is a conversion factor from ppm to $mg \cdot m^{-3}$, F2 is a conversion factor from second to day, volume of air in the floating chamber, and surface of the floating chamber. The value is either accepted or rejected, depending on the correlation coefficient (R^2) of the regression curve (Lambert and Fréchette, Chap. 2).

Other measurements, such as GPS position, weather conditions, wave height, water and air temperature, water color and transparency (Secchi disk), depth, pH (Beckman 200 and Oakton 300), alkalinity (titration), and wind velocity (Extech Instruments 407112) and direction were made at each site.

Table 8.1. General characteristics of the major Canadian aquatic ecosytems sampled in 1993-2003

Ecosystem	Flooding year	pH	Water temp [°C]	Lat. [°]	Long. [°]	Years sampled	CO_2 ($mg \cdot m^{-2} \cdot d^{-1}$)				CH_4 ($mg \cdot m^{-2} \cdot d^{-1}$)				N_2O ($mg \cdot m^{-2} \cdot d^{-1}$)			
							N	Mean	S.D.^{2}	Range	N	Mean	S.D.^{2}	Range	N	Mean	S.D.^{2}	Range
BRITISH-COLUMBIA																		
Reservoirs																		
Alouette	1928	7.1	20.3	49.34	122.41	2002	5	-407	383	-1088 - -171								
Arrow-Lower	1969	9.1	19.9	49.84	118.10	2002	5	-1032	286	-1319 - -637	2	6.6	0.42	6.3 - 6.9	6	0.20	0.17	-0.04 - 0.44
Arrow-Narrows		8.9	18.7	50.05	117.92	2002	6	-972	481	-1786 - -466	6	52.9	60.0	6.9 - 148.7	7	-0.03	0.52	-1.22 - 0.49
Arrow-Upper		7.9	12.9	50.74	117.95	2002	10	1039	1811	-1236 - 3666	9	23.0	25.0	-6.8 - 62.6	21	0.06	0.22	-0.59 - 1.39
Buntzen	1914	6.4	15.9	49.35	122.86	2002	4	1411	264	1023 - 1589								
Duncan	1965	8.4	18.9	50.34	116.93	2002	6	-810	470	-1636 - -301	3	10.0	14.0	-0.1 - 27.1	8	0.21	0.53	-0.73 - 1.07
Jones	1952	7.8	17.8	49.23	121.61	2002	4	-213	290	-529 - 161								
Kootenay		8.3	16.0	49.75	116.88	2002	18	-142	939	-1344 - 1495	14	23.5	44.0	4.9 - 177.8	25	0.04	0.25	-0.52 - 0.62
Seven Mile	1979	8.4	22.2	49.03	117.40	2002	6	-731	398	-1380 - -371	10	109.5	113.0	27.7 - 347.7	10	-0.14	0.14	-0.33 - 0.10
Stave	1911	6.8	18.8	49.33	122.30	2002	10	602	177	354 - 934								
Waneta		8.4	21.7	49.01	117.55	2002	6	-469	299	-1045 - -265	9	38.8	44.6	5.0 - 124.9	9	-0.05	0.36	-0.74 - 0.46
Whatshan	1951	7.8	20.8	50.00	118.14	2002	1	-5			3	5.8	5.64	0.1 - 11.3	8	0.26	0.41	-0.20 - 1.03
Williston-Finlay	1961	8.2	13.9	56.09	124.02	2002	7	704	413	328 - 1334								
Williston-Parsnip	1969	8.1	15.1	55.49	123.36	2002	8	1758	567	839 - 2703								
Williston-Peace	1979	8.3	11.8	56.07	122.79	2002	9	920	329	413 - 1460								
Total reservoirs		8.0	17.1			2002	105	198	1162	-1786 - 3666	56	42.1	66.7	-6.8 - 347.7	94	0.05	0.38	-1.22 - 1.39
Lakes																		
Charlie		8.2	15.5	56.30	120.96	2002	4	763	433	275 - 1300	1	2.7						
Chehalis		7.1	17.0	49.44	122.02	2002	4	245	142	85 - 377								
Chilliwack		7.4	16.7	49.06	121.42	2002	5	777	130	648 - 984								
Moberly		8.2	13.3	55.82	121.77	2002	5	1706	857	840 - 2780								
Slocan		7.9	17.7	49.84	117.45	2002	4	49	540	-419 - 640	5	15.3	12.6	3.9 - 33.0	10	0.21	0.58	-0.30 - 1.38
Trout		8.0	16.2	50.56	117.39	2002	1	-412			1	<0.1			6	-0.03	0.22	-0.38 - 0.28
Total lakes		7.8	16.3			2002	23	706	778	-419 - 2780	7	11.3	12.4	<0.1 - 33.0	16	0.12	0.48	-0.38 - 1.38
Rivers																		
Columbia		8.4	17.7	49.07	117.61	2002	2	-424	21	-439 - -410					2	0.10	0.12	0.01 - 0.19
Harrison		7.5	14.3	49.26	121.94	2002	3	1053	470	563 - 1501								
Total rivers		7.8	15.7	49.18	120.21	2002	5	462	470	-439 - 1501					2	0.10	0.12	0.01 - 0.19
MANITOBA/ONTARIO																		
Reservoirs																		
Great Falls	1928	7.5	22.6	50.28	95.54	2002	10	5754	3487	694 - 11670	9	15.3	29.0	-54.8 - 43.2	10	0.09	0.09	-0.06 - 0.22
Lac Bonnet		7.9	23.9	50.15	95.43	2002	4	3447	957	2641 - 4819	4	23.8	29.0	0.0 - 66.4	8	0.03	0.15	-0.25 - 0.30
Pine Falls	1952	7.7	23.2	50.43	95.79	2002	11	3404	1837	1278 - 7093	11	-5.0	324.0	-756.8 - 629.5	14	0.08	0.12	-0.08 - 0.37

Table 8.1. (cont.)

Ecosystem	Flooding year	pH	Water temp [°C]	Lat. [°]	Long. [°]	Years sampled	CO_2 (mg•m^{-2}•d^{-1})				CH_4 (mg•m^{-2}•d^{-1})				N_2O (mg•m^{-2}•d^{-1})			
							N	Mean	S.D.[2]	Range	N	Mean	S.D.[2]	Range	N	Mean	S.D.[2]	Range
Pointe du Bois		7.8	22.2	50.18	95.15	2002	7	3102	1783	-464 - 4994					10	0.08	0.14	-0.11 - 0.32
Seven Sisters Falls	1931	7.5	22.7	50.10	95.53	2002	16	4979	3736	460 - 11279					17	0.07	0.13	-0.09 - 0.46
Slave Falls		7.7	21.9	50.10	95.10	2002	8	2336	1028	992 - 3533	1	113.0			8	0.07	0.28	-0.58 - 0.57
Total reservoirs	1937	7.7	22.8			2002	56	4086	2896	-464 - 11670	25	11.6	211.0	-756.8 - 629.5	67	0.07	0.16	-0.58 - 0.57
Lakes																		
Bereton		7.2	23.8	49.90	95.54	2002	4	1795	549	1001 - 2264								
Betula		7.7	23.8	50.08	95.58	2002	3	2949	2995	1025 - 6029								
Bird		7.4	23.9	50.48	95.32	2002	4	1315	436	787 - 1856								
Bonnet		7.8	22.4	50.34	95.93	2002	10	3396	1519	1135 - 5617								
Falcon		8.1	22.9	49.71	95.26	2002	4	733	1188	-32 - 2505								
Jessica		7.9	24.9	50.01	95.50	2002	5	393	1758	-688 - 3495								
Shoal		8.1	23.7	49.61	94.88	2002	6	3597	5195	-725 - 10893	8	435.5	620.0	13.5 - 1763.6	12	0.01	0.18	-0.44 - 0.30
Sturgeon		7.7	26.5	49.84	94.44	2002	3	-227	135	-357 - -87								
West Hawk		8.0	23.9	49.77	95.18	2002	4	-111	164	-308 - 78								
White		8.2	24.7	50.03	95.54	2002	4	-840	489	-1438 - -272								
Winnipeg		8.4	23.7	50.69	96.58	2002	6	895	412	211 - 1457								
Lake of the Woods		7.6	22.0	49.45	94.30	2002	15	-4434	2843	1786 - 9467	3	50.1	61.7	-20 - 93	15	0.02	0.24	-0.41 - 0.40
Total lakes		7.9	23.8	50.04	95.46	2002	53	2193	2789	-1438 - 10893	8	330	549	13.5 - 1763.6	12	0.01	0.21	-0.44 - 0.40
Rivers																		
Lee		8.2	24.7	50.33	95.84	2002	5	330	1076	-1437 - 10893								
Gray		8.0	7.7	45.03	74.67	2003	8	1736	1180	-226 - 2780								
ONTARIO/QUÉBEC																		
Rivers																		
Outaouais		7.3	14.4	45.61	74.60	2003	36	2200	914	-6 - 6241								
St. Lawrence		8.1	17.6	45.63	73.68	1999, 2003	150	438	1576	-2406 - 7719	3	36.4	7.1	28.5 - 42.3				
QUÉBEC																		
Reservoirs																		
Baskatong	1927	6.3	13.8	46.76	76.00	2002	19	1161	481	144 - 2006	3	3.2	0.7	2.5 - 3.8	9	0.03	0.20	-0.37 - 0.22
Bersimis	1959	6.4	14.0	49.39	69.69	2002 - 2003	12	1485	1258	0 - 4424	3	< 0.1	< 0.1	< 0.1 - < 0.1	6	0.08	0.05	0.01 - 0.14
Cabonga	1928	6.1	17.3	47.30	76.66	1996 - 1997, 2002	160	1381	1178	-1429 - 11260	153	13.9	12.0	0.9 - 67.9	23	0.20	0.35	-0.32 - 1.06
Caniapiscau	1984	6.5	17.1	54.40	69.86	2003	28	669	1029	-12 - 4212	20	9.8	6.8	-3.0 - 24.1	47	0.05	0.46	-0.87 - 1.29
EOL	1979	6.3	16.5	53.27	76.66	2003	18	1161	515	47 - 1980	9	3.8	4.5	-2.3 - 9.7	22	0.13	0.25	-0.39 - 0.66
Gouin	1964	6.5	18.3	48.56	74.57	1999, 2003	15	665	602	0 - 2132	10	2.7	3.6	0.0 - 11.6				
Lac St-Jean	1956	5.9	12.8	49.64	70.31	2003	12	1480	642	526 - 2443								

Table 8.1. (cont.)

Ecosystem	Flooding year	pH	Water temp [°C]	Lat. [°]	Long. [°]	Years sampled	CO_2 ($mg \cdot m^{-2} \cdot d^{-1}$)				CH_4 ($mg \cdot m^{-2} \cdot d^{-1}$)				N_2O ($mg \cdot m^{-2} \cdot d^{-1}$)			
							N	Mean	S.D.[2]	Range	N	Mean	S.D.[2]	Range	N	Mean	S.D.[2]	Range
Laforge 1	1993	6.3	15.1	54.23	72.71	1993-1997, 2001, 2003	342	2062	1601	21 - 10271	326	27.3	67.0	0.0 - 724.9	24	-0.11	0.33	-0.78 - 0.63
Laforge 2	1984	6.5	17.4	54.57	70.15	2003	11	833	1279	-277 - 4197	11	7.5	1.2	5.1 - 9.0	21	0.18	0.12	-0.73 - 1.57
La Grande 1	1979	6.2	8.7	53.90	77.91	2003	11	1667	839	715 - 3371	4	8.8	2.2	6.5 - 12.3	10	0.21	0.25	-0.34 - 0.55
La Grande 3	1984	6.4	11.5	53.72	75.68	2003	35	1707	1278	-251 - 5045	17	8.1	14.0	-3.0 - 45.9	42	0.08	0.44	-1.30 - 1.19
La Grande 4	1983	6.3	14.4	54.36	73.13	2003	27	1178	677	-1196 - 2594	16	10.8	8.6	-3.0 - 31.1	29	0.11	0.3	
Manic 1	1951	6.3	11.9	49.21	68.35	1999, 2002-2003	7	3054	1508	0 - 4295	3	11.3	9.8	0 - 18.4	2	0.23	0.21	-0.71 - 0.76
Manic 2	1965	6.7	18.3	49.46	68.38	1999	10	848	1250	0 - 3003	10	6.0	8.8	0.0 - 22.8				
Manic 3	1971	6.6	16.4	50.14	68.62	1999	7	306	403	48 - 1186	7	1.1	1.3	0.2 - 3.7				
Manic 5	1964	6.7	11.0	51.20	68.69	1999, 2001-2003	61	1407	1180	-3409 - 4002	29	6.1	9.6	< 0.1 - 42.2	16	0.17	0.18	-0.43 - 0.24
Opinaca	1980	6.2	17.2	52.47	76.37	2003	85	1885	906	622 - 5376								
Outaouais	1962	7.5	20.9	45.56	74.40	2003	3	1282	133	-435 - 1377								
Outardes 3	1969	6.5	14.8	49.57	68.81	1999	1	85			1	0.1						
Outardes 4	1968	6.5	14.6	50.16	68.72	1999, 2001-2003	33	2187	2003	0 - 9076	11	0.9	3.8	-7.3 - 8.4	16	0.09	0.24	-0.42 - 0.53
Péribonka		6.4	19.5	48.76	71.61	2003	2	2504	561	2107 - 2901								
Robertson	1994	6.0	13.1	51.00	59.53	2001-2003	50	1408	779	8 - 5031	27	6.1	5.4	-5.0 - 22.7	30	0.13	0.27	-0.51 - 0.87
Robert-Bourassa	1979	6.4	12.7	53.68	77.07	1993 - 1994, 1997, 1999 - 2001, 2003	204	1706	226	-228 - 16721	157	7.9	15.0	-8.3 - 115.7	75	0.14	0.42	-1.38 - 1.29
SM 2		5.7	16.4	50.31	66.64	2001-2003	48	1506	914	278 - 3601	26	4.1	6.5	-25.7 - 9.5	38	0.06	0.18	-0.34 - 0.38
SM 3	1998	6.1	11.5	51.40	67.02	2001-2003	79	5484	3134	49 - 15618	30	2.7	4.2	-4.9 - 14.7	35	0.04	0.5	-1.15 - 1.42
Toulnoustouc	1957	6.3	12.4	50.06	67.83	2002 - 2003	12	1393	838	645 - 3370	3	0.1	0.13	-0.1 - 0.2	10	0.10	0.34	-0.47 - 0.69
Total reservoirs[1]		6.3	14.6				870	1508	1471	-3408 - 16720	520	8.8	12	-25.7 - 724.9	396	0.10	0.36	-1.38 - 1.57
Lakes																		
Baskatong region		8.4	15.0	46.74	75.87	2002	14	-389	599	-688 - 1033								
Bersimis region		6.6	13.9	49.13	69.17	2002	4	670	440	19 - 998					3	0.12	0.11	<0.01 - 0.22
Cabonga region				47.07	76.72	2002	37	935	471	235 - 2424								
Caniapiscau region		6.5	17.2	54.99	69.62	2003	7	536	560	2 - 1533	5	-0.5	1.4	-3.0 - 0.4	14	0.03	0.67	-0.91 - 1.31
Eastmain region		6.4	20.2	52.12	75.95	2003	194	1002	702	-655 - 2925								
Gouin region		5.9	19.3	48.56	73.81	1999, 2003	10	1525	1177	285 - 4289	5	6.6	3.8	0.8 - 10.7				
Laforge 1 region		6.4	17.6	54.27	72.45	1995 - 2003		2256	1196	47 - 5439	8	0.5	0.83	-0.3 - 2.2	12	0.03	0.18	-0.42 - 0.28
La Grande 3 region		6.6	14.3	53.76	74.22	2003	4	771	675	19 - 1662	3	0.9	1.5	-2.6 - 0.4	7	0.14	0.25	-0.25 - 0.46
La Grande 4 region		6.7	17.2	54.07	72.84	2003	1	1024			1	0.3			2	-0.23	1.10	-0.31 - -0.14
Manic 2 region		6.5	19.5	49.86	68.54	1999	5	1125	1805	15 - 4205	5	6.7	10.8	0.1 - 25.7				

Table 8.1. (cont.)

Ecosystem	Flooding year	pH	Water temp [°C]	Lat. [°]	Long. [°]	Years sampled	CO_2 (mg•m^{-2}•d^{-1})				CH_4 (mg•m^{-2}•d^{-1})				N_2O (mg•m^{-2}•d^{-1})			
							N	Mean	S.D.^{2}	Range	N	Mean	S.D.^{2}	Range	N	Mean	S.D.^{2}	Range
Manic 3 region		6.6	18.2	50.50	68.49	1999	5	678	578	52 - 1550	5	1.1	0.8	0.1 - 2.0				
Manic 5 region		6.6	13.4	51.29	69.06	1999, 2001-2002	33	682	538	21 - 2404	20	-8.0	29.0	-124.5 - 4.3	11	0.10	0.22	-0.28 - 0.41
Opinaca region		6.8	15.8	52.76	76.59	2003	24	1101	496	300 - 2504					4	0.13	0.12	-0.02 - 0.24
Outardes 4 region		6.1	16.9	50.17	69.00	1999, 2001-2002	12	1489	871	62 - 3440	5	1.4	1.1	0.1 - 3.1	2	0.03	0.04	<0.01 - 0.07
RB region		6.9	13.9	53.52	77.39	1999-2001, 2003	80	1357	1488	-224 - 7008	51	2.6	9.0	-7.9 - 62.2	10	0.07	0.25	-0.26 - 0.47
Robertson region		6.0	13.9	51.12	60.60	2001-2003	23	887	410	-326 - 1510	11	1.5	5.8	-2.7 - 18.6	14	0.03	0.23	-0.54 - 0.35
Saguenay region		6.4	15.9	49.26	70.59	2003	26	997	915	-575 - 3144								
SM 2 region		5.3	13.3	50.58	66.68	2001-2003	19	1220	607	639 - 2778	3	2.1	2.8	0.3 - 4.6	6	0.16	0.77	-0.71 - 1.45
SM 3 region		6.4	11.6	51.23	65.60	2001-2003	31	1299	2791	-5723 - 10947	23	-1.1	11.9	-51.1 - 9.7	15	-0.02	0.11	-0.41 - 0.25
Total lakes		6.5	16.5				551	1013	1095	-5722 - 10946	150	0.6	13.4	-124 - 62	100	0.05	0.35	-0.9 - 1.45
Rivers																		
Cabonga region		6.3	15.8	47.23	76.73	2002	3	1684	315	1382 - 2012	1	10.7			2	-0.18	3.19	-0.43 - 0.07
Caniapiscau region		6.5	19.0	54.95	69.49	2003	3	602	1409	-904 - 1887					4	0.22	0.82	-0.40 - 0.79
Eastmain region		6.6	16.1	52.13	75.42	2003	28	965	565	-47 - 1845								
La Grande 1 region		6.3	10.1	53.61	77.85	2001, 2003	8	1738	961	591 - 3057	5	4.5	1.3	3.0 - 6.0	5	0.39	0.40	-0.06 - 1.01
Manic region		4.6	18.7	50.22	66.58	2003	2	1338	703	840 - 1836								
Montreal region		7.3	13.8	45.62	73.71	2003	60	2587	1771	-8 - 11163								
Outaouais region		7.3	14.9	45.21	74.32	2003	31	2377	1386	-6 - 6241								
RB region		6.6	16.0	53.65	77.43	2000, 2001	4	1343	542	769 - 2039	4	<0.1	5.6	-7.9 - 5.2	3	0.11	0.38	-0.31 - 0.47
Saguenay region		6.4	17.9	48.75	72.19	2003	14	569	508	-24 - 1390								
Total rivers		7.0	14.8				161	1976	1536	-904- 11163	10	3.3	4.2	-7.9 - 10.7	15	0.14	0.26	-0.63 - 1.01
Estuaries																		
Bersimis region		6.4	14.9	48.93	68.68	2002	5	2807	1070	1080 - 3778	2	39.3	3.0	37.1 - 41.5	2	0.34	0.13	0.25 - 0.43
Montreal region		8.8	21.9	45.26	74.16	2003	2	-863	144	-965 - -761								
Robertson region		7.1	10.8	51.00	59.04	2001-2003	9	85	939	-1068 - 1234	1	<0.1			5	-0.09	0.15	-0.35 - 0.08
SM region		6.5	11.3	50.16	66.62	2002	5	1083	1013	-727 - 1595	3	2.5	4.3	-0.4 - 7.5	5	0.40	1.54	-0.71 - 3.12
Total estuaries		6.9	12.7				21	880	1521	-1068 - 3778	6	14.4	19.5	-0.4 - 20.5	12	0.19	0.96	-0.71 - 3.12
NEWFOUNDLAND																		
Reservoirs																		
Red Indian		6.8	20.8	48.78	56.65	2003	12	764	430	361 - 1792								
Maelpaeg			18.2	48.21	56.63	2003	16	1376	501	477 - 2156								

Table 8.1. (cont.)

Ecosystem	Flooding year	pH	Water temp [°C]	Lat. [°]	Long. [°]	Years sampled	CO_2 ($mg \cdot m^{-2} \cdot d^{-1}$)				CH_4 ($mg \cdot m^{-2} \cdot d^{-1}$)				N_2O ($mg \cdot m^{-2} \cdot d^{-1}$)			
							N	Mean	S.D.[2]	Range	N	Mean	S.D.[2]	Range	N	Mean	S.D.[2]	Range
Upper Salmon (Long Pond)	1967	5.8	14.7	47.95	55.90	2003	11	1906	541	1137 - 3199								
Upper Salmon (Cold Sping Pond)	1983	5.9	17.4	48.18	56.30	2003	16	1923	678	1083 - 3402								
Hinds	1980		18.3	48.99	57.04	2003	16	2105	812	832 - 4164								
Cat Arm	1985		17.8	50.05	56.95	2003	28	2257	1053	696 - 4886								
Maelpaeg (Granite Lake)			17.9	48.20	56.96	2003	18	3263	498	2535 - 4405								
Sandy	1925		20.8	49.25	57.03	2003	14	2510	1398	681 - 4993								
Total reservoirs		6.2	18.1				131	2089	1047	361 - 4993								
Lakes																		
Ahwachan-Jeech		6.8	19.7	48.09	56.10	2003	4	498	143	374 - 703								
Little Gull		7.1	22.8	48.37	55.47	2003	6	-501	230	-828 - -137								
Maelpaeg		5.7	19.6	48.29	56.78	2003	8	1036	245	736 - 1400								
Portland			17.4	50.19	57.57	2003	14	1223	495	470 - 2285								
River Ponds			18.0	50.52	57.38	2003	4	1232	163	1056 - 1388								
Shefield			17.8	49.33	56.57	2003	10	1053	162	764 - 1326								
Total lakes		6.4	19.0				46	867	648	-828 - 2285								

1: Reservoir > 10 years old 2. S.D. = standard deviation

8.2.3 Statistical Analyses

Exploratory analyses were done using statistical factor analysis and canonical analysis (Legendre and Legendre 1998). Then, using the major parameters responsible for the variability in GHG fluxes, a multiple regression analysis (backward stepwise) was conducted. Finally, when adequate results were obtained, a simple regression analysis was done with a single variable. Comparisons of mean fluxes between water bodies were done with Anova and Tukey analyses. When applicable, the level of acceptance of the results was $p<0.05$. Statistical analyses were done with Statistica or Statgraph software.

8.3 Results and Discussion

8.3.1 Spatial Variation of GHG Emissions

A total of 2612 CO_2 diffusive fluxes were measured, not including duplicates. In Québec, the mean values are 1013±1095 mg $CO_2 \cdot m^{-2} \cdot day^{-1}$ in natural lakes, 1976±1536 mg $CO_2 \cdot m^{-2} \cdot day^{-1}$ in rivers and 1508±1471 mg $CO_2 \cdot m^{-2} \cdot day^{-1}$ in reservoirs (Table 8.1). These emissions are comparable to those reported by Duchemin et al. (1995) and Duchemin et al. (1999) over boreal reservoirs, as well as those reported by Tremblay et al. (2001) and Lambert and Fréchette (2001, 2002) from Quebec's lakes and reservoirs. Similarly, in Finland the mean CO_2 emission in the Lokka and Porttipahta reservoirs, during open water season, are the same order of magnitude with 1700 and 3400–4000 mg $CO_2 \cdot m^{-2} \cdot day^{-1}$, respectively (Kortelainen 1998; Martikainen et al. 1996).

For CH_4, a total of 1144 diffusive fluxes, not including duplicates, were measured. The means fluxes are 0.6±13 mg $CH_4 \cdot m^{-2} \cdot day^{-1}$, in natural lakes, 3.3±4.2 mg $CH_4 \cdot m^{-2} \cdot day^{-1}$ in rivers and 8.8±12.0 mg $CO_2 \cdot m^{-2} \cdot day^{-1}$ in reservoirs (Table 8.1). The sampling covered only diffusive fluxes which are considered the major contribution to emissions from boreal reservoirs (Duchemin et al. 1995; Vaisanen et al. 1996; Hellsten et al. 1996), unlike tropical reservoirs where the average proportion (about 40%) of ebullitive fluxes is significant (Table 8.2). Our measured values are comparable to those from temperate or boreal forest ecosystems with values ranging from 0.1 to >25 mg $CH_4 \cdot m^{-2} \cdot day^{-1}$ (Lamontagne et al. 1973; Ford and Naiman 1988; Naiman et al. 1987; Chanton and Martens 1988). Shallow reservoirs with flooded peatland could have CH_4 ebullitive emissions (Duchemin 2000; Huttunen et al. 2002).

Table 8.2. Diffusive and ebullitive CH_4 fluxes in tropical reservoirs

Reservoir	Diffusion [$mg \cdot m^{-2} \cdot d^{-1}$]	Ebullition [$mg \cdot m^{-2} \cdot d^{-1}$]	[%]	Reference
Itaipu			4–7	Rosa et al. (2002ab)
Tucuruí			6–19	Rosa et al. (2002ab)
Segredo			17–25	Rosa et al. (2002ab)
Xingó			7–39	Rosa et al. (2002b), Duchemin et al. (2000)
Miranda			11–40	Rosa et al. (2002ab)
Samuel			11–56	Rosa et al. (2002ab)
Petit-Saut	770	530	40.8	Galy-Lacaux et al. (1997)
Barra Bonita			14–75	Rosa et al. (2002ab)
Curua-Una[a]	20	12	37.5	Duchemin et al. (2000)
Curua-Una[b]	16	65	80.2	Duchemin et al. (2000)
Serra da Mesa			63–92	Rosa et al. (2002ab)
Três Marias			83–87	Rosa et al. (2002ab)

a Dry season.
b Rain season.

We have measured a total of 773 N_2O fluxes with values ranging from -1.38 to 3.10 mg $N_2O \cdot m^{-2} \cdot d^{-1}$. These values are low compared to the CO_2 and CH_4 fluxes, as was stated by IAEA (1996). These values are consistent to the values measured on natural lakes with values varying from 0.1 to 0.7 (Downes 1991; Mengis et al. 1997) for the temperate regions and around 3.5 mg $N_2O \cdot m^{-2} \cdot d^{-1}$ for the Great Lakes (Lemon and Lemon 1981). Values ranging from 0.2 to >25 are also observed on rivers of the temperate regions (Deck 1981; de Angelis and Gordon 1985; Hemond and Duran 1989; McMahon and Dennehy 1999).

Variations were observed in the fluxes of CO_2 (Fig. 8.2), CH_4 (Fig. 8.3) and N_2O (Fig. 8.4) from British Columbia (West coast) to Newfoundland (East coast) representing a transect of fluxes spread over more than 5000 km (Fig. 8.1) covering different habitats of Canadian boreal ecosystems. These values include measures from reservoirs only older than 9 years for CO_2 and 4 years for CH_4 to avoid the large fluxes from young reservoirs (see below). Spatial disparity is high both in the means of ecosystem type and between different types in the same province. The strong similitude between the various ecosystems (lake, river and reservoir) is shown by the general overlap of standard deviation within a province. Similar overlaps also occur in reservoirs older than 10 years and lakes in boreal regions in Finland (Hellsten et al. 1996), Sweden (Bergstrom et al., in press), and in semi-arid western USA (Therrien et al., Chap. 9).

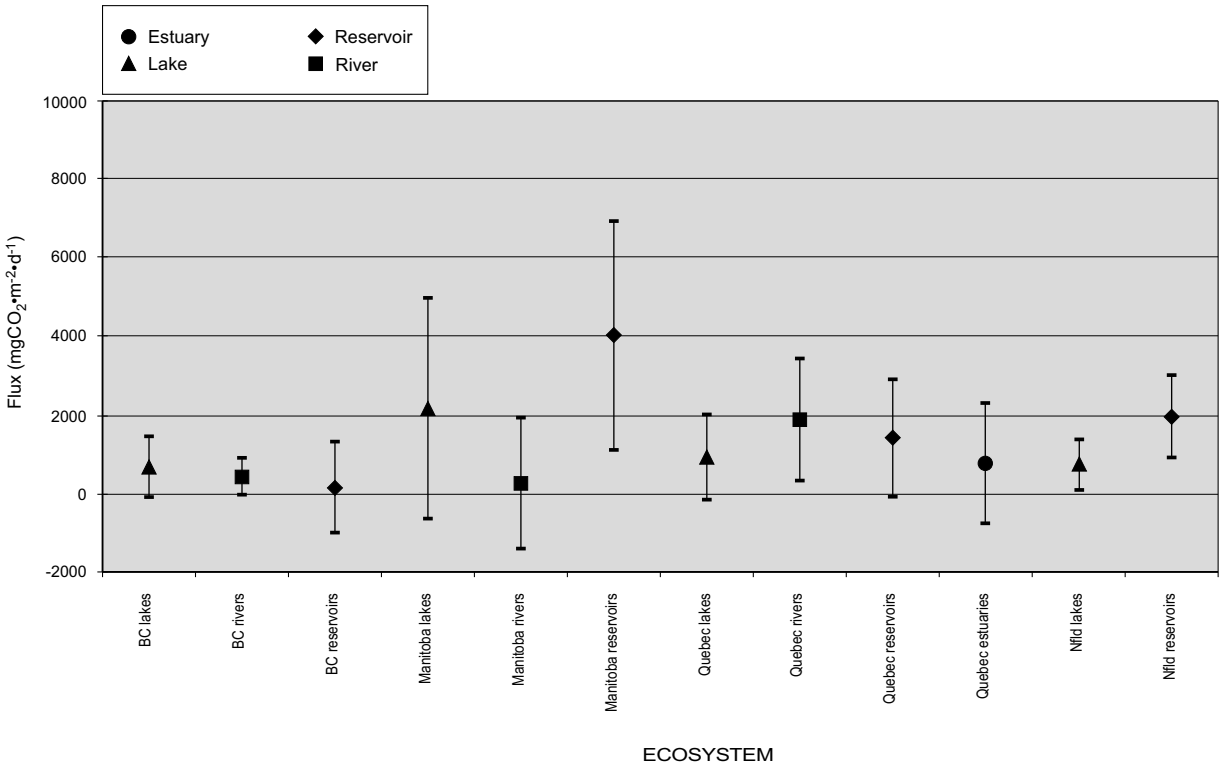

Fig. 8.2. Mean value and standard deviation of gross fluxes of CO_2 at the air-water interface in different ecosystems and provinces of Canada. Extreme individual ecosystem averages from at least 3 fluxes are shown. The mean for reservoirs is for 10 years old or more. In Manitoba, only Shoal lake and Lake of the Woods were considered since they feed the Winnipeg River System where are built the 7 reservoirs

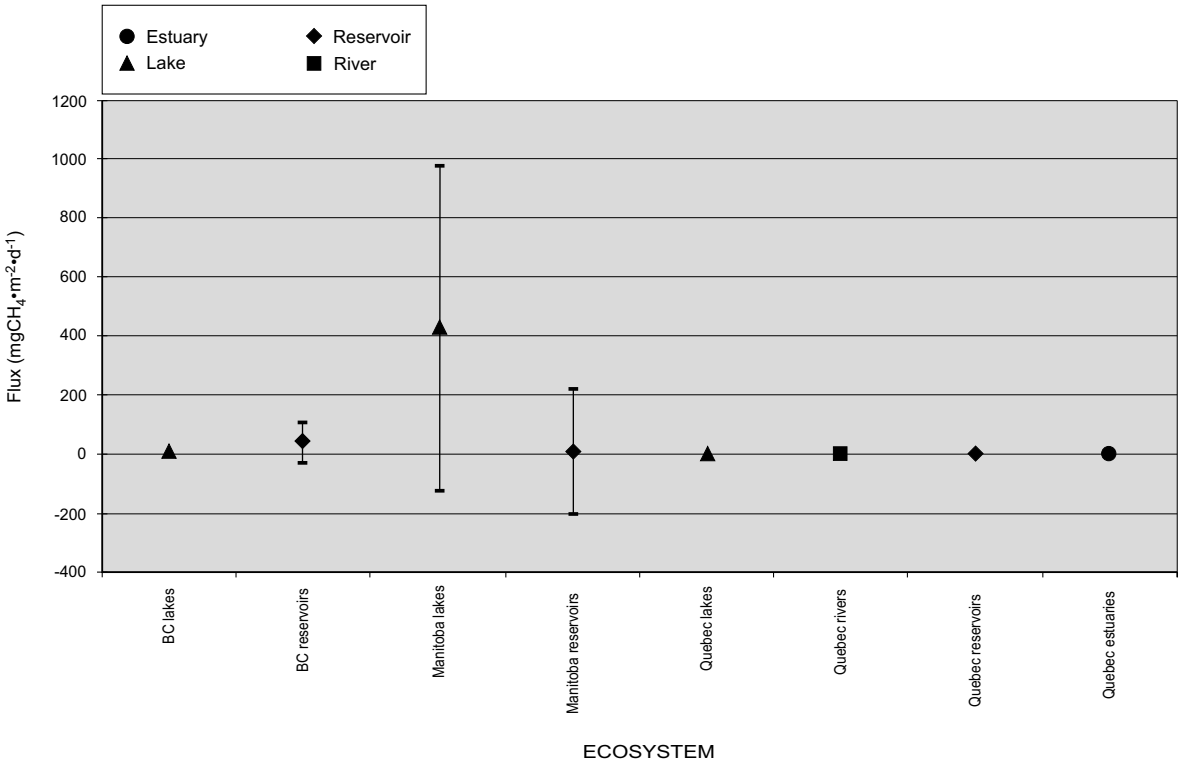

Fig. 8.3. Mean value and standard deviation of gross diffusive fluxes of CH_4 at air-water interface in different ecosystems and provinces of Canada. Extreme individual ecosystem averages from at least 3 fluxes are shown. The mean for reservoirs is for 5 years old or more. In Manitoba, only Shoal lake and Lake of the Woods were considered since they feed the Winnipeg River System where are built the 7 reservoirs

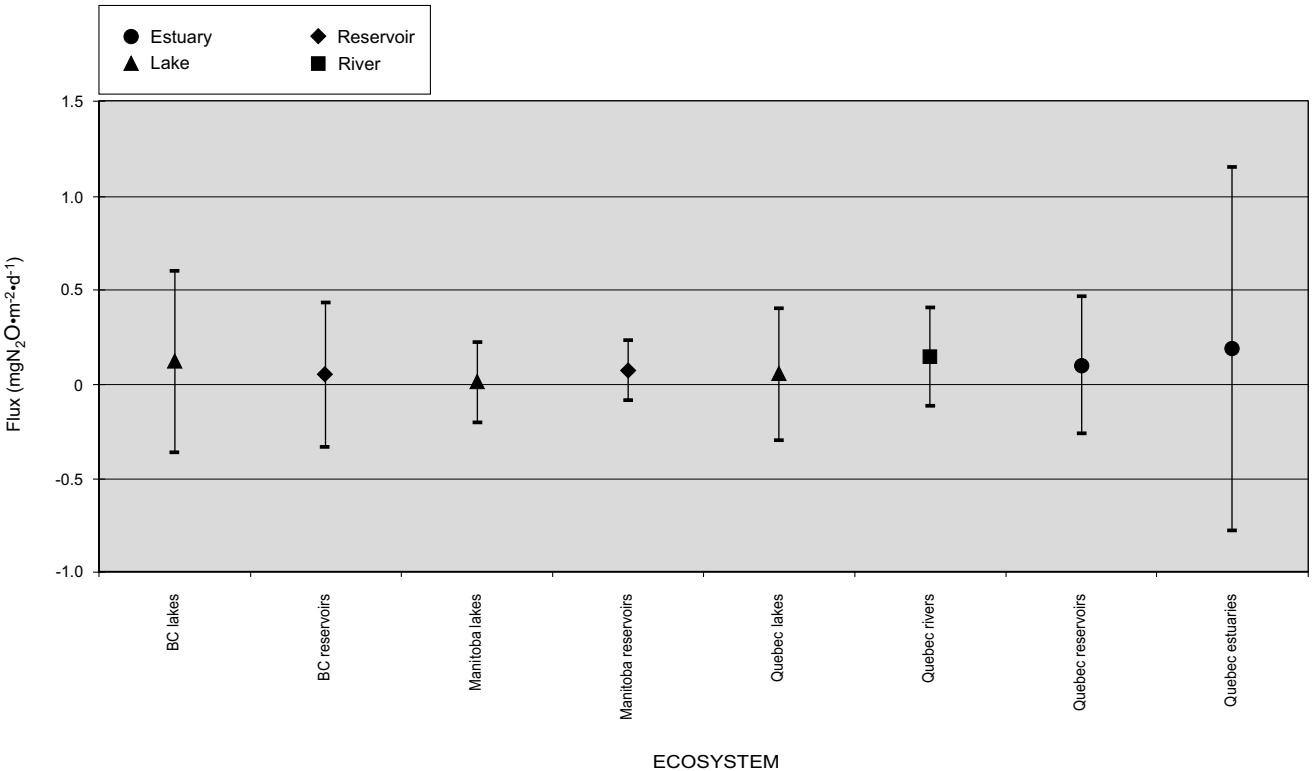

Fig. 8.4. Mean value and standard deviation of gross diffusive fluxes of N_2O at the air-water interface in different ecosystems and provinces of Canada. Extreme individual ecosystem averages from at least 3 fluxes are shown. In Manitoba, only Shoal lake and Lake of the Woods were considered since they feed the Winnipeg River System where are built the 7 reservoirs

All the available variables (latitude, longitude, depth, area, reservoir age, pH, etc.), measured during the GHG sampling, were analysed to identify possible sources of variation in air-water interface CO_2 (Table 8.3) and CH_4 (Table 8.4) fluxes. None of them showed a high correlation with GHG fluxes. However, pH and water temperature are related to CO_2 fluxes, with a high significance ($p<0.05$), but with a relatively small proportion of the variance explained ($R^2 = 0.350$ and 0.235 respectively). It is well known that pH influences the CO_2 concentration in the water by favouring the formation of bicarbonate instead of CO_2 dissolved in the water (Clark and Fritz 1997) at pH higher than 8. This leads to an undersaturation of dissolved CO_2 which promotes the absorption of atmospheric CO_2. Therefore, the very low mean fluxes measured in waterbodies of British-Columbia (Fig. 8.2) are probably related to high water pH (Table 8.1). When we consider the whole Canadian dataset, the mean gross flux of CO_2 was 1684±1840 mg $CO_2 \cdot m^{-2} \cdot d^{-1}$ ($n = 1744$) for pH < 7.9, while it was -15±991 mg $CO_2 \cdot m^{-2} \cdot d^{-1}$ ($n = 253$) for pH ≥ 7.9, both statistically different ($p<0.05$). As for the CH_4 the mean gross fluxes were 68.9±210 ($n = 524$) and 4.5±36 ($n = 105$), for pH <7.2 and for pH≥7.2 respectively, also statistically different ($p<0.05$). Despite the absence of significant correlations, a discrepancy in flux values occurs also in relation with wind speed, the average CO_2 flux being significantly higher when it exceeds 3 $m \cdot s^{-1}$ (Table 8.5). Similar findings have been noted for two of Quebec's boreal reservoirs (Duchemin et al. 1995).

Table 8.3. Regressions of gross CO_2 flux versus measured variables at the air-water interface of aquatic ecosystems in the Canadian boreal region

Variable	Probability	Coefficient of determination [R^2]
pH	<0.0001	0.350
Water temperature (°C)	0.0148	0.235
Year of filling (reservoir)	<0.0001	0.093
Age (reservoir)	<0.0001	0.086
Longitude (degree)	<0.0001	0.080
Month of sampling	<0.0001	0.062
Wind ($m \cdot s^{-1}$)	0.0247	0.061
Latitude (degree)	<0.0001	0.045
Wind direction (degree)	<0.0001	0.038
Hour of sampling (blocks of 3 hours)	<0.0001	0.026
Transparency (m)	0.0051	0.015
Wind peak ($m \cdot s^{-1}$)	0.0055	0.050

The variables listed in the table are those which were significant ($p<0.05$).

Table 8.4. Regressions of gross CH_4 flux versus measured variables at the air-water interface of aquatic ecosystems in the Canadian boreal region

Variable	Probability	Coefficient of determination [R^2]
Water temperature (°C)	0.0033	0.326
Longitude (degree)	<0.0001	0.246
Depth (m)	0.0158	0.159
Latitude (degree)	0.0401	0.010
Year of filling (reservoir)	<0.0001	0.058
Month of sampling	0.0065	0.001

Note: The variables listed in the table are those which were significant ($p<0.05$).

Table 8.5. GHG fluxes in relation with wind speed, sample depth and water temperature for various Canadian aquatic ecosystems, 1993 to 2003

	CO_2 [mg·m^{-2}·d^{-1}]			CH_4 [mg·m^{-2}·d^{-1}]			N_2O [mg·m^{-2}·d^{-1}]		
	N	Mean	C. I.	N	Mean	C. I.	N	Mean	C. I.
Wind speed [m-s^{-1}]									
< 3	1388	1470*	93	540	18.9	4.6	475	0.08	0.04
≥ 3	1010	1853*	112	420	16.2	10.4	273	0.09	0.04
Sample depth [m]									
≤ 3	772	1565	133	373	39.0*	12.6	110	0.03	0.05
> 3	1665	1683	84	628	6.8*	2.8	609	0.10	0.03
Water temperature [°C]									
≤ 17[a]	1128	1360*	97	337	9.2*	1.8	238	0.08	0.03
> 17[a]	1665	1683*	99	727	23.0*	7.0	609	0.08	0.04

C.I.: Confidence interval ($\alpha = 0.05$).
* denotes significant difference between fluxes.
a: For CH_4, groups are ≤ 14 and > 14°C.

In Manitoba, despite the relatively high mean pH, the CO_2 and CH_4 average fluxes are quite high for all aquatic ecosystems (Fig. 8.2 and 8.3, Table 8.1). Besides depth, which is lower at the stations sampled in Manitoba, but have no known influence on CO_2 air-water fluxes, input of carbon from the drainage basin through leaching could explain a significant part of this variation. In fact, freshwater lakes, rivers and reservoirs have been suggested to play a major role in the transfer of terrestrially-fixed carbon (up to 70%) to the atmosphere, although they account for less than 0.4 percent of the earth's surface (Wetzel 1975; Hope et al. 1996; Aronsen et al. 2002). Moreover, it has been shown that a part of CO_2 emissions can be explained by the relationship between DOC and bacterial ac-

tivity (Paterson et al. 1997; Jansson et al. 2000; Tadonléké et al., Chap. 19) as well as the ratio production/respiration (P/R) (del Giorgio and Peters 1994; Tadonléké et al., Chap. 19; Planas et al., Chap. 20).

The influence of the input of carbon from the watershed is also shown by our CO_2 fluxes measured in the St. Lawrence River (Table 8.6). The mean CO_2 flux increases downstream, between Cornwall (Ontario) and Lake Saint-Pierre, with a drop in the middle (Lake Saint-Louis). The increases are related to carbon input from Montréal's highly urbanized-industrialized area and the high organic biomass of Lake Saint-Pierre. A similar downstream increase of CO_2 emissions, extrapolated from a rise in partial pressure (*p*CO2), was measured in the Amazon River (Devol et al. 1987). However, this downstream increase in CO_2 emission is not observed when reservoirs are in series. Three examples are given with five reservoirs downstream of one another in Manitoba (on the Winnipeg River system) as well as in Québec (La Grande complex, Manic-Outardes complex, Table 8.1) indicating no cascade effect in GHG emissions from hydroelectric complexes.

Table 8.6. CO_2 fluxes along the St. Lawrence River

Area	Km	Flux	N	C. I.	Area	Km	Flux	N	C. I.
Cornwall	200	37	16	425	Montréal	320	481	62	401
Lake St. François	220	-177	11	375	Lake St. Pierre	450	1510	25	802
Lake St. Louis	280	-15	36	383					

Flux in $mg \cdot m^{-2} \cdot d^{-1}$;
c.i.: Confidence interval ($p<0.05$).

There is no relationship between average CO_2 fluxes and latitude for all the boreal reservoirs sampled. However, the fluxes increase inversely with latitude when we extend our dataset to tropical regions (Fig. 8.5, Table 8.7, Therrien 2003). Higher temperature and more organic matter leaching from watersheds to the aquatic systems in tropical regions would be the major factors explaining this gradient. This pattern varies according to the type of aquatic ecosystem (Table 8.7). While estuaries and rivers exhibit similar increases from North to South, lakes seem to present a surprisingly inverse pattern, the lowest fluxes being observed in the tropical region while the highest are from the present study. These results indicate that the water quality and the productivity of the systems may influence the flux of CO_2 either in or out of the water body. Aronsen et al. (2002) have observed lower emissions of CO_2 in lakes with low total organic carbon (TOC) than in lakes with high TOC. Similarly, Kortelainen (1998) has measured CO_2

Table 8.7. Fluxes of CO_2 from different regions and aquatic ecosystems

Ecosystem	Country	Region	Flux [$mg \cdot m^{-2} \cdot d^{-1}$][1]	Reference
Lake	French Guiana	Tropical	-734 (-1232 - -52)	Therrien (2004)
	USA	Temperate	50	Quay et al. (1986)
	USA	Temperate	119	Riera et al. (1999)
	Sweden	Arctic	279	Karlsson (2001)
	USA	Sub-tropical	707 (-879 - 10804)	Therrien et al. (2004)
	Sweden	Boreal	790	Aronsen (2001)
	USA	Arctic	920	Kling et al. (1991)
	Canada	Boreal	(220 - 2597)	Heisslein et al. (1980) in del Giorgio and Peters (1994)
	Canada	Boreal	1049 (-5723 - 10947)	This study
River	Brazil	Tropical	(66 - 374)	Wissmar et al. (1981)
	Panama	Tropical	(-425 - 850)	Therrien (2004)
	Canada	Arctic	313	Kling et al. (1991)
	USA	Sub-tropical	1934 (-301 - 7293)	Therrien et al. (2004)
	Canada	Boreal	1884 (-904 - 11163)	This study
	Brazil	Tropical	20880	Richey et al. (1988)
	Brazil	Tropical	19012	Richey et al. (1990)
	French Guiana	Tropical	36110 (6543 - 110563)	Therrien (2004)
Reservoir	Sweden	Boreal	128	Bergström et al. (2004)
	USA	Boreal	220 - 1300	Kelly and Rudd (unpublished), cited in St-Louis et al. (2000)
	Canada	Boreal	530 - 2200	Shellhase et al. (1997) in St-Louis et al. (2000)
	Finland	Boreal	1530	Hellsten et al. (1996)
	Canada	Boreal	1875 (-3409 - 16721)	This study

Table 8.7. (cont.)

Ecosystem	Country	Region	Flux [mg-m^{-2}-d^{-1}][1]	Reference
	Panama	Tropical	(1000 - 5000)	Therrien (2004)
	French Guiana	Tropical	4692 (203 - 14664)	Therrien (2004)
	Brazil	Tropical	171 - 8475	Rosa et al. (2002ab)
Estuary	Canada	Boreal	880 (-1068 - 3778)	This study
	Germany	Boreal	7922	Frankignoulle et al. (1998)
	Netherlands	Boreal	(3081 - 7042)	Frankignoulle et al. (1998)
	Netherlands/Belgium	Boreal	(11443 - 29047)	Frankignoulle et al. (1998)
	United Kingdom	Boreal	(3961 - 12763)	Frankignoulle et al. (1998)
	France	Boreal	(2200 - 4841)	Frankignoulle et al. (1998)
	Portugal	Boreal	10562 - 33448	Frankignoulle et al. (1998)

Average flux or range of extreme means of individual water body; extreme values in parenthesis.

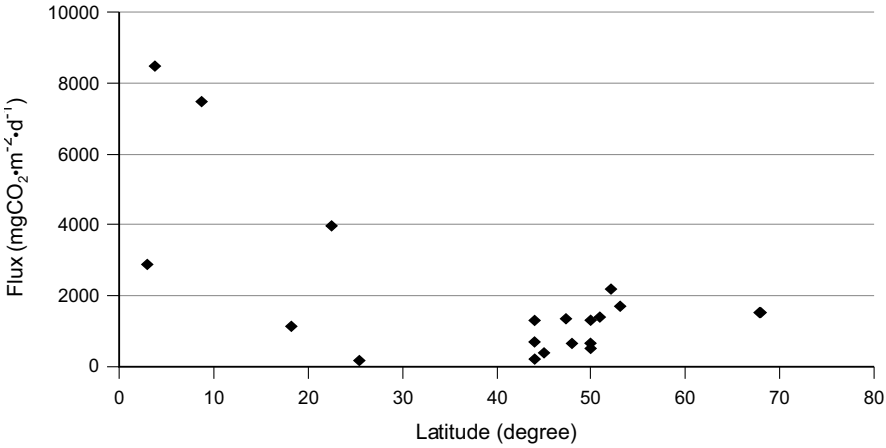

Fig. 8.5. CO_2 gross fluxes in reservoirs versus latitude. Data from Rosa et al. (2002ab), Duchemin et al. (2000), Kelly and Rudd unpublished and Shellhase et al. 1997 in St-Louis et al. (2000), Hellsten et al. (1996), this study

emissions over 175 natural Finnish lakes, all of which were supersaturated with respect to CO_2. Highest supersaturation was found in small eutrophic lakes and the lower supersaturation in the largest and deepest lakes. Moreover, in a literature review, Therrien (2003) has highlighted that gross CO_2 emissions generally increase from oligotrophic lakes to eutrophic lakes.

As for CO_2, none of the available variables analysed to identify possible sources of variation in air-water interface CH_4 fluxes showed a high correlation (Table 8.4). However, water temperature was related to CH_4 fluxes with a high significance ($p<0.05$), but with a relatively small proportion of the variance explained ($R^2 = 0.326$). Comparison of fluxes versus water temperature confirms the presence of this trend (Table 8.5). Despite a coefficient of determination (0.246), longitude was not adequately related to CH_4 fluxes. Similarly, we observe a highly significant trend between water temperature and depth with CH_4 fluxes at the water-air interface but with a relatively small coefficient of determination.

Despite the general absence of significant correlations, the CH_4 mean flux is significantly higher when the depth of sampling stations is less than or equal to 3 m (Table 8.5). Similar findings have been noted concerning ebullitive fluxes (Keller and Stallard 1994; Galy-Lacaux et al. 1997; de Lima et al. 2002; Rosa et al. 2002a; Huttunen et al. 2002). No differences were found relating to average wind speed (0–12 m-s^{-1}), but discrepancy occurs when squalls (up to 15 m-s^{-1}) occur during sampling, as pointed out

by Duchemin et al. (1995), the fluxes being higher by a factor of 7–12 times depending on the depth of stations.

Unlike CO_2 or CH_4, no significant ($p < 0.05$) relationship could be established between the N_2O fluxes and all the variables measured.

8.3.2 Temporal Variation of GHG Emission from Reservoirs

The evolution of CO_2 and CH_4 emissions over time was assessed using only the results obtained in Québec. Because of provincial disparity and it representativeness, to our knowledge, this is the biggest database of GHG fluxes from water bodies worldwide. Three reservoirs have been sampled since their filling, or within the first 10 years after impoundment as well as many reservoirs of different ages (up to 90 years old). The figures 8.6 and 8.7 show a rapid increase in the GHG emissions shortly after flooding and then a return to values observed in natural lakes or rivers within 10 years for CO_2 and 4 years for CH_4. Mean values for CO_2 were 2566±2296 mg $CO_2 \cdot m^{-2} \cdot d^{-1}$ ($n = 476$) for reservoirs < 10 years old and 1508±1771 mg $CO_2 \cdot m^{-2} \cdot d^{-1}$ ($n = 870$) for reservoirs 10 years old or more. Mean values for CH_4 were 24±58 mg $CH_4 \cdot m^{-2} \cdot day^{-1}$ ($n = 383$) for reservoirs < 5 years old and 9±12 mg $CH_4 \cdot m^{-2} \cdot day^{-1}$ ($n = 493$) for reservoirs 5 years old or more. Both CO_2 and CH_4 mean values are statistically different between old and young reservoirs. These CO_2 results illustrate the pattern stated by IAEA (1996). The CH_4 figure is also consistent with those measured in French Guiana on Petit-Saut Reservoir (Galy-Lacault 1997; Delmas et al., Chap. 12) and from other tropical reservoirs in Panama and Brazil (Keller and Stellard 1994; Duchemin et al. 2000) with smaller emissions for older reservoirs, around 10–50 mg $CH_4 \cdot m^{-2} \cdot d^{-1}$, than those for younger reservoirs with values of 500–3000 mg $CH_4 \cdot m^{-2} \cdot d^{-1}$. However, unlike diffusive emission, ebullitive fluxes do not show any distinct pattern in tropical reservoir and may have an effect on the duration of the general emissions of GHG from tropical reservoirs (Rosa et al. 2002b; Delmas et al., Chap. 12). No pattern is observed with the N_2O flux and reservoir age (Fig. 8.8).

Monitoring of the La Grande Complex reservoirs (Québec) showed a definite trophic surge immediately after filling, related to the enhanced bacterial decomposition of the labile carbon from the newly inundated organic matter and subsequent nutrient release. The surge lasted for only 9–10 years (Schetagne 1994; Chartrand et al. 1994). A similar trend was also observed by Grimard and Jones (1982). The increase in CO_2 emissions following reservoir creation is probably related to this trophic surge and the return to lower CO_2 fluxes after 9–10 years is likely caused by the

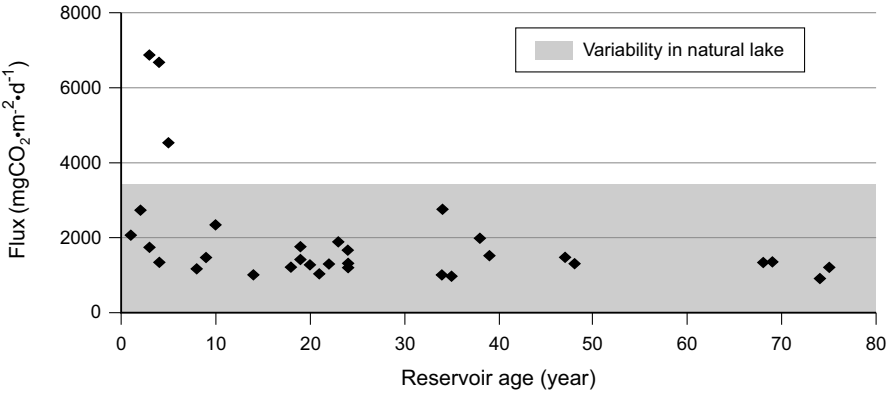

Fig. 8.6. Evolution of gross fluxes of CO_2 at the air-water interface in boreal reservoirs of the province of Quebec

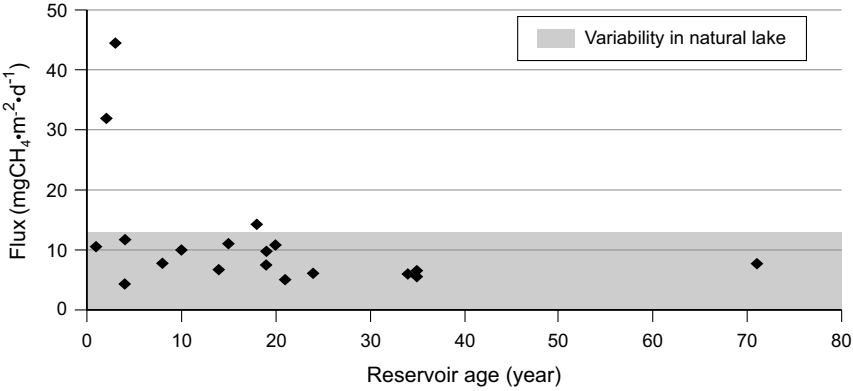

Fig. 8.7. Evolution of gross fluxes of CH_4 at the air-water interface in boreal reservoirs of the province of Quebec

depletion of the inundated labile carbon and a decrease of bacterial/plankton activities (Marty et al., Chap. 17; Tadonléké et al., Chap. 19; Tremblay et al. 1998). The time needed to return to values representative of natural conditions is usually within 10–15 years in boreal ecosystems according to the ratio of land area flooded to annual volume and the amount - quality of the organic matter flooded (Chartrand et al. 1994; Lucotte et al. 1999). After the trophic surge, it is believed that the carbon involved in CO_2 emissions is derived from inputs of organic matter from the watershed. The absence of a link between CO_2 emission and the inundated biomass has already been noted for old boreal reservoirs in Québec

(Duchemin 2000) and in Finland (Huttunen et al. 2002), and for tropical reservoirs in Brazil (Rosa et al. 2002a).

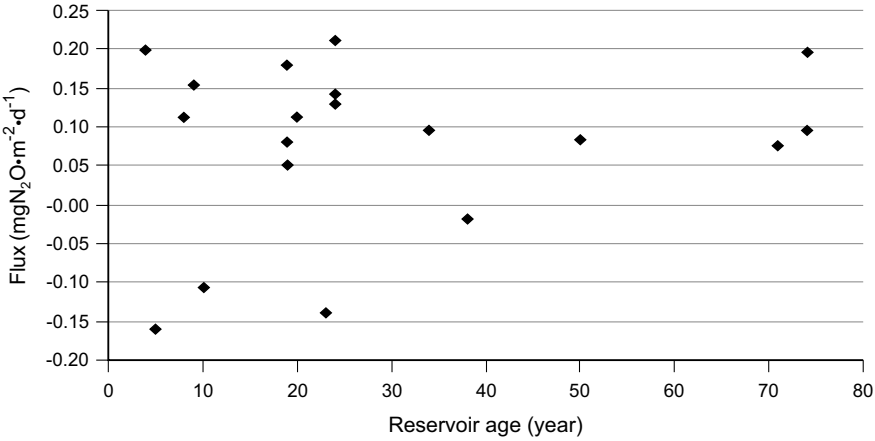

Fig. 8.8. Evolution of gross fluxes of N_2O at the air-water interface in Canadian boreal reservoirs

8.3.3 Fluxes in CO_2 Equivalent Carbon

The Global Warming Potential (GWP) of GHG can be expressed in CO_2 equivalent carbon (Table 8.8). Reservoirs are given an average value similar to lakes for B.-C., lower than lakes for Manitoba, and superior to lakes for Québec and Newfoundland, even when only old reservoirs are considered. Nevertheless, the means are generally around 2000 mg CO_2 eq.·C·m^{-2}·d^{-1}, which is an order of magnitude lower than for tropical reservoirs. For 7 reservoirs sampled monthly for 2 years, Rosa et al. (2002a) measured an average GWP for CO_2 and CH_4 of about 31700 mg CO_2 eq.·C·m^{-2}·d^{-1}, with a range in means of 5300 mg CO_2 eq.·C·m^{-2}·d^{-1} (Segredo Reservoir) to 59200 mg CO_2 eq.·C·m^{-2}·d^{-1} (Très Marias Reservoir).

8.4 Conclusion

Our results confirm the temporary increase in gross CO_2 and CH_4 fluxes at the air-water interface after the impoundment of boreal reservoirs. The

Table 8.8. Gross GHG flux in CO_2 equivalent-carbon for several aquatic ecosystems in the Canadian boreal region

Province	Type of ecosystem	CO_2 flux	CH_4 flux in CO_2·eq.	N_2O flux in CO_2·eq.	Total in CO_2·eq.
British-Columbia	Lake	706	260	36	1002
	River	462		29	491
	Reservoir	198	969	16	1183
Manitoba	Lake	2193	8580	4	10777
	River	330			330
	Reservoir	4086	267	22	4375
Ontario-Quebec	St. Lawrence River	438	837		1275
Quebec	Lake	1013	14	15	1027
	River	1076	75	43	2094
	Reservoir	2566	547	27	3140
	Reservoir[a]	1508	202	27	1737
	Estuary	880	330	55	1265
Newfoundland	Lake	867			867
	Reservoir	2089			2089

Flux in $mg \cdot m^{-2} \cdot d^{-1}$. The GWP, in CO_2 equivalent carbon, are of 23 for the CH_4 and of 296 for the N_2O for a 100 years time-horizon (IPCC, 2001).
[a]: Reservoirs older than 9 years for CO_2 and 4 years for CH_4.

duration of that burst is less than 10 years. After that period, there is generally a high similarity between fluxes in reservoirs and other surrounding aquatic ecosystems (lakes, rivers, estuaries). This suggests an input of carbon from the watershed instead of a long term decay of the newly inundated organic matter and indicate that the processes leading to GHG emissions are similar in both reservoirs and reference systems. More over, this study and other papers confirm that natural lakes and rivers are naturally significant emitters of CO_2, CH_4 and N_2O. The global average of Global Warming Potential, expressed in CO_2 equivalent carbon, shows no major differences between aquatic ecosystems, and the values are an order of magnitude lower in boreal regions than they are in tropical regions. To correctly estimate the net GHG emissions from reservoirs it is, therefore, essential to determine the emissions from the various reference ecosystems in the watershed, before and after creation of the reservoir. This will make it possible to assess net GHGs emissions for which the reservoirs are responsible and allow the comparison of energy production methods adequately.

9 CO_2 Emissions from Semi-Arid Reservoirs and Natural Aquatic Ecosystems

Jean Therrien, Alain Tremblay and Robert B. Jacques

Abstract

Carbon dioxide (CO_2) gross fluxes were measured at the air-water interface of 57 aquatic ecosystems in the western semi-arid region of the USA in April 2003. Fluxes were obtained with a floating chamber connected to an automated NDIR instrument. The results showed a strong similarity between lakes and reservoirs, as is also the case in boreal regions. The values ranged from -1500 to 10800 mg $CO_2 \cdot m^{-2} \cdot d^{-1}$ for both natural systems and reservoirs. These values are similar to those observed in boreal regions. Although several limnological parameters can influence the fluxes of CO_2, only the pH was significantly related with the CO_2 gross fluxes, which decrease with increasing pH.

9.1 Introduction

CO_2, the world's main greenhouse gas (GHG), is emitted from both natural aquatic ecosystems (lakes, rivers, estuaries, wetlands) and manmade reservoirs (Cole et al. 1994; Hope et al. 1994; IAEA 1996; Makhov and Bazhin 1999; Takahashi et al. 1999; Wickland et al. 2001; Borges et Frankignoulle 2002; Gurney et al. 2002; Richey et al. 2002). In the case of reservoirs, the amount of CO_2 emitted at the air-water interface varies over time. An initial increase occurs immediately after filling of the reservoir, related to the decomposition of a fraction of newly inundated labile organic matter (Chamberland 1992; Schetagne 1994). In boreal reservoirs, a gradual return to natural conditions follows and is generally observed within 10 years (Chamberland 1992; Rudd et al. 1993; Tremblay et al. 2004). The magnitude of the fluxes, for both reservoirs and natural systems, depends on the physico-chemical characteristics of the water body and on the input

of carbon (or organic matter) from the watershed (Duchemin et al. 2000; Rosa et al. 2002; Huttunen et al. 2002ab; Therrien 2003).

The role of the GHG emissions from freshwater reservoirs and their contribution to the increase of GHG concentrations in the atmosphere is actually well discussed worldwide (Rosa and Scheaffer 1994, 1995; Fearnside 1996; Gagnon and van de Vate 1997; St-Louis et al. 2000; Tremblay et al. in Press). This is particularly true for tropical regions where the quantity of flooded organic matter may be quite significant. However, semi-arid regions store limited amount of carbon both in phytomass and soil. Flooded organic matter coupled with warm temperatures enhance the GHG emission by favouring the decomposition of organic matter under anoxic conditions (Goodland et al. 1992; Fearnside 1995; Hamilton et al. 1995). To our knowledge, there are few emission measurements available from these environments although they are at the heart of the debate concerning methods of energy production.

Hydro-Québec and its partners have adapted a technique to measure gross GHG emissions at the air-water interface that allows for a high rate of sampling in a short period of time, while increasing the accuracy of the results and decreasing the confidence intervals of the average flux measured (see Chap. 2). Since 2002, the research has been extended to other provinces and countries, in order to compare the results with those obtained by other methods, and to better assess the gross emissions of GHG from aquatic ecosystems in boreal, semi-arid and tropical regions. This was done also to adequately estimate the contribution of reservoirs versus natural water bodies in these regions, as well as to compare properly the methods of energy production. In 2003, the sampling program was conducted in semi-arid region of the western United States of America (USA), where many reservoirs were built in the 1950's and 1960's for different uses (water management, hydroelectric generation, irrigation, etc.). These sites are easily accessible.

9.2 Material and Methods

9.2.1 Study Areas

Natural lakes (7), rivers (4) and manmade reservoirs (46) were sampled in the semi-arid western region of the USA in April 2003. These water bodies were sampled in the states of Utah (April 16^{th}-21^{st}), Arizona (April 9^{th}-15^{th}) and New Mexico (April 5^{th}-8^{th} and 22^{nd}-25^{th}), with some on the Arizona – California and Arizona – Nevada borders (Figs. 9.1-9.4). This semi-arid

Fig. 9.1. Locations of the semi-arid U.S.A. western states regions where gross fluxes of CO_2 at air-water interface were sampled in 2003

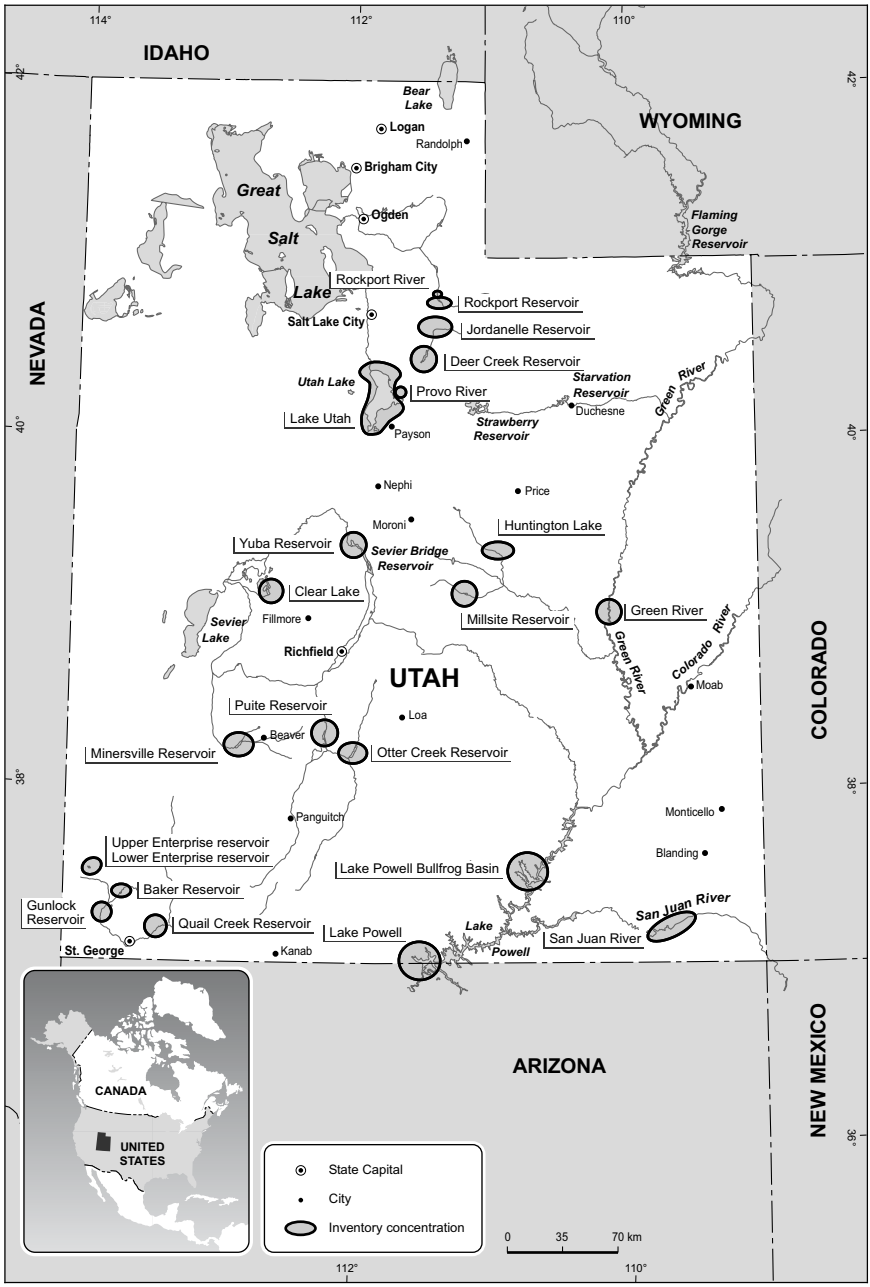

Fig. 9.2. Locations of the semi-arid Utah State water bodies sampled in 2003

Fig. 9.3. Locations of the semi-arid Arizona State water bodies sampled in 2003

region is characterized by a desert or steppe dry climate, with usually hot summers (21 to sometimes over 32ºC in July) and cool winters (-1 to 21ºC in January), less then 50 cm of annual water precipitation, and an altitude above 1000 m with mostly evergreen needleleaf trees and broadleaf shrub vegetation (Espenshade and Morrison 1980).

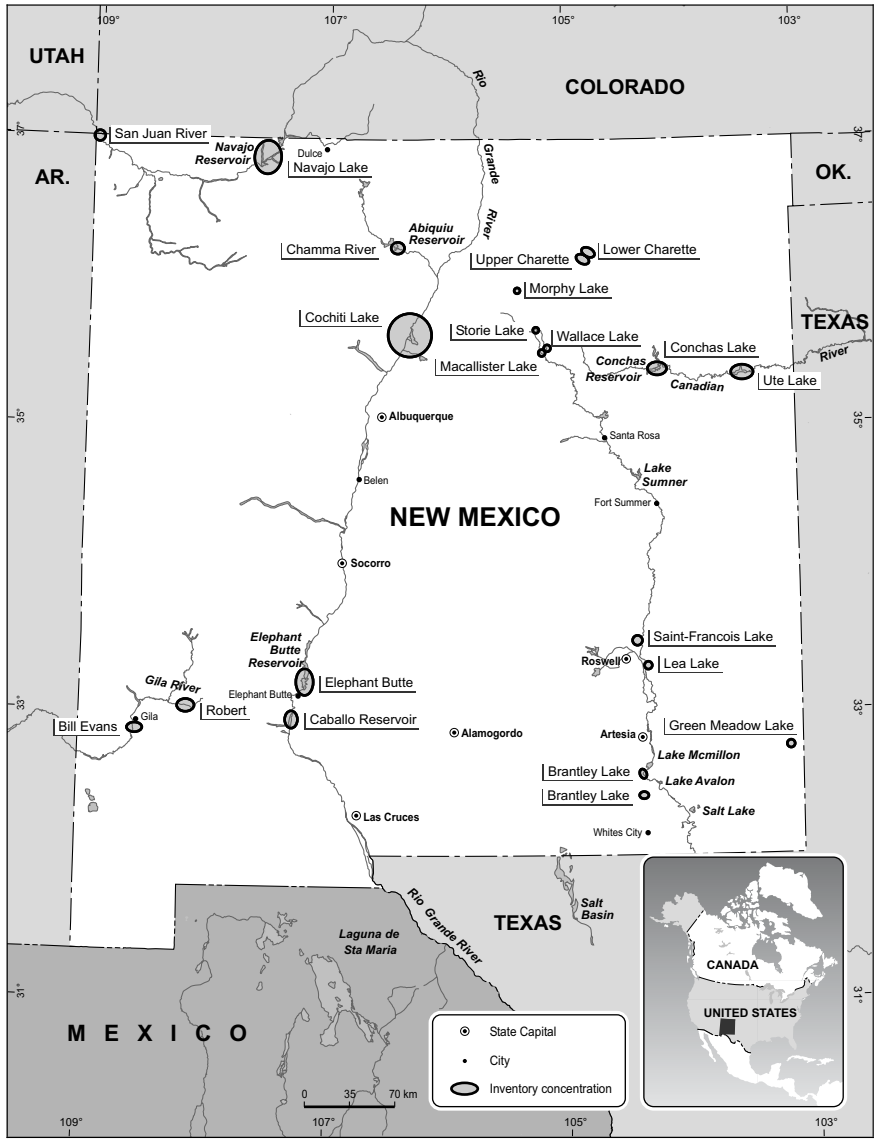

Fig. 9.4. Locations of the semi-arid New Mexico State water bodies sampled in 2003

9.2.2 Measurement of CO_2 Flux and Other Variables

The CO_2 fluxes were measured with a floating chamber linked to a Non-Dispersive Infrared (NDIR) instrument (PP-System model Ciras-SC) which takes continuous CO_2 readings with an accuracy of 0.2 to 0.5 ppm in the range of 350-500 ppm. The NDIR data logger (Campbell Scientific, model CR10X) stores a value every 20 seconds over a sampling period of 5-10 min. More details about the apparatus are available in Lambert and Fréchette (Chap. 2). Several locations were sampled from each site with a minimum of two fluxes per location. A regression curve is fitted on the results for every flux measured, and its slope determines the average flux (mg CO_2-m^{-2}-day^{-1}) using the following equation:

$$\text{Flux} = \text{slope} \times F1 \times F2 \times \text{volume} \times \text{surface-area}^{-1} \qquad (9.1)$$

where F1 is a conversion factor from ppm to $mg{\cdot}m^{-3}$, F2 is a conversion factor from second to day, volume of air in the floating chamber (0.018 m^3), and surface-area of the floating chamber (0.204 m^2). The value is accepted depending on the correlation coefficient (R^2) of the regression curve.

Other measurements generally made at each site included GPS position, weather conditions, wave height, water and air temperature, water color and transparency (Secchi disk), water depth, pH (Beckman 200 and Oakton 300), alkalinity (titration), and wind velocity (Extech Instruments 407112) and direction.

9.2.3 General Chemical Characteristics of the Water Bodies

Water chemistry data of the water bodies (Table 9.1) were obtained from the Utah Department of Environmental Quality, the Arizona Department of Environment Quality - Clean Lakes Program, the New Mexico Department of Game and Fish, the New Mexico Department of Environment - Surface Water Quality Bureau, the Bitter Lake National Wildlife Refugee, the Las Vegas National Wildlife Refugee, and the U.S. Environmental Protection Agency (EPA) website (May-September 2003). The years of flooding of reservoirs were obtained from the Arizona Department of Environmental Quality - Clean Lakes Program, the New Mexico Department of Game and Fish, the Utah Department of Environmental Quality, and several institutions (U.S. Army Corps of Engineers and the U.S. Bureau of Reclamation). The data presented in Table 9.1 are means obtained for April, when available, or from March to May to match the sampling period. Only exceptionally were data taken from another season.

Table 9.1. General characteristics of the semi-arid water bodies

Water body name	Flooding year	Surface area	$CaCO_3$	Chlo.a	CO_2 c.	Cond.	N Kjeldahl	O_2 sat.	pH	Transp.	SS	Water temp.	Turb.	CO_2	N	S.D.
ARIZONA																
Lakes																
Ashurst Lake		26							9.00			11.8		-488	6	261
Pecks Lake		13	325	1.54		510	1.16	68	8.04	1.5	319	6.1	11.5	2260	4	940
Roper Lake		5.3	160	2.20		6100	0.91	92	9.00	1.4	3394	15.2	1.6	276	2	1215
Stoneman Lake		28	320			653	0.79	138	9.14		413	16.4	24.5	-423	6	228
River																
Colorado River									8.06			13.3		3331	9	2156
Reservoirs																
Alamo Lake Reservoir	1968	422							8.93			23.8		-730	3	648
Apache Lake Reservoir	1927	421	180			1640	0.73	64	7.54	2.2	1043	20.8		-927	9	329
Arivaca Lake Reservoir	1970	13				218		88	9.16		142	24.3		42	7	777
Bartlett Lake Reservoir	1939	330	300			596	0.75	102	8.18	1.1	376	14.3	11.0	359	10	119
Bunch Reservoir	1929	3.2							7.87			9.0		146	2	1049
Horseshoe Lake Reservoir	1945	174	298	2.70		667		64	8.22	1.0	439	17.3	4.9	1251	8	1397
Lake Powell Wahweap Bas. Res.	1963	26 646*				803			8.00	14.3		14.7		823	6	453
Lyman Reservoir		164							8.30					747	1	
Parker Canyon Reservoir	1926	102							8.56			14.1		697	2	1554
Patagonia Lake Reservoir	1968	42				1208		93	8.25		783	22.3		2243	9	1343
Pena Blanca Lake Reservoir	1958	7.3				113		81	7.59		73	10.5		152	7	1178
Pleasant Lake Reservoir	1927**	246				905		93	8.51	6.0	585	22.5	0.4	-510	15	232
Roosevelt Lake Reservoir	1911	2 139	210	1.93		2300	0.64	94	8.20	0.3	840	26.2	17.0	-1116	9	293
Upperlake Mary Reservoir	1940	74		5.48		50	0.58	81	7.55	0.9	68	19.2	11.4	3104	8	942
ARIZONA-CALIFORNIA																
Reservoir																
Havasu Lake Reservoir	1938	3169	170	0.56		881	1.00	105	8.57	3.5	569	19.5	0.4	2092	6	806

Table 9.1. (cont.)

Water body name	Flooding year	Surface area	$CaCO_3$	Chlo.a	CO_2 c.	Cond.	N Kjeldahl	O_2 sat.	pH	Transp.	SS	Water temp.	Turb.	CO_2	N	S.D.
ARIZONA–NEVADA																
Reservoir																
Lake Mead Reservoir	1935	1802							8.33			14.5		1154	3	720
ARIZONA–UTAH																
River																
San Juan River			138		1.00	658		121	8.29		526	20.1	19.2	293	7	496
NEW MEXICO																
Lake																
Lea Lake		10							7.85			17.7		3641	1	
River																
Chamma River														1340	1	
Reservoirs																
Bill Evans Reservoir	1968	25							8.38			13.0		318	2	440
Brantley Lake Reservoir	1980	1243							8.30					-234	7	209
Caballo Reservoir	1941	4654							8.50			15.5		518	10	402
Cochiti Lake Reservoir	1975	486							8.26			12.7		1587	12	1176
Conchas Lake Reservoir	1935	3885							8.50			12.6		1313	10	220
Elephant Butte Reservoir	1947	16187												1100	5	571
Green Meadow Lake Reservoir	1950	5.7							8.16			14.0		-10	1	
Lower Charette Lake Reservoir	1930	300							8.60			16.0		926	2	325
Macallister Lake Reservoir	1960	40							8.70			9.5		1215	2	74
Morphy Lake Reservoir	1939	15							8.19			15.1		-341	1	
Navajo Lake Reservoir	1963	6070							8.55			13.4		753	14	707
Robert Lake Reservoir	1963	29							8.04			9.0		685	1	
Upper Charette Lake Reservoir	1930	100							8.84			7.7		927	1	
Ute Lake Reservoir	1963	3318							8.42			14.7		701	14	156
Wallace Lake Reservoir	1920	40							8.18			18.0		2436	2	696

Table 9.1. (cont.)

Water body name	Flooding year	Surface area	$CaCO_3$	Chlo.a	CO_2 c.	Cond.	N Kjeldahl	O_2 sat.	pH	Transp.	SS	Water temp.	Turb.	CO_2	N	S.D.
UTAH																
Lakes																
Clear Lake		49												360	6	131
Utah Lake		15869	258	23.75	1.67	1783	1.17	103	8.44	0.3	1 065	9.1	83.1	2862	6	3992
River																
Green River			152		2.00	563		96	8.20		354	14.8	407.0	4278	5	1856
Reservoirs																
Baker Dam Reservoir	1950	1	222	0.35	1.33	417	0.43	103	8.44	2.6	248	18.1	1.7	820	4	350
Deer Creek Reservoir	1941	486	153	5.45	1.00	426		91	8.28	4.1	249	12.3		-289	3	160
Gunlock Reservoir	1970	44	216	2.20	1.00	466	0.20	100	7.55	2.5	318	18.6	6.3	993	9	701
Huntingdon Lake Reservoir	1966	37							8.36			10.0		513	2	47
Jordanelle Reservoir	1993	541							8.32			6.3		-153	1	
Lake Powell Bullfrog Basin Res.	1963	26646*		1.00		821	0.45		8.30	3.7		22.7		575	12	104
Lower Enterprise Reservoir	1920	13							8.28			10.7		329	3	60
Millsite Reservoir	1974	71	230	0.98	1.00	470	0.10	106	8.24	3.5	256	16.1	1.3	1908	2	253
Minersville Reservoir	1914	162	238	1.63	1.00	540	0.50	85	8.60	2.4	338	18.0	2.3	183	8	61
Otter Creek Reservoir	1915	413	216	0.70	1.00	359	0.70	108	8.75	1.9	230	17.0	2.0	1246	3	291
Piute Reservoir	1915	411	228	6.66	1.50	475	0.33	107	8.52	1.1	251	19.1	11.8	517	8	318
Quail Creek Reservoir	1985	97	166	1.50	2.00	1111	0.10	108	7.80	3.0	586	18.5	0.6	380	6	154
Rockport Reservoir	1957	195	218	0.20	1.00	359		96	8.41	3.3	244	16.6	1.4	1544	3	189
Upper Enterprise Reservoir	1912	43	102	1.05	1.00	191	3.15	92	8.15	1.7	145	17.6	5.9	-20	3	128
Yuba Reservoir	1914	1786		0.80		1376		108	8.65	0.5		15.4		1390	3	132

Note: The values presented above are generally from April or, when unavailable, an average from March to May. Few exceptions concern variable with low seasonal fluctuations. All units are in $mg{\cdot}L^{-1}$, except surface area (ha), chlorophyll *a* ($\mu g{\cdot}L^{-1}$), conductivity ($\mu mho{\cdot}cm^{-1}$), dissolved O_2 saturation (%), transparency (m), water temperature (ºC), turbidity (NTU), CO_2 and C.I. ($mg{\cdot}m^{-2}{\cdot}d^{-1}$). Abbreviations are: Chlo. *a* (chlorophyll *a*), CO_2c. (CO_2 concentration in water), Cond. (conductivity), N (N Kjeldahl), O_2 sat. (dissolved O_2 saturation), Transp. (transparency – Secchi disk), SS (suspended solids), Water temp. (water temperature), Turb. (turbidity), CO_2 (CO_2 air-water interface flux), N (number of stations), S.D. (standard deviation).

* The whole area is listed for the two basins (Wahweap and Bullfrog) of the Lake Powell Reservoir.

** Upgraded in 1996.

9.2.4 Statistical Analyses

Exploratory analyses were done with matrices of measured data or global chemical data joined with average fluxes for each water body, using one or more of the following: multidimensional scaling, cluster analysis (weighted average), statistical factor analysis, and canonical analysis (Legendre and Legendre 1998). Then, using the major variables responsible for the variability in CO_2 fluxes, a multiple regression analysis (backward stepwise) was pursued. Finally, when adequate results were obtained, a simple regression analysis was done with a single variable. Comparisons of the means of fluxes between water bodies were done with Anova and Tukey analyses. When applicable, the level of acceptance of the results was $p<0.05$. All the statistical analyses were done with Statistica or Statgraph software.

9.3 Results and Discussion

A total of 312 fluxes plus the duplicates were measured with individual fluxes ranging from -1495 to 10804 mg $CO_2 \cdot m^{-2} \cdot d^{-1}$. The mean gross emissions of CO_2 measured in the southwest USA showed values of 664 ± 1091 mg $CO_2 \cdot m^{-2} \cdot d^{-1}$ (n=259) for reservoirs with extreme means of -1116 ± 293 mg $CO_2 \cdot m^{-2} \cdot d^{-1}$ (n=9, Roosevelt Lake, Arizona) and 3104 ± 942 mg $CO_2 \cdot m^{-2} \cdot d^{-1}$ (n=8, Upper Lake Mary, Arizona) (Fig. 9.5, Table 9.1). For lakes, the global average is 874 ± 2214 mg $CO_2 \cdot m^{-2} \cdot d^{-1}$ (n=31), with extreme means of -488 ± 261 mg $CO_2 \cdot m^{-2} \cdot d^{-1}$ (n=6, Ashurst Lake, Arizona) and 2862 ± 3992 mg $CO_2 \cdot m^{-2} \cdot d^{-1}$ (n=6, Utah Lake). For rivers, the values obtained are respectively 2489 ± 2284 mg $CO_2 \cdot m^{-2} \cdot d^{-1}$ (n=22), 293 ± 496 mg $CO_2 \cdot m^{-2} \cdot d^{-1}$ (n=7, San Juan River, Utah) and 3331 ± 2156 mg $CO_2 \cdot m^{-2} \cdot d^{-1}$ (n=9, Colorado River, Arizona-California) (Fig. 9.5, Table 9.1).

These emissions are similar to those reported by Duchemin et al. (1995, 1999) over boreal reservoirs as well as those reported by Lambert and Fréchette (2001, 2002) from Quebec's lakes and reservoirs with values ranging from -308 to 1850 mg $CO_2 \cdot m^{-2} \cdot d^{-1}$ for the natural lakes and values from 980 to 3300 mg $CO_2 \cdot m^{-2} \cdot d^{-1}$ for the reservoirs. Similarly, in Canadian lakes and reservoirs, Tremblay et al. (2004) measured emissions of the same order of magnitude with values ranging from -50 to 1706 mg $CO_2 \cdot m^{-2} \cdot d^{-1}$ for the natural lakes, from -333 to 1053 mg $CO_2 \cdot m^{-2} \cdot d^{-1}$ in rivers and values from -852 to 1402 mg $CO_2 \cdot m^{-2} \cdot d^{-1}$ for the reservoirs.

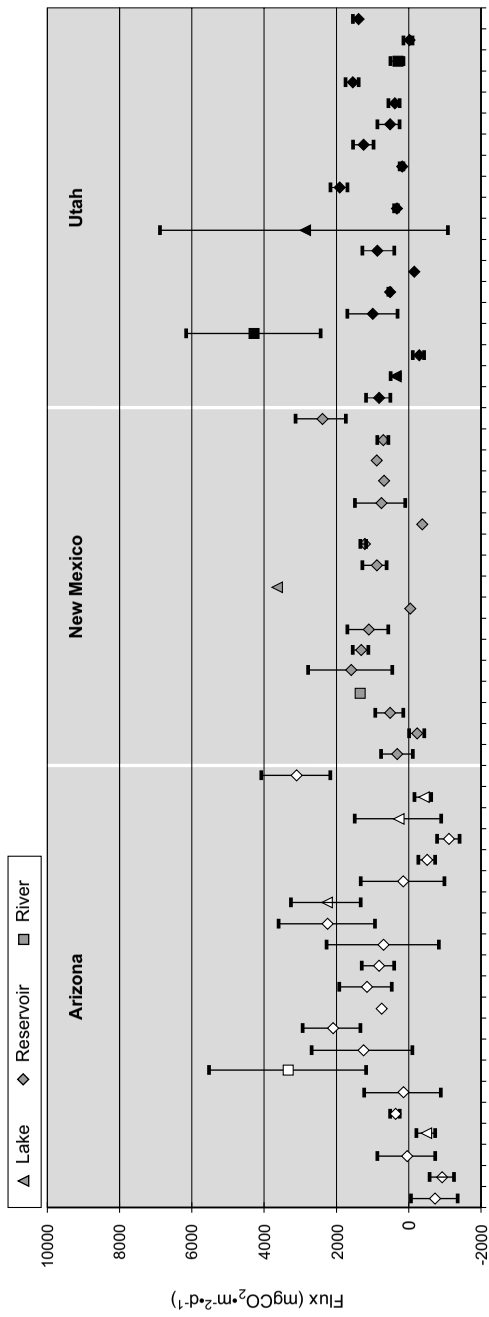

Fig. 9.5. Mean value and standard deviation of gross fluxes of CO_2 at air-water interface in semi-arid U.S.A. western states

In three reservoirs and five rivers from Panama, Therrien (2003), have measured mean gross emissions of CO_2 varying from -425 to 850 mg $CO_2 \cdot m^{-2} \cdot d^{-1}$ in rivers and from 1100 to 5000 mg $CO_2 \cdot m^{-2} \cdot d^{-1}$ in reservoirs. These aquatic systems have temperatures similar to those of the Arizona-Utah-New Mexico region but they are situated in tropical environments implying that there is more organic matter leaching from the watershed to the aquatic systems.

The strong similitude between the various ecosystems (lake, river and reservoir) with a wide overlap of means and standard deviation is clearly shown in Fig. 9.5. This is probably related to the fact that most of the reservoirs sampled in Arizona-Utah-New Mexico are more than 20 years old, with only one being under 20 years old (Table 9.1). Thus, the burst occurring in the first 10 years after the creation of the reservoir and the related release of nutrients, enhanced bacterial activity and the decomposition of the labile carbon (Chamberland 1992; Rudd et al. 1993; IAEA 1996) has ended. Similar overlaps have been obtained for reservoirs of 10 years old or more in boreal regions in North America (Fig. 9.6, Therrien 2003), Finland (Hellsten et al. 1996), and Sweden (Bergstrom et al. in Press). In Fig. 9.6, the average obtained by pooling all the water bodies of each type of ecosystem shows more clearly the similarity between the fluxes measured in semi-arid lakes and old reservoirs. The rivers show the highest average emissions.

Individual comparisons are given by state in Table 9.2 for water bodies with more than 2 fluxes. It shows rare significant differences between natural lakes and reservoirs. This reflects the similarity between water bodies. It may also be influenced by the low number of samples in some cases and by the high variability in the measurement of CO_2 fluxes. The CO_2 fluxes can vary depending on the time of day (Carignan 1998), or on the presence of wind, when outgassing occurs as the waves created by the wind are broken (Wanninkhof et al. 1985, 1987). Nevertheless, measurements taken at different locations on a water body are still one of the best indicators of the gross mean emissions for comparison purposes.

All the available variables, physico-chemical or other (latitude, longitude, depth, area, reservoir age, etc.), either measured during the GHG sampling or gathered through databank reviews, were analysed to identify possible sources of variation in air-water interface CO_2 fluxes (Table 9.3). Only the pH showed significant influence ($R^2 = 0.373$) on the results obtained (Fig. 9.7). The CO_2 emissions decrease as the pH increases, leading generally to negative emissions (CO_2 absorption) at pH higher than 8.5. In fact, higher pH (>7) favours the formation of bicarbonate instead of CO_2

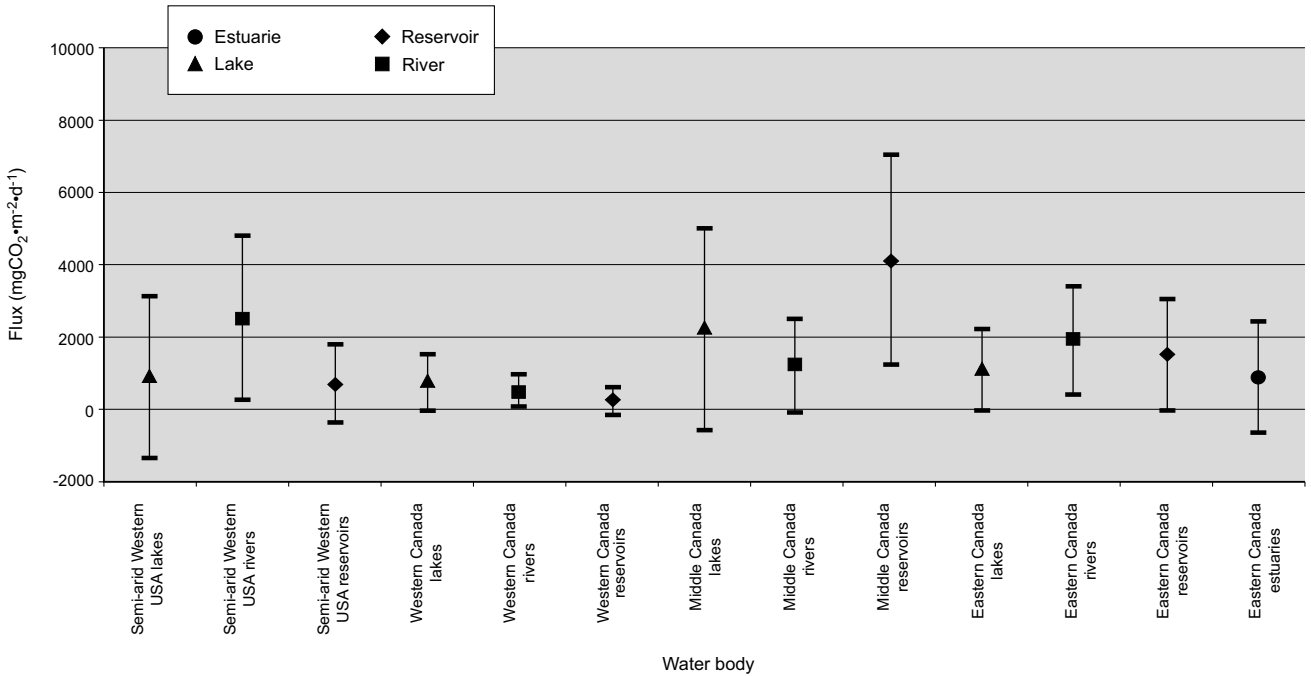

Fig. 9.6. Mean value and standard deviation of gross fluxes of CO_2 at air-water interface in different water body types of several North American regions. Reservoirs are 10 years old or more. Data taken from, Therrien (2003) and Tremblay et al. (Chap. 8)

Table 9.2. Statistical comparisons of gross CO_2 flux means at the air-water interface for water bodies in the USA semi-arid western region

Water body	Group	Water body	Group
Arizona State		**Utah State**	
Colorado River	A	Green River	A
Upperlake Mary Reservoir	A	Utah Lake	AB
Pecks Lake	ABCD	Rockport Reservoir	ABC
Patagonia Lake Reservoir	AB	Yuba Reservoir	ABC
Havasu Lake Reservoir	ABD	Otter Creek Reservoir	ABC
Lake Mead Reservoir	ABCDEFG	Gunlock Reservoir	BC
Horseshoe Lake Reservoir	BCDE	Baker Dam Reservoir	BC
Lake Powell Wahweap	BCDEF	Lower Enterprise Reservoir	BC
Basin Reservoir		Upper Enterprise Reservoir	BC
Bartlett Lake Reservoir	CEFGH	Lake Powell Bullfrog	C
San Juan River	CDEFGH	Basin Reservoir	
Pena Blanca Lake Reservoir	EFGH	Piute Reservoir	C
Arivaca Lake Reservoir	EFGH	Quail Creek Reservoir	C
Stoneman Lake	EFGH	Clear Lake (pond)	C
Ashurst Lake	EFGH	Minersville Reservoir	C
Alamo Lake Reservoir	EFGH	Deer Creek Reservoir	C
Pleasant Lake Reservoir	GH	**New Mexico State**	A
Apache Lake Reservoir	GH	Cochiti Lake Reservoir	AB
Roosevelt Lake Reservoir	H	Conchas Lake Reservoir	AB
		Elephant Butte Reservoir	ABC
		Navajo Lake Reservoir	BC
		Ute Lake Reservoir	BC
		Caballo Reservoir	C
		Brantley Lake Reservoir	

Note: Different letters in the group column denote a significant difference in the CO_2 flux means. Comparison made between water bodies with more than 2 samples.

dissolved in the water (Clark and Fritz 1997) leading to an undersaturation of dissolved CO_2 which promotes the absorption of atmospheric CO_2. Tremblay et al. (2004) observed a similar effect of pH in British Columbia (Canada) lakes and reservoirs where both lakes and reservoirs were absorbing CO_2 at pH higher than 8.

Other possible sources of CO_2 flux variation are known, such as wind, water temperature, depth of the photic zone (water transparency), nutrient exports from the watershed, or soil type (Servais et al. 1984; Wanninkhof et al. 1985, 1987; Devol et al. 1995; Duchemin et al. 1995; IAEA 1996; Striegl et Michmerhuizen 1998; Duchemin 2000; Huttunen et al. 2002a;

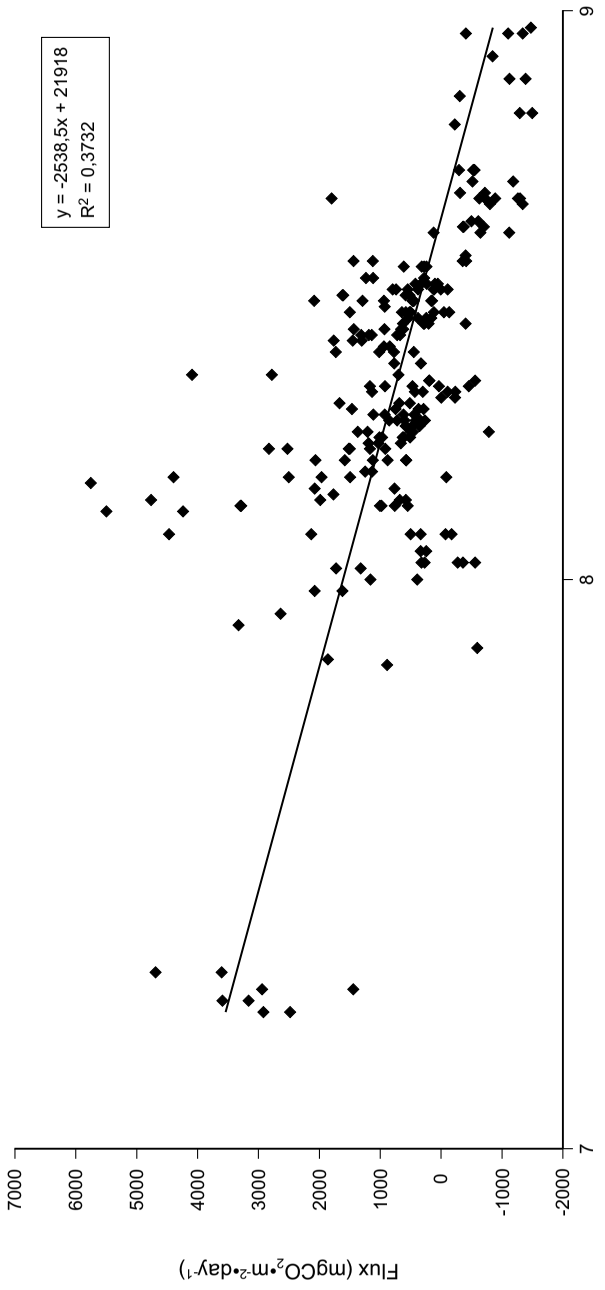

Fig. 9.7. Relation between air-water interface gross CO_2 flux and pH in U.S.A. western states reservoirs

Table 9.3. Regressions of gross CO_2 flux at the air-water interface with variables for water bodies in the USA semi-arid western region

Set of data	Variable	Probability	Coefficient of determination (R^2)
Field data	Latitude (degree)	<0.0001	0.051
	Longitude (degree)	0.0332	0.019
	Wind peak ($m \cdot s^{-1}$)	0.0053	0.002
	Depth (m)	0.0002	0.012
	Transparency (m)	0.0018	<0.001
	Air temperature (degree C)	0.0285	0.014
	pH	<0.0001	0.373
	Alkalinity ($mg \cdot L^{-1}$)	0.0006	0.081
Fluxes with physico-chemical data from Databank	Chlorophyll a ($\mu g \cdot L^{-1}$)	0.0077	0.121
	Conductivity ($\mu mho \cdot cm^{-1}$)	0.0028	0.014
	N Kjedahl ($mg \cdot L^{-1}$)	0.0495	0.001
	pH	0.0019	0.001
	Suspended solids ($mg \cdot L^{-1}$)	0.0022	0.006
	Water temperature (degree C)	0.0016	0.090

Note: The variables listed in the tables are those which could explain most of the variance in the multiple regression analysis for each of the two datasets.

Rosa et al. 2002). Many of them are related with phytoplankton production, and therefore, with the Production/Respiration ratio which is linked to the CO_2 fluxes. In an autotrophic state, a water body will have a P/R>1 and the carbon fixation by photosynthesis will lead to a decrease in the pCO_2 (Watson et al. 1993; Carpenter et al. 2001). In an heterotrophic state, the P/R is <1 and the respiration dominates, leading to an increase in the pCO_2 (see Chap. 15-18). In the cluster analysis done with the field data, the fluxes were the last merging group, indicating the absence of a strong link with any other variable. A similar lack of relation has been observed in other studies (Duchemin 2000; Lambert and Fréchette 2002; Rosa et al. 2002), showing the difficulty to identify clear patterns with the sampling of a gas when its concentration can be affected by numerous interacting factors, but varying differently. However, freshwater lakes, rivers and reservoirs have been suggested to play an important role in the transfer of terrestrially-fixed carbon to the atmosphere, although they account for less than 0.4 percent of the earth's surface (Wetzel 1975; Hope et al. 1996). Moreover, according to Aronsen et al. (2002), CO_2 fluxes from natural freshwater lakes of boreal watersheds are the major removal pathway of 30 to 70% of the terrestrial carbon exported from the watershed.

9.4 Conclusion

Our study showed that, as was observed in old (>10 years) boreal reservoirs, the mean CO_2 gross fluxes measured at the air-water interface in the western semi-arid region of the USA showed high similarity between lakes and reservoirs. The range of values measured is also similar to that observed in boreal regions, particularly in the Canadian West Coast, and in some tropical areas of Panama. More over, this study and other articles confirm that natural lakes and rivers are naturally significant emitters of CO_2 and that the behavior of reservoirs older than 10 years is similar to natural systems, indicating that the sources of carbon as well as the processes leading to GHG emissions are similar in both reservoirs and natural lakes or rivers.

10 A Comparison of Carbon Dioxide Net Production in Three Flooded Uplands (FLUDEX, 1999-2002) and a Flooded Wetland (ELARP, 1991-2002) Using a Dynamic Model

Raymond H. Hesslein, Rachel A. Dwilow, Kenneth G. Beaty
and Mark E. Lyng

Abstract

We used a dynamic model to estimate the net carbon dioxide production (NCP) of three experimentally flooded upland areas (FLUDEX) over a period of 4 years and NCP from a flooded wetland (ELARP) over 12 years (2 year pre-flooding, 10 years post-flooding). The 3 flooded upland areas had been chosen to have differing amounts of carbon stored in soils and vegetation. Estimates of NCP ranged from 33-55 mmole·m^{-2}·d^{-1} in the first year and decreased steadily to 13-30 mmole·m^{-2}·d^{-1} in the fourth year. The NCP from the reservoir with the lowest carbon stock was always lowest, the other two were similar. The NCP estimated for the wetland rose from 45 mmole·m^{-2}·d^{-1} in the first year of flooding to 178 mmole·m^{-2}·d^{-1} in the years 7-9. A decrease to 126 mmole·m^{-2}·d^{-1} was seen in the last year. Overall the model did a good job of simulating the measured results and provided a consistent methodology for comparison of NCP. In this boreal forest area of northwest Ontario flooding of wetland area results in much higher NCP and over a much greater duration than upland flooding.

10.1 Introduction

Although hydroelectric production in temperate zones is generally regarded to produce considerably less CO_2 per energy output than fossil fuel combustion, considerable effort has been put into furthering the understanding of Net CO_2 Production (NCP) in reservoirs (St. Louis et al. 2000; Duchemin et al. 1995;

Kelly et al. 1994). Two important purposes will be served by the improved knowledge; better planning and management of new and existing hydroelectric reservoirs and more precise accounting of GHG budgets for carbon credit systems.

Two series of experiments were carried out at the Experimental Lakes Area in northwestern Ontario, Canada (Fig. 10.1) to improve the understanding of NCP from flooded wetland and upland areas. The wetland flooding was carried out as the ELARP project (Experimental Lakes Area Reservoir Project) and the upland flooding as the FLUDEX (Flooded Upland Dynamics Experiment). Characteristics of the basins are given in Table 10.1. The sites of the FLUDEX reservoirs were chosen based on the amounts of stored carbon in the area to be flooded and as such are referred to as High C, Medium C, and Low C. Aspects of the experiments which included intensive studies of mercury as well as GHGs have been described in a number of publications. Production and fluxes of GHGs in particular have been discussed in Kelly et al. (1997); Matthews et al. (2003); Matthews et al. (under review); Venkiteswaran et al. (under review).

Fig. 10.1. The location of the Experimental Lakes Area

Table 10.1. Some physical characteristics of the FLUDEX and ELARP reservoirs

	High C reservoir	Medium C reservoir	Low C reservoir
Water surface area (m^2)	7400	5000	6300
Catchment runoff area (m^2)	47800	7300	900
Total site area (m^2)	55200	12300	7200
Reservoir volume (m^3)	6870	4270	7120
Mean depth (m)	0.9	0.9	1.1
	ELARP prior to flooding	ELARP after flooding	
Water surface area (m^2)	23900	180000	
Catchment runoff area (ha)	7770000	7770000	
Reservoir volume (m^3)	13000	200000	
Mean depth (m)	0.6	1.1	

NCP for 1999-2001 in the 3 FLUDEX reservoirs been assessed by an accounting of inflows and outflows in a recent article by Matthews et al. (under review) and further interpreted using stable carbon isotopes by Venkiteswaran et al. (under review). CO_2 fluxes to the atmosphere from the ELARP reservoir were assessed for 1991-1994 by Kelly et al. (1997). The purpose of the assessment of the CO_2 net production presented in this chapter is to establish a model that provides a means for estimating and comparing the NCP in general and exists as a predictive tool for application to other reservoir systems. The estimates of fluxes in this analysis were not expected to necessarily agree with those in the previous publications, partly because different data were used. This work uses only the routine physical, hydrological and chemical analyses produced by the ELA field and chemical analytical units.

In this study we used a dynamic model developed in STELLA (High Performance Systems Inc. New Hampshire, USA.) to estimate the NCP from 3 upland boreal forest areas flooded from 1999-2002 (FLUDEX), and a flooded wetland from 1991-2002 (ELARP). The model consists of 3 linked sub-models: a water budget, an alkalinity budget, and an inorganic carbon budget all of which operate simultaneously.

10.2 Methods

10.2.1 The model

The software platform STELLA was chosen for the model because no code needs to be written (just the appropriate equations describing processes) and construction with the building blocks provided by the software is quite sim-

ple. As well, it is relatively easy to incorporate real data sets such as daily hydrologic flow and to produce graphical output either in STELLA or linked to a spreadsheet such as EXCEL.

For all aspects of the model (Fig. 10.2), each of the reservoirs is represented as a well mixed unit. Because the reservoirs have depths of only about 1 m, they do not stratify vertically except for short periods. This has been verified by temperature profiles (Andy Majewski, unpublished data). The model assumes horizontal uniformity although this is probably not always the case. Because of these assumptions, the model produces estimates of the average concentrations in the reservoirs. Real measurements against which these are compared may show variance if horizontal variability exists.

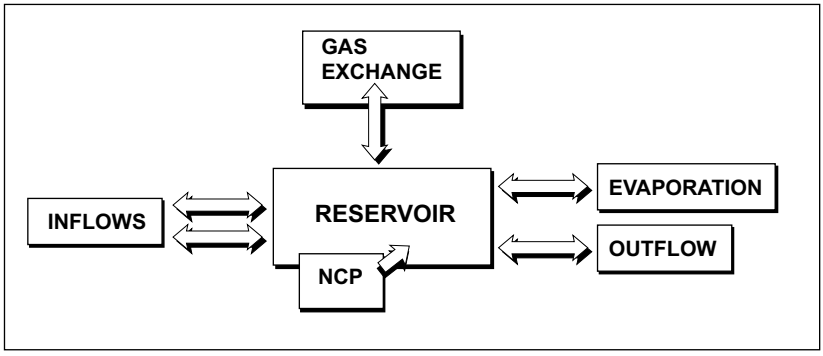

Fig. 10.2. A schematic representation of the model

Because inflow and outflow of water is critical to all of the chemical budgets of reservoirs, the hydrologic sub-model is the base of the main model. In the case of the FLUDEX reservoirs the water budget is quite simple. The water is pumped from nearby Roddy Lake at a metered rate and for each of the reservoirs outflow is measured at a calibrated weir. Natural terrestrial drainage is small for the Medium and Low C reservoirs (<2% of the water inputs) and yields only 5-15% of the water input to the High C reservoir (Matthews et al. under review). Because the reservoirs have water residence times of 5-8 days (Matthews et al. under review), which is equivalent to about 12-20 $cm \cdot d^{-1}$ (mean depth of about 1 m) even major precipitation events have only a short term influence. Evaporation pans were immersed in High C and Low C sites to give direct measurements of evaporative loss. These data were used along with pan data from the meteorological site (about 1 km away) to arrive at an estimate of reservoir evaporation. Because the reservoir hydrology was dominated by the water volumes pumped into them, evaporation was only 2-3% of outflow. In all 3 of the FLUDEX reservoirs there is significant

seepage from the dams and from some bedrock fractures under the reservoirs. This amounted to 13-20% from the High C and Medium C reservoirs and 50-65% from the Low C reservoirs. The outflow is therefore calculated as the sum of pumped and natural inflows minus evaporation and minus the change in volume calculated from the measured reservoir level.

$$\text{Outflow} = \text{Pump inflow} + \text{drainage inflow} - \text{evaporation} + \text{volume}_t - \text{volume}_{t+1}$$

The major inflow for Lake 979, the ELARP reservoir, is the outflow of Lake 240 which has a drainage area of 721 ha and has a monitored weir. One additional stream flows into the lake from the east. It drains an area of 70 ha. Flow from this stream is not monitored but can be estimated to be the same per unit area of drainage as the Northwest inflow to Lake 239, which is monitored and is only 2 km away. Other undefined terrestrial drainage is also estimated to be the same per unit area as the Northwest stream inflow of Lake 239. Direct precipitation is estimated from the measured precipitation at the Rawson Lake meteorological site, 2 km away. The catchment of the Northwest inflow is similar in surface area (56 ha), soil characteristics, and fire history. The average water residence time for the filled reservoir over the study period was about 33 days, but it varies from as little as 2 days in wet periods to infinite during dry periods when there is no flow even from Lake 240. Because the volume of water in the reservoir changes with the difference between inflows and outflows, any cumulative error, however small instantaneously, could result in significant emptying or overfilling of the reservoir in the model. In order to avoid this problem we have used measured reservoir level data to fix the volume of the reservoir. As with the FLUDEX reservoirs, the outflow is calculated as the sum of pumped and natural inflows minus evaporation and minus the change in volume calculated from the measured reservoir level. This calculated outflow differs from the measured outflow by less than 3% in any 1 year.

Once the hydrological flows are known, the chemical flows can be calculated as the product of the hydrological flow and the chemical concentrations, either measured or calculated. For both the FLUDEX and ELARP reservoirs all outflowing waters, including seepages, are assumed to have the concentrations of the well mixed reservoir. Of the 3 components of DIC (dissolved inorganic carbon as defined by Stainton et al. 1977); CO_2, HCO_3 and CO_3, only CO_2 is acted on by gas exchange, therefore the model must calculate the concentration of CO_2 as well as DIC. Solving the carbonate equilibria equations is complex and if they were solved using the time resolution required by the model, the computation time would increase significantly. However, because the pH in the ELARP and FLUDEX waters never exceeds 7.5 and is normally

between pH 6.0-7.0, CO_2 can be accurately estimated as the (DIC-alkalinity) where:

$$\text{Alkalinity} = HCO_3^- + 2*CO_3^= + OH^- - H^+ \text{ and } DIC = CO_2 + HCO_3^- + CO_3^=$$

This assumption results in an error of less than 1% in estimating the alkalinity (alkalinity typically near 100 ueq l^{-1}) and less than 15 ppm CO_2 (usually much less).

The use of the above simplification means that the model requires an alkalinity budget but not a pH (hydrogen ion) budget. Alkalinity (Gran Titration, Freshwater Institute Chemistry Laboratory) was measured in all of the inflows and outflows for which there was hydrological flow data as well as in the reservoir itself. These measurements were made once per week or 2 weeks during the open water season. We used a linear interpolation of the data to produce daily alkalinity values. These data were multiplied by the measured daily water inflow to produce the alkalinity inputs and the alkalinity of the model reservoir multiplied by the modeled daily outflow to produce outputs. The model has an adjustable function to generate or remove alkalinity from the reservoir at a constant rate as required to fit the measured data.

For the ELARP reservoir, the DIC sub model is set up in the same way as the alkalinity budget except that the additional flux between water and air is added. This flux is calculated as the product of the MTC (Mass Transfer Coefficient) and the gradient in CO_2 concentration between water and air. The MTC is calculated from the wind velocity using the equation:

2.07+.215*(wind velocity)^1.7 (Cole and Caraco 1998)

The wind velocity used as an input to the model was measured at a height of 10 m at meteorological station at ELA. The NCP in the model is proportional to the area of the reservoir and the temperature of the water. The logic is that the flooded peat is the organic substrate and that it is not limiting, and that the bacteria which produce the CO_2 behave according to the rule of a doubling of activity for each increase in temperature of 10°C. Although there have been no specific studies to determine the temperature response of the bacteria in the flooded sites it is generally accepted that bacterial enzymes behave in this way in the temperature range of 0 to 30°C. The equation is:

10^((.03*Tc)+Fittingcon)

where Tc is the temperature in °C, 10^((.03*Tc) gives a value of 1 at 0°C and doubles for each 10°C. and Fittingcon is the constant used to set the areal CO_2 production rate. For example, for Fittingcon = 1, the flux is 10 mmole·m^{-2}·d^{-1} at 0°C., 20 mmole·m^{-2}·d^{-1} at 10°C, and 40 mmole·m^{-2}·d^{-1} at 20°C. This a real rate is then multiplied by the area of the reservoir which is calculated from the water level and the bathymetric data.

The dissolved inorganic carbon sub-model for the FLUDEX reservoirs is essentially the same as that for the ELARP reservoir except that the calculation of the MTC is done using 0.1+0.215*(wind velocity)*.4)^1.7). This equation was developed based on the data of Matthews et al. (2003) while using the form of the equation of Cole and Caraco (1998). The parameters in that equation, developed for open lake surfaces, do not account for the extreme protection from wind that the flooded trees and small size of the reservoir provide. The other difference in the FLUDEX model is that the temperature of the water is simplified as a constant of 20°C. The temperature regime in the FLUDEX reservoirs has less seasonal change because the flooding season is only 115 days versus about 152 for ELARP and because the water is replaced rapidly from Roddy Lake.

10.2.1 Running the Model and Calibrating to the Measured Data

The goal in this application of the model was to estimate the NCP in the reservoir. We deem this goal to be achieved if the DIC concentrations calculated by the model match those measured in the reservoir. The aim in calibration is therefore to produce the best fit between the measured and modeled values. The sub models for water, alkalinity and DIC were calibrated in that order. As noted above, the fit between the modeled and measured hydrological flows was very good so no calibration or adjustment of this part of the model was necessary. The model allows a constant net production of alkalinity which can be adjusted to achieve a best fit to the measured alkalinity data. Once an acceptable value for the net production of alkalinity has been found, the model can be calibrated for net production of CO_2. The calibration is carried out by minimizing the sum of the squared differences between the modeled DIC and linearly interpolated measured values of DIC evaluated at each time step. After determining the best value for net production of CO_2, the differences between modeled and measured values were examined versus time for trends that might lead to a more complete understanding of the net production.

10.3 Results

10.3.1 ELARP

The model produced an excellent simulation of the outflow of water as is shown by the 1996 results in Fig. 10.3. Negative outflow is possible in the model because it is calculated from the volume minus inflows. The best fits to

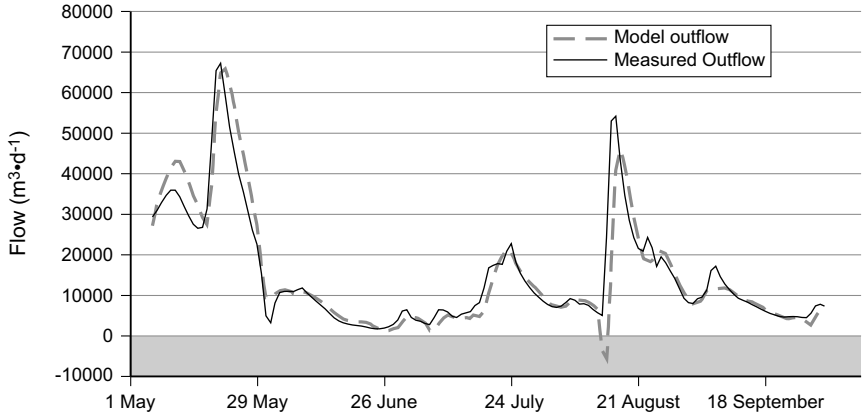

Fig. 10.3. Measured and modeled outflow from the ELARP reservoir

the constant production of alkalinity for all years are shown in Table 10.2. All of the values fall between -0.5 and -3.5 mmole·m^{-2}·d^{-1}. This small removal of alkalinity is probably due to the addition of organic acids from the flooded wetland.

The best estimates of the NCP (Fig. 10.4, Table 10.2) show an increase in production of about 2.5 x after flooding and a consistent rise to a level about 10 x pre-flooding, or 180 mmole·m^{-2}·d^{-1} by 1999-2001. The average mass transfer coefficient for gas exchange is about 0.8 m·d^{-1} and the outflow averages 0.03 m·d^{-1} (33-day residence time, 1 m meter mean depth), therefore most of the NCP is lost to the atmosphere (Fig. 10.4). The gas exchange losses were smaller than the outflow losses prior to flooding because the area of the pre-flood Lake 979 was much smaller, the NCP was much lower, and the flow was the same (the water residence time was 10 x shorter).

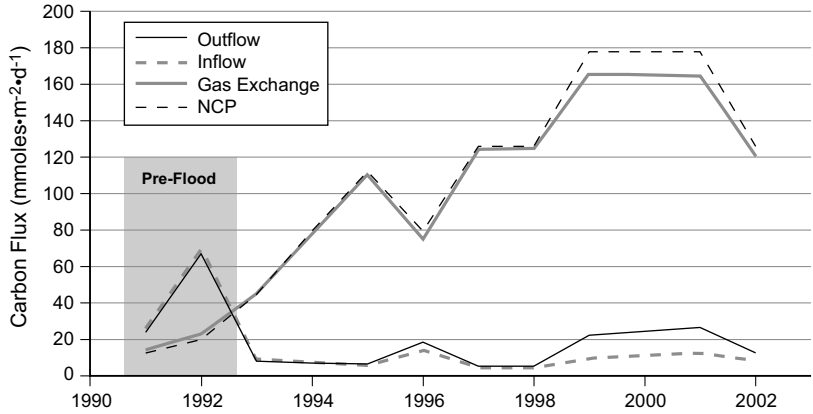

Fig. 10.4. Carbon fluxes to and from the ELARP reservoir 1991-2002

Table 10.2. A summary of best fit fluxes for FLUDEX and ELARP

Reservoir	Year	Fluxes (mmole·m^{-2}·d^{-1})				
		Alkalinity	Inflows	Gas Exchange	Outflows	NCP
High C	1999	1	15	18	35	38
High C	2000	1	21	21	43	43
High C	2001	1	14	12	27	25
High C	2002	-1	16	15	31	30
Medium C	1999	0	21	20	56	55
Medium C	2000	1.5	25	20	47	43
Medium C	2001	1	21	13	39	32
Medium C	2002	-1	17	9	24	16
Low C	1999	1	17	13	38	33
Low C	2000	1	20	13	37	29
Low C	2001	1	17	6	27	16
Low C	2002	-0.5	17	6	25	13
ELARP pre	1991	-1	26	14	24	13
ELARP pre	1992	-3.5	70	23	67	20
ELARP	1993	-2.2	9	45	8	45
ELARP	1994	-1	7	78	7	79
ELARP	1995	-1.7	6	110	7	112
ELARP	1996	-2.3	14	75	18	79
ELARP	1997	-1.4	4	124	5	126
ELARP	1998	-1.3	4	125	5	126
ELARP	1999	0.7	10	166	22	178
ELARP	2001	-0.5	12	165	27	178
ELARP	2002	-0.75	9	120	13	126

10.3.2 FLUDEX

The best estimates for the alkalinity production in the FLUDEX reservoirs were near 1 mmole·m^{-2}·d^{-1} (Table 10.2). The NCP of all 3 reservoirs declined over the 4-year period (Fig. 10.5). The most dramatic decline was in the Medium C reservoir which fell quite linearly from 55 mmole·m^{-2}·d^{-1} in 1999 to 16 mmole·m^{-2}·d^{-1} in 2002. The High C reservoir declined only from 37 mmole·m^{-2}·d^{-1} in 1999 to 30 mmole·m^{-2}·d^{-1} in 2002. The Low C reservoir had consistently the lowest NCP over the 4-years and declined from 33 mmole·m^{-2}·d^{-1} in 1999 to 13 mmole·m^{-2}·d^{-1} in 2002. Because the average mass transfer coefficients for gas exchange are only about 0.1 m·d^{-1} and the outflows average just above 0.1 m·d^{-1} (7.5-day residence time, 0.9 m mean depth) slightly more than half of the NCP is lost by outflow, much of which may degas downstream.

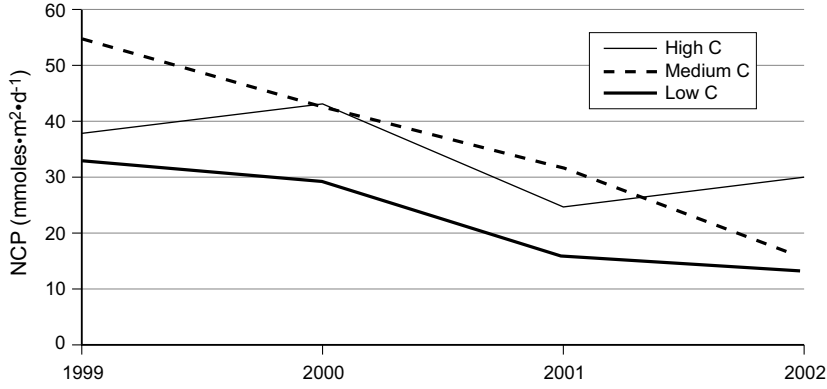

Fig. 10.5. NCP (Net CO_2 Production) in the FLUDEX reservoirs (1999-2002)

The differences (actual interpolated DIC - model DIC) between the predicted DIC in the FLUDEX reservoirs and the linearly interpolated measured values show a slight increase with time (Fig. 10.6). The model is underestimating the DIC as the summer proceeds. Because the fitting procedure minimizes the least square differences, the mean of the differences are approximately zero. This trend in differences is much more pronounced in the results for the ELARP reservoir than for the FLUDEX reservoirs (Fig. 10.7).

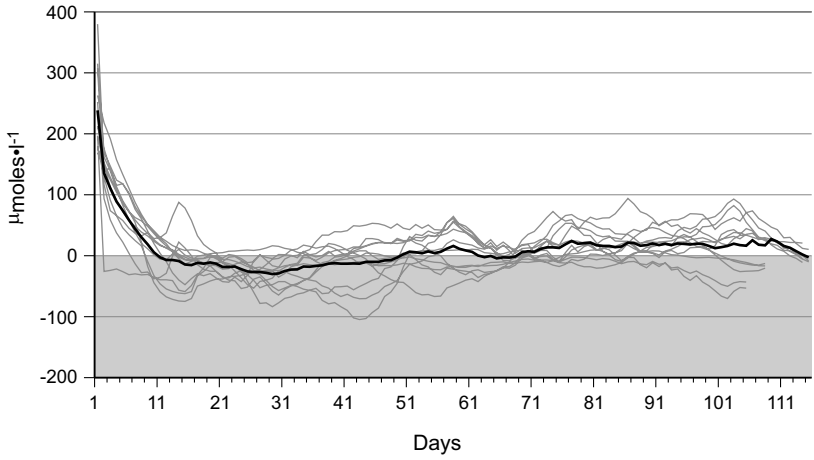

Figure 10.6

Fig. 10.6. Differences between measured and modeled DIC for best fit runs of the FLUDEX reservoirs. The heavy line is the mean for the 12 runs

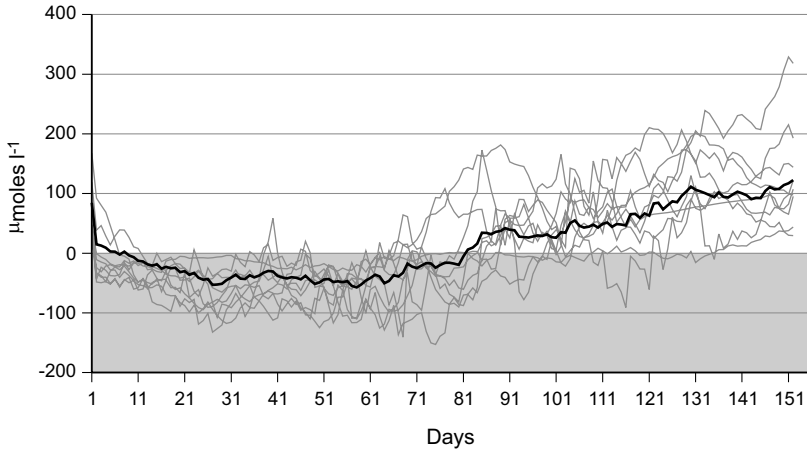

Fig. 10.7. Differences between measured and modeled DIC for best fit runs of the ELARP reservoir. The heavy line is the mean for the 11 years

10.4 Discussion

Three questions need to be answered to assess the value of the model: 1. How well does the model output fit the data? 2. How "real" are the results? Because there are many parameters which contribute to the final output we will examine independent evidence for choosing their values. 3. How useable or transportable is the model for other applications?

If we use the ELA DIC measurements as the measure of fit, the model does a good job of simulation for the FLUDEX reservoirs (Fig. 10.6). This suggests that the concept of constant values for NCP throughout the flooded periods is reasonable. There are a number of uncertainties which make it difficult to assess the fit more thoroughly. Part of this is due to potential variability in the data. Because the DIC samples are take at a single place and time only once every 2 weeks, it is possible that the actual DIC data is not representative of the average for the reservoir, which the model simulates. The only information with respect to this variability is the more comprehensive data of Matthews et al. (under review) who mention that "There were no consistent differences or noticeable spatial patterns in either CO_2 or CH_4 concentrations, but morning concentrations were higher than evening concentrations". Because the flux to the atmosphere represents nearly 50% of the net output of CO_2, the knowledge of the MTC is very important. As described by Matthews et al. (2003), the formulations relating wind speed from the 10 m meteorological tower and MTC from small lakes (Cole and Caraco 1998)

were inadequate to explain the MTC determined in the FLUDEX reservoirs by loss of added SF_6. We have tried to produce a formulation that more adequately represents the wind in these sheltered areas, but without extensive testing it is not possible to accurately estimate the errors in the gas flux term. This is not likely to be as large a problem with large reservoirs that have less protection from the wind and where formulations for MTC such as that of Cole and Caraco (1998) should be more representative.

The trends of the differences between the measured DIC and the modeled value for ELARP (Fig. 10.7) show that the assumption of a constant net production modified only by temperature does not adequately describe the system. In all flooded years the differences between the model and measured values of DIC increase, starting about 60-80 days after flooding, and continue to the end of the flooding period (about 152 days). It is possible that the temperature of the surface water is not the best representation of the bacterial environment producing the CO_2. It is believed that most of the CO_2 production is due to the breakdown of peat and other solid organic matter (Kelly et al. 1997). Because most of this type of organic matter is exposed to the air and frozen in the winter, there may be a temperature lag relative to that of the water in the central area, the sediments of which do not freeze. Much of the peat now floats in the reservoirs but typically the amount of floating peat increases through the season. This could increase the rate of decomposition because of exposure to higher temperatures and oxygen. Alternatively, the differences may be due to photosynthetic activity and respiration which is not presently specified in the model. Higher net photosynthetic rates early in the summer could be due to longer day length as well as the lack of accumulated fixed carbon for respiration. Later in the season less carbon may be fixed and more respired. The temperature effect may not be seen in the FLUDEX reservoirs because all of the area is frozen and flooded each year and the temperature of the water is more constant. The photosynthetic effect may not be apparent because much of the carbon fixed in the reservoirs remains (personal communication, David Findlay) when the reservoirs are drained after a shorter flooding season than ELARP (115 vs 152 days).

As stated, the purpose of this presentation is to evaluate the use of the model, not to critique the estimates of NCP by Matthews et al. (under review). It is however appropriate to compare the results over the period 1999-2001 for the purpose of assessing potential errors. Figure 10.8 shows a comparison of DIC inputs, DIC in outflow, and diffusive fluxes of CO_2. Differences in the inputs are very small because the calculations are based on the same data and differences result only from the methods of interpolation and integration. Differences in the estimates of diffusive fluxes and outflow could be due to 2 other sources. Matthews et al. (under review) used a different set of CO_2 data for estimating the diffusive flux from that which they used for

outflow calculations. The current model treats the reservoir as a single well mixed unit and calculations of both the diffusive flux and the outflow are based on that value. In addition, the model estimates the mass transfer coefficient from a single equation (based on Matthews et al. (2003) for all 3 reservoirs and a single set of wind velocity data. Matthews et al. (under review) use a variety of data to estimate MTC for different reservoirs and different years (Cory Matthews, personal communication) but do not present that data. Their estimates of these fluxes are, on average, higher than those of the model. From the data available there is really no way to simply decide which are the best estimates. As described by Matthews et al. (2003), the estimates of MTC vary between 0.2 and 1.5 cm hr^{-1} and do not consistently follow the wind velocity. Without much more extensive testing and understanding of the physics of diffusive gas exchange in these very sheltered systems it is hard to have a high level of confidence in the precision of the estimate of MTC.

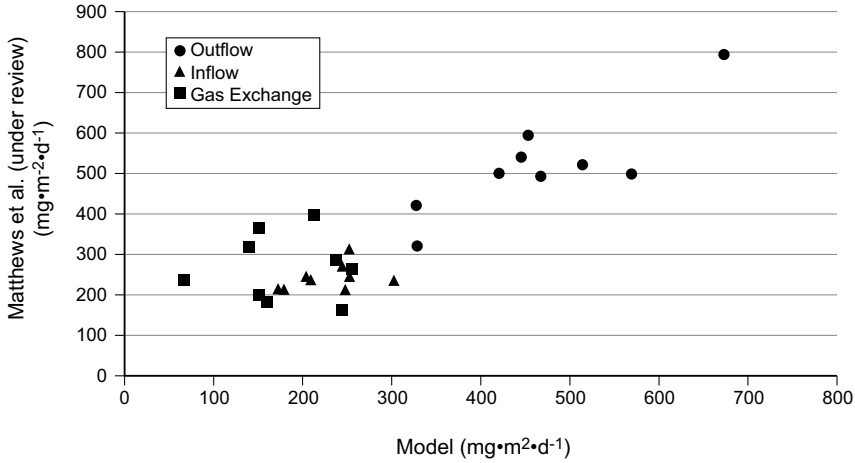

Figure 10.8

Fig. 10.8. A comparison of the fluxes from the best fit model runs for the FLUDEX reservoirs with the estimates of Matthews et al. (under review)

A comparison of NCP estimates for the ELARP reservoir with published results can only be done for the 2 pre-flood years and the first 2 post-flood years (Kelly et al. 1997). Kelly et al. (1997) estimated the pre-flood average flux (1991-1992) from the pond surface to be 0.32 $g{\cdot}m^{-2}\ y^{-1}$. Our model estimates 0.15 $g{\cdot}m^{-2}\ y^{-1}$ in 1991 and 0.24 $g{\cdot}m^{-2}\ y^{-1}$ in 1992. They estimated an average post-flood (1993-1994) flux of 0.55 $g{\cdot}m^{-2}\ y^{-1}$ for the whole flooded area and 1.0 $g{\cdot}m^{-2}\ y^{-1}$ for the former pond area. Our model estimates a mean net

production from the whole area of 0.54 $g{\cdot}m^{-2}\ y^{-1}$ for 1993 and 0.95 $g{\cdot}m^{-2}\ y^{-1}$ for 1994. Considering that the data used and the methods of estimation were different, the agreement is quite good.

The long term trends in the ELARP and FLUDEX reservoirs are very different. Although the NCP was quite similar in the first year of flooding in all 4 of the reservoirs, the NCP in the FLUDEX reservoirs followed a very different path from ELARP in subsequent years. In fact the NCP for the FLUDEX reservoirs had dropped to nearly the pre-flood levels of the ELARP reservoir by the fourth year. The NCP for ELARP continued rising to 6-10 times the pre-flood values 7-10 years after flooding. One hypothesis to explain this difference is that the NCP will be in some way proportional to the availability of organic matter for decomposition. The ELARP site flooded areas with large amounts of peat (Kelly et al. 1997 estimated 10^2 $kg{\cdot}m^{-2}$). The FLUDEX sites were estimated to have in their soils and vegetation 4.6, 3.5, and 3.1 $kg{\cdot}m^{-2}$ of organic carbon (Matthews et al. (under review)). NCP for the FLUDEX reservoirs was from 0.02- 0.08 $kg{\cdot}m^{-2}$ per flooded season or about 0.6-2.2% of the stored carbon per season. The losses from ELARP ranged from 0.23-0.33 $kg{\cdot}m^{-2}$ per season during the years of higher NCP (1997-2002) or 0.23-0.33% of the stored carbon per season. There is no expectation that all of the stored carbon is available for decomposition since we know that lakes in this area accumulate carbon in their sediments over thousands of years (Kipphut et al. 1978). Although the decline in the NCP in the FLUDEX reservoirs is not due to carbon limitation based on the total amount in storage, with both FLUDEX and ELARP there is a general trend for higher NCP with higher initial carbon stocks. This suggests that the more readily decomposed portion of the carbon stocks are limited in quantity, at least in the FLUDEX sites, and that the rate of decomposition (NCP) is controlled in some way by parameters such as organic surface area or exposure. In the FLUDEX reservoirs these parameters are relatively constant, so depletion of the easily decomposed carbon may dominate the trends. However, in the ELARP reservoir large masses of peat separated from the bottom forming floating islands. This process which began in 1993 could have significantly increased the surface area and access of oxygen to the carbon stocks.

Finally we must assess the transportability of the model and it applications in a truly predictive sense. In order to apply the model for estimation of the NCP of a hydroelectric reservoir, the required data could be quite easily collected. Hydrologic flows and temperatures are typically well known. Wind speed and other meteorological measurements are easily collected. A weekly or twice weekly program to collect data for DIC and alkalinity or DIC and dissolved CO_2 should provide an adequate database. Horizontal variability could be checked by an occasional survey. The addition of a module for the estimation of photosynthetic carbon fixation would improve the fit of the

model especially if the fixation was large and would help to understand variations in measured CO_2. The model cannot be used to predict ahead of time changes in annual NCP as were observed over years in both the FLUDEX and ELARP experiments. This requires a more complete understanding of the availability of stored carbon for decomposition.

10.5 Conclusions

NCP estimates for the 3 FLUDEX reservoirs showed a consistent decline (20-70%) over the 4 seasons of flooding. Although only 0.6-2.2% of the carbon stores in the flooded areas were converted to CO_2 each year, NCP was generally higher in reservoirs with higher carbon stores (Medium C reservoir had the highest NCP in years 1 and 3). The assumption that NCP was constant over the 115 day flooded period worked well. NCP estimates for the ELARP reservoir over 12 years (2 years pre-flood, 10 years post-flood) showed a consistent increase to a level 6-10 times the NCP of the original pond. This level was relatively stable from 7-10 years post-flooding. The maximum NCP estimated for the ELARP reservoir was 3-4 times that for the FLUDEX reservoirs.

Our conceptually simple dynamic model does a good job in estimating the NCP from 4 experimental reservoirs over 4 to 10 years. Data requirements for the model can be met with measures that are generally available from large hydroelectric reservoir sites. The model cannot be used to predict changes in NCP due to changes in the availability of carbon for decomposition from year to year.

11 Gross Greenhouse Gas Emissions from Brazilian Hydro Reservoirs

Marco Aurelio dos Santos, Bohdan Matvienko, Luiz Pinguelli Rosa, Elizabeth Sikar and Ednaldo Oliveira dos Santos

Abstract

This paper presents the results of gross carbon dioxide and methane emission measurements in several Brazilian hydro reservoirs. The term 'gross emissions' means gas flux measurements from the reservoir surface without correcting for natural pre-impoundment emissions by natural bodies such as the river channel, seasonal flooding and terrestrial ecosystems. The net emissions result from estimating pre-existing emissions by the reservoir. Measurements were carried in the Miranda, Barra Bonita, Segredo, Três Marias, Xingó, Samuel and Tucuruí reservoirs, located in two different climatological regimes. Additional data were used here from measurements taken at the Itaipu and Serra da Mesa reservoirs. Emissions of carbon dioxide and methane in each of the reservoirs selected, whether through bubbles or diffusive exchange between water and atmosphere, were assessed by sampling, with subsequent extrapolation of results to obtain a value for the reservoir. A great variability was found in the emissions, linked to the influence of various factors, including temperature, depth at the point of measurement, wind regime, sunlight, physical and chemical parameters of water, the composition of the local vegetation and the operational regime of the reservoir.

11.1 Introduction

The principal objective of this chapter is to present a methodology for accounting for the greenhouse gases emitted from different Brazilian hydroelectric reservoirs.

Experimental measurements of gas emissions from reservoirs were made to precisely determine emissions of methane (CH_4) and carbon dioxide (CO_2) gases both in the form of bubbles that form in the bottom of the lake from decomposition of organic matter and that were emitted to the atmosphere by molecular diffusion.

The measurements, made in two field surveys, consist of the collection of gas flow data, wind regimes, temperature and pH of water in the reservoirs studied.

In order to obtain an average for each reservoir as a whole from the results of experimental observations, in only some points of the reservoir and some days of the year, criteria for extrapolation had to be adopted. For emissions through bubbles, which do not occur at greater depths, a weighted average was created for the entire reservoir; and for diffusive emissions, which were found to be independent of depth, a simple average of the values measured was used.

With quantification of the emissions of the reservoirs studied, a comparison was made with emissions of hypothetical thermoelectric plants of the same capacity.

We also present a comparison between the gaseous exchange measurement method using “small chambers” with the method using larger chambers, used by other research groups.

11.2 Material and Methods

11.2.1 Site Description

Greenhouse gas measurements were carried out in the Miranda, Barra Bonita, Segredo, Três Marias, Xingó, Samuel and Tucuruí dams, located in two different climate systems. Additional data were used from measurements taken at the Itaipu and Serra da Mesa dams (Fig. 11.1).

These reservoirs range from latitudes of 2^{o} S to 25^{o} S, and vegetation types include equatorial rainforests, subtemperate forests, Atlantic forest, cerrado and caatinga (semi-arid), which includes the principal Brazilian ecosystems. The ages since flooding of the hydroelectric reservoirs range from one to twenty years, which gives the study good temporal representation. Table 11.1 below provides a brief description of the reservoirs studied.

Fig. 11.1. Location of hydroelectric facilities studied and referenced

11.3 Methodology

The measurement methodologies were essentially the same in all cases.

At each of the selected dams, emission of carbon dioxide and methane were assessed by sampling production through bubbles or diffusive water-air exchanges and extrapolating these findings to obtain a value for each dam.

The samples were collected using a set of 16 bubble collector funnels (cones of synthetic sheet on an aluminum framework, with a diameter of 75 cm and coupled to gas collecting bottles).

Table 11.1. Major Characteristics of the Hydroelectric Reservoirs Studied and Referenced

Station	Latitude	Biome	Capacity [MW]	Area of reservoir [km^2]	Density of generating capacity [$W \cdot m^{-2}$]
Miranda	18°55'S	Cerrado	390	50.6	7.71
Três Marias	18°13'S	Cerrado	396	1040	0.38
Barra Bonita	22°31'S	Mata Atlântica	140.76	312	0.45
Segredo	25°47'S	Mata Atlântica	1260	82	15.37
Xingó	9°37'S	Caatinga	3000	60	50.00
Samuel	8°45'S	Amazônica	216	559	0.39
Tucuruí	3°45'S	Amazônica	4240	2430	1.74
Serra da Mesa[a]	13°50'S	Cerrado	1275	1784	0.71
Itaipu[a]	25°26'S	Mata Atlântica	12600	1549	8.13

[a]: Reservoirs studied in parallel surveys.

The funnels were deployed under the surface of the water (at around 1 m of depth) coupled to plastic bottles that served as buoys and anchored by stones of around 10kg each attached to a rope. The choice of the sampling site and the arrangement of funnels was determined by parameters such as the year the reservoir was filled, depth, presence of semi-submersed vegetation, and geographic region of the reservoir.

The funnels remained at the site for 24 hours, during which period the bubbles released from the bottom were captured. Then the collecting bottles were hermetically sealed under the water and collected for later laboratory analysis.

Diffusion chambers are mechanisms that resemble small inverted cups, with a total volume of 75 ml and able to contain a submersed "bubble" of atmospheric air at a shallow depth (around 20 cm below the surface) with a contact surface of 22 cm^2, through which there is an exchange of gases, here called diffusion. After 3, 6, and 12 minutes of contact, a sample of the "bubble" is taken to the laboratory and the change in the concentration of each gas is estimated chromatographically, allowing for the calculation of the emission or uptake rate, as the case may be.

To obtain rates of emission by bubbles, average values were used for four different depth ranges, and approximate mathematical functions were established which described the emission rates as a function of depth. One of the functions used was a straight line, and the others were exponential functions.

Multiplying the pairs corresponding to the area and rate, the total mass of gas emitted from each depth range of the reservoir was obtained. The sum of these values represents the total mass emitted by the entire reservoir. From the total masses, the reservoir's average emission rate for each gas was calculated.

The measurements were made according to a well-established routine, in contrast with the "generalization" of the results, which requires a certain care and could constitute a source of uncertainty affecting the final results. Because of the existing conditions, the measurements needed to be limited, not only in spatial terms but also in time. In fact only two measurements series were possible, separated by an interval of 6 months. This low frequency also constituted a source of uncertainty, but for practical reasons it was not possible to increase the frequency.

A detailed description of the methodology used for assessing the spatial and temporal representativity of gas sampling is in annex and could be read in Matvienko et al. 2001; Rosa et al. 2001; Rosa et al. 2002; Rosa et al. 2003.

11.4 Results and Discussion: Gross Emissions of CO_2 and CH_4 from Brazilian Power Dams

Fourteen sampling surveys were carried out between 1998 and 1999. These measurements were carried out in the Miranda, Barra Bonita, Segredo, Três Marias, Xingó, Samuel and Tucuruí dams, located in two different climate systems. Additional measurements were performed at the Itaipu and Serra da Mesa dams (Fig. 11.1).

Measurement methodologies were essentially the same in all cases, as described in the previous section. Summary results of GHG emissions for the various power dams studied are presented in Fig. 11.2 in terms of average gross CO_2 and CH_4 emissions ($kg{\cdot}km^{-2}{\cdot}d^{-1}$).

The intensity of these emissions varied widely, due to several factors, including temperature, measurement point depth, wind system, sunlight, physical and chemical water parameters, biosphere composition and the operating system of the dam in question.

An important observation was the relatively low correlation between emissions and the age of the dam, possibly because these emissions result not only from the decomposition of pre-existing terrestrial biomass, but also organic matter swept down the upstream drainage basin (carbon from biomass and soil, as well as sewage and waste waters) in addition to organic matter produced in the dam itself (i.e. phytoplankton).

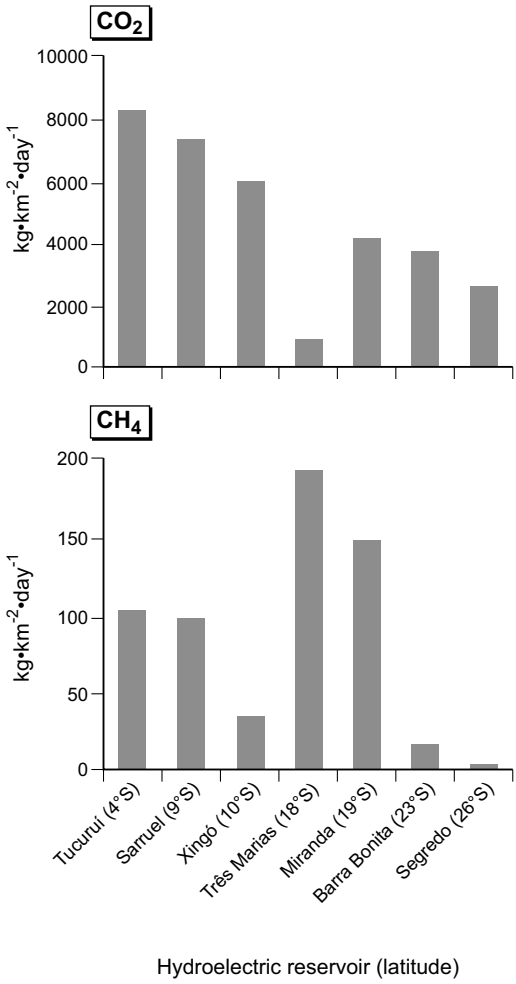

Fig. 11.2. Emissions of CO_2 and CH_4 from Power Dams studied, in $kg \cdot km^{-2} \cdot d^{-1}$

All this suggests greater difficulties in separating out the anthropogenic emissions (the purpose of this study) from emissions that would occur even without the dam. The portions transported by bubbles and by molecular diffusion are totaled, and total emissions from the reservoir are obtained for the period of time considered.

The emission rate was calculated based on the data obtained in the experimental measurements, arriving at an average value for the two surveys of each reservoir. This value will be used for the extrapolation to a one-year period. The results are the product of two data collection surveys, and

the extrapolation of the values adopted is a conservative hypothesis for emissions from power dams, since the emissions are projected as constants over the period of time (Tables 11.2 and 11.3).

Due to these factors, together with the limited number of dams studied, and the space and time constraints of the samples, these findings are somewhat uncertain. Bearing in mind that the estimated values for hydro-power plants include emissions that are not fully anthropogenic, the hydro-power plants studied generally had lower emissions than their thermo-based counterparts.

The best performances were seen in hydro-power plants with greater power densities (capacity x flooded area – $W{\cdot}m^2$), such as Itaipu, Xingó, Segredo and Miranda, well above even that of thermo-power plants using state-of-the-art technology.

Figures 11.3 to 11.5 below present the average values of CO_2 and CH_4 emissions measured as well as results from others studies. Along with the seven reservoirs, we also present data from the reservoirs of Curuá-Una (through bubbles), where we carried out an experiment with Canadian scientists in 1997, and from Itaipu and Serra da Mesa, which were the objects of specific studies commissioned by the respective companies.

In general, for methane emitted from ebullition, there was a trend towards decline between the samples taken in the first and second research survey. Newer reservoirs tend to produce more emissions through bubbles than older ones.

Except for Três Marias, all the reservoirs displayed a strong correlation between the increase in the age of the reservoir and the reduction of gas flow. This effect can be easily verified in the case of CH_4 bubbles, as shown in Fig. 11.3, which shows on the *x* axis number of years between filling of the reservoir and sampling, and on the *y* axis, the average flow of carbon equivalent of methane emitted through bubbles.

For carbon dioxide emitted by bubbles the situation is different. Along which having much lower emissions than for methane (around 100 times less), it was not possible to discern any type of dependence with the age of the reservoir. The low levels of CO_2 in bubbles could be explained by its high solubility in water, resulting in low separation of gas by bubbles.

Figure 11.4 shows this reservoir age-independent behavior of emissions.

The other process of gas transport was molecular diffusion. In this case, no pattern was found in the average data that would explain the decline in emissions of methane and carbon dioxide.

The average data for emissions by molecular diffusion from the two surveys are represented in Fig. 11.4 and 11.5 for CH_4 and CO_2,

Table 11.2. Results of the First Survey Measuring Greenhouse Gases in the Seven Hydroelectric Reservoirs

Dam	Gas flux by bubbles [$mg \cdot m^{-2} \cdot d^{-1}$]		Gas flux by diffusion [$mg \cdot m^{-2} \cdot d^{-1}$]		Sum of ebullitive and diffusive fluxes [$mg \cdot m^{-2} \cdot d^{-1}$]		Range Values [$mg \cdot m^{-2} \cdot d^{-1}$]			
	CH_4	CO_2	CH_4	CO_2	CO_2	CH_4	CO_2 Bubbles	CO_2 Diffusion	CH_4 Bubbles	CH_4 diffusion
Miranda	29.2	0.3	233.3	4981.3	4980	262.4	0.03–0.5	16–61182	0.002–175.6	20–4572
Três Marias	273.1	3.5	55.3	-138.5	-142	328.2	0.006–8.3	33–(-10060)	0.001–1205	0.9–241
Barra Bonita	4.8	0.2	14.4	6434.2	6434	19.2	0.008–0.77	1614–33424	0.002–21	3.1–29
Segredo	1.7	0.1	8.3	4789.1	4789	9.9	0.002 -2	0.0001–46857	0.004–29	0.002–64
Xingó	1.9	0.01	28	9837.1	9837	29.99	0.004–0.06	29–89203	0.01–15	3.3–142
Samuel	19.3	0.6	164.3	8087.6	8087	183.6	0.004–3.5	2313–16345	0.0001–67	4.9–2375
Tucuruí	13.2	0.14	192.2	10433	10433	205.4	0.002–0.96	1314–142723	0.01 -106	0.03–2.889
Itaipu	0.5	<1	12.4	1205	1205	12.9	0.01–0.74	-2646–7980	0.01–3.04	1.39–47
Serra da Mesa	111	1.9	10	1317.9	1316	121	0.03–3.9	(-485.67)–2500	2.4–440	2.9–94

Table 11.3. Results of the Second Survey Measuring Greenhouse Gases in the Seven Hydroelectric Reservoirs

Dam	Gas flux by bubbles [$mg \cdot m^{-2} \cdot d^{-1}$]		Gas flux by diffusion [$mg \cdot m^{-2} \cdot d^{-1}$]		Sum of ebullitive and diffusive fluxes [$mg \cdot m^{-2} \cdot d^{-1}$]		Range Values [$mg \cdot m^{-2} \cdot d^{-1}$]			
	CH_4	CO_2	CH_4	CO_2	CO_2	CH_4	CO_2 Bubbles	CO_2 Diffusion	CH_4 Bubbles	CH_4 diffusion
Miranda	18.5	0.2	27.4	3796	3796	45.9	0.01–0.87	223–41358	0.03–72.6	2.19–168.2
Três Marias	55.9	4.01	8.4	2373	2369	64.3	0.01–23.3	168–7346	0.04–402.5	0.66–70.75
Barra Bonita	3.1	0.05	19.5	1537	1537	22.6	0.002–0.19	83–20391	0.0004–15.48	5.1–59.3
Segredo	1.9	0.03	5.7	601	601	7.6	0.02–0.25	165–16218	0.01–15.4	2.14–14.59
Xingó	19.6	0.09	30.6	2440	2440	50.2	0.0004–1.9	341–17239	0.78–407.3	3.54–92.9
Samuel	13.6	0.4	10.8	6808	6807	24.4	0.01–1.2	2200–24283	0.07–37.6	6.13–17.16
Tucuruí	2.5	0.07	10.9	6516	6516	13.4	0.03–0.5	457–32291	0.92–21.2	4.44–28.53
Itaipu	0.6	<<1	7.9	-864	-864	8.5	0.001–0.009	-4061–(-120)	0–1.9	0.9–57.30
Serra da Mesa	66.3	1.5	39.2	3973	3972	105	0.06–37.4	(-6048)–10178	0.15–2546.9	(-24.3)–355

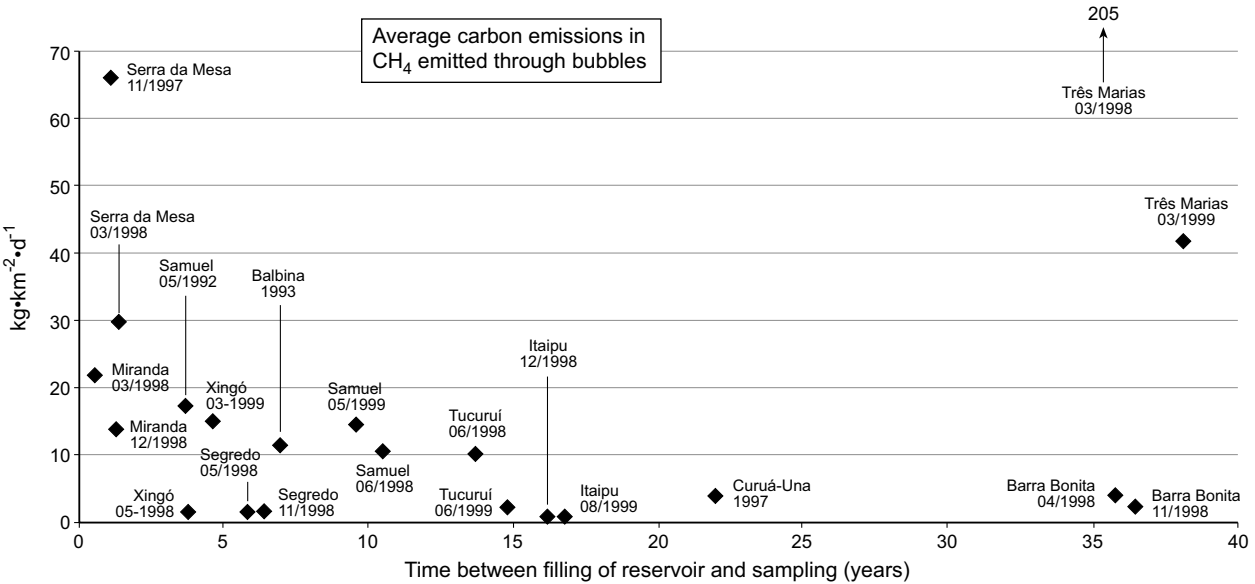

Fig. 11.3. Average carbon emissions in CH_4 emitted through bubbles in Brazilian hydroelectric reservoirs

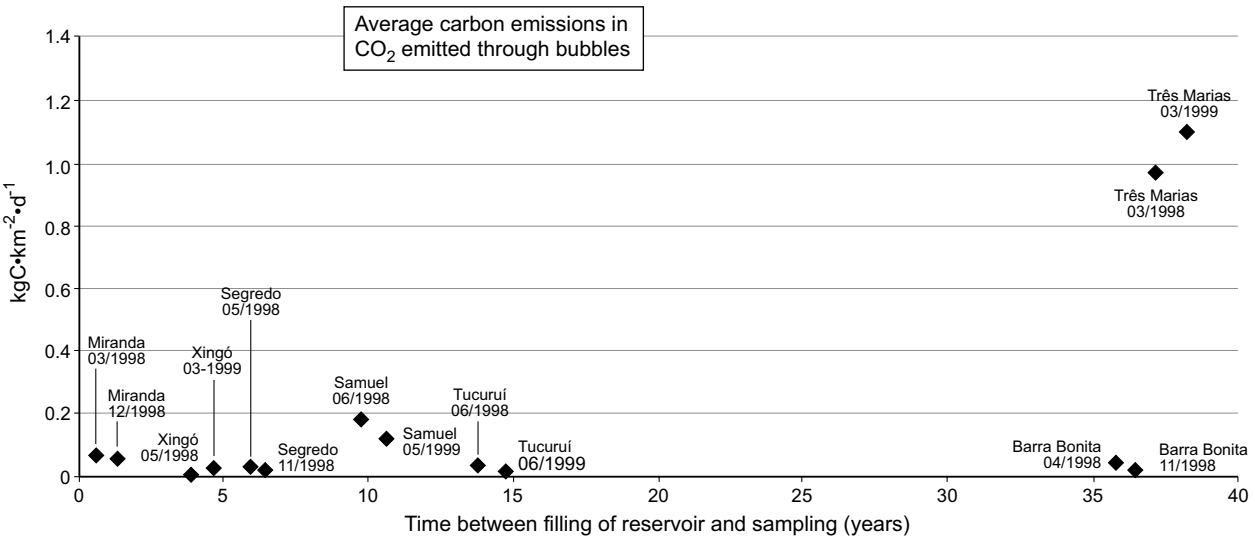

Fig. 11.4. Average carbon emissions in CO_2 emitted through bubbles in seven Brazilian hydroelectric reservoirs

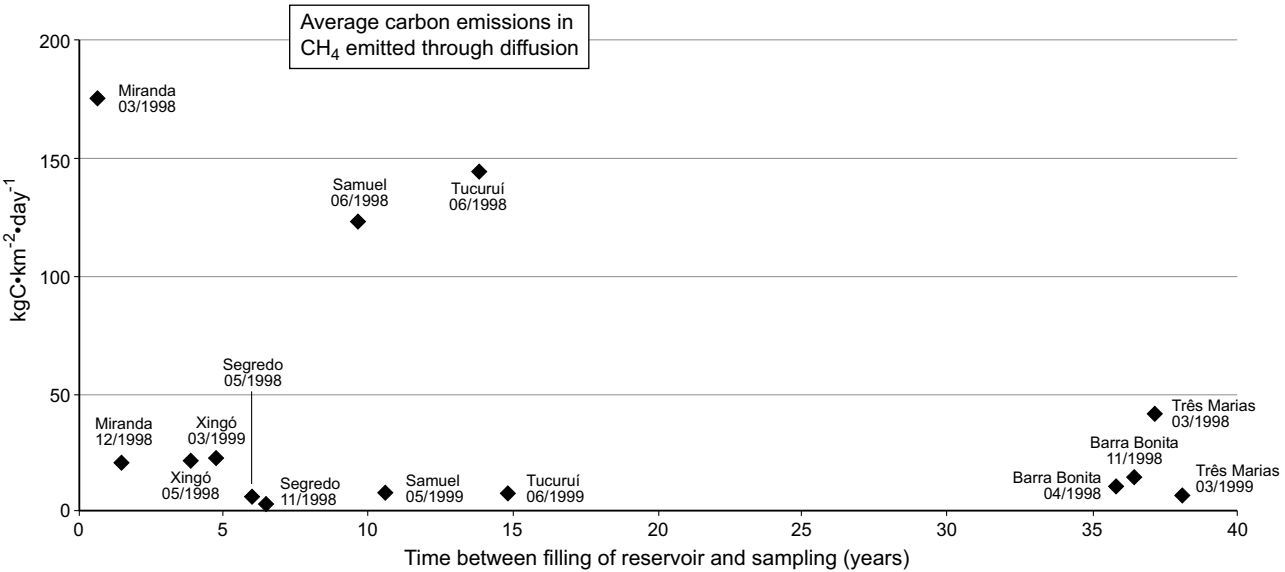

Fig. 11.5. Average carbon emissions in CH_4 emitted through diffusion in seven Brazilian hydroelectric reservoirs

respectively, which compare emissions with the age of the reservoirs. The behavior is very different from that found for methane by bubbles. For diffusion, reservoirs that have been filled for longer periods of time produce both gases in greater quantities than recently filled reservoirs – there is no apparent dependency of flows on the age of the reservoir.

The flows of gases through diffusion are much greater than by bubbles, especially in the case of carbon dioxide, which has greater water solubility. All the CO_2 (99.99%) that is released to the atmosphere is through molecular diffusion of the gas in water. For CH_4, there is a range of variation from 14% to 90% of gas emission by molecular diffusion.

It should be noted however that when the results are compared with the same reservoir, there is a tendency towards lower average results in the second research survey. However, more measurements are required for a more rigorous conclusion.

11.5 Concluding Remarks and Future Orientations

This study has shown that although hydro-power is not a zero emission energy source in terms of atmospheric greenhouse emissions, these dams performed better than thermo-power plants in most cases analyzed. This indicates that they offer a feasible solution for reducing greenhouse gas emissions by the power sector, in comparative terms.

The comparisons between the reservoirs studied show a large variation in the data on greenhouse gas emissions, which would suggest that more care should be taken in the choice of future projects by the Brazilian electrical sector.

The intensity of gas emissions in a reservoir is not invariant over time. There are fluctuations with irregular periods of duration. However, the variation is modulated by a set of influences, principally temperature, wind regime, sun exposure, physical and chemical parameters of the water, and composition of the biosphere.

The emission of CH_4 by hydroelectric reservoirs is always unfavorable, since even if the carbon has originated with natural sources, it is part of a gas with higher GWP in the final calculation.

Emissions of CO_2 can be attributed in part to the natural carbon cycle between the atmosphere and the water of the reservoir. Another part could be attributed to the decomposition of organic material, caused by the hydroelectric dam.

For CO_2, these influences could combine in such a way that emissions could be a tenuous function of latitude, such that in higher latitudes the

reservoirs would tend to have lower emissions. However this relation does not always exist, as for example with methane.

The data from the two research surveys do not allow a long-term temporal analysis of the behavior of emissions, because of the logistical and financial restrictions imposed.

The influence on the greenhouse effect which a reservoir has should be judged by its effect on three parameters: the CH_4/CO_2 ratio, permanent carbon in sediment and carbon runoff to sea.

The methane/carbon dioxide ratio is important because methane is a more effective hothouse gas than carbon dioxide. If a reservoir promotes methane formation to a larger degree than a river system, then it is augmenting the greenhouse effect. Anoxic conditions in reservoir sediments favor methane formation.

On the other hand, a reservoir may be serving as a carbon sink, perhaps through the production of insoluble humic substances immune to further decomposition in its sediment. Additionally, the runoff to the sea of dissolved humic substances may be favored by the presence of a reservoir.

In all the reservoirs studied, carbon dioxide is emitted mostly by diffusion. However, since this gas is part of the natural carbon cycle, in some measurements there was uptake of CO_2 in the reservoir through photosynthesis of primary production of the reservoir. In the case of methane, this gas is always emitted, whether through bubbles or molecular diffusion.

In some reservoirs it was observed that the plant operating regime could also influence the emission of gases. Depending on the operation of the plant, the reservoir could empty quickly, allowing shallow dendritic arms to be periodically exposed to colonization by terrestrial vegetation. These regions have an intense methane generation because of the decomposition of this vegetation. This effect occurred in the Três Marias and Samuel reservoirs.

These main topics should be developed in a near future:

1. The mean values obtained until now have a level of uncertainty and new research on GHG emission from hydro reservoirs require improvements like on line measurements;
2. The experimental measures and assessment of specific sites can give only a partial view as emissions from reservoirs vary greatly from one to another. However, such studies are necessary to supply data on the variability issue;
3. The full life-cycle assessment should be included in future studies, as well as consider emissions pre-existing dam construction. Carbon cycle studies, like the preliminary experiment conducted here should be en-

couraged, to determine carbon origin (natural and anthropogenic) in the whole watershed area;
4. It is important to include in the IPCC a discussion of the role of the GWP index in comparing thermo power and hydro reservoir emissions.
5. The carbon emitted to the atmosphere by the free surface of the water in hydroelectric reservoirs comes in part from organic material carried from the headwaters areas to the bed of large rivers and to the hydroelectric reservoirs. If this carbon, in the case of CO_2 emissions, is from biomass, then it was previously removed from the atmosphere and thus its emission does not result in increased greenhouse effect. Thus the problem emerges of quantifying these contributions and the emissions of CH_4 and N_2O. This requires studies of the carbon cycle in the watershed/reservoir system.

11.6 Annex

11.6.1 Procedures for Capturing Bubbles

In most cases, the funnels were placed along a transect going from the most shallow regions to the deepest. Around five funnels were placed in the most shallow regions, and the number was reduced in the direction of the deeper areas.

The funnels were submersed and all air was removed to avoid contamination by atmospheric air. Then the collecting bottles, full of water, were coupled to the funnel.

The choice of the sampling site and the arrangement of funnels was determined by parameters such as the density of the flooded vegetation, the year the reservoir was filled, depth, presence of semi-submersed vegetation, and geographic region of the reservoir.

We also took into account the time the boat takes to reach the sampling site, as well as the site's representativeness of the reservoir as a whole.

The funnels usually remained for 24 hours at the site, where during this period the bubbles emanating from the bottom were captured. The collection bottles were then hermetically sealed while still underwater and collected for later laboratory analysis. On some occasions however, a time of less than 24 hours was used, and the values obtained were extrapolated to the exact time of the experiment.

Based on the experience accumulated in gas sampling with funnels, it is clear that there is a strong inverse correlation between depth and gas emis-

sions by bubbles. For this reason a larger number of funnels was deployed in the more shallow regions, where more gas was released.

11.6.2 Calculation of Averages of Greenhouse Gases Emissions by Bubbles

Average rates of gas emissions, in units of $mg \cdot m^{-2} \cdot d^{-1}$, calculated for each reservoir, are descriptive parameters to be used in future estimates of gas emissions in reservoirs not studies.

Normally the total area of the reservoirs is known, but not the "area which emits". Thus, emission rates referring to the total area were determined, along with the ratios of "area which emits".

For each reservoir, the area which emits was estimated based on the first degree experimental equations, which describe the bubble emissions *y* of the gas as a function of the depth *x* of the sampled site. For each reservoir, the equation *y(x)* was obtained, and based on this the value of *xo* was calculated, such that: $y(xo) = 0$.

In this model, each reservoir emits in the belt between the shore and the geometric site of depth *xo*. Thus is defined the "emitting area".

To calculate the size of the "emitting area", it would be necessary to obtain the cartographic tables of the area of each reservoir as a function of depth, which supposedly exists for each project. However, only fragments of these tables were found.

To make up for this lack, a simply pyramid model was established. In this model, the reservoir is treated as an inverted pyramid, whose base is the water surface and the height is the depth *h* at the dam. Based on consideration of a succession of situation where the water level drops progressively, it is possible to define a set of pairs of values consisting of areas *Ai* of the water surface with the corresponding values *hi* of depths at the dam. The values *Ai* in this model are proportional to the square of *hi*, with *c* the constant of characteristic proportionality for each reservoir.

$$Ai = c\ hi \tag{11.1}$$

For all reservoirs, the areas *A* of the water surface and the depths *h* at the dam are known, allowing calculation of the constant *c*.

Using this value *c* and the value *xo*, the emitting area *Ae* can be calculated almost immediately.

But first the area *An*, which does not emit, is calculated:

$$An = c\ (h - xo) \tag{11.2}$$

The emitting area is

$$Ae = A - An \quad (11.3)$$

Thus, using the pyramid model, it is not necessary to fully reproduce the cartographic table of the reservoir to estimate the "emitting area".

For example, for the Três Marias hydroelectric facility, in the second measurement survey of CH_4 by bubbles presents:

$$y = 153.20 - 6.35x \quad (11.4)$$

1. From this equation, one can calculate at what depth *x* the rate *y* is null:
   $0 = 153.2 - 6.35\ x$
   $x = 24.12$ m
   thus, at depth of 24.12 or deeper there is no more emissions by bubbles.

2. Using Eq. 11.4, average emissions from the shore to the depth at which emissions are null can be calculated. The average value given by this equation is half of the maximum emissions:
   $y = 76.6$ mg $CH_4 \cdot m^{-2} \cdot d^{-1}$

3. For the pyramid model, the constant c is calculated using Eq. 11.1, with the total area and maximum depth of the reservoir:
   $c = A / hmax^2$
   $c = 1009.32 / 50.20^2\ km^{-2} \cdot m^{-2}$
   $c = 0.40052\ km^{-2} \cdot m^{-2}$

4. Eq. 11.2 provides the non-emitting area:
   $An = c\ (h - xo)^2$
   $A24.12 = 0.40052 \times (50.20 - 24.12)^2$
   $A24.12 = 272.53\ km^2$

5. The emitting area, according to Eq. 11.3, is:
   $Ae = 1009.32\ km^2 - 272.53\ km^2$
   $Ae = 736.79\ km^2$

6. Then the mass M emitted per day is calculated:
   $M = 736.79 \times 106\ m^2 \times 76.6$ mg $CH_4 \cdot m^{-2} \cdot d^{-1}$
   $M = 56.44 \times 109$ mg $CH_4 \cdot d^{-1}$

7. Dividing M by the total area of the reservoir gives the average emissions of the reservoir:
   $Em = 56.44 \times 109$ mg $CH_4 \cdot d^{-1} / 1009.32 \times 106\ m^2$
   $Em = 55.92 \times$ mg $CH_4 \cdot m^{-2} \cdot d^{-1}$

11.6.3 Measurement Procedures for Diffusion Rates

The chambers used in the present research resulted from a long process of refinement, inspired by the equipment used by Lucotte et al. (1997).

The original equipment was proposed to measure gas exchange in the water-air interface. A chamber of transparent acrylic was used, better described as a box with no cover, used upside down and touching the surface of the water so as to imprison a certain volume of air.

If there are emanations of, for example, carbon dioxide, its concentration in the volume of air in the canister would grow over time, and the graph of concentration vs. time allows the calculation of the rate of diffusion. Difficulties found with these chambers include warming of the gaseous contents by solar radiation, difficulty of handling in the presence of waves, susceptibility to the occasional capture of bubbles, and duration of around 5 times that needed by the smaller chambers owing to the large volume in comparison to area (because of a thick gaseous layer – around 20 cm). The modifications introduced were:

- Miniaturization of the chamber, reducing the volume from typically 20L to 40mL, which lowers the thickness of the gaseous layer to 2 cm, allowing the reduction of time to 12 minutes.
- Simultaneous use of three identical chambers for exchange times of 3 min., 6 min. and 12 min., thereby avoiding the possible effect of reduction of volume resulting from the repeated sampling in only one chamber.
- Use of miniaturized chamber in a slightly submersed position, thus obtaining immunity from the action of waves and temperature changes.

11.6.4 Principle of Exchange Rates Measurement

In the experiment the minimum number of equilibrations to determine the rate of exchange would be two, with a duration, for example, of 3 and 6 minutes. But as will be discussed below, by adding a third equilibration, for example with a 12 minute duration, it is possible to increase the reliability of the measurement through redundancy.

The volume of 50 mL of air in each chamber has a contact surface with the water of 22 cm^2, as if the chamber were a glass inverted over 22 cm^2 of natural surface, but with the difference that the chamber is submersed. The same processes of gaseous exchange that takes place in the natural surface happens at the 22 cm^2 surface of the submersed chamber.

In a typical equilibration experiment, a visit was made to the site to be sampled and with the boat anchored at a site of the desired depth the equilibration experiment was carried out as follows. First, a volume of ~500 mL of air was drawn with a piston pump equipped with a transference tube. This air was taken from around 10cm above the surface of the water.

Around 35 mL of this air was transferred to a test tube, for later measurement of the concentrations of the gases being investigated.

The chambers were filled with the 50 mL of air in the following way: the transference tube of the pump was linked to the valve of the chamber, then the chamber was submersed and filled with water and left hanging from its buoy. Next 50 mL of air is then transferred from the pump, causing the expulsion of an equal volume of water from inside the chamber. The time of the start of equilibration was then noted, the valve of the chamber was closed and the transference tube disconnected. Thus the chamber and buoy begin to float almost freely, bobbing in the waves. A cord tied to the buoy keeps it within reach.

When the time of equilibration is up, for example three minutes, the chamber is closed while still under water, which is possible through a piston that each chamber is equipped with, which along with closing it, serves later to expel the air from it. This was done after connecting the chamber to a test tube through a transference tube, with the appropriate manipulation of its valve and its piston. Thus, in three equilibration experiments, three samples of air were obtained, from equilibration times of 3, 6, and 12 minutes.

For example, in one of the experiments in the Xingó reservoir three samples were obtained.

The respective results of the analysis, together with that of the original 9C3 initial unequilibrated sample, are shown listing the concentration y of CO2 as a function of time t of equilibration.

The function $y(t)$, which represents the concentration of CO_2 , in ppm, in the chamber after t minutes of equilibration, can be described by an exponential function of the form:

$$y = C + A \exp(-k.t)$$

This formula is the theoretical conclusion resulting from a simple supposition, which is that the rate of exchange of gas dy/dt, between the water of the reservoir and the air of the chamber, would be proportional to the difference of the concentrations C in the water and y in the air of the chamber. Symbolically,

$$dy/dt = k (C - y)$$

where k is the constant of proportionality. Through integration, the function given above is obtained, where A is the arbitrary constant of the integration.

This function allows the calculation of the true rate of diffusion – the rate that prevails between the surface of the water and the atmosphere. In the equilibration experiment with chambers, the saturation effect needs to be taken into account. The saturation occurs because the volume contained in the chamber is small compared to the area of the exchanging surface.

Two observations could be made about the saturation effect: (a) even in the presence of saturation, at the first instant the exchange rate inside the chamber is identical to that which exists at the free surface of the water. This equality exists because the exchange rate is proportional to the difference of the concentrations (C - y), and at the first instant the concentration y within the chamber still was not affected by the saturation effect because it is identical to the concentration outside the chamber. (b) The saturation is theoretically predictable and the extent to which the experiments follow the prediction is a measure of the reliability of the results.

To solve the function $y(t) = C + A\ exp(-k.t)$, an algebraic approach was used: time t is the independent variable, the concentration y is the dependent and C, A, and k are three constants whose values are to be determined. If y and t were known experimentally, as they are through the chamber experiments, the function can be written as an equation in which C, A, and k are three unknowns. Using three pairs of experimental data, there are thus three equations with three unknowns.

$$411.5 = C + A\ exp(-k.0)$$
$$603.5 = C + A\ exp(-k.3)$$
$$749.5 = C + A\ exp(-k.6)$$

This set characterizes a system of three equations with three unknowns. When solved for the constants the following numerical values are obtained:

$$C = 1212.9\ ppm$$
$$A = -\ 801.4\ ppm$$
$$k = 0.0913\ min^{-1}$$

By using algebra, only three of the four experimental pairs of (y, t) can be used. The fourth experimental pair, although it contains information, cannot be used in determining the constants in this formalism, since because of its exactness, the algebraic procedure does not tolerate small experimental deviations within a set where there is redundancy of data, and it collapses in the presence of the smallest experimental errors.

However, such deviations are perfectly tolerable through another method – the statistical method. This allows the use of a redundant data set, in this case a greater number of equations (4) than the number of unknowns (3). It determines the function of the experimental set, even redundant, defining a function of quadratic deviation *S*, something similar to variance, and imposes the condition that the set of the three constants *C*, *A*, and *k* would be that which produces a minimum deviation *S*:

$$S = S\ (yi - (C + A.\exp(-ti.k)))^2$$

where (yi, ti) are experimental pairs of concentration and time. The minimization of *S* implies that their partial derivatives in relation to *C*, to *A*, and to *k* should be simultaneously null (solved by computer):

$$\partial S/\partial C = 0\ \partial S/\partial A = 0\ \partial S/\partial k = 0$$

There is some difference between the three constants obtained previously by the algebraic method and these obtained by the statistical minimization of *S*. The statistical method if better, however, because it uses a larger number of data points.

Another advantage of the statistical method is that it allows the computation of a deviation function to measure how much the data measured differ from the ideal function. In this work we define an *s* relative to the constant *C,* as follows:

$$s(\%) = 100\ .\ S1/2/\ (n\ C)$$

where *n* is the number of experimental pairs of data (here $n = 4$). It could be said that *s* is a kind of percentage deviation of a typical experimental point from the ideal value of the function. The deviation *s* is useful in judging the reliability of an equilibration data set. Estimates of emissions of CO_2 with a small *s* are more reliable than those with a large *s*.

The example given above with the samples from Xingó was a case of emissions of CO_2 from water to air. The true emission rate prevails in the chamber only in the first instant of equilibration, when the concentration of CO_2 within the chamber is identical to its concentration in the air of the surface of the reservoir. In the following instants the growing saturation within the chamber reduces the emission rate. However, a small algebraic manipulation allows the calculation of the true rate based on the function that can be determined for adjustment of the data:

$$y = C + A\ \exp(-k.t)$$

For its time derivative:

$$dy/dt = -\ A\ k\ \exp(-k.t)$$

This derivative represents the variation *T* of concentration *y* within the 50 mL volume of the chamber over time, which in this example was an increase. This derivative can be calculated for any instant *t*, including for the initial instant, using for the variable *t* the appropriate value.

In the initial instant *t = 0*, and we thus have:

$$(dy/dt)t=0 = - A\ k$$
$$\text{or, } T = - A\ k$$

Using the values of the constants *A = -762,54* and k = 0,09972, found by statistical techniques, the result is:

$$T = 76.04\ (ppm \cdot min^{-1})$$

which is the rate by which the concentration of CO_2 would increase within the chamber in the first instant of equilibration.

The rate *T*, which is identical to *dy/dt*, is itself obtained using the four pairs of experimental equilibration data, fitting the function *y(t)* to this data and calculating *dy/dt* at the instant *t=0*.

This rate T, which describes the increase over time of concentration within the chamber could be transformed into the rate *Q* which measures the mass of CO_2 per minute or per day crossing the contact interface of 22 cm^2 between the water and the air of the chamber. This transformation is made as follows:

$$Q = \text{T ppm/min x 10-6 ppm-1 x 50 mL x 1440 min}\cdot d^{-1} \text{ x}$$
$$\text{44 mg } CO_2\cdot\text{mmol 22 x 10-4 m}^2 \text{ x 25.11 mL}\cdot\text{mmol}^{-1}$$

or

$$Q = 57.35\ T \text{ mg } CO_2\cdot m^{-2}\cdot d^{-1}$$

The fraction consists of the volume of air in the chamber, which is 50 (mL), the factor 1440 min/day, which converts days to minutes, the millimolar mass of CO_2, which is 44 mg $CO_2\cdot mmol^{-1}$, the area of the chamber, 22.10-4 m^2, and the millimolar volume of an ideal gas, which in Xingó at the time of the experiments was 22.11 $mL\cdot mmol^{-1}$ (for a more exact value, the temperature and pressure at the site are needed, to make the calculation $p\ V = n\ R\ T$). It should be noted that there are units in the fraction which are cancelled, resulting in mg $CO_2\cdot m^{-2}\cdot d^{-1}$. For CH_4, Q = 20.85 T mg $CH_4\cdot m^{-2}\cdot d^{-1}$, since its millimolar mass is 16 mg $CH_4\cdot mmol^{-1}$.

In summary, for the equilibration experiments in Xingó the rate Q (mg $CO_2\cdot m^{-2}\cdot d^{-1}$) is obtained from the rate *T* (ppm/min), multiplying *T* by the factor 57.35.

The example used here results in:

$$Q = 4361 \text{ mg } CO_2\cdot m^{-2}\cdot d^{-1}$$

which value, derived from the samples, constitutes emissions of CO_2. The deviation *s* associated to this value was 0.56%.

The hypothesis that the speed of gaseous exchange between the water and the air contained in the chamber would be proportional to the difference of the respective concentrations, and that it results in the form of the function that describes the equilibration, was fully justified in the course of this research. The concentration of CO_2 (or methane) in the initial instant inside the chamber is identical to the concentration in the ambient air, and it is thus useful to examine the effect of wind, which affects concentrations in the air.

If there are constant emanations of gas from the water to the atmosphere, in the absence of winds, a layer of, for example, high CO_2 concentrations would be established over the water, and this would diffuse through the air to higher altitudes where the global average partial pressure prevails.

The turbulence established by the wind has two effects. "Pulses" of air with lower concentrations are brought to the water's surface, either from the shore or from higher altitudes, and thus in addition to diffusion, CO_2 has a second escape route from the lake –convection. Thus, in the presence of wind, a fluctuation in the concentration of CO_2 in the atmospheric air is established, which is shown when is brought into the laboratory as a sample of the "initial instant". Such a fluctuation explains the continual variability of the conditions of gaseous exchange between water and air, and doesn't lead to error, but rather to a more realistic analysis of the situation.

The aquatic environment provides a sink for dissolved CO_2, which is photosynthesis by phytoplankton. Photosynthesis converts CO_2 into organic compounds at a rate of, typically, 100–300 mg $C{\cdot}m^{-2}{\cdot}d^{-1}$, using rates found in the Broa reservoir as an example. But concomitantly with photosynthesis, respiration and methanogenesis liberate CO_2 throughout the food chain.

Depending on the relative activities of photosynthesis and the food chain there could be diffusion or absorption of atmospheric CO_2. During the night photosynthesis stops because of the lack of light, but respiration and methanogenesis continue. For this reason there should be an investigation of not only the daily rates of diffusive exchange of CO_2 but also the nocturnal. For the same reason, variations could be expected in the rates of diffusion as a function of the intensity of light, as conditions change between, for example, intense sun, fog, heavy clouds, etc.

Coexisting with these factors cited above, which tend to introduce seemingly chance fluctuations, is the content of CO_2 dissolved in the water and acting in the direction of stabilization. The water is a reservoir of dissolved CO_2. In relatively shallow water of around 30 m of depth, with a concen-

tration of (500 mol $CO_2 \cdot m^3$, there is ~1500 mol $CO_2 \cdot m^{-2}$, which is of an order of magnitude that primary production manages to consume in one day. In the atmospheric column with 360 ppm of CO_2, there is ~1000 mol $CO_2 \cdot m^{-2}$. The two values are of the same order of magnitude – the total mass of CO_2 resident in the atmosphere and the total mass dissolved in the shallow water that interact with each other in each square meter of contact surface.

Thus it should not be expected that one of these two reservoirs would dominate over the other, imposing a rigid constancy of concentrations. Rather, one should expect moderate fluctuations without drastic changes in CO_2 concentrations in the course of a day.

Over longer periods, it is possible that photosynthesis as well as gaseous exchange are always present, although with pulsating intensity, and the gaseous exchange is not capable of altering the concentrations quickly, since their effect would be moderated by the ballast of the two reservoirs.

For comparisons of two reservoirs, there is an additional method available to quantify the rate of gaseous exchange through the interface: if the concentrations of a gas in the water and in the air close to the interface were measured, and if the wind conditions were simultaneously evaluated, it is expected that there would be a good correlation of the set of these parameters with the rate of exchange. Such a procedure, because of its greater simplicity, would permit an increase in the number of sites sampled, within the available resources.

For a comparison between the results obtained with the dynamic chambers and static chambers, three series of measurements were obtained in the Tucuruí, Samuel and Itaipu reservoirs. The measurements at Tucuruí and Samuel suggest that the static chamber was underestimating the rates by approximately a factor of two.

The experiment at Itaipu was carried out with the air in the static chamber circulated by an external pump at a rate of de 1.5 $L \cdot min^{-1}$, between the pump with around 10 mL of volume and the 18 L chamber. The effect of pumping was only that of circulating the air within the chamber.

The pump was linked to the chamber by two tubes, one of which removed air from the chamber and the other returned it. The difference between the rates measured with the dynamic and static chambers were reduced significantly.

To reduce the effect of internal warming of the chamber, direct solar radiation was blocked in the chamber in the two reservoirs studied, by covering the chamber with a white woven fabric which blocked direct sunlight but allows diffused light to pass. It became clear that the static chamber was vulnerable to sunlight and temperature. Alternatively, covering the chamber with aluminum foil would block any light from entering, making

the internal environment of the chamber still more artificial, and possibly changing photosynthetic activity in the interior.

The ratio *C/G* compares the rates obtained using small and large chambers. A ration of 1 indicates agreement, which in fact was obtained when the air in the large chamber was circulating. With the variability of measurements reported, the average 1.0 of the ratio *C/G* is surprising.

Comparison of the performance of small and large chambers was carried out using the methane diffusion rates. Methane was chosen rater than carbon dioxide, because it is a simpler system. All the results obtained in the surveys reported here of diffusive exchange of methane have shown that there was only diffusion of this gas to the air and never absorption.

For carbon dioxide, there was both diffusion and absorption, with absorption occurring in almost half of the cases. Among the sources and sinks of carbon dioxide that exist in the surface layers of the water, there was sometimes dominance of one and sometimes of others.

The methane-water-air system, with the dominance of only diffusion, is less complicated than that of carbon dioxide, and it is thus more appropriate for the comparison of performance of the chambers.

Acknowledgements

We express our deepest gratitude to Eletrobras, Furnas, Itaipu and the Ministry of Science and Technology for financing work and discussing important points in this paper with us.

12 Long Term Greenhouse Gas Emissions from the Hydroelectric Reservoir of Petit Saut (French Guiana) and Potential Impacts

Robert Delmas, Sandrine Richard, Frédéric Guérin, Gwénaël Abril, Corinne Galy-Lacaux, Claire Delon and Alain Grégoire

Abstract

This paper summarizes, in a first part, results of greenhouse gas emissions from the hydroelectric reservoir of Petit Saut in French Guiana obtained during the three first years after impoundment (1994-1997). Results from three years of measurements have been extrapolated to estimate trends in methane emissions and the carbon budget of the reservoir over a 20-year period. Extrapolations were made using the global warming potential concept to calculate cumulative greenhouse gas emissions at a 100-year time horizon and to compare these emissions to potential emissions from thermal alternatives. In a second part, we analyze new data from long term continuous observations (1994-2003) of methane concentrations in the reservoir and flux data obtained during a recent campaign in May 2003. These data confirm predicted trends and show some suitable adjustments. They constitute a unique data base which is used for the development of a model to simulate both water quality and greenhouse gas emissions from tropical artificial reservoirs.

12.1 Introduction

Over the two last decades increasing concentrations of greenhouse gases (GHG) in the atmosphere contributing to an enhanced greenhouse effect have become a major environmental issue. The main contributor to this effect is, by far, fossil fuel combustion. Until recently, it was believed that

hydroelectric energy was a clean energy source compared to thermal energy production, with almost no impact on the greenhouse effect. The creation of artificial lakes modifies biosphere-atmosphere exchanges on a local scale. Carbon dioxide and methane are mostly produced from organic matter decomposition under anaerobic conditions, generating a source of greenhouse gases. From theoretical considerations Gagnon and Chamberland (1993), Svensson and Ericson (1993), and Rosa and Shaeffer (1994) suggested that artificial reservoirs could constitute an anthropogenic source of greenhouse gases. This was confirmed by the first flux measurements on boreal reservoirs (Kelly et al. 1994; Duchemin et al. 1995). More recently, Fearnside (1995) calculated that some tropical reservoirs may emit more greenhouse gases than thermal power plants of equivalent power output. Field measurements conducted on Petit Saut reservoir in French Guiana, since reservoir impoundment in 1994, confirmed that tropical reservoirs can be quite a significant source of both carbon dioxide (CO_2) and methane (CH_4) (Galy-Lacaux et al. 1997). Results presented in this last paper also highlighted the influence of methane produced within the reservoir on water quality showing that methane oxidation could be responsible for high oxygen depletion in the whole hydro system, including both the reservoir and the river downstream of the dam. A recent global scale assessment of GHG emissions from reservoirs (Saint-Louis et al. 2000), suggests that artificial reservoirs, whose total area is of the order of 1500000 km², could be a major anthropogenic source of methane representing 64 $MT \cdot y^{-1}$, 90% of emissions occurring from tropical latitudes. It is now recognized that artificial reservoirs are a GHG source, however, such global estimates are highly speculative since they rely on a very limited number of data sets. More work is clearly needed in order to better define the order of magnitude of this source and to compare it with emissions from other land surfaces, both natural (wetlands) and anthropogenic (rice paddy fields).

In this paper we first review results from the literature dealing with emission trends over 20 years from the Petit Saut reservoir (Galy-Lacaux et al. 1999). We then on a calculate, on a 100-year time scale, the net GHG emissions from this reservoir and compare the results with GHG emissions from thermal alternatives (Delmas et al. 2001). These results allow some preliminary conclusions to be drawn about hydroelectric energy and greenhouse gas emissions. The regular measurements of chemical parameters of the reservoir water column between 1997 and 2002 allow for the evaluation of the accuracy of the comparison between hydroelectric and thermal energy production. A new program was launched at the beginning of 2003 in order to reduce uncertainties pertaining to this question. This program includes new observations and modeling of which the first recent results are presented in the last section of this chapter.

12.2 Experimental Site and Campaigns

12.2.1 The Petit Saut Reservoir

Petit Saut is a hydroelectric dam, built by Electricité de France (EDF), in the tropical forest of French Guiana on the Sinnamary river, some 60 km upstream of its outlet to the Atlantic (5°03'N, 53°02'W) (Fig. 12.1) (Sissakian et al. 1997). Filling of the reservoir began in January 1994. The maximum depth of the reservoir (35 m) was reached in June 1995. This depth corresponds to the immersion of about 365 km² of primary forest with the creation of 105 km² of small islands (Huynh et al. 1996). The total amount of flooded biomass, including above-ground vegetation (170 T(C)/ha) and soil carbon (100 T(C)/ha) was around 10 million tons of carbon (Galy Lacaux et al. 1999). At maximum operating level the reservoir volume is close to 3500 million m^{-3} and the annual mean discharge of the Sinnamary river is 267 $m^3 \cdot s^{-1}$. The average turnover time is estimated to be about six months. At Petit Saut four turbines provide maximum power of 115 MW (mega Watts). For this dam the ratio between installed capacity and inundated area is therefore 0.32 MW·km² corresponding to about 11.5 MW per MT of carbon flooded. This ratio is two times less than the average ratio for hydroelectric reservoirs of the Amazon region (excluding Balbina dam in Brazil).

To solve the problems of deoxygenation observed in the downstream Sinnamary during the turbining tests, resulting from oxidation of methane generated in the reservoir, a two-falls aerating weir was built in the plant outlet canal (Gosse et al. 1997). Operational since March 1995, the weir allows the power station to function continuously while guaranteeing a minimum dissolved oxygen concentration of 2 $mg \cdot L^{-1}$ in the downstream Sinnamary and preserving fish life in the river. The weir resulted in a strong degassing of dissolved methane with close to 80% of dissolved methane in turbined water being released into the atmosphere at the weir level (Galy-Lacaux et al. 1997; see also Richard et al. Chap. 23). Such a system is specific to the Petit Saut reservoir and is not present in other hydroelectric dams in South America.

12.2.2 Measurements

Diffusive and bubbling fluxes of CH_4 and CO_2 at the reservoir surface, dissolved gas concentrations (CH_4, CO_2 and O_2) and profiles of physico-chemical characteristics in the water column (conductivity, pH, redox po-

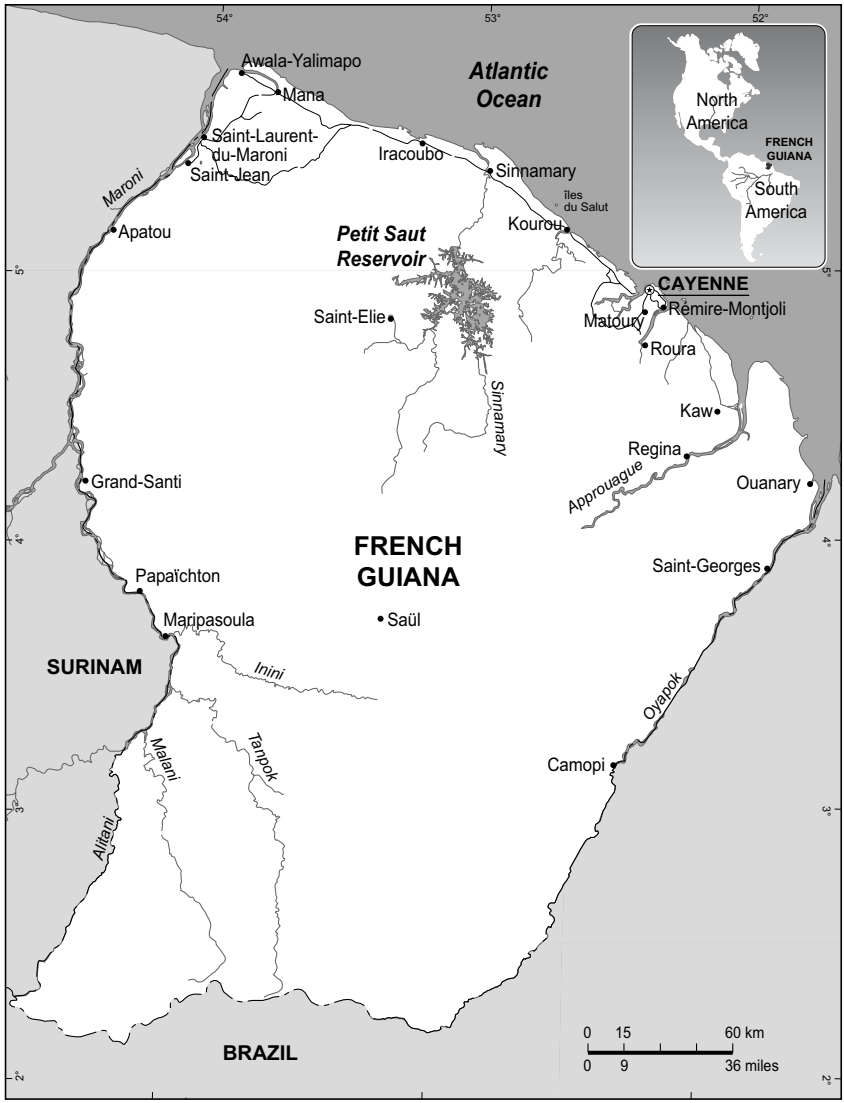

Fig. 12.1. Map of the Petit-Saut reservoir located in South America-French Guiana

tential and temperature) were measured during seven research campaigns carried out at Petit Saut between January 1994 and September 1997. An additional campaign was also conducted in 1995 on three reservoirs in the forested region of the southern Ivory Coast (Buyo, Taabo and Ayame), in order to investigate older reservoirs. Average characteristics of Petit Saut

(water flow and residence time, type of vegetation) correspond well with those of Buyo reservoir, which started to be filled 15 years earlier (Galylacaux et al. 1999; see also Chap. 23).

Diffusive fluxes (CH_4, CO_2) were measured using floating static chambers. Fluxes were calculated from the slope of the regression line of gas concentration in the chamber as a function of time (Delmas et al. 1992). Methane and carbon dioxide emission by bubbling were measured with a set of 12 inverted polyethylene funnels that only collect gas bubbles (Keller and Stallard, 1994). Degassing fluxes (CH_4, CO_2) induced by the aerating weir were determined using the average concentration of dissolved gas in the reservoir water column and the daily total water flow calculated from the EDF hydrological budget. Dissolved gas concentrations were measured by the headspace technique in samples taken at various depths (MacKay and Shiu, 1981). Analyses of gas concentrations were performed by gas chromatography using a flame ionization detector for CH_4 and a thermal conductivity detector for CO_2. Commercial standards of various concentrations adapted to the type of measurements were used for calibration. The reproducibility of the standards for each set of analysis was greater than 95%. In addition to dissolved CH_4 and CO_2 concentrations, probes were used to measure profiles of dissolved oxygen and other parameters (temperature, conductivity, redox potential) in the water column at each station of the reservoir.

In order to follow the long term evolution of parameters, vertical profiles of dissolved oxygen and methane concentrations were regularly measured once or twice a month at a station located on the reservoir axis, at 20 km from the dam since the beginning of 1998. An additional experiment was conducted in May 2003 to monitor trace gas fluxes and dissolved gas concentrations in the whole hydro-system 8 years after the filling of the reservoir.

12.3 Results

12.3.1 Observed and Predicted Emissions Over 20 Years

Concentrations and Emission Trends

The assessment of trends in emissions is based on the evolution of methane concentrations observed over three and half years after impoundment and on data collected in the Buyo reservoir in the Ivory Coast. These data suggest an expression for the time dependence of the average dissolved meth-

ane concentration in the reservoir water column, over 20 years after impoundment:

$$C(t) = [10.5 + 3.5 \cos(2\pi/12)t] \exp^{-0.015t} \quad (12.1)$$

where C(t) is dissolved methane concentration in $mg \cdot l^{-1}$ and t the time in months. The coefficient of decrease (0.015) is chosen to make the dissolved CH_4 concentration in Petit Saut reservoir, 17 years after impoundment, equal to the one measured at Buyo. The 10.5 and 3.5 mg L^{-1} amplitude coefficients were calculated by adjustment to the first three years of data taken at Petit Saut. The cosine function, with a periodicity of 12 months, describes the variations of dissolved CH_4 concentrations related to annual fluctuations of the Sinnamary water flow. Expression (12.1) is shown in Fig. 12.2, together with 1994 to 1996 data from Petit Saut. A similar expression was calculated to describe the evolution of dissolved CO_2, based on the relationship between CH_4 and CO_2 concentrations. The two parameters are linearly correlated with a regression coefficient r = 0.92, and a regression line expressed as:

$$(CO_2) = 6.11(CH_4)+22.5 \text{ (Galy-Lacaux et al. 1999)} \quad (12.2)$$

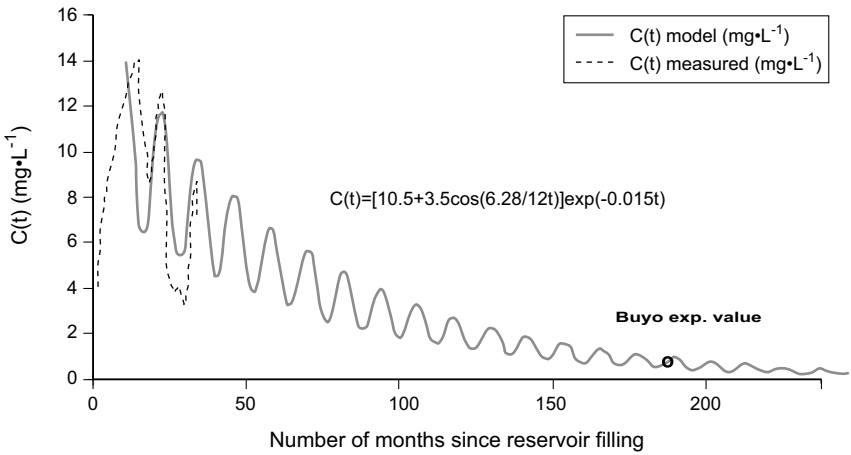

Fig. 12.2. Modeled Variations of dissolved CH_4 concentrations in the Petit Saut reservoir over a 20-year period based on the three first years of measurements and data from an older reservoir with similar characteristics, in Ivory Coast (Buyo)

Seasonal variations were shown to be linked to lake dynamics driven by rainfall variations (Galy Lacaux et al. 1999) according to the equation.

$$\frac{dC}{dt} = \frac{P - F - L}{V} - \frac{q_{in}.C}{V} \tag{12.3}$$

C is the concentration of dissolved methane. The term (P-F-L) represents the sum of vertical methane fluxes throughout the reservoir (production at sediment level, diffusion at the surface, and oxidation in the water column). If we assume that vertical methane fluxes (P-F-L) do not vary dramatically over time; then Eq. 12.3 shows that temporal variations of methane concentrations are primarily determined by the reservoir inflow (q_{in}). The term (q_{in}.C)/V introduces a dilution term directly proportional to q_{in} that explains most of the seasonal variations in the concentration of dissolved gases.

Greenhouse gas emissions from the Petit Saut reservoir result from three distinct processes: diffusion at the lake surface, bubbling in shallow zones (with water depth less than 10 m), and degassing of turbined water by the aerating weir.

Following a sharp increase immediately after the beginning of impoundment, the diffusive flux of methane at the lake surface dramatically decreased about one year later as a consequence of methanotrophic bacterial community development at the oxycline level. Bacteria were shown to be inhibited by light as long as the oxycline was very close to the surface (Dumestre et al. 1999). As a consequence the methane concentrations between the surface and the oxycline are depleted compared with those observed in the anoxic epilimnion. The diffusive flux was maximum (up to 3 $g{\cdot}m^{-2}{\cdot}d^{-1}$) within the first year of reservoir filling, then it rapidly decreased, due to methane oxidation at the oxycline level, down to values of the order of a few $mg{\cdot}m^{-2}{\cdot}d^{-1}$. To extrapolate diffusive emissions over a 20-year period, we assign a sharp decrease in emission rates after the second year and a flux equal to zero 5 years after impoundment. The emissions decrease from 35 Gg (CH_4) during the first year after impoundment to zero 5 years later (Fig. 12.2). Emission from gas bubbles is difficult to assess since measurements are only available for the first and the fourth year after impounding. In 1994, bubbling emission from the whole reservoir was estimated, from a limited data set, to be in the order of 120 $mg{\cdot}CH_4{\cdot}d^{-1}$. In 1997, based on a significant number of measurements, the same estimate provides a value a factor of 10 lower (12.7 $mg{\cdot}CH_4{\cdot}d^{-1}$). We do not have information on the long term evolution of methane emissions from gas bubbles by such reservoirs. However, results from the Ga-

tun Lake in Panama (Keller and Stallard, 1994) suggest that this type of emission may persist over time.

Emission from water degassing downstream of the dam is the most important term of the global methane flux from this hydrological system. About 80% of dissolved methane in evacuated water is emitted into the atmosphere by water degassing downstream of the dam. This emission has taken place since March 1995, when an aerating weir was built in the plant outlet canal in order to eliminate methane from the water and, therefore, prevent the oxygen consumption by methane oxidation in the river (P. Gosse 1994; P. Gosse et al. 1997). The remaining methane fraction is, for a major part, biologically oxidized along the river course (Galy-Lacaux et al. 1997; Richard et al. Chap. 23). Methane concentrations higher than 3000 ppm were measured in the air plume produced by the water fall. Compared with the two other emission mechanisms, gas emission from water degassing only depends on the average dissolved methane concentration in the water column and on the water outflow. The assessment of long term variations of emission from degassing is therefore easier to quantify. The variation in degassing flux over 20 years, shown in Fig. 12.3, is calculated from the analytical algorithm representing the evolution of dissolved methane concentration over 20 years and from a theoretical variation of the Sinnamary river flow. The water degassing flux is clearly dominant in overall methane emission from the reservoir. This is a typical feature of reservoirs in comparison with natural lakes or wetlands. In the particular case of the Petit Saut reservoir, this flux takes place in the near downstream of the dam, due to the presence of the artificial overflow weir

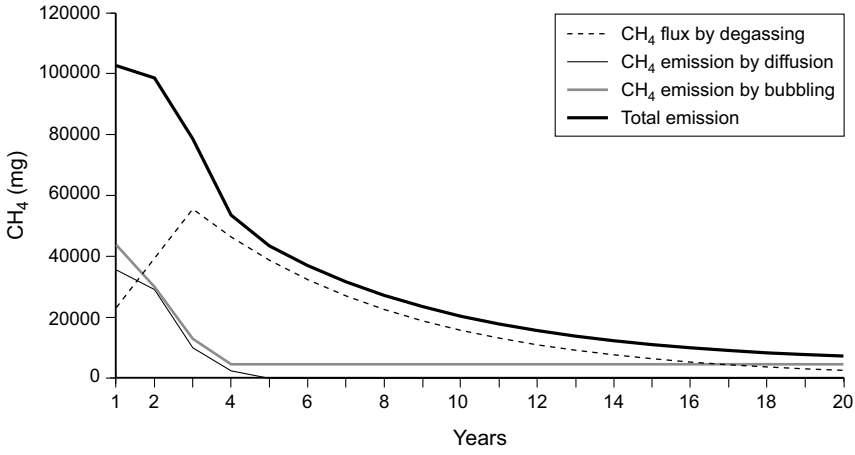

Fig. 12.3. Estimated methane emission trends, over a 20-year period, from the Petit Saut reservoir

(P. Gosse et al. 1997). Waterfalls can be naturally present in the river courses of others reservoirs, and the efficiency for water degassing and aeration can be different. However, according to our results, the contribution of the two other emission types, i.e diffusion and bubbling, is important during the first three years after impoundment. This results in maximum total emissions of more than 80 Gg (CH_4) y^{-1} for a reservoir of about 365 km^2 in which dense equatorial forest was flooded. The overall emission is reduced by a factor of 10 within a 20-year time frame; this figure is sustained by field measurements taken in similar old reservoirs.

The first estimate of carbon dioxide and methane emissions from the Petit Saut reservoir over a 20-year period relies on field measurements of the various fluxes taken at Petit Saut, and on extrapolations based on the temporal pattern of average dissolved methane concentrations established from Petit Saut and Ivory Coast data an on the relationship between methane and carbon dioxide. Diffusive and bubbling fluxes were measured during experimental campaigns at Petit Saut. CO_2 diffusive flux increased to up to 5 $g{\cdot}CO_2{\cdot}m^{-2}{\cdot}d^{-1}$ after impoundment at the beginning of 1995 and then it showed seasonal variations related to dissolved gas concentrations driven by the lake dynamics. This flux did not display the same decrease as methane flux since CO_2 is not consumed by bacteria but only by photosynthesis in the euphotic layer. Profiles of dissolved CO_2 concentrations do not show any dramatic decrease in the surface layer as was the case in the CH_4 profiles. However, the net emission into the atmosphere depends directly on the difference in partial pressure between the water surface layer and the atmosphere and wind stress, and is obviously affected by concentration changes in water. Because of the limited set of measurements of CO_2 compared to CH_4, the long term evolution of average CO_2 concentration in water is deduced from the methane as the two parameters are linearly correlated with a regression coefficient $r = 0.92$ (see Eq. 12.2).

Two types of results were derived from the above considerations: a carbon balance of the reservoir 20 years after reservoir filling (Table 12.1) and a comparison between greenhouse gas emissions from the reservoir and from thermal alternatives.

Carbon Budget of the Reservoir

The carbon losses from the reservoir in the form of both CO_2 and CH_4 over 20 years are dominated by the outlet flux of dissolved gases (2160 ± 400 Gg (C)). The diffusive emission at the lake surface represents 1300 ± 300 Gg (C), whereas emission of gas bubbles is much less important (130 ± 35 Gg (C)). The inlet flux of dissolved CO_2 (440 ± 90 Gg (C)) must

Table 12.1. Carbon balance of the hydroelectric reservoir of Petit Saut 20 years after reservoir filling

Type of emission	CH_4 Gg CH_4	CO_2 Gg CO_2	Released carbon $\Sigma C = C\text{-}CH_4 + C\text{-}CO_2$ Gg C
Emission by diffusion	77 ± 10	4700 ± 1000	1300 ± 300
Emission by bubbling	166 ± 46	75 ± 15	145 ± 40
Outlet flux	450 ± 170	6500 ± 1000	2160 ± 400
Inlet flux	0	-1600 ± 340	-440 ± 90
Total	693 ± 226	9675 ± 2300	3200 ± 800

be deduced from the loss terms. The total carbon loss from the reservoir over 20 years, in the form of volatile carbonaceous species is estimated to be 3.2 Tg (C). We estimated the carbon pool from the total amount of organic matter submitted to decomposition in the Petit Saut reservoir to be 270 Mg(C) ha^{-1}, that is about 10 Tg (C) for the entire reservoir. The carbon loss calculated is about one third of the initial carbon pool and represents certainly the main part of the biodegradable fraction of the submerged organic matter. The remaining part corresponds to the lignin-containing fraction of tree trunks, big branches and roots which decomposes over tens to hundreds of years in anaerobic conditions (Junk & Nunes de Mello, 1987).

Comparison of GHG Emissions from the Reservoir and from Thermal Alternatives

The data base obtained from the measurements taken between 1994 and 1999 at Petit Saut was used to estimate the long term impact of a tropical reservoir on the additional greenhouse effect in comparison with thermal alternatives for electric energy production. Temporal variations of greenhouse gas emissions from the Petit Saut reservoir were estimated over a 100-year period. These emissions were calculated in equivalent CO_2 using the concept of GWP (Global Warming potential) as detailed in Delmas et al. (2001). These emissions are highest in the three first years after impoundment and then decrease exponentially following the Eq. 12.1 representing the time evolution of dissolved methane concentration in the reservoir. Cumulated emissions at the end of the period reach 42.3 MT CO_{2eq}.

To calculate greenhouse gas emissions from equivalent (115 MW) thermal power plants, we used emissions factors of three greenhouse gases (CO_2, CH_4, N_2O) for oil, coal and natural gas combustion. Calculations are made over a period of 100 years with a methane GWP varying with time and with a constant GWP value (290) for N_2O. Emissions are dominated by CO_2 for the three plant types, although significant contributions of ni-

trous oxide (12%) for coal combustion, and of methane (24%) for gas combustion are observed. As expected, the gas power plant (64.3 MT CO_{2eq}) appears to be the 'cleanest' in terms of greenhouse effect in comparison with oil (77.4) and coal (98.2) plants. The comparison between reservoir and thermal power plants is shown on Fig. 12.5. At 100 years, GHG emissions from the reservoir appear to be less than those of either type of thermal alternatives. The figure shows that, due to high emissions following impoundment, the reservoir is a greater emitter in the three first decades, and a smaller one during the last decades, as reservoir emissions decrease. According to these curves, the equivalence between the hydroelectric reservoir of Petit Saut and thermal power plants would occur after 25 years for coal, 35 years for oil, and 57 years for gas plants. Although uncertainties in these calculations are very large our results show that, in spite of a low ratio between energy produced and flooded area, GHG emissions from the Petit Saut reservoir after 100 years, are lower, but of the same order of magnitude as emissions from equivalent thermal alternatives.

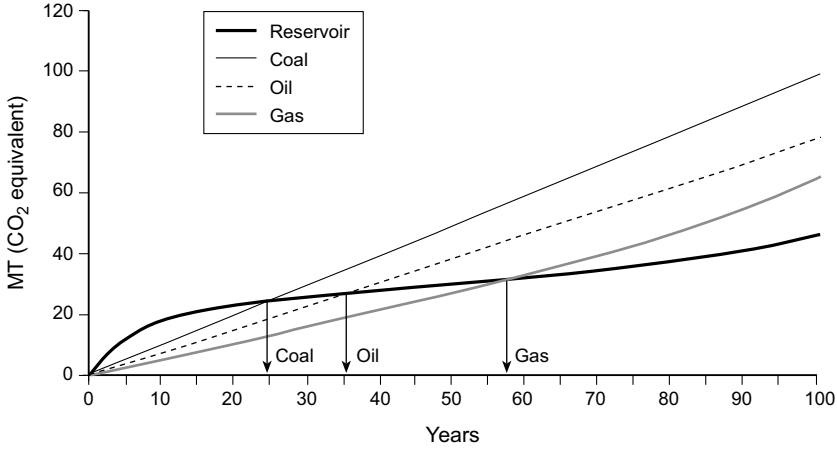

Fig. 12.4. Comparison of cumulative GHG emission at a 100-year time-scale, from the Petit Saut reservoir and of emission from equivalent (115 MW) thermal power plants (coal, oil, and gas)

Gross GHG emissions from the reservoir over its expected lifetime (100 years), are estimated at 42.3 MT ($CO_{2\ eq}$) (Fig. 12.5). After 20 years, the emission trend adopted (constant and rather low emissions) is not sustained by observations and is thus subject to large uncertainties. Net reservoir GHG emission calculations that take into account natural emissions from soil and vegetation suppressed after impoundment (6.2-18.1 MT) will

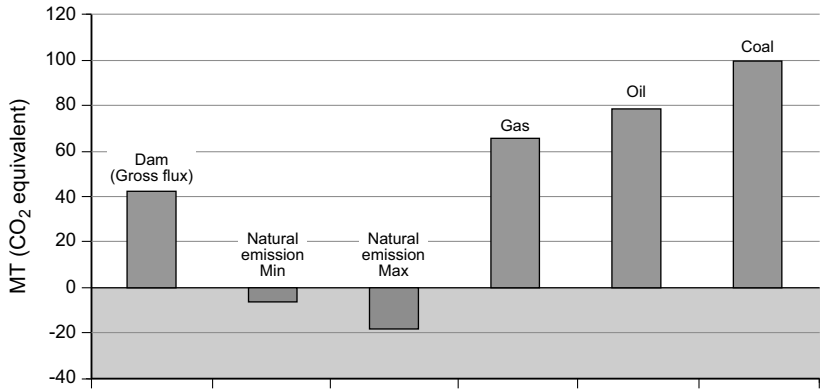

Fig. 12.5. Comparison of greenhouse gas emissions on a 100-year time-scale of Petit Saut reservoir of natural emissions from soils and of emissions from thermal alternatives

thus range between 24-36 of CO_{2eq} with an average value of 30 MT of CO_{2eq}. However, it is assumed that, when comparisons between dam and thermal power plants are made dam energy production over the 100-year period is always highest corresponding to the nominal power of the station (115 MW). The installed capacity of a dam represents what would be generated if all turbines were operated year-round, during about 8700 h, with a maximum water level of the reservoir (35 m), and in the absence of the aerating weir. This would represent an energy production of about 1 TWh per year. Energy production under real conditions of functioning is regulated by energy demand and reservoir capability. However greenhouse gas emissions from the reservoir remains the same whatever the level of energy production, while emissions from thermal power plants follow its variations. If we assume that, on average over a long period, the energy production from the dam only corresponds to 50% of the installed capacity, this would reduce the emissions from corresponding thermal alternatives by a factor of two. The comparison between dam and thermal power plants must be based on net greenhouse gas emissions from the reservoir which are about 30 MT CO_{2eq}. With this figure, the average greenhouse gas emissions in equivalent CO_2 over a 100-year period are 0.60 kg/kWh for the dam, 0.77, 0.98, and 0.64 kg/kWh for oil, coal and gas power plants respectively.

In spite of large uncertainties linked to the extrapolations of emission trends over a 100-year period, it seems that a reservoir such as Petit Saut, where the ratio between installed capacity and inundated area is low, is equivalent or better in terms of greenhouse gas emissions than any thermal

alternatives. Over a 100-year period GHG emission from the dam is estimated to be approximately the same as emission from a gas power plant and may be less than emissions from oil and coal plants.

12.3.3 Long Term Data and Recent Flux Measurements

Results presented in the previous sections have already been published (Delmas et al. 2001; Galy-Lacaux et al. 1997, 1999). In this section we examine new results of long term observations of methane profiles measured on a monthly basis between 1994 and 2003. We also use data from an experiment conducted in May 2003 to evaluate the fate of gas fluxes throughout the whole hydro-system, from the river upstream of the reservoir to the Sinnamary river mouth in the Atlantic, eight years after reservoir filling. These new data allow some comparisons to be made with predicted emissions previously published (Delmas et al. 2001).

Changes in average methane concentrations in the water column and of water residence time in the reservoir from 1995 to 2003 are shown on Fig. 12.6a along with the modeled variations published several years earlier. The comparison between modeled and experimental concentrations shows that the expression correctly reproduces the mean trend. Seasonal variations are however underestimated. The decrease of methane in the reservoir is due to a reduction of the available biodegradable carbon pool initially immerged, while seasonal variations are linked to reservoir dynamics since water residence time is governed by rainfall pattern and water resource management as explained in Sect. 12.3.1. The water residence time is simply calculated on a monthly basis as the ratio of the reservoir volume to the outflow. This figure confirms the interpretation presented in Sect. 12.3.1: an increase in the water outflow leads to a decrease in the residence time and is followed, within a month, by a decrease in methane concentration. The delayed correlation between water residence time and methane concentration is maximum ($r = 0.48$) for $dt = 1$ month (Fig. 12.6b). This occurs during the rainy season with significant differences from year to year according to rainfall variations; the sinusoidal variation is clearly a rough approximation of the reality, however, the methane trend over the 8 years of measurements is close to the modeled trend. Furthermore, it was shown in Richard et al. (Chap. 23) that using the sinusoidal function gives rather acceptable results for the methane fluxes from the dam with adequate values of monthly flow discharges. This sustains our previous extrapolation trends based on the modeled trend. However, the comparison between modeled and experimental concentrations of methane and flow discharges within the reservoir and at its outlet allows a

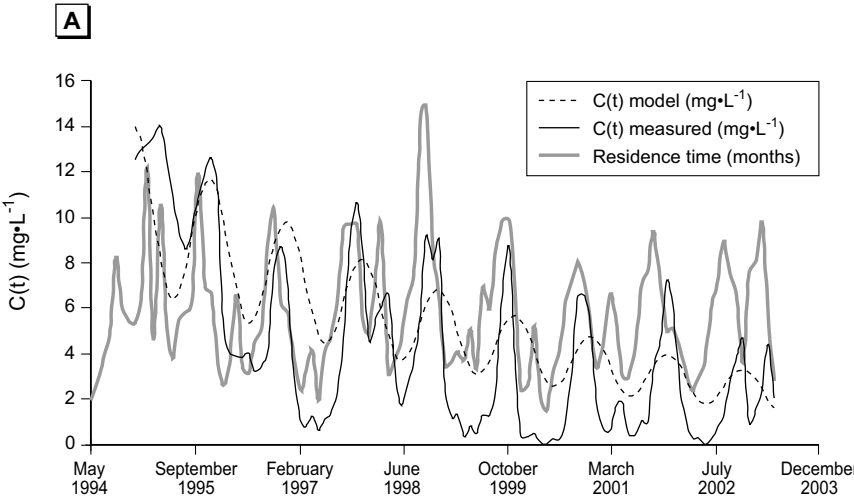

Fig. 12.6a. Evolutions of average methane concentrations in the water column and of water residence time in the reservoir calculated from the daily hydrologic budget of the reservoir, from 1995 to 2003, and comparison with model simulation

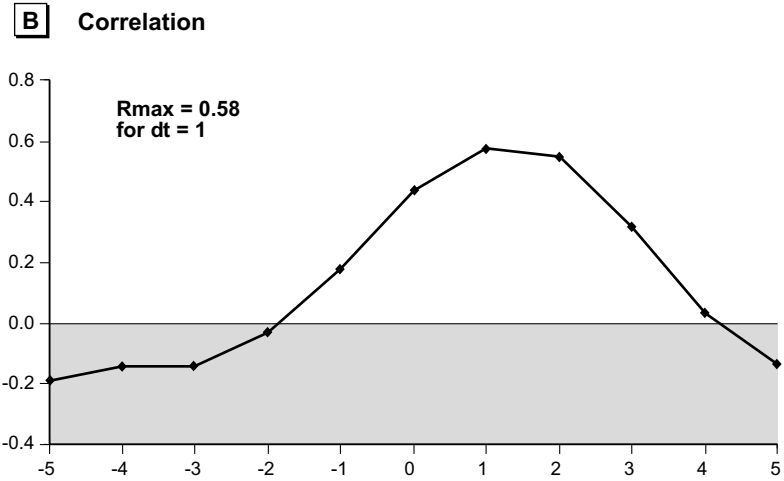

Fig. 12.6b. Delayed correlation between methane concentration and water residence time within the reservoir

more quantitative assessment of the three most important terms of the calculated carbon budget of the reservoir over 20 years (Table 12.1). These terms are the emissions of CH_4 and CO_2 by degassing at the dam outlet and the CO_2 emission by diffusion at the lake surface. Richard et al. (Chap. 22) showed that downstream emissions of CH_4 over the first 9 years were pre-

viously overestimated by probably one third in the previous long term GHG forecasts, due to the representativity of the sinusoidal function and a too schematic yearly profile of flow discharges. Although the CO_2/CH_4 ratio in the turbined water has become lower than previously selected (see Chap. 22), there should not be an overestimation of more than 30% for the previous forecasts of downstream CO_2 emissions, as the May 2003 campaign reveals that in the downstream Sinnamary, there is a high level of CO_2 emissions to the atmosphere which can be linked to the degradation of non volatile compounds released by the dam. As the downstream GHG fluxes are dominant in the budget, it means that previously calculated greenhouse gas emissions from the reservoir over 100 years might be some 20% lower than previously assessed. However, it appears that the CO_2 emission by diffusion at the lake surface might have been underestimated as it was still high in 2003.

Flux data obtained in May 2003, and shown in Table 12.2, confirm that diffusive methane emissions at the surface are quite low (less than 100 mg $CH_4 \cdot m^{-2} \cdot d^{-1}$) while CO_2 fluxes remain significant (around 5000 $mg \cdot m^{-2} \cdot d^{-1}$). Flooded forest sites emit twice as much CH_4 as sites located on the Sinnamary river bed. Surface wind has a strong influence on diffusive flux to the atmosphere, fluxes increase by a factor of 2 for wind speeds greater than 3 $m \cdot s^{-1}$. On the upstream river, CH_4 fluxes are very low (6 $mg \cdot CH_4 \cdot m^{-2} \cdot d^{-1}$) whereas CO_2 fluxes are two to three times higher than on the lake (4522 on the lake and 13000 $mg \cdot CO_2 \cdot m^{-2} \cdot d^{-1}$ on the upstream river). Downstream of the dam (< 50 km), fluxes are enhanced by a factor of 9 to 10 for both gases. N_2O fluxes remain constant in the whole system. We must note that chamber measurements on a water surface may underestimate diffusive emissions during high wind periods, because of the exclusion of natural turbulence at the air-water interface within the chamber, however, the turbulence in the water surface layer is little affected by the chamber (Kremer et al. 2003). This effect on average fluxes is difficult to quantify, since wind is generally very low except in the afternoon when thermal effects generate surface winds with velocity up to 8 $m \cdot s^{-1}$. In addition rainfall also affects surface layer turbulence (by dissipation of rain drop kinetic energy) and, therefore, air-water gas exchanges (Ho et al. 1997). Flux measurements in the downstream section of the Sinnamary river confirm that gas release downstream of the dam remains an important source of GHG, at least for methane.

Table 12.2. Results of Greenhouse gas flux measurements on the Petit Saut reservoir and the Sinnamary river in May 2003 (Courtesy from Louis Varflavy and Alain Tremblay, Hydro-Québec

Sites	Flux CH_4 Mean, (σ), n [mg m^{-2}·day^{-1}]			Flux N_2O Mean, (σ), n [mg m^{-2}·day^{-1}]			Flux CO_2 Mean, (σ), n [mg m^{-2}·day^{-1}]		
A. Petit Saut Reservoir									
All sites	87	(29)	53	3.7	(2.1)	53	4522	(1238)	83
Flooded forest sites	121	(28)	20	3.7	(1.9)	20	5302	(1060)	28
Sites on Sinnamary river bed	66	(29)	33	3.7	(2.3)	33	4125	(3334)	5
Sites with average wind speed< 3 m/s	34	(10)	36	3.2	(2.2)	36	2943	(820)	57
Sites with average wind speed > 3 m/s	199	(68)	17	3.9	(2.1)	17	7985	(2157)	26
B. Synnamary River									
Upstream the reservoir	6	(2)	2	3.2	(2.6)	2	13000	(459)	2
Downstream the Dam (< 50 km)	948	(264)	12	4.4	(2.3)	12	44140	(17030)	21
Downstream the Dam (> 50 km)	9	(8)	8	4.1	(2.2)	8	38020	(18835)	11
Estuary	2	(3)	4	3.8	(0.6)	4	16625	(10350)	5

Table 12.3 shows the carbon balance of the whole system in May 2003 including inlet fluxes of CO_2 and particulate (POC) and dissolved (DOC) organic carbon. The lake surface remains the main source of carbon to the atmosphere due to CO_2 fluxes from the water body (450 T(C)·d^{-1}). Methane emissions by diffusion from the lake surface (24 T(C)·d^{-1}) are almost the same as emissions occurring downstream of the dam including degassing at the aerating weir level and diffusion to the atmosphere along the river. Atmospheric concentrations greater than 1000 ppm were observed in the plume downwind of the aerating weir. We must note that at present, the weir is less efficient for degassing since it was lowered from 5 to 2 m height (65% now versus 80% when it was 5 m high). The total outlet flux of C from the reservoir to the atmosphere and the ocean remains, 10 years after impoundment, at least 4 times higher than the inlet flux of C from the river to the lake, since bubbling flux is missing. The inlet flux of carbon into the reservoir in this period of high waters is 153±31 T(C)·d^{-1} while the total outlet flux is 709±175 T(C)·d^{-1}. This means that the reservoir is still a net source of carbon to the atmosphere. Without the dam, for an equivalent river length (120 km length and 100 m width), transfer of C to the atmosphere would be around 50 t(C)·d^{-1}. That implies that the initial pool

Table 12.3. Carbon balance of the whole system (Upstream river, Lake and downstream river) during the May 2003 campaign (high waters). Note that the bubbling flux is missing in this balance. A rough estimate based on a few measurements give 3.67 ± 0.15 t (C)·d^{-1}

		Nature	T(C)/d	Total T(C)·d^{-1}	
				Average T(C)·d^{-1}	σ
Inlet flux[2]		TOC[1]	149	153	31
		CO_2[1]	4		
		CH_4	<0,1		
Outlet flux[3]	Diffusive flux from the lake surface	CO_2	450	474	131
		CH_4	24		
	Degasing on the weir	CO_2(40%)	46	62	6
		CH_4(65%)	15		
	Diffusive flux from the downstream river	CO_2	60	64	24
		CH_4	4		
	Export to the estuary	CO_2	40	109	14
		CH_4	1		
		TOC	54		
	Total			709	75

[1] Data from Richard & Horeau (1996) and Galy-Lacaux (1996)
[2] Mean river discharge = 265 m^3·s^{-1}
[3] Mean turbined water discharge = 125 m^3·s^{-1}

of C is still decomposing and participating in the flux to the atmosphere. Fluxes along the river course downstream of the dam are especially high since the water released through the turbines comes from the hypolimnion were CO_2 concentrations are enriched by diffusion from the sediment and organic matter degradation in the anoxic hypolimnion and at the oxic-anoxic interface. Downstream of the dam, the decomposition of organic matter is enhanced, therefore, a net carbon flux from the Sinnamary river catchments (7000 km^2 from the source to the ocean) to the coastal ocean is observed.

12.4 Conclusion and Perspective

It is now recognized that hydroelectric reservoirs, and more generally all types of artificial reservoirs, are sources of greenhouse gases. Emissions are dominated by CO_2 at boreal and probably at temperate latitudes, whereas, at tropical latitudes, methane emission becomes significant.

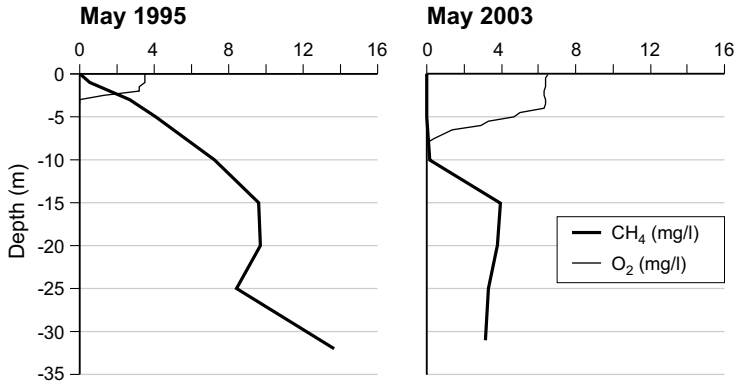

Fig. 12.7. Examples of observed evolution of dissolved methane and oxygen profiles in the water column of the Petit Saut reservoir in May 1995 and May 2003

Concerning artificial reservoirs as a whole, a question remains open: what is the magnitude (even the order of magnitude) of the corresponding methane source? In addition, for any new construction project of a hydroelectric dam it is now necessary to predict more precisely the potential greenhouse gas production to correctly assess the carbon credits linked to the project. It is no longer believed that hydroelectricity is a clean energy, especially in the tropical regions where energy demand is rapidly increasing and potential sites for dam construction are still numerous. However, we should keep in mind that a case by case comparison is necessary since many tropical reservoirs emit very low GHG amounts (Tremblay and Lambert, 2004).

12.4.1 Future Initiatives

As it is not possible to carry out field studies everywhere in the world, we decided to start in 2003 a new program based on the development of a reservoir model including the hydrodynamic functioning and the carbon cycle. The model is schematically represented in Fig. 12.8. It will rely first on a 2D finite differences hydrodynamic model with atmospheric and hydrological forcing. This model called SYMPHONIE was developed for coastal oceanography applications and it is adapted to the reservoir, for more details see: Estournel et al. 2001; Auclair et al. 2001. Biogeochemical modules will be coupled to this model; they will describe the potential capacity of the initial stock of organic matter (soil, above ground vegetation, trunks) sequestered during the reservoir filling and of the organic

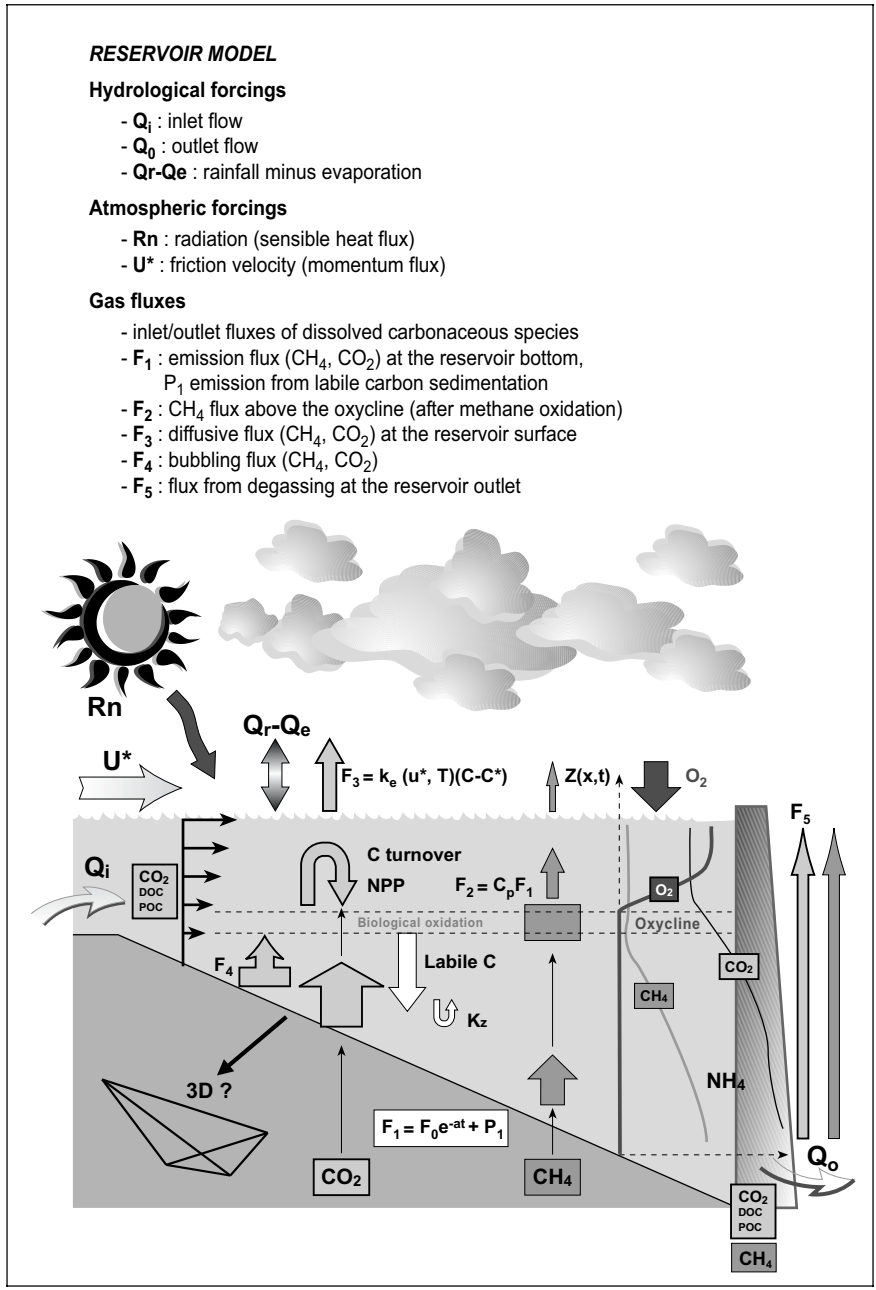

Fig. 12.8. Schematic representation of a 2D reservoir model to simulate greenhouse gas emissions from a tropical reservoir

matter (POC, DOC) coming from the river catchments to produce carbon dioxide and methane. The methanogenic activity is determined by anoxic incubations. CH_4 and CO_2 produced by organic matter degradation in sediments (flooded forest, autochthonous and allochthonous organic matter) diffuse in the water column (Kz: turbulent diffusivity and F_1: molecular diffusion). If methane concentrations are above methane solubility, CH_4 is emitted directly in the atmosphere by bubbling in low deep regions of the lake (F_4). Carbon dioxide and methane produced in the lake sustain a carbon turn-over including sedimentation of labile C via photosynthesis (Net Primary Production, NPP) and bacterial production (e.g.: methanotrophic activity). The methanotrophic activity will be parameterized thanks to laboratory experiment of methane oxidation. Oxidation rates are determined in laboratory experiments at variable methane concentrations on water samples taken from different depth (oxic epilimnion and oxic-anoxic interface) in order to calculate Kinetics parameters (Michaëlis-Menten). Oxygen necessary for methane oxidation is produced in the lake by photosynthesis or comes from exchanges with atmosphere. The remaining CH_4 and the additional CO_2 can reach the sub-surface (F_2). Gas transfer at the air-water interface (F_3) will be parameterized taking into account surface concentrations and wind speed at 10 m above the lake surface. Water containing DOC, POC, CO_2 and CH_4 reach the estuary passing through turbines. The turbulence induced by the two-fall weir allow a large degassing of methane (65%) and carbon dioxide (40%) to the atmosphere (F_5).

In a second step, these modules will be coupled to a 3D finite volume model in order to represent seasonal drawdown and subsequent changes in emissions from the reservoir. A series of new field campaigns is planned in order to derive appropriate parameterizations for modeling and establish the carbon balance of the reservoir 10 years after impoundment.

Acknowledgments

We are pleased to thank Philippe Gosse (EDF) for disclosing, calculating and writing the main differences between the CH_4 and CO_2 fluxes downstream of dam over the first 9 years and those previously forecast. Many thank also to Louis Varfalvy and Alain Tremblay (Hydro-Québec) for providing us the complete set of GHG flux measurement taken at Petit Saut during our last campaign in May 2003.

Processes leading to GHG Production

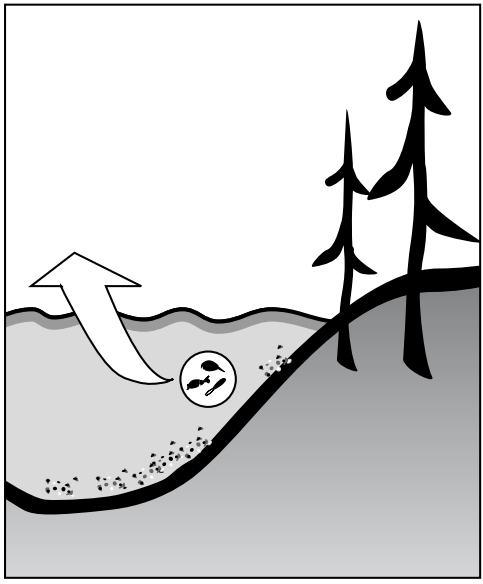

13 Production of GHG from the Decomposition of *in vitro* Inundated Phytomass and Soil

Normand Thérien and Ken Morrison

Abstract

A set of experiments was designed to measure the production of carbon dioxide and methane during decomposition of inundated samples of representative vegetation and soil samples originating from the James Bay territory over a period of approximately one year. Controlled laboratory conditions were set for water temperature (4-22°C), pH (4.5-7.0) and dissolved oxygen concentration (< 2 mg·L^{-1} and > 2 mg·L^{-1}). These conditions covered the range of conditions under which vegetation and soil are submitted during permanent flooding in newly created hydroelectric reservoirs. Representative phytomass samples consisted of spruce needles (*Picea mariana sp.*), alder leaves (*Alnus sp.*), lichen (*Cladonia sp.*), green moss (*Pleurosium sp.*) and herbaceous plants (mixed species). Representative forest soil samples consisted of lichen (*Cladonia sp.*) humus and green mosses (*Pleurosium sp.*) humus with Sphagnum moss (*Sphagnum sp.*) used as a representative ground component (phytomass) for wetlands. Production of carbon dioxide over time was observed from all samples under the given experimental conditions. The quantities of carbon dioxide produced from the vegetation samples were largest under oxic conditions at the higher temperature. The average cumulative quantities produced over 345 days ranged from 201 mg CO_2·g^{-1} (dry weight) to 447 mg CO_2·g^{-1} (dry weight) with the largest quantities produced from green moss. For the soil samples, the largest quantities of carbon dioxide produced occurred also at the higher temperature but were 15–40% larger under anoxic conditions. Under such conditions, the average cumulative quantities produced over 320 days from lichen humus and green moss humus were 72 g CO_2·m^{-2} and 140 g CO_2·m^{-2} respectively. Small quantities of methane were produced from the soil samples but only under the most favourable temperature and pH conditions and were higher under anoxic conditions.

pH conditions and were higher under anoxic conditions. Under such conditions, the average cumulative quantities of methane produced over 320 days from lichen humus and green moss humus were 0.21 g $CH_4 \cdot m^{-2}$ and 0.56 g $CH_4 \cdot m^{-2}$ respectively. Production of methane from vegetation samples was significant only for the higher temperature under anoxic conditions. Under such conditions, the average cumulative quantities produced over 345 days were largest for green moss with a value of 1.72 mg $CH_4 \cdot g^{-1}$ (dry weight). Results have shown that, under the most favourable conditions for decomposition, the production of carbon dioxide and methane from inundated phytomass and humus soil samples was still very active after 345 and 320 days respectively. Rates of production of CO_2 and CH_4 calculated from the cumulative quantities released from the flooded vegetation and soil samples under the given experimental conditions represent a reference data set from which production of CO_2 and CH_4 emitted from reservoirs under field conditions can be estimated (Thérien and Morisson, Chap. 25).

13.1 Introduction

The creation of hydroelectric reservoirs implies the flooding of vast areas of land. For example, reservoirs of Phase I of the La Grande River hydroelectric complex in northern Quebec cover an area of 11400 km^2 out of which 9700 km^2 are submerged lands. In such undertakings, considerable amounts of vegetation and large areas of soils are covered with water and various dissolved and particulate organic and inorganic materials are released to the water column over time through leaching, decomposition and mechanical attrition (Morrison and Thérien 1991). These releases start immediately upon the flooding of vegetation and soils and continue as the more labile components decompose with time. The magnitude of the releases is generally a function of the environmental conditions existing during flooding but also after the reservoir is completely filled (Thérien et al. 1982). The amounts of material being released are a function of the area of the lands covered by water and therefore varies with the water level in the drawdown zone of a reservoir. Water quality is impacted in several ways. Leaves and needles of trees and shrubs, herbaceous plants, ground covering mosses and the more labile components of the soil decompose. This process consumes important quantities of oxygen that may lead to anoxic conditions. Carbon dioxide and methane are the end products of this process (Duchemin and Lucotte 1995). Furthermore, as a result of leaching and decomposition of the submerged phytomass and inundated soils, nutrients

that stimulate primary productivity such as inorganic nitrogen and inorganic phosphorous compounds are produced. Also, metals contained in the vegetation and soils, such as lead and mercury, can be released and transformed in the water column (Morrison and Thérien 1992; Grondin et al. 1995) promoting, for example, bioaccumulation of mercury in fish (Brouard et al. 1990) and other aquatic components (Genivar 1995).

In general, the quantities of materials released in the water column of the reservoir are a function of the nature of the vegetation substrates and the types of soil being flooded. The concentration of materials in the water is generally a function of the flushing rate and the dilution processes occurring within the reservoir. It also depends on the history of the environmental conditions the reservoir has been submitted to since flooding (Thérien et Morrison 1995a; Morrison and Thérien 1995). As a consequence, concentration levels of materials in water obtained from in situ measurements would reflect a combination of the environmental conditions (temperature, pH, dissolved oxygen, etc.) and of the hydrologic processes having acted since flooding occurred. The end result is that positive identification of the controlling variables becomes more than often untraceable. Also, specific contributions from distinct vegetation substrates and types of soil are not discernable. These observations are the main reasons why, in order to assess the distinct effects of the many factors acting on the water quality during the creation of reservoirs, early studies had focussed on designing experiments that used microcosms to follow the time evolution of the water quality variables of interest (Maystrenko and Denisova 1972). These microcosms generally consisted of representative vegetation and soil samples originating from the territory targeted for flooding that were inundated and submitted to controlled environmental conditions. Unfortunately, because of the specific nature of the samples used in these studies, the observed results were not always applicable to other territorial settings. In many instances, the set of environmental conditions were not known or fully controlled. Also, in some cases, the integrity of the original samples used during the experiment was not conserved (i.e. initial shredding of the vegetation samples). In other situations, the samples were not submitted to environmental conditions that were representative or reflected the complete spectrum of environmental conditions that would exist in a newly created reservoir. These observations are the main reasons for which two sets of distinct in vitro experiments were carried out in this work. They were undertaken in order to measure the quantities of materials released in water from selected inundated vegetation samples and soil samples respectively (Thérien and Morrison 1995a, 1995b). These experiments were designed to use samples of vegetation and soil more specifically representative of northern Quebec. They were also designed to

use the representative spectrum of environmental conditions to be found in newly created reservoirs. Measurements of several inorganic and organic compounds released in water as a function of time were done including mercury and the production of carbon dioxide and methane. Results pertaining to the release of soluble inorganic and organic carbon, nitrogen, phosphorous and mercury compounds in water have already been reported (Morrison and Thérien 1994, 1996). Unpublished results pertaining to carbon dioxide and methane are presented here.

13.2 Methodology

The experimental protocol was developed by N. Therien of Université de Sherbrooke and accepted by A. Chamberland and R. Schetagne of Hydro-Québec.

13.2.1 Field Site and Sample Collection

Samples of typical vegetation and soil as well as river water were collected from unperturbed areas in the vicinity of the LG-4 development on La Grande Rivière in Quebec, Canada (54°N 73°W). Species were selected on the basis of dominance, and are thus representative of vegetation and soil in the region.

Vegetation Samples

Vegetation samples consisted of foliage from coniferous trees, foliage from deciduous trees, herbaceous plants, ground covering mosses of forest soil and ground vegetation of wetlands. The tree species selected were black spruce (*Picea mariana*) and alder (*Alnus sp*). Ground covering vegetation samples for forest soil consisted of lichen (*Cladonia sp*) and green moss (*Pleurozium sp.*). Ground vegetation samples selected for wetlands were sphagnum moss (*Sphagnum sp.*). Herbaceous plants were not selected on the basis of species but rather as a composite sample of representative non-ligneous plants. Tree foliage, herbaceous plants and forest soil moss samples were kept frozen until use, while sphagnum moss samples were maintained at 4°C until use. River water collected in the fall was kept at ambient indoor temperatures until its use the months that followed.

Soil Samples

Two types of spruce forest soils were selected; the first being soil covered by lichen and the second, soil covered by green moss. In both cases, the vegetation ground cover (lichen and moss) was carefully removed in preparation for soil sampling. A 300 mm diameter x 150 mm height open-end metallic cylindrical canister was then pushed down with a gentle rotation movement on the soil surface (the thin rim cutting through the organic matter). The whole assembly (cylinder with the soil within) was then removed from the surrounding soil carefully removing any excess material to provide a neat cylindrical sample of soil having a height of 150 mm. These samples held the top organic horizon of soil (humus) which sat on top of mineral soil. The thickness of the organic horizon was often less than 150 mm, especially for lichen humus. The samples were kept frozen until use.

13.2.2 Experimental Setup

Soil samples were transferred into 300 mm diameter x 300 mm height cylindrical quartz 22 L containers. Vegetation samples were placed in Teflon TFE mesh baskets, and each basket was placed in a given container. Each basket held 100 g (wet weight) of material except for alder leaves and sphagnum moss for which the baskets held 50 g and 200 g respectively. In each case, the samples were covered with river water leaving an air space above the water. Each container was sealed with a glass cover to prevent any loss of gas. Through a hole in each cover was a Teflon TFE fitting through which passed Teflon TFE tubes for water addition-withdrawal, Teflon FEP tubes for gas entry and exit as well as a very fine permeable Teflon FEP tube for oxygenation throughout the water column for the experiments that required oxic conditions. Oxygenation was carried out by attaching the tubes to a pressurized O_2 cylinder (ZERO grade). The containers were isolated from light in order to prevent algal growth. The container setup is shown in Fig. 13.1.

13.2.3 Experimental Conditions

The following ranges of values were used to define the experimental conditions the inundated samples of vegetation and soil were submitted to continuously during the experiment. These ranges included feasible typical

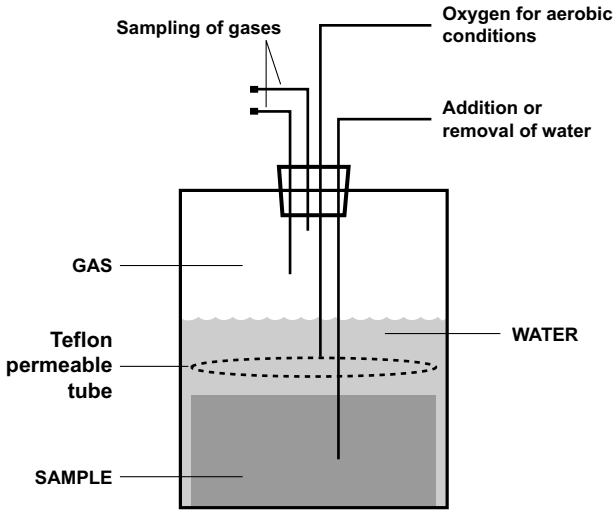

Fig. 13.1. Container setup with the vegetation or soil sample immersed in water

limits for water temperature, pH and levels of dissolved oxygen found in northern reservoirs during their distinct stages of development after flooding (Roy et al. 1986):

T1:	reservoir bottom water temperature during winter [4°C-5°C]
T2:	reservoir surface water temperature during summer [20°C-22°C]
P1:	low pH [4.5–5.0]
P2:	moderately acidic pH [6.0–6.5]
A1:	anoxic condition [< 2 mg dissolved $O_2 \cdot L^{-1}$]
A2:	oxic condition [≥ 2 mg dissolved $O_2 \cdot L^{-1}$]

From these observations, the following combinations of conditions listed in Table 13.1 (out of a total of 8 combinations possible) were selected as representative of the most frequent sets of conditions that exist during the evolution of a newly created reservoir in northern Quebec (David 1979; Roy et al. 1986).

Since the experiments were done in triplicate for the two types of soil samples with three blank containers used (no sample), 33 containers were used. Because of the limited number of experimental setups at the time, the experiments with the soil samples had to be done prior to the ones planned with the vegetation samples.

Because six distinct types of vegetation samples were used, full experimentation with the above sets of experimental conditions was not possible

Table 13.1. Experimental conditions used for the experiment

Conditions	Typical corresponding conditions in reservoir
T1A1P1	Deep zone. High humic content.
T1A2P2	Littoral zone during the cold season, well aerated, low humic content and low to moderate decomposition of organic matter.
T1A2P1	Littoral zone during the cold season, well aerated, high humic content and/or highly active decomposition of organic matter.
T1A1P2	Littoral zone during the cold season, low level of dissolved oxygen, low humic content and low to moderate decomposition of organic matter.
T2A1P2	Littoral zone during the summer season, stratification with limited aeration, low humic content and low to moderate decomposition of organic matter.
T2A2P2	Littoral zone during the summer season, well aerated, low humic content and low to moderate decomposition of organic matter.

considering the available experimental setups available and the on-going experimental logistics. Measurements and analysis were not limited to the production of carbon dioxide and methane but included other inorganic and organic compounds dissolved in water. Since the experiments done with the soil samples had indicated that a change in pH from level P1 to P2 (or P2 to P1) had no significant effect on the production of carbon dioxide and methane (Thérien et Morrison 1995a), the set of experimental conditions selected for the vegetation samples was reduced to the following combinations: T1A1, T1A2, T2A1 and T2A2. All experiments were done in triplicate for the vegetation samples consisting of tree foliage and ground covering mosses and required 63 containers including 3 blank containers. Six other containers were used with the herbaceous plants under the two following combinations of limiting conditions: T1A1 and T2A2.

At the start of the experiment, a known volume of river water was added to each container in order to flood the soil or vegetation sample. For the containers operating under anoxic condition (A1), oxygen dissolved in water was degassed by bubbling nitrogen in the water column and oxygen in the air above the water was flushed out with nitrogen.

Monitoring of pH, water temperature and level of dissolved oxygen was done on a daily basis. pH and level of dissolved oxygen were adjusted to fall in the proper range selected for the experiment. For the vegetation samples, pH was periodically adjusted to be in the 6.5–7.0 range. Details of these operations are available elsewhere (Thérien et Morrison, 1995a,b).

Temperature T2 was the room temperature [20°C–22°C] where the containers under conditions T2A1 and T2A2 were located. Temperature A1 was the temperature set at 5°C inside large refrigerators where the contain-

ers under conditions T1A1 and T1A2 were held. Containers under experimental conditions T1A1 and T2A1 were not supplied with oxygen or air after the start of the experiment. Condition A2 is the level of dissolved oxygen $\geq 2\ mg{\cdot}L^{-1}$ for which the rate of oxidation of organic matter is essentially unaffected (Perez, 1989). Condition A1 is the level of dissolved oxygen $< 2\ mg{\cdot}L^{-1}$.

Immersion of the soil and vegetation samples in water of the closed containers lasted 320 days and 345 days respectively. Gas production measurement cycles were done about every two weeks during the early stages of the experiment but were extended to about once every 4–6 weeks afterwards.

13.2.4 Measurements of Carbon Dioxide and Methane

At the end of each immersion cycle, the gas produced in the gaseous space above the water in the container was circulated from the container through a Drierite® drying column to an infrared spectrometer (ULTRAMAT 22P, Siemens) in a closed loop circuit. The infrared spectrometer was equipped with a carbon dioxide detection cell [0-10000 ppmv] and a methane detection cell [0-5000 ppmv]. These cells permitted the simultaneous measurements of the volumetric concentrations of carbon dioxide and methane of the dry gaseous mixture. The cell detectors were calibrated before and after each measurement cycle using a certified composition gas mixture of carbon dioxide and methane in air for the container operating under oxic conditions (A2). A similar calibration was done using a certified composition gas mixture of carbon dioxide and methane in nitrogen for the container operating under anoxic conditions (A1).

At the end of a measurement cycle, the gaseous mixture above the water column was flushed out with grade ZERO air or grade ZERO nitrogen for containers operating under the oxic conditions (A2) or anoxic conditions (A1) respectively. The gaseous mixture flushed out of the containers was passed through a column containing ascarite. The quantity of carbon dioxide trapped on ascarite was used as a check on the spectrometric measurement but also as a back-up measurement when concentration exceeded the upper detection limit of the cell. The water column in the container was degassed of dissolved carbon dioxide and methane by letting the system equilibrate by introducing in the gas space above the water, grade ZERO air or grade ZERO nitrogen for the container operating under oxic conditions (A2) or operating under anoxic conditions (A1) respectively.

13.2.5 Production of Gases

Carbon dioxide and methane produced by the decomposition of the inundated soil sample or the vegetation sample during a measurement cycle were contained in the gaseous mixture above the water column but also as gases dissolved in water. The number of moles of carbon dioxide and methane in the gaseous mixture above the water column is given by:

$$n_{1,i} = C_i \,.\, V_{\text{gaseous mixture}} \qquad i \in [CO_2, CH_4] \tag{13.1}$$

where C_i is the gas concentration of carbon dioxide or methane as measured by the spectrometer cell and $V_{\text{gaseous mixture}}$ is the volume of the gaseous mixture above the water column of the container.

Carbon dioxide and methane dissolved in water are computed from the assumption that gases in the gaseous mixture above the water column are in equilibrium with the gases dissolved in water. According to Henry's law:

$$X_i = K_{Hi} \,.\, p_i \tag{13.2}$$

where $p_i = [n_{1,i} \cdot n_t] \,.\, P_{\text{gaseous mixture}}$

Because of the small production of methane, pressure P of the gaseous mixture inside the sealed containers was essentially atmospheric during a measurement cycle. Therefore, the ideal gas relationship is used and,

$$n_t = P_{\text{gaseous mixture}} \cdot V_{\text{gaseous mixture}} \,/\, (R.T_{\text{gaseous mixture}}) \tag{13.3}$$

The number of moles of carbon dioxide or methane dissolved in the water column is then calculated by:

$$n_{2,i} = X_i \cdot V_{\text{water}} \tag{13.4}$$

Finally, the total molar production of carbon dioxide or methane produced during an immersion cycle is:

$$n_{\text{Total},i} = n_{1,i} + n_{2,i} \tag{13.5}$$

13.3 Results and Discussion

13.3.1 Soil Samples

Table 13.2 gives the average cumulative mass of carbon dioxide and methane produced from the two types of soil samples immersed in water during 320 days.

Table 13.2. Average cumulative mass of carbon dioxide and methane produced from the two types of soil samples immersed in water during 320 days

Conditions	Lichen humus [$g \cdot CO_2 \cdot m^{-2}$]	Moss humus [$g \cdot CO_2 \cdot m^{-2}$]	Lichen humus [$g \cdot CH_4 \cdot m^{-2}$]	Moss humus [$g \cdot CH_4 \cdot m^{-2}$]
T1A1P1	27.2 ± 8.3	45.6 ± 13.6	0.00 ± 0.00	0.00 ± 0.00
T1A2P2	26.1 ± 9.6	50.1 ± 22.5	0.00 ± 0.00	0.00 ± 0.00
T1A1P2	17.1 ± 3.1	41.1 ± 6.1	0.00 ± 0.00	0.01 ± 0.00
T2A1P2	71.5 ± 30.8	142.2 ± 0.2	0.21 ± 0.17	0.56 ± 0.41
T2A2P2	61.3 ± 5.9	100.2 ± 21.7	0.03 ± 0.03	0.13 ± 0.02

X ± s: Arithmetic average (triplicate) ± standard deviation

One observation is that carbon dioxide produced during an interval of 320 days under the most favourable conditions for decomposition [T2A1P2 and T2A2P2] is about 250–300 times the quantity of methane produced during the same time interval. Another observation is that carbon dioxide produced from the lichen humus soil sample is about half the carbon dioxide produced from the green moss humus soil sample during that time interval. However, a fuller and better appreciation of the effects of temperature, pH and the level of dissolved oxygen on the production of carbon dioxide and methane is obtained looking at the production of these gases as a function of time. Figure 13.2 shows the evolution of carbon dioxide produced by lichen humus as a function of time since initial immersion of the soil sample in water. Figure 13.3 shows similar results for the green moss humus. The curves represent the average cumulative quantities produced by the soil samples submitted to the experimental conditions defined in Table 13.1. Figure 13.4 and Fig. 13.5 show the average cumulative quantities of methane produced by the same soil samples for the experimental conditions producing methane. From these curves and the results of Table 13.2, a qualitative assessment can be made of the individual influence of temperature, pH and the level of dissolved oxygen on the cumulative production of carbon dioxide and methane and the rates of production. Table 13.3 indicates the relative importance of these factors by a (+) sign if

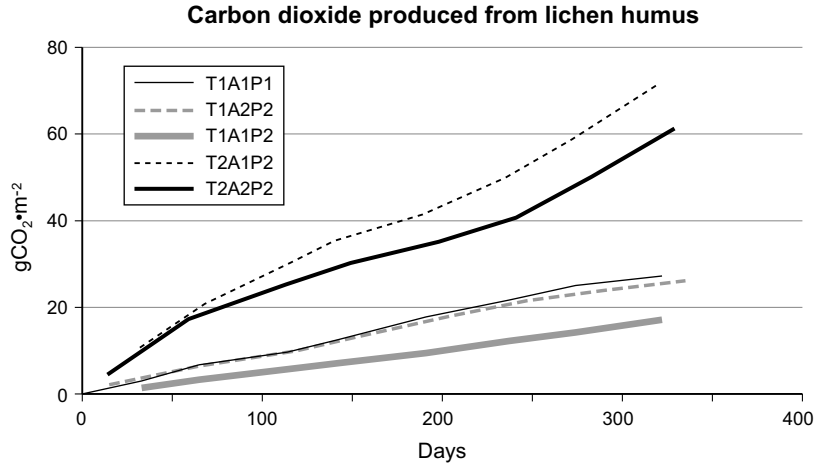

Fig. 13.2 Evolution of carbon dioxide produced from lichen humus under different sets of experimental conditions

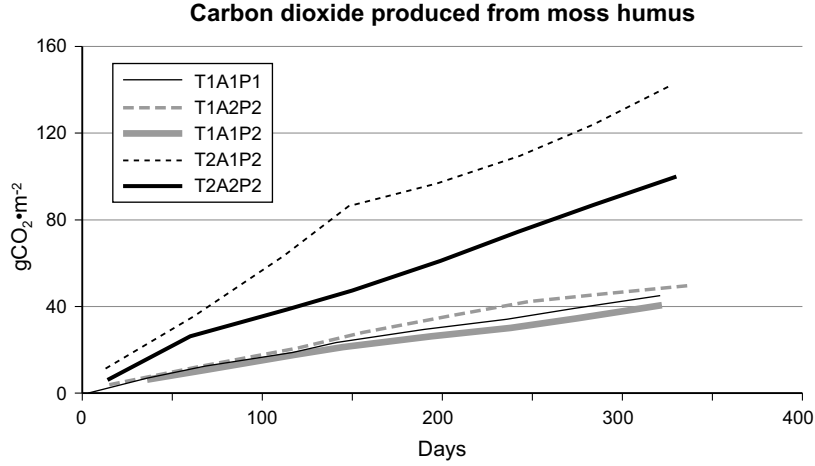

Fig. 13.3 Evolution of carbon dioxide produced from green moss humus under different sets of experimental conditions

the factor tends to increase the production of gas, a (-) sign when it tends to reduce it or a (0) sign if there appears to be no marked increase or decrease.

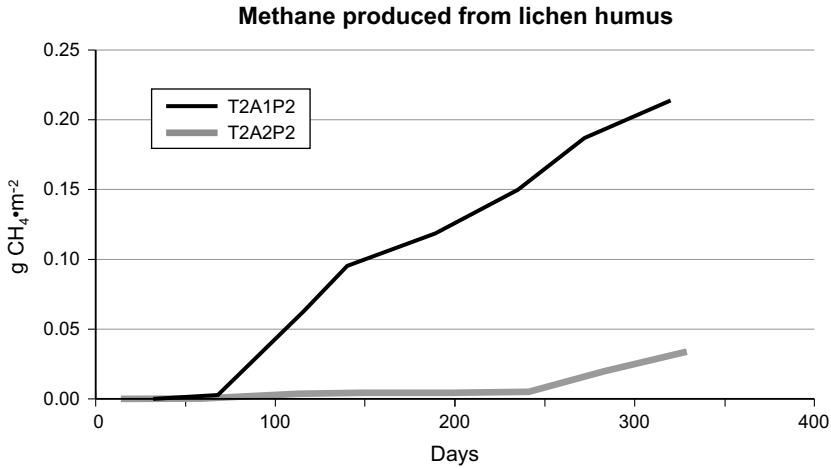

Fig. 13.4 Evolution of methane produced from lichen humus under different sets of experimental conditions

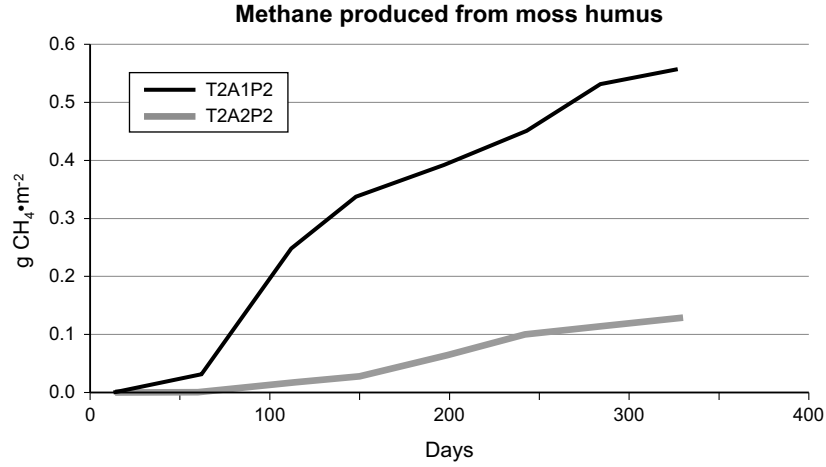

Fig. 13.5 Evolution of methane produced from moss humus under different sets of experimental conditions

Effects of Favourable Conditions for Decomposition

Comparison of the production of carbon dioxide under the experimental conditions T1A1P1 and T2A2P2 indicates significant differences. Under the more favourable conditions for decomposition of organic matter T2A2P2 (Brezonik 1994; Dickinson 1974) the production of carbon

Table 13.3. Comparison of the influence of temperature, pH and the level of dissolved oxygen on the cumulative quantity of gases produced from soil samples immersed in water during 320 days

Gas	Humus	+ TAP	+ P	+ A[T1]	+ A[T2]	+ T[A1]	+ T[A2]
CO_2	Lichen	+,++	-,0	0,+	-,0	++	++
CH_4	Lichen	0,+	0	0	--	++	0,+
CO_2	Green moss	+,++	0	0	-	++	+,++
CH_4	Green moss	+	0	0	--	++	+

A sign that is repeated (++) or (--) indicates an important contribution of the factor to the production of gases.

Notes:
+ TAP: from conditions T1P1A1 to conditions T2A2P2
+ P: from pH [P1] to pH [P2] under conditions T1A1
+ A[T1]: from anoxic [A1] to oxic [A2] conditions at temperature T1
+ A[T2]: from anoxic [A1] to oxic [A2] conditions at temperature T2
+ T[A1]: from temperature [T1] to temperature [T2] under anoxic conditions [A1]
+ T[A2]: from temperature [T1] to temperature [T2] under oxic conditions [A2]

dioxide is observed to be as high as three times the production under the less favourable conditions T1A1P1. Also, no methane is produced under conditions T1A1P1. Under conditions more favourable to the production of methane (Brezonik 1994; Sikora and Keeney 1983), that is for the higher temperature T2 and anoxic conditions A1, the production of methane reaches values that are from 4 to 7 times the values observed under conditions T2A2P2.

Effects of the Level of Dissolved Oxygen

The level of dissolved oxygen has no significant effect on the production of carbon dioxide under cold temperatures [T1A1P2 and T1A2P2] for the two types of soil samples. At higher temperatures [T2A1P2 and T2A2P2], the average rate of production of carbon dioxide (slope of the curves shown in Fig. 13.2 and Fig. 13.3) under anoxic conditions is greater than the one under oxic conditions during the first 5 months of the experiment. However, there is no significant difference in the average rate of production of carbon dioxide thereafter. The net result is that the average quantities of carbon dioxide produced during the first 320 days of the experiment under anoxic conditions are about 20 to 30% higher than the quantities produced under oxic conditions. These observations are coherent with known results reported in the literature (Dickinson 1974; Sikora and Keeney 1983). In effect, in flooded soils and sediments, methane fermentation is a two-step process acting simultaneously by which large quantities

of carbon may be released as CH_4 and CO_2 (Wetzel 1975). In the first step, organic acids and alcohols are produced with a variety of inorganic compounds from hydrolysis and fermentation of the carbohydrates, glycerols and proteins contained in the organic layer of soil or sediments. These organic acids (i.e. acetic acid and propionic acid) and alcohols are converted by bacteria operating strictly under anaerobic conditions to produce CH_4 and CO_2 from the methyl carbon: $CH_3COOH \rightarrow CH_4 + CO_2$.

For both types of soil samples, the production of methane was found to be significant only under anoxic conditions [A1] at higher temperature [T2].

Effects of pH

For the range of pH considered in this work for both types of soil, pH has no significant effect [T1A1P1 and T1A1P2] on the production of carbon dioxide and methane. A similar finding was reported by Duchemin (2000) and Lambert and Fréchette (2002) indicating that for boreal reservoirs in Northern Quebec no relationship was established between greenhouse gases emission and pH.

Effects of Temperature

For both types of soil, an increase in the water temperature has a very significant effect on the production of methane under anoxic conditions [T1A1P2 and T2A1P2]. In effect, there is virtually no production of methane at colder temperatures [T1] but a significant increase in production is observed at higher temperatures [T2]. Again, these results are in agreement with data reported in the literature (Brezonik 1994). Also, for both types of soil, the quantities of carbon dioxide produced under oxic conditions [T1A2P2 and T2A2P2] and anoxic conditions [T1A1P2 and T2A1P2] are greatly increased (3 to 5 times) at higher temperature [T2].

13.3.2 Vegetation Samples

Table 13.4 gives the average cumulative mass of carbon dioxide produced from the five types of vegetation samples immersed in water during 345 days. Table 13.5 gives similar results for methane.

The average cumulative quantities of carbon dioxide produced as a function of time are shown in Fig. 13.6 to Fig. 13.11. Similarly, Fig. 13.12 compares the average cumulative quantities of methane produced from the leaves of deciduous and coniferous trees under conditions T2A1 as a

Table 13.4. Average cumulative mass of carbon dioxide produced from different vegetation samples immersed in water during 345 days

Phytomass	T1A1 [mg $CO_2 \cdot g^{-1}$ dry]	T1A2 [mg $CO_2 \cdot g^{-1}$ dry]	T2A1 [mg $CO_2 \cdot g^{-1}$ dry]	T2A2 [mg $CO_2 \cdot g^{-1}$ dry]
Alder leaves	26.8 ± 2.5	133.0 ± 31.9	77.4 ± 9.2	374.7 ± 40.2
Spruce needle	21.3 ± 1.7	53.0 ± 14.1	32.9 ± 1.6	200.8 ± 11.7
Lichen	18.1 ± 4.2	110.6 ± 27.3	14.2 ± 0.5	269.2 ± 15.9
Green moss	24.4 ± 1.5	110.8 ± 37.8	21.6 ± 0.9	447.0 ± 34.5
Sphagnum moss	10.8 ± 1.3	44.7 ± 1.5	17.2 ± 2.8	207.7 ± 1.1
Herbaceous plant	31.7 ± 9.6	-	-	238.0 ± 1.4

X ± s: Arithmetic average (triplicate) ± standard deviation

Table 13.5. Average cumulative mass of methane produced from different vegetation samples immersed in water during 345 days

Phytomass	T1A1 [mg $CH_4 \cdot g^{-1}$ dry]	T1A2 [mg $CH_4 \cdot g^{-1}$ dry]	T2A1 [mg $CH_4 \cdot g^{-1}$ dry]	T2A2 [mg $CH_4 \cdot g^{-1}$ dry]
Alder leaves	0.0000 ± 0.0000	0.0000 ± 0.0000	0.0006 ± 0.0005	0.0000 ± 0.0000
Spruce needle	0.0000 ± 0.0000	0.0000 ± 0.0000	0.0037 ± 0.0014	0.0000 ± 0.0000
Lichen	0.0000 ± 0.0000	0.0000 ± 0.0000	0.0000 ± 0.0000	0.0000 ± 0.0000
Green moss	0.0000 ± 0.0000	0.0000 ± 0.0000	1.722 ± 0.8542	0.0021 ± 0.0036
Sphagnum moss	0.0000 ± 0.0000	0.0000 ± 0.0000	0.168 ± 0.0476	0.0000 ± 0.0000
Herbaceous plant	0.0000 ± 0.0000	-	-	0.0004 ± 0.0006

X ± s: Arithmetic average (triplicate) ± standard deviation

function of time. Fig. 13.13 shows similar results for green moss and sphagnum moss under the same experimental conditions.

As shown in Fig. 13.14, the rates of carbon dioxide produced from the vegetation samples under oxic conditions are strongly controlled by temperature.

On the average, the cumulative quantities of carbon dioxide produced by the vegetation samples immersed in water during 345 days under conditions T2A2 are about 3 times the cumulative quantities produced under conditions T1A2. As shown in Fig. 13.15, except for alder leaves, temperature has a less marked effect on the quantities of carbon dioxide produced from the vegetation samples under anoxic conditions.

Conversely, oxic conditions are a significant factor controlling the rate of production of carbon dioxide at a given temperature. This is shown in Fig. 13.16 for the experiment conducted at higher temperatures [T2] and in Fig. 13.17 for the experiment conducted at colder temperatures [T1].

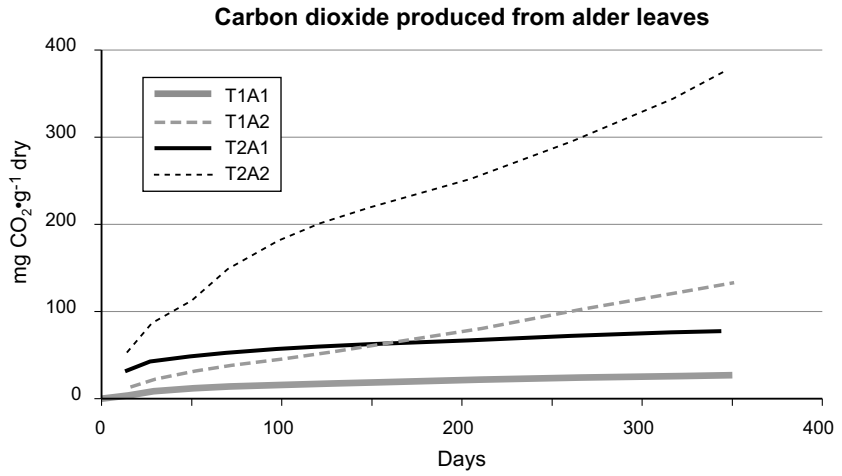

Fig. 13.6 Evolution of carbon dioxide produced from alder leaves under different sets of experimental conditions

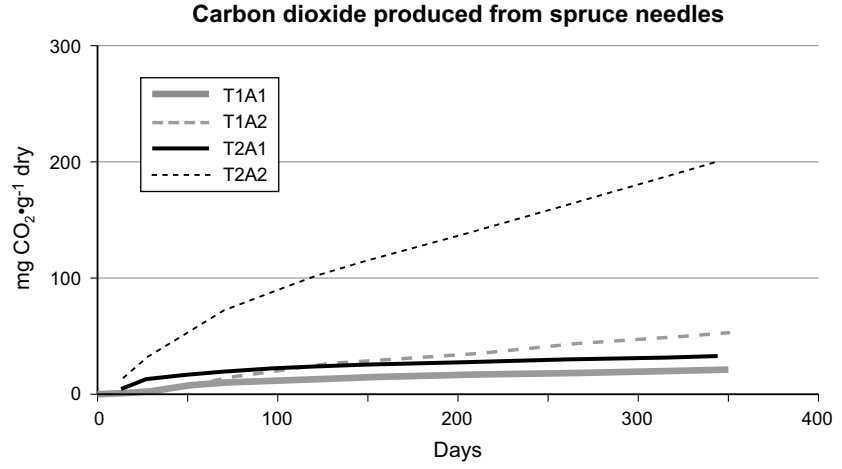

Fig. 13.7 Evolution of carbon dioxide produced from spruce needles under different sets of experimental conditions

At higher temperatures under oxic conditions [T2A2], the cumulative quantities of carbon dioxide produced during 345 days from the tree leaves immersed in water are about 5 to 6 times greater than the quantities produced under anoxic conditions at the same temperature [T2A1]. For the mosses, they are about 10 to 20 times greater under similar conditions. Under colder temperatures [T1], a similar increase in the production of

carbon dioxide is observed for the experiment conducted under oxic conditions relative to anoxic conditions. For example, under oxic conditions [T1A2], the cumulative quantities of carbon dioxide produced are about 2 to 6 times greater than the quantities produced under anoxic conditions at the same temperature [T1A1]. However, the effect on the production of carbon dioxide is much less marked than the production observed at higher temperatures.

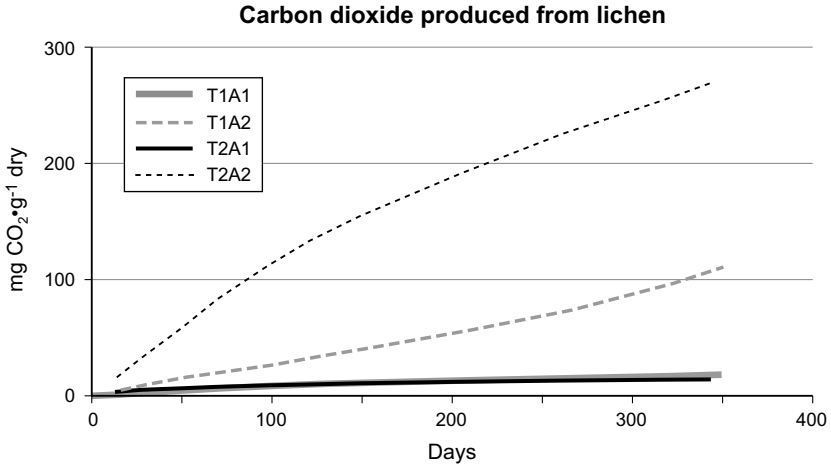

Fig. 13.8 Evolution of carbon dioxide produced from lichen under different sets of experimental conditions

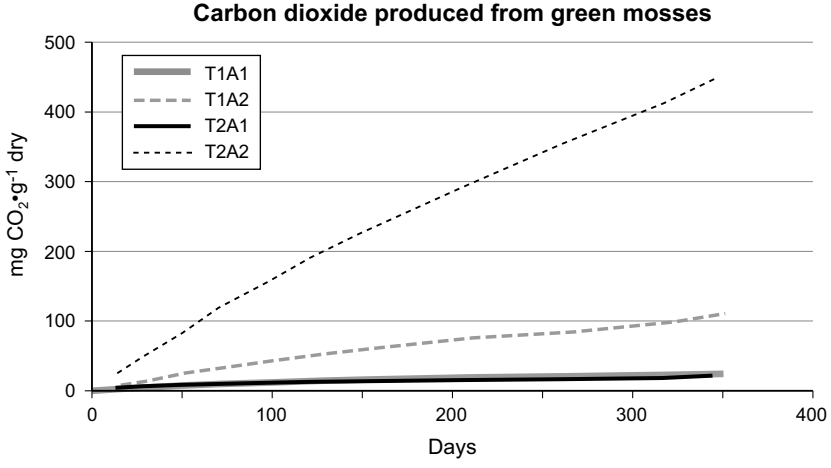

Fig. 13.9 Evolution of carbon dioxide produced from green moss under different sets of experimental conditions

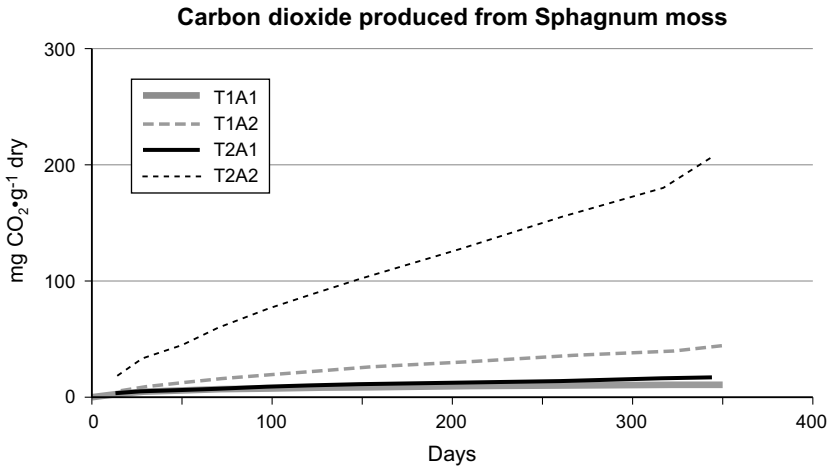

Fig. 13.10 Evolution of carbon dioxide produced from Sphagnum moss under different sets of experimental conditions

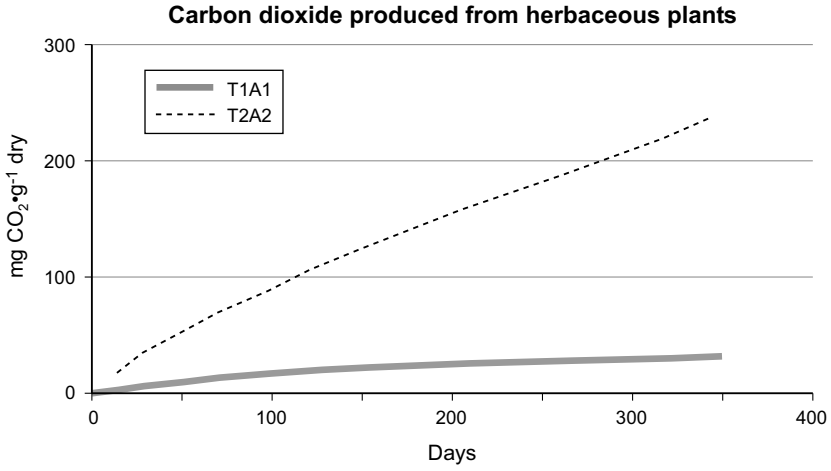

Fig. 13.11 Evolution of carbon dioxide produced from herbaceous plants under different sets of experimental conditions

The results show that the highest rate of production of carbon dioxide is obtained under oxic conditions at higher temperatures [T2A2] with cumulative quantities produced over 345 days significantly greater than the ones obtained under experimental conditions T2A1, T1A2 and T1A1. The quantities of carbon dioxide produced are generally increasing for experiments

conducted from conditions T1A1 → T2A1 → T1A2 → T2A2. An exception is for lichen and green moss for which the quantities of carbon dioxide produced under conditions T2A1 are not significantly different than those produced under conditions T1A1.

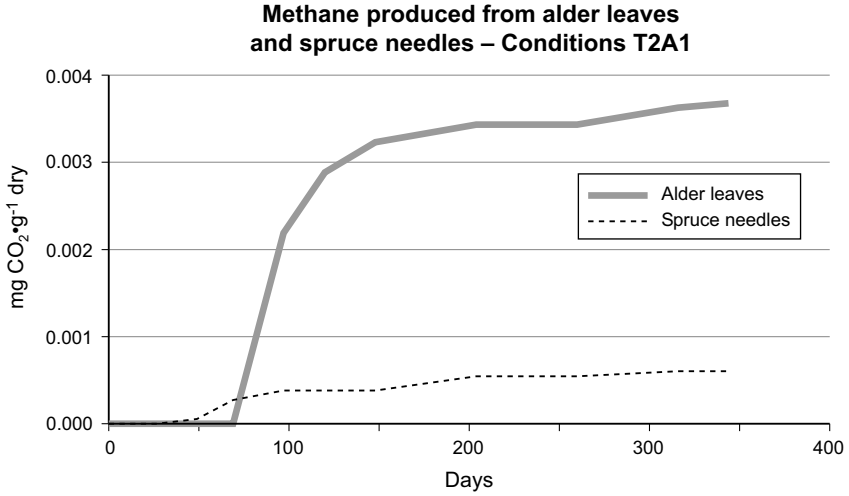

Fig. 13.12 Evolution of methane produced from alder leaves and spruce needles under different sets of experimental conditions

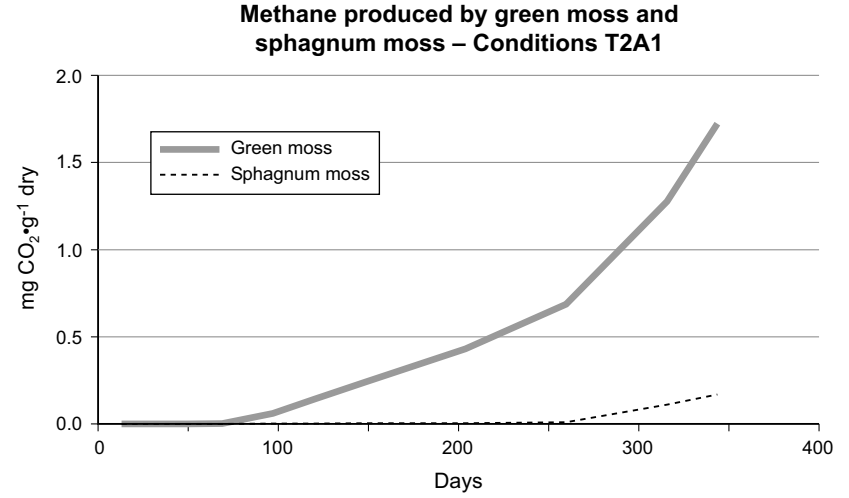

Fig. 13.13 Evolution of methane produced from green moss and sphagnum moss under different sets of experimental conditions

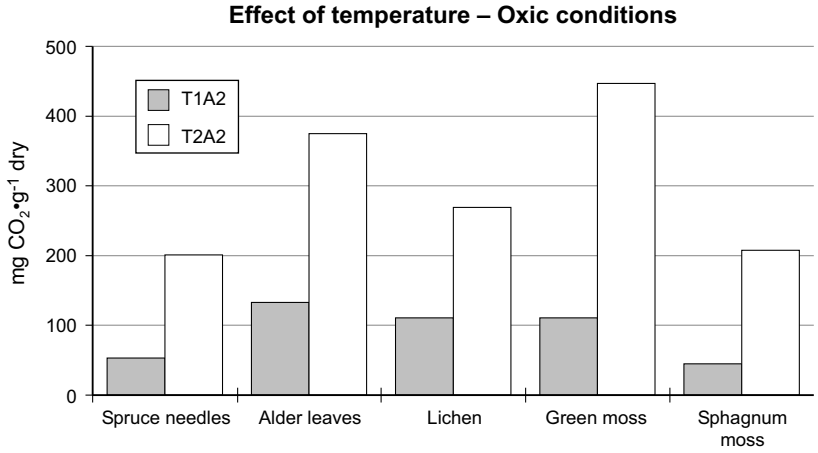

Fig. 13.14 Effect of temperature on the quantities of carbon dioxide produced from vegetation samples immersed in water during 345 days under oxic conditions

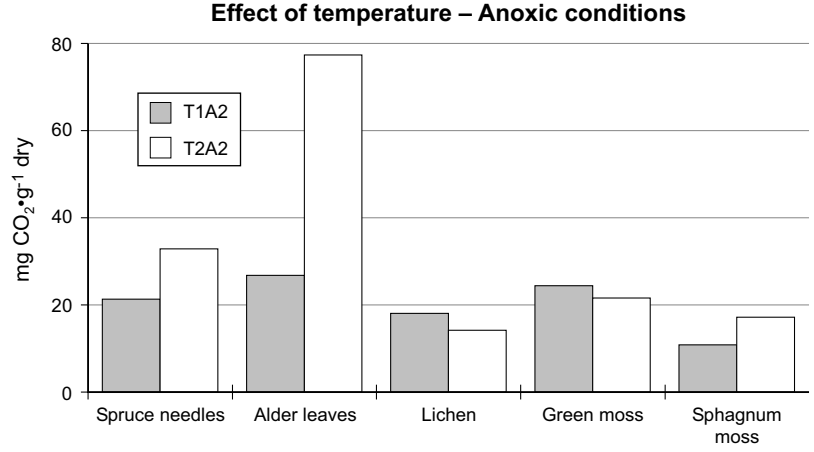

Fig. 13.15 Effect of temperature on the quantities of carbon dioxide produced from vegetation samples immersed in water during 345 days under anoxic conditions

On the basis of the quantities of carbon dioxide produced during 345 days, alder leaves and green mosses appear to decompose more easily since they produce about 375–450 mg $CO_2 \cdot g^{-1}$ (dry weight) as compared to 200–275 mg $CO_2 \cdot g^{-1}$ (dry weight) for the other types of vegetation samples. However, even after 345 days, the cumulative quantities of carbon

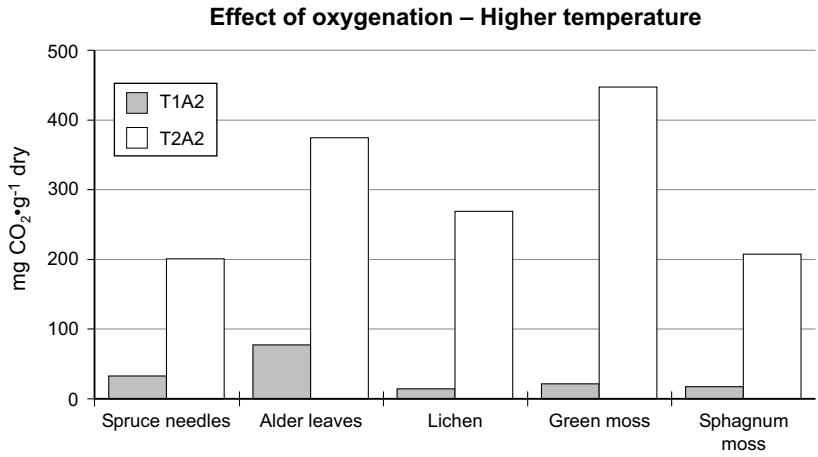

Fig. 13.16 Effect of the level of dissolved oxygen on the production of carbon dioxide from vegetation samples immersed in water during 345 days under higher temperature

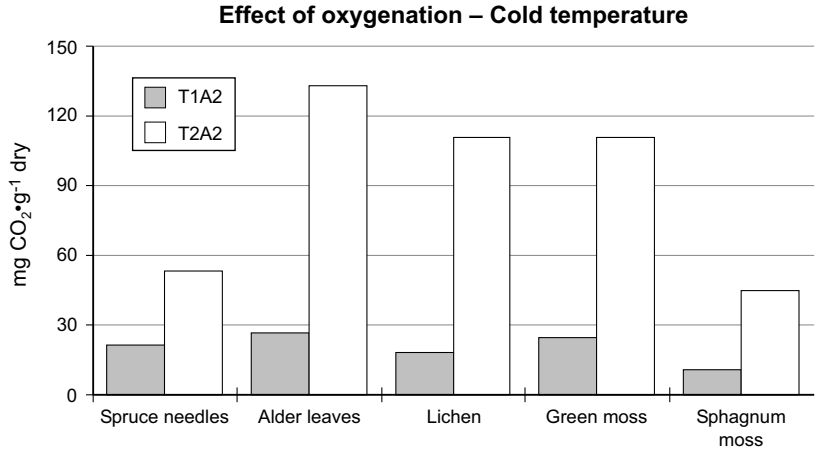

Fig. 13.17 Effect of the level of dissolved oxygen on the production of carbon dioxide from vegetation samples immersed in water during 345 days under cold temperature

dioxide produced under anoxic conditions [T1A2 and T2A2] have not levelled off. In some cases, the rate of production of carbon dioxide (slope of the curve) even appears to increase slightly (i.e. alder leaves). This is an indication that decomposition is still very active even after a year of immersion in water under the given experimental conditions. Under anoxic

conditions, the rate of production is significantly smaller and the evolution of the cumulative quantities of carbon dioxide produced as a function of time appears to be asymptotic.

For methane, no production of gases has been observed before 3 months after the initial immersion of vegetation samples in water. For sphagnum moss, methane was observed only after 9 months and, for lichen, no methane production was observed during the whole experiment. The latency periods for the production of methane are significantly much greater than the ones for the production of carbon dioxide that was detected during the first measurement cycle (15 days). Also, the production of methane occurred essentially at higher temperatures [T2] with the more significant production occurring under conditions T2A1 from green moss and, to a lesser extent, from sphagnum moss. Methane produced from alder leaves and spruce needles is negligible and the evolution of the cumulative quantities produced as a function of time is clearly asymptotic. It has been observed that the rate of production of methane from green moss increased during the last two months of the experiment. However, for all the vegetation samples put to test, the cumulative quantities of methane produced during the length of the experiment were not significant when compared to the cumulative quantities of carbon dioxide produced during that time.

13.4 Conclusion

The quantities of carbon dioxide and methane produced from the decomposition of vegetation and soil samples immersed in water and submitted to a set of controlled environmental conditions has been measured as a function of time for a period of about a year.

The results are important since the samples selected were representative of the labile vegetation and soil components of the James Bay territory that would be flooded when creating a new hydroelectric reservoir. They are also important because the sets of conditions for temperature, pH and level of dissolved oxygen in water, selected for the experiments, cover the range of conditions normally found in newly created reservoirs of northern Quebec. The results have permitted to identify the important controlling factors of carbon dioxide and methane production under these conditions. The cumulative quantities of CO_2 and CH_4 released from the flooded vegetation and soil samples under the given experimental conditions represent a reference data set from which rates of production of CO_2 and CH_4 can be calculated. In effect, rates of production under similar water temperature, dissolved oxygen and pH conditions, under the assumption that all other

environmental conditions or factors remain constant, will virtually be the same whether the volume of water is contained in a glass jar (in vitro) or is part of a reservoir (in situ). Differences in the rates of production would inevitably be observable between results from in vitro and in situ experiments when the assumption that all environmental conditions other than water temperature, dissolved oxygen and pH is not validated. The magnitude of these differences would generally be a function of the importance of the other environmental conditions or factors (that would not have been taken into account by the in vitro experiment) on the rate of production of CO_2 and CH_4. Under the assumption that water temperature, dissolved oxygen and pH are the main factors for the production of CO_2 and CH_4 from flooded vegetation and soil then production of CO_2 and CH_4 emitted from reservoirs under field conditions can be estimated. Since field conditions for water temperature, dissolved oxygen and pH will generally be different from the conditions used in the experiments these rates would need be adjusted generally through interpolation. Extrapolation would rarely be used except possibly for water temperature below 5°C. Therefore, from the knowledge of the quantity of phytomass flooded and of the soil area inundated, the rate of CO_2 and CH_4 emitted from a newly created reservoir can be computed (Thérien and Morisson, Chap. 25 below).

For both the soil samples and the vegetation samples, water temperature was found to be a controlling factor for the production of carbon dioxide. The level of oxygenation of the water was found to be another key factor. pH was not found to have any significant effect for the range of pH used.

For the vegetation samples, production of carbon dioxide was the highest under oxic conditions [> 2 mg dissolved oxygen$\cdot L^{-1}$] and higher water temperatures [20°C–22°C]. The production of carbon dioxide was the lowest under cold temperatures [5°C]. Irrespective of the water temperature, production of carbon dioxide was highest under oxic conditions [> 2 mg dissolved oxygen$\cdot L^{-1}$]. Under the most favourable experimental conditions [20°C–22°C; > 2 mg dissolved oxygen$\cdot L^{-1}$], alder leaves and green moss produced the highest quantities of carbon dioxide during the length of the experiment (345 days). On the average, 375 g $CO_2 \cdot g^{-1}$ (dry weight) was observed for alder leaves and 450 g $CO_2 \cdot g^{-1}$ (dry weight) for green moss respectively. Under the same favourable experimental conditions, other types of vegetation represented by spruce needles, lichen, sphagnum moss and herbaceous plants produced lower quantities of carbon dioxide with values in the range of 200–275 g $CO_2 \cdot g^{-1}$ (dry weight). An important result is that, under the more favourable conditions for the production of carbon dioxide [20°C–22°C; > 2 mg dissolved oxygen$\cdot L^{-1}$], the rate of production of carbon dioxide had not declined even after 345 days of experimentation.

For the less favourable experimental conditions, corresponding to anoxic conditions and low temperatures [< 2 mg dissolved oxygen·L^{-1}, 5°C], production of carbon dioxide was the lowest with values in the range 11–32 g CO_2·g^{-1} (dry weight).

For the soil samples, production of carbon dioxide was very significant at higher temperatures under oxic conditions but higher production was obtained under anoxic conditions. Under such conditions [20°C–22°C; < 2 mg dissolved oxygen·L^{-1}], the average quantities of carbon dioxide produced during the length of the experiment (320 days) were 143 g CO_2·m^{-2} and 71.5 g CO_2·m^{-2} for the green moss humus soil sample and the lichen humus soil sample respectively. At the higher temperature [20°C–22°C], the rate of production of carbon dioxide from both types of soil had not declined with time even after 320 days.

For both vegetation and soil samples, production of methane was significant only under anoxic conditions and higher temperatures [< 2 mg dissolved oxygen·L^{-1}; 20°C–22°C]. Even under these conditions, favourable to the production of methane, the quantities produced were low. The average quantities of methane produced during the length of the experiment (320 days) were 0.56 g CH_4·m^{-2} from the green moss humus soil sample and 0.21 g CH_4·m^{-2} from the lichen humus soil sample, respectively. These quantities are about 300 times less than the quantities of carbon dioxide produced under the same conditions. For the vegetation samples, production of methane during the length of the experiment (345 days) was the highest for green moss with an average value of 1.7 mg CH_4·g^{-1} (dry weight). For the other vegetation samples, production of methane was in the range of 0.0004 mg CH_4·g^{-1} (dry weight) to 0.1680 mg CH_4·g^{-1} (dry weight) with an average value of 0.0350 mg CH_4·g^{-1} (dry weight). Again, these values are very low compared to carbon dioxide produced from the vegetation samples.

Acknowledgements

This work was supported by Hydro-Québec, reference number VPENV-92-ADC-057-00.

14 Diffusive CO_2 Flux at the Air-Water Interface of the Robert-Bourassa Hydroelectric Reservoir in Northern Québec : Isotopic Approach (^{13}C)

Jean-François Hélie and Claude Hillaire-Marcel

Abstract

Hydroelectric reservoirs and lakes in boreal Québec produce greenhouse gases (GHG) mainly in the form of CO_2. No method exists, however, which can directly measure the flux of CO_2 across the air-water interface and the methods that are currently used are only representative of a small surface area and a specific time period. The objective of the current study is to improve and validate an isotopic approach to estimate the annual CO_2 flux across the air-water interface. The model requires the calibration of isotopic fluxes into and out of the interface. When applied to the Robert-Bourassa hydroelectric reservoir in boreal Québec, this model estimated an average CO_2 diffusive flux across the air-water interface of 225±51 mg $CO_2 \cdot m^{-2} \cdot d^{-1}$ in the summer of 2000 and of 446±93 mg $CO_2 \cdot m^{-2} \cdot d^{-1}$ in the summer of 2001. These average fluxes are representative of the whole ice-free period.

14.1 Introduction

Hydroelectric reservoirs and lakes in boreal Québec produce greenhouse gases (GHG) (eg. Duchemin 2000; Duchemin et al. 1999; Duchemin et al. 1995). In order to estimate net GHG emissions stemming from a hydroelectric installation, three types of potential emissions need to be considered: 1) those generated from the construction of the dam and the causeways; 2) those generated indirectly from the flooding of a forested territory (soil and vegetation) which previously participated in carbon exchanges;

and 3) those generated at the air-water interface from the excessive pressure of GHGs present in the reservoir stemming from the oxidation of organic matter (photolysis or bacteria) in the water column and the adjacent sediments. The GHGs produced from the construction of a hydroelectric reservoir can be easily estimated by accounting for the use of fossil fuels by machines and the production of cement (Gagnon and van de Vate 1996). It is difficult to estimate the effects of the loss of forested territory which previously participated in carbon exchanges with the atmosphere, as there is still no scientific consensus as to the role boreal forests play in the global carbon cycle. Some studies suggest that the boreal forest acts as a small sink for carbon (e.g. Barr et al. 2002). Other studies state that the carbon balance in boreal forests is a lot more complex and they suggest that it can act as either a source or a sink for atmospheric carbon (e.g. Arain et al. 2002; Liu et al. 2002; Wang et al. 2002; Wirth et al. 2002; Yarie and Billings 2002). In the current chapter we will, therefore, only address the third component, that is, GHG fluxes to the atmosphere.

The principal GHGs emitted from the surface of hydroelectric reservoirs are carbon dioxide (CO_2), methane (CH_4) and nitrous oxide (N_2O). Even though the global warming potential (GWP) of methane is 23 times greater than that of CO_2 (Cubasch et al. 2001), the molar concentrations of CH_4 in the surface layers of boreal reservoirs are 50 to 825 times smaller than those of CO_2 (Duchemin et al. 1995). Similarly, even though the GWP of N_2O is 296 greater than that of CO_2, the molar concentrations of N_2O in the surface layers of boreal reservoirs are at least 4000 times smaller than those of CO_2 (Huttunen et al. 2002). Since the principal GHG found in the surface waters of reservoirs is, hence, CO_2, the estimates of the fluxes at the air-water interface made in this chapter will concentrate on CO_2.

No method exists which can directly measure the flux of CO_2 across the air-water interface and, hence, allow for estimates to be made of surface waters covering large areas. Fluxes must consequently be estimated through indirect measurements. The most common current methods of measurement include: i) micrometeorological towers (flux towers); ii) floating chambers; and iii) calculations based on an equation of the diffusion of a gas across the air-water interface. Recent studies have shown that one method may overestimate GHG fluxes by a factor of 2 to 18 relative to another method (Duchemin et al. 1999; Matthews et al. 2003). Additionally, these three methods only represent a small area of surface water and one time point. They, therefore, require continuous sampling over a large area in order to determine a mean annual flux from the total surface area, an approach which is very expensive.

A first proposal for the calculation of CO_2 fluxes across the air-water interface using the value of ^{13}C in dissolved inorganic carbon (DIC) was

made in 2000 within the framework of an exploratory isotopic study of the Robert-Bourassa reservoir (Hillaire-Marcel et al. 2000; Luther 2000). Under the assumption that the mean residence time of "isotopic" DIC is longer than the mean chemical residence time (Broecker and Peng 1974), the fluxes calculated with this type of model could be representative of a longer time period. Hence, the principal objective tackled here is to improve and validate an isotopic approach in order to estimate the annual CO_2 flux across the air-water interface. The study concentrates primarily on the Robert-Bourassa reservoir. It has three aims: firstly, to determine the mean diffusive flux for the ice-free period; secondly, to determine the loss of CO_2 from the turbines; and thirdly, to determine the role of spring-time snowmelt. In order to estimate total annual emissions of CO_2 from the reservoir as a whole, it is necessary to account for all three components. In this study, however, we will only address the mean diffusive flux at the air-water interface for the ice-free season.

14.2 Materials and Methods

14.2.1 Study Site

The Robert-Bourassa reservoir (RB – previously known as La Grande 2 or LG-2) is situated in the boreal zone of Quebec (53° 45'N/77° W) and was created from the damming of the La Grande river. The impoundment of the reservoir began at the beginning of 1978 and was finished in the fall of 1979 (Dussault and Boudreault 1980). This reservoir covers a surface area of approximately 2835 km^2 (at maximum height) containing a volume of 61 930 x 10^6 m^3, has a mean depth of 22 m, a maximum depth of 150 m and an annual average fluctuation level of 3 m (Hayeur 2001; Schetagne 1989). The mean water residence time is of approximately 6 months (Schetagne 1989). The RB reservoir is fed upstream to the east by a series of reservoirs (Caniapiscau, Laforge 2, Laforge 1, La Grande 4 and La Grande 3) and the Kanaaupscow river and, to the south, by the deviation of the Boyd-Sakami which includes the Opinaca reservoir (Fig. 14.1).

In such, the RB reservoir is fed by the watersheds of the La Grande, Caniapiscau, Eastmain and Opinaca rivers which overall cover a surface area of 177 000 km^2 (Hayeur 2001). The La Grande complex, situated in the Superior clay geologic belt, is primarily characterized by granites and granitic gneiss. The deposits from the Tyrell seas cover between 50 and 75% of the area of the RB reservoir (Dussault and Boudreault 1980). The region to the east is covered by moraines and rocky outcrops (Texier

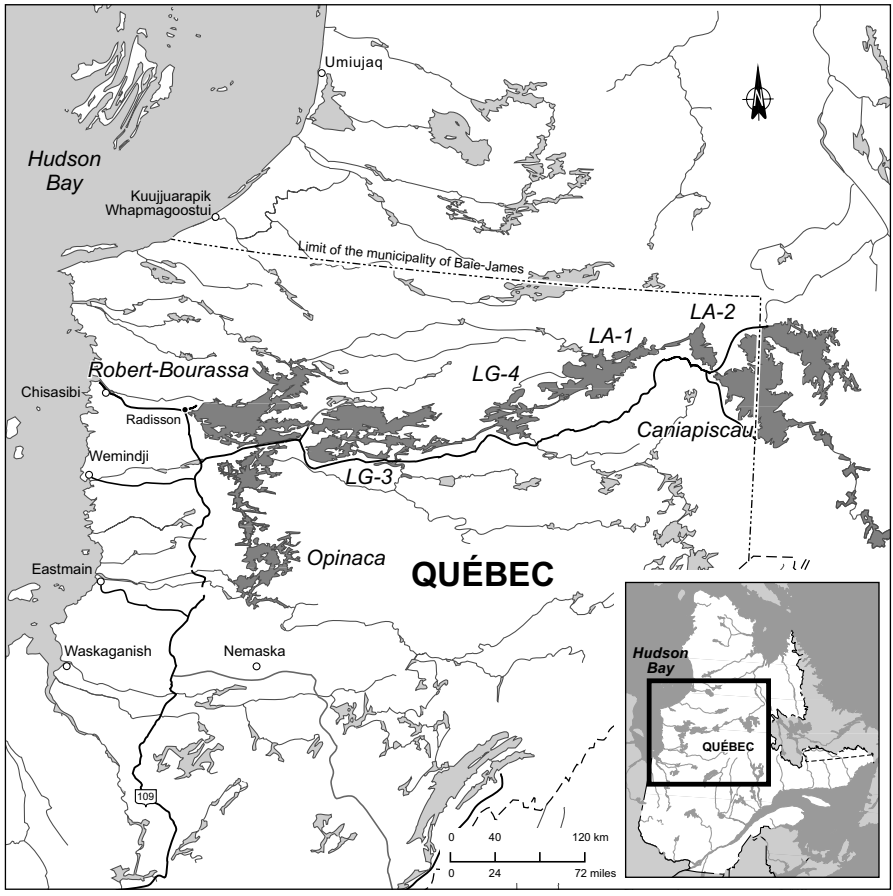

Fig. 14.1. Map of the location of the Robert-Bourassa reservoir in the province of Québec

1974). While wetlands and peatlands represent 10% of the soils, podsols represent 90% of the watershed soils and have organic horizons of less than 15 cm thickness (Grondin et al. 1995). Lakes, marshes and peatlands also represent about 10% of the actual flooded surface (Dussault and Boudreault 1980). In this region, the boreal forest is dominated by *Picea mariana* (black spruce) and *Pinus banksiana* (grey pine), while the soils are covered with *Cladina* sp. (caribou moss) as well as *Sphagnum* sp. ad *Pleurozium* (sphagna – Grondin et al. 1995). Average monthly temperatures vary between -23°C in January (minimum recorded at -56°C) and 14°C in July (maximum recorded at 34°C), and mean annual rainfall is 765 mm (Hayeur 2001).

14.2.2 Sampling Scheme

Three field campaigns were undertaken at the reservoir in the summers of 2000, 2001 and 2002. A monthly sampling campaign was also undertaken over a period of twelve months between 2001-2002. Five sampling protocols were used between the field campaigns (see Hélie 2004). However, in this study we will only use the data collected during the 2000 and 2001 campaigns. The surface water of the reservoirs (Fig. 14.1) was sampled in both calm and unstable meteorological conditions during these field campaigns. The sampling during each campaign was made from a hydroplane, where 10 to 15 sites were visited in only one day between 10:30 and 15:30 for each of the meteorological conditions.

14.2.3 In situ Sampling Measurements

Water temperature, pH, alkalinity, air temperature and wind speed were measured at each site, and samples were collected for ^{13}C analysis of both dissolved inorganic and organic carbon of the water and for ^{13}C in the air above the reservoirs (^{13}C-DIC, ^{13}C-DOC and ^{13}C-CO_{2air}, respectively). Samples were also taken for C:N analysis and ^{14}C activity of the dissolved organic matter. Here, we only present results of the ^{13}C of DIC. The other analysis will be treated elsewhere.

In order to measure the value of ^{13}C in the DIC, water was collected in a 125 ml brown glass Qorpak™ bottle, to which a spatula-tip of mercuric chloride ($HgCl_2$) was added for stabilization. The sample was subsequently stored at 4°C. Upon arrival in the laboratory, 1.5 ml of the samples was injected through rubber septa into 3 ml containers with a helium atmosphere and containing a few drops of orthophosphoric acid (100% H_3PO_4). Up to 50 samples were placed on a heating plate and heated to 40°C for at least one hour for reaction to take place. A Gilson™ autosampler was used to collect the CO_2 that was produced upon reaction, which was then isolated from the other gases with the help of a MultiFlow™ system and injected under continuous flow into a triple collection Isoprime™ mass spectrometer. The results of the ^{13}C-DIC analysis are presented in Table 14.1 in Sect. 14.4 and are given a notation of delta (δ) ‰ in accordance to the international V-PDB standard (Coplen 1995).

Table 14.1. Isotopic flux ratios calculated from samples taken across the reservoir on calm days during the 2000 and 2001 summer field campaigns

	Station	$\delta^{13}DIC_{mes}$	$\delta^{13}DIC_{prod}$	$\delta^{13}DIC_{eq}$	F_{prod}/F_{eq}
2000	1 (A)	-7.9	-21.89	-2.19	0.41
	2 (B)	-7.8	-21.73	-2.43	0.38
	3 (C)	-9.4			
	4 (D)	-8.3	-21.51	-2.91	0.41
	7	-11.5	-24.06	-4.36	0.56
	8	-10.0	-24.89	-4.19	0.39
	10	-9.2	-22.61	-4.01	0.39
	9	-10.5			
	13	-10.3	-24.54	-4.24	0.42
	Mean strong	-9.4	-23.03	-3.48	0.42±0.06
	5 (E)	-6.6	-23.10	-2.50	0.25
	6 (F)	-6.1	-21.66	-2.06	0.26
	14	-9.3	-24.44	-4.14	0.34
	18	-7.0	-23.00	-3.80	0.20
	20	-6.8	-22.06	-3.16	0.23
	Mean weak	-7.1	-22.85	-3.13	0.26±0.05
2001	7	-11.16	-21.22	-2.79	0.83
	8	-9.76	-20.78	-3.00	0.61
	9	-9.53	-20.69	-2.58	0.62
	10	-9.08	-21.16	-2.83	0.52
	13	-10.06	-20.95	-2.84	0.66
	17	-10.44	-19.89	-1.87	0.91
	Mean strong	-10.01	-20.78	-2.65	0.69±0.15
	1	-6.75	-19.75	-1.41	0.41
	2	-7.61	-20.44	-2.10	0.43
	3	-6.74	-19.79	-1.85	0.37
	4	-6.87	-19.62	-1.67	0.41
	5	-7.08	-19.78	-1.67	0.43
	6	-7.05	-19.35	-1.06	0.49
	12	-8.43	-19.77	-1.72	0.59
	14	-8.26	-20.16	-2.12	0.52
	15	-7.61	-20.62	-2.68	0.38
	Mean weak	-7.38	-19.92	-1.81	0.45±0.07

$\delta^{13}DIC_{mes}$ is the content of ^{13}C of DIC measured at the surface of the reservoir; $\delta^{13}DIC_{prod}$ is the content of ^{13}C of DIC produced within the reservoir and estimated from the $\delta^{13}C\text{-}DOC$ also measured at the surface of the reservoir; and $\delta^{13}DIC_{eq}$ is the content of ^{13}C of DIC in equilibrium with atmospheric CO_2.

14.3 Model Construction

It has been shown that the dissolved CO_2 in the Robert-Bourassa reservoir stems from the degradation of dissolved organic matter (DOM – Hélie 2004). It has also been observed that this DOM decomposes without any notable isotopic fractionation (^{13}C) and that the CO_2 produced in the reservoir has a ^{13}C value of -28 ‰ (the measured value across the Robert-Bourassa reservoir). The CO_2 in this reservoir, therefore, is enriched in ^{13}C relative to this latter value and the only source of isotopically "heavy" CO_2 is from the atmosphere. Therefore, the ^{13}C value of the measured CO_2 in the reservoir at steady state is the result of an isotopic mixture of isotopically "light" CO_2, stemming from DOM decomposition, and isotopically "heavy" CO_2 originating from the air above the reservoir (Fig. 14.2).

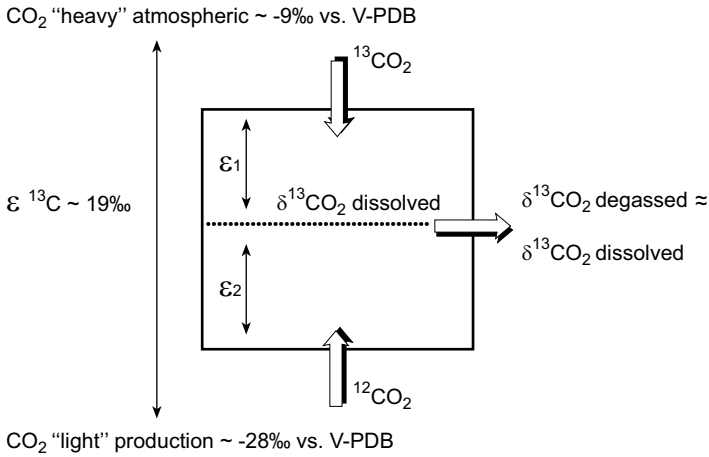

Fig. 14.2. Conceptual model of isotopic fluxes (^{13}C) in the Robert-Bourassa reservoir

The ratios of isotopic fluxes are reported as the ratios of the fractionation (δ) factors of each of the extremes of the mixture relative to the value of ^{13}C of dissolved CO_2 measured in the reservoir ($\delta^{13}CO_{2\ dissolved}$):

$$\frac{FCO_{2\ prod.}}{FCO_{2\ atm.\ eq.}} = \frac{\varepsilon_1}{\varepsilon_2} = \frac{\delta^{13}C_{degassed} - \delta^{13}C_{atm.\ eq.}}{\delta^{13}C_{prod.} - \delta^{13}C_{degassed}} \qquad (14.1)$$

Where: $FCO_{2\ prod.}$ is the isotopically "light" CO_2 flux produced from the decomposition of DOM; $FCO_{2\ atm.\ eq.}$ is the isotopically "heavy" CO_2 flux from the air above the reservoir; ε_1 is the isotopic separation factor between atmospheric CO_2 and the dissolved CO_2 measured in the reservoir

(degassed CO_2); ε_2 is the isotopic separation factor between the CO_2 produced from oxidation of DOM and the dissolved CO_2 measured in the reservoir (degassed CO_2); $\delta^{13}C_{degassed}$ is the value of the ^{13}C of CO_2 emitted from the surface of the reservoir (~$\delta^{13}C$ of dissolved CO_2 measured at the surface of the reservoir); $\delta^{13}C_{atm.\ eq.}$ is the value of ^{13}C of CO_2 dissolved in the water in equilibrium with the air above the reservoir (~$\delta^{13}C$ of global atmospheric $CO_2 \approx 8$ ‰ - ≤ 1 ‰); and $\delta^{13}C_{prod.}$ is the value of ^{13}C of CO_2 produced in the reservoir from the oxidation of DOM. The model is graphically represented in Fig. 14.3. It should be noted that the model output is not expressed as a flux but rather as a ratio of the isotopic fluxes. It, therefore, requires calibration in order to obtain a chemical flux of CO_2 at the air-water interface. This calibration is site specific as it strictly depends on the properties of the air-water interface (roughness).

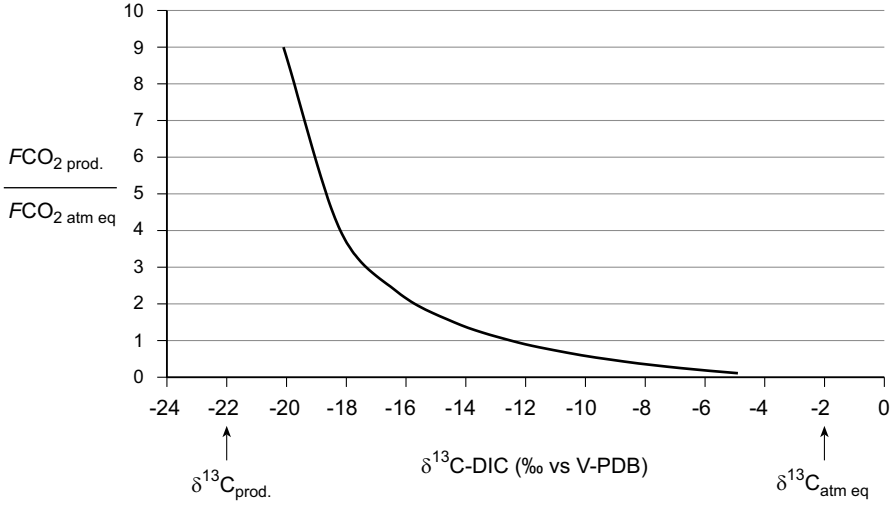

Fig. 14.3. Graphical representation of the isotopic mixing model at two extremes

14.4 Estimation of the $FCO_{2\ prod.}/FCO_{2\ atm.\ eq.}$ for the Robert-Bourassa Reservoir

In order to estimate the isotopic fluxes at the surface of the Robert-Bourassa reservoir using Eq. 14.1, we need to determine the following three ^{13}C values: $\delta^{13}C_{degassed}$, $\delta^{13}C_{prod,}$ and $\delta^{13}C_{atm.\ eq.}$. The ^{13}C value of the DIC from degassing can be measured directly from the surface water sample of the reservoir. The value of ^{13}C of CO_2 dissolved in the water in

equilibrium with the atmosphere can also be measured directly from the air sample taken above the reservoir. However, it has been shown that the atmospheric CO_2 above the Robert-Bourassa reservoir is depleted in ^{13}C relative to the average value (Hélie 2004). Since we attribute this depletion to ^{13}C depleted CO_2 degassing from the reservoir, we cannot use the otherwise very variable in nature values of atmospheric $\delta^{13}C$ CO_2 from just above the reservoir. Instead, we will use the average isotopic composition of global atmospheric CO_2, which is approximately -8 ‰ (anonymous 2001), and can constitute a maximum limit for the isotopic composition of atmospheric CO_2 involved in the exchanges at the interface. In all cases, the use of this value of -8 ‰ can only lead to a slight overestimation of the effluxing CO_2. Finally, it has also been determined that the DIC present in the Robert-Bourassa reservoir stems from the in situ decomposition of DOM (Hélie 2004) and that the measured ^{13}C value of CO_2 produced is, in fact, the same as that measured in the DOM. Similarly, it has been shown that photosynthetic activity alters very little, if any, of the ^{13}C values of DIC from the surface of the reservoir. We will, therefore, use the values of the ^{13}C of DIC measured for the degassing, those of DOC for the $\delta^{13}C_{prod.}$ and the average global value of atmospheric CO_2 for the $\delta^{13}C_{atm.\ eq.}$. One must, nonetheless, transform the values of the ^{13}C of CO_2 into $\delta^{13}C$ of DIC by partitioning the isotopic composition of CO_2 between CO_2 and bicarbonate (one can assume that the carbonate ions are negligible due to the pH) with the use of pH, temperature and alkalinity (see details in Clark and Fritz 1997). Therefore, Eq. 14.1 becomes:

$$\frac{FCO_{2\ prod.}}{FCO_{2\ atm.\ eq.}} \approx \frac{\delta^{13}C_{meas.\ DIC} - \delta^{13}C_{eq.\ DIC}}{\delta^{13}C_{prod.DIC.} - \delta^{13}C_{meas.\ DIC}} \qquad (14.2)$$

Where: $\delta^{13}C_{meas.\ DIC}$ is the measured value of ^{13}C of DIC measured in the surface water of the reservoir; $\delta^{13}C_{eq.\ DIC}$ is the value of ^{13}C of DIC in equilibrium with dissolved atmospheric CO_2; and $\delta^{13}C_{prod.DIC}$ is the value of ^{13}C of DIC in equilibrium with CO_2 stemming from the oxidation of the DOM (measured $\delta^{13}C$-DOC). During the summer campaigns of 2000 and 2001, we measured the values of ^{13}C of DIC and DOC in the surface waters of the Robert-Bourassa reservoir. The results of the values calculated from these data are presented in Table 14.1.

We identified zones of strong and weak CO_2 production in the Robert-Bourassa reservoir, where the values of ^{13}C of DIC are lower and higher, respectively (Hélie 2004). In order to estimate the average CO_2 flux from the whole reservoir, one must establish the mean contribution of fluxes from the production zone. These averages appear in the grey cells of Ta-

ble 14.1. *High mean* represents the average for the zone of high production and *low mean*, the average for the zone of low production.

Even though measurements were made during rough conditions, we only use the data collected during calm periods (and, hence, effective fluxes), since the system in not at steady state during rough conditions (Hélie 2004). Steady state conditions are necessary in order to use the model. Additionally, if these steady state conditions are observed, it is an indication that the chemical flux of CO_2 at the air-water interface is exclusively maintained by the production of CO_2 stemming from the oxidation of DOM in the reservoir and:

$$F^{13}CO_{2\ prod.} = FCO_{2\ prod.} \approx FCO_{2\ degassed} \tag{14.3}$$

Where: $F^{13}CO_{2\ prod.}$ is the isotopic flux due to the oxidation of DOM; $FCO_{2\ prod.}$ is the chemical flux due to the oxidation of DOM; and $FCO_{2\ degassed}$ is the chemical flux of CO_2 from degassing (emitted at the air-water interface).

14.5 Estimating $FCO_{2\ atm.\ eq}$ and Mean CO_2 Flux at the Air-Water Interface

The difference of ^{13}C values from the two end member mixtures is of about 19 ‰ ($\varepsilon^{13}C$ in Fig. 14.1). At such a scale, the entering flux, $F^{13}CO_{2\ atm.\ eq.}$, is equivalent to a theoretical CO_2 flux under atmospheric pressure in an aqueous environment whose pCO_2 is zero. Therefore:

$$F^{13}CO_{2\ atm.\ eq.} \approx FCO_{2\ atm.\ eq.} \tag{14.4}$$

The only method, of the three presented at the beginning of this chapter, which can be used to estimate $F^{13}CO_{2\ atm.\ eq.}$ and, therefore, $FCO_{2\ atm.\ eq.}$ is the one based on the gas diffusion equation at the air-water interface. The diffusion of a gas at the air-water interface is given by Fick's first law:

$$F = k \cdot \Delta c \tag{14.5}$$

Where: F is the gas flux across the air-water interface; k is the transfer coefficient; and Δc is the difference in the concentration of the gas on each side of the interface. Since the isotopic flux assumes a net flux without $^{13}CO_2$ in the reservoir, the chemical flux is calculated based on a zero concentration of CO_2 in the water. Since the CO_2 in the air above the reservoir surface was not measured, we use, as a first approximation, the mean

global value of 370 µatm (GLOBALVIEW-CO_2 2002). Therefore, Eq. 14.5 becomes:

$$F = k \cdot [(K_H \cdot [CO_2]_{air}) - 0] \quad (14.6)$$

Where: K_H is Henry's constant for the dissolution of CO_2 in water.

The transfer velocity (k) is, nonetheless, a lot more difficult to determine. In the literature it is known as the transfer coefficient, or the piston velocity, or the transfer velocity; and is usually expressed in cm h^{-1}. This value has no physical attribute but can be thought of as the height of water that is in equilibrium with the atmosphere at a given unit of time (Duchemin et al. 1999); and is a function of water turbulence (Jähne et al. 1987). The most common source of turbulence, in water surfaces, is the wind (Clark et al. 1995). Many studies have tried to link the k value to wind speed (McGillis et al. 2001; Jean-Baptiste and Poisson 2000; Cole and Caraco 1998; Hamilton et al. 1994; Wannikof 1992; Wannikof et al. 1991; Wannikof and Bliven 1991; Upstill-Goddard et al. 1990; Watson et al. 1991; Wannikof et al. 1987; Wannikof et al. 1985). Results from tunnel experiments suggest that three different linear relationships exist according to wind speed: one for wind speeds of less than 2–3 $m \cdot s^{-1}$; one for wind speeds between 2–3 and 11–13 $m \cdot s^{-1}$; and one for wind speeds above 11–13 m s^{-1}. The first break delineates the appearance of capillary waves (Livingstone 1993) and the second one delineates the appearance of breaking waves which draw air bubbles into the water (Broeker and Siems 1984). Although the relationship between wind speed and the transfer coefficient for winds of >3 m s^{-1} is satisfying in natural environments, it is almost always bad for low wind conditions (eg. Cole and Caraco 1998; Clark et al. 1995; Livingstone and Imboden 1993) for which very few data exist.

It is, nonetheless, possible to find in the literature estimates of the relationship between the transfer coefficient and low wind speeds. It is, however, not possible to estimate directly the transfer coefficient of CO_2 since it is not an inert gas and whose composition can be easily modified by biological activity and physico-chemical conditions. In natural environments, we evaluate the CO_2 transfer coefficient based on an inert gas: Sulfur Hexafluoride (SF_6). The transfer coefficients of these two gases are related through (Jähne et al. 1987):

$$\frac{K_{gas1}}{K_{gas2}} = \left(\frac{Sc_{gas1}}{Sc_{gas2}}\right)^{-n} \quad (14.7)$$

Where: k_1 and k_2 are the transfer coefficients of gases 1 and 2, respectively; Sc_1 and Sc_2 are the Schmidt numbers of gases 1 and 2, respectively and n is the Schmidt exponent. The Schmidt number is the ratio between

the kinematic viscosity of water and the coefficient of gas diffusion and it can be calculated for CO_2 with the application of the following relationship (Wannikof 1992):

$$S_{cCO2} = 1911.1 - (118.11 \cdot t) + (3.4527 \cdot t^2) - (0.041320 \cdot t^3) \qquad (14.8)$$

Where: t is the water temperature in °C. The transfer coefficient of SF_6 is almost always normalized to a Schmidt number of 600. The Schmidt exponent (n) seems to be dependent on water roughness. It is uniform for winds of less than 3 m s^{-1} where it takes a value of ⅔, and uniform for winds of more than 3 m s^{-1} where it takes a value of ½ (Jähne et al. 1987). Ensuing, the transfer coefficient (k) of CO_2 for calm conditions (winds < 3 m s^{-1}) can be calculated as follows:

$$k_{CO2} = k_{600} = \left(\frac{600}{Sc_{CO2}}\right)^{⅔} \qquad (14.9)$$

measured according to the water temperature of the reservoir and for a transfer coefficient of SF_6 normalized to a Schmidt number of 600. Herein, we calculate the transfer coefficient of CO_2 for the Robert-Bourassa reservoir according to two different estimates of k_{600} (Table 14.2). The wind speed was measured 2 m above the surface of the reservoir at each sampling station. Hence, the transfer coefficient calculated from the instantaneous wind speed gives an instantaneous value for the k_{600}. Since the values of ^{13}C of DIC take into account longer term carbon balances as compared with concentrations of dissolved CO_2 (eg. Broeker and Peng 1974; Szaran 1997), we need to calculate the k_{600} from a mean wind speed measured over the reservoir over a longer time period other than just on the day of sampling. Broeker and Peng (1974), for example, estimated that isotopic equilibration in the mixed layer of the ocean takes 150 times longer than for chemical equilibrium. We will, accordingly, estimate k_{600} based on wind speeds measured over a period of one month. The transfer coefficient will, hence, be more representative of the period of DIC isotopic equilibration, than that calculated from instantaneous wind speed. The average wind speed, measured at a height of 10 m above the Robert-Bourassa reservoir (u_{10}), was 3.64 m·s^{-1} and 4.13 m·s^{-1} for the months preceding the summer campaigns of 2000 and 2001, respectively. These averages were based on hourly measurements taken by Dr. Yves Bégin (Centre d'Études Nordiques de l'Université Laval) from three meteorological stations positioned on three islands in the Robert-Bourassa reservoir (Île Centrale, Île de Confusion and Île aux Neiges).

Table 14.2. Estimates of k_{600} based on mean monthly wind speeds (u) during the 2000 and 2001 summer field campaigns

		Equation	k_{600} [cm·hr^{-1}]	Reference
2000	a.	$k_{600} = 2.07 + 0.215 \cdot u_{10}^{1.7}$	4.00	Cole and Caraco (1998)
	b.	$k_{600} = 3.3 + 0.026 \cdot u_{10}^{3}$	4.55	McGillis et al. (2001)
2001	a.	$k_{600} = 2.07 + 0.215 \cdot u_{10}^{1.7}$	4.47	Cole and Caraco (1998)
	b.	$k_{600} = 3.3 + 0.026 \cdot u_{10}^{3}$	5.13	McGillis et al. (2001)

The majority of the equations which relate wind speed to the transfer coefficient take the form of:

$$k_{600} = a \cdot (u_{10})^b \tag{14.10}$$

Where: u_{10} is the wind speed measured 10 m above the surface of the water. This suggests that for a zero speed wind, the transfer coefficient is zero and that the flux across the air-water interface is also zero. This is very unlikely. On the other hand, in Table 14.2 it can be seen that the relationships have a non-zero k. Since the transfer coefficient is not zero, we can calculate a flux at zero wind speed. Relationships marked with a represent weaker transfer coefficients than those marked with b. Relationship a was determined from data taken from small lakes with surface areas of <1 km^2, while relationship b was determined from data from ocean surfaces. It seems that for a given wind speed, water roughness is greater in the ocean than in a small lake, a factor likely caused by fetch (eg. Jähne et al. 1987). Since the surface area of the Robert-Bourassa reservoir is quite large (2835 km^2) and its fetch is likely intermediate between the ocean and a small lake, it is reasonable to assume that k_{600} in this reservoir should correspond to values intermediate between relationship a and b.

It must be noted that while the transfer coefficients were estimated for a period longer than the sampling period, the dissolved CO_2 concentrations are instantaneous. It is, therefore, not possible to estimate mean annual emissions from the air-water interface with only measurements of dissolved CO_2 and the obtained transfer coefficient. Such estimates remain instantaneous, exactly the situation we are trying to avoid in this study. The model which uses stable isotopes to calculate fluxes, therefore, remains pertinent.

Nevertheless, based on relationships a and b in Table 14.2, the flux ratios ($FCO_{2\ prod.}/FCO_{2\ atm.\ eq.}$) in Table 14.1, and the relationships [14.2] to [14.10], we can calculate an average $FCO_{2\ prod.}$ for strong and weak CO_2 production rates during the 2000 and 2001 field campaigns. At steady state, assuming variation in the isotopic flux ratios (due to the variation in value of ^{13}C of DIC) and that the reservoir surface roughness lies between

those of small lakes and the ocean, in the summer of 2000 the Robert-Bourassa reservoir emitted 271±91 and 179±51 mg $CO_2 \cdot m^{-2} \cdot d^{-1}$ in the strong and weak production zones, respectively. In the summer of 2001 emissions were 544±169 and 348±88 mg $CO_2 \cdot m^{-2} \cdot d^{-1}$ in the strong and weak production zones, respectively.

These fluxes are low when compared to those measured from the same reservoir and at the same time of year as in 1993 by Duchemin (2000). When comparing the two zones of production described in the present study, Duchemin (2000) reports fluxes of 720±220, 680±290 and 720±925 mg $CO_2 \cdot m^{-2} \cdot d^{-1}$ in the weak production zone and 1370±890 mg $CO_2 \cdot m^{-2} \cdot d^{-1}$ in the strong production zone, in the month of August 1993. It is important to point out that we do not know if the measurements undertaken by Duchemin (2000) were taken under equilibrium conditions (steady state conditions), after strong winds or in intermediate conditions. Additionally, these fluxes were measured with the floating chamber technique, a method susceptible to overestimation of CO_2 fluxes relative to other measurement techniques. Measurements of CO_2 flux obtained in parallel with floating chambers (FC) and with the Thin Boundary Layer equation (TBL) in La Grande hydroelectric reservoir complex show that the FC fluxes are 2.5 times greater than those obtained with the TBL (Duchemin et al. 1999). Additionally, a recent study undertaken in a small experimental reservoir in Ontario which compared the two methods, showed that the fluxes obtained with FC were 9 to 23 times greater than those measured with TBL where k_{600} was determined with SF_6 (Matthews et al. 2003). One should note, however, that the FC used by Mathews et al. (2003), tends to slightly overestimate (~2 to 3 times) those reported by Duchemin (2000). The FC systems of Matthews et al. (2003) do not have the elongation underwater such as those of Duchemin (2000), which entrains a certain amount of relative movement of water under the most important chamber, hence, increasing turbulence which induces degassing and higher fluxes. No matter what the case, the fluxes measured by Duchemin (2000) still remain 2 to 3 times higher than those reported herein.

14.6 Estimate of the Mean Annual Diffusive CO_2 Flux from the Robert-Bourassa Reservoir

We estimate that each of the previously described production zones (strong and weak production) represents approximately half of the total surface area of the Robert-Bourassa reservoir (2835 km^2) (Hélie 2004). A link has been made between the zone of water circulation and the zones of strong

CO_2 production (determined from the values of ^{13}C of the DIC). The reservoir emitted an average of 225±51 and 446±93 mg $CO_2 \cdot m^{-2} \cdot d^{-1}$ during the summers of 2000 and 2001, respectively. Additionally, the surface of the reservoir is free of ice for ~150 days per year (Duchemin 2000). Following this, the reservoir emitted $(9.56 \pm 1.17) \cdot 10^{10}$ and $(18.97 \pm 3.96) \cdot 10^{10} \cdot g \cdot CO_2$ to the atmosphere by diffusion across the air-water interface in 2000 and 2001, respectively. The flux measured in stable conditions in August is, however, not necessarily representative of the whole ice-free period. Meanwhile, the annual balance calculated in 2001 and 2002 based on monthly time steps shows that the value of ^{13}C of the DIC is lower in June and higher in October compared to August (Hélie 2004). Therefore, the CO_2 flux in stable conditions should be overall higher in June and lower in October compared to August. For a first approximation, we assumed that the flux calculated for the month of August could provide an estimate of the mean flux for stable conditions for the whole 150 ice-free days.

14.7 Comments and Conclusions

The use of carbon stable isotopes to estimate annual CO_2 fluxes across the air-water interface has shown to be pertinent since the CO_2 isotopic residence time is much longer than its purely physico-chemical residence time. We know that the values of ^{13}C of DIC in lakes and reservoirs take into account the carbon balance over time periods longer than a month. Hence, an "isotopic" model to calculate the CO_2 fluxes at the air-water interface can be retained. The two end-members of the isotopic mixture used as inputs for the model were identified as, on the one hand, the CO_2 stemming from the oxidation of DOM in the reservoir (this would have the same isotopic composition as the DOC) and, on the other hand, the average global atmospheric CO_2 isotopic composition, resolved to be ~ -8‰. We also decided that it was easier to work with DIC instead of dissolved CO_2, since the CO_2 produced in the reservoir is divided between the different carbonate species and its isotopic composition is consequently altered. The isotopic model, therefore, presents an isotopic flux ratio $FCO_{2prod.}/FCO_{2atm.\ eq.}$, representative, respectively, of the isotopic fluxes produced in the reservoir and the isotopic flux entering an aquatic environment from atmospheric sources where the dissolved CO_2 concentration would be zero. It is, therefore, necessary to calibrate this flux ratio in order to obtain the chemical CO_2 flux at the air-water interface.

This calibration is made by estimating the isotopic flux entering the reservoir ($FCO_{2atm.\ eq}$). This was achieved by using the classic diffusion equa-

tion. In order to use this equation we had to estimate the transfer coefficient based on wind speed. Since the flux ratio accounts for carbon balance on a monthly basis, we had to use an average monthly wind speed measured at several points in the reservoir. Several equations exist that address the relationship between wind speed and the transfer coefficient. Nonetheless, only two equations exist, that produce a non-zero flux for a zero wind speed. One is based on the data taken from a small lake (Cole and Caraco 1998) and the other, based on data from the ocean (McGillis et al. 2001). It was assumed that the transfer coefficients in the reservoir were intermediate between those calculated for the small lake and the ocean. We, therefore, calculated minimum and maximum CO_2 fluxes at the air-water interface based on these relationships and took into account the different CO_2 production zones established elsewhere (Hélie 2004).

With the help of the isotopic model and the calibration of the flux ratios, we estimate that the Robert-Bourassa reservoir emitted, by diffusion across the air-water interface, between 225±51 and 446±93 mg $CO_2 \cdot m^{-2} \cdot d^{-1}$ during the summers of 2000 and 2001, respectively.

When attempting to estimate the average CO_2 flux across the air-water interface using carbon stable isotopes, one must first sample the water surface during stable conditions. It is not, necessarily, essential to measure during rough conditions, since it is considered a phenomenon which leads to the temporary decrease in dissolved CO_2 in the water column prior to a return to calm conditions. One must, however, map the areas of strong CO_2 production in order to establish the mean flux ratios which are representative of the whole water body. Finally, one must calibrate the flux ratio. The method presented herein, has the advantage of also accounting for the long-term carbon balance.

Table 14.3. Estimates of mean $FCO_{2prod.}$ for the regions of strong and weak CO_2 production during the 2000 and 2001 summer field campaigns

		Sc_{CO2} –	k_{600} [cm·hr^{-1}]	k_{CO2} [cm·hr^{-1}]	$[CO_2]_{sat}$ [mmol·cm^{-3}]	$F_{atm\ eq}$ [mmol·m^{-2}·d^{-1}]	$F_{atm\ eq}$/ F_{prod}	F_{prod} [mg·CO_2·m^{-2}·d^{-1}]
	2000							
a	strong	614.80	4.00	3.94	1.49E-05	14.08	0.42±0.06	217±37
b		614.80	4.55	4.78	1.49E-05	17.07	0.42±0.06	317±45
a	weak	596.47	4.00	4.02	1.46E-05	14.10	0.26±0.05	159±31
b		596.47	4.55	4.87	1.46E-05	17.10	0.26±0.05	192±38
	2001							
a	strong	631.61	4.47	4.32	1.51E-05	15.68	0.69±0.15	478±103
b		631.61	5.13	5.29	1.51E-05	19.20	0.69±0.15	585±127
a	weak	665.47	4.47	4.17	1.56E-05	15.63	0.45±0.07	308±48
b		665.47	5.13	5.10	1.56E-05	19.14	0.45±0.07	377±59

15 The Use of Carbon Mass Budgets and Stable Carbon Isotopes to Examine Processes Affecting CO_2 and CH_4 Production in the Experimental FLUDEX Reservoirs

Cory J.D. Matthews, Jason J. Venkiteswaran, Vincent L. St. Louis and Sherry L. Schiff

Abstract

The FLooded Uplands Dynamics EXperiment (FLUDEX) was initiated to quantify carbon dioxide (CO_2) and methane (CH_4) production in boreal reservoirs, and to better understand underlying biogeochemical processes (dissolved inorganic carbon [DIC] production, net primary production [NPP], methanogenesis, and CH_4 oxidation) governing CO_2 and CH_4 production in flooded boreal landscapes. The study experimentally flooded three upland boreal forest sites with different organic carbon (OC) storage in soils and vegetation over three seasons (June to September 1999-2001). Mass budgets of all reservoir inorganic carbon (inorganic C) and CH_4 inputs and outputs were calculated to quantify net reservoir CO_2 and CH_4 production, and isotopic ratio mass budgets were calculated to quantify biogeochemical processes controlling net reservoir CO_2 and CH_4 production.

The three reservoirs produced both CO_2 and CH_4 during each of the three flooding seasons, but neither CO_2 nor CH_4 production was related to overall mass of flooded OC. Net reservoir CO_2 production in the second and third flooding seasons (408 to 479 kg C ha^{-1}) was lower than in the first flooding season (703 to 797 kg C ha^{-1}), while reservoir CH_4 production steadily increased with each successive flooding season (from 3.2 to 4.6 kg C ha^{-1} in 1999 to 29.7 to 35.2 kg C ha^{-1} in 2001). Over three flooding seasons, NPP ranged from 77 to 273 kg C ha^{-1} and consumed 15 to 40% of gross reservoir CO_2 production. CH_4 oxidation was negligible during the first flooding season, but reduced gross reservoir CH_4 production

by 50% during the second flooding season, and by 70 to 88% during the third flooding season. However, despite decreases in net reservoir CO_2 production and increases in CH_4 oxidation over the study period, the overall total global warming potential (GWP) of the FLUDEX reservoirs remained constant due to successive increases in net CH_4 production.

15.1 Introduction

Hydroelectric power generation has become an attractive alternative to thermal power generation because it is widely accepted as a carbon-free source of energy (Hoffert et al. 1998; Victor 1998). However, emissions of the carbon-based greenhouse gases (GHGs) carbon dioxide (CO_2) and methane (CH_4) from reservoirs created for hydroelectric power generation and other purposes result from microbial decomposition of organic carbon (OC) stored in flooded soil and plant complexes. Moreover, flooded terrestrial plants no longer assimilate CO_2 through photosynthesis and flooded soils stop consuming CH_4, presenting additional burdens on atmospheric GHG levels. St. Louis et al. (2000) estimate reservoirs are responsible for 7% of the global warming potential (GWP) of all anthropogenic GHG emissions, and argue reservoir GHG emissions should be included in global carbon cycling models and national GHG inventories.

Approximately two-thirds of Canada's installed electrical energy generating capacity is hydroelectric based, with plans for expansion of current reservoir systems flooding boreal landscapes (Bodaly et al. 2004). Boreal forests act as a small CO_2 sink with respect to the atmosphere due to long-term carbon accumulation in soils (Schlesinger 1990), and dry upland boreal soils are an important sink for atmospheric CH_4 via microbial oxidation (Crill 1991; Amaral and Knowles 1997). While all boreal reservoirs studied to date emit both CO_2 and CH_4 to the atmosphere (Duchemin et al. 2000; Kelly et al. 1997; Rosenberg et al. 1997; St. Louis et al. 2000), the degree to which reservoirs influence atmospheric CO_2 and CH_4 levels is uncertain. Extensive pre-flood landscape CO_2 and CH_4 flux data from past studies (except for Kelly et al. 1997) is lacking, so our understanding of the net effect of reservoir creation on boreal landscapes is incomplete. Furthermore, GHG flux data alone provides no information on within-reservoir carbon cycling processes controlling GHG emissions.

Over the past decade, two long-term ecosystem-scale manipulations were conducted at the Experimental Lakes Area (ELA) in northwestern Ontario to assess the effects of reservoir creation on carbon dynamics in boreal landscapes. The Experimental Lakes Area Reservoir Project

(ELARP) was initiated to determine if reservoirs are significant sources of GHGs to the atmosphere by monitoring ecosystem carbon exchange in a lowland boreal wetland prior to and after flooding. The wetland, which theoretically provided a worst-case scenario for long-term decomposition and GHG production due to large OC stores held in peat, changed from a small carbon sink of approximately 7 $g{\cdot}C{\cdot}m^{-2}{\cdot}yr^{-1}$ before impoundment to a relatively large carbon source of 130 $g{\cdot}C{\cdot}m^{-2}{\cdot}yr^{-1}$ to the atmosphere after impoundment (Kelly et al. 1997). Continued monitoring of dissolved CO_2 and CH_4 in reservoir surface waters shows levels are still elevated, ten years after initial flooding (St. Louis et al. 2004).

The FLooded Uplands Dynamics EXperiment (FLUDEX) was designed as a companion experiment to the ELARP to examine the relationship between reservoir GHG production and OC storage in flooded soils and vegetation. Four biological processes governing net reservoir GHG production (gross dissolved inorganic carbon [DIC] production from decomposition, DIC consumption via net primary production [NPP], methanogenesis [CH_4 production], and CH_4 consumption via CH_4 oxidation) were quantified in three small experimental reservoirs flooding forests ranging in landscape OC storage. Regulated flooding of the three sites allowed for controlled monitoring of all reservoir inorganic carbon (inorganic C) and CH_4 inputs and outputs, and inorganic C and CH_4 mass budgets were constructed to quantify net GHG production in each of the FLUDEX reservoirs. Stable carbon isotopic ratios were determined for each of the budget terms to evaluate the relative contributions of gross DIC production, NPP, methanogenesis, and CH_4 oxidation to net reservoir GHG production.

15.2 Methods and Rationale

15.2.1 Study Site and Reservoir Construction

The FLUDEX was located at the Experimental Lakes Area (ELA) in northwestern Ontario (Fig. 15.1), where three upland forest sites differing in OC storage in vegetation and soils were chosen for flooding. The High C site (OC storage of 45860 kg C ha^{-1}) was characterized by a moist forest community (jack pine [*Pinus banksiana*], Labrador tea [*Ledum groenlandicum*], leatherleaf [*Chamaedaphne calyculata*] and *Sphagnum* spp.) and a drier upland area dominated by jack pine and *Polytrichum* spp. mosses (Table 15.1). The Medium C site (34390 kg C ha^{-1}) was comprised of a jack pine and birch (*Betula papyrifera*) forest, with an understory of

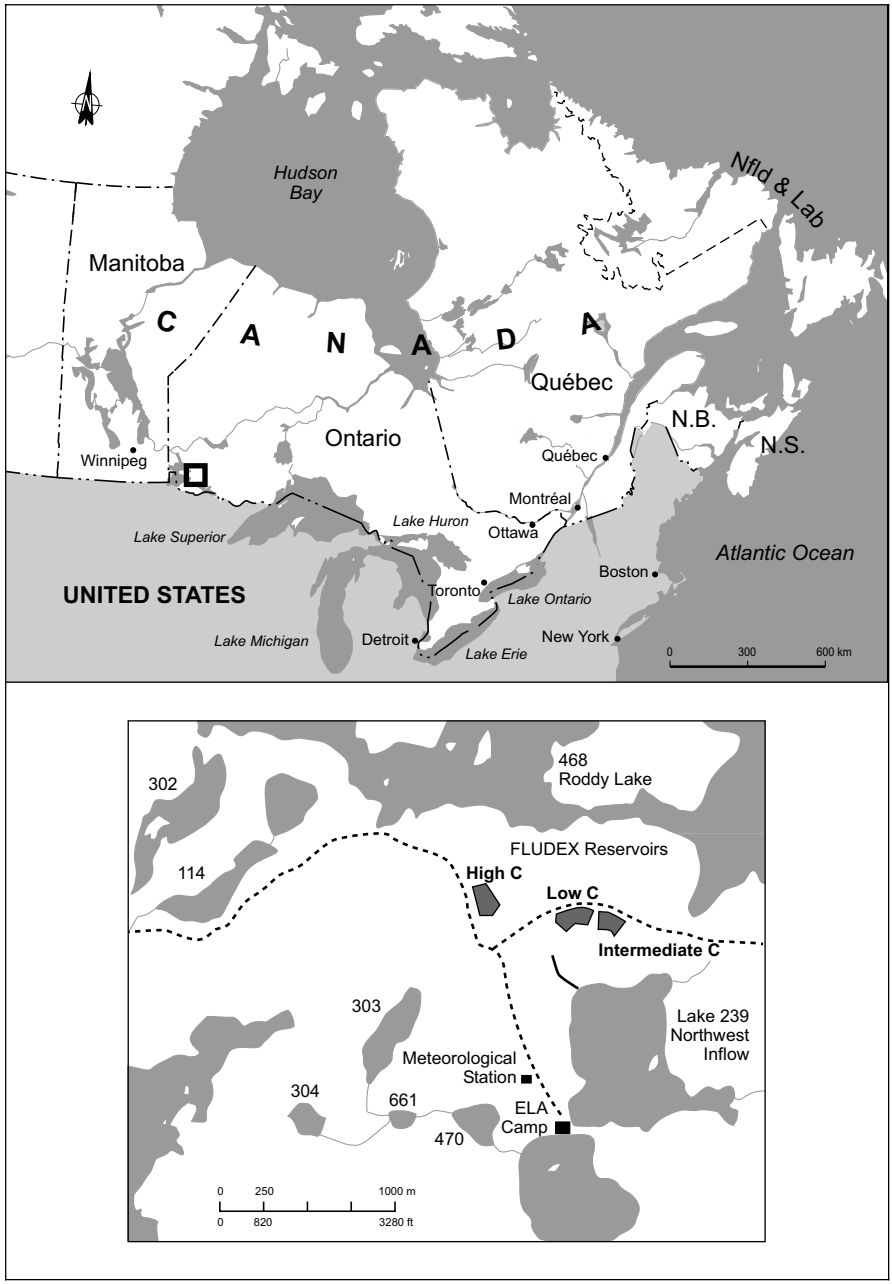

Fig. 15.1. Map of Ontario showing location of the ELA (top) and map showing the location of the FLUDEX reservoirs at the ELA (bottom)

Table 15.1. Summary of carbon stores in the FLUDEX sites prior to flooding

Dominant vegetation (percent coverage)[+]	High C Site *Pinus/Ledum/ Sphagnum* (53%) *Pinus/Polytrichum* (47%)	Medium C Site *Pinus/Betula* (100%)	Low C Site *Pinus/Vaccinium* (73%) *Polytrichum/ Cladina* (22%) Organic pillows (5%)
Carbon in trees[+] (kg C ha^{-1})	26210	27600	19570
in foliage (kg C ha^{-1})	1970	2730	1770
in bark (kg C ha^{-1})	2440	3760	1970
in wood (kg C ha^{-1})	21800	21110	15830
Carbon in shrubs[+] (kg C ha^{-1})	1350	130	200
Carbon in litter and fungal/ humic layer* (kg C ha^{-1})	15400	5700	8700
Carbon in mineral layer* (kg C ha^{-1})	2900	1500	2400
Total soil carbon (including litter)* (kg C ha^{-1})	18300	7200	11100
Total carbon in above ground vegetation[+] (kg C ha^{-1})	27560	27730	19770
Total carbon (kg C ha^{-1})	45860	34930	30870

Data marked [+] are from Heubert 1999 and data marked * are from Boudreau 2000

alder (*Alnus* spp.) and blueberry shrub (*Vaccinium* spp.), and a groundcover of various mosses and herbs (Table 15.1). The Low C site (30870 kg C ha^{-1}) contained a jack pine/blueberry shrub community, a lichen/exposed bedrock community, and an organic pillow community consisting of lichens (*Cladina* spp.), mosses (*Polytrichum* spp.), and some grasses (Table 15.1).

Wooden and gravel dikes were built along the low-lying contours of each site to create the reservoirs. Dikes were not built where the natural slope of the land exceeded flood height, creating 'shorelines' open to catchment input. During flooding seasons (June to September, 1999 to 2001), surface water from a nearby oligotrophic lake was pumped to the reservoirs via aluminium irrigation pipe. Water exited each reservoir via a gauged v-notch weir. Reservoir surface areas ranged from 5000 to 7400 m^2, and average depths ranged from 0.9 to 1.1 m (Table 15.2). Reservoirs were emptied from October to May to simulate seasonal fluctuations in water depth at the perimeter of large northern hydroelectric reservoirs.

Table 15.2. Physical characteristics of the FLUDEX reservoirs

	High C reservoir	Medium C reservoir	Low C reservoir
Water surface area (m^2)	7400	5000	6300
Catchment area (m^2)	47800	7300	900
Reservoir volume (m^3)	6870	4270	7120
Mean depth (m)	0.9	0.9	1.1

15.2.2 Theoretical Approach to Quantification of Net Reservoir CO_2 and CH_4 Production, Gross DIC Production and NPP, and CH_4 Production and CH_4 Oxidation

Decomposition of flooded soils and vegetation produced CO_2 and CH_4 that either dissolved into the reservoir water column (forming DIC and dissolved CH_4), or fluxed directly to the atmosphere via ebullition. Reservoir DIC was consumed via NPP and dissolved CH_4 was consumed via microbial CH_4 oxidation by methanotrophic bacteria. The balance of these processes governed net reservoir DIC and dissolved CH_4 production, and along with ebullition CO_2 and CH_4 fluxes, was considered net reservoir CO_2 and CH_4 production. Reservoir CO_2 and CH_4 production was determined from inorganic C and CH_4 mass budgets that included total reservoir inorganic C and CH_4 inputs (DIC and CH_4 added via pumped inflow water, precipitation, and catchment input) and total reservoir inorganic C and CH_4 outputs (DIC and CH_4 removed via outflow water, dike seepage/fracture flow, and drawdown; and diffusive surface and ebullition CO_2 and CH_4 fluxes) throughout the flooding season (Fig. 15.2). Inorganic C and CH_4 inputs and outputs were determined by multiplying dissolved DIC and CH_4 concentrations (measured frequently throughout the flooding seasons) in each of the budget components by water volumes entering and exiting the reservoirs (monitored throughout the flooding season using flow meters and v-notch weirs). CO_2 and CH_4 outputs via diffusive gas exchange were estimated using SF_6-derived gas transfer velocities and dissolved surface CO_2 and CH_4 concentrations, and CO_2 and CH_4 outputs via ebullition were measured directly. Total seasonal inorganic C and CH_4 inputs were subtracted from total seasonal inorganic C and CH_4 outputs to determine net reservoir CO_2 and CH_4 production during each flooding season.

Stable carbon isotopes analysis was used in conjunction with carbon mass budgets to quantify processes involved in net reservoir DIC and dissolved CH_4 production. Briefly, during physical, chemical, and biological processes, one of the two stable carbon isotopes (^{12}C and ^{13}C) is preferred or

discriminated against. This fractionation changes the relative proportion, or ratio, of the stable isotopes in a compound and imparts an isotopic signature reflective of the source and processes that formed the material (Kendall and Caldwell 1998). Furthermore, the isotopic composition of the remaining source material also reflects those processes. Analysis of DIC isotopic ratios gives information about the relative rates of gross DIC production from decomposition and DIC consumption via NPP. Similarly, CH_4 carbon isotopic ratios can be used to identify methanogenic pathways (Whiticar et al. 1986; Whiticar 1999) and CH_4 consumption via CH_4 oxidation.

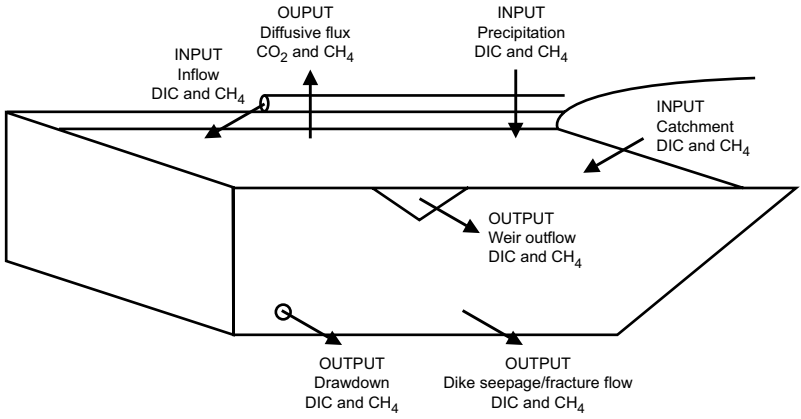

Fig. 15.2. Schematic of reservoir CO_2/DIC and CH_4 outputs incorporated in inorganic C and CH_4 mass budgets used to calculate net reservoir CO_2 and CH_4 production

Stable carbon isotopic ratios ($\delta^{13}C$) of components in the inorganic C and CH_4 budgets were either measured or estimated to construct DIC and dissolved CH_4 isotopic ratio mass budgets (direct emissions of CO_2 and CH_4 to the atmosphere via ebullition did not alter reservoir DIC/dissolved CH_4 concentrations or $\delta^{13}C$-DIC/$\delta^{13}C$-CH_4 values, so ebullition $\delta^{13}C$-CO_2/$\delta^{13}C$-CH_4 values were not included in isotopic ratio mass budgets). $\delta^{13}C$ values in pumped inflow water, catchment input, outflow water, and drawdown were measured, whereas $\delta^{13}C$ values in diffusive surface CO_2 and CH_4 fluxes, precipitation, and dike seepage and fracture flow were calculated/estimated. The difference between the isotopic ratio inputs and outputs yielded the carbon isotopic ratio of net DIC and dissolved CH_4 production.

Once net reservoir DIC and dissolved CH_4 production (i.e., excluding ebullition fluxes) were quantified using inorganic C and CH_4 mass budg-

ets, and the $\delta^{13}C$ value of net reservoir DIC and dissolved CH_4 production was calculated using DIC and dissolved CH_4 isotopic ratio mass budgets, $\delta^{13}C$ values were assigned to gross DIC production, NPP, methanogenesis, and CH_4 oxidation (see below) to quantify each process and determine its influence on net reservoir DIC and dissolved CH_4 production. Both gross DIC production and NPP were quantified using the following equation:

$$(\text{gross DIC mass} \times \delta^{13}\text{C gross DIC}) - (\text{NPP mass} \times \delta^{13}\text{C NPP}) = (\text{net DIC mass} \times \delta^{13}\text{C net DIC}) \quad (15.1)$$

where net DIC mass and $\delta^{13}C$ net DIC were calculated from mass and isotopic ratio mass budgets, $\delta^{13}C$ gross DIC and $\delta^{13}C$ NPP were assigned (see below), and gross DIC mass and NPP mass were calculated by substituting either of the following equations into Eq. 15.1 to solve for either gross DIC or NPP mass:

$$\text{gross DIC mass} = \text{net DIC mass} + \text{NPP mass} \quad (15.2)$$

$$\text{NPP mass} = \text{gross DIC mass} - \text{net DIC mass} \quad (15.3)$$

The percentage of CH_4 produced in the reservoirs that was oxidized was determined using the Rayleigh equation (Clark and Fritz 1997):

$$r = r_o \times f^{\alpha-1} \quad (15.4)$$

where r is the oxidized $\delta^{13}C$-CH_4 value (calculated from isotopic ratio mass budgets), r_o is the unoxidized $\delta^{13}C$-CH_4 value (experimentally determined; see below), α is the CH_4 oxidation enrichment factor (experimentally determined; see below), and f is the fraction of unoxidized CH_4 (remaining CH_4).

15.2.3 Inorganic C and CH_4 Mass Budgets and Stable Carbon Isotopic Ratio Mass Budgets

DIC and CH_4 concentrations and $\delta^{13}C$ values in pumped inflow water, precipitation, and catchment input. Inflow water was collected at midday for three consecutive days bi-weekly for DIC and CH_4 concentration analysis and weekly for $\delta^{13}C$-DIC analysis. Inflow CH_4 concentrations were not sufficient for $\delta^{13}C$-CH_4 analysis, so inflow $\delta^{13}C$-CH_4 values were calculated based on the $\delta^{13}C$ of atmospheric CH_4 (-47.4‰; Quay et al. 1999) (no fractionation correction was necessary). Inflow water volumes were quantified using an in-line flow meter attached to pipes transporting pumped inflow to the reservoirs. Bi-weekly DIC and CH_4 inputs via inflow were determined by multiplying average bi-weekly inflow DIC and CH_4

concentrations by inflow water volume over the two-week period, and summed to obtain seasonal inputs.

DIC and CH_4 inputs via precipitation were determined by multiplying precipitation volume over the flooding season by average precipitation DIC and CH_4 concentrations. Precipitation data were collected at the ELA meteorological station less than 1 km from the reservoirs. δ^{13}C-DIC in rain was calculated using fractionation factors between the various carbonate species (Clark and Fritz 1997) present at rain pH. The nearby ephemeral Lake 114 inflow stream (L114IF) was sampled as a substitute for catchment input DIC/CH_4 concentrations and δ^{13}C-DIC (L114IF CH_4 concentrations were not sufficient for δ^{13}C-CH_4 analysis). The soil and vegetation characteristics of the FLUDEX and L114 catchments were similar, as were δ^{13}C-DIC values. Seasonal DIC and CH_4 inputs via catchment input into the reservoirs were estimated by multiplying average L114IF DIC and CH_4 concentrations by total catchment input water volumes over the flooding season. Catchment water inputs were estimated by adjusting flow volume data collected at a nearby terrestrial flow monitoring site so that it was proportionate to reservoir catchment area.

DIC and CH_4 concentrations and δ^{13}C values in weir outflow, dike seepage/fracture flow, and drawdown. Water was collected for DIC and CH_4 concentration analysis midday at the outflow weir of each reservoir for three consecutive days bi-weekly, and weekly for δ^{13}C-DIC and δ^{13}C-CH_4 analysis. Weir outflow volumes were calculated using continuous stage level recorders located at the outflow weir of each reservoir. Bi-weekly DIC and CH_4 outputs via weir outflow were determined by multiplying average bi-weekly outflow DIC and CH_4 concentrations by outflow water volume over the two-week period, and summed to obtain seasonal outputs.

Dike seepage and bedrock fracture flow volumes were channelled into a gauged weir outside of each reservoir. Dike seepage and bedrock fracture flow could not be reliably sampled for DIC and CH_4 concentration and δ^{13}C analysis, so weir outflow DIC and CH_4 concentrations were used to estimate seasonal DIC and CH_4 loss via dike seepage and bedrock fracture flow. These estimates were conservative because weir outflow DIC and CH_4 concentrations were lower than DIC and CH_4 concentrations in bottom and porewater that contributed to seepage and fracture flow. δ^{13}C values of routinely collected surface water (monthly) and outflow water (weekly) represented dike seepage and bedrock fracture flow components in the isotopic ratio mass budgets.

DIC and CH_4 outputs during drawdown were estimated by multiplying water column DIC and CH_4 concentrations at 20 cm increments starting 2 cm above the soil/water interface (SWI) by volumes corresponding to

each of those depth profiles (determined from reservoir storage-discharge curves). Carbon storage in each depth profile was then summed to obtain the total amount of carbon in the reservoirs at the time of drawdown. $\delta^{13}C$ values were also measured at corresponding depths throughout the water column to quantify the drawdown term in isotopic ratio mass budgets.

Diffusive surface and ebullition CO_2 and CH_4 fluxes, and $\delta^{13}C$ of gas exchange. Sulfur hexafluoride (SF_6) gas was used to determine gas transfer coefficients (k) at the surface of each reservoir, which were then used with dissolved surface CO_2 and CH_4 concentrations (measured for three consecutive days bi-weekly) to estimate diffusive CO_2 and CH_4 fluxes (Matthews et al. 2003). CO_2 and CH_4 fluxes over each two-week period were summed to determine seasonal CO_2 and CH_4 losses via surface diffusion. $\delta^{13}C$ values for diffusive CO_2 and CH_4 gas exchange were calculated from surface water DIC concentration and $\delta^{13}C$ data. Reservoir $\delta^{13}C$-DIC values, pH, temperature, and fractionation factors between carbonate species (Clark and Fritz 1997) were use to calculate gas exchange $\delta^{13}C$-CO_2 values. No pH or temperature correction was needed for $\delta^{13}C$-CH_4.

To quantify ebullition, five bubble traps (inverted stoppered funnels) were deployed continuously on the reservoir surface. Bubble accumulation in the traps was measured weekly to bi-weekly, at which time fresh bubbles were collected for CO_2/CH_4 concentration and $\delta^{13}C$-CO_2/$\delta^{13}C$-CH_4 analysis by disturbing the flooded soils with a pole. Bubble CO_2 and CH_4 concentrations were multiplied by the volume of accumulated bubbles over the deployment period to determine CO_2 and CH_4 ebullition fluxes. Seasonal CO_2 and CH_4 losses via ebullition flux were determined by summing CO_2 and CH_4 losses over each deployment period.

15.2.4 $\delta^{13}C$ Values of Gross DIC Production, NPP, CH_4 Production and Oxidation

Gross DIC production. While gross DIC production encompasses all DIC generating processes in the reservoirs (decomposition of soil and vegetation, DOC mineralization, UV photodegradation of DOC to CO_2, and photorespiration), flooded soils and vegetation were expected to be the main source of reservoir DIC because they contained large OC stores available for decomposition (comparatively small amounts of OC were available for decomposition via either inflow or catchment DOC inputs [see below]). Gross DIC production was therefore assigned a $\delta^{13}C$ value reflecting flooded soil and vegetation $\delta^{13}C$ values. Prior to flooding, soil cores and samples of common plant species were collected for $\delta^{13}C$ analysis from 5 to 25 locations in each site.

δ^{13}C-DIC values added to the reservoir across the SWI were independently assessed using submerged benthic chambers deployed on flooded soil surfaces. 'Dark' chambers, covered in foil to omit light, were deployed alongside 'light' (transparent) chambers. Chamber water samples were collected at the beginning and end of a four to six hour period for δ^{13}C-DIC analysis to determine the δ^{13}C value of DIC entering the water column from flooded soils. Transparent chamber fluxes incorporated photosynthetic uptake of CO_2, and the resulting δ^{13}C-DIC value reflected photosynthesis occurring within the chamber (i.e., daytime soil fluxes). δ^{13}C of dark chamber DIC, however, represented fluxes unaltered by photosynthesis (nighttime fluxes), and should more closely match δ^{13}C values of decomposing soils and vegetation.

Net primary production. Reservoir NPP was assigned a δ^{13}C-DIC value based on calculated δ^{13}C-CO_2 values (from reservoir δ^{13}C-DIC values) and photosynthetic fractionation. The photosynthetic enrichment factor should equal -19‰ if reservoir periphyton, the dominant photoautotroph community in the reservoirs, were not CO_2-limited (Hecky and Hesslein, 1995). Algae were not likely CO_2-limited because reservoir DIC concentrations were 250 to 400 μmol L^{-1} and pH ranged from 6.0 to 6.5.

The photosynthetic enrichment factor used to calculate NPP δ^{13}C-DIC values was verified by measuring isotopic ratios in reservoir periphyton. Since photosynthetic fractionation will cause algae to have lower δ^{13}C values than reservoir δ^{13}C-DIC, comparing the δ^{13}C values in periphyton and reservoir δ^{13}C-DIC yields the photosynthetic enrichment factor. Periphyton was collected monthly from pine dowels hung at five sites in each reservoir to act as surrogate substrate for periphyton, and analysed for δ^{13}C. Periphyton collected from tree branches after reservoir drawdown was also analysed for δ^{13}C.

CH_4 production and CH_4 oxidation. Each methanogenic pathway produces CH_4 with an isotopic ratio specific to that pathway. Methyl-type fermentation results in δ^{13}C-CH_4 values of -35‰ to -25‰ different from source compounds, while CH_4 produced via CO_2 reduction has δ^{13}C-CH_4 values -55‰ from source CO_2 (Whiticar 1999). Soil and vegetation samples collected for δ^{13}C analysis prior to flooding (see gross DIC production section) provided the δ^{13}C value of source compounds for methyl-type fermentation.

CH_4 oxidation increases the δ^{13}C-CH_4 of the remaining CH_4 (Raleigh fractionation), and the percentage of original CH_4 that was oxidized can be calculated from δ^{13}C-CH_4 values prior to oxidation and the CH_4 oxidation enrichment factor. Water from dark benthic flux chambers (CH_4 oxidation is light-mediated; King 1990) and anoxic porewater δ^{13}C-CH_4 values provided the best reference for unoxidized δ^{13}C-CH_4 values. Water was col-

lected from light and dark submerged benthic chambers (see gross DIC production methods) for δ^{13}C-CH_4 analysis. The CH_4 fractionation factor was determined experimentally using water from the FLUDEX reservoirs to set up methanotroph incubations (Venkiteswaran and Schiff 2004). Porewater and water column samples were also collected for δ^{13}C-CH_4 analysis to assess differences in δ^{13}C-CH_4 below and across the SWI, and throughout the water column.

15.2.5 Analytical Methods

DIC/CO_2 and CH_4 concentrations. All water and gas samples collected for CO_2/DIC and CH_4 concentration analysis were analysed using a Varian 3800 gas chromatograph (GC) equipped with a flame ionization detector (FID) and a ruthenium methanizer. Six or seven standards ranging from 75 to 1000 ppm for CO_2 and 1.6 to 75 ppm for CH_4 were used to calibrate the GC. Standard calibration curves with an $r^2 > 0.99$ were accepted for analyses and a standard was analysed after every 10 samples to check the GC calibration. Analytical precision was ±10% for both CO_2 and CH_4. Duplicate injections of gas samples showed results to be reproducible within <±5%.

DIC/CO_2 and CH_4 Stable Isotopic Ratios. All analyses for δ^{13}C-DIC/CO_2 and δ^{13}C-CH_4 were performed on a gas chromatograph-combustion-isotopic ratio mass spectrometer (GC-C-IRMS). CH_4 was combusted to CO_2 in a Micromass combustion furnace, after which the two pulses of CO_2 flowed into a MicroMass Isochrom IRMS where masses 44, 45, and 46 were measured. Analysis of each sample was performed in duplicate and was framed by two automated pulses of reference gas. An isotopic ratio standard was analysed after no more than ten samples. Precision of δ^{13}C-DIC/CO_2 analysis was ±0.3‰ and ±0.5‰ for δ^{13}C-CH_4 analysis. Analysis of isotopic ratios in soil, vegetation, and periphyton were performed on an elemental analyzer-isotopic ratio mass spectrometer (EA-IRMS). Precision of δ^{13}C analysis was ±0.2‰. Isotopic ratios are reported in delta notation (δ), as per mil (‰) values relative to Vienna Pee Dee Belemnite (VPDB).

15.3 Results and Discussion

15.3.1 Inorganic C and CH_4 Budgets and Net Reservoir CO_2 and CH_4 Production

DIC and CH_4 concentrations in inflow water were similar during all three flooding seasons (Table 15.3). Average DIC and CH_4 concentrations in catchment input into the High C reservoir over 1999 to 2001 were 690 ± 140 and 0.7 ± 0.1 μmol L^{-1}, respectively. Average DIC concentration in precipitation over 1999 to 2001 was 40 ± 20 μmol L^{-1}; CH_4 levels were below the detection limit of 0.01 μmol L^{-1}. Outflow DIC concentrations decreased with each flooding season, while outflow CH_4 concentrations generally increased with each flooding season (Table 15.3). Diffusive surface CO_2 fluxes were highest during the first year of flooding, but decreased in the second and third flooding seasons (Table 15.3). Contrarily, surface diffusive CH_4 fluxes increased with each successive flooding season (Table 15.3). During the first flooding season, ebullition CO_2 and CH_4 fluxes were negligible, but increased during the second and third flooding seasons (Table 15.3).

Total inorganic C and CH_4 outputs (outflow, seepage, drawdown, diffusive surface flux, and ebullition flux) were always greater than total reservoir inorganic C and CH_4 inputs (inflow, precipitation, and catchment input) in all three reservoirs during each flooding season (indicating the FLUDEX reservoirs were net CO_2 and CH_4 producers during each flooding season). However, neither net CO_2 nor net CH_4 production was related to overall OC storage in the flooded sites. Net reservoir CO_2 production (i.e., including ebullition) in 1999 was 703, 797, and 704 kg C ha^{-1} in the High, Medium, and Low C reservoirs (Table 15.4). In 2000, net reservoir CO_2 production was 479, 408, and 470 kg C ha^{-1} in the High, Medium, and Low C reservoirs. In 2001, net reservoir CO_2 production was 445, 478, and 414 kg C ha^{-1} in the High, Medium, and Low C reservoirs. With the exception of the Medium C reservoir in 2000 and 2001, net CO_2 production declined in all reservoirs with each flooding season (Table 15.4).

Unlike net reservoir CO_2 production, net reservoir CH_4 production steadily increased with each successive flooding season (Table 15.5). Net reservoir CH_4 production (including ebullition) in 1999 was 4.6, 3.2, and 3.5 kg C ha^{-1} in the High, Medium, and Low C reservoirs. In 2000, net reservoir CH_4 production was 16.8, 12.8, and 24.9 kg C ha^{-1} in the High, Medium, and Low C reservoirs. In 2001, net reservoir CH_4 production was 30.5, 29.7, and 35.2 kg C ha^{-1} in the High, Medium, and Low C reservoirs

Table 15.3. Summary of DIC and dissolved CH_4 in reservoir inflow, outflow, and surface water, and of surface diffusive and ebullition CO_2 and CH_4 fluxes from the FLUDEX reservoirs during all three flooding seasons (values are means ± std deviation)

	High C Reservoir			Medium C Reservoir			Low C Reservoir		
	1999	2000	2001	1999	2000	2001	1999	2000	2001
Inorganic C									
Inflow DIC ($\mu mol \cdot L^{-1}$)	130 ± 3	126 ± 6	120 ± 6	130 ± 3	126 ± 6	120 ± 6	130 ± 3	126 ± 6	120 ± 6
Outflow DIC ($\mu mol \cdot L^{-1}$)	380 ± 40	340 ± 40	240 ± 50	430 ± 75	290 ± 60	260 ± 25	320 ± 50	250 ± 30	190 ± 10
Surface CO_2 ($\mu mol \cdot L^{-1}$)	260 ± 10	180 ± 30	140 ± 30	290 ± 10	150 ± 40	130 ± 20	190 ± 10	110 ± 30	85 ± 10
Surface diffusion ($mg \cdot CO_2 \cdot m^{-2} \cdot d^{-1}$)	1390 ± 120	970 ± 310	1150 ± 280	1010 ± 190	590 ± 240	660 ± 200	1240 ± 230	730 ± 400	860 ± 200
Ebullition ($mg \cdot CO_2 \cdot m^{-2} \cdot d^{-1}$)	0.03 ± 0.04	1.7 ± 2.5	7.7 ± 8.2	0.4 ± 0.5	1.3 ± 1.9	6.1 ± 5.2	0.0	2.9 ± 3.6	6.0 ± 5.7
CH_4									
Inflow ($\mu mol \cdot L^{-1}$)	0.11 ± 0.04	0.11 ± 0.03	0.13 ± 0.03	0.11 ± 0.04	0.11 ± 0.03	0.13 ± 0.03	0.11 ± 0.04	0.11 ± 0.03	0.13 ± 0.03
Outflow ($\mu mol \cdot L^{-1}$)	1.1 ± 1.2	3.6 ± 2.1	2.5 ± 1.7	0.9 ± 0.9	3.3 ± 1.3	4.3 ± 2.1	0.7 ± 0.7	2.2 ± 1.0	3.2 ± 0.6
Surface ($\mu mol \cdot L^{-1}$)	1.4 ± 0.1	3.3 ± 2.4	3.6 ± 3.2	0.8 ± 0.03	2.2 ± 1.4	2.5 ± 1.7	0.7 ± 0.04	1.9 ± 1.2	2.5 ± 0.8
Surface diffusion ($mg \cdot CH_4 \cdot m^{-2} \cdot d^{-1}$)	2.6 ± 2.9	7.4 ± 5.4	9.5 ± 4.6	1.0 ± 1.2	3.4 ± 2.3	5.2 ± 3.4	1.7 ± 2.0	5.3 ± 4.0	10.6 ± 4.0
Ebullition ($mg \cdot CH_4 \cdot m^{-2} \cdot d^{-1}$)	0.1 ± 0.02	7.0 ± 10.0	30.7 ± 34.0	0.1 ± 0.3	5.2 ± 9.5	26.6 ± 23.3	0.0	17.5 ± 22.1	29.1 ± 28.3

(Table 15.5). The year-to-year increase in CH_4 emissions in the FLUDEX reservoirs is important because including direct and indirect effects, CH_4 is 23 times more effective as a GHG than CO_2 over a 100 year period (Dentener et al. 2001). Therefore, over three seasons, relatively small increases in CH_4 production offset larger decreases in CO_2 production from a GWP perspective (Fig. 15.3).

15.3.2 Gross Reservoir DIC Production and Consumption Via NPP

Outflow δ^{13}C-DIC values were always more negative than inflow values (Table 15.6), indicating DIC with a δ^{13}C value more negative than that in inflow was added within the reservoirs. Pre-flood soil and vegetation δ^{13}C values ranged from -30‰ to -26‰. While some studies report little or no fractionation during heterotrophic decomposition of soil organic carbon (Flanagan and Ehleringer 1998; Lin and Ehleringer 1997), others have shown selective decomposition of soil components and/or fractionation during early stages of decomposition produces δ^{13}C-DIC values different from source material (Fogel and Cifuentes 1993). Laboratory incubations of soil and vegetation from FLUDEX reference sites indicated DIC produced in the early stages of soil decomposition was 2 to 3‰ greater than source soil OC (Baril 2001; Boudreau 2000; Venkiteswaran unpublished data). To reflect the slight enrichment observed in laboratory incubations, gross DIC production was assigned a δ^{13}C value of -27‰ for inorganic C isotopic ratio mass budget calculations.

Gross reservoir DIC production quantified using Eqs. 15.1 and 15.2 indicated that over the first three flooding seasons, reservoir DIC production was not related to initial landscape OC storage. However, there was a noticeable temporal trend in reservoir DIC production, with values decreasing from the first to third flooding seasons (Table 15.4). In 1999, gross DIC production was 851 kg C ha^{-1}, 969 kg C ha^{-1}, and 849 kg C ha^{-1} in the High, Medium, and Low C reservoirs, respectively. In 2000, gross DIC production was 661 kg C ha^{-1}, 633 kg C ha^{-1}, and 680 kg C ha^{-1} in the High, Medium, and Low C reservoirs. In 2001, gross DIC production was similar to in 2000, with the High, Medium, and Low C reservoirs producing 520 kg C ha^{-1}, 657 kg C ha^{-1}, and 686 kg C ha^{-1}, respectively (Table 15.4).

Net DIC production δ^{13}C-DIC values determined from inorganic C isotopic ratio mass budgets ranged from -24.8‰ to -20.1‰ (Table 15.4). Net DIC production δ^{13}C-DIC values were therefore not similar to soil or

Table 15.4. Inorganic C mass budget/isotopic ratio mass budget of total seasonal inorganic C inputs and outputs into the FLUDEX reservoirs in 1999, 2000, and 2001

	High C Reservoir mass (kg C ha^{-1}) and $\delta^{13}C$ (‰)						Medium C Reservoir mass (kg C ha^{-1}) and $\delta^{13}C$ (‰)						Low C Reservoir mass (kg C ha^{-1}) and $\delta^{13}C$ (‰)					
	1999		2000		2001		1999		2000		2001		1999		2000		2001	
Inputs																		
Inflow	169	-3.4	194	-8.7	167	-7.0	248	-3.4	217	-8.7	222	-6.9	248	-3.4	268	-8.8	251	-6.9
Precipitation	0	-8.0	1	-8.0	0	-8.0	0	-8.0	1	-8.0	0	-8.0	0	-8.0	1	-8.0	0	-8.0
Catchment input	41	-25.7	128	-25.7	56	-25.7	8	-25.7	29	-25.7	13	-25.7	0	-25.7	2	-25.7	1	-25.7
Total inputs	210	-7.8	323	-15.5	223	-11.6	256	-4.1	247	-10.7	235	-8.0	248	-3.5	271	-8.9	252	-7.0
Outputs																		
Diffusive flux	389	-25.5	278	-21.4	324	-25.0	263	-26.1	162	-19.4	188	-24.2	337	-24.7	216	-21.3	210	-18.8
(range)	(370 to 407)		(263 to 293)		(301 to 346)		(252 to 273)		(153 to 171)		(174 to 200)		(316 to 359)		(210 to 222)		(194 to 226)	
Weir outflow	378	-16.5	407	-17.9	249	-15.9	602	-16.9	369	-15.5	406	-15.3	194	-15.7	196	-14.9	185	-13.6
Wall seepage	101	-16.6	84	-17.9	58	-15.9	155	-17.1	101	-15.9	88	-15.3	147	-15.7	88	-15.3	51	-13.6
Fracture flow	0	n/a	0	n/a	0	n/a	0	n/a	0	n/a	0	n/a	233	-15.7	199	-15.3	172	-13.6
Drawdown	45	-17.0	33	-15.0	35	-17.0	33	-16.0	23	-16.7	30	-14.0	41	-16.0	41	-16.0	47	-12.0
Total outputs	913 (894 to 931)	-20.4	802 (787 to 817)	-19.0	666 (643 to 688)	-20.4	1053 (1042 to 1063)	-19.2	655 (646 to 664)	-16.6	712 (698 to 724)	-17.6	952 (931 to 974)	-18.9	740 (734 to 746)	-17.0	665 (649 to 681)	-15.1
Net DIC production	703 (684 to 721)	-24.2	479 (464 to 494)	-21.4	443 (420 to 465)	-24.8	797 (786 to 807)	-24.0	408 (399 to 417)	-20.1	477 (463 to 489)	-22.4	704 (683 to 726)	-24.4	469 (463 to 475)	-21.7	413 (397 to 429)	-20.1
Gross DIC production	851 (832 to 869)	-27.0	661 (646 to 676)	-27.0	520 (497 to 542)	-27.0	969 (958 to 979)	-27.0	633 (624 to 642)	-27.0	657 (643 to 669)	-27.0	849 (828 to 871)	-27.0	680 (674 to 686)	-27.0	686 (670 to 702)	-27.0

Table 15.4. (cont.)

	High C Reservoir mass (kg C ha^{-1}) and $\delta^{13}C$ (‰)						Medium C Reservoir mass (kg C ha^{-1}) and $\delta^{13}C$ (‰)						Low C Reservoir mass (kg C ha^{-1}) and $\delta^{13}C$ (‰)					
	1999		2000		2001		1999		2000		2001		1999		2000		2001	
Net primary production	148	-40.4	182	-41.8	77	-39.8	172	-40.8	225	-39.4	180	-39.3	145	-39.7	211	-38.9	273	-37.5
Ebullition (range)	0.01 (0.01 to 0.01)	-25.2	0.48 (0.21 to 0.74)	-16.4	1.77 (1.00 to 2.54)	-13.6	0.07 (0.07 to 0.07)	-26.5	0.43 (0.22 to 0.64)	-17.5	1.48 (0.71 to 2.25)	-14.2	0	n/a	0.84 (0.57 to 1.11)	-14.7	1.46 (0.91 to 1.99)	-16.4
Net CO_2 production (Net DIC production + Ebullition)	703 (684 to 721)		479 (464 to 495)		445 (421 to 468)		797 (786 to 807)		408 (399 to 418)		478 (464 to 491)		704 (683 to 726)		470 (464 to 476)		414 (398 to 431)	
Gross CO_2 production (Gross DIC production + Ebullition)	851 (832 to 869)		661 (646 to 677)		522 (498 to 545)		969 (958 to 979)		633 (624 to 643)		658 (644 to 671)		849 (828 to 871)		681 (675 to 687)		687 (671 to 704)	

Table 15.5. CH_4 mass budget/isotopic ratio mass budget of total seasonal CH_4 inputs and outputs into the FLUDEX reservoirs in 1999, 2000, and 2001

	High C Reservoir mass ($kg{\cdot}C{\cdot}ha^{-1}$) and $\delta^{13}C$ (‰)						Medium C Reservoir mass ($kg{\cdot}C{\cdot}ha^{-1}$) and $\delta^{13}C$ (‰)						Low C Reservoir mass ($kg{\cdot}C{\cdot}ha^{-1}$) and $\delta^{13}C$ (‰)					
	1999		2000		2001		1999		2000		2001		1999		2000		2001	
Inputs																		
Inflow	0.1	-47.4	0.1	-47.4	0.2	-47.4	0.2	-47.4	0.2	-47.4	0.2	-47.4	0.2	-47.4	0.2	-47.4	0.2	-47.4
Precipitation	0.0	n/a	0.0	n/a	0.0	n/a	0.0	n/a	0.0	n/a	0.0	n/a	0.0	n/a	0.0	n/a	0.0	n/a
Catchment input	0.0	n/a	0.0	n/a	0.0	n/a	0.0	n/a	0.0	n/a	0.0	n/a	0.0	n/a	0.0	n/a	0.0	n/a
Total inputs	0.1	-47.4	0.1	-47.4	0.2	-47.4	0.2	-47.4	0.2	-47.4	0.2	-47.4	0.2	-47.4	0.2	-47.4	0.2	-47.4
Outputs																		
Diffusive flux (range)	2.7 (2.5 to 2.9)	-72.3	5.7 (5.2 to 6.2)	-55.2	7.3 (6.0 to 8.5)	-37.7	1.0 (1.0 to 1.0)	-89.5	2.7 (2.4 to 3.0)	-68.0	4.0 (3.5 to 4.6)	-50.1	1.9 (1.7 to 2.2)	-80.2	4.2 (4.1 to 4.4)	-57.0	7.1 (6.6 to 7.5)	-49.3
Weir outflow	1.4	-72.3	4.3	-53.9	2.8	-40.7	1.7	-89.2	4.6	-64.8	6.0	-50.1	0.6	-79.9	1.8	-56.2	3.1	-50.4
Wall seepage	0.3	-72.3	0.9	-55.1	0.9	-36.8	0.4	-89.2	0.9	-67.8	1.2	-50.6	0.4	-79.9	1.0	-53.5	0.7	-50.0
Fracture flow	0.0	n/a	0.0	n/a	0.0	n/a	0.0	n/a	0.0	n/a	0.0	n/a	0.6	-79.9	2.3	-53.5	2.4	-50.0
Drawdown	0.3	-72.3	0.4	-50.0	0.6	-37.0	0.2	-89.2	0.4	-52.0	0.6	-48.0	0.2	-79.9	1.1	-60.0	2.2	-48.0
Total outputs	4.7 (4.5 to 4.9)	-72.3	11.3 (10.8 to 11.8)	-54.5	11.6 (10.3 to 12.8)	-38.3	3.3 (3.3 to 3.3)	-89.3	8.6 (8.3 to 8.9)	-65.6	11.8 (11.3 to 12.4)	-50.0	3.7 (3.5 to 4.0)	-80.1	10.4 (10.3 to 10.6)	-56.1	15.5 (15.0 to 15.9)	-49.5
Net dissolved CH_4 production	4.6 (4.4 to 4.8)	-73.0	11.2 (10.7 to 11.7)	-54.6	11.4 (10.1 to 12.6)	-38.2	3.1 (3.1 to 3.1)	-92.1	8.4 (8.1 to 8.7)	-65.9	11.6 (11.1 to 12.2)	-50.1	3.5 (3.3 to 3.8)	-82.0	10.2 (101. to 10.4)	-56.2	15.3 (14.8 to 15.7)	-49.5
Ebullition (range)	0.0 (0.0 to 0.0)	-72.3	5.6 (2.5 to 8.7)	-54.2	19.1 (11.5 to 26.7)	-55.4	0.1 (0.1 to 0.1)	-89.2	4.4 (2.5 to 6.2)	-49.7	18.1 (8.2 to 27.8)	-53.5	0.0	n/a	14.7 (11.0 to 18.4)	-48.4	19.9 (13.5 to 25.9)	-55.9
Net CH_4 production (net dissolved CH_4 production + ebullition)	4.6 (4.4 to 4.8)		16.8 (13.2 to 20.4)		30.5 (21.6 to 39.3)		3.2 (3.2 to 3.2)		12.8 (10.6 to 14.9)		29.7 (19.3 to 40.0)		3.5 (3.3 to 3.8)		24.9 (21.1 to 28.8)		35.2 (28.3 to 41.6)	

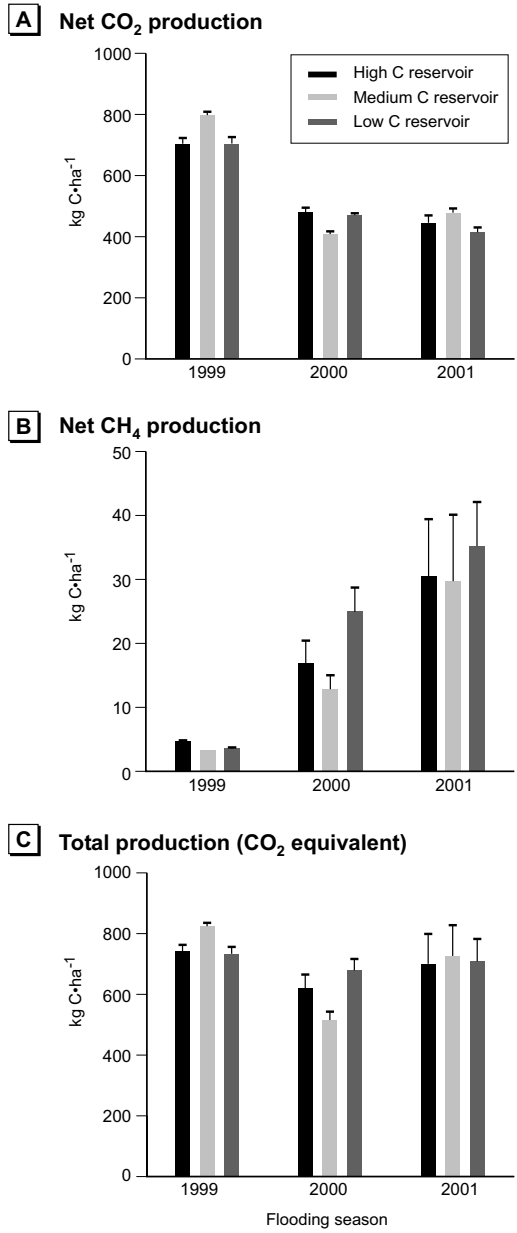

Fig. 15.3. Net CO_2 and CH_4 production in the High, Medium, and Low C reservoirs over the first three flooding seasons. Total production as CO_2 equivalents was determined by adding CO_2 production to CH_4 produced in CO_2 equivalents (calculated by multiplying CH_4 production by a GWP of 23 [Dentener and others 2001])

Table 15.6. Isotopic ratios of DIC and dissolved CH_4 in inflow and outflow, and of ebullition CO_2 and CH_4 fluxes (values are means ± std deviation)

	High C Reservoir			Medium C Reservoir			Low C Reservoir		
	1999	2000	2001	1999	2000	2001	1999	2000	2001
Inorganic C									
Inflow DIC (‰)	-3.5 ± 0.9	-8.7 ± 3.8	-6.9 ± 1.3	-3.5 ± 0.9	-8.7 ± 3.8	-6.9 ± 1.3	-3.5 ± 0.9	-8.7 ± 3.8	-6.9 ± 1.3
Outflow DIC (‰)	-16.8 ± 1.0	-18.2 ± 1.3	-15.7 ± 1.6	-17.3 ± 1.7	-15.8 ± 2.7	-15.3 ± 1.1	-15.7 ± 1.0	-14.9 ± 2.9	-13.6 ± 1.6
Ebullition CO_2 (‰)	No data	-21.2 ± 10.7	-13.6 ± 4.2	No data	-17.9 ± 2.3	-14.2 ± 2.5	No data	-15.3 ± 2.6	-16.4 ± 1.8
CH_4									
Outflow (‰)	-72.3 ± 4.5	-58.1 ± 16.2	-40.7 ± 15.5	-89.2 ± 0.1	-70.7 ± 16.7	-51.1 ± 6.7	-79.9 ± 3.4	-59.0 ± 23.6	-51.1 ± 6.3
Ebullition (‰)	No data	-69.9 ± 20.8	-55.4 ± 4.4	No data	-63.6 ± 18.2	-53.5 ± 3.0	No data	-52.8 ± 11.9	-56.0 ± 1.3

vegetation δ^{13}C-DIC values (-30‰ to -26‰) even if DIC produced by decomposition was slightly enriched, indicating water column and benthic NPP affected reservoir δ^{13}C-DIC values. Further support for substantial carbon assimilation via reservoir NPP was provided by submerged chamber results. δ^{13}C-DIC values added to light benthic chambers (-17.9‰) were greater than that added to dark chambers (-24.4‰) (photosynthesis removes more negative δ^{13}C-DIC, leaving less negative δ^{13}C-DIC remaining). The mean net DIC production δ^{13}C-DIC value (-21.5‰) lies midway between the light and dark benthic chamber δ^{13}C-DIC values, and reflects an integration of reservoir processes occurring during both day and night.

Based on outflow δ^{13}C-DIC values (Table 15.6) and a photosynthetic enrichment value of -19‰, periphyton in August and September were expected to exhibit δ^{13}C values ranging from approximately -39 to -34‰. Periphyton samples collected from wooden dowels in August and September had δ^{13}C values ranging from -39 to -29‰, indicating some bacterial and detrital accumulation in dowel periphyton. Bacteria in periphyton would have had δ^{13}C values approximately equal to reservoir δ^{13}C-DOC values (-29 to -26‰), and detritus would have had isotopic signatures similar to reservoir vegetation (approximately -29‰). Periphyton collected from branches after the flooding season had δ^{13}C values closer to expected values (-39 to -35‰). Most likely, bacteria and detritus on periphyton surfaces was sloughed off when exposed after drawdown.

Because periphyton δ^{13}C values more or less matched expected values using an enrichment factor of -19‰ relative to reservoir δ^{13}C-DIC values, an enrichment factor of -19‰ was used to calculate reservoir NPP δ^{13}C values, which ranged from -41.8 to -37.5‰ (Table 15.4). NPP calculations using Eqs. 15.1 and 15.3 showed approximately 15 to 40% of gross reservoir DIC production was removed by NPP (Table 15.4). In 1999, NPP was 148 kg C ha^{-1}, 172 kg C ha^{-1}, and 145 kg C ha^{-1} in the High, Medium, and Low C reservoirs, respectively. In 2000, NPP was 182 kg C ha^{-1}, 225 kg C ha^{-1} and 211 kg C ha^{-1} in the High, Medium, and Low C reservoirs, respectively. In 2001, NPP was 77 kg C ha^{-1}, 180 kg C ha^{-1}, and 273 kg C ha^{-1} in the High, Medium, and Low C reservoirs, respectively (Table 15.4). The difference between light and dark benthic chamber δ^{13}C-DIC values indicated 15 to 33% of reservoir DIC was consumed via photosynthesis (data not shown). With the lower estimate of 15%, NPP ranged from 140 to 170 kg C ha^{-1} in 1999, 100 to 110 kg C ha^{-1} in 2000, and 70 to 90 kg C ha^{-1} in 2001. However, these estimates account only for NPP directly on the bottom surface, and do not incorporate photosynthetic CO_2 uptake by extensive sheets of periphyton that grew on submerged tree branches.

While stable carbon isotopic ratio analysis showed considerable amounts of DIC were removed from the reservoirs through NPP, the final

fate of photosynthetically-fixed carbon in the FLUDEX reservoirs is unclear. Likely, important quantities of DIC produced in the reservoirs and later stored in algal material was eventually released as CO_2 to the atmosphere upon decomposition of algal tissues after reservoir drawdown. Therefore, gross CO_2 production estimates (gross DIC production + ebullition CO_2 fluxes) likely more closely approximate reservoir CO_2 emissions than do estimates of net CO_2 production.

15.3.3 CH_4 Production and Oxidation

Source compounds (soil, vegetation, and DOC) for methyl-type fermentation had $\delta^{13}C$ values of approximately -30‰ to -26‰, so CH_4 produced via methyl-type fermentation in the FLUDEX reservoirs would have had $\delta^{13}C$-CH_4 values between -65‰ and -51‰. Net dissolved CH_4 production $\delta^{13}C$-CH_4 values ranged from -92.1 to -73.0‰ in 1999 (Table 15.5), indicating the main CH_4 production pathway was CO_2 reduction with little subsequent CH_4 oxidation. Net dissolved CH_4 production $\delta^{13}C$-CH_4 values were between -65.9 and -54.6‰ in 2000 and between -50.1 and -38.2‰ in 2001 (Table 15.5), indicating CH_4 was produced via methyl-type fermentation and underwent some subsequent CH_4 oxidation (unoxidized $\delta^{13}C$-CH_4 values entering submerged benthic chambers were approximately -60‰, so net dissolved CH_4 production $\delta^{13}C$-CH_4 values greater than -60‰ indicated CH_4 oxidation occurred). During the 2000 and 2001 flooding seasons, porewater $\delta^{13}C$-CH_4 values ($\geq$ -70‰) were not low enough to indicate significant CO_2 reduction.

Porewater and water column $\delta^{13}C$-CH_4 values showed CH_4 oxidation occurred in the upper portion of flooded soils because $\delta^{13}C$-CH_4 values increased by 3 to 9% across the SWI, but remained unchanged after entering the water column (data not shown). Benthic chamber data also showed CH_4 oxidation occurred at or below the SWI. Water column $\delta^{13}C$-CH_4 values matched $\delta^{13}C$-CH_4 values of light benthic chambers (in the presence of light, more oxidized CH_4 was added to the chambers), while porewater $\delta^{13}C$-CH_4 values matched those of dark benthic chambers (unaltered CH_4 entered the chambers in the absence of light).

The percentage of reservoir CH_4 that was oxidized was determined using Eq. 15.4. Net reservoir dissolved CH_4 production $\delta^{13}C$-CH_4 (Table 15.5) represented oxidized $\delta^{13}C$-CH_4 values. Porewater and dark chamber $\delta^{13}C$ values, which ranged from -70 to -91‰ (data not shown), provided the best reference for unoxidized $\delta^{13}C$-CH_4 values. Experimentally determined CH_4 oxidation enrichment factors were similar in all FLUDEX reservoirs (-13 ± 1‰; Venkiteswaran and Schiff 2004). With the

exception of the first flooding season, CH_4 oxidation consumed considerable quantities of CH_4 in the FLUDEX reservoirs. In 2000, approximately 50% of the CH_4 produced was oxidized in all reservoirs, and in 2001, 70 to 88% of the CH_4 produced was oxidized.

Methane oxidation was therefore important in lowering the overall atmospheric GHG impact of the FLUDEX reservoirs through conversion of CH_4 to CO_2. However, CH_4 mass budgets showed net reservoir CH_4 production increased with each successive flooding season despite concurrent increases in CH_4 oxidation (i.e., methanogenesis increased at a faster rate than CH_4 oxidation). Increased reservoir CH_4 production led to increased ebullition CH_4 fluxes (Tables 15.3 and 15.5), because low solubility of CH_4 in water enhanced bubble formation during seasons of high CH_4 production. In the second and third flooding seasons, ebullition CH_4 fluxes were the most important route of CH_4 evasion from the reservoirs, when they were nearly double diffusive surface and outflow CH_4 losses (Table 15.5). Ebullition $\delta^{13}C$-CH_4 values indicated CH_4 in bubbles was subjected to less oxidation than CH_4 dissolved in the water column (about 50 to 75%) (note: bubbles were not oxidized in the water column; rather, CH_4 entered bubbles in the zone where CH_4 oxidation was occurring, and underwent oxidation prior to bubble formation). Therefore, with increases in reservoir CH_4 production (and consequently, greater ebullition CH_4 fluxes), there was a relative decrease in the proportion of reservoir CH_4 that was oxidized.

15.3.4 Reservoir GHG Production, OC Storage, and Timescale

Reservoir GHG production (CO_2 and CH_4 production) was not related to overall OC storage in the FLUDEX sites. Mineralization of DOC in inflow or catchment inputs would have produced DIC and obscured differences in reservoir DIC production due to landscape OC mineralization. Reservoirs had small catchment areas, so catchment inputs were not large (furthermore, the High C reservoir, with the largest catchment area, had similar, if not lower, CO_2 and CH_4 production as the Medium and Low C reservoirs). Inflow DOC mineralization was considered a small contribution to overall reservoir DIC for several reasons. Prior to entering the reservoirs, inflow DOC was subjected to upwards of 15 years (the water residence time of the lake from which inflow was drawn) of microbial and ultra-violet degradation and was unlikely to have suddenly degraded during the 5 to 9 days it was in the reservoirs. Moreover, high DOC concentrations (from within reservoir origin) decreased UV penetration in the reservoir, preventing further photodegradation of refractory lake DOC. Most importantly,

reservoir DOC mass budgets indicate the FLUDEX reservoirs were net DOC producers, exporting considerable quantities of DOC (data not shown) in outflow water. Exported DOC produced from soil and vegetation decomposition is not included in our estimates of reservoir GHG production.

Similar GHG production in the three reservoirs suggests that, at least over the short-term, total landscape OC storage is not a good indicator of subsequent reservoir GHG production. Even when wood biomass is excluded from site OC storage estimates (decomposition of wood is minimal in northern reservoirs [Smith 1991] and a vegetation decomposition study using litterbags showed little to no decomposition of wood in the FLUDEX reservoirs [Hall 2003]), net reservoir GHG production was not related to OC storage (altered estimates: High C site: 24060 kg C ha^{-1}; Medium C site: 13820 kg C ha^{-1}; Low C site: 15040 kg C ha^{-1}).

During initial stages of flooding, factors other than the amount of landscape OC storage, such as the susceptibility of carbon-containing compounds to microbial degradation (lability), may have a greater influence on reservoir GHG production. Incubations of soil and vegetation characteristic of the dry forest communities in the Medium and Low C reservoirs had greater decomposition rates than the moist forest community that characterized 50% of the High C reservoir (Baril 2001). Furthermore, plant tissues in the Medium and Low C reservoirs decomposed faster than the same tissues in the High C reservoir (Hall 2003). Reservoir GHG production may more closely match landscape OC storage over the long-term, when more resistant OC complexes are left to be mineralized.

Few studies (Galy-Lacaux 1997, 1999; Kelly et al. 1997) have monitored GHG emissions from the same reservoir over a period of time. Over the first three flooding seasons in the FLUDEX reservoirs, there was a decline in reservoir CO_2 production accompanied by an increase in reservoir CH_4 production. While future trends in net reservoir CH_4 production cannot be predicted from this short-term study, long-term effects of reservoir creation on boreal forest uplands depends primarily on changes between terrestrial and reservoir carbon cycling affecting CH_4 production and oxidation. OC in forest soils and vegetation is originally sequestered as CO_2 from the atmosphere, and each molecule of CH_4 produced in reservoirs presents a net GHG emission to the atmosphere because CH_4 has a greater GWP than CO_2. Furthermore, prior to flooding, soils in all FLUDEX sites consumed CH_4 at rates of -1.1 to -0.7 mg CH_4-C·m^{-2}·d^{-1} (data not shown); the loss of the CH_4 sink in undisturbed forest soils represents a net source of CH_4 to the atmosphere for as long as the reservoirs exist.

15.3.5 Extrapolation of FLUDEX Results to Other Studies

The FLUDEX and the ELARP. The flooded ELARP wetland, with OC stores of ~1000000 kg C ha^{-1}, represented substantially higher OC storage relative to the FLUDEX reservoirs. Does a relationship between landscape OC storage and subsequent GHG production emerge when FLUDEX and ELARP reservoirs are compared? Although the FLUDEX and ELARP reservoirs shared important characteristics (all were flooded during the same time interval, located in the same vicinity, and small in scale), major differences in water residence times confound direct comparisons of CO_2 and CH_4 surface water concentrations and concentration-based processes (i.e., surface diffusive fluxes) between the FLUDEX and ELARP reservoirs. For example, surface diffusive fluxes of both CO_2 and CH_4 from the pond surface of the ELARP reservoir during the first three years of flooding were up to approximately 3 and 12 times greater, respectively, than emissions from the FLUDEX reservoirs on an areal basis (Table 15.7), but this could be due largely to longer water residence times in the ELARP reservoir (which would allow for dissolved CO_2 and CH_4 concentrations to accumulate). Inorganic C and CH_4 mass budgets do not exist for the ELARP reservoir, so net GHG production rates comparable to the FLUDEX reservoirs are not available. Nevertheless, some comparisons between the FLUDEX and ELARP reservoirs can be made.

Ebullition CO_2 and CH_4 fluxes can be directly compared between the FLUDEX and ELARP reservoirs. Mean FLUDEX CH_4 ebullition fluxes in 2000 and 2001 (5 to 30 $mg{\cdot}CH_4{\cdot}m^{-2}{\cdot}d^{-1}$) were comparable to CH_4 ebullition fluxes from the ELARP reservoir (~20 $mg{\cdot}CH_4{\cdot}m^{-2}{\cdot}d^{-1}$; Kelly et al. 1997). However, comparable ELARP ebullition fluxes relative to FLUDEX ebullition fluxes are misleading because ebullition fluxes were measured only over deeper water in the center of the original wetland pond of the ELARP reservoir. Bubble production in the flooded peatland portion of the ELARP reservoir caused large mats of peat to become dislodged and float on the water surface around the shallow margins of the flooded wetland (Scott et al. 1999). CH_4 fluxes from peat increased from approximately 64 $mg{\cdot}CH_4{\cdot}m^{-2}{\cdot}d^{-1}$ when submerged to 440 $mg{\cdot}CH_4{\cdot}m^{-2}{\cdot}d^{-1}$ when floating (Scott et al. 1999), about 4 to 10 times greater than ebullition fluxes from the FLUDEX reservoirs. This increase occurred primarily because floating peat lies at the surface of the water column so that CH_4 produced within the peat islands fluxes directly to the atmosphere with minimal oxidization by methanotrophic bacteria (Scott et al. 1999).

Temporal trends in GHG production in the ELARP reservoir indicate flooded wetlands produce GHGs for a longer period of time than flooded

Table 15.7. CO_2 and CH_4 fluxes from the surfaces of the FLUDEX reservoirs, the ELARP reservoir, and boreal/temperate reservoirs of different ages and sizes.[+] (fluxes for additional reservoirs are presented in Tremblay et al., Chap. 8)

Reservoir	Location	Age (years)	Area (km^2)	Flux $mg \cdot CO_2 \cdot m^{-2} \cdot d^{-1}$	Flux $mg \cdot CH_4 \cdot m^{-2} \cdot d^{-1}$	Reference
High C	Ontario	3	0.0074	970-1390*	2.6-9.5*	This study
Medium C	Ontario	3	0.0050	590-1010*	1.0-5.2*	This study
Low C	Ontario	3	0.0063	730-1240*	1.7-10.6*	This study
ELARP	Ontario	1–2	0.2	1100-3700	50-90	Kelly et al. 1997
Laforge-1	Québec	2–10	960	80-10270	0.0-724.9	Duchemin et al. 1995 Therrien 2003
Laforge-2	Québec	19	286	-280-4200	5.1-9.0	Therrien 2003
La Grande-1	Québec	24	70	720-3370	6.5-12.3	Therrien 2003
La Grande-2	Québec	17	2835	300-6500	0.5-53	Duchemin et al. 1995
La Grande-3	Québec	19	2420	-250-5050	-3.0-45.9	Therrien 2003
La Grande-4	Québec	20	765	-1200-2590	-3.0-31.1	Therrien 2003
Opinica	Québec	12–13	1000	2200-4300	4-15	Kelly et al. 1994
Robert-Bourassa	Québec	12–19	2500	160-12000	1-100	Kelly et al. 1994; Duchemin et al. 1995; Duchemin et al. 2000
Caniapiscau	Québec	19	4275	-7-4210	-3.0-24.1	Therrien 2003
Revelstoke[§]	British Columbia	8	120	1560-3000	————	Schellhase et al. 1997
Kinsbasket[§]	British Columbia	19	430	460-600	————	Schellhase et al. 1997
Arrow[§]	British Columbia	22	520	570-1770	————	Schellhase et al. 1997
Whatshan[§]	British Columbia	40	15	540-790	————	Schellhase et al. 1997

[+]Fluxes presented are based on dissolved surface concentrations of CO_2 and CH_4, which are highly dependant on reservoir water residence times. Differences in water residence times for the following reservoirs are not accounted for; therefore, direct comparison of fluxes from different reservoirs should be done with caution.

*Range of mean seasonal diffusive surface fluxes (Table 15.3) only (losses via ebullition and outflow water are not included, as they are in estimates of net reservoir CO_2 and CH_4 production).

[§]As cited in St. Louis et al. 2000.

uplands. While CO_2 production in the FLUDEX reservoirs declined over three flooding seasons, dissolved surface concentrations of both CO_2 and CH_4 in the ELARP reservoir remain as high 10 years post-flood as during the first few seasons after flooding (St. Louis et al. 2004). Furthermore, the amount of stored carbon in the ELARP wetland is predicted to sustain current fluxes for approximately 2000 years, while current GHG production rates in the FLUDEX reservoirs cannot last more than 100 years if fuelled only by soil and vegetation decomposition. Greater ebullition CH_4 fluxes and prolonged GHG production in the ELARP reservoir compared to the FLUDEX reservoirs is especially important considering existing (and anticipated) hydroelectric developments flood large expanses of low-lying peatlands. Overall OC storage may be useful in predicting long-term GHG production from reservoirs flooding ecosystems with vastly different OC storage (e.g., boreal wetlands vs. boreal uplands).

The FLUDEX and actual hydroelectric complexes. Extreme differences between reservoir surface area, volume, and average depth make direct comparisons between the FLUDEX reservoirs and actual reservoirs unreasonable. For example, La Grande reservoir in northern Québec has an average depth of 22 m and an area of 2840 km^2 (Duchemin et al. 1995). Cold temperatures in deep reservoirs likely slow decomposition rates at the SWI, and development of stable thermoclines may allow anoxic conditions to develop quicker in larger reservoirs. Large reservoirs are likely to receive much greater allochthonous OC inputs via watershed run-off, and depending on river supply to the reservoirs, sedimentation rates will vary and influence decomposition rates in larger reservoirs.

However, with average depths of about 1 m, the FLUDEX reservoirs are comparable to shoreline margins of larger reservoirs. Winter drawdown of the FLUDEX reservoirs also mimicked the seasonal drawdown of many northern hydroelectric reservoirs, which exposes shoreline areas during winter months. Furthermore, despite differences in morphology and hydrology between the FLUDEX and real reservoirs, diffusive surface CO_2 and CH_4 fluxes from the FLUDEX reservoirs and reservoirs in Quebec and British Columbia are comparable (Table 15.7). Biogeochemical processes controlling GHG production in the FLUDEX reservoirs may therefore be similar to those occurring in large reservoirs. Although such small experimental systems may not directly represent real-world systems in size and hydrology, conclusions and detailed information on carbon cycling (both spatial and temporal) drawn from the FLUDEX reservoirs is unmatched by other reservoir studies. Mechanistic data received from these experiments will no doubt provide valuable input to models of carbon processes occurring in real hydroelectric complexes flooding similar landscapes.

15.4 Conclusions

The FLUDEX is one of a few detailed investigations of biogeochemical processes leading to CO_2 and CH_4 production in reservoirs. Regulated flooding of upland forest sites allowed for mass and isotopic ratio mass budgets incorporating reservoir inorganic C and CH_4 inputs and outputs to be calculated, providing valuable information about the relative roles of GHG sources and sinks controlling net reservoir GHG production. Net reservoir GHG production in these newly-created reservoirs was not related to the mass of OC stored in flooded soils and vegetation. Stable carbon isotopes analysis showed reservoir NPP consumed 15 to 40% of gross reservoir CO_2 production; however, this did not represent a true inorganic C sink within the reservoirs, as algal material decomposed after reservoir drawdown. Therefore, gross CO_2 production is likely a better approximation of the effect of reservoir creation on atmosphere CO_2 levels.

CH_4 oxidation was negligible during the first flooding season, but by the third flooding season, consumed up to 88% of methane produced in the reservoirs. CH_4 oxidation was therefore very important in lowering the overall impact of the FLUDEX reservoirs on atmospheric GHG levels. However, despite the year-to-year increases in reservoir CH_4 oxidation, there was an increase in net reservoir CH_4 production with each successive flooding season (i.e., methanogenesis increased at a greater rate than CH_4 oxidation). CH_4 emitted via ebullition, which accounted for a greater percentage of net reservoir CH_4 production with each successive flooding season, was subjected to less oxidation than that which was dissolved in the reservoir water column.

Overall decomposition rates (as measured by gross reservoir CO_2 production) decreased from the first to third flooding seasons; however, relatively smaller increases in CH_4 production with each successive flooding season kept the GWP of the FLUDEX reservoirs relatively constant. While it is unclear whether the observed trends in GHG production in the FLUDEX reservoirs will continue over longer time scales, this study has contributed a better understanding of processes governing GHG production in reservoirs. The experimental FLUDEX reservoirs are comparable to shallow shoreline regions of large hydroelectric complexes, and results from this study may be incorporated into models of GHG production in similarly flooded landscapes.

16 Mass Balance of Organic Carbon in the Soils of Forested Watersheds from Northeastern North America

François Courchesne and Marie-Claude Turmel

Abstract

The objective of this chapter is to establish the functional links between the organic carbon (C) dynamics in soils, the biogeochemical C cycle of forested watershed and the potential changes in the sequestration of atmospheric C by forest soils in response to changing climatic conditions. After an introductory statement on greenhouse gases and their effects on climate, the second part of the chapter describes the properties, functions and biogeochemical cycling of organic carbon (C) in forest soils. The third part of the chapter presents the results of an extensive review of organic C mass balance studies conducted in forested watersheds of northeastern North America. The soil and plant C pools and fluxes are quantified and results are compared to those obtained from other environments, such as southeastern United States and Western and Central Europe. The potential contribution of soils to the emission of greenhouse gases is critically discussed through an evaluation of the net role of soils on organic carbon (C) cycling and on its transport from terrestrial to aquatic environments. Based on the available data and evidences, it appears that the question as to whether soils from northern forests will behave as a net source or sink of C under a warmer climate cannot yet be answer unequivocally.

16.1 Introduction

16.1.1 Emission of Greenhouse C Gases

Carbon dioxide (CO_2), methane (CH_4), nitrous oxide (N_2O), and tropospheric ozone (O_3) and chlorofluorocarbons (CFCs) are known as the

greenhouse gases (GHGs). Their concentrations in the atmosphere significantly increased since the middle of the 18th century with industrialisation and demographic expansion. For example, the world mean CO_2 concentration increased from 280 ppmv (preindustrial concentration) to 360 ppmv (actual concentration) while N_2O was at 288 ppbv against 310 ppbv today; CH_4 increased from 0.8 ppmv to 1.72 ppmv (Bazzaz and Sombroek 1996). The changes in CO_2 and N_2O originate from the use of fossil fuels, agriculture, deforestation and biomass burning whereas the CH_4 production mostly takes its source in agricultural activities. The increase in tropospheric ozone is caused by human pollution in cities (e.g. use of fossil fuels). It results from photochemical reactions with NO_x, CH_4 and carbon monoxide (CO).

The GHGs play a major role on climatic conditions. Indeed, their presence in the atmosphere is associated to increases in air temperature and, thus, could affect the biogeochemical *equilibrium* established in terrestrial ecosystems. For example, general circulation models have projected a global warming in the order of 0.9 to 3.5 ^oC by 2100 due to human activities (Intergovernmental Panel on Climate Change 1996), a large part of it being linked to GHGs. Some of the known effects of increasing temperature on ecosystems are: faster rates of reactions, higher biomass production, increased decay of organic materials and, longer growing season at higher latitude and altitude (Rawson 1992; Chadwick and Graham 2000).

Carbon dioxide could act as a fertilizer on biomass production because it is essential for plant nutrition and it has a positive effect on photosynthesis. Thus, biomass production could be higher following an increase in CO_2 concentration. Forest growth or regrowth after burning could also be stimulated (Tans et al. 1990). Moreover, Wolfe and Erickson (1993) found that transpiration by plants was reduced by higher CO_2 levels because plant stomata are more contracted and/or the number of stomata per leaves decreases. Under such conditions, the use of water is considered to be more efficient. However, the presence of GHGs is not only associated with positive effects on ecosystems. The reduction of stratospheric ozone and the increase of tropospheric ozone both have negative impacts on plants. For example, a reduction of stratospheric ozone results in higher ultraviolet-B (UV-B) radiation. In turn, elevated UV-B reduces photosynthesis and leaf area for many plant species, and increases plant sensitivity to water deficit (Runeckles and Krupa 1994).

Higher air temperatures due to GHGs are not only thought to positively affect soil C status through biomass production or forest growth. Indeed, the decomposition of soil organic matter (SOM) is also considered to be proceeding more rapidly under higher CO_2 levels or air temperature. This would accelerate the turnover rate of many nutrients like N, P, S and base

cations (e.g. Ca, K, Mg) and could diminish the magnitude of the soil C reserve. Yet, increases in CO_2 also apparently stimulate mycorrhizal activity and make soil P more easily available whereas N fixation is more abundant (Allen et al. 1996). Mineral weathering of the substratum could also increase under warmer air and soil temperature (Chadwick and Graham 2000). This results in a fresh supply of macronutrients (Ca^{2+}, Mg^{2+}, and K^{+}) and micronutrients (Cu^{2+}, Mn^{2+}, Zn^{2+}) to the soil available pools and, subsequently to biota. Increased weathering could in turn reduce atmospheric CO_2 levels, a feed-back process known to contribute to the regulation of long-term climate changes (Raymo 1994). Another effect of global warming on soil could be the production of larger litter amounts, a litter that has a higher C/N ratio. The N content in organic layers is a major factor limiting litter decomposition (Homann and Harrison 1992). Reducing the input of N could potentially reduce the rate at which the nutrients become available.

16.1.2 Contribution of Soils from Forest Ecosystems

Because forest vegetation and forest soils have a large capacity to release and store C, mass balance estimates of C budgets are essential to establish the contribution of forest ecosystems to the global terrestrial C cycle. Indeed, forest ecosystems cover 65% of the land surface and they contain 90% and 80%, respectively, of the total vegetation and soil C pools (Gower 2003). Forest also assimilates up to 67% of all the CO_2 that is removed from the atmosphere by terrestrial ecosystems. Together temperate and boreal forests represent close to 320 Pg of C stored as soil organic C (Table 16.1). Their rate of C accumulation also rank among the highest measured for terrestrial ecosystems. In this context, even a slight change in the rate of C flux to or from forest soils, or a change in the C sink-source balance, could result in a significant effect on atmospheric CO_2 levels. Nonetheless, the role of forest ecosystems in the global C cycle has not always been considered at a level that entirely reflects the extent of their potential impact on global climate changes.

The objective of this review is to establish the links between the organic C dynamics in soils, the biogeochemical C cycle of forested watershed and the potential changes in the sequestration of atmospheric C by forest soils in response to changing climatic conditions. The key role played on a global basis by temperate and boreal forests under mid-latitudes on C sequestration (Falkowski et al. 2000) justifies our focus on ecosystems and watersheds from Northeastern North America. After an introductory statement on GHGs and their effect on climate, the second part of the

Table 16.1. Distribution of soil organic matter by ecosystem type (from Schlesinger 1977 and Schlesinger 1991)

Ecosystem type	Rate of accumulation [g·C·cm^{-2}·yr^{-1}]	Mean soil organic matter [kg·C·m^{-2}]	World area [ha x10^{8}]	Total world soil organic carbon [Pg·C]	Total world litter [Pg·C]
Tropical forest	2.3-2.5	10.4	24.5	255	3.6
Temperate forest	0.7-12	11.8	12.0	142	14.5
Boreal forest	0.8-15.3	14.9	12.0	179	24.0
Woodland and shrubland		6.9	8.5	59	2.4
Tropical savanna		3.7	15.0	56	1.5
Temperate grassland		19.2	9.0	173	1.8
Tundra and alpine	0.2-2.4	21.6	8.0	173	4.0
Desert shrub		5.6	18.0	101	0.2
Extreme desert, rock and ice		0.1	24.0	3	0.02
Cultivated		12.7	14.0	178	0.7
Swamp and marsh		68.6	2.0	137	2.5
Totals			147.0	1456	55.2

chapter describes the organic C dynamics and functions in forest soils with emphasis on the biogeochemical cycle of organic C, the role of forest soils in the C cycle, the nature and characteristics of SOM, the function of organic substances in soils and the links between C and other elemental cycles in soils. The third part of the chapter presents the results of an extensive review of organic C mass balance studies conducted in forested watersheds of Northeastern of North-America. The soil and plant C pools and fluxes are quantified and results are compared to those obtained from other environments, such as Southeastern United States and Western and Central Europe. Finally, the potential contribution of soils to the emission of greenhouse gasses will be discussed through an evaluation of the net role of soils on organic C cycling and on its transport from terrestrial to aquatic environments.

16.2 Organic Carbon in Forest Soils

The global C cycle encompasses the four spheres, the atmosphere, biosphere, hydrosphere and lithosphere, where different carbon pools are established (Fig. 16.1). A variety of exchange mechanisms (e.g. assimilation, respiration, erosion, sedimentation) are active and transfer C within and between those spheres. The fluxes exist either under the gaseous, the dissolved or the solid state. Here we will focus on the biogeochemical cycle of organic C in forested ecosystems and on its contribution to the global C cycle.

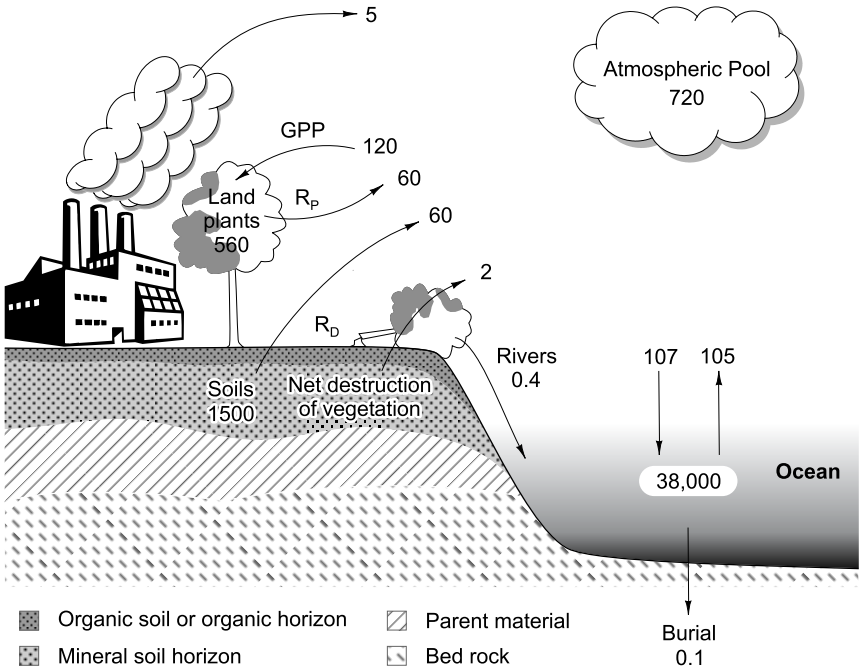

Fig. 16.1. The global carbon cycle. All pools are expressed in units of Pg C while annual fluxes are in units of Pg C yr^{-1} (modified from Schlesinger 1991)

16.2.1 Biogeochemical Cycle of Organic Carbon in Forested Ecosystems

In terrestrial ecosystems whether desert, forest, wetland or agricultural land, the biogeochemical cycle of organic C is strongly dependent on the nature of the plant cover (Schlesinger 1991) and thus, on climate. The plants provide the necessary biomass (leaves, roots, shoots, branches, fruits) that lead to the accumulation of organic matter (OM) in the ecosystem. The net primary production (NPP) of the biomass is defined as the gross primary production of plant minus plant respiration. The air temperature and the amount of precipitation are the two main factors controlling the NPP (Lieth 1975). Thus, the soil organic C content will fluctuate as a function of the NPP, the vegetation type and the environmental conditions with warm and wet climates having higher mean SOM than cold and/or dry environments (Table 16.1). Mean values of 11.8 to 14.9 $kg{\cdot}C{\cdot}m^{-2}$ as SOM are proposed for temperate and boreal forests, respectively. Not surprisingly, forest ecosystems represent close to 70% of the total world litter flux to soil surfaces.

In a forest ecosystem, photosynthesis pumps CO_2 from the atmosphere (Fig. 16.2). The C is then transferred from an oxidized state (CO_2) to reduced forms, and it is stored in leaves, branches, wood and roots. The leaching of the forest canopy as throughfall and stemflow together with litterfall deposition constitute the main aboveground fluxes controlling the input of C to the soil surface. The subsequent formation of a humus layer at the surface of soils by the biota will tend to reach a steady-state between litterfall inputs and the decomposition of these organic detritus. The microbial processes involved in the transformation and cycling of OM is strongly influenced by microclimatic (e.g. air and soil temperature, available moisture) and by chemical (e.g. acidity, redox status) conditions prevailing at the soil surface. Moreover, the dominant tree species (e.g. coniferous or deciduous) will control the abundance and degradability of litter inputs and the properties of the humus layer produced (Strobel et al. 2001). For the belowground compartment, the decomposition of roots and microbes, and the exudation of organic metabolites represent a major vector of organic C input to soils.

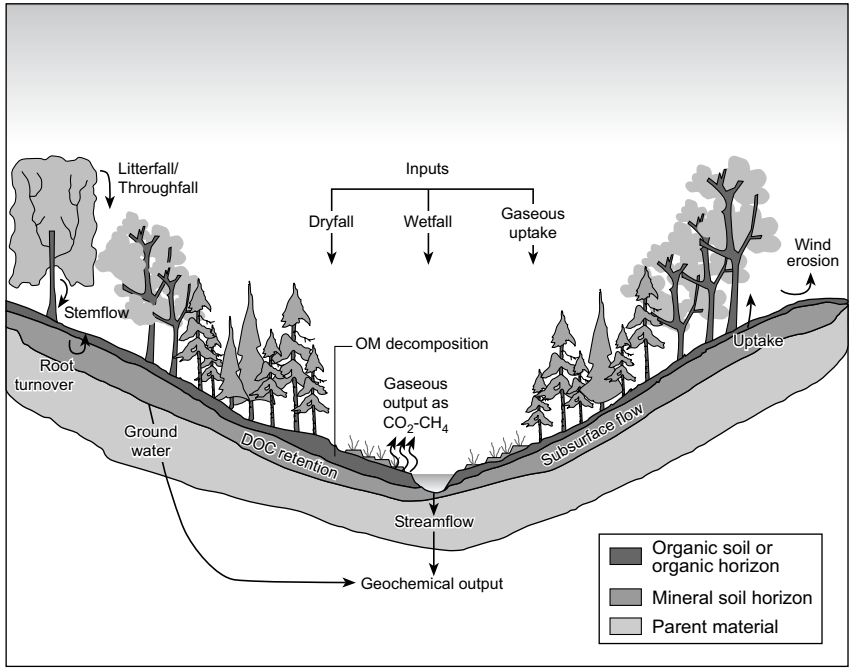

Fig. 16.2. The biogeochemical cycle of organic carbon in a forested ecosystem

The C in throughfall, stemflow and in organic horizon leachates is present as dissolved organic carbon (DOC) and comprises simple organic acids (e.g. oxalic and citric acids), for about 20% of the total concentration and a series of more complex and recalcitrant substances such as fulvic (FA) and humic (HA) acids (Herbert and Bertsch 1995). The mean DOC concentrations in precipitation, throughfall and stemflow vary from 1 to 350 mg C L^{-1} in forested catchments (Table 16.2). When such solutions percolate in mineral horizons, the DOC concentrations decrease markedly, notably in the upper B horizons (Bhf, Bf). The main mechanism responsible for DOC retention is anion exchange that leads to the formation of strong mineral-organic matter associations in the mineral soil. The retention of DOC is strongly correlated to the abundance of Al and Fe oxides and hydroxides in soils and, to lesser extent, to clay content (Qualls et al. 2002). The organic compounds then accumulate in the soil and form surface coatings on individual mineral grains and bridges linking grains to form aggregates. The net result is the creation of a secondary solid phase OM accumulation in soil profiles of forest ecosystems.

Table 16.2. Summary of literature on dissolved organic carbon (DOC) concentrations in pedosphere compartments in forested catchment, from precipitation to streams (from Dalva and Moore 1991)

Compartments	Range of DOC [mg L^{-1}]		Mean DOC [mg L^{-1}]
	min	max	
Precipitation	1.0	5.5	2.1
Throughfall	3.7	70	15
Stemflow	22	350	90
Organic soil horizon	4.8	68	49
Mineral soil horizon	2.8	55	12
Stream	1.0	11.5	4.8

Losses of matter complete the C cycle of forested watersheds (Fig. 16.2). These fluxes can take the form of gaseous C losses due to soil respiration (e.g. CO_2 released from root activity and by decomposers) and dissolved C losses in the soil solution that is leached out of the soil system towards surface or ground waters. The total amount of C lost on a yearly basis as DOC from a given landscape will depend on soil C storage and on microbial activity (Brooks et al. 1999) but also on watershed properties like the dominant hydrological flowpaths (Dosskey and Bertsch 1994), the presence of disturbances (Qualls et al. 2000) and the abundance of organic soils and wetlands (Bishop et al. 1990). Solid phase losses due to the erosion of the soil surface by running water and wind can occur in forested

ecosystems but they constitute a much smaller C output than in agricultural areas.

16.2.2 Key Role of Forest Soils in the Organic Carbon Cycle

As indicated before, the soils play a key role in the organic C cycle of forested ecosystems. In the soil, the biota transforms and redistributes C under different chemical forms that can subsequently be used by plants and other living organisms. The decomposition of the litter by micro and macro fauna, bacteria, mycetes, algae and fungi is the main mechanism through which the OM is incorporated and eventually accumulated in the soil system. In fact, the organic C content in soils reflects the balance between, on the one hand, the rate of litter deposition on the soil surface plus the input of organic residues in the substrate (e.g. exudates, decomposing roots) versus, on the other hand, the rate of OM decomposition (mineralization, humification) by the soil biota, and erosional losses. It follows that the amount and rate of OM accumulation in soils reflects the net result of these two sets of fluxes. Consequently, OM accumulation in soils will vary among ecosystem types and, for a given ecosystem, in response to perturbations like harvest or fire. For example, studies on soil chronosequences showed that under the cool and wet climate of the boreal forest, the OM accumulation could reach rates as high as 15.3 $g{\cdot}C{\cdot}m^{-2}{\cdot}yr^{-1}$ (Table 16.1). For other ecosystems, like the tundra, where more constraining environmental conditions prevail, the OM accumulation rates are slower by more than one order of magnitude (Schlesinger 1991). Eight years after whole tree harvest, Johnson et al. (1995) documented a significant decrease in the soil C pool in the organic horizons at Hubbard Brook. However, data from a Norway spruce mixed forest in Finland showed no significant differences in soil C up to three years after forest clear-cutting (Finér et al. 2002). Moreover, species rotation, notably planting red alder (*Alder rubra* Bong.) on sites previously colonised with Douglas fir (*Pseudotsuga menziesii* Franco), increased soil C concentration and stocks in organic and mineral horizons (Cole et al. 1995).

The C pumped from the atmosphere by photosynthesis is subsequently released in the soil during the decomposition of the SOM. Part of this released C is used for biota nutrition and, hence, is biochemically transformed. The microorganisms of the soil then convert C into cell materials, to CO_2 or into dissolved or solid phase organic substances. Following the initial breakdown of fresh organic residues by the macrofauna, mineralization and humification processes represent the two phases leading to the complete transformation of the organic C inputs to soils. The mineraliza-

tion of the fresh OM first liberates simple organic and inorganic solutes, gases and nutrient elements under ionic form (K^+, Ca^{2+}, Mg^{2+}). The remaining solid phase organic C is assimilated by the soil decomposers and is either accumulated in body tissues or will be transformed into humus (Baldock and Nelson 2000). The humification process is also mediated by microorganisms and produces organic materials of colloidal nature (HA and FA), including insoluble substances called humin. These humic substances are produced by the combination of mineralization residues.

The rate at which microorganisms decompose OM is strongly influenced by factors such as soil temperature, moisture status, redox conditions, soil pH and OM types (Gregorich and Janzen 2000). For example, under acidic and partly anaerobic conditions, the soil microbial biomass and diversity is generally low, reflecting the adverse environment prevailing. Moreover, under theses conditions, coniferous trees often dominate the higher vegetation of forest ecosystems. The composition of the forest litter will then be rich in lignin, a substance that is only slowly decomposed by microorganisms (Schlesinger 1991). As a result, the overall OM decomposition rate will be slower under these environmental conditions compared to a well aerated and/or less acidic forest soil supporting a larger diversity of decomposers and higher microbial counts. Moreover, Park and Matzner (2003), recently published data indicating that the size of the source C pools (here quantified in terms of forest floor depths) was a control on OM transformation.

Humic substances are relatively stable and can be stored in soils for several hundreds or thousands of years (Wang et al. 1996; Raymond and Bauer 2001). The ^{14}C dates used to establish the age of soil organic C reflect the dynamic nature of the soil system where both new and old organic C fractions are mixed. Early work by Scharpenseel et al. (1968) lists mean residence time (MRT) values ranging from 930 to 2570 years for Bh horizons of Podzols. De Coninck (1980) reported MRT between 1500 and 4000 years for HS in podzolic B horizons. The apparent ^{14}C age of OM in the Bh horizon of Podzols along a soil catena increased from 180±80 to 2840±90 BP towards the base of the slope indicating a change in the nature and properties of OM (Bravard and Righi 1990). In Sweden, Tamm and Holmen (1967) mentioned MRT between 330 and 465 years for Podzols. Estimates for litter turnover in temperate forest obtained by dividing the litter pool by the annual production yields values ranging from 2 to 45 years, depending on how woody debris are taken into account (Matthews 1997). Amundson (2001) presented values of 9 to 61 years for C residence time in soils of temperate and boreal forests with the latter having the longest residence times. The MRT of C in soils also varies from the top of the solum, with mean MRT values of about 10 years, to the deeper

horizons of the profile where MRT could reach 1000 years (Schlesinger 1977). Despite method limitations, these results clearly indicate that the soils act as a long term reservoir for the storage of C.

16.2.3 Nature and Properties of Organic Substances in Soils

The SOM is defined by Schnitzer (2000) as the sum of all organic carbon-containing substances in the soil. The SOM consists of a mixture of plant and animal residues in various stages of decomposition, organic substances that were synthesised microbially and/or chemically and the bodies of live and dead microorganisms (Schnitzer and Khan 1978). The organic substances incorporated to the soil materials are generally operationally differentiated according to some of their specific characteristics like solubility or molecular mass. This approach is needed because the structure, chemical composition and properties of organic substances, notably humic substances or humus, are still poorly known. Although many definitions exist in the literature, the term humus is here used to represent a complex and heterogeneous mixture of humification products that is, the strongly decomposed organic materials presenting no macro or microscopic remnant of plant structure and known to be resistant to further decomposition. The result of the humification process in soils appears as a dark-coloured, partly aromatic, acidic, hydrophilic, molecularly flexible polyelectrolytic OM. The humic substances can compose up to 80% of the total SOM (Table 16.3).

Table 16.3. The percentage distribution of soil organic matter in the different components (from Stevenson and Cole 1999)

Type of material	Percentage of the soil organic matter [% by weight]
Non humic substances	
Lipids (simple organic acids to more complex fats, waxes and resins)	1 to 6%
Carbohydrates	5 to 25%
Proteins/peptides/amino acids	9 to 16%
Other	Trace
Humic substances	Up to 80%

The SOM can be divided in two groups of substances: humic and non-humic substances (Baldock and Nelson 2000). The humic substances are macromolecules with complex chemical structures and are essentially

composed of C, H, N, S, and O. They have a colour varying from yellow to black and a molecular mass ranging from a few hundred to several hundred thousand Daltons (Table 16.4). The humic substances can operationally be separated into humic acids, fulvic acids and humin according to their solubility in an alkali (pH 10 to 13) and an acidic (pH < 2) solution. Based on this approach, the FA is the SOM fraction that is soluble both in acid and alkali solutions, the HA is insoluble when the alkaline extract is acidified while humin is insoluble in alkali and acid.

Table 16.4. Chemical composition and main characteristics of humic and fulvic acids

	Humic acid	Fulvic acid
Chemical composition ($g \cdot kg^{-1}$)[a]		
C	564	509
H	55	33
N	41	7
S	11	3
O	329	448
Other characteristics[b]		
Colour	Brown to black	Yellow to yellowish brown
Molecular mass (Daltons)	Up to 100000	2000-9000
Solubility in water	Lower	Higher
Total acidity ($cmol \cdot kg^{-1}$)[c]	560-890	640-1420
Functional groups ($cmol \cdot kg^{-1}$)[c]		
COOH	150-570	520-1120
Phenolic OH	210-570	30-570
Alcoholic OH	20-490	260-950
Total carbony (C = O)	10-560	120-420
Methoxyl (OCH_3)	30-80	30-120

[a]: Schnitzer 1991.
[b]: van Breemen and Buurman 1998.
[c]: Stevenson and Cole 1999.

Table 16.5 shows the distribution of humic substances in a Podzol profile, a soil order typically formed under forested vegetation in Northeastern North America. The humin dominates quantitatively the bulk of the humic substances. For all three types of organic materials, two distinct maxima are observed: one peak is found at the surface of the profile in the organic horizons whereas a second peak can be noted at the top of the podzolic B horizon. These humic substances accumulate in the surface horizons because of the seasonal input of fresh organic materials. Dissolved organic compounds are subsequently leached from the O to the mineral profile

where they accumulate in the illuvial B horizon. Here, the FA and HA concentrations surpass that of humin because of their higher solubility. The FA penetrates slightly deeper in the profile than HA since it is more soluble than the former in an acidic soil.

Table 16.5. Quantification of total C and humic substances for 18 soil profiles of the Bear Brook Watershed in Maine (USA). Values represent the average and one standard deviation except for humin which was obtained by difference (from David et al. 1990)

Horizon	Total C [g·kg^{-1}]	Humic acid [g·kg^{-1}]	Fulvic acid [g·kg^{-1}]	Humin [g·kg^{-1}]
O	383 ± 15	84 ± 15	35 ± 16	263
E	19 ± 46	6 ± 40	4 ± 39	9
B				
0-2 cm	42 ± 29	14 ± 39	15 ± 31	13
2-7 cm	37 ± 31	12 ± 45	15 ± 31	10
7-25 cm	27 ± 22	9 ± 37	12 ± 17	6
BC	13 ± 28	3 ± 41	8 ± 26	2
C	7 ± 54	2 ± 73	4 ± 51	1

The presence of humic substances impacts on most soil processes because of their unique physico-chemical characteristics. Valuable information on the characteristics of these organic compounds was gained using a range of analytical methods: total chemical analyses, oxidative degradation, IR spectroscopy, 13C NMR spectroscopy and electron spin resonance. For example, it was shown that HA contains more C but less O than FA and that total acidity is significantly higher in FA (Table 16.4). The first 3-D model published for HA has an elementary composition of $C_{308}H_{335}O_{90}N_5$ and a molecular mass of 5548 g mol^{-1} (Schluten and Schnitzer 1993). The chemical structure of humic substances is also dominated by aliphatic structures (50% of C) and aromatic rings (30–35% of C). Moreover, humic substances are known to have large surface areas and to present high levels of oxygen-containing functional groups such as carboxyl (COOH) and phenolic or alcoholic hydroxyls (Table 16.4). These acidic groups are capable to attack mineral grain surfaces, to complex metallic ions and to participate in a variety of organic-inorganic interactions (Schnitzer 2000). Indeed, oxidative degradation has shown that the structure of humic substances contains void that can accommodate, and trap, organic and inorganic soil constituents. Comparatively little is known on the chemical structure of humin; work by Preston et al. (1989) suggests that humin could essentially be HA bound to soil minerals.

The non-humic substances are described as discrete and identifiable organic compounds such as sugar acids, fats, proteins, amino acids, lignin, waxes and other lipids (Table 16.3). These compounds represent between 10 to 50% of all SOM, depending on the soil environment. The best examples of non-humic substances are the low-molecular-mass organic acids (LMMOA) present in forest soils (Table 16.6). As their name suggests, they have a low-molecular-mass ranging from 46.03 g mol^{-1}, in the case of formic acid to 192.2 g mol^{-1} for citric acid (Fox 1995). These acids are ubiquitous in forest soils and bear abundant carboxyl and hydroxyl functional groups. They are mainly the product of root and microbial exudation (McKeague et al. 1986) and of the leaching of fresh leaf surfaces. It follows that the highest LMMOA concentrations in soils are generally reached during and immediately following a rainy periods because they are easily leached and removed by dialysis from leaves (Pohlman and McColl 1988). However, these acids can readily be decomposed by photooxidation and consumed by microorganisms (McColl et al. 1990). Yet, the solubility of LMMOA is high and these compounds are able to form strong complexes with metallic ions like Al, Cu, Fe and Pb (McColl and Pohlman

Table 16.6. Molecular mass of selected low molecular mass organic acids (LMMOA) found in forest soils (from Fox 1995)

Organic acid	Molecular mass [g $mole^{-1}$]
Acetic	60.05
Aconitic	174.11
Benzoic	122.13
Cinnamic	148.17
Citric	192.12
Formic	46.03
Fumaric	116.07
Gallic	169.11
Lactic	90.08
Maleic	116.07
Malic	134.09
Malonic	104.06
p-hydroxybenzoic	138.12
Phtalic	166.13
Protocatechuic	166.13
Oxalic	90.04
Salicylic	138.12
Succinic	118.09
Tartaric	150.09
Vanillic	168.15

1986). Moreover, their reactivity, due to their acidic behaviour in most forest soils, is also elevated and promotes the weathering of primary mineral (Huang and Schnitzer 1986). Because of these two key properties, and despite their relatively short residence time in soils, LMMOA are considered to strongly influence soil genesis, in particular the formation of acidic forest soils like Podzols and Brunisols (Lundström 1993).

16.2.4 Functions of Organic Carbon in Soils

The functions of organic C in soils are numerous and are commonly subdivided into three broad groups: biological, physical and chemical (Baldock and Nelson 2000). Obviously, many interactions exist between these groups of functions. For example, the ability of SOM to chelate metals in turn plays a significant role on the stabilization of the soil structure and, also, on the capacity of the soil to act as a source of micronutrients. Table 16.7 summarizes the properties and the associated functions of OM in soils. The properties presented specifically correspond to key soil processes (van Breemen and Buurman 1998).

From the biological perspective, the crucial functions of OM are to serve as a substrate for soil macro- and microorganisms and to constitute a reservoir of macro- (N, P, S, K, Ca, Mg) and micronutrients (Cu, Mn, Zn) essential for plant growth and health. The OM can act as a source of nutrients either during the OM decomposition process and/or after complexing dissolved trace metals. By acting as binding or coating agents, OM also contributes significantly to the creation and stabilization of structural units (aggregates), a fundamental physical process in soils. The development of aggregates in turn augments water retention, insures the transport of water and gases, and protects the soil against erosion by runoff and wind. From the chemical point of view, the abundance of negative charges and associated cation exchange capacity (CEC), the high proton buffering potential and the strong metal complexation capacity associated to organic materials point to a vital role for SOM on soil fertility and quality (Baldock and Nelson 2000).

The podzolization phenomenon provides a good example illustrating some of the functions of organic C in forest soils. Indeed, there are five distinct podzolization theories and all of these theories confer a central role to the action of dissolved organic substances, either fulvate anions and/or low molecular mass organic acids (Courchesne and Hendershot 1997; van Breemen and Buurman 1998). One of the key features of Podzols results from the chelation of metals, mainly Fe and Al, by complexing dissolved organic substances such as fulvic acids. Once chelated by FA, the metals

Table 16.7. Properties and functions of organic matter in soil (from Baldock and Nelson 2000)

Property	Function
Biological properties	
Reservoir of metabolic energy	OM provides the metabolic energy which drives soil biological processes.
Source of macronutrients	The mineralization of SOM can significantly influence (positively or negatively) the size of the plant available macronutrient (N, P, and S) pools.
Ecosystem resilience	The build up of significant pools of OM and associated nutrients can enhance the ability of an ecosystem to recover after natural or anthropogenic perturbations.
Stimulation and inhibition of enzyme activities and plant and microbial growth	The activity of enzymes found in soils and the growth of plants and microorganisms can be stimulated or inhibited by the presence of soil HS.
Physical properties	
Stabilization of soil structure	Through the formation of bonds with the reactive surfaces of soil mineral particles, OM is capable of binding individual particles and aggregations of soil particles into water-stable aggregates at scales ranging from <2μm for organic molecules through 10 mm for plant roots and fungal hyphae.
Water retention	OM can directly affect water retention because of its ability to absorb up to 20 times its mass of water and indirectly through its impact on soil structure and pore geometry.
Low solubility	Ensures that the bulk of the organic materials added to the soil are retained in the soil profile.
Color	The dark color which soil organic matte imparts on a soil may alter soil thermal properties.
Chemical properties	
Cation exchange capacity	The high charge characteristics of SOM enhance retention of cations (e.g., Al^{3+}, Fe^{3+}, Ca^{2+}, Mg^{2+}, $NH4^{+}$ and transition metal micronutrients).
Buffering capacity and pH effects	In slightly acidic to alkaline soils, OM can act as a buffer and aids in the maintenance of acceptable soil pH conditions.
Chelation of metals	Stable complexes formed with metals and trace elements enhance the dissolution of soil minerals, reduce losses of soil micronutrients, reduce the potential toxicity of metals and enhance the availability of phosphorus.
Interactions with xenobiotics	Organic matter can alter the biodegradability, activity and persistence of pesticides in soils.

can be mobilized in a chemical environment that should otherwise promote their precipitation. These organo-metallic complexes are then transported to and accumulated in the podzolic B horizon. Here, the arrest of the chelates often results from their low solubility or their reaction with positively charged oxide surfaces. The precipitation of chelates down the profile initiates the formation of surface coatings that progressively link the individual mineral grains together thus favouring the establishment of resilient soil structural units. Yet, part of the precipitated organic components will subsequently be used as a source of C by microbes, a reaction that will entrain the progressive destabilization of chelates.

16.2.5 Links between Carbon and Other Elemental Cycles in Forest Soils

The following section aims at underlining the key role played by soil organic C on the biogeochemical cycle of elements in forest ecosystems. Selected examples will be used to establish the tight coupling existing between cycles but the intention is not to propose an exhaustive inventory of all potential links.

Carbon Control on N, P and S Cycles

The elements N, S and P are fundamental to the health and productivity of forests and are often limiting to plant growth in natural ecosystems. The biogeochemical cycles of these three elements is closely and functionally linked to the cycle of SOM. Yet, the movement, storage and accumulation of N, P and S, notably in organic forms are poorly understood in forest soils (David et al. 1995). Moreover, the biogeochemical cycles of all these nutrients have been altered by human activities through stresses like the combustion of fossil fuels, deforestation and fertilizer additions. The predicted long-term changes in climatic conditions could also affect the N, P and S cycles because the magnitude of SOM production and decomposition may be impacted.

A conceptual model integrating the mechanisms involved in C, N, P and S cycling in soils and the role of SOM was proposed by McGill and Cole (1981). Their model is based on the observation that the largest N, P and S pools are in the organic horizons with a secondary accumulation in the B. Two mineralization processes are involved: biological mineralization for C, N and C-bonded S and biochemical mineralization for organic P and ester-SO_4. The first is a process mediated by microbial activity that releases N and S from SOM. The second mineralization process is thought to release P and S through enzymatic activity. In all cases, the litter quality and

composition plays a major role in the organic N, P and S production and transport in the forest floor (Johnson 1995) mostly because the level of N in the plant litter is a limiting factor for the litter decomposition (Schimel and Firestone 1989). Reduction in available N following exposure to increased CO_2 was shown to constrain microbes and decrease microbial respiration (Hu et al. 2001). Obviously, the ambient environmental conditions (temperature, humidity and pH) will also control the decomposition of SOM and the production of organic and inorganic N, P and S.

Adapting the model to forest soils indicates that the decomposition of OM in the forest floor (FF) controls the cycling of C, N and S while microbial demand is also strongly involved in regulating P cycling and availability (Fig. 16.3). Accordingly, the mineralization of organic P could occur rather independently of C mineralization (David et al. 1995). The organic compounds produced by microbial activity and following SOM transformation are eventually leached from the organic to the mineral horizons (B) where most of the dissolved organic substances are retained by

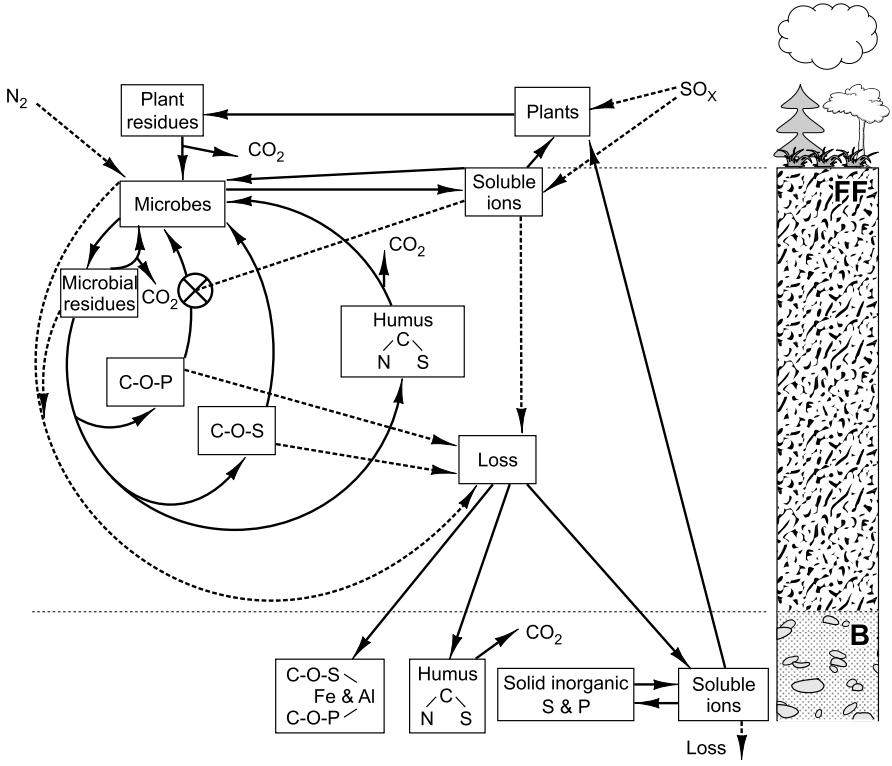

Fig. 16.3. Conceptual model of C, N, S and P cycling in northern Podzols (modified from McGill and Cole, 1981)

soil particles, in particular oxides of Al and Fe. The hydrophilic organic compounds tend to move deeper in the soil profile whereas the hydrophobic substances are preferentially sorbed in the upper part of the B horizon. This retention process contributes to the high organic N, P and S levels commonly measured in the solid phase of B horizons from podzolized forest soils. The amounts of inorganic P and S (notably SO_4) then increase with depth in the profile with almost all P being in inorganic forms in the soil parent material.

Carbon Control on Cationic Macronutrients and Micronutrients

The sustained availability of cationic macro- (Ca, K, and Mg) and micronutrients (Cu, Mn, Zn) for plant is also closely linked to the organic C cycle. Three major ecosystem processes contribute to the supply of cationic nutrients to the soil solution. First, the fragmentation, leaching and decomposition of the fresh forest litter liberate, under dissolved forms, the major cations that were bound to organic residues and to dead plant parts. Solutions collected under fresh litterfall have clearly established the extent and significance of this cationic influx to the soil surface (Courchesne and Hendershot 1988). Second, the dissolved organic compounds produced during SOM decomposition have an acidic behaviour that renders them extremely efficient, often more than inorganic acids of the same concentration, at weathering mineral surfaces. Because these organic acids are leached towards the mineral horizons by percolating waters, they can attack the mineral particles, weather them and solubilize the cations that composed the mineral structure. Thirdly, the high negative charges associated with organic compounds make OM a dominant component of the CEC of soils. The cation exchange capacity (CEC) allows the retention of nutrient cations, and of nutrient trace metals, at the surface of soil particles. This pool of nutrients can be released to the soil solution to meet the nutritional demand of the biota. The CEC of any soil is significantly increased by OM additions.

Other processes associated to SOM play a role on the cations cycle such as the adsorption of dissolved organic matter (DOM) in forest soil horizons, generally B horizons rich in Al and Fe oxides. This mechanism not only results in the immobilization of organic compounds but it also favours the retention by soils of the macronutrients or micronutrients that are bound to DOM. This process is known to reduce the losses of soluble inorganic and organic nutrients from the soil environment (Qualls et al. 2002). The cations are then stored in the soils as organic compounds or can be progressively made available to the biota through the decomposition of the organic complexes by microbes (Lundström 1993).

Carbon Control on Toxic Trace Metals

Toxic metals refer to trace metals that have no known metabolic function essential for plant growth (e.g. Cd, Pb). Consequently, their presence in soils could potentially and adversely affect the biota, with all living components of forest ecosystems being sensitive to toxic metal at specific metal concentrations (Kabata-Pendias and Pendias 1992). These metals are generally present in trace amounts in soil parent materials and bedrock but are locally concentrated by human activities (mining, smelting and industrial activities) and are subsequently deposited onto forests via atmospheric deposition, either in the dissolved or particulate form.

The free ionic forms (Cd^{2+}, Pb^{2+}) of these metals are considered the most toxic for living organisms, from bacteria to plants. However, the presence of organic substances in soils and the reactivity that OM confers to soil materials can partly counteract this toxic effect. The key processes at play are the adsorption of toxic metals on cation exchange sites produced by SOM and the complexation of metals by dissolved organic ligands. Similarly to major cations, the cationic forms of toxic metals are attracted by the negative charges associated to SOM and are immobilized at the surface of soil particles. Although these retained metals can be released to the solution, the occlusion of metals in organic structures and their long-term retention is known to occur in forest soils (Keller and Domergue 1996). Moreover, the strong affinity existing between dissolved organic substances (e.g. FA, HA, LMMOA) and trace metals like Pb lead to the chelation of free metal ions in the soil solution. Chelation is thought to reduce the toxicity of trace metals for most types of biota (Vaughan et al. 1993; Laurie and Manthey 1994). The formation of persistent organometallic complexes is further enhanced in the rhizosphere where root exudates rich in complexing organic acids abound (Legrand et al. 2004).

In many forest ecosystems that are not contaminated by the atmospheric deposition of trace metals, maximum trace metal concentrations are commonly measured in the organic horizons present at the soil surface (Dudka et al. 1995). This metal accumulation results from the biocycling of elements associated to the growing cycle of trees, a cycle that transfers up to 4 Mg of C per ha^{-1} yr^{-1} as litterfall to the surface of forest soil (Table 16.8). Once freed from the fresh litter material, the metals are complexed by the SOM of the F and H horizons thus contributing to the observed metal build up. In the Hermine, a small pristine forested catchment of the Lower Laurentians, the meter-scale spatial Cd patterns in organic F and H horizons where shown to be highly correlated to the origin of the forest litter with the biocycling of Cd by Yellow birch (*Betula alleghaniensis*) being the main factor (Manna et al. 2002).

Table 16.8. Synthesis of soil dissolved organic carbon (concentration and fluxes), total soil organic carbon (pools) and total plant organic C (stock and fluxes) from different watershed studies: Northeastern North America

Northeastern North America	Soil order	Overstory vegetation [gender]	Soil dissolved organic carbon [DOC]		Soil organic C	Total organic C in overstory biomass		References/ Principal investigators
			DOC concentrations[b c] [mg·L^{-1}]	DOC Fluxes[b] [kg·ha^{-1}·yr^{-1}]	Total organic C [kgha^{-1}][a] O = forest floor M = mineral soil	C stock [kg·ha^{-1}][a]	C fluxes as litterfall [kg·ha^{-1}·yr^{-1}][a]	
Huntington Forest–hardwood (New York, USA) 75-80 year-old	Spodosols	*Acer Fagus Betula*			O : ~22462 M : 269791	~99950	~2630	M.J. Mitchell; D.J. Raynal; E.H. White; R. Briggs; J. Shepard; T.Scott; M. Burke; J. Porter
Whiteface Mountain–conifer (New York, USA) mature forest	Spodosols	*Abies Picea*			O : ~70700 M : 221900	~76400	~1300	A. Friedland E. Miller
Howland Forest–conifer (Maine, USA) unmanaged forest since 1977	Spodosols	*Picea* *Oa:* *Bs (10cm):* *Bs (25cm):*	77.6 (15.1) 9.0 (0.5) 3.8 (0.4)	31.2 (7) (for the solum)	O : ~75350 M : 152768	~103500	~1050	I. Fernandez
Hubbard Brook Forest–hardwood (New Hampshire, USA) mature forest	Spodosols	*Fagus Acer Betula*		Th: 132 O: 263 Up B: 54.5 Lw B: 23.0	O : ~75350 M : 152768		1490	Johnson et al. 1995
Harvard Forest–conifer/hardwood (Massachusetts, USA)	Inceptisols	Conifer: *Pinus*	Conifer: Th: 13-37 Oa: 14-75 B: 26 (5.2)	Th: 139 Oa: 398 B: 167				Currie et al. 1996

Table 16.8. (cont.)

Northeastern North America	Soil order	Overstory vegetation [gender]	Soil dissolved organic carbon [DOC]		Soil organic C	Total organic C in overstory biomass		References/ Principal investigators
			DOC concentrations[b c] [mg·L^{-1}]	DOC Fluxes[b] [kg·ha^{-1}·yr^{-1}]	Total organic C [kgha^{-1}][a] O = forest floor M = mineral soil	C stock [kg·ha^{-1}][a]	C fluxes as litterfall [kg·ha^{-1}·yr^{-1}][a]	
Harvard Forest– conifer/hardwood (Massachusetts, USA) (cont.)		Hardwood: *Quercus* *Betula* *Acer*	Hardwood Th: 11-60 Oa: 5.7-45 B: 21 (3.9)	Th: 117 Oa: 225 B: 123				
Turkey Lake- hardwood (Ontario, Canada)	Podzols	*Acer* *Betula*			O: ~16500 M: 159283	~120030	~1865	I.K. Morrison N.W. Foster
Mount St-Hilaire– hardwood/mixed (Quebec, Canada)	Podzols	Hardwood *Acer* *Fraxinus* *Fagus* *Quercus*	Hardwood A: 46.0 B: 16.6					Dalva and Moore 1991
		Mixed *Tsuga* *Fagus* *Pinus* *Quercus*	Mixed A: 49.2 B: 19.4					
Montmorency Forest– conifer (Quebec, Canada) Mature forest–60 years old		*Abies* *Picea*			O: 30000 M: 70000	73000	4400	www.rnc.gc.ca (18th of March 2004)

Table 16.8. (cont.)

Northeastern North America	Soil order	Overstory vegetation [gender]	Soil dissolved organic carbon [DOC]		Soil organic C	Total organic C in overstory biomass		References/ Principal investigators
			DOC concentrations[b c] [mg·L^{-1}]	DOC Fluxes[b] [kg·ha^{-1}·yr^{-1}]	Total organic C [kgha^{-1}][a] O = forest floor M = mineral soil	C stock [kg·ha^{-1}][a]	C fluxes as litterfall [kg·ha^{-1}·yr^{-1}][a]	
Hermine Watershed–hardwood (Quebec, Canada)	Podzols	*Acer* *Fagus* *Betula*	Th: 9.4 (0.4) LFH: 28.8 (11) Up B: 3.0 (2) LwB: 2.5 (1)	Th: 93 (49) LFH: 235 (45) Up B: 38 (10) LwB: 17 (4)	O: 100998 M: 218799 (to bedrock)		1914–2146 (mean of 2030)	Unpublished data from Courchesne; Côté; Fyles and Hendershot Fyles et al. 1994
Ontario's forest ecosystem (Ontario, Canada) Modelling				Region: Boreal Cool temperate Moderate temperate	C Stock in soil (O+M) 9761 kg C x10^9 1148 kg C x10^9 37 kg C x10^9	C Stock in soil 1336 kg Cx10^9 336 kg Cx10^9 30 kg Cx10^9	16.3 (kg Cx10^{9}yr^{-1})	Liu et al. 2002

[a]: The symbol~ means that the organic carbon content is estimated from the organic matter content times a factor of 0.5.
[b]: Standard deviations are in parentheses.
[c]: Th means throughfall solutions.

16.3 Organic C Pools and Fluxes in Forest Watersheds

The objective of this section was to gather and compile data from a wide range of experimental sites from Northeastern North America where data on organic C pools and fluxes are available in the literature. Bringing together all these data (Table 16.8) on our current knowledge of organic C budgets will help to produce a picture of C cycling in the forested ecosystems of Northeastern North America. The emerging trends will subsequently be compared to those obtained in similar forested environments of Southeastern North America (Table 16.9) and of Northwestern Europe (Table 16.10).

16.3.1 Forest Ecosystems from Northeastern North America

The total soil organic C pool in forest soils from Northeastern North America covers a wide range and was estimated to vary from 100 to 320 Mg C ha^{-1} yr^{-1} (Table 16.8). The differences between these estimates must however be considered with caution because the total soil depth included in the calculations differs substantially among sites. For example, the depth reaches 125 cm at the Hermine site whereas it is of about 50 cm at Howland Forest. These data are nonetheless the best estimates available in the literature. Using the carbon budget model of the Canadian Forest Sector, regional estimates of total soil C in soils of boreal forest ecosystems of Alberta yielded values of 83 to 156 Mg C ha^{-1} (Banfield et al. 2002). Estimates for Ontario's forest were of 155 Mg C ha^{-1} (Liu et al. 2002). Differences in the size of soil organic C pools are known to be related to a range of bioclimatic factors (e.g. temperature, precipitation) but are also strongly dependent on the time since disturbance (e.g. wildfire, harvest), showing that the type of forest management practices impacts significantly on C storage in forest soils (Grigal and Ohmann 1992).

The total organic C pool is generally divided in two zones in the soil profile of forest ecosystems: the organic horizons (L, F and H) present at the surface of the profile and the upper part of the B horizons. Quantitatively, the B horizon generally constitutes a larger pool of C because it is thicker and has a much higher bulk density than the organic C–rich forest floor. One of the dominant soil orders in forest ecosystems of Northeastern North America are Spodosols (a soil order that is very close to the Podzolic order used in Canada) or soils that have developed podzolic features such as an accumulation of Al and Fe oxides in the B horizon. These podzolic soils are known to contain the greatest C amounts among forest soils (Vejre et al. 2003). Indeed, organic substances are not only accumulating

Table 16.9. Synthesis of soil dissolved organic carbon (concentration and fluxes), total soil organic carbon (pools) and total plant organic C (stock and fluxes) from different watershed studies: Southeastern North America

Southeastern North America	Soil order	Overstory vegetation [gender]	Soil dissolved organic carbon [DOC]		Soil organic C	Total organic C in overstory biomass		References/ Principal investigators
			DOC concentrations[b c] [mg·L^{-1}]	DOC Fluxes[b] [kg·ha^{-1}·yr^{-1}]	Total organic C [kgha^{-1}][a] O = forest floor M = mineral soil	C stock [kg·ha^{-1}][a]	C fluxes as litterfall [kg·ha^{-1}·yr^{-1}][a]	
Coweeta Forest–hardwood (North Carolina, USA) Native forest	Inceptisols	*Quercus*	Th: 9.07 (0.5) Oa: 32.90 (2.0) A: 15.50 (0.2) AB: 9.20 (0.1) B: 2.03 (0.05) C: 0.52 (0.05)	Th: 130 (5) Oa: 402 (25) A: 137 (2) AB: 68 (1) B: 11.7 (0.5) C: 2.9 (0.5)	O: ~13651 M: 132380	~132380	~2491	Qualls et al. 2002 W.T. Swank; L.J. Reynold; J.M. Vose
Coweeta Forest–conifer (North Carolina, USA) Planted forest in 1957	Ultisols	*Pinus*			O: ~14062 M: 38369	~126587	~3236	W.T. Swank; J.M. Vose
Duke Forest–conifer (North Carolina, USA) Planted forest in 1966-1967	Ultisols	*Pinus*			O: ~31500 M: 34848	~63532	~2458	D. Binkley
Southern Appalachians–hardwood (North Carolina, USA)	Inceptisols Ultisols	*Quercus* *Carya* *Acer*	Th: 9 (2) Oi: 33 (3) Oa: 33 (4)	Th: 130 (20) Oi: 410 (30) Oa: 405 (50)				Qualls and Haines 1991
Great Smoky Mountains (Tennessee-North Carolina, USA)								
Beech site–hardwood	Inceptisols	*Fagus*		Plot 1	O: ~14532 M: 62705	~101650	~1122	Johnson and Lindberg 1992
				Plot 2	O: ~14405 M: 84326	~ 80240	~ 914	

Table 16.9. (cont.)

Southeastern North America	Soil order	Overstory vegetation [gender]	Soil dissolved organic carbon [DOC]		Soil organic C	Total organic C in overstory biomass		References/ Principal investigators
			DOC concentrations[b c] [mg·L^{-1}]	DOC Fluxes[b] [kg·ha^{-1}·yr^{-1}]	Total organic C [kgha^{-1}][a] O = forest floor M = mineral soil	C stock [kg·ha^{-1}][a]	C fluxes as litterfall [kg·ha^{-1}·yr^{-1}][a]	
Great Smoky Mountains (Tennessee-North Carolina, USA) (cont.)								
Becking site–conifer Old grow: 200-300 year-old	Inceptisols	*Picea Abies*			O: ~83045 M: 68895	~128945	~ 955	
Great Smoky Mountains (Tennessee-North Carolina, USA)	Inceptisols	*Picea*		Plot 1	O: ~75550 M: 90677	~132320	~ 885	Johnson and Lindberg 1992
Tower site–conifer Old grow: 200-300 year-old				Plot 2	O: ~54450 M: 132941	~154200	~2708	
Upper Atlantic Coastal Plain–Mixed (South Carolina, USA)	Ultisols	*Pinus Quercus Carya*	Th: 35(21.8) A (10 cm): 25.5(7.1) E (30 cm): 13.7(6.1) E (100 cm): 1.8(0.3)	A (10 cm): 128 E (30 cm): 55 E (100 cm): 6				Dosskey and Bertsch 1997
Florida Slash Pine Forest–conifer (Florida, USA) Indigenous forest	Spodosols	*Pinus*			O: ~18700 M: 74915	~68065	~2227	H.L. Gholz

Table 16.9. (cont.)

Southeastern North America	Soil order	Overstory vegetation [gender]	Soil dissolved organic carbon [DOC]		Soil organic C	Total organic C in overstory biomass		References/ Principal investigators
			DOC concentrations[b c] [mg·L^{-1}]	DOC Fluxes[b] [kg·ha^{-1}·yr^{-1}]	Total organic C [kgha^{-1}][a] O = forest floor M = mineral soil	C stock [kg·ha^{-1}][a]	C fluxes as litterfall [kg·ha^{-1}·yr^{-1}][a]	
Grant Memorial Forest–conifer (Georgia, USA) Decimated by bark beetle in 1978	Ultisols	*Pinus*			O: ~13357 M: 151781	~87110	~5158	H.L. Ragsdale; J. Dowd
Oak Ridge Forest–conifer (Tennessee, USA) Undisturbed forest	Inceptisols	*Pinus*		Plot 1	O: ~7067 M: 51189	~58565	~1298	Johnson and Lindberg 1992
				Plot 2	O: ~7067 M: 68702	~59865	~1750	
Walker Branch Watershed–hardwood (Tennessee, USA) Agricultural and forestry practices before 1942	Ultisols	*Quercus Carya*			O: 5730 M: 78900	177858	4551	Johnson et al. 1981 Sanderman et al. 2003
Calhoun Experimental Forest–conifer (South Carolina, USA) Planted forest in 1956-1957	Ultisols	*Pinus*	Th: 7.5 O: 34.0 E(15cm): 24.0 Bt(60cm): 1.5 C(600cm): 0.6	O: 251 E: 154 Bt: 9 C: 4	O: 34900 M: 96000	123600	2475	Richter et al. 1995

[a]: The symbol~ means that the organic carbon content is estimated from the organic matter content times a factor of 0.5.
[b]: Standard deviations are in parentheses.
[c]: Th means throughfall solutions.

Table 16.10. Synthesis of soil dissolved organic carbon (concentration and fluxes), total soil organic carbon (pools) and total plant organic C (stock and fluxes) from different watershed studies: Northwestern Europe

Northwestern Europe	Soil order	Overstory vegetation [gender]	Soil dissolved organic carbon [DOC]		Soil organic C	Total organic C in overstory biomass		References/ Principal investigators
			DOC concentrations[b c] [mg·L^{-1}]	DOC Fluxes[b] [kg·ha^{-1}·yr^{-1}]	Total organic C [kgha^{-1}][a] O = forest floor M = mineral soil	C stock [kg·ha^{-1}][a]	C fluxes as litterfall [kg·ha^{-1}·yr^{-1}][a]	
Nordmoen–conifer (Norway) Mature forest	Entisols	*Pinus* *Picea*			O: ~31643 M: 56753	~76900	~1643	I. Rösberg A.O. Stuanes
Protos experimental site–conifer (Birkens, Norway)	Podzols Cambisols	*Picea*	Th: 13.1 Oa: 47.8 (14.7) E: 22.4 (8.4) B: 6.2 (0.7)	Th: 161 Oa: 363 E: 174 B: 63				Mulder and Clarke 2000
Kangasvaara catchment–conifer (Finland)	Podzols	*Picea* *Pinus* *Betula* *Populus*			O: 21244 (4256) M: 31614 (1024)	81932 (living biomass)		Finér et al. 2002
Gårdsjön–conifer (Sweeden) Mature forest, 80-100 years old	Podzols	*Picea* *Pinus*		Th: 68.2	O: 60055 M: 160827			Hultberg and Skeffington 1998

Table 16.10. (cont.)

Northwestern Europe	Soil order	Overstory vegetation [gender]	Soil dissolved organic carbon [DOC]		Soil organic C	Total organic C in overstory biomass		References/ Principal investigators
			DOC concentrations[b c] [mg·L^{-1}]	DOC Fluxes[b] [kg·ha^{-1}·yr^{-1}]	Total organic C [kgha^{-1}][a] O = forest floor M = mineral soil	C stock [kg·ha^{-1}][a]	C fluxes as litterfall [kg·ha^{-1}·yr^{-1}][a]	
Sävar (North East Sweeden)	Cambisol		*Picea abies*		O: 5000 M: 55000	50000		Alriksson and Eriksson 1998
			Pinus sylvestris		O: 6000 M: 57500	45000		
			Pinus concerta		O: 7000 M: 70000	42500		
			Larix sibirica		O: 6000 M: 53000	57500		
			Betula pendula		O: 5000 M: 60000 (M = 15 cm)	60000		
Maglehems Ora–hardwood (South Sweeden)	Cambisols Arenosols	*Fagus*		Th: 41.1 B: 37.8				Bergkvist and Folkeson 1992
Nitrex Experimental Sites–conifer	Spodosols	*Pinus*		Forest floor				Gundersen et al. 1998
(Klosterhede, Denmark)			Klosterhede	103				
(Aber, UK)			Aber	350				
(Spleud, Netherlands)			Spleud	130				
(Ysselsteyn, Netherlands)			Ysselsteyn	190				
				Below roots				
			Klosterhede	51				
			Aber	43				
			Spleud	23				
			Ysselsteyn	190				

Table 16.10. (cont.)

Northwestern Europe	Soil order	Overstory vegetation [gender]	Soil dissolved organic carbon [DOC]		Soil organic C	Total organic C in overstory biomass		References/ Principal investigators
			DOC concentrations[b c] [mg·L^{-1}]	DOC Fluxes[b] [kg·ha^{-1}·yr^{-1}]	Total organic C [kgha^{-1}][a] O = forest floor M = mineral soil	C stock [kg·ha^{-1}][a]	C fluxes as litterfall [kg·ha^{-1}·yr^{-1}][a]	
Oude Maat–hardwood (Netherlands) Undisterbed forest since 1939	Inceptisols Entisols Molisols	*Quercus* *Betula* *Alnus* *Populus*	10 cm 20 cm 40 cm 60 cm 90 cm	302 (25) 190 (29) 106 (26) 47 (11) 45 (11)				Pape et al. 1989
Solling–conifer (Germany)	Inceptisols	*Picea*	Top B: 21.5(5.2) Low B: 6.3(4.1)	Th: 100 10cm: 170(20) 100 cm: 43(5)	O: 46000 M: 79000		1500	Borken et al. 1999; Bredemeier et al. 1995
Solling–Unterlüß (Germany) *Fagus sylvatica* (131-150 year-old) *Picea abies* (90-115 year-old) *Pinus sylvestris* (54-103 year-old)	Inceptisols	Solling: Unterlüß:	10 cm: 20-92 100 cm: 2-17 10 cm: 21-110 100 cm: 2-17	224-356 13-21 235-370 17-42	O: 90000-124000 O: 75000-127000			Borken et al. 2004
Steinkreuz site–hardwood (Germany) mature forest 130 year-old	Cambisol	*Fagus* *Quercus*	Th: 11.9-16.4 Oi: 27.9-44.0 Oa: 63.1-75.9 20cm: 14.6-21.0 60cm: 3.9-7.5	53.4- 94.6 85.9- 208.2 188.7- 353.1 48.1- 93.2 7.7- 26.7	Oi: 40.8% (6cm) Oa: 25.4% (2 cm) M: 2.5% (0-6 cm) M: 0.82% (6-40 cm) M: 0.20% (40-48 cm)		2443	Solinger et al. 2001

[a]: The symbol~ means that the organic carbon content is estimated from the organic matter content times a factor of 0.5.
[b]: Standard deviations are in parentheses.
[c]: Th means throughfall solutions.

on the forest floor but metallic oxides can also retain DOC from percolating soil waters to create a second C store in Bhf and Bf horizons.

The DOC concentrations and fluxes differ widely between sites and are highest in the forest floor leachates and in throughfall solutions (Table 16.8). Within the mineral soil, DOC concentrations decrease sharply in the upper B, below the eluvial Ae horizon. The concentration further decreases in the lower B to reach a relatively constant level at the base of the solum. Fluxes of DOC follow a similar pattern. As such, DOC concentrations below the solum range from 2.5 to about 20 mg DOC L^{-1} with fluxes ranging from 17 to 167 kg DOC $ha^{-1}{\cdot}yr^{-1}$. This soil flux generally corresponds well to the total dissolved C output in the stream of a watershed. The annual litterfall input to the soil surface ranges from 1.05 to 4.40 $Mg{\cdot}C{\cdot}ha^{-1}{\cdot}yr^{-1}$ (Table 16.8). It fluctuates yearly at a given site in response to growth conditions and spatially as a function of forest type (e.g. evergreen or deciduous).

Litterfall flux is not the only organic C input to forest soils. Indeed, belowground fluxes through root mortality and rhizo-deposition are very significant contributors to the C soil budget. Indirect evidences from the Hermine suggest that fine root mortality and litterfall are of a similar magnitude in term of C flux to the soil (Courchesne et al. 2001). Similarly, Richter et al. (1999) estimated that rhizo-deposition amounted to about 50% of the litterfall C flux to soils in a catchment from South Carolina (USA). Yet, data on root mortality, rhizo-deposition and subsequent organic C input to soil are virtually unavailable at the watershed scale. Similarly, field measurements of organic C outputs from forest soils in the form of CO_2 fluxes are few at the catchment scale and simulation models are often used to quantify this C efflux (Pumpanen et al. 2003). The magnitude of the CO_2 efflux is underlined by modelling work indicating that it could amount to more than 85% of the total C losses in a wetland (Clair et al. 2002). Recognizing these uncertainties, we elected to calculate a simple annual soil organic C output to input ratio using losses as DOC in seepage waters divided by litterfall deposition. Values range from 0.84% at the Hermine to 2.97% at Howland Forest with Hubbard Brook occupying an intermediate position at 1.54%. In other words, the amount of organic C deposited to the soil surface as litterfall during one year could supply dissolved DOC at the base of the solum for a period of 30 to 120 years. Yet, a relatively conservative soil respiration efflux of 50 $mg{\cdot}C{\cdot}m^{-2}{\cdot}h^{-1}$ (Borken et al. 2004) would be more than sufficient to balance the mean annual litterfall C input reported in Table 16.8. Clearly, more work is needed to complete C budgets, notably with respect to root turnover, and, hence, to establish the watershed-scale current dynamics of organic C.

16.3.2 Forest Ecosystems from Southeastern North America

The available data on the soil organic carbon pool in forest of Southeastern North America vary from 52 to 186 Mg C ha^{-1}, a range that is lower than that of soils of the northeast (Table 16.9). This is in general agreement with data collected by Amunsdon (2001). The main soil organic C pool is still generally observed in the mineral portion of the soil profiles although some old and relatively undisturbed forests (e.g. Great Smoky Mountains) growing on Inceptisols have developed a very thick organic layer that contains more C than the underlying B horizons. None of the listed Northeastern forest sites show a similar inversion in the distribution of soil organic C pools between soil horizons (Table 16.8).

The DOC concentrations in the solutions of the lower soil horizons are restricted to values between 0.5 and 2 mg C L^{-1}, a level much smaller than that of Northeastern forests. Accordingly, DOC fluxes below the solum average about 5 $kg{\cdot}C{\cdot}ha^{-1}{\cdot}yr^{-1}$, reflecting the low dissolved C content. The most abundant soils in forests of Southeastern United States are Ultisols with associated Inceptisols and Spodosols. The Ultisols are highly weathered, deep and acidic soils formed on geologically old areas (Buol et al. 1989). They are characterized by the accumulation of clay-size materials, notably kaolinite, combined with abundant Fe oxides. These properties allow the strong retention of anions such as most DOC compounds and explain the low efflux of organic C in soil leachates.

Litterfall fluxes exceed those measured in colder environments and can reach over 5 $Mg{\cdot}C{\cdot}ha^{-1}{\cdot}yr^{-1}$ (Table 16.9). The simplified soil organic C output (losses as DOC in seepage waters) to input (litterfall deposition) ratio yields values of 0.12% (Coweeta Forest) to 0.16% (Calhoun Forest). These ratios are an order of magnitude lower than results for watersheds of the northeast indicating that the annual organic C output as dissolved C in soil leachates is a very small component of the annual organic budget in these catchments. Indeed, the dissolved output of organic C represents between 0.002 and 0.003% of the total organic C currently stored in these soils.

16.3.3 Forest Ecosystems from Northwestern Europe

The information gathered for European watersheds presenting environmental conditions similar to those existing in Northeastern North America reveal that soil organic C storage is somewhat less at 53 to 220 $Mg{\cdot}C{\cdot}ha^{-1}$ whereas DOC concentrations (2 to 17 $mg{\cdot}DOC{\cdot}L^{-1}$) and fluxes (7 to 63 $kg{\cdot}C{\cdot}ha^{-1}{\cdot}yr^{-1}$) below the solum cover comparable ranges (Table 16.10). Annual litterfall deposition varies from 1.50 to 2.44 $Mg{\cdot}C{\cdot}ha^{-1}{\cdot}yr^{-1}$ (Table 16.8). The work of Valentini et al. (2000) for the period 1996 to 1998

established that many European forest ecosystems currently act as a C sink. The simplified organic C output to input ratio is 0.70 and 2.88% for the Solling and Steinkreuz catchments, respectively. These estimates indicate that the annual litterfall flux is equal to 35 to 140 years of DOC output below the solum, a range that is very similar to that of forests from Northeastern North America. At Solling, the annual output of DOC represents 0.03% of the total organic C currently stored in soils. The range for forests of Northeastern North America is similar at 0.005 to 0.015%, indicating that northern ecosystems of Europe and North America are potentially more sensitive to changes in the rate of organic C transfers (as DOC) from terrestrial to aquatic systems than forested areas of warmer climates.

16.3.4. Carbon Pools and Fluxes in Northern Wetlands

The interest for northern wetlands in the study of the global C cycle originates from the fact that they constitute an ecosystem type, like peat-accumulating wetlands, where considerable amounts of organic C are accumulated and stored in proportion to their total surface area (Dean and Gorham 1998). Indeed, wetland ecosystems present environmental conditions favouring the accumulation of C in organic soil such as a hydrologic regime that favours anoxic conditions, a short growing season accompanied by long periods of cold temperature and a vegetation assemblage well adapted to acid and anoxic conditions, mainly coniferous, that decomposes slowly. Available estimates of organic C storage in wetlands vary from 16%, or 257 Pg C, to 33%, or 455 Pg C, of the global soil C pool (Post et al. 1982; Gorham 1991; Eswaran et al. 1993). It should be noted that these C levels only represent an approximation of the real wetlands C pool because data on the depth and bulk density of organic horizons or soils are often missing. Wetlands are thus generally viewed as a major sink for atmospheric C although some warns that spatial and temporal variability of C fluxes are large and that wetlands can act both as a C source or sink depending on environmental conditions (Blodau 2002).

Figure 16.4 synthesize the results of 21 different studies on C pools and fluxes in wetlands (Trettin et al. 1995). The soil C stock (50–1300 t C ha^{-1}) is the largest C pool in the whole wetland ecosystem. The above- and below-ground vegetation biomass constitute the other major C pool in wetlands, with the overstory vegetation varying from 15 to 52 t C ha^{-1}, whereas the root biomass fluctuates from 5.7 to 16.5 t C ha^{-1}. The understory vegetation represents a minor organic C stock in these systems (Fig. 16.4). The annual storage of C in trees (aboveground and roots)

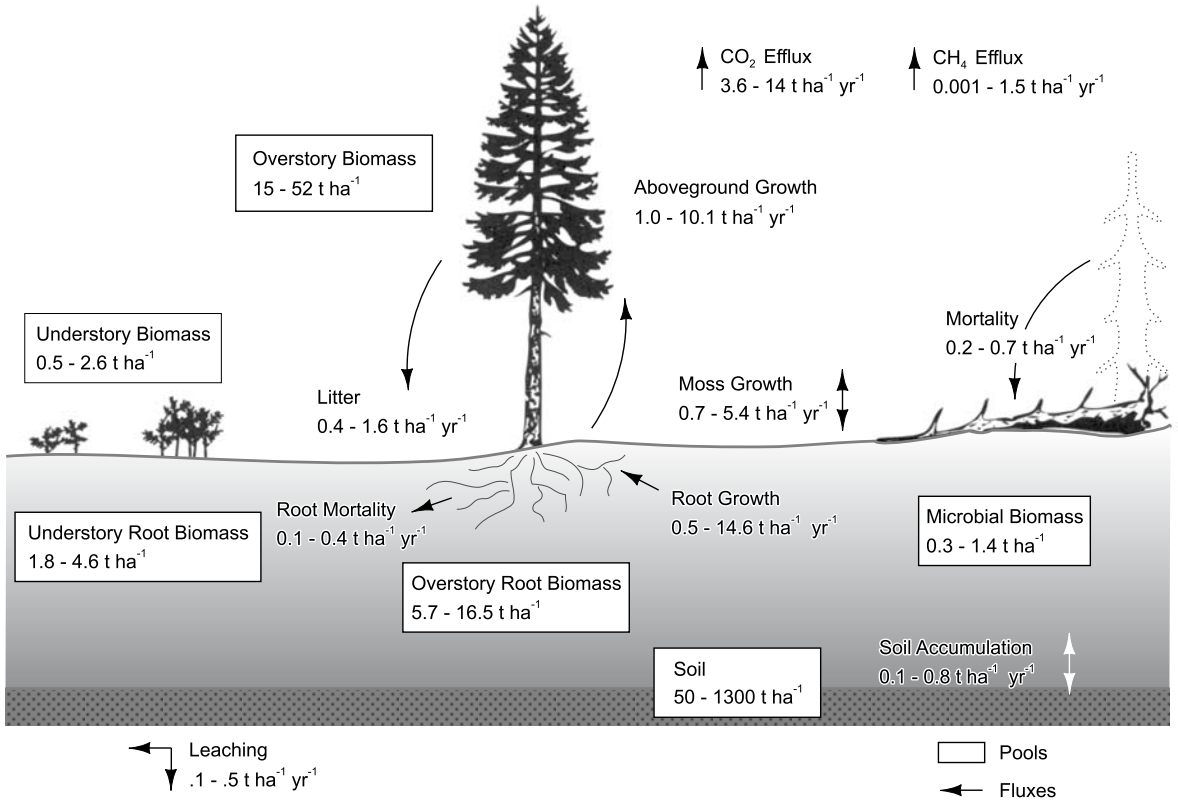

Fig. 16.4. Pools and fluxes of C in northern forested wetlands. The values are from 21 different studies covering the period 1972 to 1993 (modified from Trettin et al. 1995)

encompasses a wide range of values and represents a significant fraction of the standing C stock. Moss growth rates are also variable and are of a magnitude comparable to that of yearly aboveground tree growth. The range of rates of soil C accumulation (0.1–0.8 t C $ha^{-1}yr^{-1}$) somewhat integrates the temporary effects of variations in ecosystem processes and of perturbations (warmer temperature, drier summer, parasite infestation, fires).

The CO_2 and CH_4 effluxes constitute the major vector for C loss from wetlands (Fig. 16.4). They are closely linked to soil temperature. As such, the C effluxes are higher during the summer period and are controlled by the rate of SOM decomposition (Kim and Verma 1992; Bartlett and Harris 1993; Dunfield et al. 1993). The CO_2 is mostly produced by plant respiration and aerobic peat decomposition while CH_4 is the result of anaerobic decomposition (Clair et al. 2002). The water table level also strongly influences the GHGs effluxes with CO_2 fluxes increasing when the water table is low whereas CH_4 emissions tend to increase when groundwater levels are higher. The C losses via deep leaching as DOC are not well documented as indicated by the paucity of data on this DOC flux from wetlands (Blodau 2002). Data in Fig. 16.4 nonetheless suggest that deep leaching of DOC is small compared to gaseous C outputs and that it represents a secondary component of the organic C budget of wetlands. Other evidences reveal that the outflux of C from wetlands in surface waters is however significant at 10 to 15% of total C output (Clair et al. 2002). Moreover, several studies showed that the DOC concentrations in streams or lakes increase with the proportion of the watershed occupied by wetlands, notably under high flow conditions (Dalva and Moore 1991; Koprivnjak and Moore 1992; Judd and Kling 2002).

Although wetlands represent such a major pool of organic C, the relative response of gaseous and dissolved C losses from wetlands to changes in climatic conditions are still poorly known. Recent work in the United Kingdom indicates that the observed increased export of DOC in freshwaters results from the release of DOC from peatlands under rising temperature (Freeman et al. 2001). They showed that the activity of the enzyme phenol oxidase increased with temperature and that it could contribute to the higher DOC export from peatlands. They concluded that the key terrestrial pool of organic C existing in wetlands could progressively be transferred to the oceans and that this flux was likely to increase further if global temperatures were to increase. Looking at gaseous losses of C, Clair et al. (2002) predicted that a climate changes generated by the doubling of atmospheric CO_2 could cause a doubling of the annual losses of C as CO_2 and CH_4 to reach 1.1% of the total biomass. In this context, the wetland would be converted from a C sink to an active source of GHGs

to the atmosphere. In short, the predictions of the evolution of C fluxes to and from northern wetlands under changing climatic conditions are still very uncertain mostly because of the complexity of the processes involved and, unfortunately, because of methodological difficulties (Blodau 2002).

16.4 Implications for the Emission of Greenhouse Gases

Two key questions asked by the scientific community concerning the potential role of soils on the global C cycle in a changing climatic environment are: 1) Will soil behave as a net source of C to the atmosphere under a warmer climate because of increased SOM decomposition? Or 2) Will NPP be stimulated to the extent that soil will behave as a sink of C under increasing air temperature? In other words, will a positive or a negative feed-back be established between the soils and the atmosphere in terms of net C fluxes?

16.4.1 Net Role of Soils on the Cycling of Organic Carbon in Terrestrial Ecosystems

The environmental consequences and problems associated with the emission of GHG to the atmosphere forced scientists to seek a better understanding of the global C cycle. The connections between carbon balance of terrestrial and aquatic ecosystems, and climate are key to this issue. In particular, new knowledge on the role of soils on C storage and sequestration and, thus, on the C cycling, was needed. Consequently, integrated efforts were initiated for a wide spectrum of spatial and temporal scales over the last decade to study the distribution of organic C in soils and C exchanges between soils and the atmosphere. In this context, two positions emerged in the scientific community as to the net effect of future climatic changes on the storage of C in soils. Some studies contend that the soil will continue to act as a sink for atmospheric CO_2 (Tans et al. 1990; Schlesinger 1991) while others submit that GHG-related climate warming will cause soil to become a net source of C to the atmosphere (Houghton and Woodwell 1989; Schimel et al. 1991a,b).

Many studies have shown that C release from soils under a warmer climate will increase because heterotrophic respiration will exceed photosynthesis. In short, soils could become a source of C because air warming will stimulate the decomposition rate of SOM more than NPP. Kirschbaum (2000) adds that the changes in SOM are likely to be very slow with their effect on atmospheric CO_2 being small over the next decades to centuries.

The key role of respiration as the main determinant of C balance in forest ecosystems of Europe was also documented by Valentini et al. (2000). Based on data collected along an elevation gradient, Trumbone et al. (1996) observed a strong dependence of soil organic C turnover time on air temperature and, therefore, suggested that soil could become a source of C if global temperature were to increase. Davidson et al. (2000) further advocated that evidences were in favour of a strong climatic control on the storage of C in terrestrial ecosystems. Goulden et al. (1998) added that climatic changes that promote soil thawing under boreal forest are likely to increase the efflux of CO_2 to the atmosphere because warming at high latitudes would submit previously unexposed organic C compounds to microbial activity. However, recent work by Kulmala et al. (2004) point to an interesting feed-back between increased photosynthesis due to CO_2 fertilization and climate. Their study of pine forest in Finland indeed showed that a CO_2-driven increase in forest biomass could enhance the production of organic aerosols, a phenomenon known to cool climate.

Looking at the decomposition of soil organic C, Giardina and Ryan (2000) found no evidence that decomposition rates C in forest mineral soils, consequently CO_2 production, increased with higher air temperature. Their results originated from a range of 82 sites distributed over five continents and showed that the soil turnover is remarkably constant over a large gradient in mean annual air temperature, in contrast to Trumbone et al. (1996) and Davidson et al. (2000). They nonetheless recognize that some specific conditions could produce a different response of SOM decomposition rates to temperature changes. Schimel et al. (2001) computed global C budgets and established that the terrestrial biosphere (including forest soils) behaved as a C sink in the 1990s and that this sink was mostly located in extratropical areas of North America and Eurasia. They also demonstrated that the evolution of this terrestrial sink was largely due to changes in land use (Schimel et al. 2000). A four-decade-long field study of C accumulation by a re-establishing pine forest ecosystem showed that the forest was a strong C sink and that 20% of the newly accumulated C was found in the forest floor while less than 1% was traced back in mineral horizons (Richter et al. 1999). The trees accounted for 80% of the C sink.

Others scientists have underlined the large uncertainties that exists regarding the magnitude of key C fluxes (e.g. impact of clear cutting, root turnover, erosional losses, CO_2 effluxes from soils), in particular those that are strongly influenced by human activities (Amundson 2001). In this respect, a crucial concern is our incomplete understanding of many microbial mechanisms involved in C transformation, sequestration and translocation in soils and of their response to a changing climate (Fontaine et al. 2004). Obviously, these observations cast a healthy doubt on the reliability of

available data on C fluxes and stores and on their potential use to predict future changes. More generally, some scientists have stressed the fact that the direction and extent of the net effect of changes in climatic conditions on the storage of organic C in soils are, as observed currently in terrestrial environments, likely to vary considerably among forest ecosystems and as a function of future large-scale anthropogenic perturbations (Houghton et al. 1999; Gower 2003).

Finally, and as pointed out by Conant et al. (2003), better estimates of the spatial variability of soil carbon pools in soils are urgently needed to increase the precision of measurements and to make the often modest temporal changes occurring in soil C detectable. This is particularly relevant in strongly heterogeneous forest soils of hilly and mountainous landscapes. Harmon (2001) further suggested that the spatial and temporal scales at which the field studies are performed could play a significant role on the conclusion reached as to the role of forest soil on organic C sequestration. For example, the first 20 cm of the soil could respond to a change in atmospheric CO_2 inputs while the rest of the profile does not (Schimel et al. 1994). Clearly, the scientific debate on whether soils from northern forests will behave as a net source or sink of C under a warmer climate has yet to settle.

16.4.2 Changes in the Transport of DOC from Terrestrial to Aquatic Ecosystems

In the literature, there are some suggestions that global warming could increase DOC export to aquatic environments (Post et al. 1982). Indeed, and because DOC fluxes to surface waters are strongly dependent on hydrology, this process could be accentuated by higher precipitation levels (Michalzik et al. 2001). Similarly, high pulses of DOC to streams have been documented following prolonged dry periods (Biron et al. 1999). However, it is difficult to predict changes in the C cycle only on the basis of precipitation and temperature changes, either on the short or the long term. The temporal variability in the DOC export is indeed caused by a series of environmental factors like the flowpath of water in soils, the perturbation regime and frequency, the abundance and position of wetlands in the watershed and, the balance between ecosystem productivity and decomposition (Brooks et al. 1999; Tranvick and Jansson 2001). Yet, few literature examples based on field measurements integrate this level of functional complexity.

For example, in Sweden an annual temperature reduction was accompanied by an increase in DOC concentrations in both lakes and streams in the 1970s and 1980s. The changes in precipitation and runoff were invoked to

explain these observations (Freeman et al. 2002). In Northwestern Ontario, higher DOC concentrations were also measured in headwater streams where increasing air temperatures and dryer conditions had been recorded. However, lower DOC concentrations were recorded in lakes located downstream because the low water availability favoured the retention of DOC by soils in the upstream segment of the watershed. Clearly, the dominant hydrologic pathway determined if the DOC was to be retained by soil materials or exported towards the aquatic system (Moore 1998; Freeman et al. 2001). As such, there is no definite consensus as to magnitude and direction of the effects of global warming on DOC export fluxes with results varying considerably between ecosystems. Human disturbances (e.g. clear cutting, changes in land use, drainage of wetlands) could add to this complexity by affecting the production DOC and thus the export of DOC towards aquatic environments.

17 Planktonic Community Dynamics over Time in a Large Reservoir and their Influence on Carbon Budgets

Jérôme Marty, Dolors Planas, Bernadette Pinel-Alloul and Ginette Méthot

Abstract

The aim of this chapter was to determine the influence of zooplankton organisms on carbon cycling within reservoirs and lakes from Northern Quebec. The first part of the paper presents results from LG-2 reservoir where zooplankton dynamics were followed from 1 year prior to impoundment to 6 years after flooding. In terms of community structure, flooding was associated with an increase in zooplankton biomass with the strongest effects observed for cladocerans and rotifers. This increase was related to changes in the physical characteristics of the sampled sites (water residence time, temperature and turbidity), chemical characteristics of the water (total phosphorus) and the abundance of resources (Chl. *a*).

The second part of the chapter is a comparison of zooplankton community structure expressed as limnoplankton (AFDW) for several reservoirs of different age (1 to 35 years old). We related the average size of organisms to the algal biomass and finally to the carbon fluxes measured between the water and the atmosphere. We found that part of the larger carbon fluxes observed in young reservoirs compared to older reservoirs may be explained by a top-down control of primary producers by zooplankton.

17.1 Introduction

In the past decade, a growing interest has focused on the role of the biota in the global carbon cycle. Freshwater ecosystems represent an important component of the land in northern regions and particularly in Quebec,

where they cover about 15% of the land surface (Canadian Centre for Remote Sensing, 2001). Consequently, carbon cycling within freshwater ecosystems may contribute to an important part of the total carbon cycling for the north, which has been widely ignored by scientists in the past. Recent studies have shown that the carbon dioxide (CO_2) flux from limnetic habitats to the atmosphere may represent up to 50% of the continental losses of organic plus inorganic carbon to the ocean (Cole et al. 1994). Among the factors regulating the carbon balance in freshwater ecosystems, dissolved organic carbon (DOC) plays a major role (Hope et al. 1996). Lake and catchment characteristics (Sobek et al. 2003), drainage ratio, turnover time (Rasmussen et al. 1989) as well as climatic factors (i.e. precipitation, temperature) are also indirectly related to carbon cycling since they regulate dissolved organic carbon inputs to lakes and rivers. Thus, atmospheric CO_2 is regulated by a number of complex physical, chemical and biological processes and in aquatic sciences, an intensive debate over whether aquatic ecosystems are sinks or sources of CO_2 to the atmosphere continues (Cole et al. 2000, Carignan et al. 2000, Del Giorgio & Duarte 2002, Karl et al. 2003).

Within the last decade, the issue of whether reservoirs are sinks or sources of CO_2 has been raised with regards to hydroeletric reservoirs, since future trends in the building of dams will depend on their global impact to the environment (Rosenberg 2000).

The ability of aquatic ecosystems to buffer atmospheric CO_2 is related to the amount of gross primary production and to the amount of respired carbon (Lyche et al. 1996, Planas et al. 2003). If we are interested in greenhouse gases (GHG) emissions and in particular, the CO_2 dynamics in aquatic systems, particular attention should be addressed to determine the relative contribution of algae and bacterial communities to carbon cycling in freshwaters. However, if we are interested in the mechanisms determining the structure of those communities, many physical, chemical and biological variables must also be considered. One of the biological variables able to influence both algal and bacterial communities is their zooplankton consumers.

Zooplankton communities play a very important role in food-web dynamics because of their central position within the trophic web. They are key to the transfer of carbon from primary producers to higher levels (planktivorous fish) (Galbraith 1967, Hutchinson 1971, Christoffersen et al. 1993) and are able to assimilate carbon from a wide range of sources including microbial organisms (bacteria, ciliates and flagellates) (Sherr & Sherr 1984, Sanders & Wickham 1993, Havens et al. 2000, Adrian et al. 2001, Zöllner et al. 2003, Marty et al. 2003).

Thus, the entire zooplankton community through its impact on food-web structure, is able to influence the limnetic carbon cycle and the state of the ecosystem to act as a sink or source of carbon (Schindler et al. 1997).

The ecology of reservoirs has been relatively well documented in the literature. Most studies have focused on short-time scale observations, getting a "snap shot" image of mechanisms from reservoirs. However, such an approach may not be relevant in the case of reservoirs since, because of their recent history as a new ecosystem, they behave much more dynamically than natural lakes in many of their limnological variables (Thornton 1990). Thus, long-term data sets are necessary to describe the structure and functioning of communities as well as their resilience within these types of systems (Bonecker et al. 2001).

The aims of this chapter are 1-to describe the structure of the zooplankton community in a large reservoir over a long period of time, from one year before impoundment to 6 years after flooding; 2- to determine the most important environmental variables that have an influence on zooplankton community structure in these systems and 3- to compare the zooplankton community structure between reservoirs of different ages to assess its potential effect on carbon dynamics.

17.2 Materials and Methods

17.2.1 Long-term Data Set (1978-1984)

Study Area

The James Bay project is the most ambitious hydroelectric project attempted in Canada. The damming of the river La Grande (53° 54'N, 76° 78'W) consisted in the building of a series of 6 dams as well as two 2 major diversions, resulting in the creation of 9 reservoirs covering a total surface of 17 228 km^2 with an installed capability of 15 244 MW. The reservoir LG-2 (or Robert-Bourassa) was first flooded in November 1978 and was filled within a year, covering a surface area of about 2500 km^2. LG-2 reservoir has a mean depth of 22 m, with a maximum depth of 150 m in front of the dam. Water residence time (WRT) is about 6 months.

An intensive monitoring program was performed by the Société d'Énergie de la Baie James (SEBJ) to determine flooding effects on physical, chemical and biological variables. This program started one year before flooding (1978) and last 6 years after impoundment (1979-1984). A series of 6 stations were chosen: 3 stations were originally situated along the La Grande river (LG2400, LG2402 and LG2406) and 3 others over an-

cient lakes flooded by the reservoir (LG2403, LG2404 and LG2405) (Fig. 17.1). Also, a natural lake (Detcheverry) was sampled to represent an unperturbed ecosystem within the same area. More detailed descriptions of the sites are given in Pinel-Alloul & Méthot (1984), Schetagne & Roy (1985) and Méthot & Pinel-Alloul (1987).

Material and Methods

Sampling was performed during the ice-free period (May to October) for 7 years (1978 to 1984) to cover pre-impoundment (1978), impoundment (1979) and post-impoundment (1980-1984) phases. All variables were sampled twice a month for the overall period, for each selected station. A large set of physical and chemical variables were measured in the field (i.e.: temperature, dissolved oxygen, conductivity, water transparency), derived from field measurements such as water residence time or determined in the laboratory from a composite water sample collected in the euphotic zone of the water column (nutrients, chlorophyll *a*, pH, inorganic (% O_2) carbon) (Table 17.1). All chemical analyses were made following standard procedures (APHA-AWWA-WPCF, 1975) and are described in detail in Schetagne & Roy (1985). Carbonic acid concentration (H_2CO_3) was calculated from bicarbonate concentration using Henry's constant (Kh) corrected for temperature and pH (Sigg et al. 1992). The partial pressure of CO_2 (pCO_2) was also estimated from bicarbonate concentration and pH, with appropriate corrections for temperature (Kling et al. 1992).

Zooplankton was collected at the same frequency as described above, with a Clarck-Bumpus sampler (75 µm mesh) by oblique tows from 25 m to the surface at deep stations or through the entire water column at shallow stations. All samples were fixed with 5% formalin. Zooplankton abundance ($nb{\cdot}m^{-3}$) was determined for each species and then converted to biomass ($mg{\cdot}m^{-3}$) using specific dry weight estimates for cladocerans and copepods (Dumont et al. 1975, Pinel-Alloul & Méthot 1979) and volumetric formula for rotifers (Bottrell et al. 1976). Biomass estimates were computed for each zooplankton group (cladocerans, calanoids, cyclopoids, nauplii and rotifers) and summed to calculate total zooplankton biomass.

A multiple regression model was constructed which predicts total zooplankton biomass based on environmental variables during the flooding of LG-2. Variables were entered into the model using a mixed stepwise procedure, with probability to enter and leave set to 0.05. Data were log-transformed to respect residual homogeneity and normality.

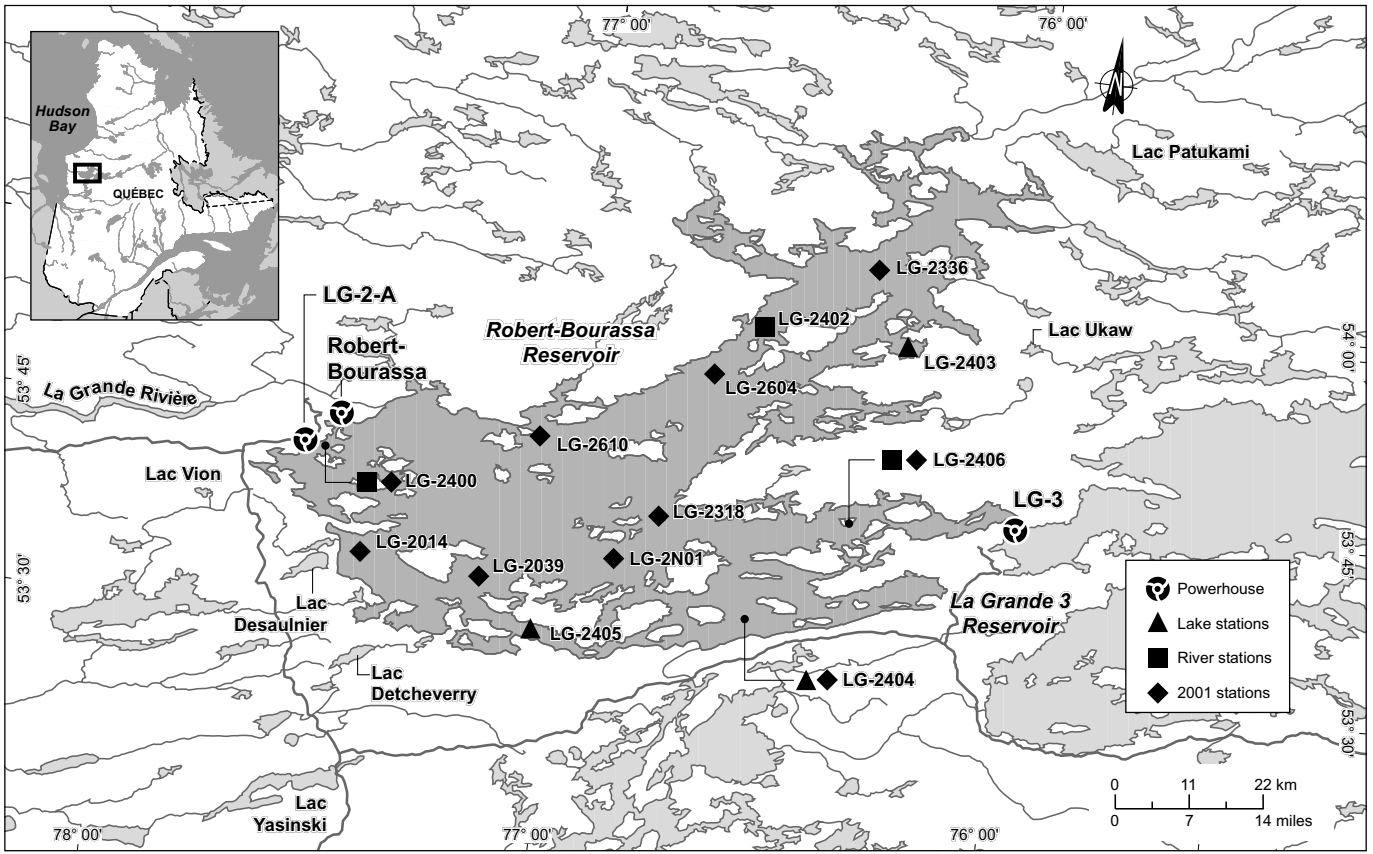

Fig. 17.1. Location of the sampling sites in the LG-2 reservoir, for the long-term data set and for 2001 sampling

Table 17.1. Physical and chemical characteristics in lacustrine and riverine stations of LG-2 and in a reference lake, from 1978 to 1984. Data represents the annual means for each station, with minimal and maximal values

Status	Station	Total phosphorus ($\mu g \cdot l^{-1}$)	Chl.a ($\mu g \cdot l^{-1}$)	pH	Turbidity (utn)	Water residence time (years)	H_2CO_3 ($mg \cdot l^{-1}$)	% O_2	pCO_2 (μatm)
Reference Lake	SB400	4.8 (2-18)	1.1 (0.5-2.4)	7 (6.6-7.3)	0.5 (0.1-2.5)	-	4 (2.8-6.5)	95 (85-103)	1004 (460-2336)
Lake stations	LG2403	12 (5-18)	2.8 (n.d.-8.5)	6.4 (5.9-6.9)	0.8 (0.4-1.9)	2.5 (2.5-2.5)	11.7 (8.6-16.3)	87.5 (67-100)	1516 (572-4107)
	LG2405	16.5 (4-33)	2.9 (0.6-8.4)	6.5 (6.1-7.1)	1.1 (0.5-2.3)	-	12.9 (7-21.2)	80.6 (36-95)	1895 (513-4579)
	LG2404	12.8 (5-27)	2.1 (0.6-4.8)	6.3 (6-6.7)	2.3 (0.6-9.8)	0.07 (0-0.2)	11.4 (6.2-16.7)	92 (78-105)	1354 (458-3026)
Riverine stations	LG2400	11.1 (5-18)	1.7 (n.d.-5)	6.3 (5.9-6.7)	1 (0.4-5)	1.2 (0-2.5)	17.2 (5.6-23.3)	86 (57-110)	1668 (653-3847)
	LG2402	11.7 (0.7-25)	2.1 (0.1-7.2)	6.4 (5.9-6.8)	0.9 (0.2-3.8)	1.1 (0-1.5)	13.2 (4.9-26.6)	87 (64-106)	1423 (419-4180)
	LG2406	10.5 (4-18)	1.6 (0.2-4.6)	6.4 (6-6.8)	1 (0.2-5.9)	0.7 (0-2.5)	9.7 (8.6-11.5)	96 (71-115)	1388 (528-2485)

17.2.2 Recent Data Set

During the past 3 years (2001-2003), a new research project has been conducted in the major hydroelectric reservoirs of Quebec to assess the contribution of the biological component of the carbon cycle to carbon emissions from reservoirs to the atmosphere. Similar to the long-term data set, environmental variables were measured at several stations within various reservoirs, and in addition, planktonic metabolism (Planas et al. 2003) and CO_2 flux arising from the water column to the atmosphere were also measured.

Study Area

In 2001, sampling was carried out in two reservoirs of La Grande river with 10 sampling sites visited twice on the LG-2 reservoir (Fig. 17.1) and 2 sites on LA-1, a more recently flooded reservoir (7-years), as well as a series of 7 natural lakes situated near the two reservoirs.

In 2002, 2 other reservoirs were sampled in the North shore of the St Lawrence region: the Manic-5 reservoir (35 years) and the recently flooded reservoir SM-3 (1 year). Six stations were sampled on each reservoir as well as 6 reference lakes situated in the same region (for station localization, see Fig. 18.5, Planas et al. 2004).

Zooplankton Biomass Estimates

Zooplankton was sampled with a 53 μm mesh sized net (diameter: 0.2 m), from 1 m above the sediments to the surface or from a maximum depth of 30 m for the deepest stations. Sampled volumes varied from 15 to 950 L depending on site depth. Zooplankton were first narcotised with carbonated water and then preserved in 4% formaldehyde.

In the laboratory, each zooplankton sample (250 ml) was divided into two equal volumes with a Folsom splitter for taxonomic and limnoplankton analyses. Both sub-samples were then fractionated into 4 size classes by sequential screening through Nitex nets (500 μm, 200 μm, 100 μm and 53 μm) to determine the size spectra of the community for biomass calculations.

To estimate limnoplankton biomass corresponding to sestonic particles, the size fractions from half of the original sample (125 ml), as previously described, were filtered onto on a pre-combusted GF/C (Whatman) glass fibre filter, dried at 40°C for 24 hours and ash-combusted at 500°C for 12 hours. Limnoplankton organic biomass was calculated for each size fraction as the difference between the dry weight and ash weight, ex-

pressed in mg of ash-free dry weight (AFDW) of limnoplankton per unit volume. Here, the term limnoplankton is defined as the seston fraction larger than 53 μm, including zooplankton plus algae and detritus (the two latter particularly in size fractions <200 μm). A full description of the limnoplankton analyses has been presented in previous studies (Masson & Pinel-Alloul 1998, Patoine et al. 2000).

All limnoplankton data were averaged for each reservoir (all stations within a single reservoir) and over time. General differences among sites were tested on log-transformed data using one-way ANOVA and specific differences among sites were determined by comparing means using Tukey-Kramer HSD test.

The specific weight (mg.ind.) of main taxonomic groups was determined using a large 110 um plankton net (0.5 m. diameter) to obtain a large number of organisms. To obtain a precise measurement of weight, organisms were sorted and then placed in filtered water to allow gut evacuation and then directly placed in a pre-weighted capsule and frozen in liquid nitrogen. In the laboratory, organisms were freeze-dried to avoid loss of volatile organic compounds and then weighed on a Sartorius M2P scale. Weights were averaged for the overall community, per sites.

17.3 Results

17.3.1 Long-term Variation in Zooplankton Community (1978-1984)

Impoundment had a great impact on total zooplankton biomass (TZB) in both inundated rivers and lakes (Fig. 17.2). A gradual increase in zooplankton biomass was observed during the first 5 years of the study. If we consider the first 3 years (pre-impoundment period and one year after flooding: 1978-1980), TZB was higher in lakes stations (19-44 $mg{\cdot}m^{-3}$), compared to the reference lake (21-17 $mg{\cdot}m^{-3}$) and river stations (0.18-14 $mg{\cdot}m^{-3}$). During the following two years (1981-1982), zooplankton biomass was comparable in both types of impounded stations and reached maximum values (42-58 $mg{\cdot}m^{-3}$) equivalent to 3 to 4 times the biomass from reference lake and 2.7 to 300 times the biomass observed the year previous to impoundment (1978) in the river La Grande. The decrease and stabilization of zooplankton biomass began in 1983. Although double that in the reference lake, zooplankton biomass declined to a level close to the one shown in 1978 in flooded lakes.

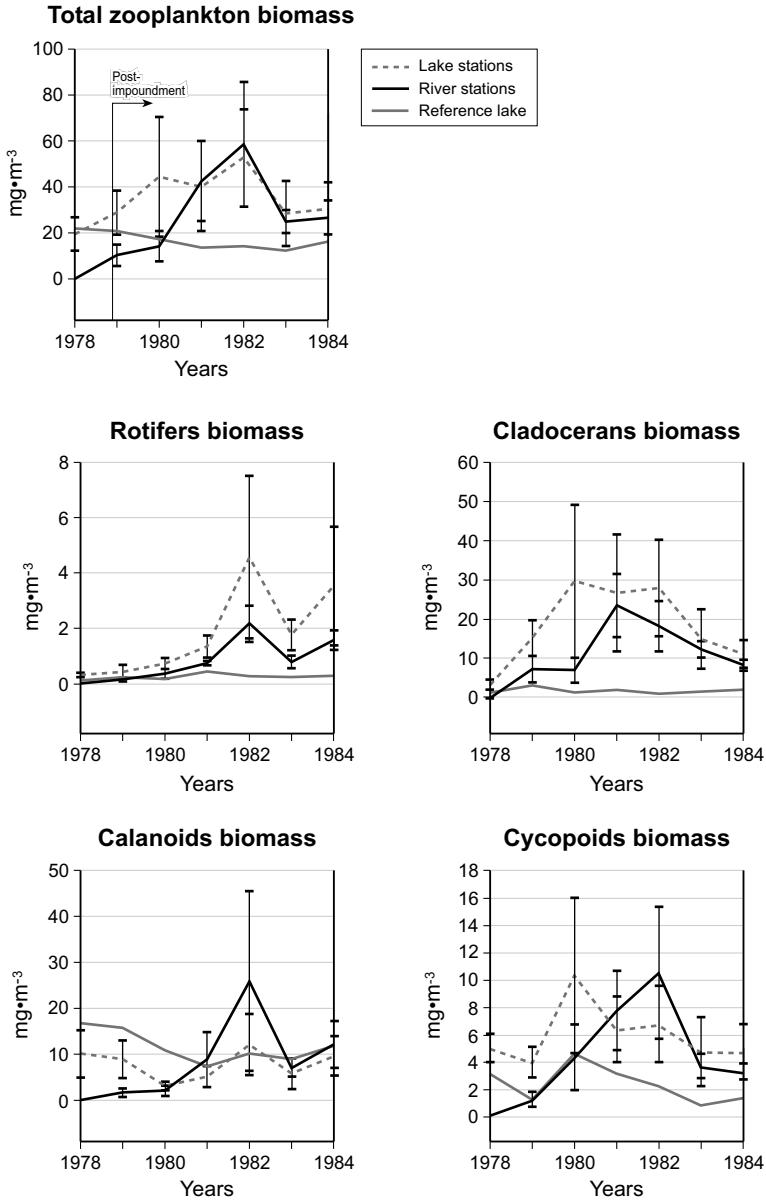

Fig. 17.2 Annual variations (1978-1984) in zooplankton biomass in lake and river stations of LG-2 reservoir and in the reference lake (data are presented as the mean ± SE)

The response of each taxonomic group to impoundment is also presented in Fig. 17.2. The most significant increase in biomass was observed for cladocerans: almost absent before impoundment in river stations (0.04 $mg{\cdot}m^{-3}$) and low in biomass in lake stations (3.3 $mg{\cdot}m^{-3}$), they were the most predominant group after 1979 with maximum values reached in 1980, the year following flooding in lake stations (30 $mg{\cdot}m^{-3}$) and 2 years (1981) after flooding for river stations (23 $mg{\cdot}m^{-3}$). In lake stations, a decrease in the development of calanoids and cyclopoids copepods at the beginning of the impoundment (1978-79) was concomitant to an increase in rotifers biomass.

Environmental variables that entered in the multiple regressions model to predict total zooplankton biomass are presented in Table 17.2 in the selection order. We observed that zooplankton biomass could be predicted with physical (water residence time, temperature and turbidity), chemical (total phosphorus) and biological variables (chl. *a*), explaining 67% of TZB variance. The order in which variables entered the model indicates how was the variable significant to predict TZB considering the last entered variable. Thus, water residence time was the best predicting variable, followed by temperature, total phosphorus, chl. *a* and turbidity (Table 17.2).

Table 17.2. Multiple regression model for prediction of total zooplankton biomass during flooding period of LG-2 reservoir

Variables	Coefficient	S.E.	t	p(t)	r^2	VIF	Partial correlation
Zooplankton biomass					0.67		
Intercept	0.19	0.24	0.76	0.44		1.07	
Water residence time	0.59	0.04	14.22	<0.0001		1.55	0.63
Temperature	2.08	0.18	10.99	<0.0001		1.31	0.37
Total phosphorus	53.2	16.96	3.14	0.002		1.07	0.22
Chl. a	0.45	0.17	2.56	0.011		1.35	0.39
Turbidity	-0.528	0.23	-2.3	0.022		1.44	-0.38

n=261, F=105.5, p(F)<0.0001, r^2-adj=0.66

17.3.2 Relation with Water Quality and Trophic Status

After impoundment, changes in water quality were observed in most physical and chemical variables (Schetagne & Roy 1985). Change in productivity is illustrated in Fig. 17.3. Mean total phosphorus (TP) concentration for the 7 years period was 13.8 $\mu g{\cdot}L^{-1}$ in the lakes stations, 11.1 $\mu g{\cdot}L^{-1}$

in the river stations and 4.8 µg·L^{-1} in the reference lake. TP increased during the first 3 years after impoundment until 1981 and then decreased slowly the following years (Table 17.1). Nutrient increase was concomitant to this of phytoplankton biomass expressed as chl. *a*: during the three years following flooding, chl. *a* increased from 1 to 3 µg·L^{-1}. In the reference lake, TP and chl. *a* concentrations remained stable during the 1979-1984 time period with respectively 4.8 µg·L^{-1}and 1.1 µg·L^{-1} in average for the overall period (Fig. 17.3). We noticed an increase in chl. *a*, for all studied sites for the year 1981, suggesting a certain coherence among ecosystem and the potential role of large scale influences on the dynamic of plankton.

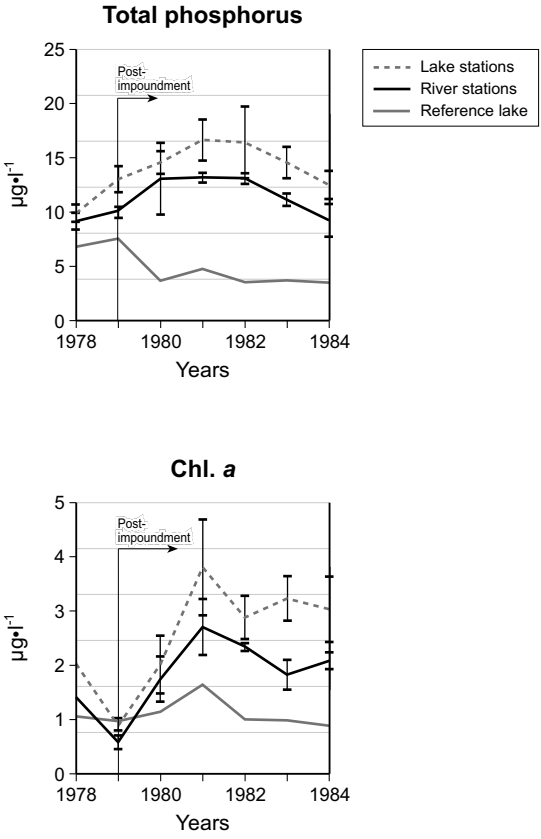

Fig. 17.3 Annual variations (1978-1984) in total phosphorus and *chl.a* in lake and river stations of LG-2 reservoir and in the reference lake (data are presented as the mean ± SE)

Changes in the concentration of carbonic acid (H_2CO_3), pCO_2, the percentage of oxygen and pH are reported in Fig. 17.4. The pCO_2 values from all sites (reservoir or lake) show that all ecosystems were over-saturated in CO_2, even prior to flooding. In LG-2 reservoir, H_2CO_3 concentration and pCO_2 were 0.083 mmol·L^{-1} and 1500 µatm. respectively, which is about 50% higher than in the reference lake (0.053 mmol·L^{-1} and 1004 µatm.). An increase was observed for 2 years after flooding, followed by a gradual decrease. Over the 7 years, no difference was detected between lake and river stations, except between reservoir stations and the natural lake, with values higher in the reservoir, even 5 years after flooding. The percentage of oxygen decreased from 95 to 80% during the first 3 years after flooding and then increased to a stable value (89%) in 1983 and 1984. However, lower oxygen saturation values persisted in the reservoir compared to the reference lake, even 7 years after flooding. Finally, mean pH tended to be lower in both types of reservoir stations (6.3) compared to the reference lake (7).

17.3.3 Recent Data Set: A Comparison between Reservoirs

Limnoplankton

Total limnoplankton biomass expressed in AFDW varied from 7.75 to 50 mg·m^{-3} among sampled reservoirs and lakes. Natural lakes, LG-2 and SM-3 reservoirs had a comparable total limnoplankton biomass (21.9 to 24.5 mg·m^{-3}) whereas the highest biomass was observed in LA-1 station and the lowest in MA-5. On average, total limnoplankton biomass (4.7 mg·m^{-3}) in the older reservoirs (MA-5, LG-2) was lower than in the young reservoirs (LA-1, SM-3) but didn't differ significantly among reservoirs when considered together (Fig. 17.5).

Within the total limnoplankton, the largest size-fraction (>500 µm) represented 11 to 32% of total biomass. Taxonomic observations under a binocular stereomicroscope showed that the >500 µm fraction corresponded mostly to cladocerans such as *Daphnia* spp. and *Holopedium* sp., adult calanoids and cyclopoids such as *Epischura* sp., *Leptodiaptomus* sp. and *Mesocyclops* sp. The maximum biomass for this fraction was observed in the recent SM-3 and LA-1 reservoirs with values twice to six times higher compared to the older reservoirs MA-5 and LG-2 (Table 17.3). AFDW for the >500 µm fraction (4.7 mg·m^{-3}) was higher in the lake than in the older reservoirs and lower than in the young reservoirs but did not differ significantly from reservoirs when they were all considered together (Fig. 17.5).

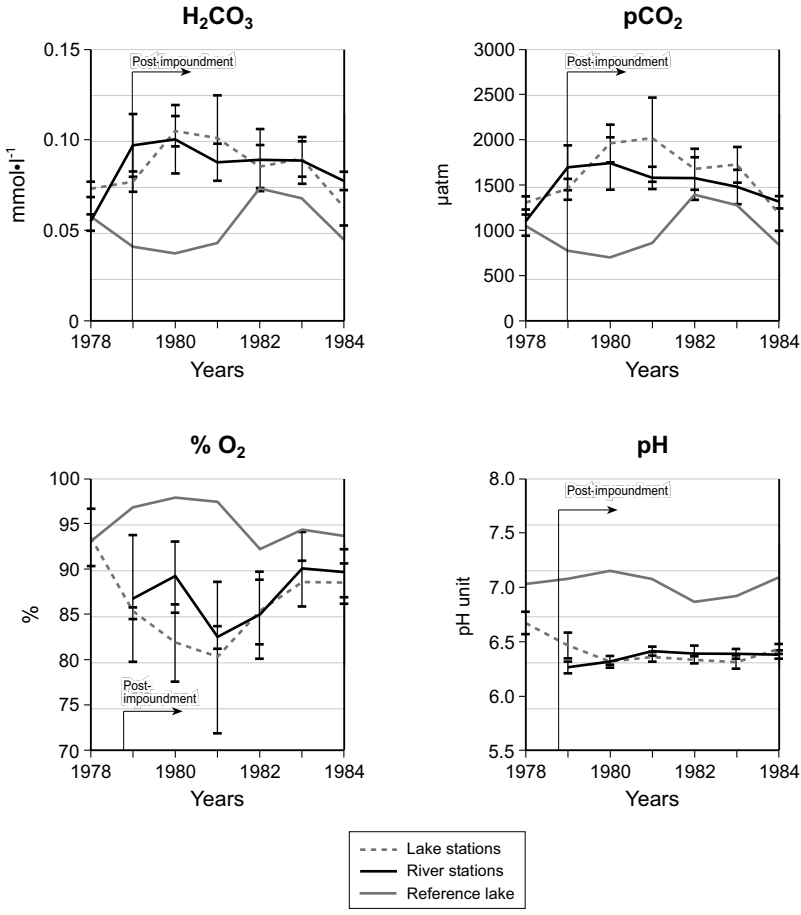

Fig. 17.4 Annual variations (1978-1984) in carbonic acid (H_2CO_3), pCO_2, oxygen and pH in lake and river stations of LG-2 reservoir and in the reference lake (data are presented as the mean ± SE)

The 200-500 µm fraction accounted for 20 to 30% of total limnoplankton biomass and corresponded to smaller cladocerans such as *Bosmina* sp. and immature copepods. There was no general difference between sites (P=0.07) detected with one-way ANOVA, although Tukey-Kramer test showed significantly higher values in LA-1 and LG-2 reservoirs than in MA-5 reservoir (Fig. 17.5).

The 100-200 µm fraction was composed of nauplii and large rotifers such as *Kellicottia longispina* as well as a large amount of colonial algae such as *Tabellaria sp*. Because of this large algal contribution, this fraction

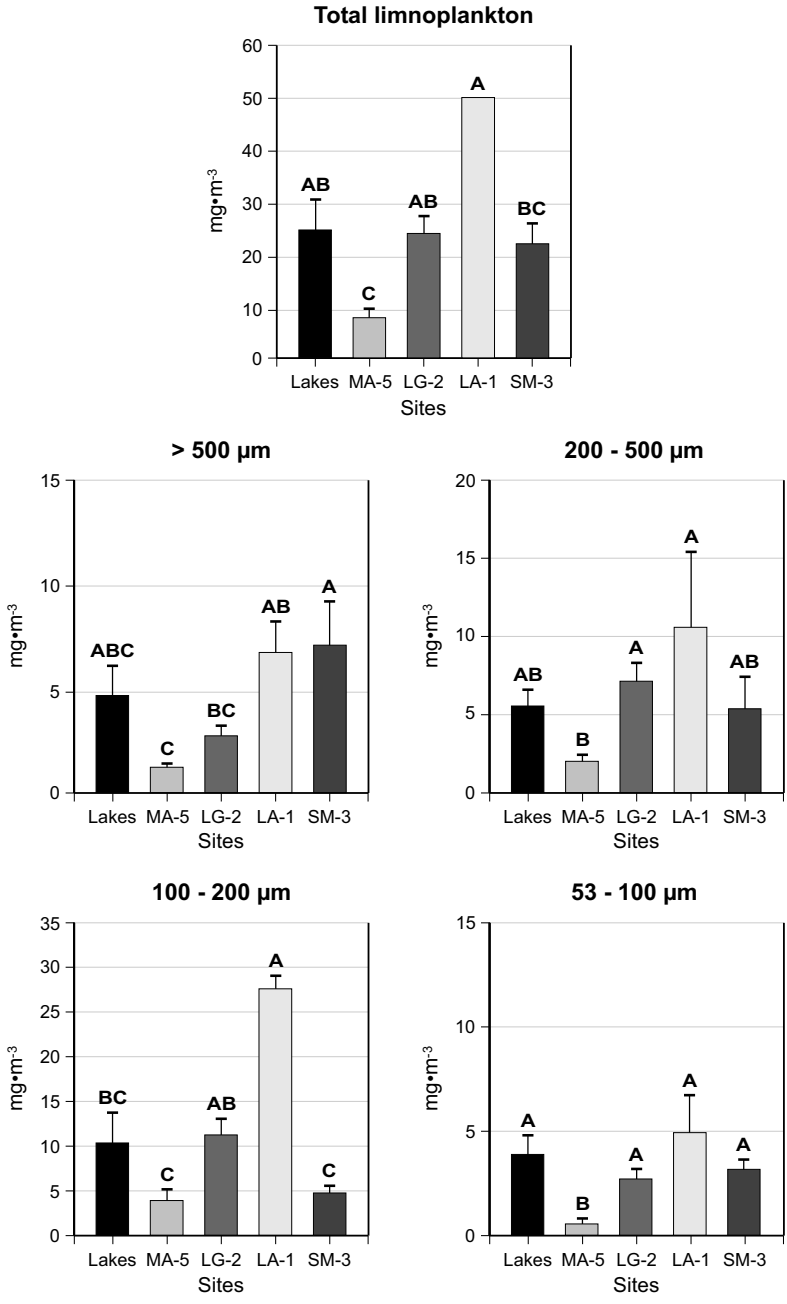

Fig. 17.5 Ash free dry weight (mg. AFDW·L^{-1}) of seston for a group of northern Quebec lakes and reservoirs. Levels not connected by the same letter are significantly different. Data are shown as the mean ± SE

Table 17.3. Limnoplankton biomass expressed as ash free dry weight (mg·AFDW·L^{-1}) according to size fraction, in a series of 4 reservoirs from Northern Quebec and in natural lakes. Data are presented as the means over sampling period and stations, with minimal and maximal values

	Lakes	LA-1	LG-2	Manic-5	SM-3
N	9	2	12	6	5
Total limnoplankton	24.5 (2.9-63.3)	49.9 (49.8-50)	23.8 (10.7-46.9)	7.7 (4.4-9.7)	21.9 (12.8-34.6)
>500 µm	4.7 (0.4-13.8)	6.8 (5.3-8.3)	2.8 (1-7.3)	1.2 (1-1.5)	7.1 (2.4-16.2)
200-500 µm	5.5 (0.9-9.7)	10.6 (5.7-15.4)	7.1 (1.7-13.4)	2.0 (1.2-2.6)	5.38 (2.9-13.8)
100-200 µm	10.3 (0.9-35)	27.6 (26.1-29.1)	11.2 (4.8-23.2)	3.9 (1.31-5.3)	4.8 (2.3-7.7)
53-100 µm	3.9 (0.7-10.1)	4.9 (3.1-6.7)	2.7 (1.1-6.0)	0.5 (0-0.9)	3.2 (1.6-4.9)

accounted for 24% (SM-3) to 55% (LA-1) of total limnoplankton biomass. A significant biomass difference of this fraction was observed among sites (P=0.01) with values significantly lower in North shore of the St Lawrence region, MA-5 and SM-3 and higher in LA-1. No difference was observed between natural lakes and LG-2 reservoir (Fig. 17.5).

Finally, the 53-100 μm fraction was characterized by small rotifers (*Keratella cochlearis, Polyarthra vulgaris*), algae and organic matter; and accounted for a minor proportion to total biomass (7-16%). Only MA-5 was significantly lower in biomass compared to other sites (Fig. 17.5).

Zooplankton Specific Weight

Zooplankton weight variation among sites is presented in Fig. 17.6. Organisms from the La Grande River region (LG-2, LA-1) were smaller compared to the ones in the North shore of the St Lawrence region (MA-5, SM-3). The lowest weights were observed in the LG-2 reservoir (1.7 $\mu g \cdot ind^{-1}$) and then in LA-1 (2.7 $\mu g \cdot ind^{-1}$). The maximum value (26.7 $\mu g \cdot ind^{-1}$) was observed in the recently flooded reservoirs SM-3 with organisms in average 15 times heavier compared to LG-2. Organisms from MA-5 reservoir and natural lakes had a comparable weight (8.5 and 13 $\mu g \cdot ind^{-1}$).

17.4 Discussion

One of the most consistent features of new reservoirs is the temporary increase, called “trophic upsurge”, of all trophic levels following impoundment. This phenomenon was first observed in Russian reservoirs (Baranov 1962) and also in western and eastern Canada by Duthie & Ostrofsky (1975) and Pinel-Alloul & Méthot (1984). Trophic upsurge is characterized by an initial increase in nutrient concentration (in particular phosphorus), originating from the degradation of labile organic compounds (soils and vegetation compounds) that boosts the overall productivity of the reservoir for about a decade, until nutrients become re-equilibrated to the initial conditions. In LG-2, the trophic upsurge of zooplankton lasted 4 years (1980 to 1984), but no strong depression in productivity was observed the following years, since nutrient concentrations remained stable at least until 5-years after impoundment (Fig. 17.3). Variation in the intensity and length of the trophic upsurge may be observed among reservoirs. It depends on the initial trophic state of the flooded ecosystem but also on landscape characteristics such as soil thickness, type of vegetation and its degradability (St Louis et al. 2000), watershed slope and human activity

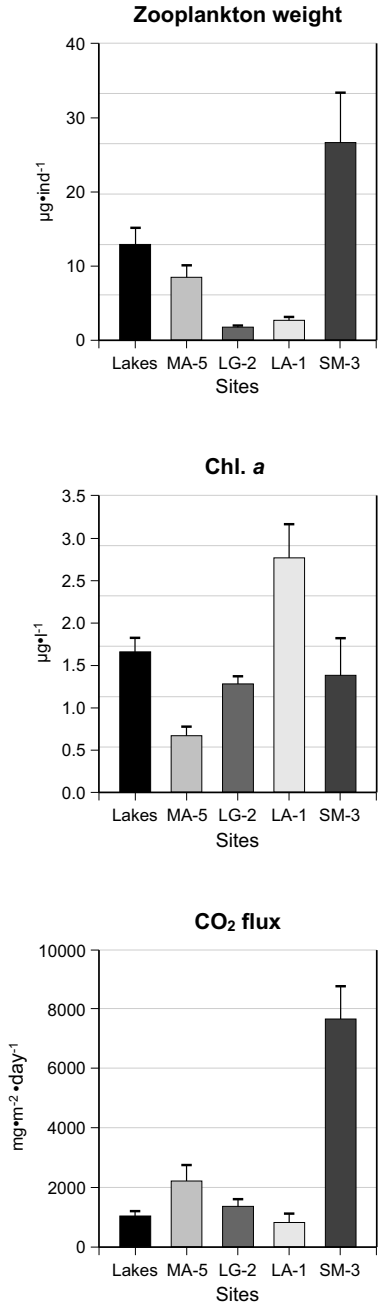

Fig. 17.6 Comparison of zooplankton weight, phytoplankton biomass and evasive CO_2 flux for a group of northern Quebec lakes and reservoirs. Data are presented as the mean ± SE

(Marzolf 1990a). The recent data on LG-2 (limnoplankton and chl. *a* concentrations), 23 years after impoundment, suggest that the trophic state of the reservoir may even be lower than the one prior to impoundment. This could be explained by the fact that hydrological variables such as water residence time and temperature play a more important role in reservoirs compared to natural lakes, at least for zooplankton community (Naselli-Flores & Barone 1994, 1997, Velho et al. 2001).

During LG-2 flooding, all zooplankton taxonomic groups responded to the trophic upsurge but cladocerans and rotifers were the most sensitive to flooding (Fig. 17.2) since they are generally more adapted to variable hydrological characteristics of reservoirs (Branco et al. 2002). A comparable result for cladocerans was observed in the recent data set where the AFDW for the >500 μm fraction was higher in recent reservoirs compared to older ones. Zooplankton community within reservoirs is usually dominated by fast-growing organisms (r-strategists species) such as cladocerans (Paterson et al. 1997) and rotifers (Nogueira 2001). Copepods, because of their longer development time, are often absent in reservoirs where they experience washout if water residence time is shorter than their development time (McLaren 1963).

The difference between river and lake stations illustrates that biological response to impoundment may differ with the type of flooded water body. Considering the type of reservoir or the type of stations within a single reservoir is important in the case of zooplankton since most groups are limited in their development in flowing water. The damming of rivers creates non-flowing or low-flow habitats for organisms in regions where they did not exist previously (Marzolf 1990b), whereas impoundments which include natural lakes create flowing habitats in previously non-flowing water bodies. During LG-2 flooding, the impoundment of the La Grande river induced contrasting effects of trophic upsurge on zooplankton since both rivers and lakes were flooded. Lake stations were characterized by higher biomass compared to river stations. This could be explained by the fact that reservoirs differ from lakes in many of their physical and chemical characteristics and the most important of which, in the case of planktonic communities, are variables related to water residence time, temperature, nutrients and turbidity. In LG-2, the minor increment in zooplankton biomass was observed in stations characterized by low water residence time such as LG2400 situated close to the dam and also in stations close to the inflow of water coming from a distinct geologically area, covered by the sediment of the Tyrrel Sea, with a more variable regime (LG2404). The importance of hydrology on zooplankton biomass was confirmed in the multiple regressions model when a majority of the variables that entered the model were related to hydrology.

We hypothesize that food web structure may determine the degree of the ecosystem to act as a sink or source of carbon. In lakes, Schindler et al. (1997) observed that the presence of large grazer organisms could be related to a decrease in primary production in turn associated to an increase in the partial pressure of CO_2 (pCO_2) at the air-water interface. Considering the long-term data set from the LG-2 reservoir, there was no clear impact from zooplankton on phytoplankton biomass. Instead, the observed trophic upsurge supports a stronger bottom-up impact due to high nutrient availability rather than a top-down control from higher level of the food-web, which is illustrated by the selection of total phosphorus and chl.*a* as variables to predict TZB. This result is consistent with other studies from recently flooded reservoirs (Paterson et al. 1997, Holz et al. 1997, Thouvenot et al. 2000) or natural lakes (Hessen 1989, Jürgens 1994).

It is difficult to link biological variables to the amount of carbon exchanged with the atmosphere since no direct fluxes were measured during LG-2 flooding. To a lower extent, carbonic acid concentration and pCO_2 can be related to the importance of biological processes occurring in the water column and therefore that to the ability of the ecosystem to act as a source or sink of carbon. Photosynthetic activity is usually related to a change in oxygen concentration as well as an increase in pH due to the removal of carbonic acid. On the other hand, when respiration occurs, carbon is released and a decrease in oxygen and pH may be observed in the water column. The higher pCO_2 values in LG-2 after flooding (Fig. 17.4) suggest that this reservoir was probably acting more as a source than a sink of CO_2 to the atmosphere. Both decreases in oxygen and pH validate the fact that respiration might play a major role over photosynthesis during the early years of LG-2. This is not surprising considering that in recently flooded reservoirs, the decomposition of large amounts of organic matter implies CO_2 production through respiration process (Duchemin et al. 1995, Houel 2003).

When comparing zooplankton specific weight and chl. *a* (Fig. 17.6), reservoirs with large-bodied zooplankton organisms were characterized by a lower phytoplankton biomass. For instance, reservoirs with the heaviest zooplankton organisms (SM-3 and MA-5) had the lowest chl. *a* concentration. Surprisingly, the weight of organisms differed more according to the regions rather than reservoirs age. Regional characteristics such as temperature may explain such difference since ice-free period tend to be shorter for northern ecosystems. Also, reservoir characteristics such as water residence time may limit the development of organisms and, therefore, modulate their potential impact on algae.

In the recent data set, direct flux measurements of CO_2 arising from the water column were performed, enabling to relate carbon production to bio-

logical processes such as planktonic production and respiration (Planas et al. 2003). Data on zooplankton show that carbon flux between the water and the atmosphere may also be influenced by food-web structure. Large organisms were able to suppress more effectively phytoplankton and a greater proportion of carbon was released to the atmosphere. Moreover, we found a negative correlation between zooplankton weight and the ratio between production (AGP) and respiration (R) ($r=-0.98$, $p=0.004$), suggesting the strong effect of food-web structure not only on phytoplankton biomass but also on the metabolic balance of plankton. Finally, we also performed stable isotope analysis on zooplankton, phytoplankton and organic matter to determine the contribution of allochthonous and autochthonous sources of carbon to zooplankton. Preliminary results show that zooplankton organisms rely more on phytoplankton rather than detrital material in reservoirs compared to lakes. Carbon stable analysis confirmed the top-down effect of zooplankton organisms on the algal community as suggested in Fig. 17.6: we found that organisms from younger reservoirs were strongly depleted in $\delta^{13}C$ compared to older reservoirs and natural lakes. Also, we were able to correlate the carbon signatures of organisms with carbon fluxes measured at the water-atmosphere interface ($r=-0.86$; $p=0.0005$), with the most depleted carbon signatures measured in sites where high carbon fluxes were recorded (Marty et al., in preparation).

17.5 Conclusions

This study confirms the importance of zooplankton community in the planktonic food-webs from reservoirs through bottom-up and top-down control. During the flooding of LG-2, the increase in food resources allowed zooplankton biomass to increase as predicted according to the theory of trophic upsurge. However, if zooplankton were not limited by food resource, physical characteristics of reservoirs played a major role in structuring zooplankton communities. Water residence time and temperature were most important for the prediction of zooplankton biomass since lower residence time and higher temperature allowed cladocerans and rotifers to respond the most to flooding.

If the long term monitoring of LG-2 suggests a bottom-up effect on zooplankton, data on other studied reservoirs revealed the potential top-down impact from zooplankton on primary producers and in turn, on the global carbon cycle. More specifically, we found that zooplankton community structure is able to influence the ability of reservoirs to act as a sink or a source of carbon for the atmosphere.

18 Production and Consumption of Methane in Soil, Peat, and Sediments from a Hydro-Electric Reservoir (Robert-Bourassa) and Lakes in the Canadian Taiga

Louis B. Jugnia, Réal Roy, Maria C. Pacheco-Oliver, Carlos B. Miguez, Charles W. Greer

Abstract

Functional and structural aspects of the indigenous methanogenic and methanotrophic microbial populations were assessed in soil, peat and sediment from a hydroelectric reservoir (Robert-Bourassa) located in the subarctic Taiga. Three locations (un-flooded, seasonal flooding, and permanent flooding) in the reservoir were selected for sampling of forest soil and peat soil. Lakes located near the reservoir were also sampling for comparison with nearby unperturbed aquatic systems. Using samples incubated in microcosms at 5, 10 and 25°C, methane production and oxidation were quantified by gas chromatography. Structural aspects included bacterial counts of methanotrophic bacteria, and PCR amplification using 16S rDNA universal primers and primers specific for genes involved in methanogenesis or methanotrophy.

Methanogenesis in the different systems appeared to depend on a combination of environmental factors, including the amounts and quality of organic carbon, and the abundance of oxidizing ions (Fe^{3+}, SO_4^{2-}). Periodically flooded or flooded peats contributed more to methane production than unflooded peats, soils and natural lake sediments. Similarly, methane oxidation rates were higher in peat soils than in flooded soils or lake sediments. The lowest rate of methane oxidation was observed in the forest soil, which was a typically undisturbed soil where the rate of CH_4 production was close to the lower range of values observed in this study. This parallel evolution between the potential rate of methanogenesis and CH_4

oxidation suggests an association between CH_4 oxidation activity and CH_4 supply. Methanogenesis appeared more sensitive to temperature increases than methanotrophy.

The nucleotide sequences of PCR amplified and cloned *mcrA* fragment, a gene specific to methanogenesis revealed that many of the sequences obtained from the soils in this study were closely related to only uncultured clones of methanogens. Methanotrophic bacterial abundance was higher in flooded peat and lake sediment than in flooded soil, but abundance of methanotrophic bacteria in unflooded peat was lower than in unflooded forest soil. PCR amplification of genes specific to methanotrophic bacteria suggested that flooding of soil leads to a shift in populations of methanotrophic bacteria.

A comparison of methane production and oxidation values obtained during this study indicated that essentially all of the methane produced in peat, forest soil and sediment could be oxidized within the system with little net atmospheric emission.

18.1 Introduction

The atmospheric concentration of methane has increased dramatically since the industrial revolution and this may be a driving factor in global climate change. Methane (CH_4) is a very potent greenhouse gas. Compared to CO_2, methane absorbs infrared radiation more effectively (Conrad 1996; Crutzen 1991) and has a global warming potential 21 times that of CO_2 (IPCC 1992). In addition to this warming effect, CH_4 participates in chemical reactions in the atmosphere that lead to the formation of tropospheric ozone, itself a green house gas. This ozone formation amplifies the direct green house effect of methane by approximately 70% (Moss 1992).

Two modes of origin for methane are commonly recognised: biogenic methane produced by living organisms and abiogenic chemically-produced (thermocatalytic) methane. In the literature, the CH_4 resulting from the degradation of organic matter by anaerobic microbes is commonly referred to as biogenic CH_4. It is formed by strictly anaerobic methanogenic archaea (methanogens) (Zinder 1993), which occupy a diverse range of anaerobic habitats, e.g. marine and freshwater sediments, marshes, swamps, flooded soils, bogs and intestinal tracts of animals. In the presence of oxygen, a substantial part of the produced CH_4 can be oxidized by methane oxidizing bacteria (methanotrophs) and thus be retained in the system as biomass carbon or emitted as CO_2 (Roslev et al. 1997) (Hanson and Hanson 1996).

Microbial production and oxidation of methane are performed by natural microbial populations involved in the biochemical cycle of carbon. An environment is a CH_4 source when CH_4 production by methanogenic archaea is greater than its consumption by methanotrophic bacteria. On the contrary, if methane oxidation is greater than its production, the environment is a sink for methane. A change in the equilibrium between sources and sinks can lead to increased atmospheric emission. A particular concern is the increase in the atmospheric methane concentration as a consequence of anthropogenic activities, such as the creation of reservoirs for energy or water supply (irrigation or drinking water) schemes. In northern Quebec, the development of hydroelectric facilities that provide energy for urban zones located in the south has led to the flooding of large areas of land, including forests, lakes and peat bogs. Flooding associated with the creation of reservoirs modifies biogeochemical cycles (Friedl and Wüest 2002), which includes changing the carbon balance of peatlands from CO_2 and CH_4 sinks (consumption) to CO_2 and CH_4 sources (production) (Duchemin et al. 1995; Kelly et al. 1997; St. Louis et al. 2000).

Since flooding of terrestrial habitats could enhance production of methane, knowledge of the CH_4 sources and sinks and of the factors and organisms involved in the CH_4 cycling is essential in order to develop mitigation strategies. However, few studies have investigated the potential activities of methane metabolism in soil, peat and sediment from cold continental climates under various flooding and temperature regimes. Changes in methanogenic and methanotrophic activities induced by the flooding of soils will influence the net flux of methane from reservoirs. This chapter discusses results of our investigation of microbial methane metabolism in soil, peat and sediment from hydroelectric reservoirs in the Canadian taiga.

18.2 Material and Methods

18.2.1 Site Description and Sample Collection

Soils and sediments were collected from different sampling sites at the Robert-Bourrassa Reservoir (53°N, 77°W) situated in the mid-north Canadian shield taiga at ca. 1500 km from Montreal, Canada. The pedology of the boreal forets/taiga soil domain, is dominated by two major features, i.e., well drained podzolic soils and peatlands. These soils cover about 60% and 10%, respectively and the remaining 30% of soil cover is organic forest soils with poor drainage conditions intermediate between those of podzolic soils and peatlands. The taiga forest is dominated by sparsely dis-

tributed small black spruce (*Picea mariana*) trees, with thick cladine (*Cladonia sp.*) and golden hypnum (*Pleurozium sp.*) cover on the ground. The climate in the region is of the cold continental type; with annual precipitation around 80 cm and a temperature range of -35°C to 23°C with an average of -3°C.

The Robert-Bourassa reservoir was created in 1979 and has a total area of 2835 km^2. This reservoir is part of a major hydroelectric complex including 6 other reservoirs (Caniapiscau, Eastmain-Opinaca, LaForge 1 and 2, La Grande 3 and 4) with a total surface area of 12941 km^2 within the La Grande complex watershed (175000 km^2). The sampling sites were selected to represent the main types of submerged taiga forest soils, lake sediments and peat bogs during the flooding of the reservoir. The soil in the taiga forest is typically a ferro-humic podzol with an eluviated A horizon (Ae) and an iron-rich B horizon (Bf) (Canadian Survey Committee 1978). In addition, samples were collected from peat bogs dominated by sphagnum (*Sphagnum* sp.) and from sediments of natural lakes Vion (53°39'N, 77°48'W), Patukami (54°14'N, 75°54'W) and Yasinski (53°17'N, 77°29'W). (See map in Chap. 21 by Planas et al. for more details on the geographic localization of Robert Bourrassa Reservoir and lakes). These lakes were selected to compare methane metabolism in glacial lakes and in reservoirs. For lake and reservoir sediments, triplicates of the top 5 cm were collected with an Ekman dredge in the deepest zone of each lake. For peat bogs and soils, samples from the organic layer were collected along a transect running from a central site in the non-vegetated point in the reservoir to the vegetated area, representing flooded, periodically flooded and undisturbed (un-flooded) areas.

18.2.2 Physico-Chemical Variables

Organic carbon content was determined by loss-on-ignition at 550°C for 2 hours, and ion concentrations by automated colorimetric methods (Traacs Auto Analyser). Nitrites were determined by the automated cadmium reduction method based on the Griess reaction. Sulfate was determined by the automated methylthymol blue reaction and iron was analysed by the ferrozine assay (Lovley and Phillips 1987b) as modified by Achtnich et al. (1995).

18.2.3 Bacterial Methane Metabolism

Analytical Methods

Analysis of methane was performed by gas chromatography on a SRI 8610 C gas chromatograph (SRI, Torrance, CA, USA) equipped with a flame ionization detector (FID) operated at 150°C (Roy and Greer 2000). A stainless steel column (2 m x 3.1 mm) packed with Porapak-Q (Supelco, Mississauga, On, Canada) was used for separation at 60°C with helium as a carrier gas at a flow rate of 20 ml min^{-1}. For gas determinations, 0.2 ml of the gas sample was injected into the GC system with simultaneous integration of peaks using the Peak Simple II software (SRI, Torrance, CA, USA). Gas standards were injected at the beginning and at the end of each day of analysis. A gas standard that contained 7092 ppmv of each of the following gases: CH_4, CO_2 and C_2H_2 was prepared at the beginning of each day of analysis.

Methanogenesis Activity

For methanogenesis, experiments were performed in anaerobic soil microcosms consisting of 20 g (wet weight) of soil and 60 ml of deionized water in 120-ml glass serum bottles capped with Teflon-lined rubber stoppers and sealed with aluminium crimps. Thereafter, the incubation flasks were evacuated for 15 min and backfilled with N_2 three times. Methane was measured over time by gas chromatography as described in Sect. 18.2.3. Additional experiments of CH_4 production in the presence of precursors (acetate or CO_2/H_2 mixture) and competitive inhibitors (Fe^{3+} and SO_4^{2-} ions) of methanogenesis were also conducted at 25°C. Sediments from Lake Yasinski were used for experiments with precursors and samples from flooded peat in the experiment with inhibitors. Microcosms were prepared with triplicate samples (with addition) and controls (no addition). The effect of Fe^{3+} and SO_4^{2-} on CH_4 production by methanogens was tested by adding separately, aqueous solutions of magnesium sulfate and ferric chloride at a final concentration of 5 mM per flask. The effect of precursors was measured in microcosms: 1) by addition of acetate at a final concentration of 10 mmoles per flask and flushed with N_2 or 2) by flushing with a 20.5% (v/v) CO_2/H_2 mixture. CH_4 production during these experiments was measured as previously described.

Methane Oxidation Activity

Experiments for methanotrophy were performed in aerobic soil microcosms consisting of 10 g (wet weight) of soil and 10 ml of deionized water in 120-ml glass serum bottles capped with rubber stoppers and sealed with aluminum crimps. To each flask, 0.5 ml of pure methane was added by syringe after withdrawal of an equal volume of the gas phase. At the beginning of the experiment, the final concentration of CH_4 in each incubation flask was around 5000 ppmv. The rates of CH_4 consumption were measured by the decrease of CH_4 in the headspace of the serum bottles over time. Methane in the flask's headspace was determined by gas chromatography (GC) using a 0.5 ml sample gas volume as described in Sect. 18.2.3 (Analytical Methods).

Plate Counts and DIG Detection of Methanotrophic Bacteria

The number of culturable methanotrophic bacteria in samples was estimated by the spread plate technique. Homogenized soil (10g) was serially diluted in sterile 1% (w/v) sodium pyrophosphate (pH= 6.8) and 0.1 ml samples were subsequently plated onto ammonium mineral salts agar (Whittenbury et al. 1970). Colonies were counted after 2 weeks of incubation at 25°C in gastight jars containing 25% v/v methane in air. Colonies were then lifted onto nylon membranes (82 mm), the cells were lysed, and the DNA was fixed onto the membranes (Greer et al. 1993). Membranes were hybridized using methanotrophic-specific DNA probes. Three probes were used for the detection of *pmoA*, type I 16S rDNA, and type II 16S rDNA. Probes were labelled with DIG (Digoxigenin) using the DIG DNA Labeling and Detection Kit (Roche Molecular Biochemicals). The number of probe-positive colonies was determined and the corresponding colony locations were confirmed on the original plate.

Diversity of Methanogens and Methanotrophs

Diversity of methanogens and methanotrophs was studied by PCR amplification of 16S rDNA genes or functional genes (*pmoA*, *mmoX*, *mcrA*) specific to each group of bacteria. Total DNA was extracted directly from soils and sediments using the method of Flemming (1994) as described in Pacheco-Oliver et al. (2002). MicroSpin columns (Pharmacia) were used for DNA purification and DNA purity was verified by PCR using universal eubacterial 16S rDNA primers f27/r1492 (Lane 1991). Interfering material, causing false negative amplification, was removed by further purification on a MicroSpin column (Pharmacia) containing polyvinylpolypyrrolidone (PVPP) (Berthelet et al. 1996).

A Perkin Elmer Cetus model 480 thermal cycler was used for all amplifications. For methanogens, extracted DNA was used as the template for the PCR amplification of Archea-specific [16S rDNA 4fa and 1492rp1 (McDonald et al. 1999) and 1Af and 1100r (McDonald et al. 1999)], and ME1 and ME2 for the methanogens-specific gene *mcrA* (McDonald et al. 1999). For methanotrophs, sequences of primers used for amplification of functional (*mmoX* and *pmoA*) and phylogenetic (group-specific 16S rDNA) genes were those previously described Bourne et al. (2001); Costello and Lidstrom (1999); Holmes et al. (1995a); Holmes et al. (1995b); Miguez et al. (1997). Briefly, the 16S rDNA genes were PCR amplified from total DNA extracted from soil and sediment using the methanotroph phylogenetic group-specific reverse primers Type 2b, Mm1007 and Mb 1007 in combination with the bacteria-specific forward primer f27 (Costello and Lidstrom 1999; Holmes et al. 1995a). Three different reverse *pmoA* primers were used in conjunction with the A189 forward primer to ascertain the molecular profile of the methane-oxidizing community. These three primer sets target the *pmoA* gene with varying specificity and provide a great deal of insight into the diversity of the *pmoA* genes from methanotrophs studied in various environments.

The reaction product of PCR amplification of the methanogen-specific gene *mcrA* was verified for size and purity (0.7% w/v agarose gels), cut and extracted from the gel with the Qiaex II gel extraction kit (Qiagen). Purified DNA was ligated into the plasmid vector pCR2.1-TOPO vector with the TOPO TA cloning kit (Invitrogen) and the hybrid vector was used to transform *Escherichia coli* Top 10 competent cell by following the manufacturer's instructions. Transformants were screened on Luria-Bertani agar plates containing 40 μg ml^{-1} X-Gal (5-bromo-4-chloro-3-indolyl-b-galactopyranoside) and 50 μg Kanamycin ml^{-1}. For each environmental sample, 10 clones with *mcrA* inserts were randomly selected and grown overnight in 5 ml of LB broth medium containing 50 μg Kanamycin ml^{-1}. Plasmids from these clones were isolated using the QIA spin mini-prep kit (Qiagen) and screened by gel electrophoresis to determine whether they contained the appropriately sized inserts. The inserts were digested with endonucleases Eco RI, Rsa-I and Taq 1 and analysed by agarose gel electrophoresis. Clones were grouped on the basis of similar banding patterns. One clone of each group was then sequenced by PCR using the dRhodamine Terminator cycle sequencing kit and an ABI prism sequencer (Applied Biosystems).

18.2.4 Statistics

Rates of methane oxidation were computed by linear regression of CH_4 concentration over time through the linear portion of the plot (Sokal and Rohlf 1981) using the JMP software (Sall et al. 2001). Methane oxidation rates were then compared statistically by ANCOVA (Sokal and Rohlf 1981) using the JMP software (Sall et al. 2001).

18.3 Results

18.3.1 Methanogenesis

Physico-Chemical Aspects

The chemical characteristics of the samples are summarized in Table 18.1. Organic matter content was relatively higher in soil (18.3 to 99.2 $mg{\cdot}g^{-1}$ dry weight) than in lacustrine sediments (2.05 to 12.3 $mg{\cdot}g^{-1}$ dry weight). Nitrate concentrations varied from 0.76 to 3.99 µM, while those of sulfate varied from 78 to 243 µM with a high concentration in Lake Patukami (1247 µM). Ferric ion concentrations were relatively low (53-389 µM) in peat and un-flooded soils, and high (1571-2539 µM) in lacustrine sediments, permanently and periodically flooded forest soils.

Table 18.1. Mean (standard error) values of organic matter (OM) content (mg·g of fresh weight) and some chemical ions concentrations in interstitial water ($\mu mole{\cdot}l^{-1}$) of samples from the ecosystems studied

	Sites	OM	NO_3^-	SO_4^{2-}		Fe^{3+}	
Lakes	Vion	11.4 (0.0)	2.07 (0.49)	184.5	(2.16)	1570	(37.9)
	Yasinski	2.05 (0.0)	2.03 (1.07)	243.2	(31.3)	2440	(43.4)
	Patukami	12.3 (0.0)	1.86 (0.52)	1247	(19.3)	2540	(36.6)
Peat	Flooded	73.5 (0.0)	2.11 (0.70)	78.5	(2.16)	389	(15.6)
	Periodically flooded	84.7 (0.01)	2.33 (1.32)	88.4	(6.91)	275	(10.1)
	Un-flooded	99.2 (0.02)	1.36 (0.64)	165.8	(12.55)	53.3	(21.9)
Soil	Flooded	18.3 (0.00)	1.46 (0.59)	160.5	(1.60)	1681	(54.1)
	Periodically flooded	62.7 (0.01)	3.99 (3.51)	171.4	(5.47)	2062	(56.5)
	Un-flooded	89.1 (0.00)	0.76 (0.06)	195.2	(5.67)	149	(15.6)

The Potential Rate of Methane Production in Relation to Temperature

Measurable rates of CH_4 production occurred in all samples when incubated at 25°C. CH_4 production occurred with no lag phase in flooded and periodically flooded peat microcosms incubated at 25°C or after a lag phase ranging from 5 to 60 days for all the other cases (Table 18.2). Acetylene suppressed CH_4 production in soils and sediment microcosms (Fig. 18.1A).

Table 18.2. Approximate lag phase extents (days) and potential methane production rates (headspace ppmv·d^{-1}) of samples incubated at different temperatures (mean value ± 1 SD), Different letters in superscript within columns and a particular system indicate significant differences at $p < 0.05$)

	Sites	5 °C		10 °C		25 °C	
		Rates	lag	Rates	lag	Rates	lag
Lakes	Vion	< 2ppmv·d^{-1}		3.99 (0.66)	40	241.4 (12.8)^{c}	5
	Yasinski	< 2ppmv·d^{-1}		< 2ppmv·d^{-1}		6.45 (1.72)^{b}	25
	Patukami	< 2ppmv·d^{-1}		< 2ppmv·d^{-1}		24.5 (6.13)^{a}	60
Peat	Flooded	273 (57)^{b}	15	367 (47)^{b}	40	581.7 (67.1)^{b}	0
	Periodically flooded	207 (29)^{b}	30	313 (39)^{b}	25	571 (67.5)^{b}	0
	Un-flooded	16 (3.8)^{a}	60	21 (16)^{a}	40	264 (6.1)^{a}	15
Soil	Flooded	< 2ppmv·d^{-1}		6.83 (1.26)	40	306 (20.6)^{c}	10
	Periodically flooded	< 2ppmv·d^{-1}		32.8 (4.52)	20	239 (15.2)^{b}	15
	Un-flooded	< 2ppmv·d^{-1}		< 2ppmv·d^{-1}		11.2 (3.61)^{a}	50

Production was detected at 10°C in lake Vion, permanently and periodically flooded soil, and at 5°C only in peat soils (Table 18.2). Potential rates of CH_4 production observed at 25°C were: high (571-582 ppmv·d^{-1}) in periodically or permanently flooded peat, moderate (239-306 ppmv·d^{-1}) in un-flooded peat, Lake Vion, periodically or permanently flooded soil, and low (6-24 ppmv·d^{-1}) in Lake Yasinski, Lake Patukami and un-flooded soil (Table 18.2). CH_4 production rates increased with a significant difference ($p < 0.05$) between flooded, periodically flooded and un-flooded forest soils at 25°C (Table 18.2). This tendency was also observed at 5 and 10°C with peat soil, but a significant difference ($p < 0.05$) was registered only between un-flooded peat and permanently or periodically flooded peat (Table 18.2).

Addition of either Fe^{3+} or SO_4^{2-} in our incubation flasks increased the lag phase and decreased the rate of CH_4 production (Fig. 18.2A). Methane production rate was lower in soils to which SO_4^{2-} rather than Fe^{3+} was added (Fig. 18.2A). For example, the total decrease in activity over an

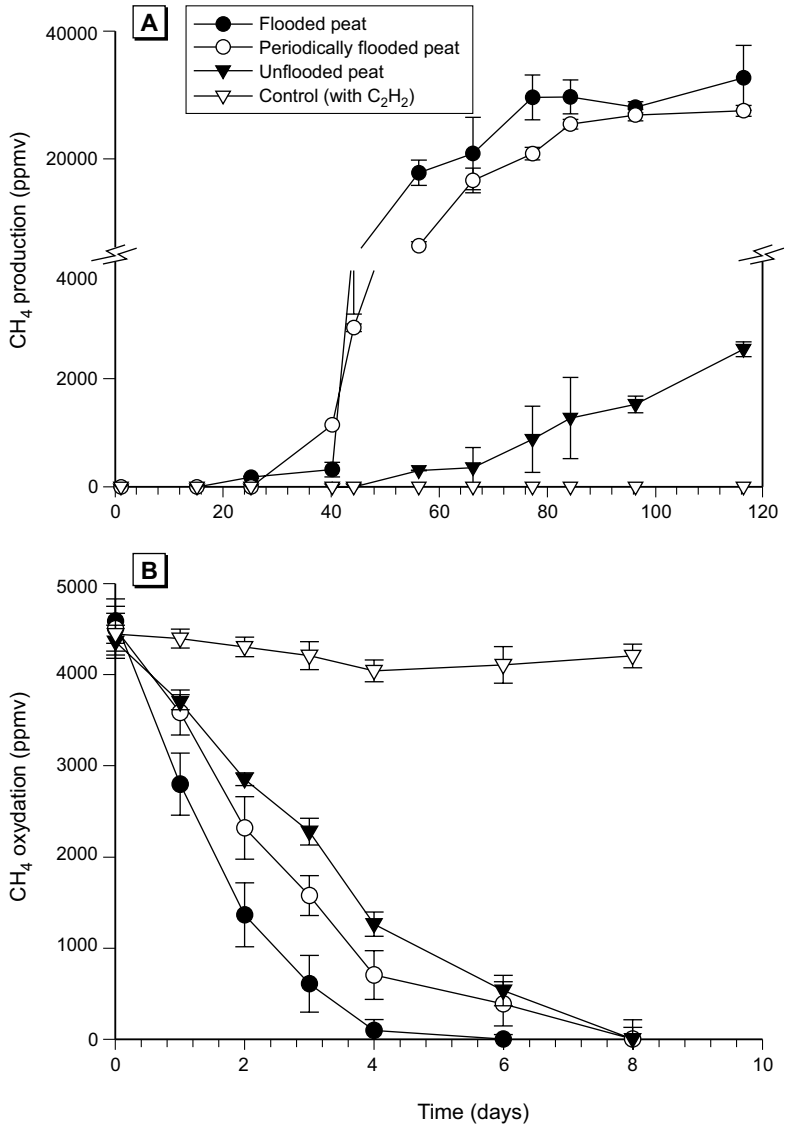

Fig. 18.1. Methane production (A) and uptake (B) in samples from peat incubated in microcosms at 10°C. Control flasks were incubated with C_2H_2, an inhibitor of methane producing and methane oxidizing bacteria. Data are averages of triplicate flasks with error bars equivalent to ± 1 SD

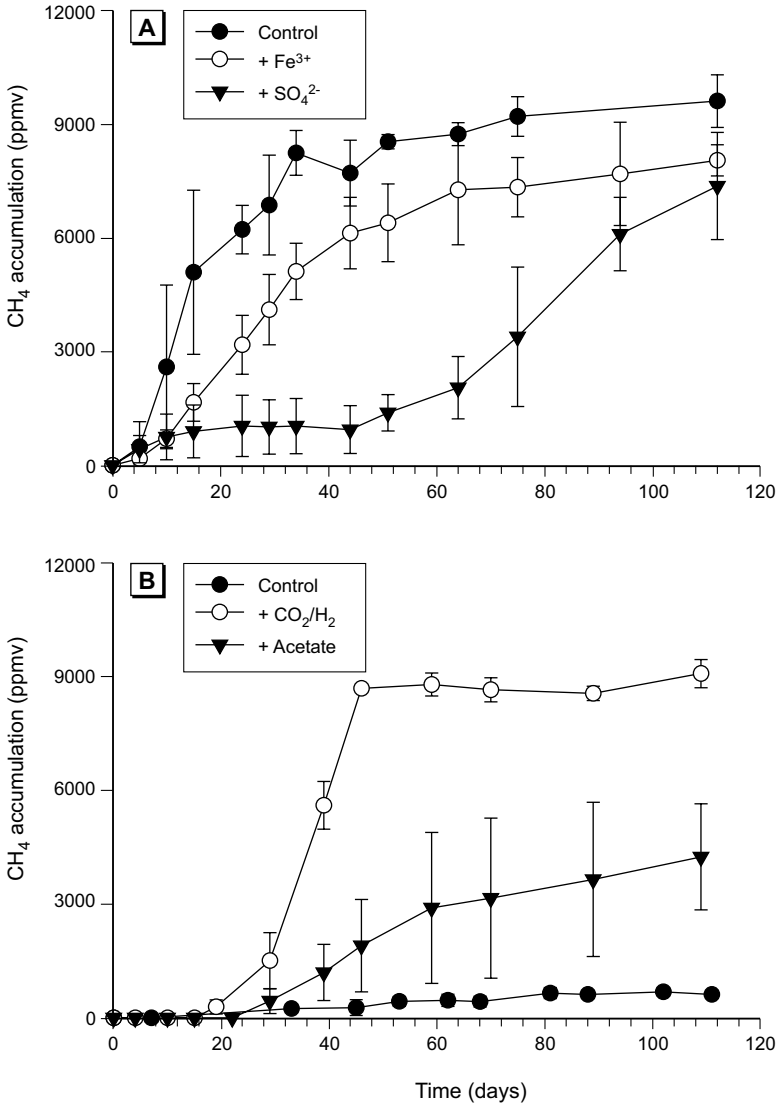

Fig. 18.2. Methane production at 25°C in experimental microcosms during experiment in the presence of Fe^{3+} and SO_4^{2-} as inhibitors (A) or acetate and CO_2+H_2 as precursors (B) of methanogenesis. Samples from flooded peat and Lake Yasinski were used for experiments with inhibitors and precursors, respectively. Data are averages of triplicate flasks with errors bars equivalent to ± 1SD

incubation period range of 0 to 60 days was about 20% and 90% in samples treated with Fe^{3+} and SO_4^{2-}, respectively. The main reason for this difference is the longer lag phase following the addition of SO_4^{2-} (45 days) than following the addition of Fe^{3+} (5 days). Methane production in sediments from Lake Yasinski did not exceed 2000 ppmv over 120 days of incubation. Following the addition of methanogenic precursors methane concentration increased up to 4000 and 9000 ppmv in the flask headspace following the addition of acetate or CO_2/H_2, respectively, after a lag phase of about 20 days (Fig. 18.2B).

Molecular Analysis of Methanogenic Archaea

Extracted DNA from soil, peat and sediment samples gave positive amplification with the universal eubacterial primers (Table 18.3). No amplification occurred in some cases with Archaea-specific 16S rDNA primers, while the *mcrA* gene detected methanogens in the same samples (Table 18.3). Sequence analysis targeting the *mcrA* gene encoding the α subunit of the methyl coenzyme M reductase, indicated that all the clones were assigned to the class Euryarchaeota, and all were close relatives of methanogens from lakes, landfills or wetlands and there was clustering closely related to a species from un-flooded soil *Methanosarcina acetivorans* (Table 18.4).

Table 18.3. PCR amplification results for methanogen genes in terrestrial samples from various systems in the Canadian taiga

	Sites	f27/1492	1Af/1100Ar	4fa/1492rp1	ME1/ME2
Lakes	Vion	+	+	-	+
	Yasinski	+	+	+	+
	Patukami	+	+	+	+
Peat	Flooded	+	+	+	+
	Periodically flooded	+	+	+	+
	Un-flooded	+	+	+	+
Soil	Flooded	+	-	-	+
	Periodically flooded	+	-	+	+
	Un-flooded	+	-	-	+

Phylogenetic Primers:
f27/1492 : Universal eubacteria
1af/1100ar: Archaea bacteria
4fa/1492rp1: Archaea bacteria
Functional Primers:
ME1/ME2: methyl conenzyme reductase A (Apha subunit)

Table 18.4. Nucleotide sequence identities of Archaeal mcrA clones

Strain	Number of clones	Best mcrA match NCBI Blast (Accession number)	Description	% Identity
Lake Vion	2/10	Uncultured euryarchaeote clone novmcr55 methyl-coenzyme M reductase subunit A (mcrA) gene (AF525522)	Hypereutrophic lake	94
Lake Yasinski	2/10	Uncultured euryarchaeote clone novmcr57 methyl-coenzyme M reductase subunit A (mcrA) gene (AF525523)	Hypereutrophic lake	94
Lake Patukami	2/10	Uncultured Methanobacterium sp. clone OS82 methyl-coenzyme M reductase alpha subunit (mcrA) gene (AF414030)	Methanogen populations in landfill	93
Flooded Peat	3/10	Uncultured Methanobacterium sp. clone OS82 methyl-coenzyme M reductase alpha subunit (mcrA) gene (AF414030)	Methanogen populations in landfill	93
Per.* Flooded Peat	5/10	Uncultured methanogenic archaeon partial mcrA gene for methyl-coenzyme M reductase subunit A (AJ489763)	Methanogen Archaea in Finnish oligotrophic fen	94
Flooded Soi1	2/10	Uncultured Methanobacterium sp. clone OS82 methyl-coenzyme M reductase alpha subunit (mcrA) gene (AF414030)	Methanogen populations in landfill	94
Per.* Flooded Soil	2/10	Uncultured Methanobacterium sp. clone OS82 methyl-coenzyme M reductase alpha subunit (mcrA) gene AF414030	Methanogen populations in landfill	94
Un-Flooded Soil	7/10	Methanosarcina acetivorans (AE011175)	Genome of M. acetivorans	95

* Periodically

18.3.2 Methanotrophy

Potential Methane Oxidation Rates in Relation to Temperature

Methane was consumed in all soil and sediment microcosms at all temperatures (5, 10 and 25°C). In the presence of the inhibitor, acetylene, methane in soil or sediment microcosms did not decrease with time (Fig. 18.1B). Methane oxidation rates were higher in flooded soils, compared to periodically flooded and un-flooded forest soils. This tendency was also observed in peat soil at 10°C, whereas samples from lake sediments did not show a clear pattern at any of the three temperatures (Table 18.5). Methane oxidation rates were highest in peat (593-1399 ppmv·d^{-1}) and the minimum value was within the upper range of values observed in lake and soil samples (Table 18.5). Uptake rates in lake sediment, periodically flooded soil and flooded soil varied from 120 to 376 ppmv CH_4·d^{-1}, which was greater than that obtained in un-flooded soil (62-146 ppmv CH_4·d^{-1}) (Table 18.5).

Table 18.5. Potential methane oxidation rates (headspace ppmv·d^{-1}) of samples incubated at different temperatures (Mean value ± S.D., different letters within rows indicate significant differences at $p < 0.05$)

	Sites	5°C	10°C	25°C
Lake	Vion	132 (10.5)[a]	134 (16.5)[a]	230 (24)[b]
	Yasinski	158 (7.24)[a]	164 (10.8)[a]	336 (27)[b]
	Patukami	120 (6.93)[a]	180 (11.3)[b]	228 (42.6)[b]
Peat	Flooded	741(113.86)[a]	988 (61.3)[a]	1097 (66.6)[b]
	Periodically flooded	593 (38.67)[a]	712 (87.9)[b]	910 (75.6)[b]
	Un-flooded	617 (30.48)[a]	619 (61.9)[a]	1399 (155)[b]
Soil	Flooded	159 (3.58)[a]	237 (19.5)[a]	376 (53.5)[b]
	Periodically flooded	147 (9.91)[a]	177 (8.26)[a]	228 (18.0)[a]
	Un-flooded	61.7 (4.39)[a]	71.5 (6.77)[a]	146 (9.77)[b]

Temperature affected methane oxidation differently in soil, peat and sediment systems (Table 18.5). Lake Yasinski sediment had a significantly ($p < 0.05$) higher rate of methane oxidation with an increase from 10°C to 25°C but no increase when these sediments were incubated below 10°C (Table 18.5). This pattern was also observed for flooded and un-flooded soil, and peat (Table 18.5). The rate of methane oxidation in periodically flooded systems (peat or soil) did not significantly increase when incubated above 10°C, but it significantly decreased when incubated at 5°C (Table 18.5).

Colony Counts and DNA Analysis

Counts of methanotrophic bacteria ranged from 3.0 x 10^4 to 1.9 x 10^6 cfu·g·soil^{-1}. There was a 10 fold (10^5-10^6) difference between the various lake sediments. Counts varied by as much as 100 fold (10^4-10^6) between flooded, periodically flooded and un-flooded peat and soil samples (Table 18.6). Three different DNA probes were used to screen colonies for methanotrophic bacteria. More pmoA probe-positive colonies were counted in lake sediment (92-98% of cfu) that in soil (69-91% of cfu) or peat (44-81% of cfu) samples. The two other 16S rRNA probes for type I and II methanotrophs revealed a variable degree of prevalence of type I over type II methanotrophs (Table 18.6).

Table 18.6. Colony forming unit (CFU) counts and hybridization analyses for methanotroph genes in terrestrial samples from various systems in the Canadian taiga

		CFU [x 10^4·g of soil]	pmoA [% CFU]	16S rDNA Type 1 [% CFU]	16S rDNA Type 2 [% CFU]
Lake	Vion	190	92	66	3
	Yasinski	144	96	58	14
	Patukami	14	98	74	11
Peat	Flooded	124	68	26	6
	Periodically flooded	74	81	54	16
	Un-flooded	3	44	7	3
Soil	Flooded	8	75	25	45
	Periodically flooded	14	91	23	34
	Un-flooded	116	69	74	7

PCR amplification of genes coding for 16S rRNA and functional genes from environmental DNA allows for the detection and identification of non-culturable bacteria in addition to cultivable bacteria. Total community DNA extracted from our samples served as template for PCR amplification with different primers (Table 18.7). 16S rDNA was detected in all of our samples using universal primer r1492. With primers 2b, known to amplify 16S rDNA of type II methanotrophs, we recorded positive amplification in all cases. Mb 1007 and Mm 1007 reverse primers that target type I methanotrophs belonging to *Methylobacter* and *Methylomonas* respectively, were amplified with DNA templates from lake Yasinski, Lake Vion and flooded forest soil. As noted in Table 18.7, amplification was observed in all the

Table 18.7. PCR amplification results for methanotrophs genes in terrestrial samples from various systems in the Canadian taiga

		Phylogenic primers				Functional primers			
						pMMO			sMMO
		r 1492	Type 2b	Mb 1007	Mm 1007	A682	A650	Mb661	mmoX
Lake	Vion	+	+	+	+	-	+	+	+
Lake	Yasinski	+	+	+	+	+	+	+	+
Peat	Flooded	+	+	-	-	-	-	+	+
Soil	Flooded	+	+	+	+	+	-	+	+
Soil	Periodically flooded	+	+	-	-	+	-	+	+
Soil	Un-flooded	+	+	-	-	+	+	+	+

Phylogenetic Primers:		Annealing Temperature °C
R1492	Universal eubacteria	60
Ms1020	*Methylosinus/Methylocystis*	54
Type 2b	Type II Methanotrophs	60
Mb1007	Methylobacter	58
Mm1007	Methylomonas	58

Functionnal Primers:	Annealing Temperature °C
A682 pMMO (pmoA)	55
A650 pMMO (pmoA)	56
Mb661 pMMO (pmoA)	52
mmoX sMMO (mmoX)	55

DNA samples using the Mb661 primer set, and variable amplification occurred with the other two primers A682 and A650 in samples from the different sites. The mmoX functional gene was also amplified in all the samples tested.

18.4 Discussion

The potential rates of CH_4 production and oxidation were measured under conditions favouring the process under study; they should reflect either the size of the active population or indicate that the potential is greatest where the populations are most active.

18.4.1 Methanogenesis

High rates of CH_4 production always occurred in permanently or periodically flooded systems with high concentrations of organic matter (Tables 18.1 & 18.2). The importance of organic matter in methanogenesis has previously been reported (Parashar et al. 1991; Yagi and Minami 1990; Crozier et al. 1995; Yavitt and Lang 1990). In our sites, this importance is substantiated by results from Lake Yasinki where low CH_4 production can be related to the low concentration of organic matter found in this system. Supplements of acetate or CO_2/H_2 in samples from Lake Yasinski increased methane accumulation by about 5 and 10 times, respectively, over that of the control. Also, methane production with acetate addition was apparently lower than with CO_2/H_2 mixture (Fig. 18.2) suggesting that methanogenesis in Lake Yasinski sediment was substrate limited, and that the majority of active methanogens were likely hydrogenotrophic methanogens rather than acetoclastic methanogens. This result could be confirmed by combining microbiological studies with the determination of the isotopic signature ($^{13}C/^{12}C$ ratio) of CH_4 produced. Indeed, hydrogenotrophic methanogenesis leads to the production of more negative ^{12}C enriched CH_4 than acetate-dependent methanogenesis (Whiticar 1999).

In un-flooded peat and soil, low rates of CH_4 production did not reflect the high concentration of organic matter (Table 18.1 & 18.2). Among factors that could explain this discrepancy, we suspect the availability of labile organic material, humic substance and the population size of methanogens. The importance of organic matter in limiting the rate of methanogenesis has been reported elsewhere in sediment from acidic bog Lake Grosse Fuchskuhle (Germany) (Casper et al. 2003) and in peat where the organic matter was relatively recalcitrant (Yavitt and Lang 1990). Al-

though Stewart and Wetzel (1982) and Cervantes et al. (2000) have both reported adverse effects of humic substances on methanogenesis, it is unlikely that this would cause the difference between soil and flooded and un-flooded peat, since they were sampled in adjacent sites. More likely, as Mayer and Conrad (1990), Fetzer et al. (1993) and Peters and Conrad (1995) all reported, the small methanogenic population in forest soils is responsible for the slower rate of methanogenesis. Another possible explanation of this low rate is that some methane oxidation occurred in aerobic microsites remaining in our sample from previously well aerated un-flooded systems. This phenomenon is well known in normal conditions on the field. This may account for lower rate of methane production initially (2 to 3 days) but not over a longer period of time such as those reported here.

CH_4 production rates in Lake Patukami and Lake Yasinski were as low as in un-flooded soil, whereas the production rate in Lake Vion was as high as those observed in permanently or periodically flooded soil (Table 18.2). These differences in methane production rates in these systems must be viewed within the environmental context, which encompasses the microbial and chemical properties of the systems. For example, we suspect that inflows from peats surrounding Lake Vion, may account for the high CH_4 production rate compared to the other lakes. Recently, Casper et al. (2003) reported a similar observation in Lake Grosse Fuchskuhle (Germany) where peat in the catchment influenced sediment methane production within the lake. Moreover, as was observed previously for peat (Moore and Knowles 1990), the highest methane production during this study occurred in peat soils. In forest soil, the main reason for the low rate of methanogenesis might be rather intrinsic to the system since it seems to be linked to the small methanogenic population. Besides the low number of methanogenic bacteria in un-flooded soil, the sequential reduction of ions such as nitrate, iron, and sulfate following the onset of anaerobiosis after flooding of soil, may also explain the differences in methane production rates and the observed variable lag phases of 5 to 60 days.

Lag phases in methanogenesis observed in the sediment of Lake Vion, Lake Patukami, periodically and permanently flooded soils were similar to those reported for rice soil (Lindau et al. 1993; Roy et al. 1997; Wang et al. 1992; Yagi and Minami 1993; Yao et al. 1999) and forest soil (Peters and Conrad 1995; Peters and Conrad 1996). The presence of ions that inhibit methanogenesis (Fe^{3+} and SO_4^{2-}) in our samples may have affected the rate of methanogenesis observed during this study. Negative effects of Fe^{3+} and SO_4^{2-} ions were seen more in systems with low concentrations of organic matter such as Lake Yasisnki. It is well known that under carbon limitation, methanogens will be out-competed for acetate or hydrogen by sulfate-

reducing bacteria (Lovley et al. 1982; Lovley and Phillips 1987a). Studies on rice soils (Achtnich et al. 1995; Roden and Wetzel 1996; Roy et al. 1997; Wang et al. 1993) and forest soils (Peters and Conrad 1996) showed that the initiation of methanogenesis followed the reduction of nitrate, ferric iron, and sulfate. During this study, methanogenesis in permanently or periodically flooded peat occurred without a lag phase. Moore and Knowles (1989) reported a significant influence of the water table depth on methane emissions from peatlands. Sphagnum peat bogs are characterized by low mineral content (Dedysh et al. 1998) and addition of Fe^{3+} or SO_4^{2-} to flooded peat led to a decrease in the CH_4 production rate and the appearance of a lag phase (Fig. 18.2A). Then, it seems that as in un-flooded soil, both the lag phase and low methane production rates in un-flooded peat could at least partially be related to the low population of methanogenic bacteria.

In un-flooded soil, the global concentration of all the different ions analysed was lower than those in any sediment of the three lakes considered. Un-flooded soil exhibited the longest lag phase and the lowest CH_4 production rate compared to the lakes. An explanation of this observation may be that upland soil, normally well aerated and with no known history of methanogenesis, may exhibit slower sequential reduction (Peters and Conrad 1996). In sediment from Lake Yasinski, the sulfate concentration was relatively high but 5 times lower than the sulfate concentration measured in Lake Patukami. Such a high sulfate concentration may explain the long lag phase observed with samples from this lake. It is still unclear why such a high sulfate concentration was observed in sediment from Lake Patukami. In the context of emission of greenhouse gases by hydro-electric reservoirs, more attention should be given to this observation. Forest soils in the Canadian taiga are usually podzols that have higher levels of Fe^{3+} than peat soil. Areas with high Fe^{3+} or sulfate would be more likely to produce less methane than soil with low sulfate or Fe^{3+} concentrations. Un-flooded systems showed the lowest amount of methane production per day. The permanent and periodically flooded systems had the highest daily methane production. These systems were distinguished from each other by a distinctive hydrologic regime characterized by variable flooding duration. The increase in methane production rates in permanent and periodically flooded systems suggests that, after a dry period, rewetting the surface layers may stimulate methanogenesis or, more probably, methane stored in pores is expelled (Moore and Knowles 1990). Likewise, permanent or periodic flooding might cause the release of nutrients (Grimard and Jones 1982) and/or soluble organic substrates (Zsolnay and Görlitz 1994) required for bacterial metabolism (Jugnia et al. 1999) and for the methanogenic archaea.

The maximum methane production rates at 25°C, between permanently and periodically flooded soils and peat systems, were very similar. This indicates that periodically flooded sites may show significant methane production at least during the warm months of the year. At 5°C and 10°C, rates of methane production were below the limit of detection in our samples except in peats. Williams and Crawford (1984), Yavitt et al. (1988) also reported low methane production at 4°C and 10°C in peat from wetlands in Minnesota and Appalachian peatland, respectively. In contrast, Svensson (1984) found that virtually no methane production occurred at 6°C in peat from a Swedish wetland. Rates of methane production increased with increasing temperature, but this relationship is best displayed in peat systems where methane production was markedly greater at 25°C than at 5°C. It appears that low temperatures constrain microbial the activity of the methanogenic archaea.

Comparative nucleotide sequence analyses of representative clones with other *mcrA* genotypes revealed that many of the sequences obtained in this study were closely related to only uncultured clones for which physiological and other properties remain unknown. This illustrates both the incomplete nature of the microbial database and also the need for further basic research in this area. Although the community structure of our samples was unclear when using PCR amplification of the *mcrA* gene, it is likely that acetate-consuming methanogens dominated in the majority of our samples. In fact, except in Lake Yasinski acetate was the most ubiquitous and most representative organic acid produced (data not shown). Amongst acetate users within the methanogens, species belonging to the genera Methanosarcina and Methanosaeta are well known. These genera represent about 90% of the archaeal population (Casper et al. 2003) and have been found in various environmental samples including Lakes sediments (Casper et al. 2003; Zepp Falz et al. 1999), peat bogs (McDonald et al. 1999; Nercessian et al. 1999), sludges (McHugh et al. 2003) and rice field soils (Chin et al. 1999). A more detailed analysis of our samples will be performed using 16S probes (Raskin et al. 1994) directed at different physiological groups within the methanogens, to highlight their potential linkage with acetate production.

18.4.2 Methanotrophy

Potential Methane Oxidation

All the samples studied acted as sinks for methane and this clearly showed the ubiquity of CH_4 oxidation (Hanson and Hanson 1996). The absence of

methane oxidation in the presence of acetylene indicated that CH_4 oxidation was dependent on methane-oxidizing bacteria.

Potential methane oxidation, like methane production, was greatest in peat samples. As already reported (Bender and Conrad 1992; Schnell and King 1995) high methane production provided more substrates for methane-oxidizing bacteria and resulted in higher rates of methane consumption in peat soils. Also, this indicates that peat soils with high methane production supporting large populations of active methane-oxidizing bacteria are likely to respond to increased methane production following flooding. Such a response by the soil methanotrophs would tend to decrease CH_4 fluxes from flooded forest soils to the atmosphere. The CH_4 formed in flooded soils and sediments can migrate to the surface and emitted into the atmosphere by diffusion, ebullition or transport through vascular plants adapted to life in flooded environments. However, less CH_4 might be emitted from diffusion after flooding with oxygen-containing water, because CH_4 may get converted to CO_2 at the oxic surface of the sediment or within the water body of lakes and reservoirs systems. This conversion is more likely to occur in deep waters, where CH_4 undergoes efficient microbial oxidation to CO_2, whereas CH_4 from shallow waters may form bubble escaping to the atmosphere.

The lowest rate of methane oxidation was observed in the forest soil samples, namely undisturbed soils where the rate of CH_4 production was close to the lower range of values observed in this study. This could be an indication of the lack of substrates for methanotrophs in this system. Methane oxidation rate in soils and peat increase after flooding, matching the increase tendency already observed with methane production rates under the same conditions. Likewise, we found that in permanent or periodically flooded peat and soil, both relatively high potential activities for methane production and oxidation occurred. This parallel evolution between the potential rate of methanogenesis and CH_4 oxidation, is similar to the report by Boom et al. (1997) suggesting an association between CH_4 oxidation activity and CH_4 supply in recently drained or intermittently flooded terrestrial ecosystems. This observation is also consistent with previous results that confirm the positive correlation between methanotrophy and methanogenesis, the highest methanotrophic activity being observed in methanogenic environments (Jean Le Mer 2001).

Colony Hybridization Analysis and PCR Amplification

The hybridization of methanotrophic bacterial colonies to pmoA gene probe was generally lower in peat than in soils or lakes sediments (Table 18.6). A low pH, a low mineral content, and a weak buffering capacity

characterize sphagnum peat bogs (Dedysh et al. 1998). A neutral medium (pH = 6.8) (Whittenbury et al. 1970), such as the one used in this study with a salt content of about 0.5 to 1 $g \cdot l^{-1}$ (in contrast to 5 to 50 $mg \cdot l^{-1}$ in peat water (Dedysh et al. 1998)), may not have been appropriate for the growth of indigenous methanotroph populations. Accordingly, some methanotrophs may have eluded isolation under the employed culture conditions, resulting in an underestimate of the viable population of type II methanotrophs usually found to be dominant in peat bogs (Dedysh et al. 2001; Dedysh et al. 1998; McDonald et al. 1995).

The total viable counts of methanotrophs in lake sediment and soil were similar (8×10^4 - 1.9×10^6 $cfu \cdot g \cdot soil^{-1}$) and close to counts reported for a humisol (9.7×10^4 - 1.3×10^5 $cfu \cdot g \cdot soil^{-1}$) (Megraw and Knowles 1987). Type I methanotrophs were detected in lake sediments by colony hybridization analysis (Table 18.6). PCR amplification of 16S rRNA genes from methanotrophic bacteria from Lake Yasinski and Lake Vion was positive with the Mb 1007 and Mm 1007 reverse primers, which target type I methanotrophs belonging to the *Methylobacter* and *Methylomonas* genera, respectively. These observations with lake sediment were similar to those of Costello and Lidstrom (1999) and Costello et al. (Costello et al.) in sediments from Lake Washington. Colony hybridization analysis indicating type II methanotrophs in flooded and periodically flooded soil was consistent with positive PCR amplification of 16S rDNA genes from type II methanotrophs using the type 2b primers. Supporting this finding, all soils and sediment were positive for the *mmoX* gene, encoding sMMO, more common in type II methanotrophs (Table 18.7).

The functional pMMO primers used in this study (A682 and A650) target the *pmoA* gene differently. The A189/A650 primer combination targets uncultured novel organisms, which may be atmospheric methane oxidizers. Undisturbed forest soils and lake sediments gave positive amplification with A650 and lake sediment, but periodically flooded and flooded soils or flooded peat were not positive. These results suggest that although flooding of soil may not alter the overall function of soil methanotrophic bacteria, it may alter the population composition. A forthcoming nucleotide sequence analysis of the amplification products may provide a better understanding of the possible shifts in soil methanotrophic populations following flooding.

Methane Oxidation in Relation to Temperature

The activity of the methanotrophic bacteria in the different systems investigated was affected by the incubation temperature. Rates of methane oxidation generally increased significantly within the lower temperature range

(5°C and 10°C), except for samples from Lake Yasinski, un-flooded soil, and un-flooded peat. At the higher temperature range (10°C-25°C), rates of methane oxidation also significantly increased for most soils except for Lake Yasinski sediment, periodically flooded soil and peat. There are some previous observations that soil temperature correlates positively with CH_4 uptake (Crill 1991; Priéme and Christensen 1997; Saari et al. 1998), although CH_4 uptake in general is only weakly influenced by temperature (Born et al. 1990; King et al. 1990; Koschorreck and Conrad 1993). It is unclear why the un-flooded soil and peat did not show an increase in methane oxidation at the lower temperature range while the flooded/periodically flooded soils did, or why the periodically flooded soil and peat did not show an increase of methane oxidation at the higher temperature range. It is possible that the low methane production rate from static soil incubations could explain some of these differences. However, for most soils and peat we observed a longer lag phase for methane production than for methane oxidation and the concentration of methane used in methane oxidation experiments was much higher compared to the initial rates of methane production. Could the population composition of the indigenous methanotrophic bacteria account for some of these differences, as already suggested by the different responses of flooded soil to PCR amplification with primer A650 for pmoA? For instance, type I methanotrophs usually have higher rates of methane assimilation than type II methanotrophs (Leak and H. 1986). This observation may be important in relation to methane production: the flooded soil and peat may respond better at low temperatures to an increase in methane production than un-flooded soil or lake sediment at low temperature.

18.5 Methane Biogeochemistry and Concluding Remarks

We can evaluate the potential importance of methane oxidation by comparing production and oxidation values obtained during this study. This comparison indicates that essentially all of the methane produced in peat, forest soil and sediment could be oxidized within the system, with little net atmospheric emission (Fig. 18.3). This may explain the small contribution to greenhouse gas of methane from hydroelectric reservoirs (Duchemin et al. 1995). While our experimental methods do not enable us to precisely know the amount of methane produced or oxidized, our study certainly show that there is a large potential for oxidation of methane within all the different systems investigated. Similar to the conclusion regarding methane oxidation in the Appalachian moss-dominated peatlands (Yavitt et al. 1988), our

observation provided evidence that methane oxidation could be an important process moderating the amount of methane emitted after flooding of soils in the Canadian taiga.

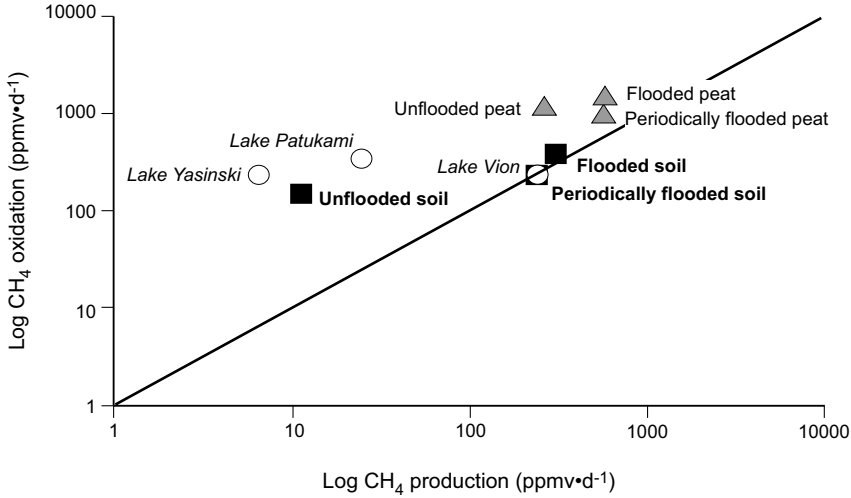

Fig. 18.3. Relations between methane production and methane oxidation at 25°C within the main systems investigated during our study

Forests and wetlands in the boreal zone contain large amounts of organic matter in vegetation and soils (Kauppi et al. 1997). Biogeochemical processes in reservoir or lakes are linked to the immediate terrestrial ecosystems in their catchment, from which they receive allochtonous carbon via streams and through groundwater and surface water inflow. The increased availability of easily degradable allocthonous organic matter can increase CH_4 emissions from lakes and reservoir by enhancing the CH_4 production (Huttunen et al. 2003). However, our observations during this study suggest that the importance of methane production and oxidation activities were linked. This indicates that carbon from the catchment entering lakes and reservoirs would probably fuel methane production, which would largely be oxidized within the system at the water-sediment interface and through the water column leading to negligible CH_4 emissions from those systems.

Our data also showed a large range of values for rates of methane production and methane oxidation, thus indicating that considerable variability exists among processes and among terrestrial systems in this region. These observations directly affect the study of methane biogeochemistry in hydro-electric reservoirs in the north since land flooding includes different

types of terrestrial systems. Rather than considering a reservoir as a simple large system, each part of the reservoir may have a distinctive substrate quality that governs its capacity to produce and consume methane, leading to huge spatial variations. In agreement with laboratory studies by Dunfield et al. (1993) methanogenesis is more sensitive to temperature increases than methanotrophy. Even if this difference is, at least, partly due to differences in diffusion constraints in the field (Born et al. 1990), this will tend to amplify the decrease in net emissions at low temperatures in the field.

Acknowledgments

This work was supported by a discovery grant from NSERC to RR and a NSERC/Hydro-Quebec strategic grant to DP.

19 Bacterial Activity in the Water Column and its Impact on the CO_2 Efflux

Rémy D. Tadonléké, Dolors Planas and Serge Paquet

Abstract

As part of a comprehensive study intended to elucidate mechanisms that drive carbon dioxide (CO_2) emissions from hydroelectric reservoirs, we examined bacterial abundance and production in the water column of three hydroelectric reservoirs of different ages and their nearby lakes, in relation to temperature, dissolved organic carbon (DOC), Chlorophyll *a*, phytoplankton production and CO_2 fluxes from these ecosystems to the atmosphere. The summer values of bacterial production and bacterial specific production in each reservoir were similar to those in the nearby lakes. There was no clear evidence that the age of the reservoir *per se* had a strong effect on the measured bacterial activities, even though the highest values of these activities were found in the youngest reservoir. DOC and nutrient availability were among the major factors driving bacterial activities. DOC was indeed positively related to bacterial production, bacterial specific production and the proportion of bacteria with high nucleic acid content (i.e. bacteria with higher activity = % HNA) in these sites, where nutrients were, most of the time, found to be limiting for bacterial growth. Among the bacterial variables tested, the % HNA appeared to be important in determining changes in CO_2 emissions at least in reservoirs, where it explained 38% of the variance of CO_2 fluxes to the atmosphere. Such a relationship was not found in lakes. These results indicate that examining different aspects of the functioning of bacterial communities may help to understand the mechanisms underlying CO_2 emissions from aquatic ecosystems, and suggest that the relative importance of factors driving bacterial activities and CO_2 efflux may be quite different in lakes versus reservoirs.

19.1 Introduction

Due to climatic warming, there has been an increasing interest in the greenhouse gas (GHG) production by different ecosystems both at a regional and a global scale. Among these gases is carbon dioxide (CO_2), which has been estimated to contribute ~ 70% of the GHG effects on the atmosphere. It is now known that average CO_2 concentrations in many lakes are above atmospheric equilibrium (Cole et al. 1994), turning these lakes into net sources of CO_2 to the atmosphere. Whether an ecosystem in a net sink or source of CO_2 to the atmosphere is greatly influenced by the balance between the planktonic primary production (sink of CO_2) and community respiration (source of CO_2), and has been a subject of debate among aquatic ecologists (e.g. del Giorgio et al. 1997; Carignan et al. 2000).

One decade ago, Rudd et al. (1993) published a paper in which they pointed out that hydroelectric reservoirs are significant but often neglected sources of CO_2 and methane to the atmosphere. Following the flooding of reservoirs, the amount of degradable material generally increases in the system (e.g. Paterson et al. 1997) because of the presence of both the flooded material and the allochthonous material imported from catchments. This likely has strong implications on the dynamics of greenhouse gases, and particularly CO_2, in these ecosystems, since the net heterotrophy of an aquatic system (i.e. the system is a source of CO_2 to the atmosphere) has been attributed to bacterial degradation of allochthonous organic carbon (Tranvik 1988; del Giorgio et al. 1997). The amount of this readily degradable organic matter in new reservoirs is expected to decrease over the course of time.

Following the controversy triggered by the paper of Rudd et al. (1993), many studies have been initiated in order to determine the actual amount of emissions of GHG from hydroelectric reservoirs or to compare these amounts with other anthropogenic sources (e.g. Gagnon & Chamberland 1993; Svensson & Ericson 1993; Kelly et al. 1997; Duchemin 2000; St. Louis et al. 2000). Even though some studies in the early 90's were conducted with the aim of understanding the mechanisms that drive these emissions from hydroelectric reservoirs, the number of such studies is very low and they have dealt mainly with the decomposition of the flooded biomass (e.g. Thérien 1991). It is only recently that comprehensive studies dealing with GHG emissions in these man-made ecosystems have began (e.g. Duchemin 2000; Barette & Laprise 2002; Huttunen et al. 2002). Among these studies are those initiated in 1992 by Hydro-Quebec in its hydroelectric reservoirs. In 2000, in addition to the usual measurements of

methane and CO_2 in Hydro-Quebec's hydroelectric reservoirs located in the boreal region of the province of Québec (Canada), measurements of biological variables in the water column were included in the investigation program conducted in these ecosystems by the Chaire de recherche en environnement Hydro-Québec/NSERC/UQAM. These biological variables included planktonic primary production and community respiration (Chap. 20), zooplankton compartment (Chap. 17), as well as bacterial abundance and production. The activities of these biological compartments are among the factors that should be taken into account in the estimation of the actual amounts of GHG due to the creation of an hydroelectric reservoir (net emissions), in addition to the fact that they may help explain the fluxes measured over the reservoir (gross emissions).

In this chapter, we examined the bacterial abundance and production in the water column of three of these hydroelectric reservoirs and their nearby lakes, in relation to temperature, chlorophyll *a*, phytoplankton production and dissolved organic carbon, some of the factors known to be important in the dynamics of bacterioplankton communities. Reservoirs of different ages were included in the research program in order to test whether they differ in the measured variables according to their age. We finally tested whether bacterioplankton activities were important in determining changes in the measured CO_2 emissions from the studied ecosystems. In this study, we considered the heterogeneity in the activity of bacterial communities (active versus less active), in contrast to most previous studies that have attempted to relate bacteria to CO_2 emissions in hydroelectric reservoirs (e.g. Huttunen et al. 2002).

19.2 Study Sites and Methods

The three reservoirs under study are Sainte Marguerite 3 (SM-3), La Grande 2 (LG-2, now known as Reservoir Robert-Bourassa) and Manicouagan 5 (MA-5). They were flooded in 2000, 1979 and 1967, respectively. The number of nearby lakes sampled was 3 for SM-3, 4 for LG-2 and 3 for MA-5. All of these ecosystems are situated in the north part of the Canadian Shield in the province of Québec. SM-3 and MA-5 are located in the "Cote nord" region (50°-52˚N, 66°-70˚W), while LG-2 is located in the eastern part of the James Bay region and belongs to the hydroelectric complex of the Lagrande River (52°-54°N, 68°-78°W). The three reservoirs also differ in terms of morphometry. LG-2 is the largest of all (surface area = 2835 km^2), followed by MA-5 (1942 km^2) and SM-3 (253 km^2). LG-2 has many sub-basins and bays with relatively shallow

depths, while SM-3 and M-5 are canyon-type and circular-type reservoirs, respectively, with relatively high depths. Further details on the study sites, including lakes and the sampled stations, can be found in Chap. 20 (Planas & Paquet) of this volume.

LG-2 and nearby lakes were sampled in 2001, while the two other reservoirs and their nearby lakes were sampled in 2002. The data presented here are from samples collected in June-August (i.e. summer) in the different ecosystems. Prior to sampling, water temperature was measured in situ, every 0.5 or 1m from surface to the deeper layers, using either a temperature/O_2-meter (YSI 5718 DO probe) or a multi-parameter probe (YSI 6600). The temperature values presented here are mean values in the epilimnion or in the euphotic zone (when the water column was not thermally stratified). For simplification, we will use the terms "upper waters" to designate these two parts of the water column.

Samples were taken every 0.5 m in the entire water column for stations with depths < 4 m and in the upper waters for the other stations. These samples were pooled thereafter and sub-samples for bacterial abundance analyses were preserved with formaldehyde (final concentration 2% v/v) and stored at 4ºC.

Samples for dissolved organic carbon (DOC) analyses were taken with sterile and acid-washed Tygon™ tubes, which allow integration of samples from the surface to the bottom of the layer of interest (see above). These samples were filtered through pre-ignited (450˚C, 4h) filters and collected in pre-ignited bottles. They were thereafter spiked with 0.1N $HgCl_2$, and stored in the dark and cold (4˚C) until analysis. DOC concentrations were determined using a Shimadzu TOC-5000A analyzer by the high temperature catalytic oxidation method.

Bacterial abundance and production were determined as described in Tadonléké et al. (In press). Briefly, bacterial abundance was determined on formaldehyde-preserved samples using flow cytometry after staining of bacterial cells with the nucleic acid dye SYBR Green II. A plot of green fluorescence measured at 530 ± 30 mn (FL1) versus 90° light scatter (SSC, a parameter related to cell size) was used to discriminate and count stained bacteria. This method allows the distinction of at least two bacterial subgroups characterized by high and low apparent nucleic acid content. In each cytogram, all the stained bacteria were counted (total bacterial abundance). In addition, two main sub-groups (for simplification) were separated and counted according to their nucleic acid content: bacteria with high nucleic acid content (HNA) and bacteria with low nucleic acid content (LNA) (Lebaron et al. 2001). The nucleic acid content of bacterioplankton cells is now considered by many microbial ecologists as an index of bacterioplankton activity. Several studies indicate that active bacterial

cells tend to have higher nucleic acid content (e.g. Lebaron et al. 2001). HNA are thus considered in this study as bacteria that have higher activity, compared to LNA.

Bacterial production was estimated from radioactive Leucine (Leu) incorporation (Kirchman 1993), after 60 to 90 mn incubations of subsamples. Labelled bacteria were collected on 0.2 μm polycarbonate filters, incubated for 10 mn and rinsed twice with 5ml of cold 5% trichloroacetic acid. Filters were analyzed later by liquid scintillation. Rates of Leu incorporation were converted to carbon production using the conversion factor of 3.1 kgC·mol·Leu^{-1} (Kirchman 1993).

The other data related to bacterial variables in this study (i.e. Chlorophyll *a* [Chl *a*], phytoplankton volumetric gross production [VGP] and CO_2 fluxes from the studied ecosystems) are already presented in Planas & Paquet (Chap. 18). These data are used here only for correlation purpose.

In this study, we compared each reservoir to (i) its nearby lakes and (ii) the other reservoirs to test the effect of age. Such comparative studies involving reservoirs of different ages and lakes located in their respective catchments are scarce. The comparison was done using the non-parametric Kruskall-Wallis rank sum test. To detect the source of the significant differences between the three reservoirs, the Tukey-Kramer comparison test was applied when the Kruskall-Wallis test was significant. Regression analyses were used to test empirical relationships between variables. For these analyses, data were $\log_{10}$ transformed (except temperature and percentage) to stabilize the variance and attain homoscedasticity. The probability level at which the statistical analyses were accepted as significant was ≤ 0.05.

19.3 Results

19.3.1 Temperature and DOC

The temperature of the upper waters in each reservoir was significantly lower than that found in its nearby lakes ($P < 0.05$), but similar to that observed in the other reservoirs under study ($P = 0.34$) (Fig. 19.1.1). These lower temperatures in reservoirs are consistent with the fact that reservoirs are more variable than natural lakes in terms of hydrology (Wetzel 1990).

In two of the studied reservoirs (SM-3 and LG-2), DOC concentration tended to be lower than in the nearby lakes (Fig. 19.1.2). However, no significant difference was found between the two types of ecosystems, as it

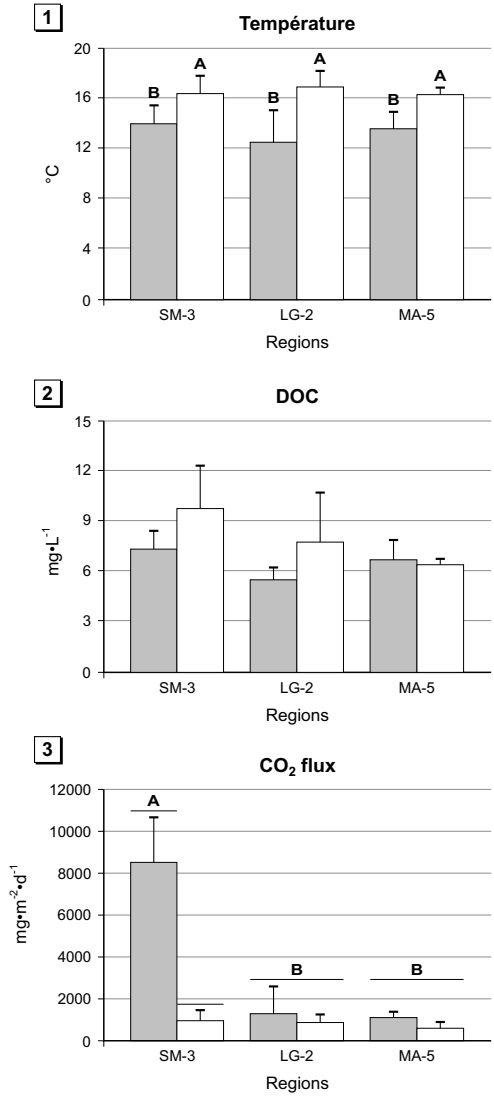

Fig. 19.1. Across-system comparison of (1) the mean summer temperature, (2) dissolved organic carbon concentration in the upper waters of the study sites and (3) CO_2 fluxes from the studied ecosystems. Reservoirs are placed from the youngest to the oldest from left to right.

Note that comparison involves only (i) each reservoir and its nearby lakes and (ii) the three reservoirs of different ages. Values that are similar are indicated by the same letter, whereas those that are significantly different are indicated by different letters. Black histograms represent reservoirs whereas white histograms represent lakes

was also observed for the MA-5 region ($P > 0.07$). Among reservoirs, the DOC concentration increased from LG-2 (which has an intermediate age) to the youngest reservoir SM-3, via M-5 (the oldest reservoir), the value in LG-2 being significantly lower than those in the two other reservoirs ($P = 0.0049$).

The average CO_2 fluxes from reservoirs to the atmosphere were similar to those from lakes in LG-2 and MA-5 regions, in contrast to the SM-3 region, where the young reservoir SM-3 had an average flux significantly higher than that from its nearby lakes. Among reservoirs, the youngest one SM-3 exhibited CO_2 fluxes significantly higher than the two others (Fig. 19.1.3)

19.3.2 Bacterial Abundance and Production in the Study Sites

Total bacterial abundance significantly differed between reservoirs and lakes only in the LG-2 region. Among reservoirs, MA-5 (the oldest) had significantly lower total bacterial abundance, compared to SM-3 and LG-2 (Fig. 19.2.1). The abundance of bacteria with high nucleic acid content (HNA) averaged 1.13 (sd = standard deviation = 0.31), 0.65 (sd = 0.11) and 0.49 (sd = 0.18) x 10^6 cells·mL^{-1} in SM-3, LG-2 and MA-5, respectively. The values in the corresponding set of lakes averaged 1.07 (sd = 0.47), 0.99 (sd = 0.34) and 0.57 (sd = 0.35) x 10^6 cells·mL^{-1}, respectively. These average HNA abundances were similar in lakes and in the reservoir in each region, but significantly higher in the youngest reservoir SM-3, compared to the two others. Among the tested variables that may control bacterial communities, Chl *a* and phytoplankton gross production (VGP) were significantly and positively related to both total bacterial abundance and HNA abundance (Table 19.1). DOC was also significantly and positively correlated with the percentage of HNA (% HNA) and explained 25% of its variance (not shown).

Neither bacterial production (BP) nor bacterial specific production (BSP = bacterial production/total bacterial abundance = production per bacterial cell) was significantly different between reservoir and lakes in each of the three regions during the summer ($P > 0.08$), even though values in SM-3 and MA-5 tended to be higher than in their respective nearby lakes (Fig. 19.2.2; 19.2.3). When reservoirs were compared to each other, there was no clear evidence that the age of the reservoir per se had a strong effect on BP and BSP, even though the highest values of these activities were found in the youngest reservoir SM-3, which also had the highest HNA abundance, % HNA and CO_2 evasive fluxes. Indeed, BP was highest

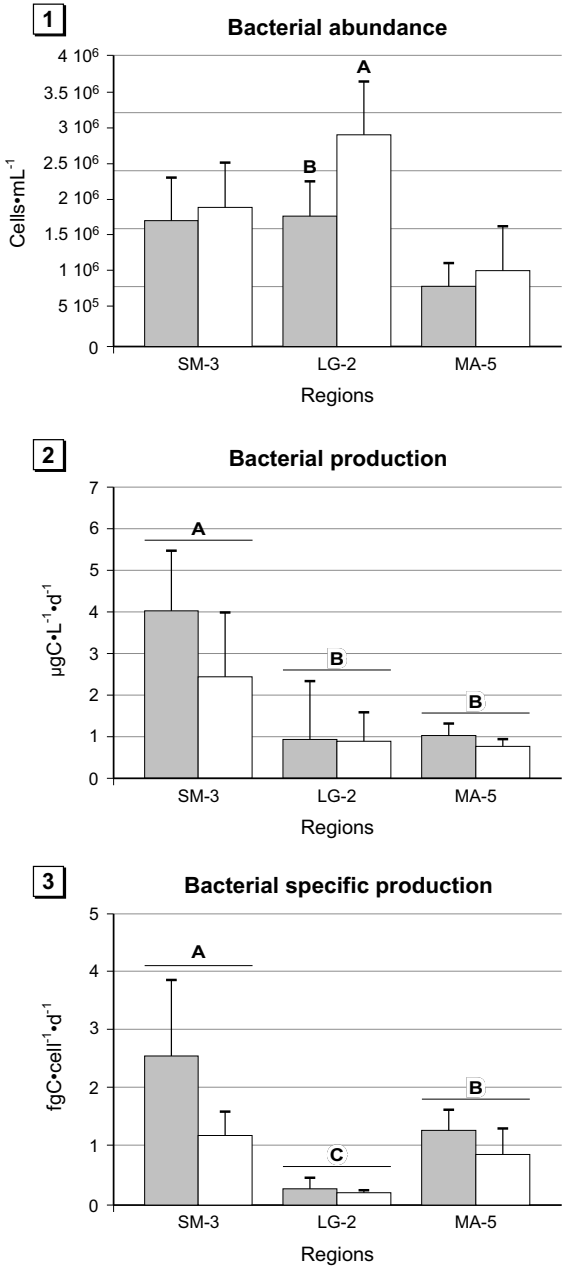

Fig. 19.2. Across-system comparison of (1) total bacterial abundance, (2) bacterial production and (3) bacterial specific production (bacterial production/total bacterial abundance) in the upper waters of the study sites. Statistical comparison and position of reservoirs as in Fig. 19.1

Table 19.1. Significant relationships between the variables under study

Y	X	Equation	R^2	P
Total bacterial abundance	Chl *a*	Y = 5.93 (0.09) + 0.69 (0.22)X	0.23	0.0043
	VGP	Y = 5.36 (0.16) + 0.5 (0.09)X	0.45	0.0001
HNA abundance	Chl *a*	Y = 5.69 (0.08) + 0.55 (0.2)X	0.18	0.011
	VGP	Y = 5.38 (0.18) + 0.29 (0.1)X	0.19	0.011
Bacterial production	DOC	Y = - 0.41 (0.35) + 0.95 (0.43)X	0.14	0.035
Bacterial specific production	DOC	Y = 3.96 (0.71) + 2.27 (0.87)X	0.18	0.014
	Temperature	Y = 4.72 (0.48) + 0.07 (0.03)X	0.14	0.031
CO_2 fluxes	Bacterial production	Y = 2.7 (0.17) + 0.97 (0.39)X	0.17	0.019
	% HNA (all data)	Y = 2.02 (0.34) + 0.02 (0.006)X	0.25	0.0047
	% HNA (reservoirs)	Y = 1.82 (0.40) + 0.027 (0.007)X	0.38	0.0024

P is the probability, numbers in the parentheses are standard errors of estimates. Acronyms as in the text.

in SM-3 but was not significantly different between the two other reservoirs. BSP was significantly different between the three reservoirs ($P < 0.003$), but the lowest value was found in LG-2 rather than in the oldest reservoir MA-5 as it could be expected (Fig. 19.2.2 and 19.2.3). In contrast to bacterial abundances, BP and BSP were not correlated with either Chl *a* or VGP. BP and BSP were rather correlated with DOC concentrations. BSP further correlated positively with water temperature (Fig. 19.3.1, Table 19.1).

When we plotted bacterial variables against the measured CO_2 fluxes from the studied ecosystems, we found that only BP and % HNA were significantly correlated with these fluxes (Table 19.1). When these two bacterial variables were included in a multiple regression model, only the % HNA occurred as independent variable, explaining 25% of the across-site variance of CO_2 fluxes. Separation of reservoir data from lake data showed that the relationship between % HNA and CO_2 fluxes was non significant for lakes ($P = 0.61$) and significant and positive for reservoirs. For the latter relationship, the percentage of the variance of CO_2 fluxes explained by % HNA was 38% (Fig. 19.3.2, Table 19.1)

19.4 Discussion

19.4.1 Factors Affecting Bacterioplankton Activities (i.e. Production, Specific Production and% HNA)

Our results suggest that DOC (in terms of both quantity and quality) was an important factor determining within and among-ecosystem variations in

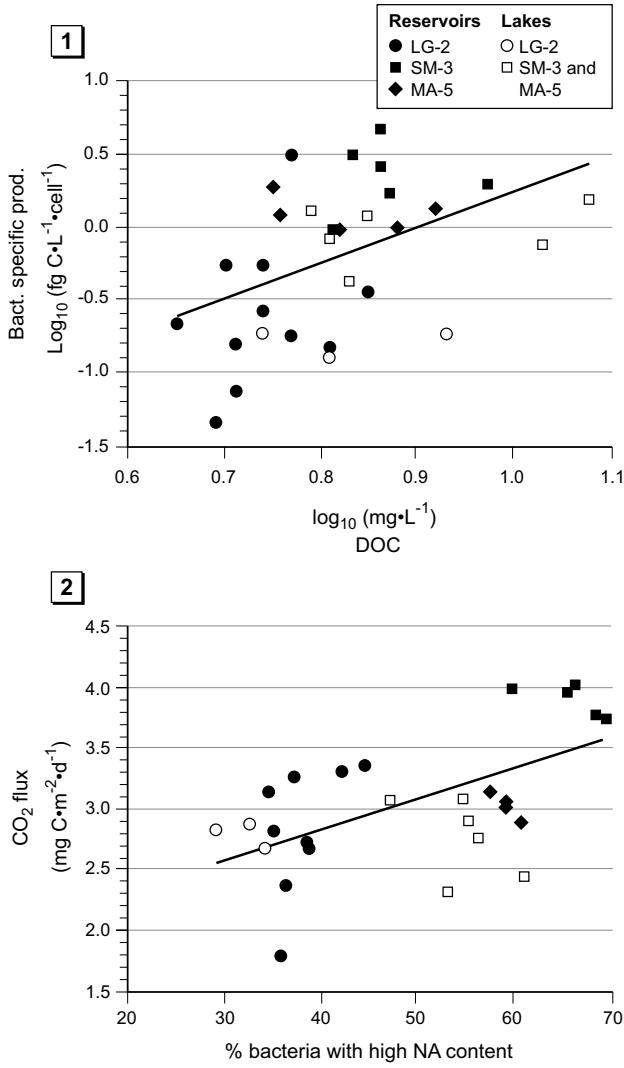

Fig. 19.3. Relationship between (1) the bacterial specific production (BSP = bacterial production per cell) and the dissolved organic carbon (DOC) concentration and (2) the measured evasive CO_2 fluxes and the percentage of bacteria with high activity (i.e. bacteria with high nucleic acid content = % HNA in the text) in the study sites.

Filled symbols represent data from reservoirs, with filled circles for LG-2, filled squares for SM-3 and filled diamonds for MA-5. Open symbols represent data from lakes, with open circles for the LG-2 region and open squares for SM-3 and MA-5 regions. Note that the % of bacteria with high nucleic acid content was not log-transformed. See Table 19.1 for equations

bacterial activities during this study, as it has been found in other studies. Indeed, the increasing trend in the bacterial specific production from LG-2 to SM-3 via MA-5 coincided with the increasing trend in DOC concentrations in these respective reservoirs (Fig. 19.1.2; 19.2.3). A similar pattern was found for the proportion of bacteria with high nucleic acid content (i.e. bacteria with higher activity), which significantly increased from 37% in LG-2 to 66% in SM-3 via 58% in M-5 ($P < 0.002$). In lakes, the pattern in DOC was also similar to that in bacterial production, with an increasing trend from lakes in the MA-5 region to lakes in the SM-3 region via lakes in the LG-2 region (Fig. 19.1.2; 19.2.2). In addition, among all the studied ecosystems, the youngest reservoir (SM-3) had the highest bacterial production, bacterial specific production and HNA abundance and proportion. Finally, DOC was positively correlated, and had the strongest relationships (compared to other tested variables), with bacterial production and bacterial specific production (Table 19.1). New reservoirs are expected to have more nutrient and labile DOC from the flooded soils (Grimard & Jones 1982; Paterson et al. 1997). That the highest % HNA was found in the youngest reservoir SM-3 is in agreement with this expectation. Newly flooded material has been found to strongly stimulate bacterial communities in the experimental Reservoir 979 in the Canadian Shield boreal region (Paterson et al. 1997). These results are also consistent with those from other boreal aquatic freshwaters. Positive cross-system relationships between bacterial production and DOC have been reported, for example, in Swedish humic lakes spanning a larger range of DOC concentration (Jansson et al. 2000).

Our results are consistent with the expectation that newly flooded reservoirs will have higher bacterial activities, compared to older reservoirs, but they also suggest that once the trophic upsurge period (which is expected to last 10 to 15 years) is over, the age of the reservoir per se does not have a strong effect on bacterial activities in these man-made ecosystems when they are still oligotrophic. Indeed, no significant difference was found between the 24 year-old reservoir LG-2 and the 36 year-old reservoir MA-5 in terms of bacterial production. In addition, the lowest bacterial specific production and abundance of bacteria with high activity were found in the reservoir LG-2 rather than in the oldest reservoir MA-5 (which is supposed to have lower amount of labile DOC), as it could be expected. In a comparative study involving two Finnish reservoirs flooded in 1967 and 1970, Huttunen et al. (2002) found that bacterial production was higher in the older of these two reservoirs. However, this older reservoir was also eutrophic, whereas the other reservoir was mesotrophic. We are not aware of any other study that has examined summer bacterial activities in reservoirs of different ages, which could allow further comparison. Based on average

Chl *a* concentrations (which were < 1.5·µg L^{-1}) our study sites were rather oligotrophic. The rates of bacterial production measured during this study, especially in LG-2 and MA-5, are similar to those reported for other humic boreal freshwaters where nutrient limitation of bacteria has been demonstrated (e.g. Jansson et al. 1996). Our experimental studies involving removal of bacterial grazers or nutrient addition in dilution-regrowth of natural sub-samples of bacterioplankton confirmed nutrient limitation of bacteria in LG-2 and MA-5 [(Tadonléké et al. (in press); Tadonléké et al. (in prep.)]. In such pristine boreal oligotrophic environments, factors such as the type of soil and biomass flooded, the amount of precipitation, the morphometry (e.g. deep versus shallow) and the water residence time of the ecosystem, all known to influence DOC and nutrient supply, are likely very important in determining variations among ecosystems.

19.4.2 Bacterioplankton Activities and Variations in CO_2 Fluxes to the Atmosphere

The results of this study indicate that the proportion of bacteria with high activity (% HNA) was an important factor determining changes in the CO_2 fluxes, at least in reservoirs. Indeed, the % HNA alone explained 38% of the variance of CO_2 fluxes and was also positively related to DOC concentration in reservoirs (R^2 = 0.45, P = 0.0003). Such R^2 are rather good, given that in a narrow trophic gradient, and particularly in unproductive waters, across-site relationships between variables are often weak or non significant. As the percentage of bacteria with high nucleic acid content (% HNA) is considered by many microbial ecologists as the number active bacteria, our results thus suggest that higher DOC concentrations (and likely quality) resulted in increases in the number of metabolically active bacteria in the system and thus in bacterial respiration of organic matter, which likely resulted in increases in CO_2 fluxes. To our knowledge, such significant relationship between active bacteria and CO_2 fluxes has not yet been reported in aquatic systems, although bacteria are known as the major decomposers of organic matter. Since % HNA, but not total bacterial abundance was correlated with the measured fluxes in this study, our results suggest that considering the heterogeneity of bacterial communities (and not bacteria as an homogenous compartment) may help improve our understanding of the functioning of aquatic ecosystems in terms of CO_2 fluxes, as it has been found for trophic dynamic studies (del Giorgio et al. 1996; Tadonléké et al. In press). We thus suggest that different aspects of the functioning of bacterial communities (including their activity structure based on indexes such as the % HNA) should be considered when attempt-

ing to understand the mechanisms that contribute to CO_2 emissions from aquatic ecosystems.

We did not find a significant relationship between % HNA and CO_2 fluxes in lakes, as we did find in reservoirs (Fig. 19.3.2). Compared to reservoirs, the number of points involved in this relationship for lakes was lower, which calls for caution in interpretation of the latter relationship. However, together with the finding that bacterial activities and DOC concentration in each reservoir were similar to those in its nearby lakes, whereas lake waters were significantly warmer than reservoir waters (Fig. 19.1.1, 19.1.2; 19.2.2, 19.2.3), these results, not only support the idea that water temperature was not the major factor driving among-site variations in bacterial activities during this study, but also suggest that the relative importance of factors driving bacterial activities and CO_2 evasive flux may be quite different in lakes versus reservoirs. This hypothesis remains to be tested. Comparative studies involving these aspects, in particular with different reservoirs and their respective natural nearby lakes, are scarce, although the two types of ecosystems may be different in terms of hydrologic characteristics, phytoplankton-total phosphorus ratio and zooplankton structure (Pinel-Alloul & Méthot 1984; Soballe & Kimmel 1987; Wetzel 1990). Factors such as water temperature, wind speed and the amount of biomass flooded are also known to affect CO_2 fluxes from waters to the atmosphere and may help explain the unexplained variance for reservoirs and the lack of significant relationship between these fluxes and % HNA in lakes.

19.4.3 Contribution of Bacterioplankton Activities to CO_2 Fluxes from Freshwaters to the Atmosphere

In addition to biological processes (plankton photosynthesis and respiration), other factors are known to have influence on CO_2 concentrations in freshwaters. For example, the inflow of streams and groundwater contributes dissolved CO_2 through direct inputs of CO_2 (Kratz et al. 1997) or via bicarbonate ions that are converted to CO_2 after entering the lakes (Dillon & Molot 1997). Ultra violet degradation of DOC can also lead to the production of CO_2, either directly or via enhanced bioavailability (Granéli et al. 1996; Bertilsson & Tranvik 1998).

It is only recently that researchers have initiated comprehensive studies intended to estimate the relative contribution of the different sources of CO_2 emitted from freshwaters to the atmosphere (Sobek et al. 2003). Few of these studies and of those intended to highlight factors that cause variations in the concentration of CO_2 (and its evasive fluxes) in the water col-

umn have been conducted in reservoirs (e.g. Duchemin 1999; Barette & Laprise 2002; Huttunen et al. 2002), compared to natural lakes (e.g. del Giorgio et al. 1999; Kelly et al. 2001; Striegl et al. 2001; Jonsson et al. 2003; Sobek et al. 2003). Given that many of the world's rivers are either impounded or facing impoundment in the near future and that large reservoirs (> 0.5 km^3) represent a significant fraction (~ 20%) of the global mean runoff (Kalff 2002), understanding these processes and the contribution of bacterial degradation of organic matter to CO_2 fluxes from reservoirs is important to identify environmental changes that occur due to their creation and thus to estimate their global warming potential. Ideally, this must be done in comparison with natural nearby lakes and should include data from the pre-flooding period.

The respiration of organic matter is thought to be a major factor causing changes in CO_2 concentrations in aquatic systems. However the relative importance of benthic versus planktonic respiration remains to be elucidated. In temperate lakes along a trophy gradient, links have been found between the carbon fluxes to the atmosphere and planktonic respiration (e.g. del Giorgio et al. 1999). Recently, from their analysis of 33 unproductive and relatively shallow boreal lakes of different humic content in Sweden, Sobek et al. (2003) suggested that benthic respiration, which is often neglected, is a major source of CO_2 in boreal lakes. Jonsson et al. (2003) have reached the same conclusion for other Swedish lakes. These authors found that pelagic respiration did not fully account for the calculated net CO_2 fluxes in many of the 51 shallow and relatively shallow boreal lakes that they studied. In 16 of these lakes, they calculated that benthic respiration represented a high proportion of these fluxes and that the relative importance of this source was greater in lakes with high DOC content, while the planktonic respiration was most important in lakes with low DOC content (see Table 4 and Fig. 5 in Jansson et al. 2003). In lake Örträsket (Sweden), benthic respiration has been estimated to contribute about 40% of the total net CO_2 production (Jonsson et al. 2001). As noted earlier, such studies are scarce in reservoirs. Barrette & Laprise (2002) developed a model in order to predict CO_2 emissions from hydroelectric reservoirs. When applied to the hydroelectric reservoir LA-1 (James Bay region, Québec), their model underestimated the measured CO_2 fluxes during summer and particularly in the deep station. Barrette & Laprise (2002) attributed the observed discrepancy to the fact that bacterial production of CO_2 in the water column was not accounted for in their model. In this reservoir LA-1, Duchemin (1999) also noted that the dominant source of CO_2 emitted to the atmosphere at the deep station was the CO_2 formed by a fermentative oxidation of organic matter present in the water column. It thus seems that the relative importance of planktonic versus benthic respiration depends on

the depth and, more generally, on the morphometric characteristics of the ecosystems. Kelly et al. (2001) found, for example, that the partial pressure of CO_2 in the water column was positively related to the ratio of epilimnetic area to epilimnetic volume.

One important thing to note is that most of these studies that have attempted to highlight the mechanisms of GHG production from freshwaters do not really tell us about the relative importance of bacterial communities in this production of CO_2, especially in the water column. The evaluation of the actual contribution of bacteria to CO_2 emissions from these freshwater ecosystems needs bacterial respiration data, which are not often reported. The relatively low number of studies reporting bacterial respiration in natural ecosystems is due to methodological problems associated with direct measurements of this bacterial process. These measurements require that the other planktonic organisms be inhibited or separated from bacteria. The effects of such inhibition and physical separation on bacterial metabolism are poorly known. On the other hand, estimation of bacterioplankton respiration from planktonic community respiration measurements using conservative values of bacterial growth efficiency and algal respiration may lead to wrong conclusions, because (i) the bacterial growth efficiencies reported in nature are considerably variable and the causes of this variability are poorly understood (del Giorgio & Cole 1998) and (ii) the contribution of bacterioplankton respiration to total planktonic respiration varies across a trophic gradient and strongly decreases in eutrophic environments (e.g. Biddanda et al. 2001). The latter finding points out the necessity of studying several reservoirs of different ages and trophic status, in order to examine to what extent eutrophication affects the relative importance of the different sources of CO_2 in these ecosystems. In pelagic environments were nutrients are scarce, the energetic costs of bacterial growth seem to be higher (compared to eutrophic environments). In such environments, bacterioplankton respiration has been found to contribute more than 75% of the planktonic community respiration (e.g. Biddanda et al. 2001). Similar results are expected in our study sites, given that bacterial production was low and generally limited by nutrients. Because no measurements of bacterial respiration were done during our study, we are currently attempting to exploit the existing models that have been developed in order to estimate bacterioplankton respiration from bacterioplankton production rates (e.g. del Giorgio & Cole 1998). These models will allow us to estimate the relative contribution of bacterial respiration in the water column to CO_2 fluxes to the atmosphere in the reservoirs SM-3, MA-5 and LG-2 and their nearby lakes. Understanding the contribution of bacterial respiration to CO_2 fluxes and their relationship with the ecosystem morphometry may help (i) determine the catchment surface that should be

flooded and (ii) improve models for studying CO_2 emissions from reservoirs.

19.5 Conclusion

The results of this study confirm the idea that newly flooded reservoirs tend to be more productive than old ones, but they also suggest that once the period of trophic upsurge is over the age of the reservoir per se is not important in determining among-ecosystem variations in bacterioplankton activities in oligotrophic reservoirs. Dissolved organic carbon concentration appeared to be among the major factors causing variations in bacterioplankton activities within and among the studied ecosystems. The percentage of bacteria with higher activity (considered as active bacteria) best explained the variations in CO_2 efflux in reservoirs but was not correlated at all with CO_2 evasive fluxes in lakes, which suggests that the relative importance of mechanisms underlying CO_2 emissions from these two types of ecosystems might be quite different. This hypothesis remains to be tested using a larger data set.

20 Production-Consumption of CO_2 in Reservoirs and Lakes in Relation to Plankton Metabolism

Dolors Planas, Serge Paquet and Annick Saint-Pierre

Abstract

We present data on metabolism, primary production and respiration, and their relationship to CO_2 effluxes of a three-year study conducted in north-eastern Canada, in two distinct boreal regions where large hydroelectric reservoirs have been established. In each region, the youngest and oldest reservoirs were sampled, as well as three to four natural lakes surrounding each reservoir.

The trophic status of all the sampled ecosystems ranged from oligotrophic, in lakes and the oldest (23 and 35 years-old) reservoirs, to mesotrophic in the youngest (1 and 7 years-old) reservoirs. The areal gross primary production (AGP) to areal planktonic respiration (APR) ratio varied from lower than 1 to higher than 1 in any given system. Differences in the AGP/APR ratio were related to season; lower in spring, higher in summer, both in reservoirs and in lakes. Within reservoirs differences in the ratio were also a function of the maximum depth of the sampled station. The AGP/APR ratio tended to be higher in the deeper than in the shallower stations. A very strong relationship ($r^2 = 0.93$) was found between CO_2 evasive fluxes and the total respiration of the system. The contribution of gross primary production (GPP) to total planktonic respiration (TPR) was higher in lakes (from > 50 to 200%) than in reservoirs. In reservoirs, the % of GPP to TPR varied by < 10% in the spring in the older oligotrophic reservoir, to more than 100% in the 7 year-old mesotrophic reservoir in summer.

20.1 Introduction

During the last decade, there has been an increasing interest in greenhouse gas (GHG) emissions coming from large hydroelectric reservoirs (Rudd et al. 1993; Duchemin et al. 1995; Fearnside 1997; Kelly et al. 1997; Duchemin 2000; Huttunen et al. 2002; Rosa et al. 2003). It is now evident that even for reservoirs located in the northern latitudes, where climate is cold and nutrient concentrations are low in comparison to temperate and/or southern regions, the gross GHG emissions may contribute to the regional biogeochemical carbon (C) cycle (St. Louis et al. 2000).

The origin of CO_2 supersaturation in temperate aquatic ecosystems, may be due to the degradation of organic carbon or the inputs of dissolved inorganic carbon by surface, sub-surface or groundwater (Krats et al. 1997; Carignan 1998). In boreal regions, with a large C-storage in soils, it is likely that the main source of CO_2 is the in situ degradation of organic carbon coming from terrestrial ecosystems in the dissolved organic form (DOC) or buried in reservoirs (e.g., Kling et al. 1991; Cole et al. 1994). In aquatic ecosystems, this allochthonous C, may constitute a large stable C pool that would be slowly and constantly degraded by heterotrophic bacteria and/or sunlight (Fenchel & Jorgensen 1977; Allard et al. 1994; Granéli et al. 1996; Curtis & Schindler 1997; Reche et al. 1999). Studies on DOC utilization as a source of energy for aquatic ecosystems date back to the beginning of the last century (Naumann 1918, cited in Karlsson et al. 2002), but have been greatly expanded upon in recent years, particularly in lakes and in oceans (Emerson, et al. 1997; Williams 1998; Cole et al. 2002; del Giorgio & Duarte 2002; Karlsson et al. 2002; Hanson et al. 2003). In contrast with oceans and natural lakes, reservoir data of C-processes and C-fluxes is very limited, particularly in boreal regions (Rudd et al. 1993; Kelly et al. 1997; Duchemin 2000; Barette and Laprise, in Chap. 24).

Studies done in Northern reservoirs have measured the C fluxes at the sediment-water (Duchemin et al. 1995; Houel 2003) and/or water-atmosphere interfaces (Kelly et al. 1994, 1997; Schellhase et al. 1997; Duchemin 2000; Huttunen et al. 2002) without considering the biological or physical processes that are important in the CO_2 biogeochemical cycle. Furthermore, the studies of GHG emissions from reservoirs have mainly emphasized the bacterial degradation of forest soil, which had been flooded by dammed rivers and lakes, and from this postulate models were constructed to estimate the duration of the phenomena (Dionne & Thérien 1997), and the amount of GHG produced at the bottom of the reservoir, which was released to the water-air interface (Barrette & Laprise 2002; Barette in Chap. 20). A recent study on the degradation of flooded soils in

boreal reservoirs of different ages has shown that no more than 20% of the GHG fluxes to the atmosphere could be explained by the bacterial degradation of flooded soils, and has suggested that this decomposition would take place only in the first years of inundation (Houel 2003). From these results, a new hypothesis on the origin of the carbon in the GHG emissions, after the first years of a reservoirs' initial flooding, proposes that carbon might originate from the bacterial mineralization of DOC of terrestrial origin. Following this hypothesis, Weissenberger et al. (1999) estimated that for Northern Quebec hydroelectric reservoirs, current GHG atmospheric emissions could be the result of the degradation of only 10% of the DOC entering the system.

One way to verify the importance of allochthonous organic matter degradation in the carbon budget of reservoirs is to analyze the biological processes contributing to the production and consumption of organic matter in aquatic ecosystems in the form of community metabolism, algal photosynthesis (P) and total community respiration (R). The ratio between P/R would allow us to recognize if the system is a source ($P/R < 1$) or a sink ($P/R > 1$) of carbon, and hence to estimate the relative importance of the allochthonous inputs which supply the energy of that system, and contribute to CO_2 over saturation.

In this chapter, we will discuss the results of a study on: 1) pelagic metabolism in large hydroelectric reservoirs and surrounding lakes of Northern Québec (Canada); 2) the comparison, in a given region, of metabolism in reservoirs of different ages (e.g. the youngest and the oldest); 3) the relationship between CO_2 produced in reservoirs and CO_2 emissions to the atmosphere; 4) the comparison of the metabolism and CO_2 mass balances of reservoirs and of surrounding lakes, in order to verify if in a given region with similar physiognomic characteristics, metabolism and its relationship to CO_2 emissions are comparable between man-made lakes and natural lakes. In the discussion, only CO_2 emissions were taken into consideration since in Northern Canada boreal reservoirs, CO_2 is the main component of GHG (Duchemin 2000).

20.2 Study Site

The locations of the study site are located in Fig. 20.1. Two of the studied reservoirs, Robert-Bourrasa (LG2) and Laforge 1 (LA1), are located in the La Grande hydroelectric complex of the James Bay territory (between 49° and 55°N and 78° and 68°W, in northern Québec). Seven studied lakes

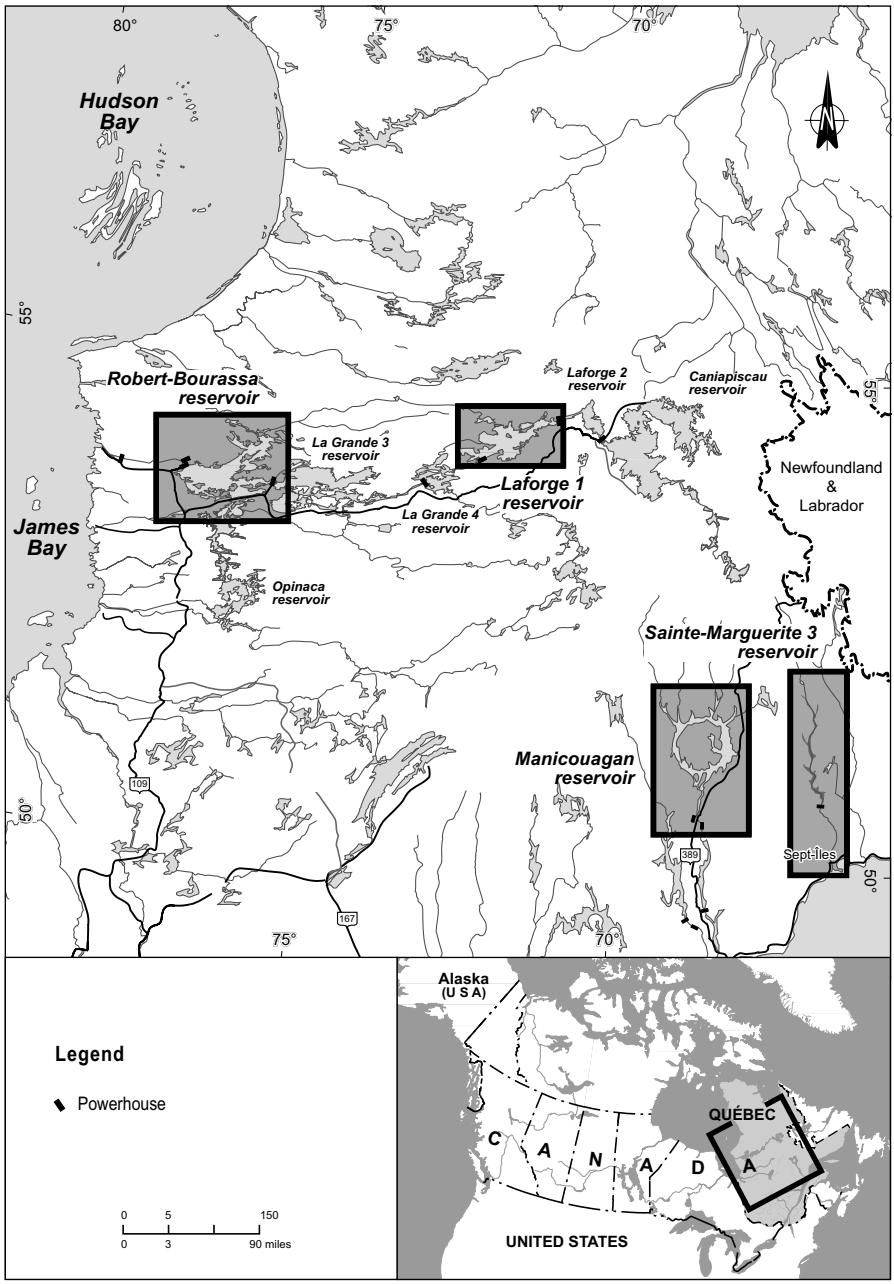

Fig. 20.1. Location of the studied regions

are located in the watershed of these reservoirs. Two other reservoirs, Sainte-Marguerite 3 (SM-3) and Manic 5 (MA-5), and six lakes are located in the Manicouagan and Sainte-Marguerite hydroelectric complex of the "Côte-Nord" region (50° and 52°N and 70° and 66°W; in eastern Québec). Of the four reservoirs that we studied, SM-3 was the youngest (1-year old) and had the smallest surface area, followed by 7-year old LA-1 with an intermediate surface area. The 23-year old reservoir, LG-2, was the largest in our study, and the oldest (35-years old) and deepest reservoir was MA-5 (Table 20.1).

Both sample regions are geologically similar and lie in the Canadian Shield, one of the oldest continental geological formations originating in the Precambrian Era. The Canadian Shield is a granite pedestal covered with glacial till, and in some areas (LG-2 southern basin) by clay and sand deposits from the ancient Tyrrell Sea, which covered the southern part of the James Bay area during the last deglaciation period. Both regions differ in relief and climate. The "Côte-Nord" is more mountainous than the James Bay area, and its climate is slightly more temperate.

20.3 Methods

Sampling — Two sessions of sampling were done during the ice-free season in each region. The first sampling took place just after the spring thaw, and the second in mid-summer. LA1 and three surrounding lakes were sampled in 2000, and LG-2 and four surrounding lakes in 2001. Some stations of LA1 were also sampled in 2001. The SM-3 and MA-5 reservoirs and six surrounding lakes were sampled in 2002. The majority of sampling was done from the pontoons of a hydroplane, but the closest littoral stations were sampled from a boat.

Integrated 60 L water samples for planktonic biomass and metabolism measurements were taken with a Van Dorn bottle, in the upper layers of the water column, mixed layer (Z_{mix}) or the photic layer (Z_{phot}), depending of the stratification conditions. Temperature (°C) and photosynthetic available radiation (PAR, $\mu E \cdot m^{-2} \cdot sec^{-1}$) were measured *in situ*. The Z_{mix} was defined by the depth at which there was a temperature decrease of 1°C or more per meter, and the Z_{phot} limit was calculated as the layer where PAR was >1% of the sub-surface light. At each station, water samples were pooled in opaque styrofoam thermally-insulated HDPE Nalgen™ jars.

Phytoplankton biomass and metabolic measurements — All of the samples used for biomass and metabolism analyses were subsampled from the

Table 20.1. Reservoir ages during sampling and some morphological characteristics of the 18 ecosystems considered in the study

Region	Names	Long.	Lat.	Age	Area (km^2)	Volume (hm^3)	Zmax (m)	Zmean (m)	ε_{PAR}
SM-3	SM-3 reservoir	66°48’	50°48’	1	246 ± 2	11907 ± 126	145	48.4 ± 0.21	1.15 ± 0.24
	Grand Lac Aux								1.38 ± 0.22
	Cèdres Lake	67°07’	52°02’	-					
	Houdan Lake	67°04’	51°13’	-					0.94 ± 0.15
	Grand Lac Germain								0.80 ± 0.07
	Lake	66°42’	51°07’	-					
LA-1	LA-1 reservoir	72°13’	54°20’	7	1074 ± 44	6138 ± 364		5.72 ± 0.10	0.95 ± 0.42
	Km 12 Lake	72°40’	54°08’	-	2.15	10.11	30	4.70	0.57
	Km 17 Lake	72°44’	54°08’	-	0.25	0.40	10	1.60	0.86 ± 0.13
	Km 75 Lake	72°32’	54°22’	-	0.18	0.45	9.4	2.50	1.04 ± 0.09
LG-2	LG-2 reservoir	77°02’	53°37’	23	2630 ± 13	55412 ± 573	150	21.07 ± 0.09	1.20 ± 0.33
	Désaulnier Lake	77°32’	53°34’	-	10.62	86.08	32	7.56	1.22 ± 0.01
	Yasinski Lake	77°29’	53°17’	-	41.00	197.65	31	4.37	1.33 ± 0.02
	Patukami Lake	75°53’	54°14’	-	42.46	247.12	132.5	5.44	0.76 ± 0.21
	Ukau Lake	76°00’	53°55’	-	3.30	16.33	20.5	4.84	1.68 ± 0.89
MA-5	MA-5 Reservoir	68°39’	51°09’	35	1950 ± 1	120058 ± 669	350	61.56 ± 0.32	0.84 ± 0.27
	Matonipi Lake	69°45’	51°51’	-					1.08 ± 0.03
	Du Chaunoy Lake	69°48’	51°32’	-					0.34
	Berté Lake	68°33’	50°47’	-					0.60 ± 0.05

Long. = longitude, Lat. = latitude, Age = time since reservoir have been fill to the sampling year, Zmax = maximum depth, Zmean = mean depth and ε_{PAR} = light extinction coefficient of photosynthetic available radiation (400 – 700 nm)

homogenized integrated 60 L samples collected at each station. Phytoplankton biomass was estimated by chlorophyll-a (chla) analysis, approximately 1 L of water was filtered in triplicates on a Whatman GF/C™ glass fiber filter, and filters were keep frozen at -80°C until processed using a 90% hot ethanol solution, following a Sartory & Groββelaar (1984) extraction procedure. The chla absorbance readings, before and after acidification, were done on a Pye-Unicam (UV-300) model spectrophotometer using 4 cm light path cells.

For each station, immediately upon returning from the field, homogenized water subsamples were distributed, in triplicate, into 300 ml Pyrex BOD clear (18) and dark (3) bottles. The bottles were incubated in a six-wheeled rotating incubator with a light range of between 1000 $\mu E \cdot m^{-2} \cdot s^{-1}$ in the first wheel, to < 30 $\mu E \cdot m^{-2} \cdot s^{-1}$ in the fifth and last wheel for clear bottles, the dark bottles were placed in the sixth wheel. The incubator design follows that of Shearer et al. (1985), with modifications described by Carignan et al. (2000) to simulate the light gradients usually found in Eastern Canadian Shield lakes. Light in the incubator was provide by a metal-halide lamp (Phillips MH1000, 1,000 W) and the incubator was filled with bulk water taken in the study region. Prior to starting incubation, the water temperature was adjusted to ± 1°C of that measured in situ and it was kept constant with a recirculation cooler (VWR model 1179).

Production and respiration data were obtained by measuring changes in dissolved oxygen (O_2) concentration after incubations. The period of incubation was 4 h for the production measurements, and 12 h for the respiration estimations following Carignan et al. (2000). At the beginning of the incubation, four replicate clear BOD bottles were filled to estimate the initial O_2 concentration in the water. The O_2 concentrations were measured using a high precision Winkler method as described in Carignan et al. (1998), and titrations were done on a Brinkman-Metrohm Titrino 716/A10 using a platinum Pt-titrode probe. We estimated net production (NP) and planktonic community respiration (R) by subtracting initial O_2 from O_2 concentrations measured after incubation of clear and dark bottles, respectively. Gross photosynthesis (GP) was calculated by adding R to NP, assuming that the diurnal respiration rate was representative of the nocturnal respiration rate. Areal planktonic community respiration was estimated by multiplying volumetric planktonic community respiration (VR) by the sampling depth.

We used the computer models PSPARMS and DPHOTO (version 4) developed by Fee (1990) to estimate photosynthetic parameters and to calculate the numerical integration of areal daily gross photosynthetic rates (AGP; mg $C \cdot m^{-2} \cdot d^{-1}$). Volumetric GP rates were calculated by dividing AGP values by sampled depth. Daily solar irradiance data ($Watt \cdot m^{-2}$), reg-

istered in permanent meteorological towers located close to the reservoirs, were provided by the Centre d'Études Nordiques (CEN) of Laval University (Québec City, Canada) for the James Bay region or by Environment Canada for the "Côte Nord" region. For a better comparison of our data with data published in other studies, we transformed the O_2 production (P) and consumption rates (R) to C using a photosynthetic quotient of 1.25 moles of O_2 per mole of CO_2 (Williams & Robertson 1991).

In 2001 and 2002, CO_2 evasive flux measurements were done simultaneously to water sampling at each station. In 2001, the flux measurements were done with 36 L static chambers and gas was sampled with a syringe at regular intervals, following the procedure described in Duchemin et al. (1995). In 2002, we used a different chamber model (18 L volume) and direct measurement of CO_2 concentration through time with a nondispersive infrared gas analyzer (NDIR) as describe in Chap. 3.

Statistical analysis — Log or other data transformations were done when necessary to control the variance, the homoscedasticity and the linearity of the relationships.

One-way analysis of variance (ANOVA with GLM for unbalanced categories) was done on data within reservoirs or lakes, or between lakes and reservoir, followed by a Tukey multivariate means comparison test for between region comparisons, and t-tests for reservoir and lakes means comparisons within a given region. To explore the relationship between CO_2 evasive flux and metabolism, or metabolism and certain environmental variables, we used linear regressions. Two approaches were taken, firstly data from all sampling stations were used to explain the inter-site response, and secondly to analyze the complete systems mass balance of the different components of the CO_2 cycle. Mass balance calculations were only done for the system where we had bathymetric measurements (the four reservoirs and four lakes of the La Grande complex).

20.4 Results and Discussion

20.4.1 Phytoplankton Biomass

In general, pelagic chla concentrations were low in all of the ecosystems sampled, ranging from 0.13 to 4.38 $\mu g \cdot L^{-1}$ (mean = 1.38 $\mu g \cdot L^{-1}$) for reservoirs, and 0. 50 to 1.82 $\mu g \cdot L^{-1}$ (mean = 1.11 $\mu g \cdot L^{-1}$) for lakes (Table 20.2). The pelagic chla concentrations in lakes and the oldest reservoirs were within the range of the lowest concentrations usually found in Canadian Shield waters (e.g., Brunskill & Schindler 1971; Fee et al. 1992; Planas et al. 2000) and indicate ultra-oligotrophic to oligotrophic status. Younger

reservoirs, particularly LA-1, tend to have higher maximum chla concentrations, signifying an oligo-mesotrophic status (Table 20.2, Fig. 20.2). A higher trophic status could be expected in younger reservoirs as a result of the increase in limiting nutrients due to the decomposition of flooded terrestrial organic matter, as described by the trophic upsurge theory (e.g., Baranov 1962; Ostrofsky 1978).

Table 20.2. Range of phytoplankton biomass (Chlorophyll a, CHLA), areal gross production (AGP), areal planktonic respiration (APR) and AGP/APR ratio measured in upper layer (mixing zone or photic zone) of reservoirs and lakes

Regions	Type	N	CHLA ($mg \cdot L^{-1}$) Min.-Max.	AGP ($mg\ C \cdot m^{-2} \cdot d^{-1}$) Min.-Max.	APR ($mg\ C \cdot m^{-2} \cdot d^{-1}$) Min.-Max.	AGP/APR Min.-Max.
SM-3	Reservoir	12	0.13-4.38	53-415	20-288	0.27-3.42
	Lakes	6	0.56-1.12	57-206	57-232	0.48-1.93
LA-1	Reservoir	14	1.16-3.93	89-683	80-1360	0.21-3.92
	Lakes	5	0.90-1.70	56-144	35-335	0.43-1.62
LG-2	Reservoir	19	0.55-1.86	29-329	22-330	0.25-8.89
	Lakes	8	1.18-1.82	75-201	28-187	0.63-4.99
MA-5	Reservoir	11	0.19-1.34	14-257	6-177	0.36-2.63
	Lakes	5	0.50-1.28	42-187	5-390	0.36-0.99

Phytoplankton biomass in reservoirs would be dependent of the age. However the highest biomass does not occur in the youngest reservoir SM-3 ($1.38 \pm 0.32\ \mu g \cdot L^{-1}$), but in 7 year-old LA-1 ($2.13 \pm 0.21\ \mu g \cdot L^{-1}$). The 1-year old SM-3 reservoir probably had not reached the phytoplankton biomass peak yet, as would be expected by the trophic upsurge theory, and its chla concentrations were intermediate between LA-1 and the two older reservoirs (23-year old LG-2 and 35-year old MA-5, with chla ranges of $1.39 \pm 0.32\ \mu g \cdot L^{-1}$ and $0.67 \pm 0.08\ \mu g \cdot L^{-1}$ respectively; Fig. 20.2).

Regional differences were found between lakes. The lakes of the James Bay region had significantly higher chla concentrations than those of the "Côte Nord" region (Fig. 20.2, Table 20.2). The James Bay lakes had the highest mean chla (LG-2 lakes = $1.16 \pm 0.11 \mu g \cdot L^{-1}$ and LA-1 lakes = $1.44 \pm 0.10\ \mu g \cdot L^{-1}$). In the "Côte Nord" lakes no significant differences were found in chla concentrations between SM-3 ($0.86 \pm 0.13\ \mu g \cdot L^{-1}$) and MA-5 ($0.83 \pm 0.16\ \mu g \cdot L^{-1}$).

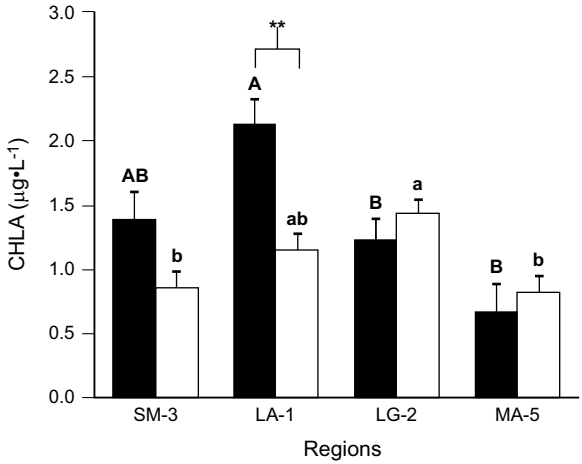

Fig. 20.2. Mean (± standard error) of phytoplankton biomass measured by chlorophyll-a (Chla) in reservoirs (black bars) and lakes (white bars). Significant differences (Tukey multiple means comparisons, $\alpha < 0.05$) between reservoir means are indicated by different capital letters, and differences between lake means by different lower case letters. Significant differences between reservoirs and lakes for a given region are also shown (t-test, ** = $p < 0.01$)

20.4.2 Areal Gross Production

AGP of phytoplankton was significantly higher in LA-1 than in the other reservoirs, or surrounding lakes. This rate was three times higher than the rate for any of the other reservoirs or lakes (337 ± 42 mg $C{\cdot}m^{-2}{\cdot}d^{-1}$ for LA-1 and between a mean of 107 ± 64 and 138 ± 27 mg $C{\cdot}m^{-2}{\cdot}d^{-1}$ for the other lakes and reservoirs, respectively Fig. 20.3). Although the AGP rates of LA-1 were higher than those of the other reservoirs sampled in our study, they were fairly low when compared to the rates measured in other man-made lakes, including those of boreal region (Huttunen et al. 2002; Knoll et al. 2003). Thus, AGP rates measured in northern boreal hydroelectric reservoirs in Finland ranged between 272 and 1640 mg $C{\cdot}m^{-2}{\cdot}d^{-1}$ (Huttunen et al. 2002). On the 12 small Ohio reservoirs studied by Knoll et al. (2003) only three had AGP rates lower than 500 mg $C{\cdot}m^{-2}{\cdot}d^{-1}$, the rates in the other nine reservoirs were from 500 up to 1500 mg $C{\cdot}m^{-2}{\cdot}d^{-1}$. Though, the AGP rates measured in LA-1 were high when compared with those measured in unperturbed Canadian boreal lakes or deep lakes from other boreal regions (Carignan et al. 2000; Arvola et al. 1993; Fee et al. 1992). No significant differences were found in our study between the AGP rates of the other three reservoirs sampled (LG-2, MA-5, SM-3, ($p > 0.05$), or between those

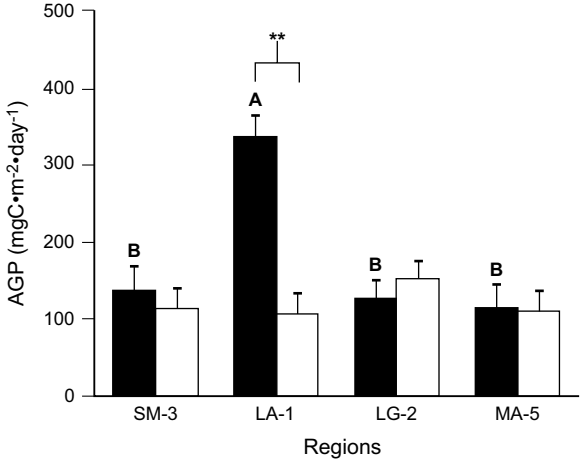

Fig. 20.3. Mean (± standard error) Areal Gross Production (AGP) measured in reservoirs (black bars) and lakes (white bars). Significant differences (Tukey multiple means comparisons, $\alpha < 0.05$) between reservoir means are indicated by different capital letters, and differences between lake means by different lower case letters. Significant differences between reservoirs and lakes for a given region are also shown (t-test, ** $= p < 0.01$)

reservoirs and their surrounding lakes ($p > 0.05$) (Table 20.2, Fig. 20.3). The AGP rates in these former ecosystems were within the values cited in the literature for oligotrophic ecosystems (Wetzel 2001).

20.4.3 Areal Planktonic Respiration

Areal planktonic respiration (APR) showed a similar trend to that of AGP values; differences between reservoirs being related to age (Fig. 20.4). The APR in LA-1 was four times higher than in older reservoirs (459 ± 116 mg $C{\cdot}m^{-2}{\cdot}d^{-1}$ for LA-1, 128 ± 14 mg $C{\cdot}m^{-2}{\cdot}d^{-1}$ in LG-2 and 114 ± 23 mg $C{\cdot}m^{-2}{\cdot}d^{-1}$ in MA-5). The SM-3 reservoir had respiration rates (176 ± 31 mg $C{\cdot}m^{-2}{\cdot}d^{-1}$), which were intermediate between those of LA-1 and, LG-2 and MA-5 (Fig. 20.4). Excluding LA-1, mean APR values for the lakes were similar to those of the reservoirs of the same region (Fig. 20.4). In lakes of the LA-1 region, the mean APR value was less than half of the rate measured in the reservoir, but these differences were not significant due to the large APR variability in those lakes.

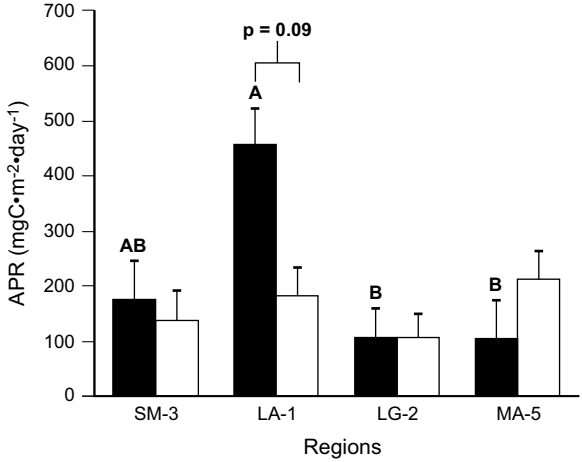

Fig. 20.4. Mean (± standard error) Areal Planktonic Respiration (APR)) measured in reservoirs (black bars) and lakes (white bars). Significant differences (Tukey multiple means comparisons, $\alpha < 0.05$) between reservoir means are indicated by different capital letters, and differences between lake means by different lower case letters. Significant differences between reservoirs and lakes for a given region are also shown (t-test, * = $p < 0.05$)

To our knowledge, no pelagic APR rates have been published for reservoirs. If we compare our APR rates (Table 20.2) to those measured in boreal lakes, our results are within the mean areal planktonic respiration measured by Carignan et al. (2000).

20.4.4 Spatial Variation of the Production: Respiration Ratio

The range of the AGP/APR ratio, measured in the upper layers of the water column was greater in reservoirs than in lakes (Table 20.2, Fig. 20.5). Between reservoirs, the mean AGP/APR ratio, when data from all of the stations were considered, was close to 1 in MA-5, LA1 and SM-3 (1.27 ± 0.37, 1.20 ± 0.40 and 1.13 ± 0.37, respectively), indicating that production was almost in equilibrium with respiration, and it was higher than 1 in LG-2 (2.06 ± 0.29). In contrast, the mean AGP/APR in lakes was generally lower than in reservoirs for any region (LA-1 area, 0.86 ± 0.40; LG-2 area, 1.88 ± 0.35; SM-3 area 0.97 ± 0.40), and very low in MA-5 (0.58 ± 0.40). Our ratio ranges (Table 20.2) and mean values (1.3 in reservoirs and 1.0 in lakes) were comparable with the few existing data where both metabolic processes (primary production and total respiration) were measured, as in oligotrophic boreal lakes (e.g., P:R mean = 1.7 in Carignan et al. 2000).

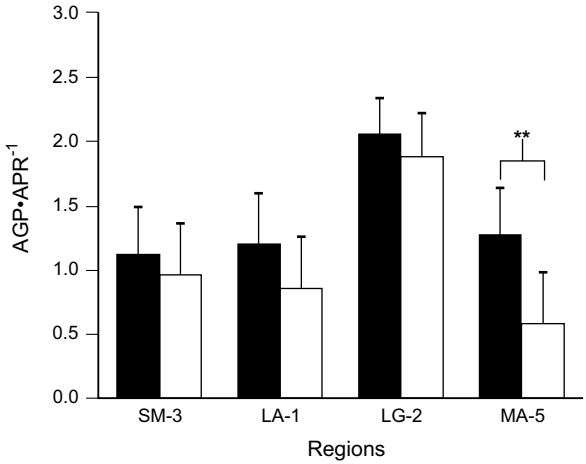

Fig. 20.5. Mean (± standard error) AGP/APR ratio of reservoirs (black bars) and lakes (white bars). Significant differences (Tukey multiple means comparisons, $\alpha < 0.05$) between reservoir means are indicated by different capital letters, and differences between lake means by different lower case letters. Significant differences between reservoirs and lakes for a given region are also shown (t-test, ** = $p < 0.01$)

Due to the size of the studied reservoirs and the difference within reservoir morphology and hydrology, it was important to analyze the spatial distribution of the AGP/APR ratio within reservoirs. Both James Bay reservoirs (LA-1 and LG-2) were dendritic in shape and had a large surface area to maximum depth ratio. On the other hand, the two "Côte-Nord" reservoirs (SM-3 and MA-5) were both canyon shaped and had a small surface area to maximum depth ratio (Table 20.1). Reservoir spatial heterogeneity has been considered more often in canyon reservoirs than in dendritic reservoirs, and it has been related to the influence of the characteristics of inflow waters and of reservoir mean depth (Thorton 1990; Conde et al. 1996; Nogueira et al. 1999; Armengol et al. 1999; Zanata & Espindola 2002)

Figure 20.6 presents the spatial distribution of the AGP/APR values measured at the different stations for the four studied reservoirs. In reservoir LA-1, which had the smallest surface area, three stations were located at the main axis at the water flow, LA206A, LA1903 and LA143C (Fig. 20.6a, E, D and B), another, LA1907 (Fig. 20.6a C), was located in a side bay, over a former lake. Two stations were situated close to dams, one on the LA-2 dam, which is the inflow of LA-1, and the other at the outflow

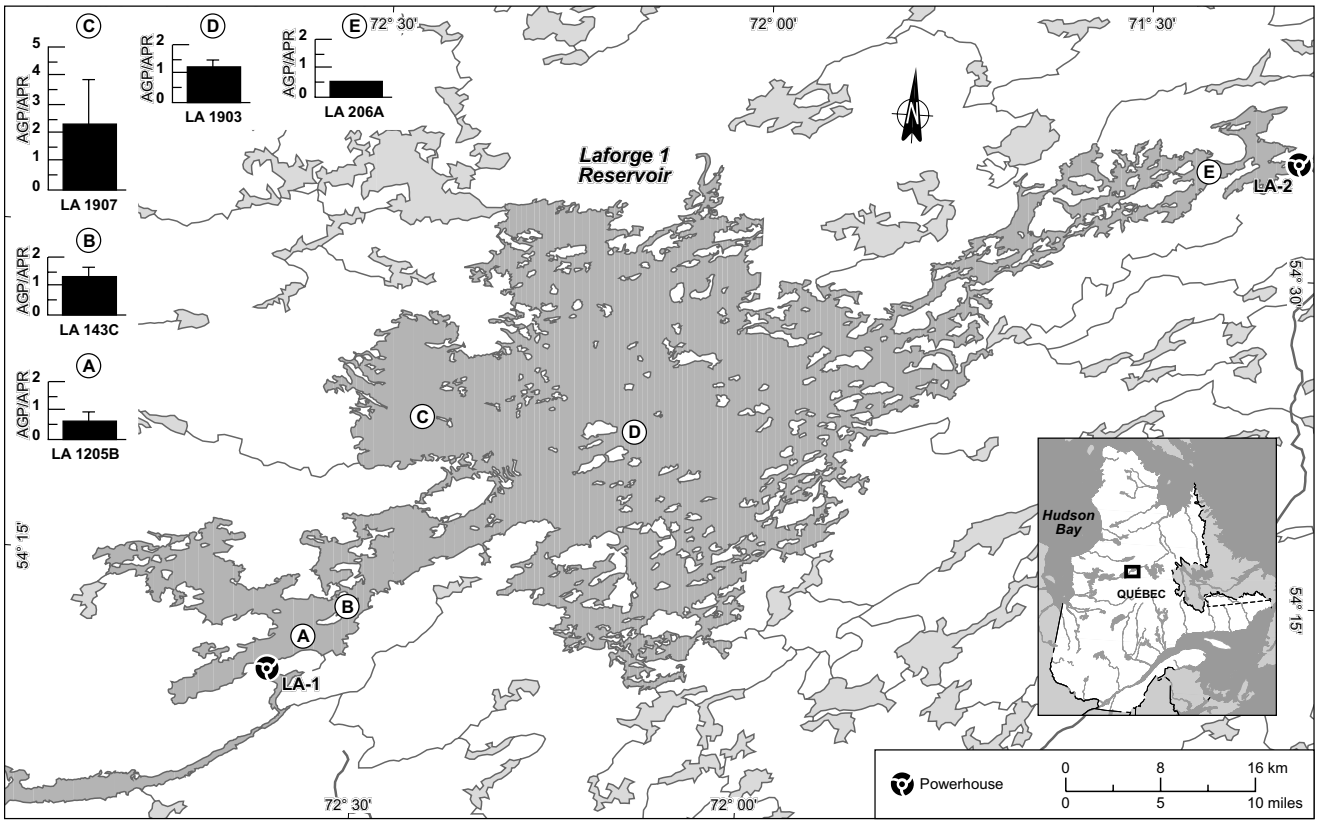

Fig. 20.6. Spatial distribution of the spring and summer mean (± standard error) AGP/APR ratio value at each sampled station in the four reservoirs: a) LA-1, b) LG-2, c) MA-5 and d) SM-3

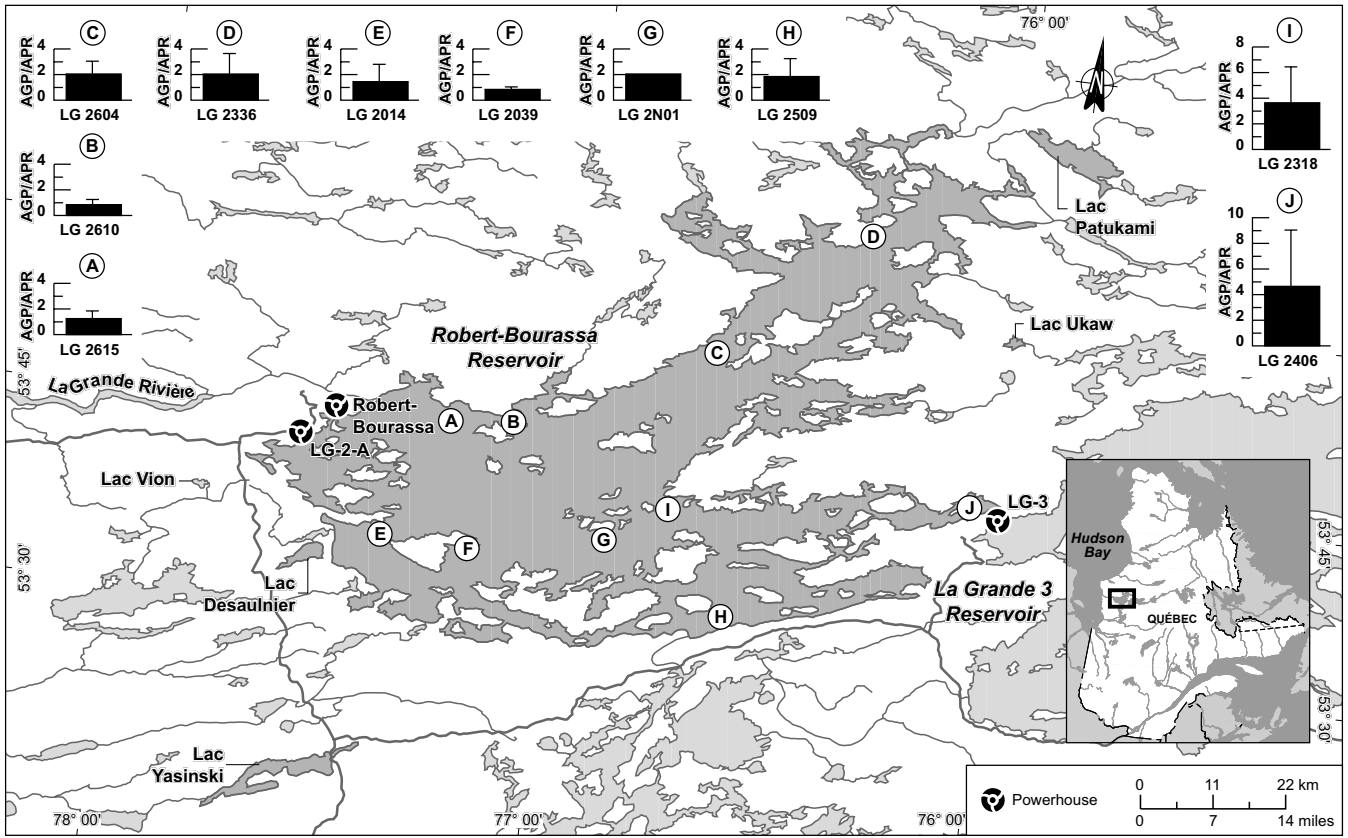
C
D
E
F
G
H
I
B
A
J
AGP/APR
LG 2604
LG 2336
LG 2014
LG 2039
LG 2N01
LG 2509
LG 2318
LG 2610
LG 2615
LG 2406
76° 00'
Lac Patukami
Lac Ukaw
Robert-Bourassa Reservoir
LaGrande Rivière
53° 45'
Robert-Bourassa
LG-2-A
Lac Vion
LG-3
53° 30'
Lac Desaulnier
La Grande 3 Reservoir
Hudson Bay
QUÉBEC
Lac Yasinski
78° 00'
77° 00'
Powerhouse
0 11 22 km
0 7 14 miles

Fig. 20.6. (cont.)

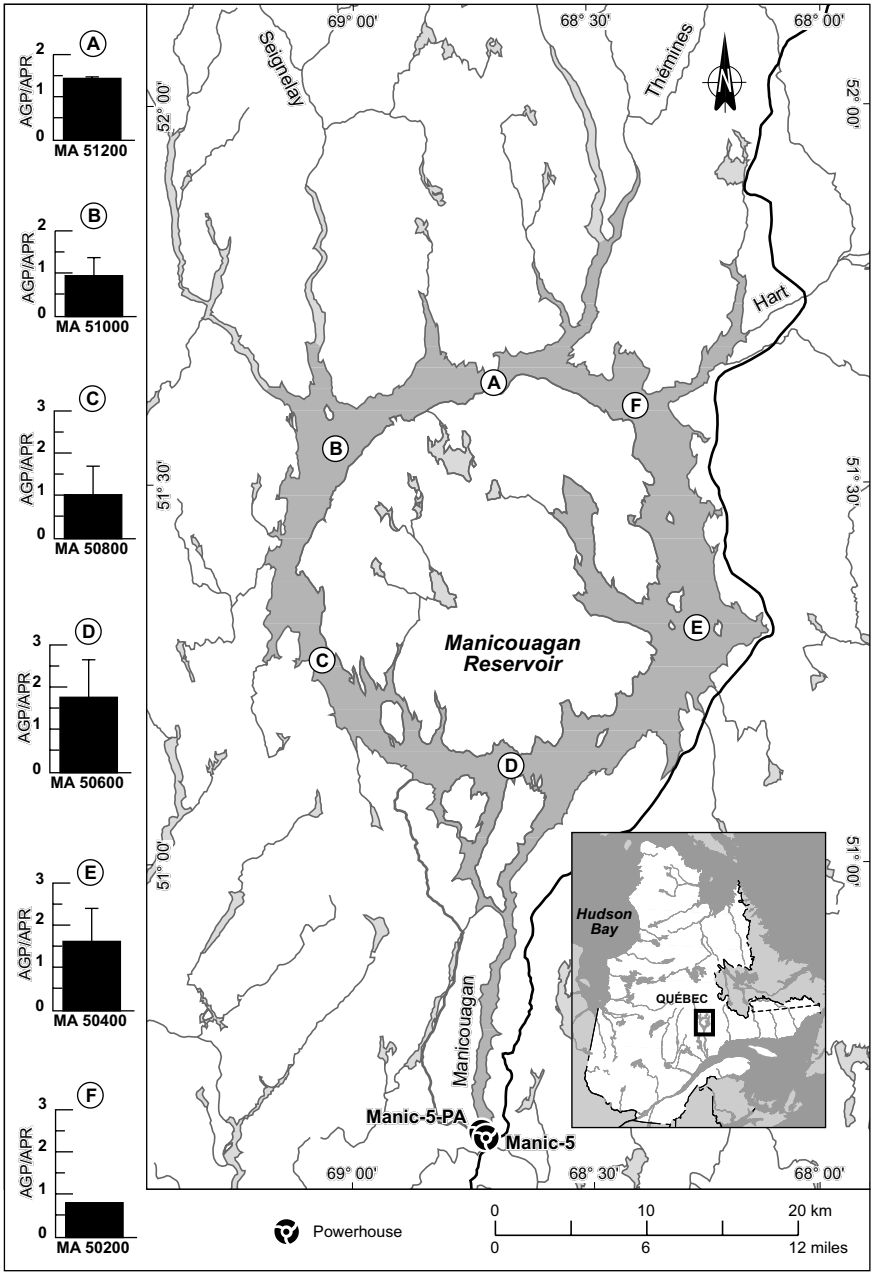
A
AGP/APR
MA 51200
B
MA 51000
C
MA 50800
D
MA 50600
E
MA 50400
F
MA 50200
69° 00'
68° 30'
68° 00'
52° 00'
51° 30'
51° 00'
Seigneulay
Thémines
Hart
Manicouagan Reservoir
Manicouagan
Manic-5-PA
Manic-5
Hudson Bay
QUÉBEC
Powerhouse
0 10 20 km
0 6 12 miles

Fig. 20.6. (cont.)

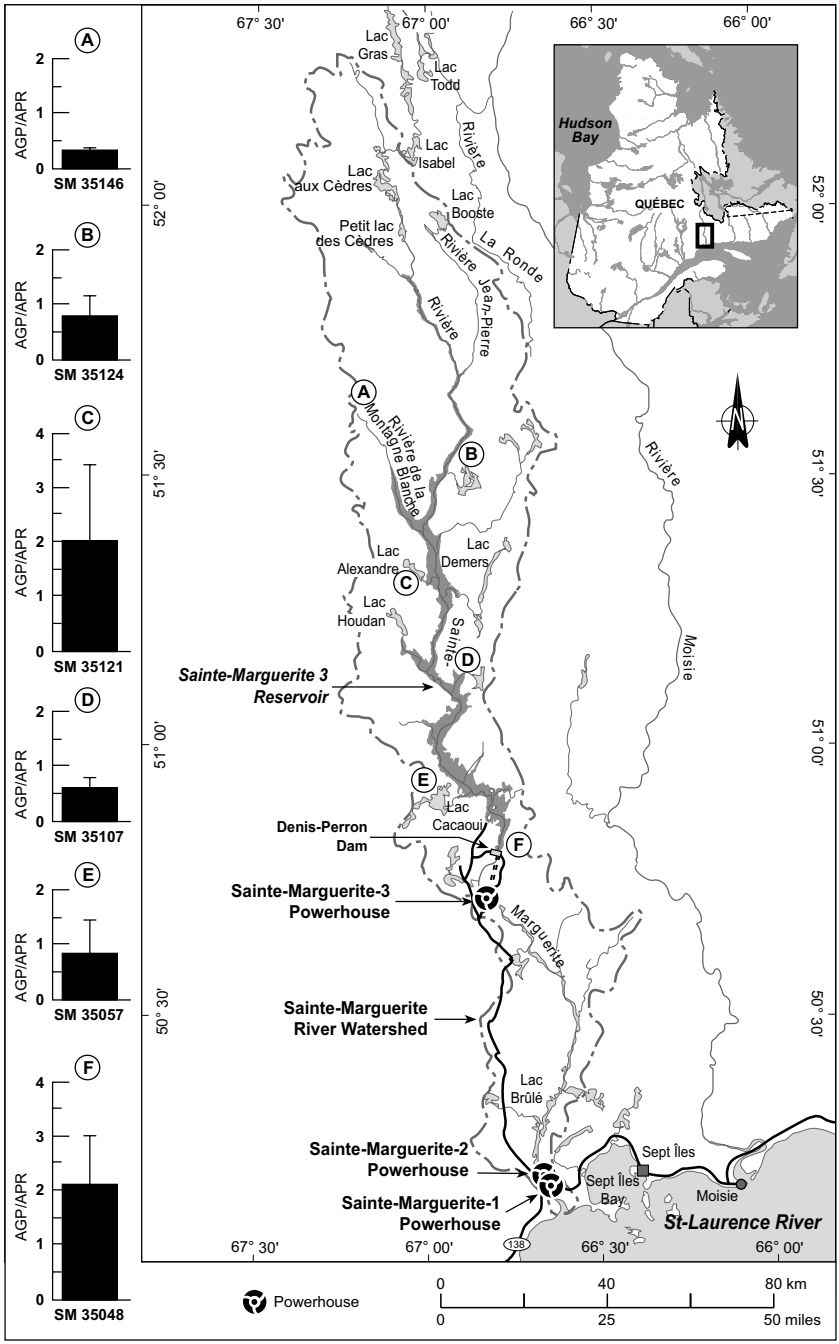
A
AGP/APR
SM 35146
B
SM 35124
C
SM 35121
D
SM 35107
E
SM 35057
F
SM 35048
67° 30'
67° 00'
66° 30'
66° 00'
52° 00'
51° 30'
51° 00'
50° 30'
Lac Gras
Lac Todd
Lac Isabel
Lac aux Cèdres
Lac Booste
Petit lac des Cèdres
Rivière La Ronde
Rivière Jean-Pierre
Rivière
Rivière de la Montagne Blanche
Lac Alexandre
Lac Demers
Lac Houdan
Sainte-
Moisie
Sainte-Marguerite 3 Reservoir
Lac Cacaoui
Denis-Perron Dam
Sainte-Marguerite-3 Powerhouse
Marguerite
Sainte-Marguerite River Watershed
Lac Brûlé
Sainte-Marguerite-2 Powerhouse
Sainte-Marguerite-1 Powerhouse
Sept Îles
Sept Îles Bay
Moisie
St-Laurence River
Hudson Bay
QUÉBEC
138
Powerhouse
0 40 80 km
0 25 50 miles

Fig. 20.6. (cont.)

of LA-1 (Fig. 20.6a, E and D). The AGP/APR ratio in this reservoir was lower than 1 in both, the inflow and at the outflow stations, and closes to the equilibrium (AGP/APR ~1) at LA1903 and LA143C, and AGP/APR > 2 in LA1907 (Fig. 20.6a, D,B and C).

In LG-2, the reservoir with the largest surface area of the four reservoirs studied, we sampled 10 stations. Two of the 10 stations, LG2406 and LG2509 were located close to the outflow of the main tributaries, LG3 and Sakami reservoirs (Fig. 20.6b; J and H). Five stations (LG2318, LG2NO1, LG2039, LG2610, LG2615) were located along the main water flow axis of La Grande Rivière (Fig. 20.6b, I, G, F, B and A), two others,LG2336 and LG2604, were situated on the northern part of the reservoir, near a small tributary, the Canapuskuu River (Fig. 20.6b D and C), and the remaining station, LG2014, was located in the southern part of the LG-2 dam (Fig. 20.6b E). In the main inflow of the La Grande River the AGP/APR ratios were high, and decreased along the main axis from upstream to downstream. Although the northern stations of LG-2 had AGP/APR ratios higher than 1, they were half as productive as the first two stations of the main axis under the influence of the LG-3 water discharge. The ratios in these northern stations were similar to those of the southern stations positioned at the outflow of the Sakami reservoir. The AGP/APR ratios in the remaining stations, downstream of the reservoir, were near equilibrium.

The MA-5 reservoir has a peculiar shape (donut-shaped, Fig. 20.6c) resulting from an ancient meteoritic impact. Three main tributaries are located at the North part of the reservoir and three stations were nearby them, one between stations MA51200, MA50200 and MA51000 (Fig. 20.6c, A, F and B). In the opposite site of the inflow lies the reservoir outflow that has created a delta near which the MA50600 (Fig. 20.6c, D) station was located. The two remaining stations, MA50400, MA50800, were positioned more or less in the middle, between the main tributaries and the outflow, one at each arm of the reservoir (Fig. 20.6c, E and C). The AGP/APR ratio did not have a clear pattern in MA-5. The AGP/APR ratios < 1 were measured at the west and at the north-east stations, the latter close to a tributary. AGP/APR ratios ≥ 1 were found in the other stations, with the highest ratio in the south near the outflow of MA-5 reservoir. The latter results contrast with those of the other reservoirs mentioned before, where AGP/APR ratios were lower towards the outflow as compared with the central and up reservoir stations.

The SM-3 reservoir was built in a narrow valley surrounded by high mountains (Fig. 20.6d). Morphologically, this reservoir may be considered the most typically canyon-shaped reservoir in our study. The canyon has a narrow constriction near the middle of the reservoir, separating two wide basins. In this reservoir we sampled six stations, three upstream and three

downstream of the central constriction. Stations SM35146 and SM35124 may be considered representative of inflow waters (Fig. 20.6d, A and B). The first was located in the bed of one tributary and the second at the junction of this tributary with the main water inflow, the St. Marguerite River, (Fig. 20.6d, B). The third station in this basin, SM35121 was located a few km north of the constriction (Fig. 20.6d, C). In the southern basin of the reservoir, the three remaining stations, SM35107, SM35057 and SM35048 were distributed at equal distance between the constriction and the dam (Fig. 20.6d, D, E and F). In this reservoir, the AGP/APR ratio presented an upstream-downstream pattern in each basin, with lower than 1 to higher than 1 AGP/APR ratios. The southern stations in each section had AGP/APR ratios two to three times higher than in those of the other sampling sites. Once again, this "Côte-Nord" reservoir behaves differently than the two reservoir located in Bay James region in relation to the spatial distribution.

The spatial distribution of AGP/APR in the reservoirs of the two northern Quebec regions does not always follow the reservoir continuum concept, particularly in the older reservoir (LG-2). In the LG-2 reservoir, the highest P/R ratio was measured in the upstream stations. More productive waters upstream of the LG-2 reservoir may be explained by is intermediate position in the reservoir cascade series of La Grande River. Thus, the source water for LG-2, coming from LG-3, was probably less turbid that in normal reservoirs fed by a river or from the shallow reservoir like LA-2, reduced turbidity results in more light for primary production. However, the pattern of decreasing AGP/APR ratios downstream was not present in the upstream LA-1 reservoir, where the main inflow was also the outflow of reservoir, LA-2. In LA-1 the more productive stations were located in the middle of the reservoir, as would be predicted by the canyon reservoir concept. In the youngest reservoir sampled, SM-3, lower AGP/APR ratios were found at the stations located in shallower waters, where respiration rates were driven by the degradation of newly flooded soil and vegetation.

In the studied reservoirs the highest AGP/APR ratios were measured at the stations located in the deepest waters. In general in our study, Z_{max} at each station appeared to be a good predictor of the differences in the metabolic processes that occur at the spatial scale ($AGP/APR = 0.69\ lo_{g10}\ (Z_{max}) + 0.11$, $r^2 = 0.21$, F ratio = 8.4 and Prob. > F = 0.0067; Fig. 7). In the deepest stations we also measured the highest light penetration (light extinction coefficient = ε_{par}). The relationship of ε_{par} and Z_{max} in these reservoirs fits a quadratic function determined by the geographic localization of the reservoirs and the characteristics of the landscape flooded (Fig. 8). On the left side of the curve, low Z_{max} and high light penetration, we had the

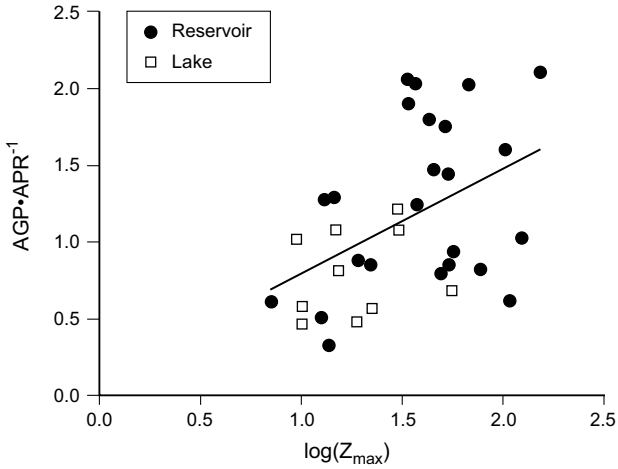

Fig. 20.7. Relationship between the AGP/APR ratio and $\log_{10}$ maximum depth (Z_{max}) at the corresponding station, for reservoirs (●) and lakes (□)

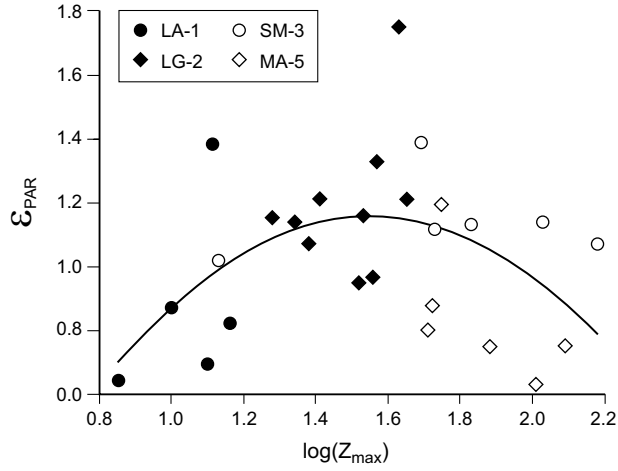

Fig. 20.8. Relationship between the light extension coefficient (ε_{PAR}) and $\log_{10}$ maximum depth (Z_{max}) for reservoir stations (LA-1 = ●, LG-2 = ■, SM-3 = ○ and MA-5 = □)

LA-1 stations located over former lake basins. At the other end of the x-axis the deepest station, also with very low ε_{par}, correspond to "Côte Nord" reservoir SM-5. Intermediate Z_{max} values were found in LG-2 and MA-5 reservoirs, which had the highest ε_{par}. It has been shown that mean depth, bottom characteristics associated with the type of ecosystem flooded (for-

est, bog and lake) as well as light, are important variables that explain biological processes in reservoirs, particularly primary production (Soballe & Kimmel 1987; Hejzlar et al. 1989; Thébault et al.1999; Fernandez-Rosado et al. 1994).

20.4.5 Gross Primary Production and Total Respiration Mass Balance and their Relationship to CO_2 Flux at the Water-Air Interface

In the studied ecosystems, to ascertain the importance of the metabolic processes in CO_2 emission, we compared mean planktonic total water column respiration (CO_2 production) and mean CO_2 fluxes in the air-water interface for the two sampled seasons, spring and summer. This comparison was only possible in the lakes and reservoirs where evasive CO_2 atmospheric flux was measured simultaneously with water sampling. We calculated total planktonic respiration (TPR) by the extrapolation of respiration rates measured in the upper layers to the whole depth, with the assumption that respiration rates are constant through the water column. The relationship was very strong ($\log_{10}$ CO_2 flux = 0.67 + 0.90 $\log_{10}$ TPR, $r^2 = 0.93$, $F = 198.8$ and $p < 0.0001$; Fig. 20.9). The relative contribution of TPR to CO_2 evasive fluxes varied widely in relation to the type of ecosystem, and in some cases with the sampling period (spring/summer). In reservoirs, the means percentage of TPR contributed more than 100% to CO_2 evasion; it

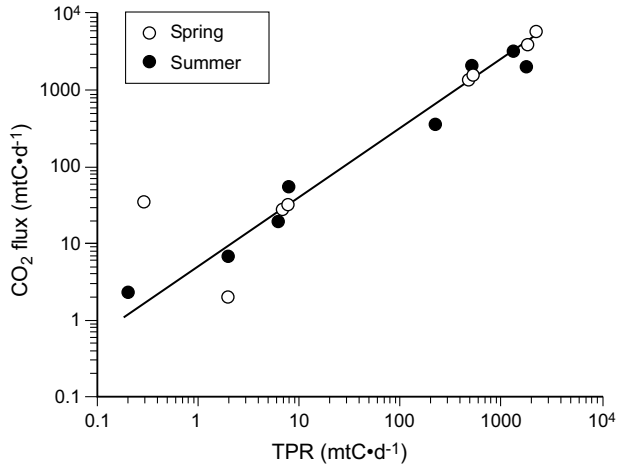

Fig. 20.9. Relationship between evasive CO_2 flux and the total plankton respiration (TPR) for the four reservoirs and four lakes in the LG-2 region for spring (○) and summer (●)

was lower in spring than in summer with 136% and 193% respectively. In lakes, except Lake Desaulnier in spring, the percentage of respiration contribution to CO_2 effluxes was lower than in reservoirs and rather similar between seasons (Table 20.3). Contribution to CO_2 evasive fluxes between reservoirs was independent of the age of the reservoir even in spring or summer (Table 20.3).

To compare the importance of autochthonous vs. allochthonous C contribution to respiration, and hence to CO_2 supersaturation, we calculated the % of GPP over TPR. In all ecosystems, the autochthonous contribution to total respiration was lower in the spring than in the summer, and its contribution in reservoirs was lower than in lakes in any season. In reservoirs, mean autochthonous carbon contribution to respiration was 20 and 50% in spring and summer, respectively, indicating a higher allochthonous C-respiration in earlier open waters season than in the middle of summer (Table 20.3). Between reservoirs, as expected, the lowest autochthonous carbon contribution to respiration occurred in the youngest reservoir, SM3. Reservoir LA-1, the shallowest and the most productive of the four reservoirs studied, presented the highest % of contribution of GPP to PTR of all reservoirs, with a summer contribution of over 100%. In lakes the mean % contribution of GPP to TPR represented 78 and over 100% in spring and summer, respectively (Table 20.3).

In this study, in general, the % of contribution of autochthonous C to the total ecosystem respiration was negatively related to the mean depth of the ecosystem (Fig. 20.10). This relationship was very strong for reservoirs ($\log_{10}$ GPP/PRT = 2.64-0.96 $\log_{10}$ Zmoy, $r_2 = 0.83$, F = 29.05, $p = 0.0017$). Due to the fact that respiration was only measured in the upper part of the water column, we likely over-estimated total respiration in the deepest reservoirs. If we considered the % of contribution of GPP to planktonic respiration only in the upper part of the water column, where metabolic processes were measured, we found that in summer there was an excess of autochthonous production over respiration in all reservoirs except the youngest one (SM-3). When this excess of autochthonous C produced in the photic zone sink as POC to the aphotic zone, we could predict that respiration rates would be much lower toward the bottom in reservoirs with higher mean depth than those lower mean depth. Thus, for a similar GPP in the photic zone, different degrees of dilution of the sedimenting organic matter could explain the negative relationship between the percent of contribution of autochthonous C to respiration with mean depth (Fig. 20.10).

In conclusion, most of the biological indicators mean values, such as phytoplankton biomass, areal gross primary production and areal planktonic respiration were similar for older reservoirs and lakes in a given

Table 20.3. Spring and summer carbon (C) mass balance in reservoirs and in lakes for: evasive CO_2 fluxes (CO_2 flux); C-fixed by phytoplankton (GPP), or C-respired by planktonic organisms in the mixing zone (PRphot) or in the entire ecosystem (TPR); and the relative contribution (%) of total planktonic respiration (TPR) to CO_2 fluxes, % contribution of GPP to TPR (GPP/TPR) and to planktonic respiration in the photic zone (PRphot; GPP/PRphot)

	Sites	CO_2 flux ($mt \cdot d^{-1}$)	TPR ($mt \cdot d^{-1}$)	TPR/CO_2 %	GPP ($mt \cdot d^{-1}$)	GPP/TPR %	PRphot ($mt \cdot d^{-1}$)	GPP/PRphot %
Spring	LA-1	1430	488	125.13	237	48.57	287	82.58
	LG-2	3986	1827	168.06	298	16.31	464	64.22
	MA-5	6125	2203	131.88	265	12.03	196	135.20
	SM-3	1641	530	118.42	32	6.04	36	88.89
	Reservoir means			135.87		20.74		92.72
	LDESA	5	1.94	146.97	1.4	72.16	0.081	
	LPATU	33	7.71	85.67	4.4	57.07	2.605	
	LUKAU	3	0.29	37.98	0.4	137.93	0.035	
	LYASI	28	6.75	88.39	2.9	42.96	0.961	
	Lake means			89.75		77.53		
Summer	LA-1	374	224	219.61	322	143.75	151	213.25
	LG-2	3259	1320	148.51	442	33.48	270	163.70
	MA-5	2072	1786	316.06	178	9.97	172	103.49
	SM-3	2126	512	88.30	47	9.18	50	94.00
	Mean			193.12		49.10		143.61
	LDESA	7	1.94	101.62	1.9	97.94	0.081	
	LPATU	20	6.17	113.12	6.7	108.59	1.298	
	LUKAU	2	0.20	36.67	0.4	200.00	0.007	
	LYASI	57	7.94	51.08	6.7	84.38	0.838	
	Mean			75.62		122.73		

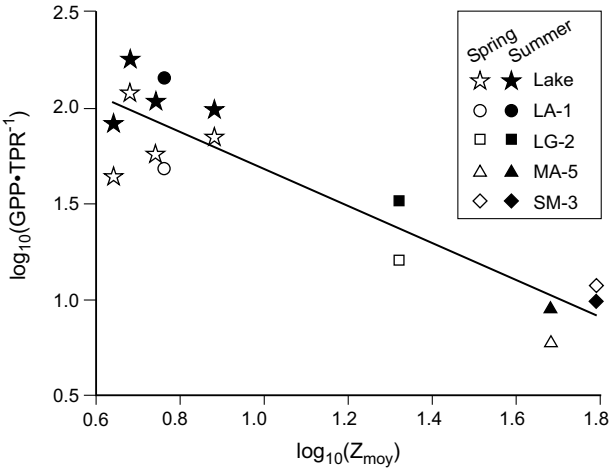

Fig. 20.10. Relationship between gross primary production (GPP) / plankton total respiration (PTR) ratio and mean depth of reservoirs or lakes.

Spring values for lakes (X), summer values for lakes (+), LA-1 in spring (○), LA-1 in summer (●), LG-2 in spring (□), LG-2 in summer (■), MA-5 in spring (◊), MA-5 in summer (♦),SM-3 in spring (△) and SM-3 in summer (▲)

region. The greatest differences between systems were measured in one of the young reservoirs, LA-1, where mean planktonic biomass and the metabolic processes were the highest measured in our study sites. In the youngest reservoir, SM-3, sampled only one year after it was filled to the maximum level, not significant mean differences were found for any variable measured when we compared to the oldest reservoirs (LG-2 and MA-5) and the studied lakes but the maximum values of phytoplankton biomass and areal gross production were mesured in SM-3. Except in the youngest reservoir SM-3, autochthonous organic matter production in the upper layer of reservoirs was in excess of respiration in summer and in spring. Total planktonic community respiration in reservoirs and lakes predicted more than 90% of the CO_2 fluxes measured at the air-water interface. The contribution of planktonic gross primary production to total planktonic C-respiration was lower in reservoirs than in lakes, and it was negatively related to mean depth in reservoirs. The negative relationship between respiration rates with mean depth may be explained by the overestimation of respiration rates in the deepest part of the reservoir, when respiration rates were extrapolated from the mixing or photic zone to the aphotic zone. Real measurements of respiration rates in the deep layer of reservoirs need to be done to ascertain the relative importance of the biological processes to CO_2 emissions. In reservoirs built in pristine areas, the importance of mor-

phometric parameters, such as depth, was emphasized by several relationships, either at the small scale (stations level) or at the entire ecosystem level (mass balance) implying the importance of the ecosystem size in predicting reservoir processes. Finally, the greatest achievement of this study is to show that planktonic metabolisms process could easily explain the CO_2 effluxes of hydroelectric Northern Québec reservoirs even by the amount of C release by TPR or by the linear relationship found with the effluxes response to the TPR variations.

21 Impacts of Ultraviolet Radiation on Aquatic Ecosystems: Greenhouse Gas Emissions and Implications for Hydroelectric Reservoirs

Julie Bastien

Abstract

Ultraviolet radiation (UV) affects carbon dynamics in aquatic ecosystems. Photooxidation of dissolved organic matter (DOM) can produce greenhouse gases (GHG) and the effects of UV on primary and secondary production can influence the flux of carbon (C) between aquatic ecosystems and the atmosphere. Products of photooxidation include: DOM of lower molecular weight, carbon dioxide (CO_2) and carbon monoxide (CO). Lower molecular weight DOM can be more easily utilized by microorganisms. Secondary microbial production and the production of CO_2 from aerobic respiration are, therefore, favored. However, the harmful effects UV have on phytoplankton diminish the rate of CO_2 fixation. The fluxes of CO_2 in reservoirs are influenced in the same manner as natural lakes since reservoirs older than 10 years are comparable to lakes. The largest distinction to be made between reservoirs and lakes is their surficial aerial coverage, which is generally much larger for reservoirs. This factor may help explain the differences observed in carbon fluxes from natural lakes and reservoirs. Following the literature review, a first gross estimate was made of the importance of the production of GHGs resulting from photooxidation relative to other processes. The results show that when making a calculation of the balance of net CO_2 emissions from aquatic ecosystems and hydroelectric reservoirs, photooxidation needs to be taken into consideration as it can account for between 6 and 28% of total emissions.

21.1 Introduction

It is well known that ultraviolet radiation (UV) affects carbon dynamics in aquatic ecosystems (Williamson et al. 1999; Bertilsson & Trawvick 2000; Erikson III et al. 2000; Granéli et al. 1996, 1998; Morris and Hargreaves 1997). UV radiation acts differently on biotic and abiotic process: photooxidation, variability in the photosynthetic capacity and the rate of microbial respiration, etc. The effects of UV on DOM can result in the production of greenhouse gases (GHG). This chapter presents a review of the literature. Particular attention is paid to the role of UV in DOM decomposition, its impact on biological production and the production of GHGs in natural aquatic ecosystems and reservoirs.

21.2 Ultraviolet Radiation and Dissolved Organic Matter

The ultraviolet spectrum (280–400 nm) is divided into three regions: UV-A (315–400 nm), UV-B (280–315 nm) and UV-C (200–280 nm) (Hessen 2002). Photosynthetically available radiation (PAR) is found in the 400 to 700 nm region (Häder 1997). Stratospheric ozone absorbs radiation differently according to the wavelength: UV-C is completely absorbed, most of the UV-B is absorbed, and UV-A is only slightly absorbed (Häder 1997; Granéli et al. 1998; Smith et al. 1992). The amount of UV-B received at the surface of the earth is, therefore, dependent on the thickness of the ozone layer.

The amount of radiation received below the surface of the water depends on both the amount of radiation received just above the water surface and on the reflectivity of the air-water interface (Hessen 2002). Between 10 and 12% of the radiation is reflected by the water surface. Only the absorbed solar radiation can chemically (photooxidation) influence the ecosystem and lead to the production of GHGs and low molecular weight carbon compounds (Zepp and Cline 1977). UV-B can penetrate, on average, between 5 and 20 m depth in marine waters (Herndl et al. 1997) and up to between 0.04 and 4 m in freshwaters (Reche et al. 1999; Wetzel et al. 1995; Williamson et al. 1999: Table 21.1).

In the water column suspended organic and inorganic material, microorganisms and, most importantly DOM, contribute to the attenuation of radiation with depth through absorption, diffusion and reflection (Arts et al. 2000; Eriksson III et al. 2000; Hessen 2002; Obernosterer et al. 1999; Smith et al. 1999; Schindler et al. 1996; Zepp et al. 1998). Additionally, shorter wavelengths (UV: 280–400 nm), usually considered more harmful

than longer wavelengths (PAR: 400–700 nm), are preferentially absorbed. Dissolved organic matter, therefore, protects living organisms from the detrimental effects of UV, by limiting the depth of UV penetration. Dissolved organic matter acts as a protecting filter (sun-block) for aquatic organisms in lake environments in the same way as the stratospheric ozone does for terrestrial environments (Jerome and Bukata 1998).

Table 21.1. Comparison of different physico-chemical parameters in oceans and lakes

Parameter	Lakes	Oceans
Mean depth (m)	~30	3800
Depth of UV-B penetration (m)	0.04–4	5–20
DOM (mg C L^{-1})	1–50	0.43–0.96
Surface coverage	~2% earth's surface	~68% earth's surface

Source: Reche et al. 1999; Herndl et al. 1997; Mopper et al. 1991; Wetzel et al. 1995; Williamson et al. 1999; Benner and Biddanda 1998; Peltzer and Hayward 1996.

UV and DOM can both play an indirect role in the production of GHGs through their influence on primary and secondary production, or a direct role through the degradation of DOM to smaller molecules and to CO_2. All these processes take place in both marine and freshwater systems (Zepp et al. 1998). Their relative importance, however, can vary. The concentration of DOM is higher in freshwater than in marine systems (Table 21.1) (Morris et al. 1995; Laurion et al. 1997), and explains the weaker UV penetration in freshwaters. UV plays an important role in aquatic ecosystems both through its absorption and its reaction with DOM.

21.2.1 Types of Dissolved Organic Matter

Dissolved organic matter is composed of dissolved organic carbon (DOC) and organic compounds containing sulfur (S), nitrogen (N) and phosphorus (P). Decomposition of DOC is ten times greater than that of particular organic carbon and is additionally accelerated by photolysis and its subsequent bioavailability, contributing to the efflux of CO_2 to the atmosphere (Wetzel et al. 1995). The majority of freshwater (>50%) (Corin et al. 1996; Ertel 1990; Herndl et al. 1997; Wetzel et al. 1995; Davies-Colley and Vant 1987; Reche et al. 1999; Moran and Hodson 1990) and marine (Petterson et al. 1997) DOM is composed of dissolved humic substances (DHS). Dis-

solved humic substances are dark colored, acidic and are composed primarily of aromatic molecules (Gastonguay et al. 1995). The chromophores contained in the humic substances strongly absorb UV (Frimmel 1994; Morris et al. 1995) and serve as initiators of photoreactions (Yiyong 1996). Chromophores are chemical groups or residues which give the dark color to the material, allowing it to absorb the radiation. The unsaturated conjugated bonds and the free electron pairs of the heteroatoms of the humic molecules act as chromophores for humic substances (Corin et al. 1996; Kulovaara et al. 1996).

Humic (HA) and fulvic (FA) acids[1] originating from the decomposition of terrestrial plant material are the principal components of DOM. During decomposition of humic substances, humic acids are degraded to fulvic acids, which are in hand degraded to CO_2 and H_2O (Gastonguay et al. 1995). The relative proportion of humic and fulvic acids determines the colour of the water and influences UV absorption. The fulvic fraction is more photosensitive than the humic fraction (Molot and Dillon 1997; Kulovaara et al. 1996) due to its less polymerized compounds (Wetzel 2001) and lower proportion of aromatic structures (Corin et al. 1996). The HA:FA ratio is lower in forest soils (~0.7) than in prairie soils (~2.3) (Stevenson 1994). Lakes and reservoirs situated in forested regions receive more fulvic acids and are, therefore, more susceptible to photooxidation.

21.2.2 Dissolved Organic Matter Quality

Dissolved organic matter can be qualitatively characterized according to its age and origin. DOM age is correlated to the position occupied by DOM in the water column. This concept pertains to marine environments with very deep water columns. Young DOM (days to months) is found in the surface waters, while old DOM is found at depths of more than 1000 m where it can be more than 1000 years old (Benner and Biddanda 1998).

Dissolved organic matter can be of autochthonous or allochthonous origin. Autochthonous DOM in aquatic ecosystems, is produced by photosynthesis (Häder 1997), extracellular release and exudation mechanisms, or by the degradation of plankton and macrophytes (e.g. mortality, grazing, biodegradation, photodegradation) (Obernosterer et al. 1999). Allochthonous DOM, by contrast, originates from the terrestrial input from the watershed (Hessen 2002). This material is, therefore, produced outside the aquatic ecosystem. The quantity of allochthonous DOM will vary according to the

[1] By definition, humic acids precipitate in acid solutions (pH 2) but dissolve at higher pH. Fulvic acids are soluble at all pHs (Wetzel 2001).

ratio of watershed surface area to lake surface area. The majority of Northern American temperate lakes receive their carbon from inputs from the watershed (Engstrom 1987; Gennings et al. 2001). The proportion of allochthonous and autochthonous DOM is, therefore, influenced by the degree of aquatic productivity, precipitation, terrestrial inputs and elevation (Williamson et al. 1996).

The optical properties of DOM differ according to its origin. Allochthonous DOM absorbs more visible and UV radiation than autochthonous DOM which is less sensitive to this radiation (Donahue et al. 1998; Thomas and Lara 1995). Allochthonous DOM is, therefore, more susceptible to photochemical mineralization to CO_2 and CO (Moran et al. 2000; Opsahl and Benner 1998). However, allochthonous DOM is usually considered more recalcitrant to biodegradation (Lindell, et al. 1995; Moran et al. 2000), although it can support a certain degree of bacterial growth (Moran and Hodson 1990). Several factors can explain this difference. Firstly, allochthonous DOM is generally older than freshwater autochthonous DOM, because prior to reaching the lake or the river it has circulated within the watershed. Secondly, allochthonous DOM is primarily composed of humic substances, that is, of heterogeneous polymeric high molecular weight compounds (Bertilsson and Tranvik 2000; Moran and Hodson 1990). Allochthonous DOM biodegradation is also slower than autochthonous DOM biodegradation due to its lower nitrogen content[2] (Wetzel 2001). However, since photooxidation creates smaller and more bioavailable molecules, the kinetics of photooxidation positively increases the kinetics of biodegradation (Gennings et al. 2001; Moran et al. 1999; Miller 1998). The latter being limited by photooxidation in waters dominated by humic substances. This is the case in the majority of boreal lakes and reservoirs (De Haan 1993).

The origin of DOM influences the formation of dissolved inorganic carbon (DIC). Lakes with high primary production (high chlorophyll concentrations and high concentration of autochthonous DOM) produce less DIC (Bertilsson and Tranvik 2000). Dissolved organic carbon will, therefore, be more easily mineralized in humic oligotrophic lakes than in eutrophic lakes high in algal productivity. The daily photodegradation rate of humic substances in lakes is of the same magnitude as the rate of photosynthetic DIC fixation (De Haan 1993). Humic substances are the principle source of substrate utilized in photochemical reactions resulting in DIC and carboxylic acid production (Kieber et al. 1990). The content of DHS originating from the degradation of lignaceous and herbaceous organic matter is,

[2] The C:N ratio for allochthonous DOM is 50:1 and for autochthonous DOM 12:1 (Wetzel 2001).

therefore, important (Bertilsson and Tranvik 1990). A significant quantity of DHS is likely to be present in flooded areas (reservoirs) as has been shown by the increase in total organic carbon in the first years following impoundment (Hayeur 2001).

21.2.3 Photoreactions and DOM

While the degradation of humic substances is slow, photolysis increases degradation both directly and indirectly by propagating biodegradation (Amador et al. 1989; Geller 1986; Herndl et al. 1997) to a point where daily variations in DOC are observable (Corin et al. 1996; Doney et al. 1995; Kieber et al. 1989; Mopper and Stahovec 1986; Petterson et al. 1997). Photodegradation also produces strong oxidants ($\cdot O_2^-$, $\cdot OH^-$, H_2O_2) (Corin et al. 1996; Wannikof and Knox 1996; Zepp et al. 1998; Haag and Hoigne 1985; Mopper et al. 1991; Mopper and Zhou 1990), which are, in part, responsible for photobleaching[3] (Reche et al. 1999). Iron (Fe) and copper (Cu) play an important role in freshwater and marine ecosystems through their participation in processes invoked by UV (Faust and Zepp 1993; Palenik et al. 1991) that produce and consume peroxydes (Scully et al. 1996) and other oxidants (Zepp et al. 2003).

According to the first law of photochemistry, only absorbed radiation can produce photochemical changes (Miller 1999). When a humic molecule absorbs a photon of a given energetic level, it becomes unstable and undergoes a variety of changes such as chemical reactions, light emission and physical deactivation, prior to returning to a stable state (Zepp and Cline 1977). Once a given level of energy is absorbed, either through the breaking of a bond or through electron activation, new products can be formed (Miller 1999). The photoproducts include volatile compounds (CO_2, CO) and bioavailable low molecular weight carbonic compounds (Corin et al. 1996; Miller and Moran 1997; Vähätalo et al. 1999). Carbon dioxide (CO_2) and CO volatilization are the primary cause of DOM loss from aquatic ecosystems (Miller and Moran 1997).

Production of Low Molecular Weight Compounds

It appears that the majority of DOM from all origins is resistant to biological mineralization (Ertel 1990; Salonen and Vähätalo 1994). Since the

[3] Photobleaching is the process by which optical properties of the material are changed (Morris and Hargreaves 1997): the pigments lose their color and, hence, their capacity to absorb radiation is altered (Moran et al. 2000; Hongve 1994).

concentration of DOM in lakes is not continuously increasing despite autochthonous production and relatively continuous allochthonous inputs, other processes must contribute to the destruction/transformation of the recalcitrant fraction of this material (Granéli et al. 1998). Ultraviolet radiation can degrade high molecular weight DOM to low molecular weight compounds (<1000 Da) that are more easily bioassimilated such as carboxylic acids (formic, acetic, citric, and levulinic acids), aldehydes (formeldahyde, acetaldehyde), ketoacids (glyoxylate, pyruvate) and aliphatic mono- and di-basic acids (Bertilsson and Tranvik 1998, 2000; Corin et al. 1996; Dahlén et al. 1996; Ertel 1990; Häder 1996; Kieber et al. 1989; Lindell et al. 1995; Miller and Moran 1976; Mopper and Stahovec 1986; Opsahl and Benner 1998; Palenik et al. 1991; Salonen and Vähätalo 1994; Zepp et al. 1998). Carboxylic acid production rates are equivalent to 30% of DIC production rates. Table 21.2 is a compilation of rates of photooxidation found in the literature. Without the UV induced transformation of terrestrial DOM into low molecular weight compounds, this material would remain biologically and chemically inert (Gennings et al. 2001). Moreover, a portion of the low molecular weight compounds are volatile (Mopper and Stahovac 1986).

Production of Dissolved Inorganic Carbon

Ultraviolet radiation can also mineralize DOM to DIC (HCO_3^-, CO_3^{2-}, CO_2) (Ertel 1990; Petterson et al. 1997; Dahlén et al. 1996; Vodacek et al. 1997), carbon monoxyde (CO) (Moran and Zepp 1997) and carbonyl sulphide (COS) (Andreae and Ferek 1992; Uher and Andreae 1997). Carbon dioxide and CO are the principle gases formed by photooxidation (Johannessen and Miller 2001; Gao and Zepp 1998; Moran and Zepp 1997; Häder 1997; Opsahl and Benner 1998; Miller and Zepp 1995). Moreover, the principal source of CO production is DOM photooxidation in the epilimnion (Doney et al. 1995; Johnson and Bates 1996; Schmidt and Conrad 1993; Valentine and Zepp 1993; Wilson et al. 1970; Zepp et al. 1998; Zuo and Jones 1995). Only a small portion of CO comes from anaerobic production in the hypolimnion (Conrad et al. 1983). Approximately 15 to 20 times more DIC than CO is produced from photooxidation (Miller and Zepp 1995; Miller and Moran 1997). Dissolved inorganic carbon and CO production is ubiquitous in lakes (Bertilsson and Tranvik 2000). The production of DIC from DOC seems to be the most rapid photochemical process of DOC transformation (Eriksson III et al. 2000). On average we can estimate photochemical mineralization rates of DOC to be approximately 4 $\mu M\ C\ h^{-1}$ (Amon and Benner 1996). According to various authors,

Table 21.2. Photooxidation rates (production of DIC, CO or carboxylic acids) in aquatic ecosystems after several authors and under different experimental parameters

Authors	Photooxidation rate[a]	Exposure time and other parameters[b]
Granéli et al. 1996	75 $mgC \cdot m^{-2} \cdot d^{-1}$ (DIC)	24 h; solar radiation; mean of 5 Swedish lakes (clear to humic)
Moran and Zepp 1997	77–126 $mgC \cdot m^{-2} \cdot d^{-1}$ (DIC)	Estimate for the oceans
Anesio and Granéli 2003	2.6 $mgC \cdot m^{-2} \cdot d^{-1}$ (DIC)	24 h; solar radiation; Swedish lake
Granéli et al. 1998	24 $\mu gC \cdot L^{-1} \cdot h^{-1}$ (DIC)	6 h; solar radiation (UV-A: 520 $kJ \cdot m^{-2}$); mean of 10 lakes.
Bertilsson and Tranvik 2000	86 $\mu gC \cdot L^{-1} \cdot h^{-1}$ (DIC) 15 $\mu gC \cdot L^{-1} \cdot h^{-1}$ (CA)	12 h; UV-B: 1.5 $W \cdot m^{-2}$; UV-A: 17.4 $W \cdot m^{-2}$; PAR: 5 $W \cdot m^{-2}$; 38 lakes
Bertilsson and Tranvik 1998	19 $\mu gC \cdot L^{-1} \cdot h^{-1}$ (CA)	8 h; solar radiation (UV-A: 710 $kJ \cdot m^{-2}$); lacustrine environment
Dahlén et al. 1996	2 $\mu g\ C \cdot L^{-1} \cdot h^{-1}$ (CA)	89 h; UV-B: 0.003 $W \cdot m^{-2}$; UV-A: 5.1 $W \cdot m^{-2}$; humic lake
Miller and Moran 1997	1.6 $\mu M \cdot C \cdot h^{-1}$ (DIC) 0.1 $\mu M \cdot C \cdot h^{-1}$ (CO)	4 h; measured after 2 weeks of biological degradation; marine environment; simulated solar radiation
Gao and Zepp 1998	22 $\mu M \cdot C \cdot h^{-1}$ (DIC) 1.5 $\mu M \cdot C \cdot h^{-1}$ (CO)	4 h; Satilla River; simulated solar radiation

[a] Photooxidation rates (variable units) of DIC, CO and carboxylic acids (CA) including oxalic acid, manolic acid, formalic acid and acetic acid.
[b] The experimental conditions vary highly between the studies, with some authors using natural solar radiation and others using simulated radiation. Some studies are from freshwaters and others from marine environments.

the proportion of mineralizable DOC varies between 15 and 65% (Moran et al. 2000; Salonen and Vähätalo 1994). Photodecarboxylation is the principal mechanism through which DIC is produced from DOC (Amon and Benner 1996; Miller and Moran 1997). In molecules containing aromatic structures, it is the carboxylic acid functional groups that undergo decarboxylation and not the aromatic structures themselves (Budac and Wan 1992).

The wavelength of radiation is important for determining the rate of photoreactions involving DOM. Few studies have considered the effect of wavelength when measuring the quantum yield (number of photoreactions

per photon absorbed). Shorter wavelengths are more energetic with regards to photooxidation (Bertilsson and Tranvik 2000; Vähätalo et al. 2000; Kulovaara et al. 1996). Therefore, between 290 and 390 nm, the quantum yield decreases with increasing wavelength. UV-B (280–315 nm) is, therefore, more important in terms of photooxidative capacity than UV-A (315–400 nm), and produces more CO_2 and CO per photon mole. However, photoreactions do take place at depths greater than the level of UV-B penetration (0.04 to 4 m in lakes; Reche et al. 1999; Wetzel et al. 1995), indicating that UV-A also participates in these reactions (Granéli et al. 1996; Opsahl and Benner 1998; Reche et al. 1999). In fact the profile of reactions resembles the profile of UV-A penetration (Bertilsson and Tranvik 1998). The experiments undertaken by Granéli et al. (1998) further show that PAR and UV-A are more important for photooxidation than UV-B[4]. Actually, even though the energy absorbed per photon is greater at shorter wavelengths (UV-B), the total absorbed energy is greater at longer wavelengths (UV-A and PAR), because a greater amount of these latter wavelengths reach the surface of the earth.

Lignin Photodegradation

A part of the DOM in lakes derives from surface runoff of decomposed terrestrial vegetation (allochthonous DOM). Lignin is a phenolic polymer derived from the bark of lignaceous vegetal species (Ertel 1990). Lignin may be partly responsible for the color of water (Wang et al. 1988). Lignin is very resistant to degradation and only a few specialized microorganisms are able to degrade it (Paul et al. 1999). However, lignin may be depolymerized, through CuO oxidation, into smaller and more soluble phenolic compounds (Ertel 1990). Once in soluble form, lignin is very vulnerable to photodegradation (Opsahl and Benner 1998). Additionally, photochemical reactions further increase lignin solubility by increasing the proportion of hydroxyl, carboxyl and ketonic groups, and by decreasing the amount of methoxyl groups (Opsahl and Benner 1998; Vähätalo 1999). The residence time of lignin in oceans is 250 years, equivalent to less than a tenth of the residence time of lignin in terrestrial ecosystems (Ertel 1990). This would suggest that soluble lignin is removed from aquatic systems, and that photodegradation is the most likely mechanism (Ertel 1990). Furthermore, even when in particulate form, lignin can be modified and mineralized by photochemical reactions (Vähätalo 1999).

[4] 44%, 39% and 17% of the DIC photoproduced stems from PAR, UV-A and UV-B radiation, respectively (Granéli et al. 1998).

The production of more labile and degradable lignin compounds following lignin photodegradation, indicate that the processes of photodegradation and biodegradation can interact (Paul et al. 1999). Nonetheless, photodegradation remains a more important process for lignin degradation than biodegradation. Assuming the presence of significant quantities of dissolved lignin, photodegradation of DOM in reservoirs is likely possible. In fact, dissolved lignin is preferentially photooxidized relative to the remaining DOM fraction (Ertel 1990). The mixing of bottom waters rich in lignin compounds with surface waters will have a profound impact on the availability of lignin for photodegradation.

21.2.4 Ionic Conditions

Ionic conditions can influence photooxidation at several scales. Firstly, the absorption spectrum of different DOM compounds is dependant on pH (Williamson et al. 1996). Secondly, in a study by Reche et al. (1999), it was noted that more photobleaching took place under alkaline conditions. Color loss results in a decreased absorption capacity by photons, therefore, diminishing the photooxidation potential (Miller 1999). In fact, it seems as though photooxidation rates are higher in more acidic environments. The clarity of the water resulting from low microbial growth in acidic environments allows for deeper radiation penetration (Yan et al. 1996) and, therefore, favors photooxidation (Schindler et al. 1997b). In the presence of acids, the aromatic portions of DOM molecules can be oxidized to H_2O and CO_2 (Donahue et al. 1998). It has been shown in the literature that in more acidic lakes (pH<5.8) a higher ratio is observed between CO_2 emissions to the atmosphere and the storage of CO_2 in the sediments than in more neutral lakes (pH 6–8) (Anesio and Granéli 2003). In fact at pHs <6.5 free volatile inorganic carbon species (CO_2)[5] dominate (Wetzel 2001). However, under these acid conditions a greater photolitic mineralization of DOM to DIC would also be observed (Anesio and Granéli 2003; Gennings et al. 2001; Table 21.3). In acid lakes, the proportion of CO_2 stemming from photooxidation is greater than that from respiration. According to Anesio and Granéli (2003), atmospheric acid deposition in lakes will have an equally important impact on long-term carbon exchanges in aquatic ecosystems as the thinning of the ozone layer.

[5] Between pH 6.5 and 10.5, HCO_3^- will dominate, and at pHs > 10.5 CO_3^{2-} will dominate (Wetzel 2001).

Table 21.3 DIC production (photooxidation in μg $C \cdot L^{-1} \cdot h^{-1}$ ± s.d., n=3) following 24 h exposure to UV under different pH conditions

pH	Photooxidation ($\mu g \cdot C \cdot L^{-1} \cdot h^{-1}$)
4.5	31.8 ± 1.5
5.7	28.7 ± 1.3
6.8	23.7 ± 1.4
8.6	18.4 ± 0.8

Source: Anesio and Granéli 2003

21.3 Ultraviolet Radiation and Microorganisms

The effects of UV on carbon storage capacities are not restricted to release from decomposition but are also related to the fixation capacity of phytoplankton (Paul et al. 1999) and to the productivity of bacterioplankton. In fact, exposure of DOM to UV can lead to the production of substances that can either favour or limit microbial growth (Obernosterer et al. 1999). UV can also directly affect microorganisms, in some cases lethally (Obernosterer et al. 1999; Häder et al. 1998).

21.3.1 Plankton

Ocean-atmosphere CO_2 exchange is in part related to biological activity. Phytoplankton is responsible for the utilization of nearly half of the atmospheric carbon stored in the oceans. Those regions characterized by high phytoplankton productivity tend to be undersaturated relative to the atmosphere and, consequently, act as sinks rather than sources of carbon. A decrease in the phytoplankton community due exposure to UV can, therefore, reduce the efficiency of oceans to act as sinks for atmospheric carbon and increase the effluxes of greenhouse gases (GHG) to the atmosphere as a result of a decrease in the retention of DIC produced in situ (Häder et al. 1998; Kondratyev and Varotsos 2000). This results in CO_2 concentrations closer to equilibrium (water-atmosphere) and, hence, a smaller capacity for the ocean to absorb atmospheric CO_2.

Notwithstanding, UV radiation can have contrasting effects on the phytoplankton. The transformation of Fe^{3+} into the more soluble form of Fe^{2+} caused by UV radiation, favors the assimilation of this essential nutrient by the phytoplankton (Häder 1997; Palenik et al. 1991). The increase in availability of micronutrients, such as iron (Fe) and manganese (Mn), resulting from exposure to UV radiation can lead to a strong increase in

phytoplankton productivity and, therefore, in the rate of carbon fixation (Morel and Price 1990).

Bacterioplankton biomass and productivity can be as equally important as phytoplankton biomass and productivity (Häder et al. 1998; Herndl et al. 1997). Bacteria are responsible for a large part of aerobic respiration (CO_2 production), the whole of anaerobic respiration (CH_4 production) and a large part of the remineralization of organic nutrients (DIC production). There are some aquatic ecosystems in which secondary bacterial production is greater than primary phytoplankton productivity (Cole 1999). These are said to be net heterotrophic systems: a larger amount of carbon is consumed than stocked. The respiration in these systems is sufficient to generate CO_2 supersaturation (Cole 1999).

Methane (CH_4) and nitrous oxide (N_2O) are produced by bacteria living in the sediments: anaerobic methanogenic bacteria and nitrifying and denitrifying bacteria, respectively (Eriksson III et al. 2000; Schmidt and Conrad 1993; Svensson 1998). Microorganisms living in the sediments are protected from solar radiation. UV radiation, therefore, has little or no effect on the production of these GHGs in aquatic ecosystems (Eriksson III et al. 2000).

Nonetheless, the efficiency of carbon storage is not only a function of the phytoplankton, but also of the trophic interactions such as those between phytoplankton and zooplankton. In certain communities, for example, UV affects grazing zooplankton more than phytoplankton. When the phytoplankton are limited by grazers, an increase in UV radiation will result in an increase in primary production and, hence, carbon uptake (Williamson 1995; Bothwell et al. 1994; Schindler et al. 1997a). The differential effect of UV on algae and zooplankton will reduce the impacts of grazing and will compensate for photosynthetic inhibition (Häder 1997).

An additional ecological effect of UV radiation differentiates eutrophic and oligotrophic lakes. This hypothesis is based on the fact that macrozooplankton (predators) migrate vertically towards the bottom during the day leaving a possibility for the small zooplankton (preys) to find refuge in the epilimnion (Kondratyev and Varotsos 2000). In oligotrophic lakes, UV radiation can penetrate the whole depth of the epilimnion and, hence, greatly diminish the refuge area for small zooplankton which are limited by the presence of the thermocline. In oligotrophic lakes, therefore, the damaging UV rays can be more harmful for small zooplankton than in eutrophic lakes.

21.3.2 Harmful Effects of UV on Microorganisms

The intensity of the radiation received at the surface of the earth varies according to the type of radiation due to their selective absorption by the ozone layer. Even when only 1% of the radiation reaching the earth's surface is composed of UV-B (due to absorption by the ozone, amongst others), small variations in the quantity of UV-B received can influence biological systems (Williamson 1995). A simultaneous increase in UV-B radiation and decrease in photosynthetically available radiation (PAR), for example, increases the harmful effects on organisms and decreases the primary production, respectively. Consequently, less carbon is captured through photosynthesis and more is released through respiration.

Genetic influences of UV on organisms can be either direct via DNA absorption of UV (formation of thymine dimers), or indirect via the formation of free radicals and subsequent alteration of DNA or other cellular constituents. Direct photochemical degradation of DNA is primarily related to the effects of UV-B and, therefore, increases abruptly below 320 nm (Bothwell et al. 1994).

UV radiation photobleaches cellular pigments (Hongve 1994). The damage caused to the photosynthetic equipment is less dependent on the length of the wavelength. It is equally affected by UV-A and UV-B (Hessen 2002). UV-A radiation can be beneficial through stimulating photoreparatory mechanisms as it can be detrimental through damaging the photosystem (Smith et al. 1992; Williamson 1995). The quantity of and the time of exposure to solar radiation are the primary factors influencing the carbon mechanisms in phytoplankton communities (Mousseau et al. 2000; Köhler et al. 2001).

The effects of UV go further than simple photoinhibition through damage to the pigments and the chloroplasts: the cell itself can be damaged or destroyed (Xenopoulos et al. 2000). Effects on the growth integrate effects undergone at different stages. A decrease in growth can be due to the effects on various physiological and photosynthetic processes. UV-A and UV-B affect the protists' (flagellates, ciliates) capacity to feed on bacteria. UV radiation can, therefore, influence the capacity of carbon transfer to higher trophic levels. Additionally, UV radiation can affect the motility and orientation functions of microorganisms (Häder 1997; Herndl et al. 1997; Kondratyev and Varotsos 2000).

UV radiation interacts with both DOM and microorganisms. However, the global effects of UV on large scale productivity are not as noticeable as those on decomposition. With this in mind, changes in carbon storage are primarily related to changes in decomposition and, therefore, to carbon release (Paul et al. 1999; Table 21.4).

Table 21.4. Review of the effects of different physico-chemical and biological parameters on photochemically formed GHG (i.e. produced or induced by UV)

Parameter	Emission of photooxidatively formed GHGs
Young DOM	+
Allochthonous DOM	+
Acidity	+
Presence of iron	+
Damaging effects of UV on phytoplankton	+
Damaging effects of UV on bacterioplankton	–

21.4 Photooxidation in Reservoirs

Thus far we have discussed the issue of photooxidation in natural aquatic environments being dependent upon a suite of physico-chemical (DOM, acidity) and biological (type of microorganism and the damaging effects of UV) parameters. In terms of hydroelectric reservoirs, it has been shown that following the period of changes caused by impoundment, these systems will act like natural lakes in terms of their water quality (Chartrand et al. 1994; Schetagne 1994), biological productivity (Chartrand et al. 1994; Hayeur 2001) and GHG emissions (Tremblay et al. Chap. 8). It is, therefore, logical to use our knowledge of natural lakes in order to grossly estimate the role of UV radiation in GHG emissions from reservoirs.

21.4.1 Vegetation

The color of a water body is a good indicator of its content in humic substances (Pace and Cole 2002). In boreal Québec, the waters are generally dark colored. This is due, amongst other reasons, to the presence of peatlands and the boreal forest, two environments that produce large quantities of humic substances (Payette and Rochefort 2001). The majority of large Canadian hydroelectric reservoirs (e.g. Gouin, Sainte Marguerite, La Grande, Laforge, Robertson) are influenced by this acidic type of vegetation. Acidity favors DOM mineralization to DIC, mainly through an increase in photooxidation (Anesio and Graneli 2003; Donahue et al. 1998; Gennings et al. 2001). Peatlands are rich in humic substances: they are considered to be carbon sinks (Blodau 2002). Photooxidation in reservoirs where peatlands were flooded allows for the degradation of a portion of organic matter (once dissolved) which would otherwise not be degraded.

21.4.2 Residence Time

The age of allochthonous DOM in a reservoir depends upon the residence time of the DOM in the reservoir. This time period can vary from a few days (La Grande 1, 15 days) to several months (Caniapiscau, 26 months) (Therrien et al. 2002). Reservoirs and large lakes with long residence times tend to have smaller quantities of DOM and a less pronounced coloration due to higher rates of photo- and biomineralization (Pace and Cole 2002). However, in these types of reservoirs the sedimentation of DOM is favored (Engstrom 1987), hence, diminishing the amount of dissolved material available for photooxidation.

21.4.3 Temperature and Ice

Freezing and thawing are likely to be important factors in Canadian hydroelectric reservoirs. This type of climatic influence changes the nature and the distribution of humic substances (Frimmel 1994; Belzile et al. 2002). Additionally, the combination of ice formation on the reservoir and the changes in water table levels and thermal expansion, facilitates the mechanical degradation of partially submerged trees prior to photochemical degradation. The action of the ice and the water level is most effective on trees whose tops are still above the water (and still rooted), hence, usually just a few years after the filling of the reservoir.

21.4.4 Estimate of the Rate of Photooxidation in Reservoirs

Current knowledge suggests that shallow tropical basins are more important sources of GHGs than the cold and deep basins of boreal reservoirs (WCD 2000). Regional differences may be attributed to several factors. In warm climates (tropical environments), biodegradation takes place at a higher rate than in colder regions. Additionally, CH_4 emissions from aquatic ecosystems and reservoirs are generally more important in tropical regions than in boreal regions. In fact, in boreal regions CH_4 fluxes stemming from aquatic systems are lower since the waters are mostly well oxygenated. The waters in tropical regions are often anoxic due to the higher water temperatures and the large quantity of dissolved and particulate organic matter (Duchemin 2000; Rosa et al. 2002). Anaerobic CH_4 production is, therefore, favored. Carbon dioxide is also produced from aerobic dissolved and particulate organic matter degradation and from oxidation of CH_4 (Rosa et al. 2002).

But what about GHG emissions related only to photooxidation? Firstly, photooxidation is a phenomenon which involves several variables (Doney et al. 1995). Although the portion of DOC which is photolabile is large, it is variable according to its location. Additionally, humic substances have poorly defined structures (Frimmel 1994), which further complicates the estimation of their photodegradation into CO_2. We also, still do not know the extent of biodegradation following the production of low molecular weight molecules by UV radiation. Coagulation/flocculation of DOM is another mechanism which favors DOM loss, but whose importance is unknown and seemingly variable (Molot and Dillon 1997). Other factors such as cloud cover, the thickness of the ozone layer, the depth of the water column, etc., can also greatly influence the estimation of photochemical mineralization of DOM (Vähätalo et al. 1996).

Despite the different interactions, it is possible to use indicators in order to estimate the rate of photooxidation. Zika (1990) suggested using hydrogen peroxide (H_2O_2) as an indicator. The presence of H_2O_2 testifies to the photooxidation of DOM; it is a by-product of the reaction. The potential photoreactivity of a natural lake or reservoir may also be estimated by measuring the concentration and the rate of production of H_2O_2. Meanwhile, even if the majority of the H_2O_2 comes from photooxidation, a small fraction is also produced by biological activity and atmospheric deposition (Zika 1990).

Herein, we have attempted to grossly estimate the size of CO_2 fluxes originating from photochemical processes (Table 21.5). In order to calculate total CO_2 fluxes, the surface area of the water body was multiplied by the unitary CO_2 flux (measured as mg $C{\cdot}m^{-2}{\cdot}d^{-1}$). The flux of photoproduced CO_2 was calculated in the same manner but using a unit of flux of photoproduced CO_2 of 75 $mgC{\cdot}m^{-2}{\cdot}d^{-1}$, a mean taken from Granéli et al. (1996). The authors measured photooxidation rates in 5 boreal lakes with different concentrations of humic substances. Photooxidation rates varied between 44.3 and 171.1 $mgC{\cdot}m^{-2}{\cdot}d^{-1}$, depending on the lake. The estimated values of photoproduced CO_2 fluxes, implies certain simplifications of the processes and causes. Firstly, we consider a homogeneous water column, implying that the same processes occur both in the centre and at the margins of the lake or reservoir, when in reality spatial variability exists. In addition, the flux of photoproduced CO_2 is estimated using a unitary value which is the same for all lakes and reservoirs, when in reality variability is to be expected between lakes and reservoirs according to latitude, altitude, physico-chemical parameters, environmental variables, etc. Nonetheless, these estimates underline the important role photooxidation plays in GHG emissions from aquatic environments.

Table 21.5 Estimates of total CO_2 fluxes and CO_2 fluxes stemming uniquely from photooxidation ($Gg{\cdot}d^{-1}$), emitted from the total surface of several lakes and reservoirs in Quebec and Ontario

Lake/Reservoir	Surface Area [km^2]	Unit CO_2 Flux[a] [$mgC{\cdot}m^{-2}{\cdot}d^{-1}$]	Total CO_2 Flux [$Gg{\cdot}C{\cdot}d^{-1}$]	Photoproduced CO_2 Flux[b] [$Gg{\cdot}C{\cdot}d^{-1}$]
Lake Superior	82100	271	22	6.2 (28%)
Lake Michigan	57800	271	16	4.3 (28%)
Lake Huron	59600	271	16	4.5 (28%)
Lake Erie	25700	271	7	1.9 (28%)
Lake Ontario	18960	271	5.1	1.4 (28%)
La Grande 3 reservoir	2420	449	1.1	0.18 (17%)
La Grande 3 reservoir (before flooding)	245	449	0.11	0.018 (17%)
Lake Mistassini	2335	271	0.63	0.18 (28%)
Manic 5 reservoir	1806	419	0.76	0.14 (18%)
Manic 5 resevoir (before flooding)	377	419	0.16	0.028 (18%)
Gouin reservoir	1357	224	0.30	0.10 (33%)
Lake à l'Eau-Claire	1383	271	0.37	0.10 (28%)
Lake Bienville	1249	271	0.34	0.094 (28%)
Lake St. Jean	1003	271	0.27	0.075 (28%)
Pipmuacan reservoir	802	512	0.41	0.060 (15%)
Sainte-Marguerite 3 reservoir (< 10 yrs)	252	1218	0.31	0.019 (6%)
Average typical lake	15	271	0.0041	0.0011 (28%)

[a] measured in the field for reservoirs (Therrien et al. 2004). An average of 271 $mgC{\cdot}m^{-2}{\cdot}d^{-1}$ was used for lakes, based on measurements taken in the Côte Nord of the James Bay. All fluxes are in $mgC{\cdot}m^{-2}{\cdot}d^{-1}$.
[b] Estimated from a photooxidation rate of 75 $mgC{\cdot}m^{-2}{\cdot}d^{-1}$ (mean from Granéli et al. 1996; Table 21.5); in parenthesis: percentage of the total CO_2 flux.
Source (for the aerial surfaces): Statistics Canada 2003; Hydro-Quebec 2002.

Following the physico-chemical transition period (10 years after flooding), the principal factor explaining the larger portion of GHG produced in reservoirs relative to lakes is their larger surface area. For example, La Grande 3 produces 10 times more GHG since impoundment, uniquely due to the increase in size (for comparison, the calculation of the total CO_2 flux for the period prior to flooding was made with the same value per unit surface area of 449 $mgC{\cdot}m^{-2}{\cdot}d^{-1}$; Table 21.5). Comparatively, Lake Superior produces 20 times more CO_2 than La Grande 3 after impoundment, and 200 times more than La Grande 3 prior to flooding despite a lower unit flux of 271 $mgC{\cdot}m^{-2}{\cdot}d^{-1}$. Additionally, the Sainte-Marguerite 3 reservoir,

which has the highest fluxes per unit of surface area (1218 $mgC \cdot m^{-2} \cdot d^{-1}$), produces less CO_2 over the total surface area than the other reservoirs. Following these initial estimates, photooxidation would account for between 6 and 28% of the total emissions of CO_2 according to the water body (Table 21.5). Fluxes of photoproduced CO_2 are likely underestimated in young reservoirs (<10 years) such as Sainte-Marguerite 3, where there is an important input of organic matter.

21.5 Conclusion

Ultraviolet radiation (UV) could play an important role in the emission of greenhouse gases (GHGs) such as carbon dioxide (CO_2) and carbon monoxide (CO). Photooxidation products result from the interaction of photochemical, biological and physical processes (Mopper and Stahovec 1986). In aquatic environments, GHG production depends more particularly on the content of DOM and biological production.

Dissolved organic matter reactivity can differ when exposed to UV radiation as a result of both its age and the origin of the DOM. Dissolved organic matter photooxidation produces both lower molecular weight compounds which are more biodegradable, and volatile products such as CO_2 and CO. Ionic conditions play a role in photooxidative reactions.

The effect of UV radiation on the emission of GHGs is not straightforward since UV also affects aquatic microorganisms in a varied manner. UV radiation physically affects microorganisms: photosynthetic carbon fixation decreases and respiration increases with exposure to strong UV radiation. However, the degradation from UV of DOM into lower molecular weight compounds increases the availability of nutrients and favors microbial mineralization.

Microbial mineralization stimulation by UV combined with photomineralization of DOM and the inhibition of algal productivity by UV, can result in a net decrease in carbon accumulation and can change the ecosystem balance between respiration and production (Bertilsson and Tranvik 2000; Eriksson III et al. 2000; Granéli et al. 1996, 1998; Morris and Hargraeves 1997). Dissolved organic matter photodegradation will increase carbon fluxes from aquatic ecosystems to the atmosphere (Granéli et al. 1998). UV radiation, therefore, plays an important, if not principal, role in the loss of total organic carbon from aquatic ecosystems (Gennings et al. 2001).

Reservoirs are similar to lakes in terms of their water quality, biological production and GHG emissions 10 years after impoundment (Schetagne

1994; Therrien et al. 2002). In the short-term, the production of dissolved inorganic carbon (DIC) and GHGs is amplified by the flooding of the forests and the consequent dissolution of organic matter and lignin. The difference that is observed when comparing total emissions is mostly attributable to the difference in aerial coverage. The rate of photooxidation in reservoirs depends, in part, upon the type of vegetation that has been flooded, the age of the DOM and the temperature of the water. According to a first estimate, photooxidation can contribute between 6 and 28% to the total GHG emissions stemming from aquatic ecosystems. When measuring net emissions from hydroelectric reservoirs and natural lakes one should, therefore, account for photooxidation processes.

22 Impact of Methane Oxidation in Tropical Reservoirs on Greenhouse Gases Fluxes and Water Quality

Sandrine Richard, Philippe Gosse, Alain Grégoire, Robert Delmas and Corinne Galy-Lacaux

Abstract

This chapter presents a summary of water quality data (physico-chemical) from 10 years of measurements in the Petit Saut hydroelectric reservoir in French Guiana. Methane oxidation in and downstream of the reservoir are of particular interest. In the first part of the paper we discuss both the primary factors influencing the water quality and the patterns of stratification, methane production and oxidation in the reservoir. Secondly, we present data of methane emissions and oxidation downstream of the dam. We demonstrate that the oxidation of the dissolved CH_4 was a major oxygen consumer downstream of the dam. The results indicate that the aerating weir built in the plant outlet canal guarantees the minimum regulatory concentration of 2 $mg{\cdot}L^{-1}$ of dissolved oxygen as delineated by the scientific community of Petit Saut, following observations of the resistance to hypoxia in a tropical environment. This long term database, which helped in detecting changes over time (dissolved gases concentrations, CH_4 oxidation velocity) will be used to improve the models developed to simulate both water quality and greenhouse gas emissions in a tropical reservoir environment.

22.1 Introduction

There are many large hydroelectric reservoirs located in tropical zones (Table 22.1). The corresponding impact studies must take into account the

Table 22.1. Characteristics of some tropical reservoirs

Reservoir	Country	Impounding of the reservoir	Volume km^3	Reservoir Area km^2	Residence time month	Installed capacity MW	Vegetation Type	Flooded biomass Mg C ha^{-1}
Ayamé I	Ivory Cost	1959	0.9	180	8.7	22	Dry Forest	170
Brokopondo	Surinam	1964	24	1600	26	180	Rain Forest	270
Buyo	Ivory Coast	1980	8.3	895	8	220	Rain Forest	270
Nam Gnum	Laos	1968	7	390	9	135	Dry Forest	200
Nam Leuk	Laos	1999	0. 2	13	6	39	Dry Forest	200
Petit Saut	France	1994	3.5	365	6	116	Rain Forest	270
Theun Hinboun	Laos	1998	0.02	6	< 0.1	210	Dry Forest	200
Tucurui	Brazil	1985	45.5	2875	1.7	3960	Rain Forest	300
Taabo	Ivory Coast	1979	0.6	69	2	220	Forest-Savannah	160

complexity and the fragility of the ecosystems of these regions, often covered by forests.

The vegetation biomass of a tropical rainforest can be dense, at Petit Saut reservoir studied in French Guiana (South America), it was estimated at 270 T(C) ha^{-1}. Field measurements conducted on this reservoir since its impoundment in 1994 confirm that a tropical reservoir can be a significant source of carbon dioxide (CO_2) and methane (CH_4) due to the decomposition of this vegetation (Gagnon and Chamberland 1993; Svensson and Ericson 1993; Rosa and Shaeffer 1994; Galy-Lacaux et al. 1997a and b; Gosse et al. 2000).

The water quality results at Petit Saut – which are presented hereunder – highlight the influence of methane which was responsible for a high oxygen consumption in the whole hydrosystem, including both the reservoir and the river downstream of the dam. The main consequence for the management of the power station was the accentuation of the deoxygenation observed from the beginning of the filling in the Sinnamary River downstream of the dam (Gosse and Grégoire 1997; Richard 1996). Electricité de France decided in September 1994 to build an aerating weir with two drops in the plant's tailrace canal, in order to bring atmospheric oxygen into the river and to emit into the atmosphere a high proportion (around 80%) of oxygen-demanding dissolved methane. Operational since March 1995, the weir has enabled the power station to function continuously, while guaranteeing a minimum dissolved oxygen (DO) concentration of 2 mg L^{-1} in the downstream Sinnamary (Gosse et al. 2000; Richard et al. 2003).

22.2 Site and Measurement Descriptions

22.2.1 The Example of the Petit Saut Reservoir and the Downstream River

The Petit Saut dam is located on the Sinnamary River in French Guiana (5°03 N, 53°02 W) (Fig. 22.1). It was constructed in the humid tropical forest by EDF's (Electricité de France) National Centre for Hydroelectric Engineering (CNEH). January 1994 marked the beginning of the filling phase. Full supply level, 35 m ASL (above sea level) in depth, was reached in June 1995; the reservoir stretches across approximately 365 km^2 of inundated primary forest and has created 105 km^2 of small islands. Its total storage capacity is 3500 10^6 m^3, useful storage is between 35 and 29.5 m ASL in depth, the minimum operating level. The total amount of flooded

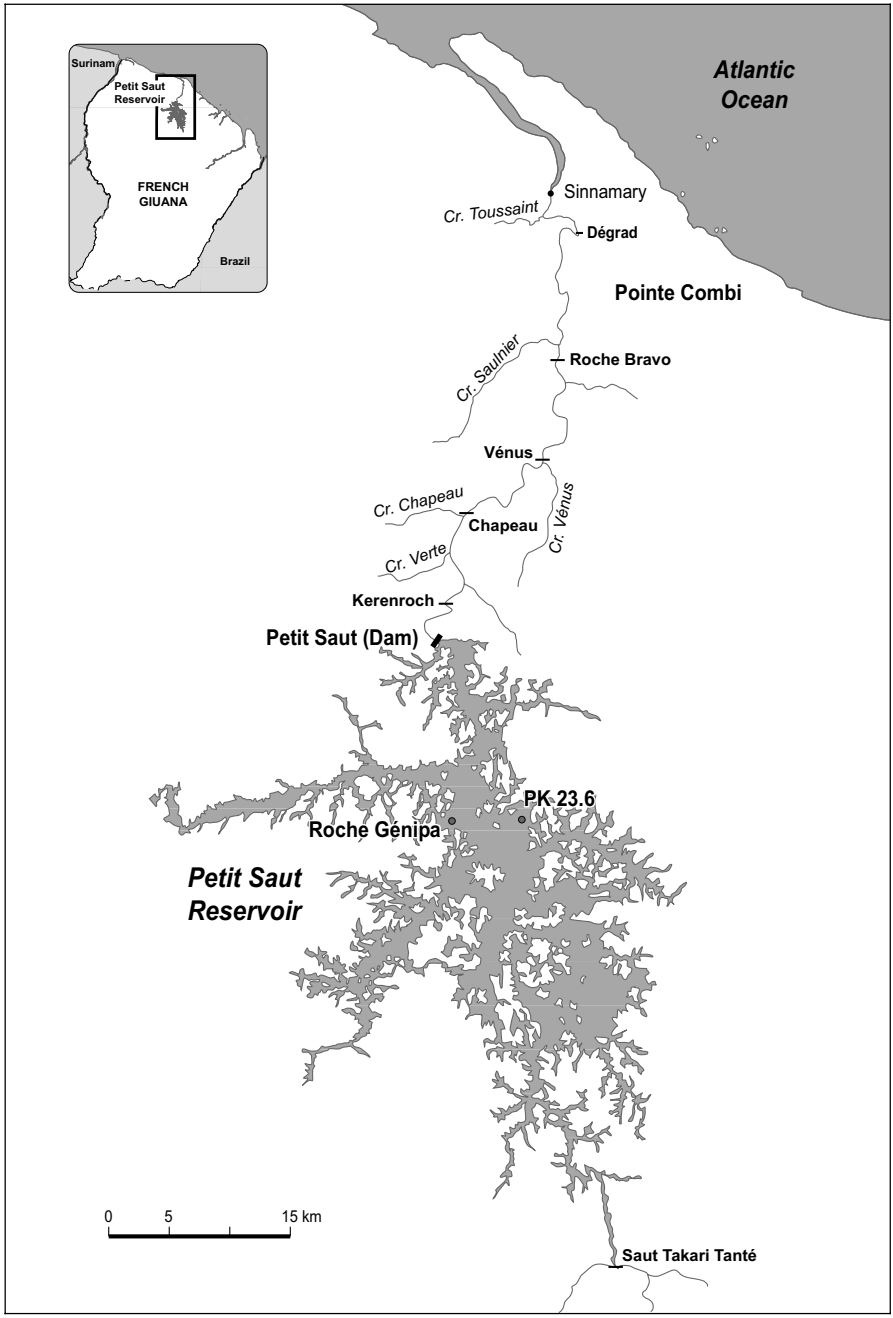

Fig. 22.1. Location of the main measurement stations in the Sinnamary drainage basin (French Guiana)

biomass, including aboveground vegetation (170 T(C) ha^{-1}) and soil (100 T(C) ha^{-1}), is around 10 million tons of carbon. The average flow of the Sinnamary River at the dam site is close to 265 $m^3 \cdot s^{-1}$. The retention time is approximately 6 months (Sissakian 1992). The installed capacity is 116 MW generated by four 29 MW turbine units. For this dam, the ratio between installed capacity and inundated area is therefore 0.32 MW per km^2 corresponding to 11.6 MW per MT of carbon. In 1995, an aerating weir was built in the plant tailrace canal in order to improve air-water gas exchanges and to increase the oxygen content in the Sinnamary River (Gosse and Grégoire 1997; Gosse et al. 1997).

22.2.2 Measurements

Profiles of physico-chemical characteristics in the water column were measured since the impounding of Petit Saut (around 25 parameters such as conductivity, pH, redox potential, temperature, mineral composition, dissolved organic carbon, total organic carbon, metals…). Additional campaigns were also conducted in 1995 on three reservoirs in the forested region of southern Ivory Coast (Buyo, Taabo and Ayame) Galy-Lacaux et al. 1999), and in 2001 and 2002 in East Asia (Laos) (Richard 2001a and 2002; Richard and Zouiten 2001). The average characteristics of Petit Saut (water flow and residence time, type of vegetation) compare quite well with those of some African and Asian reservoirs (Table 22.1).

Dissolved gas concentrations (CH_4 and CO_2) were measured by the headspace technique in samples taken at various depths (MacKay and Shiu 1981). Analyses of gas concentrations were performed by gas chromatography using a flame ionization detector for CH_4 and a thermal conductivity detector for CO_2. Commercial standards with various concentrations adapted to the type of measurements were used for calibration. The reproducibility of the standards for each set of analyses was greater than 95%.

Since the beginning of 1998, vertical profiles of dissolved oxygen and methane concentrations are regularly measured once or twice a month at a station located in the reservoir axis at 20 km from the dam (Roche Génipa), in order to follow the long-term evolution of these parameters.

Downstream, three stations are investigated: the turbines, the weir (downstream) and Pointe Combi (40 km downstream of the dam).

22.3 Water Quality and Methane Oxidation in the Reservoir

The chemical and biochemical processes taking place at high temperatures in the lower layers of a tropical reservoir, in relation to the decomposition of the submerged biomass, leads to the formation of greenhouse gases (CH_4, CO_2, H_2S, etc). The consumption of oxygen resulting from these phenomena can maintain the lower layers of the lake in a permanent anoxic state, at least during the first few years after impounding. The thickness of the oxygenated surface layers may be reduced for several years (Fig. 22.2), despite the reoxygenation by atmospheric air or by phytoplankton photosynthesis.

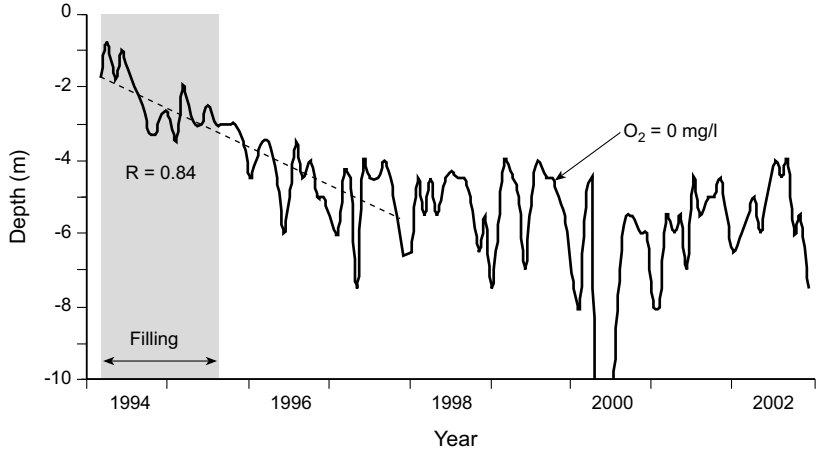

Fig. 22.2. Oxycline position in Petit Saut reservoir since impoundment

22.3.1 Stratification and General Water Quality

During the filling phase of Petit Saut reservoir (18 months), a stratified lake was formed in which the oxygenated upper layer gradually increased in thickness from less than 1 m at the beginning of the impoundment to close to 7 m, 5 years later. The level of oxygen remained undersaturated at the surface, never exceeding 4 mg L^{-1} during the first five months; later, conditions improved and saturated oxygen was progressively measured (8 mg L^{-1}) in the surface layer. High levels of dissolved oxygen are found during the dry season, when there is a maximum amount of sunlight and a high level of photosynthesis.

The water column is still characterised by the complete absence of oxygen in the hypolimnion. This phenomenon appeared within 10 days after filling began and has continued with varying intensity. Temperature profiles show that the reservoir remains stratified almost throughout the year (Richard 1996; Richard et al. 1997 and 2000). We saw a partial destratification in May 2000, due to a major rise in the river discharge (around 3000 $m^3 \cdot s^{-1}$).

From upstream to downstream in the reservoir, we can observe a longitudinal succession with a river zone, a transition zone and a lacustrine zone.

For all the parameters, a vertical gradient is only observed in the transition zone, the lacustrine zone, the axis of the lake (old river bed) and the coastal zones, because of the existence of a gradient between the bottom and the top of the lake. In the river zone, the water quality is the same as in the river but most of the vegetation is flooded at high water level. The transition zone is characterised by the presence of low concentrations of dissolved oxygen in the whole water column, and in the lacustrine zone, stratification is observed throughout the year with an oxygenated epilimnion (surface) and an anoxic hypolimnion (bottom). The measurements stations are mainly in the lacustrine zone.

This stratification was observed in several reservoirs located in South America: Brokopondo in Surinam (Leentvaar 1967, 1973, 1984 et 1993; Heide 1982), Samuel (Matsumara-Tundisi et al. 1989; Falotico 1993; Tundisi 1989; Figueiredo et al. 1994), Tucuruí (Champeau et al. 1986; Froehlich et al. 1993; Peireira 1994; Figueiredo et al. 1994), Curuá-Una (Junk et al. 1989; Darwish 1982) and Balbina in Brazil (Fearnside 1989; Eletronorte 1992 and 1993; Froehlich et al. 1993; Figueiredo et al. 1994). We observed the same type of stratification in Nam Leuk located in Laos (Richard 2001a and 2002; Richard and Zouiten 2001).

The high mean retention time (6 months at Petit Saut) maintains the thermal stratification (Darwish 1982). The large size of the reservoir has prevented the homogenisation of the whole water column. The hypolimnion is anoxic and enriched by the permanent diffusion of compounds due to organic degradation (i.e., ammonium, phosphate, dissolved organic carbon, methane) and matter released from the geological substrate (iron, manganese, silicon).

Conductivity can be selected as an indicator of the state of the reservoir. The mean conductivity (22 to 75 $\mu S \cdot cm^{-1}$), since the start of the filling phase, has shown a general trend of enrichment, reaching its maximum level during the period from October 1994 to February 1995 (Fig. 22.3). The mineralization observed is very high, compared with other reservoirs

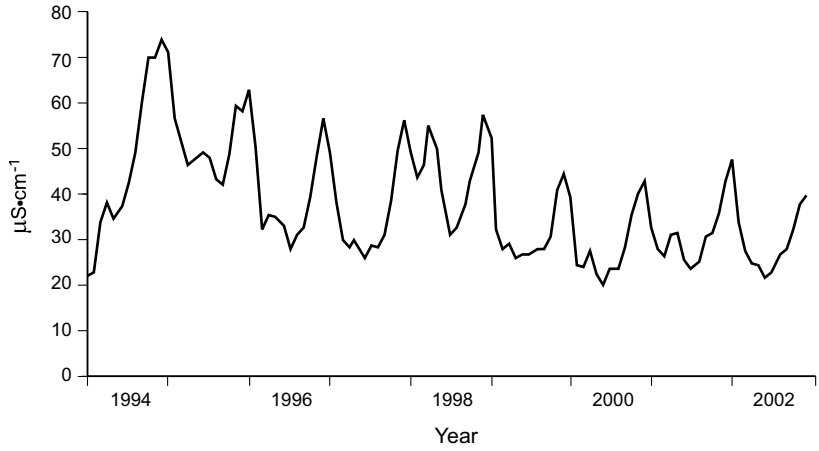

Fig. 22.3. Average conductivity ($\mu S \cdot cm^{-1}$) in the water column of Petit Saut reservoir (central part) since impounding (time origin = January 1994)

like Samuel with a maximum of 45 $\mu S \cdot cm^{-1}$ (Falotico 1993), Balbina with a maximum of 50 $\mu S \cdot cm^{-1}$ (Eletronorte 1993; Froehlich et al. 1993) and Curuá-Una where the conductivity is less than 30 $\mu S \cdot cm^{-1}$ (Darwish 1982; Junk et al. 1981). Following this period of maxima the values became more moderate. The enrichment was observed during each dry season, and from January through March 1998 due to exceptional climatic conditions associated with *El Niño* . The values reflect the opposing forces of production and variable dilution induced by rainfall. The bottom of the reservoir shows a high level of degradation. In the water column itself, a gradient between the bottom and the top of the lake is the result of dilution and bacterial consumption phenomena (Fig. 22.4) (Richard 1996; Richard et al. 1997). The values from the other reservoirs are substantially lower and could be explained by a difference in the period or the location of measurement level. We note, however, that their hierarchy corresponds to the ranking of the lakes according to the general organic matter retention times, as defined above.

The higher mineralisation at the bottom of the lake depends not only on production, but also on the dilution capabilities of the environment and the quantity of water capable of ensuring it. It is therefore related to the inflows of water that vary over time. The accumulation and decomposition of organic waste on the bottom lead to a modification in the physicochemical quality of the environment and its reactive capacities.

The pH decreased as soon as impounding began. This decrease is linked to the dissolving of the humic acids in the organic matter decomposed by

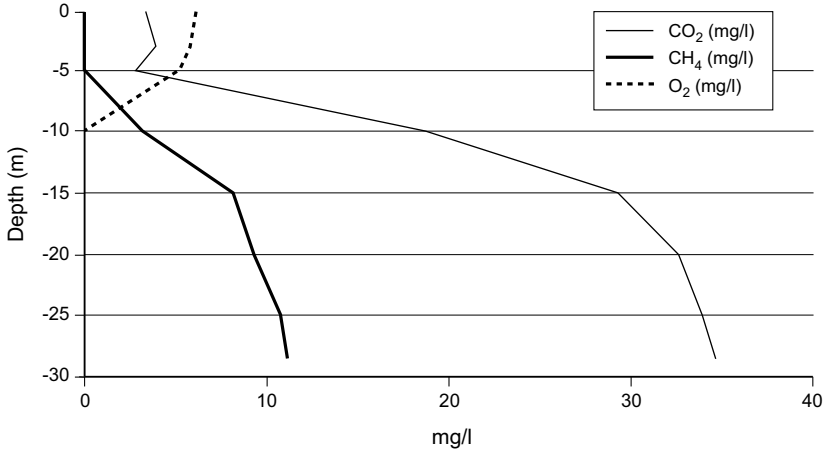

Fig. 22.4. Vertical profiles of dissolved oxygen, dissolved methane and carbon dioxide in Petit Saut reservoir in January 2002

respiration. Before the impounding, the mean value was 6.3. In the anoxic layer the mean value is around 5.6 in the reservoir of Petit Saut. At Brokopondo, most of the measurements range between 5.4 and 5.8 (Heide 1982), values in agreement with those found at Petit Saut.

At the base of the water column, the redox potential reaches low values, mostly inferior to 100 or 50 mV and can, in certain circumstances, be negative. Redox potential is lower in the sediments. Concentrations of hydrogen sulphide have also been measured, with a maximum of 50 $\mu g \cdot L^{-1}$ at the bottom in December 1994 (Lacaux et al. 1994a, b and 1995) and lower concentrations later (Dumestre 1998).

In the bottom layers of the reservoir, the high ammonium values correlated with the conductivity and the mean retention time and are an expression of the anaerobic decomposition process. The concentrations of ammonium measured at Petit Saut are close to those observed at Balbina (Electronorte 1993; Froehlich et al. 1993; Richard 1996).

The orthophosphate concentrations found at Petit Saut (maximum 3 $\mu molP \cdot l^{-1}$) are the same as those found at Balbina (Eletronortre 1993). Falotico (1993) mentions maximum values of 0.4 $\mu molP \cdot l^{-1}$ at Samuel, or 10 times less. The total phosphorus reached 12 $\mu molP \cdot l^{-1}$ at Petit Saut, and did not exceed 3 $\mu molP.l^{-1}$ at Curuá-Una (Darwish 1982).

Given the anoxia on the bottom, the absence of nitrates and the very low sulphate concentrations, the role of electron acceptors necessary for biochemical degradation reactions is dominated by the metals with different degrees of oxidation, such as ferrous and manganitic derivatives (De Groot

1991). This reduction results in more soluble derivatives whose accumulation is favoured not only by the changing redox balance, but also by the acidification of the environment. The phenomenon is even more perceptible when anoxia conditions are accentuated by the increase of the water retention time or the increase of the organic matter retention time. The results obtained at Curuá-Una (Darwish 1982) are mostly at the limit of detection. No metal dosing was carried out at Samuel (Falotico 1993). At Balbina, Fe^{2+} and Fe^{3+} concentrations were analyzed (Eletronorte 1993), with values reaching 11.3 $mg{\cdot}L^{-1}$ for the Fe^{2+}, like at Nam Leuk with 14 $mg{\cdot}L^{-1}$, concentrations in the same range as those measured at Petit Saut.

The mobilization of the other components of the lateritic mineral substrate (Si, Al) is not directly linked to the redox potential modifications, but is highly dependant on the pH, whose values are very close to the range of insolubility for the hydroxides corresponding to these elements. They therefore only participate in a very small manner in the mineralization of the bottom water.

22.3.2 Methane Production and Oxidation in the Reservoir

In Petit Saut reservoir, methane is produced in the sediment and probably in the water column (Dumestre 1998). Average concentrations of dissolved methane were calculated from profiles, with a linear interpolation between experimental points usually located at 0, 3, 5, 10, 15, 20, 25 and 30 m of depth. Methane concentrations increased during the first months of reservoir impounding up to a maximum average value in the water column of 14 $mg{\cdot}L^{-1}$ in the central part of the reservoir in May 1995, with a maximum of 24 $mg{\cdot}L^{-1}$ at the bottom of the reservoir. At the same time, the oxygen concentration in the surface layer was undersaturated and lower than 4 $mg{\cdot}L^{-1}$. Then periodical variations were observed. They are correlated with water flow variations in the reservoir inducing changes in the accumulation of dissolved gases (Galy-Lacaux 1996; Galy-Lacaux et al. 1997a and b). In French Guiana, the rainy season extends from December to July and the dry season from August to December.

After May 1995, the first minimum value of the mean dissolved methane concentration was observed in September 1995 (8.6 $mg{\cdot}L^{-1}$), followed by a maximum in January-February 1996 (13 $mg{\cdot}L^{-1}$). The following minimum value was observed in April 1996. From December 1996 to January 1997, the average methane concentration was at a maximum of about 10 $mg{\cdot}L^{-1}$. From April-June 1997, methane profiles indicated a sharp decrease in the average concentration in the reservoir reaching the lowest

value ever observed (around 1 $mg{\cdot}L^{-1}$). This minimum should be interpreted in light of the peculiar hydrology of the reservoir. It corresponds to a period of exceptionally high rainfall. Then after June 1997, concentrations increased slightly again and were equal to about 2 $mg{\cdot}L^{-1}$ in August 1997. Later, an enrichment was observed each dry season, with two exceptional climatic events: in 1998 El Niño (a dry season within the rainy season), and in 2000, a major rising of the river (around 3000 $m^3{\cdot}s^{-1}$) (Fig. 22.5) (Richard et al. 2000).

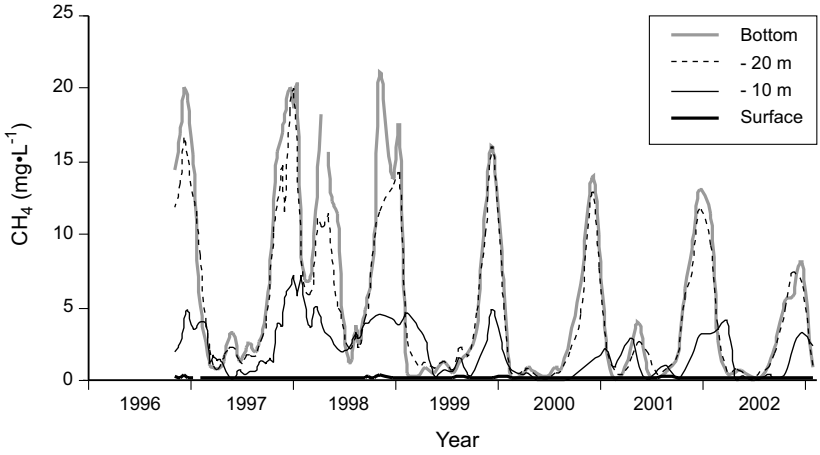

Fig. 22.5. Dissolved methane in Petit Saut reservoir (central part)

Using the 1994-1995 measurements and a vertical profile of methane measured in a comparable African reservoir which was 17 years old when it was sampled, an equation was proposed in 1996 to represent the evolution of average CH_4 concentration in the water column of Petit Saut reservoir (near the dam) over the first 20 years:

$$C(t) = [10.5 + 3.5 \cos(2\pi/12)t] \exp^{-0.015t}$$

where C(t) is the dissolved methane in $mg{\cdot}L^{-1}$ and t is the time expressed in months (Fig. 22.6) (Galy-Lacaux et al. 1999). It is a rather acceptable formulation for the 1994-2002 period, when considering the methane fluxes in the water released by the dam (see Chap. 22.4.3). We observed a decrease in CH_4 in March 1995 in the surface layer, due to its oxidation, in relation to the development of a high quantity of methanotrophic bacteria. These bacteria managed to stop definitely the diffusive methane emissions towards the atmosphere, with an associated significant consumption

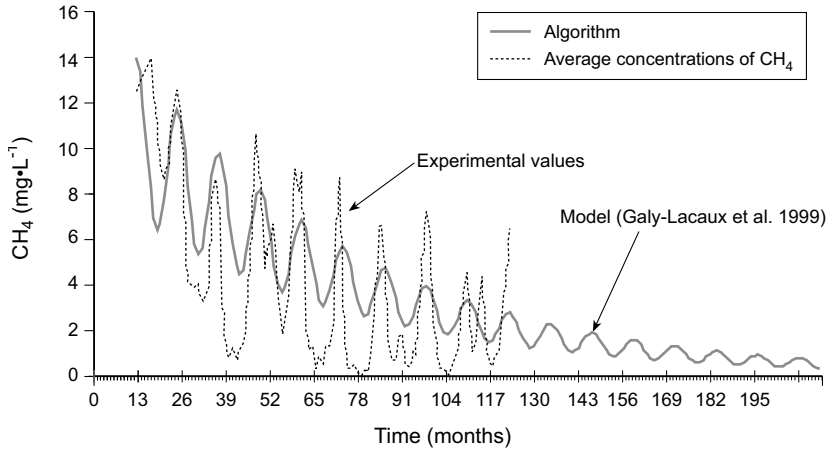

Fig. 22.6. Comparison between measured and predicted average concentrations of dissolved methane in the water column of Petit Saut reservoir (central part) since impoundment

of dissolved oxygen at the oxycline level (Dumestre 1998). In December 1995, Dumestre measured a very high velocity – 0.27 $mgCH_4 \cdot L^{-1} \cdot hour^{-1}$ – of methane oxidation at depth – 4 m, which is a level of consumption much higher than previous published data (Dumestre 1998). Excessive illumination seems to have inhibited the growth of the methanotrophic bacteria during the first year after the beginning of filling (Dumestre et al. 1999a and b). The increase in the thickness of the surface oxygenated layer (less than 50 cm in 1994) following a decrease in other more classical oxidation processes progressively alleviated the effect of light when it reached 2m at the end of 1994. Furthermore, the deepening of the oxycline offered more space for the development of methanotrophic bacteria which are aerobic under the oxycline, the accumulation of methane occurs during the dry season. It was roughly assessed that the dissolved oxygen consumption in the reservoir between 1995 and 1997 was around 0.3 $Tg \cdot year^{-1}$, including methane oxidation (which played a role from the second semester of 1994), activity of more classical bacteria (which started beginning of 1994), phytoplankton respiration and chemical consumptions (such as the transformation of Fe^{2+} in Fe^{3+}).

A rather close relationship between methane concentrations and carbon dioxide is observed in the hypolimnion of Petit Saut reservoir (Fig. 22.7). When CH_4 is equal to zero, the concentration of CO_2 is around 13 $mg \cdot L^{-1}$. This is the concentration close to that measured in flowing water in French Guiana rivers (around 20 $mg \cdot L^{-1}$).

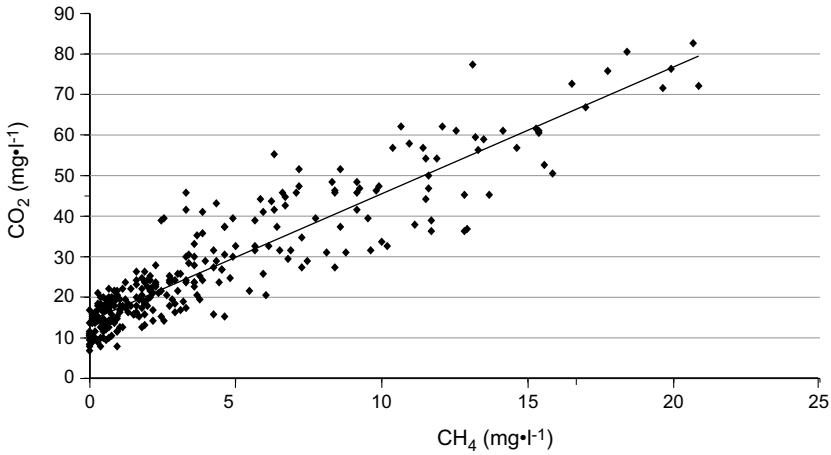

Fig. 22.7. Relationship between dissolved methane and carbon dioxide in the hypolimnion (1998-2001) $(CO_2) = 3.152(CH_4)+14.32$ r = 0.92

Deoxygenation has also occurred, for example, in the reservoirs of Brokopondo, Nam Gnum and Ayamé, where, during the first years after their creation, the water bodies were of very poor quality (Heide 1982). They now have an epilimnion roughly fifteen meters thick that is well oxygenated and devoid of methane (Galy-Lacaux et al. 1999; Richard et Zouiten 2001).

22.3.3 Principal Factors Influencing Water Quality

The quality and quantity of submerged vegetation are also important factors in explaining the evolution of water quality. Hence, compared with Petit Saut, where the flooded vegetation is a "moist" type primary tropical forest, at Nam Leuk and Nam Gnum, it is the "dry" type with notably little leaf litter. At the Laotian sites a partial recuperation at the end of the rainy seasons is typical. Even more so, when reservoir is built in regions of savannah at these same latitudes, like at Taabo, the water quality problems are much less severe (Table 22.2). If the easily degradable forest litter, leaves and herbaceous plants provoke a rapid anoxia in the bottom layers, the tree trunks resist degradation for many long years. Junk and Nunes de Mello (1987) give degradation times between 10 and 100 years. Lake Brokopondo, 39 years after its impoundment, still has tree trunks in place, as does Nam Ngun impounded in 1968. The quality of the organic matter to be degraded is, therefore, an important factor that affects water quality, as well as the quantity of carbon. Hence, the consequences will be different if we flood a tropical primeval forest or a savannah.

Table 22.2. Average concentration of dissolved CH_4 on the vertical in different tropical reservoirs (close to the dam)

Reservoir	Age years	Sample date	Season	Average CH_4 concentration (mg L^{-1})
Buyo*	15	Dec.-95	Beginning of dry season	0.34
Ayamé*	36	Dec.-95	Beginning of dry season	0.38
Nam Ngum**	34	Apr.-01	End of dry season	0.10
Nam Leuk**	2	Apr.-01	End of dry season	7.57
Nam Leuk**	2	Sept.-01	End of dry season	2.43
Nam Leuk***	2	Avr.-02	End of dry season	0.72

* C. Lacaux et al. (1999)
** Richard (2001a and b, 2002)
*** Richard (2002)

The availability and the renewal of dissolved oxygen is what will mainly determine the water quality in the reservoir (Goodland 1979; Tundisi 1988; Fearnside 1989). At Tucuruí, where the retention time is one month, the water quality remains acceptable. Stratification of the central zone only takes place during low flow periods. During this period, the hypolimnion is anoxic. During the rainy season, the whole water body in the central zone is oxygenated and the bottom layers in the littoral zone remain anoxic (Pereira 1989 and 1994). At Curuá-Una where the renewal time is low (1 month), Darwish (1982) carried out a surveillance program from November 1977 to May 1978. The most unfavourable station presented oxygenation conditions from the surface to the bottom during the last two months of the study, but the concentrations remained low (0.5 mg L^{-1}). Junk et al. (1981) indicated that the stratification of Curuá-Una was not pronounced, and no oxygen was present at the surface during their measurements. Amazonian reservoirs in general don't present marked temperature gradients on the vertical, but this doesn't make the thermocline more fragile, as the temperatures are high.

Junk et al. (1981) and Darwish (1982) indicated that 63% of the dissolved oxygen in the Curuá-Una reservoir had come from surface diffusion, 27% from the upstream tributaries and 10% from primary production. At Petit Saut, it was assessed that, between 1995 and 1997, the oxygen input into the reservoir was around 0.3 Tg $year^{-1}$, with rather comparable fluxes from primary production and surface diffusion (0.1-0.15 Tg $year^{-1}$) and a flux of 0.05 Tg $year^{-1}$ from upstream tributaries (Gosse et al. 2000). It is important to note that the presence of dissolved oxygen in the epilimnion not only depends on the primary production, wind, currents and

aeration, but also on the reservoir's morphology and the amount of water flowing into the lake. An hypolimnion, rather independent from the epilimnion (the oxygen does not diffuse), can persist in case of a moderate renewal by inflows from the tributaries, as occurs in the central part of Petit Saut reservoir where there is an absence of total destratification. The permanence of the stratification is shown by Heide (1982) at Brokopondo. This author also attributes this absence of mixing to the presence of flooded trees that impede the action of the wind. Manosowski (1986) and Paiva (1977) have also demonstrated this phenomenon. These conditions can favour the development of macrophytes that may react, in turn, to the influence of the wind and the circulation of water.

The retention time of waters in the reservoir is an essential parameter in the comprehension of the phenomena occurring in reservoirs, but it is important to associate it with other parameters such as reservoir morphology and bathymetry, and spatial circulation and turbulence in the different zones of the lake. The Petit Saut reservoir, like all of the Amazonian reservoirs, is heterogeneous. It is made up of zones with variable retention times, averaging 6 months for the whole of the reservoir. Certain zones have long renewal times (up to 14 months at Crique Aimara and 27 months at Crique Bonne Nouvelle, according to Sissakian 1992). Even though each zone may react in a different manner, the depth of the epilimnion appears to be rather uniform spatially. It should be noted that the dendritic pattern of reservoirs affects the circulation and the renewal of water. The passage of water coming from tributaries takes place in a preferential manner in the axis of the former riverbed. This phenomenon is also described by Leentvaar (1966) and Heide (1982) at Brokopondo. At Theun Hinboun, the intense renewal of the water body does not lead to dissolved oxygen problems in the reservoir, 3 years after its creation, despite an initial biomass in the reservoir area (identical to Nam Leuk).

On the basis of carbon production measurements performed by Vaquer et al. (1997), the input of carbon by phytoplankton growth was close to 0.03 Tg $year^{-1}$ in Petit Saut reservoir (Gosse et al. 2000). It is comparable to the organic part (0.02 Tg $year^{-1}$) of the poorly labile carbon flux coming from the upstream tributaries and ten times lower than the gaseous emission of carbon (CH_4 and CO_2) to the atmosphere assessed by Galy-Lacaux et al. (1997) for the 1994-1997 period. This shows the importance of carbon production coming from the submerged soil in the first years after filling.

The emissions of methane and dissolved carbon dioxide towards the atmosphere arise from three different processes: diffusion at the lake surface, gas bubble flux in shallow zones of the lake, and water degassing downstream from the dam. The last process is examined in the next chapter.

22.4 Methane Emission and Oxidation Downstream of the Reservoir

The early hypothesis (Gosse 1994) of a major contribution of dissolved methane (DM) in the dissolved oxygen (DO) sink observed in the downstream river during the turbining tests was proven (Chap. 22.4.1). It justified the building of an aerating weir in the plant outlet canal (Chap. 22.4.2). Operational since March 95, the weir allows an immediate reoxygenation of the water and a significant local elimination of methane towards the atmosphere. Thanks to the weir, over 2 mg L^{-1} of DO is maintained in the river at Pointe Combi, the minimum regulatory concentration set in conjunction with the Scientific Committee, following observations made on the resistance of fish to hypoxia in a tropical environment.

The oxidation of the residual DM and other compounds released by the dam, and the low inflows of the downstream tributaries led to the formation in the downstream river (from the dam outlet confluence down to the estuary) of a DO sag curve whose minimum was mainly located between Roche Bravo (31 km downstream of the dam) and Pointe Combi (40 km) over the March 1995-2000 period. The downstream DM concentrations observed at Petit Saut and their contribution to the atmospheric methane emissions and the DO budget of the downstream river are detailed in Chap. 22.4.3 to 22.4.8.

The analysis of dissolved gases along the river, downstream of new tropical dam lakes, have rarely been the subject of such in-depth research, especially for methane. Some DO data were collected: at Balbina, Eletronorte (1993) found that the downstream DO did not reach 1 mg·L^{-1} and that the situation was improving 200 km downstream, at the confluence with Rio Jatapu. At Curuá-Una, characterised by a low renewal time (1 month), a DO content greater than 5 mg·L^{-1} was measured during the November 1977-May 1978 (Darwich 1982).

22.4.1 Evidence of a Consumption of Dissolved Oxygen in the Downstream Sinnamary River Due to an Oxidation of Dissolved Methane

The significant role of dissolved methane (DM) oxidation on the dissolved oxygen (DO) balance of the river downstream from the Petit Saut dam, was demonstrated in 5 chronological steps (Gosse et al. 2000):

Evidence in June-August 1994 of an Oxygen Demand of Gaseous Origin Added by the Turbined Water into the Downstream River

Before the first testing of the hydroelectric plant turbines in June 1994, the guaranteed instream flow of around 100 $m^3 \cdot s^{-1}$ was released exclusively by the bottom gates. Although the mean DO concentration in the reservoir had been close to zero since February 1994, the DO concentration in the whole downstream Sinnamary was exceeding 4 $mg \cdot L^{-1}$ (Fig. 22.8): the reason was the atmospheric equilibrium of DO (close to 8 $mg \cdot L^{-1}$ at 25°C) obtained immediately downstream of the jet and the hydraulic jump generated at the gates outlet. On the contrary, without air mixing, the DO concentration was nil in the turbined water and in the plant outlet canal which enters the river 300 m downstream. The surprise came from the high amount of dilution flow which had to be released by the bottom gates to exceed 2 $mg \cdot L^{-1}$ of DO at Pointe Combi during the turbining tests. It was shown by a DO model (Gosse, 1994) that the only way to correctly reproduce the observed DO profiles in the river was to consider that the 2 day DO demand in the turbined water was greater than in the bottom gates outlet, with a difference progressively increasing from at least 2.5 $mg \cdot L^{-1}$ in mid-June 1994 to close to 10 $mg \cdot L^{-1}$ end of August-beginning of September 1994. As the turbine inlet from the reservoir is a few metres above the inlet of the bottom gates, and as the survey in the reservoir at the time (Richard, 1996) was revealing poorer chemical conditions with increasing depth, it was considered (Gosse 1994) that this additional DO demand in the turbined water could only be of gaseous origin and generated in the deoxygenated reservoir, and that – thanks to the high local air-water mixing – the gaseous DO demand downstream of the bottom gates had been low.

Theoretical Assessment – Early September 1994 – of a DM Concentration of Several $mg \cdot L^{-1}$ in the Turbined Flow End of August-Beginning of September 1994

Without any measurement of reduced gases, DM role was the more convincing assumption for explaining such a high gaseous DO demand, as excessively higher concentrations had to be considered for the other potential candidate H_2S (Gosse 1994; Gosse and Grégoire 1997). This proposal came as a surprise to the GHG team whose last measurements resulting from samples taken in March 1994 were indicating a mean level of DM in the reservoir of only 0.3 $mg \cdot L^{-1}$.

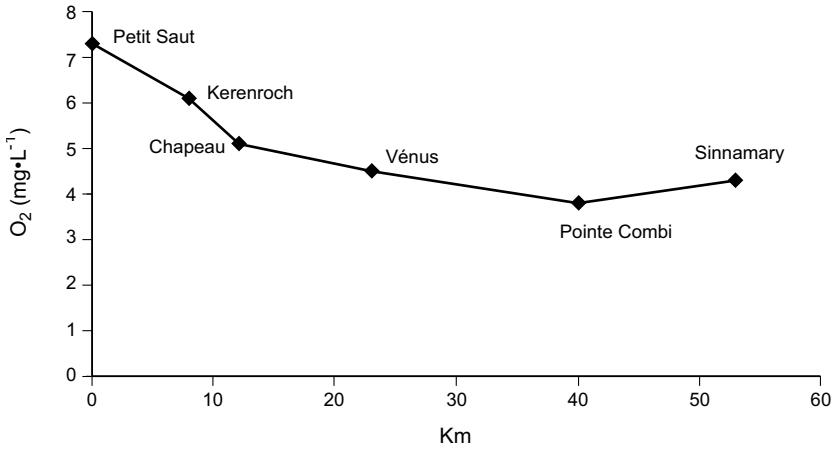

Fig. 22.8. Longitudinal profile of dissolved oxygen ($mg{\cdot}L^{-1}$) in Sinnamary Estuary from the dam to the estuary entrance, end of March 1994

Experimental Confirmation of DM Presence End of September 1994

Galy-Lacaux (1996) measured a high concentration (3 $mg{\cdot}L^{-1}$) of DM in the turbined water and a very low concentration (0.2 $mg{\cdot}L^{-1}$) downstream of the bottom gates in the samples taken beginning of September 1994.

Experimental Confirmation — from October 1994 — of a DO Sink of Gaseous Origin Contained in the Bottom Layers of the Reservoir and in the Turbined Water

The method applied by (Richard 1996) consisted in comparing the consumption of DO in bottles containing either unagitated water or water having being strongly agitated to establish a gaseous equilibrium with the atmosphere. Gaseous DO consumption was mainly observed in less than one and a half days.

In situ Measurements – from December 1994 to September 1995 – Proving Rapid DM Oxidation in the River

Galy-Lacaux (1996) and Galy-Lacaux et al. (1997) firstly showed that all the DM present in the water downstream of the dam had disappeared at Pointe Combi, and secondly – using emission measurements by gas chambers – calculated that no much more than 20% of the DM present in the Sinnamary 300 m downstream of the dam was emitted to the atmosphere along the 40 km. That proved the predominance of the oxidation of DM in

the progressive disappearance of DM downstream of the weir. It was also a confirmation of the high speed of DM oxidation in the downstream river, as between one day and two days are necessary for a water body released at the dam to travel 40 km, for a discharge between 240 $m^3 \cdot s^{-1}$ and 100 $m^3 \cdot s^{-1}$. The involvement of methanotrophic bacteria in the DM oxidation was shown in 1996 by J. F Dumestre (1998).

22.4.2 Building of an Aerating Weir in the Plant Outlet Canal in Order to Guarantee 2 mg L^{-1} of DO in the Downstream Sinnamary River

To honour the minimum requirement of 2 $mg \cdot L^{-1}$ during the turbining tests, it was necessary in September 1994 to dilute the turbined flow by a discharge from the bottom gates four times greater. It was not a viable situation for a normal exploitation of the hydroelectric plant, which had to come into service in 1995. Consequently, EDF decided at end of September 1994 to build an aerating weir in the outlet canal in order to create an exchange of gases (oxygen and methane) between air and water, taking the entire technically possible head (Gosse and Grégoire 1997). The weir (Fig. 22.9) is a 85 m wide cascade of 2 consecutive waterfalls. It is a metallic structure of 5 hexagons (side = 7 m) delimited by upstream and downstream walls, the top of which is 5.8 m and 3.4 m above sea level, respectively.

The weir, installed in March 1995 showed a good aeration efficiency, with close to 80% of the DM eliminated from the turbined water and a DO concentration immediately downstream of the weir close to 90% of the saturation level for turbined discharge up to 200 $m^3 \cdot s^{-1}$. This aeration efficiency decreased after December 2001 due to a voluntary reduction in the height of the upper wall (and therefore the upper nappe) in order to better satisfy the higher electricity demand. The lowering of the weir was possible as higher margins above the DO threshold of 2 $mg \cdot L^{-1}$ were observed in the downstream Sinnamary, due to a decrease of the DO demand in the river. Some characteristics of the aerating efficiency of the weir are given here under. More details on the weir structure and its efficiency can be found in Gosse and Grégoire (1997), Gosse et al. (1997b) and Richard et al. (2003).

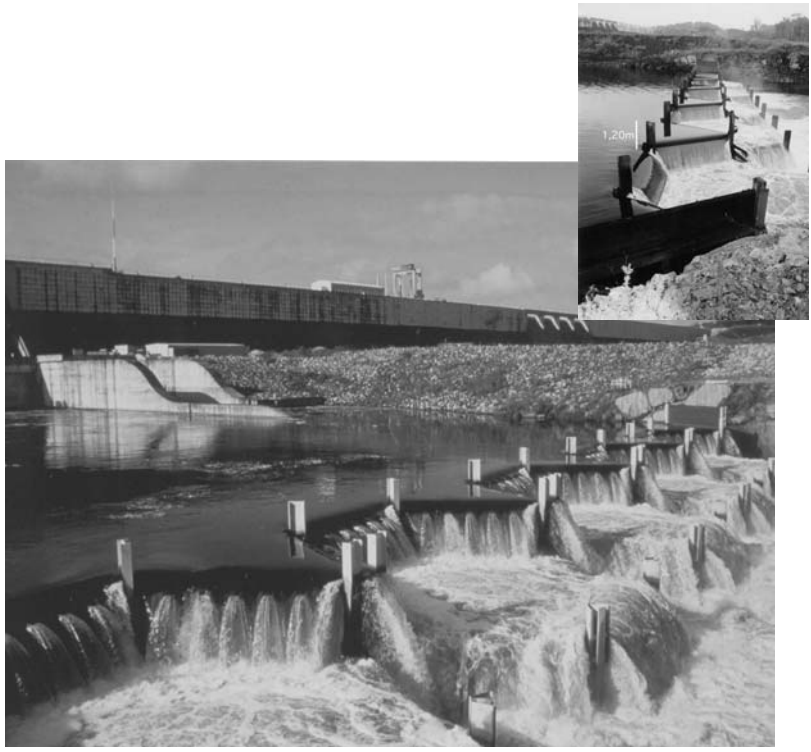

Fig. 22.9. Aerating weir in the power plant outlet canal before and after its first lowering

22.4.3 Historical Reconstruction (1994-2002) of the DM Concentrations and Fluxes in the Water Crossing the Dam

Over the years, between 1994-2002, the flow crossing the dam was mainly turbined or passed through the bottom gates. DM concentrations in the reservoir at the intakes of the turbine circuit and the bottom gates are close, with a difference in altitude of only a few metres between the two intakes. There is only a slight difference in the concentration of non volatile compounds observed in the near downstream of the corresponding outlets.

DM concentrations in the water intake of the dam can be determined by 3 methods: direct DM measurement in the water entering the turbines (with some uncertainty due to the heterogeneity to be considered from one turbine to another) when the plant is running; DM measurement in the first hectometres downstream of the dam which gives the water intake concentration, if the percentage of DM elimination to the atmosphere at the im-

mediate outlet of the dam has been correctly assessed; exploitation of DM concentrations measured in the reservoir along a vertical in the central part near the dam (Galy Lacaux et al. 1997-1999 and Delmas et al. 2001 chose this last method and the average value for their GHG emissions forecasts).

The first method is favoured here, as a lot of DM data were collected in the turbine entrances (weekly step in 1995, 15 days step from 1996 to 1998, monthly step the following years) and as the method is more representative of the flow released by the dam, which was mainly turbined and released by the bottom gates during the 9 years.

2 types of special events must be considered however:

- the use of the surface valve from March 1995 till October 1996 in order to inject a partial flow of better water quality into the plant outlet canal. The DM concentration in this outlet was representative of the surface of the reservoir. But the discharges involved were low.
- the use of the flood gates, for the rare floods which were too strong to be evacuated only by the bottom gates.

If we assume that the impact of the slightly higher DM concentrations in the bottom gates – by comparison to the turbine circuits – is compensated by the impact of the lower DM concentrations appearing when the upper flood gates are used, DM concentrations and DM fluxes in the water crossing the dam can be assessed by using the DM concentrations measured in the turbines entrance (given in Fig. 22.10): by multiplying for each month of the March 1995-December 2002 period, the average value of DM measurements in the turbine entrance by the corresponding monthly discharge released by the dam, we find that DM concentrations and DM fluxes in the water crossing the dam were respectively equal to 4.75 $mg{\cdot}L^{-1}$ and 1.1 $kg{\cdot}s^{-1}$ on average over the 94 months (mean annual flow close to 250 $m^3{\cdot}s^{-1}$).

The average DM concentration and the DM flux in the water crossing the dam become respectively equal to 4.7 $mg{\cdot}L^{-1}$ and 290000 tons (1.03 $kg{\cdot}s^{-1}$) over the 1994-2002 period, including the first 14 months characterized by the following increase in DM concentrations: 0 $mg{\cdot}L^{-1}$ in January 1994, 0.25 $mg{\cdot}L^{-1}$ in March (GHG team measurement in the reservoir), 0.8 $mg{\cdot}L^{-1}$ in June 1994 (Gosse 1994), 3 $mg{\cdot}L^{-1}$ in September (GHG team measurement) , and 12 -14 $mg{\cdot}L^{-1}$ range over the December 1994-February 1995 period (GHG team and Hydreco measurements).

A slightly greater flux — 340000 tons (1.2 $kg{\cdot}s^{-1}$) — is obtained over the same period when replacing the 1995-2002 DM measurements by the Galy Lacaux (1996) sinusoidal function given in Chap. 22.3.2 (with $t = 0$ corresponding to 1 January 1995). This formula was used in the previous

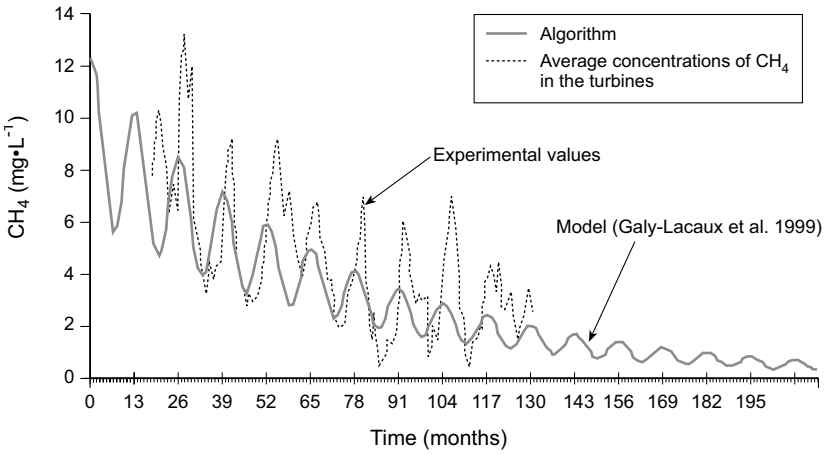

Fig. 22.10. Comparison of the Galy-Lacaux et al. algorithm with the average monthly concentrations of dissolved CH_4 ($mg{\cdot}L^{-1}$) measured in the turbines entrance (time origin = January 1994)

downstream GHG forecasts calculated by Galy Lacaux et al. 1997-1999 and Delmas et al. 2001 who proposed a mean downstream DM flux of 395000 tons – 1/3 greater than the flux based on measurements – the surplus being mainly due to the difference between the predicted and the real flow discharges downstream of the dam.

22.4.4 Efficiency of DM Elimination in the Near Downstream of the Dam (1994-2002)

In the very near downstream of the dam, significant amount of DM contained in the flow crossing the dam can be emitted to the atmosphere by aeration processes taking place either at the outlet of the bottom gates or at the weir built in the plant outlet canal.

For a good assessment over the 1994-2002 of this local elimination, it is necessary to consider 4 periods:

- from Januray 1994 (beginning of reservoir filling) until March 1995, period during which there was no aerating weir in the plant outlet canal. The bottom gates and – episodically – the turbine circuits (during the short turbine tests of the June-September 1994 period) were used.
- from March 1995 (aerating weir on operation) till October 1996, period during which the flow was mainly turbined, but with some small addition from the bottom gates or the surface valve at the dry seasons in

order to guarantee 2 $mg{\cdot}L^{-1}$ of DO in the downstream river. But the potential benefit of the surface valves was limited for DM, as these valves release the flow into the plant outlet canal immediately upstream of the aerating weir.

- from October 1996 till December 2001, period during which the flow was turbined normally, under the initial configuration of the aerating weir.
- from end of December 2001 till December 2002, period during which the flow was turbined normally, under a new configuration of the aerating weir (division roughly by 2 of the height of the upper fall due to a lowering of 1.2 m of the top of the upper wall)

For the last 3 periods, the bottom gates (and exceptionnaly the flood gates) were also used to release the peak discharges entering the reservoir.

Aeration Efficiency at the Bottom Gates Outlet

For a discharge of 100 $m^3{\cdot}s^{-1}$ released by the dam through the bottom gates, it can be assumed that around 95% of the DM contained in the water is emitted to the atmosphere in the air-water mixing taking place at the outlet: in September 1994, the outlet DM concentration was around 0.15 $mg{\cdot}L^{-1}$ for an average value of 3 $mg{\cdot}L^{-1}$ in the turbine outlet; at the end of February 1995, the outlet DM concentration was 0.45 $mg{\cdot}L^{-1}$ for a value exceeding 8 mg L^{-1} in the turbine entrance.

Aeration Efficiency of the Weir Built in the Plant Outlet Canal

It was experimentally assessed in 1996 that, for a discharge released by the dam through the turbines, the weir was eliminating 82% of the DM contained in the water at 80 $m^3{\cdot}s^{-1}$ and 75% at 230 $m^3{\cdot}s^{-1}$, the upstream concentration of DM being around 5 $mg{\cdot}L^{-1}$ (Gosse and Grégoire 1997). The use of the monthly uptream and downstream measurements taken in 1999 and 2000 gives a slightly better aeration efficiency, with a percentage of elimination of 80% on average (standard deviation of 3%) for a discharge in the 160-270 $m^3{\cdot}s^{-1}$ range and upstream DM concentrations varying from 2 to 7 $mg{\cdot}L^{-1}$. The lowering of the upper fall in December 2001 led to a decrease in the efficiency of DM elimination close to 10% (Richard et al. 2003). Over the year 2002, the monthly upstream (turbine entrance point) and downstream (0.8 km downstream of the dam) DM concentrations give a mean percentage of DM emission to the atmosphere equal to 68%, whereas the percentage was equal to 79% over the 3 years 1999-2001.

Global Efficiency of DM Elimination in the Near Downstream of the Dam

For an assessment of the percentage of DM eliminated in the near downstream of the dam under aeration processes, it has to be considered, firstly, that the efficiency of DM elimination decreases when the discharge increases, secondly, that a release of water both through the gates and the weir affect the elimination efficiency at the 2 sites as the downtream altitude of the river is dependent on the total discharge released at the dam (the moderate secondary effect of the tide is disregarded). However, a situation with outlet daily and monthly discharges outside the (turbined) range 150-270 $m^3 \cdot s^{-1}$ is not frequent since June 1995 (end of the first filling of the reservoir). Much higher discharges leading to the opening of the bottom gates can be observed during the high peak of the rainy season, mainly in May or June: in June 1999 and May 2000, for a turbined discharge of 250 $m^3 \cdot s^{-1}$ in both cases, and a bottom gates discharge of respectively 400 and 300 $m^3 \cdot s^{-1}$, it was measured that there was respectively 57% and 60% less DM in the near downstream of the river-plant outlet canal confluence than in the water entering the turbines circuits.

Using daily discharges crossing the dam through the different outlets and aeration efficiencies of the 2 main aerating structures (bottom gates and aerating weir) at those discharges, it can be assessed that close to 80% of the DM flux released by the dam over the 1994-2002 period was emitted to the atmosphere immediately downstream of the dam.

It is a greater value than the percentage of CO_2 emitted to the atmosphere under the same aeration processes: according to the monthly values collected by Hydreco, this percentage was close to 65% on average on the 3 years 1999-2001, with a mean CO_2 concentration close to 20.5 $mg \cdot L^{-1}$ in the turbine entrance – 6.6 times the mean DM concentration – and close to 13.5 $mg \cdot L^{-1}$, 0.8 km downstream of the dam. The 6.6 ratio between DM and dissolved CO_2 in the flow crossing the dam is lower than the ratio obtained between CO_2 and DM by Galy-Lacaux et al. (1999) and Delmas et al. (2001), in their prediction of outlet fluxes from the dam over 20 years (Table 12.1, chap. 12). The ratio is 14, based on a formula – given in chap. 12 – determining CO_2 fluxes from CH_4 values. However, it does not mean that their forecast of downstream CO_2 emissions by Petit Saut dam (Table 12.1) are significantly overestimated. CO_2 emissions to the atmosphere which take place in the downstream Sinnamary and are not linked to DM oxidation have also to be taken into account. The joint Hydro-Québec – Hydreco – CNRS – EDF campaign performed in May 2003 shows that these emissions are high.

22.4.5 DM Emissions to the Atmosphere in the Sinnamary River Downstream of the Aerating Weir

Downstream of the weir built in the plant outlet canal, the proportion of DM emitted to the atmosphere could not be very high during the first years following the reservoir impoundment for 2 main reasons:

- rapid oxidation of DM accelerating the disappearance of DM in the water, limiting the DM stock which can be emitted to the atmosphere downstream
- unfavourable physical conditions for an important exchange of gases at the water-air interface in the first 20 km: low slope of the bed (less than 0.003%), deepness of the river – the mean depth between the weir and Pointe Combi can be approached by the formula $H = 1.56\ Q^{0.193}$ with Q discharge crossing the dam in $m^3 \cdot s^{-1}$ – and very low winds usually.

Galy-Lacaux (1996) and Galy-Lacaux et al. (1997a) assessed that only around 20% of the DM remaining in the river immediately downstream of the weir was escaping to the atmosphere between the weir and Pointe Combi. The asssesment was based on measurements of gas emissions to the atmosphere performed in 1995 by the GHG team, with a closed chamber drifting along the river. 2 discharges were studied: 220 $m^3 \cdot s^{-1}$ in 5 sections of the river between the aerating weir and Crique Venus (23 km downstream of the dam) in September 1995 (Galy-Lacaux 1996); 100 $m^3 \cdot s^{-1}$ in 2 sections (1 km and 6 km downstream of the dam) in May 1995 (Lacaux and Delmas 1995). At 220 $m^3 \cdot s^{-1}$ the measured emission fluxes of DM are rather well described at all the 5 points by the equation $F = 0.075\ M$, with F flux ($g \cdot m^{-2} \cdot hour^{-1}$) and M the DM concentration in the river which was in the 0.1-0.6 $mg \cdot L^{-1}$ range, whereas the equation $F = 0.02\ M$ is better suited for the 2 measurements points at 100 $m^3 \cdot s^{-1}$ (Gosse et al. 1998).

Using the formula of H given here above and using the 2 formulae of F at 100 $m^3 \cdot s^{-1}$ and 220 $m^3 \cdot s^{-1}$ – with an interpolation for intermediate discharges – Gosse et al. (2002) proposed the following schematic model for the average DM disappearance in the river between the dam and Pointe Combi over the 1994-1998 period.

$$dM / dt = - K_2\ M - D_3$$

with

$M\ (mg \cdot L^{-1}) =$ DM concentrations in the river (considered homogeneous in the cross section, which is an acceptable hypothesis except for the first kilometres when there is a mixing of turbined flow with water coming from the bottom gates)

T (s), time = the time needed to cross the dam–Pointe Combi stretch being described by the equation T (in days) = 66 $Q^{-0.75}$; and the dilution effect of downstream tributaries being neglected, as their total flow generally represents less than 5% of Q

K_2 (s^{-1}) = coefficient of physical exchanges of methane at the water-atmosphere interface, equal to 0.075/H at 220 m^3 s^{-1} ($K_2 = 0.41 \cdot d^{-1}$)

D_3 ($mg \cdot CH_4 \cdot L^{-1} \cdot s^{-1}$) = DM loss due to DM oxidation inside the water column, which is calibrated, by reducing the discrepancy between the calculated and typical measured profiles of DM along the river during the 1994-1998 period.

Using the model, it was assessed (Gosse et al. 2002) that for the 1995-1998 period, close to 30% of the DM present in the river downstream of the aerating weir was emitted to the atmosphere for a turbined discharge between 220 $m^3 \cdot s^{-1}$ and the mean annual discharge of the Sinnamary (260 $m^3 \cdot s^{-1}$), the rest being oxidized inside the water column. It appeared that the formulation $D_3 = d.M_0$, with d (constant approaching $0.6 \cdot d^{-1}$) and M_0 (the upstream DM concentration) was a rather acceptable simplified formulation to describe DM oxidation and the longitudinal decrease in DM concentrations, in conjunction with the K_2 formulation derived from the emission measurements of the GHG team and the very schematic hydrodynamics chosen in the model.

The percentage of DM which is emitted to the atmosphere downstream of the weir is much more important since end of 1999. The analysis of the longitudinal DM profiles collected by Hydreco shows that since that date, DM remains significantly present at Pointe Combi (0.2 $mg \cdot L^{-1}$ or more at the dry season), even for discharges lower than 200 $m^3 \cdot s^{-1}$, which did not happen the years before for similar levels of DM in the Sinnamary, in the near downstream of the aerating weir (Fig. 22.11). As there is no reason why the aeration coefficient at the surface should be lower from 1999 (on the contrary it could be slightly higher due to the improvement of the water quality over the years), the persistence of DM suggests a lower speed of DM oxidation in the river, which could be due to a lower population of active methanotrophic bacteria coming from the reservoir. The hypothesis of a new benthic production of methane is not considered as it would lead to worse DO conditions, which is not the case.

There are two direct consequences of the downstream persistence of DM in the river since end of 1999: firstly, it means that for a same flow

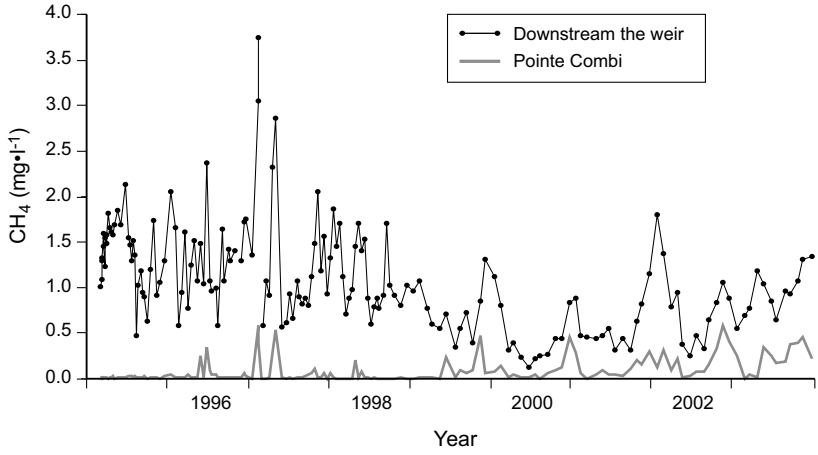

Fig. 22.11. Dissolved methane concentrations ($mg \cdot L^{-1}$) downstream of the aerating weir installed in the power plant outlet canal and at Pointe Combi (40 km downstream of the dam). A general progressive decrease is observed after 1997 at the upstream point due to an improvement of water quality in the reservoir. The increase at this point after 2001 is due to the partial lowering of the aerating weir (end of 2001 and end of 2002). The dissolved methane concentration at Pointe Combi is greater after 1998 due to a decrease in the methane oxidation velocity along the river stretch

discharge and for a same concentration of DM downstream of the aerating weir, the DM flux emitted to the atmosphere in a downstream cross section is greater today than before end of 1999. The potential stock of DM which can be emitted to the atmosphere is less subject to a decrease by oxidation; secondly, it means that the aeration conditions at the surface downstream of Crique Venus – an area which was not studied by the GHG team as there were DM depleted at the time – are much more important today than before for correctly assessing the DM flux emitted to the atmosphere downstream of the dam: this is an area where the aeration at the surface is more and more influenced by tidal currents and wind action and imperfectly described by the flow discharges released by the dam.

DM emissions to the atmosphere and associated DM concentrations in the river were recently measured during a joint Hydro-Québec–Hydreco–CNRS–EDF campaign performed one day of May 2003 for a 150 $m^3 \cdot s^{-1}$ discharge (emission measurements given by A. Tremblay, L. Varfalvy, G. Abril and F. Guérin, oral communication). Three points of the river were studied. In the upper stretch of the downstream river (between 1 and 2 km downstream of the dam), the measured emission flux is coherent with the 1995 measurements: the adjustment of the coefficient k in the formula

$F = kM$ giving the DM emitted flux F ($g \cdot m^{-2} \cdot h^{-1}$) from the DM concentration in the river (M in $mg \cdot L^{-1}$) gives a value of k between 0.04 and 0.045 in the near downstream of the dam and at Crique Venus respectively for the May 2003 campaign, which is an intermediate value of those obtained at 100 $m^3 \cdot s^{-1}$ and 220 $m^3 \cdot s^{-1}$ in 1995. At the third point (Pointe Combi), k appeared to be greater – close to 0.1 – under the influence of active wind and tide action, due to the proximity of the sea.

On the basis of the high value of k obtained in the downstream part of the river (Pointe Combi) for the June 2003 campaign, which is higher than the k values obtained along the dam-Crique Venus stretch during the 1995 campaign at 220 $m^3 \cdot s^{-1}$, it can be calculated – using and Gosse et al.'s model with adapted values of K_2 and d – that at least 45% of the DM flux present in the river downstream of the aerating weir was emitted to the atmosphere over the 2001-2002 period for the mean flow discharge along the 40 km downstream stretch. This is directly linked with the decrease of the oxidation velocity. Since end of 2001, this higher downstream emission tends to compensate the reduction in DM emission at the aerating weir, whose height was reduced.

22.4.6 A New Assessment of the Methane Emissions to the Atmosphere in the Downstream Sinnamary River (1994-2002 Period)

From the assessment of the DM flux crossing the Petit Saut dam (Chap. 4.3) and the DM flux emitted to the atmosphere donwnstream of the dam in the immediate (Chap. 4.4) and far (Chap. 4.5) fields, it is possible to propose an assessment of around 250000 tonnes for the methane emissions to the atmosphere in the downstream Sinnamary over the 1994-2002 period, and an assessment of around 40000 tonnes for the methane fluxes oxidised in the downstream river. This oxidation generates dissolved CO_2 but this production is not sufficient by comparison to the aeration exchanges at the surface to provoke an increase of dissolved CO_2 concentrations along the river, which, according to Hydreco measurements, were equal on average to 13.5 $mg \cdot L^{-1}$ and 11.5 $mg \cdot L^{-1}$, 0.8 km and 40 km (Pointe Combi) downstream of the dam over the January 1999-September 2001 period, a.

It can be considered that the constant value of 85% selected by Galy-Lacaux et al. (1997) and Delmas et al. (2001) – in their GHG emissions forecasts – for the percentage of DM emitted to the atmosphere from the downstream discharges of the dam, is rather acceptable on average over the 9 years 1994-2002 period (floods excluded), with the poorest represen-

tativity for the first 14 months, during which DM emission was much greater as the bottom gates were mostly used to feed the downstream Sinnamary.

22.4.7 Extrapolation of CH_4 Findings to Other Morphological Conditions

There are reasons to suggest that the building of the weir which locally increased the methane emissions to the atmosphere has not increased significantly the total downstream emissions of DM to the atmosphere, as it favoured DM oxidation by methanotrophic bacteria in the downstream river. Without specific effort to maintain the river oxygenated when turbining , i.e. without weir building in the plant outlet canal, the downstream river would have been anaerobic most of the time of the 1994-2002 period. Consequently no major methane oxidation would have taken place along the dam-Pointe Combi stretch., favouring an emission to the atmosphere of around half of the upstream DM flux.. Due to the high stock of DM which would have entered the estuary (around 2-3 $mg{\cdot}L^{-1}$ on average), high DM emissions to the atmosphere would have been present in the estuary at the surface due to wind and tide currents. The DO depletion in the river and intermittently at the bottom of the estuary would probably have led to DM production in the water column, probably generating an additional source of DM emission to the atmosphere.

If the slope of the downstream river had been very steep, no aerating weir would have been necessary to increase DO concentrations. The physical exchanges of gases at the water-air interface would have been naturally very high, with a rapid emission of DM to the atmosphere and an insignificant DM disappearance by oxidation, despite the better conditions for atmospheric oxygenation of the river and consequently better conditions for DM oxidation.

22.4.8 The Role of DM Oxidation in the DO Budget of the Downstream Sinnamary

DM started to play a major role in DO consumption during the short turbining tests performed between June and September 1994 (Chap. 22.4.4). Before that, the discharge was only released by the bottom gates which were delivering a water with less than 0.1 $mg{\cdot}L^{-1}$ of DM, if we consider the DM content downstream of the bottom gate outlet in September 1994 (0.2 $mg{\cdot}L^{-1}$) and the average DM concentration of 0.3 $mg{\cdot}L^{-1}$ on the vertical in the reservoir in March 1994 (Gosse et al. 2000). The DO decrease of

3 to 4 $mg{\cdot}L^{-1}$ from the dam to Pointe Combi during the March-May 1994 period was generated by a chemical and biological consumption which was not linked to gases.

From October 1994 to February 1995, the DM concentration just downstream of the dam (water coming only from the bottom gates) gradually increased and reached 0.45 $mg{\cdot}L^{-1}$ at the end of the period (Fig. 22.12). From March 1995 to March 1998, with the power station in operation and the aerating weir in place, the DM concentration just downstream of the weir was close to 1.3 $mg{\cdot}L^{-1}$ on average (Fig. 22.11), representing a potential DO demand exceeding 4 $mg{\cdot}L^{-1}$ on average. As the non-methane-related chemical and biological consumption of oxygen has further decreased in the water released by the dam (assessed experimentally at less than 2 $mg{\cdot}L^{-1}$ in 2 days), oxidation of DM has been considered as a major DO sink in the downstream Sinnamary from March 1995 to 1998 (Gosse et al. 2000). However, using a DO model which takes into account the aeration mechanisms at the surface, it was shown (Gosse et al. 2002) that a DO demand which was not experimentally detected in the dam outlet had to be added, in order to correctly reproduce the DO concentrations at Pointe Combi. (Fig. 22.13). The nature of this additional DO sink which was represented as a benthic demand (with possible values exceeding 2 $g{\cdot}O_2{\cdot}m^{-2}{\cdot}d^{-1}$) in a modelling exercise (Gosse et al. 2002) still has to be determined. It can be both benthic and contained in the flow, and is linked to the degradation of non volatile compounds released by the dam. The moderate level of the 2 days BOD measured at Pointe Combi (1.2 $mg{\cdot}L^{-1}$ on average in 2002-2003 at 25°C) – which is lower than 0.8 km downstream of the dam (1.7 $mg{\cdot}L^{-1}$ on average) suggests that the non benthic sink cannot be very high.

DM played a lesser role in the DO budget of the downstream river after 1998 for 2 main reasons: general decrease in DM concentration in the reservoir and consequently downstream of the dam (before lowering the aerating weir); decrease in the DM oxidation velocity.

22.5 General Conclusion

Dissolved methane, which in a tropical environments had not been studied very closely until the last few years, has proven to be one of the most important parameters in terms of oxygen consumption and GHG emission at Petit Saut site.

The originality was the installation of a weir downstream of the turbines to reoxygenate the anoxic waters and to expulse methane in order to

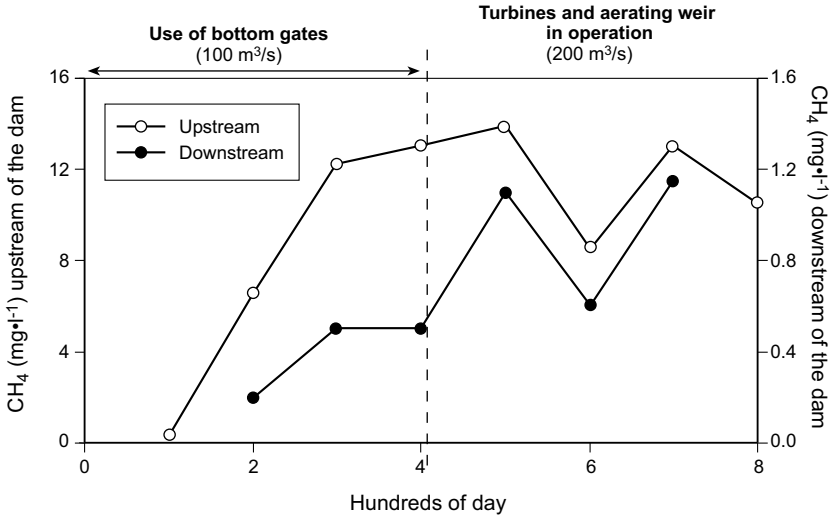

Fig. 22.12. Dissolved methane (mg·L^{-1}) upstream the dam (water column average) and in the Sinnamary 300m downstream of the dam, in 1994 and 1995 (in hundreds days from January 1994)

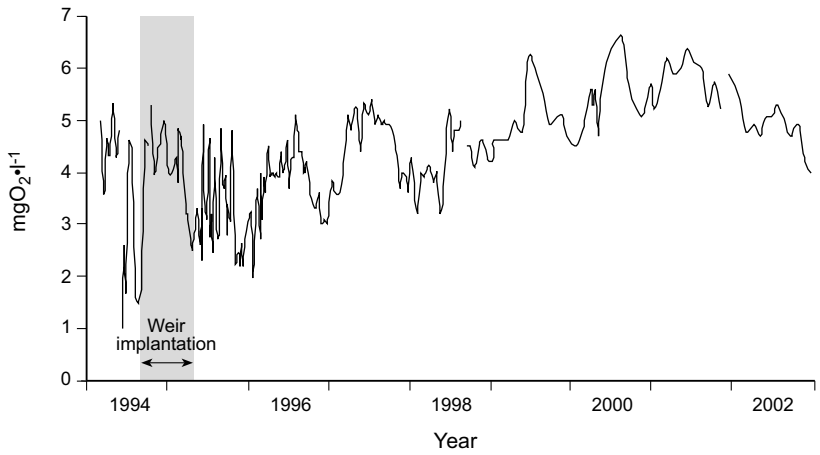

Fig. 22.13. Dissolved oxygen (DO) in mg·L^{-1} at Pointe Combi (from 1994 to 2002). Thanks to the weir built in the plant outlet canal which brought DO and eliminated dissolved methane (and its damaging oxidation) a concentration of 2 mg·L^{-1} of DO was guaranteed. The general progressive increase from 1996 is correlated with the decrease in the consumed quantity of methane (Fig. 22.11). The decrease after end of 2001 is due to the lowering of the weir which has slightly reduced the DO upstream concentration and increased the methane content

reduce its oxygen demand in the downstream river and guarantee the dissolved oxygen threshold of 2 $mg{\cdot}L^{-1}$ determined for the maintenance of aquatic life in the Sinnamary. The oxygen demand of the remaining methane has decreased the last years, offering possibilities for lowering the weir.

The long term acquisition of information inside and downstream of the Petit Saut reservoir helps in detecting changes over time (DO and DM improvements in the reservoir and resulting DM emissions, DM oxidation velocity in the downstream river). In conjunction with data collection on older reservoirs, it will allow an improvement in the forecasts of aquatic ecosystems functioning and evolution in tropical reservoirs.

Acknowledgements

We thank all the Hydreco staff and specially Cécile REYNOUARD and Benoit BURBAN for technical supports; and EDF for its constant financial support to the environmental measurement programme.

Modelling

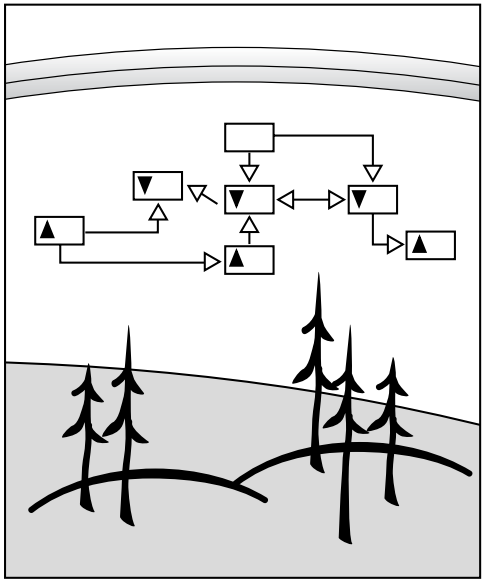

23 Using Gas Exchange Estimates to Determine Net Production of CO_2 in Reservoirs and Lakes

Raymond H. Hesslein

Abstract

The net contributions to the atmosphere of GHG's from reservoirs and lakes are made up of fluxes in inflows, outflows, and gas exchange. The rates of production, which are primarily due to bacteria and algae, and the transport coefficients due to hydrologic flows, wind velocity etc. can both vary considerably over time. Achieving accurate estimates of the net production requires an understanding of the variability of these various functions and requires sampling protocols adequate to define the parameters over the period of study. Several sampling protocols have been used each with strengths and weaknesses. This paper discusses the methods used for data collection and data interpretation for the gas exchange fluxes. Serious potential errors in estimates are identified for data based on infrequent sampling. Alternate protocols are recommended which use models of wind histories and estimates of diurnal changes due to photosynthesis. The recommended approach is to use high resolution measurements of parameters supplemented by models to understand the variability prior to designing programs to estimate fluxes.

23.1 Introduction

The contribution of greenhouse gases that a reservoir (or any water body) makes to the environment is equal to the net production of GHG's in the reservoir. This definition is different from the "net GHG emissions" as defined by the World Commission on Dams (WCD 2000) which considers only the incremental emission due to the creation of reservoirs. There are a number of approaches to determining the net production. In principle, net production in the water column and sediments could be measured, how-

ever spatial and temporal heterogeneity in both locations make the task very difficult. Alternately, a budget of inputs and outputs from the body can be assessed and the net calculated by differences. The inputs and outputs are typically surface water inflows, surface outflows and gas transfer at the air water interface. Ground waters are generally of lesser importance especially in riverine systems. Estimation of the fluxes in surface flows can be made by monitoring flows and concentrations. In hydroelectric reservoirs, flows are typically very well known and a variety of methods are available for measuring gas concentrations.

23.2 Methods Used to Estimate Gas Exchange

The parameters required for calculating the flux of GHG's at the air water interface using Fick's Law (Flux = (Cw-Cw) * MTC) are the concentrations in air and water and the mass transfer coefficient (MTC). The MTC is not directly measurable but is generally estimated from relationships with wind velocities. Estimates of the gas fluxes using Fick's Law can be made in water or in air. The methods for estimation in air are described briefly, but for reasons outlined below this chapter will focus on measurements made in or on the water.

Methods for estimating gas fluxes based on measurements in air are known as micrometeorological methods. There are two approaches taken. In one case the concentration in the air moving up is measured along with the upward velocity and the concentration in air moving down is measured along with the downward velocity. The difference between the integral of the product of concentration and velocity over time of the upward and downward measurements gives the net flux. Because the vertical velocity field in air is highly variable and changes rapidly, the instruments must make measurements of concentration and velocity very rapidly. These instruments, usually a sonic anemometer and a high speed gas analyzer, must be mounted on a rigid tower above the water surface. In order to have confidence in the data one must be assured that the measurement, made at a single location, is representative of the whole water body. The surrounding land can have an influence, depending on wind velocities and thermal convection, which can result in locations which are biased to upward or downward velocities. This can be especially problematic for small water bodies but is not generally important for large hydroelectric reservoirs.

An alternate approach for estimation of fluxes in air is to measure concentrations at two heights over the water body, calculate the gradient, and multiply by a MTC. In this approach the concentrations are often measured

by lasers averaging over whole water bodies. The MTC can be estimated from mean eddy mixing coefficients measured or calculated in relation to wind speed. The laser technique is fairly new and there are few publications giving results or comparing results with other methods of estimation.

Because of the effort and expense in setting up the equipment for the estimation of fluxes in the air over the water body, most estimates of gas fluxes to and from water bodies have been made using measurements in or on the water. Two fundamentally different methods have been used. The most common applies Fick's Law with estimates of the MTC from measurements of wind speed.

Two models have been used to produce an estimate of flux (MacIntyre et al. 1995). The Thin Boundary Layer (TBL) model assumes that the transfer is controlled by a thin boundary at the water surface across which the transport is at molecular rates and that the concentration at the air-water interface (upper surface of the boundary layer) is in equilibrium with respect to solubility with the gas concentration in the air. The second model used is the Surface Renewal Model (SRM) which assumes that eddies replace the surface film of water at a rate which depends on the turbulence in the water. Both models define the MTC based on wind speed either by setting the thickness of the boundary layer in the TBL or driving the turbulence in the SRM. Because the relationship between the wind and the MTC for both models is empirical, the only practical difference between the models is that the relationship between the MTC for individual gases with different molecular weights is slightly different. Given the uncertainties in the estimation of the MTC from wind velocities, this difference is in most cases of minor importance.

The second method for estimating gas fluxes across the air-water interface is the use of a flux box, helmet, or floating chamber (FC) (Kremer et al. 2003). Designs vary, but generally this is a shallow box (15-20 cm) about 0.5 m square with one 0.5 m square side open. The box has a floatation collar which allows the box to float open side down on the water with the rim 1-2 cm under the water. The box is flushed with air, placed on the water and a series of 2 or more measurements of the concentration of the gas(es) of interest made in the box over a period of generally 10 minutes or so. The gas flux is then calculated as the change in concentration times the volume of the box divided by the area of the interface and the time over which the measurements were made. Measurements of gas concentrations in the water and in outside air are not always made, in which cases MTC values cannot be calculated.

23.3 Discussion of the Methods

Regardless of which of the two methods is used, the results must answer two important questions. First, how accurate are the flux estimates from the method and second, how well can longer term total flux from the water body be estimated from the data collected? The ideal way to answer the question of accuracy is to test both methods under a variety of weather conditions on a water body with a known gas flux. Experiments of this sort have been accomplished with the use of deliberate tracers. For example, sulfur hexafluoride (SF_6), a gas which is inert in water bodies, has been used and the "true" flux calculated by the change in mass of SF_6 in the water body. In fact, this has been the method of choice for defining the empirical relationship between wind speed and MTC which is used for the TBL/SRM methods. In this way the accuracy of the MTC is calibrated by these deliberate tracer experiments and only the relative performance of other gases is at issue. There are few field calibrations of the FC. In some instances where FC fluxes have been compared to fluxes determined by tracers, the chamber fluxes have been much higher. Hartman and Hammond (1984) suggested that this was a result of chamber movement from wind or waves introducing turbulence at the walls and was less important at low wind speeds. However, Matthews et al. 2003 also saw much higher fluxes (3-7 times) from chambers than with the TBL model calibrated by SF_6 in very sheltered water bodies. Kremer et al. 2003 recently reviewed published and unpublished data where the FC method and TBL could be compared and concluded that there was a range of conditions, generally with winds of 2-8 m s^{-1} and relatively small waves without whitecaps, when properly used FCs could be expected to produce good flux estimates.

The answer to the second question concerning the calculation of fluxes applicable over long periods of time require that the data be considered in the context of the history of gas flux of the water body over the period to be estimated. Just how well any set of measurements will answer this question will depend on the characteristics of the measurement schedule and the characteristics of the water body. Estimates made using both the TBL/SRM and the FC methods are essentially instantaneous. Clearly, if a single measurement is made annually on a system that has a highly variable flux, the estimate of integral net production is going to be very uncertain. In order to more fully understand the implications of sampling frequency and lake variability, we will explore what is known about variability of CO_2 in natural waters.

The flux of CO_2 from inflow and outflow, algal photosynthesis and respiration, sediment and water column bacterial metabolism and gas exchange control the CO_2 budgets in most water bodies. It is hard to generalize about the variability of each of these sets of processes in different water bodies, but the character of each can be described. Inflow and outflow fluxes can vary a great deal seasonally and diurnally in reservoirs due both to the change in water flows and the concentrations of CO_2. In rapidly flushed systems daily measurements might be required to adequately characterize the integral fluxes. In lakes with long residence times the flows may only be of occasional and minor importance. The net of algal photosynthesis and respiration are generally driven by availability of light in the short term and vary over a 24 hour cycle. In nutrient rich environments the diurnal changes in CO_2 can be very large and non-linear (Schindler and Fee 1973, Carignan 1998,) while in very oligotrophic lakes the effect may be small. Bacterial production of CO_2 in the sediments and water may vary significantly between water bodies, but the temporal trends are smoother because changes in substrate supplies and temperature are relatively slow. Gas exchange fluxes can change rapidly because of the high variability in wind velocity. The concentration of CO_2 can also change rapidly due to the processes above and due to the gas exchange itself. Sellers et al.(1995), using hourly measurements of wind velocity, CO_2 in air and CO_2 in water for one week showed a range of hourly fluxes of 0-132 $mmol \cdot m^{-2} \cdot d^{-1}$. Even integrated over 24 hour periods, the range was 4.6-32.9 $mmol \cdot m^{-2} \cdot d^{-1}$ compared to an average flux for the week of 18.2 $mmol \cdot m^{-2} \cdot d^{-1}$.

If we use as an example a lake with only a constant flux from the sediment and gas exchange flux, the concentration of CO_2 in the water will vary inversely with the preceding wind velocity. In a variable wind field the flux to the atmosphere might vary greatly but the net production would still be constant. The greatest flux would occur during high wind following a period of low wind which had allowed the CO_2 to accumulate. Given a long enough period of constant wind of any velocity, the flux to the atmosphere would have to equal the constant flux from the sediments. The context for any instantaneous measure of flux must include the history of the wind.

How well can we address variability in flux with the floating chamber data? The main advantage of the FC method is that it gives a direct estimate of the flux into the chamber by the change in mass over the time of measurement. Measurements can be made in a short time and the equipment can be simple and inexpensive. However, there are many disadvantages. Generally the measurements cannot be carried out in rough weather. This potentially eliminates the periods of highest flux. As mentioned above, the accuracy of the method is in doubt, wind and wave induced mo-

tion of the chamber have been suggested as causing overestimates and the reduction of both turbulence and surface cooling suggested to cause underestimates. Kremer et al. (2003) have recommended criteria for use, but no comprehensive understanding is available for applying corrections. Because the measurements are made over a short period of time they are thought to represent fluxes only for the immediate conditions. While successive or continuous measurements by FCs are in principle possible, we know of no such studies. There is therefore little knowledge of how to extrapolate these instantaneous fluxes over time. While histories of wind velocity in areas are often available and might be of some use if the gas concentrations in the water were known, these are often not measured because the FC measurement does not require them. The lack of this information makes extrapolation over time impossible.

The extrapolation of fluxes estimated by the concentration gradient x MTC method is straight forward. The method has been calibrated by many deliberate tracer experiments over a range of water bodies and weather conditions. If the continuous record of concentrations in air and water are known along with continuous wind records, continuous flux estimates can be made and the integral over any period should be accurate. This assumes that the wind velocities and concentrations are applicable across the entire water. Continuous records of wind speed can be collected for water bodies relatively easily or can be approximated from records of nearby weather stations. Recent developments in instrumentation (Sellers et al. 1995, Carignan 1998) have provided some continuous records of concentration in air and water, but these records are not available to estimate fluxes in most studies. In the absence of continuous records, estimates are usually based on simple averages of fluxes estimated at the time measurements are made. However, if continuous wind records are available improved interpolation of fluxes between concentration measurements is possible.

23.4 Using a Model to Assist Interpretation

We can, for example, model a lake that has no inflow or outflow, a mean depth of 5 m, well mixed, and a net production of CO_2 of $5x10^{-3}$ mole·m^{-2}·d^{-1}. At steady state or averaged over the long term the flux to the atmosphere must equal this production rate. If the MTC is 0.25 m·d^{-1}, the steady state concentration in the water will be 20 x 10^{-3}·mole·m^{-3} above that of water in equilibrium with the atmosphere. If the wind is increased so that the MTC is doubled (after 10 days in Fig. 23.1), the initial flux

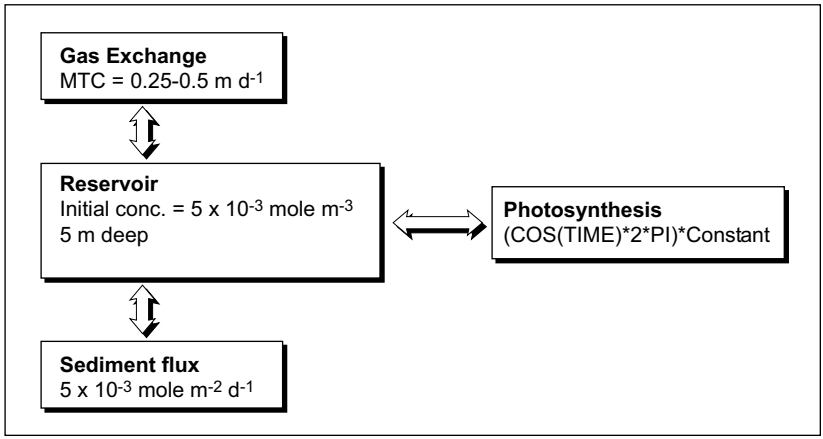

Fig. 23.1. Schematic of the model set up in STELLA

will double (10×10^{-3}·mole·m^{-2}·d^{-1}), and then decrease to the original steady state value (by day 60, Fig. 23.1). The new steady state concentration will be half or 10×10^{-3} mole·m^{-3}. If the MTC is reduced by half again the flux will drop initially to 2.5×10^{-3} mole·m^{-2}·d^{-1} (by day 60 in Fig. 23.1) and the concentration will return to the original value of 20×10^{-3} mole·m^{-3}. With a moderate change in wind velocity from 2 to 5 and back to 2 m·s^{-1} we see that the instantaneous concentration can vary by a factor of two and the instantaneous flux by fourfold. The situation in the very short term could be worse because the wind could be even more variable. Although this might suggest that the only solution to getting accurate estimates of the flux would be to have nearly continuous measurements of wind and CO_2, this is perhaps not the case.

If we can assume that the net production is constant over the period and if continuous wind measurements are available we can calculate the true flux by iteratively solving the flux equations. The model used is the same numerical model used to produce the data in Fig. 23.1 except that the true flux is not known. If, for instance, a measurement of concentration was available only for day 100, and wind data was continuous, an estimate of the true flux could be made for that instant. The concentration on day 100 is 18.6×10^{-3} mole·m^3 and the MTC is 0.25 m/d giving an instantaneous flux of 4.65×10^{-3} mole·m^{-2}·d^{-1}. If we use these values respectively as the concentration on day 0 and the net production from day o to 100, the model will slightly underestimate the concentration on day 100 (17.2 vs 18.6×10^{-3}, Fig. 23.2). We can iteratively find the true net production by changing the estimate of net production until the concentration in the

model matches our data on the sampling date. If we had weekly analyses, we could model each week separately or we could model the whole period and select the net production that gave us the best approximation of all of the measurements.

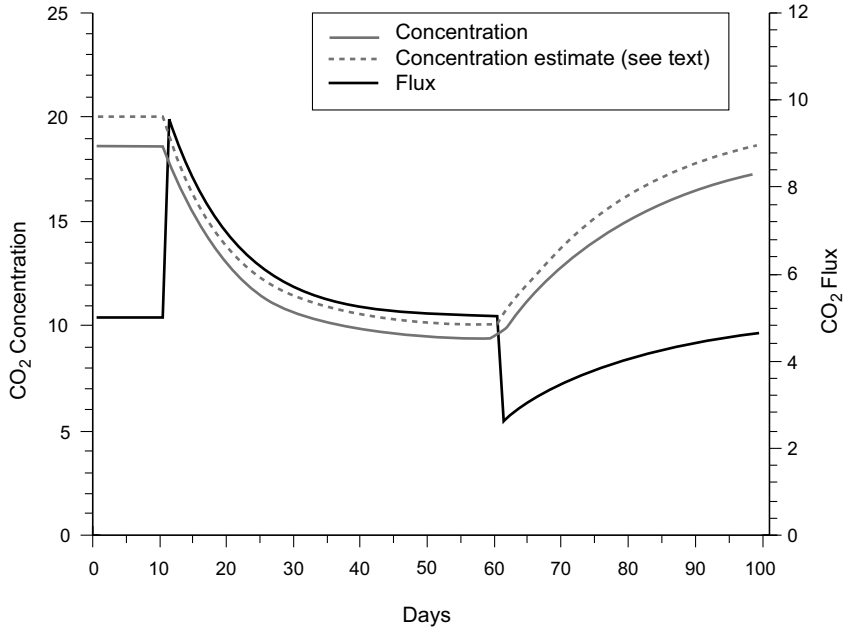

Fig. 23.2. Model predictions of concentrations in water and flux at the air-water interface with changing gas Mass Transfer Coefficient

An important question that arises is: From how long in the past must we run the model? The concentration at any point in time is a consequence of the history of the wind, but the farther back in time we go, the less the effect on the present concentration. The period of influence depends on the residence time of the CO_2. If the system had an MTC = 0, no CO_2 would be lost and the residence time would be infinite. The longer the model ran, the higher the CO_2 concentration would be. If on the other hand the MTC was 5 m/d, then the residence time of the CO_2 with respect to gas exchange would be 1 day and the wind even a few days before the measurement would have little influence on the concentration. Numerically this can be tested in the model by starting earlier and using longer and longer wind histories. At some point the concentration on day 100 will change very little. The simple solution might be to start the model very early, however, as the confidence that wind history is long enough improves, the assumption

that the net production is constant over the period becomes less certain. The assumption of constant flux has been discussed in a model application (Hesslein et al. Chap. 10, this volume).

23.5 Other Sources of Variability

Of course, in reality, wind variation is not the only factor affecting the concentration in the lake. Bacterial production of CO_2 might be relatively constant, but flow variations and diurnal photosynthetic influences might also be important in controlling the instantaneous CO_2 from which the flux is calculated. The same approach can be taken for this variability as for the wind alone. We must effectively have some idea of the history of the flow or photosynthesis. Let's examine how important the variation in CO_2 due to photosynthesis can really be in the instantaneous flux calculation. Carignan (1998) observed diurnal changes in the difference in the concentration of CO_2 between air and water of twofold (about 4 umol·L^{-1}). The changes were fairly consistent over a 7 day period. Schindler and Fee (1973) showed a much larger change in CO_2, about 50 umol·L^{-1} (approximately equivalent to 750-1000 ppm), with the daytime values below the detection limit of about 10 ppm. Again the variations were fairly consistent over 5 days. These variations are primarily due to photosynthesis, but may be modified by diurnal changes in wind (lower velocities at night) which are common. One way to include the photosynthetic variation in the model would be to add a diurnal curve of the estimated value and re-run the fitting procedure now with wind and photosynthesis. The output might look like Fig. 23.2. In this case the variation in concentration (Fig. 23.2a) caused by the photosynthetic simulation is about +- 15%. The variation in the flux (Fig. 23.2b) is the same because the MTC is constant over long periods in the model. In a highly variable wind field the error in estimating the mean flux or the net production could of course be much worse.

All of the above discussion of the treatment of variance has dealt with concentrations of CO_2 in the water not in the air. Sometimes the concentration in the air is measured along with the concentration in the water so that the instantaneous gradient can be accurately estimated. Alternatively, an average value is used for the concentration in air, usually near the present global average of about 375 ppm. If the concentrations of CO_2 in the water are near the value in the air, i.e. the gradient is small, it is important to have confidence in the value for air used if accurate estimates of fluxes are to be achieved. The best known records of CO_2 in the atmosphere (Keeling et al. 1982) have been collected for the purpose of estimating the global

mean, not local values. While seasonal cycles are clear in these records, they tell us little about the variation over small water bodies or even in continental locations influenced by land based photosynthesis and respiration. A one month long record from Winnipeg, MB (Fig. 23.3) shows diurnal and other variation spanning 340 to 440 ppm. This data is from a location at the edge of the city which is an open, flat, prairie region. Biswas et al. (2003) document a range of CO_2 of 403-653 ppm over one year in air above Sundarban mangrove environment, Bay of Bengal, India. The minimum values were observed during mid day with higher winds and the maximum values during the night with thermal inversions. Wind direction and season also influenced the CO_2 concentration in air. On small lakes surrounded by forest the variance could be much higher. Sellers et al. (1995) show a record of CO_2 over Lake 979 (25 hectares) at the Experimental Lakes Area, in the boreal forest of northwestern Ontario with a range of 375-560 ppm in a 24 hour period.

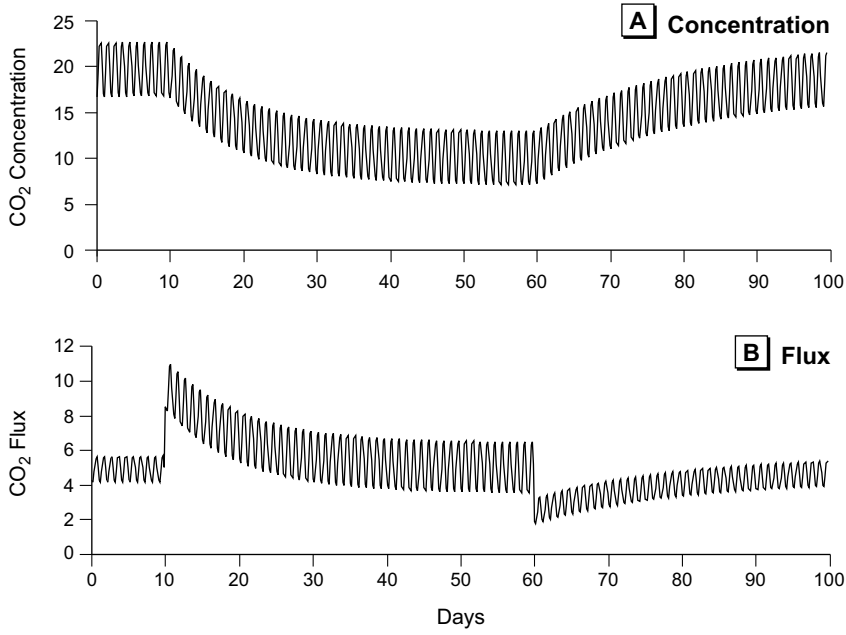

Fig. 23.3. Model predictions of concentrations with simulation of changing MTC and photosynthetic influence. b. Model predictions of concentrations with simulation of changing MTC and photosynthetic influence

At least part of the cause of the variation in CO_2 over Lake 979 is the prevalence of periods of low wind speeds. At high wind speeds we expect

the vertical turbulence in the atmosphere to be high and the horizontal mixing rapid so that the concentrations in the air reflect at least regional features such as is probably the case much of the time in the Winnipeg data in Fig. 23.3. At very low wind speeds much smaller features may be of importance. The air may be stable over the water and the CO_2 flux from the water itself may influence the concentration near the interface. Also, the lake may be surrounded by hills like Lake 979 and cool nighttime air may flow down from the forests onto the lake, carrying high CO_2 concentrations from forest respiration.

Accurately documenting the concentration of CO_2 in air so that an accurate estimate of the gradient can be made would require continuous measurements. However, the problem that this variance poses to the estimation of net production may not be so serious. Since the MTC increases rapidly with increasing wind velocity (Fig. 23.4) the bulk of the flux throughout short term variations will occur at higher wind speed. In the calculations of flux, the periods of low wind speed which allow larger change in the CO_2, will have little weight in the longer term integral. Sellers et al. (1995) demonstrated this with calculations from continuous measurements over one week. Ignoring two full days of the lowest wind speeds caused their weekly flux estimate to drop by only 8%.

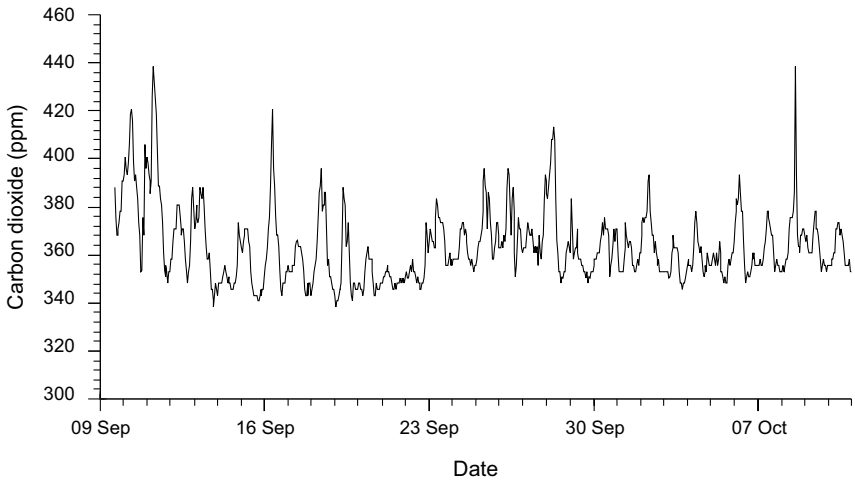

Fig. 23.4. CO_2 in air at the fresh air intake of the Freshwater Institute, Winnipeg, MB. Canada. Measured with a Li-Cor LI-6262 IRGA

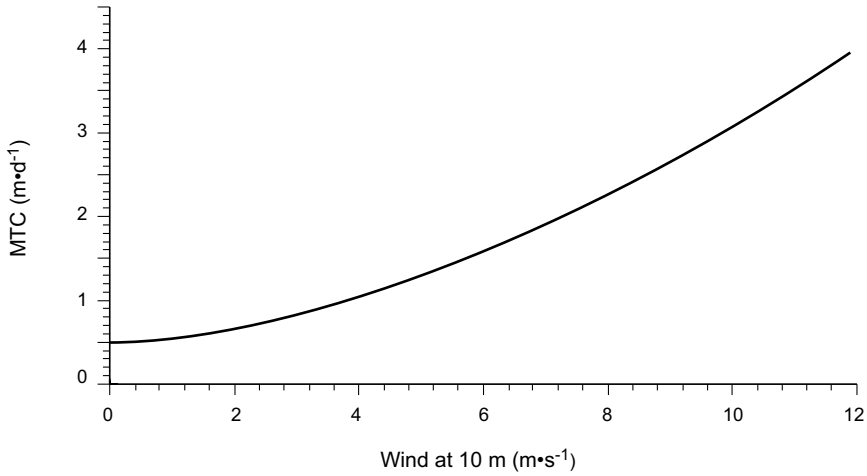

Fig. 23.5. The relationship between wind velocity and MTC (mass transfer coefficient) calculated from the equation of Cole and Caraco (1998)

23.6 Conclusion

In conclusion we must emphasize how important it is that measurements or calculations of instantaneous fluxes of gases at the air water interface be placed in the proper context for the accurate estimation of net production. When taking into consideration the more comprehensive data sets for CO_2 in freshwater systems available in the literature, it is apparent that the precision of the measurement of CO_2 is not the most important source of error. Natural variability due to flow, wind, and photosynthesis causes much larger changes than are likely to result from sampling methods or analytical techniques. Two approaches are possible to address the problem. 1. High frequency measurements can be made, probably at least every four hours to resolve photosynthetic effects. This can be achieved with modern instrumentation. 2. Alternately, fewer measurements of CO_2 could be made, but the characteristics of the lake such as photosynthetic rates would have to be relatively well defined and at least continuous wind velocities would have to be available to adequately model the flux. I would recommend that in the absence of continuous monitoring, an instrument package of the type described by Carignan (1998) be used for at least a few periods to characterize the variation before a monitoring schedule is designed. This would also provide the information required to chose the appropriate model parameters.

24 A One-Dimensional Model for Simulating the Vertical Transport of Dissolved CO_2 and CH_4 in Hydroelectric Reservoirs

Nathalie Barrette and René Laprise

Abstract

The goal of this project consisted in developing a mathematical model capable of simulating the physical processes responsible for the vertical transport of dissolved greenhouse gases (GHG) in hydroelectric reservoirs. This combined approach of measurement and numerical modeling confirmed certain hypotheses concerning the missing CO_2 source and the amount of methane oxidation. Moreover, a relation between differences in GHG emission patterns and reservoir depth was revealed. The numerical model developed in this study can be used to determine sampling strategies based on the temporal and spatial distributions of a given reservoir.

24.1 Introduction

The first research projects on greenhouse gas emissions from hydroelectric reservoirs focused on field measurements. The researchers concentrated primarily on developing sampling and analytical techniques for geographically limited measurements of gas fluxes at the air-water interface. The researchers initially ran into some very concrete obstacles, namely: (i) there was no existing apparatus capable of conducting continuous 24-hour sampling of the GHG and related concentration profiles in the water during the whole ice-free period; (ii) as the time spent out on the reservoir was often limited for reasons of safety, sampling was excluded during certain periods of the year, namely the spring thaw, autumn turn-over and strong wind events; (iii) given that the analysis of each sample required a considerable amount of laboratory time, sampling was restricted; (iv) since the selected study sites had to be accessed by boat in a short amount of time if the sam-

ple was to be successfully analyzed, certain sectors of the reservoirs were not included in the sampling; and, finally (v) because the measurement campaigns were primarily carried out in geographically isolated places, the costs involved were quite high. Despite all these constraints, the numerous data gathered during the first measurement campaigns clearly identified that hydroelectric reservoirs emit GHG in the form of CO_2 and CH_4 (Duchemin et al. 1995; Duchemin et al. 1999). In order to counterbalance these constraints in the experimental approach, we developed a model that would allow us to make greater use of this data and obtain better temporal and spatial coverage. The model was intended to complement the experimental approach initially used in studies of GHG in hydroelectric reservoirs.

In particular, the mathematical computer model we have developed is able to simulate the physical processes underlying the vertical transport of dissolved gases in hydroelectric reservoirs, from the flooded soil to the air-water interface. In an ideal context, a numerical model that simulates CO_2 and CH_4 at the surface of hydroelectric reservoirs would have included all of the production, fixation and transport processes of these gases from the moment they are created until they escape into the atmosphere. Nonetheless, at the time this project was conducted (1995-1999), there was only partial knowledge about the production and fixation processes. Since the processes could not be explicitly defined in the numerical model, they were incorporated in the model based on our field estimates and the data from the literature.

We began this project by looking for an existing lake model that: (i) was based on the physical laws controlling the heat fluxes both in the lake and between the lake and atmosphere; (ii) was driven by a restricted number of observed or estimated weather variables; (iii) did not require any adjustment of the lake's physical parameters; (iv) was sensitive to the physical characteristics of the lake (bathymetry and turbidity); (v) simulated evaporation for various periods of integration; and (vi) was valid for a great diversity of lakes and climates.

Based on this model, we (i) studied the temporal and spatial distribution of the CO_2 and CH_4 flux at the surface of a northern reservoir; (ii) examined the temporal and spatial distribution (three stations at different depths) of the dissolved CO_2 and CH_4 profiles in a northern reservoir; (iii) considered the sensitivity of the vertical transport of dissolved gases to different meteorological parameters; and (iv) estimated the annual CO_2 and CH_4 emissions in various reservoirs.

In this chapter, we first describe the methods used to calculate the energy balance components. We then provide a detailed description of the parameterization of turbulent diffusion, convective transport and ice for-

mation, as well as the various methods used for the calculation of gas fluxes at the air-water interface. We also give an overview of the main results of the sensitivity tests and validation model. Finally, we provide an example of how the model can be applied by calculating an estimate of the annual CO_2 emissions from the Laforge-1 and La Grande-2 reservoirs (Fig. 24.1).

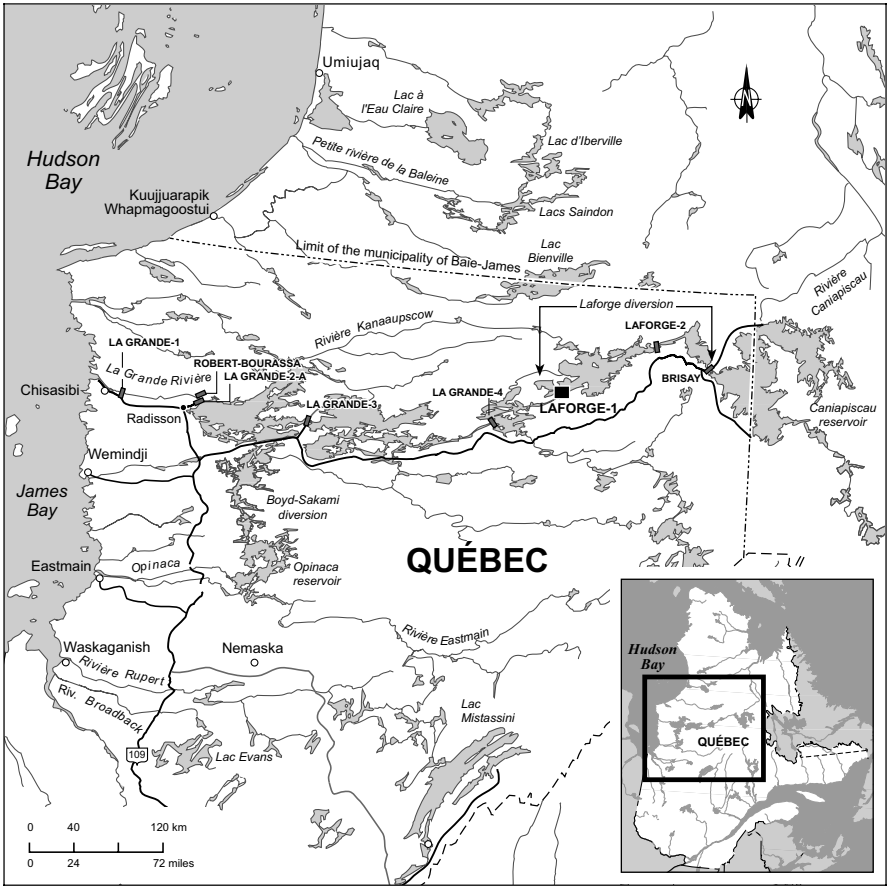

Fig. 24.1. Map of the study area

24.2 Thermodynamic Lake Models

There are two main categories of simple thermodynamic lake models, namely mixed-layer models and turbulent diffusive models. A mixed-layer model initially assumes the existence of an homogeneous layer below the

surface, whereas a turbulent diffusive model is able to describe the vertical profile of properties such as temperature and constituent concentrations. The main advantage of the mixed-layer equation is the shorter computing time, since all the characteristics of the upper part of the lake are represented by a single prognostic equation (Henderson-Sellers 1987).

For our study, however, vertical transport profiles were required in order to assess gas fluxes at the air-water interface. The lake model used in this study is an extension of the 1-D lake model initially developed by Hostetler (1987) and Hostetler and Bartlein (1990). It is a numerical column model of vertical transport of mass and heat by diffusion and convection. The model uses several meteorological variables as input data, namely air temperature, humidity, wind speed and net balance of solar and terrestrial radiation. Some additions were made to the original version of Hostetler's model: 1) constituent equations for CO_2 and CH_4 were added and 2) two different techniques were used to calculate the gas fluxes at the air-water interface: a bulk aerodynamic technique (BAT) (McFarlane and Laprise 1985) and a method using a thin boundary layer model (TBL) (Hamilton 1992).

24.3 Description of the Hostetler Lake Model

24.3.1 Energy Balance Equations

To simulate the evolution of the thermal lake profile, the energy balance at the surface (SEB) and internal energy balance (IEB) must be considered. The SEB is the algebraic sum of all the energy fluxes at the lake's air-water interface and is written (Hostetler, 1987):

$$\Delta Q_s = K_d - K_r + L_{ra} - L_u - Q_e - Q_h + Q_{ice} \qquad (24.1)$$

where ΔQ_s: variation of the energy stored in the lake ($w \cdot m^{-2}$)
- K_d: total incident solar radiation (direct and diffusive) ($w \cdot m^{-2}$)
- K_r: reflected solar radiation ($w \cdot m^{-2}$)
- L_{ra}: incident terrestrial radiation ($w \cdot m^{-2}$)
- L_u: emitted terrestrial radiation ($w \cdot m^{-2}$)
- Q_e: latent heat flux lost due to evaporation ($w \cdot m^{-2}$)
- Q_h: sensible heat flux given to (>0) or received from (<0) the atmosphere ($w \cdot m^{-2}$)
- Q_{ice}: latent heat flux due to melting (>0) or freezing (<0) of ice ($w \cdot m^{-2}$)

Moreover, the IEB looks at the energy exchanges which take place in the total volume of the lake. The IEB is written (Hostetler 1987):

$$\Delta Q_S = Q_{surf} + Q_{abs} \tag{24.2}$$

where Q_{surf}: heat flux absorbed by the surface layer ($w \cdot m^{-2}$)
Q_{abs}: absorption of penetrating solar radiation under the surface ($w \cdot m^{-2}$)

Two terms can be added, namely the heat flux added or withdrawn by water arrival in the lake and the heat flux added or withdrawn through the bottom of the lake.

By regarding the lake as a series of horizontal layers of finite thickness, the energy balance of one of the layers below the water surface can be written:

$$\delta q_S = q_{abs} + (q_{din} - q_{dout}) + (q_{cin} - q_{cout}) \tag{24.3}$$

where δq_S: variation in the energy stored in the layer ($w \cdot m^{-2}$)
q_{abs}: solar energy absorbed by the layer ($w \cdot m^{-2}$)
q_{din}: diffusive heat flux entering the layer ($w \cdot m^{-2}$)
q_{dout}: diffusive heat flux out of the layer ($w \cdot m^{-2}$)
q_{cin}: convective heat flux entering layer ($w \cdot m^{-2}$)
q_{cout}: convective heat flux out of the layer ($w \cdot m^{-2}$)

The coupling of Eqs. 24.1, 24.2 and 24.3 constitutes the basis for the construction of a lake model capable of simulating the evolution of the thermal profile starting with the net energy balance. The equations used to calculate the terms in Eq. 24.1 are provided in greater detail in Barrette (2000).

24.3.2 Turbulent Diffusion

The heat flux inside the lake is transported by turbulent (eddy) diffusion. Turbulent diffusion implies a turbulent exchange of heat induced either by the mechanical forcing of the atmosphere (wind) or by the thermal stratification of the lake (density gradient). The turbulent diffusion process plays an important role in determining a lake's thermal structure. It is noteworthy that the majority of the heat transfer occurs vertically (horizontal homothermy), and, under these conditions, a water column model should be enough to describe the evolution of the lake's temperature profile.

Mathematical Equation for Heat

By considering that the lake temperature is related to z (depth) and t (time), the equation expressing temperature change can be written as follows (Hostetler 1987):

$$\frac{\partial T}{\partial t} = \frac{\partial}{\partial z}\left[\left(k_m + K(z,t)\right)\frac{\partial T}{\partial z} \right] + \frac{1}{c}\frac{\partial [\phi]}{\partial z} \tag{24.4}$$

where T: temperature (°C)
t: time (s)
z: depth (m)
k_m: molecular diffusion ($m^2 \cdot s^{-1}$)
K: eddy diffusion ($m^2 \cdot s^{-1}$)
c: water heat capacity ($J \cdot Kg^{-1} \cdot °C^{-1}$)
ϕ: heat source term ($w \cdot m^{-2}$)

The first term on the right of Eq. 24.4 represents heat transfer by turbulent and molecular diffusion, and the second term, heating by direct absorption of solar radiation.

To complete Eq. 24.4, it is necessary to specify both the boundary and initial conditions. The condition at the lake surface is a function of energy balance, that is:

$$\left(k_m + K(z,t)\right)\frac{\partial T}{\partial z}\Big|_{z=0} = K^* + L_{ra} - L_u \pm Q_e \pm Q_h \pm Q_{ice} \tag{24.5}$$

Assuming no energy exchange between the sediments and lake, then the conditions at the bottom of the lake are:

$$(k + K(z,t))\frac{\partial T}{\partial z}\Big|_{z=b} = 0 \tag{24.6}$$

However, this last boundary condition can be replaced by an interactive boundary between the lake bottom and its water volume.

Initial conditions are necessary to describe the lake's water temperature profile at the initial time. For lack of adequate observations, isothermal conditions are often chosen. The temperature at initial time is thus defined as:

$$T[0,z] = T_0, \text{ for } 0 \le z \le b \tag{24.7}$$

However, any other non-isothermal profile can be used for the initial conditions.

Mathematical Equation for Passive Tracers

An equation similar to 24.4 can also be used for the transport of tracers in the water column, such as CO_2 and CH_4. Equation 24.5 becomes, in the case of tracer diffusion:

$$\frac{\partial \varphi}{\partial t} = \frac{\partial}{\partial z}\left[\left(k_m + K(z,t)\right)\frac{\partial \varphi}{\partial z}\right] \tag{24.8}$$

where φ : tracer concentration ($g \cdot m^{-3}$)

To complete Eq. 24.8, it is necessary to specify the boundary conditions as well as the initial conditions. To evaluate tracer flux at the surface of the reservoir, we will use various methods which we will present in Sect. 24.4.

Fluxes at the bottom of the reservoir are set in the model using the benthic fluxes (corresponding to the organic degradation of flooded soil and the bacterial activity in the biofilm just below the flooded soil) measured during the sampling period, whereas the initial concentration profiles vary according to the season and the depth of the station being studied.

Numerical Technique

Numerical techniques make it possible to replace continuous partial derivative equations by algebraic equations which can be solved on a computer. The diffusion equation is a second order, parabolic partial derivative equation with two independent variables (z and t). Parabolic equations are typically found in evolving diffusion problems such as heat equations. There are two basic methods to solve such equations: explicit and implicit methods. The implicit Crank-Nicholson method (Nougier 1987) offers numerical stability at the cost of minor algebraic complexity and thus was used for the resolution of Eqs. 24.4 and 24.8. The solution with this method is based on a temporal grid with a one-hour resolution and a vertical mesh varying according to the depth of the station being studied.

Calculation of the Turbulent Diffusion Coefficient (K)

Henderson-Sellers (1985) proposed a method for a turbulent diffusion formula in neutral conditions which does not require any empirical adjustment. In this method, the coefficient of turbulent diffusion in neutral conditions is given by:

$$K_0(z) = (kw^* z/P_0)\, e^{(-k_{ek}z)} \tag{24.9}$$

where v_k: Von Karman constant (0.4)
P_0: Prandtl number in neutral conditions (1.0)
w^*: friction velocity ($m \cdot s^{-1}$)
k_{ek}: latitude parameter

The friction velocity is given by:

$$w^* = 1.2x10^{-3}\, U \tag{24.10}$$

where U is wind speed ($m \cdot s^{-1}$) above the lake.

The k_{ek} term represents a parameter which depends on the latitude of the Ekman profile and is given by:

$$k^* = 6.6\, (\sin \phi)^{1/2}\, U^{-1.84} \tag{24.11}$$

where ϕ: latitude of the lake.

The turbulent diffusion coefficient in stratified conditions is given by:

$$K(z) = (kw^* z/P_0)\, e^{(-kz)}\, (1+37\, Ri^2)^{-1} \tag{24.12}$$

where the Richardson number is given by:

$$Ri = \{-1+[1+40N^2k^2z^2/(w^{*2}\, e^{(-2k^*z)})]^{1/2}\}/20 \tag{24.13}$$

and where the Brunt-Väisälä frequency, N^2, is given by:

$$N^2 = -\frac{g}{\rho_w}\frac{\partial \rho_w}{\partial z} \tag{24.14}$$

The density of water, ρ_w, is calculated as a function of temperature, salinity, if applicable, and pressure (Henderson-Sellers 1985).

The method suggested by Henderson-Sellers (1985) has the advantage of not requiring that parameters be empirically adjusted to the specific lake. This approach thus allows the simulation of the energy balance and the monitoring of a lake or reservoir's thermal profile without carrying out a specific adjustment for the lake other than to specify its depth and to provide the required surface flux.

24.3.3 Convective Adjustment

Convective adjustment is based on the assumption that considerable anomalies of temperature, resulting in an unstable profile (i.e., a layer of hot water under a layer of cold water) cannot last for long periods of time (Henderson-Sellers and Davies 1988). Thus, when an abnormal temperature variation occurs during the simulation, the model calls upon a convection scheme intended to bring the temperature back towards a neutral isothermal profile. For a temperature anomaly taking place at a depth z_a, the convective adjustment is carried out to preserve the energy:

$$Tz_a = \int_{-z_a}^{0} A(z)T(z)dz \Big/ \int_{-z_a}^{0} A(z)dz \tag{24.15}$$

where $T\,z_a$ is the new isothermal temperature at a depth z_a.

This convective scheme makes it possible to simulate the shallow convective mixtures (under the surface) and the deep convective mixtures which take place in early spring, late in the autumn and during the winter. Convection, when it occurs, will also mix the concentration profiles of the dissolved gases CO_2 and CH_4.

24.3.4 Ice Model

The ice model used by Hostetler and Bartlein (1990) is a modified version of the Patterson and Hamblin (1988) model. This model is based on the physics and thermodynamics which control the transport of heat through fresh water, ice and the atmosphere.

The principle postulates at the base of this model are as follows: (i) there is formation of ice when the water surface temperature is 0°C and less, and melting when the temperature is 0°C and more; (ii) increasing or melting ice varies in an exponential way over time (due to the changes in surface fluxes in the presence of ice); (iii) the fusion heat is added or subtracted from the surface energy balance depending on whether there is ice formation or melting; (iv) there is only molecular diffusion under the ice cover (i.e., no turbulent diffusion); (v) the convective movements persist under the ice cover. These postulates follow the work of Pivovarov (1973), Ragotzkie (1978) and Oke (1978).

When the temperature of the air is higher or equal to the melting point, the equation of the surface energy balance becomes:

$$-Q_l = K_d - K_r + L_{ra} - L_u - Q_e - Q_h + L_i\rho_i(dh/dt) \quad \text{if } T_a > T_m \quad (24.16)$$

where Q_l: upwards heat flux, just above ice surface
L_i: latent heat of fusion
ρ_i: ice density ($g \cdot m^{-3}$)
dh/dt: melting rate of surface ice
T_m: fusion temperature of ice (0°C)
T_a: surface air temperature (°C)

The calculation of the terms Lu, Qe and Qh is adapted for ice (Brutsaert 1982). For example, for the Qe calculation, we use the latent heat of sublimation rather than the latent heat of vaporization.

The rate of ice formation or melting at the ice-water interface is determined by the surface energy balance and is expressed by:

$$-Q_f + Q_w = L_i\rho_i(dh/dt) \quad (24.17)$$

where Q_f represents the sum of Q_l and solar radiation absorbed by the ice layer. The Q_w term is the heat flux coming from the volume of water under the ice and is expressed as:

$$Q_w = -K_w \frac{\partial T}{\partial z} \quad (24.18)$$

where K_w is the thermal conductivity of water and T, the water temperature.

The total thickness of the ice is thus determined by Eqs. 24.16, 24.17 and 24.18.

24.4 Calculation of CO_2 and CH_4 Fluxes at the Air-Water Interface

To calculate CO_2 and CH_4 fluxes on the reservoir's surface, two different approaches were tested: the technical bulk aerodynamic technique (BAT) and the thin boundary layer model (TBL). The first formula uses turbulent exchange coefficients whereas the second is similar to a mixed-layer model.

24.4.1 Bulk Aerodynamic Technique (BAT)

This aerodynamic equation uses the turbulent exchange coefficient which represents the mechanical interaction between the movement within the atmospheric mixed-layer and the water surface. To calculate GHG fluxes on the surface, a drag coefficient (C_D) is used which is a function of stability and surface roughness. The equation used for the calculation of GHG surface flux is written (Peixoto and Oort 1992):

$$F_{GHG} = C_D\, U\, \rho_a\, ([GHG]_w - [GHG]_a) \tag{24.19}$$

where C_D: drag coefficient
U: wind speed ($m \cdot s^{-1}$)
ρ_a: air density ($g \cdot m^{-3}$)
$[GHG]_w$: surface water GHG concentrations ($g \cdot m^{-3}$)
$[GHG]_a$: surface air GHG concentrations ($g \cdot m^{-3}$)

The drag coefficient is a function of the Richardson number which is a measurement of stability in the atmosphere. As in the Canadian GCM, the Richardson number is calculated using the following expression (McFarlane and Laprise 1985):

$$Ri_B = g\, z_1\, T_a^{-1}\, (T_a - T_w)\, U^{-2} \tag{24.20}$$

where g: gravitational acceleration ($m \cdot s^{-2}$)
z_1: height of the anemometer (m)
T_a: air temperature (°C)
T_w: water surface temperature (°C)

Finally, the drag coefficient is evaluated using the following expressions according to whether the situation is unstable ($Ri_B < 0$) or stable ($Ri_B \geq 0$) (Henderson-Sellers 1987):

$$C_D = C_{D0}\, (1 + 24.5\, |C_{D0}\, Ri_B|^{0.5}) \quad \text{if } Ri_B < 0 \tag{24.21}$$

$$C_D = C_{D0}\, (1 + 11.5\, Ri_B)^{-1} \quad \text{if } Ri_B \geq 0 \tag{24.22}$$

where $C_{D0} = v_k^2\, (\ln(z_1/z_w))^{-2}$, v_k and z_w represent the von Kármán constant and the height of the surface roughness respectively.

24.4.2 Thin Boundary Layer (TBL)

The TBL approach was developed initially by Whitman (1923) to study the absorption of the HCl gas through an air-liquid interface in an experimental system. Liss (1967) was the first to adapt this method to natural

systems. The GHG flux ($mmol \cdot m^{-2} \cdot h^{-1}$) at the air-water interface is expressed in the following way:

$$F_{GHG} = k_{GHG} ([GHG]_w - [GHG]_{equil}) \quad (24.23)$$

where k_{GHG}: GHG piston velocity ($cm \cdot h^{-1}$)
$[GHG]_w$: surface water GHG concentrations ($mmol \cdot m^{-3}$)
$[GHG]_{equil}$: water GHG concentrations at in situ temperature and pressure and in equilibrium with the atmospheric GHG concentrations ($mmol \cdot m^{-3}$)

The value of k_{GHG} is calculated using the following expressions, according to whether the wind speed is higher or lower than 3 $m \cdot s^{-1}$:

$$K_{GHG} = k_{600} (600^{0.67}) (sc^{0.67})^{-1} \quad \text{if } v < 3 \text{ m} \cdot s^{-1} \quad (24.24)$$

$$K_{GHG} = k_{600} (600^{0.5}) (sc^{0.5})^{-1} \quad \text{if } v \geq 3 \text{ m.s}^{-1} \quad (24.25)$$

where k_{600}: piston velocity standardized for SF6 gas
sc: Schimdt number

An experiment conducted with SF6 gas by Crusius and Wanninkof (1991) made it possible to determine two linear equations expressing the evolution of k600 according to wind speed. The values of k600 are calculated using the following expressions:

$$k_{600} = 0.76 \text{ v} \quad \text{if } v < 3 \text{ m} \cdot s^{-1} \quad (24.26)$$

$$k_{600} = (5.6 \text{ v}) - 14.4 \quad \text{if } v \geq 3 \text{ m} \cdot s^{-1} \quad (24.27)$$

The Schimdt number is calculated in the following way:

$$sc = kiv / dc_{GHG} \quad (24.28)$$

where kiv: kinematic viscosity (poise)
dc_{GHG}: diffusion coefficient for GHG ($cm^2 \cdot s^{-1}$)

The terms kiv and dc_{GHG} are calculated from:

$$kiv = h (\rho_W + 0.033) \quad (24.29)$$

$$dc_{GHG} = (3.39 \times 10^{-7} T_s) + 9.1 \times 10^{-6} \quad (24.30)$$

where h: water viscosity (poise)
ρ_W: water density ($g \cdot ml^{-1}$)
T_s: water surface temperature (°C)

This method is described in detail by Hamilton (1992). It is worth noting that this method has been used to estimate the flux of CO_2 and CH_4 at

the surface of the reservoirs since the very beginning of the research project on greenhouse gases (Duchemin et al. 1999). This technique requires less laboratory analysis and is faster for sampling than the static chamber method.

The lake model presented here requires very few specific adjustments to the lake or reservoir being studied, thereby allowing a broader use than many other models in terms of variety of climates and aquatic environments.

The BAT method seems to compare best with the measurements (Fig. 24.2), while the TBL method tends to generate an excessive occurrence of weak fluxes (<500 $mg{\cdot}m^{-2}{\cdot}d^{-1}$). Though this problem is also encountered in the BAT method, it is less common. In addition, both methods reproduce too few events exceeding 3000 $mg{\cdot}m^{-2}{\cdot}d^{-1}$ (Fig. 24.2). For all the simulated cases, the TBL method produced a wider range of values of GHG fluxes and concentrations than did the BAT method.

24.5 Results

24.5.1 Model Definition of Atmospheric GHG Concentrations and GHG Sources and Sinks

The emission of GHG into the atmosphere from reservoirs naturally depends on the atmospheric GHG concentrations. Analysis of the CO_2 atmospheric concentration measured at the LA-1 reservoir led us to conclude that the CO_2 atmospheric concentration defined in the model needed to include seasonal variability. Based on the literature (Pearman and Hyson 1981; Fraser et al. 1986) and local observations, an algebraic function fitting the seasonal variations of atmospheric CO_2 was developed for the model. The methane concentrations observed at LA-1 indicated that the seasonal variations were small enough (<1%) to be ignored. Thus, a constant value equivalent to 2.02 ppmv was assigned to the CH_4 atmospheric concentration and a CO_2 atmospheric concentration varying from 370 ppmv to 393 ppmv was set to represent the annual cycle.

The GHG sources set in the model for the ice-free period correspond to the organic degradation of flooded soil and the bacterial activity in the biofilm just below the flooded soil. These sources were estimated using the benthic values of fluxes measured at the LA-1 reservoir between 1994 and 1997. Average values were calculated by considering only the chambers having been submerged in water for a period of more than 15 hours. The averages thus obtained are 1121 $mg{\cdot}m^{-2}{\cdot}d^{-1}$ and 5 $mg{\cdot}m^{-2}{\cdot}d^{-1}$ for CO_2 and

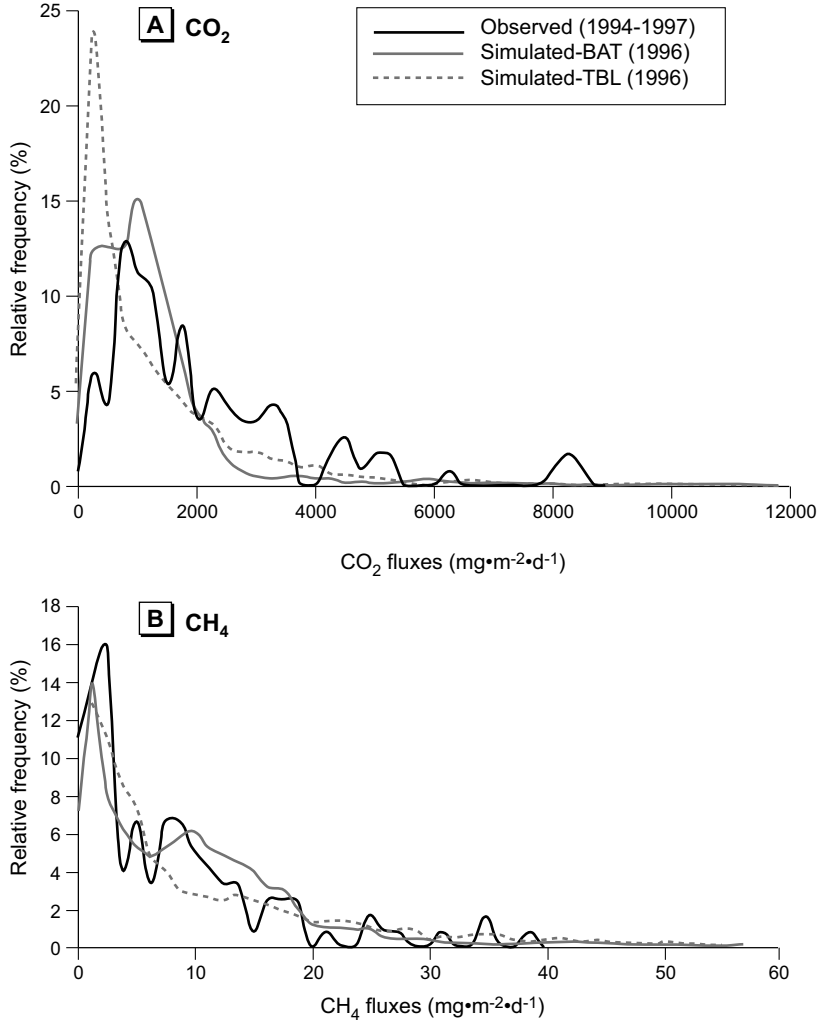

Fig. 24.2. Relative frequencies of observed and simulated CO_2 and CH_4 surface fluxes, LA-1 reservoir

CH_4 respectively. Duchemin (2000) observed that benthic fluxes were rather insensitive to the station depth and the type of flooded ground, and did not vary much from one reservoir to another. The same source values were thus defined for the various stations being studied with the model.

GHG fluxes toward the atmosphere were negligible when ice sheets were present, thus resulting in an accumulation of dissolved gases in the water column for the winter period under the ice sheet. For the ice-covered

period, the principal source of CO_2 and CH_4 was considered to come only from the organic degradation of the flooded soil, and the biofilm was assumed to be inactive during this period. Averages were calculated based on the gas fluxes measured at the level of the soil-water interface (subsurface water) in the LA-1 reservoir between 1994 and 1998. The averages thus obtained are 77 $mg{\cdot}m^{-2}{\cdot}d^{-1}$ and 2 $mg{\cdot}m^{-2}{\cdot}d^{-1}$ for CO_2 and CH_4 respectively.

24.5.2 Sensitivity Test and Validation

Sensitivity of the Model to Initial Conditions

A series of experiments were designed to assess the sensitivity of the model to the initial temperature and dissolved GHG concentrations, and to determine the adjustment time. The sensitivity tests were done using measurements taken in 1995 at the LA-1 reservoir. Basic principles suggest that the adjustment time is proportional to the square of the depth of the station. Hence, for a shallow station, the initial temperature and dissolved GHG concentrations do not greatly influence behaviour in the reservoir in the medium and long term, whereas for a deep station, the initial values influence the results for more than 3 months. The experiments carried out on the validation and application of the model thus allowed for a sufficiently long adjustment period (9 to 12 months), in particular in the case of deep stations, so that the effect of the initial conditions is negligible.

Sensitivity of the Model to Weather Variables

From the analysis of measurements, Duchemin (2000) concluded that the weather variables that had the strongest influence on the variations of the GHG fluxes at the surface of the reservoirs are surface air temperature and wind speed. The response of the model to these two weather variables and their influence on the transport of dissolved GHG in the reservoir and their emission into the atmosphere were studied.

It is reasonable to think that an increase in wind speed would result in an increase in GHG surface fluxes due to more intense ventilation on the surface. However, the results of the sensitivity simulations carried out for a deep station instead show a readjustment of the temporal distribution of GHG surface fluxes.

It was generally found that, in the case of a deep station, wind speed modifies the structure of the thermal profile and the asymptotic temperature values, whereas for a shallow station, the profile is more uniform and changes are limited solely to the asymptotic temperature values (Barrette

2000; Barrette and Laprise 2002). Changes in wind speed generate some differences in dissolved GHG concentration profiles, which are more significant in the case of deep stations than in that of shallow stations.

Comparison of Model-Simulated Results with Observations for the Freezing-Thawing Cycle and Temperature Profile

The model successfully reproduces the freezing-thawing cycle for the LA-1 reservoir. The thaw date simulated by the model (June 15) corresponds to 1996 observations. The Canadian Ice Centre estimated the maximum ice thickness accumulated on the surface of the lakes in the La Grande (James Bay) region to be 1.2 m in 1996; the model simulated a maximum thickness of 1.4 m.

In general, the model concurs with observations of water temperature profiles (Barrette 2000; Barrette and Laprise 2002). Nevertheless, the model tends to over-estimate water temperature values at the beginning of the summer by ≅1°C, and to underestimate them towards the end of the summer by ≅2°C (Barrette 2000; Barrette and Laprise 2002). It is noteworthy that the water level of the LA-1 reservoir is subject to fluctuation during the ice-free period; these fluctuations can result in significant changes in the thermal characteristics of water in the reservoir, and these were not considered in the model.

Comparison of Model-Simulated Results with Observations for Carbon Dioxide

The model accurately reproduces the observed profiles of dissolved CO_2 concentrations in the water column for the ice-break-up date, June 15. Later in the ice-free season, however, the model underestimates the values of dissolved CO_2 concentrations, these differences increasing through July and August. Simulations successfully reproduce the observed distributions of dissolved CO_2 concentrations in the water column in the case of shallow stations. For deeper stations, however, the model underestimates the range of distribution; this may be due to the fact that the model simulates several episodes with thermocline, whereas the presence of such a thermocline was, somewhat surprisingly, never recorded.

Duchemin (2000) observed that the concentrations of dissolved CO_2 in the water were higher under the ice-cover than during the ice-free period. In fact, they observed that the dissolved CO_2 concentrations ranged between 5 $g{\cdot}m^{-3}$ and 15 $g{\cdot}m^{-3}$ for the winter period. The model simulates this interval relatively well, with values ranging between 1 $g{\cdot}m^{-3}$ and 12 $g{\cdot}m^{-3}$

depending on the simulated station (Barrette 2000; Barrette and Laprise 2002).

The deterioration of simulated results in the summer, as noted previously, indicates that the defined source intensity is insufficient during the ice-free period. This missing source might be related to bacterial production in the water column as described by Duchemin (2000). The incubation experiments with water column samples taken from LA-1 in 1996 showed that the bacterial production of CO_2 in the water column is negligible at the beginning of June but high at the end of July (Duchemin 2000). They estimated that the carbon dioxide formed by a fermentative oxidation of organic matter present in the water column represented between 20% to 100% of the observed atmospheric CO_2 fluxes and that this source was dominant at deep stations. The model results (obtained thus far without consideration of bacterial production) also show that it is at the deep stations that the most significant differences occur between the simulated and observed values of CO_2 fluxes. Assuming that the CO_2 source present in organic degradation of flooded soil is adequately defined in the model, and that the modelled surface fluxes are of the order of observed CO_2 fluxes, the deficit associated with the missing source in the model (fermentative oxidation of organic matter in the water column) varies from 20% at the shallow station to 70% at the deep station. The degradation of organic material in the water column thus seems to correspond, in both qualitative and quantitative terms, to the missing source highlighted in the analysis of simulated results.

Finally, it is also possible that the difference in the underestimation between early spring and late summer is also due in part to the absence of seasonal effects in the regulation of the CO_2 sources associated with the degradation of organic material in the flooded soil. A review of the literature reveals that temperature is one of the most important parameters determining the CO_2 production/fixation processes (Svesson 1984; Whalen et al. 1991; Raich and Schlesinger 1992; Dunfield et al. 1993; Moosavi and Crill 1996). Duchemin (2000) noted that benthic fluxes varied with the seasons. Several scientists are working to develop biogeochemical models of CO_2 production and fixation in various natural environments (e.g. Falloon et al. 1998; Martens et al. 1998; Hulzen et al. 1999).

Comparison of Model-Simulated Results with Observations for Methane

A first series of simulations was performed without taking into account the oxidation of methane in the water column above the flooded soil. The results obtained showed significant over-estimations of methane concentra-

tions (Barrette 2000). Duchemin (2000) estimated that 50 to 75% of the CH_4 produced in the flooded soil was oxidized before reaching the atmosphere. Incubation experiments with the water column samples also showed that the CH_4 oxidation rates are more significant at the beginning of the summer than at the end of August (Duchemin 2000), thus perhaps explaining why the model more adequately simulates dissolved CH_4 concentrations at the end of August than at the beginning of the summer. Finally, it is worth noting that, according to Duchemin (2000), oxidation is more significant above a flooded peat bog than above a flooded forest floor. The most significant differences between the simulated and observed values of dissolved CH_4 concentrations were, moreover, noted at the station located above a flooded peat bog.

The ability of the model to reproduce the frequency distribution of observed CH_4 fluxes was assessed. Overall, the results were substantially improved with the addition of methane oxidation. However, the regulation of oxidation had to be refined by including the seasonal effects. Indeed Duchemin (2000) observed, from incubation experiments, that the methane oxidation rates varied substantially in response to the season. Moreover, they noted significant variations in relation to the sampling depth. Further measurements must therefore be taken in order to establish a parametric function for methane oxidation rates in terms of the most influential factors.

24.5.3 Application: Comparison of the Annual CO_2 Emissions for Two Reservoirs in Central Northern Québec

In this last section of this chapter, the model is used to estimate the amount of CO_2 emitted by the LA-1 and LG-2 reservoirs in 1997. It is worth restating that the simulated annual emissions of CO_2 probably underestimate the real emissions because the CO_2 source associated with bacterial activity in the water column was not accounted for in the model. Nevertheless, it is believed that the model can be used as starting point for a distributed comparison of hydroelectric installations. Indeed, in his statistical analysis of GHG fluxes, Duchemin (2000) highlighted the need for integrating such inter-basin analysis in the development of a long-term sampling strategy. According to this author, neglecting such an analysis when developing a tool for evaluating GHG emissions would considerably decrease the effectiveness of this tool.

Simulations of the column model were run for the LA-1 and LG-2 reservoirs with conditions that corresponded to the weather variables observed at each reservoir. The purpose was to evaluate how the physi-

ographic characteristics of these reservoirs influence the vertical transport towards and the emission of CO_2 into the atmosphere. Ideally, the proper evaluation of the annual emissions of CO_2 for all of these reservoirs would have required detailed knowledge of the reservoirs' bathymetry. This information would have made it possible to evaluate, for each reservoir, the surface occupied by the various depth categories. Unfortunately, we do not have access to this data and the evaluation of the annual emissions of CO_2 per reservoir had to be modelled using a simple representative depth. The average depths of the LA-1 and LG-2 reservoirs are around 4 m and 20 m respectively. The CO_2 sources were set the same for both reservoirs because Duchemin (2000) observed that benthic fluxes did not vary significantly from one reservoir to another. The CO_2 sources were set as defined in Sect. 24.5.1.

It is noteworthy that despite the assumption in the model that the two reservoirs had identical CO_2 sources, the different physiographic characteristics of the reservoirs as well as local weather conditions and geographical position are able to produce different simulated CO_2 emission patterns. The model hence simulates higher 1997 annual emission for LG-2 (198 $g{\cdot}m^{-2}{\cdot}an^{-1}$) than for LA-1 (179 $g{\cdot}m^{-2}{\cdot}an^{-1}$) (Fig. 24.3). These simulated values are in apparent contradiction with the estimated values of 258 $g{\cdot}m^{-2}{\cdot}an^{-1}$ for LG-2 and 320 $g{\cdot}m^{-2}{\cdot}an^{-1}$ for LA-1 deduced by Duchemin (2000) based on his samples taken during the period from 1993 to 1997. As explained before, the substantially lower simulated values result from missing sources in the model. The fact that the ratios of LG-2/LA-1 annual values differ in the model and the observation-based estimates may in part result from the absence of measurements taken during the strong autumnal peak emission at LG-2, thus resulting in a substantial underestimation of real fluxes at LG-2. It is hoped that the model simulation can contribute to the development of more effective sampling strategies, based on the characteristics of the GHG emission pattern associated with each reservoir.

24.6 Conclusion

With the advent of fast and affordable computers, numerical modelling is rapidly becoming a powerful integrating tool for studying complex phenomena. One advantage of physically based numerical models is that they constitute virtual laboratories where a large number of experiments can be performed inexpensively and in a relatively short lapse of time. The interpretation of such simulated results, however, is directly related to the state of the quantitative, observation-based knowledge of the phenomenon. In

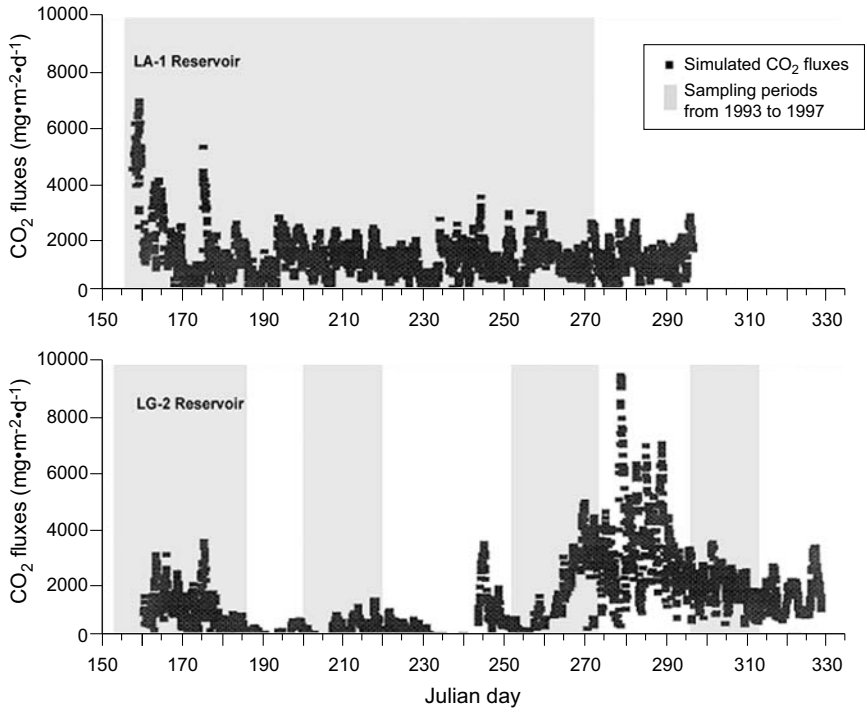

Fig. 24.3. Simulated CO_2 fluxes at air-water interface for LA-1 and LG-2 reservoirs in 1997 and the sampling periods from 1993-1997

other words, modelling can constitute an excellent complementary tool to field and laboratory experiments, but it cannot replace the actual study of a phenomenon or process.

This increasing complexity has allowed the models to be used by an ever-greater public, extending from scientific researchers to political decision makers. In fact, the models' results are increasingly used by public authorities to devise strategies in fields such as agriculture, forestry, economy or health (IPCC, 2001).

The research presented in this chapter illustrates the relevance of the complementary approaches of experimentation and modelling. While some of the physical processes, such as those associated with the transport of the dissolved GHG towards the surface, are well understood and can be correctly modelled, others such as the chemical and biological processes underlying GHG sources, remain elusive. Nonetheless, the model developed for this study has contributed to a better understanding of the processes and has confirmed certain hypotheses currently under study in field experiments.

The combined approaches of measurement and numerical modelling, for example, have confirmed certain hypotheses concerning the missing source of CO_2, the amount of methane oxidation and the existence of an intense fall peak in GHG emission for deep reservoirs. In addition, differences in GHG emission patterns related to the depth of the station were highlighted. For example, it was noted that the shallow stations respond less strongly and exhibit less variability to weather forcing than do the deep stations. In fact, the shallow stations usually present a well-mixed layer over the entire depth, and so are less affected by a change in meteorological conditions (Tremblay et al. 2004, Chap. 8).

The numerical model developed in this research can be used to study the temporal and spatial distribution of dissolved GHG concentration profiles and surface fluxes of GHG. It could therefore be used to improve sampling strategies based on the characteristics of temporal and spatial distributions associated with each reservoir. For example, shallow reservoirs such as LA-1 that present a greater homogeneity of GHG emissions need not be subjected to considerable sampling. However, deep reservoirs such as LG-2 require more intensive sampling, with special care being taken to target the spring and autumn peak periods, since they make a significant contribution to the annual GHG emission average (Tremblay et al. 2004, Chap. 8). A numerical model can also be used as an experimental laboratory to study and understand the relations between certain weather variables and GHG surface fluxes.

In its current state, this model cannot be used to evaluate the net carbon emissions from hydroelectric reservoirs. Before this becomes possible, experimental research must provide more information concerning the processes that drive the production and fixation of GHG in hydroelectric reservoirs. Further research on these subjects could lead to the establishment of a production/fixation model based on variables such as water temperature, dissolved oxygen, nutritive elements and the nature of the organic matter.

Furthermore, given the possibility that most of the GHG emitted at the surface of the hydroelectric reservoirs originates from terrigenous carbon from runoff, the optimal model will have to incorporate the whole system, i.e., all the driving processes of the exchange, transport, production and consumption of carbon inside the drainage basin area, including the hydroelectric reservoirs.

25 Modelling the GHG emission from hydroelectric reservoirs

Normand Thérien and Ken Morrison

Abstract

A mechanistic model has been constructed to compute the fluxes of CO_2 and CH_4 emitted from the surface of hydroelectric reservoirs. The structure of the model has been designed to be adaptable to hydroelectric reservoirs of different sizes and configurations and the reservoir can be partitioned into one, two or three vertical volumetric zones. Each zone may accommodate a number of influents and effluents including turbined flow and discharged flow. Each zone consists of a surface water layer (0–10 m) and a bottom water layer (>10 m). The model considers advective and diffusive mass transfers of dissolved CO_2 and CH_4 between zones and water layers, the rates of CO_2 and CH_4 produced from the decomposition of flooded vegetation and soil in the reservoir, and, mass transfer of CO_2 and CH_4 at the water-air interface. Global mass balance equations are solved to compute the magnitude of the advective flows between zones and water layers. Component mass balance equations are solved to compute the concentrations of CO_2 and CH_4 as a function of time in the surface and bottom water layers of each of the zones of the reservoir. The rates of CO_2 and CH_4 emitted from the surface water layer are computed using the two-film theory. Data from the Robert-Bourassa reservoir, a large operational hydroelectric reservoir, has been used as input data to the model. Results from the model were first compared with experimental data available for the calculation of dissolved CO_2 concentration in the surface water layer. Secondly, results from the model were compared with fluxes of CO_2 and CH_4 emitted from that reservoir as calculated from the experimental determination of dissolved CO_2 in water. Also, they were compared with direct measurements of the fluxes at the water-air interface. It has been observed that concentrations of CO_2 computed by the model are in the range

of values reported for the surface water layer. No data was available for comparison with concentration of CH_4. Emissions of CO_2 computed by the model were in the range of fluxes calculated from the experimental determination of dissolved CO_2 in water. The computed flux as a function of reservoir age was also coherent with the CO_2 flux measurements data. The transitional emissions of CO_2 resulting from the decomposition of flooded vegetation and soil were found to be significant during not more than 6 to 8 years depending of the volumetric zones of the reservoir considered. Simulations were done under two distinct scenarios for the CO_2 content of the influents to the reservoir. The first scenario used data which reflected the contribution of carbon originating from the drainage basin. The second scenario assumed the CO_2 concentration in the influent water to be at equilibrium with the atmospheric CO_2. From the simulation results and the data available an important finding is that the main source of carbon contributing to the GHG emission from the hydroelectric reservoir after the transitional emissions of CO_2 due to the decomposition of the flooded vegetation and soil have faded away appears to be essentially the carbon originating from the drainage basin.

The results have also indicated that fluxes of CH_4 computed from the model are grossly underestimating the values reported from the direct measurements of CH_4 emissions. Analysis of the results have indicated the source of the discrepancies which lies with the very low production of CH_4 as indicated from the vegetation and soil decomposition data used by the model. Suggestions to improve the model forecasting of CH_4 emissions are indicated.

25.1 Introduction

GHG emission from hydroelectric reservoirs related to the decomposition of flooded vegetation and soil has been the subject of intense examination this last decade. It is part of a larger interest in GHG emission from natural aquatic systems in general that include oceans, estuaries, rivers, lakes and wetlands. Among the main factors affecting GHG emission from reservoirs reports from the IPCC (1995, 2001) have indicated:

- the type of reservoir;
- the residency time of the reservoir;
- the age of the reservoir;
- the nature of the vegetation flooded and type and extent of the soil inundated;
- the quantity of biomass inundated;

- the topography of the reservoir;
- temperature and climate (latitude and seasons) including wind;
- the operational conditions (drawdown).

Many authors have studied the effects of these factors and the results have been reported in part by Duchemin (2000) and synthesized recently by Therrien (2003). A global observation is that increases in the fluxes of CO_2 and CH_4 emitted from the hydroelectric reservoirs generally occur immediately after flooding. In the early years following flooding, the major sources of carbon for CO_2 and CH_4 emitted from hydroelectric reservoirs come from the decomposition of the flooded vegetation and soil. For reservoirs located in the boreal and temperate regions the transitional increase in the flux of CO_2 was estimated to have a duration of less than 10 years (Chamberland 1992, 1993; Rudd et al. 1993). After this interval of time, these authors and others (cited in Therrien 2003) concluded that the carbon originating from the drainage basin was essentially the main source of carbon contributing to the GHG emission from hydroelectric reservoirs. However, these affirmations were made mostly by deduction from the observations about the evolution of water quality variable such as dissolved organic carbon as a function of time (Chamberland 1992, 1993), or partially from assumed rate of emissions and similitude with others processes (Rudd et al. 1993). However, no formal demonstration is known to the authors.

Synthesis of information in the literature has led Therrien (2003) to conclude that sampling and flux measurements of GHG emitted from reservoirs and natural aquatic systems give variable results that limit statistical comparisons and often only permit the identification of the trends. The main causes for these variations are the day-night and seasonal GHG emission cycles, the effects of environmental factors and the various methodologies used for sampling and analysis. It is the major reason why the construction of a model was undertaken to compute the quantities of CO_2 and CH_4 emitted from a reservoir based on some hypothesis about the main processes operating and the effect of specific factors. In fact, the general structure of many of the existing water quality models could accommodate the additional development required to include modules of computation for the emission of these gases from a reservoir. Since decomposition of the flooded vegetation and soil was a principal issue here, the approach was to use the existing water quality model developed for hydroelectric reservoirs located in Northern Quebec which already referred to the decomposition of flooded vegetation and soil to compute the more conventional water quality variables (Thérien 1999). In effect, the water quality model already imbedded the data bank including the kinetic parameters characterizing the

decomposition of the labile vegetation components and types of soil when flooded with water.

The structure of the water quality model already offered the following characteristics that were identified by the IPCC (1995, 2001) as influential factors for GHG emission:

- segmentation of the reservoir by zones to represent at best the type, morphology and topography of the reservoir;
- specification of the inflows and volume of the reservoir (residence time);
- specification of the level of water as a function of time (operational conditions);
- specification of the monthly water temperature and the months during which the surface of the reservoir is ice-free (temperature and climate);
- specification of the densities of the labile components of vegetation and the fractions of the terrestrial surface occupied by different types of soil (type and quantity of biomass inundated; type and extent of soil inundated);
- solution of the mass balance equations for flows and mass concentration as a function of time since flooding (age of reservoir).

Additional required variables included the velocity of the wind, which is known to play a role at determining the magnitude of GHG emission at the water-air interface (Duchemin et al 1995, 2000).
Construction of the computational modules for GHG emission required:

- to complement the existing data bank with the additional kinetic parameters related to the production of CO_2 and CH_4 resulting from the decomposition of the labile vegetation components and types of soil already known. Data reflecting the temporal dynamics of gas production under several sets of controlled experimental conditions was already available for several labile vegetation components and types of soil (see Chap. 13). This data has been used in this work to define mathematical functions describing adequately the evolution with time of the cumulative quantities of gases produced under each set of environmental conditions. Values for the kinetic parameters of these functional relationships were then estimated by calibration.
- to integrate a fundamental expression for the mass transfer at the water-air interface (Brezonik 1994) with field validated relationships to include effects of water temperature and wind velocity (Banks 1975; Banks et al. 1977).

Details of the formulation of the model and the results obtained are described below.

25.2 Model formulation

25.2.1 Basic configuration of the reservoir

Volumetric zone

The modelling of GHG emission from hydroelectric reservoirs is done through the construction of complementary computational modules, one for CO_2 emission and one for CH_4 emission, to an existing water quality model derived for hydroelectric reservoirs (Thérien 1999). An earlier version of the water quality model allowed the user to segment the volume of a given reservoir into N volumetric zones. For example, the Robert-Bourassa reservoir and the Opinaca reservoir had been segmented into 9 and 7 volumetric zones respectively (Thérien 1999). To use such a model the user had to furnish specific data for each of the zones of the reservoir. This proved to be a severe requirement since the data was not always available. Models with a smaller number of volumetric zones were also constructed. Results from these simpler models were very satisfactory as they captured the essential characteristics of the dynamics and magnitude of the water quality variables simulated. Therefore, the structure of the model was designed to be adaptable to any given reservoir and allow flexibility in use. The present version of the model allows the user to segment the volume of a given reservoir into a maximum of three volumetric zones as can be seen in Fig. 25.1.

Each zone may receive up to three distinct influents, which may consist of rivers or the effluents from an upstream reservoir. It may also receive input flows from adjacent zones of the reservoir. Each zone may also output flows through turbined effluent, discharged effluent (overflow) or flows to adjacent zones of the reservoir.

Surface and bottom water layers

Each volumetric zone is made up of two vertical layers of water, a surface water layer and a bottom water layer. The surface water layer consists of the upper 10 m of water in the reservoir in contact with the atmosphere. Initially, the depth of this layer starts at 0 and builds up to 10 m as the water level in the reservoir rises after flooding is initiated. As soon as the water level in the reservoir reaches a height of 10 m the model considers the

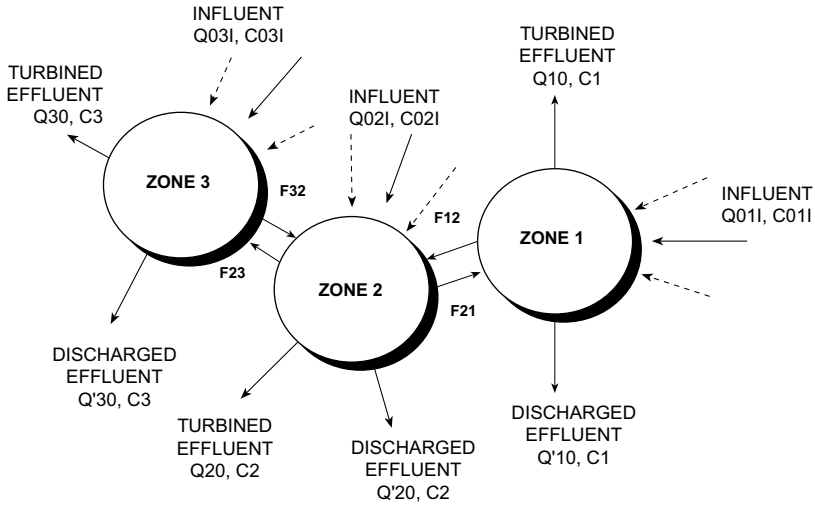

Fig. 25.1. Three zone configuration of an hydroelectric reservoir considering hydraulic flow and mass balance

The significance of the symbols shown on Fig. 25.1 are as follows:

Q01i, Q02i, Q03i: Volumetric flowrate of influent i to zone 1, 2 or 3. Up to three influents per zone are allowed (i = 1, 2, 3).

Q10, Q20, Q30: Volumetric flowrate of the turbined effluent from zone 1, 2 or 3. A maximum of one turbined effluent per zone is allowed with at least one turbined effluent from all of the zones considered.

Q'10, Q'20, Q'30: Volumetric flowrate of the discharged effluent from zone 1, 2 or 3. A maximum of one discharged effluent per zone is allowed with at least one discharged effluent from all of the zones considered.

C01i, C02i, C03i: Mass concentration of influent i (i = 1, 2, 3) to zone 1, 2 or 3.

C1, C2, C3: Mass concentration in zone 1, 2 or 3.

F12, F21: Mass flowrate from zone 1 to zone 2 or, conversely, from zone 2 to zone 1 resulting from bi-directional advective and diffusive flows.

F23, F32: Mass flowrate from zone 2 to zone 3 or, conversely, from zone 3 to zone 2 resulting from bi-directional advective and diffusive flows.

construction of a bottom water layer. The height of the bottom layer is continuously variable and follows the water level fluctuations in the reservoir. Figure 25.2 illustrates these two layers and indicates the many processes that affect the concentration of a given water quality variable in each of these layers.

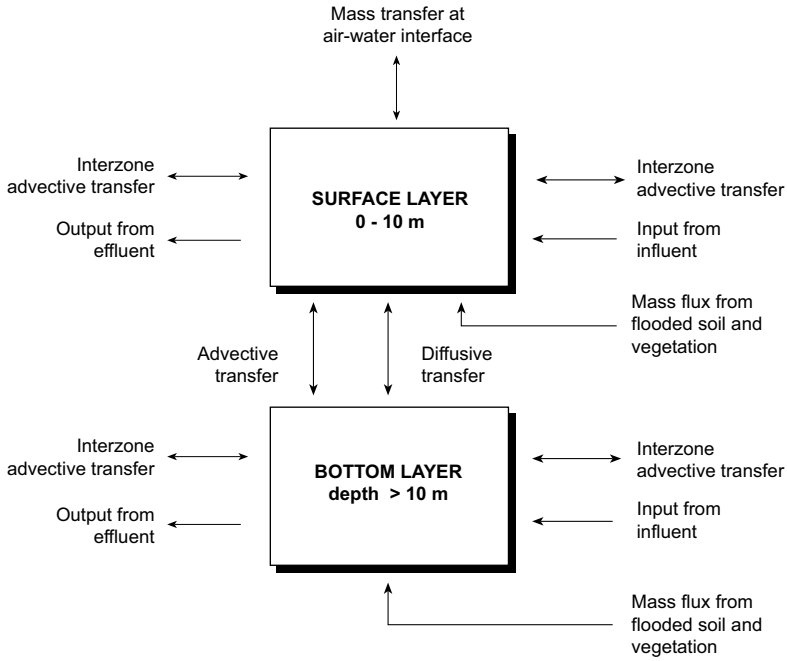

Fig. 25.2. Surface water layer and bottom water layer showing advective, diffusive and mass transfer from flooded soil and vegetation

Stratum of soil

The whole reservoir is not flooded instantaneously and phytomass and soil present on the territory will be inundated progressively with time. The amounts of material released in the water as a result of the decomposition of the inundated vegetation and soil will also be released progressively with time. To account for the quantities of phytomass and the areas of soil that will be inundated as flooding progress in time the whole reservoir is segmented vertically into N stratum each having a height of 1 m. The whole terrestrial area is then partitioned vertically into N sub-areas of soil. These sub-areas are calculated from data about the surface area inundated as a function of the water level in the reservoir. Also, as the water level

rises in the reservoir after flooding the model stores the time at which each stratum is been flooded. This permits to do three things:

- initiate the flux of material released to the water column as soon a stratum is being flooded and under the environmental conditions existing at that time; and,
- keep track of the duration of time pre-flooded stratum have been submitted to decomposition and adjust, accordingly, the flux of material released to the water column taking into account the history of environmental conditions having affected the stratum;
- distribute the flux of material being released from each flooded stratum into the surface water layer and bottom water layer according to where the moving surface layer is at that time.

25.2.2 Constitutive equations of the model

The general mass balance equation for a given water quality variable of zone j of the reservoir is given by:

$$d\,Mj / dt = d\,[Cj \,.\, Vj] / dt = Fin,j\,(t) - Fout,j\,(t) + NPj\,(t) \qquad (25.1)$$

with

$$Fin,j = Qin,j \,.\, Cin,j \qquad (25.2)$$

$$Fout,j = Qout,j \,.\, Cj \qquad (25.3)$$

and the volumetric mass balance written for zone j is given by:

$$d\,Vj / dt = Qin,j\,(t) - Qout,j\,(t) \qquad (25.4)$$

where

Fin,j: Influent mass flowrate to zone j at time t (mass $time^{-1}$)
Fout,j: Effluent mass flowrate from zone j at time t (mass $time^{-1}$)
Qin,j: Influent volumetric flowrate to zone j at time t (volume $time^{-1}$)
Qout,j: Effluent volumetric flowrate from zone j at time t (volume $time^{-1}$)
Mj: Total mass in zone j at time t
Vj: Volume of water in zone j at time t
Cj: Mass concentration in zone j at time t (mass $volume^{-1}$)
Cin,j: Influent mass concentration to zone j at time t (mass $volume^{1}$)
NPj: Rate of change of mass in zone j at time t due distinct biochemical and physical processes contributing to a change in mass in zone j (mass $time^{-1}$)

Substitution of Eq. 25.4 into Eq. 25.1 provides a simpler mass rate expression, which is used in the model:

$$Vj \cdot d\,Cj / dt = Qin,j\,[Cin,j - Cj] + NPj\,(t) \qquad (25.5)$$

Similar equations can be written for the mass concentration variable in the surface and bottom water layers and are available elsewhere (Thérien 1999).

In the case of carbon dioxide and methane the term NPj in Eq. 25.5 is defined as:

$$NPj = \Sigma\, P_k,j \qquad (25.6)$$

P_k,j represents the rate of change of mass of component i in zone j due to process k. Table 25.1 indicates the five distinct processes considered by the model for the computation of the concentration of carbon dioxide and methane in the surface water layer (0–10 m). The bottom water layer (> 10 m) considers only four of these processes (k = 2,…,5).

Table 25.1. Processes considered by the model which contribute to the change in concentration of carbon dioxide and methane in the surface and bottom water layers of a volumetric zone of the reservoir

k	Process
1	Mass transfer at the water-air interface
2	Production of gases from decomposition of flooded vegetation and soil
3	Biodegradation of organic matter in the water volume
4	Interzone and interlayer mass tranfer
5	Input from influents and output from effluents

25.3 Mass transfer of CO_2 and CH_4 at the water-air interface

The kinetics of gas transfer is simple at the macroscopic level since the transfer rate is first order dependent on the difference between the actual concentration C and the saturation value C* (Brezonik 1994):

$$V \cdot (dC / dt) = K \cdot A \cdot (C^* - C) \qquad (25.7)$$

K is the gas transfer coefficient (units of length time^{-1}) and it varies with the nature of the gas and environmental conditions. However, quantification of the factors affecting this coefficient requires and understanding of the mechanism of transfer. The most common mechanistic model for gas transfer is the two-film model developed by Whitman (1923). In its formu-

lation a gaseous film is assumed at the atmosphere side of the water-air interface and a liquid film is assumed on the water side of the interface. Surface renewal models have also been proposed (Higbie 1935; Danckwerts 1951, 1955) with other models combining film theory and surface renewal models (Dobbins 1964) or considering the boundary-layer profile (McCready and Hanratty 1984; Hanratty 1991). However, these models all lead to the same general form of transfer equation as the two-film model [Eq. 25.7], which is used in this work.

Regardless of whether gas transfer is limited by the liquid film, the gas film, or both, transfer rates vary with environmental conditions. The gas transfer coefficient K is not constant for a given gas. However, as pointed out by Brezonik (1994), it is not practical to measure K for all the substances of interest (i.e. CO_2, CH_4) over the range of conditions needed to predict transfer rate in the ambient environment. Instead, values applicable to field conditions are estimated from relationships based on reference compounds whose transfer coefficients have been measured under a wide range of environmental conditions. Water and O_2 are used as reference compounds because the transfer rates of each are controlled exclusively by one of the film (gas for water, liquid for O_2) and because numerous studies have measured these coefficients under field conditions. This approach has been used in this work.

Therefore, the mass transfer of CO_2 or CH_4 at the water-air interface is based on the concept of atmospheric reaeration of a water body. For this case, the transfer of oxygen at the interface is expressed as:

$$V \cdot (dC_{DO} / dt) = K_{LDO} \cdot A \cdot (C_{DO}^* - C_{DO}) \qquad (25.8)$$

where

C_{DO}^*: Dissolved concentration of dissolved oxygen in water at saturation (mass volume^{-1})

C_{DO}: Dissolved concentration of dissolved oxygen in water (mass volume^{-1})

K_{LDO}: Dissolved oxygen interfacial transfer coefficient (length time^{-1})

A: Surface area between the water and the atmosphere (length^2)

V: Volume of water (length^3)

25.3.1 Wind effect

For lakes and reservoirs, or large open bays, the effect of wind may be significant in oxygen transfer creating turbulence that results in increased

reaeration. Banks (1975) and Banks and Herrera (1977) have explored this effect and suggested the following relationship, which is used in this work.

$$K_{LDO}(T_o) = 0.728\,[V]^{1/2} - 0.317\,V + 0.0372\,[V]^2 \qquad (25.9)$$

V is the wind velocity in m/s at 10 m above the water surface and K_{LDO} is the wind driven oxygen transfer coefficient in $m \cdot d^{-1}$. The reference temperature $T_o = 20°C$.

25.3.2 Water temperature effect

The effect of water temperature on the oxygen transfer coefficient has also been studied by Holley (1975) and Zison et al. (1978), which suggest the following relationship, which is used in this work:

$$K_{LDO}(T) = K_{LDO}(T_o)\,.\theta^{T-T_o} \qquad (25.10)$$

The numerical value of θ depends on the mixing condition of the water bodies with values reported in the range 1.005 to 1.030. In practice, a value of $\theta = 1.024$ is often used (Thomann and Mueller 1987) as is done here.

25.3.3 Mass transfer coefficient for carbon dioxide and methane

As pointed earlier, the mass transfer coefficients K_{LCO2} and K_{LCH4} are estimated from knowledge of the mass transfer coefficient K_{LDO} of dissolved oxygen in water, which has been measured under a wide range of environmental conditions. Individual relationships between the mass transfer coefficient of the compound of interest (CO_2 or CH_4) in the rate-limiting film and K_{LDO} have been derived from theoretical considerations using the two-film theory, the surface-renewal models or the mixed two-film and surface renewal model of Dobbins (Brezonik 1994). These relationships applied to CO_2 and CH_4 have the following general formulations:

$$K_{LCO2} / K_{LDO} = (D_{LCO2} / D_{LDO})^n \qquad (25.11)$$

$$K_{LCH4} / K_{LDO} = (D_{LCH4} / D_{LDO})^n \qquad (25.12)$$

where

K_{LCO2}: CO_2 interfacial transfer coefficient (length $time^{-1}$)
K_{LCH4}: CH_4 interfacial transfer coefficient (length $time^{-1}$)
D_{LCO2}: Diffusivity of CO_2 in water ($length^2 \cdot time^{-1}$)
D_{LCH4}: Diffusivity of CH_4 in water ($length^2 \cdot time^{-1}$)

n is a parameter taking values between 0.5 and 1 according to which theory or model has been considered for the derivation. However, field and laboratory determinations of the mass transfer coefficients for several compounds of interest have indicated a more restricted range of values with n taking values between 0.5 to 0.67 with the higher values observed under conditions of low turbulence and a value of 0.5 obtained under conditions of high turbulence. For example, field-scale tracer measurements in two lakes at two wind speeds indicated values of n averaging 0.51 (Watson et al. 1991). Therefore, a value of n = 0.50 has been used in the model to reflect turbulence and wind-induced mixing in large reservoirs.

The classic two-film gas-transfer model and its surface-renewal relatives implicitly assume that the interface itself poses no barrier to gas transfer; resistance is caused only by diffusion through the gas and/or liquid films (Brezonik 1994). As indicated above, relationships (25.11) and (25.12) refer to diffusivity of CO_2 and diffusivity of CH_4 in water. Thus, the use of these relationships is valid only when the resistance offered by the liquid film controls the global mass transfer of each of these compounds. This is generally the case for highly volatile compounds and unreactive gases when Henry's Law constant H is more than $3.5\ 10^3$ mm·Hg·L·mol^{-1} (Liss and Slater 1974). This is the case for methane with H = $7.8\ 10^5$ mm·Hg·L·mol^{-1}.

If a compound reacts rapidly with water, its rate of removal within the liquid film will be enhanced, thus increasing the concentration gradient in the film and enhancing diffusive transport (Brezonik 1994) and the interfacial coefficient computed by relationships such as the one above may not be adequate. Compounds in this category include strong acids and weakly acidic compounds such as CO_2. The possibility that chemical enhancement is significant for CO_2 transfer in water has received much attention. Schindler et al. (1972) and Emerson (1975) have reported chemical enhancement of CO_2 transfer in a small freshwater lake submitted to a set of controlled experiments. However, Emerson (1975) further indicated that this lake is probably an extreme case, and most freshwaters should have small chemical enhancements. Also, it was indicated that for large and medium-size lakes with moderate alkalinity and pH $\leq \sim 8$, chemical enhancements should be negligible (Brezonik 1994). Therefore, relationships (25.11) and (25.12) appear to provide a sound theoretical basis for computation of the interfacial transfer coefficients and are used by the model.

Finally, the rate of transfer of CO_2 at the water-air interface of zone j (mg time^{-1}) is expressed as:

$$P_{1,CO2,j} = K_{LCO2} \cdot A_j \cdot (C_{CO2}^* - C_{CO2}) \qquad (25.13)$$

with the emission of CO_2 (mg·length^{-2}·time^{-1}) given by:

$$\text{Emission of } CO_2 = K_{LCO2} \,.\, (C_{CO2}^* - C_{CO2}) \qquad (25.14)$$

Similarly for CH_4 (mg time^{-1}):

$$P_{1,CH4,j} = K_{LCH4} \,.\, A_j \,.\, (C_{CH4}^* - C_{CH4}) \qquad (25.15)$$

with the emission of CH_4 (mg·length^{-2}·time^{-1}) given by:

$$\text{Emission of } CH_4 = K_{LCH4} \,.\, (C_{CH4}^* - C_{CH4}) \qquad (25.16)$$

The following relationships were used for the saturation concentration C_{CO2}^* (mg·L^{-1}) and C_{CH4}^* (mg·L^{-1}) as a function of temperature (°C):

$$C_{CO2}^* = 0.17782341 + 0.95320673 \,.\, \exp\,(\,-\,T / 22.987342\,) \qquad (25.17)$$

$$C_{CH4}^* = 0.021545186 + 0.044000599.\, \exp\,(\,-\,T / 21.747661) \qquad (25.18)$$

25.3.4 Effect of ice formation

When ice forms during the colder months of the year the interfacial transfer coefficient would theoretically take a value approaching zero. However, since the ice sheet is never a perfect barrier to gas exchange this coefficient would generally not be equal to zero. The default value used by the model during this interval of time is one-tenth the value that would be computed for open water at the current water temperature (~ 0°C). The model allows the user to specify other values if so desired during the months ice forms (a fraction from 0 to 1 of the value computed under ice free conditions for the cold season). The model computes the quantities of gases not emitted that would be trapped during the months the reservoir is covered with ice and emits the accumulated amount the month the ice cover breaks.

Production of gases from the decomposition of flooded vegetation and soil

The model uses the results obtained from a set of experiments designed to measure the production of carbon dioxide and methane during decomposition of representative vegetation and soil samples originating from the James Bay territory. Table 25.2 indicates the nature of the vegetation samples originating from trees, shrubs and ground cover with the organic components for the forest soil and the wetlands considered by the model.

Table 25.2. Nature of the phytomass and types of soil considered by the model

Phytomass	Forest soil	Wetlands
Alder leaves	Humus of lichen	Sphagnum moss
Spruce needle	Humus of green moss	
Lichen		
Green moss		
Herbaceous plant		

These experiments were done under oxic conditions, which reflected aerobic conditions (A2) and anaerobic conditions (A1). They were also done under a set of temperatures reflecting cold-water temperature (T1) and warmer water temperature (T2) with a range of pH (P1, P2) reflecting pH found generally in the water column of reservoirs. Table 25.3 gives a summary of the experimental conditions found in Chap. 13 of this book, which describes these experiments.

Table 25.3. Experimental conditions used during the production of gases from the decomposition of flooded vegetation and soil

T1 :	Reservoir bottom water temperature during winter [4°C–5°C]
T2:	Reservoir surface water temperature during summer [20°C–22°C]
P1:	Low pH [4.5–5.0]
P2:	Moderately acidic pH [6.0–6.5]
A1:	Anoxic condition [< 2 mg dissolved $O_2 \cdot L^{-1}$]

For all of the vegetation and soil samples of Table 25.2, analysis of the data generated under the set of environmental conditions given above has indicated that the cumulative amount of CO_2 produced as a function of time is generally well approximated by the following relationship:

$$M(t) = M_{max} \,.\, [1\text{-}\exp(\text{-}R.t)] \tag{25.19}$$

where

M(t): Mass produced at time t (mass)

M_{max}: Ultimate (asymptotic) quantity produced under the most favourable condition (mass)

R: Rate constant ($time^{-1}$)

t: Time evolved since flooding (time)

For methane, the cumulative amounts produced as a function of time has been found to be more adequately represented by the following set of relationships:

$$\text{For } t \leq 60 \text{ days: } M(t) = 0 \tag{25.20}$$

$$\text{For } t > 60 \text{ days: } M(t) = M_{max} \,.\, [1\text{-}\exp(\text{-}R.\{t\text{-}60\})] \tag{25.21}$$

In both cases the rate of gas produced under a given set of environmental conditions is given by the following relationship (valid when t > 60 days for methane):

$$dM(t)/dt = R \,.\, [M_{max} - M(t)] \tag{25.22}$$

with M(0) = 0 for carbon dioxide and M(60) = 0 for methane. This relationship indicates that the maximum rate of production of carbon dioxide occurs just after flooding [strictly at time = 0 according to Eq. 25.22]. For methane, the maximum rate of production would occur after a delay of 60 days. In both cases, the rate of gas produced would then continuously decrease from the maximum value to reach a zero value as $t \rightarrow \infty$. Under a constant set of environmental conditions (constant R) the quantities of gases produced during a time interval $\Delta t = t_2 - t_1$ is then given by:

$$M(\Delta t) = M(t_2) - M(t_1) = M_{max}.[\exp(\text{-}R.t_1) - \exp(\text{-}R.t_2)] \tag{25.23}$$

This relationship can also be written as:

$$M(\Delta t) = [M_{max} - M(t_1)].\{1\text{-}\exp[\text{-}R.(\Delta t)]\} \tag{25.24}$$

where $[M_{max} - M(t_1)]$ represents the known potential quantity of gas that could be produced at a later time. This last formula is used by the model to compute the quantity of gas produced at different time intervals Δt, each corresponding to a distinct set of environmental conditions (R values) existing in the reservoir since flooding.

Therefore, the rate of CO_2 produced in a given stratum (mg time^{-1}), that is the amount of CO_2 produced in the given time interval Δt, is the sum of the quantities of CO_2 produced by the n individual components of flooded phytomass and soil indicated in Table 25.2. It is expressed here as:

$$P_{2,CO2,j} = \Sigma_n \,[M_{n,CO2,max} - M_{n,CO2}(t_1)].\{1\text{-}\exp[\text{-}R_{n,CO2}.(\Delta t)]\} \tag{25.25}$$

Similarly for CH_4:

$$P_{2,CH4,j} = \Sigma_n \,[M_{n,CH4,max} - M_{n,CH4}(t_1)].\{1\text{-}\exp[\text{-}R_{n,CH4}.(\Delta t)]\} \tag{25.26}$$

Finally, the global rates of CO_2 and CH_4 produced in the surface water layer and in the bottom water layer of a given zone are the sum of the quantities given by relations (25.25) and (25.26) for an individual stratum

taking into account the respective number of strata in each of the two water layers.

25.3.5 Effect of oxic conditions

Generally, based on observations from the Robert-Bourassa reservoir and the Opinaca Reservoir, aerobic conditions prevailed in the surface water layer (0–10 m) of the reservoir. However, at the bottom of these reservoirs conditions leading to anaerobic conditions sometimes existed (< 2 mg DO L^{-1}). Therefore, rate constants R reflecting production of carbon dioxide and methane under aerobic (A2) and anaerobic (A1) conditions were retained in the model.

25.3.6 Effect of water temperature

Water temperature had a significant effect on the rate of production of carbon dioxide and methane from the decomposition of vegetation and soil samples (See Chap. 13). Therefore, rate constants R associated with cold temperature (T1) and warm temperature (T2) were retained in the model.

25.3.7 Effect of pH

The arithmetic average and standard deviation of pH measurements done in the Robert-Bourassa and Opinaca reservoirs during the 20 year period following initial flooding has been calculated for both the surface water layer (0–10 m) and the bottom water layer of these reservoirs. Table 25.4 and Table 25.5 show the results at individual and pooled sampling stations for the Robert-Bourassa reservoir and the Opinaca reservoir, respectively.

The relative difference between the average pH for the surface water layer (pooled stations) and the average pH of the bottom water layer (pooled stations) is less than 5% for the Robert-Bourassa and less than 3.6% for the Opinaca reservoir. Moreover, the relative differences of the average pH between individual stations for any of the two reservoirs are less than 8%.

Also, production of carbon dioxide and methane from flooded soil samples was not very sensitive to pH for experiments done over a larger range of pH [pH1 $\in$ (4.5–5.0), pH2 $\in$ (6.0–6.5)] that included the values reported in Table 25.4 and Table 25.5 for both these reservoirs. Results from experiments done with vegetation samples submitted to different pH

Table 25.4. Arithmetic average and standard deviation of pH measurements done in the Robert-Bourassa reservoir during the period 1978 – 1995

Surface	G2400	G2402	G2403	G2404	G2405	G2406	All stations	All stations
							Average	Standard deviation
Average	6.28	6.42	6.43	6.26	6.40	6.35	6.357	0.073
Standard deviation	0.238	0.220	0.249	0.220	0.357	0.155		
Bottom								
Average	6.04	5.89	6.11	5.93	6.19	6.06	6.037	0.112
Standard deviation	0.203	0.274	0.380	0.458	0.282	0.370		

Table 25.5. Arithmetic average and standard deviation of pH measurements done in the Opinaca reservoir during the period 1978–1995

	EM400	EM401	EM402	EM403	EM421	All stations	All stations
Surface							
Average	5.95	6.03	6.18	6.19	5.58	5.986	0.248
Standard deviation	0.249	0.307	0.289	0.175	0.405		
Bottom							
Average	5.77	5.90	5.65	5.91	5.63	5.772	0.133
Standard deviation	0.421	0.370	0.450	0.394	0.196		

conditions were only for lichen and spruce needles (Morrison 1991). The results were highly variable and consideration of which in the model offered no hope of a greater precision. Also, for boreal reservoirs in Northern Quebec no relationship was established between GHG emission and pH (Duchemin 2000; Lambert et Fréchette 2002). For all the above reasons, the effect of pH on the rate constants R was not included in the model.

25.3.8 Kinetic parameters

Table 25.6 gives the kinetic parameters M_{max} and R of Eq. 25.24 for the cumulative amount of CO_2 produced from the decomposition of the flooded vegetation and soil samples to reflect the effects of oxic conditions and water temperature. Table 25.7 gives similar information for the production of CH_4.

The values indicated in these tables reflect rate constants derived for temperatures T1 and T2, which cover a range of values near the ones

Table 25.6. Kinetic parameters R and Mmax for the production of carbon dioxide from vegetation and soil samples flooded under several sets of environmental conditions

Kinetics parameter	Units	Alder leaves	Spruce needle	Lichen	Green moss	Sphagnum moss	Herbaceous plants	Lichen humus	Green moss humus
R (T1A1)	1/year	2.30E-01	2.50E-01	7.26E-02	6.21E-02	1.89E-01	2.96E-01	1.56E-01	2.04E-01
R (T1A2)	1/year	7.72E-01	4.61E-01	2.57E-01	2.31E-01	5.41E-01	-	2.83E-01	2.84E-01
R (T2A1)	1/year	9.53E-01	4.92E-01	7.58E-02	5.70E-02	2.30E-01	-	1.51E+00	1.53E+00
R (T2A2)	1/year	5.01E+00	2.78E+00	1.14E+00	9.41E-01	2.91E+00	2.08E+00	1.13E+00	8.95E-01
Mmax	mg/g	2.45E+02	1.68E+02	4.11E+02	6.98E+02	1.42E+02	2.11E+02		
Mmax	g/m^2							2.48E+01	5.30E+01

Table 25.7. Kinetic parameters R and Mmax for the production of methane from vegetation and soil samples flooded under several sets of environmental conditions

Kinetics parameter	Units	Alder leaves	Spruce needle	Lichen	Green moss	Sphagnum moss	Herbaceous plants	Lichen humus	Green moss humus
R (T1A1)	1/year	1.00E-06	1.00E-06	1.00E-06	1.00E-06	1.00E-06	1.00E-06	3.65E-07	3.65E-07
R (T1A2)	1/year	1.00E-06	1.00E-06	1.00E-06	1.00E-06	1.00E-06	-	3.65E-07	3.65E-07
R (T2A1)	1/year	4.34E+01	5.00E+00	1.00E-06	6.15E-02	5.31E-02	-	5.73E-01	1.37E+00
R (T2A2)	1/year	1.00E-06	1.00E-06	1.00E-06	2.54E-05	1.00E-06	1.00E+02	6.38E-02	2.35E-01
Mmax	mg/g	3.83E-04	4.71E-03	0.00E+00	1.40E+01	2.24E-01	7.60E-05		
Mmax	g/m^2							4.48E-01	6.92E-01

found in hydroelectric reservoirs on the James Bay territory. However, monthly values of the water temperature in these reservoirs can differ significantly from T1 and T2 at times. In order to compute the rate constant R(T,Ai) corresponding to the reservoir water temperature T at any given time the model uses the following linear relationship relating the rate constants R(T1,Ai) and R(T2,Ai), i=1,2:

$$R(T,Ai) = R(T1,Ai) + (T-T1).(R(T2,Ai)-R(T1,Ai))/(T2-T1) \qquad (25.27)$$

This equation is an approximation of more elaborate formulations expressing an exponential dependence to temperature. However, it is generally valid for microbial processes (production of gas through decomposition of organic matter) when, as is the case here, the range of temperature variations is small (Brezonik 1994).

Mass transfer between adjacent zones

At any given time water flows from one volumetric zone of the reservoir to another (when the reservoir is configured using more than one zone). Each zone may also be submitted to inflows from influents or outflows through turbined flow or discharged flow. In each case large masses of water transit in the system. Therefore, advective mass transfer of dissolved carbon dioxide and dissolved methane would occur between zones. The model considers such transfer through Eq. 25.1.

Mass transfer between the surface and bottom layers of water

As the water level in the reservoir changes with time (rising or falling due to the drawdown) the volume of water in the surface layer of water (of constant depth = 10 m) is not constant but varies according to the bathymetry of the reservoir and the volume of water contained in the reservoir as a function of the level of water. At any given time, the model computes the volumetric flow to transfer from the bottom layer to the surface layer (or vice-versa) in order to satisfy the global mass (volumetric) balance equations. Advective mass transfer of dissolved carbon dioxide and dissolved methane from one layer to another occurs through this exchange of water.

When the water level in the reservoir is constant during a given interval of time no advective mass transfer occurs between the surface and bottom water layers. However, during that time interval diffusive mass transfer can occur. To account for this possibility, the model includes a diffusive mass transfer term in the mass balance equation written for each of the two water layers. Therefore, consideration of the advective mass transfer and diffusive mass transfer of dissolved carbon dioxide and dissolved methane

is done trough equations similar to Eq. 25.1 which are written and solved for the surface and the bottom water layers of each zone of the reservoir.

Biodegradation of organic matter from the influents

Because reservoirs may have long hydraulic residency times, the structure of the model allows, as an option, the consideration of both dissolved organic carbon and particulate organic carbon entering with the influents to be decomposed further in the reservoir to produce CO_2 and CH_4. If required, this provides a means of taking into account additional biodegradation of organic material that originates from the drainage basin to contribute further to the emission of GHG from a reservoir. The model assumes a rate of production of CO_2 and CH_4, which is first-order with respect to the concentration of dissolved organic carbon and particulate organic carbon. The rates of production of CO_2 and CH_4 (mg time^{-1}) for zone j are expressed as:

$$P_{3,CO2,j} = V_j \,.\, [\, K_{CO2,DOC} \,.\, DOC + K_{CO2,POC} \,.\, POC \,] \qquad (25.28)$$

$$P_{3,CH4,j} = V_j \,.\, [\, K_{CH4,DOC} \,.\, DOC + K_{CH4,POC} \,.\, POC \,] \qquad (25.29)$$

where

DOC: Dissolved organic carbon in water (mass volume^{-1})

POC: Particulate organic carbon in water (mass volume^{-1})

$K_{CO2,DOC}$: Rate constant for the biodegradation of DOC to CO_2 [mass CO_2 (mass DOC)$^{-1}$ time^{-1}]

$K_{CO2,POC}$: Rate constant for the biodegradation of POC to CO_2 [mass CO_2 (mass POC)$^{-1}$ time^{-1}]

$K_{CH4,DOC}$: Rate constant for the biodegradation of DOC to CH_4 [mass CH_4 (mass DOC)$^{-1}$ time^{-1}]

$K_{CH4,POC}$: Rate constant for the biodegradation of POC to CH_4 [mass CH_4 (mass POC)$^{-1}$ time^{-1}]

V_j: Volume of water in zone j (length^3)

25.3.9 Numerical solution of the constitutive equations

The mass balance equations for each of the surface water layers and bottom water layers are solved numerically using the transition matrix approach (Dorf 1967) providing a quasi-analytic solution for the set of differential equations. This numerical approach has been used in the past for modeling the dynamics of ecological systems (Patten 1971). It is also a part of the numerical algorithm of the Finneco Model (Kinnunen et al.

1982; Kauranne 1983); a water quality model used for lakes and reservoir in Finland. The numerical computations for the concentration of the water quality variables are done with a time step of one month.

Data required

The model requires the following input data:

- densities ($g \cdot m^{-2}$) of the phytomass components (Table 25.2) that will be flooded;
- percentage of the terrestrial area to be flooded that are occupied by the three types of soil;
- kinetic parameters for the production of CO_2 and CH_4 from decomposition of the vegetation and soil components (built-in the model);
- influent concentration of dissolved CO_2 and CH_4;
- relationship for the terrestrial area flooded per zone of the reservoir as a function of the water level;
- relationship for the surface area (water-air interface) per zone of the reservoir as a function of the water level;
- relationship for the volume of water per zone of the reservoir as a function of the water level;
- water level in the reservoir as a function of time;
- influent flow rates as a function of time;
- water temperature of the reservoir as a function of time.

The following represents optional requirements:

- kinetic parameters for the biodegradation of DOC and POC to CO_2 and CH_4 (required only when one wants to consider this effect);
- influent concentration of DOC and POC (required only when one wants to consider biodegration of DOC and POC to CO_2 and CH_4 in the reservoir);
- influent water temperature as a function of time (required when one cannot furnish concentrations of CO_2 and CH_4 in the influents which are then computed as being at equilibrium with CO_2 and CH_4 in the atmosphere). By default, inflows enter the surface water layer of the reservoir. However, the model allocates the inflows to the surface water layer or the bottom water layer of zone j according to density of the incoming water relative to the density of water in the reservoir (determined by water temperature of the reservoir) when the influent water temperature is furnished.
- average wind velocity (when the user does not want to use default values provided by the model and reflecting average monthly wind veloci-

ties reported at weather stations nearest the latitude and longitude of the reservoir of interest);
- month of ice formation and first month free of ice (when the user does not want to use default values provided by the model and reflecting known average values reported for other reservoirs near the latitude and longitude of the reservoir of interest).

General computational algorithm

Figure 25.3 gives a general view of the key computational steps and the required information or data required for the computation.

25.4 Results and discussion

25.4.1 Input data to the model

In order to illustrate the magnitude and transient characteristics of the CO_2 and CH_4 emissions computed by the model and to compare the results to field measurements a simulation was done using the Robert-Bourassa reservoir.
This reservoir was chosen because:

- it is a large operational and representative hydroelectric reservoir of Northern Quebec;
- a very extensive set of data related to water quality variables is available (summarized in Lalumière 2001) and has been used in the past for testing water quality models (Thérien 1999a,b);
- the nature, density and distribution of the labile vegetation components and types of soil of the territory before flooding have been well documented (Poulin et al. 1992);
- kinetic parameters for the production of CO_2 and CH_4 from the decomposition of organic material are available for the key vegetation components and types of soil for that reservoir (Chap. 13, this book);
- field measurements of emissions of GHG are available for this reservoir (Therrien 2003).

Figure 25.4 illustrates the nine zone segmented reservoir with the Kanaaupscow river entering zone 1, the effluent from the LG3 reservoir entering zone 2 and the influent from EOL-Sakami entering zone 3. Turbined and discharged flows are effluents from zone 4. Active current flow

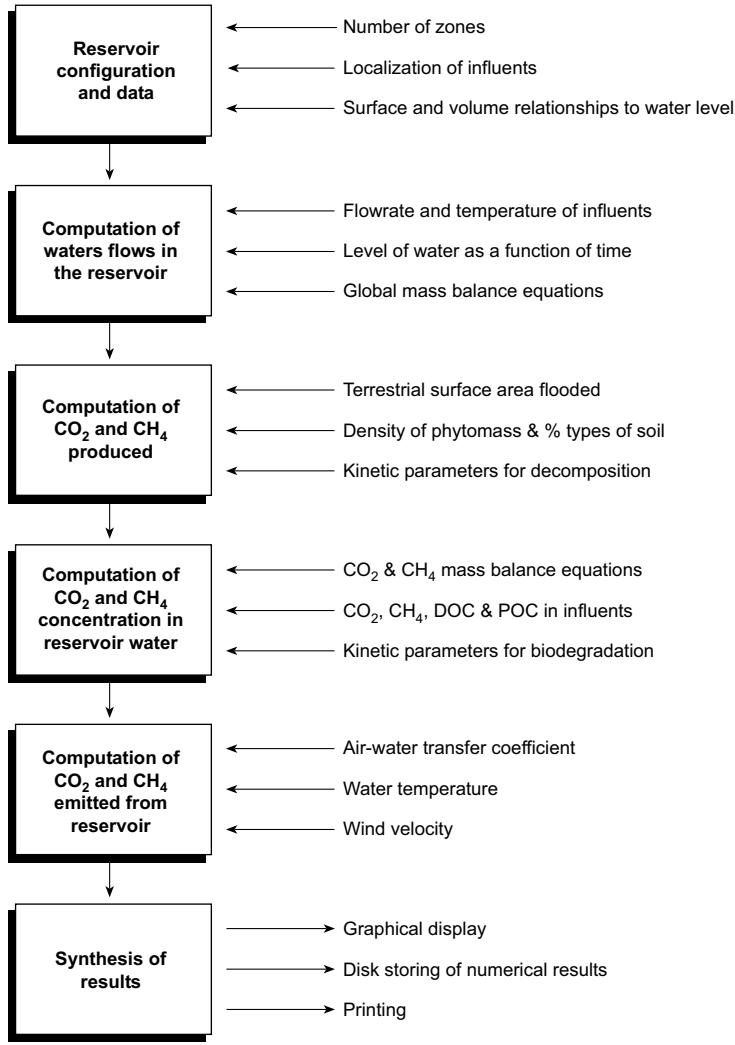

Fig. 25.3. General computational algorithm of the model

zones refer to zones where advective transfer of material dominates with a high rate of mixing. Bay type flow zones refer to zones where advective transfer of material still occurs between an adjacent zone but diffusive transfer plays a larger role.

The flooding of the reservoir was initiated November 1978. Figure 25.5 shows the water level of water in Robert-Bourassa reservoir as a function

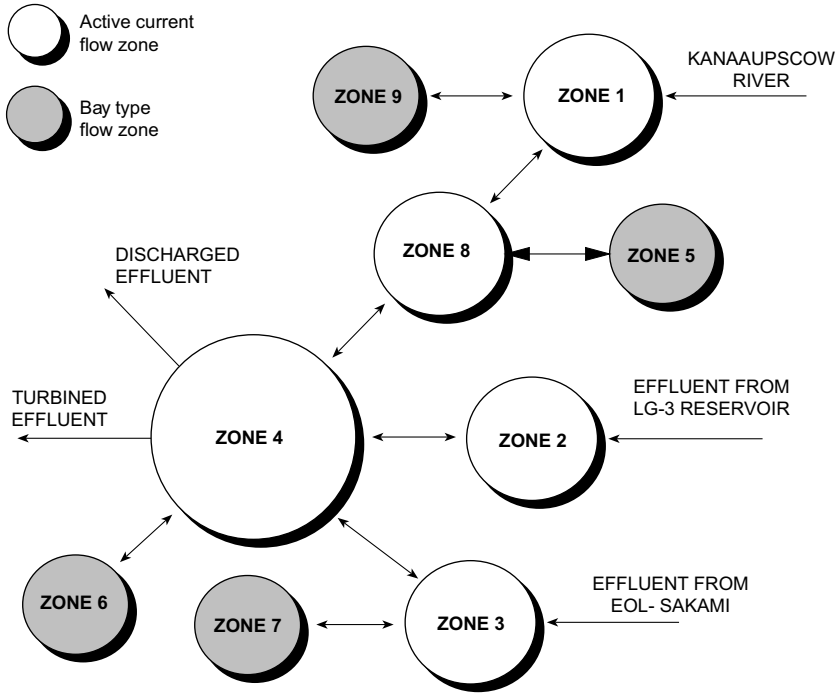

Fig. 25.4. Nine zone configuration of the Robert-Bourassa reservoir

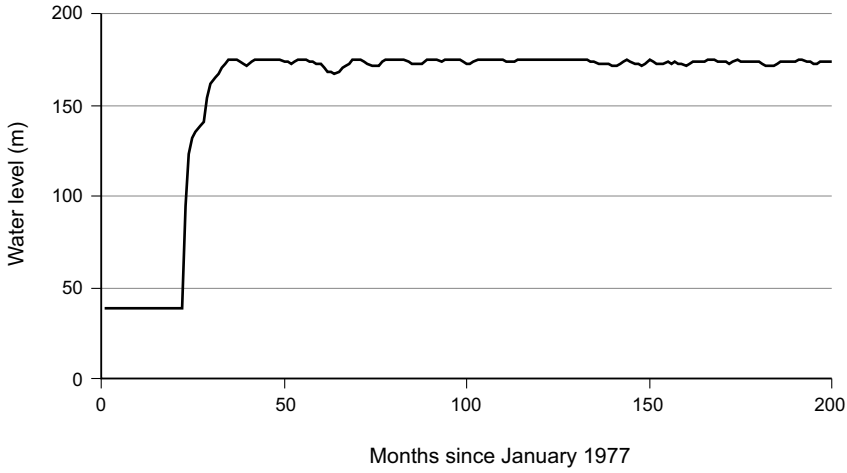

Fig. 25.5. Water level in Robert-Bourassa reservoir as a function of time since January 1977. Flooding in November 1978

of time since January 1977 whereas Fig. 25.6 shows the average monthly flowrates of influents to the reservoir. Figure 25.7 shows the average monthly water temperature in the reservoir and Fig. 25.8 shows the average monthly water temperature of the influents.

Concentrations of dissolved CO_2 and CH_4 in the influents as required by the model can be specified in one two ways:

- the values are reported from direct measurements;
- the concentrations are assumed to be at equilibrium with the concentration of these gases in the atmosphere at the given water temperature of the influents.

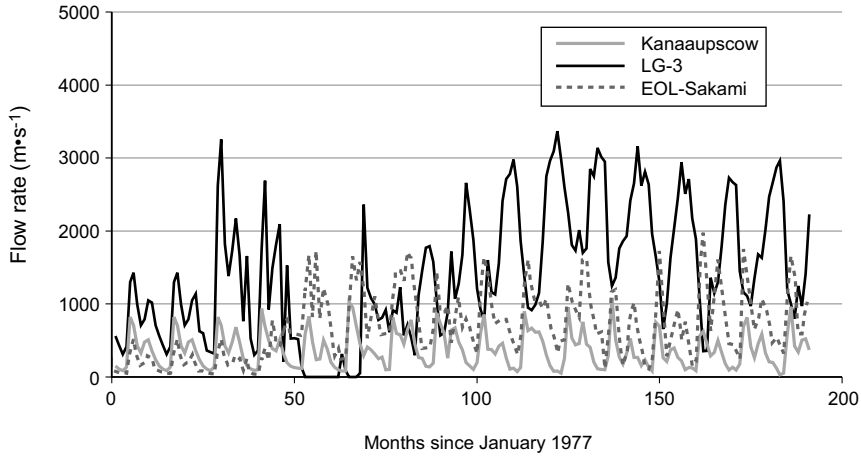

Fig. 25.6. Average monthly flowrate of influents to Robert-Bourassa reservoir as a function of time since January 1977. Flooding in November 1978

Dissolved CO_2 can also be calculated from alternate measurements of inorganic carbon (C_{INORG}) and the acid carbonate (HCO_3). In effect, on the assumption that inorganic carbon is essentially the sum of acid carbonate and dissolved carbon dioxide (which is almost always true since carbonates are negligible) one can compute the missing value from:

$$CO_2 = C_{INORG} - HCO_3$$

Generally, measurements for C_{INORG} and HCO_3 are available (summarized in Lalumière 2001). However, this approach would provide acceptable results only if the quantity of CO_2 originally in the water sample is conserved from the moment it is sampled to the moment it is being determined analytically.

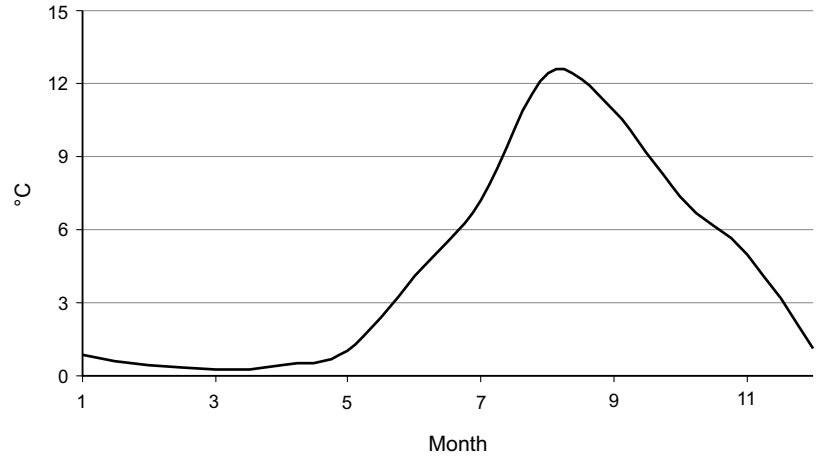

Fig. 25.7. Average monthly water temperature in Robert-Bourassa reservoir

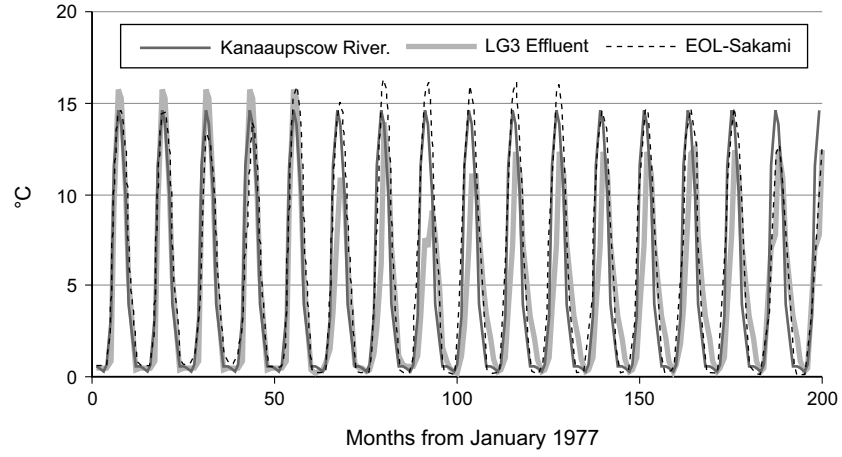

Fig. 25.8. Average monthly water temperature of influents to Robert-Bourassa reservoir

The model requires the concentrations of dissolved CO_2 and CH_4 in the water of the influents to be known. However, no direct measurements of dissolved CO_2 and CH_4 in the water of the influents was available. For that reason, the concentration of dissolved CH_4 in the water of the influents was assumed to be at equilibrium with the concentration of CH_4 in the atmosphere at the water temperature of the influents. However, since concentrations of C_{INORG} and HCO_3 in these influents had been reported con-

centration of dissolved CO_2 was calculated using the method described above. Figure 9 shows the concentration of CO_2 in the water of the influents where they are compared to the concentration of CO_2 in the water of the influent calculated at equilibrium with the atmospheric CO_2 at the average water temperature of the influents. An important observation is that the concentrations of CO_2 in the influents as calculated from field data (C_{INORG} and HCO_3) are not at equilibrium with the atmospheric CO_2.

Carbon originating from the drainage basin appears to be essentially the main source of carbon contributing to the higher concentrations of CO_2 measured in the water of the influents to the Robert-Bourassa reservoir. This CO_2 enrichment has also been observed in rivers and has been shown to depend largely on the nature of the vegetation and soil of the drainage basin (Eckardt and Moore 1990; Hinton et al. 1998 and Hope et al. 1997).

Since the field data did not extend further than 1986 and no particular trends as a function of time was observed a constant average value for the concentration of CO_2 in water for each of the influents was used for the simulations done with the model. Table 25.8 gives the average value ± standard deviation with the number of data available.

Table 25.8. Kinetic parameters R and Mmax for the production of methane from vegetation and soil samples flooded under several sets of environmental conditions

Kanaapscow River [mg·L^{-1}]	From LG-3 Reservoir [mg·L^{-1}]	EOL/Sakami River [mg·L^{-1}]	CO_2 at saturation [mg·L^{-1}]
N = 42	N = 45	N = 47	N = 204
3.70 ± 1.79	2.46 ± 1.53	2.55 ± 1.69	0.98 ± 0.14

The average wind velocity used in this work during the ice-free water months for the Robert-Bourassa reservoir is 4.2 m·s^{-1}. It is representative of the average of the wind velocities measured in 2000 and 2001 during field determinations of CO_2 and CH_4 flux emitted from the surface of the Robert-Bourassa reservoir (Lambert 2001, 2002) as shown in Table 25.9. The average wind velocity was 3.69 ± 1.93 m·s^{-1} considering all measurements and 4.05 ± 1.61 m·s^{-1} when considering only wind velocities other than the ones reflecting calm situations (wind velocities < 0.1 m·s^{-1}), which are not representative of windy situations. The value of the water-air interface transfer coefficient K_{LDO} calculated from Eq. 25.9 for a wind velocity of 4.2 m·s^{-1} is 0.82 m·d^{-1}. This value is in the range of values reported for different water bodies as one can observe in Table 25.10.

Table 25.9. Wind velocities measured ($m \cdot s^{-1}$) during CO_2 and CH_4 flux measurements done at the Robert-Bourassa reservoir in 2000–2001

Station	Site	Month	Year	Wind velocity [$m \cdot s^{-1}$]	Wind velocity[a] [$m \cdot s^{-1}$]
G2664	36b	October	2001	6	6
G2664	36	October	2001	6	6
G2669	34	October	2001	3	3
G2666	6	October	2001	3	3
G2664	4	October	2001	2.7	2.7
G2663	3	October	2001	4	4
G2662	2	October	2001	4	4
G2661	1	October	2001	4	4
G2610	3034	July	2001	4.5	4.5
G2604	3030	July	2001	0.07	
G2610	3005	June	2001	6	6
G2615	3006	June	2001	2.6	2.6
G2336	3017	July	2001	4.2	4.2
G2604	3018	July	2001	6	6
G2645	3027	July	2001	1.5	1.5
G2336	3028	July	2001	0.07	
G2402	404	August	2000	2.3	2.3
G2403	405	August	2000	3.5	3.5
G2405	414	August	2000	2	2
G2629	418	August	2000	3.5	3.5
G1207	425	August	2000	7.6	7.6
G2628	426	August	2000	4.6	4.6
			Average	3.69 ± 1.93	4.05 ± 1.61

[a]: Not considering wind velocity < 0.1 $m \cdot s^{-1}$.

Table 25.10. Values of the water-air mass transfer coefficient ($m \cdot d^{-1}$) for dissolved oxygen for different water bodies

Water bodies	K_{LDO} [$m \cdot d^{-1}$]	Reference
Lake & reservoir	0.97 (V = 5 $m \cdot s^{-1}$)	Banks (1975)
Estuaries	0.9 – 2.1	Thomann and Mueller (1987)
Lakes	0.3 – 1.5	Thibodeaux (1979)
Great lakes	1.15 – 1.75	Brezonik (1994)

Finally, Table 25.11 gives the density of phytomass components on the territory used for the simulation and Table 25.12 gives the percentage of the total terrestrial surface occupied by representative types of soil.

Table 25.11. Density of phytomass components ($kg \cdot h^{-1}$ dry weight) on the Robert-Bourassa territory before flooding

Phytomass	Representative phytomass	Density
Coniferous needles	Spruce needles	3294
Deciduous leaves	Alder leaves	281
Lichen	Lichen	2565
Green moss	Green moss	443
Herbaceous plants	Herbaceous plants	1609

Table 25.12. Percentage of terrestrial surface (%) occupied by different representative types of soil

Soil	Representative component	Total terrestrial surface
Forest soil I	Lichen humus	55.6
Forest soil II	Green moss humus	9.6
Wetlands	Sphagnum moss	34.8
Total		100.0

25.4.2 Simulation with the model

The structure of the model takes into account the influx of CO_2 and CH_4 to the reservoir by the influents. As shown in Fig. 25.9, the enrichment of CO_2 in the water of the influents already reflected the contribution of the organic material from the drainage basin. Therefore the simulations done here have not considered any additional decomposition in the reservoir of the organic material entering with the influents. To this end, the rate constants $K_{CO2,DOC}$, $K_{CO2,POC}$, $K_{CH4,DOC}$ and $K_{CH4,POC}$ were all considered equal to zero.

CO_2 emissions

At any given time the concentration of CO_2 computed from the model will differ from zone to zone of the reservoir. In effect, density of the phytomass flooded, the area of soil inundated, the influx of CO_2 from the influent to a given zone and the hydraulic residency time vary from zone to zone and these various factors have a direct impact on the mass balance of CO_2 of any given zone. Therefore, results will be different from zone to zone according to heterogeneity of conditions affecting the CO_2 mass balance in these zones.

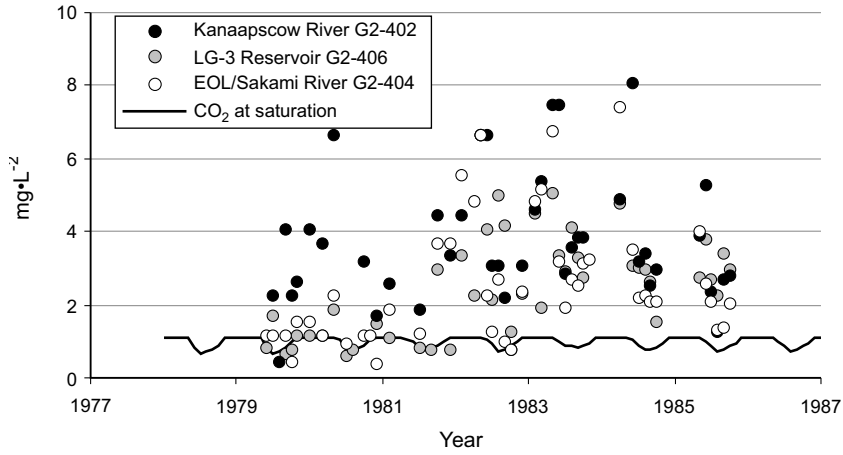

Fig. 25.9. Concentrations of carbon dioxide in the influents to Robert-Bourassa reservoir as calculated from measurements of C_{INORG} and HCO_3

Figure 25.10 illustrates simulation results obtained for the concentration of CO_2 in active current flow zones 1, 2 and 3 of the segmented reservoir shown in Fig. 25.4. Figure 25.11 illustrates similar results for bay type flow zones 6, 7 and 9. As can be observed from both sets of results, the magnitude of the CO_2 concentration profiles for the active flow zones will generally be lower than for bay type flow zones since residency time will be shorter with an increase in mixing for these zones. Also, the transitional increase in concentration in CO_2 due to the decomposition of the flooded vegetation and soil for the active current flow zones is somewhat shorter in duration than for bay type flow zones. However the difference is not very large as can be seen in Fig. 25.12 illustrating the extreme of two CO_2 concentration profiles computed for the reservoir. The duration for which the CO_2 concentration profile due to the decomposition of the flooded vegetation and soil is significantly different from the CO_2 concentration profile due to the influx of CO_2 by the influents can be observed to range typically from 5 to 7 years. After that interval of time the carbon originating from the drainage basin is essentially the main source of carbon contributing to the CO_2 concentration profile observed in the reservoir.

Finally, Fig. 25.13 compares the monthly concentrations of dissolved CO_2 computed from the model for zone 4 with values of CO_2 calculated from daily measurements of inorganic carbon (C_{INORG}) and acid carbonates (HCO_3) reported for that zone (sampling station G2400 of the Robert-Bourassa reservoir). Large variability in the data is observed which is not unusual for individual daily measurements. Nonetheless, the model

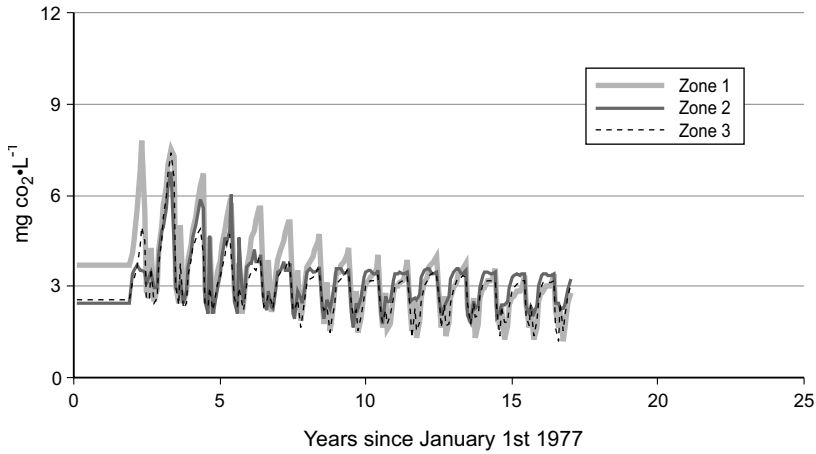

Fig. 25.10. Concentration of CO_2 in the surface water layer of active current flow zones of the segmented Robert-Bourassa reservoir. Flooding in November 1978

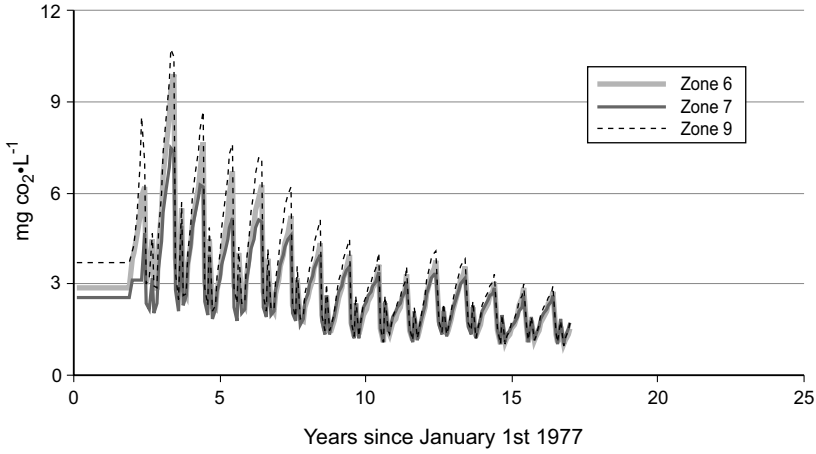

Fig. 25.11. Concentration of CO_2 in the surface water layer of bay type flow zones of the segmented Robert-Bourassa reservoir. Flooding in November 1978

computations (monthly basis) are in the range of the experimental data (daily basis).

Figure 25.14 shows the corresponding monthly fluxes of CO_2 (reported here on a daily basis) computed by the model as influenced by the water temperature in the reservoir. They are compared with the fluxes calculated from the previously determined CO_2 concentration and with individual

flux measurements of CO_2 reported recently for the Robert-Bourassa reservoir (Lambert 2001, 2002; Therrien 2003).

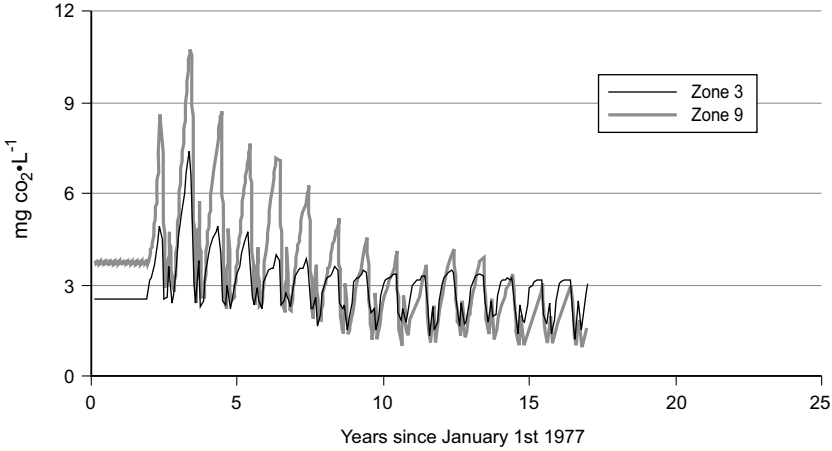

Fig. 25.12. Comparison of the CO_2 concentration profiles in the surface water layer of a bay type flow zone and of an active current flow zone of the segmented Robert-Bourassa reservoir. Flooding in November 1978

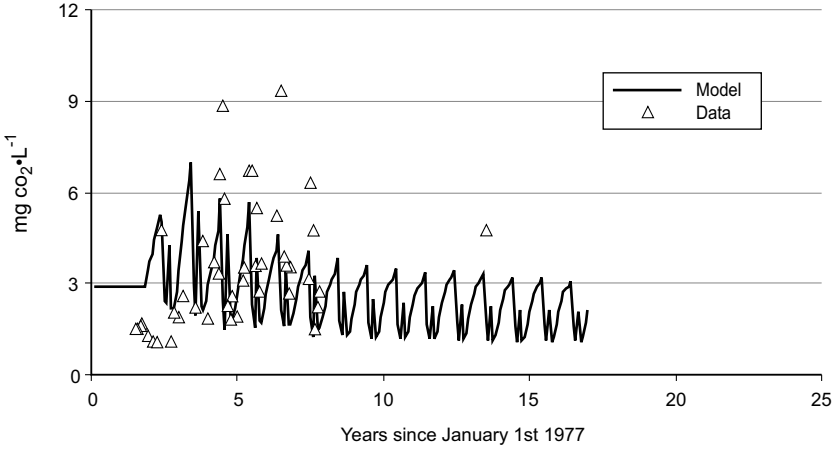

Fig. 25.13. Concentration of CO_2 dissolved in the surface water layer of zone 4 of the segmented Robert-Bourassa reservoir compared with data

Simulations done with this model version (a 9 zones segmented reservoir) were restricted to a time interval of 17 years. However, the monthly fluxes computed already show an asymptotic behaviour, which is nearly

achieved. As Table 25.13 indicates, the fluxes of CO_2 computed compare fairly well with the flux measurements when the comparison is done at comparable times.

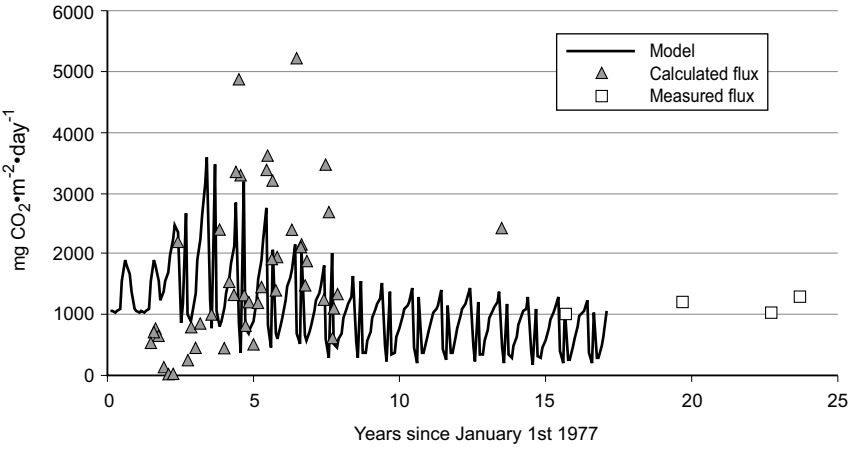

Fig. 25.14. Fluxes of CO_2 emitted from zone 4 of the segmented Robert-Bourassa reservoir compared to calculated fluxes and direct flux measurements

Table 25.13. Comparisons of fluxes of CO_2 computed from the model and measured in Robert-Bourassa reservoir

Date	Type of results	Emission [mg·CO_2·m^{-2}·d^{-1}]
August 1992	Field measurement[1]	999
August 1997	Field measurement[1]	1212
August 2000	Field measurement[1]	1026
August 2001	Field measurement[1]	1289
August (1990–1993)	Averaged monthly values from model	1093 ± 62

[1] Lambert (2001, 2002), Therrien (2003)

An important finding resulting from the model computations is that the transitional increase in the fluxes of CO_2 due to the decomposition of the flooded vegetation and soil in the reservoir is significant only during an interval of time not exceeding 6–8 years. These observations appear to confirm the estimations made in the past for boreal reservoirs (Chamberland 1992, 1993; Rudd et al. 1993) and support the statement that after this interval of time the carbon originating from the drainage basin is essentially

the main source of carbon contributing to the GHG emission from hydroelectric reservoirs.

Such a conclusion becomes more apparent when the fluxes of CO_2 computed by the model are expressed on a yearly basis. Figure 25.15 illustrates the yearly average of CO_2 emitted from zone 4 and compares it with the results of a complementary simulation done with the model neglecting the influent influx of CO_2 from the drainage basin (which is achieved by considering the concentration of CO_2 in the influents to be at equilibrium with the atmospheric CO_2 only). There is no CO_2 emitted from the influents to the atmosphere under the assumption that the concentration of CO_2 in the influent is at equilibrium with the atmospheric CO_2 since the driving force is zero (see Eq. 25.14). Under this hypothetical scenario the influx of CO_2 by the influents to the reservoir does not contribute any additional release of CO_2 from the reservoir other than the CO_2 emitted from the decomposition of the flooded vegetation and soil. Eventually, the rate of emission of CO_2 under the assumed condition will tend towards zero as can be observed in Fig. 25.15.

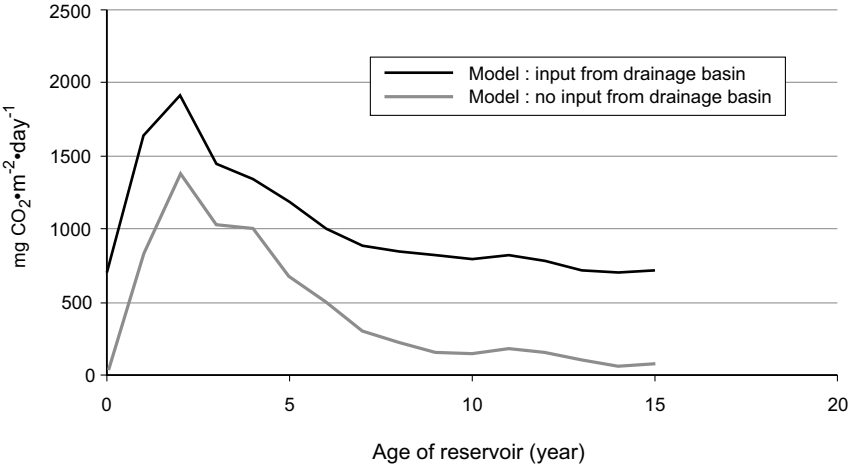

Fig. 25.15. Yearly averaged fluxes of CO_2 emitted from zone 4 of the Robert-Bourassa reservoir considering the influent influx of CO_2 from the drainage basin or neglecting it completely (influent dissolved CO_2 at equilibrium with the atmospheric CO_2 only)

Again, these results are coherent with the assumption that carbon originating from the drainage basin is the major source of carbon emitted through the water-air interface of the reservoir but only after the transi-

tional flux of CO_2 due to the decomposition of the flooded vegetation and soil has vanished.

CH_4 emissions

Figure 25.16 shows the concentration of dissolved CH_4 in zone 4 of the nine zone segmented Robert-Bourassa reservoir as computed by the model. No direct measurement of CH_4 was available to check upon these values but they are very small values as they are essentially the concentration of CH_4 at equilibrium with the atmosphere at the water temperature of the reservoir. The corresponding values for the flux of CH_4 emitted at the water-air interface of the reservoir are illustrated in Fig. 25.17 where they are compared with the flux measurements of CH_4 reported recently for the Robert-Bourassa reservoir (Lambert 2001, 2002; Therrien 2003).

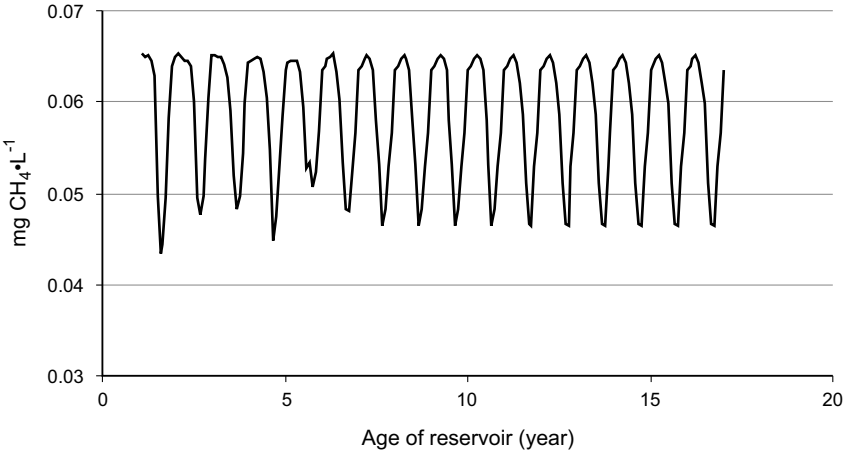

Fig. 25.16. Concentration of dissolved CH_4 in the surface water layer as computed by the model for zone 4 of the nine zone segmented Robert-Bourassa reservoir

Large discrepancies are observed but they are no surprise. In effect, kinetic parameters R and Mmax given in Table 25.7 for the production of CH_4 from the decomposition of flooded vegetation and soil are extremely small values compared to the ones reported for the kinetic parameters related to the production of CO_2. Therefore, the use of these parameters by the model will contribute negligible quantities of CH_4 to the incoming CH_4 entering the reservoir through the influents. The most probable cause for these discrepancies is that the kinetic parameters furnished in Table 25.7 underestimate the true value of these parameters. Again, this would not be

a surprise considering that no production of methane occurred before 60 days and that even after a period of one year production of methane was still very active for some of the vegetation and soil components (see Chap. 13).

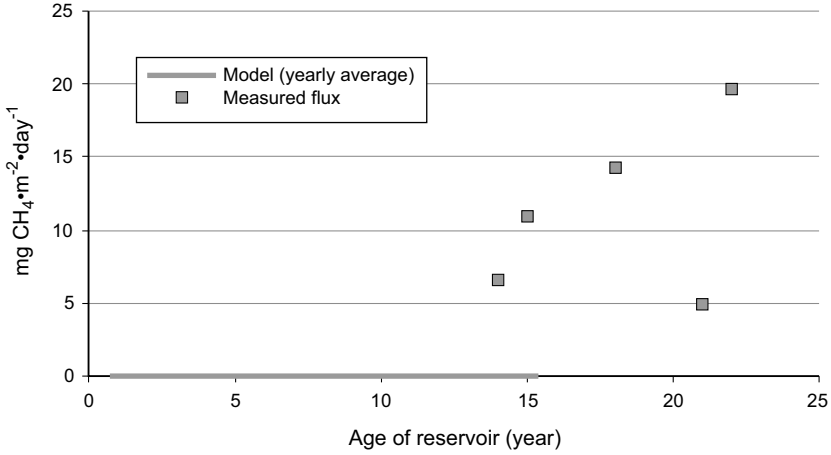

Fig. 25.17. Yearly average of the flux of CH_4 emitted from zone 4 of the nine zone segmented Robert-Bourassa reservoir

In order to improve the predictive capabilities of the model for the production of methane, some options appear. They are all based on the availability of recent field data measurements for CH_4 emissions from newly created as well as for equilibrated reservoirs and others water bodies (Lambert 2001, 2002; Therrien 2003).

These options are:

- a re-calibration of the kinetic parameters for the production of methane from flooded vegetation and soil using the available data for reservoirs for which input data sets can be furnished to run the model;
- the analysis of the concentration of dissolved methane in rivers to see if similar concentrations in the influents to a reservoir could explain the emissions of methane reported in reservoirs;
- the analysis of the concentration and flux of methane emitted from lakes since long-term evolution of some of the characteristics of reservoirs offer similarities of processes (Tremblay et al. 2001).

25.4.3 Limitations of the Model

This version of the model does not:

- take into account the dynamics of the primary production including the photosynthesis-respiration of the primary trophic level of the reservoir;
- consider the increased productivity of the whole aquatic ecosystem the early years after flooding with the corresponding increase in respiration from the biotic components;
- compute the degree of oxidation of methane in the water column and the corresponding extent of transformation to carbon dioxide.

Also, computations of the interfacial mass transfer K_{LCO2} and K_{LCH4} by the model using relationships (25.11) and (25.12) are valid if the transfer of CO_2 and CH_4 in water occurs by diffusion only. This condition does not appear to restrict the use of relationship (25.11) for CO_2 emitted from boreal reservoirs since CO_2 transfer by bubbling is very small (< 1%) compared to transfer by diffusion (Therrien 2003). Generally, transfer of CH_4 by bubbling in boreal reservoirs is small compared to transfer by diffusion but this is not always the case as has been reported recently (Therrien 2003). For some of the boreal reservoirs for which emission by bubbling was observed (Duchemin 2000), the use of relationship (25.12) could underestimate the emission of CH_4 at the interface by as much as 30%.

25.5 Conclusion

25.5.1 Model characteristics

The model derived here is built around fundamental mass balance equations for CO_2 and CH_4, which permit the *rigorous* treatment of input, output, production and transformation of these compounds. The solution of these mass balance formulations, represented by differential equations, permits the computation of their evolution as a function of time. This allows the user to include explicitly as input data to the model variables that vary with time such as water temperature, wind velocity, influent flow rate, influent water quality, water level and so on.

The structure of the model is limited to the consideration of a finite number of spatial vertical and horizontal segmentations of the reservoir. The current version of the model offers up to three zones (horizontal segmentation of a reservoir) and two water layers per zone. The choice made represented a compromise in term of flexibility to the user (wanting to represent at best the morphological configuration of its reservoir) and the re-

quirements that follow in providing the bathymetric related data per zone and layers.

The structure and formulation of the model permit the consideration of numerous processes affecting the mass balance of CO_2 and CH_4 such as the ones considered here but others can be added to the structure easily (i.e. transformation of methane to CO_2 in the water column).

The input data required to run the model, except for kinetic oriented data related to the decomposition of flooded vegetation and soil components, are generally available from the Hydro-Quebec environmental data bank.

Such a model has the capability to do sensitivity analysis and to characterize the influence of uncertainties in the values of parameters or variables on the model response. This is useful since the results permit the discrimination between less sensitive and critical parameters. Also, these results permit the more precise identification of areas for which priority of development should be given.

25.5.2 Performance of the model

The model does not compute directly the emissions of CO_2 and CH_4 from the reservoir but computes first the concentrations of CO_2 and CH_4 dissolved in the water of the surface and of the bottom layers of each of the zones of the reservoir. The rates of transfer of CO_2 and CH_4 at the water-air interface of each zone is then computed from the concentrations of CO_2 and CH_4 dissolved in the water of the surface layer according to the driving forces which are the water temperature and wind velocity.

The first step offered an opportunity to do an indirect check upon the mass transfer at the water-air interface by comparing the computed results with available data for the concentration of CO_2 and CH_4 dissolved in water. This check was important because any large discrepancy at this stage would have been indicative of a value for the interface mass transfer coefficient that was either too large or too small. The comparisons made have indicated that concentrations of CO_2 computed by the model are in the range of values reported for the surface water layer.

Comparisons of flux have indicated that emissions of CO_2 computed by the model were in the range of fluxes calculated from the experimental determination of dissolved CO_2 in water. The computed flux of CO_2 as a function of reservoir age was also coherent with the CO_2 flux measurements data.

An important finding is that the transitional increase in the fluxes of CO_2 computed from the model and due to the decomposition of the flooded

vegetation and soil in the Robert-Bourassa reservoir is significant only during an interval of time not exceeding 6–8 years. Also, the results from the model are coherent with the assumption that carbon originating from the drainage basin is the major source of carbon emitted through the water-air interface of the reservoir after the transitional flux of CO_2 due to the decomposition of the flooded vegetation and soil has faded away.

Fluxes of CH_4 computed from the model have been shown to underestimate grossly the values reported from the direct measurements of CH_4 emissions. Analysis of the results have indicated the source of the discrepancies which lies with the very low production of CH_4 as indicated from the vegetation and soil decomposition data used by the model. Suggestions to improve the model forecasting of CH_4 emissions are indicated.

Acknowledgements

This work was supported by Hydro-Québec.

26 Synthesis

Alain Tremblay, Louis Varfalvy, Charlotte Roehm and Michelle Garneau

Abstract

The objectives of this chapter are to present a comprehensive review of the current state of knowledge and to identify the gaps in the greenhouse gas issues in hydroelectric reservoirs and natural ecosystems. It has become essential to integrate our knowledge of the carbon cycle at the larger temporal and spatial scales in order to properly assess the magnitude of GHG fluxes from reservoirs[1] and natural ecosystems. The information available comes from small scale and short term (1 to 10 years) studies mostly from boreal regions but also from semi-arid and tropical regions. Natural variability of GHG fluxes due to regional climatic variations and their impacts on whole biological production are far more important than the techniques available to measure them. Therefore, one must keep in mind that the uncertainties in the GHG fluxes are related to natural spatial and temporal variations of fluxes and not necessarily from the measurement techniques themselves. This synthesis is based on the findings of over ten years of studies reported by research teams from many universities, governmental agencies and power utilities.

[1] To define the magnitude of GHG fluxes we calculate gross and net emissions. The gross emissions are those measured at the water-air interface. The net reservoir emissions are gross emissions minus pre-impoundment natural emission (both terrestrial and aquatic ecosystems) at the whole watershed level, including downstream and estuary. These definitions come from the WCD (2000).

26.1 Greenhouse Gases in Natural Environments

26.1.1 Terrestrial Ecosystems

Forests and wetlands are dynamic ecosystems in terms of carbon cycling. Overall, the carbon pool of forests is similar among climatic regions but the allocation between soils and vegetation varies with latitude. Higher latitudes are characterized by slow decomposition rates and short growing seasons (Chap. 6, Malhi et al. 1999). Typical soils of boreal forests have a higher organic carbon content (24±94%) than soils from temperate (10±77%) or tropical forests (11±63%). However, the estimates of the organic carbon sequestered in the vegetation of tropical forest are two to five times higher (15-23 $kg{\cdot}C{\cdot}m^{-2}$) compared to boreal and temperate forests (4-6 $kg{\cdot}C{\cdot}m^{-2}$) (Chap. 6, Goodale et al. 2002; FAO 2001; Malhi and Grace 2000).

Current estimates of GHG budgets of forests indicate that these ecosystems act as carbon sinks regardless of climatic region. The sequestering of GHGs by forests is the result of the balance between a substantial uptake of CO_2 by biomass and CO_2 release through soil respiration, oxidation of CH_4 by methanotrophic bacteria, and a more or less significant emission of N_2O from soil, a by-product of nitrification and denitrification reactions. According to estimated GHG budgets, the boreal forest sink (-873 $mg{\cdot}CO_2\text{-}eq.{\cdot}m^{-2}{\cdot}d^{-1}$) is weaker than the temperate and tropical ones (-1 288 and -1 673 $mg{\cdot}CO_2\text{-}eq.{\cdot}m^{-2}{\cdot}d^{-1}$, respectively). Boreal forests, during particularly warm and dry years, can be net sources of CO_2 (Chap. 4, Goulden et al. 1998; Lindroth et al. 1998; Carrara et al. 2003). The duration of growing seasons, which lengthens from higher to lower latitudes, contributes to such a pattern. Unlike boreal and temperate forests, the N_2O flux seems to play an important role in the GHG budget of tropical forests, representing an average loss of 30% (in CO_2-eq.) of the NEE. This is due to a relatively high N_2O emission rate from tropical forest soils as well as to the global warming potential of N_2O, which is about 300 times higher than that of CO_2 (IPCC 2001; Livingston et al. 1988; Clein et al. 2002). Furthermore, such as the estimated range of GHG fluxes for the tropical forest suggests, GHG production in the form of N_2O could exceed, at some sites, the CO_2 uptake, transforming the sites into GHG sources (2758 $mg{\cdot}CO_2\text{-}eq.{\cdot}m^{-2}{\cdot}d^{-1}$) (Chap. 4).

Natural disturbances are expected to increase in frequency and extent under conditions of a changing climate (IPCC 2001). The forest GHG budgets do not, however, take into account the influence of natural disturbances (fire, insect defoliation, wind throw) on large-scale carbon dynam-

ics of northern forests. Over wide areas, these natural disturbances (especially fire) can result in significant short and long-term emissions and they should be taken into account to more accurately assess the long-term carbon storage or the net biome production of an ecosystem (Amiro et al. 2001; Kasischke and Bruhwiler 2002, Chap. 4 and 6).

Wetlands cover 3% of the Earth's surface but represent approximately 30% of the terrestrial soil carbon pool. Wetlands cover around 30% of the circumboreal landscape (Gorham 1991; McLaughlin 2004). They have a strong propensity to emit CH_4 because of their water-saturated soils that favor anaerobic decomposition of organic matter. Tropical wetlands, dominated by marshes and swamps, emit large amounts of CH_4 into the atmosphere (71 $mg{\cdot}CH_4{\cdot}m^{-2}{\cdot}d^{-1}$) compared to northern peatlands (34 $mg{\cdot}CH_4{\cdot}m^{-2}{\cdot}d^{-1}$) resulting in a global GHG budget of about 11000 $mg{\cdot}CO_2\text{-}eq.{\cdot}m^{-2}{\cdot}d^{-1}$ and 1400 $mg{\cdot}CO_2\text{-}eq.{\cdot}m^{-2}{\cdot}d^{-1}$ for tropical and boreal wetlands, respectively. However, these budgets only indicate the order of magnitude of the GHG fluxes, since they are calculated from few available data. As for the forests, the wetland GHG fluxes vary with environmental and climatic parameters (Chap. 6, McLaughlin 2004). Moreover, GHG budgets estimated for wetlands do not generally take into account ponds which are potential sources of GHG (Kling et al. 1991; Roulet et al. 1994; Waddington and Roulet 2000) and export of DOC (Carroll and Crill 1997; Alm et al. 1999b; Waddington and Roulet 2000). These exports could significantly change the GHG budgets of wetlands.

Most of the information available in the literature covers partial or complete growing season for a few years (Chap. 4). Very few studies across ecosystem types even consider a complete annual cycle in estimates of carbon budgets. Since GHG fluxes vary among seasons and between years according to climatic conditions, it is important to look at both the time scale and the spatial scale used to estimate net GHG budgets for terrestrial ecosystems. For example, it is generally believed that pristine young forest ecosystems, after a growth over a period of 30 to 50 years (sink of carbon), reach a stage of maturity that lasts for a few years (neither a sink or a source of carbon) and then slowly decay (source of carbon) (Grace et al. 1995, International Science Conference, 2000). In view of the high variability encountered at small scales in the GHG fluxes, a temporal scale a 100 years and a spatial scale at the drainage basin level would be more appropriate to assess GHG mass balance in terrestrial ecosystems. This approach will minimize the seasonal or local variation due to natural climatic and biological variability and give more realistic estimates of GHG net fluxes.

26.1.2 Aquatic Ecosystems

Although inland waters cover less than two percent of the earth's surface, they may contribute to an important part of the total carbon cycling since a significant part of the terrestrial organic carbon moves through rivers and lakes before reaching estuaries and oceans. In fact, recent studies have shown that up to 15% of the annual forest carbon production is exported through the drainage system and that CO_2 flux from limnetic habitats to the atmosphere may represent up to 50% of the continental losses of organic carbon to the ocean (Cole et al. 1994; Dillon and Molot 1997). This is particularly true for the northern hemisphere where most of the freshwater lakes are found. The export of carbon from terrestrial to aquatic ecosystems, in the form of DOC and DIC, may contribute to improve carbon budgets (Richey et al. 2002, Chap. 6).

Approximately 90% of the organic carbon in lakes and rivers is in the dissolved phase (DOC) and 10% as particulates (POC) (Naiman 1982; Hope et al. 1994; Pourriot and Meybeck 1995). DOC and POC exceed the amount of organic carbon present as living material in the form of bacteria, plankton, flora and fauna (Wetzel 2001). The major source of material and energy in most aquatic systems is from allochthonous inputs of terrestrial organic matter. The amount of organic matter reaching a lake and the chemical composition of these organic compounds change seasonally with the volume of flow in relation to time in the stream, and the growth and decay cycle of terrestrial and marsh vegetation (Chap. 6, 8 and 9). Compared to runoff, groundwater flow contributes small amounts of DOC (around 5%) to aquatic ecosystems (Devol et al. 1987; Cole et al. 1989; Prairie et al. 2002; Schiff et al. 2001).

Much of the DOC pool consists of refractory compounds that are chemically complex and resistant to microbial degradation (Lindell et al. 1995; Moran et al. 2000). The labile dissolved organic compounds are recycled rapidly, even at low concentrations, and represent the major carbon pathways of energy transformations. The labile organic compounds are used either by bacteria or phytoplankton, transformed within living organisms and transferred to the top of the food chain. While the refractory complex compounds can be broken into smaller fractions by ultraviolet light (Chap. 21), and assimilated or used by bacteria (Gennings et al. 2001), most refractory compounds settle to the lake sediments.

Lakes and rivers act as transit zones for carbon between terrestrial ecosystems and estuaries, and are generally a source of gases to the atmosphere. There seems to be a positive relationship between the amount of carbon entering the lake, calculated as the drainage / lake surface ratio, and the magnitude of the emissions at the water-air interface (Engstrom 1987;

Sobek et al. 2003, Chap. 8). Since allochthonous terrestrial inputs to a lake are generally defined by the characteristics of its drainage basin and are relatively constant in time, emission of CO_2 to the atmosphere or its emission further downstream should also be relatively constant in the long term (Wetzel 2001). For deep water lakes, the contribution of organic carbon from lake sediments is very small in comparison to the terrestrial drainage basin input. However, for shallow lakes, the magnitude of the sediment carbon fluxes could be significant, since water temperature is generally higher and favors decomposition of the organic matter in the sediments (Chap. 5, 11, 22).

Carbon is transformed by the primary producers (bacteria, phytoplankton) or the secondary consumers (zooplankton, benthos, fish), as it moves up in the food chain and it is respired or consumed at different rates according to the productivity of the system. In addition to the water chemistry, these respiration rates will influence the quantity of CO_2 dissolved in the water and the CO_2 fluxes at the water-air interface. Approximately 90% of natural boreal lakes are over saturated in CO_2 and emit between 50 to 10000 $mg{\cdot}CO_2{\cdot}m^{-2}{\cdot}d^{-1}$ to the atmosphere (e.g. Cole et al. 1994; Prairie et al. 2002; Therrien 2003). Rivers from boreal and temperate zones have fluxes higher than or in the same order of magnitude as lakes (Hinton et al., 1998; Hope et al., 1997; Cole and Caraco 2001; Sobek et al. 2003). Lakes having a pH higher than 8, either caused by high primary production or buffered by the alkaline soils of the drainage basin, tend to be under saturated in CO_2. These systems have lower emissions or act as CO_2 sinks (Chap. 8, 9).

Most lakes, rivers and varzéas from tropical regions tend to have higher CO_2 emissions than those in boreal regions (Richey et al. 2002, Chap. 22). While CH_4 fluxes at the water-air interface are small and N_2O fluxes are negligible (Therrien, Chap. 8, 9) in both tropical and boreal regions, CH_4 emissions can be significant in shallow areas such as beaver dams, rice fields and varzéas (Chap. 4, 6, 22).

Sub-surface sediments often present anoxic conditions which enhance CH_4 production and increase CH_4 concentrations. Both CH_4 production and diffusion across the sediment-water interface increase with whole lake productivity from oligotrophic to eutrophic lakes (Chap. 5). However, more than 95% of the CH_4 sediment production is oxidized in the water column and/or at the sediment-water interface contributing very little directly to lake GHG emissions (Lidstrom and Somers 1984; Frenzel et al. 1990; King 1990; King and Blackburn 1996). The sediment CH_4 production usually increases with lake depth as water anoxic conditions are more frequently found. Nevertheless, in shallow warm waters and sediments rich in organic matter of tropical regions, e.g. *varzéas*, or very eutrophic lakes

of temperate regions, CH_4 can form bubbles that will not be oxidized and could contribute to GHG emissions (Chap. 5, 11, Keller and Stallard 1994; Huttunen et al. 1999, Fig. 26.1). In shallow areas (< 1 m) the CH_4 emitted at the water-air interface represents up to 45% of the CH_4 production at the sediment-water interface (Scranton et al. 1993; Duchemin et al. 1995; Duchemin et al. 2000; Huttunen et al. 2002) and up to 10% of CH_4 production in deeper areas (>3 m) (Rudd et Taylor 1980). Sediment GHG production in certain environments can, therefore, represent a significant proportion of the gas emitted at the lake water-air interface (Chap. 5).

26.1.3 Estuaries

Estuaries are sites of intense sedimentation processes of materials from either surface runoff or eroded from land and transported in rivers. Along with this inert material, there is also heterotrophic bacterial respiration occurring, and the majority of the bacteria are attached to the particles and plankton.

Tidal marshes are generally a long-term net sink of atmospheric CO_2 leading to a net burial of organic matter in the sediment (Smith and Hollibaugh 1993; Gattuso et al. 1998). However, due to an intense recycling of sedimentary organic matter at low tide, tidal flats and marshes emit large amounts of CO_2 directly to the atmosphere. Lateral transport of CO_2 from tidal flats and marshes can also significantly contribute to the high pCO_2 measured in adjacent estuarine waters. Estuaries are very dynamic heterotrophic ecosystems with CO_2 emissions to the atmosphere varying between 44 and 44000 $mg \cdot m^{-2} \cdot d^{-1}$ (Chap. 7). Estuarine plumes are sites of intense primary production and show large seasonal variations; therefore at any one time, some plumes behave as a net sink of CO_2 while others are a net source. Because of high organic matter content of the sediments and low oxygen concentration in tidal flats and marshes, there are also moderate CH_4 emissions to the atmosphere varying from 0.32-8 $mg \cdot m^{-2} \cdot d^{-1}$.

Despite the fact that about 60% of the fresh water discharge and organic carbon inputs to oceans occur at tropical latitudes, most of the reported CO_2 fluxes in estuaries are from temperate latitudes (Ludwig et al. 1996). In any case the carbon dioxide source from inner estuaries and sources or sinks from riverine plumes could represent significant components of regional cycles and perhaps the global carbon cycle. However, CH_4 emissions from estuaries seem to be a minor contributor to global methane emissions (Chap. 7, Bange et al. 1994).

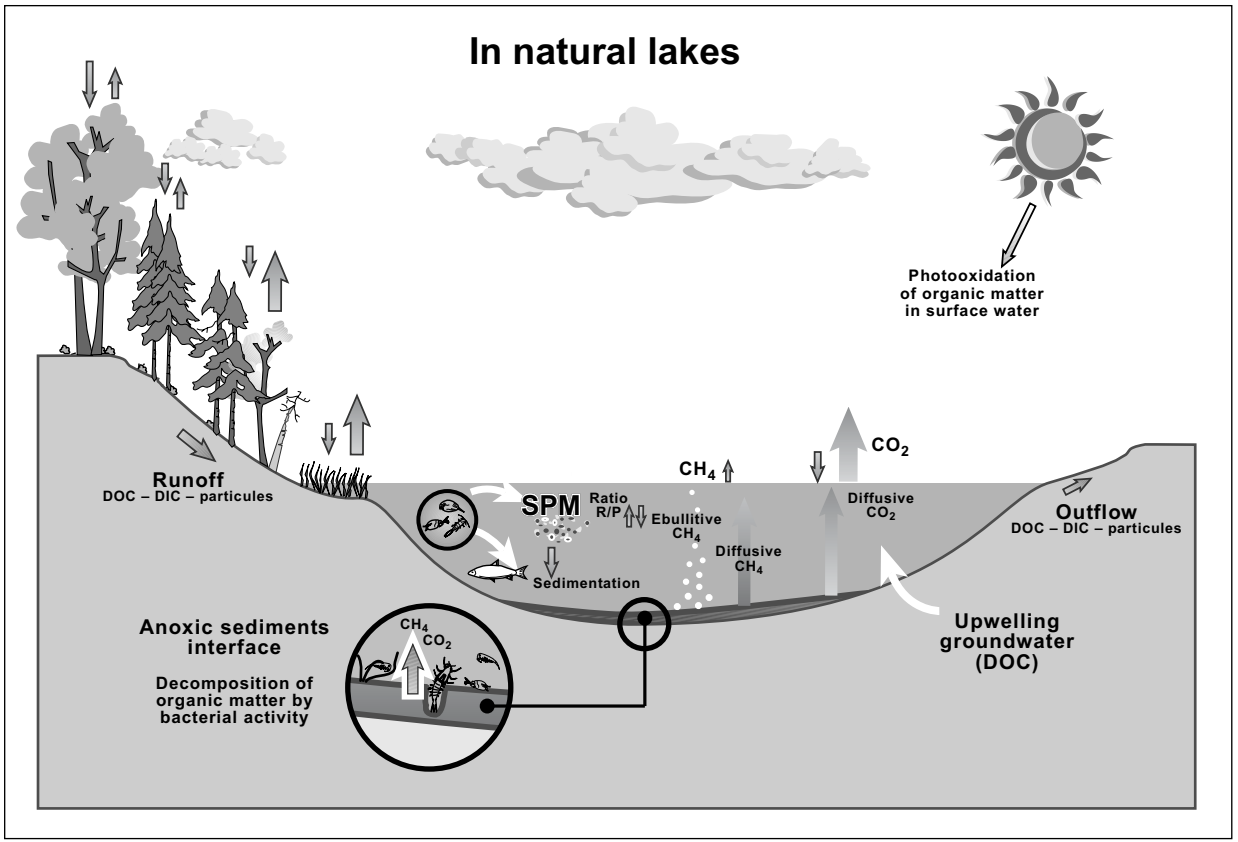

Fig. 26.1. Major processes occurring in natural lakes

26.2 The Issue of Greenhouse Gases in Hydroelectric Reservoirs

According to the IAEA (1996) and others (Table 26.1), energy generated with the force of water is one of the cleanest ways to generate electricity in terms of greenhouse gas emissions. This trend was confirmed by most of the studies made on boreal reservoirs during the last decade for which the average gross GHG emissions are one to two orders of magnitude lower than those from thermal alternatives. However, emissions from tropical reservoirs could, under certain conditions, exceed those from thermal alternatives (cf. the Petit Saut reservoir in French Guiana and some Brazilian reservoirs). Nevertheless, a worldwide debate on the role of freshwater reservoirs and their contribution to the increase of GHG in the atmosphere is on going. There is a concurrent debate on the comparison of energy generation methods (Rosa and Scheaffer 1994, 1995; Fearnside 1996; Gagnon and van de Vate 1997; St. Louis et al. 2000; Tremblay et al. 2003). As a

Table 26.1. Full Energy Chain Greenhouse Gas Emission Factors in $g \cdot CO_2 \cdot equiv./kWh(e) \cdot h^{-1}$ (modified from IAEA 1996)

Energy source	Emission Factor* g CO_2 equiv./ kWh(e).h
Coal (lignite and hard coal)	940 - 1340
Oil	690 - 890
Gas (natural and LNG)	650 - 770
Nuclear Power	8 - 27
Solar (photovoltaic)	81- 260
Wind Power	16 - 120
Hydro Power	4 - 18
Boreal reservoirs (La Grande Complexe)[1]	~ 33
Average boreal reservoirs[2]	~ 15
Tropical reservoirs (Petit-Saut)[3]	~ 455 (gross) / ~ 327 (net)
Tropical reservoirs (Brazil)[4]	~ 6 to 2100 (average: ~160)

*: Rounded to the next unit or the next tenth respectively for values < or > 100 $g \cdot CO_2 \cdot equiv./kWh(e) \cdot h^{-1}$.
1: La Grande Complexe, Quebec, 9 reservoirs, 15 784 MW, ~ 174 km^2/TWh, (Hydro-Quebec 2000).
2: According to average reservoir characteristics of 63 km^2/TWh, (Hydro-Québec 2000).
3: Petit-Saut, French Guiana, 115 MW, 0.315 MW/km^2 (Chap. 12).
4: 9 Brazilian reservoirs from 216 to 12 600 MW, total power = 23 518 MW, total surface = 7867 km^2.

result, much research has been done over the last 10 years to better understand the processes leading to GHG emissions from reservoirs and to determine the duration of these emissions.

The chemical, morphological and biological processes determining the fate of carbon in reservoirs are similar to those occurring in natural aquatic ecosystems. However, some of these processes might be temporally modified in reservoirs due to the flooding of terrestrial ecosystems which results from the creation of reservoirs (Chartrand et al. 1994; Schetagne 1994; Deslandes et al. 1995). In boreal reservoirs, environmental follow-up programs have clearly shown that these changes generally last less than 10 years (Chap. 1). However in tropical reservoirs, these changes can extend over a longer period of time according to the conditions of impoundment.

The conclusions drawn in this section are based on results from the world's largest environmental programs. One must keep in mind, that most of the data come from research and measurements in boreal regions (mainly Canada) and, to a lesser extent, from a follow-up environmental program of Petit Saut reservoir in tropical French Guiana. This section also benefits from many field measurements undertaken in tropical regions of Panama and Brazil, the semi-arid region of the southeastern of United States, and other areas of the boreal region (Figs 26.1-26.5, Table 26.2).

26.2.1 Flooded Soils and Sediments

In vitro experiments have been made by flooding different types of soils and reproducing different environmental conditions reflecting impoundments of boreal terrestrial ecosystems (Chap. 13). These experiments have revealed significant releases of CO_2 and CH_4 to overlying waters. Regardless of the environmental conditions applied over 340 days, total amounts of cumulative carbon ranged from 200 to 450 mg $CO_2.g^{-1}$ and was about 1.7 mg $CH_4.g^{-1}$ for flooded vegetation. For flooded soils, average cumulative quantities produced over the same period ranged from 72 and 140 $g.CO_2.m^{-2}$ and from 0.2 to 0.6 $g.CH_4.m^{-2}$ (Chap. 13). For the living part of the vegetation, a significant proportion of the initial carbon content was released to the water phase in first 6 months with the largest quantities coming from green mosses. For the flooded soils, which support a far greater mass of organic matter, only a small fraction of the initial carbon pool was released to the water column over the duration of the experiment. Due to the great variability of the carbon burden in soil samples, the percentage of the initial carbon pool which is released is difficult to accurately estimate.

Table 26.2. Environmental impacts of the creation of reservoirs, in terms of greenhouse gases, in boreal, semi-arid and tropical regions

Type of impact	Boreal reservoirs	Semi-arid reservoirs	Tropical reservoirs
CO_2 emissions	Diffusive CO_2 >95% Ebulittive CO_2 <5% <10 years	Diffusive CO_2 >95% Ebulittive CO_2 <5% <10 years	Diffusive CO_2 >95% Ebulittive CO_2 <5% >10 years
CH_4 emissions	Diffusive CH_4 >95% Ebullitive CH_4 <5% <10 years	Diffusive CH_4 >95% Ebullitive CH_4 <5% <10 years	Diffusive CH_4 >60% Ebullitive CH_4 >30% >10 years
Erosion in the draw down zone, active release of organic matter	<10 years	<10 years	<10 years
Release of nutrients from flooded soils to the water column	<10 years	<10 years	<10 years
Enhanced bacterial activity in flooded soils and water column	<10 years	<10 years	>10 years
Decomposition of a fraction of the flooded organic matter	<10 years	<10 years	<10 years
Presence of anoxic zone	Mostly negligible <10 years	Mostly negligible <10 years	Maybe very important in some reservoirs >10 years
Methanogenesis at the sediment-water interface	Negligible <10 years	Negligible <10 years	Maybe very important in some reservoirs >10 years
Contribution of allochthonous DOC to methanogenesis	Negligible	Negligible	Maybe important according to presence of anoxic zone
Macrophyte growth in the drawdown zone	Negligible	Negligible	Maybe important in some reservoirs
Degassing downstream of the dam	Mostly negligible	Mostly negligible	Maybe very important in some reservoirs

In boreal reservoirs, *in situ* measurements of flooded soils confirm that only a small fraction of the carbon pool is released to the water column (Houel 2002). Indeed, after a decade most flooded soils, except those eroded in the drawdown zone at the rim of the reservoirs, show no significant loss of carbon content (Houel 2003). These results are related to small physical structural changes and a partial degradation of organic matter upon flooding. While bacterial activity is intense enough to provoke a strong oxygen demand in the flooded soils and in the bottom waters for a few years after impoundment (Schetagne 1994), losses of carbon in these flooded soils are smaller than the inherent variability in the carbon content encountered of nearby soils (Figs. 26.2-26.3). Nevertheless, organic matter in podzolic soils appears more sensitive to degradation after flooding than that of peatlands which are already saturated under pre-flood conditions. Ligneous components of flooded vegetation remained virtually unaffected after many decades, with spruce tree trunks having lost less than 1% of their biomass after 55 years of flooding in the Gouin reservoir (boreal Québec, Van Coillie et al. 1983). Furthermore, results from artificial reservoirs (ELARP and FLUDEX, Chap. 15) having similar GHG emissions, demonstrated that the composition of the organic matter was more important than the quantity. Experimental reservoirs allow a better understanding of the mechanisms related to GHG fluxes. However, due to their shallow depth and small surface area, the results can not be easily extrapolated to larger reservoirs.

In tropical French Guiana, the results of the Petit Saut reservoir showed a rapid increase in GHG emissions following flooding (Chap. 12, 22, Galy-Lacaux et al. 1997, 1999). The large amount of flooded vegetation coupled with the high mean water temperature ($> 25^{o}C$) enhanced the decomposition of organic matter and the consumption of dissolved oxygen in the water column, creating anoxic conditions that favor CH_4 production at the soil-water interface. Seven years after impoundment, sediment CH_4 production decreased by 30% (Chap. 12, 22). However, carbon input from the drainage basin may have maintained anoxic conditions favorable for CH_4 production and which may extend the period of CH_4 production in some tropical reservoirs (Chap. 12, 22, Figs. 26.4-26.5).

There is a convergence in the results that clearly illustrates that, in both boreal and tropical reservoirs, the contribution of flooded soils of the reservoir carbon pool is important in the first few years following impoundment (Chap. 9, 11, 12). After this period, terrestrial allochthonous input of DOC can exceed, by several times, the amount of POC and DOC produced within the reservoir through soil leaching or primary production (Wetzel 2001). In reservoirs, this is particularly important since the water residence

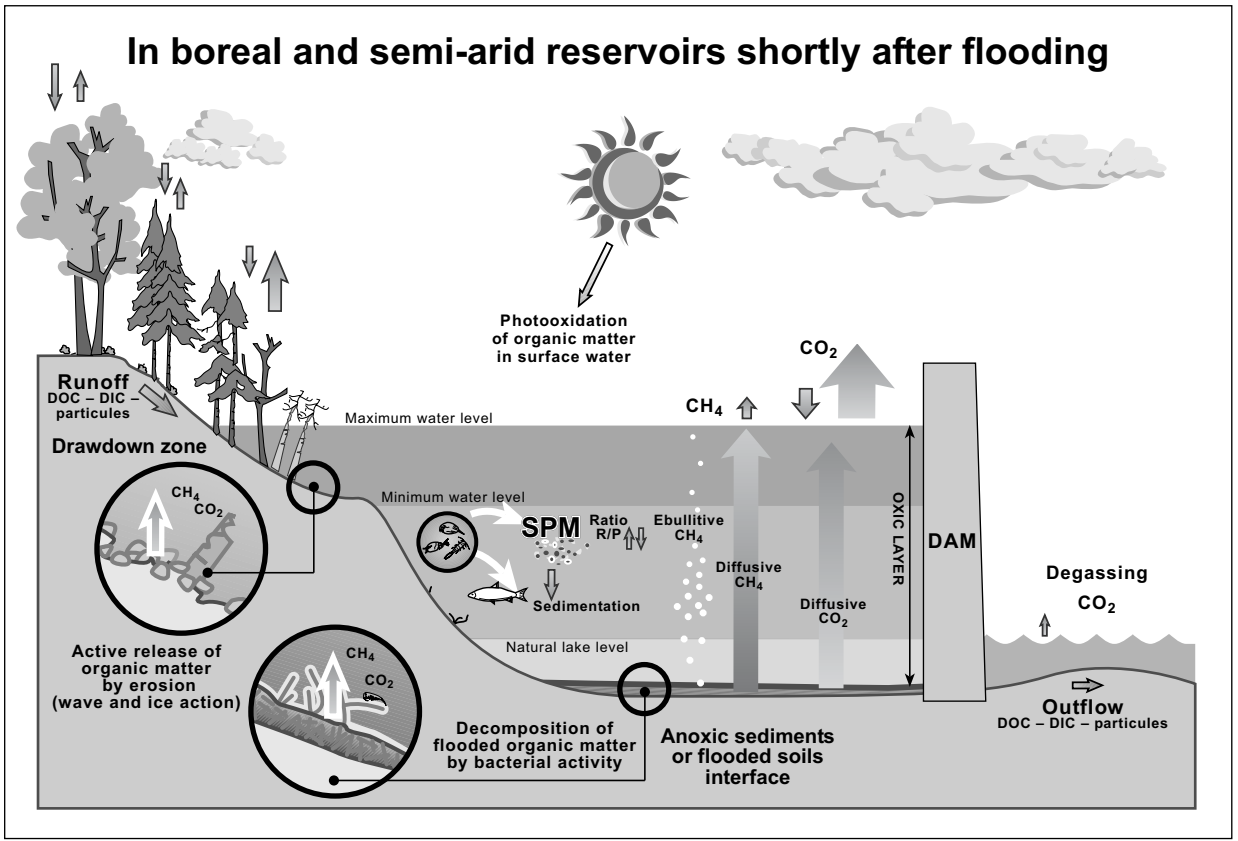

Fig. 26.2. Major processes occurring in boreal and semi-arid reservoirs shortly after flooding (<10 years)

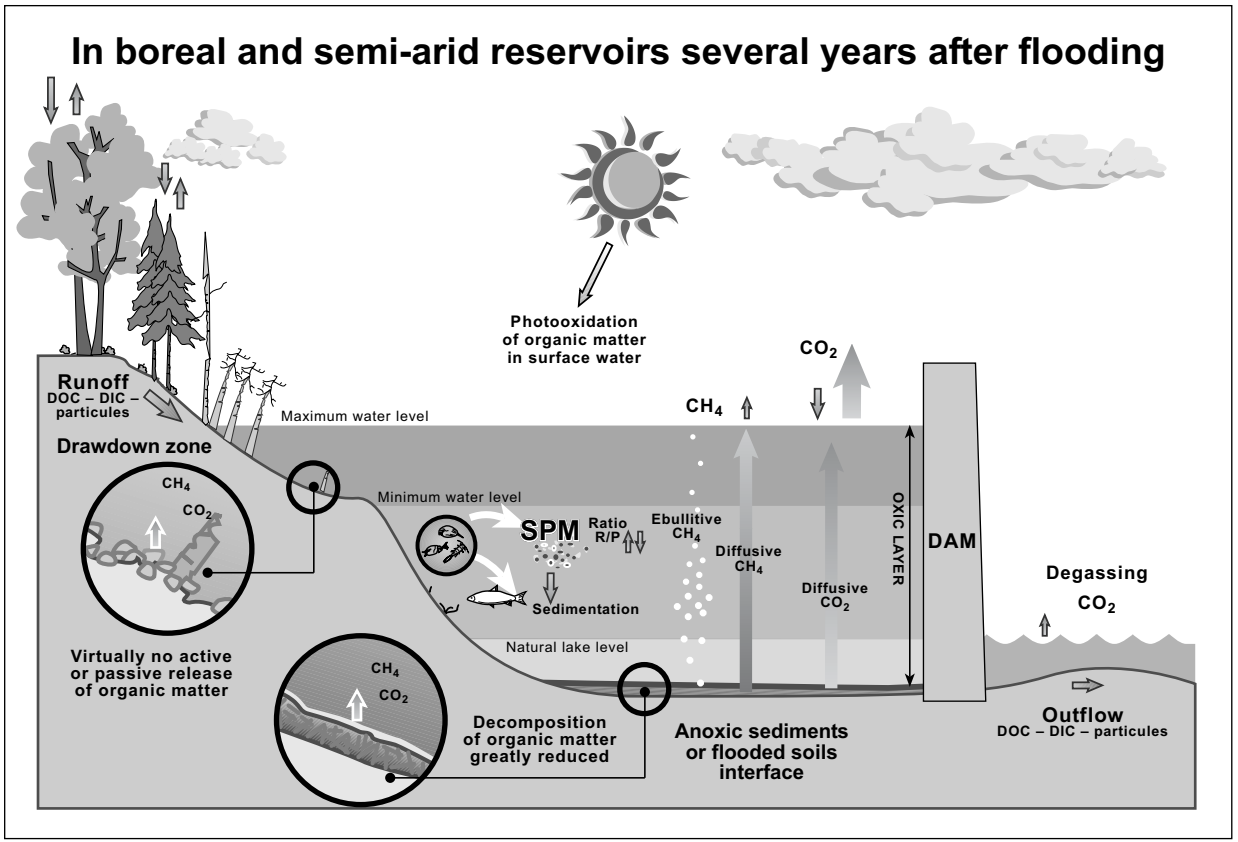

Fig. 26.3. Major processes occurring in boreal and semi-arid reservoirs several years after flooding (>10 years)

time is generally shorter, from a few weeks to a few months, in comparison to several years to many decades in the case of lakes (Chap. 8). The GHG emissions model which predicts that after 5 to 8 years, the contribution of carbon from flooded soils are very small and that the major source of carbon is allochthonous terrestrial matter, further supports this. Moreover, in the shallow experimental FLUDEX and ELARP reservoirs, where the allochthonous terrestrial inputs are very small, there was a decrease in the overall DIC and CO_2 production following the maximum production. However, it is still difficult to determine if the CO_2 emissions are related to the loss of carbon from the flooded soils or from the decomposition of algal biomass produced in reservoirs (Chap. 15).

26.2.2 Water Column

The water column hypolimnion (lower) and epilimnion (upper) are affected differently by external parameters. The hypolimnion is little affected by external processes and generally characterized by molecular diffusion of gas from the soil-water interface to the few meters above (Chap. 5, 22, Duchemin 2000). The epilimnion is generally thicker, from 1 or 2 m to 30-50 m. This layer is generally perturbed by external parameters such as wind, waves, UV light radiation, and gas exchange with the atmosphere (Chap. 10, 12, 13, 14, 20, 22).

In boreal Québec, results from the La Grande complex show that intensive decomposition of flooded organic matter is short lived due to the rapid depletion of readily decomposable fraction (Chap. 1, Schetagne 1994). Water quality modifications resulting from this decomposition, such as dissolved oxygen depletion, increased CO_2 production and release of nutrients, last up to 8 to 14 years after impoundment. The duration depends on the reservoir's hydraulic and morphological characteristics (Schetagne 1994; Chartrand et al. 1994). The *in vitro* flooding experiments confirmed that, at the temperature (around 10-20^{o}C) of the water of the La Grande complex, virtually all of the labile carbon was decomposed within a few years and mostly within the first few months (Chap. 13). Additionally, an experimental model predicting water quality, indicated a similar trend; after a period of less than 10 years, the water quality in boreal reservoirs was comparable to that of natural lakes (Chap. 25). Moreover, in the tropical Petit Saut reservoir there was very intensive decomposition of the flooded organic matter resulting in a rapid consumption of most of the dissolved oxygen in the water column. Water quality modifications due to the decomposition were more severe that those observed in boreal reservoirs. This resulted in a mostly permanent stratification where the oxygenated

upper layer gradually increased in thickness from less than 1 m after impoundment to close to 7 m, 5 years after impoundment. Although there is a clear improvement in the water quality after 5 years, in contrast to boreal reservoirs the water quality modifications may last longer than 10 years (Chap. 12, 22).

The ratio of areal gross primary production to planktonic respiration, which reflects community metabolism, varies with the seasons and within a water body but is similar between lakes and reservoirs older than 7 years (Chap. 20). This ratio indicates that the lowest autochthonous carbon contribution to respiration occurs in younger reservoirs as well as in the shallow areas of reservoirs where organic matter from soil is released. This is further supported by similar bacterial activity between lakes and reservoirs older than 7 years, although there is no clear evidence that the age of the reservoir had a strong effect on measured bacterial activity (Chap. 18, 19). Nevertheless, the time after impoundment does have an effect on DOC and nutrient availability which are positively related to bacterial activities (Figs. 26.2-26.5).

Similarly, the zooplankton community was also affected by the higher primary production in the years following impoundment, where community biomass increased. Zooplankton, however, were affected by the water residence time and water temperature and not by food availability. In boreal reservoirs, these conditions favored the growth of cladoceran and rotifer communities and influenced the dynamics of carbon exchange with the atmosphere. For example, total planktonic community respiration in reservoirs and lakes, accounted for more than 90% of the CO_2 fluxes measured at the water-air interface (Chap. 20).

26.2.3 Exchange at the Water-Air Interface

Allochthonous terrestrial inputs of carbon, water chemistry, sediment dynamics and biological production in a system will determine the concentration of CO_2 and CH_4 dissolved in the water, and ultimately affect GHG fluxes at the water-air interface. However, the mechanisms occurring at the water-air interface are quite complex and make it inherently difficult to estimate exchange coefficients (e.g. k_{600}) required to calculate GHG fluxes with indirect methods (TBL, concentration gradients, etc.) (Chap. 2, 3, 14, Guérin et al. 2003; Duchemin et al. 1995). Therefore, direct measurements of fluxes at the water-interface integrate all the processes and indicate the actual direction of the fluxes, either out of the system (source of GHG) or into the system (sink of GHG). These direct methods are comparable to indirect methods with less than a 20% variation between the techniques

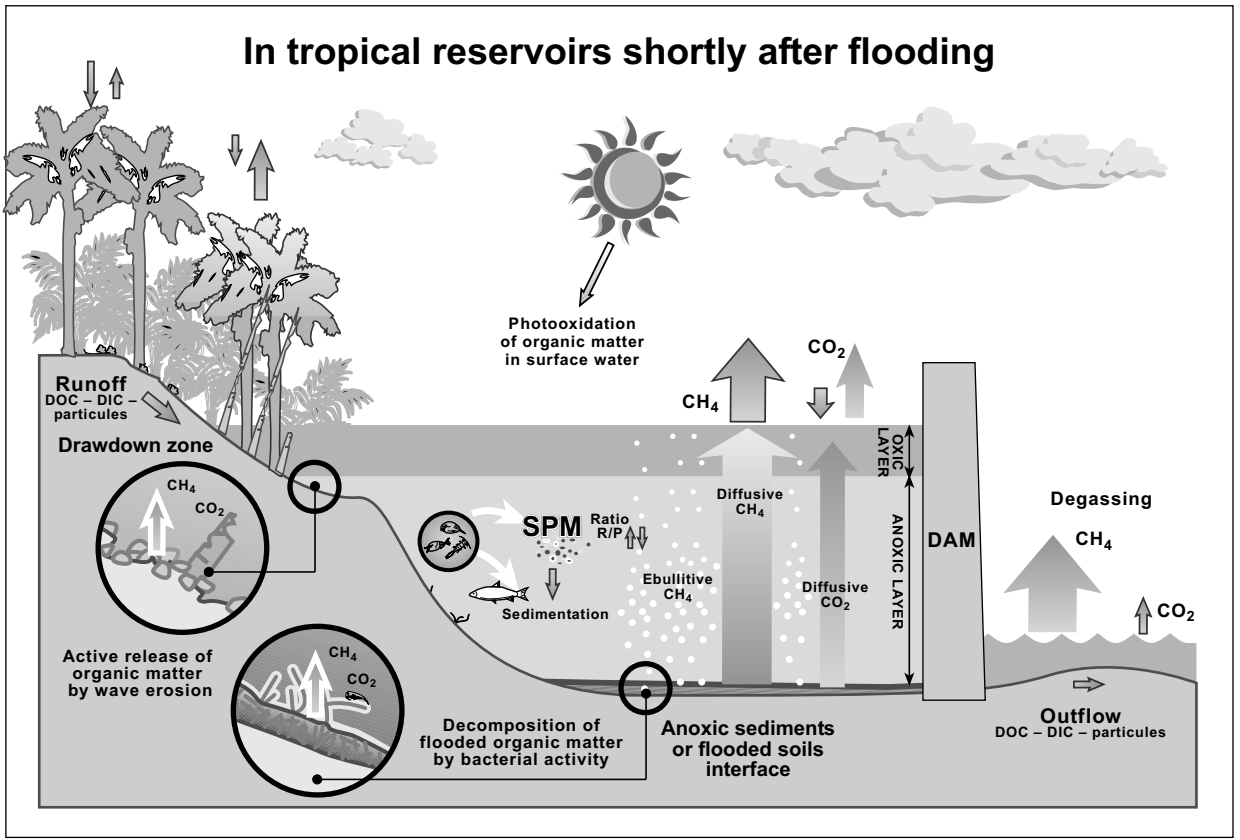

Fig. 26.4. Major processes occurring in tropical reservoirs shortly after flooding (<10 years)

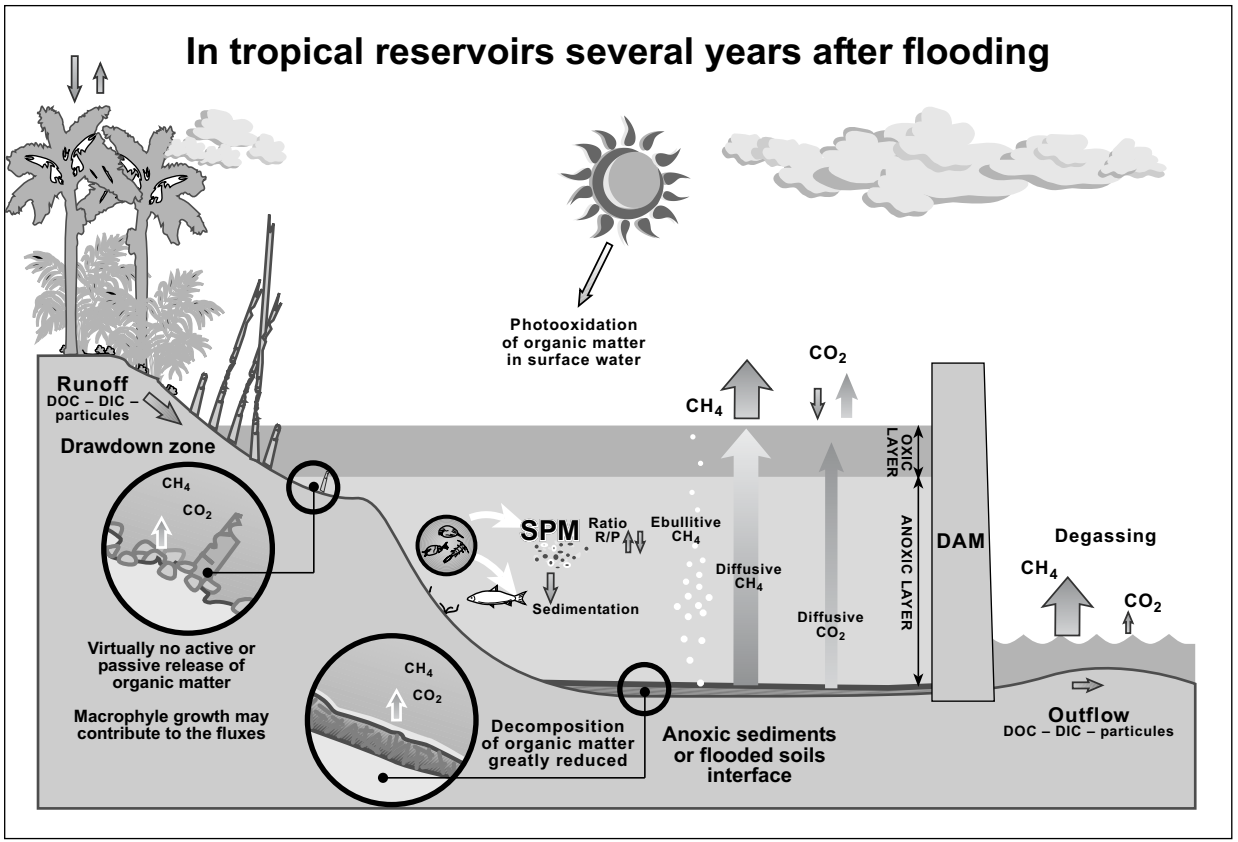

Fig. 26.5. Major processes occurring in tropical reservoirs several years after flooding (>10 years)

(Lannemezan 2004). The errors associated with the techniques to measure GHG fluxes are smaller than the natural GHG variations, it is therefore, more important to adequately assess both the spatial and the temporal variations of GHG fluxes.

Fluxes in boreal reservoirs are usually 3 to 6 times higher than those from natural lakes when they reach their maximum at 3 to 5 years after impoundment. In boreal reservoirs older than 10 years, fluxes ranged between -1800 to 11200 mg $CO_2 \cdot m^{-2} \cdot d^{-1}$ and are similar to those of natural systems with flux ranged from -460 to 10800 mg $CO_2 \cdot m^{-2} \cdot d^{-1}$. Generally, degassing and ebullition emissions are not reported for boreal regions because diffusive emissions are considered the major pathway. Methane emissions are very low in these ecosystems; however, they can be substantial in some tropical areas where the ebullition pathway is important (Chap. 11, 12, 22).

In Québec, for which the largest dataset is available (10 years of systematic measurements) the evolution of CO_2 and CH_4 emissions over time was determined on a set of reservoirs of different ages (from 2 years old to 90 years old). The results indicated a rapid increase in the GHG emissions shortly after flooding, followed by a return to values (10 years for CO_2 and 4 years for CH_4) measured in natural lakes or rivers. The mean values range from -50 to 120 mg $CO_2 \cdot m^{-2} \cdot d^{-1}$ for reservoir and range from -124 to 1700 mg $CO_2 \cdot m^{-2} \cdot d^{-1}$ for natural lakes. Despite fewer data available similar patterns are observed in most of the studied reservoirs in boreal (Finland, British-Columbia, Manitoba, New Foundland–Labrador), semi-arid (Arizona, New Mexico, Utah) and tropical regions (Panama, Brazil, French Guiana, Chap. 8, 9, 11, 12). In tropical regions, the time to return to natural values is sometimes longer depending on the water quality conditions. For example, when anoxic conditions occur CH_4 production decreases slowly and might be maintained for longer periods by carbon input from the drainage basin. However, such situations are rare in most of the studied reservoirs (Chap. 11, 12).

While direct measurements indicate the magnitude of GHG fluxes, these fluxes may not be necessarily due the reservoir effect but instead may be related to other parameters such as the input of carbon from the drainage basin and atmospheric exchange. As was previously mentioned, it is difficult to separate the contribution of each parameter to the carbon cycle. However, the use of stable isotopes tracers (^{13}C, ^{15}N, ^{18}O) has allowed for a differentiation to be made between terrestrial and atmospheric CO_2 (Chap. 15). This technique can discriminate between the contribution of decomposition from organic matter stored in the flooded soils and the autochthonous organic matter produced by primary production (Chap. 15). Surface emissions obtained by direct measurements are usually overesti-

mated in comparison to emissions resulting from reservoir processes alone. For example, average CO_2 diffusive fluxes estimated on the Robert-Bourassa reservoir (La Grande complex) with the stable isotopes technique were 2 to 3 times lower than those obtained with direct measurement techniques. In that view, models developed for water-air gas exchange can help to determine the contribution of the major mechanisms responsible for GHG emission from water bodies. The results from such a model calibrated on two boreal reservoirs (northern Québec) have indicated that wind and water temperature both influence the GHG fluxes (Chap. 21).

26.2.4 Reservoir Characteristics

Mechanical action of wind, waves, ice and physical reservoir characteristics have an effect on carbon cycle and may significantly impact GHG emissions from water bodies. The proportion of the total land area flooded in the drawdown zone is a good indicator of the magnitude and duration by which active wave action will transfer carbon from flooded soils to the water column. This erosion of organic material increases the availability of carbon (dissolved or particles) and of nutrients for primary production. In shallow areas otherwise protected from wave action, this active process plays a role during prolonged periods, where organic matter has not been eroded. For example, at the La Grande complex reservoir, the flooded soils are generally thin, rapidly eroded and subsequently deposited in deeper colder areas that are less favorable for bacterial decomposition (Chartrand et al. 1994) (Figs. 26.2-26.3, Table 26.2). Moreover, in shallow areas with reduced water dilution rates, fluxes of CO_2 and CH_4 are 2 or 3 times higher than in natural lakes, confirming that a certain amount of carbon and nutrients from flooded soils are recycled and maintained in the water column for periods longer than 10 years.

Periodically or permanently flooded soils or peat contribute more to methane production than unflooded substrates (Chap. 18). As a result, methane oxidation rates are higher in peat than in flooded forest soils or lake sediments. The lowest rates of methane oxidation are observed in the forest soils, typically undisturbed soils, where the rates of CH_4 production are close to the lowest range of values in the reservoirs. Most of the CH_4 produced in the shallow areas of reservoirs can be potentially oxidized in the water column. Therefore, the GHG emissions from flooded substrates in shallow areas in the drawdown zone are probably not important over the long term because most of the soils in these zones are rapidly eroded (Table 26.2, Figs. 26.2-26.5). Indeed, results from La Grande complex reservoirs, have shown that erosion of organic material in the drawdown zone

was highest during the first few years and decreased rapidly within 5 to 10 years (Chartrand et al. 1994, Chap. 8). Similar results were found in the Petit Saut reservoir (Lannemezan, 2004).

The ratio of land area flooded to annual volume of water flowing through the reservoir is another indicator of the magnitude of the post impoundment increase in labile carbon and nutrients. The annual volume of water flowing through a reservoir is considered a key factor because: (1) it is an indicator of the diluting capacity of nutrients and carbon released into the water column, (2) it plays a role in the extent of oxygen depletion and thus methane production, and (3) contributes to the export of nutrients and carbon out of the reservoir, reducing autochthonous production.

Reservoirs built in mountain valleys are generally deep, cover a small land surface area, have short water residence times, and have large water volumes for energy production. These mountains reservoirs are, therefore, the most effective in terms of GHG emissions per unit of energy generated. On the other hand, reservoirs built on mountain plateaus are the least effective in terms of GHG emissions per unit of energy generated. They are generally shallow reservoirs, with very large flooded land surfaces and where the water residence time is longer (Chap. 8, 9, 11 12).

26.2.5 Assessment of Net GHG Emissions from Reservoirs

The higher emissions of GHGs from reservoirs in the first years after impoundment are a direct consequence of the flooding of forest, soil and peat sediments. They are related to the release of labile carbon and nutrients made available to producer organisms upon flooding. However, after a period of about 10 years, all water quality and biological parameters, as well as GHG fluxes, indicate that reservoirs behave like natural lakes (Chap. 8, 17 18, Schetagne 1994; Chartrand et al. 1994; Therrien 2003). Therefore, reservoirs should be considered as such when estimating long-term net GHG emissions.

For natural lakes, allochthonous terrestrial inputs are generally defined by the biophysical characteristics of the drainage basin which are relatively constant in time; thus the emission of CO_2 to the atmosphere should also be relatively constant in time. This is probably even more important for reservoirs since water residence times are much shorter than they are for natural lakes.

This monograph and many other studies suggest that natural lakes and rivers are substantial emitters of CO_2 and CH_4 while estuaries and terrestrial ecosystems can be either sources or sinks of GHGs according to the stage of their succession (Chap. 4, 6). Moreover, the results in this mono-

graph demonstrate that the creation of reservoirs has a direct impact on the increased production of GHG during the first years after impoundment. Therefore, to correctly estimate net GHG emissions from reservoirs, it would be essential to determine the emissions from the various ecosystems in the watershed, prior to and following the creation of the reservoir. However, quantification of the changes in GHG emissions due to flooding is very complex, time consuming, and quite costly, since it requires an understanding of the carbon cycle at the drainage basin level. This includes the downstream river portion from the dam to the estuary. Because of this complexity, such quantifications are rarely undertaken. Nonetheless, a methodology for determining net emissions for which the reservoirs are responsible needs to be developed (WCD 2000). An approach has been put forward by the WCD which suggests reporting the GHG emissions as net emissions: for (1) evaluating individual future reservoir sites, such as hydroelectric dams, and (2) estimating global inventories of anthropogenic changes in the sources and sinks of CO_2 and CH_4. Several major biogeochemical parameters influencing GHG emissions from tropical and boreal regions (such as initial carbon stocks, hydrodynamics, water residence time, DOC and POC inputs and outputs, etc.) were also identified as issues that needed more research (WCD 2000). Moreover, since they are large temporal and spatial variations in GHG fluxes from both aquatic and terrestrial ecosystems, we suggest to use a time scale on the order of 100 years that would integrate much of the natural variations at the drainage basin scale as proposed by the WCD (2000).

According to this global approach, net reservoir emissions should be lower than those directly measured at the water-air interface usually reported in this monograph or in the literature. A first estimation of net emission was done on Petit Saut reservoir and showed that net emissions are about 30% lower than those directly measured on the reservoir (Chap. 12). A study using stable isotopes performed on Robert-Bourassa reservoir suggests a similar trend (Chap. 8, 14, Therrien 2003).

26.2.6 Comparison of GHG Emissions from Various Energy Sources

Sustainable energy planning requires comparison of the advantages and disadvantages of different energy sources in terms of "full-energy-chain" emission factors (i.e. from cradle to grave) of the most harmful pollutants (SO_x, NO_x, PM, etc.), as well as the emissions factors of the major greenhouse gases (CO_2, CH_4, N_2O, etc.) included in the Kyoto protocol (US

DOE 1998, Spath et al. 1999, Dones et al. 1999, Spath and Mann 2000, US EPA 2000, Hydro-Québec 2000, IAEA 2001).

According to the GHG emission factors reported for hydro reservoirs both by IAEA (1996) and by various studies performed during the last decade on a variety and a great number of reservoirs (Table 26.1), it can be concluded that the energy produced with the force of water is very efficient, with factors of emission between one and two orders of magnitude lower than the thermal alternatives (Table 26.1). However in some cases, tropical reservoirs, such as the Petit Saut reservoir in French Guiana or some Brazilian reservoirs, GHG emissions could, during a certain time period, significantly exceed emissions from thermal alternatives. Similar values have been reported in the literature (e.g., Rosa and Scheaffer 1994, 1995; Fearnside 1996; Gagnon and van de Vate 1997). GHG emission factors from thermal power plants would be smaller using the most effective technology such as combined-cycle gas-fired power plants for which "full-energy-chain" emissions factors are in the range of 400 – 500 g CO_2 equiv./ $kWh(e) \cdot h^{-1}$. As the costs related to the reduction of GHG emissions with this technology are not very high (Spath 2000; US EPA 2000), this technology is already used worldwide. The use of clean coal technologies reducing significant amount of GHG emissions is also feasible (US.DOE 1998), however at much higher costs.

In view of the context of this monograph, only the emission factors from GHG were considered; however, full scale environmental comparisons between the energy options should also include other pollutants (SO_x, NO_x, PM, etc.). From the point of view of GHG emissions, the results presented in this monograph and the data appearing in Table 26.1 provide the following general observations:

- GHG emission factors from hydroelectricity generated in boreal regions are significantly smaller than corresponding emission factors from thermal power plants alternatives (i.e. from < 2% to 8% of any kind of conventional thermal generation alternative);
- GHG emission factors from hydroelectricity generated in tropical regions cover a much wider range of values (for example, a range of more than 2 order of magnitude for the 9 Brazilian reservoirs). Based on a 100 year lifetime, these emissions factors could either reach very low or very high values, varying from less than 1% to more than 200% of the emission factors reported for thermal power plant generation;
- Net GHG emission factors for hydro power, should be at first sight 30% to 50% lower than the emission factors currently reported.

26.2.6 Conclusion and Unresolved Issues

With this synthesis we have taken our understanding of the dynamics of GHGs in reservoirs a step forward. The processes leading to GHG emissions in boreal, semi-arid and tropical reservoirs are similar (Table 26.2, Figs. 26.1-26.5). The main differences are related to the much greater presence of anoxic conditions in tropical reservoirs, which favour and sustain methanogenesis over longer time periods (>10 years). Additionally, in boreal and semi-arid regions, GHG emissions are similar between natural lakes and reservoirs older than 10 years within the same drainage basin. This monograph has addressed many issues raised at the expert meeting workshop of the World Commission on Dams held in Montreal in 2000. While several studies were performed on various boreal and tropical reservoirs addressing the processes responsible for GHG emissions and attempts were made to assess net emissions of GHG over large drainage basins and on time scales of 100 years, many issues still need to be addressed.

Since estimates of GHG emissions should be based on time scales > 100 years, it is crucial to develop tools (e.g., model of Chap. 12) to predict the GHG emissions for future reservoir projects including the impacts of long term climate change (www.cics.uvic.ca/scenarios). Use of predictive models will be very important for decreasing overall costs of the projects and reduce their impacts.

To adequately use such models, the following information has to be generated:

- inter calibrate sampling and measuring GHG techniques and optimize sampling strategies in order to increase spatial and temporal coverage;
- measure GHG over a wider range and diversity of reservoirs to determine temporal and spatial heterogeneity for both ebullitive and diffusive emissions;
- measure GHG from reference sites, such as rivers, lakes, forested areas and wetlands in order to determine temporal and spatial heterogeneity;
- determine the proportion of GHGs emitted in relation to the carbon inputs from flooded soils or sediments and from the drainage basin;
- determine the transience of carbon in reservoirs, natural lakes and downstream to estuaries.

Integration of fluxes at the landscape/catchment level prior and after flooding taking into account land cover changes is essential before major conclusions can be drawn. Sampling comparing between reservoir and natural lake fluxes per unit area is insufficient. The data generated by such studies will greatly improve, among other issues, our ability to adequately assess GHG emissions from reservoirs and natural environments.

References

Abe DS, Adams DD, Sidagis Galli CV, Sikar E, Tundisi JG (submitted) Sediment carbon gases (CH_4 and CO_2) in the Lobo-Broa Reservoir, São Paulo State, Brazil: concentrations and diffuse emission fluxes for carbon budget considerations. (submitted to Lakes and Reservoirs)

Abe DS, Kato K, Adams DD, Terai H, Tundisi JG (2000) Contribution of free-living and attached bacteria to denitrification in the hypolimnion of a mesotrophic Japanese lake. Micr Environ 15:93-101

Abril G, Etcheber H, Delille B, Frankignoulle M, Borges AV (2003) Carbonate dissolution in the turbid and eutrophic Loire estuary. Mar Ecol Prog Ser 259:129-138

Abril G, Etcheber H, Le Hir P, Bassoullet P, Boutier B, Frankignoulle M (1999) Oxic/anoxic oscillations and organic carbon mineralization in an estuarine maximum turbidity zone (The Gironde, France). Limnol Oceanogr 44:1304-1315

Abril G, Iversen N (2002) Methane dynamics in a shallow, non-tidal, estuary (Randers Fjord, Denmark). Mar Ecol Prog Ser 230:171-181

Abril G, Nogueira M, Etcheber H, Cabeçadas G, Lemaire E, Brogueira MJ (2002) Behaviour of organic carbon in nine contrasting European estuaries. Estuar Coast Shelf Sci 54:241-262

Adams DD (1991) Gas composition of Hamilton Harbour sediments: changes during the 1980-1990 decade. Canada Centre for Inland Waters, National Water Research Institute, Burlington, Ontario, Canada, Internal report

Adams DD (1992) Sediment pore water geochemistry of Taupo Volcanic Zone lakes with special reference to carbon and nitrogen gases. Taupo Research Laboratory File Report 135, Dept. Marine Freshwater Research, D.S.I.R., Taupo, New Zealand

Adams DD (1994) Sampling sediment pore water. In: Mudroch A, MacKnight SD (eds) CRC Handbook of techniques for aquatic sediments sampling, 2nd ed. CRC Press, Boca Raton, pp 171-202 (chap. 7)

Adams DD (1996) Aquatic cycling and hydrosphere to troposphere transport of reduced trace gases: a review. In: Adams DD, Seitzinger SP, Crill PM (eds) Cycling of reduced gases in the hydrosphere. Mitt Internat Verein Limnol, Mitteilungen 25, E. Schweizerbart'sche Verlagsbuchhandlung (Nägele u. Obermiller), Stuttgart, Germany, pp 1-13

Adams DD (1999) Methane, carbon dioxide and nitrogen gases in the surficial sediments of two Chilean reservoirs: diffusive fluxes at the sediment water interface. In: Rosa LP, Aurélio dos Santos M (eds) Dams and climate change.

Proceedings of an International Workshop on Hydro Dams, Lakes and Greenhouse Gas Emissions, COPPE Report, Rio de Janeiro, pp 50-77

Adams DD, Baudo R (2001) Gases (CH_4, CO_2 and N_2) and pore water chemistry in the surface sediments of Lake Orta, Italy: acidification effects on C and N gas cycling. J Limnol 60:79-90

Adams DD, Dinkel C, Mengis M, Wehrli B (in preparation) Sediment pore water methane: a comparison of two sampling and measuring techniques. (submitted to Environ Sci Tech)

Adams DD, Fendinger NJ (1986) Early diagenesis of organic matter in the recent sediments of Lake Erie and Hamilton Harbor: I. Carbon gas geochemistry. In: Sly PG (ed) Sediments and water interactions. Springer-Verlag, New York, pp 305-315

Adams DD, Matisoff G, Snodgrass WJ (1982) Flux of reduced chemical constituents (Fe^{2+}, Mn^{2+}, NH_4 and CH_4) and sediment oxygen demand in Lake Erie. Hydrobiologia 92:405-414

Adams DD, Naguib M (1999) Carbon gas cycling in the sediments of Plußsee, a northern German eutrophic lake, and 16 nearby water bodies of Schleswig-Holstein. Arch Hydrobiol Spec Issues Adv Limnol 54:91-104

Adams DD, Ochola SO (2002) A review of sediment gas cycling with reference to Lake Victoria and sediment gas measurements in Lake Tanganyika. In: Odada EO, Olago DO (eds) The East African Great Lakes: limnology, paleolimnology and biodiversity. Advances in Global Research book series, Kluwer Publishers, Dordrecht, The Netherlands, pp 277-305

Adams DD, van Eck GThM (1988) Biogeochemical cycling of organic carbon in the sediments of the Grote Rug reservoir. Arch Hydrobiol, Ergebnisse der Limnologie 31:319-330

Adams DD, Vila I, Pizarro J, Salazar C (2000) Gases in the sediments of two eutrophic Chilean reservoirs: potential sediment oxygen demand and sediment-water flux of CH_4 and CO_2 before and after an El Niño event. Verh Internat Verein Limnol 27:1376-1381

Adams JM, Constable JVH, Guenther AB, Zimmerman P (2001) An estimate of natural volatile organic compound emissions from vegetation since the last glacial maximum. Chemosphere. Global Change Science 3:73-91

Adrian R, Wickham SA, Butler NM (2001) Trophic interactions between zooplankton and the microbial community in contrasting food webs: the epilimnion and deep chlorophyll maximum of a mesotrophic lake. Aquat Microb Ecol 24:83-97

Aitkenhead JA, McDowell WH (2000) Soil C:N ratio as a predictor of annual riverine DOC flux at local and global scales. Glob Biogeochem Cycles 14:127-138

Alexeyev, V.A.; Birdsey, R.A., eds. 1994. Carbon in ecosystems of forests and peatlands of Russia. Krasnoyarsk, Siberia, Institute for Forest Research. [in Russian].

Allard B, Borén H, Petterssonn C, Zhang G (1994) Degradation of humic substances by UV irradiation. Environ Int 20:97-101

Allen GP, Salomon JC, Bassoulet P, Du Penhoat Y, De Grandpré C (1980) Effects of tides on mixing and suspended sediment transport in macrotidal estuaries. Sediment Geol 26:69-90

Allen Jr LH, Baker JT, Boote KJ (1996) The CO_2 fertilization effect: higher carbohydrate production and retention as biomass and seed yield. In: Bazzaz F, Sombroek W (eds) Global climate change and agricultural production. Wiley & Sons, Toronto, Ontario, Canada

Aller RC (1998) Mobile deltaic and continental shelf muds as suboxic, fluidized bed reactors. Mar Chem 61:143-155

Alm J, Saarnio S, Nykänen H, Silvola J, Martikainen PJ (1999a) Winter CO_2, CH_4 and N_2O fluxes on some natural and drained boreal peatlands. Biogeochemistry 44:163-186

Alm J, Schulman L, Silvola J, Walden J, Nykänen H, Martikainen PJ (1999b) Carbon balance of a boreal bog during a year with an exceptionally dry summer. Ecology 80:161-174

Alm J, Talanov A, Saarnio S, Silvola J et al. (1997) Reconstruction of carbon balance for microsites in a boreal oligotrophic pine fen, Finland. Oecologia 110:423-431

Alriksson A, Eriksson HM (1998) Variations in mineral nutrient and C distribution in the soil and vegetation compartments of five temperate tree species in NE Sweden. For Ecol Manage, Forest Ecol Manage 108:261-273

Amador JA, Alexander M, Zika RG (1989) Sequential photochemical and microbial degradation of organic molecules bound to humic acid. Appl Environ Microbiol 55:2843-2849

Amaral JA, Knowles R (1997) Localization of methane consumption and nitrification activities in some boreal forest soils and the stability of methane consumption on storage and disturbance. J Geophys Res 102:29255-29260

Ambus P, Christensen S (1995) Spatial and seasonal nitrous oxide and methane fluxes in Danish forest, grassland and agroecosystems. J Environ Qual 24(5):993-1001

Amiro BD, Todd JB, Wotton BM, Logan KA, Flannigan MD (2001) Direct carbon emissions from Canadian forest fires, 1959-1999. Can J Forest Res 31(3):512-525

Amon RMW, Benner R (1996) Photochemical and microbial consumption of dissolved organic carbon and dissolved oxygen in the Amazon River system. Geochimica et Cosmochimica Acta 60(10):1783-1792

Amouroux D, Roberts G, Rapsomanikis S, Andrea MO (2002) Biogenic gas (CH_4, N_2O, DMS) emission to the atmosphere from near-shore and shelf waters of the Northwestern Black sea. Estuar Coast Shelf Sci 54:575-587

Amundson R (2001) The carbon budget in soils.Annu Rev Earth Planet Sci 29:535-562

Andreae MO, Ferek RJ (1992) Photochemical production of carbonyl sulfide in seawater and its emission to the atmosphere. Glob Biogeochem Cycles 6:175-183

Anesio AM, Graneli W (2003) Increased photoreactivity of COD by acidification: implications for the carbon cycle in humic lakes. Limnol Oceanogr 48(2):735-744

Anonyme (2001) Stable isotopic composition of atmospheric carbon dioxide (13C and 18O). University of Colorado, Institute of Arctic and Alpine Research NOAA, Climate Monitoring and Diagnostics Laboratory, Carbon Cycle Group. ftp://ftp.cmdl.noaa.gov/ccg/

APHA-AWWA-WPCF (1975) Standard methods for the examination of water and waste-water, 14th ed. American Public Health Association, American Water Works Association, Water Pollution Control Federation, New York

Apps MJ, Kurz WA (1991) Assessing the role of Canadian forests and forest sector activities in the global carbon balance. World Resource Rev 3(4):333-343

Arain MA, Black TA, Barr AG et al. (2002) Effects of seasonal and interannual climate variability on net ecosystem productivity of boreal deciduous and conifer forests. Can J For Res 32(5):878-891

Araújo TM, Higuchi N, Carvalho JA Jr (1999) Comparison of formulae for biomass content determination in a tropical rain forest site in the state of Pará, Brazil. For Ecol Manage 117:43-52

Armengol J, Garcia JC, Comerma M, Romero M, Dolz J, Roure M, Han BH, Vidal A, Simek K (1999) Longitudinal processes in canyon type reservoirs: the case of Sau (N.E. Spain). In: Tundisi JG, Straskraba M (eds) Theoretical reservoir ecology and its applications. International Institute of Ecology, Brasilian Academy of Sciences and Backhuys Publishers, Brazil, pp 313-345

Arneth A, Kelliher FM, Mcseveny TM, Byers JN (1998) Net ecosystem productivity, net primary productivity and ecosystem carbon sequestration in a *Pinus radiata* plantation subject to soil water deficit. Tree Physiol 18:785-793

Aronsen G (2001) Carbon dioxide emissions from lakes: regulations and effects on the carbon budget of the Boreal zone. UMEÄ University, Sweden

Aronsen G, Sobek S, Bergstrom AK, Tranvik L, Agren A, Jansson M (2002) The flux of CO_2 from boreal lakes in a landscape perspective. Proceedings of the American Society of Limnology and Oceanography, 10–14 June 2002, Victoria, British-Columbia

Arts MT, Robarts RD, Kasai F, Waiser MJ, Tumber VP, Plante AJ, Rai H, de Lange HJ (2000) The attenuation of ultraviolet radiation in high dissolved organic carbon waters of wetlands and lakes on the northern Great Plains. Limnol Oceanogr 45(2):292–299

Arvola L, Karusalmi A, Tulonen T (1993) Observation of plankton communities and primary production and bacterial production of Lake Paanajärvi, a deep subartic lake. Oulanka Report 12:93-107

Aselmann I, Crutzen PJ (1989) Global distribution of natural freshwater wetlands and rice paddies, their net primary productivity, seasonality and possible methane emissions. J Atmosph Chem 8:307-358

Atjay GL, Ketner P, Duvigneaud P (1979) Terrestrial primary production and phytomass. In: Bolin B, Degens ET, Kempe S, Ketner P (eds) The global carbon cycle. SCOPE 13, Wiley and Sons, New York, pp 129-182

Auclair AND (1985) Postfire regeneration of plant and soil organic carbon pools in a *Picea mariana-Cladonia stellaris* ecosystem. Can J For Res 15:279-291

Auclair F, Marsaleix P, Estournel C (2001) The penetration of the northern current over the gulf of Lions (Mediterranean) as a downscaling problem. Oceanologica Acta 26(6):529-544

Badr O, Probert SD, O'Callaghan PW (1991) Origins of atmospheric methane. Appl Energy 40:189-231

Baldocchi DD, Falge E, Gu L et al. (2001) FLUXNET: A new tool to study the temporal and spatial variability of ecosystem-scale carbon dioxide, water vapor, and energy flux densities. Bull Am Meteorol Soc 82(11):2415-2434

Baldocchi DD, Hicks BB, Meyers TP (1988) Measuring biosphere-atmosphere exchanges of biologically related gases with micrometeorological methods. Ecology 69:1131-1340

Baldock JA, Nelson PN (1999) Soil organic matter. In: Sumner ME (ed) Handbook of Soil Science. CRC Press, Boca Raton, Florida

Banfield GE, Bhatti JS, Jiang H, Apps MJ (2002) Variability in regional scale estimates of carbon stocks in boreal forest ecosystems: results from West-Central Alberta. For Ecol Manage 169:15-27

Bange HW, Bartell UH, Rapsomanikis S and Andrea MO (1994) Methane in the Baltic and North Seas and a reassessment of the marine emissions of methane. Glob Biogeochem Cycles 8:465-480

Bange HW, Dahlke S, Ramesh R, Meyer-Reil LA, Rapsomanikis S, Andrea MO (1998) Seasonal study of methane and nitrous oxide in the coastal waters of the southern Baltic Sea. Estuar Coast Shelf Sci 47:807-817

Bange HW, Rapsomanikis S, Andrea MO (1996) The Aegean Sea as a source of atmospheric nitrous oxide and methane. Mar Chem 53:41-49

Banks RB (1975) Some features of wind action on shallow lakes. J Environ Eng Div 101(EE5): 813-827

Banks RB, FF Herrera (1977) Effect of wind and rain on surface reaeration, J Environ Eng Div 103(EE3): 489-504

Baranov IV (1962) The storage lakes of the U.S.S.R. and their importance for fishery. Izv.Gos.Nauchno-Issled.Inst.Ozern.Rybn.Khoz. pp 139-183

Barette N, Laprise R (2002) Numerical modeling: a complementary tool for studying CO_2 emissions from hydroelectric reservoirs. (Glob Biogeochem Cycles 16:751-761

Barford CC, Wofsy SC, Goulden ML et al. (2001) Factors controlling long- and short-term sequestration of atmospheric CO_2 in a mid-latitude forest. Science 294:1688-1691

Baril M (2001) ^{13}C in dissolved inorganic carbon from the decomposition of flooded reservoirs. BSc thesis, University of Waterloo, Waterloo, Ontario

Barr AG, Griffis TJ, Black TA et al. (2002) Comparing the carbon budgets of boreal and temperate deciduous forest stands. Can J For Res 32(5):813-822

Barrette N (2000) Réservoirs hydroélectriques du moyen nord québécois: mesures et modélisation numérique des flux et des concentrations de gaz à effet de serre. PhD thesis, Sciences de l'Environnement, Université du Québec à Montréal, Canada

Barrette N, Laprise R (2002) Numerical modeling: a complementary tool for studying CO2 emissions from hydroelectric reservoirs. Glob Biogeochem Cycles 16(4):1128-1139

Bartlett DS, Bartlett KB, Hartman JM et al. (1989) Methane emissions from the Florida Everglades: Patterns of variability in a regional wetland ecosystem. Glob Biogeochem Cycles 3:363-374

Bartlett KB, Bartlett DS, Harris RC, Sebacher DI (1987) Methane emissions along a salt marsh salinity gradient. Biogeochemistry 4:183-202

Bartlett KB, Crill PM, Bonassi JA, Richey JE, Harriss RC (1990) Methane flux from the Amazon river floodplain: emissions during rising water. J Geophys Res 95(D10):16773-16788

Bartlett KB, Crill PM, Sebacher DI, Harriss RC, Wilson JO, Melack JM (1988) Methane flux from the central Amazonian floodplain. J Geophys Res 93(D2):1571-1582

Bartlett KB, Harriss RC, Sebacher DI (1985) Methane flux from coastal marshes. J Geophys Res 90:5710-5720

Bartlett KB, Harriss RC (1993) Review and assessment of methane emissions from wetlands. Chemosphere 26:261-320

Bates TS, Kelly KC, Johnson JE, Gammon RH (1996) A reevaluation of the open ocean source of methane to the atmosphere. J Geophys Res 101:6953-6961

Batjes NH (1996) Total carbon and nitrogen in the soils of the world. Eur J Soil Sci 47:151-163

Batjes NH, Dijkshoorn JA (1999) Carbon and nitrogen stocks in the soils of the Amazon region. Geoderma 89:273-286

Bazzaz F, Sombroek W (1996) Global climate change and agricultural production. Wiley & Sons,Toronto, Ontario

BC Hydro (1994) Carbon project-reservoir study. Strategic R&D project. Final report prepared by Powertech Labs Inc.

Bellisario L, Bubier J, Moore T, Chanton J (1999) Relationship between net ecosystem productivity and CH_4 flux in Northern wetlands. Glob Biogeochem Cycles 13:81-91

Belzile C, Gibson JAE, Vincent WF (2002) Colored dissolved organic matter and dissolved organic carbon exclusion from lake ice: implications for irradiance transmission and carbon cycling. Limnol Oceanogr 47(5):1283-1293

Benner R, Biddanda B (1998) Photochemical transformation of surface and deep marine dissolved organic matter: effects on bacterial growth. Limnol Oceanogr 43(6):1373-1378

Bergeron Y (1991) The influence of island and mainland lakeshore landscapes on the boreal forest fire regimes. Ecology 72:1980-1992

Bergkvist B, Folkeson L (1992) Soil acidification and element fluxes of a *Fagus sylvatica* forest as influenced by simulated deposition. Water Air Soil Poll 65:111-133

Bergström AK, Algesten G, Sobek S, Tranvik L, Jansson M (2004) Emission of CO_2 from hydroelectric reservoirs in northern Sweden. Arch Hydrobiol 159: 25-42

Berner RA (1980) Early diagenesis: a theoretical approach. Princeton University Press, Princeton

Bertilsson S, Tranvik LJ (1998) Photochemically produced carboxylic acids as substrates for freshwater bacterioplanckton. Limnol Oceanogr 43(5):885-895

Bertilsson S, Tranvik LJ (2000) Photochemical transformation of dissolved organic matter in lakes. Limnol Oceanogr 45(4):753-762

Bhatti JS, Apps MJ, Tarnocai C (2002) Estimates of soil organic carbon stocks in central Canada using three different approaches. Can J For Res 32:805-812

Biddanda B, Ogdahl M, Cotner J (2001) Dominance of bacterial metabolism in oligotrophic relative to eutrophic waters. Limnol Oceanogr 46:730-739

Birdsey RA (1996) Carbon storage for major forest types and regions in the conterminous United States. In: Sampson NR, Hair D (eds) Forests and global change, vol 2. American Forests, Washington, DC, pp 1-25

Birdsey RA, Heath LS (1995) Carbon changes in US forests. In: Joyce LA (ed) Productivity of America's forests and climate change. USDA Forest Service General Technical Report RM-271, pp 56-70

Birdsey RA, Plantinga AJ, Heath LS (1993) Past and prospective carbon storage in US forests. For Ecol Manage 58:33-40

Biron P, Roy AG, Courchesne F, Hendershot WH, Côté B, Fyles J (1999) The effects of antecedent moisture conditions on the relationship of hydrology to hydrochemistry in a small forested watershed. Hydrol Process 13:1541-1555

Bishop KH, Grip H, O'Neill A (1990) The origins of acid runoff in a hillslope during storm events. J Hydrol 116:25-61

Biswas H, Mukhopadhayay SK, De TK, Sen S, Jana TK (2004) Biogenic controls on the air water carbon dioxide exchange in the Sundarban mangrove environment, NE coast of Bay of Bengal, India. Limnol Oceanogr 49: 95–101

Black TA, Chen WJ, Barr AG et al. (2000) Increased carbon sequestration by a boreal deciduous forest in years with a warm spring. Geophys Res Lett 27(9):1271-1274

Blais AM (2003) Synthèse des connaissances sur les stocks de carbone dans le sol et la végétation des forêts et tourbières boréales, tempérées et tropicales. Rapport préparé par Environnement illimité inc. pour Unité Environnement, Hydro-Québec Production, Montréal

Blodau C (2002) Carbon cycling in peatlands - a review of processes and controls. Environ Rev 10:111-134

Bodaly RA, Rolfhus KR, Penn AF, Beaty KG, Hall BD, Hendzel LH, Mailman M, Majewski AR, Matthews CJD, Paterson MJ, Peech KA, St.Louis VL, Schiff SL, Venkiteswaran JJ (2004) The use of experimental reservoirs to explore the impacts of hydro-electric developments on methylmercury and greenhouse gas production: The FLUDEX experiment. Environmental Science and Technology (submitted)

Boeckx P, Van Cleemput O (1997) Methane emission from a freshwater wetland in Belgium. Soil Sci Soc Am J 61(4):1250-1256

Bonecker CC, Lansac-Toha FA, Velho LFM, Rossa DC (2001) The temporal distribution pattern of copepods in Corumbá Reservoir, State of Goiás, Brazil. Hydrobiologia 453/454:375-384

Boon PI (2000) Carbon cycling in Australian wetlands: the importance of methane. Verh Internat Verein Limnol 27:37-50

Boon PI, Sorrell BK (1995) Methane fluxes from an Australian floodplain wetland: the importance of emergent macrophytes. J N Am Benthol Soc 14:582-598

Borges AV, Delille B, Schiettecatte LS, Gazeau F, Abril G, Frankignoulle M (2004a) Gas transfer velocities of CO_2 in three European estuaries (Randers Fjord, Scheldt and Thames). Limnol Oceanogr (in press)

Borges AV, Frankignoulle M (2002) Distribution and air-water exchange of carbon dioxide in the Scheldt plume off the Belgian coast. Biogeochemistry 59:41-67

Borges AV, Vandenborght JP, Schiettecatte LS, Gazeau F, Ferrón-Smith S, Delille B, Frankignoulle M (2004b) Variability of the gas transfer velocity of CO_2 in a macrotidal estuary (The Scheldt). Estuaries (in press)

Borken W, Xu YJ, Besse F (2004) Leaching of dissolved organic carbon and carbon dioxide emission after compost application to six nutrient-depleted forest soils. J Environ Qual 33:89-98

Borken W, Xu YJ, Brumme R, Lamersdorf N (1999) A climate change scenario for carbon dioxide and dissolved organic carbon fluxes from a temperate forest soil: drought and rewetting effects. Soil Sci Soc Am J 63:1848-1855

Botch MS, Kobak KI, Vinson TS, Kolchugina TP (1995) Carbon pools and accumulation in peatlands of the former Soviet Union. Glob Biogeochem Cycles 9(1):37-46

Bothwell ML, Sherbot DMJ, Pollock CM (1994) Ecosystem response to solar ultraviolet-B radiation: influence of trophic-level interactions. Science 265:97-100

Botkin DB, Simpson LG (1990) Biomass of the North American boreal forest. Biogeochemistry 9:161-174

Bottrell HH, Duncan A, Gliwicz ZM, Grygierek E, Herzig A, Hillbricht-Ilkowska A, Kurasawa H, Larsson P, Weglenska T (1976) A review of some problems in zooplankton production studies. Norw J Zool 24:412-456

Boudreau NM (2000) Sources of CH_4, CO_2 and DOC in newly flooded boreal upland reservoirs. MSc thesis, University of Waterloo, Waterloo, Ontario

Bouillon S, Frankignoulle M, Dehairs F, Velimirov B, Eiler A, Abril G, Etcheber H, Borges AV (2003) Inorganic and organic carbon biogeochemistry in the Gautami Godavari estuary (Andhra Pradesh, India) during pre-monsoon: the local impact of extensive mangrove forests. Glob Biogeochem Cycles 17:1114

Bourassa J (2001) Banque de données UQAM sur les émissions de gaz à effet de serre. Bilan statistique. Direction Environnement, Hydro-Québec, Montréal

Bousquet P, Peylin P, Ciais P et al. (2000) Regional changes of CO_2 fluxes over land and oceans since 1980. Science 290:1342-1346

Bouwman AF (1986) Gaseous nitrogen emissions from undisturbed terrestrial ecosystems: assessment of their impacts on local and global nitrogen budgets. Biogeochemistry 2:249-279

Bouwman AF (ed) (1990) Soils and the greenhouse effect. Wiley & Sons, New York

Bowden RD, Steudler PA, Melillo JM, Aber JD (1990) Annual nitrous oxide fluxes from temperate forest soils in the North-eastern United States. J Geophys Res 95:13997-14005

Bowling DR, Tumispeed AA, Delany AC, Baldocchi DD, Greenberg JP, Monson RK (1998) The use of relaxed eddy accumulation to measure biosphere-atmosphere exchange of isoprene and other biological trace gases. Oecologia 116:305-315

Bradbury IK, Grace J (1983) Primary production in wetlands. In: Gore AJP (ed) Ecosystems of the World, 4A. Mires: swamp, bog, fen and moor. Elsevier Scientific Publishing Company, Amsterdam Oxford New York, pp 285-310

Branco CWC, Rocha MIA, Pinto GFS, Gomara GA, De Filippo R (2002) Limnological features of Funil Reservoir (Rio de Janeiro,. Brazil) and indicator properties of rotifers and cladocerans of the zooplankton community. Lakes Reserv Res Manage 7:87-92

Brasse S, Nellen M, Seifert R, Michaelis W (2002) The carbon dioxide system in the Elbe estuary. Biogeochemistry 59:25-40

Bravard S, Righi D (1990) Podzols in Amazonia. Catena 17:461-475

Brezonik PL (1994) Chemical kinetics and process dynamics in aquatic systems, Lewis Publishers, Boca Raton, Florida

Bridgham SD, Updegraff K, Pastor J (2001) A comparison of nutrient availability indices along an ombrotrophic-minerotrophic gradient in Minnesota wetlands. Soil Sci Soc Am J 65:259-269

Broecker HC, Siems W (1984) The role of bubbles for gas transfer from water to air at higher windspeeds. Experiments in the wind-wave facility in Hamburg In: Gas transfer at water surfaces. Brutsaert W, Jirka GH (eds) D. Reidel Boston pp 229-236

Broecker WS, Peng TH (1974) Gas exchange rates between air and sea. Tellus 26:21-35

Brooks PD, McKnight DM, Bencala KE (1999) The relationship between soil heterotrophic activity, soil dissolved organic carbon (DOC) leachate, and catchment-scale DOC export in headwater catchments. Water Resour Res 35:1895-1902

Brouard D, Demers C, Lalumière R, Verdon R (1990) Rapport synthèse: évolution des teneurs en mercure des poissons du complexe hydroélectrique La Grande (Québec) (1978-1989). Rapport conjoint Vice-présidence Environnement, Hydro-Québec et Groupe Environnement Schooner inc.

Brown S, Iverson LR, Prasad A, Liu D (1993) Spatial distribution of carbon densities and pools in vegetation and soils in tropical Asian forests. Geocarto Int 8:45-59

Brown S, Lugo AE (1992) Above ground biomass estimates for tropical moist forests of the Brazilian Amazon. Interciencia 17:8-18

Brumme R, Beese F (1992) Effects of liming and nitrogen fertilization on emissions of CO_2 and N_2O from a temperate forest. J Geophys Res 97:12851-12858

Brunskill GJ, Schindler DW (1971) Geography and bathymetry of selected lakes bassins, Experimental Lakes Area, northwestern Ontario. J Fish Res Board Can 28:139-155

Brutsaert WH (1982) Evaporation into the atmosphere: theory, history and applications. D. Reidel, Hingham

Bubier J, Crill P, Modelade A, Frolking S, Linder E (2003) Peatland responses to varying interannual moisture conditions as measured by automatic CO_2 chambers. Glob Biogeochem Cycles 17(2):1066

Bubier JL, Moore TR, Roulet NT (1993) Methane emissions from wetlands in the midboreal region of northern Ontario, Canada. Ecology 74:2240-2254

Budac D, Wan P (1992) Photodecarboxylation: mechanism and synthetic utility. Photochem Photobiol 67:135-166

Buol SW, Hole FD, McCraken RJ (1989) Soil genesis and classification Iowa State University Press, Ames

Burke IC, Yonker CM, Parton WJ, Cole CV, Flach K, Schimel DS (1989) Texture, climate and cultivation effects on soil organic matter content in U.S. grassland soils. Soil Sci Soc Am J 53:800-805

Burke RAJ, Barber TR, Sackett WM (1988) Methane flux and stable hydrogen and carbon isotope composition of sedimentary methane from the Florida Everglades. Glob Biogeochem Cycles 2:329-340

Butterbach-Bahl K, Gasche R, Huber C, Kreutzer K, Papen H (1998) Impact of N-input by wet deposition on N-trace gas fluxes and CH_4-oxidation in spruce forest ecosystems of the temperate zone in Europe. Atmos Environ 32(3):559-564

Cai WJ, Pomeroy LR, Moran MA, Wang Y (1999) Oxygen and carbon dioxide mass balance for the estuarine-intertidal marsh complex of five rivers in the southeastern U.S. Limnol Oceanogr 44:639-649

Cai WJ, Wang Y (1998) The chemistry, fluxes and sources of carbon dioxide in the estuarine waters of the Satilla and Altamaha Rivers, Georgia. Limnol Oceanogr 43:657-668

Cai WJ, Wiebe WJ, Wang Y, Sheldon JE (2000) Intertidal marsh as a source of dissolved inorganic carbon and a sink of nitrate in the Satilla River-estuarine complex in the southeastern US. Limnol Oceanogr 45:1743-1752

Cameron WM, Pritchard DW (1963) Estuaries. In: Hill MN (ed) The Sea, vol 2. Wiley–Interscience, New York, pp 306-324

Camill P, Lynch JA, Clark JS, Adams JB, Jordan B (2001) Changes in biomass, aboveground net primary production, and peat accumulation following permafrost thaw in the boreal peatlands of Manitoba, Canada. Ecosystems 4:461-478

Cannell MGR, Milne R (1995) Carbon pools and sequestration in forest ecosystems in Britain. Forestry 68:361-378

Canuel R, Duchemin E, Lucotte M (1997) Handbook on greenhouse gases sampling and analytical techniques. International Workshop on Greenhouse Gases, Santarém, Brazil

Cao M, Gregson K, Marshall S (1998) Global methane emission from wetlands and its sensitivity to climate change. Atmos Environ 32(19):3293-3299

Capone DG, Kiene RP (1988) Comparison of microbial dynamics in marine and freshwater sediments: contrasts in anaerobic carbon catabolism. Limnol Oceanogr 33:725-749

Carignan R (1998) Automated determination of carbon dioxide, oxygen, and nitrogen partial pressures in surface waters. Limnol Oceanogr 43(5):969-975

Carignan R, Planas D, Vis C (2000) Planktonic production and respiration in oligotrophic shield lakes. Limnol Oceanogr 45:189-199

Carignan R, Blais AM, Vis C (1998) Measurement of primary production and community respiration in oligotrophic lakes using the Winkler method. Can J Fish Aquat Sci 55:1078-1084

Carini S, Weston N, Hopkinson C, Tucker J, Giblin A, Vallino J (1996) Gas exchange rates in the Parker river estuary, Massachussets. Biol Bull 191:333-334

Carpenter SR, Cole JJ, Hodgson JR, Kitchell JF, Schindler DE (2001) Trophic cascades, nutrients, and lake productivity: whole-lake experiments. Ecol Monogr 71:63-186

Carrara A, Kowalski AS, Neyrinck J, Janssens IA, Curiel Yuste J, Ceulemans R (2003) Net ecosystem CO_2 exchange of mixed forest in Belgium over 5 years. Agric Forest Meteorol 119:209-227

Carroll P, Crill PM (1997) Carbon balance of a temperate poor fen. Glob Biogeochem Cycles 1997:11349-11356

Casper P (1992) Methane production in lakes of different trophic status. Arch Hydrobiol Beih Ergebn Limnol 37:149-154

Casper P (1996) Methane production in littoral and profundal sediments of an oligotrophic and a eutrophic lake. Arch Hydrobiol Spec Iss Adv Limnol 48:253-259

Casper P, Adams DD (in prep) The biogeochemical cycling of carbon (CH_4 and CO_2) and nitrogen (N_2) gases across an environmental gradient of north German lakes. (submitted to Biogeochemistry)

Casper P, Chan OC, Furtado ALS, Adams DD (2003b) Methane in an acidic bog lake: the influence of peat in the catchment on the biogeochemistry of methane. Aquat Sci 65:36-46

Casper P, Furtado A, Adams DD (2003a) Biogeochemistry and diffuse fluxes of greenhouse gases (methane and carbon dioxide) and dinitrogen from the sediments in oligotrophic Lake Stechlin. In: Koschel R, Adams DD (eds) Lake Stechlin: an approach to understand an oligotrophic lowland lake. Arch Hydrobiol Spec Iss Adv Limnol 58:53-71

Casper P, Maberly SC, Hall GH, Finlay BJ (2000) Fluxes of methane and carbon dioxide from a small productive lake to the atmosphere. Biogeochemistry 49:1-19

Casper SJ (1985) Lake Stechlin: a temperate oligotrophic lake. Monographiae Biologocae, vol 58, Dr. W. Junk Publishers, Dordrecht Boston Lancaster

Castro MS, Steudler PA, Melillo JM, Aber JD, Millham S (1993) Exchange of N_2O and CH_4 between the atmosphere and soil in spruce-fir forests in the northeastern United States. Biogeochemistry 18:119-135

CCMF (1997) Critères et indicateurs de l'aménagement durable des forêts. Rapport technique du Conseil canadien des ministres des forêts

Chadwick OA, Graham RC (1999) Pedogenic processes. In: Sumner ME (ed) Handbook of soil science. CRC Press, Boca Raton, Florida

Chamberland A (1992) Greenhouse gas emissions from large reservoirs in northwestern Quebec (James Bay territory): Paper presented at the 9th World Clean Air Congress, Montreal, Sept 1992. Hydro-Québec, Environnement

Chamberland A (1993) Caractérisation des gaz à effet de serre émis par les plans d'eau du nord-ouest Québécois. Hydro-Québec Environnement

Chambers JQ, Higuchi N, Schimel JP (1998) Ancient trees in Amazonia, Nature 391:135-136

Champeau A, Gregoire A, Vaquer A (1986) Mission août 1986 en Guyane et sur les sites de Brokopondo (Surinam) et Tucuruí (Brésil). Rapport de mission E.D.F.

Chanton JP, Crill PM, Bartlett KB, Martens CS (1989) Amazon capims (floating grass mats): a source of ^{13}C-enriched methane to the troposphere. Geophys Res Lett 16:799-802

Chanton JP, Martens CS (1988) Seasonal variations in ebullutive flux and carbon isotopic composition of methane in a tidal freshwater estuary. Glob Biogeochem Cycles 2:289-298

Chanton JP, Martens CS, Kelley CA (1989) Gas transport from methane-saturated, tidal freshwater and wetland sediments. Limnol Oceanogr 34:807-819

Chartrand N, Schetagne R, Verdon R (1994) Enseignements tirés du suivi environnemental au complexe La Grande. In : Dix-huitième Congrès international des Grands Barrages, Comptes rendus, 7-11 novembre 1994, Durban (South Africa). Paris: Commission Internationale des Grands Barrages, pp 165-190

Chen JM, Ju W, Cihlar J et al. (2003) Spatial distribution of carbon sources and sinks in Canada's forests. Tellus Ser B 55:622-641

Chen WJ, Black TA, Yang PC et al. (1999) Effects of climatic variability on the annual carbon sequestration by a boreal aspen forest. Glob Change Biol 5:41-53

Chhabra A, Palria S, Dadhwal VK (2003) Soil organic carbon pool in Indian forests. For Ecol Manage 173:187-199

Chou WW, Wofsy SC, Harriss RC et al. (2002) Net fluxes of CO_2 in Amazonia derived from aircraft observations. J Geophys Res 107(D22), 4614, 10.1029/2001D001295

Christoffersen K, Riemann B, Klysner A, Sondergaard M (1993) Potential role of fish predation and natural populations of zooplankton in structuring a plankton community in eutrophic lake water. Limnol Oceanogr 38:561-573

Cicerone R, Oremland RS (1988) Biogeochemical aspects of atmospheric methane. Glob Biogeochem Cycles 2:299-327

Clair TA, Arp P, Moore TR, Dalva M, Meng FR (2002) Gaseous carbon dioxide and methane, as well as dissolved organic carbon losses from a small temperate wetland under a changing climate. Environ Pollut 116:S143-S148

Clark DA (2002) Are tropical forests an important carbon sink? Re-analysis of the long-term plot data. Ecol Appl 12(1):3-7

Clark ID, Fritz P (1997) Environmental isotopes in hydrogeology. CRC Press, Boca Raton, Florida

Clark JF, Schlosser P, Wanninkhof R, Simpson HJ, Schuster WSF, Ho DT (1995) Gas transfer velocities for SF_6 and ^3He in a small pond at low wind speeds. Geophys Res Lett 22:93-96

Clark JF, Wanninkhof R, Schlosser P, Simpson HJ (1994) Gas exchange rates in the tidal Hudson River using a dual tracer technique. Tellus 46B:274-285

Clark KL, Gholtz HL, Moncrieff JB, Cropley F, Loescher HW (1999) Environmental controls over net exhanges of carbon dioxide from contrasting Florida ecosystems. Ecol Appl 9(3):936-948

Clein JS, McGuire AD, Zhang X et al. (2002) Historical and projected carbon balance of mature black spruce ecosystems across North America: the role of carbon-nitrogen interactions. Plant and Soil 242:15-32

Cloern JE (1996) Phytoplankton bloom dynamics in coastal ecosystem: a review with some general lessons from sustained investigation of San Francisco Bay, California. Rev Geophys 34:127-168

Cole DW, Compton JE, Homann PS, Edmonds RL, van Migroet H (1995) Comparison of carbon accumulation in Douglas fir and Red alder forests. In: McFee WW, Kelly JM (ed) Carbon forms and functions in forest soils. Soil Science Society of America, Madison, Wisconsin

Cole JJ (1999) Aquatic microbiology for ecosystem scientists: new and recycled paradigms in ecological microbiology. Ecosystems 2:215-225

Cole JJ, Caraco FC, Kling GW, Kratz TK (1994) Carbon dioxide supersaturation in the surface waters of lakes. Science 265:1568-1570

Cole JJ, Caraco NF (1998) Atmospheric exchange of carbon dioxide in a low-wind oligotrophic lake measured by the addition of SF_6. Limnol Oceanogr 43:647-656

Cole JJ, Caraco NF (2001) Carbon in catchments: connecting terrestrial carbon losses with aquatic metabolism. Mar Freshwater Res 52:101-110

Cole JJ, Caraco NF (2001) Emissions of nitrous oxide (N_20) from a tidal, freshwater river in the Hudson River, New York. ENVI 35:991-996

Cole JJ, Caraco NF, Strayer DL, Ochs C, Nolan S (1989) A detailed organic carbon budget as an ecosystem-level calibration of bacterial respiration in an oligotrophic lake during midsummer. Limnol Oceanogr 34:286-296

Cole JJ, Pace ML, Carpenter SR, Kitchell JF (2000) Persistence of net heterotrophy in lakes during nutrient addition and food web manipulations. Limnol Oceanogr 45:1718-1730

Cole JJ, Carpenter SR, Kitchell JF, Pace ML (2002) Pathway of organic carbon utilization in small lakes: results from a whole lake ^{13}C addition and coupled model. Limnol Oceanogr 47:1664-1675

Conant RT, Smith GR, Paustian K (2003) Spatial variability of soil carbon in forested and cultivated sites: implications for change detection. J Environ Qual 32:278-286

Conde D, Pintos W, Gorga J, De-Leon R, Chalar G, Sommaruga R (1996) The main factors inducing chemical spatial heterogeneity in the Salto Grande, a reservoir on the Uruguay River. Arch Hydrobiol Suppl 113:571-578

Conkling BL, Hoover CM, Smith WD, Palmer CJ (2002) Using forest health monitoring data to integrate above and below ground carbon information. Environ Pollut 116:S221-S232

Conrad R, Aragno M, Seiler W (1983) Production and consumption of carbon monoxide in a eutrophic lake. Limnol Oceanogr 28(1):42-49

Coplen TB (1995) Discontinuance of SMOW and PDB. Nature 375: 285

Corin N, Backlung P, Kulovaara M (1996) Degradation products formed during UV-irradiation of humic waters. Chemosphere 33:245-255

Courchesne F, Hendershot WH (1988) Cycle annuel des éléments nutritifs dans un bassin forestier: contribution de la litière fraîche. Can J For Res 18:930-936

Courchesne F, Hendershot WH (1997) La genèse des Podzols. Géogr Phys et Quatern 51:235-250

Courchesne F, Roy AG, Biron PM, Côté B, Fyles J, Hendershot WH (2001) Fluctuations of climatic conditions, elemental cycling and forest growth at the watershed scale. Environ Monit Assess 67:161-177

Crill PM (1988) Sources of atmospheric methane in the south Florida environment. Glob Biogeochem Cycles 2(3):231-243

Crill PM (1991) Seasonal patterns of methane uptake and carbon dioxide release by a temperate woodland soil. Glob Biogeochem Cycles 5(4):319-334

Crill PM, Bartlett KB, Harriss RC et al. (1988) Methane flux from Minnesota peatlands. Glob Biogeochem Cycles 2(4):371-384

Crump BC, Baross JA, Simenstad CA (1998) Dominance of particle-attached bacteria in the Columbia River estuary, USA. Aquat Microb Ecol 14:7-48

Crusius J, Wanninkhof RH (1991) Refining the gas exchange-wind speed relationship at low wind speeds on lake 302N with SF_6. Limnol Oceanogr

Cubasch U, Dai X, Ding Y et al. (2001) Technical summary. In: Houghton JT, Ding Y, Griggs DJ et al. (eds) Climate Change 2001: The Scientific Basis. Contribution of Working Group I to the Third Assessment Report of the Intergovernmental Panel on Climate Change, Cambridge University Press, New York

Cummings DL, Kauffman JB, Perry DA, Hugues RF (2002) Aboveground biomass and structure of rainforests in the southwestern Brazilian Amazon. For Ecol Manage 163:293-307

Currie WS, Aber JD, McDowell WH, Boone RD, Magill AA (1996) Vertical transport of dissolved organic C and N under long-term N amendments in pine and hardwood forests. Biogeochemistry 35:471-505

Curtis PJ, Schindler DW (1997) Hydrological control of dissolved organic carbon mass balances in central Ontario lakes. Biogeochemistry 36:125-138

Curtis PS, Hanson PJ, Bolstad P, Barford CC, Randolph JC, Schmid HP, Wilson KB (2002) Biometric and eddy-covariance based estimates of ecosystem carbon storage in five eastern North American deciduous forests. Agric Forest Meteorol 113:3-19

D'Arcy P, Carignan R (1997) Influence of catchment topography on water chemistry in southeasthern Quebec shield lakes. Can J Fish Aquat Sci 54:2215-2227

Dadhwal VK, Nayak SR (1993) A preliminary estimate of biogeochemical cycle of carbon for India. Sci & Cult 59: 9-13

Dahlén J, Bertilsson S, Pettersson C (1996) Effects of UV-A irradiation on dissolved organic matter in humic surface waters. Environ Int 22(5):501-506

Dalva M, Moore TR (1991) Sources and sinks of dissolved organic carbon in a forested swamp catchment. Biogeochemistry 15:1-19

Dame R, Chrzanowski T, Bildsteine K, Kjerfve B, McKellar H, Nelson D, Spurrier J, Stancyk S, Stevenson H, Vernberg J, Zingmark R (1986) The outwelling hypothesis and North Inlet, South Carolina. Mar Ecol Prog Ser 33:217-229

Danckwerts PV (1951) Significance of liquid-film coefficients in gas-absorption. Introduction of the surface renewal concept. Ind Eng Chem 43:1460-1467

Danckwerts PV (1955) Gas absorption accompanied by chemical reaction. AIChE J 1:456-463

Darwich AJ (1982) Estudos limnológicos na represa hidrelétricas de Curuá-Una (Santarém P.A.). Para obtenção do grau de Mestre em Ciências Biológicos, Manaus, Brasil

David M (1979) Étude bibliographique sur la qualité des eaux, SEBJ, Direction Environnement, Montréal

David MB, Fuller RD, Fernandez IJ, Mitchell MJ, Rustad LE, Vance GF, Stam AC, Nodvin SC (1990) Spodosol variability and assessment of response to acidic deposition. Soil Sci Soc Am J 54:541-548

David MB, Vance GF, Krzyszowska AJ (1995) Carbon controls on spodosol nitrogen, sulfur and phosphorus cycling. In: McFee WW, Kelly JM (eds) Carbon forms and functions in forest soils. Soil Science Society of America, Madison, Wisconsin

Davidson EA, Lefebvre PA (1993) Estimating regional carbon stocks and spatially covarying edaphic factors using soil maps at three scales. Biogeochemistry 22:107-131

Davidson EA, Trumbone SE, Amundson R (2000) Soil warming and organic carbon content. Nature 408:789-790

Davies-Colley RJ, Vant WN (1987) Absorption of light by yellow substance in freshwater lakes. Limnol Oceanogr 32(2):416-425

De Angelis MA, Gordon L (1985) Upwelling and river runoff as sources of dissolved nitrous oxyde to the Alsea estuary, Oregon. Estuar Coast Shelf Sci 20:375-386

De Angelis MA, Lilley MD (1987) Methane in surface waters of Oregon estuaries and rivers. Limnol Oceanogr 32:716-722
De Angelis MA, Scranton MI (1993) Fate of methane in the Hudson river and estuary. Glob Biogeochem Cycles 7:509-523
De Coninck F (1980) Major mechanisms in the formation of spodic horizons. Geoderma 24:101-128
De Groot CJ (1991) The influence of FeS on the inorganic phosphate system in sediments. Verh Internat Verein Limnol 24:3029-3035
De Haan H (1993) Solar UV-light penetration and photodegradation of humic substances in peaty lake water. Limnol Oceanogr 38(5):1072-1076
De Lima IBT, Victoria RL, Novo EMLM, Feigl BJ, Ballester MVR, Ometto JP (2002) Methane, carbon dioxide and nitrous oxide emissions from two Amazonian reservoirs during high water table. Verh Int Ver Theor Angew Limnol 28:438-442
Dean WE, Gorham E (1998) Magnitude and significance of carbon burial in lakes, reservoirs, and peatlands. Geology 26:535-538
Deck BL (1981) Nutrient-element distributions in the Hudson estuary, Ph.D. dissertation, Columbia University, New York
Del Giorgio P, Duarte CM (2002) Respiration in the open ocean. Nature 420:379-384
Del Giorgio PA, Cole JJ (1998) Bacterial growth efficiency in natural aquatic systems.Ann Rev Ecolog Syst 29:503-541
Del Giorgio PA, Cole JJ Caraco NF, Peters RH (1999) Linking planktonic biomass and metabolism to net gas fluxes in northern temperate lakes. Ecology 80:1422-1431
Del Giorgio PA, Cole JJ, Cimbleris A (1997) Respiration rates in bacteria exceed phytoplankton production in unproductive aquatic systems. Nature 385:148-151
Del Giorgio PA, Gasol JM, Vaqué D, Mura P, Agusti S, Duarte CM (1996) Bacterioplankton community structure: protists control net production and the proportion of active bacteria in a coastal marine community. Limnol Oceanogr 41:1169-1179
Del Giorgio PA, Peters RH (1994) Patterns in planktonic P:R ratios in lakes: influence of lake trophy and dissolved organic carbon. Limnol Oceanogr 39:772-787
Delaune RD, Pezeshki SR (2003) The role of soil organic carbon in maintaining surface elevation in rapidly subsiding U.S. Gulf of Mexico coastal marshes. Water Air Soil Poll 3:167-179
Delmas R, Galy-Lacaux C, Richard S (2001) Emissions of greenhouse gases from the tropical hydroelectric reservoir of Petit Saut (French Guiana) compared with emissions from thermal alternatives. Glob Biogeochem Cycles 15(4):993-1003
Delmas RA, Servant J, Tathy JP, Cros B, Labat M (1992) Sources and sinks of methane and carbon dioxide exchanges in mountain forest in equatorial Africa. J Geophys Res 97:6179-6196

DeLucia EH, Hamilton JG, Naidu SL et al. (1999) Net primary production of a forest ecosystem with experimental CO_2 enrichment. Science 284:1177-1179

Denmead OT (1991) Sources and sinks of greenhouse gases in the soil-plant environment. Vegetatio 91:73-86

Dentener F, Derwent R, Dlugokencky E et al. (2001) Atmospheric chemistry and greenhouse gases. In: Houghton JT, Ding Y, Griggs DJ et al. (eds) Climate change 2001: the scientific basis. Contribution of Working Group I to the Third Assessment Report of the Intergovernmental Panel on Climate Change, Cambrigdge University Press, New York

Desjardins RL, Hart RL, MacPherson JI, Schuepp PH, Verma SB (1992) Aicraft — and tower — based fluxes of carbon dioxide, latent, and sensible heat. J Geophys Res 97:18477-18485

Deslandes JC, Guénette S, Prairie Y, Roy D, Verdon R, Fortin R (1995) Changes in fish populations affected by the construction of the La Grande complex (phase I), James Bay region, Quebec. Can J Zool 73: 1860-1877

Detwiller RP, Hall CAS (1988) Tropical forests and the global carbon cycle. Science 239:42-47

Devol AH, Quay PD, Richey JE, Martinelli LA (1987) The role of gas exchange in the inorganic carbon, oxygen, and ^{222}Rn budgets of the Amazon River. Limnol Oceanogr 32:235-248

Devol AH, Richey JE, Clark WA, King SL, Martinelli LA (1988) Methane emissions to the troposphere from the Amazon floodplain. J Geophys Res 93(D2):1583-1592

Devol AH, Forsberg BR, Richey JE, Pimentel TP (1995) Seasonal variation in chemical distributions in the Amazon (Solimoes) river: a multiyear time series. Glob Biogeochem Cycles 9:307-328

Dickinson CH (1974) Decomposition of litter in soil. In: Dickinson CH, Pugh GJF (eds) Biology of plant litter decomposition, vol 1. Academic Press, New York pp 633-658

Dillon PJ, Molot LA (1997) Dissolved organic carbon mass balance in central Ontario lakes. Biogeochemistry 36:29-42

Dionne D, Therien N (1997) Minimizing environmental impacts of hydroelectric reservoirs through operational control: a generic approach to reservoirs in northern Quebec. Ecol Model 105:41- 63

Dise NB (1993) Methane emission from Minnesota peatlands: spatial and seasonal variability. Glob Biogeochem Cycles 7(1):123-142

Dittrich M, Casper P, Koschel R (2000) Changes in the porewater chemistry of profundal sediments in response to artificial hypolimnetic calcite precipitation. Arch Hydrobiol Spec Iss Adv Limnol 55:421-432

Dixon RK, Brown S, Houghton RA, Solomon AM, Trexler MC, Wisniewski J (1994) Carbon pools and flux of global forest ecosystems. Science 263:185-190

Dobbins WE (1964) BOD and Oxygen relationships in streams J Sanit Eng Div 90: 53-78

Donahue WF, Schindler DW, Page SJ, Stainton MP (1998) Acid-induced changes in DOC quality in an experimental whole-lake manipulation. Environ Sci Tech 32:2954-2960

Dones R, Ganther U, Hirschberg S (1999) Greenhouse gas total emissions from current and future electricity and heat supply systems. Paul Scherer Inst., Switzerland, Proceedings of the 4th International Conference on GHG Control Technologies, Pergamon, 1999

Doney SC, Najjar RG, Stewart S (1995) Photochemistry, mixing and diurnal cycles in the upper ocean .J MarRes 53:341-369

Dong Y, Scharffe D, Lobert JM, Crutzen PJ, Sanhueza E (1998) Fluxes of CO_2, CH_4 and N_2O from a temperate forest soil: the effects of leaves and humus layers. Tellus Series B 50(3):243-252

Dorf RC (1967) Modern Control Systems. Addison-Wesley, Reading, Mass.

Dosskey MG, Bertsch PM (1994) Forest sources and pathways of organic matter transport to a blackwater stream: a hydrologic approach. Biogeochemistry 24:1-19

Dosskey MG, Bertsch PM (1997) Transport of dissolved organic matter through a sandy forest soil. Soil Sci Soc Am J 61:920-927

Downes MT 1991 The product and consumption of nitrate in an eutrophic lake during early stratification. Arch Hydrobiol 122:257-274

Duchemin E (2000) Hydroélectricité et gaz à effet de serre: évaluation des émissions des différents gaz et identification des processus biogéochimiques de leur production. PhD thesis. Université du Québec à Montréal

Duchemin E, Canuel R, Ferland P, Lucotte M (1999) Étude sur la production et l'émission de gaz à effet de serre par les réservoirs hydroélectriques d'Hydro-Québec et des lacs naturels (volet 2). Rapport scientifique, Hydro-Québec, Dir. princ. Planification tratégique

Duchemin E, Lucotte M (1995) Production of the greenhouse gases CH_4 and CO_2 by hydroelectric reservoirs of the boreal region, Glob Biochem Cycles 9(4):529-540

Duchemin E, Lucotte M, Canuel R (1999) Comparison of static chamber and thin boundary layer equation methods for measuring greenhouse gas emissions from large water bodies. Environ Sci Tech 33:350-357

Duchemin E, Lucotte M, Canuel R, Queiroz AG, Almeida DC, Pereira HC, Dezincourt J (2000) Comparison of greenhouse gas emissions from an old tropical reservoir with those from other reservoirs worldwide. Verh Int Ver Theor Angew Limnol 27:1391-1395

Dudka S, Ponce-Hernandez R, Hutchinson TC (1995) Current level of total element concentrations in the surface layer of Sudbury's soils. Sci Total Environ 162:161-171

Dueñas C, Fernandez MC, Carretero J, Liger E (1999) Methane and carbon dioxide fluxes in soils evaluated by ^{222}Rn flux and soil air concentration profiles. Atmos Environ 33(27):4495-4502

Dumas P (2001) Rapport méthodologique. Amélioration et validation de la méthode d'analyse des gaz à effet de serre dans l'eau et l'air. Étude des

contenants utilisés pour l'échantillonnage. Centre d'expertise en toxicologie humaine, Institut national de santé publique du Québec
Dumas P (2002) Analyse des gaz à effet de serre: méthane et dioxyde de carbone. Été 2001. Direction de toxicologie humaine, Institut national de santé publique du Québec
Dumestre JF (1998) Ecologie microbienne de la retenue de Petit Saut. Thèse d'Université, Toulouse
Dumestre JF, Guézennec J, Galy-Lacaux C, Delmas R, Richard S, Labroue L (1999) Influence of light intensity on methanotrophic bacterial activity in the Petit Saut reservoir, French Guiana. Appl Environ Microbiol 65:534-539
Dumestre JF, Vaquer A, Gosse P, Richard S, Labroue L (1999b) Bacterial ecology of a young hydroelectric reservoir (French Guiana): evidence of reduced compound exhaustion and bacterial community adaptation. Hydrobiologia 400:75-83
Dumont HJ, Van de Velde I, Dumont S (1975) The dry-weight estimate of biomass in a selection of Cladocera, Copepoda and Rotifera from the plankton, periphyton and benthos of continental waters. Oecologia 19:97
Dunfield P, Knowles, Dumont R, Moore T (1993) Methane production and consumption in temperate and subarctic peat soils: response to temperature and pH. Soil Biol Biochem 25:321-326
Dussault D, Boudreault J (1980) Réseau de surveillance écologique du complexe La Grande : description du milieu. Direction Environnement, Hydro-Québec
Duthie HC, Ostrofsky ML (1975) Environmental impact of the Churchill Falls (Labrador) hydroelectric project: a preliminary assessment. J Fish Res Board Can 32:117-125
Duxbury JM, Bouldin DR, Terry RE, Tate RL (1982) Emissions of nitrous oxide from soils. Nature 298:462-464
Dyck BS, Shay JM (1998) Biomass and carbon pool of two peatlands in the experimental lakes area, Northwestern Ontario. Can J Bot 77:291-304
Eamus D, Hutley LB, O'Grady AP (2001) Daily and seasonal patterns of carbon and water fluxes above a north Australian savanna. Tree Physiol 21:977-988
Eckhardt BW, Moore TR (1990) Controls on dissolved organic carbon concentrations in streams of southern Quebec. Can J Fish Aquat Sci 47:1537-1544
Edwards GC, Neumann HH, Den Hartog G, Thurtell GW, Kidd G (1994) Eddy correlation measurements of methane fluxes using a tunable diode laser at the Kinosheo Lake tower site during the Northern wetlands study (NOWES). J Geophys Res 99(D1):1511-1517
Efremova et al. (1997) Reserves and content of carbon in bog ecosystems of Russia. Pochvovedenie 12:1470-1477 [in Russian]
Ehman JL, Schmid HP, Randolph JC et al. (2002) An initial intercomparison of micrometerological and ecological inventory estimates of carbon sequestration in a mid-latitude deciduous forest. Glob Change Biol 8:575-589
Eletronorte (1992) Fitomassa da área do reservatório da Uhe Balbina. Rapport Eletronorte Brasilia DF

Eletronorte (1993) Diagnóstico da qualidade da água. Fases rio, enchimento e reservatório. Rapport Eletronorte Brasilia DF

Emerson S (1975) Chemically enhanced CO_2 gas exchange in a eutrophic lake: a general model. Limnol Oceanogr 20:743-53

Emerson S, Quay P, Karl D, Winn C, Tupas L, Landry M (1997) Experimental determination of the organic carbon flux from open-ocean surface waters. Nature 389:951-954

Engstrom DR (1987) Influence of vegetation and hydrology on the humus budgets of Labrador lakes. Can J Fish Aquat Sci 44:1306-1314

Environment Canada (1997) CO_2/Climate report: 1994-1995 in review: an assessment of new developments relevant to the science of climate change. 97(Spring)-1

Erickson III DJ, Zepp RG, Atlas E (2000) Ozone depletion and the air-sea exchange of greenhouse and chemically reactive trace gases. Chemosphe. Global Change Science 2:137-149

Ertel JR (1990) Photooxidation of dissolved organic matter: An organic geochemical perspective. In: Effects of solar radiation of biogeochemical dynamics in aquatic environments. Woods Hole Oceanography. Technical Report WHOI-90-90, p.79-81

Espenshade M (1980) Goode's World Atlas. Rand McNally, Chicago

Estournel C, Broche P, Marsaleix P, Devenon J-L, Auclair F, Vehil R (2001) The Rhone river plume in unsteady conditions: numerical experiment results. Estuar Coast Shelf Sci 53:25-38

Eswaran H, Van den Berg E, Reich P (1993) Organic carbon in soils of the world. Soil Sci Soc Am J 57:192-194

European Environment Agency (2001) Annual European Community greenhouse gas inventory, 1990-1999. Technical Report No. 60, 11 April 2001

Falkowski P, Scholes RJ, Boyle E, Canadell J, Canfield D, Elser J, Gruber N, Hibbard K, Högberg P, Linder S, Mackenzie FT, Moore III B, Pederson T, Rosenthal Y, Seitzinger S, Smetacek V, Steffen W (2000) The global carbon cycle: a test of our knowledge of earth as a system. Science 290:291-296

Falloon PD, Smith P, Smith JU, Szabo J, Coleman K, Marshall S (1998) Regional estimates of carbon sequestration potential: linking the Rothamsted carbon model to GIS databases. Biol Fertil Soils 27:236-241

Falotico MHB (1993) Característica limnológicas e aspectos da composição e distribuição da comunidade zooplanctônica em sua fase de enchimento (reservatório de Samuel-Rondônia). Para obtenção de grau de Mestre em Ciências da Engenheria Ambiental, Universitade de Sâo Paulo

Fan SM, Goulden ML, Munger JW et al. (1995) Environmental controls on the photosynthesis and respiration of a boreal lichen woodland: a growing season of whole-ecosystem exchange measurements by eddy correlation. Oecologia 102:443-452.

Fang J, Chen A, Peng C, Zhao S, Ci L (2001) Changes in forest biomass carbon storage in China between 1949 and 1998. Science 292:2320-2322

FAO (2001) Global forest resources assessment 2000. FAO Forestry Paper 140 http://www.eldis.org/static/DOC6658.htm

Faust BC, Zepp RG (1993) Photochemistry of aqueous iron (III)-polycarboxylate complexes: roles in the chemistry of atmospheric and surface waters. Environ Sci Tech 27:2517-2522

Fearnside PM (1989) Brazil's Balbina dam: environment versus the legacy of the pharaohs in Amazonica. Environ Manage 13:401-423

Fearnside PM (1996) Hydroelectric dams in Brazilian Amazonia: response to Rosa, Schaeffer and dos Santos. Environ Conserv 23:105-108

Fearnside PM (1997) Greenhouse-gas emissions from Amazonian hydroelectric reservoirs: the example of Brazil's Tucurui dam as compared to fossil fuel alternatives. Environ Conserv 24:64-75

Fearnside PM (1997) Greenhouse gases from deforestation in Brazilian Amazonia: net committed emissions. Climatic Change 35:321-360

Fearnside PM, de Alencastro Graça PML, Rodrigues FJA (2001) Burning of Amazonian rainforests: burning efficiency and charcoal formation in forest cleared for cattle pasture near Manaus, Brazil. For Ecol Manage 146:115-128

Fearnside PM (1995) Hydroelectric dams as sources of greenhouse gases. Environ Conserv 22(1):7-19

Fee EJ (1990) Computer programs for calculating in situ phytoplankton photosynthesis. Can Tech Rep Fish Aquat Sci no 1740

Fee EJ, Shearer JA, DeBruyn ER, Schindler EU (1992) Effects of lake size on phytoplankton photosynthesis. Can J Fish Aquat Sci 49:2445-2459

Féher M, Martin PA (1995) Tunable diode laser monitoring of atmospheric trace gas constituents, Spectrochimica Acta Part A 51:1579-1599

Fenchel T, Jorgensen BB (1977) Detritus food chain of aquatic ecosystems: the role of bacteria. Adv Microb Ecol 1:1-58

Fendinger NJ, Adams DD (1986) A headspace equilibration technique for measuring dissolved gases in sediment pore water. Intern J Environ Anal Chem 23:253-265

Fendinger NJ, Adams DD (1987) Nitrogen gas supersaturation in the recent sediments of Lake Erie and two polluted harbors. Water Res 21:1371-1374

Fernandez-Rosado MJ, Lucena J, Niell FX (1994) Space-time heterogeneity of the chlorophyll-a distribution in La Concepción reservoir (Istan, Malaga): representative models. Arch Hydrobiol 129:311-325

Fiedler S, Sommer M (2000) Methane emissions, groundwater levels, and redox potentials of common wetland soils in a temperate-humid climate. Glob Biogeochem Cycles 14(4):1081-1093

Figueiredo A, Froehlich S, Menezes CF, Miyai R (1994) Reservatoriós na Amazonia. Rapport Eletronorte Brasil

Finér L, Mannerkoski H, Piirainen S, Starr M (2002) Carbon and nitrogen pools in an old-growth, Norway spruce mixed forest in eastern Finland and changes associated with clear-cutting. For Ecol Manage 174:51-63

Flanagan LB, Ehleringer JR (1998) Ecosystem-atmosphere CO_2 exchange: interpreting signals of change using stable isotope ratios.Trends Ecol and Evol Amst 13:10-14

Fogel ML, Cifuentes LA (1993) Isotope fractionation during primary production. In: Engel MH, Macko SA (eds) Organic geochemistry. Plenum, New York, pp 73-98

Fontaine S, Bardoux G, Abbadie L, Mariotti A (2004) Carbon input to soil may decrease soil carbon content. Ecol Lett 7:314-320

Ford TE, Naiman RJ (1988) Alteration of carbon cycling by beaver: methane evasion rates from boreal forest streams and rivers. Can J Zool 66:529-533

Forsyth DJ, Howard-Williams C (1983) Lake Taupo: ecology of a New Zealand lake. New Zealand Department of Scientific and Industrial Research (DSIR Information Series, 158) Wellington

Forsyth DJ, McColl RHS (1975) Limnology of Lake Ngahewa, North Island, New Zealand. N Z J Mar Freshwater Res 9:311-332

Fox TR 1(995) The influence of low-molecular-weight organic acids on properties and processes in forest soils. In: McFee WW, Kelly JM (eds) Carbon forms and functions in forest soils. Soil Science Society of America, Madison, Wisconsin

Franken ROG, Van Vierssen W, Lubberding J (1992) Emissions of some greenhouse gases from aquatic and semi-aquatic ecosystems in the Netherlands and options to control them. Sci Total Environ 126:277-293

Frankignoulle M, Abril G, Borges A, Bourge I, Canon C, Delille B, Libert E, Théate JM (1998) Carbon dioxide emission from European estuaries. Science 282:434-436

Frankignoulle M, Bourge I, Wollast R (1996) Atmospheric CO_2 fluxes in a highly polluted estuary (The Scheldt). Limnol Oceanogr 41:365-369

Frankignoulle M, Middelburg J (2002) Biogases in tidal European estuaries: the BIOGEST project. Biogeochemistry 59:1-4

Fraser C, Roulet NT, Moore TR (2001) Hydrology and dissolved organic carbon biogeochemistry in a large peatland. Hydrol Process 15:3151-3166

Fraser PJ, Elliott WP, Waterman LS (1986) Atmospheric CO_2 record from direct chemical measurements during the 19th century. In: Trabalka JR, Reichle, DE (eds) The changing carbon cycle: a global analysis. Springer-Verlag, New York, pp 66-88

Freeman C, Evans DC, Monteith DT, Reynolds B, Fenner N (2001) Export of organic carbon from peat soils. Nature 412:785

Freeman C, Ostle N, Kang H (2001) An enzymatic 'latch' on a global carbon store. Nature 409:149

Frenzel P, Thebrath B, Conrad R (1990) Oxidation of methane in the oxic surface layer of a deep lake sediment (Lake Constance). FEMS Microb Ecol 73:149-158

Freshwater Institute – FLUDEX Project (2001) The upland flooding project (FLUDEX). Experimental lakes area. Summary report for 2000 prepared by the research team of Freshwater Institute, University Alberta, University of Wisconsin, University of Manitoba, University of Waterloo and David Huebert, consulting botanist from Winnipeg

Freshwater Institute – FLUDEX Project (2002) The upland flooding project (FLUDEX). Experimental lakes area. Summary report for 2001 prepared by

the research team of Freshwater Institute, University Alberta, University of Wisconsin, University of Manitoba, University of Waterloo and David Huebert, consulting botanist from Winnipeg

Frimmel FH (1994) Photochemical aspects related to humic substances. Environ Int 20:373-385

Froehlich S, Figueiredo A, Miyai R (1993) Características físico-químicas de reservatórios na Amazônia: UHE Tucuruí e Balbina. Monographia a presentada no Curso Internacional de Limnologia e Manejo de Águas Interiores, Sâo Carlos SP

Frolking S, Crill PM (1994) Climate controls on temporal variability of methane flux from a poor fen in southeastern New Hampshire: measurement and modeling. Glob Biogeochem Cycles 8(4):385-397

Furrer G, Wehrli B (1996) Microbial reactions, chemical speciation, and multicomponent diffusion in porewaters of a eutrophic lake. Geochim Cosmochim Acta 60:2333-2346

Fyles IH, Shaw CH, Apps MJ et al. (2002) The role of boreal forests and forestry in the global carbon budget: a synthesis. In: Shaw CH, Apps MJ (eds) The role of boreal forests and forestry in the global carbon budget. Proceedings of IBFRA 2000 Conference (May 8-12, 2000), Edmonton, Canada, Canadian Forest Service, Natural Resources Canada, Northern Forestry Centre, pp 1-21

Fyles JW, Côté B, Courchesne F, Hendershot WH, Savoie S (1994) Effects of base cation fertilization on soil and foliage nutrient concentrations, and litterfall and throughfall nutrient fluxes in a sugar maple forest. Can J For Res 24:542-549

Gagnon L, Chamberland A (1993) Emissions from hydroelectric reservoirs and comparison of hydroelectric, natural gas and oil. Ambio 22:568-569

Gagnon L, van de Vate JF (1997) Greenhouse gas emissions from hydropower, the state of research in 1996. Ener Pol 25:7-13

Galbraith MGJ (1967) Size-selective predation on *Daphnia* by rainbow trout and yellow perch. Trans Am Fish Soc 96:1-10

Galchenko VF, Lein A, Ivanov M (1989) Biological sinks of methane. In: Andrea MO, Schimel DS (eds) Exchange of trace gases between terrestrial ecosystems and the atmosphere. Wiley and Sons, New York, pp 59-71

Galy-Lacaux C (1996) Modification des échanges de constituants mineurs atmosphériques liés à la création d'une retenue hydro-électrique. Impact des barrages sur le bilan de méthane dans l'atmosphère. Thèse de doctorat de l'Université Paul-Sabatier (Toulouse III)

Galy-Lacaux C, Delmas R, Dumestre JF, Richard S (1997) Évolution temporelle des émissions gazeuses et des profils de gaz dissous. Estimation du bilan de carbone de la retenue de Petit-Saut deux ans après sa mise en eau. Hydroécol Appl 9(1-2):85-115

Galy-Lacaux C, Delmas R, Jambert C, Dumestre JF, Labroue L, Richard S, Gosse P (1997) Gaseous emissions and oxygen consumption in hydroelectric dams: a case study in French Guyana. Glob Biogeochem Cycles 11(4):471-483

Galy-Lacaux C, Delmas R, Kouadio G, Richard S, Gosse P (1999) Long-term greenhouse gas emissions from hydroelectric reservoirs in tropical forest regions. Glob Biogeochem Cycles 13:503-517

Gammon RH, Charlson RJ (1993) Origins, atmospheric transformations and fate of biologically exchanged C, N and S gases. In: Wollast R, Mackenzie FT, Chou L (eds) Interactions of C, N, P and S biogeochemical cycles and global change. NATO Series, vol 14, Springer-Verlag, Berlin, pp 283-304

Gao H, Zepp RG (1998) Factors influencing photoreactions of dissolved organic matter in a coastal river of the southeastern United States. Environ Sci Tech 32:2940-2946

Gastonguay L, Champagne GY, Ladouceur M, Lacasse R (1995) Dosage électrochimique des substances humiques dans les eaux des réservoirs hydroélectriques. Rapport IREQ-95-010, Hydro-Québec, Montréal

Gattuso JP, Frankignoulle M, Wollast R (1998) Carbon and carbonate metabolism in coastal aquatic ecosystems.Ann Rev Ecolog Syst 29:405-434

Geller A (1986) Comparison of mechanisms enhancing biodegradability of refractory lake water constituents. Limnol Oceanogr 31(4):755-764

Genivar (1995) Régime alimentaire des poissons du complexe La Grande et teneurs en mercure dans leurs proies (1993-1994), Rapport préliminaire présenté à la Vice-présidence Environnement et Collectivités, Hydro-Québec, Genivar groupe-conseil, Québec, décembre 1995

Gennings C, Molot LA, Dillon PJ (2001) Enhanced photochemical loss of organic carbon in acidic waters. Biogeochemistry 52:339-354

Genxu W, Ju Q, Guodong C, Yuanmin L (2002) Soil organic carbon pool of grassland soils on the Qinghai-Tibetan Plateau and its global implication. Sci Total Environ 291:207-217

Giardina C, Ryan M (2000) Evidence that decomposition rates of organic carbon in mineral soil do not vary with temperature. Nature 404:858-861

Gifford RM, Cheney NP, Noble JC, Russell JS, Wellington AB, Zammit C (1992) Australian land use, primary production of vegetation and carbon pools in relation to atmospheric carbon dioxide concentrations. In: Gifford RM, Barson MM (eds) Australia's renewable resources: sustainability and global change. Bureau of Rural Resources, Canberra, pp 151-187

GLOBALVIEW-CO_2: Cooperative atmospheric data integration project - Carbon dioxide (2002) CD-ROM, NOAA CMDL, Boulder, Colorado [Also available on Internet via anonymous FTP to ftp://ftp.cmdl.noaa.gov, Path: ccg/co2/GLOBALVIEW]

Glooschenko WA, Tarnocai C, Zoltai S, Glooschenko V (1993) Wetlands of Canada and Greenland. In: Whigham DF, Dykyjová D, Heju S (eds) Handbook of vegetation science. Wetlands of the world: inventory, ecology and management. Kluwer Academic Publishers, Dordrecht, The Netherlands, pp 415-514

Goni MA, Thomas KA (2000) Sources and transformation of organic matter in surface soils and sediments from a tidal estuary (North Inlet, South Carolina, USA). Estuaries 23:548-564

Gonsiorczyk T (2002) Wechselwirkungen zwischen der Sediment- und Gewässerbeschaffenheit in geschichteten Seen unterschiedlicher Trophie – Vergleichende Sedimentuntersuchengen zum C-, N- und P-Umsatz. Thesis, Brandenburgische Techische Universität, Cottbus, Germany

Goodale CL, Apps MJ, Birdsey RA et al. (2002) Forest carbon sinks in the northern hemisphere. Ecol Appl 12(3):891-899

Goodland R (1979) Environmental optimisation in hydro-development of tropical forest regions. In: Panday RS (ed) Proceeding of the symposium "Man made lakes and human health", Paramaribo, University of Surinam. pp 10-20

Goodland R, Anastacio J, Rajendra P (1992) Can hydro-reservoirs in tropical moist forests be environmentally sustainable? Environ Conserv 20:122-130

Goodroad LL, Keeney DR (1984) Nitrous oxide emission from forest, marsh, and prairie ecosystems. J Environ Qual 13:448-452

Goosen NK, Kromkamp J, Peene J, van Rijswijk P, van Breugel P (1999) Bacterial and phytoplankton production in the maximum turbidity zone of three European estuaries: the Elbe, Westerschelde and Gironde. J Mar Sys 22:151-171

Gorham E (1991) Northern peatlands: role in the carbon cycle and probable responses to climatic warming. Ecol Appl 1:182-195

Gosse P (1994) Hypothèse d'une influence des gaz formés en anaérobiose dans le réservoir de Petit Saut sur les baisses d'oxygène dissous dans le Sinnamary aval. Rapport EDF-DER

Gosse P, Delmas R, Dumestre JF, Galy-Lacaux C, Labroue L, Malatre K, Richard S (2000) Demonstration of the determining role of dissolved methane in the consumption of dissolved oxygen, in an equatorial river. XXVII SIL Congress, Dublin (August 1998), Verh Internat Verein Limnol 2:1-6

Gosse P, Dumestre JF, Richard S (1998) Puits d'oxygène dissous lié à la consommation du méthane dans le Sinnamary en aval du barrage de Petit Saut. Electricité de France EDF/HE31/98/24, Paris

Gosse P, Dumestre JF, Richard S (2002) Dissolved methane and oxygen modelling in an equatorial river downstream of a new reservoir. Verh Internat Verein Limnol 28:1894-1898

Gosse P, Grégoire A (1997) Artificial re-oxygenation of the Sinnamary, downstream of Petit Saut dam. Hydroécol appl 9(1/2):23-56

Gosse P, Sabaton C, Travade F (1997) EDF experience in improving releases for ecological purposes. In: Holly F, Gulliver J. (eds) Energy and water sustainable development. Theme D. ASCE, San Francisco, pp 453-458

Gosse P, Sissakian C et al. (2000) Des réponses à 125 questions posées sur l'évolution de l'écosystème aquatique du Sinnamary après la mise en eau du réservoir hydroélectrique de Petit Saut (Guyane). Electricité de France, Centre National d'Equipement Hydraulique

Goulden ML, Munger JW, Fan SM, Daube BC, Wofsy SC (1996) Exchange of carbon dioxide by a deciduous forest: response to interannual climate variability. Science 271:1576-1578

Goulden ML, Wofsy SC, Harden JW et al. (1998) Sensitivity of boreal forest carbon balance to soil thaw. Science 279:214-217

Gower ST (2003) Patterns and mechanisms of the forest carbon cycle. Ann Rev Environ Res 28:169-204

Gower ST, Vogel JG, Norman JM, Kucharik CJ, Steele SJ, Stow TK (1997) Carbon distribution and aboveground net primary production in aspen, jack

pine and black spruce stands in Saskatchewan and Manitoba, Canada. J Geophys Res 102:28977-28985

Grace J, Lloyd J, McIntyre J et al. (1995) Carbon dioxide uptake by an undisturbed tropical rain forest in Southwest Amazonia, 1992 to 1993. Science 270:778-780

Granberg G, Mikkelä C, Sundh I, Svensson BH, Nilsson M (1997) Sources of spatial variation in methane emission from mires in northern Sweden: A mechanistic approach in statistical modeling. Glob Biogeochem Cycles 11:135-150

Graneli W, Lindell M, Marçal De Faria B, Esteves FDA (1998) Photoproduction of dissolved inorganic carbon in temperate and tropical lakes – dependence on wavelength band and dissolved organic carbon concentration. Biogeochemistry 43:175-195

Graneli W, Lindell MJ, Tranvik LJ (1996) Photo-oxidative production of dissolved inorganic carbon in lakes of different humic content. Limnol Oceanogr 41:698-706

Granier A, Ceschia E, Damesin C et al. (2000) The carbon balance of a young beech forest over a two-year experiment. Functional Ecology 14:312-325

Granier A, Pilegaard K, Jensen NO (2002) Similar net ecosystem exchange of beech stands located in France and Denmark. Agric Forest Meteorol 114:75-82

Granli T, Bockman OC (1994) Nitrous oxide from agriculture. Norw. J. Agric. Sci. Suppl 12:19-23

Gregorich EG, Janzen HH (2000) Microbially mediated processes: decomposition. In: Sumner ME (ed) Handbook of Soil Science. CRC Press, Boca Raton, Florida

Grelle A, Lindroth A (1996) Eddy-correlation system for long-term monitoring of fluxes of heat, water vapour and CO_2. Glob Change Biol 2:297-307

Griffis TJ, Black TA, Morgenstern K et al. (2003) Meteorological and ecophysiological controls on the carbon balances of three old growth boreal forests. Agric Forest Meteorol 117:53-71

Griffis TJ, Rouse WR, Waddington JM (2000) Inter-annual variability of net ecosystem CO_2 exchange at a subarctic fen. Glob Biogeochem Cycles 14(4):1109-1121

Grigal DF, Ohmann LF (1992) Carbon storage in upland forest of the Lake States. Soil Sci Soc Am J 56:935-943

Grimard Y, Jones HG (1982) Trophic upsurge in new reservoirs: a model for total phosphorus concentrations. Can J Fish Aquat Sci 39:1473-1483

Grondin A, Lucotte M, Mucci A, Fortin B (1995) Mercury and lead profiles and burdens in soils of Québec (Canada) before and after flooding. Can J Fish Aquat Sci 52:2493-2506

Guenther A (2002) The contribution of reactive carbon emissions from vegetation to the carbon balance of terrestrial ecosystems. Chemosphere 49:837-844

Gundersen P, Emmett BA, Kjonaas OJ, Koopmans CJ, Tietema A (1998) Impact of nitrogen deposition on nitrogen cycling in forests: a synthesis of NITREX data. For Ecol Manage 101:37-55

Gurney KR, Law RM, Denning AS et al. (2002) Towards robust regional estimates of CO_2 sources and sinks using atmospheric transport models. Nature 415:626-630

Gächter R, Wehrli B (1998) Ten years of artificial mixing and oxygenation: no effect on the internal phosphorus loading of two eutrophic lakes. Environ Sci Tech 32:3659-3665

Haag WR, Hoigne J (1985) Photo-sensitized oxidation in natural water via OH radicals. Chemosphere 14:1659-1671

Hahn M, Gartner K, Zechmeister-Boltenstern S (2000) Greenhouse gas emission (N_2O, CO_2, CH_4) from three different soils near Vienna (Austria) with different water and nitrogen regimes. Die Bodenkultur 51(2):115-125

Hall BD (2003) The impact of reservoir creation on the biogeochemistry cycling of methyl and total mercury in boreal upland forests. PhD Thesis, University of Alberta, Edmonton, Alberta

Hamilton JD (1992) Methane and carbon dioxide flux ponds and lakes of the Hudson Bay lowlands. PhD thesis, University of Manitoba, Canada

Hamilton JD, Kelly CA, Rudd JWM, Hesslein RH, Roulet NT (1994) Flux to the atmosphere of CH_4 and CO_2 from wetland ponds on the Hudson Bay lowlands (HBLs). J Geophys Res 99(D1):1495-1510

Hamilton JG, Delucia EH, George K, Naidu SL, Finzi AC, Schlesinger WH (2002) Forest carbon balance under elevated CO_2. Oecologia 131(2):250-260

Hamilton SK, Sippel SJ, Melack JM (1995) Oxygen depletion and carbon dioxide and methane production in waters of the Pantanal wetland of Brazil. Biogeochemistry 30:115-141

Hanratty TJ (1991) Air-water mass transfer. In: Wilhems SC, Gulliver JG (eds) Proceedings of the 2nd International Symposium. American Society of Civil Engineers, New York

Hanson PC, Bade DL, Carpenter SR, Kratz TK (2003) Lake metabolism: relationship with dissolved organic carbon and phosphorus. Limnol Oceanogr 48:1112-1119

Happell JD, Chanton JP (1993) Carbon remineralization in a North Florida swamp forest: Effects of water level on the pathways and rates of soil organic matter decomposition. Glob Biogeochem Cycles 7(3):475-490

Harding RB, Jokela EJ (1994) Long-term effects of forest fertilization on site organic matter and nutrients. Soil Sci Soc Am J 58:216-221

Harmon ME (2001) Carbon sequestration in forests. J Forestry April:24-29

Harriss RC, Gorham E, Sebacher DI, Bartlett KB, Flebbe PA (1985) Methane flux from northern peatlands. Nature 315:652-654

Harriss RC, Sebacher DI (1981) Methane flux in forested freshwater swamps of the southestearn United States. Geophys Res Lett 8(9):1002-1004

Harriss RC, Sebacher DI, Bartlett KB, Bartlett DS, Crill PM (1988) Sources of atmospheric methane in the south Florida environment. Glob Biogeochem Cycles 2(3):231-243

Harriss RC, Sebacher DI, Day FPJ (1982) Methane flux in the Great Dismal Swamp. Nature 297:673-674

Hartman B, Hammond D, D E (1984) Gas exchange rates across sediment-water and air-water interfaces in South San Francisco Bay. J Geophys Res 89:3593-3603

Havens KE, Work KA, East TL (2000) Relative efficiencies of carbon transfer from bacteria and algae to zooplankton in a subtropical lake. J Plankton Res 22:1801-1809

Hayeur G (2001) Synthèse des connaissances environnementales acquises en milieu nordique de 1970 à 2000. Hydro-Québec, Montréal

Healy RW, Striegl RG, Russell TF, Hutchinson GL, Livingston GP (1996) Numerical evaluation of static chamber measurements of soil-atmosphere gas exchange: identification of physical processes. Soil Sci Soc Am J 60:740-747

Heath LS, Birdsey RA, Williams DW (2002) Methodology for estimating soil carbon for the forest carbon budget model of the United States (2001) Environ Pollut 116:373-380

Hecky RE, Hesslein RH (1995) Contributions of benthic algae to lake food webs as revealed by stable isotope analysis. J N Am Bentholog Soc 14:631-653

Hejzlar J, Straskraba M, Budejovice Č (1989) On the horizontal distribution of limnological variables in Rimov and other stratified Czechoslovak reservoirs. Arch Hydrobiol Beih Ergenn Limnol 33:41-55

Hélie JF (2004) Géochimie et flux de carbone organique et inorganique dans les milieux aquatiques de l'est du Canada: exemples du Saint-Laurent et du réservoir Robert-Bourassa -approche isotopique-. Thèse de doctorat, Université du Québec à Montréal

Hélie JF, Hillaire-Marcel C (2003) Utilisation des isotopes stables ($^{13}CO_2$) pour la quantification des émissions de GES à partir des réservoirs hydroélectriques pour la période 2000-2002, Université du Québec à Montréal. Chaire de recherche en environnement Hydro-Québec/CRSNG/UQAM

Hellsten S, Martikainen PJ, Vaisanen T, Niskanen A, Huttunen JT, Heiskanen M, Nenonen O (1996) Measured greenhouse gas emissions from two hydropower reservoirs in northern Finland. IAEA Advisory Group Meeting on Assessment of Greenhouse Gas Emissions from the Full Energy Chain for Hydropower, Nuclear Power and other Energy Sources, Hydro-Québec Montreal (Canada), March 1996

Hemond HF, Duran AP (1989) Fluxes of N_2O at the sediment-water and water-atmosphere boundaries of a nitrogen-rich river. Water Resour Res 25(5):839-846

Henderson-Sellers A (1985) New formulation of eddy diffusion thermocline models. Appl Math Model 441-446

Henderson-Sellers A (1987) One-dimensional modelling of thermal stratification in oceans and lakes. Environ Softw 2(2):78-84

Henderson-Sellers A, Davies AM (1988) Thermal stratification modelling for oceans and lakes. In: Annual review of numerical fluid mechanics and heat transfer, vol II: Hemisphere Pub., Washington, pp 86-156

Hendzel L (2002) Nitrous oxide fluxes from the FLUDEX reservoirs. In: The upland flooding experiment (FLUDEX), Experimental Lakes Area, Summary report for 2001. appendix 12. Freshwater Institute, Winnipeg, Canada

Herbert BE, Bertsch PM (1995) Characterization of dissolved and colloidal organic matter in soil solution: a review. In: McFee WW, Kelly JM (eds) Carbon forms and functions in forest soils. Soil Science Society of America, Madison Wisconsin

Herndl GJ, Brugger A, Hager S, Kaiser E, Obernosterer I, Reitner B, Slezak D (1997) Role of ultraviolet-B radiation on bacterioplankton and the availability of dissolved organic matter. Vegetatio 128:43-51

Hessen D, Nygaard K (1992) Bacterial transfer of methane and detritus: implications for the pelagic carbon budget and gaseous release. Arch Hydrobiol Beih Ergebn Limnol 37:139-148

Hessen DO (1989) Factors determining the nutritive status and production of zooplankton in a humic lake. J Plankton Res 11:649-664

Hessen DO (2002) UV radiation and arctic ecosystems. Springer, Berlin

Hesslein RH (1976) An in situ sampler for close interval pore water studies. Limnol Oceanogr 21:912-914

Huebert D (1999) Experimental lakes area upland flooding project vegetation analysis, 2nd edition. Freshwater Institute, Manitoba, Canada

Higbie R (1935) The rate of absorption of a pure gas into a still liquid during short periods of exposure. Trans Am Inst Chem Eng 31:365-89

Hillaire-Marcel C, Bilodeau G, Luther L, Varfalvy L (2000) Rapport sommaire sur l'utilistation des isotopes stables aux fins de quantification des émissions de GES. Chaire de recherche en environnement Hydro-Québec/CRSNG/ UQÀM, Université du Québec à Montréal

Hinton MJ, Schiff SL, English MC (1998) Sources and flowpaths of dissolved organic carbon during storms in two forested watersheds of the Precambrian Shield. Biogeochemistry 41:175-197

Ho DT, Larry LF, Bliven F, Wanninkhof R, Schlosser P (1997) The effect of rain on air-water exchange. Tellus 49B:149-158

Hoffert M, Caldeira K, Jain AK, Haites EF, Harvey LDD, Potter SD, Schlesinger ME, Schneider SH, Watts RG, Wigley TML, Wuebbles DJ (1998) Energy implications of future stabilizations of atmospheric CO_2 content. Nature 395:881-884

Holley ER (1975) Oxygen transfer at the air-water interface. In: Rumer RR jr et al Interfacial transfer processes in water resources. Report 75-1, State University of New York at Buffalo

Hollinger DY, Goltz SM, Davidson EA, Lee JT, Tu K, Valentine HT (1999) Seasonal patterns and environmental control of carbon dioxide and water vapor exchange in an ecotonal boreal forest. Glob Change Biol 5:891-902

Hollinger DY, Kelliher FM, Schulze ED et al. (1995) Initial assessment of multi-scale measures of CO_2 and H_2O flux in the Siberian taiga. J Biogeogr 22(2-3):425-431

Holz JC, KD Hoagland, Spawn RL, Popp A, Andersen JL (1997) Phytoplankton community response to reservoir aging, 1968-92. Hydrobiologia 346:183-192

Homann PS, Harrison RB (1992) Relationships among N, P, and S in temperate forest ecosystems. In: Johnson-Lindberg (ed) Atmospheric deposition and

forest nutrient cycling. Ecological Studies, vol 91, Springer-Verlag, New York
Homann PS, Sollins P, Chappell HN, Stangenberger AG (1995) Soil organic carbon in a mountainous, forested region: relations to site characteristics. Soil Sci Soc Am J 59:1468-1475
Hongve D (1994) Sunlight degradation of aquatic humic substances. Acta Hydrochim Hydrobiol, 3:117-120
Hope D, Billet MF, Cresser MS (1997) Exports of organic carbon in two river systems in NE Scotland. J Hydrol 193:61-82
Hope D, Billet MF, Cressner MS (1994) A review of the export of carbon in river water: fluxes and processes. Environ Pollut 84:301-324
Hope D, Kratz TK, Riera JL (1996) Relationship between pCO_2 and dissolved organic carbon in northern Wisconsin lakes. J Environ Qual 25:1442-1445
Hostetler SW (1987) Simulation of lake evaporation with an energy balance-eddy diffusion model of lake temperature: model development and validation, and application to lake-level variations at Harney-Malheur Lake, Oregon. PhD thesis, University of Oregon
Hostetler SW, Bartlein PJ (1990) Simulation of lake evaporation with application to modelling lake level variations of Harney-Malheur Lake, Oregon. Water Resour Res 26(10):2603-2612
Houel S (2003) Dynamique de la matière organique terrigène dans les réservoirs boréaux. Thèse de doctorat en sciences de l'environnement, Université du Québec à Montréal
Houghton RA (1999) The annual net flux of carbon to the atmosphere from changes in land use 1850-1990. Tellus 51B:298-313
Houghton RA (2003) Why are estimates of the terrestrial carbon balance so different? Glob Change Biol 9(4):500-509
Houghton RA, Hackler JL, Lawrence KT (1999) The U.S. carbon budget: contributions from land-use change. Science 285:574-578
Houghton RA, Lawrence KT, Hackler JL, Brown S (2001) The spatial distribution of forest biomass in the Brazilian Amazon: a comparison of estimates. Glob Change Biol 7:731-746
Houghton RA, Woodwell GM (1989) Global climatic change. Sci Amer 260:36-47
Hu S, Chapin III FS, Firestone MK, Field CB, Chiariello NR (2001) Nitrogen limitation of microbial decomposition in a grassland under elevated CO_2. Nature 409:188-191
Huang PM, Schnitzer M (1986) Interactions of soil minerals with natural organics and microbes. Soil Science Society of America Spec. Publ. 17, Madison, Wisconsin
Hultberg H, Skeffington R (1998) Experimental reversal of acid rain effects: the Gårdsjön Roof project. Wiley, England
Hulzen JB, Segers R, van Bodegom PM, Leffelaar PA (1999) Temperature effects on soil methane production: an explanation for observed varability. Soil Biol Biochem 31:1919-1929

Huntington TG (1995) Carbon sequestration in an aggrading forest ecosystem in the Southeastern U.S.A. Soil Sci Soc Am J 59:1459–1467

Hutchinson BP (1971) The effect of fish predation on the zooplankton of ten Adirondack lakes, with particular reference to the alewife, *Alosa pseudoharengus*. Trans Am Fish Soc 100:325-335

Huttunen JT, Vaisanen TS, Heikkinen M, Hellsten S, Nykanen H, Nenonen O, Martikainen PJ (2002b) Exchange of CO_2, CH_4 and N_2O between the atmosphere and two northern boreal ponds with catchments dominated by peatlands or forests. Plant and Soil 242:137-146

Huttunen JT, Vaisanen TS, Hellsten S, Martikainen PJ (2002) Fluxes of CH_4, CO_2 and N_2O in hydroelectric reservoirs Lokka and Porttipahta in the northern boreal zone in Finland. Glob Biogeochem Cycles 16:1-17

Hydro-Québec. Banque Intégrée réservoirs. [En ligne] (2002) [http://banque-integree.hydro.qc.ca/reservoirs/html/index.html], consultée le 31-06-03

Häder DP (1997) The effects of ozone depletion on aquatic ecosystems. Academic Press, Texas

Häder DP, Kumar HD, Smith RC, Worrest RC (1998) Effects on aquatic ecosystems. J Photochem Photobiol, B: Biol 46:53–68

IAEA, Hydro-Québec (1996) Assessment of greenhouse gas emissions from the full energy chain for hydropower, nuclear power and other energy sources. Working material: papers presented at IAEA advisory group meeting jointly organized by Hydro-Québec and IAEA (Montréal, 12-14 March, 1996), Montréal, International Atomic Energy Agency et Hydro-Québec

International Geosphere-Biosphere Programme (1996) Global change. Global wetland distribution and functional characterization: trace gases and the hydrologic cycle. Workshop report, Santa Barbara, 16-20 May

Inubushi K (1993) Methane production and emission in tropical peat soil. Japan InfoMAB Newsletter 13:4-7

IPCC (1995) Climate change. The science of climate change: contribution of WGI to the Second Assessment report of the Intergovernmental Panel on Climate Change, Cambridge University Press, New York

IPCC (1995) Climate Change 1994: radiative forcing of climate change and an evaluation of the IPCC IS92 emission scenarios. Intergovernmental Panel on Climate Change, Cambridge University Press, New York

IPCC (1995) IPCC Second Assessment Climate Change. A Report of the Intergovernmental Panel on Climate Change. Intergovernmental Panel on Climate Change, Geneva

IPCC (1996) Technical summary. In: Watson RT et al. (eds) Climate Change 1995. Cambridge University Press, New York

IPCC (2001) Climate change 2001: Summary for policymakers and technical summary of the Working Group II report. Cambridge University Press, New York

IPCC (2001) Climate change 2001: Synthesis report. A contribution of working groups I, II and III to the third assessment report of the Intergovernmental Panel on Climat Change. Cambridge University Press, New York

IPCC (2001) Climate change 2001: the scientific basis. Contribution of Working Group I to the Third Assessment Report of the Intergovernmental Panel on Climate Change. Cambridge University Press, New York

IPCC (2002) IPCC Expert group meeting on factoring out direct human-induced changes in carbon stocks and GHG emissions from those due to indirect human-induced and natural effects. Report of meeting, Geneva, Switzerland, 16-18 September

Ittekkot V, Lanne RWPM (1991) Fate of riverine particulate organic matter. In: Degens ET, Kempe S, Richey R (eds) Biogeochemistry of major world rivers. SCOPE 42, Wiley and Sons, New York, pp 233-242

Jackson RB, Banner JL, Jobbágy EG, Pockman WT, Wall DH (2002) Ecosystem carbon loss with woody plant invasion of grasslands. Nature 418:623-626

Janssens IA, Freibauer A, Ciais P et al. (2003) Europe's terrestrial biosphere absorbs 7 to 12% of European anthropogenic emissions. Science 300:1538-1542

Janssens IA, Lankreijer H, Matteucci G et al. (2001) Productivity overshadows temperature in determining soil and ecosystem respiration across European forests. Glob Change Biol 7:269-278

Janssens IA, Samson DA, Cermak J, Meiresonne L, Riguzzi F, Overloop S, Ceulemans R (1999) Above and below ground phytomass and carbon storage in a Belgian Scots pine stand. .Annals of Forest Science 56:81-90

Jansson M, Bergstrom AK, Blomqvist P, Drakare S (2000) Allochtonous organic carbon and phytoplankton/bacterioplankton production relationships in lakes. Ecology 81:3250-3255

Jansson M, Blomqvist P, Jonsson A, Bergstrom AK (1996) Nutrient limitation of bacterioplankton, autotrophic and mixotrophic phytoplankton and heterotrophic nanoflagellates in the Lake Ortrasket. Limnol Oceanogr 41:1552-1559

Jarvis PG, Dolman AJ, Schulze E-D et al. (2001) Carbon balance gradient in European forests: should we doubt 'surprising' results? A reply to Piovesan and Adams. Journal of Vegetation Science 12:145-150

Jarvis PG, Linder S (2000) Constraints to growth of boreal forests. Nature 405:904-905

Jarvis PG, Massheder JM, Hale SE, Moncrieff JB, Rayment M, Scott SL (1997) Seasonal variation of carbon dioxide, water vapor, and energy exchanges of a boreal black spruce forest. J Geophys Res 102(D24):28953-28966

Jayakumar DA, Naqvi SWA, Narvekar PV, George MD (2001) Methane in coastal and offshore water of the Arabian Sea. Mar Chem 74:1-13

Jean-Baptiste P, Poisson A (2000) Gas transfer experiment on a lake (Kerguelen Islands) using ^{3}He and SF_6. J Geophys Res 105 (C1):1177-1186

Jerome JH, Bukata RP (1998) Tracking the propagation of solar ultraviolet radiation: dispersal of ultraviolet photons in inland waters. J Great Lakes Res. 24(3):666-680

Jobbágy EG, Jackson RB (2000) The vertical distribution of soil organic carbon and its relation to climate and vegetation. Ecol Appl 10:423-436

Johannessen SC, Miller WL (2001) Quantum yield for the photochemical production of dissolved inorganic carbon in seawater. Mar Chem 76:271-283

Johnson CE, Driscoll CT, Fahey TJ, Siccama TG, Hughes JW (1995) Carbon dynamics following clear-cutting of a Northern hardwood forest. In: McFee WW, Kelly JM (eds) Carbon forms and functions in forest soils. Soil Science Society of America, Madison, Wisconsin, pp. 463-488

Johnson DW (1995) Role of carbon in the cycling of other nutrients in forested ecosystems. In: McFee WW, Kelly JM (eds) Carbon forms and functions in forest soils. Soil Science Society of America, Madison, Wisconsin, pp.299-328

Johnson DW, Cole DW, Horng FW, van Miegrot H, Todd DE (1981) Chemical characteristics of two forested Ultisols and two forested Inceptisols relevant to anion production and mobility, Oak Ridge National Laboratory, Environmental Sciences Division, Publication no1670, Oak Ridge, Tennessee

Johnson DW, Lindberg SE (1992) Atmospheric deposition and forest nutrient cycling. (Ecological Studies, vol 91) Springer-Verlag, New York

Johnson JE, Bates TS (1996) Sources and sinks of carbon monoxide in the mixed layer of the tropical South Pacific Ocean. Glob Biogeochem Cycles 10:347-359

Joiner DW, Lafleur PM, McCaughey JH, Bartlett PA (1999) Interannual variability in carbon dioxide exchanges at a boreal wetland in the BOREAS northern study area. J Geophys Res 104:27663-27672

Jones JB, Mulholland PJ (1998a) Carbon dioxide variation in a hardwood forest stream: an integrative measure of whole catchment soil respiration. Ecosystems 1:183-196

Jones JB, Mulholland PJ (1998b) Methane input and evasion in a hardwood forest stream: effects of subsurface flow from shallow and deep pathways. Limnol Oceanogr 43:1243-1250

Jonsson A, Karlsson J, Jansson M (2003) Sources of carbon dioxide supersaturation in clearwater and humic lakes in northern Sweden. Ecosystems 6:224-235

Jonsson A, Meili M, Bergstrom AK, Jansson M (2001) Whole-lake mineralization of allochthonous and autochthonous organic carbon in a large lake (Örträsket, N. Sweden). Limnol Oceanogr 46:1691-1700

Judd KW, Kling GW (2002) Production and export of dissolved C in arctic tundra mesocosms: the role of vegetation and water flow. Biogeochemistry 60:213-234

Junk WJ (1997) General aspects of floodplain ecology with special reference to Amazonian floodplains. In: Junk WJ (ed) The central Amazon floodplain: ecology of a pulsing system. Springer-Verlag, Berlin, pp 3-20

Junk WJ, Bailey RE, Sparks A (1989) The flood pulse concept in river floodplain systems. Can Spec Publ Fish Aquat Sci 106:110-127

Junk WJ, Nunes de Mello JAS (1987) Impactos ecologicos das represas hidrelétricas na Bacia Amazônica brasiliera. Tübinger Geograph Stud 95:367-385

Junk WJ, Robertson BA, Darwich AJ, Vieira I (1981) Investigacões limnológicas e ictiológicas em Curuá-Una, a primeira represa hidrelétrica na Amazônia Central. Acta Amazonica 11:689-716

Justic D, Rabalais N, Turner RE (1995) Stoichiometric nutrient balance and origin of coastal eutrophication. Mar Pollut Bull 30:41-46

Jürgens K (1994) Impact of *Daphnia* on planktonic microbial food webs: a review. Marine microbial food webs 8:295-324

Jähne B, Münnich KO, Bösinger R, Dutzi A, Hubert W, Libner P (1987) On the parameters influencing air-water gas exchange. J Geophys Res 92 (C2):1937-1949

Kabata-Pendias A, Pendias H (1992) Trace elements in soils and plants. 2nd ed, CRC Press, Boca Raton, Florida

Kalff J (2002) Limnology: inland water ecosystems. Prentice Hall, Upper Saddle River, NJ

Kankaala P, Bergström I (2004) Emission and oxidation of methane in *Equisetum fluviatile* stands growing on organic sediment and sand bottoms. Biogeochemistry 67:21-37

Karl DM, Laws EA, Morris PM, Wiliams PJL, Emerson S (2003) Metabolic balance of the open sea. Nature 426:32

Karlsson J (2001) Pelagic energy mobilization and carbon dioxide balance in subarctic lakes in northern Sweden. Doctoral dissertation, Umea University, Sweden

Karlsson J, Jansson M, Jonsson A (2002) Similar relationship between pelagic primary and bacterial production in clearwater and humic lakes. Ecology 83:2902-2910

Kasischke ES, Bruhwiler LM (2003) Emissions of carbon dioxide, carbon monoxide, and methane from boreal forest fires in 1998, J Geophys Res 108(D1), 8146, doi:10.1029/2001JD000461

Kauffman JB, Cummings DL, Ward DE, Babbitt R (1995) Fire in the Brazilian Amazon: 1. biomass, nutrient pools, and losses in slashed primary forests. Oecologia 104:397-409

Kauppi PE (1992) Carbon budget of temperate zone forests during 1951-2050. In: Apps MJ, Price DT (eds) Forest ecosystems, forest management and the global carbon cycle. (NATO ASI Series, vol 140) Springer-Verlag, Berlin Heidelberg, pp 191-198

Kauppi PE, Mielikäinen K, Kuusela K (1992) Biomass and carbon budgets of European forests, 1971 to 1990. Science 256:70-74

Kauppila P, Meeuwig JJ, Pitkänen H (2003) Predicting oxygen in small estuaries of the Baltic Sea: a comparative approach. Estuar Coast Shelf Sci 57:1115-1126

Kauranne T (1983) Computer program documentation for the lake model Finneco and the river model QUAL-II. Oy International Business Machines, Ab National Board of Waters, Helsinki

Keddy PA (2000) Wetland ecology: principles and conservation. Cambridge University Press, Cambridge

Keeling CD, Bacastow RB, Whorf TP (1982) Measurements of the concentration of carbon dioxide at Mauna Loa Observatory (Hawaii). In: Clark WC (ed) Carbon dioxide review. Oxford University Press, New York

Keeling CD, Chin JFS, Whorf TP (1996) Increased activity of Northern hemispheric vegetation inferred from atmospheric CO_2 measurements. Nature 382:146-149

Keil RG, Mayer LM, Quay PD, Richey JE, Hedges JI (1997) Loss of organic matter from riverine particles in deltas. Geochim Cosmochim Acta 61:1507-1511

Keller C, Domergue FL (1996) Soluble and particulate transfers of Cu, Cd, Al, Fe and some major elements in gravitational waters of a Podzol. Geoderma 71:263-274

Keller M, Goreau TJ, Wofsy SC, Kaplan WA, McElroy MB (1983) Production of nitrous oxide and consumption of methane by forest soils. Geophys Res Lett 10:1156-1159

Keller M, Kaplan WA, Wofsy SC (1986) Emissions of N_2O, CH_4 and CO_2 from tropical forest soils. J Geophys Res 91(D11):11791-11802

Keller M, Reiners WA (1994) Soil-atmosphere exchange of nitrous oxide, nitric oxide, and methane under secondary succession of pasture to forest in the Atlantic lowlands of Costa Rica. Glob Biogeochem Cycles 8(4):399-409

Keller M, Stallard RF (1994) Methane emission by bubbling from Gatun Lake, Panama. J Geophys Res 99:8307-8319

Kelley CA, Marteens CS, Chanton JP (1990) Variations in sedimentary carbon remineralization rates in the White Oak River estuary, North Carolina. Limnol Oceanogr 35:372-383

Kelley CA, Martens CS, Ussler W III (1995) Methane dynamics across a tidally flooded riverbank margin. Limnol Oceanogr 40:1112-1129

Kelly CA, Fee E, Ramlal PS, Rudd JW, Hesslein RH, Anema C, Schindler EV (2001) Natural variability of carbon dioxide and net epilimnetic production in the surface waters of boreal lakes of different sizes. Limnol Oceanogr 46:1054-1064

Kelly CA, Rudd JWM, Bodaly RA et al. (1997) Increases in fluxes of greenhouse gases and methyl mercury following flooding of an experimental reservoir. Environ Sci Tech 31:1334-1344

Kelly CA, Rudd JWM, St.Louis VL, Moore T (1994) Turning attention to reservoir surfaces, a neglected area in greenhouse studies. Eos 75:332-333

Kendall C, Caldwell EA (1998) Fundamentals of isotope geochemistry, chap 2. In: Kendall C, McDonnell JJ (eds) Isotope tracers in catchment hydrology. Elsevier, Amsterdam, pp 51-86

Kern JS, Turner DP, Dodson RF (1997) Spatial patterns of soil organic carbon pool size in the Northwestern United States. In: Lal R, Follett R, Stewart BA (eds) Soil Processes and the carbon cycle. Advanced Soil Science, CRC Press, Boca Raton, Florida, pp 29–43

Ketchum RH (1983) Estuarine characteristics. Ecosystems of the world 26:1-14

Kieber RJ, McDaniel J, Mopper K (1989) Photochemical source of biological substrates in sea water: implications for carbon cycling. Nature 341:637-639

Kieber RJ, Zhou X, Mopper K (1990) Formation of carbonyl compounds from UV-induced photodegradation of humic substances in natural waters: fate of riverine carbon in the sea. Limnol Oceanogr 35(7):1503-1515

Kim J, Verma SB (1992) Soil surface CO_2 flux in a Minnesota peatland. Biogeochemistry 18:37-51

Kim J, Verma SB, Billesbach DP, Clement RJ (1998) Diel variation in methane emission from a midlatitude prairie wetland: significance of convective through flow in *phragmites australis*. J Geophys Res D21:28029-28039

King GM (1990) Regulation by light of methane emissions from a wetland. Nature 345:513-515

King GM, Blackburn TH (1996) Controls of methane oxidation in sediments. In: Adams DD, Seitzinger SP, Crill PM (eds) Cycling of reduced gases in the hydrosphere. Mitt Internat Verein Limnol, Mitteilungen 25, E. Schweizerbart'sche Verlagsbuchhandlung (Nägele u. Obermiller), Stuttgart, pp 25-38

Kinnunen K, Nyholm B, Niemi J, Frisk T, Kylä-Harakka T, Kauranne T (1982) Water quality modeling of finnish water bodies, Publication of the Water Research Institute, Report 46, Vesihallitus – National Board of Waters, Helsinki

Kipphut GW (1978) An investigation of sedimentary processes in lakes. PhD Thesis, Columbia University, New York

Kirchman DL (1993) Leucine incorporation as a measure of biomass production by heterotrophic bacteria. In Kemp PF, Sherr BF, Sherr EF, Cole JJ (eds), Handbook of methods in aquatic microbial ecology. Lewis Publishers, Boca Raton, Florida pp 509-512

Kirschbaum MUF (2000) Will changes in soil organic carbon act as a positive or negative feedback on global warming? Biogeochemistry 48:21-51

Kling GW, Kipphut GW, Miller MC (1991) Arctic lakes and streams as gas conduits to the atmosphere: implications for tundra carbon budgets. Science 251:298-302

Kling GW, Kipphut GW, Miller MC (1992) The flux of CO_2 and CH_4 from lakes and rivers in artic Alaska. Hydrobiologia 240:23-36

Klinger LF, Zimmerman PR, Greenberg JP, Heidt LE, Guenther AB (1994) Carbon trace gas fluxes along a successional gradient in the Hudson Bay lowland. J Geophys Res 99:1469-1494

Klopatek JM (2002) Below ground carbon pools and processes in different age stands of Douglas-fir. Tree Physiol 22:197-204

Knohl A, Schulze ED, Kolle O, Buchmann N (2003) Large carbon uptake by an unmanaged 250-year-old deciduous forest in Central Germany. Agric Forest Meteorol 118(3-4):151-167

Knoll LB, Vanni MJ, Renwick WH (2003) Phytoplankton primary production and photosynthetic parameters in reservoirs along a gradient of watershed land use. Limnol Oceanogr 48:608-617

Kokorin AO, Lelyakin AL, Nazarov IM (1996) Calculation of CO_2 net sinks/emissions in Russian forests and assessment of mitigation options. Environ Manage 20(suppl. 1):S101-S110

Kolchugina TP, Vinson TS (1993) Carbon sources and sinks in forest biomes of the former Soviet Union. Glob Biogeochem Cycles 7:291-304

Kolchugina TP, Vinson TS, Shwidenko AZ, Dixon RK, Kobak KL, Botch MS (1992) Carbon balance of forest biomes (undisturbed ecosystems) in the former Soviet Union. In: Proceedings of the IPCC Workshop, University of Joensuu, Finland, pp 52-62

Köhler J, Schmitt M, Krumbeck H, Kapfer M, Litchman E et PJ Neale (2001) Effects of UV on carbon assimilation of phytoplankton in a mixed water column. Aquat Sci 63:294-309

Körtzinger A (2003) A significant CO2 sink in the tropical Atlantic Ocean associated with the Amazon River plume. Geophys Res Lett 30:2287

Kondratyev KA, Varotsos CA (2000) Atmospheric ozone variability. Springer, Chichester, pp 368-438

Koprivnjak JF, Moore TR (1992) Sources, sinks, and fluxes of dissolved organic carbon in sub-arctic fen catchments. Arctic Alpine Res 24:204-210

Kormann R, Müeller H, Werle P (2001) Eddy flux measurements of methane over the fen Murnauer Moos (11°11'E, 47°39'N) using a fast tunable diode laser spectrometer. Atmos Environ 35(14):2533-2544

Kortelainen P (1998) Finnish lakes as sources of greenhouse gases: CH_4, CO_2 and N_2O supersaturation in 12 Finnish lakes before and after ice-melt. In: Proceedings of International Workshop of hydro dams, lakes and greenhouse emissions, 4-5 December 1998, Copacabana, Rio de Janeiro

Koschel R, Adams DD (eds) (2003) Lake Stechlin: an approach to understand an oligotrophic lowland lake. Arch Hydrobiol Spec Iss Adv Limnol, vol 58, E. Schweizerbart'sche Verlagsbuchhandlung (Nägele u. Obermiller), Stuttgart

Koyama T (1990) Gases in lakes, their production mechanism and degassing (CH_4 and H_2) of the earth. In: Geochemistry of gaseous elements and compounds, Theophrastus Publications, Zographou, Athens, pp 271-335

Krankina ON, Dixon RK (1994) Forest management options to conserve and sequester terrestrial carbon in the Russian Federation. World Resour Rev 6:88-101

Krankina ON, Harmon ME, Winjum JK (1996) Carbon storage and sequestration in the Russian forest sector. Ambio 25:284-288

Kratz TK, Schindler J, Hope D, Riera JL, Bowser CJ (1997) Average annual carbon dioxide concentrations in eight neighboring lakes in northern Wisconsin, USA. Verh Internat Verein Limnol 26:335-338

Kremer JN, Nixon SW, Buckley B, Roques P (2003) Technical note: conditions for using the floating chamber; method to estimate air-water gas exchange. Estuaries 26(4A):985-990

Kremer JN, Reischauer A, D'Avanzo C (2003) Estuary-specific variation in the air-water gas exchange coefficient for oxygen. Estuaries 26:829-836

Ku TT, Hinkley ED, Sample JO (1975) Long path monitoring of atmospheric carbon monoxide with a tunable diode laser system. Appl Opt 14:854-861

Kühl M, Steuckart C, Eickert G, Jeroschewski P (1998) A H2S microsensor for profiling biofilms and sediments: application in an acidic lake sediment. Aquat Microb Ecol 15:201-209

Kuivila KM, Murray JW, Devol AH, Lidstrom ME, Reimers CE (1988) Methane cycling in the sediments of Lake Washington. Limnol Oceanogr 33:571-581

Kulmala M, Suni T, Lehtinen KEJ, Dal Maso M, Boy M, Reissel A, Rannik U, Aalto P, Keronen P, Hakola H, Back JB, Hoffmann T, Vesala T, Hari P (2004) A new feedback mechanism linking forests, aerosols, and climate. Atmos Chem Phys 4:557-562

Kulovaara M, Corin N, Backlund P, Tervo J (1996) Impact of UV_{254}-radiation on aquatic humic substances. Chemosphere 33(5):783-790

Kurz WA, Apps MJ (1993) Contribution of northern forests to the global carbon cycle: Canada as a case study. Water Air Soil Poll 70:163-176

Kurz WA, Apps MJ (1999) A 70-year retrospective analysis of carbon fluxes in the canadian forest sector. Ecol Appl 9:526-547

Lacaux C**,** Delmas RA (1995) Aménagement hydroélectrique de Petit Saut (Guyane). Modification des échanges biosphère atmosphère de constituants mineurs atmosphériques. Rapport de mission, rapport de convention GP 7540, EDF Laboratoire d'Aérologie, Université Paul Sabatier

Lacaux C, Delmas RA, Labroue L (1994a) Aménagement hydroélectrique de Petit Saut (Guyane). Modifications des échanges biosphère-atmosphère de constituants mineurs atmosphériques. Rapport scientifique n° 1, rapport de convention GP 7540, EDF Laboratoire d'Aérologie, Université Paul Sabatier

Lacaux C, Jambert C, Delmas RA, Labroue L (1994b) Aménagement hydroélectrique de Petit Saut (Guyane). Modifications des échanges biosphère-atmosphère de constituants mineurs atmosphériques. Rapport scientifique n° 2, rapport de convention GP 7540, EDF Laboratoire d'Aérologie, Université Paul Sabatier

Lafleur PM (1999) Growing season energy and CO_2 exchange at a subarctic boreal woodland. J Geophys Res 104(D8):9571-9580

Lafleur PM, McCaughey JH, Joiner DW, Bartlett PA, Jelinski DE (1997) Seasonal trends in energy, water, and carbon dioxide fluxes at a northern boreal fen. J Geophys Res (BOREAS Special Issue) 102(D24):29009-29020

Lafleur PM, Roulet NT, Admiral SW (2001) Annual cycle of CO_2 exchange at a bog peatland. J Geophys Res 106(D3):3071-3081

Lafleur PM, Roulet NT, Bubier JL, Moore TR (2003) Interannual variability in the peatland-atmosphere carbon dioxide exchange at an ombrotrophic bog. Glob Biogeochem Cycles 17(2), 10.1029/2002GB001983

Lal M, Singh R (2000) Carbon sequestration potential of Indian forests. Environ Monit Assess 60:315-327

Lal R, Kimble JM (2001) Importance of soil bulk density and methods of its measurement. In: Lal R, Kimble JM, Follett RF, Stewart BA (eds) Assessment methods for soil carbon. Lewis Publishers, Boca Raton, p 31-44

Lalumière R (2001) Réseau de suivi environnemental du complexe La Grande : suivi de la qualité de l'eau des secteurs La Grande-2-A et La Grande-1 (1978-2000). Rapport synthèse préparé par le Groupe conseil Génivar inc. pour la direction Expertise et Support technique de production de l'unité Hydraulique et Environnement d'Hydro-Québec

Lambert M (2000) Analyse statistique de données sur les émissions de gaz à effet de serre des réservoirs. Banque de données GES Hydro-Québec-UQAM. Direction Environnement, Hydro-Québec, Montréal

Lambert M, Fréchette JL (2001) Campagne d'échantillonnage sur les émissions de gaz à effet de serre des réservoirs et des lacs environnants. Rapport de terrain 2000, Direction Environnement, Hydro-Québec, Montréal

Lambert M, Fréchette JL (2002) Campagne d'échantillonnage sur les émissions de gaz à effet de serre des réservoirs et des lacs environnants, rapport de terrain 2001. Direction Environnement, Hydro-Québec, Montréal

Lambert M, Fréchette JL, Dumas P, Tremblay A, Varfalvy L (2001) Development of ex-situ GC/MS analysis technique for greenhouse gas samples collected by floating chambers and a hydroplane. Proceedings of the 28th Congress of the Societas Internationalis Limnologiae (SIL), February 4-10th, Melbourne, Australia

Lamontagne RA, Swinnerton JW, Linnenbom VJ, Smith WD (1973) Methane concentrations in various marine environments. J Geophys Res 78:5317-5324

Lamontagne S, Carignan R, D'Arcy P, Prairie YT, Paré D (2000) Element export in runoff from eastern Canadian Boreal Shield drainage basins following forest harvesting and wildfires. Can J Fish Aquat Sci 57 (suppl. 2):118–128

Larsen JA (1980) The Boreal Ecosystem, Academic Press, New York

Larzillière M et al. (1997-2002) Développement et parachèvement du développement d'un appareil (Laser IR) de mesure de gaz à effet de serre et réalisation de mesures quantitatives sur différents lacs artificiels et naturels et les réservoirs hydroélectriques. Projet de recherche et de développement coopératif (RDC). No Dossier CRDPJ 228063-99. Rapports annuels 1997 à 2002

Laurance WF, Fearnside PM, Laurance SG, Delamonica P, Lovejoy TE, Rankin-de-Merona JM, Chambers JQ, Gascon C (1999) Relationship between soils and Amazon forest biomass: a landscape-scale study. For Ecol Manage 118:127-138

Laurie SH, Manthey JA (1994) The chemistry and role of metal ion chelation in plant uptake processes. In: Manthey JA, Crowley DE, Luster DG (eds) Biochemistry of metal micronutrients in the rhizosphere. CRC Press, Boca Raton, Florida

Laurion I, Vincent WF, Lean DRS (1997) Underwater ultraviolet radiation: development of spectral models for northern high latitude lakes. Photochem Photobiol 65(1):107-114

Law BE, Thornton PE, Irvine J, Anthoni PM, Van Tuyl S (2001) Carbon storage and fluxes in Ponderosa pine forests at different developmental stages. Glob Change Biol 7:755-777

Lebaron Ph, Servais P, Agogué H, Courties C, Joux J (2001) Does the high nucleic acid content of individual bacterial cells allow us to discriminate between active cells and inactive cells in aquatic systems? Appl Environ Microbiol 67:1775-1782

Lee X, Fuentes JD, Staebler RM, Neumann HH (1999) Long-term observation of the atmospheric exchange of CO_2 with a temperate deciduous forest in southern Ontario, Canada. J Geophys Res 104:15975-15984

Leentvaar P (1967) The artificial Brokopondo lake of the Suriname river, its biological implications. Atas do simposio sobre a biota Amazonica 3:127-140

Leentvaar P (1973) Lake Brokopondo. In: Ackermann WC, White GF, Worthington EB (eds) Man-made lakes: their problems and environmental effects. American Geophysical Union, Washington, DC, pp 186-196

Leentvaar P (1984) The Brokopondo barrage lake in Suriname, south America, and the planned Kabalebo project in west Suriname. In: Hydro-Environmental indices: a review and evaluation of their use in the assessment of the environmental impacts of water projects. IHP Technical documents in hydrology, UNESCO, pp 49-56

Leentvaar P (1993) The man-made Lake Brokopondo. In: Oubster PE (ed) Freshwater Ecosystem of Surinam, Kluwer Academic Pub, Netherlands,. pp 227-237

Legendre P, Legendre L (1998) Numerical Ecology. 2nd ed, Elsevier, Amsterdam

Lemon E, Lemon D (1981) Nitrous oxide in freshwaters of the Great Lake basin. Limnol Oceanogr 26:867-879

Lerman A (1979) Geochemical processes: water and sediment environments. Wiley and Sons, New York

Lidstrom ME, Somers L (1984) Seasonal study of methane oxidation in Lake Washington. Appl Environ Microbiol 47:1255-1260

Lieth H (1975) Modeling the primary productivity of the world. In: H Lieth, Whittaker RH (eds) Primary productivity of the biosphere. Springer-Verlag, New York

Liikanen A, Flöjt L, Martikainen P (2002) Gas dynamics in eutrophic lake sediments affected by oxygen, nitrate, and sulfate. J Environ Qual 31:338-349

Liikanen A, Huttunen JT, Murtoniemi T, Tanskanen H, Väisänen T, Silvola J, Alm J, Martikainen PJ (2003a) Spatial and seasonal variation in greenhouse gas and nutrient dynamics and their interactions in the sediments of a boreal eutrophic lake. Biogeochemistry 65:83-103

Liikanen A, Martikainen PJ (2003) Effect of ammonium and oxygen on methane and nitrous oxide fluxes across the sediment-water interface in a eutrophic lake. Chemosphere 52:1287-1293

Liikanen A, Ratilainen E, Saarnio S, Alm J, Martikainen PJ, Silvola J (2003b) Greenhouse gas dynamics in boreal, littoral sediments under raised CO_2 and nitrogen supply. Freshwater Biol 48:500-511

Lilley MD, De Angelis MA, Olson (1996) Methane concentrations and estimated fluxes from Pacific Northwest rivers. In: Adams DD, Seitzinger SP, Crill PM (eds) Cycling of reduced gases in the Hydrosphere. E. Schweizerbart'sche Verlagbuchhandlung, Stuttgart, pp 187-196

Lin G, Ehleringer JR (1997) Carbon isotopic fractionation does not occur during dark respiration in C3 and C4 plants. Plant Physiol 114:391-394

Lindell M, Graneli W, Tranvik L (1995) Enhanced bacterial growth in response to photochemical transformation of dissolved organic matter. Limnol Oceanogr 40:195-199

Lindroth A, Grelle A, Moren AS (1998) Long-term measurements of boreal forest carbon balance reveal large temperature sensitivity. Glob Change Biol 4:443-450

Lipschultz F (1981) Methane release from a brackish intertidal salt-marsh embayment of Chesapeake Bay, Maryland. Estuaries 4:143-145

Liski J (1995) Variation in soil organic carbon and thickness of soil horizons within a boreal forest stand. Effect of trees and implications for sampling. Silva Fennica 29(4):255-266

Liski J, Westman CJ (1995) Density of organic carbon in soil at coniferous forest sites in southern Finland. Biogeochemistry 29:183-197

Liss PS (1967) Process of gas exchange across an air-water interface. Deep Sea Res 20:221-238

Liss PS, Slater PG (1974) Flux of gases across the sea-air interface. Nature 247:181-184

Litvak M, Miller S, Wofsy SC, Goulden M (2003) Effect of stand age on whole-ecosystem CO_2 exchange in the Canadian boreal forest. J Geophys Res 108(D3):6-11

Liu J, Peng C, Apps M, Dang Q, Banfield E, Kurz W (2002) Historic carbon budgets of Ontario's forest ecosystems. For Ecol Manage 169:103-114

Livingston GP, Hutchinson GL (1995) Enclosure-based measurement of trace gas exchange: applications and sources of error. In: Matson PA, Harriss RC (eds) Biogenic trace gases: measuring emissions from soil and water. Blackwell Science, London, pp 14-51

Livingston GP, Vitousek PM, Matson PA (1988) Nitrous oxide flux and nitrogen transformations across a landscape gradient in Amazonia. J Geophys Res 93(D2):1593-1599

Livingstone DM, Imboden DM (1993) The non-linear influence of wind-speed variability on gas transfer in lakes. Tellus 45B:275-295

Lorke A, Müller B, Maerki M, Wüest A (2003) Breathing sediments: the control of diffusive transport across the sediment-water interface by periodic boundary-layer turbulence. Limnol Oceanogr 48:2077-2085

Lucotte M, Schetagne R, Thérien N, Langlois C, Tremblay A (1999) Mercury in the biogeochemical cycle: natural environments and hydroelectric reservoirs of Northern Québec (Canada). Springer-Verlag, New York

Ludwig W, Probst JL, Kempe S (1996) Predicting the oceanic input of organic carbon by continental erosion. Glob Biogeochem Cycles 10:23-41

Lundström US (1993) The role of organic acids in the soil solution chemistry of a podzolized soil. J Soil Sci 44:121-133

Luther L (2000) Suivi isotopique ($^{13}CO_2$) du métabolisme du carbone et des émissions de CO_2 dans un réservoir hydroélectrique du Nouveau-Québec. Mémoire de Maîtrise, Université du Québec à Montréal

Lyche A, Andersen T, Christoffersen T, Hessen DO, Berger Hansen PH, Klysner A (1996) Mesocosm tracer studies. 2. The fate of primary production and the

role of consumers in the pelagic carbon cycle of a mesotrophic lake. Limnol Oceanogr 41:475-487

Macdonald JA, Skiba U, Sheppard LJ, Ball B, Roberts JD, Smith KA, Fowler D (1997) The effect of nitrogen deposition and seasonal variability on methane oxidation and nitrous oxide emission rates in an upland spruce plantation and moorland. Atmos Environ 31(22):3693-3706

MacIntyre S, Melack JM (1995) Vertical and horizontal transport in lakes: linking littoral, benthic, and pelagic habitats. J N Am Benthol Soc 14:599-615

MacIntyre S, Wanninkhoff R, Chanton JP (1995) Trace gas exchange in freshwater and coastal marine environmnets. In: Mason P, Hariss R (eds) Biogenic trace gases: Measuring emissions from soil and water (Methods in Ecology) Blackwell Science, Cambridge, Massachusetts, pp 52-97

Mackay D, Shiu WY (1981) A critical review of Henry's law constants for chemicals of environmental interest. J Phys Chem 10:1175-1199

Maddock JEL, Santos MBP, Prata KR (2001) Nitrous oxide emission from soil of the Mata Atlantica, Rio de Janeiro State, Brazil. J Geophys Res 106(D19):23055-23060

Magenheimer JF, Moore TR, Chmura GL, Daoust RJ (1996) Methane and carbon dioxide flux from a macrotidal salt marsh, Bay of Fundy, New Brunswick. Estuaries 19:139-145

Makhov GA, Bazhin NM (1999) Methane emission from lakes. Chemosphere 38:1453-1459

Malhi Y, Baldocchi DD, Jarvis PG (1999) The carbon balance of tropical, temperate and boreal forests. Plant Cell Environ 22:715-740

Malhi Y, Grace J (2000) Tropical forests and atmospheric carbon dioxide. Trends Ecol Evol 15:332-337

Malhi Y, Nobre AD, Grace J et al. (1998) Carbon dioxide transfer over a Central Amazonian rain forest. J Geophys Res 103:31593-31612

Mancinelli RL (1995) The regulation of methane oxidation in soil. Ann Rev Microbiol 49:581-605

Manies KL, Harden JW, Kramer L, Parton WJ (2001) Carbon dynamics within agricultural and native sites in the loess region of western Iowa. Glob Change Biol 7:545-555

Manna S, Courchesne F, Roy AG, Turmel MC, Côté B (2002) Trace metals in the forest floor, litterfall patterns and topography. Transactions of the 17th World Congress of Soil Science, Bangkok, pp 1306.1-1306.9

Marino R, Howard RW (1993) Atmospheric oxygen exchange in the Hudson river: dome measurements and comparison with other natural waters. Estuaries 16:433-445

Markkanen T, Rannik U, Keronen P, Suni T, Vesala T (2001) Eddy covariance fluxes over a boreal Scots pine forest. Bor Environ Res 6:65-78

Martens CS, Albert DB, Alperin MJ (1998) Biogeochemical processes controling methane in gassy coastal sediments, Part 1. A model coupling organic matter flux to gas production, oxydation and transport. Continent Shelf Res 18:1741-1770

Martens CS, Goldhaber (1978) Early diagenesis in transitional sedimentary environments of the White Oak River estuary, North Carolina. Limnol Oceanogr 23:428-441

Martens CS, Kelly CA, Chanton JP (1992) Carbon and hydrogen isotope characterization of methane from wetlands and lakes of the Yukon-Kuskokwim Delta, western Alaska. J Geophysical Res 97(D15):16,689-16,701

Marty J, Pinel-Alloul B, Carrias JF (2003) Zooplankton responses to experimental nutrients and planktivorous fish addition and top-down effects on phytoplankton and ciliate communities (submitted to Freshwater Biol)

Marzolf GR (1990b) Reservoirs as environments for zooplankton. In: Thornton KW, Kimmel BL, Payne FE (eds) Reservoir limnology: ecological perspectives. Wiley & Sons, New York, pp 195-208

Masson S, Pinel-Alloul B (1998) Spatial distribution of zooplancton biomass size fractions in a bog lake: abiotic and (or) biotic regulation? Can J Zool 76:805-823

Matsumara-Tundisi T, Tundisi JG, Saggio A, Oliveira Neto AL, Espindola EG (1989) Limnology of Samuel reservoir (Brazil, Rondônia) in the filling phase. Verh Internat Verein Limnol, 24: pp 1482-1488

Matthews CJD, Joyce EM, St.Louis VL, Schiff SL, Bodaly RA, Venkiteswaran JJ, Beaty KG (submitted) Carbon dioxide (CO_2) and methane (CH_4) production in small reservoirs flooding upland boreal forests. Ecosystems (under review)

Matthews CJD, St.Louis VL, Hesslein RH (2003) Comparison of three techniques used to measure diffusive gas exchange from sheltered aquatic surfaces. Environ Sci Tech 37:772-780

Matthews E (1997) Global litter production, pools, and turnover times: estimates from measurements data and regression models. J Geophys Res 102:18,771-18,800

Mattson KG, Swank WT (1989) Soil and detrital carbon dynamics following forest cutting in the Southern Appalachians. Biol Fert Soils 7:247-253

Matvienko B, Rosa LP, Sikar E, Santos MA, de Filippo R, Cimbleris ACP (2000) Gas release from a reservoir in the filling stage. Verh Internat Verein Limnol 27:1415-1419

Maystrenko YG, Denisova AI (1972) Method of forecasting the content of organic and biogenic substances in the water of existing and planned reservoirs. Sov Hydrol ,6:515-540

McColl JG, Pohlman AA (1986) Soluble organic acids and their chelating influence on Al and other metal dissolution from forest soils. Water Air Soil Poll 31:917-927

McColl JG, Pohlman AA, Jersak JM, Tam SC, Northup RR (1990) Organics and metal solubility in California forest soils. In: Gessel SP et al. (eds) Sustained productivity of forest soils. Proceedings of the 7th North American Forests and Soils Conference (Vancouver, 24-28 July 1990), University of British Columbia, Vancouver, pp.178-195

McColl RHS (1977) Chemistry of sediments in relation to trophic conditions of eight Rotorua lakes. NZ J Mar Freshwater Res 11:509-523

McCready MJ, Hanratty TJ (1984) A comparison of turbulent mass transfer at gas-liquid and solid-liquid interfaces. In: Brutsaert W, Jirka GH (eds), Gas transfer at water interfaces. D. Reidel, New York, pp 283-292

McDowell WH, Likens GE (1988) Origin, composition, and flux of dissolved organic carbon in the Hubbard Brook Valley. Ecol monog 58:177-195

McFarlane NA, Laprise R (1985) Parameterization of sub/grid-scale processes in the AES/CCC Spectral GCM. Report 85-12 CCRN 17, Canadian Climate Program

McGill WB, Cole CV (1981) Comparative aspects of cycling of organic C, N, S, and P through soil organic matter. Geoderma 26:267-286

McGillis WR, Edson JB, Hare JE, Fairall CW (2001) Direct covarience air-sea CO_2 fluxes. J Geophys Res 106 (C8):16729-16745

McKeague JA, Cheshire MV, Andreux F, Berthelin J (1986) Organo-mineral complexes in relation to pedogenesis In: Huang PM, Schnitzer M. Interactions of soil minerals with natural organics and microbes. (Special Publication No 17), Soil Science Society of America, Madison, Wisconsin

McLaren IA (1963) Effects of temperature on growth of zooplankton and the adaptative value of vertical migration. J Fish Res Board Can 20:685-727

McMahon PB, Dennehy KF (1999) N_2O emissions from a nitrogen-enriched river. Environ Sci Tech 33:21-25

Melack JM (1996) Recent developments in tropical limnology. Verh Internat Verein Limnol 26:211-217

Mellilo JM (1996) Carbon and nitrogen interactions in the terrestrial biosphere: Anthropogenic effects. In: Walker B, Steffen W (eds) Global change and terrestrial ecosystems. Cambridge University Press, Cambridge, pp 431-450

Melloh RA, Crill PM (1996) Winter methane dynamics in a temperate peatland. Glob Biogeochem Cycles 10 (2):247-254

Mengis M, Gachter R, Wehrli B (1997) Sources and sinks of nitrous oxide (N_2O) in deep lakes. Biogeochemistry 38:281-301

Méthot G, Pinel-Alloul B (1987) Fluctuations du zooplancton dans le réservoir LG-2 (Baie James, Québec): relation avec la qualité physico-chimique et trophique des eaux. Nat Can Rev Ecol Syst, 114:369-379

Meybeck M (1993) Riverine transport of atmospheric carbon: sources, global typology and budget. Water Air Soil Poll 70:443-463

Michalzik B, Kalbitz K, Park JH, Solinger S, Matzner E (2001) Fluxes and concentrations of dissolved organic carbon and nitrogen – a synthesis for temperate forest. Biogeochemistry 52:173-205

Michalzik B, Tipping E, Mulder J, Gallardo Lancho JF, Matzner E, Bryant CL, Clarke N, Lofts S, Vicente Esteban MA (2003) Modelling the production and transport of dissolved organic carbon in forest soils. Biogeochemistry 66:241-264

Middelburg JJ, Klaver G, Nieuwenhuize J, Wielemaker A, Haas W, Vlut T, Van der Nat FJWA (1996) Organic matter mineralization in intertidal sediments along an estuarine gradient. Mar Ecol Prog Ser 132:157-168

Middelburg JJ, Nieuwenhuize J, Iversen N, Høegh N, de Wilde H, Helder W, Seifert R, Christof O (2002) Methane distribution in tidal estuaries. Biogeochemistry 59:95-119

Miller SD, Goulden ML, Menton MC et al. (2004). Biometric and micrometeorological measurements of tropical forest carbon balance. Ecol Appl 14 (in press)

Miller WL (1999) An overview of aquatic photochemistry as it relates to microbial production. In: Bell CR, Brylinski M, Johnson-Green P (eds) Microbial biosystems: new Frontiers. Proceedings of the 8th International Symposium on Microbial Ecology. Atlantic Canada Society for Microbial Ecology, Halifax, Canada, 7 p.

Miller WL, Moran MA (1997) Interaction of photochemical and microbial processes in the degradation of refractory dissolved organic matter from a coastal marine environment. Limnol Oceanogr 42(6):1317-1324

Miller WL, Zepp RG (1995) Photochemical production of dissolved inorganic matter: Significance to the oceanic organic cycle. Geophys Res Lett 22:417-420

Minkkinen K (1999) Effect of forestry drainage on the carbon balance and radiative forcing of peatlands in Finland. Academic Dissertation, Faculty of Agriculture and Forestry, University of Helsinki

Molot LA, Dillon PJ (1997) Photolytic regulation of dissolved organic carbon in northern lakes. Glob Biogeochem Cycles 11(3):357-365

Monosowski E (1986) Brazil's Tucuruí dam: development at environmental cost. In: Goldsmith E and Hildyard N (eds)The Social and environmental effects of large dams. Vol. 2: Case studies, Wakebridge Ecological Centre, Cornwall,UK, pp. 191-198

Monson RK, Turnipseed AA, Sparks JP et al. (2002) Carbon sequestration in a high-elevation, subalpine forest. Glob Change Biol 8:1-20

Mooney HA, Vitousek PM, Matson PA (1987) Exchange of materials between terrestrial ecosystems and the atmosphere. Science 238:926-932

Moore TR (1989) Dynamics of dissolved organic carbon in forested and disturbed catchments (Westland, New Zealand) 1: Maimai. Water Resour Res 25:1321-1330

Moore TR (1998) Dissolved organic carbon: sources, sinks, and fluxes and role in the soil carbon cycle. In: Lal R, Kimble JM, Follett RF, Stewart BA (eds) Soil processes and the carbon cycle. CRC Press, Boca Raton, Florida (Advances in Soil Science), pp 281-292

Moore TR, Heyes A, Roulet NT (1994) Methane emissions from wetland, southern Hudson Bay lowland. J Geophys Res 99:1455-1467

Moore TR, Knowles R (1987) Methane and carbon dioxide evolution from subarctic fens. Can J Soil Sci 67:77-81

Moore TR, Knowles R (1990) Methane emissions from fen, bog and swamp peatlands in Quebec. Biogeochemistry 11:45-61

Moosavi SC, Crill PM (1996) Controls on methane flux from Alaskan boreal wetland. Glob Biogeochem Cycles 10(2):287-296

Mopper K, Stahovec WL (1986) Sources and sinks of low molecular weight organic carbonyl compounds in seawater. Mar Chem 19:305-321

Mopper K, Zhou X, Kieber RJ, Kieber DJ, Sikorski RJ, Jones RD (1991) Photochemical degradation of dissolved organic carbon and its impact on the oceanic carbon cycle. Nature 353:60-62

Mopper, K, Zhou X (1990) Photoproduction of hydroxy radicals at the sea surface an its potential impact on marine processes. In: Effects of solar ultraviolet radiation on biogeochemical dynamics in aquatic environments. Woods Hole Oceanographic Institution, Massachusetts. Rapport technique WHOI-90-09, pp 151-157

Moraes JL, Cerri CC, Mellilo JM, Kicklighter D, Neill C, Skole DL, Steudler PA (1995) Soil carbon stocks of the Brazilian Amazon basin. Soil Sci Soc Am J 59:244-247

Moran MA, Hodson RE (1990) Bacterial production on humic and nonhumic components of dissolved organic carbon. Limnol Oceanogr 35(8):1744-1756

Moran MA, Sheldon WM, Sheldon JE (1999) Biodegradation of riverine dissolved organic carbon in five estuaries of the southeastern United States. Estuaries 22(1):55-64

Moran MA, Sheldon WM, Zepp RG (2000) Carbon loss and optical property changes during long-term photochemical and biological degradation of estuarine dissolved organic matter. Limnol Oceanogr 45(6):1254-1264

Moran MA, Zepp RG (1997) Role of photoreactions in the formation of biologically labile compounds from dissolved organic matter. Limnol Oceanogr 42(6):1307-1316

Morel FMM, Price NM (1990) Indirect effects of UV radiation on phytoplankton. In: Effects of solar ultraviolet radiation on biogeochemical dynamics in aquatic environments. Woods Hole Oceanographic Institution, Massachusetts. Rapport technique WHOI-90-09, pp 110-112

Morris DP, Hargreaves BR (1997) The role of photochemical degradation of dissolved organic carbon in regulating the UV transparency of three lakes on the Pocono Plateau. Limnol Oceanogr 42(2):239-249

Morris DP, Zagarese H, Williamson CE, Balseiro EG, Hargreaves BR, Modenutti B, Moeller R, Queimalinos C (1995) The attenuation of solar UV radiation in lakes and the role of dissolved organic carbon. Limnol Oceanogr 40(8):1381-1391

Morris JT, Whiting GJ (1986) Emission of gaseous carbon dioxide from salt-marsh sediments and its relation to other carbon losses. Estuaries 9:9-19

Morrison KA, Thérien N (1991) Experimental evaluation of mercury release from flooded vegetation and soils. Water Air Soil Poll 56:607-619

Morrison KA, Thérien N (1992) Mercury release and transformation from flooded vegetation and soils: experimental evaluation and simulation modeling. In: Watras CJ, Huckabee JW (eds) Mercury pollution: integration and synthesis. Papers presented at the International Conference on Mercury as a Global Pollutant, June 1992, Monterey, California. Lewis Publishers, Boca Raton, Florida, pp 355-365

Morrison KA, Thérien N (1994) Mercury fluxes from inundated soils under controlled environmental conditions, International Conference on Mercury as a Global Pollutant, Whistler, British Columbia, July 10-14

Morrison KA, Thérien N (1995) Changes in mercury levels in Lake Whitefish (*Coregonus clupeaformis*) and Northern Pike (*Esox lucius*) in the LG-2 reservoir since flooding. Water Air Soil Poll 80:819-828

Morrison KA, Thérien N (1996) Release of organic carbon, Kjeldahl Nitrogen and total phosphorus from flooded vegetation. Water Qual Res J Can 31(2):305-318

Mosier AR (1990) Gas flux measurement techniques with special reference to techniques suitable for measurements over large ecologically uniform areas. In: Bouwman, AF (ed) Soils and the greenhouse effect. Wiley & Sons, Chichester, pp 289-301

Mousseau L, Gosselin M, Levasseur M, Demers S, Fauchot J, Roy S, Villegas PZ, Mostajir B (2000) Long-term effects of ultraviolet-B radiation on community structure and on simultaneous transport of carbon and nitrogen by estuarine phytoplankton during a mesocosm study. Mar Ecol Progr Series 199:69–81

Mudroch A, MacKnight SD (eds) (1994) CRC Handbook of techniques for aquatic sediments sampling, 2nd ed. CRC Press, Boca Raton

Mulder J, Clarke N (2000) EU project PROTOS: production and transport of organic solutes: effects of natural climatic variation. Final report. European Commission

Mulholland PJ, Wilson GV, Jardine PM (1990) Hydrogeochemical response of a forested watershed to storms: effects of preferential flow along shallow and deep pathways. Water Resour Res 26:3021-3036

Müller B, Buis K, Stierli R, Wehrli B (1998) Evaluation and application of PVC based liquid membrane ion-selective electrodes for high spatial resolution measurements in lake sediments. Limnol Oceanogr 43:1728-1733

Müller B, Märki M, Dinkel C, Stierli R, Wehrli B (2002) In situ measurements of lake sediments using ion-selective electrodes with a profiling lander system. In: Taillefret M, Rozan TF (eds) Environmental electrochemistry, analyses of trace element biogeochemistry. ACS Symposium Series 811, American Chemistry Society, Washington, DC, pp 126-143

Müller B, Märki M, Dinkel C, Stierli R, Wehrli B (2002) In situ measurements of lake sediments using ion-selective electrodes with a profiling lander system. In: Taillefert M, Rozan TF (eds) Environmental electrochemistry: Analysis of trace element biogeochemistry. (American Chemical Society Symposium Series 811) Washington DC, pp 126-143

Müller B, Wang Y, Dittrich M, Wehrli B (2003) Influence of organic carbon decomposition on calcite dissolution in surficial sediments of a freshwater lake. Water Res 37:4524-4532

Myneni RB, Dong J, Tucker CJ, et al. (2001) A large carbon sink in the woody biomass of Nothern forests. Proc Natl Acad Sci U S A 98:14784-14789

Nabuurs GJ, Mohren GMJ (1995) Carbon relations of Dutch forests. In: Zwerver S, Van Rompaey RSAR, Kok MTJ, Berk MM (eds) Climate change research: evaluation and policy implications: Proceedings of the international climate

change research conference, Maastricht, Netherlands, 6-9 December 1994 Elsevier, Amsterdam pp 553-556

Nabuurs GJ, Päivinen R, Sikkema R, Mohren GMJ (1997) The role of European forests in the global carbon cycle - a review. Biomass and Bioenergy 13:345-358

Naguib N, Adams DD (1996) Carbon gas (CH_4 and CO_2) cycling in sediments of the Tonteich, a northern German acid pond. In: Adams DD, Seitzinger SP, Crill PM (eds) Cycling of reduced gases in the hydrosphere. Mitt Internat Verein Limnol, Mitteilungen 25, E. Schweizerbart'sche Verlagsbuchhandlung (Nägele u. Obermiller), Stuttgart, pp 83-90

Naiman RJ (1982) Characteristics of sediment and organic carbon export from pristine boreal forest watersheds. Can J Fish Aquat Sci 39:1699-1718

Naiman RJ, Melillo JM, Lock MA, Ford TE, Reice SR (1987) Longitudinal patterns of ecosystem processes and community structure in a subarctic river rontinunm. Ecology 68:1139-1156

Naselli-Flores L, Barone R (1994) Relationship between trophic state and plankton community structure in 21 Sicilian dam reservoirs. Hydrobiologia 275-276

Naselli-Flores L, Barone R (1997) Importance of water-level fluctuation on population dynamics of cladocerans in a hypertrophic reservoir (Lake Arancio, south-west Sicily, Italy). Hydrobiologia 360:223-232

Nay SM, Mattson KG, Bornmann BT (1994) Biases of chamber methods for measuring soil CO_2 efflux demonstrated with a laboratory apparatus. Ecology 75:2460-2463

Neal C, House WA, Jarvie HP, Eatherall A (1998) The significance of dissolved carbon dioxide in major lowland rivers entering the North Sea. Sci Total Environ 210/211:187-203

Nelson BW, Kapos V, Adams JB, Oliveira WJ, Braun PG, Amaral IL (1994) Forest disturbance by large blowdowns in the Brazilian Amazon. Ecology 75(3):853-858

Nelson BW, Mesquita R, Pereira JLG, Souza SGA, Batista GT, Couto LB (1999) Allometric regressions for improved estimate of secondary forest biomass in the central Amazon. For Ecol Manage 117:149-167

Neumann HH, Den Hartog G, King KM, Chipanshi AC (1994) Carbon dioxide fluxes over a raised open bog at the Kinosheo Lake tower site during the Northern Wetlands Study (NOWES). J Geophys Res 99(D1):1529-1538

Nienhuis PH (1992) Eutrophication, water management, and the functioning of Dutch estuaries and coastal lagoons. Estuaries 15:538-548

Nilsson LO (1995) Forest biogeochemistry interactions among greenhouse gases and N deposition. Water Air Soil Poll 85(3):1557-1562

Nilsson S, Shvidenko A, Stolbovoi V, Gluck M, Jonas M, Obersteiner M (2000) Full carbon account for Russia. Interim report IR-00-016, International Institute for Applied Systems Analysis, Laxenburg, Austria. [URL:] http://www.iiasa.ac.at/Publications/Catalog/PUB_AUTHOR_Nilsson,S..html

Nishio T, Koike I, Hattori A (1981) N_2/Ar and denitrification in Tama estuary sediments. Geomicrobiol J 2:193-206

Nogueira MG (2001) Zooplankton composition, dominance and abundance as indicators of environmental compartmentalization in Jurumirim reservoir (Paranapanema River), Sao Paulo, Brazil. Hydrobiologia 455:1-18

Nogueira MG, Henry R, Maricatto FE (1999) Spatial and temporal heterogeneity in the Jurumirim Reservoir, Sao Paulo, Brazil Lakes Reservoirs. Res Manage 4:107-120

Nougier JP (1987) Méthodes de calcul numérique. Masson, Paris

Nykänen H, Alm J, Lang K, Silvola J, Martikainen PJ (1995) Emissions of CH_4, N_2O and CO_2 from a virgin fen and a fen drained for grassland in Finland. J Biogeogr 22:351-358

Nykänen H, Alm J, Silvola J, Tolonen K, Martikainen PJ (1998) Methane fluxes on boreal peatlands of different fertility and the effect of long-term experimental lowering of the water table on flux rates. Glob Biogeochem Cycles 12:53-69

Nykänen H, Silvola J, Alm J, Martikainen PJ (1996) The effect of peatland forestry on fluxes of carbon dioxide, methane and nitrous oxide. In: Trettin CC, Jurgensen MF, Grigal DF, Gale MR, Jeglum J (eds) Northern forested wetlands: ecology and management. CRC Press, Boca Raton, pp 331-345

Obernosterer I, Reitner B, Herndl GJ (1999) Contrasting effects of solar radiation on dissolved organic matter and its bioavailability to marine bacterioplankton. Limnol Oceanogr 44(7):1645-1654

O'Connor DJ, Dobbins WE (1958) Mechanism of reaeration in natural streams. Trans Am Soc Civ Eng 123:641-684

Oechel WC, Hastings SJ, Vourlitis G, Jenkins M, Riechers G, Grulke N (1993) Recent change of Arctic tundra ecosystems from a net carbon dioxide sink to a source. Nature 361:520-523

Oke TR (1978) Boundary layer climates. Methuen, London

Olson JS, Watts JA, Allison LJ (1983) Carbon in live vegetation of major world ecosystems. Rep. DOE/NBB-0037, US Department of Energy, Office of Energy Research, Carbon Dioxide Research Division, Washington, DC

Olson JS, Watts JA, Allison LJ (1985) Major world ecosystem complexes ranked by carbon in live vegetation: a database. Rep. DOE/NDP-017, Environmental Science Division, Oak Ridge National Laboratory, Oak Ridge, TN

Opsahl S, Benner R (1997) Distribution and cycling of terrigenous dissolved organic matter in the oceans. Nature 386:480-482

Opsahl S, Benner R (1998) Photochemical reactivity of dissolved lignin in river and ocean waters. Limnol Oceanogr 43(6):1297-1304

Ostrofsky ML (1978) Trophic changes in reservoirs: an hypothesis using phosphorus budget models. Int Rev Gesamten Hydrobiol 63:481-499

Pacala SW, Hurtt GC, Baker D et al. (2001) Consistent land- and atmosphere-based U.S. carbon sink estimates. Science 292:2316-2320

Pace ML, Cole JJ (2002) Synchronous variation of dissolved organic carbon and color in lakes. Limnol Oceanogr 47(2):333-342

Paiva MP (1977) The environmental impact of man-made lakes in the Amazonian region of Brazil. Rapport Electrobras Rio de Janeiro

Palenik B, Price NM, Morel FMM (1991) Potential effects of UV-B on the chemical environment of marine organisms: a review. Environ Pollut 70:117-130

Panikov NS, Zelenev V (1991) Methane and carbon dioxide production and uptake in some boreal ecosystems of Russia. In: Vinson TS, Kolchugina TP (eds) Carbon cycling in boreal forests and subarctic ecosystems. EPA Report EPA/600R-93/084, Office of Research and Development, Washington, pp 125-138

Panikov NS, Dedysh SN (2000) Cold season CH_4 and CO_2 emission from boreal peat bogs (West Siberia): Winter fluxes and thaw activation dynamics. Glob Biogeochem Cycles 14:1071-1080

Panikov NS, Sizova MV, Zelenev VV, Makhov GA, Naumov AV, Gadzhiev IM (1995) Methane and carbon dioxide emission from several Vasyugan wetlands: Spatial and temporal flux variations. Ecol Chem 4:12-23

Papale D, Valentini R (2003) A new assessment of European forests carbon exchanges by eddy fluxes and artificial neural network spatialization. Glob Change Biol 9:525-535

Pape T, van Breemen N, van Oeveren H (1989) Calcium cycling in an oak-birch woodland on soils of varying $CaCO_3$ content. Plant and Soil 120:253-261

Park JH, Matzner E (2003) Controls on the release of dissolved organic carbon and nitrogen from a deciduous forest floor investigated by manipulations of aboveground litter inputs and water flux. Biogeochemistry 66:265-286

Park PK, Hager SW, Cissel MC (1969) Carbon dioxide partial pressure in the Columbia River. Science 166:867-868

Paterson MJ, Findlay D, Beaty K, Findlay W, Schindler EU, Stainton M, McCullogh G (1997) Changes in the planktonic food web of a new experimental reservoir. Can J Fish Aquat Sci 54:1088-1102

Patoine A, Pinel-Alloul B, Prepas EE, Carignan R (2000) Do logging and forest fires influence zooplankton biomass in Canadian boreal shield lakes? Can J Fish Aquat Sci 57(suppl 2):155-164

Patten BC (1971) Systems Analysis and Simulation in Ecology. Academic Press, New York

Patterson JC, Hamblin PF (1988) Thermal simulation of a lake with winter ice cover. Limnol Oceanogr 3(33):323-338

Paul N, Callaghan TV, Moody S, Gwynn-Jones D, Johanson U, Gehrke C (1999) UV-B impacts on decomposition and biogeochemical cycling. In: Rozema J (ed) Stratospheric ozone depletion: the effects of enhanced UV-B radiation on terrestrial ecosystems. Backhuys Publishers, Leiden, pp 101-114

Payette S (1992) Fires as a controlling process in the North American boreal forest. In: Shugart HH, Leemans R, Bonan GB (eds) A systems analysis of the global boreal forest. Cambridge University Press, New York, pp 144-169

Payette S, Rochefort L (2001) Écologie des tourbières du Québec-Labrador. Presses de l'Université Laval, Sainte-Foy

Pearman GI, Hyson P (1981) A global atmospheric diffusion simulation model for atmospheric carbon studies. In: Bolin B (ed), Carbon cycle modelling. Wiley & Sons, New York, pp 227-240

Peixoto JP, Oort AH (1992) Physics of climate. American Institute of Physics, New York

Peltzer ET, Hayward NA (1996) Spatial and temporal variability of total organic carbon along 140°W in the equatorial Pacific Ocean in 1992. Deep-Sea Res II 43:1155-1180

Pereira A (1989) Étude des données limnologiques de la retenue de Tucurui, Amazonie, Brésil. Rapport de stage DEA, Technique et Gestion de l'Environnement

Pereira A (1994) Contribution à l'étude de la qualité des eaux des retenues amazoniennes: application de la modélisation mathématique à la retenue de Tucuruí (Brésil). Thèse de 3ème Cycle, Ecole Nationale des Ponts et Chaussées

Perez S (1989) Procédés de boues activées sous des conditions limitantes en oxygène dissous. Mémoire, Université de Sherbrooke, Sherbrooke

Perillo GME (1995) Geomorphology and sedimentology of estuaries. (Developments in Sedimentology 53), Elsevier, Amsterdam

Pettersson C, Rahm L, Allard B, Borén H (1997) Photodegradation of aquatic humic substances: an important factor for the Baltic carbon cycle? Boreal Environ Res 2:209-215

Pfeiffer EM (1994) Methane fluxes in natural wetlands (marsh and moor) in northern Germany. Current Topics in Wetland Biogeochemistry 1:36-47

Phillips OL, Malhi Y, Higuchi N et al. (1998) Changes in the carbon balance of tropical forests: evidence from long-term plots. Science 282:439-442

Pilegaard K, Hummelshøj P, Jensen NO, Chen Z (2001) Two years of continuous CO_2 eddy-flux measurements over a Danish beech forest. Agric Forest Meteorol 107:29-41

Pinel-Alloul B, Méthot G (1979) Étude du zooplancton du réseau de surveillance écologique du complexe La Grande, Territoire de la Baie James : analyse des données (1977-1978) Rapport de recherche, Université de Montréal, CREM

Pinel-Alloul B, Méthot G (1984) Étude préliminaire des effets de la mise en eau du réservoir de LG-2 (Territoire de la Baie James, Québec) sur le seston grossier et le zooplancton des rivières et des lacs inondés. Int Revue Ges Hydrobiol 69:57-78

Pinel-Alloul B, Méthot G (1984) Preliminary study of the effects of impoundment of LG-2 reservoir (James Bay Territory, Quebec, Canada) on the net seston and zooplankton of impounded rivers and lakes. Int Revue Ges Hydrobiol 69:57-78

Pivovarov AA (1973) Thermal conditions in freezing lakes and rivers. Wiley & Sons, New York

Planas D, Desrosiers M, Groulx SR, Paquet S, Carignan R (2000) Pelagic and benthic algal responses in eastern Canadian Boreal Shield lakes following harvesting and wildfires. Can J Fish Aquat Sci 57:136-145

Planas D, Paquet S, St-Pierre A (2004) Production-consumption of CO_2 in reservoirs and lakes in relation to plankton metabolism. In:Tremblay A, Varfalvy L, Roehm C, Garneau M (eds) Greenhouse gases emissions from

natural environments and hydroelectric reservoirs: fluxes and processes, Springer-Verlag. (in press)
Pohlman AA, McColl JG (1988) Soluble organics from forest litter and their role in metal dissolution. Soil Sci Soc Am J 52:265-271
Post WM, Emanuel WR, Zinke PJ, Stangenberger AG (1982) Soil carbon pools and world life zones. Nature 298:156-159
Post WM, Izaurralde RC, Mann LK, Bliss N (1999) Monitoring and verifying soil organic carbon sequestration. In: Rosenberg NJ, Izaurralde RC, Malone EL (eds) Carbon sequestration in soils: science, monitoring and beyond. Proceedings of the St. Michaels Workshop, December 1998, Battelle Press, Columbus, pp 67-82
Poulin-Thériault, Gauthier & Guillemette Consultants inc. (1992) Caractérisation préliminaire de la phytomasse inondée des futurs complexes hydroélectriques. Rapport présenté à la vice-présidence Environnement, Hydro-Québec
Poulin-Thériault, Gauthier & Guillemette Consultants inc. (1993) Méthode de caractérisation de la phytomasse appliquée aux complexes Grande-Baleine et La Grande. Rapport présenté à la vice-présidence Environnement, Hydro-Québec
Pourriot R, Meybeck M (1995) Limnologie générale. (Collection d'écologie 25), Masson, Paris
Powell DS, Faulkner JL, Darr DR, Zhu Z, MacCleery DW (1993) Forest resources of the United States (1992) USDA Forest Service, Rocky Mountain Forest and Range Experiment Station General Technical Report, RM-234
Prairie YT, Bird DF, Cole JJ (2002) The summer metabolic balance in the epilimnion of southeastern Quebec lakes. Limnol Oceanogr 47:316-321
Preston CM, Schnitzer M, Ripmeester JA (1989) A spectroscopic and chemical investigation on the de-ashing of a humin. Soil Sci Soc Am J 53:1442-1447
Prieme A (1994) Production and emission of methane in a brackish and a freshwater wetland. Soil Biol Biochem 26(1):7-18
Pulliam WM (1993) Carbon dioxide and methane exports from a southeastern floodplain swamp. Ecol Monogr 63:29-54
Pumpanen J, Ilvesniemi H, Hari P (2003) A process-based model for predicting soil carbon dioxide efflux and concentration. Soil Sci Soc Am J 67:420-413
Qualls RG, Haines BL (1991) Geochemistry of dissolved organic nutrients in water percolating through a forest ecosystems. Soil Sci Soc Am J 55:1112-1123
Qualls RG, Haines BL, Swank WT, Tyler SW (2000) Soluble organic and inorganic nutrient fluxes in clearcut and mature deciduous forests. Soil Sci Soc Am J 61:1068-1077
Qualls RG, Haines BL, Swank WT, Tyler SW (2002) Retention of soluble organic nutrients by a forested ecosystem. Biogeochemistry 61:135-171
Quay PD, Emerson SR, Quay BM, Devol AH (1986) The carbon cycle for Lake Washington: a stable isotope study. Limnol Oceanogr 31:596-611
Quay PD, Stutsman J, Wilbur D, Snover A, Dlugokencky E, Brown T (1999). Isotopic composition of atmospheric methane. Glob Biogeochem Cycles 13:445-461

Ragotzkie RA (1978) Lakes: chemistry, geology, and physics. A Lerman Editions, New York

Raich JW, Schlesinger WH (1992) The global carbon dioxide flux in soil respiration and its relationship to vegetation and climate. Tellus 44B:81-99

Randerson JT, Chapin FS, Harden J, Neff JC, Harmon M (2002) Net ecosystem production: a comprehensive measure of net carbon accumulation by ecosystems. Ecol Appl 12(4):937-947

Rapalee G, Trumbore SE, Davidson EA, Harden JW, Veldhuis H (1998) Soil carbon stocks and their rates of accumulation and loss in a boreal forest landscape. Glob Biogeochem Cycles 12:687-701

Rask H, Schoenau J, Anderson D (2002) Factors influencing methane flux from a boreal forest wetland in Saskatchewan, Canada. Soil Biol Biochem 34(4):435-443

Rasmussen JB, Godbout L, Schallenberg M (1989) The humic content of lake water and its relationship to watershed and lake morphometry. Limnol Oceanogr 34:1336-1343

Ravindranath NH, Somashekhar BS, Gadgil M, Deying X (1992) Carbon emissions and sequestration in forests: case studies from seven developing countries, vol 3: India and China. Lawrence Berkeley Laboratory, Berkeley, LBL Report No. 32759 UC-402

Rawson HM (1992) Plant responses to temperature under conditions of elevated CO_2. Aust J Plant Physiol 40:473-490

Raymo ME (1994) The Himalayas, organic carbon burial, and climate in the Miocene. Paleoceanography 9:399-404

Raymond PA, Bauer J, Cole JJ (2000) Atmospheric CO_2 evasion, dissolved inorganic carbon production and net heterotrophy in the York River estuary. Limnol Oceanogr 45:1707-1717

Raymond PA, Bauer JE (2001) Riverine export of aged terrestrial organic matter to the North Atlantic Ocean. Nature 409:497-500

Raymond PA, Caraco NF, Cole JJ (1997) Carbon dioxide concentration and atmospheric flux in the Hudson river. Estuaries 20:381-390

Raymond PA, Cole JJ (2001) Gas exchange in rivers and estuaries: choosing a gas transfer velocity. Estuaries 24:312-317

Reche I, Pace ML, Cole JJ (1999) Relationship of trophic and chemical conditions to photobleaching of dissolved organic matter in lake ecosystems. Biogeochemistry 44:259-280

Reeburgh WS, Alperin MJ (1988) Studies on methane oxidation. SCOPE/UNEP – Mitt Geol Palaeont Inst, Univ Hamburg Sonderband 66:367-375

Regina K, Nykänen H, Silvola J, Martikainen PJ (1996) Fluxes of nitrous oxide from boreal peatlands as affected by peatland type, water table level and nitrification capacity. Biogeochemistry 35:401-418

Reid PC, Lancelot C, Gieskes WWC, Hagmeier E, Weichart G (1990) Phytoplankton of the North Sea and its dynamics: a review. Neth J Sea Res 26: 295-331

Reiners WA, Keller M, Gerow KG (1998) Estimating rainy season nitrous oxide and methane fluxes across forest and pasture landscapes in Costa Rica. Water Air Soil Poll 105(1-2):117-130

Rice AH, Pyle EH, Saleska SR et al. (2004) Carbon balance and vegetation dynamics in an old-growth Amazonian forest. Ecol Appl (in press)

Richard S (1996) La mise en eau du barrage de Petit Saut. Hydrochimie 1- du fleuve Sinnamary avant la mise en eau, 2- de la retenue pendant la mise en eau, 3- du fleuve en aval. Thèse de l'Université Aix-Marseille

Richard S (2001a) Complementary environmental study of the Nam Theun 2 hydropower scheme (RDP Laos). Water quality in the Nam Theun, the Nam Kathang, the Xé Bangfaï, and the Nam Leuk at the end of the rainy season Hydreco, Petit Saut, French Guyana

Richard S (2001b) Physico-chemical water quality in the hydroelectric reservoir of Petit Saut (French Guiana) and downstream. International Workshop on hydroelectric reservoirs and greenhouses gas emissions, Rio de Janeiro, Brazil

Richard S (2002) NT2 Hydropower project-Lao PDR: the dissolved oxygen consumption kinetics in the water turbined by the Nam Leuk power plant. Report Hydreco/EDF

Richard S, Arnoux A, Cerdan P (1997) Évolution de la qualité physico-chimique des eaux de la retenue et du tronçon aval depuis le début de la mise en eau du barrage de Petit-Saut. Hydroécol Appl 9(1-2):57-83

Richard S, Galy-Lacaux C, Arnoux A, Cerdan P, Delmas R, Dumestre JF, Gosse P, Labroue L, Sissakian C, Horeau V (2000) Evolution of physico-chemical water quality and methane emissions in the tropical hydroelectric reservoir of Petit Saut (French Guiana). Verh Internat Verein Limnol 27:1454-1458

Richard S, Grégoire A, Gosse P (2003) Efficacité d'un seuil artificiel sur l'oxygénation de l'eau et l'élimination de CH_4 contenu dans l'eau évacuée par le barrage hydroélectrique de Petit Saut (Guyane française). Conférence internationale des limnologues d'expression française (CILEF-2003) (du 27 juillet au 1er août 2003) Montréal, Canada

Richard S, Horeau V, Cerdan P (2000) Bilan des événements hydrologiques d'avril à juin 2000 sur la qualité des eaux de la retenue de Petit Saut et de la rivière à l'aval. Rapport Hydreco/EDF-CD Guyane

Richard S, Zouiten C (2001) Complementary environmental study of the Nam Theun 2 hydropower development project (RDP Laos): surface water and soil quality (August 2001). Hydreco/EDF

Richey JE, Devol AH, Wofsy SC, Victoria RL, Riberio MNG (1988) Biogenic gases and the oxidation and reduction of carbon in Amazon River and floodplain waters. Limnol Oceanogr 33:551-561

Richey JE, Hedges JI, Devol AH, Quay PD, Victoria RL, Martinelli LA, Forsberg BR (1990) Biogeochemistry of carbon in the Amazon River. Limnol Oceanogr 35:352-371

Richey JE, Melack JM, Aufdenkampe AK, Ballester VM, Hess LL (2002) Outgassing from Amazonian rivers and wetlands as a large tropical source of atmospheric CO_2. Nature 416:617-620

Richter DD, Markewitz D, Trumbone SE, Wells CG (1999) Rapid turnover of soil carbon in a re-establishing forest. Nature 400:56-58

Richter DD, Markewitz D, Wells CG et al.(1995) Carbon cycling in a Loblolly Pine forest: implications for the missing carbon sink and for the concept of soil. In: McFee WW, Kelly JM (eds) Carbon forms and functions in forest soils. Soil Science Society of America, Madison, Wisconsin

Riera JL, Schindler JE, Kratz TK (1999) Seasonal dynamics of carbon dioxide and methane in two clear-water lakes and two bog lakes in northern Wisconsin, U.S.A. Can J Fish Aquat Sci 56:265-274

Rio Workshop (2001) Rio GHG working group report. Matvienko B, Varfalvy L, Rosa LP, dos Santos MA, Delmas R (eds) Rio de Janeiro

Rochette P, Gregorich EG, Desjardins RL (1992) Comparison of static and dynamic closed chambers for measurement of soil respiration under field conditions. Can J Soil Sci 72:605-609

Roehm CL, Roulet NT (2003) Seasonal contribution of CO_2 fluxes in the annual C budget of a northern bog. Glob Biogeochem Cycles 17:1029, doi10.1029/2002.GB0001889

Rosa LP, Aurélio dos Santos M, Matvienko B, Sikar E (2002) Hydroelectric reservoirs and global warming. RIO 02 - World Climate and Energy Event, 6-11 Janvier 2002

Rosa LP, Dos Santos MA (1998) Dams and Climate Change. Proceedings of International Workshop on Hydrodams, Lakes and Greenhouse Gas Emissions (December 4-5), Rio de Janeiro

Rosa LP, dos Santos MA (2000) Certainty and uncertainty in the science of greenhouse gas emissions from hydroelectric reservoirs. A report on the state of the art for the World Commission on Dams. Final report, Alberto Luiz Coimbra Institute of Graduate Studies and Research in Engineering. Federal University of Rio de Janeiro (Coppe/UFRJ)

Rosa LP, dos Santos MA, Matvienko B, Matvienko E, Lourenço RSM, Menezes CF (2003) Biogenic gas production from major amazon reservoirs, Brazil. Hydrol Proces 17:1443-1450

Rosa LP, Matvienko B, Santos MA, Montero JPL, Sikar E, Silva MB, Santos EO (2001) Emissões de gases de efeito estufa derivados de reservatórios hidrelétricos – monitoramento e treinamento de técnicos do setor elétrico brasileiro. Projeto PPE 1486 – ANEEL/MCT/PNUD, Report, December 2001

Rosa LP, Matvienko B, Santos MA, Sikar E (2002) Carbon dioxide and methane emissions from brazilian power dams**.** Project BRA/95/G31, PNUD/ELETROBRÁS/MCT, Background Reports

Rosa LP, Schaeffer R (1994) Greenhouse gas emissions from hydroelectric reservoirs: Comment on the synopsis by Rudd et al. (Are hydroelectric reservoirs significant sources of greenhouse gases? Ambio 22(4) 1993). Ambio 23(2):164-165

Rosa LP, Schaeffer R (1995) Global warming potentials: the case of emissions from dams. Ener Pol 23(2):149-158

Rosa LP, Sikar BM, Dos Santos MA, Dos Santos EO, Sikar EM (2002b) Dam reservoirs and greenhouse gas emissions in Brazil. In: International

Symposium on Reservoir Management in Tropical and Sub-Tropical Regions, Sept. 26, 2002, Iguassu, Brazil. ICOLD 70th Annual Meeting. Volume 1, pp 439-449

Rosa LP, Sikar BM, Dos Santos MA, Sikar EM, Eletrobras C (2002a) First brazilian inventory of anthropogenic greenhouse gas emissions. Background reports: carbon dioxide and methane emissions from brazilian hydroelectric reservoirs. Ministry of Science and Technology, Brasilia

Rosenberg DM (2000) Global-scale environmental effects of hydrological alterations. BioScience 50

Rosenberg DM, Berkes F, Bodaly RA, Hecky RE, Kelly CA, Rudd JWM (1997) Large-scale impacts of hydroelectric development. Environ Rev 5:27-54

Rothfuss F, Conrad R (1998) Effect of gas bubbles on the diffusive flux of methane in anoxic paddy soils. Limnol Oceanogr 43:1511-1518

Rothfuss F, Frenzel P, Conrad R (1994) Gas diffusion probe for measurements of CH_4 gradients. In: Stal LJ, Caumette P (eds) Microbial mats: structure, development and environmental significance. Springer-Verlag, Berlin, pp. 167-172

Roulet NT, Ash R, Moore TR (1992) Low boreal wetlands as a source of atmospheric methane. J Geophys Res 97(D4):3739-3749

Roulet NT, Jano A, Kelly CA et al. (1994) Role of the Hudson Bay lowland as a source of atmospheric methane. J Geophys Res 99(D1):1439-1454

Roulet NT, Moore TR (1995) The effect of forestry drainage practices on the emission of methane from northern peatlands. Can J For Res 25(3):491-499

Roy D, Boudreault J, Boucher R, Schetagne R, Thérien N (1986) Réseau de surveillance écologique du Complexe La Grande 1978-1984: Synthèse des observations. SEBJ, Direction Ingénierie et Environnement

Roy J, Saugier B, Mooney H (2001) Terrestrial global productivity: past, present and future, Academic Press, San Diego

Rudd JWM, Hamilton RD (1978) Methane cycling in a eutrophic shield lake and its effects on whole lake metabolism. Limnol Oceanogr 23:337-348

Rudd JWM, Harris R, Kelly CA, Hecky RE (1993) Are hydroelectric reservoirs signifiant sources of greenhouse gases? Ambio 22:246-248

Runeckles VC, Krupa SV (1994) The impact of UV-B radiation and ozone on terrestrial vegetation. Environ Pollut 83:191-213

Rusch H, Rennenberg H (1998) Black alder (*Alnus glutinosa* L.) trees mediate methane and nitrous oxide emission from the soil to the atmosphere. Plant and Soil 201:1-7

Ryan MG, Hubbard RM, Pongracic S, Raison RJ, McMurtrie RE (1996) Foliage, fine-root, woody-tissue and stand respiration in *Pinus radiata* in relation to nitrogen status. Tree Physiol 16:333-343

Saarnio S, Alm J, Silvola J, Lohila A, Nykänen H, Martikainen PJ (1997) Seasonal variation in CH_4 emission and production and oxidation potentials at microsites on an oligotrophic pine fen. Oecologia 110:414-422

Saigusa N, Yamamoto S, Murayama S, Kondo H, Nishimura N (2002) Gross primary production and net ecosystem exchange of a cool-temperate

deciduous forest estimated by the eddy covariance method. Agric Forest Meteorol 112:203-215
Saleska SR, Miller SD, Matross DM et al. (in review) Carbon fluxes in old-growth Amazonian rainforests: unexpected seasonality and disturbance-induced net carbon loss
Salonen K, Vahatalo A (1994) Photochemical mineralization of dissolved organic matter in lake Skjervatjen. Environ Int 20:307-312
San Jose JJ, Montes RA, Fariñas MR (1998) Carbon stocks and fluxes in a temporal scaling from a savannah to a semi-deciduous forest. For Ecol Manage 105:251-262
Sanderman J, Amundson RG, Baldocchi DD (2003) Application of Eddy covariance measurements to the temperature dependence of soil organic matter mean residence time. Glob Biogeochem Cycles 17:1061
Sanders RW, Wickham SA (1993) Planktonic protozoa and metazoa: predation, food quality and population control. Marine Microbial Food Webs 7:197-223
Sansone FJ, Holmes ME, Popp BN (1999) Methane stable isotopic ratios and concentrations as indicators of methane dynamics in estuaries. Glob Biogeochem Cycles 13:463-474
Sansone FJ, Rust TM, Smith SV (1998) Methane distribution and cycling in Tomales Bay, California. Estuaries 21:66-77
Sarma VVSS, Kumar MD, Manerikar (2001) Emission of carbon dioxide from a tropical estuarine system, Goa, India. Geophys Res Lett 28:1239-1242
Sartory DP, Groββelaar JE (1984) Extraction of chlorophyll a from freshwater phytoplankton for spectrophotometric analysis. Hydrobiologia 114:177-187
Savage K, Moore TR, Crill PM (1997) Methane and carbon dioxide exchange between the atmosphere and northern boreal forest soils. J Geophys Res 102(D24):29279-29288
Scharpenseel WH, Tamers MA, Pietig F (1968) Altersbesttimmung von Böden durch die Radiokohlenstoffdatierungsmethode. Zeitschrift für Pflanzenernährung und Bodenkunde 119:34-52
Schellhase HU, MacIssac EA, Smith H (1997) Carbon budget estimates for reservoirs on the Columbia River in British Columbia. The Environmental Professional 19:48-57
Schetagne R (1989) Qualité de l'eau, régions de La Grande 2 et Opinaca: Interprétation des données de 1988. Réseau de suivi environnemental du Complexe La Grande, phase 1. Vice-présidence Environnement, Hydro-Québec, Montréal
Schetagne R (1994) Water quality modifications after impundment of some large northern reservoirs. Archiv Hydrobiol Adv Limnol 40:223-229
Schetagne R, Roy D (1985) Réseau de surveillance écologique du complexe LaGrande, 1977-1984.: Physico-chimie et pigments chlorophylliens. Rapport de recherche de la société d'Énergie de la Baie James, Montréal
Schiff HI, Mackay GI, Bechara J (1994) The use of tunable diode laser absorption spectroscopy for atmospheric measurements. In: Sigrist MW (ed) Air monitoring by spectroscopic techniques. Wiley & Sons, New York, pp.304-305

Schiff SL, Venkiteswaran J, Boudreau N, St.Louis VL et al. (2001) Processes affecting greenhouse gas production in flooded reservoirs: insights from carbon and oxygen isotope. Presented at the 4th International symposium on applied isotope geochemistry (AIG-4) held at the Asilomar Conference Center in Pacific Grove, California, June 21-25, 2001

Schiller CL, Hastie DR (1996) Nitrous oxide and methane fluxes from perturbed and unperturbed boreal forest sites in northern Ontario. J Geophys Res 101(D17):22767-22774

Schimel DS, Braswell BH, Holland EA, McKeown R et al. (1994) Climatic, edaphic and biotic controls over storage and turnover of carbon in soils. Glob Biogeochem Cycles 8:279-293

Schimel DS, House JI, Hibbard KA, Bousquet P et al (2001) Recent patterns and mechanisms of carbon exchange by terrestrial ecosystems. Nature 414:169-172

Schimel DS, Kittel TGF, Knapp AK, Seastedt TR, Parton WJ, Brown VB (1991b) Physiological interactions along resource gradients in a tallgrass prairie. Ecology 72:672-684

Schimel DS, Kittel TGF, Parton WJ (1991a) Terrestrial biogeochemical cycles: global interactions with the atmosphere and hydrology. Tellus, Special issue AB 43:188-203

Schimel DS, Melillo J, Tian H et al. (2000) Contribution of increasing CO_2 and climate to carbon storage by ecosystems in the United States. Science 287:2004-2006

Schimel JP, Firestone MK (1989) Nitrogen incorporation and flow through a - coniferous forest soil profile. Soil Sci Soc Am J 53:779-784

Schindler DE, Carpenter SR, Cole JJ, Kitchell JF, Pace ML (1997) Influence of food web structure on carbon exchange between lakes and the atmosphere. Science 277:248-251

Schindler DW, Brunskill GJ, Emerson S, Broecker WS, Peng TH (1972) Atmospheric carbon dioxide: its role in maintaining phytoplankton standing crops. Science 177:1192-1194

Schindler DW, Curtis PJ, Bayley SE, Parker BR, Beaty KG, Stainton MP (1997b) Climate-induced changes in the dissolved organic carbon budgets of boreal lakes. Biogeochemistry 36:9-28

Schindler DW, Curtis PJ, Parker BR, Stainton MP (1996) Consequences of climate warming and lake acidification for UV-B penetration in North American boreal lakes. Nature 379:705-708

Schindler DW, Fee EJ (1973) Diurnal variation of dissolved organic carbon and its use in estimating primary production. J Fish Res Board Can 30:1501-1510

Schlesinger WH (1977) Carbon balance in terrestrial detritus. Ann Rev Ecol Syst 8:51-81

Schlesinger WH (1984) Soil organic matter: a source of atmospheric CO_2. In: Woodwell GM (ed) The role of terrestrial vegetation in the global carbon cycle. SCOPE 23, Wiley & Sons, New York, pp 111-127

Schlesinger WH (1990) Evidence from chronosequence studies for a low carbon storage potential of soils. Nature 348:232-234

Schlesinger WH (1997) Biogeochemistry: an analysis of global change. 2nd ed Academic Press, San Diego, California
Schluten HR, Schnitzer M (1993) A state to the art structural concept for humic substances. Naturwissenschaften 80:2-30
Schmid HP, Cropley F, Su HB, Offerle B, Grimmond CSB (2000) Measurements of CO_2 and energy fluxes over a mixed hardwood forest in the Midwestern United States. Agric Forest Meteorol 103(4):357-374
Schmidt U, Conrad R (1993) Hydrogen, carbon monoxide, and methane dynamics in lake Constance. Limnol Oceanogr 38(6):1214-1226
Schnitzer M (1991) Soil organic matter: the next 75 years. Soil Sci 151:41-58
Schnitzer M (2000) A lifetime perspective. Adv Agron 68:1-58
Schnitzer M, Khan SU (1978) Soil organic matter. Elsevier, Amsterdam
Schroeder PE, Winjum JK (1995) Assessing Brazil's carbon budget: I. Biotic carbon pools. For Ecol Manage 75:77-86
Schulze ED, Heimann H (1998) Carbon and water exchange of terrestrial systems. In: Galloway JN, Melillo J (eds) Asian Change in the context of global change. (IGBP-Series, vol 3), Cambridge University Press, Cambridge, pp 145-161
Schulze ED, Wirth C, Heimann M (2000) Climate change: Managing forests after Kyoto. Science 289:2058-2:059
Schütz H, Seiler W (1989) Methane flux measurements: methods and results. In: Andreae MO, Schimel DS (eds) Exchange of trace gases between terrestrial ecosystems and the atmosphere. Wiley & Sons, New York, pp 209-228
Scott KJ, Kelly CA, Rudd JWM (1999) The importance of floating peat to methane fluxes from flooded peatlands. Biogeochemistry 47:187-202
Scranton MI, McShane K (1991) Methane fluxes in the southern North Sea: the role of European rivers. Cont Shelf Res 11:37-52
Scully NM, McQueen DJ, Lean DSR, Cooper WT (1996) Hydrogen peroxide formation: the interaction of ultraviolet radiation and dissolved organic carbon in lake waters along a 43-75°N gradient. Limnol Oceanogr 41(3):540-548
Seiler W, Conrad R (1987) Contribution of tropical ecosystems to the global budgets of trace gases, especially CH_4, H_2, CO, and N_2O. In: Dickinson RE (ed) Geophysiology of Amazonia: vegetation and climate interactions. Wiley & Sons, New York, pp 133-160
Seiler W, Conrad R, Scharffe D (1984) Field studies of methane emission from termite nests into the atmosphere and measurement of methane uptake by tropical soils. J Atmos Chem 1:171-186
Sellers P, Hesslein RH, Kelly CA (1995) Continuous measurement of CO_2 for estimation of air-water fluxes in lakes: an in situ technique. Limnol Oceanogr 40:575-581
Servais P, Debecker E, Billen G (1984) Annual cycle of gross primary production and respiration in the Viroin river (Belgium). Hydrobiologia 111:57-63
Shearer JA, DeBruyn ER, DeClercq DR, Schindler DW, Fee EJ (1985) Manual of phytoplankton primary production methodology. Can Tech Rep Fish Aquat Sci 1740:1-47

Sherr BF, Sherr EB (1984) Role of heterotrophic protozoa in carbon and energy flow in aquatic ecosystem. In: Klugg MJ, Reddy CA (eds) Current perspectives in microbial ecology. American Society for Microbiology, Washington, DC, pp 412-423

Shurpali NJ, Verma SB, Kim J, Arkebauer TJ (1995) Carbon dioxide exchange in a peatland ecosystem. J Geophys Res 100(D7):14319-14326

Shvidenko A, Nilsson S (1997) Are the Russian forests disappearing? Unasylva 48:57-64

Shvidenko A, Nilsson S, Shepashenko D (2000) Dynamics of phytomass and net primary production of Russian forests in 1961-1998: an attempt of aggregated estimation. In: Biodiversity and dynamics of ecosystems in North Eurasia, vol 4: Forest and soil ecosystems of North Eurasia. Russian Academy of Sciences, Novosibirsk, pp 110-112

Sigg L, Stumm P, Behra P (1992) Chimie des milieux aquatiques. Masson, Paris

Sikora LJ, Keeney V (1983) Further aspects of soil chemistry under anaerobic conditions. In: Gore AJP (ed) Mires: swamp, bog, fen and moor.(Ecosystems of the world, V.4) Elsevier, New York, pp 247-256

Siltanen RM, Apps MJ, Zoltai SC, Mair RM, Strong WL (1997) A soil profile and organic carbon database for Canadian forest and tundra mineral soils. Natural Resources Canada, Canadian Forestry Service, Northern Forestry Center, Edmonton

Silver JA (1992) Frequency modulation spectroscopy for trace species detection: theory and comparison among experimental methods. Appl Opt 24:707-717

Silvola J, Alm J, Ahlholm U, Nykänen H, Martikainen PJ (1996) CO_2 fluxes from peat in boreal mires under varying temperature and moisture conditions. J Ecol 84:219-228

Simmons JA, Fernandez IJ, Briggs RD, Delaney MT (1996) Forest floor carbon pools and fluxes along a regional climate gradient in Maine. For Ecol Manage 84:81-95

Simpson IJ, Edwards GC, Thurtell GW, Den Hartog G, Neumann HH, Staebler RM (1997) Micrometeorological measurements of methane and nitrous oxide exchange above a boreal aspen forest. J Geophys Res 102(D24):29331-29341

Singh KD (1993) The 1990 tropical forest resources assessment. Unasylva 44(174):10

Sissakian C (1992) Présentation de la retenue de Petit Saut en Guyane française: cartographie-partition de la retenue volumes et surfaces-intégration paysagère. Hydroécol Appl 1:121-132

Sitaula BK, Bakken LR (1993) N_2O release from spruce forest soil, relation with nitrification, CH_4 uptake, temperature, moisture and fertilisation. Soil Biol Biochem 25:1415-1421

Smagin AV, Smagina MV, Vomperskii SE, Glukhova TV (2000) Generation and emissions of greenhouse gases in peatlands. Eurasian Soil Sci 33:959-966

Smith DW (1991) Water quality changes and clearing requirements for impoundments in arctic and subarctic regions. Prog Water Tech 12:713-733

Smith KA, Clayton H, Arah JRM et al. (1994) Micrometeorological and chamber methods for measurement of nitrous oxyde fluxes between soils and the atmosphere: overview and conclusions. J Geophys Rev 99:16541-16548

Smith LK, Lewis WM (1992) Seasonality of methane emissions from five lakes and associated wetlands of the Colorado Rockies. Glob Biogeochem Cycles 6:323-338

Smith LK, Lewis WM, Chanton JP, Cronin G, Hamilton SK (2000) Methane emissions from the Orinoco River floodplain, Venezuela. Biogeochemistry 51:113-140

Smith RC, Prézelin BB, Baker KS, Bidigare RR, Boucher NP, Coley T, Karentz D, MacIntyre S, Matlick HA, Menzies D, Ondrusek M, Wan Z, Waters KJ (1992) Ozone depletion: ultraviolet radiation and phytoplancton biology in antarctic waters. Science 255:952-959

Smith REH, Furgal JA, Charlton MN, Greenberg BM, Hiriart V, Marwood C (1999) Attenuation of ultraviolet radiation in a large lake with low dissolved organic matter concentrations. Can J Fish Aquat Sci 56:1351-1361

Smith RL, Miller LG, Howes BL (1993) Geochemistry of methane in Lake Fryxell, an amictic, permanently ice-covered, Antarctic lake. Biogeochemistry 21:95-115

Smith SV, Hollibaugh JT (1993) Coastal metabolism and the oceanic organic carbon cycle. Rev Geophys 31:75-89

Soballe DM, Kimmel BL (1987) A large-scale comparison of factors influencing phytoplankton abundance in rivers, lakes and impoundments. Ecology 68:1943-1954

Sobek S, Algesten G, Bergström AK, Jansson M, Tranvik LJ (2003) The catchment and climate regulation of pCO_2 in boreal lakes. Glob Change Biol 9:630-641

Solinger S, Kalbitz K, Matzner E (2001) Controls on the dynamics of dissolved organic carbon and nitrogen in a Central European deciduous forest. Biogeochemistry 55:327-349

Sombroeck WG, Nachtergaele FO, Hebel A (1993) Amounts, dynamics and sequestrations of carbon in tropical and subtropical soils. Ambio 22:417-426

Sorrell BK, Boon PI (1992) Biogeochemistry of billabong sediments: II. Seasonal variations in methane production. Freshwater Biol 27:435-445

Spath PL, Manw MK, Kerr DR (1999) Life cycle assessment of coal-fired power production, National Renewable Energy Laboratory, US, June 1999, NREL/TP-570-25119

St.Louis VL, Kelly CA, Duchemin E, Rudd JWM, Rosenberg DM (2000) Reservoirs surfaces as sources of greenhouse gases to the atmosphere: a global estimate. BioScience 50:766-775

St.Louis VL, Rudd JWM, Kelly CA, Bodaly RA, Paterson MJ, Beaty KG, Hesslein RH, Heyes A, Majewski AR (2004). The rise and fall of mercury methylation in an experimental reservoir. Environ Sci Tech (submitted)

Stange F, Butterbach-Bahl K, Papen H, Zechmeister-Boltenstern S, Li C, Aber J (2000) A process-oriented model of N_2O and NO emissions from forest soils, 2. Sensitivity analysis and validation. J Geophys Res 105(D4):4385-4398

Statistique Canada. Altitude et superficie des principaux lacs, provinces et territoires. [En ligne, http://www.statcan.ca/francais/Pgdb/phys05_f.htm] Consulté le 15 juillet 2004

Steudler PA, Bowden RD, Melillo JM, Aber JD (1989) Influence of nitrogen fertilization on methane uptake in temperate forest soils. Nature 341:314-316

Stevenson FJ (1994) Humus chemistry. genesis, composition, reactions. 2nd ed. Wiley & Sons, New York

Stevenson FJ, Cole MA (1999) Cycles of soil: carbon, nitrogen, phosphorus, sulphur, micronutrients. 2nd ed,Wiley & Sons, New York

Stone TA, Schlesinger P, Houghton RA, Woodwell GM (1994) A map of the vegetation of South America based on satellite imagery. Photogramm Eng Remote Sensing 60(5):541-551

Striegl RG, Kortelainen P, Chanton JP, Wickland KP, Bugna GC, Rantakari M (2001) Cardon dioxide partial pressure and ^{13}C content of north temperate and boreal lakes at spring ice melt. Limnol Oceanogr 46:941-945

Striegl RG, Michmerhuizen CM (1998) Hydrologic influence on methane and carbon dioxide dynamics at two north-central Minnesota lakes. Limnol Oceanogr 43:1519-1529

Strobel BW, Bruun Hansen HC, Borggaard OK, Ansersen MK, Raulund-Rasmussen K (2001) Composition and reactivity of DOC in forest floor soil solutions in relation to tree species and soil type. Biogeochemistry 56:1-26

Stumm W, Morgan JJ (1996) Aquatic chemistry: chemical equilibria and rates in natural waters. In: Schnoor J, Zehnder A (eds) Environmental science and technology. Wiley & Sons, New York

Suyker AE, Verma SB, Arkebauer TJ (1997) Season-long measurement of carbon dioxide exchange in a boreal fen. J Geophys Res 102(D24):29021-29028

Suyker AE, Verma SB, Clement RJ, Billesbach DP (1996) Methane flux in a boreal fen: seasonal-long measurement by eddy correlation. J Geophys Res 101:28637-28647

Svensson BH (1984) Different temperature optima for methane formation when enrichments from acid peat are supplemented with acetate or hydrogen. Appl Environ Microbiol 48:389-394

Svensson BS, Ericson SO (1993) Does hydroelectric power increase global warming? Comment to the synopsis by Rudd et al. Are Hydroelectric Reservoirs Significant Sources of Greenhouse Gases? (Ambio, V. 22, No 4, 1993). Ambio 22(8):569-570

Svensson JM (1998) Emission of N_2O, nitrification and denitrification in a eutrophic lake sediment bioturbated by *Chironomus plumosus*. Aquat Microb Ecol 14(3):289-299

Sweerts JPR, Kelly CA, Rudd JWM, Hesslein R, Cappenburg TE (1991) Similarity of whole-sediment molecular diffusion coefficients in sediments of low and high porosity. Limnol Oceanogr 36:335-342

Szaran J (1997) Achievement of carbon isotope equilibrium in the system HCO_3^- (solution) – CO_2 (gas). Chem Geol 142:79-86

Tadonléké DR, Planas D, Lucotte M (in press) Microbial food web in boreal humic lakes and reservoirs: ciliates as a major factor related to the dynamics of the most active bacteria. Microb Ecol

Takahashi T, Wanninkhof R, Feely RA et al. (1999) Net sea-air CO_2 flux over the global oceans: an improved estimate based on the sea-air pCO_2 difference. In: Nojiri Y (ed) Proceedings of the 2nd International Symposium CO_2 in the Oceans - The 12th Global Environment Tsukuba, 18–22 January 1999, Center for Global Environmental Research, Tsukuba, pp 9-15

Tamm CO, Holmen H (1967) Some remarks on soil organic matter turn-over in Swedish podzol profiles. Soils and Fertilizers 31:1576

Tans PP, Fung IY, Takahashi T (1990) Observational constraints on the global atmospheric CO_2 budget. Science 247:1431-1438

Tarnocai C (1994) Amount of organic carbon in Canadian soils. In: Transactions of 15th World Congress of Soil Science, vol 6a, Commission V: Symposia. Acapulco, Mexico. International Society of Soil Science, pp 67-82

Tathy JP, Cros B, Delmas RA, Marenco A, Servant J, Labat M (1992) Methane emission from a flooded forest in central Africa. J Geophys Res 97(D6):6159-6168

Ternon JF, Oudot C, Dessier A, Diverres D (2000) A seasonal tropical sink for atmospheric CO_2 in the Atlantic ocean: the role of the Amazon river discharge. Mar Chem 68:183-201

Texier C (1974) Aperçu géologique du site LG 2. Montréal. Université du Québec à Montréal, CERSE

Thébault JM, Capblancq J, Petit M (1999) Influence de la morphométrie et du brassage vertical sur la production primaire nette du phytoplancton. Compte rendu de l'Académie des Sciences, Paris, Sciences de la vie 322:63-70

Thérien N (1991) La création de réservoirs hydroélectriques et les gaz à effet de serre. Actes du Colloque "Les enseignements de la phase I du complexe La Grande", 59e congrès de l'ACFAS, pp 26-34

Thérien N (1999) Élaboration d'un modèle prévisionnel de la qualité de l'eau adaptable aux divers réservoirs hydroélectriques du moyen-nord québécois. Rapport présenté à Service Hydraulique et environnement, Hydro-Québec, Montréal.

Thérien N, Morrison KA (1995a) Détermination des flux de matières en fonction du temps pour des échantillons types de sols inondés sous diverses conditions environnementales contrôlées: Lot 1 - Carbone, azote et phosphore / Lot 2 - Anhydride carbonique et méthane / Lot 3 - Mercure volatil, inorganique et méthylique / Lot 4 épaisseur active des sols / Lot 5 - Biodégradabilité de la tourbe et des sols. Rapport final. Vice-présidence environnement, Hydro-Québec, Montréal

Thérien N, Morrison KA (1995b) Gaz à effet de serre libérés en fonction du temps pour des substrats de phytomasse ennoyés sous diverses conditions environnementales contrôlées. Rapport final. Vice-présidence environnement, Hydro-Québec, Montréal

Thérien N, Spiller G, Coupal B (1982) Simulation de la décomposition de la matière végétale et des sols inondés dans les réservoirs de la région de la Baie de James. Canadian water resources journal 7(1):375-396

Therrien J (2003) Revue des connaissances sur les gaz à effet de serre des milieux aquatiques – Le gaz carbonique, l'oxide nitreux et le méthane. Rapport du Groupe conseil GENIVAR inc. présenté à Hydro Québec, Direction Barrages et Environnement, Montréal

Therrien J (2004) Flux de gaz à effet de serre en milieux aquatiques. Suivi 2003. Rapport du Groupe conseil GENIVAR inc. présenté à Hydro-Québec, Direction Barrages et Environnement, Montréal

Therrien J (in prep.) Campagne d'échantillonnage sur les émissions de gaz à effet de serre des réservoirs et des lacs environnants: rapport de terrain 2003. Rapport du Groupe conseil GENIVAR inc. présenté à Hydro Québec, Direction Barrages et Environnement, Montréal

Therrien J, Verdon R, Lalumière R (2002) Suivi environnemental du complexe La Grande. Évolution des communautés de poissons. Rapport synthèse 1977-2000. Groupe conseil GENIVAR inc. et Direction Barrages et Environnement, Hydro-Québec Production, Montréal

Thibodeaux LJ (1979) Chemodynamics. Wiley & Sons, New York

Thomann RV, Mueller JA (1987) Principles of surface water quality modeling and control. Harper & Row Publishers, New York

Thomas DN, Lara RJ (1995) Photodegradation of algal derived dissolved organic carbon. Mar Ecol Progr Ser 116:309-310

Thorton KW (1990) Perspectives of reservoirs limnology. In: Thorton KW, Kimmel BL and Payne FE (eds) Reservoir limnology: ecological perspectives. Wiley & Sons, New York, pp 1-13

Thouvenot A, Debroas D, Richardot M, Jugnia LB, Devaux J (2000) A study of changes between years in the structure of plankton community in a newly-flooded reservoir. Arch Hydrobiol 149:131-152

Timperley MH, Vigor-Brown RJ (1986) Water chemistry of lakes in the Taupo Volcanic Zone, New Zealand. NZ J Mar Freshwater Res 20:173-183

Tranchart S, Delisle C, Frigon C, Larzillière M (1999) Rapport d'activité 1999: Mesure des concentrations de CH_4 et de CO_2 par spectroscopie laser infrarouge. Rapport présenté à Hydro-Québec par Université Laval, Laboratoire LPAM

Tranvik LJ (1988) Availability of dissolved organic carbon for planktonic bacteria in oligotrophic lakes of different humic content. Microb Ecol 16:311-322

Tranvik LJ, Jansson M (2002) Terrestrial export of organic carbon. Nature 415:861-862

Tremblay A, Lambert M (submitted) Émissions des gaz à effet de serre de rivières et de réservoirs du Panama. Journal des sciences de l'eau

Tremblay A, Lambert M, Fréchette JL, Varfalvy L (2001) Comparison of greenhouse gas emissions from hydroelectric reservoirs and adjacent lakes. Presented to the 28th Congress of the Societas Internationalis Limnologiae, February 4-10, Melbourne, Australia

Tremblay A, Lambert M, Gagnon L (in press) CO_2 fluxes from natural lakes and hydroelectric reservoirs in Canada. Environ Manage

Tremblay A, Lucotte M, Schetagne R (1998) Total mercury and methylmercury accumulation in zooplankton of hydroelectric reservoirs in Northern Québec (Canada). Sci Total Environ 213:307-315

Tremblay A, Therrien J (2004) Gross emission of GHG from boreal reservoirs over time. In: Tremblay A, Varfalvy L, Rhoem C et al (eds) Greenhouse gases emissions from natural environments and hydroelectric reservoirs: fluxes and processes. Springer-Verlag .(in press)

Tremblay T (2002) Modélisation de la pCO_2 dans l'épilimnion et du flux de CO_2 à la surface d'un plan d'eau douce lors de variations des conditions de turbulence par le vent et par la modification de la production nette de CO_2 à l'intérieur de l'épilimnion. Rapport d'activité de synthèse présenté à C Hillaire-Marcel. UQAM-SCT

Trettin CC, Jurgensen MF, Gale MR, McLaughlin JW (1995) Soil carbon in northern forested wetlands: impacts of silvicultural practices. In: McFee WW, Kelly JM (eds) Carbon forms and functions in forest soils. Soil Science Society of America, Madison, Wisconsin

Trofimov S, Men'shikh Y, Dorofeeva TB, Goncharuk EI, Yu N (1998) Organic matter reserves and decomposition rates in the boggy soils under spruce forests of the Central forest state biospheric reserve. Eurasian Soil Sci 31:378-383

Trumbore SE, Chadwick OA, Amunson R (1996) Rapid exchange between soil carbon and atmospheric carbon dioxide driven by temperature change. Science 272:393-396

Trumbore SE, Davidson EA, Camargo PB, Nepstad D, Martinelli LA (1995) Below ground cycling of carbon in forest and pastures of Eastern Amazonia. Glob Biogeochem Cycles 9:515-528

Tundisi JG (1988) Limnologia e manejo de represas. Sao Carlos. EESC-SP/CHREA/ACIESP 1:1-506

Turcq B, Cordeiro RC, Sifeddine A, Simões Filho FFL, Albuquerque ALS, Abrão JJ (2002) Carbon storage in Amazonia during the Last Glacial Maximum: secondary data and uncertainties. Chemosphere 49:821-835

Turner DP, Koerper GJ, Harmon ME, Lee JJ (1995) A carbon budget for forests of the conterminous United States. Ecol Appl 5:421-436

Uher G, Andreae MO (1997) Photochemical production of carbonyl sulfide in North Sea water: a process study. Limnol Oceanogr 42:432-442

Uncles RJ (2002) Estuarine physical processes research: some recent studies and progress. Estuar Coast Shelf Sci 55:829-856

UNECE/FAO [United Nations Economic Commission for Europe/Food and Agriculture Organization of the United Nations] (2000) Forest resources of Europe, CIS, North America, Japan and New Zealand (industrialized temperate/boreal countries). UNECE/FAO contribution to the global forest resources assessment 2000, ECE/TIM/SP/17, United Nations, Geneva

Updegraff K, Bridgham SD, Pastor J, Weishampel P, Harth C (2001) Response of CO_2 and CH_4 emissions from peatlands to warming and water table manipulation. Ecol Appl 11(2):311-326

Upstill-Goddard RC, Barnes J, Frost T, Punshon S and Owens NJP (2000) Methane in the Southern North Sea: low salinity inputs, estuarine removal and atmospheric flux. Glob Biogeochem Cycles 14:1205-1217

Upstill-Goddard RC, Watson AJ, Liss PS, Liddicoat MI (1990) Gas transfer velocities in lakes measured with SF_6.Tellus 42B:364-377

Urban NR, Dinkel C, Wehrli B (1997) Solute transfer across the sediment surface of a eutrophic lake: I. Porewater profiles from dialysis samplers. Aquat Sci 59:1-25

Usol'tsev VA, Koltunova AI (2001) Estimating the carbon pool in the phytomass of larch forests in northern Eurasia. Russian journal of ecology 32:235-242

Vähätalo AV, Salkinoja-Salonen M, Taalas P, Salonen K (2000) Spectrum of quantum yield for photochemical mineralization of dissolved organic carbon in a humic lake. Limnol Oceanogr 45:664-676

Vähätalo AV, Salonen K, Salkinoja-Salonen M, Hatakka A (1999) Photochemical mineralization of synthetic lignin in lake water indicates enhanced turnover of aromatic organic matter under solar radiation. Biodegradation 10:415-420

Vaisanen TS, Martikainen PJ, Hellsten SK, Niskanen A, Huttunen JT, Heiskanen M, Nenonen O (1996) Importance of greenhouse gas emissions from finnish hydropower production compared to other sources of electricity, with the Kemijoki water body as an example. In: IAEA Advisory Group Meeting on Assessment of Greenhouse Gas Emissions from the Full Energy Chain for Hydropower, Nuclear Power and other Energy Sources, Montreal (Canada), March 1996

Valentine RL, Zepp RG (1993) Formation of carbon monoxide from the photodegradation of terrestrial dissolved organic carbon in natural waters. Environ Sci Tech 27(2):409-412

Valentini R, Matteucci G, Dolman AJ et al. (2000) Respiration as the main determinant of carbon balance in European forests. Nature 404:861-865

Van Breemen N, Buurman P (1998) Soil formation. Kluwer Academic Publishers, Netherlands

Van Cleve K, Barney R, Schlentner R (1981) Evidence of temperature control of production and nutrient cycling in two interior Alaska black spruce stands. Can J For Res 11:258-273

Van Coillie R., Visser SA, Campbell PGC, Jones HG (1983) Évaluation de la dégradation de bois de conifères immergés durant plus d'un demi-siècle dans un réservoir. Annales de Limnologie 19: 129-134

Van de Walle I, Mussche S, Samson R, Lust N, Lemeur R (2001) The above- and belowground carbon pools of two mixed deciduous forest stands located in East-Flanders (Belgium). Ann For Sci 58:507-517

Van der Heide J (1982) Physics and chemistry of lake Brokopondo and its affluents. In: Van der Heide J (ed.) Lake Brokopondo: filling phase limnology of a man-made lake in the humid tropics, vol II. University of Amsterdam, Academish Proefschrift, pp 37-199

Van der Nat FJ, Middelburg JJ (2000) Methane emissions from tidal freshwater marshes. Biogeochemistry 49:103-121

Van Eck GTM, Smits JGC (1986) Calculation of nutrient fluxes across the sediment-water interface in shallow lakes. In: Sly PG (ed) Sediments and water interactions. Springer-Verlag, New York, pp 289-301

Vaquer A, Pons V, Lautier J (1997) Distribution spatio-temporelle du phytoplancton dans le réservoir de Petit Saut. Hydroécol Appl 9:169-194

Varfalvy L, Delmas R, Richard S, Santos MA, Matvienko B (2002) An international collaborative project. Assessment and modeling of net greenhouse gas (GHG) emissions from hydroelectric reservoirs. Terms of reference (TOR) - Phase I. Inter-comparison of current and upcoming GHG measurement techniques and additional GHG flux measurements at the Petit Saut reservoir and at various reference sites (forested sites, wetlands, rivers, estuary), December 20, 2002

Vaughan D, Lumsdon DG, Linehan DJ (1993) Influence of dissolved organic matter on the bio-availability and toxicity of metals in soils and aquatic systems. Chem Ecol 8:185-201

Vejre H, Callesen I, Vesterdal L, Raulund-Rasmussen K (2003) Carbon and nitrogen in Danish forest soils – Contents and distribution determined by soil order. Soil Sci Soc Am J 67:335-343

Velho LFM, Lansac-Toha FA, Bonecker CC, Bini LM, Rossa DC (2001) The longitudinal distribution of copepods in Corumba Reservoir, State of Goias, Brazil. Hydrobiologia 453/454:385-391

Venkitesvaran JJ, Schiff SL, Boudreau NM, St.Louis VL, Matthews CJD, Joyce EM, Beaty KG, Bodaly RDA (submitted in 2003) Processes affecting greenhouse gas production in experimental boreal reservoirs: a stable carbon isotope approach. Ecosystems (under review)

Venkiteswaran JJ, Schiff SL (2004) Temperature dependence of carbon isotope fractionation during methane oxidation in experimental boreal reservoirs. Appl Geochem (in review)

Verma SB, Ullman FG, Billesbach D, Clement RJ, Kimm J, Verry ES (1992) Eddy correlation measurements of CH4 flux in a northern peatland ecosystem. Boundary-Layer Meteorol 58:289-304

Veyssy E, Etcheber H, Lin RG, Buat-Menard P, Maneux E (1999) Seasonal variations and origins of particulate organic carbon in the lower Garonne River at La Réole (SW France). Hydrobiologia 391:113-126

Victor DG (1998) Strategies for cutting carbon. Nature 395:837-838

Vila I, Contreras M, Montecino V, Pizarro J, Adams D (2000) Rapel: A 30 years temperate reservoir: eutrophication or contamination? In: Berman T, Hambright KD, Gat J, Gafny S, Sukenik A, Tilzer M (eds) Limnology and lake management 2000+: Proceedings of the Kinneret Symposium, Ginnosar, Israel, Sept. 1998. (Advances in limnology 55) E. Schweizerbart'sche Verlagsbuchhandlung, Stuttgart, pp 31-44

Viner AB (1987) Inland waters of New Zealand. (DSIR Bulletin. 241). Department of Scientific and Industrial Research, Wellington, New Zealand

Vitt D, Bayley SE, Jin T, Halsey L, Parker B, Craik R (1990) Methane and carbon dioxide production from wetlands in boreal Alberta. Report prepared for Alberta Environment, Edmonton

Vodacek A, Blough NV, DeGrandpre MD, Peltzer ET, Nelson RK (1997) Seasonal variation of CDOM and DOC in the middle atlantic bight: terrestrial inputs and photooxidation. Limnol Oceanogr 42(4):674-686

Vompersky SE (1994) The role of mires in the carbon circulation. In: Biogenocenic peculiarities of mires and their rational use. Report from the XI Sukachev Memory Meetings, Nauka, Moscow, p 5–37 [in Russian]

Vourlitis GL, Oechel WC (1997) The role of northern ecosystems in the global methane budget. Ecol Stud 124:266-289

Vucetich JA, Reed DD, Breymeyer A, Degórski M, Mroz GD, Solon J, Roo Zielinska E, Noble R (2000) Carbon pools and ecosystem properties along a latitudinal gradient in northern Scots pine (Pinus sylvestris) forests. For Ecol Manage 136:135-145

Waddington JM, Roulet NT (2000) Carbon balance of a boreal patterned peatland. Glob Change Biol 6(1):87-97

Waddington JM, Roulet NT, Swanson RV (1996) Water table control of CH4 emission enhancement by vascular plants in boreal peatlands. J Geophys Res 101(D17):22775-22785

Wang S, Grant RF, Verseghy DL, Black TA (2002) Modelling carbon dynamics of boreal forest ecosystems using the canadian land surface scheme. Clim Change 55:451-477

Wang WH, Beyerle-Pfnür R, Lay JP (1988) Photoreaction of salicylic acid in aquatic systems. Chemosphere 17:1197-1204

Wang Y, Amundson R, Trumbore S (1996) Rodiocarbon dating of soil organic matter. Quaternary Research 45:282-288

Wanninkhof R (1992) Relationship between wind speed and gas exchange over the ocean. J Geophys Res 97(C5):7373-7382

Wanninkhof R, Asher W, Weppernig R, Chen H, Schlosser P, Langdon C, Sambrotto R (1993) Gas transfer experiment on Georges Bank using two volatile deliberate tracers. J Geophys Res 98(C11):20 237-20 248

Wanninkhof R, Ledwell JR, Crusius J (1991) Gas transfer velocities on lakes measured with sulfur hexafluoride In: Wilhelms SC, Gulliver JS (eds) Air-water mass transfer: Selected papers from the 2nd International Symposium on Gas tranfer at water surfaces, Minneapolis, Minnesota, September 1990. American Society of Civil Engineers, New York, pp 441-458

Wanninkhof R, Ledwell JR, Broecker W, Hamilton M (1987) Gas exchange on Mono lake and Crowley lake, California. J Geophys Res 92 (C13):14567-14580

Wanninkhof R, Ledwell JR, Broecker WS (1985) Gas exchange-wind speed relation measured with sulfur hexafluoride on a lake. Science 275:1224-1226

Wanninkhof RH, Bliven LF (1991) Relationship between gas exchange, wind speed, and radar backscatter in a large wind-wave tank. J Geophys Research 96 (C2):2785-2796

Wassmann R, Thein UG, Whiticar MJ, Rennenberg H, Seiler W, Junk WJ (1992) Methane emissions from the Amazon floodplain: characterization of production and transport. Glob Biogeochem Cycles 6(1):3-13

Watson AJ, Robertson JE, Ling RD (1993) Air-sea exchange of CO_2 and its relation to primary production. In: Wollast R, Mackenzie FT and Chou L (eds) Proceedings of the NATO Advanced Research Workshop 1991, Melreux (Belgium). Springer-Verlag, New York, pp 249-258

Watson AJ, Upstill-Goddard RC, Liss PS (1991) Air-sea gas exchange in rough and stormy seas measured by a dual-tracer technique. Nature 349:145-147

Weiss R (1970) The solubility of nitrogen, oxygen and argon in water and seawater. Deep-Sea Res 17:721-735

Weiss RF (1974) Carbon dioxide in water and seawater: the solubility of a non-ideal gas. Mar Chem 2:203-215

Weissenberger S, Duchemin E, Houel S, Canuel R, Lucotte M (1999) Greenhouse gas emissions and carbon cycle in boreal reservoirs. In: Proceedings of the Internat Workshop on Hydro dams, lakes and greenhouse gas emissions. COPPE, Rio de Janeiro, pp 33-40

Wetzel RG (1975) Limnology. Saunders, Philadelphia

Wetzel RG (1990) Reservoir ecosystems: conclusions and speculations. In: Thornton KW, Kimmel BL, Payne FE (eds) Reservoir limnology: ecological perspective. Wiley & Sons, New York pp 227-238

Wetzel RG (2001) Limnology: lake and river ecosystems, 3rd ed. Academic Press, San Diego

Whalen SC, Reeburgh WS, Barber VA (1992) Oxidation of methane in boreal forest soils: a comparison of seven measures. Biogeochemistry 16:181-211

Whalen SC, Reeburgh WS, Kizer KS (1991) Methane consumption and emission from taiga sites. Glob Biogeochem Cycles 5:261-274

White E, Don BJ, Downes MT, Kemp LJ, MacKenzie AL, Payne GW (1978) Sediments of lake Rotorua as sources and sinks for plant nutrients. NZ J Mar Freshwater Res 12:121-130

Whiticar MJ (1999) Carbon and hydrogen isotope systematics of bacterial formation and oxidation of methane. Chem Geol 161:291-314

Whiticar MJ, Faber E, Schoell M (1986) Biogenic methane formation in marine and freshwater environments: CO_2 reduction vs acetate fermentation–isotope evidence. Geochimica et Cosmochimica Acta 50:693-709

Whiting GJ (1994) CO_2 exchange in the Hudson Bay lowlands: community characteristics and multispectral reflectance properties. J Geophys Res 99(D1):1519-1528

Whiting GJ, Chanton JP (1993) Primary production control of methane emission from wetlands. Nature 364:794-795

Whiting GJ, Chanton JP (2001) Greenhouse carbon balance of wetlands: methane emission versus carbon sequestration. Tellus Series B 53(5):521-528

Whiting GJ, Chanton JP, Bartlett DS, Happell JD (1991) Relationships between CH_4 emission, biomass, and CO_2 exchange in a subtropical grassland. J Geophys Res 96:13067-13071

Whitman WG (1923) Preliminary experimental confirmation of the two-film theory of gas absorption. Chem Metall Eng 29:146-148

Whittaker RH, Likens GE (1973) Carbon in the biota. In: Woodwell GM, Pecan EV (eds), Carbon and the biosphere. US Atomic Energy Commission, Symposium Series 30, National Technical Information Service, Springfield, pp 281-302

Wickland KP, Striegl RG, Mast MA, Clow DW (2001) Carbon gas exchange at a southern Rocky Mountain wetland, 1996-1998. Glob Biogeochem Cycles 15: 321-335

Widdows J, Brown S, Brinsley MD, Salkeld PN, Elliot M. (2000) Temporal changes in intertidal sediment erodability: influence of biological and climatic factors. Cont Shelf Res 20:1275-1289

Wienhold F, Frahm GH, Harris GW (1994) Measurements of N_2O fluxes from fertilized grassland using a fast response tunable diode laser spectrometer, J Geophys Res 99:16557

Wiesenburg DA, Guinasso NL (1979) Equilibrium solubilities of methane, carbon monoxide and hydrogen in water and seawater. J Chem Eng Data 24:356-360

Williams PJ leB (1998) The balance of plankton respiration and photosynthesis in open oceans. Nature 394:55-57

Williams PJ leB, Robertson JE (1991) Overall planktonic oxygen and carbon dioxide metabolisms: the problem of reconciling observations and calculations of photosynthetic coefficients. J Plankton Res 13:153-169

Wilson JO, Crill PM, Bartlett KB, Sebacher DI, Harriss RC, Sass RL (1989) Seasonal variation of methane emissions from a temperate swamp. Biogeochemistry 8:55-71

Wilson KB, Baldocchi DD (2000) Estimating annual net ecosystem exchange of carbon over five years at a deciduous forest in the southern United States. Agric Forest Meteorol 100:1-18

Wirth C, Schulze ED, Lühker B, Grigoriev S, Siry M, Hardes G, Ziegler W, Backor M, Bauer G, Vygodskaya NN (2002) Fire and site type effects on the long-term carbon and nitrogen balance in pristine Siberian Scots pine forests. Plant and Soil 242:41-63

Wissmar RC, Richey JE, Stallard RF, Edmond JM (1981) Plankton metabolism and carbon processes in the Amazon river, its tributaries, and floodplain waters, Peru-Brazil, May-June 1977. Ecology 62:1622-1633

Witman WB, Rogers JE (1991) Research needs in the microbial production and consumption of radiatively important trace gases. In: Rogers JE, Whitman WB (eds) Microbial production and consumption of greenhouse gases: methane, nitrogen oxides, and halomethanes. American Society for Microbiology, Washington, DC, pp 287-291

Wolfe DW, Erickson JD (1993) Carbon dioxide effects on plants: uncertainties and implications for modeling crop response to climate change. In: Kaiser HM, Drennen TE (eds) Agricultural dimensions of global climate change, St.Lucie Press, Delray Beach, Florida, pp 153-178

Wollast R (1983) Interaction in estuaries and coastal waters. In: Bolin B, Cook RB (eds) The major biogeochemical cycles and their interactions. SCOPE 21, Wiley & Sons, New York, pp 385-407

Woodwell PM, Rich PH, Hall CAS (1973) Carbon in estuaries. In: Woodwell PM, Pecan EV (eds) Carbon and the biosphere.(U.S. Atomic Energy Commission Symposium Series 30) NTIS, Springfield, VA, pp 221-240

Word Commission on Dams (2000) Dam reservoirs and greenhouse gases. Report on the workshop held on February 24-25, 2000, Hydro-Quebec, Montreal, World Commission on Dams Secretariat

Word Commission on Dams (2000b) Dams and global change executive summary review draft (February 2000). Rosa LP, dos Santos MA, Arnell N, Hulme M (eds) Prepared for the WCD, World Commission on Dams Secretariat, WCD Thematic Reviews, II.2 Dams and Global Change, 2000

Word Commission on Dams (2000c) Certainty and uncertainty in the science of greenhouse gas emissions from hydroelectric reservoirs: a report on the state of the art for the World Commission on Dams. Final Report (March 2000). Rosa LP, dos Santos MA (eds), prepared for WCD, World Commission on Dams Secretariat, WCD Thematic Reviews, 2000

Word Commission on Dams (2000) Thematic reviews. II.2. Dams and global change. Dams reservoirs and greenhouse gases. Report on the workshop held on February 24-25, 2000; Final minutes. Hydro-Quebec, Montreal

World Commission on Dams (2000) Workshop on dam reservoirs and greenhouse gases (February 24-25, 2000), Part III, Final Minutes, Montreal

World Meteorological Organization, Global Atmospheric Watch (2002) World Data Centre for Greenhouse Gases. WMO WDCGG Data Summary. WDCGG No 26. GAW Data

Wüest A, Piepke G, van Senden DC (2000) Turbulent kinetic energy balance as a tool for estimating vertical diffusivity in wind-forced stratified waters. Limnol Oceanogr 45:1388-1400

Yamamoto S, Murayama S, Saigusa N, Kondo, H (1999) Seasonal and interannual variation of CO_2 flux between a temperate forest and the atmosphere in Japan. Tellus Series B 51:402-413

Yarie J, Billings S (2002) Carbon balance of the taiga forest within Alaska: present and future. Can J For Res 32:757-767

Zanata LH, Espindola ELG (2002) Longitudinal processes in Salto Grande reservoir (Americana, SP, Brazil) and its influence in the formation of compartment system. Brazilian J Biol 62:347-361

Zannetti P (1990) Air pollution modeling: theories, computational methods and available software. Computational Mechanics Publications, Southampton

Zappa CJ, Raymond PA, Terray EA, McGillis WR (2003) Variation in surface turbulence and the gas transfer velocity over a tidal cycle in a macro-tidal estuary. Estuaries 26(6):1401-1415

Zhou YR, Yu ZL, Zhao SD (2000) Carbon storage and budget of major Chinese forest types. Acta Phytoecologica Sinica, 24(5):518-522 [in Chinese]

Zison SW, Mills WB, Diemer D, Chen CW (1978) Rates, constants and kinetic formulations in surface water quality modelling. Tetra Tech inc. for USEPA, ORD, Athens, GA, ERL, EPA 600-3-78-105

Zoltai SC, Matikainen PJ (1996) Estimated extent of forested peatlands and their role in the global carbon cycle. In: Apps MJ, Price DT (eds) Forest ecosystems, forest management and the global carbon cycle. NATO Advanced Science Institute Series, vol 140, Springer-Verlag, Heidelberg, p 47-58

Zöllner E, Santer B, Boersma M, Hoppe HG, Jurgens K (2003) Cascading predation effects of *Daphnia* and copepods on microbial food web components. Freshwater Biol 48:2174-2193